PROCEEDINGS

VETERINARY PATHOLOGY SERVICE
WEDNESDAY SLIDE CONFERENCE
2017-2018

JOINT PATHOLOGY CENTER
SILVER SPRING, MD 20910
2017-2018

JOINT PATHOLOGY CENTER
VETERINARY PATHOLOGY SERVICE

Case	JPC No.	Slide ID No.	Species	Lesion/condition	Tissue	Page
Conference 1	**23-Aug-17**					**1-20**
1	4017218	11-1259-7	Dog	Pulmonary amyloidosis	Lung	
2	4065317	MU1165314	Ox	Lymphocytic perivasculitis/Malignant catarrhal fever	Eye	
3	4066355	RP22064	Rabbit	Interstitial pneumonia/*Toxoplasma gondii*	Lung	
4	4099789	UMC171	Cat	Arteriolosclerosis and hyphema/hypertensive retinopathy	Eye	
Conference 2	**30-Aug-17**					**21-40**
1	4084138	16040206	Horse	Necrotizing hepatitis/Tyzzer's disease (*Clostridium piliforme)*	Liver	
2	4101299	1235813-002	Macaque	Necrotizing colitis/*Entamoeba histolytica*	Colon	
3	4066348	14-1424	Horse	Hepatic fibrosis/Pyrrolizidine alkaloid intoxication	Liver	
4	4101085	T17-15923	Dog	Compound odontoma	Gingiva	
Conference 3	**6-Sep-17**					**41-63**
1	4019127	10N0979	Cat	Perivascular histiocytisis/Globoid cell leukodystrophy	Cerebellum and brain stem	
2	4020992	11-30435	Dog	Necrotizing nephritis, hepatitis, splenitis/Canine herpesvirus-1	Kidney, liver, spleen	
3	4102122	E 1246-14	Horse	Proliferative rhinitis/*Rhinosporidium seeberi*	Nasal mucosa	
4	4101575	B17-798	Cat	Carcinoma, high grade with epithelial and mesenchymal components	Mammary gland	
Conference 4	**20-Sep-17**					
1	4101761	N761-15	Horse	Necrotizing vasculitis/*Trema micrantha* ingestion	Pons	**64-83**
2	4102434	16/545	Dog	Leiomyositis/Chronic intestinal pseudo-obstruction	Small intestine	
3	4101313	CASE 2	Ox	Pyogranulomas and Wallerian degeneration/Vaccine oil adjuvant reaction	Spinal cord	
4	4101755	CASE #2	Dog	Neuroendocrine tumor (chemodectoma)	Fibroadipose tissue	
Conference 5	**27-Sep-17**					**84-107**
1	4100988	S17-3588	Pig	Interstitial pneumonia (necrotizing), bronchopneumonia (suppurative), and arteritis (necrotizing)/PCV-2, *Aspergillus* sp., *Pneumocystis carinii*	Lung	
2	4102148	16-180	Ox	Bronchointerstitial pneumonia/BRSV	Lung	
3	4101308	16H0097	Boar	Necrotizing bronchopneumonia, lymphadenitis, hepatitis */Salmonella choleraesuis*	Lung, lymph node, liver	
4	4101307	P16-555	Pig	Fibrinonecrotizing vasculitis/Classical swine fever	Spleen	
Conference 6	**4-Oct-17**					**108-128**
1	4017935	3120125021	Guinea fowl	Lymphoma	Feathered skin	
2	4033563	12060787	Chicken	Necrotizing hepatitis/Inclusion body hepatitis (*Aviadenovirus)*	Liver	
3	4035426	T	Turkey	Skeletal muscle degeneration and necrosis/Toxic myopathy	Skeletal muscle	
4	4101090	T17-14880	Peacock	Necrotizing tracheitis/Gallid herpesvirus-1 (infectious laryngotracheitis)	Trachea	
Conference 7	**18-Oct-17**					**129-154**
1	4101076	F1753191	Goat	Thymoma; hyperkeratotic and lymphocytic dermatitis	Haired skin, mediastinal mass	
2	4102437	17-14227	Dog	Mesothelioma and branchial cysts	Pericardium	
3	4019378	S9004764	Calf	Meningoencephalitis/Sporadic bovine encephalomyelitis (*Chlamydophila pecorum)*	Brainstem and cerebellum	
4	4100736	L17-994 (no label)	Cat	Necrosuppurative bronchopneumonia/FIPV and *Bordetella bronchiseptica*	Lung	
Conference 8	**25-Oct-17**					**155-176**
1	4019838	11111437	Horse	Equine multinodular pulmonary fibrosis/ *Equine herpesvirus-5*	Lung	
2	4101759	N450-14	Cat	Bronchitis and bronchiectasis/*Aspergillus* sp.	Lung	
3	4018605	P1270-11	Cat	Feline idiopathic pulmonary fibrosis	Lung	
4	4100435	H17-0145J	Alpaca	Necrosuppurative bronchopneumonia/ *Burkholderia pseudomallei*	Lung	
Conference 9	**1-Nov-17**					**177-196**
1	4101294	17-38-W	Mouse	Pulmonary adenomas, emphysema	Lung, haired skin	
2	4101486	DX17-0022	Mouse	Histiocytic sarcoma; cystic endometrial hyperplasia	Uterus	
3	4103775	MS 15-2723	Mouse	Granulomatous hepatitis/*Schistosoma* sp.	Liver	
4	4104252	MS17-3649	Mouse	Meningoencephalitis/Zika virus	Brain	
Conference 10	**29-Nov-17**					**197-215**
1	4019375	H12/1754	Ox	Granulomatous enteritis/Johne's disease (*Mycobacterium avium* ssp. *Paratuberculosis)*	Small intestine	
2	4102431	JCP-TAMU-1 2017	Cat	Renal tubular necrosis/Lily intoxication	Kidney	
3	4102670	N-103/17	Dog	Hepatic fibrosis with macronodular hepatocellular regeneration/Copper toxicosis	Liver	
4	4050142	2014 Case 1	Ox	Histiocytosis (lymph node and liver) with birefringent pigment/2,8-dihydroxyadenine deposition ("Green liver disease")	Liver/lymph node	

Conference 11	**6-Dec-17**					**216-239**
1	4048071	SQ	Squirrel	Viral fibropapillomas/Squirrel fibroma virus	Haired skin	
2	4048228	R14-160	Salamander	Neuroepithelioma (neuromastoma)	Skin	
3	4102429	17-5139	Dolphin	Meningomyelitis and arteriosclerosis/ *Brucella seti*	Spinal cord	
4	4101227	92039	Rhinoceros	Pheochromocytoma and myelolipoma	Adrenal gland	
Conference 12	**13-Dec-17**					**240-262**
1	4102118	16L-2815	Horse	Granulomatous polyradiculoneuritis/Cauda equina syndrome	Spinal cord (cauda equina)	
2	4084210	N2015-0602	Hedgehog	Bilaterally symmetrical myelin degeneration/Wobbly Hedgehog Syndrome	Brain and spinal cord	
3	4020995	C973	Dog	Necrotizing meningoencephalitis/ *Neospora caninum*	Brain	
4	4101762	O291/16	Dog	Necrotizing meningoencephalitis (NME)	Brain	
Conference 13	**3-Jan-18**					**263-280**
1	4050462	14/327	Dog	Ocular melanosis and glaucoma	Globe	
2	4070254	K13-8163-B	Dog	Iridociliary adenoma; ferrugination of retinal vessels	Globe	
3	4095576	719/16	Guinea pig	Osseous choristoma/heterotrophic bone formation of the ciliary body	Globe	
4	4101750	NE 17-399	Penguin	Fibrous osteodystrophy (scleral ossicles)	Globe	
Conference 14	**10-Jan-18**					**281-303**
1	4019414	BB364/11	Dog	Ganglioneuromatosis	Jejunum	
2	4101493	2 (salmon colored slide)	Dog	Normal placental site involution	Uterus	
3	4102671	N-1238	Goat	Bilaterally symmetrical neuroaxonal degeneration/Copper deficiency ("Swayback")	Spinal cord	
4	4065579	2 (white colored slide)	Guinea pig	Teratoma	Ovary	
Conference 15	**17-Jan-18**					**304-325**
1	4101316	S16-1796	Owl	Necrotizing hepatitis/Columbid herpesvirus-1	Liver	
2	4100856	E 6940/16	Flamingo	Proliferative and necrotizing dermatitis/ *Avipoxvirus*	Skin	
3	4101222	LJ84	Monkey	Hemorrhagic and necrotizing pancreatitis/ *Adenovirus*	Pancreas	
4	4103279	401343	Sheep	Pulmonary adenocarcinoma	Lung	
Conference 16	**24-Jan-18**					**326-349**
1	4101317	F16-0079-3	Python	Bronchointerstitial pneumonia/ *Morelia viridis nidovirus*	Lung	
2	4101141	1704 0830	Alpaca	Ileitis & colitis/*Eimeria macusaniensis*	Ileum & colon	
3	4067142	H15-0067L	Bilby	Pyogranulomatous adrenalitis and encephalitis/ *Sporothrix* spp.	Brain & adrenal gland	
4	4100648	WSC 2017-18 Case 1	Monkey	Multiple encysted acanthocephalans	Testis	
Conference 17	**31-Jan-18**					**350-368**
1	4079216	186	Crocodile	Multiple Microsporidian spores	Liver (EM image)	
2	4021148	12-294	Horse	Necrohemorrhagic adrenalitis/Equine *herpesvirus* -1	Adrenal gland	
3	4085535	S-13-1538	Ox	Necrotizing abomasitis/Arsenic poisoning	Omasum/abomasum	
4	4101690	2017 B	Ox	Polyglucosan bodies (Lafora-like bodies)	Cerebrum (slide & EM)	
Conference 18	**7-Feb-18**					**369-388**
1	4101081	1704415	Horse	Glomus tumor	Skin	
2	4102669	NP-20/17	Pig	Necrosuppurative dermatitis and cellulitis/ *Pasteurella multocida*	Skin	
3	4102987	V165/17	Cat	Proliferative and hyperkeratotic otitis externa/Proliferative and necrotizing otitis of kittens	External ear canal	
4	4102124	S 504/16	Horse	Necrotizing vasculitis/Purpura hemorrhagica	Skin	
Conference 19	**21-Mar-18**					**389-412**
1	4048933	P46/14	Dog	Parathyroid adenoma	Parathyroid gland	
2	4101305	3855-16	Dog	Sarcoma (favor peripheral nerve sheath tumor) and Osteosarcoma	Soft tissue mass	
3	4102120	W1161-16	Dog	Adrenal necrosis (cortical and medullary)/Trilostane intoxication	Adrenal gland	
4	4048433	4079-14	Sheep	Thyroid follicular hyperplasia; follicular hypoplasia and hypotrichosis (haired skin)	Haired skin, thyroid gland	
Conference 20	**6-Apr-18**					**413-433**
1	4084197	T16-13553	Dog	Carcinoid	Gallbladder	
2	4099033	20327-15 A or C	Dog	Bridging fibrosis with micronodular hepatocellular regeneration/Lobular dissecting hepatitis	Liver	
3	4101304	10621-16	Cat	Lymphocytic cholangitis	Liver	
4	4032913	2012911922	Dog	Sarcoma	Liver	
Conference 21	**11-Apr-18**					**434-456**
1	4085100	Case 1 G9312	Monkey	Granulomatous arteritis; myocardial degeneration and necrosis	Lung; heart	
2	4101079	F1755364	Cat	Hyaline vascular necrosis	Brain	

3	4100982	G071	Guinea pig	Lymphocytic apoptosis; salivary gland epithelial necrosis/Ebola and Cytomegalovirus infection	Salivary gland & thymus	
4	4101312	16N-3473	Horse	Proliferative and necrotizing arteritis/*Strongylus vulgaris*	Aorta	
Conference 22	**18-Apr-18**					**457-480**
1	4066542	15L-2067C	Horse	T-cell rich B-cell lymphoma; neuronal degeneration and loss/Equine dysautonomia (grass sickness)	Ileum	
2	4066540	P636-14	Dog	Perivascular lymphoid proliferation	Cerebrum	
3	4066861	15-23253	Dog	Intravascular lymphoma	Liver	
4	4101495	#1	Cat	Lymphoma with angioinvasion, angiodestruction, and coagulative necrosis	Haired skin	
Conference 23	**25-Apr-18**					**481-505**
1	4100935	164361-16	Dog	Osteomyelitis and myositis/*Blastomyces dermatitidis*	Bone	
2	4018791	UFMG 247/12	Cat	Osteomyelitis/suspect *Nocardia* sp.	Bone	
3	4100931	16-41394	Dog	Metaphyseal osteomyelitis/Hypertrophic osteodystrophy	Bone	
4	4100936	109234-16	Dog	Chondrodysplasia/Mucopolysaccharidosis	Bone	
Conference 24	**2-May-18**					**506-529**
1	4101485	AP17-0483	Zebrafish	Malignant peripheral nerve sheath tumor (PNST), multiple granulomas	Whole body	
2	4101145	IP17-300	Tilapia	Branchial epithelial hyperplasia/ *Ichthyophthirius multifilis;* Epitheliocystis; filamentous bacilli; monogeaean	Head	
3	4084211	68197	Chameleon	Necrotizing hepatitis/*Ranavirus*	Liver	
4	4101578	N17-104-1	Turtle	Dysgerminoma	Ovary	
Conference 25	**9-May-18**					**530-549**
1	4102436	17B-0101	Dog	Nephroblastoma	Kidney	
2	4101577	16A351	Macaque	Chorioamnionitis/*Streptococcus* sp.	Placenta	
3	4068392	CASE 2 51304	Ox	Mycotic rumenitis/*Candida* sp. and zygomycetes	Rumen	
4	4101147	Case 2	Mouse	Embolic pneumonia/*Klebsiella pneumoniae* and acidophil macrophage pneumonia	Lung	

Joint Pathology Center
Veterinary Pathology Services

WEDNESDAY SLIDE CONFERENCE 2017-2018

Conference 1

23 August 2017

CASE I: 11-1259-7 (JPC 4017218).

Signalment: Ten-year-old, castrated male, mixed breed canine (*Canis lupis familiaris*).

History: A reportedly 10 year old male castrated mixed breed dog presented for complete necropsy following euthanasia. The dog had a three week history of lethargy, weakness, dyspnea, tachypnea and in-appetence. There was a history of a left total hip replacement and bilateral hip dysplasia. The dog had been on Deramaxx since 2003 and Tramadol since 2009. On presentation the dog was in respiratory distress with a heart rate of 180 bpm. There was pitting edema in the right front forelimb.

Gross Pathology: The dog had a body condition score of 5/5 and was in good post mortem condition. A firm, red, 1cm diameter mass was present on the dorsal antibrachium, and a soft, 7cm x 4cm white subcutaneous mass was present in the right axillary region (lipoma). The pleural cavity contained approximately 150ml of thin red fluid. Within the cranial mediastinum there was a 30 cm x 26 cm by 15 cm lobulated, poorly demarcated, white to yellow firm mass. On cut surface >75% of the mass was soft and yellow to light green (necrosis). The mass extended into the pericardium and similar masses were present within the right and left atria and auricles, and right ventricular free wall (ranging from 3-6cm in diameter). A single 2-3 cm diameter mass was present within the right cranial lung lobe, and another single 2-3 cm mass was present within the wall of the esophagus. There were multiple masses (1-4cm in diameter) within the wall of the stomach.

Gross Morphologic Diagnosis: None provided.

Laboratory results: None provided.

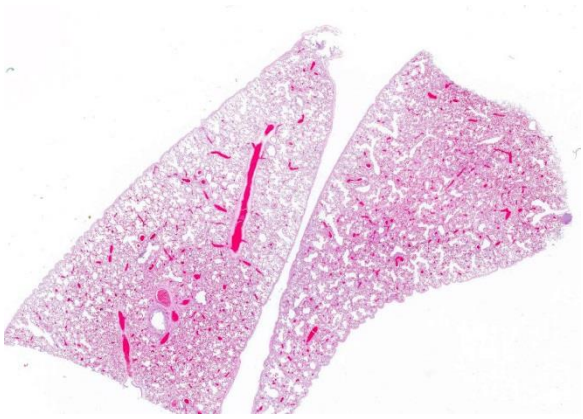

Lung, dog. Two sections are presented for evaluation.

Microscopic Description: Lung: The alveolar interstitium is randomly effaced and expanded by variably sized aggregates of amorphous homogenous eosinophilic material. In addition, similar aggregates are observed replacing the tunica media of pulmonary arteries and arterioles and occasionally of veins. The material can be also seen rarely ruptured into the alveolar air space. Occasionally, organized accumulations of fibrin, neutrophils and erythrocytes are present in arteries and arterioles which are adhered to the endothelial surface of the vessel (thrombosis). Some thrombi contain a flattened cell population adhered to the surface (endothelialization). A moderate multifocal alveolar histiocytosis is present characterized by intra-alveolar accumulations of macrophages with abundant eosinophilic vacuolated cytoplasm. Extramedullary hematopoiesis is present.

Contributor's Morphologic Diagnoses: Marked multifocal pulmonary amyloidosis characterized by deposition in arterioles and interstitium with fibrin thrombi, and mild to moderate pulmonary edema.

Contributor's Comment: Amyloid is composed insoluble protein arranged in β-pleated sheets of protein. The conformation of the protein is the primary characteristic responsible for the binding and staining of the Congo red dye. Amyloid is most commonly classified as secondary or AA

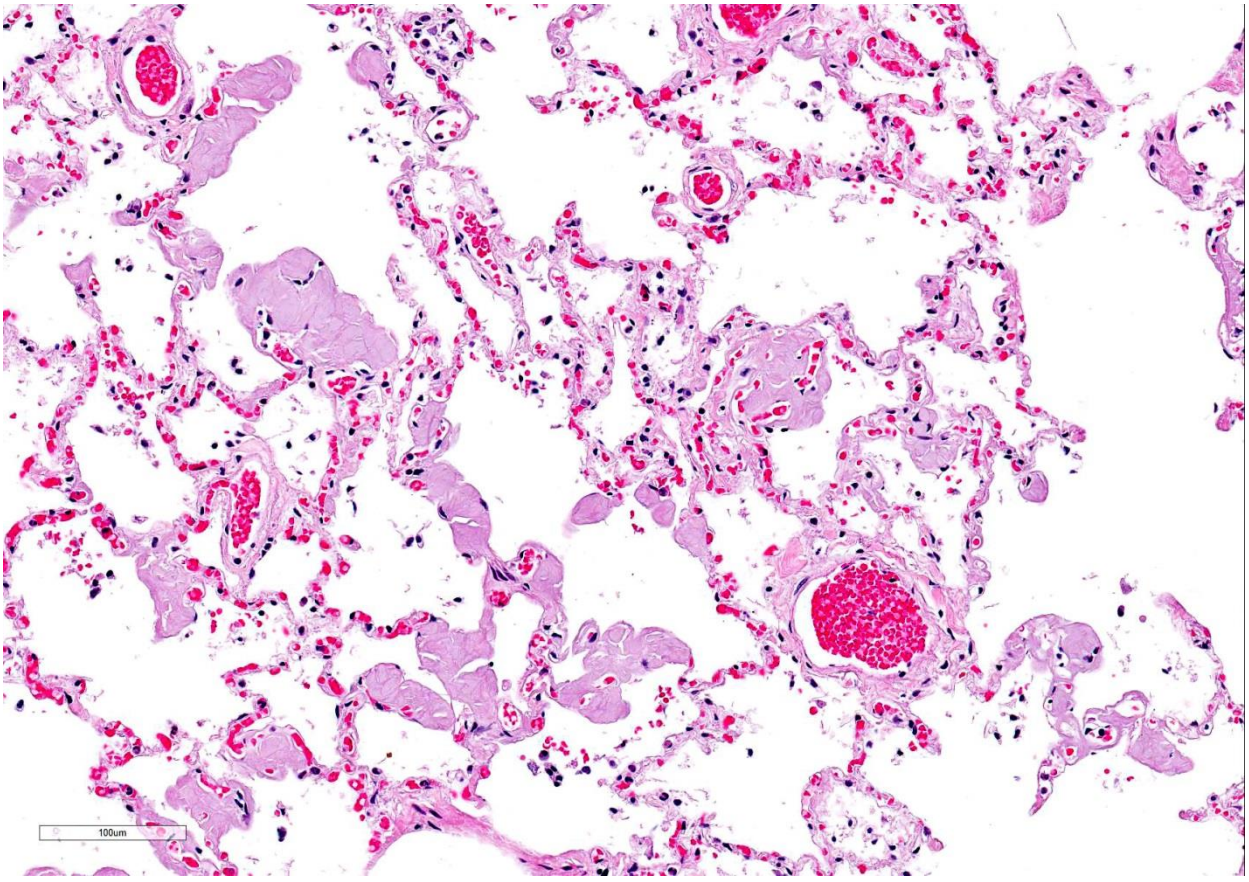

Lung, dog. Two sections are presented for evaluation. Multifocally, nodular aggregates of amyloid expand alveolar septa. (HE, 288X)

and primary or AL in veterinary medicine. AA amyloid is associated with chronic inflammation and is composed of fragments derived from serum amyloid A, a serum apolipoprotein and acute phase protein produced by hepatocytes. Familial amyloidosis in the Shar-Pei dog breed and cat breeds such as the Abyssinian and Siamese is also AA amyloid. AL amyloid is formed from immunoglobulin light chains, predominantly λ light chain fragments. This type of amyloid is commonly associated with plasma cell dyscrasias. Aβ (β-amyloid) is angiocentric cerebral deposits of amyloid recognized in the human and canine. Amyloidosis is also classified as localized or systemic with systemic involvement representing more than 60% of cases (1).

Amyloidosis is reported in several organs in species of veterinary importance but most commonly deposits in the glomerular tuft and peritubular interstitium of the kidney, the periarteriolar lymphoid sheaths in the spleen and the space of Disse in the liver.

Pulmonary amyloidosis is reported in canines and humans. Radiographically, human parenchymal amyloidosis is divided into a nodular form and a diffuse septal form (1). In canines, amyloid deposition in the tunica intima and media of large pulmonary arteries is described. This particular deposition of amyloid is derived from apolipoprotein AI and may be a age related change (2,3). The type of amyloid present in this case was not determined.

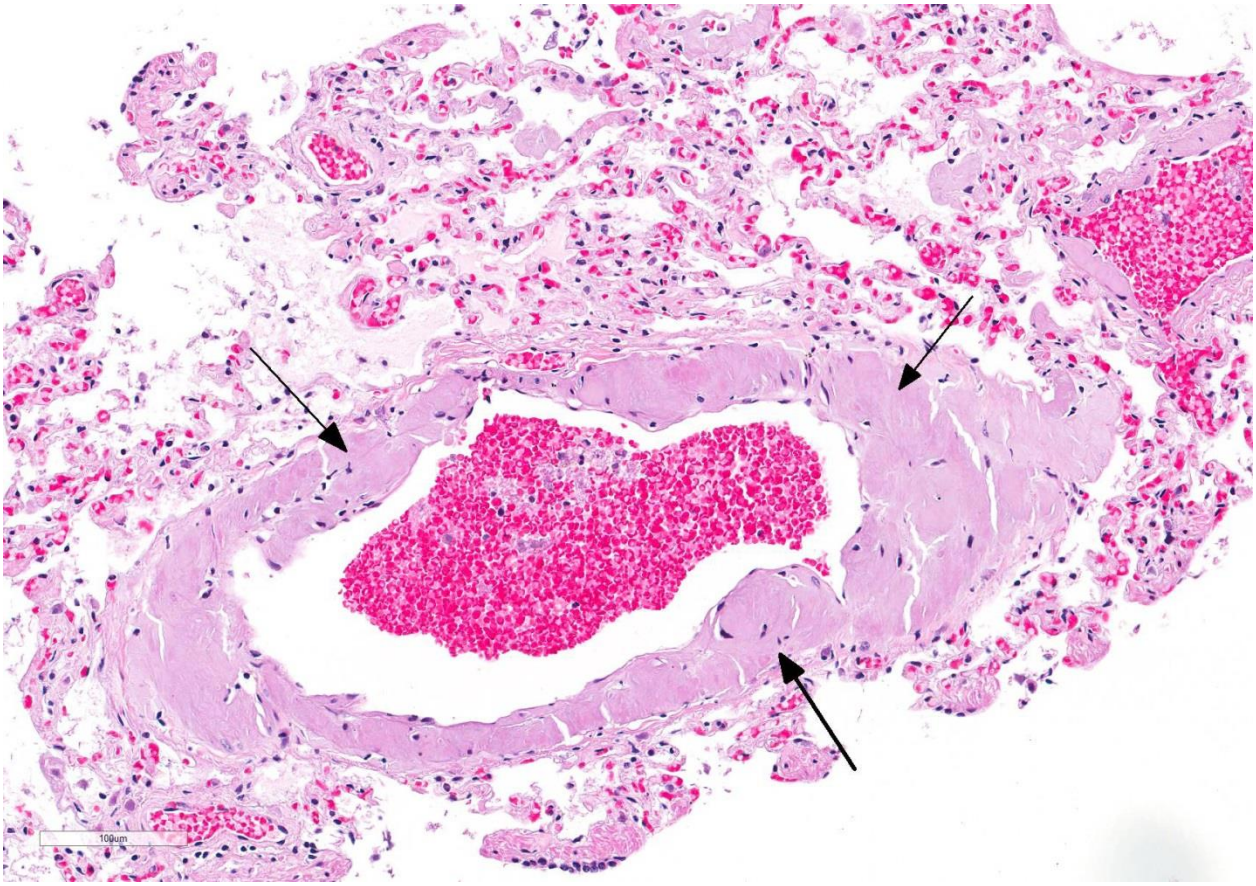

Lung, dog. Walls of pulmonary arterioles of all sizes are thickened by amyloid deposits (arrows)(HE, 288X) .

JPC Diagnosis: Lung: Amyloidosis, arteriolar, arterial, and interstitial, multifocal, marked with alveolar edema, mixed breed, *canine*.

Conference Comment: This case nicely demonstrates the histologic changes associated with pulmonary amyloidosis. A Congo red was run to highlight the apple green birefringence of the deposited amyloid and participants discussed the use of Thioflavine T viewed under a ultraviolet light as an additional amyloid marker.[3] Although the microscopic appearance is characteristic, a differential diagnosis of pulmonary arteriolar/arterial and interstitial hyalinosis was discussed. Pulmonary hyalinosis has been reported as a finding in the pulmonary artery of older dogs.[10] Hyalinosis can be differentiated from amyloid using periodic-acid shift (PAS) stain which highlights the glassy eosinophilic material.[2] The following chart was used to review the classification of different types of amyloidosis:

Clinicopathologic Category	Associated Diseases	Major Fibril Protein	Precursor Protein
Systemic (Generalized Amyloidosis)			
Primary Amyloidosis (Immune dyscrasias)	Monoclonal plasma cell proliferations	AL (Light chain amyloid)	Ig light chains (mainly λ type, but also κ type)
Secondary Amyloidosis (Reactive systemic amyloidosis)	Chronic inflammatory conditions	AA (Amyloid associated)	SAA (Serum associated amyloid)
Hereditary Amyloidosis			
Familial amyloidosis	Renal impairment	AA	SAA
Localized Amyloidosis			
Islet amyloid	Type 2 diabetes mellitus	AIAPP	Islet amyloid polypeptide
Cerebral (senile) amyloid	Cognitive disorder	Aβ (Beta-amyloid protein)	APP (amyloid precursor protein)
Pulmonary vessel amyloid	?	Apolipoprotein A-I (apoA-I)	?

Chart adapted from table 6-17 in *Robbins and Cotran Pathologic Basis of Disease*, page 258

While reviewing the chart above, participants were reminded that familial amyloidosis occurs in Shar-Pei dogs and Abyssinian cats with AA amyloid deposition in the renal interstitium as opposed to the glomeruli. In these cases, renal impairment is generally mild and amyloid is usually

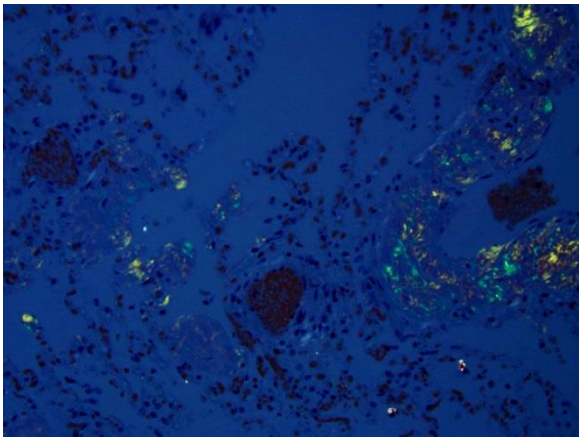

Lung, dog. Amyloid deposits within septa and arteriole walls exhibits congophilia and apple-green birefringence on a 5um section . (Congo Red, 400X)

diagnosed incidentally during necropsy.[7]

In addition, conference participants discussed the gross appearance of organs containing amyloid deposits as yellow, waxy, coalescing, nodular amorphous deposits that turns brown when stained with Lugol's iodine and deep purple with acetic acid.[7]

Finally, the conference moderator emphasized (as did the contributor's in the above comment) that in most domestic species AA amyloid deposition in the liver begins in the space of Disse with the exception of the mouse where deposition occurs in the periportal regions of the liver.[1]

Contributing Institution:
Department of Veterinary Biosciences
College of Veterinary Medicine
The Ohio State University
http://vet.osu.edu/biosciences

References:

1. Barthold SW, Griffey SM, Percy DH. Mouse. In: *Pathology of Laboratory Rodents and Rabbits.* 4th ed. West Sussex, UK: Wiley & Sons, Inc.; 2016:92.
2. Cianciolo RE, Mohr FC. Urinary system. In: Maxie MG, ed. *Jubb, Kennedy, and Palmer's Pathology of Domestic Animals*. Vol. 2. 6th ed. London, UK: Saunders Elsevier; 2016:406.
3. Cullen JM, Stalker MJ. Liver and biliary system. In: Maxie MG, ed. *Jubb, Kennedy, and Palmer's Pathology of Domestic Animals*. Vol. 2. 6th ed. London, UK: Saunders Elsevier; 2016:279.
4. Johnson KH, Sletten K, Hayden DW, O'Brien TD, Roertgen KE, Westermark P. Pulmonary vascular amyloidosis in aged dogs. A new form of spontaneously occurring amyloidosis derived from apolipoprotein AI. *Am J Pathol*. 1992 Nov;141(5):1013-9.
5. Kumar V, Abbas AK, Aster JC. Diseases of the immune system. In: *Robbins and Cotran Pathologic Basis of Disease*. 9th ed. Elsevier Saunders; 2015: 256-262.
6. Lachmann HJ, Hawkins PN. Amyloidosis and the lung. *Chronic Respiratory Disease*. 2006;3(4):203-14.
7. Miller MA, Zachary JF. Mechanisms and morphology of cellular injury, adaptation, and death. In: McGavin MD and Zachary JF, eds. *Pathologic Basis of Veterinary Disease*. 6th ed. Elsevier, Mosby Saunders; 2016: 30-31.
8. Roertgen KE, Lund EM, O'Brien TD, Westermark P, Hayden DW, Johnson KH. Apolipoprotein AI-derived pulmonary vascular amyloid in aged dogs. *Am J Pathol*. 1995 Nov;147(5):1311-7.

9. Snyder PW. Diseases of immunity. In: McGavin MD and Zachary JF, eds. *Pathologic Basis of Veterinary Disease*. 4th ed. Elsevier, Mosby Saunders; 2007: 1488.
10. Williams, K. Coronary arteriosclerosis with myocardial atrophy in a 13-year-old dog. *Veterinary Pathology*. 2003 Nov; 40(6), 695-697.

CASE II: MU1165314 (JPC 4065317).

Signalment: Two and a half-year-old, female, Charolais bovine, (*Bos taurus*).

History: This cow had a 1 month history of waxing and waning fever, malaise and nasal discharge, with epiphora and bilateral corneal opacity. Clinical signs regressed with dexamethasone treatment. She progressed to sloughing of the skin on the nose, teats, anus, vulva and coronary bands. She was euthanized due to quality of life issues. There was no history of contact with sheep.

Gross Pathology: This animal was an adequately fleshed, minimally autolyzed white adult female bovine of 500 Kg body weight. The nasal planum was crusted and ulcerated, with red underlying tissue. There was separation of the coronary bands that affected all coronary bands. All teats are covered by crusts, revealing red tissue beneath. Externally both corneas are cloudy and mottled, with reddening of the conjunctiva and milky fluid in the anterior chambers. The corneas became cloudy after fixation and sections of the eye revealed severely increased corneal thickening and exudate in the anterior chamber and behind the lens. The vitreous was cloudy as well.

Lymph nodes associated with the mammary gland, head, neck, and thorax were enlarged to 3-5 times expected volume. There were oral ulcers, particularly on the sides of the thickest part of the tongue and little mucosa remains on the dental pad. The anterior third of the esophagus was uniformly dark red and the wall approached 1 cm in thickness. The abomasal mucosa in 1-1.5 cm thick and the abomasal mucosal folds are thereby accentuated. Punctate ulcers were evident in the mucosa.

Incision of the fixed globes revealed a thickened cornea, with rust red areas of vascularization, and coagulation of exudates in the anterior chamber and vitreous, causing their partial to complete opacity.

Gross Morphologic Diagnosis: None provided.

Laboratory results: Multiple tissues and swabs were positive for herpesviral sequences that were identified as sheep-associated malignant catarrhal fever virus by sequencing. The same samples were negative for sequences of infectious bovine rhinotracheitis virus, bluetongue, BVD and epizootic hemorrhagic disease virus. NVSL

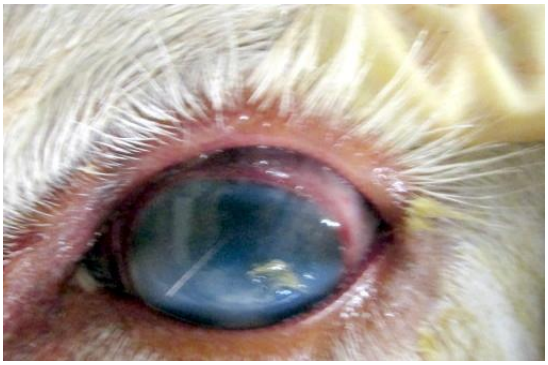

Eye, ox. The cornea is cloudy and edematous, with reddening of the conjunctivae and milky fluid in the anterior chamber. (Photo courtesy of: Veterinary Medical Diagnostic Laboratory, University of Missouri; vmdl.missouri.edu)

testing was declared negative for foot and mouth disease virus.

Microscopic Description (limited to the eye): Nearly every segment of the eye is inflamed or secondarily altered in this animal, with variability in the severity of inflammation between sites . Pink fibrillar edema fluid is present in the anterior chamber. There is pronounced edema of the corneal stroma, with attenuation, vacuolation and loss of the keratinocytes. Intense mixed, predominantly lymphocytic infiltration occurs in the limbus and extends into the cornea, as well as the conjunctiva and sclera. Small thin-walled blood vessels occur in the peripheral corneal stroma, and, beyond this, single file leukocytes align along the stromal fibers. Neutrophils contribute substantially to the population in the more central cornea. The iris and ciliary bodies also contain numerous lymphocytes, macrophages and intermixed neutrophils that exfoliate freely into the anterior and are adhered to the endothelial layer at the back of the cornea. The filtration angle is also filled with similar cells. The fibers of the vitreous are separated by fluid and leukocytes and there choroid is similarly affected. Scleral vessels and extraocular muscle and adventitia have less extensive infiltrates. Lymphocytes are visible in the walls of a few muscular vessels at the base of the iris in some sections.

Similar perivascular lesions (not shown) were associated with ulcerations were found in the skin, tongue, abomasum and in the brain, lung, kidney, heart and adrenal. Lymph nodes were enlarged, with hyperplastic cortical tissue and hemorrhages.

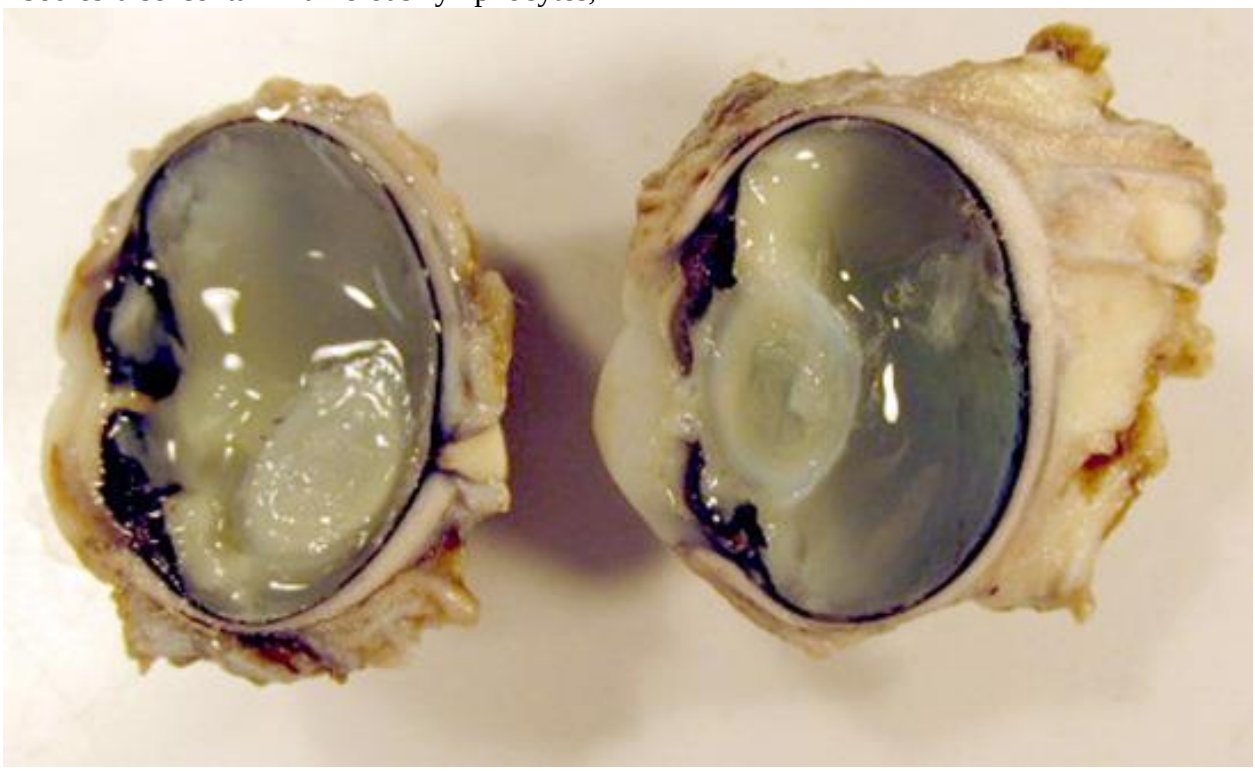

Globe, ox. The cornea is thickened and vascular, and there is coagulated exudate in the anterior and posterior changes. (Photo courtesy of: Veterinary Medical Diagnostic Laboratory, University of Missouri; vmdl.missouri.edu)

Contributor's Morphologic Diagnoses: Eye: Severe lymphocytic vasculitis and perivasculitis, uvea and cornea, with corneal edema, erosion and vascularization.

Contributor's Comment: Malignant catarrhal fever is caused by a rhadinovirus that cause polysystemic disease of cattle, bison, various deer and other ruminants (2). Most cases in cattle affect animals in the 8-24 month age range and have a mean duration of 71 days. Cattle surviving acute MCF have chronic lesions in medium caliber vessel and cornea, comprised of arteriopathy with variable recanalization. Microscopic lesions throughout the body are characterized microscopically by vasculitis. Anterior and posterior synechiae, edema and eventual fibrosis of the corneal stroma, and perforating ulcers and staphyloma are other common ocular lesions.

MCF-related rhadinoviruses have now known to be extremely variable in genetic sequences (3). OvHV-2 had some alleles that varied over 60% in genetic composition.

Globe, ox. Subgross examination of a partial section through the affected globe demonstrates an edematous thickened cornea, prominent cellular infiltrate in the uvea, ciliary body and iris leaflets, and proteinaceous exudates within the anterior segment (HE, 50X)

Translation of 9.5 polypeptides revealed only 49% amino acid identity. However, the clinical signs of MCF in cattle from viral isolates originating sheep, bison, reindeer and cattle, as related to viral genotype, did not reveal differences.

Ocular disease is consistently present in the head and eye form but milder lesions can occur in other forms as well (6). In one study, there was no correlation between the degree of corneal edema at first examination and lethal disease outcome. Corneal edema began at the limbus in natural cases, and corneal erosion was common (5). Keratinization of the corneal epithelium, pyknosis and cytoplasmic vacuolation of epithelial cells were observed (4). Corneal perforations occurred and chronic scars common. The corneal edema and uveitis improved in all surviving cattle. Posterior segment disease was frequently present, but difficult to detect to the alterations in the anterior segment (6).

A review of lesions spontaneously occurring MCF-like disease in exotic hooved stock involved cases in 15 moose, 1 roe deer and 1 red deer. Frequent gross findings involved the eye and included conjunctivitis, corneal opacity and fibrin clots in the anterior chamber. Although OvHV-2 caused some cases, CpHV-2 caused others. Most cases occurred in farmed animals and zoos (1). The microscopic appearance of lesions was similar to those in cattle. Additional novel rhadinoviruses have been described in exotic hooved stock and cervids. (1) Pigs also develop ocular lesions resulting from MCF (2).

JPC Diagnosis: Eye: Panuveitis and vasculitis, lymphoblastic and necrotizing, diffuse, severe with ulcerative keratitis and corneal edema, Charolais, bovine.

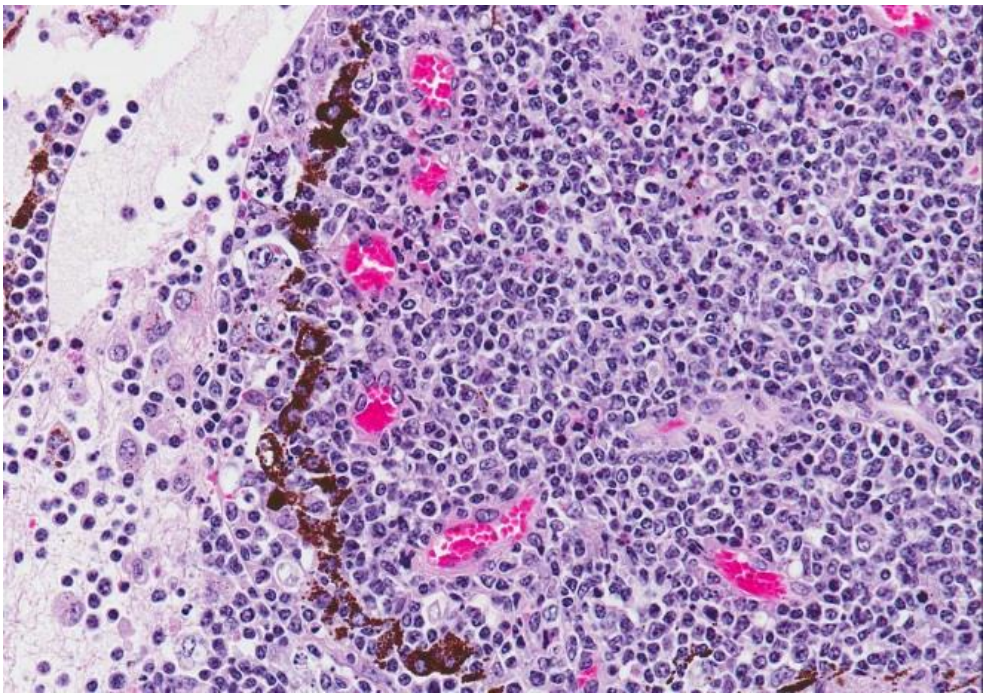

Globe, ox. The ciliary body is markedly expanded by an infiltrate of large numbers of blastic lymphocytes admixed with fewer heterophils and cellular debris. (HE 400X)

Conference Comment: There was significant slide variation in this case. Additional morphologic diagnoses generated by conference participants included conjunctivitis, keratitis, and episcleritis depending on the plane of tissue sectioned.

Malignant catarrhal fever is caused by infections with the MCF virus group of ruminant *Gammaherpesviridae* (which are known as Rhadinoviruses in older texts).[3] Of the pathogens in the MCF virus group, 6 are associated with clinical signs: *Alcelaphine herpesvirus* 1 (carried by wildebeest) and 2 (carried by hartebeest), *Ovine herpesvirus* 2 which is endemic in domestic sheep, *Caprine herpesviruses* 2 (endemic in domestic goats) and 3 (affects white tailed deer and red brocket deer), and *Ibex MCF virus* which is carried by Nubian ibex and produces disease in bongo and anoa. [5] However, most natural outbreaks are due to *Ovine herpesvirus* 2 in sheep or *Alcelaphine herpesvirus* 1 in African wildebeest.

MCF is characterized by marked T-lymphocyte hyperplasia which was prominent in conference discussion. [5] In the slides examined numerous lymphoblastic cells were present in various portions of the eye with prominent mitotic figures. The pathogenesis of MCF is presumed to start with infection of large granular lymphocytes that are subsequently transformed by the gammaherpesvirus. In fact, the OHV-2 genome has been detected in CD8+ T cells which are the predominant cell present in the perivascular inflammation. The pathogenesis of this disease is unclear, and although the invasive T cells are most likely cytotoxic T lymphocytes or T-suppressor cells the mechanism they use to cause such marked vasculitis has not yet been identified.[5]

Conference participants briefly reviewed various terms used to classify ocular inflammation such as: endophthalmitis (inflammation of the uvea, retina, and ocular cavities), panophthalmitis (inflammation of all of the ocular structures, including the sclera), anterior uveitis (inflammation of the ciliary body and iris), posterior uveitis (inflammation of the ciliary body and

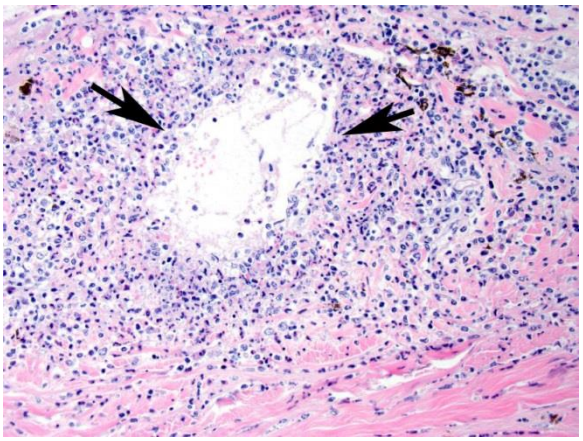

Globe, ox. The wall of a scleral venule is expanded and effaced by infiltration of blastic lymphocytes and heterophils which are admixed with cellular debris (vasculitis). (HE 400X)

choroid), panuveitis (inflammation of the iris, ciliary body, and choroid), and chorioretinitis (inflammation of the choroid and the retina).[7]

In addition, these slides contained nice examples of the tapetum lucidum which is not commonly seen in microscopic sections. The conference moderator noted that in cats and dogs the tapetum is cellular and has a "brick-like" appearance; whereas in ruminants and horses, it contains more fibrous connective tissue with fibroblasts arranged linearly. Pigs were specifically mentioned because they are lacking a tapetum lucidum.[1]

Acute severe bovine viral diarrhea (BVD) and mucosal disease was mentioned as a differential. However, MCF usually affects multiple organs that are not involved in mucosal disease like liver, kidney, bladder, eye, and brain. Also, MCF produces lymphoid hyperplasia whereas lymphoid tissue in BVDV infections is atrophic.[5]

Contributing Institution:
Veterinary Medical Diagnostic Laboratory
University of Missouri
www.vmdl.missouri.edu

References:

1. Bacha WJ, Bacha LM. *Color Atlas of Veterinary Histology*. 3rd ed. West Sussex, UK: John Wiley & Sons, Ltd.; 2012:268.
2. Li H, Gailbreath K, Flach EJ, et al. A novel subgroup of rhadinoviruses in ruminants. *J Gen Virol.* 2005;86:3021-3026.
3. O'Toole D, Li H. The pathology of malignant catarrhal fever, with emphasis on ovine herpesvirus 2. *Vet Pathol.* 2014; **51**: 437-452.
4. Russel GC, Scholes SF, Twomey DF, et al. Analysis of genetic diversity of ovine herpesvirus 2 in samples from livestock with malignant catarrhal fever. *Vet Microbiol.* 2014;172:63-71.
5. Uzal FA, Plattner BL, Hostetter JM. Alimentary system. In: Maxie MG, ed. *Jubb, Kennedy, and Palmer's Pathology of Domestic Animals.* Vol 2.6th ed. St. Louis, Missouri: Elsevier; 2016:131-136.
6. Vikøren T, Li H, Lillehaug A, et al. Malignant catarrhal fever in free ranging cervids associated with OVHV-2 and CPHV-2 DNA. *J Wildlife Dis.* 2006;42:797-807.
7. Wilcock BP, Njaa BJ. Special senses. In: Maxie MG, ed. *Jubb, Kennedy, and Palmer's Pathology of Domestic Animals.* Vol 1.6th ed. St. Louis, Missouri: Elsevier; 2016:446.
8. Whateley HE, Young S, Liggitt HD, et al. Ocular lesions of bovine malignant catarrhal fever. *Vet Pathol.* 1985;22:219-225.
9. Zemljič T, Pot SA, Haessig M, et al. Clinical ocular findings in cows with malignant catarrhal fever: ocular disease progression and outcome in 25 cases (2007-2010). *Vet Ophthalmol.* 2012;15:46-52.

CASE III: RP22064 (JPC 4066355).

Signalment: Adult, female, brush rabbit (*Sylvilagus bachmani*).

History: This animal was 1 of 2 rabbits found dead in a lion exhibit in the same week.

Gross Pathology: The rabbit had small adipose stores. There were fleas in the haircoat. The lungs were red but floated in formalin.

Gross Morphologic Diagnosis: None provided.

Laboratory results: *Toxoplasma gondii* was confirmed by PCR and sequencing performed on tissues from the second brush rabbit found in the same enclosure.

Microscopic Description: Examined is a section of lung in which alveolar lumina are diffusely flooded with proteinaceous fluid (edema) and beaded eosinophilic fibrillar material (fibrin) admixed with plump and foamy alveolar macrophages, fewer lymphocytes, nondegenerate heterophils and plasma cells and scant hemorrhage. Small amounts of fibrin and few lymphocytes, plasma cells, heterophils, and macrophages thicken alveolar septa (up to 3 times normal thickness) and surround larger pulmonary blood vessels. Within alveolar septa and lumina, there are moderate numbers of 1 - 2 µm, oval to fusiform basophilic organisms (tachyzoites) forming 15 - 30 µm in diameter clusters (presumed intrahistiocytic) or, less often, arranged individually (extracellular). Multifocally, there is scattered lytic necrosis of alveolar septa characterized by disruption and replacement of septa by small amounts of necrotic cellular and karyorrhectic debris, fibrin and the aforementioned inflammatory cells. Bronchiole lumina contain refluxed edema fluid and inflammatory cells and peribronchiolar connective tissue is edematous. Alveolar septa are rarely lined by a thin layer of brightly eosinophilic fibrin (hyaline membranes).

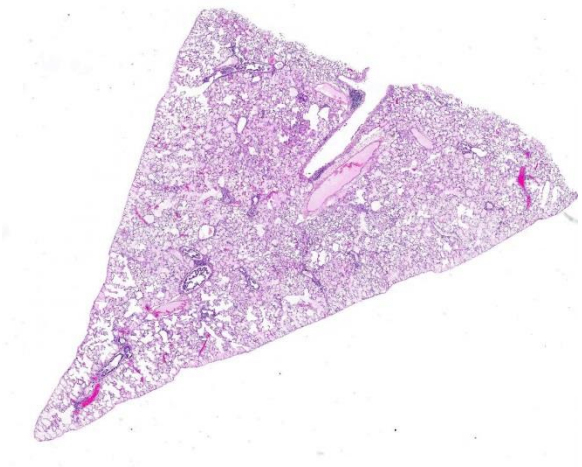

Lung, rabbit. At subgross magnification, there are multiple randomly scattered foci of hypercellularity and multifocal to coalescing areas of edema-filled alveoli. (HE, 5X)

Contributor's Morphologic Diagnoses: Lung: Moderate diffuse acute interstitial pneumonia with edema, necrosis, and intralesional protozoa (etiology: *Toxoplasma gondii*).

Contributor's Comment: Histologic findings are consistent with *Toxoplasma gondii*.[2,3] *T. gondii* are apicomplexan protozoa that affect a wide range of intermediate hosts and are closely related to other coccidia including *Neospora* spp. and *Sarcocystis* spp.[2]

The life cycle of *T. gondii* includes both an intermediate and definitive host. All warm-blooded mammals, including cats and humans, can act as intermediate hosts to complete the asexual stages of the life cycle.

The intermediate host is infected by ingesting the sporulated oocysts in food, water, or soil contaminated with cat feces, or less commonly, by ingesting tissue cysts in uncooked meat.[1,3] Sporozoites leave the oocyst and develop into tachyzoites, which invade the lamina propria and multiply in the intestines. Tachyzoites continue to multiply first in the mesenteric lymph nodes, and then reach the rest of the body through the circulation either free or within lymphocytes, macrophages, and granulocytes. Lesions associated with acute toxoplasmosis are more commonly observed during this asexual stage with rapid multiplication of tachyzoites. The most commonly associated lesions include necrosis, edema, and inflammation (Figure 1).[1-3] This case shows the lesions of an acute infection with *T. gondii*. In this rabbit, lesions were observed in the lung, heart, liver, spleen, kidney, adrenal gland, thyroid gland, stomach, small intestine, brain, skeletal muscle, mesenteric lymph node, and nasal turbinates. Tachyzoites can spread anywhere in the body, as evidenced in this case. Tachyzoites eventually encyst in a wide range of tissues, including brain, liver, lung, muscles, and retina. Tissue cysts may contain anywhere from two to hundreds of bradyzoites. Animals that survive the acute phase of the infection acquire immunity to *T. gondii*.[2]

Domestic and wild felids are the definitive hosts for *T. gondii*. Cats most commonly become infected by eating muscle containing tissue cysts. Bradyzoites are released in the gastrointestinal tract and enter the epithelial cells of the small intestines to undergo several stages of asexual and sexual multiplication. Gamonts are formed and result in oocyst formation. The prepatent period is variable and ranges from 3 – 18 days or more depending on the stage of the organism at the time of ingestion. Unsporulated oocysts are released into the feces where they sporulate within 24 hours in order to infect an intermediate host. Oocysts can remain viable in the environment for long periods of time.[1,2]

This case shows the lesions of disseminated toxoplasmosis with a rabbit as the intermediate host; the definitive host in this case is unknown. The lions may have functioned as the definitive host, or the rabbits could have acquired the infection outside of the lion enclosure. Biosecurity measures are in place to exclude feral cats and other felids from the entire facility. In general, biosecurity measures that could decrease the impact of *T. gondii* in zoos and other facilities include: not housing highly susceptible species (e.g. marsupials and primates) near felids, freezing meat that cannot be cooked prior to feeding animals, designing enclosures to exclude domestic cats and other vectors, and daily cleaning to prevent the sporulation of oocysts in the environment.[2]

JPC Diagnosis: Lung: Interstitial pneumonia, necrotizing, diffuse, moderate, with fibrin, edema, and protozoal tachyzoites (etiology consistent with

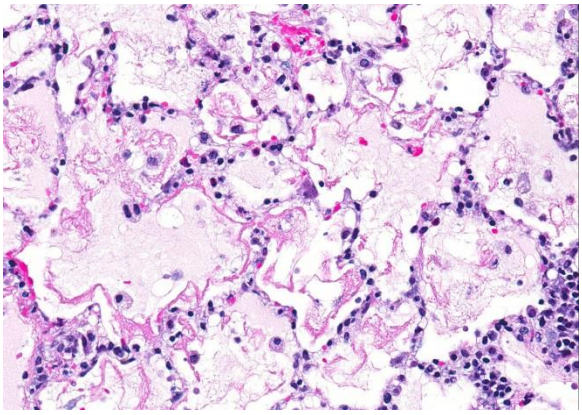

Lung, rabbit. Alveoli are flooded with edema fluid and polymerized fibrin, which often forms hyaline membranes long hypercellular, and often necrotic alveolar walls. (HE, 320X)

Toxoplasma gondii), brush rabbit, *Sylvilagus bachmani*.

Conference Comment: This case nicely demonstrates the characteristic histologic lesions associated with the interstitial pneumonia associated with systemic toxoplasmosis. Conference participants described the random areas of necrosis and identified intracellular and extracellular protozoal tachyzoites within the interstitium and epithelial cells. Participants discussed the different patterns of pneumonia, interstitial, bronchopneumonia, embolic pneumonia, bronchointerstitial pneumonia, granulomatous, and uncategorizable pneumonias.

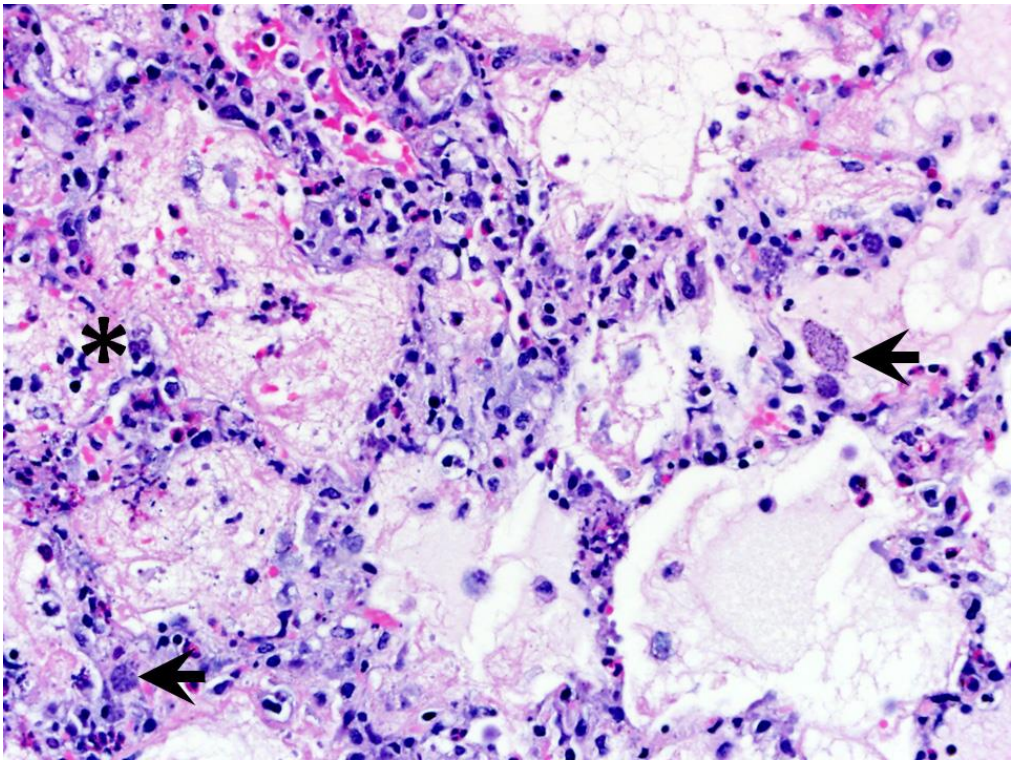

Lung, rabbit. Several intracellular and extracellular clusters of tachyzoites (arrows) are present within alveolar macrophages and alveolar septa. Tachyzoites are 1 - 2 microns in diameter with a basophilic nucleus. There is necrosis of alveolar septa with associated lymphohistiocytic and heterophilic infiltrates, fibrin, and karyorrhectic debris (asterisk). (HE, 400X) (Photo courtesy of: Wildlife Disease Laboratories, Institute for Conservation Research, San Diego Zoo Global, http://www.sandiegozooglobal.org)

The conference moderator discussed traditional bronchopneumonia, which involves an exudate originating at the bronchiolar-alveolar junction and fills bronchioles and alveoli. The characteristic distribution is cranioventral (due to gravity dispersal of inhaled pathgens) which is most commonly caused by opportunists. In contrast, bronchointerstitial pneumonia may be defined as either (1) bronchiolar necrosis and diffuse alveolar damage with destruction of both bronchiolar and alveolar epithelium, or (2) mononuclear cellular inflammation which surround airways and infiltrate alveolar septa. *Mycoplasma hyopneumonia* with its characteristic peribronchiolar and peribronchar lymphoproliferative nature was discussed as one example.[4]

Conference participants considered *Encephalitozoon cuniculi* as a potential differential for this presentation in a rabbit. *Encephalitozoon cuniculi* is a gram-positive, acid fast, obligate intracellular microsporidian that infects a variety of mammalian hosts, the domestic rabbit, being one of the most common. Historically, there has been disagreement among taxonomists about the

classification of this organism, but genomic sequencing has confirmed it as a eukaryotic fungus within the phylum Microsporidia. Transmission occurs through ingestion or inhalation of infected urine or transplacentally. Infective spores then enter circulation via infected mononuclear cells and hit initial target organs such as lung, liver, or kidney. At approximately 3 months post infection, organisms can be found within the central nervous system and produce characteristic clinical signs (head tilt, ataxia, and vestibular signs). In dwarf rabbits, phaecoclastic uveitis and cataract formation are quite common after transplacental transmission. In the lung, lesions may appear as a focal to diffuse interstitial pneumonia with mononuclear cellular infiltration. Microscopically, *E. cuniculi* and *T. gondii* can look quite similar; staining characteristics can help differentiate the two. Toxoplasma organisms are Gram-negative and do not stain with carbol fuschin stains (a type of acid fast stain, a Ziehl-Neelsen subcomponent stain).[2] Although, the contributor prudently identified toxoplasmosis using PCR, Gram stains and several acid fast stains (Ziehl-Neelsen and Fite-Faraco; we do not have access to Carbol fuschin) were performed to further rule out encephalitozoonosis. Organisms within submitted sections were strongly Gram negative, and were not highlighted with acid fast stains which confirm the contributor's diagnosis of *Toxoplasma gondii*.

Finally, conference participants discussed that Toxoplasmosis has a military and veterinary public health relevance due to its recent identification in the central nervous system of individuals suffering from various mental health disorders (bipolar disorder, post-traumatic stress disorder, schizophrenia) and related suicides.[1]

Toxoplasma	***Encephalitozoon***
Small cyst 60	Large pseudocyst up to 120
Spores not acid fast	Spores are **acid fast**
Gram negative	Gram **positive**
Do not stain with carbol fuchsin	Stain with **carbol fuchsin** (purple)
Giemsa: granulated cytoplasm	**Giemsa**: light blue cytoplasm
Stains well with **H&E**	Stains poorly with H&E
Larger organism 2-6 um	Smaller organism 1.5 x 2.5 um
Tend to invoke **necrosis**	Necrosis is not a feature

Contributing Institution:
Wildlife Disease Laboratories
Institute for Conservation Research
San Diego Zoo Global
http://www.sandiegozooglobal.org

References:

1. Ansari-Lari M, Farashbandi H, Mohammadi F. Association of Toxoplasma gondii infection with schizophrenia and its relationship with suicide attempts in these patients. *Trop Med Int Health*. 2017; 22:epub ahead of print. doi: 10.1111/tmi.12933.
2. Barthold SW, Griffey SM, Percy DM. Rabbit. In: *Pathology of Laboratory Rodents and Rabbits*. 4th ed. Oxford, UK: John Wiley & Sons, Inc.; 2016:293-295.
3. Brown CC, Baker DC, Barker IK. Alimentary system. In: Maxie MG, ed. *Jubb, Kennedy and Palmer's Pathology of Domestic Animals*. Vol 2. 5th ed. Edinburgh, UK: Elsevier Limited; 2007:270-272.
4. Caswell JL, Williams KJ. Respiratory system. In: Maxie MG, ed. *Jubb, Kennedy and Palmer's Pathology of Domestic Animals*. Vol 2. 6th ed. Edinburgh, UK: Elsevier Limited; 2016:506-511.
5. Dubey JP, Odening K. Toxoplasma and related infections. In: WM Samuel, MJ Pybus, and AA Kocan, ed. *Parasitic Diseases of Wild Mammals*, 2nd ed. Ames, IA: Iowa State University Press; 2001: 478-492.
6. Gardiner CH, Fayer R, Dubey JP. *An Atlas of Protozoan Parasites in Animal Tissues*, 2nd edition. Armed Forces Institute of Pathology. Washington, DC. 1998.

CASE IV: UMC171 (JPC 4099789).

Signalment: Sixteen-year-old, neutered male, Domestic shorthair cat (*Felis catus*).

History: The cat had an enlarged thyroid discovered during dental prophylaxis 1.5 years before death. At this time there was a grade I murmur auscultated over the left heart. Anti-thyroid medication was started but was discontinued due to miscommunication with the owner about the need for life-long therapy. Four months before euthanasia the cat was noted to be losing weight and was presented again. It was treated for hyperthyroidism and hypertension. Three weeks before euthanasia, the cat became depressed and painful over several days and was brought to an emergency service. He was found to have hyphema in both eyes, with elevated intraocular pressure in the left eye. BUN was also increased. After several days of trying unsuccessful medical therapy and pain relief, the cat was euthanized. The cardiac murmur had become grade IV of VI at three days before euthanasia.

Globe, cat: Gross view of the left eye. The anterior chamber is filled with blood and an ulcer is present near the lateral cornea. (Photo courtesy of: Veterinary Medical Diagnostic Laboratory, University of Missouri)

Gross Pathology: An aged, neutered male, silver tabby and white, short-haired feline is necropsied. The animal has body weight 4.6 kg, with adequate fat stores and minimal

autolysis. The left eye is filled with blood, and the cornea bulges forward. An ulcer covers the central cornea. Blood leaks into the fixative when the eye is immersed in formalin after removal. The left thyroid is dark brown in color and enlarged, with a length of 1.5 cm. The right thyroid is reduced in size, nodular, and atrophic. The parathyroid glands are prominent. The kidneys are pale tan in color with a slight indentation of the anterior pole of the left kidney. They are firm in texture and the cortex has a somewhat granular character, with reduced cortical width. The combined kidneys weigh 33.5 grams, 0.72% body weight (normal 1.1%).The heart, especially the left ventricle, is severely enlarged. The total heart weight is 25.2 grams, 0.54% body weight. The right ventricular free wall weighs 3.0 grams (11.0% total heart weight) and the left ventricle weight 16.0 grams (63% heart weight, .35% body weight). The left to right ventricular weight ratio is 5.33, increased). The right ventricular wall measures 2 mm in width and the left 11 mm (ratio 5.5, increased).

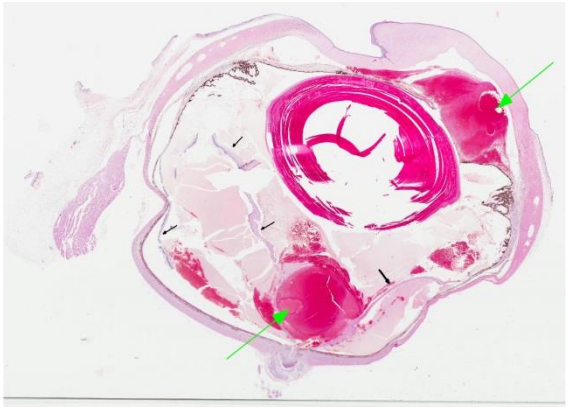

Globe, cat: There are large clots in the anterior and posterior segments (green arrows), and the retina is diffusely detached. (black arrows). (HE, 60X)

Gross Morphologic Diagnosis: None provided.

Microscopic Description: The anterior portion of the eye is filled with hemorrhage, including the angle, with extensive hemosiderosis at the root of the iris and in the meshwork. Additional hemorrhage mixes with the vitreous in parts of the posterior chamber and lies on both sides of a detached retina. The RPE is universally hypertrophic. The detached retina is severely atrophic, with reduction and mixing of the granular layers and with loss of the ganglion cells, particularly at the periphery. Scattered hemosiderophages are also present in the retina and small arterioles are thickened. Adjacent optic nerve contains few axons (not present in all slides). Thick, hyalinized arterioles occur in the choroid and retina. PAS staining highlights increased eosinophilic material in the media of small muscular vessels. A segment of corneal erosion is attended by stromal disarray, melanosis and vascularization, with mild superficial inflammation. A narrow fibrovascular membrane extends along the anterior face of the iris.

Contributor's Morphologic Diagnoses:
Hyphema with glaucoma, retinal detachment, retinal atrophy and corneal erosion with keratitis
Arteriolar degeneration (arteriolosclerosis), eye
Other pertinent final diagnoses: Thyroid adenomas, atrophy of normal thyroid, left ventricular hypertrophy, glomerulosclerosis with similar vascular lesions (not included).

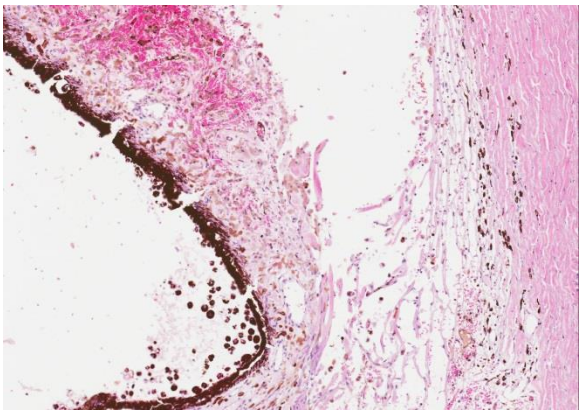

Globe cat. A hemorrhagic pre-iridal fibrovascular membrane covers the iridal root; however, the drainage angle remains open. (HE, 168X)

Contributor's Comment: This particular patient had multiple risk factors for developing hypertensive retinopathy and hyphema. A combination of thyroid-induced ventricular enlargement and renal failure, along with irregular treatment of the condition, produced a cycle of worsening disease. Histologic lesions primarily involve retinal and choroidal vessels, as in this case, with lesions ranging from fibrinoid necrosis to multi-layered onion-skin layering of medial hypertrophy and adventitial fibrosis. The animal has severe separation of the retina from the choroid with choroidal hypertrophy and hemosiderosis. Given the severity of retinal atrophy, it is likely that the cat had been blind for several weeks before hyphema was noticed clinically.

Intraocular hemorrhage is a frequent sequelum of high blood pressure in old cats.[2,5] Renal disease, hyperthyroidism and cardiac disease are commonly contributory (this cat had a trifecta). Disease is usually symmetrical but with qualitative differences between eyes. This cat also developed hyphema in the right eye, but intraocular pressure did not become elevated and no corneal ulcer was found. Hypertensive lesions can be found in the retina, choroid and rarely iris. Vascular lesions result in retinal and preretinal hemorrhage and edema; with retinal detachment because of effusion from leaky choroidal vessels. Exudative retinal separation and retinal necrosis produce atrophy of the photoreceptive and characteristic "tombstoning" of the retinal pigment epithelium. In this eye intraocular pressure was increased, resulting in secondary open angle glaucoma.

The earliest retinal changes in hypertension are arteriolar narrowing secondary to vasospasm, followed by diffuse or focal narrowing of arteriolar walls, changes that can be seen on ocular exam. In progressive disease, the blood-retinal barrier breaks down, leading to fluid leakage, bleeding and ischemia of the nerve fiber layer. Severe disease in people portends an increased risk of cardiovascular mortality.[1]

Hyphema or hemorrhage into the anterior chamber results from disruption of the blood ocular barrier, and has a number of causes, including trauma, vessel-rich neoplasms and coagulopathy. In some of these conditions, only one eye is affected. Common sequelae include cataracts, glaucoma, synechiae, corneal staining by hemoglobin, and eventual phthisis. Other organs, including brain, heart and kidneys are common targets

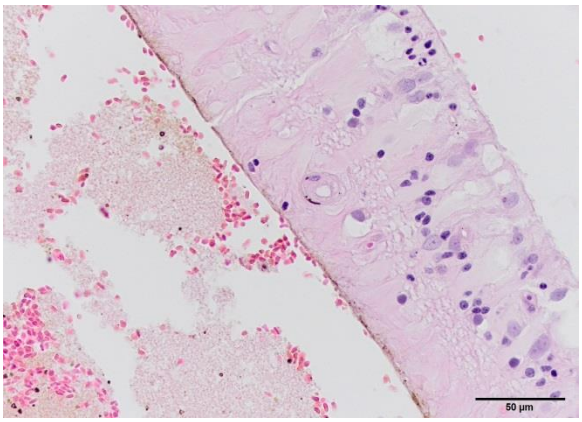

Globe cat. The detached retina is atrophic, with a few granular neurons remaining. A hyalinized arteriole is visible in the center of the retinal segment. (HE, 400X) (Photo courtesy of: Veterinary Medical Diagnostic Laboratory, University of Missouri)

of hypertension. Bleeds due to hypertension can produce clotted or unclotted blood. Use of ultrasound can be useful, if blood obscures evaluation of the back of the eye. Persistent slow bleeding and alteration of intraocular structures suggests a poor prognsis.[4]

Decreased blood flow through the vasa vasorum during hypertension results in acute hypoxia and aortic medial necrosis. In turn, decreased flow results in increased vascular tone, neovascularization, leading to reduced vasodilatory capacity, creating a self-perpetuating cycle. Kidney disease, hyperthyroidism, hyperaldosteronism, anemia and diabetes are predisposing systemic diseases. Some studies indicate that arteriosclerosis is uncommon in normotensive cats. Remodeling of small arteries and arterioles results in narrow lumen diameter and hypertrophic remodeling of the media.[3]

JPC Diagnosis: Eye: Arteriolosclerosis, multifocal, moderate with severe intraocular hemorrhage, retinal atrophy and detachment, Domestic shorthair, feline.

Conference Comment: This case provided exceptionally descriptive microscopic lesions. Intraocular hemorrhage was the most prominent microscopic finding among conference participants. There was dialogue about the top four rule outs for hemorrhage in all chambers of the eye:

(1) Trauma (often a diagnosis of exclusion)
(2) Hypertensive retinopathy
(3) Neoplasia which can rupture and hemorrhage into the eye
(4) Inflammation especially due to hematogenous uveal localization of infectious agents
(5) Coagulopathy

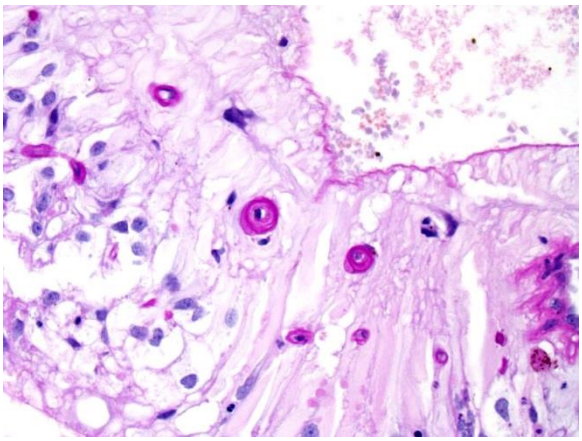

Globe cat. A periodic acid-Schiff stain demonstrates the 'onion-skinning" changes associated with the walls of small vessels in the atrophic retina. (PAS, 400X)

It was obvious amongst conference participants that neoplasia and inflammation could be ruled out. However, since participants were not provided the clinical history in this case, a conversation ensued regarding how to separate trauma from hypertension microscopically.

Vascular changes are the best way to differentiate hypertension from trauma. With systemic hypertension, there is fibrinoid necrosis of the tunica media, thickening of arteriolar walls, narrowing of the vascular lumen most likely secondary to vessel damage and leakage of blood proteins into the wall which is best seen in the choroid and retinal vessels.[6] The thickened walls and characteristic "onion-skinned" appearance were highlighted in this case with a periodic acid-Schiff stain. Based on our microscopic findings, we concur with the contributor's diagnosis of hypertensive retinopathy and discussed the clinical findings in this case (described above) to include the associations of renal failure and hypertension/elevated intraocular pressure.

Renal disease is the most common cause of hypertension in dogs and cats and may

either be a cause or an effect of hypertension. In either case, hypertension is self-perpetuating because medial hypertrophy and hyalinization of renal arteries lead to progressive nephrosclerosis, heightened hypertension, and increased pressure-induced damage in affected tissues.[4] In this case, it is not clear which was the initial development: hyperthyroidism, renal disease, or hypertrophic cardiomyopathy. However, it is likely that all three contributed to the clinical and microscopic findings in this case.

Additionally, conference participants viewed several iridal changes, resulting in discussion of the following entities (not all present in this slide): anterior synechia (adherence of the iris to the cornea with compression of the drainage angle), posterior synechia (adherence of the iris to the lens), iris bombé (posterior synechia that involves the entire circumference of the iris and blocks flow of aqueous causing increased pressure in the posterior chamber and causing bowing of the iris forward), ectropion uveae (contraction of a pre-iridal fibrovascular membrane resulting in infolding of the pupillary border to adhere to the anterior iris surface), and entropion uveae (contraction of a pre-iridal fibrovascular membrane resulting in infolding of the pupillary border to adhere to the posterior iris surface).[6]

Contributing Institution:
Veterinary Medical Diagnostic Lab and Department of Veterinary Pathobiology
http://vmdl.missouri.edu/
http://vpbio.missouri.edu/

References:

1. DellaCroce JT, Vitale AT. Hypertension and the eye. *Curr Opin Ophthalmology* 2008;19:471-498.
2. Dubielzig RR, Ketring KL, McLellan GJ, Albert DM eds. *Veterinary Ocular Pathology: a Comparative Review*. Saunders-Elsevier: St Louis MO. 2010: 5, 370-372.
3. Kohnken R, Scansen BA, Premanandan C. Vasa vasorum arteriopathy: relationship with systemic arterial hypertension and other vascular lesions in cats. *Veterinary Pathology*.2016. epub doi: 10.1177/0300985816685137.
4. Robinson WF, Robinson NA. Cardiovascular system. In Maxie G, ed. *Jubb, Kennedy, and Palmer's Pathology of Domestic Animals Vol 3*, 6th ed. Elsevier, Inc. St. Louis; 2016:59-60.
5. Telle MR, Betbeze C. Hyphema: considerations in the small animal patient. *Topics Copan Anim Med* 2015;30:97-106.
6. Wilcock BP, Njaa BL. Special senses. In Maxie G, ed. *Jubb, Kennedy, and Palmer's Pathology of Domestic Animals Vol 1*, 6th ed. Elsevier, Inc. St. Louis; 2016:447-449, 472-473.

Self-Assessment - WSC 2017-2018 Conference 1

1. True or false: The most common form of amyloidosis in veterinary medicine is systemic amyloidosis.
    a. True
    b. False

2. The virus which causes malignant catarrhal fever belongs to which of the following families:
    a. Morbillivirus
    b. Rhadinovirus
    c. Coronavirus
    d. Paramyxovirus

3. The primary cell type resulting in lesions in malignant catarrhal fever is:
    a. Macrophage
    b. T-lymphocyte
    c. B-lymphocyte
    d. Neutrophil

4. A pneumonia in which mononuclear inflammation surrounds airways and infiltrates alveolar septa is best exemplifies which type of pneumonia
    a. Bronchopneumonia
    b. Interstitial pneumonia
    c. Bronchointerstitial pneumonia
    d. Uncategorized pneumonia

5. Which of the following is the earliest retinal change associated with hypertension:
    a. Narrowing of arteriolar walls
    b. Ischemia of the nerve fiber layer
    c. Vasospasm
    d. Fluid exudation and bleeding

Please email your completed assessment to Ms. Jessica Gold at Jessica.d.gold2.ctr@mail.mil for grading. Passing score is 80%.This program (RACE program number) is approved by the AAVSB RACE to offer a total of 0.5 CE Credits, with a maximum of 12.5 CE Credits being available to any individual Veterinary Medical Professionals for the 2017-2018 Wednesday Slide Conference. This RACE approval is for the subject matter categories of: SCIENTIFIC using the delivery method of NON-INTERACTIVE DISTANCE. This approval is valid in jurisdictions which recognize AAVSB RACE; however, participants are responsible for ascertaining each board's CE requirements.
RACE does not "accredit", "endorse" or "certify" any program or person, nor does RACE approval validate the content of the program.

Joint Pathology Center
Veterinary Pathology Services

WEDNESDAY SLIDE CONFERENCE 2017-2018

Conference 2

30 August 2017

CASE I: 16040206 (JPC 4084138).

Signalment: 1 month-old, intact female, Thoroughbred horse (*Equus caballus).*

History: The owner found her dead in the stall. She was behaving normally the night before. (per rDVM)

Gross Pathology: The conjunctiva, sclera, and adipose tissue are yellow. The liver is enlarged and skeletal muscle is pale. (per rDVM)

Laboratory results: None provided.

Microscopic Description: Liver (H&E): The liver contains large, individual to coalescing, randomly-placed foci of degenerate neutrophils with fewer macrophages surrounding foci of necrotic hepatocytes admixed with cellular debris. Adjacent peripheral hepatocytes are shrunken, angular, and hypereosinophilic with small, pyknotic nuclei and contain intracytoplasmic, long, slender, parallel to cross-hatched bundles of lightly basophilic to negatively staining, 3.5 to 14 microns in length bacilli. Bile canaliculi in areas less affected by inflammation are distended multifocally with golden brown intracanalicular bile. Randomly, many sinusoids are modestly to moderately congested.

Liver (Steiner's silver stain): Myriads of multifocal to coalescing intracytoplasmic, long, slender, parallel to crosshatched bundles of argyrophilic bacilli measuring 3.5 to 14 microns in length are within hepatocytes peripheral to foci of necrosis and inflammation throughout the section.

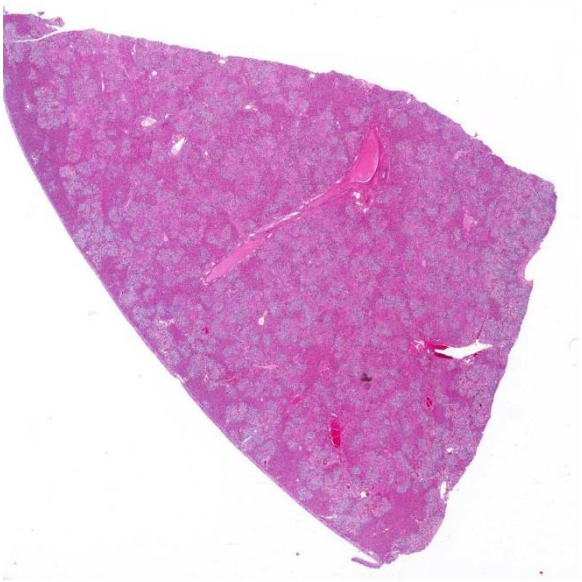

Liver, foal. There are numerous coalescing areas of pallor and hypercellularity (necrosis) forming a retiform pattern through the tissue. (HE, 6X)

Contributor's Morphologic Diagnosis: Liver: Severe, acute, multifocal to coalescing, random, necrosuppurative hepatitis with intracellular bacilli and moderate bile stasis.

Contributor's Comment: Tyzzer's disease is a bacterial infection that has been reported to affect many different species[4]. The etiologic agent, originally deemed *Bacillus pilifomis,* was reclassified in 1993 to the class *Clostridia* based on genetic sequencing of the 16S rRNA[4]. *Clostridium piliforme* is a filamentous, spore forming, gram negative, argyrophilic, obligate intracellular bacterium.

Adult horses are relatively resistant to clinical infections and harbor *C. piliforme* as part of their normal gastrointestinal microbiota. The upregulation of IL-12 has been explored in laboratory mice experimentally infected with *C. piliforme* which aids in resistance to this infection and others[7]. Foals under 6 weeks of age however are typically fatally affected. Transmission in foals is thought to be via a fecal-oral route due to coprophagia of the dam's feces during the early weeks of neonatal life[6].

Bacteria gain access to intestinal mucosal cells and by an unknown mechanism travel to and infect hepatocytes where it replicates and causes hepatocellular death. The incubation period can be as long as seven days until clinical signs first appear. At this time, nonspecific signs including anorexia, depression, fever, jaundice, and diarrhea may be observed[6]. These signs can be subtle, which is why many foals present as a "found dead" case. Due to the rapid course of disease, treatment typically is unrewarding.

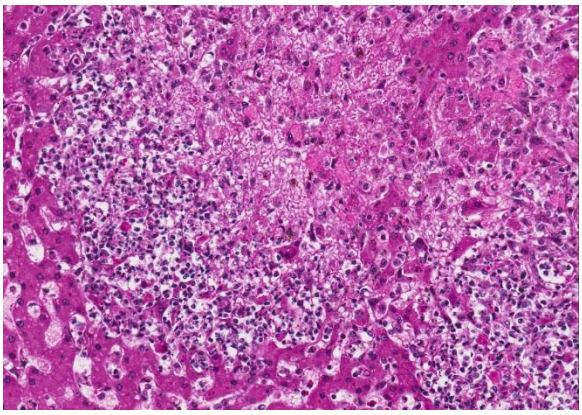

Liver, foal. Lytic necrosis predominates within the liver, with small foci of coagulative necrosis scattered throughout the section. (HE, 296X)

This case was a classic presentation of clinical disease. The age of the foal (4 weeks old) places it in the susceptible age range for acquiring the bacteria from coprophagic practices[6] and allows for a week long incubation period. Foals become coprophagic during the second week of life and continue the practice through the fifth week[6]. Typically foals born late in foaling season, from mid-March through May, have a higher prevalence of infection.[5, 6] Seventy-seven percent of cases occur in these foals where as 23% of cases occur foals born between January to early March[6]. This is thought to be due to environmental changes and diet which impact the mare's microbiota[6]. Heavy rainfalls, wildlife reservoirs, and spores contaminating the soil perpetuate the bacteria within the environment for extended periods of time[7]. Nutrient-dense diets are thought to increase incidence of infection as well and correlate with the overrepresentation of Thoroughbreds and other performance breeds associated with this disease.

The provided history of behaving normally and then finding the foal dead is also typical of this infection, especially in younger foals. Foals closer to the six weeks of age typically

display the nonspecific signs described above for 24-48 hours before death; whereas younger foals usually are found dead with no outward signs of illness[6]. Icterus is a common sequela of hepatic damage; however, hepatomegaly is not a common gross finding. We interpret this to be due to the prominent inflammatory cell infiltrate in the necrotic lesions (fig. 1). Our initial suspected diagnosis of *Clostridium piliforme* (fig. 2) was confirmed by the positive Steiner's silver stain demonstrating black, argyrophilic bacilli bordering foci of necrosis (figs. 3, 4). An antemortem diagnosis of *Clostridium piliforme* has been historically challenging as the bacteria does not grow on conventional media; however, a nested PCR has been developed for in vivo clinical diagnosis using feces as an inexpensive way of confirming the *Clostridium piliforme*[5].

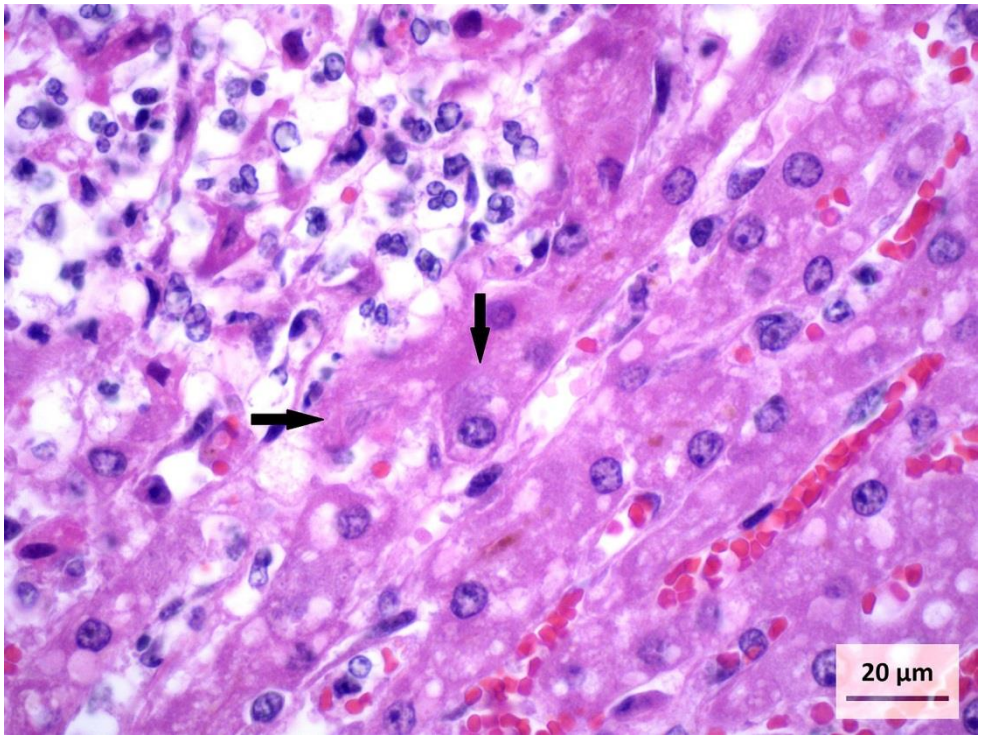

Liver, foal. At the edges of necrotic lesions, hepatocytes contain aggregates of faintly-staining intracytoplasmic filamentous bacilli within their cytoplasm. (HE, 600X) (Photo courtesy of: Oklahoma State University Center for Veterinary Health Sciences, Department of Pathobiology, http://cvhs.okstate.edu/Veterinary_Pathobiology).

JPC Diagnosis: Liver: Hepatitis, necrotizing, multifocal to coalescing, random, marked, with numerous intracytoplasmic bacilli, Thoroughbred, equine.

Conference Comment: This case demonstrates a classic example of Tyzzer's disease in a foal resulting in acute necrotizing hepatitis. Participants' description and discussion mirrored much of what was offered by the contributor. A Warthin-Starry stain was viewed during the conference which beautifully demonstrates the argyrophilic intracellular bacteria lying in sheaves or bundles within hepatocytes located at the periphery of necrotic foci.[3] As the contributor aptly notes, *C. piliforme*-induced lesions in the liver are generally acute and began as foci of coagulative necrosis. As neutrophils are recruited to phagocytize necrotic hepatocellular debris, additional tissue damage results in foci of lytic necrosis, the predominant type of necrosis in this case.

The contributor provides an excellent review of the clinical findings, pathogenesis, gross and microscopic lesions in foals. Additionally, the conference moderator reviewed several susceptible laboratory animal species which present with characteristic lesions not

necessarily associated with the classic target tissues (liver, intestine, and heart). Mongolian gerbils are particularly susceptible to *C. piliforme* infection which can additionally cause diffuse suppurative encephalitis. In rats, infection usually occurs in young animals during the postweaning period and is typically an enterohepatic disease. The typical manifestation in rats is necrotizing and hemorrhagic ileitis with adynamic ileus (also known as megaloileitis). Rabbits usually present with severe, watery colitis that result in high mortality. Microscopically, the characteristic foci of hepatic necrosis are present, as well as, severe focal to segmental necrosis of the cecal mucosa that usually extends transmurally.[1]

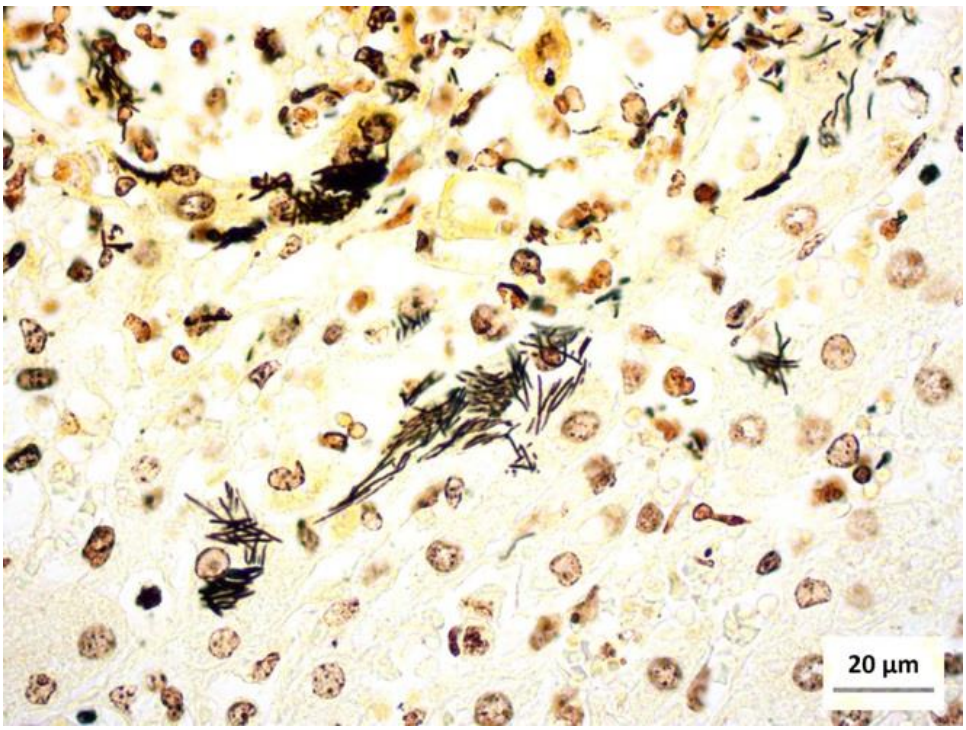

Liver, foal. Intracytoplasmic C. piliforme within hepatocytes are well-demonstrated with silver stains. (Steiner, 600X) (Photo courtesy of: Oklahoma State University Center for Veterinary Health Sciences, Department of Pathobiology, http://cvhs.okstate.edu/Veterinary_Pathobiology).

Finally, participants discussed differential diagnoses for random necrotizing hepatitis in foals. Equine herpesvirus-1 causes systemic disease in neonates including multifocal necrosis in liver, spleen, adrenal glands and other tissues with concurrent bronchointerstitial pneumonia. However, there are often prominent intranuclear inclusion bodies in hepatocytes and occasional syncytial cells in the lungs.[2] Septicemia due to *Salmonella* sp. or *E. coli* results in watery foul smelling diarrhea as well as joint lesions, pneumonia, and meningitis (with *Salmonella* sp.).[10] Lastly, sleepy foal disease, caused by *Actinobacillus equuli*, causes multifocal hepatitis, severe enteritis, and embolic nephritis.[3]

Contributing Institution:
Oklahoma State University Center for Veterinary Health Sciences
Department of Pathobiology
http://cvhs.okstate.edu/Veterinary_Pathobiology

References:

1. Barthold SW, Griffey SM, Percy DH. *Pathology of Laboratory Rodents and Rabbits.* Ames, IA: John Wiley & Sons, Inc.; 2016:137, 201-202, 275-276.
2. Caswell JL, Williams KJ. Respiratory system. In: Maxie MG, ed. *Jubb, Kennedy, and Palmer's Pathology of Domestic Animals.* Vol.

2. 6th ed. St. Louis, MO: Elsevier; 2016:568.
3. Cullen JM, Stalker MJ. Liver and biliary system. In: Maxie MG, ed. *Jubb, Kennedy, and Palmer's Pathology of Domestic Animals.* Vol. 2. 6th ed. St. Louis, MO: Elsevier; 2016:314-315, 317.
4. Duncan AJ, Carman, RJ, Olsen GJ, Wilson KH. Assignment of the gent of Tyzzer's disease to *Clostridium piliforme* comb. nov. on the basis of 16S rRNA sequence analysis. 1993. *International Journal of Systematic Bacteriology*. 1993; 43: 314-318.
5. Fosgate GT, Hird DW, Read DH, Walker RL. Risk factors for *Clostridium piliforme* infection in foals. *JAVMA*. 2002; 220: 785-790.
6. Francis-Smith K, Wood-Gush DGM. Coprophagia as seen in Thoroughbred foals. *Equine Veterinary Journal*. 1977; 9: 155-157.
7. Neto RT, Uzal FA, Hodzic E, Persiani M, Jolissaint S, Alcaraz A, Carvallo FR. Coinfection with *Clostridium piliforme* and Felid herpesvirus 1 in a kitten. *J Veterinary Diagnostic Investigation*. 2015; 27: 547-551.
8. Niepceron A, Licois D. Development of a high-sensitivity nested PCR assay for the detection of *Clostridium piliforme* in clinical samples. *The Veterinary Journal*. 2010; 185:222-224.
9. Swerczek TW. Tyzzer's disease in foals: retrospective studies from 1969 to 2010. *Canadian Veterinary Journal*. 2013; 54: 876-880.
10. Uzal FA, Plattner BL, Hostetter JM. Alimentary system. In: Maxie MG, ed. *Jubb, Kennedy, and Palmer's Pathology of Domestic Animals.* Vol. 2. 6th ed. St. Louis, MO: Elsevier; 2016:166-167, 172-173.
11. Van Andel RA, Hook RR, Franklin CL, Besch-Williford CL, Riley LK. Interleukin-12 has a role in mediating resistance of murine strains to Tyzzer's disease. *Infection and Immunity*. 1998; 66: 4942-4946.

CASE II: 1235813-002 (JPC 4101299).

Signalment: Juvenile female cynomolgus macaque, non-human primate (*Macaca fascicularis).*

History: This animal had decreased body weight, and a history of soft watery feces. It was found hypothermic and lying on floor of the cage and was humanely euthanized.

Gross Pathology: No gross pathology lesions were observed.

Laboratory results: None provided.

Microscopic Description: Colon: There are multifocal areas of segmental to full-thickness loss of mucosal architecture, with colonic crypts replaced by pale staining eosinophilia with pyknotic and karyorrhectic nuclear debris (necrosis) and some viable neutrophils. Crypts adjacent to the necrotic areas are variably lined by detached epithelial cells with pyknotic nuclei and

Colon, cynomolgus macaque. A section of colon is presented for evaluation (HE, 5X).

scant eosinophilic cytoplasm. Frequently scattered within the areas of necrosis, as well as within the submucosa, there are clusters of round protozoal trophozoites, which partially efface occasional crypts. Clusters of bacterial colonies are noted within the superficial to mid-mucosa in some areas of necrosis. The colonic lamina propria is infiltrated by a mixed population of inflammatory cells, including moderate numbers of plasma cells, fewer lymphocytes, and rare eosinophils. In some slides, the colonic serosa is infiltrated by a similar inflammatory cell population.

Some sections of colon contain gut-associated lymphoid tissue with loss of lymphocytes and variable necrosis. The protozoa stained positive with PAS and the bacteria were identified as a mixture of gram negative and gram positive organisms with a Gram Twort stain.

Contributor's Morphologic Diagnosis: Colon: Acute, multifocal, necrotizing colitis, with intralesional protozoa consistent with *Entamoeba histolytica*.

Contributor's Comment: Non-human primates held in laboratory and research settings harbor a variety of intestinal parasites that rarely cause clinical infection.[5] *Entamoeba histolytica* is a protozoan parasite that is a part of the normal fauna, but has also been shown to be pathogenic in captive non-human primates. Amebiasis affects the colon, causing diarrhea and can also cause liver abscesses, and ultimately lead to death.[1] It is of particular concern because of its zoonotic potential.[3] Clinical disease secondary to this pathogen is uncommon in the biomedical research laboratory setting and is usually secondary to stress or immunosuppression.

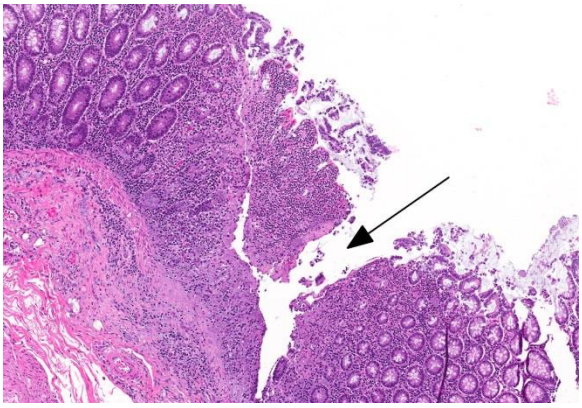

Colon, cynomolgus macaque. There are multifocal areas of full thickness mucosal necrosis (arrow) (HE, 168X).

Definitive speciation of *Entamoeba* spp. can be made using PCR-reverse line hybridization blot (RLHB), as differentiation of this protozoan from *Entamoeba dispar*, *Entamoeba nutalli*, and other species of this genera using light microscopy can be challenging.[1,3] Because of this difficulty, it has been suggested to make a combined diagnosis of *Entamoeba histolytica* and *Entamoeba dispar* unless molecular differentiation can be made. *Entamoeba nutalli* was found to be pathogenic in in Japanese macaques in a study where *Entamoeba dispar* was not identified, despite being reported to be prevalent in captive macaques. This suggests that colonies of macaques in captivity may have differing predominant causes of amebiasis.[2]

A definitive diagnosis of intestinal amebiasis may be complicated in cases of macaques infected with *Entamoeba chattoni*, as it has been shown to breach the mucosa of the cecum shortly after death.[4] In the case presented here, protozoal trophozoites are present in the submucosa with and without any associated pathology in varying areas of the slide. However, the organisms present within the mucosa and the GALT (present in some slides) are associated with pathology.

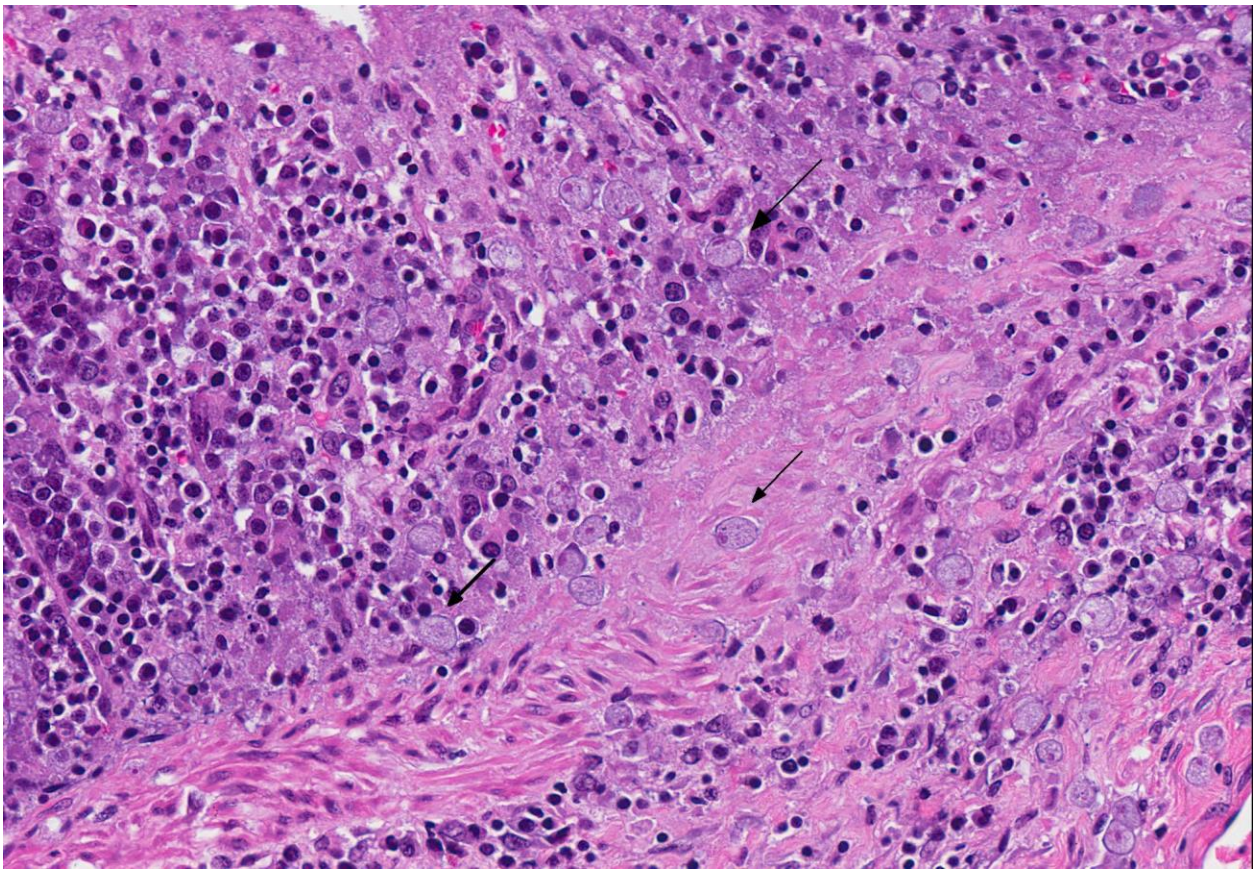

Colon, cynomolgus macaque. Within the necrotic mucosa and extending into the unaffected submucosa, there are numerous amebic trophozoites. (arrows) (HE, 400X).

JPC Diagnosis: Colon: Colitis, necrotizing, multifocal, moderate with numerous amoebic trophozoites, cynomolgus macaque, non-human primate (*Macaca fascicularis).*

Conference Comment: Conference participants discussed two species of Entamoeba: *E. histolytica* and *E. dispar* (the primary form of amoeba found in macaques).[4] Amoebic dysentery caused by *Entamoeba histolytica* is relatively common in humans and nonhuman primates, but rarely infects other species. Cats are susceptible to experimental infection, and infection in dogs is sporadic and most likely caused by ingestion of infected human feces. Dogs act as dead end hosts since they don't pass encysted amebae, and thus present little public health hazard.

Amebae are usually nonpathogenic organisms that inhabit the lumen of the large intestine, but may cause colitis due to changes in host diet or immune status, or the virulence attributes of the organism. Additionally, disease appears to be more common in animals with concurrent *Trichuris* or *Ancylostoma* infections.

The essential steps leading to tissue damage by amebae are: adhesion to mucus by lectins, enzymatic breakdown of protective mucus, and lectin-mediated adherence to host epithelium. *E. histolytica* releases cysteine proteases that cause damage to mucosal epithelium and attract inflammatory

cells, both of which lead to characteristic ulcerative colitis with "flask shaped" ulcers. Microscopically, amebae are surrounded by a clear halo with extensive pseudopodia and possess a nucleus with a dark karyosome. The cytoplasm appears foamy and they frequently phagocytize erythrocytes, which makes them difficult to distinguish from activated macrophages.[7] A periodic acid-Schiff stain was viewed during the conference which nicely highlighted intra-cytoplasmic glycogen granules within amebae; it also lightly stained goblet cells within the mucosa. Trichrome and Giemsa stains can also be used to highlight amoebic trophozoites. Due to the presence of intracytoplasmic glycogen (starch), Lugol's iodine can also be used to diagnose the presence of trophozoites via direct smear.

In humans and non-human primates, primary sites of dissemination are the liver (through the portal circulation) and less commonly, lung and brain. Fatal amebiasis with abscess formation has been reported in various primate species.[5] Recent reports in transgenic mice that overexpress Bcl-2 (anti-apoptotic gene) reveal that epithelial cell apoptosis facilitates *E. histolytica* infection in the intestinal tract.[1]

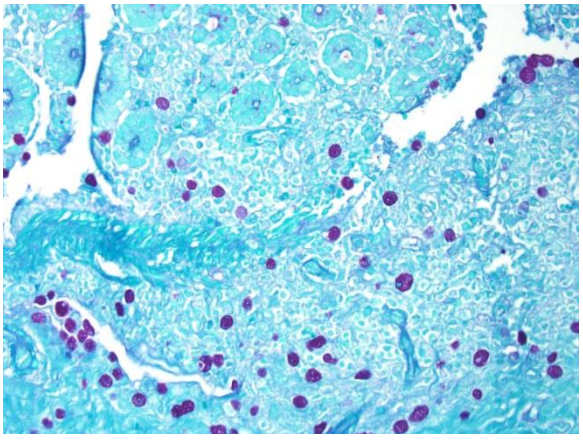

Colon, cynomolgus macaque. A PAS easily demonstrates the presence of the trophozoites. (Periodic acid-Schiff, 400X).

Conference participants discussed several ruleouts including: *Shigella flexneri* and *S. sonnei* (both are gram-negative bacilli that cause necrohemorrhagic colitis and can lead to submucosal ulceration and perforation), *Salmonella enteritidis* and *S. typhimurium* (which, although less common, cause necrotizing suppurative enterocolitis with paratyphoid nodule formation and can lead to septicemia with pyogranulomas in other organs), *Campylobacter jejuni* and *C. coli* (these are spiral bacteria evident with silver stains, and the most frequently isolated enteric pathogens causing mild colonic mucosal hyperplasia), *Yersinia enterocolitica* and *Y. pseudotuberculosis* (large colonies of gram-negative bacteria within necroulcerative enterocolitis), and *Balantidium coli* (ciliated trophozoites with a kidney-shaped macronucleus, can cause ulcerative enterocolitis which is fatal in great apes).[5] Leaf-eating primates (colobus monkey, silver-leafed monkey) are particularly susceptible to erosive and ulcerative gastritis due to a higher gastric pH (similar to the colon in other species) which is conductive to the survival of the amebae.[5] Comparatively, *Entamoeba invadens* was discussed as causing significant disease in snakes. *E. invadens* is typically spread via fecal-oral transmission and results in hemorrhagic enteritis and colitis, with subsequent spread to the liver via portal circulation to cause hepatic abscesses.[2]

Lastly, free-living (leptomyxid) amoebae were reviewed, which rarely cause disease, but may in immunosuppressed animals. *Acanthamoeba* sp., *Balamuthia mandrillaris* and *Naegleria fowleri* may result encephalitis. *Acanthamoeba* sp. and *B. mandrillaris* both cause granulomatous amoebic encephalitis. In contrast, *N. fowleri* infection is such an acute process that there are very few inflammatory cells associated with infection.[5]

Contributing Institution:
http://www.mpiresearch.com

References:

1. Becker SM, Cho KN, Guo X, et al. Epithelial cell apoptosis facilitates *Entamoeba histolytica* infection in the gut. *Am J Pathol.* 2010; 176(3):1316-1322.doi: 10.2353/ajpath.2010.090740.
2. Flanagan JP. Chelonians (turtles, tortoises). In: Miller RE, Fowler ME, eds. *Fowler's Zoo and Wildlife Medicine.* Vol. 8. St. Louis, MO: Elsevier; 2015:70.
3. Levecke B, Dreesen L, Dorny P, Verweij J, Vercammen F, Casaert S, Vercruysse J, Geldhof P. Molecular identification of *Entamoeba spp*. in captive nonhuman primates. *J Clin Microbiol*. 2010;48(8):2988-2990.
4. Purcell JE, Philipp MT. Parasitic diseases of nonhuman primates. In: Wolfe-Coote S, ed. *The Handbook of Experimental Animals the Laboratory Primate.* 1st ed. San Diego, CA: Elsevier; 2005:581-582.
5. Strait K, Else JG, Eberhard ML. Parasitic diseases of nonhuman primates. In: Abee CR, Mansfield K, Tardif S, Morris T, ed. *Nonhuman Primates in Biomedical Research: Diseases*. Vol 2. 2nd ed. San Diego, CA: Elsevier; 2012:206-209, 221-222, 599-602.
6. Tachibana H, Yanagi T, Akatsuka A, Kobayashi S, Kanbara H, Tsutsumi V. Isolation and characterization of a potentially virulent species of *Entamoeba nutalli* from captive Japanese macaques. *Parasitology.* 2009;136:1169-1177.
7. Uzal FA, Plattner BL, Hostetter JM. Alimentary system. In: Maxie, MG, ed. *Jubb, Kennedy, and Palmer's Pathology of Domestic Animals*. Vol 2. 6th ed. St. Louis, MO: Elsevier; 2016:242.
8. Verweij J, Vermeer J, Brienen A. *Entamoeba histolytica* infections in captive primates. *Parasitol Res*. 2003;90:100-103.
9. Vogel P, Zaucha G, Goodwin Sm Kuel K, Fritz D. Rapid postmortem invasion of cecal mucosa of macaques by nonpathogenic *Entamoeba chattoni*. *Am J Trop Med Hyg*. 1996;55(6):595-602.
10. Zanzani S, Gazzonix A, Epis S, Manfredi M. Study of the gastrointestinal parasitic fauna of captive non-human primates (*Macaca fascicularis*). *Parasitol Res.* 2016;115:307-312.

CASE III: 14-1424 (JPC 4066348).

Signalment: 16-year-old, female, Hafflinger horse (*Equus caballus*).

History: The animal was presented in emergency care center for acute neurological disorders (unsteadiness, fallings and decubitus, amaurosis). Despite critical care, development of a semi-comatose state and convulsions led to euthanasia.

Gross Pathology: At necropsy, the liver had an increased consistency with a variegated aspect and somewhat bulging tissue at section. The brain did not show visible changes.

Liver, horse. At subgross magnification, bridging fibrosis between portal areas forms a retiform pattern within the section. (HE, 168X)

Laboratory results: Blood analyses showed severe neutrophilic leukocytosis (Leukocytes 32,99.109/L, neutrophils 28,5.109/L, lymphocytes 2,67.109/L).
Biochemistry exam showed hyperproteinemia (80 g/L), hypoalbuminemia (25 g/L) and hyperglobulinemia (54 g/L).
A severe augmentation of gamma-GT was present (510 U/L), and increased values for GLDH (11,7 UI/L), total bilirubin (89 µmol/L), CK (> 2036 U/L), and lactates (> 12 mmol/L).
CSF fluid analysis did not show significant changes.
PCR (blood for Babesia sp., Theileria sp., and blood and CSF for Borrelia sp.) were negative.

Microscopic Description: Liver: Diffusely, there is marked fibrosis, mostly restricted to portal tract, and multifocal bridging between these portal tracts, distorting normal hepatic architecture. Isolation of individual hepatocytes by fibrosis is also present at the edges of the lobules. Diffusely, there are hepatocytes which are moderately to severely enlarged, with swollen nuclei. Cytoplasm is also enlarged and is vacuolated. In several portal tracts, bile duct proliferation is present. Multifocally, little hemorrhages and discrete infiltration of neutrophils, lymphocytes and macrophages are present.

Contributor's Morphologic Diagnosis: Liver: Hepatocellular degeneration, diffuse, marked, with megalocytosis. Generalized portal and bridging fibrosis and moderate bile duct proliferation, Haflinger, equine.

Contributor's Comment: Such changes observed in the liver are suggestive of pyrrolizidine alkaloids intoxication. These alkaloids are toxic to the liver, leading to irreversible lesions when intoxication comes to chronicity, especially in pigs, horses and cattle. These toxic alkaloids are not directly toxic, and necessitate bioactivation in hepatocytes (especially those in centrilobular region), leading to binding of these agents to proteins and nucleic acids. It results then in inhibition of mitosis, without inhibiting DNA synthesis, leading to megalocytosis. Associated to megalocytosis, there is fibroplasia and bile duct proliferation (fibroplasia is marked in cattle,

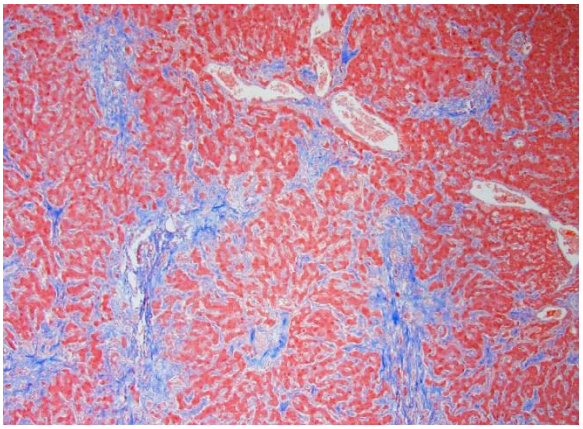

Liver, horse. A Masson's Trichrome stain highlights the extent of portal fibrosis in this section. (Masson's Trichrome, 40X)

moderate in horses and often minimal in sheep). Pyrrolizidine alkaloids are not the only toxic substances to cause such megalocytosis. Indeed, aflatoxins and nitrosamines can lead to this change in liver.[1,2]

Clinically, chronic intoxication by pyrrolizidine alkaloids is characterized by liver failure and its possible consequences (icterus and photosensitization). Secondary neurological signs can develop, known as "hepatic encephalopathy". Histopathological analysis of the brain of this horse showed presence of Alzheimer type II cells, consistent with this syndrome. In species other than the horse, spongiosis is also present in addition to Alzheimer type II cells.[3]

Many plants containing pyrrolizidine alkaloids can be ingested (*Senecio* spp., *Crotalaria* spp., *Heliotropium* spp.). In this particular case, the plant responsible for these lesions was not identified; given the wide distribution of *Senecio vulgaris* in the region where the horse lived, its consumption was very likely the origin of this chronic intoxication.[4]

JPC Diagnosis: Liver: Fibrosis, portal and bridging, diffuse, moderate with hepatocellular loss, karyomegaly and megalocytosis, and biliary hyperplasia, Haflinger, equine.

Conference Comment: This case provides a classic example of pyrrolizidine alkaloid toxicity in the liver. Participants described the dense bridging fibrosis from periportal

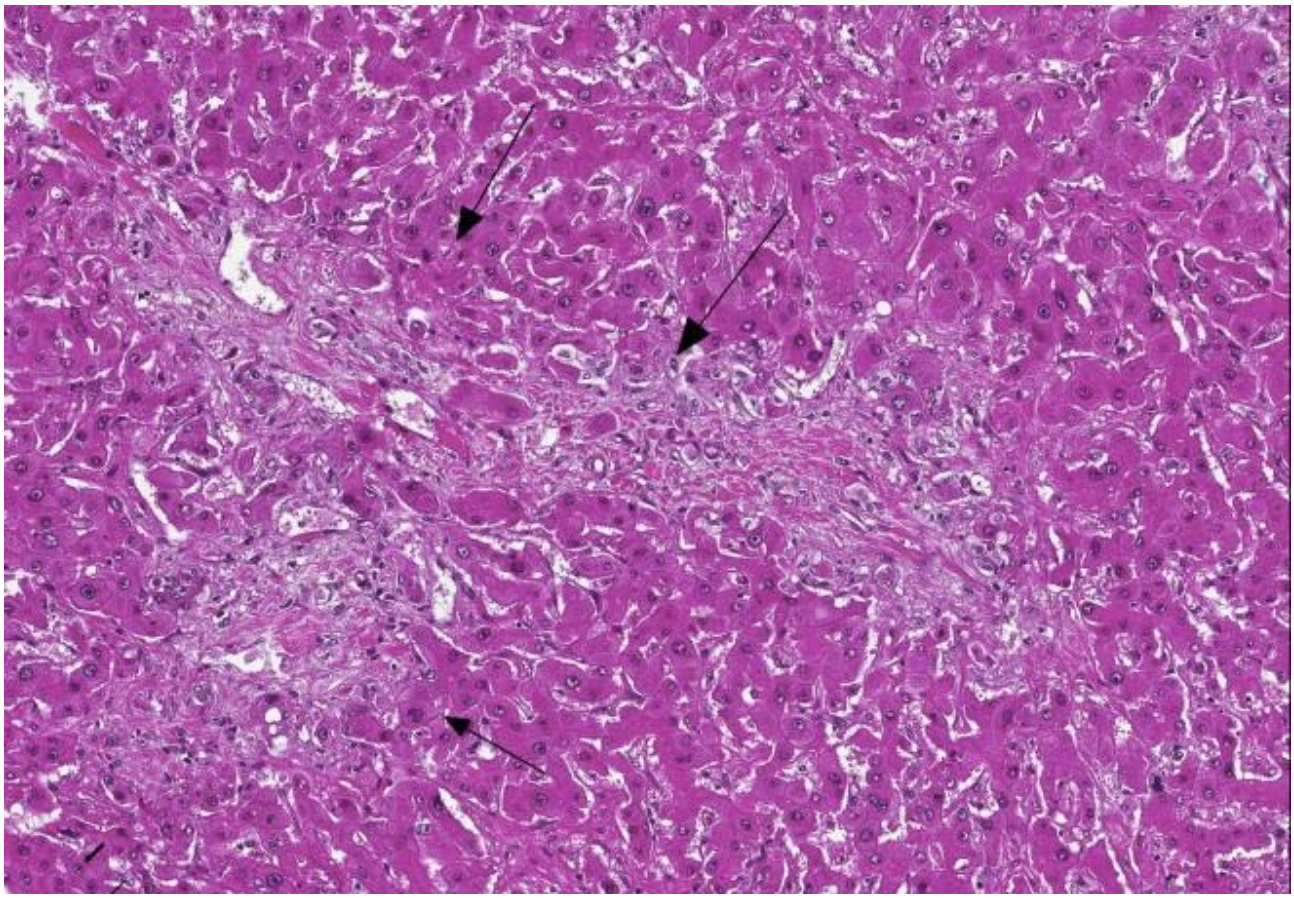

Liver, horse. Higher magnification of the portal areas demonstrates the extent of fibrosis, which encircles and replaces the hepatocytes of the limiting place, and the mild associated biliary hyperplasia. (HE, 168X)

regions that surrounds and separates hepatocytes and effaces the limiting plate as well as the ductular reaction with cholestasis. Occasionally obliterated centrilobular veins were suggestive of veno-occlusive disease. Particularly prominent are the perinuclear accumulations of bile pigment within hepatocytes and multifocal karymegalic and/or multinucleated hepatocytes which are a characteristic finding in several varieties of toxic hepatic diseases.

The contributor offers a concise review of pyrrolizzidine alkaloid toxicity including pathogenesis and clinical signs. The submitted blood work was reviewed during the conference, illustrating the degree of cholestasis and hepatocellular damage (elevated GGT and bilirubin) as well as the musculoskeletal damage and reversion to anaerobic metabolism due to persistent convulsions (elevated CK and lactate).

The moderator led a brief discussion of hepatic encephalopathy caused by hyper-ammonemia. Within the large intestine, breakdown of protein and urea by microflora occurs routinely to produce ammonia. Ammonia is also produced within the liver (hepatic deamination of amino acids) and in peripheral tissues (from metabolism of glutamate). Normally, ammonia is removed the first time through the liver via portal circulation, whereupon it enters the urea cycle. However, acute hepatic disease can result in buildup of ammonia within the circulation which passes through the blood-brain barrier, and causes a decrease in energy metabolism, astrocyte injury and edema formation, and neuronal injury. Overworked, damaged astrocytes cluster together in pairs with enlarged swollen nuclei, margination of chromatin, and prominent nucleoli to form Alzheimer type II astrocytes.[3]

Various plant species that produce different types of alkaloids were reviewed: *Compositae* (*Senecio* spp.), *Leguminosae* (*Crotalaria* spp., *Tephrosia* spp.), and *Boranginaceae* (*Heliotropium*, *Cynoglossum*, *Amsinckia*, *Echium*, *Trichodesma* and *Symphytum* spp.). *Croatalaria* sp. affects the widest range of tissues. Pyrrolizidine alkaloid toxicity depends on four factors: which alkaloids are produced, which organ is affected and the metabolic activity of target cells, the rate the alkaloid is converted to toxin versus the efficiency of glutathione conjugation, and the species, sex, and age of the animal. Monogastric species are the more susceptible to toxicity, as they lack a rumenal degradative pathways for toxin; sheep and goats have the greatest resistance. Horses are more likely to develop hepatic encephalopathy which causes head-pressing and compulsive walking and leads to idiomatic names like “walkabout” and “walking disease”.[3]

Several differential diagnoses for hepatotoxins were discussed during the conference, including aflatoxins, nitrosamines, triterpenes, methylazoxy-methanol, and indospicine.

Toxin	Produced by	Microscopic changes
Aflatoxin (B1 most potent)	*Aspergillus flavus, A. parasiticus, Penicilliu m puberulum*	Biliary hyperplasia and hemorrhagic necrosis; megalocytosis less prominent
Nitrosamines (dimethylnitrosamine)	Reaction product of trimethylamine with sodium nitrite (preservative) in herring meal	Not specific – slowly developing hepatotoxicity; megalocytosis, fatty change, bile accumulation
Triterpenes (predominately Lantadene A and C)	*Lantana camara*, an ornamental shrub native to the Americas and Africa	Focal hepatic necrosis, canalicular cholestasis; icterus and photosensitization
Methylazoxymethanol	*Cycas* or *Zamiaceae* spp. plants produce toxin	Centrilobular necrosis Cycads also produce neurotoxic animo acid β-N-methylamino-L-alanine (BMAA) – cause CNS lesions due to excitotoxicity
Indospicine (6-amidino-2-hexanoic acid)	Legumes of the genus *Indigofera*	Cattle/dogs: centrilobular necrosis, cholestasis, hepatic encephalopathy Horses: neurologic disorder "Birdsville horse disease"

Chart adapted from Cullen JM, Stalker MJ. Liver and biliary system. In: Maxie MG, ed. *Jubb, Kennedy, and Palmer's Pathology of Domestic Animals*. Vol 2. 6th ed. Philadelphia, PA: Elsevier; 2016:330-343.

Species differences with regard to target tissues and histologic lesions were also discussed. Cattle tend to develop more severe fibrosis that can lead to veno-occlusion. Sheep affected by *Heliotropium europaeum* and *Echium plantagineum* may develop severe intravascular hemolysis if liver copper content is high and hepatic mass is decreased. In pigs, pyrrolizidine alkaloids cause pulmonary emphysema with diffuse fibrosis and potential renal insufficiency. Experimental exposure in rats leads to progressive pulmonary disease, pulmonary hypertension, and cor pulmonale with necrotizing vasculitis of the pulmonary arterioles. Lastly, goats are relatively resistant, but with exceptionally high doses of *Croatalaria retusa* they develop acute lesions consisting of centrilobular hemorrhagic necrosis, midzonal hepatocyte swelling and vacuolation.

Finally, a review of photosensitization was provided by the moderator. Photo-sensitization is the inflammation of unpigmented skin (usually) due to the reaction of ultraviolet light of wavelengths 290-400 nm on photodynamic compounds that have become bound to dermal cells. Type I or primary photosensitization those

photodynamic compounds were deposited unchanged in the skin before the liver (healthy) could excrete it. Examples were given of photosensitizing plants that contain pigments from the helianthrone (St. John's Wort, buckwheat) or furocoumarin (spring parsley, bishop's weed, Dutchman's breeches, giant hogweed) family. The pigments produced by helianthrone are hypericin and fagopyrin, and furocoumarin are psoralens.

Type II photosensitization is due to defective pigment synthesis associated with several congenital conditions is specific breeds. Bovine congenital hepatopoietic porphyria ("pink tooth") is most common in Shorthorn, Ayrshire, Holstein and Jamaican cattle and causes a deficiency in uroporphyrinogen III cosynthetase which results in red-brown coloration of porphyrin in dentin and bone and skin lesions due to accumulated uroporphyrins which absorb UVA radiation. Siamese cats are also prone to congenital photosensitization and the deficiency is also thought to be uroporphyrinogen III cosynthetase. Another inherited deficiency is seen in Limousin cattle that develop bovine erythropoietic protoporphyria due to ferrochelatase deficiency with leads to protoporphyrin IX accumulation in blood and tissue. In this disease, photodermatitis is the only lesion.

Type III (hepatogenous) photosensitization is the most common form and usually accompanies cholestasis of more than a few days' duration in herbivores eating green feed that are kept in direct sunlight. Phytoporphyrin (phylloerythrin), a porphyrin produced in herbivores by rumenal microflora as a breakdown product

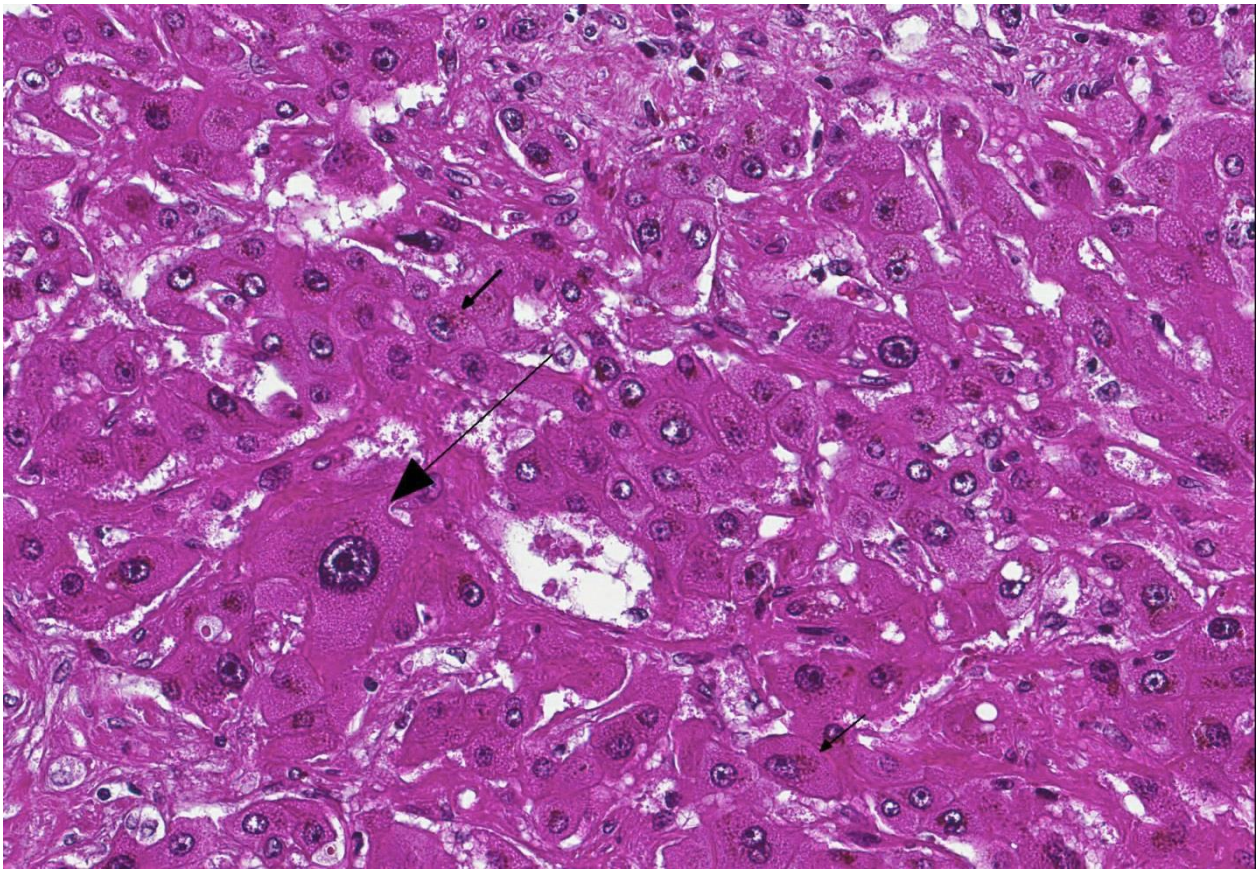

Liver, horse. Hepatocytes are diffusely swollen, effacing normal plate architecture by the accumulation of numerous intracytoplasmic vacuoles, and cell borders are distinct. Occasionally hepatocytes are increased up to 5x normal, with a single large nucleus (megalocyte) (large arrow). Hepatocytes often contain an aggregate of lipofuscin granules in proximity to the nucleus (small arrows). (HE, 400X)

of chlorophyll, is released into portal circulation, removed by hepatocytes, and excreted in bile. Cholestasis increases retention of phytoporphyrin in the blood and result in dermatitis of unpigmented areas of skin exposed to sunlight.[3]

Contributing Institution:
Anatomie Pathologique
Vetagro sup
Campus vétérinaire

References:

1. Cortinovis C, Caloni F. Epidemiology of intoxication of domestic animals by plants in Europe, *The Veterinary Journal*. 2013; 197(2):163-168.
2. Cullen JM, Brown DL. Hepatobiliary system and exocrine pancreas. In: Zachary JF, ed. *Pathologic Basis of Veterinary Disease*. 5th ed. St. Louis, MO: Mosby; 2007:439-440.
3. Cullen JM, Stalker MJ. Liver and biliary system. In: Maxie MG, ed. *Jubb, Kennedy, and Palmer's Pathology of Domestic Animals*. Vol 2. 6th ed. Philadelphia, PA: Elsevier; 2016:291-292, 294, 330-343.
4. Stalker MJ, Hayes MA. Liver and biliary system. In: Maxie MG, ed. *Jubb, Kennedy, and Palmer's Pathology of Domestic Animals*. Vol 2. 5th ed. Philadelphia, PA: Elsevier; 2007:373-374.
5. Zachary JF: Nervous system. In: Zachary JF, ed. *Pathologic Basis of Veterinary Disease*. 5th ed. St. Louis, MO: Mosby; 2007:814-815.

CASE IV: T17-15923 (JPC 4101085).

Signalment: 8-month-old, female, German Shepherd Dog (*Canis familiaris*).

History: A 5 x 5 x 3 cm gingival mass was observed on right mandible.

Gross Pathology: A multilobulated exophytic growth.

Laboratory results: None provided.

Microscopic Description: Gingiva: The mass was a non-demarcated and non-capsulated mass that contained epithelial and mesenchymal elements composed of islands of odontogenic tissue lined with a palisading columnar epithelium along a basement membrane consistent with ameloblasts supported on ample spindled to stellate mesenchymal cells (dental pulp). Multiple section consistent with a

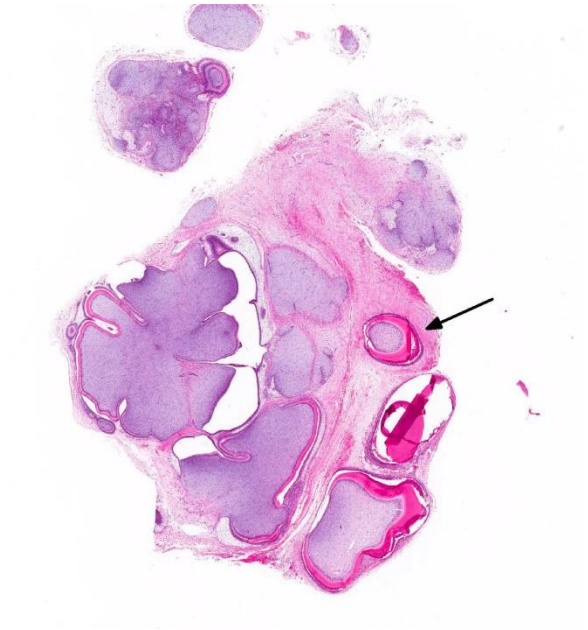

Mandible, dog: The submitted submucosal tissue demonstrates numerous well-formed tooth like structures (denticles). An arrow demonstrates one structure bearing an extremely strong resemblance to a developing tooth. (HE, 11X)

developing tooth like-structures (denticles) composed of odontoblasts, dentin and enamel were observed. Mitotic cells and malignant features were not present.

Contributor's Morphologic Diagnosis: Gingiva: Odontoma, German Shepherd dog, canine (*Canis familiaris*).

Contributor's Comment: Differential diagnoses for maxillary and mandibular swelling in immature dogs include trauma, infection, developmental disorders, and neoplastic lesions. Neoplastic oral maxillary or mandibular masses in immature, young dogs are typically of odontogenic origin.[2] Odontomas are rare[1] slow-growing masses that occur during odontogenesis, mainly in young dogs, resulting in dentition disruption and in prevention of eruption or displacement of normal teeth.[3] The masses cause swelling and deformity of mandible and/or maxilla. The cause and pathogenesis of odontomas, either in humans or nonhuman species, is unknown.[2,3] However, hereditary factors, genetic alterations during dental development, infections or trauma have been suggested to be involved in odontoma formation.[3]

Odontomas are odontogenic tumors with features of resembling the embryonic pattern of tooth development. Production of enamel, dentin, cementin, and sometimes small teeth

Mandible, dog: Higher magnification of tooth-like structures (denticles). PU= dental pulp; E=Enamel; D=Dentin (black arrows). (HE, 400X) (Photo courtesy of: The University of Georgia, College of Veterinary Medicine, Department of Pathology, Tifton Veterinary Diagnostic & Investigational Laboratory, Tifton, GA 31793; http://www.vet.uga.edu/dlab/tifton/index.php)

are characteristic. Tumors with patterns resembling normal teeth are compound odontomas, whereas a more disorganized arrangement is a characteristic of complex odontomas. Complex odontomas are composed of well-differentiated but disorganized dental hard tissues bearing no resemblance to a tooth and surrounded by a thin fibrous capsule. Compound odontomas are composed of many separate, small tooth-like structures known as "denticles", each one containing enamel, dentin, cementum, and pulp which are anatomically similar to normal teeth.[3,4] Compound odontomas are localized in the mandible or maxilla. However, in most reported cases in dogs, compound odontomas are localized in the mandible[3].

In dogs and other species, clinical signs associated with odontomas include facial or mandibular swelling, ocular symptoms, missing teeth, or tooth-like structures erupted into the oral cavity. Odontomas can become extremely large, even in very young dogs.[2]

Surgical excision is the treatment of choice for odontomas. Complete surgical excision of the mass in combination with aggressive curettage would result in a favorable outcome.[2,3] For prognostic and therapeutic considerations, it is important to differentiate odontomas from ameloblastic odontoma and ameloblastoma, which develop in old dogs.[4]

JPC Diagnosis: Gingiva: Compound odontoma, German Shepherd Dog, canine.

Conference Comment: This case provides an excellent example of a compound odontoma in a dog. The contributor's review of odontomas is excellent and mirrors much of the initial conference discussion. Conference participants described hamartomatous proliferation of odontogenic epithelium and primitive mesenchyme forming variably sized tooth-like structures in variable stages of development (denticles).

The moderator began with a review of tooth development which begins with two embryonic tissues: buccal cavity squamous epithelium (BCSE) and embryonic mesenchyme (EM). The EM forms dentin, cementum, and pulp, and the BCSE invaginates into the EM to form the dental lamina. The dental lamina grows into the adjacent tissue to form the dental bud which progresses through cap and bell stages eventually leading to crown eruption. The epithelium (BCSE) differentiates to form the ameloblastic cell layer at the outer surface of the tooth that produce enamel and the mesenchymal layer (EM) differentiates into odontoblasts, cementoblasts, and pulp (also periodontal ligament and alveolar bone) which move toward the center of the tooth and makes dentin and cementum respectively. Enamel covers the outside of the tooth and is composed of hydroxyapatite (mineral) crystal and heavily mineralized calcium salts. Dentin comprises the bulk of the tooth mass under the enamel and is slightly softer with tubules that contain odontoblast processes. Cementum covers the root of the tooth (doesn't project above gumline) and is a bone-like substance (contains basophilic reversal lines) with embedded cementocytes.[5]

The microscopic characteristics of epithelium of odontogenic origin (also known as ameloblastic epithelium) are: peripheral palisading, anti-basilar nuclei, basilar epithelial cytoplasmic clearing, and non-basilar epithelial cells (stellate reticulum) have intercellular bridges which separate the inner and outer layer of enamel epithelium during development.[3] There are

Tumor	Odontogenic epithelium	Stroma	Mesenchyme	Matrix	Species affected	Misc.
Ameloblastoma	Yes	Not essential for diagnosis	None	None	Dog, cat, horse	Keratinization may occur
Amyloid producing odontogenic tumor	Yes	Not essential for diagnosis	None	Amyloid	Dog, cat, horse	Matrix composed of enamel proteins which are still Congophilic and exhibit apple-green birefringence; IHC + for laminin
Canine acanthomatous ameloblastoma	Yes	Stellate fibroblasts in dense collagen; regularly spaced dilated, empty blood vessels	Periodontal ligament	None	Dog	Interconnected sheets of odontogenic epithelium
Ameloblastic fibroma	Yes	Loose, collagen poor, resembles dental pulp	Dental pulp	None	Young animals, cattle	Most common oral neoplasm in cattle
Ameloblastic fibro-odontoma	Yes	Loose, collagen poor, resembles dental pulp	Dental pulp	Dentin or enamel	Young animals, cattle	
Complex odontoma	Yes	Well-differentiated dentinal tissue	Dental pulp	Dentin, enamel (may be mineralized)	Dog, rodent, primates, horse	Horse, rodents produce cementum; "balls of disorganized dental hard substance"
Compound odontoma	Yes	Well-differentiated dentinal tissue; dense collagen and vascular connective tissue	Dental pulp	Dentin, mineralized enamel	Young dogs	Multiple tooth-like structures (denticles)

Chart adapted from Munday JS, Lohr CV, Kiupel M. Tumors of the alimentary tract. In: Meuten DJ, ed. *Tumors in Domestic Animals*. 5th ed. Ames, IA: John Wiley & Sons, Inc.; 2017:530-542.

two types of teeth in mammals, brachydont (carnivores) and hypsodont (ruminants and horses). Brachydont teeth are characterized by a short crown above the gingiva, constricted neck at the gumline, and a root embedded in the jawbone. Hypsodont teeth are high-crowned teeth extending past the gum line that continue to erupt throughout life.[5]

The moderator compiled a very complete description of various dental tumors classified as: epithelial with mature fibrous stroma (no odontogenic mesenchyme, not inductive) and mixed epithelial and mesenchymal (odontogenic epithelium and ectomesenchyme, inductive).

Tumors of mesenchyme or odontogenic ectomesenchyme with or without sparse odontogenic epithelium were briefly presented: Peripheral odontogenic fibromas (POFs) are composed of connective tissue consisting of delicate fibrillar collagen of varying density and evenly spaced stellate cells. Relatively small amounts of odontogenic epithelium are present in the connective tissue. At times, this tumor can be difficult to differentiate from fibrous gingival hyperplasia. However, POFs present as a single mass whereas gingival hyperplasia is multifocal and extend linearly along the gingiva.

Within the domestic animal species, cementomas have only been reported in the horse. They appear as radiopaque masses surrounding tooth roots of the incisors (most common). Microscopically they are composed of thick deposits of irregular cementum-like material with basophilic reversal lines that are fused to the base of the tooth. Osteomas can look similar but will be fused with adjacent bone, not with the tooth.

Finally, the various types of odontogenic cysts, both developmental and inflammatory, were discussed. Developmental or dentigerous cysts are the most common and occur usually in sheep and brachycephalic dogs. The epithelial lining of dentigerous cysts is thought to be derived from the reduced enamel epithelium. There are two types of inflammatory cysts: periapical (radicular) cysts which form around the apex of non-vital teeth and are due to periodontal or endodontal disease, and lateral periodontal cysts which are less common and occur lateral to the root of a vital tooth. In general, all types of odontogenic cysts have a true epithelial lining and usually an underlying loose fibrous wall.[3]

Contributing Institution:
The University of Georgia
College of Veterinary Medicine
Department of Pathology
Tifton Veterinary Diagnostic & Investigational Laboratory
Tifton, GA 31793
http://www.vet.uga.edu/dlab/tifton/index.php

References:

1. Felizzola CR, Martins MT, Stopiglia A, et al. Compound odontoma in three dogs. *J Vet Dent*. 2003; 20 (2):79-83.
2. Hoyer NK, Bannon KM, Bell CM, et al. Extensive maxillary odontomas in 2 dogs. *J Vet Dent*. 2016; 33(4):234-242.
3. Munday JS, Lohr CV, Kiupel M. Tumors of the alimentary tract. In: Meuten DJ, ed. *Tumors in Domestic Animals*. 5th ed. Ames, IA: John Wiley & Sons, Inc.; 2017:530-542.
4. Papadimitriou S, Papazoglou LG, Tontis D, et al. Compound maxillary odontoma in a young German shepherd dog. *J Small Anim Pract*. 2005; 46(3):146-50.
5. Uzal FA, Plattner BL, Hostetter JM. Alimentary system. In: Maxie MG, ed. *Jubb, Kennedy, and Palmer's Pathology of Domestic Animals.* Vol. 2. 6th ed. St. Louis, MO: Elsevier; 2016: 4-7.
6. Valentine BA, Lynch MJ, May JC. Compound odontoma in a dog. *J Am Vet Med Assoc*. 1985; 186 (2):177-9.

Self-Assessment - WSC 2017-2018 Conference 2

1. Which of the following is NOT true concerning *Clostridium piliforme* in horses
   a. Most fatal cases are seen in foals under the age of 6 weeks.
   b. Coprophagia is considered to be a part of the pathogenesis of the disease in foals.
   c. Lesions in the myocardium are most commonly associated with fatal disease in foals.
   d. Foals born late in the foaling period have a higher incidence than those born early in the foaling period.

2. Which of the following species may develop a suppurativeencephalitis in association with Clostridium piliforme?
   a. Rabbits
   b. Primates
   c. Mongolian gerbils
   d. Waterfowl

3. Which of the following is not true concerning *Entamoeba histolytic* infection in non-human primates?
   a. *E. histolytica* is a potentially zoonotic infection.
   b. The disase appears to be more common in animals with concurrent *Trichuris* infection
   c. The primary site of dissemination is the liver.
   d. Dogs, which may be infected by ingesting human feces, poses a significant health hazard in areas with poor sanitation.

4. Why are monogastrics more susceptible to pyrrolizzidine alkaloid toxicity?
   a. They find the plants more palatable than ruminants.
   b. They lack rumenal degradative pathways for the toxin.
   c. They possess significantly difference cytochrome enzymes within hepatocytes which are less efficient at breaking down the toxins.
   d. They do not possess Clubb cells in the lung which assist in detoxifying the alkaloids.

5. Dental neoplasms containing regular structures resembling normal teeth are most characteristic of the following:
   a. Compound odontomas
   b. Complex odontomas
   c. Ameloblastic odontomas
   d. Ameloblastomas

Please email your completed assessment to Ms. Jessica Gold at Jessica.d.gold2.ctr@mail.mil for grading. Passing score is 80%.This program (RACE program number) is approved by the AAVSB RACE to offer a total of 0.5 CE Credits, with a maximum of 12.5 CE Credits being available to any individual Veterinary Medical Professionals for the 2017-2018 Wednesday Slide Conference. This RACE approval is for the subject matter categories of: SCIENTIFIC using the delivery method of NON-INTERACTIVE DISTANCE. This approval is valid in jurisdictions which recognize AAVSB RACE; however, participants are responsible for ascertaining each board's CE requirements.
RACE does not "accredit", "endorse" or "certify" any program or person, nor does RACE approval validate the content of the program.

Joint Pathology Center
Veterinary Pathology Services

WEDNESDAY SLIDE CONFERENCE 2017-2018

C o n f e r e n c e 3

6 September 2017

CASE I: 10N0979 (JPC 4019127).

Signalment: 1 year-old, male, Domestic longhaired cat (*Felis catus)*.

History: This tissue was from a stray cat hit by a car 3 weeks prior to presentation to the VMTH. On presentation the cat was non-ambulatory and obtunded, had a fractured right pelvic limb, absent voluntary movement of both pelvic limbs and the left thoracic limb, and no pain perception. Due to a grave prognosis, the cat was humanely euthanized.

Gross Pathology: This cat was thin and had a healing transverse fracture of the right distal tibia. The bladder was distended and had a severely compromised thickened wall with large irregular areas of full thickness necrosis (considered the result of trauma). The brain and spinal cord were grossly normal.

Laboratory results: None provided.

Microscopic Description: Brain: There is severe bilateral, regional and symmetrical demyelination of the white matter (WM) in the brain and spinal cord of varying severity. There are widespread angiocentric accumulations of large mononuclear cells. These cells are CD18 immunoreactive (macrophages) that have abundant, distended pale finely vacuolated eosinophilic cytoplasm, eccentric nuclei, and are occasionally multinucleated. In areas of demyelination in the WM, there is scattered axonal necrosis with axonal spheroids and reactive astrogliosis. The large globoid mononuclear cells are PAS positive, but stain non-metachromatically. The gray

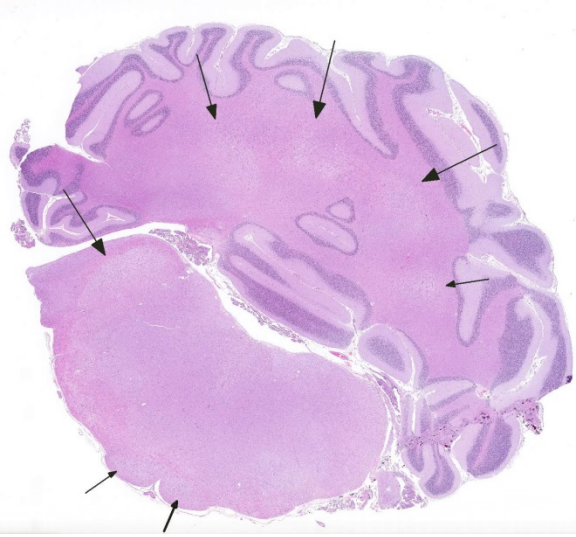

Cerebellum and brainstem, cat. There are bilaterally symmetrical areas of pallor and hypercellularity within the deep cerebellar white matter and the spinocerebellar tracts of the underlying brainstem. (HE, 6X)

matter appears unaffected.

Contributor's Morphologic Diagnosis: Brain and spinal cord: Severe bilaterally symmetrical perivascular histiocytosis and demyelination (consistent with globoid cell-like leukodystrophy).

Contributor's Comment: Globoid cell leukodystrophy is a rare lysosomal storage disease (sphingolipidosis) that involves the white matter of the central and peripheral nervous system. The disease has been described in humans (Krabbe's disease), mutant twitcher mice, rhesus monkeys, polled Dorset sheep, and domestic cats. In all affected animals except the domestic cat there is a demonstrated autosomal recessive mode of inheritance. [1,2,4,5,7] One report documents globoid leukodystrophy in 2 female kittens that resulted from inbreeding of common ancestors, which suggests a hereditary basis in cats as well.[1] Clinical signs appear at a young age (1-3 months of age) and initially consist of ataxia, hypermetria, tremors, and proprioceptive deficits which progress to blindness, anorexia, muscle atrophy, and paraplegia.

Cerebellum and brainstem, cat. Areas of pallor are also demonstrated on a Luxol fast blue stain, suggesting focal areas of demyelination. (LFB, 6X) (Photo courtesy of: University of California, Davis, Veterinary Medical Teaching Hospital, Anatomic Pathology Service.)

Death occurs by 1-2 years of age.[6]

The disease occurs due to a deficiency in galactocerebrosidase enzyme activity resulting in an accumulation of galactosylsphingosine (psychosine) within Schwann cells and oligodendrocytes.[1] It remains undetermined if accumulation of this intracellular material is a result of abnormal myelin synthesis or abnormal breakdown. Psychosine is cytotoxic thus resulting in degeneration and necrosis of oligodendrocytes and Schwann cells (hence the extensive demyelination) and extracellular release. Macrophage phagocytose and accumulate psychosine and are the hallmark 'globoid cells' seen on histopathology and typically aggregate perivascularly in the white matter.[3] Typical histological findings consist of bilaterally symmetrical white matter demyelination and striking perivascular hypercellularity characterized by numerous plump globoid macrophages.[6] The centrum semiovale, corona radiate, corpus callosum, optic tract, and cerebellar medullare are most severely affected.[6] Peripheral subpial areas are the most commonly affected portion of the spinal cord.[6] The intracytoplasmic material within macrophages is typically PAS positive, non-metachromatic, and non-sudanophilic.[1] Leukocyte immunohistochemical markers such as CD18 or MAC1 can be used to confirm globoid cells are of macrophage/microglial origin.

JPC Diagnosis: Cerebellum and brain stem: Histiocytosis, perivascular, multifocal, moderate with demyelination and gliosis, Domestic longhair, feline.

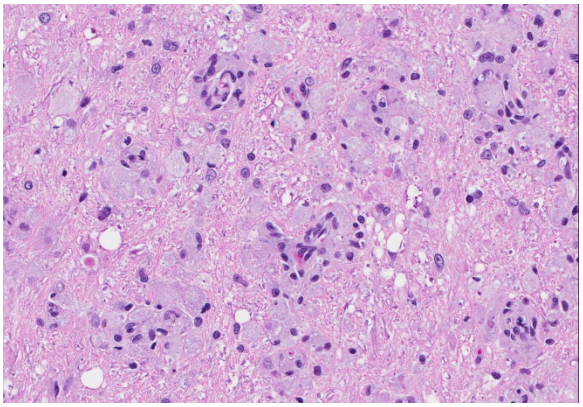

Cerebellum white matter, cat. Blood vessels are surrounded by histiocytes with abundant foamy cytoplasm, which also are present in lesser numbers within the intervening neuropil. (HE, 400X)

Conference Comment: This case nicely demonstrates lesions attributable to globoid-cell leukodystrophy (Krabbe's disease) in a young cat. Participants discussed the bilaterally symmetrical areas of pallor within deep spinocerebellar and brain stem pyramidal tracts corresponding to white matter vacuolation and histiocytosis. Histiocytes are described as having an amphophilic granular cytoplasm. There is evidence of demyelination characterized by axonal swelling (spheroids) and dilated myelin sheaths with macrophages phagocytizing myelin (Gitter cells in digestion chambers). Participants reviewed the immunohistochemical stains submitted by the contributor including Luxol fast blue that further emphasizes the severity of the demyelination and CD18 which classifies perivascular engorged cells as histiocytic in origin. Participants were reminded that the affected histiocytes are clustered around vessels in an attempt to leave the tissue but are too large to pass between endothelial cells and enter circulation.

The contributor provides a complete summary of the pathogenesis of globoid cell leukodystrophy which was also discussed by participants. The conference moderator lead participants in reviewing the broad categories of storage diseases: induced and inherited. In general, storage diseases are characterized by accumulation of a substance that exceeds the capacity of that cell to digest or dispose of that substance. Inherited storage diseases are almost always proved to be due to lysosomal deficits, and commonly occur in young animals owing to the fact that they are caused by genetic defects. Inherited storage disease categories were mentioned: sphingolipidoses, glycoproteinoses, mucopolysaccharidoses, glycogenoses, mucolipidoses, ceroid-lipofuscinoses, and Lafora disease. Induced storage diseases have been produced by ingestion of plants containing swainsonine

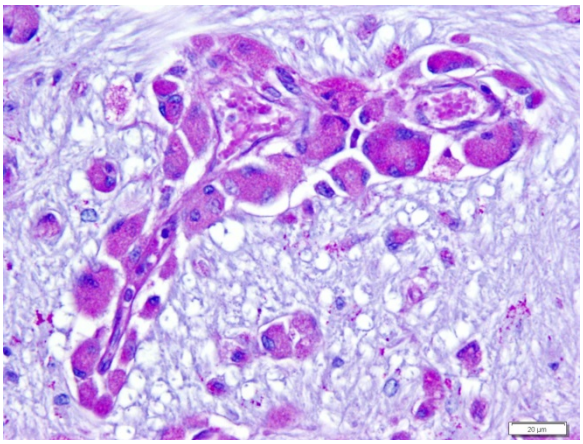

Cerebellum white matter, cat. Perivascular histiocytes stain strongly positive with a PAS stain. (periodic acid-Schiff, 400X) (Photo courtesy of: University of California, Davis, Veterinary Medical Teaching Hospital, Anatomic Pathology Service.)

(an indolizidine alkaloid) and plants of the *Trachyandra* spp. and *Phalaris* spp. genera.[1]

Finally, of the inherited storage diseases, the moderator reviewed sphingolipidoses:

Sphingolipidosis category	Common name	Deficiency	Accumulation	Cellular vacuolation	Animals affected
GM1 Gangliosidosis		β-galactosidase	GM1 ganglioside, some oligosaccharides	Neurons & macrophages	Cats, dogs, cattle, sheep
GM2 Gangliosidosis	Tay Sachs; Sandoff disease	β-Hexosaminidase	GM2 ganglioside, +/- globoside	Neurons & macrophages	Cats, dogs, Yorkshire pigs
Glucocerebrosidosis	Gaucher's disease	Glucocerebrosidase	Glucocerebroside	Neurons & macrophages (not in cerebellar Purkinje cells or spinal cord)	Sydney Silky Terrier
Sphingomyelinosis	Niemann-Pick type A	Sphingomyelinase	Sphingomyelin, cholesterol and ganglioside	Neurons & macrophages	Cats, miniature poodles
Sphingomyelinosis	Niemann-Pick type C	NPC 1 or NPC 2 proteins	NPC 1 or NPC 2 proteins	Neurons & macrophages	Cats, Boxer dogs
Galactosialidosis		β-galactosidase & α-neuraminidase	Gangliosides and oligosaccharides	Neurons & macrophages	Schipperke dogs
Galactocerebrosidosis	Globoid cell leukodystrophy; Krabbe's disease	Galactocerebrosidase (GALC)	Galactocerebroside and galactosylsphingosine (psychosine)	Macrophages only (globoid cells)	Cats, mutant Twitcher mice[4], polled Dorset sheep

Chart adapted from: Cantile C, Youssef S. Nervous system. In: Maxie MG ed. *Jubb, Kennedy, and Palmer's Pathology of Domestic Animals*. Vol. 1. 6th ed. St. Louis, MO: Elsevier; 2016:284-293.

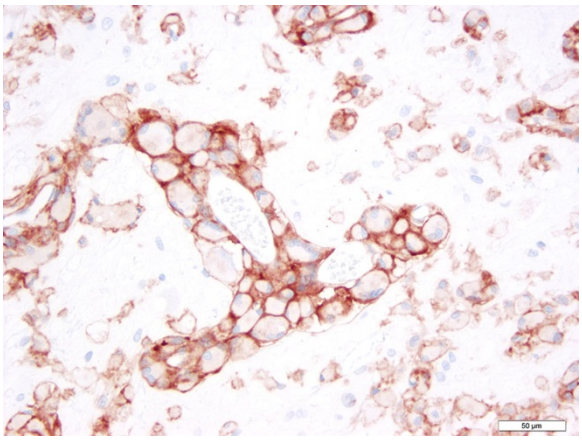

Cerebellum white matter, cat. Perivascular histiocytes also stain dense cytoplasmic positivity for CD-18. (periodic acid-Schiff, 400X) (Photo courtesy of: University of California, Davis, Veterinary Medical Teaching Hospital, Anatomic Pathology Service.)

Several attendees expressed concern with the diagnosis in this case, noting the previous history severe trauma, the lack of any mention of lesions elsewhere in the central nervous system, as well as the lack of any specific identification of material contained within macrophages in the examined sections. Moveover, as is the case with strays, there is a lack of a familial history. There was general concern that the lesion may be a long-term sequel to the severe neurologic trauma noted weeks prior to this case.

Contributing Institution:
University of California, Davis
Veterinary Medical Teaching Hospital
Anatomic Pathology Service

References:

1. Cantile C, Youssef S. Nervous system. In: Maxie MG ed. *Jubb, Kennedy, and Palmer's Pathology of Domestic Animals*. Vol. 1. 6th ed. St.

Louis, MO: Elsevier; 2016:284-293, 301-303.
2. Johnson, K. Globoid Leukodystrophy in the Cat. *J Am Vet Med Assoc.* 1970:157(12):2057-2064.
3. Kobayashi T, Yamanaka T, Jacobs J, et al. The twitcher mouse: an enzymatically authentic model of human globoid cell leukodystrophy (Krabb disease). *Brain Res*. 1980;202:479-483.
4. Krinke GJ. Neuropathologic analysis of the peripheral nervous system. In: Bolon B, Butt MT, ed. *Fundamental Neuropathology for Pathologists and Toxicologists*. Hoboken, NJ: John Wiley & Sons, Inc.; 2011:378-379.
5. Maxie MG, Youssef S: The nervous system. In: Maxie MG ed. *Jubb, Kennedy, and Palmer's Pathology of Domestic Animals.* Vol. 1. 5th ed. Philadelphia, PA: Elsevier Saunders; 2007:381-382.
6. Pritchard D, Napthine D, Sinclair A. Globoid cell leucodystrophy in Polled Dorset sheep. *Vet Path.* 1980;17:399-405.
7. Sigurdson C, Basaraba R, Mazzaferro E, Gould D. Globoid Cell-like Leukodystrophy in a Domestic Longhaired Cat. *Vet Pathol*. 2002;39:494-496.
8. Summers B, Cummings J, de Lahunta A. *Veterinary Neuropathology*. St. Louis, MO: Mosby; 1995:220-221.
9. Wenger, D, Victoria T, Rafi M, Luzi P, Vanier M, Vite C, Patterson D, Haskins M. Globoid cell leukodystrophy in Cairn and West Highland White Terriers. *J Hered*. 1999; 90:138-142.
10. Zachary JF: Nervous system. In: McGavin MD, Zachary JF eds. *Pathologic Basis of Veterinary Disease*. 4th ed. St. Louis, MO: Mosby Elsevier; 2007:931-932.

CASE II: 11-30435 (JPC 4020992).

Signalment: 2-week-old male and female intact, terrier mixed breed dogs *(Canis lupus familiaris)*.

History: An adult terrier mixed breed dog was vaccinated with canine distemper virus during pregnancy, and 7 out of 8 puppies died after birth. Upon initial presentation, 6 puppies had normal physical exams and normal temperatures, while the 7th puppy was vocalizing, dyspneic, mildly cyanotic, and had a mildly elevated lymphocyte count. This puppy was euthanized a short time later. The rest of the puppies had intermittent twitching, one puppy was hypoglycemic, and one puppy had moderate amounts of clear nasal discharge. The rest of the puppies died within the next few days.

Gross Pathology: The kidney, liver, spleen, and to a lesser extent within the lungs and small intestines were multifocal pinpoint to 1 mm, dark red foci (petechia). The thoracic cavity contained approximately 5-10 ml of yellow to red-tinged, translucent fluid. The

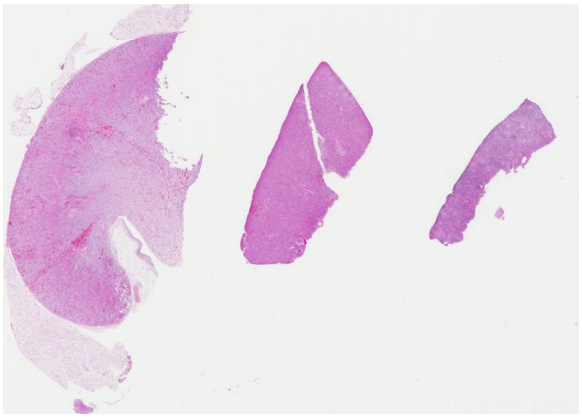

Kidney, liver, spleen, puppy. A section of each organ is submitted for examination (HE, 5X).

lungs were diffusely red and rubbery.

Laboratory results: FA was positive for canine herpesvirus.
FA was negative for canine distemper virus.
Bacteriology showed no growth in the lung and kidney.

Microscopic Description: Multifocally within sections of kidney, liver, and spleen, the parenchyma has lost differential nuclear staining and contains necrotic cellular debris and hemorrhage. The surrounding cells often have karyorrhectic nuclei with hyper-eosinophilic cytoplasm. Few nuclei contain a single, round, eosinophilic intranuclear inclusion bodies with marginated chromatin.

Additionally, tissue from the lungs and jejunum (slides not submitted) have similar multifocal regions of necrosis with few single, round, eosinophilic intranuclear inclusion bodies with marginated chromatin. The alveolar septa are also diffusely expanded by macrophages, lymphocytes, and neutrophils with type II pneumocyte hyperplasia. The grey and white matter of the cerebrum, cerebellum, and brainstem (slides not submitted) are multifocally disrupted by glial cells, macrophages, few neutrophils, and degenerating neurons. The meninges are diffusely thickened with neutrophils, lymphocytes, and macrophages.

Immunohistochemistry: The small intestine was negative for canine parvovirus, and the brain was negative for canine distemper virus.

Contributor's Morphologic Diagnosis: Kidney, liver, and spleen: Nephritis, hepatitis, and splenitis, necrotizing,

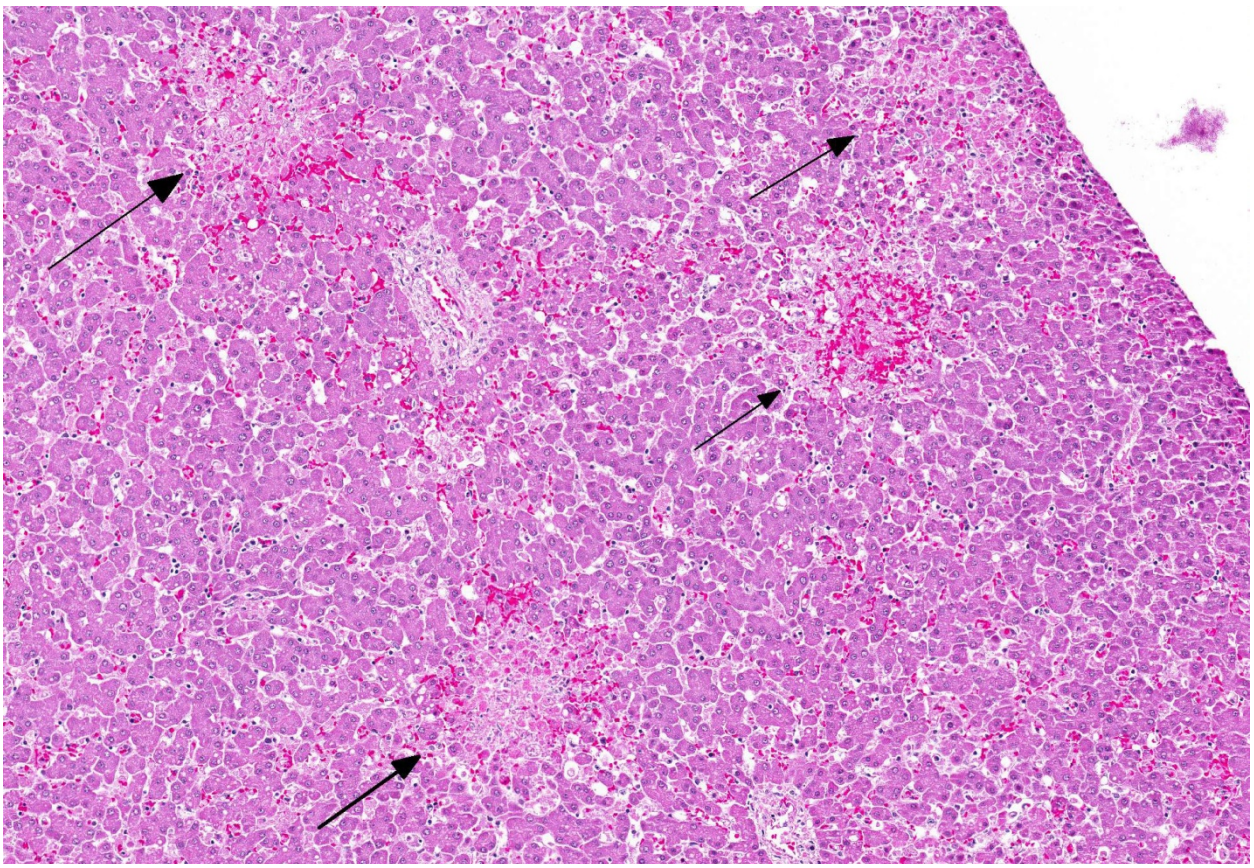

Liver, puppy. The liver contains randomly scattered areas of coagulative necrosis and hemorrhage. (arrow) (HE, 140X).

multifocal, marked, with few eosinophilic intranuclear inclusion bodies.

Etiology: Canine herpesvirus-1 (CaHV-1)

Contributor's Comment: Canine herpesvirus type 1 is a well-known entity first recognized in the 1960s and is a double stranded DNA virus in the alphaherpesvirus subfamily. The virus is deactivated in temperatures greater than 40°C and flourishes in temperatures between 34°C and 36°C; thus, by raising the body temperature, chances of survival are increased.[2, 5, 7]

The age of the dog can determine the clinical presentation of the herpesvirus infection. Dogs less than 3 weeks old generally have fatal systemic disease due to acute neonatal viremia. Dogs older than 3 weeks can have ocular and mucosal disease (either respiratory or vaginal). Naïve pregnant bitches are susceptible to systemic infection that can cause abortions or acute neonatal viremia. Latent infection is a concern for any age group if they survive the original infection and can occur following steroid administration or stress, such as pregnancy.[1, 2, 3]

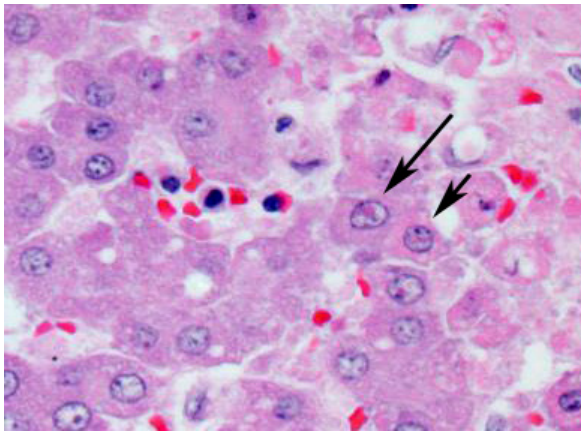

Liver, puppy. Hepatocytes at the periphery of areas of the necrosis rarely contain intranuclear viral inclusions. (arrows) (HE, 400X).

Typically, dogs less than 3 weeks of age acquire the disease in a variety of methods: *in utero*, passage through the birth canal, direct contact with oronasal secretions of the bitch, direct contact with other dogs that are shedding, and humans acting as fomites. Older dogs with ocular and/or mucosal disease are generally infected via aerosolization. Viral replication can occur in the nasopharynx, tonsils, and/or retropharyngeal and tracheobronchial lymph nodes. The virus then spreads throughout the bloodstream via macrophages to infect the liver, kidneys, lymph nodes, lungs, and centralnervous system.[1, 2, 3, 7] The incubation period is approximately 6 to 10 days and litter mortality can reach 100% over the course of a week.[2] Common clinical signs include vocalization, anorexia, hypothermia, abdominal pain, and/or incoordination.[2, 4]

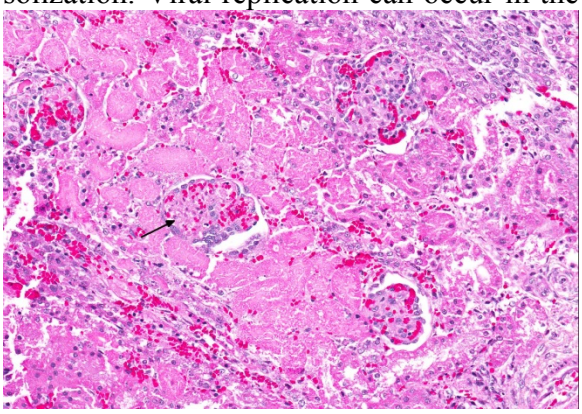

Kidney, puppy. Scattered throughout the cortex are randomly scattered areas of infarction affected glomeruli (arrow) and surrounding tubules. (HE, 324X)

Characteristic gross and histologic lesions in affected dogs less than 3 weeks of age include systemic hemorrhage and necrosis in the kidney, liver, spleen, and intestine with little associated inflammation, enlarged lymph nodes, and non-suppurative meningoencephalitis, all of which were present within this case.[2, 4, 5, 6, 7]

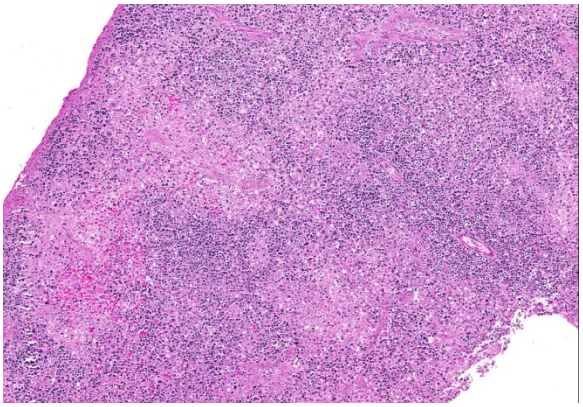

Spleen, puppy. Extensive lymphoid and splenic necrosis is characteristic of CHV-infection in puppies. (HE, 324X)

Eosinophilic intranuclear inclusion bodies were also present. Classic lesions in addition to a positive fluorescent antibody test verified canine herpesvirus. Fluorescent antibody testing and immunohistochemistry ruled out canine distemper virus and canine parvovirus as possible contributors.

JPC Diagnoses: 1. Liver: Hepatitis, necrotizing, random, multifocal to coalescing with few eosinophilic intranuclear inclusion bodies, terrier mix, canine.

2. Kidney, tubules and glomeruli: Nephritis, necrotizing, multifocal, mild.
3. Spleen: Splenitis, necrotizing, diffuse, severe.

Conference Comment: This case serves as a classic example of canine herpesvirus-1 (CaHV-1) in a puppy, causing random necrotizing hepatitis, nephritis, and splenitis. Participants described multifocal areas of coagulative necrosis in the liver and kidney, as well as diffuse necrosis in the spleen, with few eosinophilic intranuclear inclusion bodies, mild vasculitis, and fibrin thrombi (especially in the liver and glomeruli). Participants also noted that inclusions were most prominent in the liver adjacent to areas of necrosis, but were difficult to see in the kidney and spleen due to the extensive necrosis in those tissues.

In addition, participants reviewed select alphaherpesviruses from other species (cats, farm animals, and horses), which are summarized in the following chart[1, 3, 7, 8, 11]:

Alphaherpesvirus	Common name	Primary lesions
Bovine herpesvirus 1	Infectious bovine rhinotracheitis	Fibrinonecrotic membrane along trachea/larynx, bronchointerstitial pneumonia; Systemic form: Focal areas of necrosis within the alimentary tract
	Infectious pustular vulvovaginitis	Necrotizing vulvovaginitis with intranuclear inclusion bodies in epithelial cells

Bovine herpesvirus 2	Pseudo-lumpy skin disease	Eruption of superficial cutaneous nodules with a depressed center; no scar formation or deep necrotic sequestra (differentiates from true lumpy skin disease)
	Bovine mammillitis	Trauma initiates infection; swollen teats with cutaneous plaques; epithelial syncytia with Cowdry type A intranuclear viral inclusions
Porcine herpesvirus 1	Pseudorabies/Aujeszky's Disease	Abortion; non-suppurative meningoencephalitis; rhinitis, tonsillitis, pneumonia; coagulative necrosis of placenta, liver, spleen, adrenal gland
Equine herpesvirus 3	Equine coital exanthema	Papules, vesicles, pustules on genitalia or muzzles; ballooning degeneration of keratinocytes with intranuclear viral inclusions
Equine herpesvirus 5	Multinodular pulmonary fibrosis	Nodules with thick interstitial collagen with irregular alveoli lined by cuboidal cells; intranuclear viral inclusions in alveolar macrophages
Gallid herpesvirus 1	Avian infectious laryngotracheitis	Mucohemorrhagic fibrinonecrotic exudates (+/- tracheal casts) within nasal turbinates, sinuses, conjunctiva, larynx, and trachea; epithelial ulceration with formation of syncytial cells containing intranuclear viral inclusions
Gallid herpesvirus 2	Marek's disease	Herpesviral induced T-cell lymphoma; four different gross lesion patterns: (1) thickening and yellowing of peripheral nerves (2) discoloration of the iris (3) enlargement of feather follicles and (4) visceral tumors

Anatid herpesvirus 1	Duck Plague	Multifocal hemorrhages in visceral organs; severe enteritis with lymphoid tissue necrosis; foci of necrosis in liver
Feline herpesvirus 1	Feline viral rhinotracheitis	Focal ulcerative (and often eosinophilic) lesions on face or nasal planum (usually without clinical respiratory signs); ulcerative and necrotizing with large glassy intranuclear viral inclusions in epithelial cells

Contributing Institution:
University of Illinois
College of Veterinary Medicine
Veterinary Diagnostic Laboratory
Urbana, IL 61802
http://vetmed.illinois.edu/

References:

1. Cantile C, Youssef S. Nervous system. In: Maxie MG, ed. *Jubb, Kennedy, and Palmer's Pathology of Domestic Animals.* Vol 1. 6th ed. St. Louis, MO: Elsevier; 2016:382-383.
2. Carmichael LE, Greene CE. Canine herpesvirus infection. In: Greene CE, ed. *Infectious Diseases of the Dog and Cat*. 3rd ed. Elsevier; 2006: 47-53.
3. Caswell JL, Williams KJ. Respiratory system. In: Maxie MG, ed. *Jubb, Kennedy, and Palmer's Pathology of Domestic Animals.* Vol 2. 6th ed. St. Louis, MO: Elsevier; 2016:537-538, 568, 577.
4. Decaro N, Martella V, Buonavoglia C. Canine Adenoviruses and to canine Herpesvirus. *Vet Clin North Am Small Anim Pract*. 2011; 41 (6): 1097-1120.
5. Herpesvirus. *Vet Clin North Am Small Anim Pract*. 2008; 38 (4): 799-814.
6. Evermann JF, Ledbetter EC, Maes RK. Canine reproductive, respiratory, and ocular diseases due
7. Kojima A, Fujinami F, Takeshita M, Minato Y, Yamamura T, Imaizumi K, Okaniwa, A. Outbreak of neonatal
8. canine Herpesvirus infection in a specific pathogen free beagle colony. *Jpn J Vet Sci*. 1990; 52 (1): 145-154.
9. Mauldin EA, Peters-Kennedy J. Integumentary system. In: Maxie MG, ed. *Jubb, Kennedy, and Palmer's Pathology of Domestic Animals.* Vol 1. 6th ed. St. Louis, MO: Elsevier; 2016:625-627.
10. Ojkic D, Brash ML, Jackwood MW, Shivaprasad HL. Viral diseases. In: Boulianne M ed. *Avian Disease Manual.* 7th ed. Jacksonville, FL: American Association of Avian Pathologists, Inc.; 2013:30-31, 42-43, 59-60.
11. Percy DH, Carmichael LE, Albert DM, King JM, Jonas AM. Lesions in puppies surviving infection with

canine Herpesvirus. *Vet Path*. 1971; 8: 37-53.
12. Percy DH, Olander HJ, Carmichael LE. Encephalitis in the newborn pup due to a canine Herpesvirus. *Vet Path*. 1968; 5: 135-145.
13. Schlafer DH, Foster RA. Female genital system. In: Maxie MG, ed. *Jubb, Kennedy, and Palmer's Pathology of Domestic Animals.* Vol 3. 6th ed. St. Louis, MO: Elsevier; 2016:431-432, 443-445.
14. Zachary JF, McGavin MD. *Pathologic Basis of Veterinary Disease*. 5th ed. Elsevier; 2012:218, 654, 1117.

CASE III: E 1246-14 (JPC 4102122).

Signalment: 24-year-old, intact female, polo pony (*Equus ferus caballus*).

History: Only little clinical history was provided. Recurring polypoid structures had been observed in the left nostril for seven years, especially growing during the spring and summer period. The polypoid structures had formerly been diagnosed as rhino-sporidiosis seven years ago.

Gross Pathology: A tissue sample from the nasal mucosa fixed in formalin was submitted measuring 2.8 x 1.9 x 1.4 cm, containing two separate masses connected by a tissue bridge. The first mass measured 2.3 x 1.4 x 1.1 cm and the second mass was 1.9 x 1.9 x 1.2 cm in size. Both masses were partially ulcerated.

Laboratory results: None provided.

Microscopic Description: Nasal mucosa: There is a polypoid, multilobulated mass expanding the submucosa, formed by loosely fibrovascular tissue and covered by

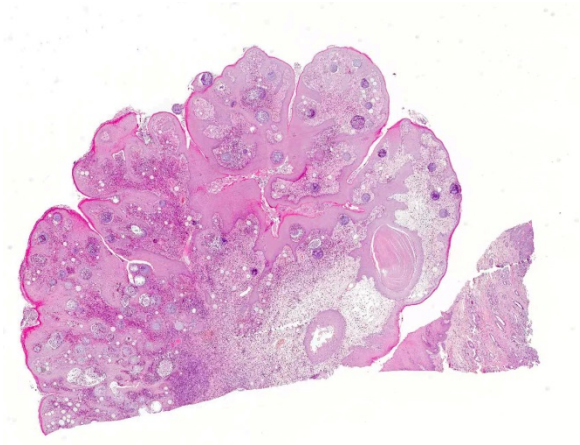

Nasal polyp, horse. At subgross magnification, a polyp composed of an edemaout collagenous core covered with hyperplastic squamous epithelium contain numerous large basophilic endosporulating sporangia in proximity to the epithelium. (HE, 15X)

hyperplastic stratified squamous epithelium. Within the fibrovascular tissue, there is marked infiltration with lymphocytes, moderate numbers of viable and degenerated neutrophils and macrophages and fewer plasma cells. Randomly distributed throughout the mass are immature to mature, partially ruptured fungal sporangia ranging from 10 to 300 µm in diameter. The smaller round immature sporangia measure 10 to 60 µm in diameter, have a central nucleus and a prominent nucleolus surrounded by loose, basophilic granular material. Their unilamellar wall is up to 2 µm thick. The intermediate sporangia measuring 60 to 200 µm in diameter show a bilamellar wall and an accumulation of ovoid, immature endospores of up to 1 µm in diameter. Large mature sporangia also have a hyaline, bilamellar wall and the immature endospores are located closer to the sporangial wall whereas the 12 µm large, eosinophilic, globular mature endospores are located more centrally. Few of the sporangia are ruptured, showing a discharge of endospores into the surrounding tissue and a marked infiltration by neutrophils. The overlying hyperplastic epithelium shows

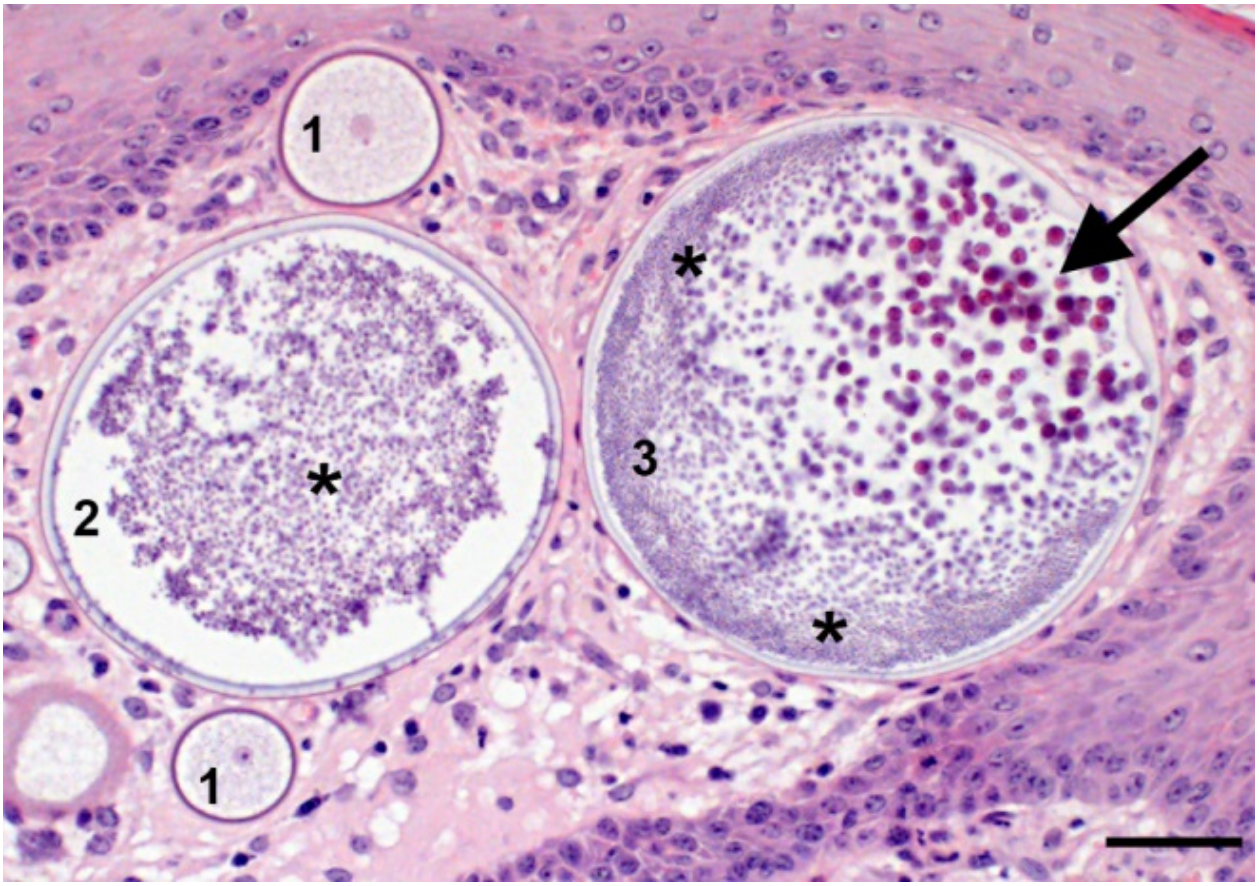

Nasal polyp, horse. Nasal mucosa with various maturation stages: 1, immature sporangium with eosinophilic, unilamellar wall, central nucleus with a prominent nucleolus surrounded by basophilic, granular material; 2, intermediate sporangium with a bilamellar wall enclosing abundant immature endospores (asterisk); 3, mature sporangium with a bilamellar wall containing immature endospores located closer to the sporangial wall (asterisks) and eosinophilic, mature endospores arranged more centrally (arrow); note the hyperplastic epithelium; Hematoxylin & Eosin, bar = 50 µm (Photo courtesy of: Department of Veterinary Pathology, Freie Universität Berlin http://www.vetmed.fu-berlin.de/en/einrichtungen/institute/we12/index.html)

multifocal keratinization and multifocal erosions with formation of serocellular crusts.

Adjacent to the mass the mucosa is lined by multifocally pseudostratified columnar epithelium and prominent seromucous glands.

Contributor's Morphologic Diagnosis: Nasal mucosa: Rhinitis, proliferative, lymphoplasmacytic and pyogranulomatous, chronic-active, focal-expansive, severe with epithelial hyperplasia and fungal sporangia consistent with *Rhinosporidium seeberi.*

Contributor's Comment: *Rhinosporidum seeberi* is a fungal-like organism causing the mucocutaneous disease Rhinosporidiosis in humans and many different animals including mammalians and birds.[3] Previously classified as a fungus, currently the agent is assigned to a new class of parasites the DRIP clade respectively the clade of the Mesomycetozoea.[6] Rhinosporidiosis is endemic in different countries in Asia and Africa with high incidence in India, Sri Lanka and Argentina. However, the disease has been reported in about 70 different countries worldwide.

Rhinosporidium seeberi's natural habitat is most likely the ground water. Infection occurs primarily via the nasal cavity through penetration of infectious spores via superficial trauma in the epithelium. The disease seems to be infective but not infectious, although the life cycle and pathogenesis are not yet fully understood. In vitro cultivation is very challenging; so far, the agent's isolation from its habitat was not successful. [1]

The typical clinical appearance of nasal or laryngeal rhinosporidiosis is single to multiple, granular, pink to red, pedunculated or sessile, polypoid growths (strawberry-like appearance).[1,6] The masses are non-infiltrating, slow-growing and painless.[5] Burgess et al.[2] hypothesized that the organism has the ability to persist subclinically for long a time.

The histopathological appearance of rhinosporidiosis seems to be the same in animals as in humans. Histological differentials include *Coccidioides immitis* and _ *(Emmonsia- new name) parvum* because of the size of the sporangia[3]; nevertheless, the identification of all different stages allows a reliable, histopathological diagnosis.[1] A periodic acid-Schiff (PAS) reaction clarifies the thick, unilamellar, eosinophilic and PAS-positive wall of immature sporangia whereas the bilamellar wall of intermediate sporangia stains partially positive for PAS, the inner layer shows positive staining for Gomori methenamine silver.[2] Endospores additionally stain positive with toluidine blue.

The treatment of choice is the complete surgical excision of the polypoid masses using electro-cautery. Recurrence is common, in which sessile polyps seem to recur more often than pedunculated polyps.

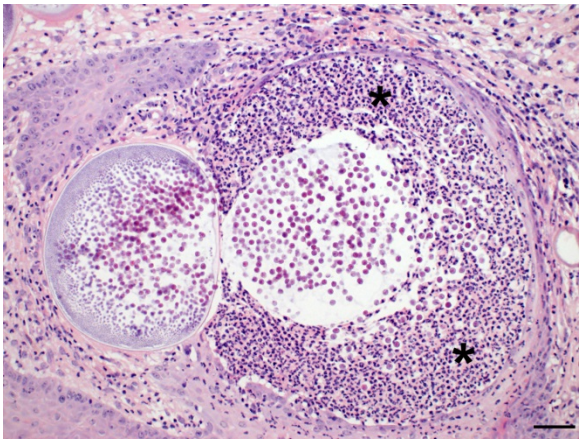

Nasal polyp, horse. Nasal mucosa with mature sporangia, the one on the right ruptured and infiltrated by high numbers of neutrophils (asterisks); Hematoxylin & Eosin, bar = 50 µm (Photo courtesy of: Department of Veterinary Pathology, Freie Universität Berlin http://www.vetmed.fu-berlin.de/en/einrichtungen/institute/we12/index.html)

Interestingly, rare cases of spontaneous regression have been reported.[1]

Rhinosporidiosis in animals and humans is an extremely rare disease in Europe[6]; the observed infections are mostly linked to former stays in endemic countries.[4] Due to globalization and the growth of international trade with animals, Rhinosporidiosis could become an emerging disease in European countries.

JPC Diagnosis: Nasal mucosa: Rhinitis, proliferative, chronic, diffuse, moderate with numerous sporangia and endospores, polo pony, equine.

Conference Comment: This case demonstrates a classic example of nasal rhinosporidiosis in a horse. Participants described nodular lesions with overlying hyperplastic mucosa that contains variably sized sporangia and endospores in different stages of maturation surrounded by inflammation and fibrous connective tissue.

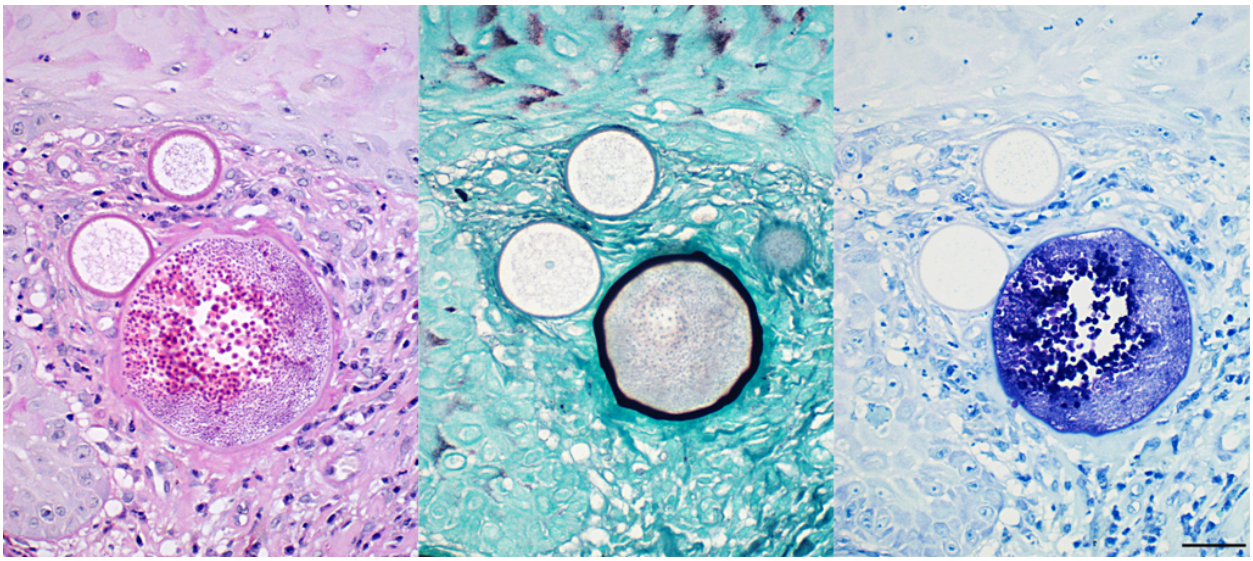

Nasal polyp, horse. Nasal mucosa with sporangia after PAS reaction (left panel), Grocott methenamine silver (middle panel) and toluidine blue staining (right panel). Immature sporangia are characterized by an eosinophilic, PAS-positive, unilamellar wall while only the outer layers of mature sporangia are fairly PAS-positive (left panel). The inner part of the bilamellar wall of the mature sporangia stains intensely positive with silver (middle panel). Mature endospores stain positive with toluidine blue (right panel); bar = 40 µm (Photo courtesy of: Department of Veterinary Pathology, Freie Universität Berlin http://www.vetmed.fu-berlin.de/en/einrichtungen/institute/we12/index.html)

The conference moderator presented the images submitted by the contributor and attendees discussed the staining patterns of sporangia and endospores. Periodic acid-Schiff (PAS) highlights endospores, unilamellar walls of juvenile sporangia, and outer walls of mature sporangia and Gomori methenamine silver (GMS) indicates the inner wall of mature sporangia. [2, 4]

Rhinosporidium seeberi exists in three forms in infective tissue. It develops as spherical sporangia (6-300 µm) which mature to develop a thick bilamellar wall. The nuclei undergo changes as well, maturing from uninucleate immature sporangia, dividing their nuclei, and forming numerous uninucleate endospores (6-7 µm) characteristic of mature sporangia. Once the sporangium matures, the endospores are released through a break in the cell wall. Free spores consequently enlarge to form sporangia and continue the tissue cycle.

Grossly, rhinosporidiosis has a nodular, polypoid appearance with numerous pinpoint white foci on the surface representing larger spherules filled with sporangiospores. Systemic dissemination is rare and the disease is seldom fatal, but can cause complications due to obstruction of airways or bleeding. Sporangia generally incite a chronic granulomatous response, whereas free endospores incite an acute neutrophilic response. Eosinophils are rare. Multinucleated giant cells are often prominent around and within empty mature sporangia having entered through the break in the cyst wall. [3, 4, 8]

There are very few differentials for *Rhinosporidium seeberi* due to their large size; they are the largest endosporulators, and characteristic location in the upper respiratory tract. Sporangia of *Coccidiodes immitis,* for example, are rarely larger than 80-200 µm. In addition, their endospores lack internal globular bodies and only their walls stain with fungal stains. Empty

sporangia may resemble *Blastomyces dermatitidis;* however, there is no broad-based budding present, and the presence of mature sporangia with endospores is not characteristic of simple yeast. Another differential is *(Emmonsia parvum- new name?)* which has much thicker trilaminar adiaspore walls.[4] Finally, a rarely seen condition that may be confused with *Rhinosporidium seeberi* is myospherulosis. Myospherulosis is a type of foreign-body reaction in which erythrocytes interact with an exogenous substance, usually ointments, or endogenous fat and form subcutaneous nodules composed of macrophages that have intracytoplasmic homogenous eosinophilic spherules. These structures stain negatively with PAS, but the intracytoplasmic spherules are positive for endogenous peroxidase identifying them as phagocytized erythrocytes.[4, 9]

Contributing Institution:
Department of Veterinary Pathology
Freie Universität Berlin
http://www.vetmed.fu-berlin.de/en/einrichtungen/institute/we12/index.html

References:

1. Arseculeratne SN. Recent advances in rhinosporidiosis and *Rhinosporidium seeberi*. *Indian J Med Microbiol.* 2002;20:119-131.
2. Burgess HJ, Lockerbie BP, Czerwinski S, Scott M. Equine laryngeal rhinosporidiosis in western Canada. *J Vet Diagn Invest.* 2012;24(4):777-780.
3. Caswell JL, Williams KJ. Respiratory system. In: Maxie MG, ed. *Jubb, Kennedy, and Palmer's Pathology of Domestic Animals.* Vol. 2. 6th ed. St. Louis, MO: Elsevier; 2016:476, 579.
4. Chandler FW, Kaplan W, Ajello L. *Histopathology of Mycotic Diseases.* Chicago, IL: Year Book Medical Publishers, Inc.; 1980:109-111.
5. Kennedy FA, Buggage RR, Ajello L. Rhinosporidiosis: a description of an unprecedented outbreak in captive swans (*Cygnus* spp.) and a proposal for revision of the ontogenic nomenclature of *Rhinosporidium seeberi*. *J Med Vet Mycol.* 1995;33:157-165.
6. Leeming G, Hetzel U, Campbell T, Kipar A. Equine rhinosporidiosis: an exotic disease in the UK. *Vet Rec.* 2007;160:552-554.
7. Leeming G, Smith KC, Bestbier ME, Barrelet A, Kipar A. Equine rhinosporidiosis in United Kingdom. *Emerg Infect Dis*. 2007;13:1377-1379.
8. Lopez A, Martinson SA. Respiratory system, mediastinum, and pleurae. In: Zachary JF ed. *Pathologic Basis of Veterinary Disease.* 6th ed. St. Louis, MO: Elsevier; 490.
9. Mauldin EA, Peters-Kennedy J. Integumentary system. In: Maxie MG, ed. *Jubb, Kennedy, and Palmer's Pathology of Domestic Animals.* Vol. 1. 6th ed. St. Louis, MO: Elsevier; 2016:560.
10. Nollet H, Vercauteren G, Martens A, Vanschandevijl K, Schauvliege S, Gasthuys F, Ducatelle R, Deprez P. Laryngeal rhinosporidiosis in a Belgian warmblood horse. *Zoonoses Public Health.* 2008;55:274-278.

CASE IV: B17-798 (JPC 4101575).

Signalment: 14-year-old, spayed, female, Domestic shorthair cat (*Felis catus*).

History: The owner identified an approximately 1cm nodule associated with the right mammary chain in December. By the following May, it had grown to approximately 4cm and became ulcerated. The right mammary chain and left inguinal mammary gland were removed surgically, and the tissue was submitted for histopathology. At the time of surgery, a single, approximately 4mm pulmonary nodule was identified on thoracic radiographs. On follow-up radiographs one month later, this nodule had enlarged and additional pulmonary nodules were identified.

Gross Pathology: The right inguinal mammary gland was expanded by a 3.7 x 3.2 x 2.8 cm firm, ulcerated mass. The right superficial inguinal lymph node was included in the sample and was also enlarged and firm.

Laboratory results: Immunohistochemistry for cytokeratin, vimentin, and smooth muscle actin was performed to characterize the neoplastic population.

IHC for cytokeratin (AE1/AE3) revealed diffuse, strong, cytoplasmic labeling of the polygonal neoplastic population. Rarely, patchy areas of spindle cells exhibit weak to moderate cytoplasmic labeling (<1% overall).

IHC for vimentin strongly stained the cytoplasm of the majority (approximately 75%) of the neoplastic spindle cells and occasional polygonal cells (<5% overall).

IHC for smooth muscle actin highlights vascular smooth muscle within and around

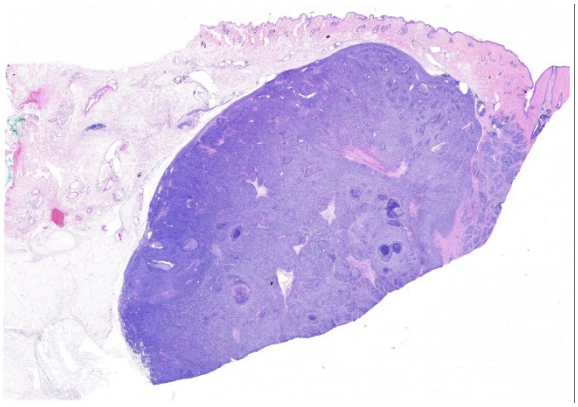

Mammary gland, cat. At subgross magnification, adjacent to the nipple, there is a well-demarcated densely cellular neoplasm. (HE, 10X)

the neoplasm and rarely individual or small groups of neoplastic cells in the epithelial or spindle cell populations (overall <1% of either population).

Microscopic Description: Mammary gland with nipple: Expanding and infiltrating the dermis and subcutis is a neoplasm composed of malignant epithelial and spindle cell populations that are typically but not always closely associated with each other.

The epithelial population is composed of polygonal cells in irregular tubules and islands with frequent central necrosis. The cells have round to oval to irregular nuclei with large amounts of vesicular to coarsely stippled chromatin and a large central nucleolus. They have moderate amounts of eosinophilic cytoplasm. They exhibit marked anisocytosis and anisokaryosis with 29 mitotic figures in 10 HPF. Near the nipple, neoplastic epithelial cells are present without the neoplastic spindle population and are instead inciting a prominent scirrhous reaction. The neoplastic epithelial cells extend along the epithelium and fill the lumen of the teat sinus, where they are mixed with corpora amylacea.

The neoplastic spindle cell population typically surrounds the epithelial population and is composed of streams of spindle cells

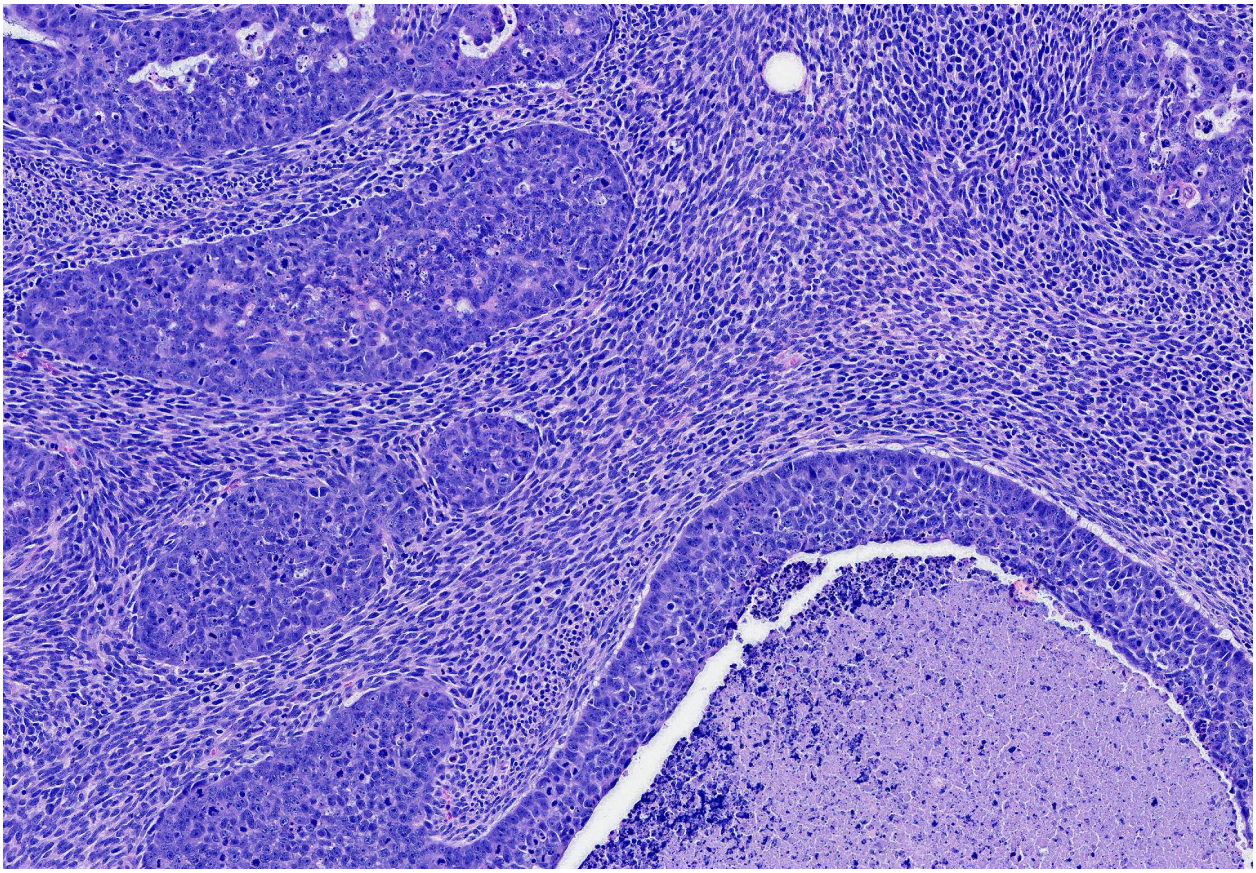

Mammary gland, cat. The neoplasm is composed of two distinct populations of neoplastic cells. Polygonal glandular epithelial cells form trabecular and islands, often with a central area of necrosis. A second population of robust spindle cells form elongate streams and bundles. (HE, 160X)

that have elongate nuclei with large amounts of coarse chromatin and a small nucleolus. They have small amounts of indistinct, eosinophilic cytoplasm. They exhibit moderate anisocytosis and anisokaryosis with 42 mitotic figures in 10 HPF. Narrow fingers of neoplastic spindle cells extend several millimeters from the main mass into the surrounding subcutaneous tissue.

The right superficial inguinal lymph node (not included) is extensively effaced by the neoplastic epithelial population and an associated scirrhous response.

Contributor's Morphologic Diagnosis: Mammary gland: Carcinosarcoma.

Contributor's Comment: Mammary neoplasia in cats occurs less commonly than in dogs but when it occurs, it is more likely to be malignant.[4] The classification of mammary neoplasia is complex and neoplasms may be composed of elements of epithelial, basal/myoepithelial, or mesenchymal origin individually or in combinations. Subtyping of feline mammary neoplasia has been based on the classification scheme published in 1999 by the World Health Organization with some publications proposing updates that would bring the feline classification scheme closer to the recently updated guidelines for canine mammary neoplasia.[4,5,9,17] Immuno-histochemistry can be helpful (or critical) in some cases to help distinguish the cell types involved in a particular neoplasm. Cells of luminal epithelial origin are expected to express so-called luminal cytokeratins (CK7, CK8, CK18, CK19). Cells of basal or

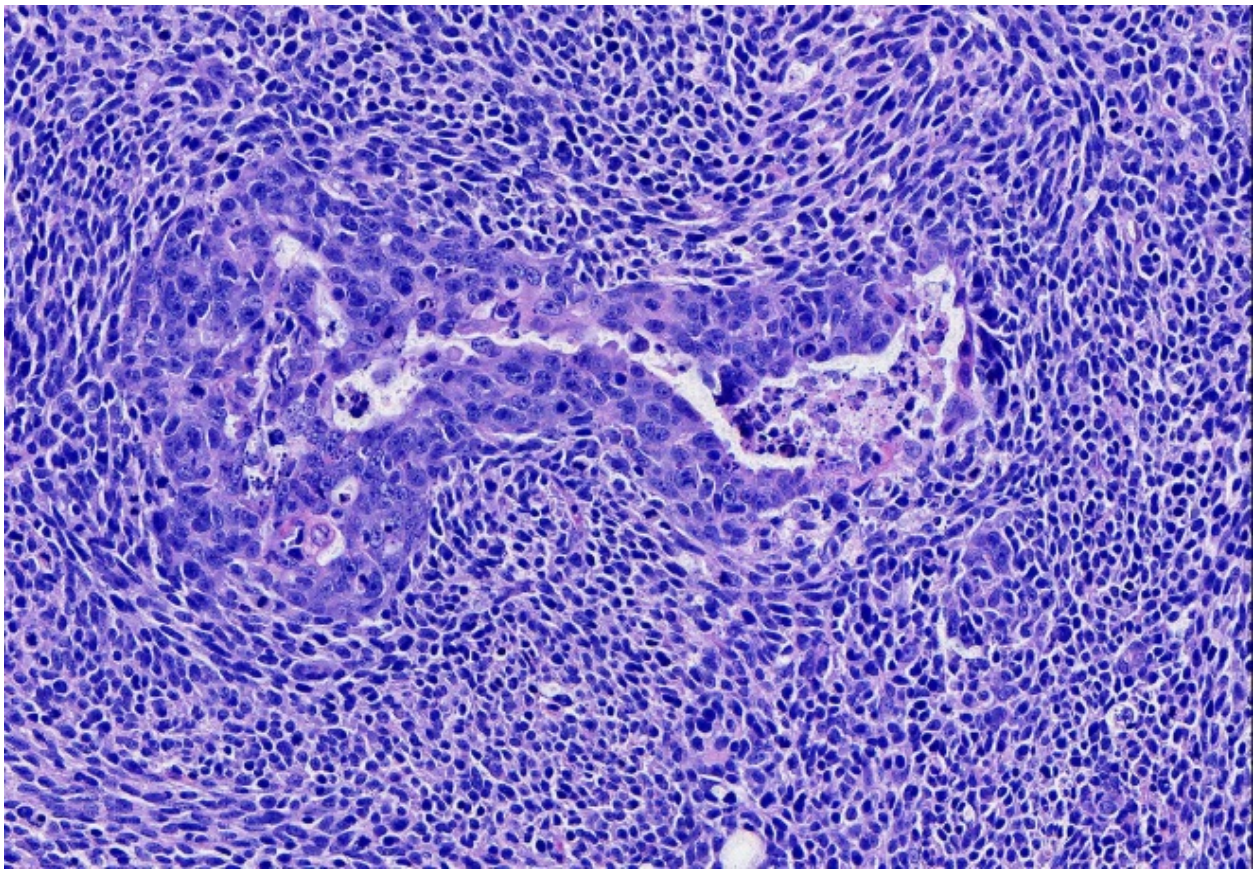

Mammary gland, cat. Higher magnification of the neoplasm. (HE, 300X)

myoepithelial origin are expected to express so-called basal cytokeratins (CK5, CK6, CK14, CK17) as well as smooth muscle actin, vimentin, calponin, and p63.[14]

In this case, proliferative epithelial and spindle cell populations were identified. Both populations had high mitotic rates, atypia, and infiltrative growth to support malignancy. Furthermore, the epithelial population was found within sections of a draining lymph node. Based on the hematoxylin and eosin stained sections, the primary differentials considered were carcinosarcoma (malignant mixed mammary tumor), carcinoma and malignant myoepithelioma, or spindle cell carcinoma arising from tubular carcinoma. The cytokeratin cocktail (AE1/AE3) used for IHC in this case recognizes cytokeratins 1, 2, 3, 4, 5, 6, 7, 8, 10, 14, 15, 16, 19, so both luminal and basal/myoepithelial cells would be expected to stain. The lack of significant cytokeratin or smooth muscle actin expression in the spindle cell population made it unlikely that this population was of myoepithelial origin and would not be expected with a diagnosis of carcinoma and malignant myoepithelioma. The lack of cytokeratin expression in the vast majority of the spindle cells would also be unexpected in a spindle cell carcinoma.[5] Given the presence of a distinct cytokeratin-expressing epithelial population and a distinct vimentin-expressing spindle cell population, a diagnosis of carcinosarcoma (malignant mixed mammary tumor) was made. Additional IHC for other markers of myoepithelium (calponin and p63) were not performed in our lab to further rule out a myoepithelial component.

Although feline mammary carcinosarcomas have appeared in several reports, they are rare and do not appear in more recent publications discussing prognostic evaluation of feline mammary neoplasia.

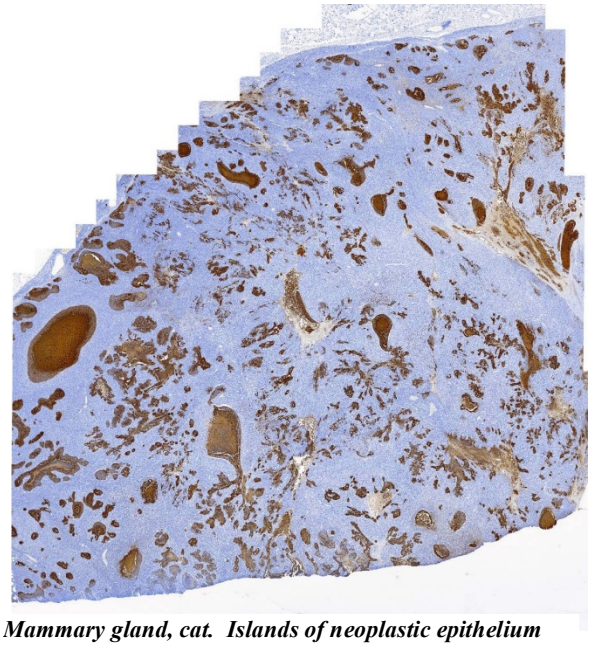

Mammary gland, cat. Islands of neoplastic epithelium stain intensively for cytokeratins. (anti-AE1/AE3, 10X) (Photo courtesy of: Cummings School of Veterinary Medicine, Tufts University http://vet.tufts.edu/foster-hospital-small-animals/departments-and-services/pathology-service/)

[2,8,10,13,17] In dogs, carcinosarcomas of the mammary gland are also rare and appear to have an aggressive course with all dogs with carcinosarcoma in one prognostic study (8 cases) exhibiting metastasis and having a median survival of only 4.2 months.[12] This particular cat had evidence of pulmonary (radiographic evidence) and lymph node (histologically confirmed) metastasis at the time of biopsy with progression of pulmonary nodules seen radiographically a month later. Mammary carcinosarcomas in dogs frequently have an osteosarcoma component,[4,5] but this was not seen in any sections from this particular case.

In cats, tumors with malignant epithelial and mesenchymal components (variably referred to as carcinosarcomas, malignant mixed tumors, or sarcomatoid carcinoma) have been rarely described in other organs, including uterus[11], salivary gland[7], prostate[16], lung[3], digital apocrine glands[6], pancreas[15], and biliary system[1].

JPC Diagnosis: Mammary gland: Carcinosarcoma, Domestic shorthair, feline.

Conference Comment: This case provided the rare opportunity to discuss the intricacies of feline mammary neoplasia, as well as the difficulties in precisely classifying the more rare variants.. Participants described a well-demarcated, multinodular neoplasm that expands the dermis composed of two types of cells: polygonal cells arranged in islands and trabeculae with central areas of comedonecrosis and spindle cells arranged in long interlacing streams separating islands of polygonal cells. Near the teat canal, there are areas of desmoplasia and large areas of necrosis with neoplastic cells present within the teat canal and lymphatic

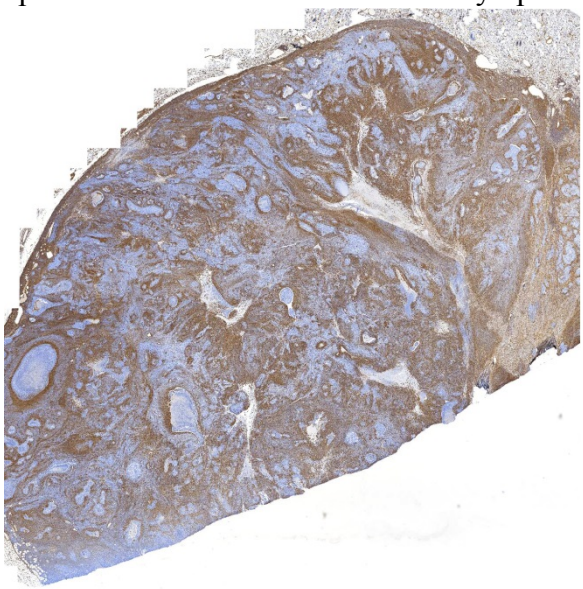

Mammary gland, cat. Spindle cells stain strongly positive for vimentin. (anti-vimentin, 10X) (Photo courtesy of: Cummings School of Veterinary Medicine, Tufts University http://vet.tufts.edu/foster-hospital-small-animals/departments-and-services/pathology-service/)

vessels.

Feline mammary tumors are much less common than their canine counterparts and are more often malignant. Consequently grading and staging are important in regards to prognosis. The Elston and Ellis grading system (used in women) has been adapted for cats as well as a more recent numeric grading system that bases tumor grade on the following criteria: lymphovascular invasion, nuclear form, and mitotic count.

Table 1: Feline-specific malignant mammary gland tumors[4]

Malignant epithelial neoplasms	
Cribiform carcinoma	Lumina lined by neoplastic cells that are very inconspicuous (compared to tubular carcinomas).
Micropapillary invasive carcinoma	In queens and males, more than 50% have a micropapillary pattern.
Comedocarcinoma	Multiple small areas of well-defined necrosis located at the center of nodules of neoplastic cells. Neutrophil infiltration is attributed to mastitis in addition to the neoplastic process.
Anaplastic carcinoma	Rare in cats.
Intraductal papillary carcinoma	Rare in cats, identical to what is seen in dogs. Malignant variant of intraductal papillary adenoma.
Ductal carcinoma	AKA "feline complex carcinoma", malignant variant of the ductal adenoma which is composed of doubled layered neoplastic cells (luminal epithelial and basal cell components) forming cords, tubules, and solid areas around slit-like lumina. Ductal carcinomas are more solid with increased basal cells and less organized structure, more mitotically active with cellular atypia, and potentially areas of squamous differentiation and keratinization.
Malignant epithelial neoplasms – special types	
Adenosquamous carcinoma	Areas of carcinoma (any type) and areas of squamous differentiation.
Mucinous carcinoma	Rare, contains an abundant mucoid matrix surrounding neoplastic epithelial cells.
Lipid-rich carcinoma	Rare in cats, identical to what is seen in dogs.
Malignant mesenchymal neoplasms – sarcomas	
Inflammatory carcinoma	Clinical diagnosis characterized by sudden onset of subcutaneous edema, erythema, and pain in the ventral abdomen. The common histologic feature is large emboli of neoplastic cells in dermal lymphatics.

Prognostic factors include: epidemiologic factors (age, breed, reproductive status), clinical factors (staging, tumor size, lymph node invasion and metastasis, aggressiveness of surgery), and histological factors (type of tumor, grade).[4]

The conference moderator led a discussion on the published classification of feline mammary tumors. Hyperplasia and benign neoplasms are rare but are similar to what's found in bitches. Malignant mammary neoplasms are split into three groups: malignant epithelial neoplasms, malignant epithelial neoplasms – special types, and malignant mesenchymal neoplasms – sarcomas.

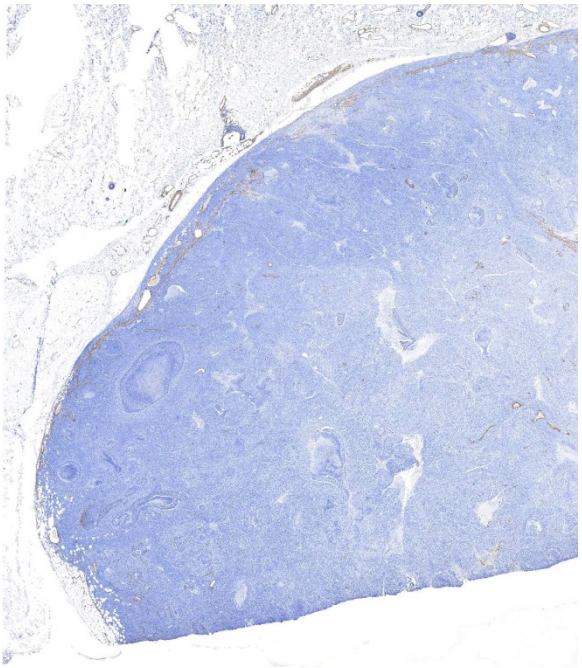

Mammary gland, cat. Neither population stain for smooth muscle actin. (anti-SMA, 10X) (Photo courtesy of: Cummings School of Veterinary Medicine, Tufts University http://vet.tufts.edu/foster-hospital-small-animals/departments-and-services/pathology-service/)

The contributor's morphologic diagnosis was discussed and debated at length. For expert evaluation, the case was sent to Dr. Michael Goldschmidt, Professor Emeritus at University of Pennsylvania, who commented that based on the morphology of the original HE slide (which was the only slide avaible to participants), a diagnosis of carcinosarcoma was perfectly acceptable. Several additional immunohistochemical stains were run to better categorize the neoplastic cell population. Both calponin and p63 were equivocal, staining some of the mesenchymal cell population but not all. Cytokeratin 5, 6, and 7 were negative for the mesenchymal cell population. Based on these results, we agree with the contributor's diagnosis of carcinosarcoma.

Contributing Institution:
Cummings School of Veterinary Medicine
Tufts University
http://vet.tufts.edu/foster-hospital-small-animals/departments-and-services/pathology-service/

References:

1. Cavicchioli L, Ferro S, Zappulli V, et al. Carcinosarcoma of the biliary system in a cat. *J Vet Diag Invest*. 2013; 25(5): 562-565.
2. Fusaro L, Panarese S, Brunetti B, Sarli G, et al. Quantitative analysis of telomerase in feline mammary tissues. *J Vet Diagn Invest*. 2009; 21:369-373.
3. Ghisleni G, Grieco V, Scanziani E, et al. Pulmonary carcinosarcoma in a cat. *J Vet Diag Invest*. 2003; 15: 170-173.
4. Goldschmidt MH, Peña L, Zappulli. Tumors of the Mammary Gland. In: Meuten DJ, ed. Tumors in Domestic Animals. 5th ed. Ames, IA: John Wiley & Sons, Inc; 2017: 723-765.
5. Goldschmidt M, Peña L, Rasotto R, Zappulli V. Classification and grading of canine mammary tumors. *Vet Pathol*. 2011;48:117-131.
6. Herraez P, Rodriguez F, Espinosa de los Monteros A, et al. Multiple primary digital apocrine sweat gland carcinosarcoma in a cat. *Vet Rec*. 2005; 157(12): 356-358.
7. Kim H, Nakaichi M, Itamoto K, Taura Y. Malignant mixed tumor in the salivary gland of a cat. *J Vet Sci*. 2008; 9(3): 331-333.
8. Mills SW, Musil KM, Davies JL, et al. Prognostic value of histologic grading for feline mammary carcinoma: a retrospective survival analysis. *Vet Pathol*. 2015;52:238-249.

9. Misdorp W, Else RW, Hellme'n E, et al. Histological classification of mammary tumors of the dog and the cat. In: World Health Organization, ed. International Histological Classification of Tumors of Domestic Animals. Second ser. Vol 7. Washington, DC: Armed Forces Institute of Pathology, American Registry of Pathology; 1999.
10. Paniago JDG, Vieira ALS, Ocarino NM, Serakides R, et al. Mammary carcinosarcoma in cat: a case report. *Arq Bras Med Vet Zootec.* 2010; 62(4): 812-815.
11. Papparella S, Roperto F. Spontaneous uterine tumors in 3 cats. *Vet Pathol.* 1984; 21:257-258.
12. Rasotto R, Berlato D, Goldschmidt MH, and Zappulli V. Prognostic significance of canine mammary tumor histologic subtypes: an observational cohort study of 229 cases. *Vet Pathol.* 2017; doi: 10.1177/0300985817698208
13. Soares M, Madeira S,Correia J, Ferreira F, et al. Molecular based subtyping of feline mammary carcinomas and clinicopathological characterization. *The Breast*. 2016; 44-51.
14. Sorenmo KU, Rasotto R, Zappulli V, Goldschmidt MH. Development, anatomy, histology, lymphatic drainage, clinical features, and cell differentiation markers of canine mammary gland neoplasms. *Vet Pathol*. 2011;48:85-97.
15. Yamamoto R, Suzuki K, Mitsumor K, et al. Pancreatic carcinosarcoma in a cat. *J Comp Path*. 2012; 147: 223-226.
16. Zambelli D, Cunto M, Bettini G, et al. Successful surgical treatment of a prostatic biphasic tumor (sarcomatoid carcinoma) in a cat. *J Fel Med and Surg*. 2010; 12: 161-165.
17. Zappulli V, Rasotto R, Caliari D, et al. Prognostic evaluation of feline mammary carcinomas: a review of the literature. *Vet Pathol*. 2015;52:46-60.

Self-Assessment - WSC 2017-2018 Conference 3

1. Which of the following is the enzymatic deficiency associated with globoid cell leukodystophy?
    a. Glucocerbrosidase
    b. Galactocerebrosidase
    c. Sphingomyelinase
    d. Galactosidase

2. Which of the following species may develop a suppurative encephalitis in association with Clostridium piliforme?
    a. Rabbits
    b. Primates
    c. Mongolian gerbils
    d. Waterfowl

3. Which of the following is not a documented source of canine herpesvirus-1 in puppies?
    a. Across the placenta
    b. Through the colostrum
    c. From humans acting as fomites
    d. From nasal secretion of the bitch

4. Why of the following is true concerning *rhinosporidium seeberi?*
    a. It has recently been reclassified as a fungus.
    b. Initial infection is through an as-yet unidentified pathway across intact intestinal mucosa.
    c. Systemic infection is common, but is generally non-fatal.
    d. Free endospores incite a neutrophilic rather than an eosinophilic response.

5. Which of the following does NOT stain myoepithelial cells:
    a. Calponin
    b. CK8
    c. Smooth muscle actin
    d. CK17

Please email your completed assessment to Ms. Jessica Gold at Jessica.d.gold2.ctr@mail.mil for grading. Passing score is 80%.This program (RACE program number) is approved by the AAVSB RACE to offer a total of 0.5 CE Credits, with a maximum of 12.5 CE Credits being available to any individual Veterinary Medical Professionals for the 2017-2018 Wednesday Slide Conference. This RACE approval is for the subject matter categories of: SCIENTIFIC using the delivery method of NON-INTERACTIVE DISTANCE. This approval is valid in jurisdictions which recognize AAVSB RACE; however, participants are responsible for ascertaining each board's CE requirements.
RACE does not "accredit", "endorse" or "certify" any program or person, nor does RACE approval validate the content of the program.

Joint Pathology Center
Veterinary Pathology Services

WEDNESDAY SLIDE CONFERENCE 2017-2018

Conference 4

20 September 2017

CASE I: N761-15 (JPC 4101761).

Signalment: 6-year-old, male, Criollo, *Equus caballus*, horse.

History: This horse lived in the metropolitan area of Porto Alegre since it was born. It had a nine day history of lethargy, sialorrhea, evolving to neurological signs of ataxia and recumbency. Euthanasia was elected due to the poor prognosis and progression of clinical signs. Two days prior to onset of clinical signs, *Trema micrantha* branches were pruned, and its leaves were readily available for consumption in the pasture the horse was hold.

Distance and close view of Trema micrantha, a fast growing and toxic plant seen in tropical and subtropical areas of the Western Hemisphere. (Photo courtesy of: Faculdade de Veterinária, Universidade Federal do Rio Grande do Sul, Setor de Patologia Veterinária, http://www.ufrgs.br/patologia/)

Gross Pathology: The brain of this horse was diffusely yellow with grayish to dark-red multifocal do coalescent friable to soft pinpoint foci, mainly involving the pons.

Laboratory results: Fragments of cerebrum, cerebellum and spinal cord were refrigerated and tested by direct fluorescent antibody test (DFAT) for Rabies virus (RABV) in a certified laboratory, following OIE recommendations, and gave negative results.

Microscopic Description: Pons: Approximately one third of the cut section (which corresponds to the pons) presents severe vasculitis and liquefactive necrosis of white and gray matter; these are characterized by multifocal transmural fibrinoid necrosis of blood vessels, which sometimes are occluded by thrombosis and associated with perivascular hemorrhage, in addition to severe vacuolation of myelin (suggestive of intramyelinic edema) and perivascular

edema. There is a moderate multifocal perivascular inflammatory infiltrate consisting predominantly of neutrophils with few lymphocytes and plasma cells. At the periphery of the areas with necrosis of blood vessels, numerous Gitter cells, Wallerian degeneration and multiple axonal spheroids are observed.

Contributor's Morphologic Diagnosis: Brain (pons): Focally extensive, liquefactive necrosis of the white and gray matter, with severe multifocal vasculitis, fibrinoid necrosis, thrombosis, perivascular hemorrhage and intramyelinic edema.

Condition: Encephalomalacia due to *Trema micrantha* poisoning

Contributor's Comment: This horse was part of a major study involving 14 horses that were poisoned by *T. micrantha* consumption in different municipalities of Rio Grande do Sul state, Brazil. This condition caused lesions that affected different regions of the CNS, but the most striking lesions were observed in pons.

T. micrantha is an arboreal species widely distributed in Brazil, within the Cannabaceae family, occurring in tropical and subtropical areas in almost all tropical and subtropical areas of South, and Central America countries[4], and in the southern counties of Florida (United States of America).[4] It is a fast growing tree up to 5-20m, that has highly palatable leaves, which are promptly consumed by herbivores, especially when branches with green leaves fall to the ground, either due to pruning or windstorms, becoming readily available for consumption,[9] as in the present case.

Presentation, horse. The horse demonstrated progressive neurologic signs of lethargy, sialorrhea, ataxia, and recumbency. (Photo courtesy of: Faculdade de Veterinária, Universidade Federal do Rio Grande do Sul, Setor de Patologia Veterinária, http://www.ufrgs.br/patologia/)

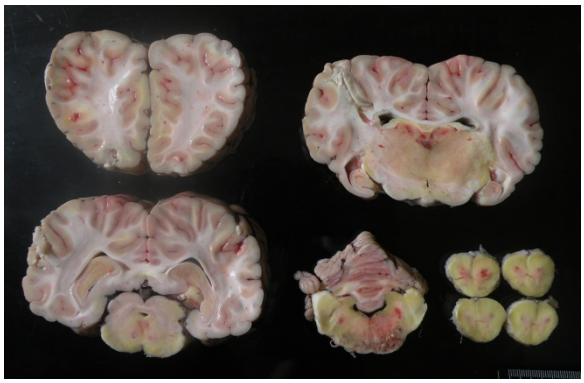

Brain, horse. The brain was diffusely yellow-gray, with numerous areas of hemorrhage and malacia. (Photo courtesy of: Faculdade de Veterinária, Universidade Federal do Rio Grande do Sul, Setor de Patologia Veterinária, http://www.ufrgs.br/patologia/)

The toxic compounds of *T. micrantha* are still unknown,[8] though a toxic compound named trematoxin obtained from *Trema tomentosa* has been described in Australia. This is a hepatotoxic glycoside associated with centrilobular necrosis in cattle, sheep, goats, horses and camels;[10] however hepatic lesions were absent in this horse, as in the majority of the remaining.

Neurological abnormalities after *T. micrantha* consumption have been related to hepatic encephalopathy, resulting in Alzheimer type II astrocytes and perivascular edema on histopathology of the CNS from the affected animals[1]. However, lesions of this horse were mainly characterized by malacia, severe fibrinoid

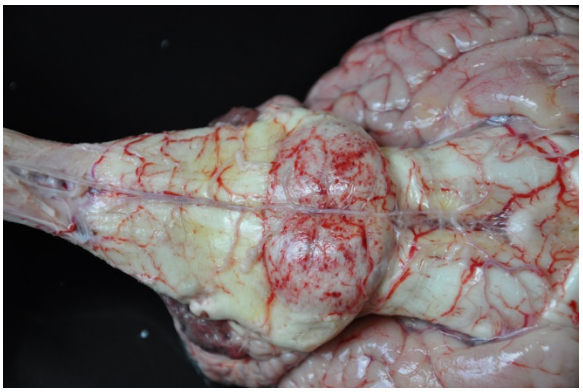

Brain, horse. Upon gross examination, perivascular hemorrhage and edema was most pronounced in the pons. (Photo courtesy of: Faculdade de Veterinária, Universidade Federal do Rio Grande do Sul, Setor de Patologia Veterinária, http://www.ufrgs.br/patologia/)

degeneration of blood vessels, thrombosis and hemorrhage. The massive necrosis and softening of the brain may be attributed to an ischemic lesion secondary to the fibrinoid necrosis of blood vessels, which resulted in extensive areas of hemorrhage and thrombosis and, consequently, areas of liquefactive necrosis, as previously described. These are not lesions usually related to hepatic encephalopathy. Still, the cause of these lesions is unknown, however it is speculated that it results from the action of an intermediary metabolite formed immediately after *T. micrantha* consumption, which would only occur in equid metabolism.[6]

Differential diagnosis of the present case included parasitic infection by *Trypanosoma evansi* and leukoencephalomalacia due to the prolonged ingestion of corn contaminated with fumonisin B1.[7] This horse did not have access to contaminated corn, and lesions differed from that condition due to the involvement of both gray and white matter. *T. evansi* infection in horses is characterized by a non-suppurative encephalitis and edema,[7] which was not observed in this horse.

In this case, *T. micrantha* consumption caused predominantly a neurological disease, with absent hepatic lesions. Thus, this neurotoxicosis should be considered in the differential diagnosis of CNS diseases in horses.

JPC Diagnosis: Brain, pons: Vasculitis, necrotizing, multifocal, marked with thrombosis, edema, and perivascular hemorrhage, Criollo, equine.

Conference Comment: This case is an unusual presentation of toxic encephalomalacia caused by *Trema micrantha* ingestion. The contributor provided an excellent review of *Trema micrantha* and *T. tomentosa* poisoning which was mirrored in much of the conference discussion. Conference participants reviewed several differentials, including gram-negative sepsis, purpura hemorrhagica, equine herpesvirus-1, listeriosis, eastern equine encephalitis (EEE), leukoencephalomalacia, *Trypanosoma evansii* and cerebrovascular accidents. Most differentials could be ruled out based on lesion distribution and host inflammatory response. Equine herpesvirus-1 is most common in the white matter of the spinal cord and characteristically results in nonsuppurative necrotizing vasculitis and

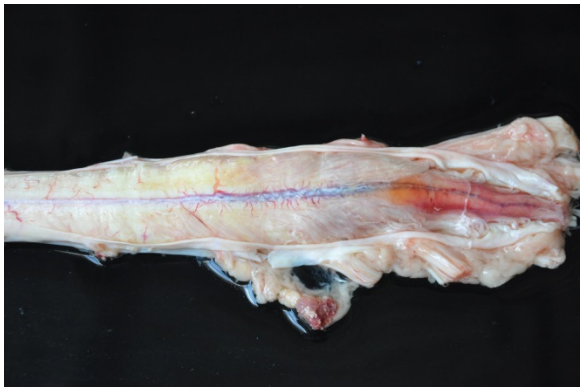

Spinal cord, horse. Areas of hemorrhage and malacia are present in the spinal cord as well. (Photo courtesy of: Faculdade de Veterinária, Universidade Federal do Rio Grande do Sul, Setor de Patologia Veterinária, http://www.ufrgs.br/patologia/)

thrombosis.[2] *Listeria monocytogenes*, is common in the brainstem, but is characterized by "microabscesses" composed of small aggregates of neutrophils within the neuroparenchyma.[2] The equine encephalitides (*Alphaviruses*) produce diffuse lesions in the grey matter with increasing severity in the cerebral cortex consisting of lymphoplasmacytic and neutrophilic necrotizing encephalitis.[2]

The differentials discussed in-depth include leukoencephalomalacia, purpura hemorrhagica, and cerebrovascular accident, because they are associated with encephalomalacia without significant inflammation of the neuroparenchyma, as is seen in this case.

Leukoencephalomalacia (LEM), also known as moldy corn poisoning, occurs in horses, donkeys, or mules fed corn laced with mycotoxin fumonisin B1 which is produced by *Fusarium verticillioides* or *F. proliferatum*, which grow in warm, moist conditions causing sporadic outbreaks of disease. Fumonisin causes encephalomalacia of the white matter in two ways (1) it damages the microcirculatory system and impairs cardiovascular function, and (2) competitively inhibits sphingosine N-acetyltransferase which leads to the accumulation of sphingosine and blocks the production of spingolipids. In this case, lesions were in both the grey and white matter of the pons. In contrast, LEM produces lesions in the white matter of the cerebrum.[2, 5]

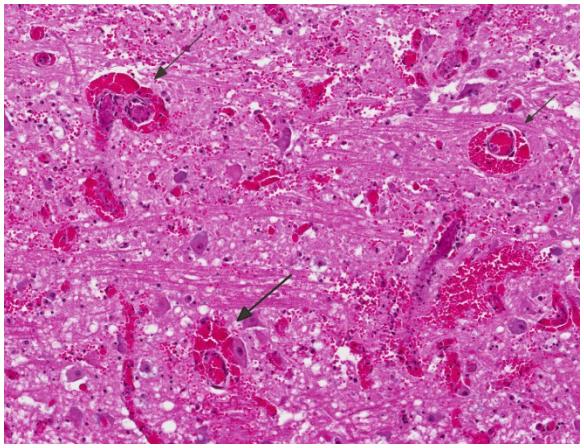

Pons, horse. Ring hemorrhages are prominent in malacic areas (arrows). The vessel at upper left is thrombosed as well (HE, 240X)

Although often associated with myositis, purpura hemorrhagica can affect many organs as it results in tissue necrosis secondary to vascular injury caused by immune-complex deposition (IgA and streptococcal M protein). In horses, purpura hemorrhagica accompanies *Streptococcus equi* infection and results in fibrinonecrotic vasculitis and hemorrhagic infarcts. Inflammatory infiltrates are rarely seen, but when seen are usually located at the periphery of areas of necrosis and *Streptococcus equi* is isolated from the lymph nodes or guttural pouch.[3]

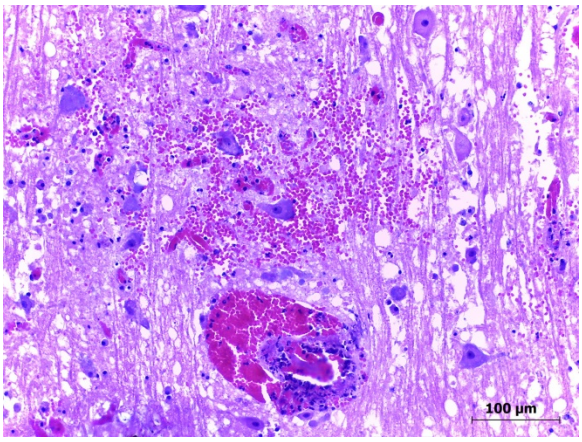

Pons, horse. Necrotizing vasculitis with degenerate neutrophils admixed with cellular debris in the vessel wall. (Photo courtesy of: Faculdade de Veterinária, Universidade Federal do Rio Grande do Sul, Setor de Patologia Veterinária, http://www.ufrgs.br/patologia/) (HE, 240X)

Cerebrovascular accidents (CVA) which are increasing in recognition in small animals

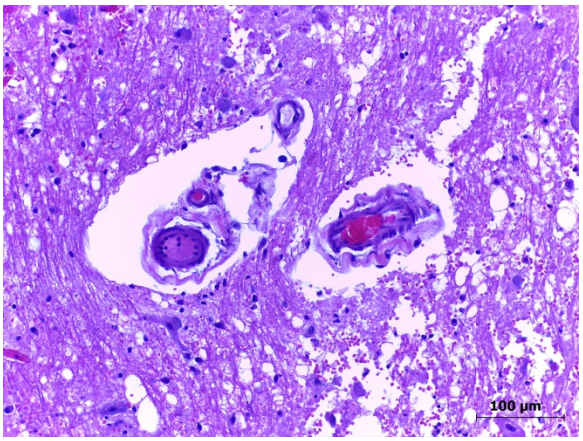

Pons, horse. Fibrinoid necrosis, with pink protein expanding vessel walls, as well as perivascular edema. (Photo courtesy of: Faculdade de Veterinária, Universidade Federal do Rio Grande do Sul, Setor de Patologia Veterinária, http://www.ufrgs.br/patologia/) (HE, 240X)

due to increasing awareness of their existence as well as sophisticated imaging techniques are often characterized by ring hemorrhage in the absence of significant inflammation. Literature on this problem in large animals is currently lacking.

Contributing Institution:
Faculdade de Veterinária
Universidade Federal do Rio Grande do Sul
Setor de Patologia Veterinária
http://www.ufrgs.br/patologia/

References:

1. Bandarra PM, Pavarini SP, Raymundo DL, et al. Trema micrantha toxicity in horses in Brazil. *EquineVet J*. 2010;42:456-459.
2. Cantile C, Youssef S. Nervous system. In: Maxie MG, ed. *Jubb, Kennedy, and Palmer's Pathology of Domestic Animals.* Vol. 1. 6th ed. St. Louis, MO: Elsevier; 2016:302, 315-316, 362-364, 376-377, 383-384.
3. Cooper BJ, Valentine BA. Muscle and tendon. In: Maxie MG, ed. *Jubb, Kennedy, and Palmer's Pathology of Domestic Animals.* Vol. 1. 6th ed. St. Louis, MO: Elsevier; 2016:229.
4. Hargis AM, Myers S. The integument. In: Zachary JF ed. *Pathologic Basis of Veterinary Disease*. 6th ed. St. Louis, MO: Elsevier; 2017:1120-1121.
5. Lorenzi H. Árvores Brasileiras. Manual de Identificação e Cultivo de Plantas Arbóreas Nativas do Brasil (Handbook for identification and cultivation of native trees from Brazil).5th ed. São Paulo, Brazil: Plantarum; 2008;01:90.(In Portuguese)
6. Miller AD, Zachary JF. Nervous system. In: Zachary JF ed. *Pathologic Basis of Veterinary Disease*. 6th ed. St. Louis, MO: Elsevier; 2017:879-880.
7. Nelson G. Elms and mulberries. In: *The trees of Florida: a reference and field guide*. 1st ed.: Pineapple Press Inc., Sarasota. Florida. 1994:48-52.
8. Pavarini SP, Bandinelli MB, Bassuino DM, et al. Novos aspectos sobre a intoxicação por *Trema micrantha* (Cannabaceae) em equídeos. *Pesq Vet Bras*. 2013;11:1339-1344.
9. Rech RR, Barros CSL. Neurologic diseases in horses. *Vet Clin North Am EqPract*. 2015;31:281-306.
10. Tokarnia CH, Brito MF, Barbosa JD, et al. Plantas Tóxicas do Brasil (Poisonous plants from Brazil). 2nd ed. Rio de Janeiro, Brazil: Helianthus; 2012:174-176. (In Portuguese)
11. Traverso SD, Corrêa AMR, Schmitz M, et al. Intoxicação experimental por *Trema micrantha* (Ulmaceae) em bovinos. *Pesq Vet Bras*. 2004;24:211-216.
12. Trueman KF, Powell MV. Suspected poisoning of camels by *Trema tomentosa* (poison peach). *Aust Vet J*. 1991;68:213-214.

CASE II: 16/545 (JPC 4102434).

Signalment: 6 years old, male, Norwegian lundehund, *Canis familiaris*, dog.

History: The dog had gastrointestinal signs for approximately 5 months. He could be normal for some days, but had recurrent episodes of diarrhea with thin watery and light-colored feces. The appetite was normal, but decreased the last two weeks. At the clinic, a thickened intestinal segment cranial to the pelvis was noted on abdominal palpation. The feces were very light in color, pale brown to almost yellow-white. The consistency was paste-like and it seemed to contain fat. X-ray and ultrasound revealed severely gas-distended and dilated intestines with almost no peristaltic movements. Exploratory laparotomy was performed. The abdominal cavity contained small amounts of yellow clear fluid, and there were no signs of peritonitis. The stomach, duodenum and pancreas were normal. Nearly all of jejunum and ileum, all the way to the ileocecal junction, was characterized by atony and dilation. There were indications of peristaltic movements, but no proper contraction of intestinal wall muscle. The cecum was small and firm and the colon had near normal diameter. No physical obstruction could be detected, and it was possible to press intestinal contents from the ileum to the colon during the explorative laparotomy. The clinical tentative diagnosis was a condition that affected the function of gut motility, a pseudo-obstruction. There were no other signs consistent with dysautonomia. The dog was euthanized.

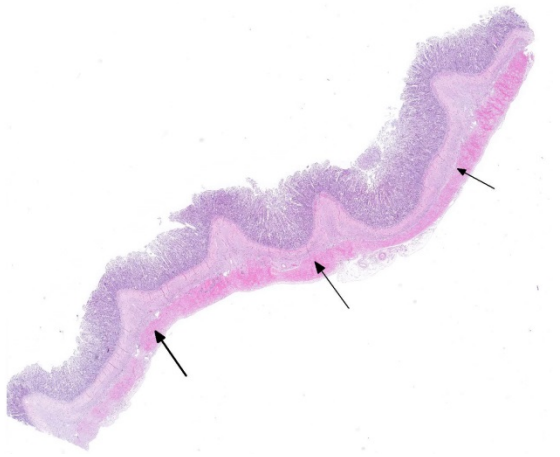

Jejunum, dog. At subgross magnification, the wall of the jejunum is markedly thinned due to marked loss of smooth muscle within the inner circular layer of smooth muscle (arrows). (HE, 5X)

Gross Pathology: The body condition of the cadaver was below normal. The small intestine was severely dilated with abundant light grey-brown content with a thin porridge-like consistency. The content of the colon was similar in color, but a little firmer. There was no hyperemia in the intestinal mucosa, and the surface of the mucosa was also otherwise normal (the breed is predisposed to intestinal lymphangiectasia).

Laboratory results: None provided.

Microscopic Description: In the inner circular layer of the lamina muscularis of the jejunum there is a multifocal to diffuse loss of smooth muscle cells due to degeneration and necrosis. This layer is affected to a variable degree, but usually the innermost part of the lamina muscularis is better preserved and the outer part, towards the Auerbach's plexus and the outer longitudinal muscle, was more severely affected. In affected areas, there was a mild multifocal inflammatory cell infiltrate composed lymphocytes, some plasma cells and histiocytic cells. In the most severely affected areas, there was near total loss of the inner circular layer of smooth muscle cells, and replacement by mild fibrosis. Except for moderate autolytic changes in the mucosa, the small intestine was otherwise normal. The lamina muscularis in stomach and colon was normal.

Contributor's Morphologic Diagnosis: Jejunum: Leiomyositis, lymphocytic, chronic with smooth muscle degeneration and necrosis.

Contributor's Comment: Chronic intestinal pseudo-obstruction (CIPO) is a syndrome characterized by gastrointestinal dilation without any physical occlusion of the lumen.[4] It is a rare condition in humans, and dogs, and single cases are also described in a cat and a horse.[1,2,3,5] Morphologically CIPO may be classified as neuropathy, mesenchymopathy or myopathy, based on predominant involvement of enteric neurons, interstitial cells of Cajal or smooth muscle cells, respectively.[1]

In domestic animals, CIPO may occur in congenital aganglionosis, other conditions associated with enteric neuronal loss or ganglioneuritis, the systemic dysautonomias and intrinsic disease of intestinal smooth muscle.[4]

In dogs, CIPO is rare and associated with intestinal leiomyositis. Affected dogs are of variable ages and breeds, they present with acute or chronic signs of vomiting, regurgitation and small bowel diarrhea.[5]

The pathogenesis is unknown, but an autoimmune inflammatory reaction affecting the intestinal lamina muscularis is suspected. Histopathology of small intestine reveals mononuclear inflammation, smooth muscle degeneration and necrosis, and fibrosis centered on areas of myofiber loss. Immunohistochemically, the lymphocytic infiltration is dominated by T lymphocytes,

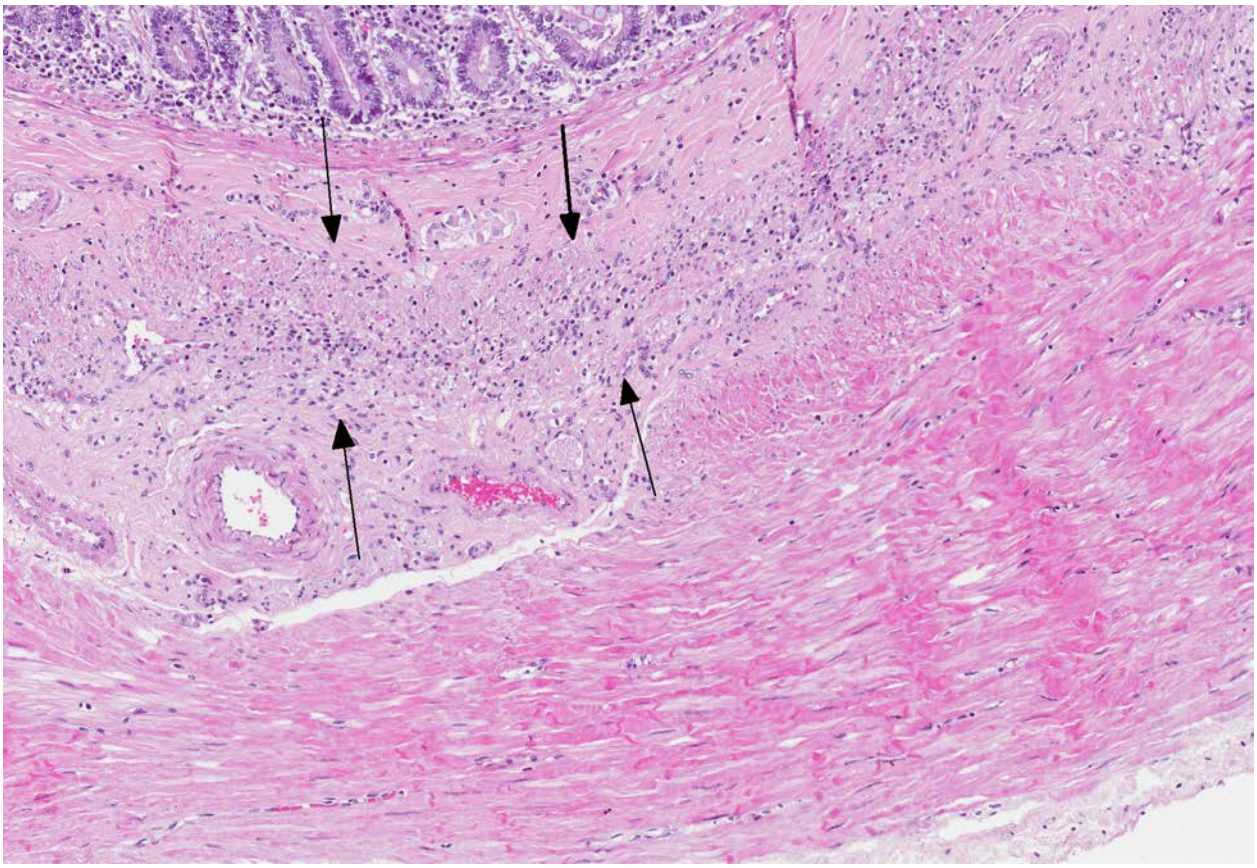

Jejunum, dog. Higher magnification of the loss of smooth muscle within the inner circular layer of smooth muscle (arrows). Lymphocyte nuclei are present within the layer as well. (HE, 5X)

with fewer B lymphocytes. The intestinal lesions may be segmental in early stages, but in chronic and severe cases, there may be near full thickness loss of smooth muscle cells in the lamina muscularis.[5]

Similar lesions, but milder may also be seen in gastric or colonic wall. In living dogs, a full-thickness intestinal biopsies is required to make a definitive diagnosis.[5]

JPC Diagnosis: Small intestine, inner circular layer: Leiomyositis, chronic, lymphocytic, diffuse, severe with smooth muscle loss and fibrosis, Norwegian lundehund, canine.

Conference Comment: This is a nice example of chronic intestinal pseudo-obstruction, a rare condition that is described most often in dogs, and results from segmental or diffuse neuromuscular dysfunction leading to a flaccid and dilated section of intestine with no physical obstruction.
In domestic animals, there are two main types of pseudo-obstruction: disorders that affect the ganglia of the myenteric plexi and those that affect the tunica muscularis. In dogs, infiltration of the tunica muscularis with inflammatory cells (predominately T-lymphocytes) and resulting fibrosis is the most common presentation (seen in this case).[6]

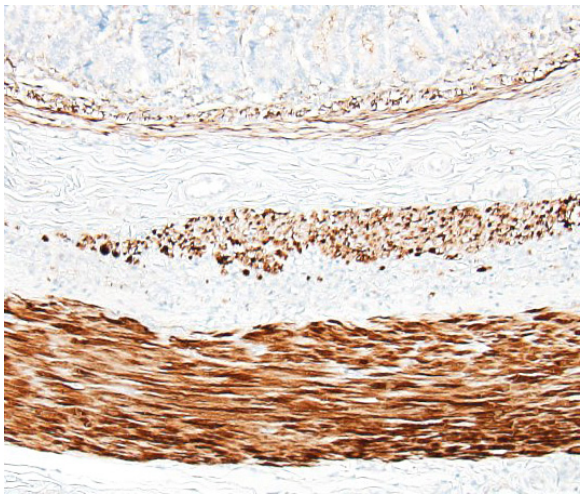

Jejunum, dog. A desmin IHC stain demonstrates the marked the loss of smooth muscle within the inner circular layer of smooth muscle. (anti-desmin, 100X)

With regard to neurpathic entities, in horses, particularly white foals born of parents with "frame overo" color patterns (white on both sides of their bodies), the myenteric plexi of the terminal ileum, cecum, and colon are affected in a congenital condition known as congenital colonic aganglionosis or "lethal white foal syndrome". Foals with this congenital abnormality are missing the ganglia within those regions of the intestine leading to fatal colic. The gene mutation observed in horses, rodents, and humans with this condition is a loss of function mutation of the endothelin receptor type B gene. This gene functions in timing of the migration of cells of the neural crest. In addition to the myenteric plexus, these foals are also lacking melanocytes in the skin (also derived from the neural crest) which explains their white color. A similar genetic condition of Clydesdale foals is associated with hypoganglionosis of the myenteric plexus resulting in megacolon. The pathogenesis in this unknown, although it does occur in older foals (4-9 months old) indicating an acquired condition.[6]

Dysautonomia or Key-Gaskell syndrome was briefly discussed as a rare entity affecting cats under 3 years of age with an unknown pathogenesis. This syndrome presents as disordered motility, with affected animals that often die due to regurgitation, prolonged starvation, or aspiration pneumonia. Affected neurons in the cranial nerve nuclei III, V, VII, and XII, ventral horns of the spinal cord and dorsal root ganglia appear chromatolytic on light microscopy. Ultrastructurally they have a

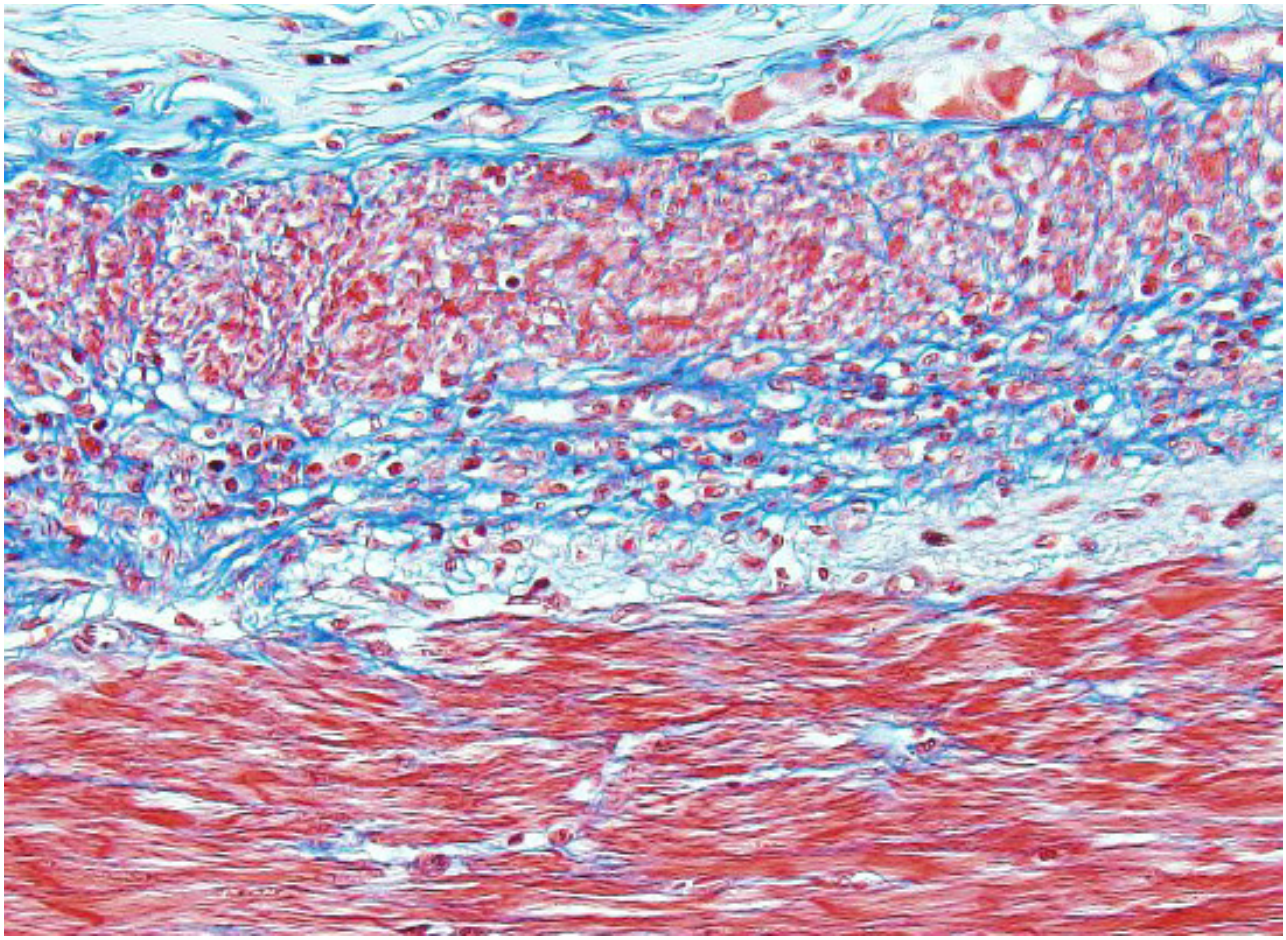

Jejunum, dog. A trichrome stain demonstrates the extent of fibrosis within the inner circular layer of smooth muscle. (Masson's trichrome, 200X)

characteristic appearance with autophagocytic vacuoles, dilated cisternae, and stacks of smooth endoplasmic membranes in their cytoplasm.[6] Lastly, proventricular dilatation disease (PDD) was reviewed caused by avian bornavirus. PDD causes flaccidity and dilation of any portion of the gastrointestinal tract in parrots, macaws, conures, and cockatoos due to lymphoplasmacytic ganglioneuritis of the myenteric plexi resulting in atrophy of the intestinal wall.[4]

The main differential myopathic condition discussed was canine immune-mediated polymyositis which may involve muscle damage by T-lymphocytes within the alimentary tract, particularly skeletal muscle of the esophagus. Polymyositis is overrepresented in German Shepherd Dogs and Newfoundlands and may occur as part of a spectrum of disease along with systemic lupus erythematosis which is diagnosed by a positive antinuclear antibody (ANA) titer. Testing for serum antibodies to type 2M myosin may aide in diagnosis of polymyositis because most affected dogs lack serum antibodies to 2M myosin.[3] In this case, immune-mediated polymyositis is not likely the cause since it is the smooth muscle in the tunica muscularis that is affected in this dog.

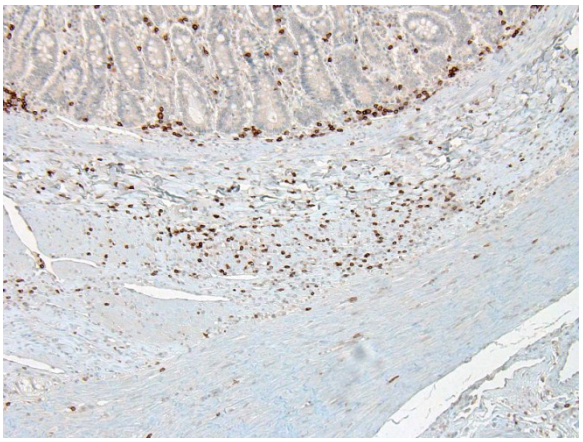

Jejunum, dog. A CD-3 IHC stain demonstrates the number of T-cells within inner circular layer of smooth muscle. (anti-CD3, 200X)

Contributing Institution:
www.nmbu.no

References:

1. Antonucci A, Fronzoni L, Cogliandro L, et al. Chronic intestinal pseudo-obstruction. *World J Gastroenterol.* 2008;14:2953-2961.
2. Chenier S, Macieira SM, Sylvestre D, Jean D. Chronic pseudo-obstruction in a horse: A case of myenteric ganglioneuritis. *Can Vet J*. 2011;52:419-422.
3. Cooper BJ, Valentine BA. Muscle and tendon. In: Maxie MG, ed. *Jubb, Kennedy and Palmer's Pathology of Domestic Animals*, Vol 1, 6th ed. St. Louis, USA: Elsevier; 2016:227-228.
4. Harvey AM, Hall EJ, Day MJ, Moore AH, Battersby IA, Tasker S. Chronic intestinal pseudo-obstruction in a cat caused by visceral myopathy. *J Vet Intern Med.* 2005;19:111-114.
5. Schmidt RE, Reavill DR, Phalen DN. Gastrointestinal system and pancreas. In: *Pathology of Pet and Aviary Birds.* 2nd ed. Ames, IA: John Wiley & Sons, Inc.; 2015:69.
6. Uzal FA, Plattner BL, Hostetter JM. Alimentary system. In: Maxie MG, ed. *Jubb, Kennedy and Palmer's Pathology of Domestic Animals*, Vol 2, 6th ed. St. Louis, USA: Elsevier; 2016:74, 77-78.
7. Zacuto AC, Pesavento PA, Hill S, et al. Intestinal leiomyositis: A cause of chronic intestinal pseudo-obstruction in 6 dogs. *J Vet Intern Med.* 2016;30:132-140.

CASE III: CASE 2 (JPC 4101313).

Signalment: 8-month-old, heifer, Nelore, *Bos taurus indicus*, Bovine.

History: Three sick cows were submitted to the Veterinary Hospital of the Universidade Federal de Minas Gerais (UFMG), as well as samples of the spinal cord of an additional cow from the same farm, collected during a field necropsy. These 4 cows were from a farm in Minas Gerais state, with a herd of 3,000 cattle, where in the past 3 years (2013-2016), 35 cows died after presenting clinical signs characterized by ataxia, paresis and paralysis of the pelvic limbs, emaciation, and sternal recumbency. Two of these cattle were euthanatized due to the severe ataxia, inability to stand, and emaciation. The herd was vaccinated against foot-and-mouth disease twice a year.

Gross Pathology: The cow was in poor body condition. Locally extensive areas of the skeletal muscle of the thoracic region (*longissimus dorsi* muscle) were replaced by numerous 0.3-0.8 mm in diameter, yellow and firm coalescent nodules (pyogranulomas) surrounded by moderate amounts of white and firm tissue (fibrous connective tissue). On the cut surface, some nodules contained yellowish and viscous fluid (purulent exudate) or whitish and viscous fluid (similar to the oily adjuvant of the foot-and-mouth disease vaccine). In the medullary canal of the subjacent vertebrae, extending from the intervertebral foramen to

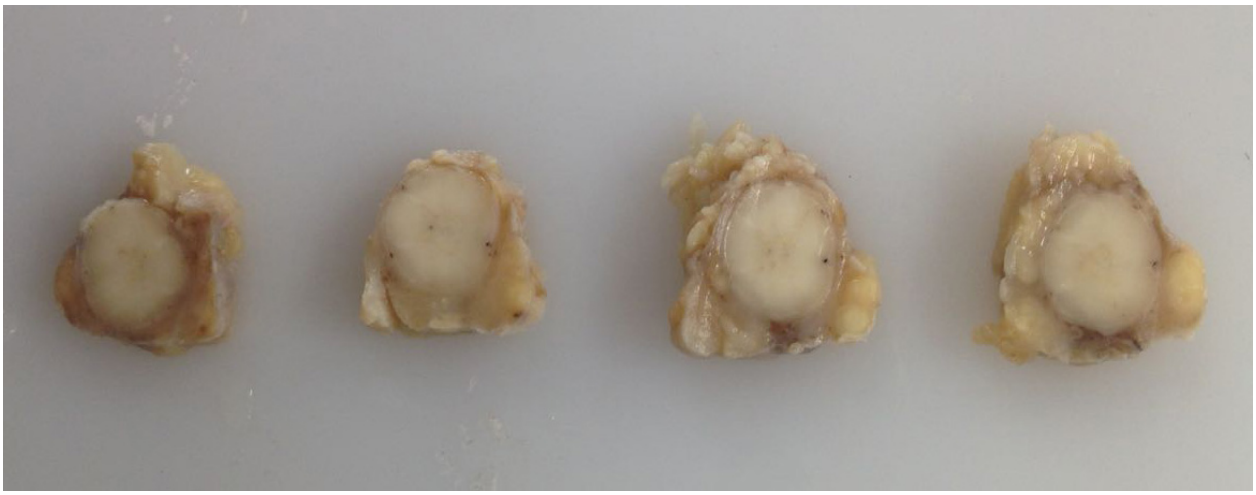

Spinal cord and dura, ox. The epidural space and dura mater were thickened due to multiple 0.3-0.8 mm in diameter, yellow and firm coalescent nodules (pyogranulomas) surrounded by moderate amounts of white and firm tissue (fibrosis). The remaining dura mater was thickened and firm (fibrosis). (Photo courtesy of: Departamento de Clinica e Cirurgia Veterinarias, Escola de Veterinaria, Universidade Federal de Minas Gerais, Belo Horizonte, Minas Gerais, Brazil, 31270-901. www.vet.ufmg.br)

the epidural space and dura mater, there were pyogranulomas identical to those described in the skeletal muscle. The remaining dura mater was thickened and firm (fibrosis).

Laboratory results: Laboratory results are pending**.**

Microscopic Description: Meninges: The dura mater is expanded, and partially or completely effaced by extensive areas of pyogranulomatous inflammation with proliferation of fibrous connective tissue. The pyogranulomas are composed by a central clear vacuole of variable sizes (ranging from 30 to 300 µm) (consistent with the space left by the oil adjuvant droplets), surrounded by variable numbers of degenerated and viable neutrophils, with aggregates of necrotic material and mineralization, and, more externally, by large numbers of epithelioid macrophages and fewer multinucleated giant cells, lymphocytes and plasma cells. These structures are further surrounded by a thick layer of dense fibrous connective tissue. Extensive areas of the dura mater are thickened by fibrous connective tissue infiltrated by low to moderate numbers of lymphocytes, plasma cells, and macrophages. Pyogranulomas and fibrous tissuesinvade or compress the adjacent nerve fibers. In the white matter of the affected sections of the spinal cord, there are numerous well-defined, large and clear vacuoles (dilated periaxonal spaces) containing either swollen axons (spheroids) or foamy macrophages (digestion chambers).

Contributor's Morphologic Diagnoses: 1. Meninges (dura mater): Pachymeningitis, pyogranulomatous and fibrosing, multifocal to coalescent, marked, with intralesional vacuoles (consistent with oil adjuvant droplets).
2. Spinal cord: Wallerian degeneration, multifocal, moderate, with spheroids and digestion chambers.

Contributor's Comment: Clinical signs and gross and histopathological findings, in these four cows, were compatible with compressive myelopathy due to pyogranulomatous reaction to the oily

Spinal cord and dura, ox. Subgross examination of the submitted section of spinal cord revelas and extensive areas of dermal fibrosis and scattered pyogranulomas extending outwards from the dura. (HE, 6X)

adjuvant of a vaccine**.** The history of previous application of the foot-and-mouth disease vaccine in the thoracic region (site of the muscular pyogranulomas) indicated its involvement with these lesions.

Compressive myelopathies in ruminants have been associated with several causes of space occupying lesions within the medullary canal, including abscesses, granulomas, physical traumas, malformations, and neoplasms[1, 2, 3]. While traumas and abscesses are apparently more common in feedlot cattle, calves, and small ruminants; neoplasms, mainly lymphomas, occur more frequently in adult dairy cows[3]. Compressive myelopathies due to postvaccinal granulomas are uncommon in cattle and occur mainly in association with foot-and-mouth disease (FMD) vaccine adjuvant[2, 3, 4]. Cases of post-vaccinal granulomas have also been related to water-in-oil adjuvant of a vaccine against *Escherichia coli* and *Campylobacter fetus* spp. *veneralis*[5] and of a vaccine against *E. coli* and *Clostridium perfringens type C*[1].

Clinical signs of compressive myelopathy related to postvaccinal granulomas include ataxia, paresis and paralysis of pelvic limbs, permanent recumbency, and progressive loss of the muscular tone.[2, 3, 4, 5] The beginning of the clinical signs occurs up to 60 days after the vaccination.[3] In the reports of the condition in Brazil, the mortality rate ranged from 0.83% to 6.0%.[2, 3, 4] Due to the similarity of the clinical signs, this condition must be included as a differential diagnosis of other two important neurological diseases in Brazilian cattle herds, rabies and botulism.[4]

An important factor for the development of the medullary lesions was the inappropriate administration of the vaccine in the muscle of a paravertebral area in the thoracic and lumbar regions. According to the orientation from the manufacturers of the vaccine and from the guidelines of the National Program for the Eradication of foot-and-mouth disease[6], this vaccine must be applied subcutaneously or intramuscularly, in the lateral cervical region. Even when applied in the recommended location, subcutaneous and muscular lesions are frequently observed in the sites of application. These lesions are either granulomas or abscesses and are an important source of economic losses due to the cost to trimming the lesion in slaughterhouses.[1] According to the owner of these cows, the application of the vaccine in the thoracic region was performed to avoid evident subcutaneous and muscular lesions in the cervical area and to facilitate the procedure when it was performed in a basic cattle handling system with straight race.

The presence of typical intralesional vacuoles (interpreted as the space left by the oily adjuvant of the vaccine, removed during the processing for the histopathological analysis) and the absence of infectious

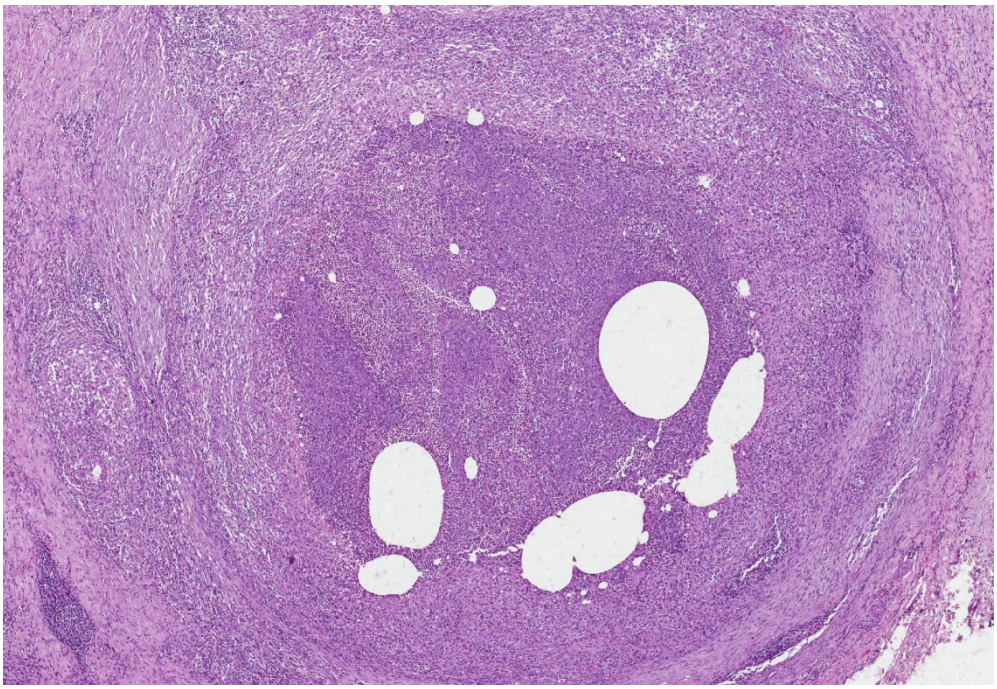

Spinal cord and dura, ox. There are multiple well-formed pyogranulomas ranging up to 2.5mm which are centered on clear vacuoles (vaccine adjuvant) (HE, 60X)

organisms in special stains (Grocott methenamine silver, Giemsa, or Ziehl-Neelsen acid-fast stains) corroborate the association of the lesions to the adjuvant. Adjuvants are important components of the vaccines and act nonspecifically, increasing the immune response against injected antigens. The adjuvant used in the FMD vaccine, that was responsible for the lesions observed in the cases, is reported as a water-in-oil emulsion.[3] The water-in-oil adjuvant used in a *Clostridium perfringens type C–E. coli* bacterin-toxoid vaccine and in a Rotavirus and Coronavirus vaccine, was also able to induce muscular lesions, such pyogranulomas, fibrosis, mineralization and necrosis.[5] Occasionally, adjuvants can cause other adverse effects, including, anaphylaxis, lymphoplasmacytic inflammation and neoplasms.[1]

Despite some studies hypothesizing an association between needle insertion into the intervertebral foramen with lesions in the medullary canal, histologic findings indicate a progression of the adjuvant due to constant rupture of the granulomas. This hypothesis is corroborated by the observation of ruptured granulomas, presence of degenerated neutrophils within the granulomas, and occasional free vacuoles among the granulomas. Migration through the tissues is a well-known property of water-in-oil adjuvants.[1, 3]

Vaccination against FMD is one of most important policies for animal health in the beef cattle industry in Brazil. FMD is a highly contagious viral disease affecting cloven-hoofed animals. It has great potential for causing severe economic loss, due its importance for commercial trade, and the requirement for total elimination of the affected herds. Brazil has no outbreaks of FMD since 2005, when outbreaks in two states led to the sacrifice of 39,845 cattle. Currently, the country has 4 zones (corresponding for 76.1% of the national territory) certified as free of the disease with use of vaccination and 1 zone (corresponding for 1.1% of the national territory) as free of the disease without using vaccination.[6]

JPC Diagnoses: 1. Spinal cord, epidural space: Pyogranulomas, multiple, with clear vacuoles, Nelore, bovine.

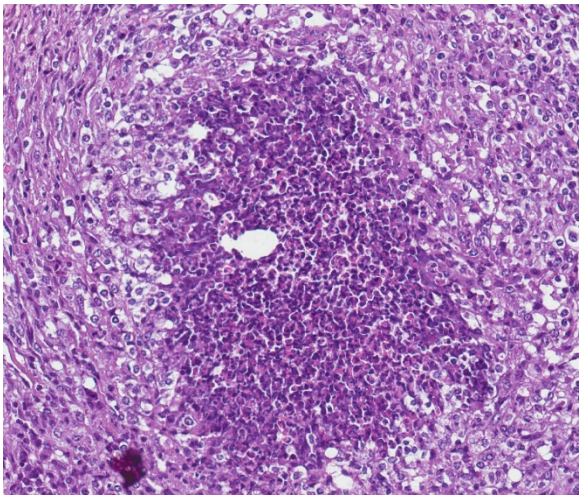

Spinal cord and dura, ox. Vacuoles representing vaccine adjuvant are surrounded by numerous degenerate neutrophils in the core of the pyogranulomas. (HE, 356X)

2. Spinal cord: Wallerian degeneration, multifocal, mild with dilated myelin sheaths and swollen axons.

Conference Comment: The contributor provided an excellent review of the gross and microscopic lesions associated with tissue migration of water-in-oil adjuvant pyogranulomas.
As mentioned above, adjuvant and associated inflammation can spread into the intervertebral foramina by direct extension through progressive rupture of the pyogranulomas and reformation of the fibrous capsule.

The risk of injection site granulomas appears to be higher in vaccines with bacterial components in them. This is theorized to be due to soft tissue damage from the bacterial endotoxin that abets extension of the inflammation through tissue planes.[5]

Conference attendees noted Wallerian degeneration (dilated myelin sheaths, swollen axons, Gitter cells in digestion chambers phagocytizing myelin) in the white matter of the spinal cord with grey matter that was relatively unaffected. These changes are characteristic of chronic compression, whereas acute compression predominately affects the grey matter.[5]

Contributing Institution:
Veterinary School
Universidade Federal de Minas Gerais
www.vet.ufmg.br

References:

8. MAPA 2017. Ministério da Agricultura , Pecuária e Abastecimento – Programa Nacional de Erradicação da Febre Aftosa. Available online: www.agricultura.gov.br/assuntos/sanidade-animal-e-vegetal/programas-de-saude-animal/programa-nacional-de-erradicação-da-febre-aftosa-pnefa
9. Marques ALA, Simões SVD, Maia LA. Compressão medular em bovinos associada a vacinação contra febre aftosa. *Ciência Rural*. 2012;42(10):1851-1854
10. McAllister MM, O´Toole D, Griggs K. Myositis, lameness and paraparesis associated with use of an oil-adjucant bacterin in beef cattle. *J Am Vet Med Assoc.* 1995;207(7):936-938.
11. O'Toole D, Steadman L, Raisbeck et al. Myositis, lameness and recumbency after use of water-in-oil adjuvanted vaccines in near term beef cattle. *J. Vet Diagn Invest*. 2005;17:23-31.
12. O'Toole D, McAllister MM, Griggs K. Iatrogenic compressive lumbar myelopathy and radiculopathy in adult cattle following injection of an adjuvanted bacterin into loin muscle: histopathology and ultrastructure. *J. Vet Diagn Invest.* 1995;7:237-244.
13. Panziera W, Rissi DR, Galiza G. et al. Pathology in practice. *J Am Vet Med Assoc.* 2016;249(5):483-485.
14. Ubiali DG, Cruz RAS, Lana MVC et al. Spinal cord compression in cattle after

the use of an oily vaccine. *Pesq Vet Bras*. 2011;31(11):997-999.

CASE IV: CASE #2 (JPC 4101755).

Signalment: 11 year old, castrated male, French bulldog, (*Canis lupus familiaris*).

History: A veterinarian found a mass at the base of the heart and tried to treat with radiation therapy. Clinically, the dog had severe coughing because of tracheal compression from the mass. A tracheostomy was performed since the larynx had collapsed. The dog was found dead by his owner 17 days after starting radiation therapy.

Gross Pathology: Necropsy was done only for the organs in the thoracic cavity. A 7x7x5 cm, reddish-tan to grayish-white, multi-nodular mass was found at the base of the heart involving the aorta, vena cava and trachea. The lungs were mildly edematous and appeared reddish-tan in color.

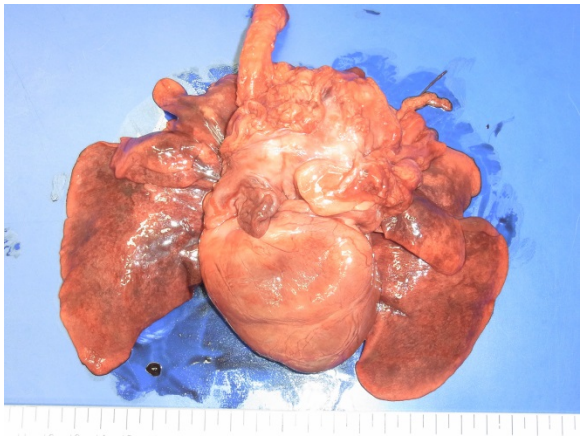

Heart base, dog. A 7x7x5 cm, reddish-tan to grayish-white, multi-nodular mass was found at the base of the heart involving the aorta, vena cava and trachea (Photo courtesy of: Laboratory of Comparative Pathology, Department of Veterinary Clinical Sciences, Graduate School of Veterinary Medicine Hokkaido University, https://www.vetmed.hokudai.ac.jp/organization/comp-pathol/e/index.html)

Laboratory results: None provided**.**

Microscopic Description: Heart: The mass is poorly demarcated and invades the right atrium wall. The neoplastic cells are polygonal arranged in cords on a moderate fibrovascular stroma. The nuclei are round to ovoid, with rare distinct nucleoli, and moderate anisokaryosis and anisocytosis.

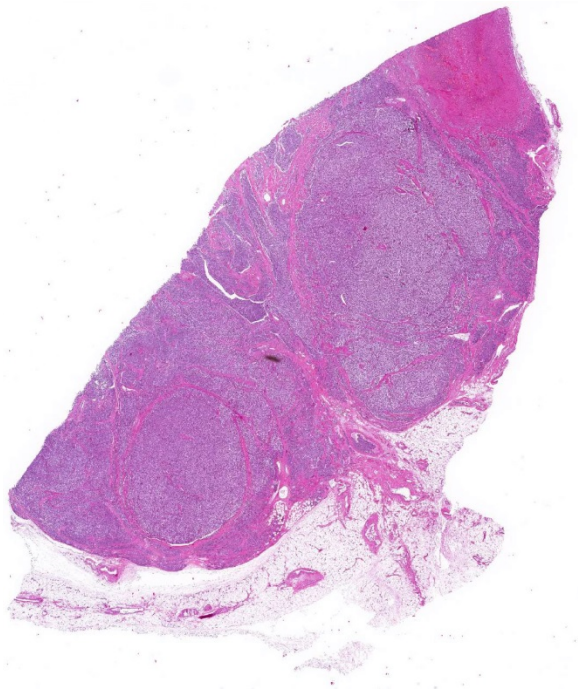

Heart base, dog. Subgross examination of the tumor of the heart base reveals a multilobulated expansile neoplasm. (HE, 5X)

Mitoses are rare. The cytoplasm is plump with fine eosinophilic granules. Atypical neoplastic cells with giant nuclei are occasionally found especially in the center of the mass. There are multifocal areas of necrosis, and vascular invasion is frequently seen with clusters of neoplastic cells in blood vessels in the less affected area of the heart.

Contributor's Morphologic Diagnosis: Heart: Aortic body carcinoma.

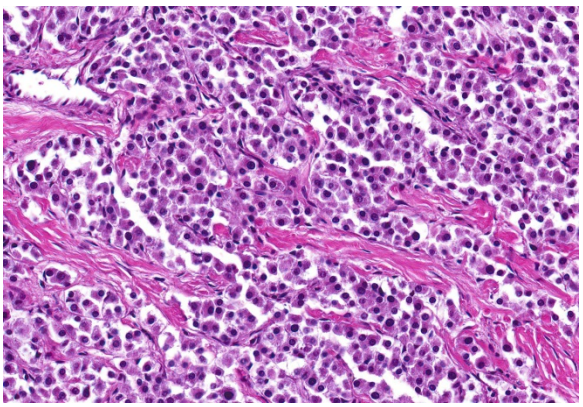

Heart base, dog. Neoplastic cells are polygonal, arranged in nests and packets, and have a moderate amount of granular cytoplasm. Nuclei are monomorphic. (HE, 400X)

Contributor's Comment: Aortic body tumor is a type of paraganglioma (chemodectoma) which is derived from cells of the neural crest. In dogs, paragangliomas are predominantly derived from the aortic or the carotid body. Aortic body tumors are more frequent than carotid body tumors in animals, whereas it is opposite in humans. Paragangliomas occur most frequently in dogs with lower incidence in cats and cattle. Brachycephalic breeds such as the Boxer and Boston terrier are highly predisposed, which implies that some genetic predisposition that is aggravated by chronic hypoxia seems to be cause of this tumor. Paraganglioma does not cause functional clinical signs, but it can compress the trachea, aorta and vena cava resulting in cardiac decompensation (hydropericardium, hydrothorax, cyanosis, ascites, edema, and passive congestion of the liver) and/or dyspnea, coughing, or vomiting.[7]

Aortic body tumors are usually benign but malignant tumors can also occur[1,8]. Aortic body carcinomas can infiltrate the wall of the pulmonary artery to form papillary projections into the lumen or invade the wall of the left atria. Aortic body carcinomas can metastasize to many organs such as the lung, liver, myocardium, kidney, lymph nodes and adrenal cortex[7]. A recent report has indicated that 9 out of the 13 dog (69%) cases showed metastasis to other organs[9]. The authors compared the characteristics of metastatic and non-metastatic aortic body carcinomas and demonstrated that metastasis is correlated with high tumor weight to body weight ratio (g/kg). However, no significant difference was found in malignant features of neoplastic cells such as pleomorphism and presence of giant cells. They concluded that those tumors are generally malignant or potentially malignant. In our case, vascular invasion of neoplastic cells and metastasis to a hilar lymph node were found. Unfortunately, we were prevented from investigating organs outside of the thoracic cavity at the request of the owner.

In humans, genetic mutations of succinate dehydrogenase complex subunit D (*SDHD*) in familial paraganglioma were first identified in 2000[2]. SDHD protein is one of the subunits consisting succinate dehydrogenase (Complex II of the respiratory chain) integrated in the inner mitochondrial membrane. SDHD forms

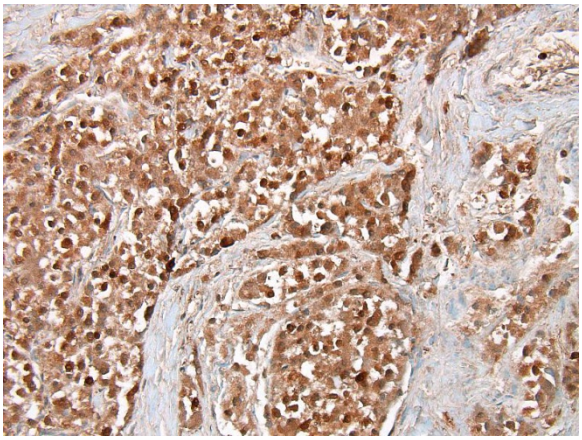

Heart base, dog. The cytoplasm of neoplastic cells stains strongly immunopositive for synaptophysin, a neuroendocrine marker. (anti-synaptophysin, 400X)

dimer with SDHC, another subunit of Complex II. The dimer can be bound to ubiquinone and water during electron transport at Complex II. Genetic mutations of *SDHD* can decrease the enzymatic activity of Complex II and lead to cellular hypoxia. Although the exact mechanism of tumorigenesis by *SDHD* mutations is still unclear, hypoxia due to decreasing Complex II activity may be associated with tumorigenesis. Indeed, people living at higher altitudes (e.g. Andes peoples), are subject to paraganglioma and hypoxia-inducible factors (HIF) affect several biological events related to tumorigenesis such as cell proliferation, metabolism and angiogenesis. Mutations of other SDH protein composing Complex II (*SDHA*, *SDHB*, *SDHC*) are also associated with paraganglioma[5,7]. Specifically, *SDHB* mutation frequently results in metastatic paraganglioma, whereas *SDHD* mutation is usually related to benign paraganglioma in the head and neck[3]. In dogs, a study indicated genetic mutations of *SDHD* and *SDHB* in some chemodectomas and pheochromocytomas[4]. Canine chemodectomas have the potential to be a model for human paraganglioma but further research is required.

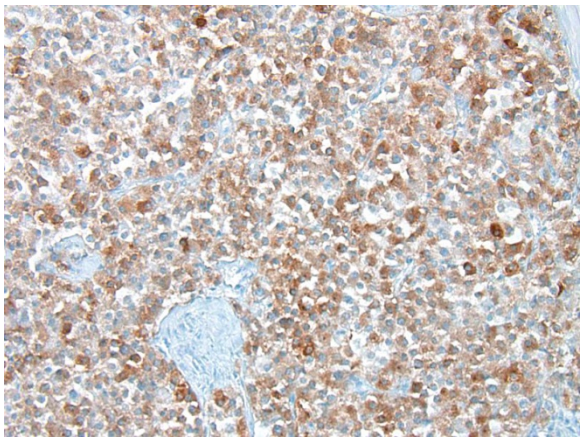

Heart base, dog. The cytoplasm of neoplastic cells stains strongly immunopositive for S-100, a marker for cells of neural crest origin. (anti-S-100, 400X)

JPC Diagnosis: Fibroadipose tissue: Neuroendocrine tumor, French bulldog, canine.

Conference Comment: This case provided a beautiful representation of a neuroendocrine tumor in a brachycephalic dog. In the slides provided, there was no myocardium present, and attendees were unable to be more definitive in their diagnoses than neuroendocrine tumor.

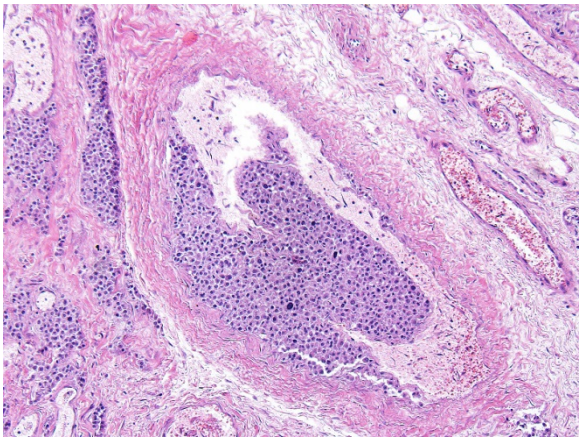

Heart base, dog. Neoplastic cells are present within vessels. Within this focus, several cells exhibit karyomegaly. (HE, 200X)

Conference participants discussed several stains that could be used to identify this as a neoplasm of neuroendocrine origin. Secretory granules of neuroendocrine cells can be identified with chromogranin A, neuron-specific enolase, synaptophysin, and S100. Churukian-Schenk, a silver-bassed, histochemical stain may also be used to identify granules. Ultrastructurally, secretory granules appear electron-dense and membrane-limited. There are also stellate or sustentacular cells with long cytoplasmic processes present in-between neoplastic cells. These cells are theorized to provide support to the chemoreceptor cells.

Malignant tumors may have decreased secretory granules and sustentacular cells, and some stains (chromogranin A) could potentially be negative.[7]

Chemoreceptor organs are located at the base of the heart (aortic body) and in the neck (carotid body) and function as sensors of variations in blood carbon dioxide content, pH, and oxygen tension and help to regulate respiration (through parasympathetic nerves) and circulation (through sympathetic nerves) based on detected changes. These organs are small and composed of chemoreceptor cells and sustentacular cells on a fine collagen and reticular fiber stroma. Chemoreceptor cells are of neural crest origin and have intracytoplasmic secretory granules that contain vasoactive factors, dopamine, norepinephrine, enkephalin peptides, and adrenomedullin. In addition to the carotid and aortic bodies, chemoreceptors are located in the nodose ganglion (vagus nerve), ciliary ganglion (orbit), pancreas, below the middle ear on the internal jugular vein, and the glomus jugulare (recurrent branch of the glossopharyngeal nerve).[7]
Participants were encouraged to read a recent article that outlines the findings in 13 cases of canine aortic body tumors in which 9 dogs had metastases and 4 did not. A recent publication on aortic body tumors in 13 dogs[9] identified tradition features of malignancy in these tumors, including pleomorphism, anisokaryosis and anisocytosis, mononuclear giant cells, and local tissue and vascular invasion, but none correlated with metastasis. Hence, these neoplasms should be all considered as potentially malignant.

Contributing Institution:
Laboratory of Comparative Pathology
Department of Veterinary Clinical Sciences
Graduate School of Veterinary Medicine

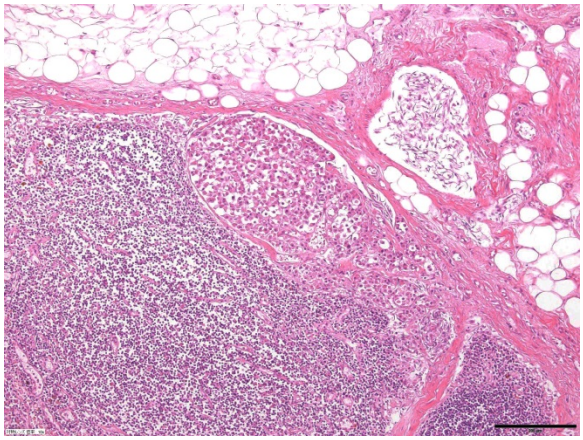

Heart base, dog. Neoplastic cells are present within the subcapsular sinus of one of the hilar lymph nodes. (Photo courtesy of: Laboratory of Comparative Pathology, Department of Veterinary Clinical Sciences, Graduate School of Veterinary Medicine Hokkaido University, https://www.vetmed.hokudai.ac.jp/organization/comp-pathol/e/index.html) (HE, 400X)

Hokkaido University
https://www.vetmed.hokudai.ac.jp/organization/comp-pathol/e/index.html

References:

15. Aupperle H, März I, Ellenberger C, Buschatz S, Reischauer A, Schoon HA. Primary and secondary heart tumours in dogs and cats. *J Comp Pathol*. 2007;136:18-26.
16. Baysal BE, Ferrell RE, Willett-Brozick JE, et al. Mutations in SDHD, a mitochondrial complex II gene, in hereditary paraganglioma. *Science*. 2000;287:848-851.
17. Favier J, Brière JJ, Strompf L, et al. Hereditary paraganglioma/pheochromocytoma and inherited succinate dehydrogenase deficiency. *Horm Res*. 2005;63:171-179.
18. Holt DE, Henthorn P, Howell VM, Robinson BG, Benn DE. Succinate dehydrogenase subunit D and succinate dehydrogenase subunit B mutation analysis in canine phaeochromocytoma

and paraganglioma. *J Comp Pathol*. 2014;151:25-34.
19. Kirmani S, Young WF. Hereditary Paraganglioma-Pheochromocytoma Syndromes. 2008 May 21 [Updated 2014 Nov 6]. In: Pagon RA, Adam MP, Ardinger HH, et al., editors. GeneReviews® [Internet]. Seattle (WA): University of Washington, Seattle; 1993-2017.
20. Rijken JA, Niemeijer ND, Jonker MA, et al. The Penetrance of paraganglioma and pheochromocytoma in SDHB germline mutation carriers. *Clin Genet*. 2017; [Epub ahead of print] doi: 10.1111/cge.13055.
21. Rosol TJ, Meuten DJ. Tumors of the endocrine glands. In: Meuten DJ, ed. *Tumors in Domestic Animals*. 5th ed. Oxford, UK: John Wiley & Sons, Inc.; 2017:828-833.
22. Treggiari E, Pedro B, Dukes-McEwan J, Gelzer AR, Blackwood L. A descriptive review of cardiac tumours in dogs and cats. *Vet Comp Oncol*. 2017;15:273-288.
23. Yamamoto S, Fukushima R, Hirakawa A, Abe M, Kobayashi M, Machida N. Histopathological and immunohistochemical evaluation of malignant potential in canine aortic body tumours. *J Comp Pathol*. 2013;149:182-191.

Self-Assessment - WSC 2017-2018 Conference 4

1. Which of the following has been identified as the main pathologic lesion in Trema tomentosa intoxication?
    a. Massive hepatocellular necrosis
    b. Encephalomalacia
    c. Myocardial necrosis
    d. Necrosis of articular cartilage

2. Which of the following best describes the myopathic form of chronic intestinal pseudoobstruction in the dog?
    a. T-cell mediated destruction and loss of the muscularis mucosae
    b. B-cell mediated destruction and loss of the muscularis mucosae
    c. T-cell mediated destruction and loss of the inner and outer longitudinal layers
    d. B-cell mediated destruction and loss of the inner and outer longitudinal layers

3. Which of the following vaccines are primarily responsible for intradural granuloma formation?
    a. Killed vaccines
    b. Modified live vaccines
    c. Oil-in-water vaccines
    d. Water-in-oil vaccines

4. Which of the following is not true concerning paragangliomas*?*
    a. Brachycephalic dogs are predisposed.
    b. A higher incidence of this tumor is seen in dogs than in cats and cattle.
    c. Affected animals generally display signs associated with epinephrine secretion.
    d. Aortic body tumors are most commonly found at the base of the heart.

5. Which of the following IHC stains would likely not be positive in an aortic body tumor:
    a. Chromagranin A
    b. Cytokerain
    c. S-100
    d. Synaptophysis

Please email your completed assessment to Ms. Jessica Gold at Jessica.d.gold2.ctr@mail.mil for grading. Passing score is 80%.This program (RACE program number) is approved by the AAVSB RACE to offer a total of 0.5 CE Credits, with a maximum of 12.5 CE Credits being available to any individual Veterinary Medical Professionals for the 2017-2018 Wednesday Slide Conference. This RACE approval is for the subject matter categories of: SCIENTIFIC using the delivery method of NON-INTERACTIVE DISTANCE. This approval is valid in jurisdictions which recognize AAVSB RACE; however, participants are responsible for ascertaining each board's CE requirements.
RACE does not "accredit", "endorse" or "certify" any program or person, nor does RACE approval validate the content of the program.

Joint Pathology Center
Veterinary Pathology Services

WEDNESDAY SLIDE CONFERENCE 2017-2018

Conference 5

27 September 2017

Corrie Brown, DVM, PhD, DACVP
Josiah Meigs and University Distinguished Professor
Department of Veterinary Pathology
College of Veterinary Medicine
University of Georgia
Athens, GA 30602

CASE I: S17-3588 (JPC 4100988).

Signalment: 8-week-old, male, breed not specified, *Sus scrofa domesticus*, porcine.

History: A piglet from an intensive pig farm, where a mortality rate increase of approximately 10% was registered in weaned piglets within a short time span, was submitted for necropsy. Affected animals displayed diarrhea that was occasionally bloody. All suckling piglets in this farm were vaccinated against porcine circovirus type 2 (PCV-2) and *Lawsonia intracellularis*.

Gross Pathology: The piglet was severely emaciated and moderately dehydrated and its hind limbs were soiled with dry, dark brown feces. The cranial lobes of the lung were bilaterally dark red and with a firm consistency, whereas the rest of the lungs were bilaterally diffusely firm, heavy and did not collapse after the thorax was opened. The intestine was filled with a small amount of brown, liquid to creamy ingesta. No further gross lesions were detected in other organs.

Laboratory results:

PCV-2 antigen immunohistochemical detection: High amount of PCV-2 antigen visible within the macrophages in the lung and lymphoid organs (spleen, Peyer´s patches, retroperitoneal and mesenteric

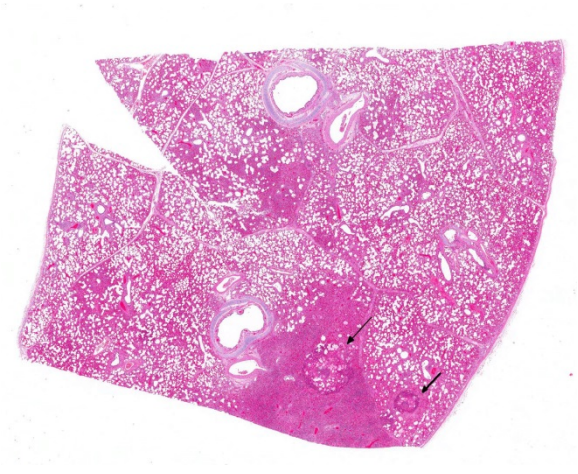

Lung, pig. At subgross magnification, there is a diffuse interstitial pneumonia with randomly scattered areas of consolidation. There are two circular areas of necrosis outlined by cellular debris (arrows). (HE, 5X)

lymph nodes, tonsils).
Bacteriology lung: High content *Pasteurella multocida*; moderate content *Streptococcus suis*.
Bacteriology intestinal content: Inconclusive (mixed microbial flora detection).
Serology: No antibodies against porcine respiratory and reproductive syndrome (PRRS) virus and classical swine fever (CSF) virus detected.

Microscopic Description: Lung: In approximately 90% of the parenchyma the alveolar septae are diffusely congested and multifocally severely thickened due to the presence of a high number of macrophages, lymphocytes and plasma cells, as well as fewer multinuclear giant cells of the foreign body type with up to five nuclei, neutrophils and accumulation of eosinophilic, foamy material (edema). The bronchus associated lymphoid tissue (BALT) is severely depleted and infiltrated by macrophages displaying moderate numbers of intra-cytoplasmatic, basophilic botryoid inclusion bodies. The bronchiolar epithelium is multifocally severely disrupted and the bronchiolar lumen is filled with a high amount of degenerated neutrophils intermingled with desquamated respiratory epithelium and occasional multinuclear giant cells. The surrounding alveoli are filled with high numbers of viable neutrophils and increased amounts of alveolar macrophages with a foamy cytoplasm, as well as a moderate number of free erythrocytes (hemorrhage) and edema. In most of the slides there are focal-extensive, hypereosinophilic areas displaying loss of cellular detail, karyorrhexis, karyolysis and pyknosis (lytic necrosis) associated with multiple, non-pigmented, septated fungal hyphae with 5-8 µm thick parallel walls and an acute angle dichotomous branching. Surrounding these necrotic areas there is a prominent granulomatous reaction characterized by the presence of high

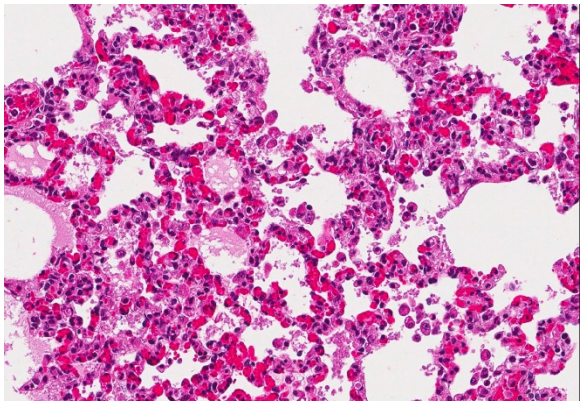

Lung, pig. Alveolar septa are widened and hypercellular with hypertrophic pulmonary intravascular macrophages and abundant granular eosinophilic alveolar contents. (HE, 360X)

numbers of degenerate and viable neutrophils, epithelioid macrophages, lymphocytes and occasionally fibroblasts and sparse collagen proliferation. The interstitial septae and the pleura are diffusely moderately edematous.

Contributor's Morphologic Diagnosis:
Lung: 1. Severe, diffuse, chronic, granulomatous, bronchointerstitial pneumonia with intralesional intra-cytoplasmatic botryoid basophilic inclusion bodies
2. Moderate, multifocal, acute, suppurative bronchopneumonia
3. Mild, focal-extensive to focal, chronic, granulomatous and necrotizing pneumonia with intralesional fungal hyphae (some slides only)

Contributor's Comment: The postmortem and histological findings are compatible with an infection with porcine circovirus type 2 (PCV-2).

PCV are small non-enveloped, single-stranded DNA viruses with a circular

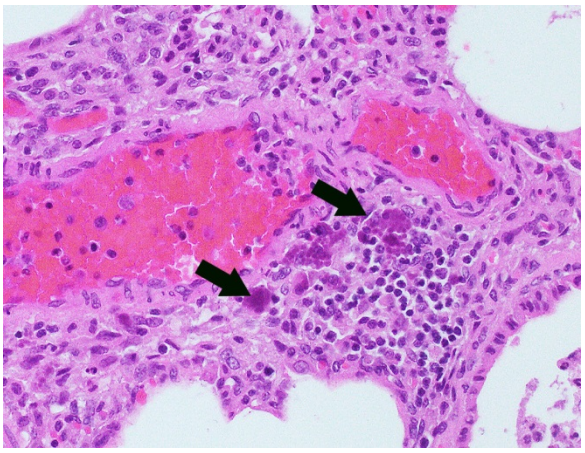

Lung, pig: The BALT is severely depleted and infiltrated by macrophages displaying moderate numbers of intracytoplasmic, basophilic botryoid inclusion bodies (arrow) (HE, 20X). (Photo courtesy of: Institute of Animal Pathology, Vetsuisse Faculty, University of Bern, Länggassstrasse 122, 3012 Bern, Switzerland (http://www.itpa.vetsuisse.unibe.ch/index_eng.html)

genome that belong to the genus *Circovirus* from the *Circoviridae* family; two genotypes (PCV-1 and PCV-2) are currently described. While PCV-1 is nonpathogenic, PCV-2 is highly virulent and was isolated for the first time in 1997 in association with postweaning multisystemic wasting syndrome (PMWS), an important, globally present swine disease of great economic impact.[1,6] Since several other often overlapping clinical syndromes were linked to PCV-2 infection in several age groups following its discovery, namely porcine respiratory disease complex (PRDC), porcine dermatitis and nephropathy syndrome (PDNS), enteric disease, reproductive failure and, more recently, PCV-2-associated cerebellar vasculitis, the term PCV-associated diseases (PCVADs) is nowadays used.[1,5,6] The most common clinical presentation is systemic PCV-2 infection (PMWS) associated with PRDC-associated pneumonia.[5] Other swine disease entities such as proliferative and necrotizing pneumonia, sow abortion and mortality syndrome, congenital hypomyelination and abortion with fetal myocarditis may also be associated to PCV-2 infection, but definite proof is still lacking.[1]

PCV-2 infection is usually slow progressing[1] and infection occurs following inhalation or ingestion of viral particles present in contaminated oronasal-pharyngeal body fluids, feces and urine. Establishment of lymphoid tissue infection in the tonsils and Peyer's patches is achieved through infection of mucosal dendritic cells, macrophages and lymphocytes, although the mechanisms that allow the virus to penetrate past the epithelial body barriers have yet to be fully elucidated. While macrophages are non-permissive to virus replication and act primarily as viral "carriers" within the organism, lymphocytes allow PCV-2 replication. Viral replication and release is associated with lymphocyte injury and lysis, which leads to severe lymphoid depletion and subsequent immunosuppression.[10]

Piglets between 5 and 12 weeks of age are usually most affected and display strong growth impairment or wasting, as well as a wide range of unspecific clinical signs, namely tachypnea, respiratory distress, fever, diarrhea, pallor, jaundice and central nervous signs. Sudden death can also occur.

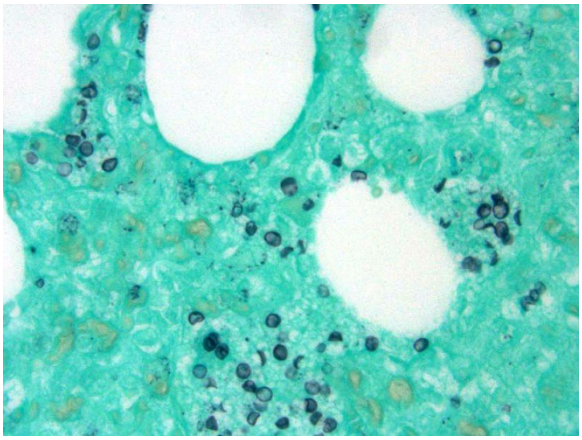

Lung, pig. A GMS stain demonstrated numerous trophozoites of Pneumocystis within alveoli. (Gomori methenamine silver, 400X)

Morbidity is usually around 5-10% and affected animals usually die or are euthanized due to poor prognosis.[1,6] The most commonly PMWS-associated lesions at necropsy include poor body condition, enlarged or atrophic lymph nodes, and interstitial pneumonia, very often associated with cranioventral bronchopneumonia.[1,5] Histologically, the most commonly found lesions include severe lymphoid depletion associated with granulomatous lymphadenitis, bronchointerstitial pneumonia, granulomatous enteritis, interstitial nephritis, meningoencephalitis, and vasculitis. Sharply demarcated, single or in grapelike clusters (botryoid) arranged, basophilic inclusion bodies can be observed in the cytoplasma of macrophages of the lymphoid system, although their presence in other locations is also described.[1,6]

Besides the above-described lung lesions of the piglet, a severe, diffuse depletion of lymph follicles associated with a severe infiltration of macrophages displaying abundant intracytoplasmatic, botryoid, basophilic inclusion bodies in the tonsils, the spleen, Peyer's patches, and in the retroperitoneal and mesenterial lymph nodes was observed. A high amount of PCV-2 antigen could be detected via immunohistochemistry both in the lymphoid organs and in the lung, thus confirming the PMWS diagnosis. Although PCV-2-associated lymphoid depletion does not always correlate with clinical disease and has also been described in subclinically infected pigs[6], it is most likely that in the present case the PCV-2 infection led to a severe immunosuppression, which allowed the infection with opportunistic bacterial (*Pasteurella multocida* and *Streptococcus suis*) and fungal (most likely *Aspergillus sp.*) pathogens.

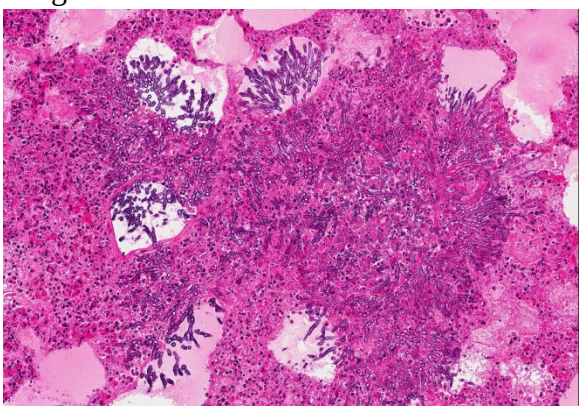

Lung, pig: Numerous septate, dichotomously branching fungal hyphae, measuring 4um in diameter, efface a pulmonary arteriole. (HE, 246X)

Interestingly, this piglet came from a farm where vaccination against PCV-2 was performed in suckling piglets. Several highly effective vaccines against PCV-2 are currently available on the market and have been widely used since 2006, which subsequently caused a reduction of the PCVAD disease prevalence;[2,4,6,7,8,9] however, occasional outbreaks in vaccinated animals have been described.[3] Even if PCV-2 infection alone is known to be sufficient to cause PMWS[1], it is quite likely that host, management, co-infections (namely with parvovirus or PRRS virus) or immuno-stimulation play a crucial role in disease progression to PCVAD.[1,7] In the present case the piglet was serologically negative for anti-PRRS virus antibodies and there was no evidence of a co-infection with other major swine pathogens. Therefore, an individual immune impairment or an individual vaccination failure due to an insufficient vaccination dosage may explain the above-described findings in the piglet.

JPC Diagnosis: 1. Lung: Pneumonia, interstitial, necrotizing, diffuse, moderate with diffuse, severe, bronchoalveolar-associated lymphoid tissue (BALT) depletion, rare intrahistiocytic botryoid inclusions, multinucleated macrophages, and intra-alveolar fungal cysts (etiology

consistent with *Pneumocystis* sp.), breed not specified, porcine.
2. Lung: Bronchopneumonia, suppurative and histiocytic, multifocal to coalescing, moderate with intra and extracellular bacilli.
3. Lung: Arteritis, necrotizing, focally extensive, severe with intraluminal fungal hyphae.

Conference Comment: This case provides a slide that is ripe with descriptive features. Participants identified the same key features as the contributor: viral interstitial pneumonia, bacterial bronchopneumonia, and intra-arteriolar fungi.

There were very few examples of botryoid intracytoplasmic viral inclusions in macrophages present within depleted BALT tissues. The moderator noted that inclusions are seen less frequently in more recent cases, which has been described but not explained in the literature. The contributors submitted images were reviewed and discussed, including immunohistochemistry for PCV-2. We thank the contributor for providing additional images, which adds to the teaching/learning value of the case.

Conference participants described the fungal hyphae as angiocentric. Although there is significant tissue damage surrounding the mass of fungal hyphae, it appears to be surrounded by a thin layer of smooth muscle which could represent either the wall of an artery or a bronchiole. Based on the pathogenesis of *Aspergillus* sp., our morphologic diagnosis is arteritis. Although *Aspergillus fumigatus* and *A. flavus* are often associated with chronic destructive bronchitis in German shepherd dogs, in other species they commonly disseminate and spread systemically to other organs. Fungal conidia and hyphae are able to block immune responses and evade killing by phagocytes. Macrophages phagocytize fungi

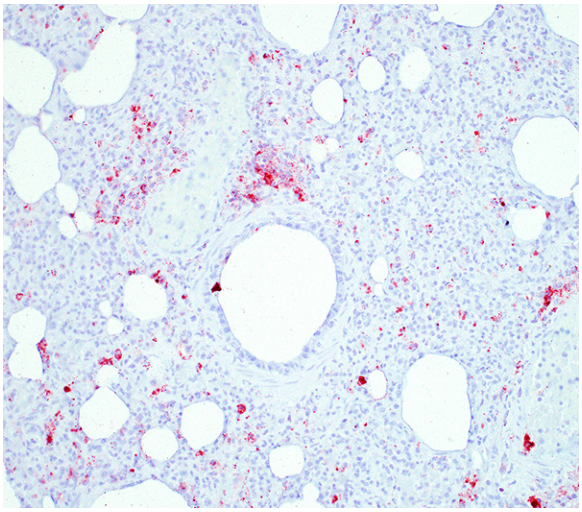

Lung, pig: Large amount of PCV-2 antigen (stained red) visible within macrophages and most prominent in the BALT (anti-PCV-2 IHC, 20X). (Photo courtesy of: Institute of Animal Pathology, Vetsuisse Faculty, University of Bern, Länggassstrasse 122, 3012 Bern, Switzerland (http://www.itpa.vetsuisse.unibe.ch/index_eng.html)

by identification of pathogen associated molecular patterns (PAMPs) using pattern recognition receptors (PRRs) expressed on the surface of macrophages and other phagocytic cells. Specifically, *Aspergillus fumigatus* uses β-glucans, melanin, and other molecules to block lysosomal killing by reactive oxygen species, phagolysosomal acidification, and other destructive mechanisms in macrophages and neutrophils to allow for systemic spread via leukocyte trafficking. In addition, hyphae can travel separately by invading endothelial cells lining capillaries and access the circulatory system, break off in the blood stream, attach to endothelium, and invade tissues at distant sites. It is postulated that ligand-receptor interactions determine where the fungal hyphae decide to stop and spread.[10]

In addition, conference attendees described small, punctate, fungal cysts that partially fill alveoli giving the spaces a honeycombed appearance. These were interpreted as secondary pulmonary pneumocystosis. *Pneumocystis carinii* is a common

secondary disease induced by immune suppression and has been associated with Porcine Respiratory and Reproductive Syndrome (PRRS) and PCV-2 in pigs. Pneumocystis is a fungus with a small uninucleate trophic form that replicates by binary fission and a larger multinucleate cyst form with 8 intracystic bodies formed by sexual replication. These intracystic bodies are released and attach to type I pneumocytes where they mature into trophic forms. Binding to type I pneumocytes, macrophages, surfactant proteins, and fibronectin is mediated by glycoprotein A (cell surface protein). Grossly, Pneumocystis results in a diffusely firm, rubbery, lung. The characteristic microscopic finding is a "honeycomb" material filling alveoli which represents intracellular and extracellular fungal bodies. The wall of the cyst form stains with Gomori methenamine silver (GMS) and Periodic acid-Schiff (PAS).[1] In this case, GMS identified numerous *Pneumocystis* sp. organisms scattered throughout the lung parenchyma often lining alveoli.

Contributing Institution:

Institute of Animal Pathology
Vetsuisse Faculty
University of Bern
Länggassstrasse 122, 3012
Bern, Switzerland
http://www.itpa.vetsuisse.unibe.ch/index_eng.html

References:

1. Caswell JL, Williams KJ. Respiratory System. In: Maxie MG, ed. *Jubb, Kennedy, and Palmer's Pathology of Domestic Animals.* Vol. 2. 6th ed. St. Louis, MI: Elsevier; 2016:527-529, 535-536.
2. Fachinger V, Bischoff R, Jedidia SB, et al. The effect of vaccination against porcine circovirus type 2 in pigs suffering from porcine respiratory disease complex. *Vaccine* 2008; 26: 1488-1499.
3. Gerber PF, Johnson J, Shen H, et al. Association of concurrent porcine circovirus (PCV) 2a and 2b infection with PCV associated disease in vaccinated pigs. *Res Vet Sci* 2013; 95: 775-781.
4. Kixmöller M, Ritzmann M, Eddicks M, et al. Reduction of PMWS-associated clinical signs and co-infections by vaccination against PCV2. *Vaccine* 2008; 26: 3443-3451.
5. López A, Martinson A. Respiratory System, Mediastinum, and Pleurae. In: Zachary JM, ed. *Pathologic Basis of Veterinary Disease.* Vol. 6th ed. St. Louis, MI: Elsevier; 2017:541.
6. Opriessnig T and Langohr I. Current state of knowledge on porcine circovirus type 2-associated lesions. *Vet Pathol* 2013; 50: 23-38.
7. Opriessnig T, Meng XJ and Halbur PG. Porcine circovirus type 2 associated disease: update on current terminology, clinical manifestations, pathogenesis, diagnosis, and intervention strategies. *J Vet Diagn Invest* 2007; 19: 591-615.
8. Pejsak Z, Podgorska K, Truszczynski M, et al. Efficacy of different protocols of vaccination against porcine circovirus type 2 (PCV2) in a farm affected by postweaning multisystemic wasting syndrome (PMWS). *Comp Immunol Microbiol Infect Dis* 2010; 33: e1-5.
9. Segales J, Urniza A, Alegre A, et al. A genetically engineered chimeric vaccine against porcine circovirus type 2 (PCV2) improves clinical, pathological and virological outcomes in postweaning multisystemic wasting syndrome affected farms. *Vaccine* 2009; 27: 7313-7321.

10. Zachary JF, Mechanisms of Microbial Infections. In: Zachary JM, ed. *Pathologic Basis of Veterinary Disease.* Vol. 6th ed. St. Louis, MI: Elsevier; 2017:219-220, 233-234.

CASE II: 16-180 (JPC 4102148).

Signalment: 6-month-old female Normande, *Bos taurus,* bovine.

History: Six of ten Normande heifers developed acute respiratory disease characterized by coughing and dyspnea. The animals had not been vaccinated against bovine respiratory disease complex and had not received antibiotic treatment recently. The heifers were grazing on a pasture of ryegrass and clover, with concentrate and silage supplementation.

Gross Pathology: Bilaterally, the cranial lung lobes showed homogeneous dark red discoloration and firm consistency (consolidation) involving approximately 30% of the pulmonary parenchyma. The affected regions were well demarcated from the non-affected adjacent parenchyma. There was moderate amount of pink stable froth admixed with mucus in the thoracic portion of the trachea, accompanied by extensive petechiation in the tracheal mucosa.

Lung, calf. There is marked collapse and consolidation of cranioventral lobes and moderate interlobular emphysema scattered throughout all lobes. (HE, 5X)(Photo courtesy of: Animal Health Platform, National Institute of Agricultural Research (INIA), Uruguay, www.inia.uy)

Laboratory results: No ancillary laboratory testing was done before the autopsy was performed. Immunohistochemistry was performed and was positive for bovine respiratory syncytial virus (BRSV) antigen within lung lesions. Additionally, PCR detected the viral genome in lung tissue.

Microscopic Description: Lung: Multifocally, bronchioles are mildly ectatic and contain intraluminal necrotic cellular debris admixed with neutrophilic and fibrinous exudate that frequently occludes their lumen. Bronchiolar epithelial cells are either necrotic and sloughed, or markedly attenuated, with loss of apical cilia. In the alveolar spaces there is an amorphous homogeneous light eosinophilic material (edema), fibrin and moderate neutrophilic and multifocal histiocytic infiltrate (alveolar macrophages), with occasional and infrequent bi- or multinucleated syncytial cells, admixed with necrotic epithelial cells with hypereosinophilic cytoplasm and pyknotic nuclei. Multiple, variably sized intracytoplasmic eosinophilic inclusion bodies are observed infrequently in some multinucleated syncytial cells. Some alveolar septae were lined by hypertrophied (type II) pneumocytes.

Contributor's Morphologic Diagnosis:

Lung, calf. There is diffuse consolidation of the alveoli and filling of airways with exudate throughout the section, as well as mild BALT hyperplasia. (HE, 5X)

Lung: Bronchointerstitial pneumonia with necrotizing and neutrophilic bronchiolitis, type II pneumocyte hyperplasia, and rare multinucleated syncytial cells with intra-cytoplasmic viral eosinophilic inclusion bodies consistent with bovine respiratory syncytial virus, moderate, acute.

Condition: Bovine respiratory syncytial virus (BRSV) pneumonia.

Contributor's Comment: The bovine respiratory disease (BRD) complex is a multifactorial disease caused by several viruses and bacteria, including BRSV, parainfluenza 3 (PI3), bovine herpesvirus 1 (BHV-1 or infectious bovine rhinotracheitis virus, IBRV), bovine viral diarrhea virus (BVDV), *Mannheimia haemolytica*, *Pasteurella multocida*, *Histophilus somni* and *Mycoplasma bovis*,[2,4,6] among other possible causes.

BRSV (genus *Pneumovirus*, family *Paramyxoviridae*) is the most important viral etiological agent of the BRD complex, given its widespread distribution and high pathogenicity, [2] and is responsible for numerous outbreaks of respiratory disease worldwide.[1,2,6] BRSV by itself causes an acute respiratory syndrome including dyspnea, tachypnea, coughing, anorexia, and hyperthermia, occasionally leading to death due to severe respiratory distress.[6] Additionally, BRSV infection predisposes calves to secondary bacterial infections, such as *M. haemolytica*, *P. multocida*, and *H. somni*. It is estimated that the economic losses in cattle with BRD are in the range of US$23.23 and US$151.18 per animal, including deaths, decrease production and prevention and treatment costs.[1] For detailed information on BRSV epidemiology, pathology and pathogenesis, diagnosis, and immunology, please refer to the excellent review by Sacco et al. 2014.

In the case presented herein, the diagnosis of BRSV was made by intralesional detection of BRSV antigen by immunohistochemistry, and by detection of the viral genome by PCR in lung tissue. In cases of respiratory disease, the histologic lesions of broncho-interstitial pneumonia with necrotizing bronchiolitis and syncytial cells are highly suggestive of BRSV and should raise a suspicion for this agent. However, the observation of syncytial cells alone is not conclusive for the diagnosis, particularly if typical inclusion bodies are not observed

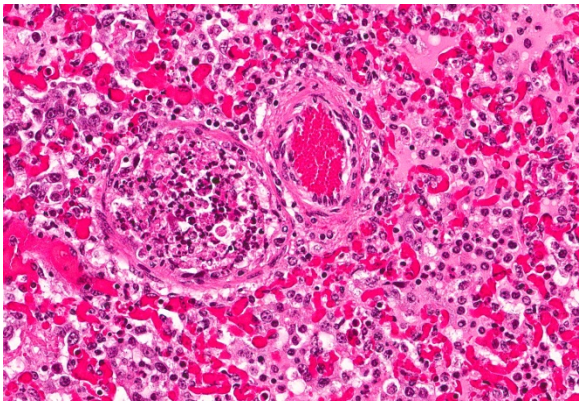

Lung, calf. Diffusely, there is necrosis of airway epithelium primarily of small bronchioles, and the lumen is filled with necrotic cellular debris as well as rare necrotic viral syncytia. (HE, 400X)

upon histologic examination. PI3 infection may also produce syncytial cells and inclusion bodies similar to those produced by BRSV. Furthermore, fibrinous bronchopneumonia caused by several bacteria induces formation of macrophagic multinucleate giant cells morphologically similar to syncytial cells in the lumen of bronchioles and alveoli. Consequently, viral detection by PCR or IHC is necessary for the etiologic diagnosis of BRSV pneumonia.[2] In this case, IBRV, PI3 and bacterial agents were ruled out in lung tissue by IHC, PCR and bacterial cultures, respectively.

In Uruguay, the distribution, frequency and economic impact of BRSV for the cattle industry are unknown. In a serologic study in 100 cattle from different regions of the country, 95% were positive to anti-BRSV antibodies by ELISA,[3] which suggests that the agent has a wide geographic distribution. However, there are few reports of BRSV-associated pneumonia in cattle in this country.[5]

JPC Diagnosis: Lung: Pneumonia, bronchointerstitial, necrotizing and fibrinosuppurative, diffuse, severe, with rare alveolar and bronchiolar multinucleated viral syncytia with intracytoplasmic viral inclusions, Normande, bovine.

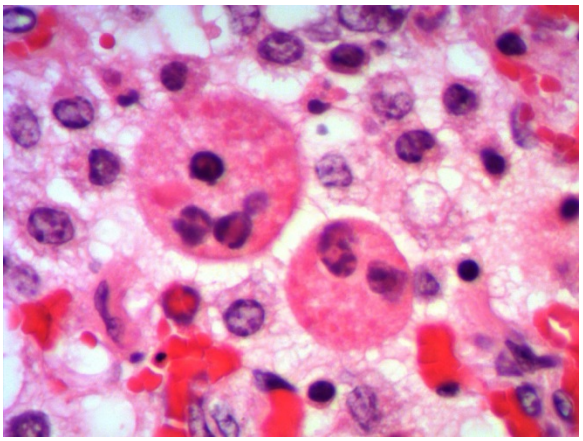

Lung, calf. Viral syncytia often contain or one more irregularly round eosinophilic viral inclusions.

Conference Comment: This is apparently a straightforward case of uncomplicated bovine respiratory syncytial virus (BRSV) in a young heifer. Uncomplicated cases are rare since BRSV impairs the mucociliary apparatus, predisposing affected animals to secondary bacterial infections.

Conference participants identified classic microscopic features of BRSV, centered on the bronchioloalveolar junction, including necrotizing bronchiolitis, alveolar edema and inflammation, and moderate numbers of viral syncytial cells within the bronchiolar and alveolar lumens containing eosinophilic intracytoplasmic viral inclusion bodies.

Attendees also discussed the possibility of bronchiolitis obliterans formation due to chronic bronchiolar damage. Bronchiolitis obliterans is a polypoid proliferation of fibrous connective tissue lined by attenuated epithelial cells that causes obstruction of airways, resulting in hypoxic vaso-constriction of the pulmonary parenchyma, pulmonary hypertension, and right heart failure.[2]

Bovine respiratory syncytial virus is common among beef and dairy herds in Europe and North America and is an important cause of acute outbreaks of respiratory disease and enzootic pneumonia in 2-week-old to 5-month-old calves.[2] BRSV is spread via aerosol and targets the ciliated cells of the conductive system and alveolar type II pneumocytes of the gas exchange component of the respiratory system. The virus (like other *Paramyxoviruses*) attaches via heparin binding domains on envelope glycoprotein G, and enters the cell using envelope

Lung, calf. A variety of cells demonstrate immunopositivity for BRSV antigen including airway epithelium and sloughed cells within the lumen (upper left), alveolar macrophages, and multinucleate syncytia (anti-BRSV, 400X) (HE, 5X)(Photo courtesy of: Animal Health Platform, National Institute of Agricultural Research (INIA), Uruguay, www.inia.uy)

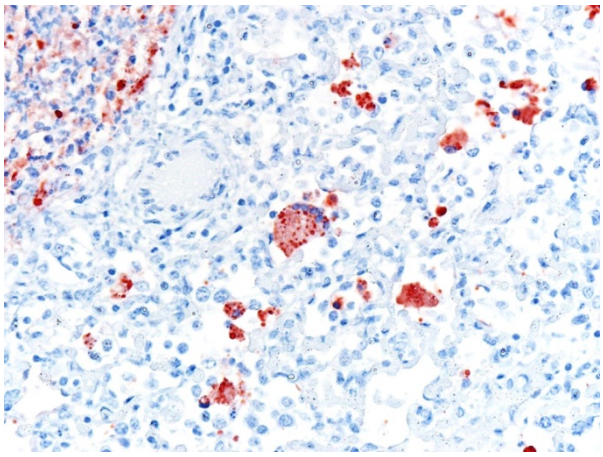

glycoprotein F, its fusion protein, which also induces the formation of syncytial cells. Viral syncytia allow interaction with and spread to adjacent unaffected cells. Once host cells are infected a cascade of pro-inflammatory cytokines is released, recruiting neutrophils, lymphocytes, and macrophages to the lesion.

Experiments in tissue culture have revealed that the virus itself does not cause very much damage to respiratory epithelium. It has been presupposed that most of the damage is due to exuberant host defense mechanisms.[7] Gross lesions associated with BRSV infection range from red, rubbery cranioventral lungs (atelectasis) to firm, heavy, edematous caudodorsal areas of lung that fail to collapse postmortem. However, there are frequent variations in the gross appearance for several reasons: (1) If calves die in respiratory distress, there is often marked subpleural and interlobular emphysema with bullae formation; and (2) Secondary bacterial bronchopneumonia can become so severe as to obscure more subtle viral lesions.[2] The microscopic lesions noted above (necrotizing bronchiolitis with syncytial cells) are highly suggestive of BRSV; however, bovine parainfluenza virus 3 (BPIV-3) must also be considered.

Bovine parainfluenza virus 3 (BPIV-3) is also a member of the *Paramyxoviridae* family. Microscopic lesions can be identical to BRSV although there are usually fewer syncytial cells and the clinical course is typically less severe. Diagnosis requires virus isolation or detection of viral antigen by immunohistochemistry or nucleic acid by RT-PCR testing (as in this case). Unfortunately, definitive diagnosis is often problematic, as viral antigen can be cleared from the body long before the secondary bacterial pneumonia results in death of the animal.[2]

Contributing Institution:

Animal Health Platform
National Institute of Agricultural Research (INIA)
Uruguay
www.inia.uy

References:

11. Brodersen BW. Bovine respiratory syncytial virus. *Vet Clin North Am Food Anim Pract* 2010. 26:323-333.
12. Caswell JL, Williams KJ. Respiratory system. In: Maxie MG, ed. *Jubb, Kennedy and Palmer´s Pathology of Domestic Animals*. Vol 2. 6th ed. St. Louis, MO: Elsevier; 2016: 504, 539-546.
13. Costa M, García L, Yunus AS, Rockermann DD, Saml SK, Cristina J. Bovine respiratory syncytial virus: First serological evidence in Uruguay. *Vet Res* 2000. 31:241-246.
14. Griffin D, Chengappa MM, Kuskak J, McVey DS. Bacterial pathogens of the bovine respiratory disease complex. *Vet Clin North Am Food Anim Pract* 2010. 26:381-394
15. Rivero R, Sallis ESV, Callero JL, Luzardo S, Gianneechini R, Matto C, Adrien ML, Schild AL. Neumonía enzoótica asociado al virus respiratorio

sincitial bovino (BRSV) en terneros en Uruguay. *Veterinaria (Montevideo).* 2013. 49:29-39.
16. Sacco RE, McGill JL, Pillatzki AE, Palmer MV, Ackermann MR. Respiratory syncytial virus infection in cattle. *Vet Pathol* 2014. 51:427-436.
17. Zachary JF. Mechanisms of microbial infections. In: Zachary JF ed. *Pathologic Basis of Veterinary Disease*. St. Louis, MO: Elsevier; 2016: 208-209.

CASE III: 16H0097 (JPC 4101308).

Signalment: 1 to 2-year-old, male, Central European boar (Eurasian wild pig), *Sus scrofa*, porcine.

History: The perished animal was detected on a hunting premise in early December. Several perished wild boars of the same age had been found during the last months.

Gross Pathology: The pig was in a moderate body condition (26 kg body weight). Signs of autolysis were mild (due to the low temperature weather conditions). The pig was moderately infected with lice. The carcass was severely cyanotic (especially snout and ears) and all lymph nodes were severely hyperemic. Multiple abscesses were seen in the mandibular lymph nodes. The lung was not collapsed and heavy. The cranial lobes and multifocally the diaphragmatic lobes of the lung were consolidated and dark red with multiple small abscesses. The trachea was filled with large amounts of pus. The liver was severely hyperemic and had multiple irregularly distributed 1 to 5 mm in diameter foci of necrosis. The spleen was severely enlarged. Embolic suppurative nephritis was present in both kidneys. There were multiple foci of necrosis in the adrenals. The stomach was severely hyperemic. The gastro-

Carcass, boar. The carcass diplays cyanosis of the snout. (Photo courtesy of: Friedrich-Loeffler-Institut, Federal Research Institut for Animal Health, Suedufer 10, D-17493, Greifswald-Insel Riems, Germany. www.fli.de)

intestinal tract including the colon was almost empty. No signs of gun-shot wounds or injuries caused by an accident (e.g. collision with a car) were detected.

Laboratory results: *Salmonella* Choleraesuis was isolated from multiple tissues.
PCRs were negative for European swine fever virus, African swine fever virus, pseudorabies virus, rabies virus and PCV-2.

Microscopic Description: Lung: There are numerous foci of necrosis which appear to be associated with the airways. They are irregular shaped, of variable size and sometimes confluent. They are surrounded by predominantly neutrophilic infiltrates. Alveoli of the adjacent pulmonary tissue are filled with fibrin, contain few neutrophils and occasionally erythrocytes. The alveolar septae are severely hyperemic. Some contain fibrin thrombi. Numerous bacterial colonies are present throughout the pulmonary tissue (both gram positive and gram negative). Salmonellae are frequently detected in the periphery of the necrotic foci and in bacterial emboli in small blood vessels.

Lymph node (mediastinal): The subcapsular region is dilated by hyperemia, hemorrhages and infiltrates of neutrophils and histiocytes. There are multifocal areas of necrosis and neutrophilic infiltration most likely associated with larger blood vessels. Small blood vessels are obliterated by fibrin thrombi and bacterial emboli. Numerous bacterial emboli are present throughout the section. Lymphoid follicles are severely depleted

Liver: Many small and irregularly distributed foci of necrosis are present throughout the hepatic tissue. Some consist of pure coagulation necrosis; others have foci of hemorrhage or are infiltrated by few neutrophils or histiocytes. The liver is severely hyperemic. In addition to erythrocytes, leucocytes and fibrin are present in hepatic arteries and veins. Sinusoids are dilated by hyperemia and leukocytostasis. Bacterial colonies and emboli occur in a multifocal distribution. They stain positive for salmonella LPS by IHC. There are a few areas with loss of hepatic tissue structure and infiltration of large numbers of long bacilli without inflammatory reaction.

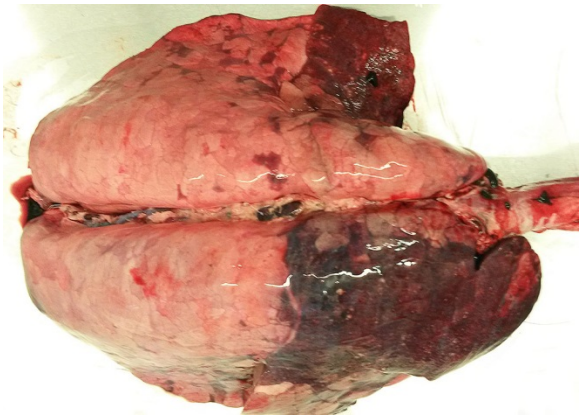

Lung, boar. The cranial ventral lobes and scattered lobules throughout the remainder of the lung are consolidated and hemorrhagic. Multiple abscesses may be seen in these areas. (Photo courtesy of: Friedrich-Loeffler-Institut, Federal Research Institut for Animal Health, Suedufer 10, D-17493, Greifswald-Insel Riems, Germany. www.fli.de)

Contributor's Morphologic Diagnosis:
Lung: Severe, diffuse acute fibrinopurulent and necrotizing bronchopneumonia with bacterial colonies, fibrin thrombi and bacterial emboli in small blood vessels.

Lymph node (mediastinal): Severe purulent and necrotizing lymphadenitis with severe hyperemia, hemorrhages and lymphatic depletion as well as fibrin thrombi and bacterial emboli in small blood vessels.

Liver: Severe multifocal acute necrotizing hepatitis with bacterial emboli in small blood vessels.

Contributor's Comment: Groups of gram-negative bacteria were seen in all tissues examined. IHC using a primary antibody against salmonella LPS (MCA2832, Bio-Rad) identified them as salmonella. In the lung, gram-positive coccoid bacteria were found in addition. Gram-labile long slender bacilli in the liver were interpreted as post mortem invasion.

Salmonella are gram-negative, aerobic to facultative anaerobic, motile, facultative intracellular bacilli. They represent one genus in the family Enterobacteriaceae. The genus *Salmonella* encompasses more than 2500 species, subspecies and serovars. *Salmonella (S.) enterica* subspecies *enterica* has the largest number of serovars (>1500) including the most important animal and human pathogens, e.g. *S. enterica* subspecies *enterica* Choleraesuis, abbreviated as *S.* Choleraesuis.

Pathogenic salmonella can be differentiated in host adapted serovars (e.g. *S.* Choleraesuis in pigs, *S.* Dublin in cattle, *S.* Typhi in humans) and serovars with a wide host spectrum (e.g. *S.* Typhimurium and many others). Host-adapted salmonella cause severe generalized disease both in young and adult hosts; serovars with a wide host spectrum cause predominantly enterocolitis in young animals.

Mandibular lymph nodes, boar. The lymph nodes are enlarged and hyperemic with small abscesses. (Photo courtesy of: Friedrich-Loeffler-Institut, Federal Research Institut for Animal Health, Suedufer 10, D-17493, Greifswald-Insel Riems, Germany. www.fli.de)

Three syndromes are associated with salmonella infections of swine[11]: (1) septicemic salmonellosis usually associated with *S.* Choleraesuis, (2) acute or chronic enterocolitis and rectal stricture associated with *S.* Typhimurium and (3) ulcerative enterocolitis and/or caseous tonsillitis and lymphandenitis associated with *S.* Typhisuis. In addition, clinically in apparent infections by numerous other salmonella serovars are possible.[4]

The main reservoir for *S.* Choleraesuis is the intestinal tracts of pigs.[4] Persistent carriers occur and shedding can be activated by stress. During acute disease, up to 10^6 *S.* Choleraesuis/g feces are excreted. Salmonella remain infectious for 3 months in wet and for 6 months in desiccated feces. Therefore contact to other pigs or environment contaminated by pigs are the main sources of infection. *S.* Choleraesuis is rarely associated with contamination of carcasses or pork products. Thus, it is unusual as cause of human disease. If human disease occurs, it is severe.

The main route of infection is the alimentary tract including the tonsils. Irrespective of the route of inoculation, *S.* Choleraesuis was most frequently recovered from the ileocecal junction, ileocolic lymph node, cecal contents, tonsil, lung and colon.[3] After crossing the mucosal barrier, infection of macrophages and dendritic cells occurs. Survival in phagocytes is an important feature of virulence and allows systemic bacterial dissemination.[11]

Lesions in septicemic salmonellosis are mainly associated with endothelial damage and microvascular thrombosis due to endotoxins, cytokines released by endotoxin activity and bacterial emboli.[3,9,11] This results in congestion of many organs, widespread hemorrhages, often as petechiae, and pulmonary edema and causes fatal disease. At necropsy, thrombosis of capillaries and venules in the dermal papillae of the skin, glomerulonephritis, paratyphoid nodules (ranging from coagulative necrosis to granulomas) in the liver, splenomegaly with small lymphoid

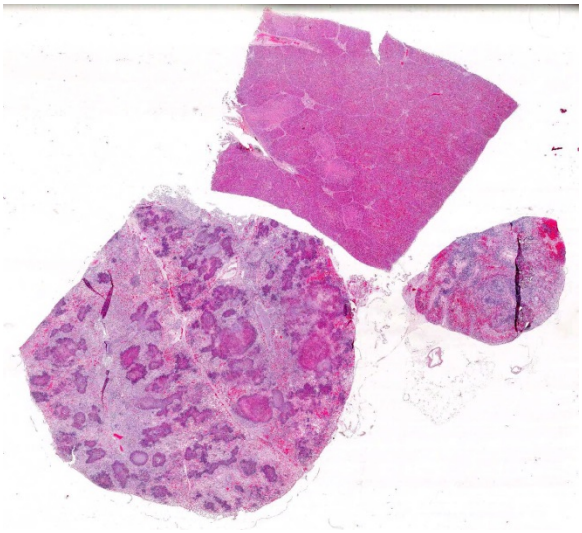

Lung, liver, and lymph node, boar. Multiple abscesses are visible at subgross magnification in the section of lung (lower left). The lymph node (right) exhibits marked lymphoid depletion and hemorrhage, and the liver (top) displays hypocellular areas of necrosis. (HE, 6X)

follicles, but histiocytic infiltrates and

meningoencephalitis are common findings. The injury to the capillaries in pulmonary interalveolar septae may result in a fulminant fibrinous bronchopneumonia.

Differential diagnoses are other causes of generalized disease with high fever (classical swine fever, African swine fever) or septicemia (pasteurellosis, streptococcal infection, erysipelas) or fibrinous pneumonia (e.g. *Actinobacillus pleuro-pneumoniae* infection).

During the 1950s and 1960s, *S.* Choleraesuis was the predominant serovar isolated from pigs worldwide. At the present time, it is still highly prevalent in domestic pigs in North America and Asia, but rare in Australia and Western Europe.[1,7] There are a few case reports of *S.* Choleraesuis in wild boars in Germany.[6,8,10,12] A survey of perished wild boars submitted to the regional diagnostic laboratory of Thuringia, Germany, detected *S.* Choleraesuis in 20% (24 pigs) of the pigs examined.[5] Further characterization of the isolates revealed that distinct isolates were circulating in herds of

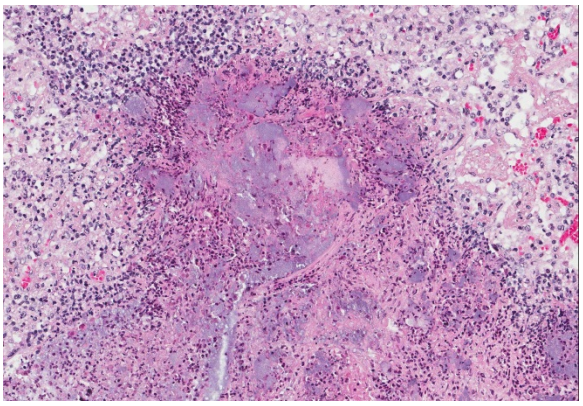

Lung, boar. Airways are necrotic and filled with large colonies of small bacilli which extend into the surrounding alveoli. Surrounding alveoli contain variable amounts of degenerate neutrophils admixed with necrotic debris, polymerized fibrin, and hemorrhage. (HE, 168X)

wild boars separated by natural barriers or arterial roads. There appears to be a higher susceptibility of young animals, because predominantly shoats and juvenile pigs were affected. The percentage of carriers and shedders without clinical signs remained unresolved. *S.* Choleraesuis infection of wild boar may serve as reservoir for domestic pigs especially if kept outdoors. Attention should be paid to game meet inspection to reduce health risks for hunters and persons preparing and consuming pork from wild boars.

JPC Diagnosis: 1. Lung: Bronchopneumonia, necrotizing multifocal to coalescing, severe with numerous large bacterial (do we want to specify / i.e.; coccobacilli?) colonies, Central European boar, porcine.
2. Liver: Hepatitis, necrotizing, multifocal, mild to moderate with occasional large bacterial colonies.
3. Lymph node: Lymphadenitis, necrotizing, acute, multifocal, marked with hemorrhage and occasional bacterial colonies.

Conference Comment: This case provided a comprehensive presentation of *Salmonella choleraesuis* in a wild boar. There were a few atypical microscopic findings noted during the conference. First, there were rare multinucleated giant cells in the liver and lymph node which is not a typical finding salmonellosis. Second, the pattern of pneumonia in the lung appears to be bronchocentric, which is unusual for S. Choleraesuis, which often presents as an embolic interstitial pneumonia.[11] Affected animals may develop bronchopneumonia as a result of secondary bacterial opportunists but in this case IHC using a primary antibody against salmonella LPS (MCA2832, Bio-Rad) demonstrated the presence of bacilli in large numbers within multiple airways. An alternate expalantion was proposed by the moderator, who

suggested the bronchogenic appearance may have resulted from an outgrowth of inflammation within the adjacent bronchial vascular tree. Finally, conference participants noted that it is unusual to see such large colonies of *Salmonella* sp. within lesions. However, after much discussion, attendees were resigned to the fact that under favorable circumstances excessively large burdens of any bacteria could form colonies in affected tissues.

The contributors comments abovesuperbly reviews the serovars of *Salmonella* sp. affecting domestic animals, porcine specific serovars and their clinical syndromes, pathogenesis, and gross findings, and the history and distribution of salmonellosis in wild boars in Europe. Salmonellae are often found in the intestinal lamina propria and regional lymph nodes of poultry and cattle, which are important reservoirs for the organism. . *Salmonella choleraesuis* is a common co-infection with hog cholera (classical swine fever), and was originally thought to be the causative agent of classical swine fever, with which it shares many gross lesions.[11]

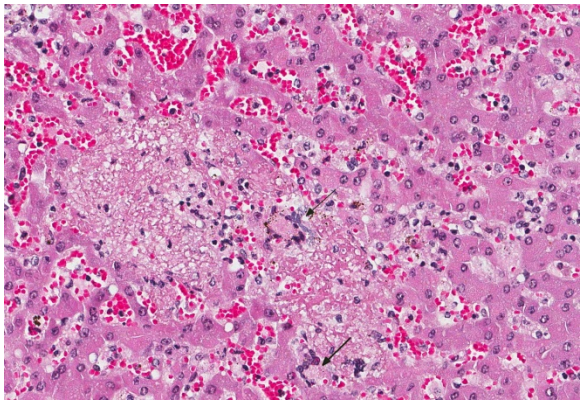

Liver, boar: There are randomly scattered foci of hepatocellular necrosis and loss throughout the section. Additional, several multinucleated cells are present in this image. (HE, 400X)

During the discussion on the pathogenesis of salmonellosis, the conference moderator pointed out that the cause of all of the microscopic changes associated with salmonellosis is due to endothelial damage resulting from endotoxin release. Endotoxin (lipopolysaccharide or LPS) is a virulence factor encoded on Salmonella pathogenicity islands (SPI-2), which are clusters of plasmid genes that can be shared among bacterial colonies. In addition to LPS, SPIs also code for other virulence factors such as fimbriae, motility, and other secreted proteins. Endotoxins induce the release ofcytokines which leads to thrombosis of capillaries and venules (Shwartzman reaction), hemorrhage, and eventual

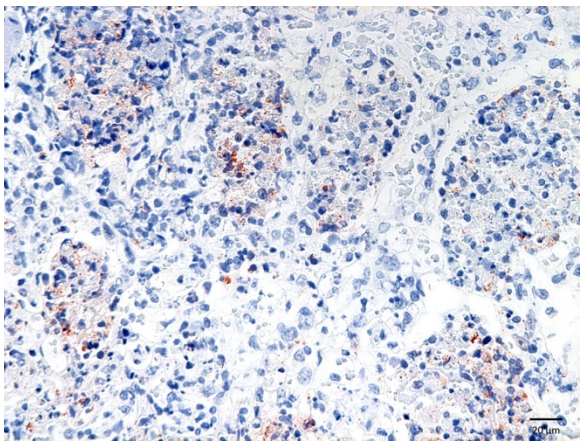

Lung, boar: Intra- and extracellular bacilli are immunopositive for antibodies against Salmonella lipopolysaccharide (anti-S. Cholerasuis MCA2832, 400X) (Photo courtesy of: Friedrich-Loeffler-Institut, Federal Research Institut for Animal Health, Suedufer 10, D-17493, Greifswald-Insel Riems, Germany. www.fli.de)

ischemic necrosis of visceral organs. Additionally, endotoxins help bacteria evade phagocytosis, decreases lysis within the phagolysosome, and renders complement useless, thus perpetuating survival and replication of the organism.[2]

Contributing Institution:
Friedrich-Loeffler-Institut
Federal Research Institut for Animal Health
Suedufer 10, D-17493
Greifswald-Insel Riems, Germany

www.fli.de

References:

1. Eddicks M, Hausleitner R, Eddicks L, et al. Detection of *Salmonella choleraesuis* var. Kunzendorf in a fattening pig with septicaemic salmonellosis. A case report. *Tierarztl Praxis*. 2016; 44:381-387.
2. Gelberg HB. Alimentary system and the peritoneum, omentum, mesentery, and peritoneal cavity. In: Zachary JF, ed. *Pathologic Basis for Veterinary Disease*. 6th ed. St. Louis, MO: Elsevier; 2016: 377-378.
3. Gray JT, Fedorka-Cray PJ, Stabel TJ, Ackermann MR. Influence of inoculation route on the carrier state of *Salmonella choleraesuis* in swine. *Vet Microbiol*. 1995; 47(1-2):43-59.
4. Griffith RW, Schwartz KJ, Meyerholz DK. Salmonella. In: Eds. Straw BE, Zimmerman JJ, D´Allaire S, Taylor DJ. *Diseases of Swine*. 9th ed. Asia: Blackwell Publishing; 2006:739-754.
5. Methner U, Heller M, Bocklisch H. *Salmonella enterica* subspecies *enterica* serovar *choleraesuis* in a wild boar population in Germany. *Eur J Wildl Res*. 2010; 56:493-502.
6. Müller M, Weber A, Tucher R, Naumann L. Case report: *Salmonella choleraesuis* as a cause of hematogenous osteomyelitis in a wild boar (*Sus scrofa*). *Tierärztl Umschau*. 2004; **59**:700-702.
7. Pedersen K, Sørensen G, Löfström C, Leekitcharoenphon P, Nielsen B, Wingstrand A, Aarestrup FM, Hendriksen RS, Baggesen DL. Reappearance of Salmonella serovar choleraesuis var. Kunzendorf in Danish pig herds. *Vet Microbiol*. 2015; 176(3-4):282-291.
8. Plötner J, Bussemer R, Otta J, Schmidt O, Winkler H. Zu einer salmonella-cholerae-suis-Infektion im Schwarzwildbestand zweier benachbarter Jagdgebiete. *Mh Vet Med*. 1979; 34:860-861.
9. Reed WM, Olander HJ, Thacker HL. Studies on the pathogenesis of *Salmonella typhimurium* and *Salmonella choleraesuis* var kunzendorf infection in weanling pigs. *Am J Vet Res*. 1986; 47(1):75-83.
10. Schulze C, Neumann G, Grütze I, Engelhardt A, Mirle C, Ehlert F, Hlinak A. Case report: Porcine circovirus type 2 infection in an European wild boar (Sus scrofa) in the state of Brandenburg, Germany. *Dtsch Tierarztl Wochenschr*. 2003; 110(10):426-428.
11. Uzal FA, Plattner BL, Hostetter JM. Alimentary system. In Maxie MG, ed. *Jubb, Kennedy, and Palmer`s Pathology of Domestic Animals*. Vol 2, 6th ed. St. Louis, MO: Elsevier; 2016:170-173.
12. Weber A, Broos H, Wachowitz R, Heil G, Schultze-Rhonhof J. *Salmonella choleraesuis* in wild boar (*Sus scrofa*) in Northern Bavaria. *Tierärztl Umschau*. 1990; 45: 411-414.

CASE IV: P16-555 (JPC 4101307).

Signalment: Juvenile, male, domestic pig, *Sus scrofa domesticus*, porcine.

History: This case is one out of four pigs from an unvaccinated control group of a vaccine development study. The pigs were experimentally infected i.m. with 10^6 $TCID_{50}$ of classical swine fever virus wild type strain Alfort/Tuebingen. They were humanely killed after developing clinical disease 15 days post infection including fever up to 41°C, apathy, changed defecation and dermal macula.

Skin, pig. There are confluent dermal hemorrhages within the skin of the caudal abdomen. (Photo courtesy of: Friedrich-Loeffler-Institut, Federal Research Institute for Animal Health, Department of Experimental Animal Facilities and Biorisk Management, Südufer 10, 17493 Greifswald – Insel Riems, Germany. https://www.fli.de)

Gross Pathology: The splenic surface showed multifocal, distinct, flame-shaped white streaks with a variably distinct peripheral plum-colored border extending 2-3 mm from and perpendicular to the acute angle. Cut sections revealed roughly wedge-shaped white areas with a variably distinct peripheral plum-colored border at the acute angle, interpreted as mild, multifocal, (ischemic) infarcts.

Other macroscopic changes in this pig were mild hydrothorax and ascites, mild, multifocal, pleural fibrosis with synechiae between parietal and visceral pleura, and moderate hyperplasia of the lymphocentrum bronchiale.

Macroscopic changes in the other pigs included mild to moderate ascites which was the only constant change observed in all four animals. Further important macroscopic changes included moderate, multifocal, irregular cherry red dermal maculae in the inguinal area in two pigs, and peripherally cherry red and white marbled hepatic and gastric lymph nodesinterpreted as blood-filled sinusoids in one pig.

Laboratory results: Classical swine fever genomic RNA was detected in multiple samples of this pig beginning 5 days post infection and up to day 15 using diagnostic real-time RT-PCR.[5] The results were clearly positive with threshold cycle values of 25.12 on the day of killing.

Microscopic Description: Spleen: Located at the acute angle and affecting 10-20% of the splenic parenchyma is a wedge-shaped area displaying diffuse, pale, eosinophilic, shadow-like histoarchitecture and a peripheral zone of moderate extravascular erythrocyte accumulation (acute hemorrhage) which extends into the adjacent normal tissue. The stromal and parenchymal cells display ill-defined cellular borders, cytoplasmic hypereosinophilic condensation, nuclear loss, pyknosis and karyorrhexis (coagulation necrosis). There is minor multifocal basophilic granular change of the necrotic debris (dystrophic mineralization). At the border to the normal appearing tissue are oligofocal medium sized arteries with pyknotic, karyorrhectic and lost endothelia and smooth muscular cells, intramural deposition of an hypereosinophilic amorphous mass (fibrin)

Spleen, pig. There are irregular white marginal infarcts with hemorrhagic seams. (Photo courtesy of: Friedrich-Loeffler-Institut, Federal Research Institute for Animal Health, Department of Experimental Animal Facilities and Biorisk Management, Südufer 10, 17493 Greifswald – Insel Riems, Germany. https://www.fli.de)

and minor and variable infiltration by degenerating neutrophils, macrophages and foreign body-type and Langhans-type

multinucleated giant cells (fibrinonecrotizing vasculitis). The lumen of multiple affected arteries is occluded by an eosinophilic fibrillary to amorphous mass with scant encased degenerating neutrophils and macrophages (fibrin-rich thrombus). The white pulp in the adjacent parenchyma is of mildly reduced cellularity and displays a mild loss of small differentiated lymphocytes with heterochromatic nuclei (lymphoid depletion) combined with a relative increase in moderately sized lymphoblastic cells with round, euchromatic nucleus, multiple mitotic figures and a mildly increased number of tingible body macrophages. The serosal mesothelial cells are multifocally enlarged and display round euchromatic nuclei (reactive change).

Contributor's Morphologic Diagnosis:
Spleen: Vasculitis, fibrinonecrotizing, oligofocal, acute, moderate, with multinucleated giant cells, arterial thrombosis, necrosis and hemorrhage (infarct).

Contributor's Comment: This case of moderate, acute, oligofocal, fibrino-necrotizing vasculitis with multinucleated giant cells, arterial thrombosis, necrosis and hemorrhage is the histopathological correlate of the grossly detected anemic infarcts at the acute angle of the spleen.

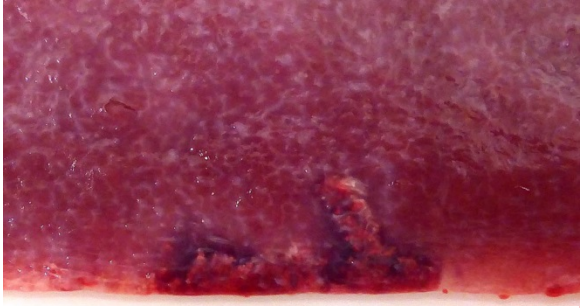

Spleen, pig. There are irregular white marginal infarcts with hemorrhagic seams. (Photo courtesy of: Friedrich-Loeffler-Institut, Federal Research Institute for Animal Health, Department of Experimental Animal Facilities and Biorisk Management, Südufer 10, 17493 Greifswald – Insel Riems, Germany. https://www.fli.de)

These infarcts at the acute angle of the spleen (there is a special German term for that: "Milzrandinfarkte") are considered as one of the most characteristic if not pathognomonic lesions present in 1 – 87% of cases of classical swine fever (CSF; synonym: hog cholera).[13]
This case from an experimental study was selected for the Wednesday Slide Conference because in contrast to most classic textbooks of veterinary pathology including Jubb, Kennedy and Palmer's Pathology of Domestic Animals and Pathologic Basis of Veterinary Disease which describe hemorrhagic infarcts in CSF,[13,14] the current case demonstrates ischemic core infarct areas, suggestive of a very early stage of an infarct pathogenesis. Furthermore, the multinucleated giant cells observed in this case are a rare feature, possibly due to a marked activation of monocytes / macrophages, which is a key element of CSF pathogenesis.[4,8]

Etiology:

Lymph node, pig. Peripheral sinuses of the gastric and hepatic nodes contain abundant hemorrhage. (Photo courtesy of: Friedrich-Loeffler-Institut, Federal Research Institute for Animal Health, Department of Experimental Animal Facilities and Biorisk Management, Südufer 10, 17493 Greifswald – Insel Riems, Germany. https://www.fli.de)

The etiologic agent of CSF is the classical swine fever virus (CSFV), a pestivirus of the flaviviridae family. It is related to the other well-known species of the genus pestivirus bovine virus diarrhea virus-1 and -2, border disease virus as well as novel pestiviruses including HoBi-like viruses (atypical pestivirus) and Bungowannah virus.[12] Notably, some of the related ruminant pestiviruses including bovine virus diarrhea virus can occasionally infect pigs,[11] leading to cross-reactive antibodies and false positive serological results.[5] In contrast, evidence of naturally occurring CSFV-infection in ruminants or other species is lacking. The CSFV is a spherical, enveloped, single-stranded, positive-sense RNA virus with a diameter of ~ 50 nm. The ~12.3 kb RNA consists of a single open reading frame encoding the four structural proteins C, E^{rns}, E1, and E2, as well as the non-structural proteins N^{pro}, p7, (NS2-3), NS2, NS3, NS4A, NS4B, NS5A, and NS5B.[12]

Epidemiology:

CSF is one of the most important diseases of domestic pigs and notifiable to the World Organization for Animal Health. The main hosts for CSFV are domestic pigs (*Sus scrofa domesticus*) and European wild boars (*Sus scrofa scrofa*). Furthermore, it has been proven experimentally that warthogs (*Phacochoerus africanus*) and bushpigs (*Potamochoerus larvatus*) are also susceptible to CSFV.[3] Currently CSF is endemic in South and Central America, parts of Eastern Europe, and Asia and represents a constant threat for all other pig producing countries.[1]

CSFV can be transmitted horizontally, mainly by the oronasal route. Furthermore, vertical *in utero* transmission is possible. The normal incubation time is four to seven days. Diseased pigs are highly viremic and shed virus at least from the beginning of clinical disease until death or the occurrence of neutralizing antibodies. Virus is shed in saliva, lacrimal secretions, urine, feces and semen.[1]

Clinical Course:

Depending on the virulence of the CSFV strain and the age and constitution of the host the clinical course of CSF can be

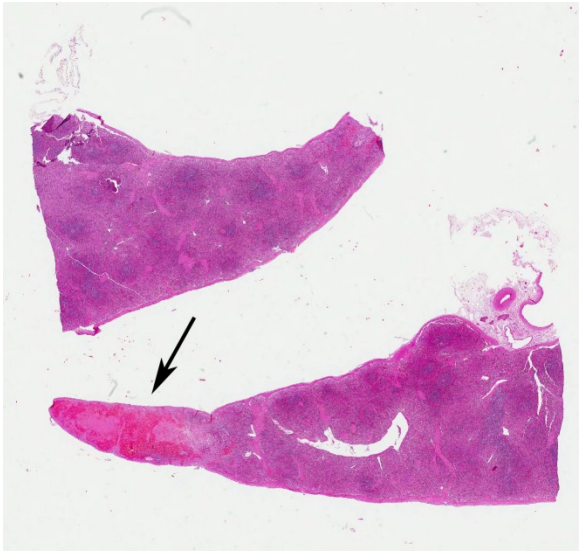

Spleen, pig. There are irregular white marginal infarcts with hemorrhagic seams. At subgross, the acute angle of the section at bottom shows an arterial infarct with peripheral hemorrhage (arrow). (HE, 5X)

peracute, acute or chronic. In the classical acute form, initial atypical clinical signs such as high fever, anorexia, gastrointestinal symptoms, weakness and conjunctivitis progress to the characteristic hemorrhagic fever and neurological symptoms with a mortality of up to 100% after 2 to 4 weeks. However, a variable proportion of pigs may not progress and recover from the disease. In the chronic form clinical symptoms such as remitting fever, depression, and wasting are usually non-specific and inevitably lead to death after a disease duration of 1 - 3 months. Furthermore, *in utero* infection is a special situation which leads to fetal death, resorption, abortion, mummification, stillbirth, malformations or birth of persistently infected piglets which show runting, late onset disease and inevitably death after 2 – 11 months.[1]

Macroscopic Changes:

Pigs may succumb to peracute CSF without any characteristic gross lesions. Characteristic macroscopic findings in acute CSF are dermal erythema and cyanosis at the margins of the ears, limbs and ventral abdomen. Petechial and ecchymotic hemorrhages can be observed in skin, larynx, epiglottis, urinary bladder, gastric mucosa, and the serosal surfaces of kidneys, lungs, and heart. The lymph nodes can present a typical marbled appearance due to hemorrhages with blood in the peripheral sinuses. Furthermore, there is necrotizing to suppurative tonsillitis, infarcts at the margin of the spleen, as well as hydropericardium, hydrothorax, and hydroperitoneum. In chronic CSF lesions include atrophic lymphatic organs, splenic infarcts, necrosis of gut associated lymphoid tissues including colonic button ulcers. Furthermore, due to the immunosuppression a magnitude of secondary and non-specific lesions can occur. Gross lesions in late onset disease in persistently infected pigs resemble those of the chronic form. Typical malformations in piglets include cerebellar hypoplasia, thymic atrophy, and deformities of the head and limbs.[1,13,14]

Pathohistologic Changes:

The most important pathohistological findings in acute CSF are multifocal necrotizing vasculitis and lymphoid necrosis and depletion in the lymphatic organs. Vasculitis is often followed by thrombosis, infarction and hemorrhages. In addition to the characteristic gross splenic infarcts, infarcts can also develop in lymph nodes, skin, tonsil, gallbladder, and large intestine. No matter if neurological clinical symptoms have been reported or not, the brain is among the best tissues to check for histological changes. They present as lymphocytic panencephalitis with marked perivascular cuffing and extravasation of blood plasma protein. Chronic cases may also present with mesangioproliferative glomerulonephritis. *In utero* infected piglets can be affected by hypomyelination inducing congenital tremors. Furthermore, the physeal growth plates may exhibit zones of persistent primary spongiosa (growth arrest lines) presumably reflecting viral destruction of osteoclasts.[13]

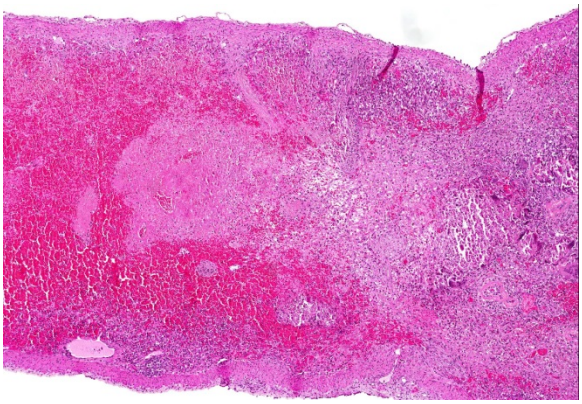

Spleen, pig. Higher magnification of the splenic infarct. An aggregate of multinucleated cells is present at right. (HE, 80X)

Pathogenesis:

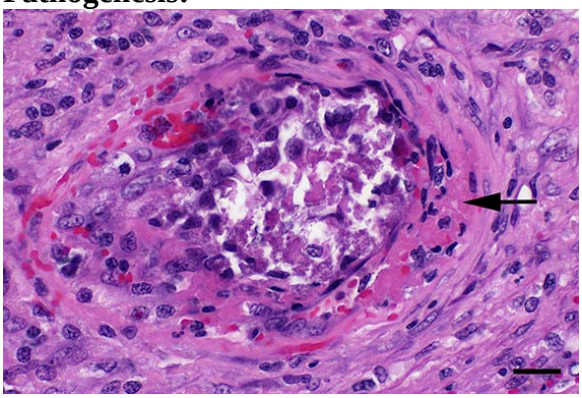

Spleen, pig. There is necrosis of the endothelium and extrusion of protein (arrow) within the wall of a medium-sized splenic arteriole. (HE, 400X)

Infection usually occurs via the oronasal route and the CSFV enters the body mainly via the epithelial cells or M-cells of the tonsillar crypts. Primary replication takes place within macrophages in the tonsils and local oropharyngeal lymph nodes, followed by mononuclear cell-associated viremia mainly to other lymphoid organs including spleen, thymus, lymph nodes and mucosa associated lymphoid tissues.[14] Furthermore, CSFV can also be found in variable amounts in all other organs of the body including skeletal muscles, heart, lung, liver, pancreas, stomach, duodenum, jejunum, ileum, kidney, urinary bladder, brain, spinal cord.[6] The CSFV envelope glycoproteins E^{rns} and E2 are responsible for attachment to the putative virus receptor CD46 together with heparan sulfates.[2] The most important host cells are macrophages and dendritic cells, but CSF can also be found in endothelial cells and various epithelial cells, lymphocytes and megakaryocytes. Although activation of macrophages is a well-known feature of CSF, multinucleated giant macrophages as observed in this case are not described.[4,8] Especially the infection of plasmacytoid dendritic cells induces secretion of large quantities of interferon α, which is a key element in the pathogenesis of CSF. The high serum level of interferon α is suggested to be the central inducer of immune cell dysregulation, which manifests as lymphocyte apoptosis, depletion and immunosuppression as well as bone marrow suppression.[10] Furthermore, a marked increase in macrophage / monocyte-derived pro-inflammatory cytokines such as TNF α, IL-1, and IL-6 is suggested to be the main mediator of systemic endotheliotoxicity. Cytokine induced activation of endothelial cells represents the basis for light microscopically visible endothelial swelling. This is followed by degeneration and necrosis of endothelial cells inducing breakdown of the endothelial barrier, fibrinonecrotizing vasculitis, activation of the clotting system, edema and hemorrhages.[14] The formation of arterial infarcts at the multifocal sites of vasculitis within the spleen leads to vascular occlusion followed by ischemic necrotic cell death of the dependent parenchyma. The anatomy of the spleen with single blood supply and minimal anastomoses is an important predisposing factor for infarction.[7] Although it is also most possibly related to some microanatomical features, it is still enigmatic why the infarcts are aligned along the acute angle of the spleen in CSF but not in other diseases with splenic infarcts such

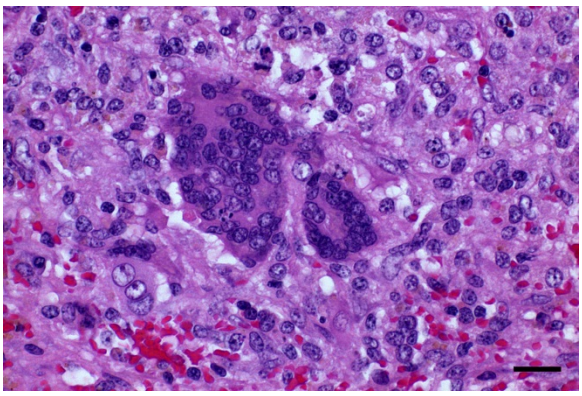

Spleen, pig. Occasional foreign body-type (left) and Langerhans-type (right) multinucleated giant macrophages can be observed within and adjacent to the foci of vasculitis. (Photo courtesy of: Friedrich-Loeffler-Institut, Federal Research Institute for Animal Health, Department of Experimental Animal Facilities and Biorisk Management, Südufer 10, 17493 Greifswald – Insel Riems, Germany. https://www.fli.de) (HE, 400X)

as African swine fever, highly-pathogenic porcine reproductive and respiratory syndrome and chronic erysipelas.[9] As can be seen in the current case, the infarcted areas initially can be pale due to the lack of blood inflow following complete arterial occlusion. This is rapidly followed by hemorrhage from damaged vessels and inflow of blood from the surrounding parenchyma with intact perfusion leading to the commonly illustrated hemorrhagic infarcts. Secondary pallor due to cell swelling, hemoglobin degradation and diffusion within the affected area usually does not take place in the spleen due to its spongy consistency.[7]

Differential Diagnosis:
A good overview concerning the differential diagnosis of porcine hemorrhagic fevers is presented in Sánchez-Vizcaíno et al. (2015).[9] Concerning splenic infarction in pigs, the most important etiologic differential diagnoses are CSF, African swine fever, highly-pathogenic porcine reproductive and respiratory syndrome, and septic and embolic infarction from other primary lesion sites such as endocarditis valvularis thromboticans in chronic erysipelas.

JPC Diagnosis: 1. Spleen, red pulp: Vasculitis, necrotizing, multifocal to coalescing with multifocal infarcts, *Sus scrofa domesticus*, porcine.
2. Spleen, white pulp: Lymphoid depletion, diffuse, severe.

Conference Comment: The contributor provides a complete review of classical swine fever. The multinucleated giant cells noted by the contributor were seen by conference participants as well. It is possible, that as the moderator suggests, these cells form because monocytes and macrophages are markedly activated as part of the CSF pathogenesis. Attendees debated this concept and pointed out that pestiviruses do not have a fusion protein and should not inherently cause fusion of affected cells.[13] Although the process of multinucleated giant cell formation in inflammation is not well understood it does require that macrophages be bathed in cytokines like IFN-γ, IL-3, IL-4, IL-13 and GM-CSF. Subsequently, membranes of adjacent macrophages express fusogenic proteins such as: DC-STAMP, β1 and β2 integrins, CD44, CD47, macrophage fusion receptor, fusion regulator protein (FRP-1; CD98), and P2X7 (ligand gated ion channel activated by ATP that forms a pore).[1]

Contributing Institution:
Friedrich-Loeffler-Institut
Federal Research Institute for Animal Health
Department of Experimental Animal Facilities and Biorisk Management
Südufer 10, 17493 Greifswald – Insel Riems, Germany.
https://www.fli.de

References:
1. Blome S, Staubach C, Henke J, Carlson J, Beer M. Classical swine fever-an updated review. *Viruses* 2017:9(4).
2. Drager C, Beer M, Blome S. Porcine complement regulatory protein CD46 and heparan sulfates are the major factors for classical swine fever virus attachment in vitro. *Arch Virol* 2015:160(3)**:**739-746.
3. Everett H, Crooke H, Gurrala R, Dwarka R, Kim J, Botha B, et al. Experimental infection of common warthogs (*Phacochoerus africanus*) and bushpigs (*Potamochoerus larvatus*) with classical swine fever virus. I: Susceptibility and transmission. *Transbound Emerg Dis* 2011:58(2)**:**128-134.

4. Gomez-Villamandos JC, Ruiz-Villamor E, Bautista MJ, Sanchez CP, Sanchez-Cordon PJ, Salguero FJ, et al. Morphological and immunohistochemical changes in splenic macrophages of pigs infected with classical swine fever. *J Comp Pathol* 2001:125(2-3)**:**98-109.
5. Hoffmann B, Beer M, Schelp C, Schirrmeier H, Depner K. Validation of a real-time RT-PCR assay for sensitive and specific detection of classical swine fever. *J Virol Methods* 2005:130(1-2)**:**36-44.
6. Liu J, Fan XZ, Wang Q, Xu L, Zhao QZ, Huang W, et al. Dynamic distribution and tissue tropism of classical swine fever virus in experimentally infected pigs. *Virol J* 2011:8**:**201.
7. Mosier DA: Vascular Disorders and Thrombosis. In: Zachary JF, ed. *Pathologic Basis of Veterinary Disease*. 6th ed. St. Louis, Missouri: Elsevier; 2017: 44-72.
8. Sanchez-Cordon PJ, Nunez A, Salguero FJ, Pedrera M, Fernandez de Marco M, Gomez-Villamandos JC. Lymphocyte apoptosis and thrombocytopenia in spleen during classical swine fever: role of macrophages and cytokines. *Vet Pathol* 2005:42(4)**:**477-488.
9. Sanchez-Vizcaino JM, Mur L, Gomez-Villamandos JC, Carrasco L. An update on the epidemiology and pathology of African swine fever. *J Comp Pathol* 2015:152(1)**:**9-21.
10. Summerfield A, Ruggli N. Immune responses against classical swine fever virus: between ignorance and lunacy. *Front Vet Sci* 2015:2**-**10.
11. Tao J, Liao J, Wang Y, Zhang X, Wang J, Zhu G. Bovine viral diarrhea virus (BVDV) infections in pigs. *Vet Microbiol* 2013:165(3-4)**:**185-189.
12. Tautz N, Tews BA, Meyers G. The molecular biology of pestiviruses. *Adv Virus Res* 2015:93**:**47-160.
13. Valli VEO, Kiupel M, Bienzle D. Hematopoietic system. In: Maxie MG, ed. *Jubb, Kennedy and Palmer's Pathology of Domestic Animals.* Vol 3. 6th ed. St. Louis, Missouri: Elsevier; 2016: 102-267.
14. Zachary JF. Mechanisms of microbial infections. In: Zachary JF, ed. *Pathologic Basis of Veterinary Disease*. 6th ed. St. Louis, Missouri: Elsevier; 2017: 132-241.

Self-Assessment - WSC 2017-2018 Conference 5

1. Which of the following cells are not initially infected by PCV-2 in swine?
    a. Lymphocytes
    b. Macrophages
    c. Mucosal dendritic cells
    d. Endothelial cells

2. Which of the following in not a syndrome associated with PCV-2 infection in swine?
    a. Cerebellar vasculitis
    b. Dermatitis and nephropathy
    c. Laminar cortical necrosis
    d. Reproductive failure

3. True or False. BRSV is not considered a potentially fatal infection in the absence of bacterial members of the Bovine Respiratory Disease Complex.
    a. True
    b. False

4. Which of the following is not considered a host-adapted serovar of *Salmonella enterica?*
    a. S. Typhimurium in cattle
    b. S. Dublin in cattle
    c. S. typhi in humans
    d. S. Choleraesuis in swine
    e.
5. Which of the following is not seen in associated with classical swine fever?
    a. Lymphoid necrosis
    b. Hypomyelination
    c. Glomerulonephritis
    d. Hydranencephaly

Please email your completed assessment to Ms. Jessica Gold at Jessica.d.gold2.ctr@mail.mil for grading. Passing score is 80%.This program (RACE program number) is approved by the AAVSB RACE to offer a total of 0.5 CE Credits, with a maximum of 12.5 CE Credits being available to any individual Veterinary Medical Professionals for the 2017-2018 Wednesday Slide Conference. This RACE approval is for the subject matter categories of: SCIENTIFIC using the delivery method of NON-INTERACTIVE DISTANCE. This approval is valid in jurisdictions which recognize AAVSB RACE; however, participants are responsible for ascertaining each board's CE requirements.
RACE does not "accredit", "endorse" or "certify" any program or person, nor does RACE approval validate the content of the program.

Joint Pathology Center
Veterinary Pathology Services

WEDNESDAY SLIDE CONFERENCE 2017-2018

C o n f e r e n c e 6

4 October 2017

CASE I: 3120125021 (JPC 4017935).

Signalment: 1-year-old, Crested Guinea fowl, *Guttera pucherani*, avian.

History: A peri-orbital mass surrounded the left eye. Growth of the mass initially started rostrally from the eye and slowly extended to the nose and the upper eyelids. Initial treatment with enrofloxacin gave transient improvement. A second treatment with the same antibiotic did not have effect. Bacterial culture yielded Staphylococci susceptible to doxycyclin. Treatment with doxycyclin was started but did not give improvement. A surgical biopsy was then taken and submitted for histopathology.

Gross Pathology: Bilaterally there was a mass of approximately 1.5cm in diameter, involving the upper eyelids and extending into the subcutis of the nose. On cut surface the mass was solid, firm and marbled pale tan to black with multifocally softer tissue with cystic spaces containing viscous mucoid material.

Laboratory results: Bacterial culture in the past: Staphylococci, not further specified.

Microscopic Description: Skin: In the dermis and subcutis, elevating the overlying epidermis, is a densely cellular, poorly demarcated, non-encapsulated, infiltrative growing, monomorphic round cell neoplasm. Neoplastic cells are organized in poorly defined lobules of large solid sheets with scant intermingled fibrovascular connective tissue. Neoplastic cells are round to oval with a small amount of pale amphophilic cytoplasm and indistinct cell borders. Nuclei are round and contain coarsely clumped chromatin and one or two

Feathered skin, guinea fowl. At subgross magnification, the dermis is expanded and largely effaced by sheets of neoplastic round cells. (HE, 5X)

moderately distinct nucleoli. Mitotic figures are 18 per 5 HPF and there is mild anisocytosis and anisokaryosis. Small numbers of neoplastic cells multifocally infiltrate the epidermis and feather follicle epithelium and there's multifocal infiltration and replacement of pre-existing muscle tissue and lacrimal glands (not present in all slides). Multifocally there are areas of necrosis characterized by pyknosis, karyorrhexis, karyolysis, loss of cellular detail and amorphous, eosinophilic debris with associated infiltration of moderate numbers of heterophils. Multifocally dispersed throughout the neoplasm there are small numbers of heterophils and macrophages with an occasional multinucleated giant cell. The overlying epidermis is multifocally ulcerated and covered with serocellular crusts (not present in all slides).

Contributor's Morphologic Diagnosis:
Skin: Lymphoma.

Contributor's Comment: Guinea fowl are terrestrial, ground-living birds that belong to the order Galliformes, family Numidae. Some ornithologists consider them to be part of the superfamily Phasanidae (including Partridges and Pheasants).

There are limited reports available on lymphoid neoplasms and neoplasms in general in guinea fowl. Pancreatic adenocarcinomas and seminomas have been reported as rare spontaneous neoplasms in guinea fowl.[3,1] Viral- induced pancreatic tumors and duodenal adenomas have been reported in guinea fowl in experimental settings.[9,2] In general, the most common naturally-occurring neoplasms in birds are lymphomas, fibromas and fibrosarcomas, and lipomas[6]; however these information are based upon a population including species of the Galliformes order but not including domestic fowl.

Lymphomatous tumors are also relatively common in domestic fowl and turkeys. Common sites of occurrence are liver, spleen, thymus and kidneys. Cutaneous and oropharyngeal lymphomas have been reported in pheasants. The neoplasms were present in the skin around the eyes, around the external ear openings and involving the hard palate.[4] Histologically, these tumors were composed of a pleomorphic mixture of lymphoblasts and lymphocytes. [4]

A similar case of a guinea fowl presenting with a periorbital lymphoma has been reported and was associated with visceral lymphomas in the spleen, lungs, kidneys, liver and ovary. [8] In our case, however, we did not perform a full necropsy and information regarding the internal organs was not available.

Most information on ocular and periorbital tumors in animals is from dogs and cats. In these animals, ocular tumors are relatively rare. Ocular tumors can arise from the eyelids and adnexa, the optic nerve and structures within the globe, and metastases are generally infrequent. The most frequent neoplasms of the eyelid and conjunctiva in dogs are squamous cell carcinoma and Meibomian adenoma. Less frequently encountered are melanocytic neoplasms, papillomas, vascular tumors, mast cell tumors and lymphomas.

In dogs, cats and cattle, multicentric lymphoma regularly involves the eye. In dogs and cats, there is predominant involvement of the uvea, whereas in cattle retrobulbar (orbital) neoplasms are more common. Only occasionally are lymphomas encountered in the tissues of the eyelids in these animals. Solitary lymphomas in the

conjunctiva and third eyelid have been reported in cats and horses.

In birds, squamous papillomas, squamous cell carcinomas, malignant melanomas, basal cell tumors and adeno(carcino)mas of the lacrimal gland have been reported in the skin and subcutis of the eyelids.[7] Lymphoma is reported as a neoplasm arising in the orbit as are infiltrative carcinomas, chondromas and teratomas.[7] An infectious etiology has not been identified in the lymphomas reported in pet birds or in the report of a periorbital lymphoma in a Guinea fowl.[7,8]

Lymphocytic neoplasms in poultry are often categorized as infectious or non-infectious. Spontaneously occurring neoplasms often involve older birds whereas viral induced neoplasms develop in relatively young birds.[5] The most important viral-induced neoplastic diseases in poultry are:

- Marek's disease, caused by Gallid herpesvirus type 2
- Avian Leukosis caused by avian leukosis virus (retrovirus)
- Reticuloendotheliosis, caused by reticuloendotheliosis virus (retrovirus).

Of these entities, Marek's disease can involve the skin.[5] Marek's disease is a disease that mainly affects chickens and only occasionally affects pheasants, quail, game fowl and turkeys. To the best knowledge of the author, Marek's disease has not been reported in guinea fowl.

JPC Diagnosis: Feathered skin: Lymphoma, crested guinea fowl (*Guttera pucherani*), avian.

Conference Comment: There are three main viral neoplastic diseases in chickens which result in lymphoid tumors: Marek's disease (MD), avian leukosis, and reticuloendotheliosis.[5]

Marek's disease is caused by an alpha herpesvirus (Gallid herpesvirus-2) and typically affects young chickens, and rarely quail, turkeys, pheasants, and jungle fowl. The herpesvirus that causes MD is classified into three serotypes. Serotype 1 is ubiquitous in chickens and varies in pathogenicity from very virulent (vv+) which is oncogenic to avirulent (mild). Serotype 2 is also common in chickens but is

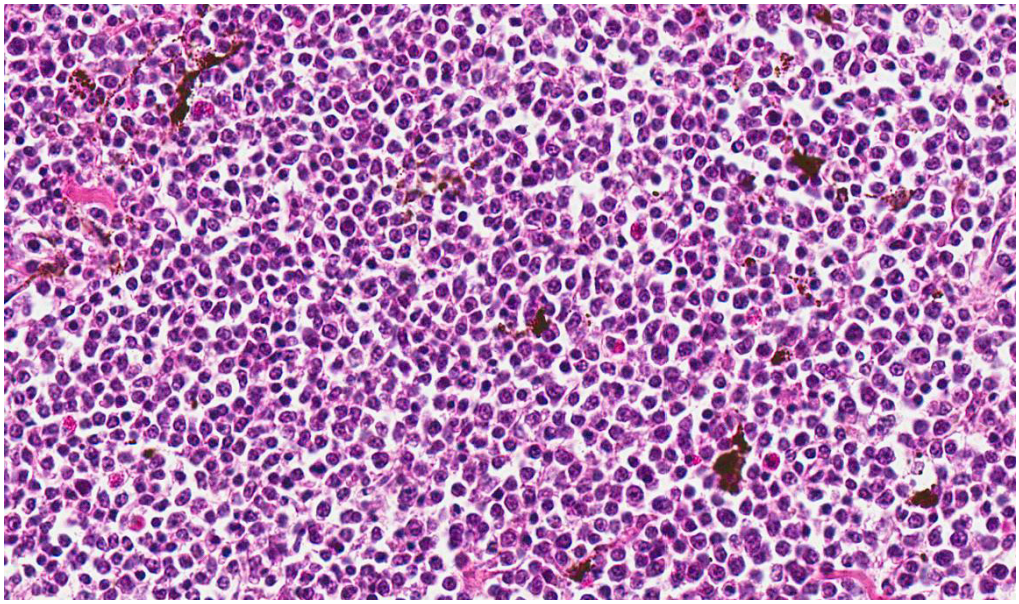

Feathered skin, guinea fowl. Neoplastic cells have distinct cell borders, a moderate amounts of finely granular eosinophilic cytoplasm, irregularly round nuclei with coarsely stippled chromatin. Moderate numbers of heterophils and plasma cells are scattered throughout the neoplasm. (HE, 400X)

non-oncogenic and serotype 3 is common in turkeys and also non-oncogenic. The virus is spread through inhalation of virus-containing feather follicle dander of infected birds which can spread across long distances. Carrier birds can be silently infected and periodically shed the virus throughout their lives. There are four different types of lesions seen in MD: (1) peripheral nerve enlargement, (2) discoloration of the iris; (3) swelling of feather follicles with skin reddening (leukosis); (4) and visceral tumors often involving heart, spleen, liver, gonads, kidneys, and proventriculus. Of the four, visceral tumors are most common and can result in depressed, cachexic birds prior to death with vague clinical signs. Microscopically, lymphomas caused by MD contain pleomorphic T-lymphocytes that carry a MD tumor-associated surface antigen (MATSA).[5] In pet birds, epitheliotropic lymphoma that appears similar to MD occurs but the etiology has not been identified.[11]

Avian leukosis (ALV) affects mature chickens and is caused by alpha retroviruses known as avian leukosis viruses which have been further classified into 10 subgroups (A through J). Retroviral strains are classified by the pathogenicity of their lesions and subgroup. Lymphoid leukosis (LL) is the most common, caused by ALV subgroup A, and characterized by gradual onset, low mortality, and neoplasia of the Bursa of Fabricius with metastasis to other visceral organs. Recently a new strain of ALV was discovered, "J", which causes myeloid leukosis (myelocytomatosis) and most likely results from recombination of endogenous and exogenous retroviruses. In contrast to MD, egg transmission is the predominate mechanism of spread in ALV. These chicks are immune tolerant and do not develop antibody but have an increased risk of death from LL. If female, these chickens will lay fewer eggs and shed the virus to their own progeny further disseminating the infection. Clinical signs of ALV are non-specific and many birds simply appear emaciated and lethargic. Tumors may be detected within the bursa of Fabricius by insertion of the clinician's finger into the cloaca. Additionally, birds with skeletal myelomatosis (subgroup J) may develop osteopetrosis of the shanks resulting in what are colloquially known as "boot shanks". Avian retroviruses cause osteopetrosis by infecting osteoblasts and making them constitutively active, while osteoclasts remain unaffected.[1,2] Microscopically, neoplastic cells are uniformly lymphoblastic and positive for immunoglobulin M and B-cell markers since they originate in the Bursa of Fabricius.[5]

Reticuloendotheliosis (RE) encompasses a variety of conditions caused by retroviruses. Only two conditions caused by this non-defective RE virus, runting syndrome and chronic lymphoma are of economic importance particularly in the southern U.S. Runting disease is induced by vaccination with RE virus-contaminated biologics of chicks less than 1 week old and characterized by stunted growth, feather abnormalities, and severe atrophy of the thymus and Bursa of Fabricius leading to immunosuppression and concurrent infections. Chronic lymphoma syndrome occurs very rarely in turkeys, ducks, quail, pheasants, geese, peafowl, prairie chickens and chickens and results in few clinical signs other than mild depression prior to death. In experimentally infected animals lesions resemble LL or MD.[5]

Diagnosis of lymphoid tumors in birds can be difficult and necessitates a complete history, thorough necropsy, immuno-

fluorescent tests for surface antigens, and molecular techniques like PCR.[5]

Contributing Institution:
http://www.uu.nl/faculty/veterinarymedicine/EN/labs_services/vpdc

References:

1. Foster RG, Lian JB, Stein G, Robinson HL. Replication of an osteopetrosis-inducing avian leukosis virus in fibroblasts, osteoblasts, and osteopetrotic bone. *Virology*. 1994;205(1):179-187.
2. Foster RG, Robinson HL. Establishment of interference in osteoblasts by an osteopetrosis-inducing avian leukosis virus. *Virology*. 1994;205(1):376-378.
3. Golbar H. M, Izawa T, Kuwamura M et al. Malignant seminoma with multiple visceral metastases in a Guinea Fowl (*Numida meleagris*) kept in a zoo. *Avian Diseases Digest*. 2009;4(1):143-145.
4. Kirev T, Toshkov IA, Mladenov ZM. Virus induced duodenal adenomas in guinea fowl. *J. Natl. Cancer. Inst.* 1987; 79 (5):1117-1121.
5. Ojkic D, Brash ML, Jackwood MW, Shivaprasad HL. Viral diseases. In: Boulianne M, ed. *Avian Disease Manual*. 7th ed. Jacksonville, FL: American Association of Avian Pathologists, Inc.; 2013:30-38.
6. Okoye JOA, Ilochi CC. Pancreatic adenocarcinoma in guinea fowl. *Avian Pathology* 1993 ;(22):401-406.
7. Pattison M, McMullin PF, Bradbury JM, Alexander DJ. *Poultry Diseases*. 6th ed. Philadelphia, PA: Elsevier; 2008:569-570.
8. Payne LN, Venugopal K. Neoplastic diseases: Marek's disease, avian leukosis and reticuloendotheliosis. *Rev. sci. tech. Off. Int. Epiz.* 2000;19(2): 544-564.
9. Reece RL. Observations on naturally occurring neoplasms in birds in the state of Victoria, Australia. *Avian Pathology* 1992;(21):3-32.
10. Schmidt RE, Reavill DR, Phalen DN. *Pathology of Pet and Aviary Birds*. 1st ed. Ames, IA: Iowa State Press; 2003:206-207.
11. Schmidt RE, Reavill DR, Phalen DN. *Pathology of Pet and Aviary Birds*. 2nd ed. Ames, IA: Iowa State Press; 2015:258-259.
12. Schnellbacher RW, Wilson S. What is your diagnosis?. *Journal of Avian medicine and Surgery* 2010; 24(3):241-244.
13. Toshkov I, Kirev T, Bannasch P. Virus induced pancreatic cancer in guinea fowl. An electron microscopical study. *Int J Pancreatol.* 1991 ;(1):51-64.

CASE II: 12060787 (JPC 4033563).

Signalment: 26-day-old, male and female, commercial white broiler chickens, *Gallus gallus domesticus*, avian.

History: Five birds were submitted from a commercial broiler facility for evaluation for gangrenous dermatitis. Three birds were deceased and two were alive at time of submission. No other history available.

Gross Pathology: Per submittal request, there were no lesions consistent with gangrenous dermatitis in the birds. Instead, the livers were swollen, friable, pale and riddled with dark red to light yellow military foci. Additionally, the kidneys were pale, swollen and friable and the spleen was mottled.

Laboratory results: Acid fast stains on tissues were negative.

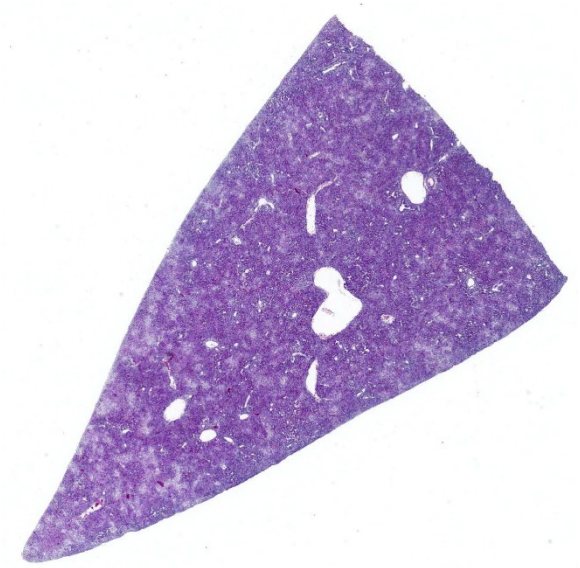

Liver, chicken. At subgross magnification, a retiform pattern of pallor (necrosis) is present throughout the section. (HE, 5X)

Microscopic Description: Liver: The hepatocellular parenchyma is interrupted by numerous, individual and coalescing foci of necrosis. The foci of necrosis are abruptly demarcated from surrounding viable parenchyma and contain necrotic cell debris along with infiltrates of intact and degenerate heterophils and scant erythrocytes (hemorrhage). Typically restricted to the margin of the viable: necrotic parenchyma, several hepatocytes exhibit large, granular to homogeneous, basophilic intranuclear inclusion bodies that peripherally displace chromatin. Lastly, multifocal portal regions have mild to moderate infiltrates by lymphocytes, plasma cells and fewer macrophages.

Contributor's Morphologic Diagnosis:
Liver: Marked, acute to subacute, necrotizing hepatitis with basophilic, intranuclear, inclusion bodies consistent with adenovirus (inclusion body hepatitis).

Contributor's Comment: Inclusion body hepatitis (IBH) was first reported from an outbreak in chickens in the United States by Helmboldt and Frazier.[3] Since that time, IBH has grown to become a ubiquitous disease with worldwide distribution. IBH occurs in chickens 3-7 weeks of age and is characterized by an abrupt increase in mortality that lasts 3-5 days and can approach 10-30%.[2,5] Affected birds exhibit an enlarged mottled liver, icterus, hemorrhages, and pale, swollen kidneys. Microscopic evaluation shows hepato-cellular necrosis with eosinophilic or basophilic intranuclear inclusion bodies.

Inclusion body hepatitis is caused by fowl adenovirus. Fowl adenoviruses are divided into at least 12 serotypes, most of which are apathogenic. IBH is typically associated with serotypes 2 and 8; whereas a different clinicopathological manifestation of fowl adenovirus infection, known as hydro-pericardium syndrome (HPS), is typically associated with serotype 4.[2,5] However, some birds have demonstrated both IBH and HPS from administration of the same strain[4],and therefore, the clinical disease form may be multifactorial related to background, co-infections, route of infection or age of the bird.

Historically, outbreaks of IBH have been associated with concurrent disease, particularly immunosuppressive agents such as infectious bursal disease (IBD) or chicken anemia virus (CAV).[1,6] In the present case, cloacal bursas from affected birds were examined at necropsy and microscopically; no lesions were identified. Additionally, serologic surveys on affected flocks did not demonstrate IBD infection in birds dying from IBH.

A PubMed search for information related to IBH returns a paucity of contemporary studies. Therefore, although this disease may no longer be commonly seen or studied, similar to infectious canine hepatitis (canine

adenovirus-1), IBH does re-emerge on occasion.

JPC Diagnosis: Liver: Hepatitis, necrotizing, multifocal to coalescing, marked with numerous basophilic intranuclear viral inclusions, *Gallus gallus domesticus*, avian.

Conference Comment: There are three genera that affect birds: (1) Aviadenoviruses (group I) which contain fowl adenoviruses (IBH), goose adenoviruses, falcon adenovirus 1, duck adenovirus 2, pigeon adenovirus 1 and turkey adenovirus 1 and 2; (2) Siadenoviruses (group II) which contain turkey adenovirus 3 (hemorrhagic enteritis, marble spleen disease) and raptor adenovirus 1; and (3) Atadenoviruses (group III) which contains duck adenovirus 1 (egg drop syndrome).[6] These ubiquitous viruses generally only cause disease in immunosuppressed birds.

Fowl adenovirus, the cause of inclusion body hepatitis, has worldwide distribution, typically affecting young chickens. Most animal species have their own adenovirus that induces hepatitis, enteritis, or respiratory disease (see chart below). With IBH, gross lesions are usually non-specific and may consist of pallor of the wattles and comb, depression, and a sudden increase in mortality within the flock. Depending on the severity of the hepatitis, there may be petechial and ecchymotic hemorrhages in the skeletal muscles of the legs. The liver is generally enlarged with mottling characterized by soft, yellow, focal areas and hemorrhage. Kidneys are often swollen

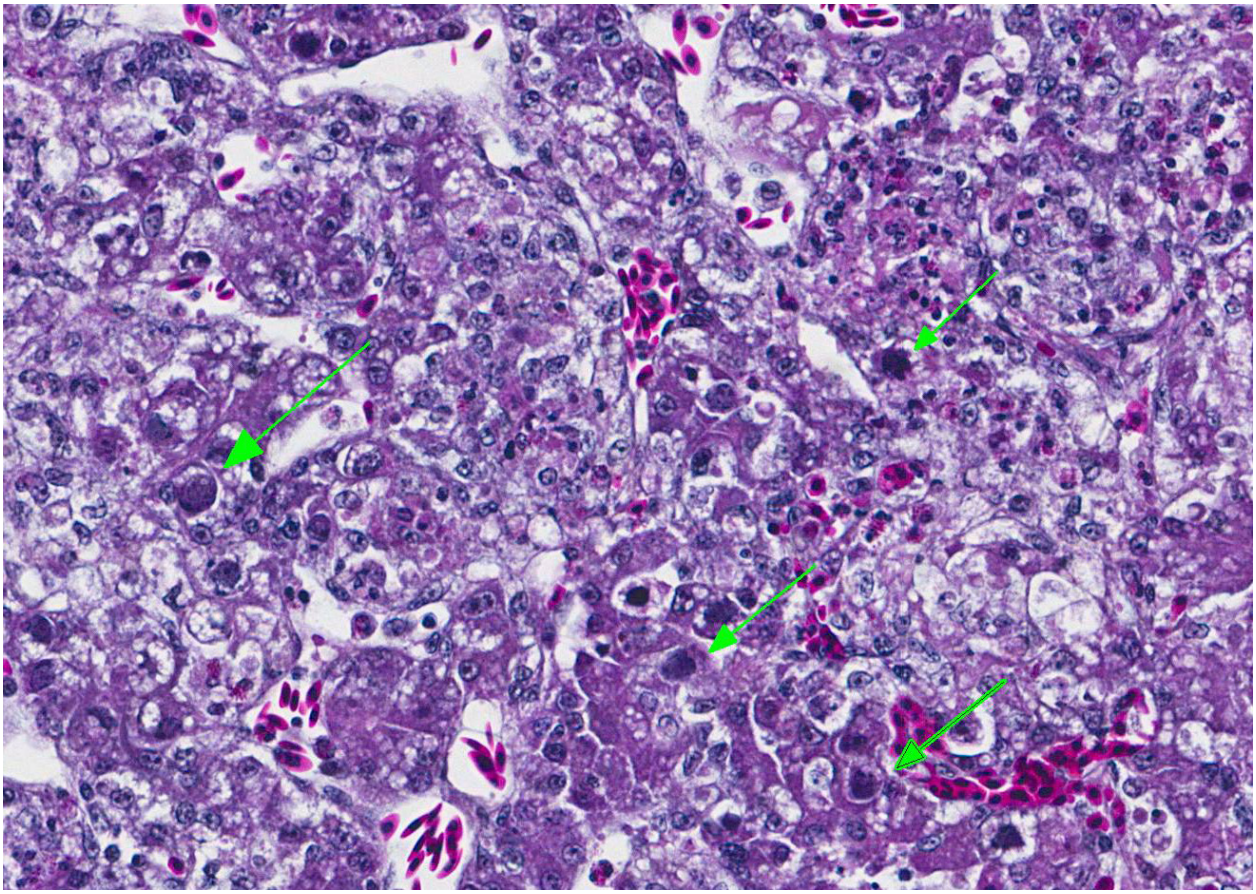

Liver, chicken. Adjacent to areas of hepatocellular necrosis and loss, the nuclei of degenerating hepatocytes are expanded by a single basophilic viral inclusion (arrows). (HE, 400X)

and mottled as well and the Bursa of Fabricius is usually reduced in size. Microscopically, there is focally extensive degeneration and necrosis of hepatocytes with the characteristic basophilic intra-nuclear viral inclusion bodies within hepatocytes adjacent to areas of necrosis. Renal lesions consist of membrano-proliferative glomerulonephritis, and the Bursa of Fabricius is grossly small due to lymphoid depletion.[6]

Hemorrhagic enteritis of turkeys (caused by turkey adenovirus) results in large basophilic intranuclear viral inclusion bodies within cells of the mononuclear phagocyte system in the spleen leading to widespread necrosis and involution of the white pulp. There is lymphoid depletion in the thymus and Bursa of Fabricius. Intestinal lesions are most prominent in the duodenum and are characterized by mucosal congestion, degeneration and necrosis of the epithelium lining the villus tips and luminal hemorrhage with mixed inflammation in the lamina propria. Adenoviral inclusions are rarely seen in intestinal epithelia, liver, bone marrow, circulating leukocytes, lung, pancreas, brain, and kidney.[6]

Egg drop syndrome is caused by a hemagglutinating adenovirus (duck adenovirus 1) and results in loss of color of pigmented eggs, decrease in production, or production of thin-shelled, wrinkly eggs in healthy looking laying hens. The virus is widespread in its natural host, waterfowl, and spread vertically and horizontally to domestic birds. In chicks infected in utero the virus remains latent until they start laying eggs. The primary site of replication is in the pouch shell gland and gross lesions other than atrophied ovaries and oviducts are not appreciated. For diagnosis, allantoic fluid can be checked for hemagglutinating activity or viral DNA detected by PCR.[6]

Table 1: Select adenoviruses in veterinary species[4]

Species	**Name/Species**	**Comment**
Dogs	Canine adenovirus 1 Canine adenovirus 2 (mastadenovirus)	- Infectious canine hepatitis - Infectious canine tracheobronchitis
Horses	Equine adenovirus 1 & 2 (mastadenovirus)	- Asymptomatic or mild respiratory disease in immunocompetent hosts - Bronchopneumonia/systemic disease in Arabian foals with SCID
Cattle	Bovine adenovirus (mastadenovirus and atadenovirus)	- 10 serotypes - Asymptomatic or mild respiratory disease - Occasionally pneumonia, enteritis, keratoconjunctivitis in calves
Swine	Porcine adenovirus (mastadenovirus)	- 4 serotypes - Asymptomatic or mild respiratory disease/enteritis; rarely encephalitis
Sheep	Ovine adenovirus (mastadenovirus and atadenovirus)	- 7 serotypes - Asymptomatic or mild respiratory disease - Occasionally severe respiratory/enteric disease in lambs

Goats	Caprine adenovirus (mastadenovirus and atadenovirus)	- 2 serotypes - Asymptomatic or mild respiratory disease
Deer	Cervine adenovirus (Odocoileus adenovirus 1; atadenovirus)	- Vasculitis, hemorrhage, pulmonary edema
Rabbits	Adenovirus 1 (mastadenovirus)	- Diarrhea
Mice	Murine adenovirus 1 & 2 (mastadenovirus)	- Murine adenovirus 1: experimental infections - Murine adenovirus 2: enterotropic; causes runting in neonates
Guinea pigs	Guinea pig adenovirus (mastadenovirus)	- Usually asymptomatic; rarely pneumonia with high mortality, low morbidity

Conference attendees also discussed two viral agents that cause immunosuppression and are common concomitant infections in IBH cases: chicken infectious anemia and infectious bursal disease (IBD).

Chicken infectious anemia (*Gyrovirus* genus, Circoviridae family) is a disease of young birds that is characterized by aplastic anemia, generalized lymphoid atrophy, intramuscular hemorrhage, and immuno-suppression. Older birds are usually not affected unless the animal has concurrent infection with infectious bursal disease. The most common method of transmission is vertical from infected hens. Also transmission in feces is common with crowded bird houses. The most common gross lesions are thymic atrophy and yellow, fatty bone marrow. Microscopically, there is thymic lymphoid depletion and atrophy of all cell lines within the bone marrow. Due to resulting immunosuppression, secondary bacterial infections like gangrenous dermatitis may be present.[6]

Infectious bursal disease (also known as "Gumboro disease") is caused by avian birnavirus and results in inflammation and atrophy of the Bursa of Fabricius with resulting immunosuppression. Avian birnavirus has two serotypes with serotype 1 being pathogenic. The virus spreads rapidly, is persistent in the environment, and infects chickens as long as they have a functional Bursa of Fabricius (1-16 weeks old). Initial clinical signs are vague: dehydration, diarrhea, tremor, ataxia, depression, anorexia, and a droopy appearance are common and may resemble coccidiosis. Microscopically, there is marked lymphoid necrosis within the Bursa of Fabricius, thymus, Harderian gland, cecal tonsils, and Peyer's patches followed by atrophy and replacement with fibrous connective tissue.[6]

It was originally thought that IBH was always be preceded by an immuno-suppressive pathogen but recently IBH has been accepted as a primary disease.[6]

Contributing Institution:

Oklahoma Animal Disease Diagnostic Laboratory and the Department of Veterinary Pathobiology
Center for Veterinary Health Sciences
Oklahoma State University
Rm 250 McElroy Hall
Stillwater, OK 74078

References:

14. Fadly AM, Winterfield RW, Olander HJ. Role of the bursa of Fabricius in the

pathogenicity of inclusion body hepatitis and infectious bursal disease viruses. *Avian Dis*. 1976; 20:467-477.
15. Gomis S, Goodhope R, Ojkic D, Willson P. Inclusion body hepatitis as a primary disease in broilers in Saskatchewan, Canada. *Avian Dis.* 2006; 50:550-555.
16. Helmbolt CF, Frazier MN. Avian hepatic inclusion bodies of unknown significance. *Avian Dis*. 1963; 7:446-450.
17. MacLachlan NJ, Dubovi EJ. *Fenner's Veterinary Virology*. 5th ed. London, UK: Academic Press; 2017:217-227.
18. Mazaheri A, Prusas C, Voss M, Hess H. Some strains of serotype 4 fowl adenoviruses cause inclusion body hepatitis and hydropericardium syndrome in chickens. *Avian Pathol.* 1998; 27:269-276.
19. Ojkic D, Brash ML, Jackwood MW, Shivaprasad HL. Viral diseases. In: Boulianne M, ed. *Avian Disease Manual*. 7th ed. Jacksonville, FL: American Association of Avian Pathologists, Inc.; 2013:10-15, 39, 55-56.
20. Philippe C, Grgic H, Nagy E. Inclusion body hepatitis in young broiler breeders associated with a serotype 2 adenovirus in Ontario, Canada. *J Appl Poult Res.* 2005; 14:588-593.
21. Toro H, Gonzalez O, Escobar C, Cerda L, Morales MA, Gonzalez C. Vertical induction of the inclusion body hepatitis/hydropericardium syndrome with fowl adenovirus and chicken anemia virus. *Avian Dis*. 2001; 45:215-222.

CASE III: T (JPC 4035426).

Signalment: 12-month-old, female, breeder hen turkeys, *Meleagris gallopavo*, avian.

History: A spike in mortality was reported in this flock of 2200 breeder hens. Affected live birds were down, unable to rise, had drooped wings and were panting. In the tom barn, the birds were using their wings to stand. Both live and dead birds were submitted to the local field veterinarian for postmortem examination.

Gross Pathology: The veterinarian noted that the majority of the birds had pale streaking of the breast and thigh muscles and some birds also had pale streaking of the myocardium. Formalin-fixed tissues, frozen tissues, bacteriology swabs and a feed sample were submitted to the laboratory for further testing**.**

Laboratory results: PCR testing of lung/trachea was negative for Avian Influenza and Avian Paramxyovirus-1 infection.
Bacterial culture of swabs from bone marrow and peritoneum was negative for bacterial pathogens.
Feed sample HPLC Ionophore Analysis: 36 ug/g salinomycin was detected. Levels of

Skeletal muscle, turkey. A single section of skeletal muscle is presented for examination. There are small areas of pallor within the muscle scattered randomly throughout the section (HE, 6X)

monensin, narasin and lasalocid were < 1 ug/g.

Microscopic Description: Skeletal muscle: Sections from the skeletal muscle from the thigh reveal widespread acute myonecrosis, with swelling, hyalinization, fragmentation and hypercontraction of myofibres. Numerous coagulated portions of myofibres are lightly mineralized and pale eosinophilic lightly fibrillar material is often present between the retracted necrotic myofibres. There is very early hypertrophy of satellite cell nuclei and low numbers of infiltrating macrophages and heterophils.

Contributor's Morphologic Diagnosis:
Skeletal muscle: Acute severe multifocal monophasic skeletal myonecrosis.

Contributor's Comment: Differential diagnoses for lesions of skeletal myopathy in turkeys include: exertional myopathy[5], nutritional myopathy associated with Vitamin E/ selenium deficiency, and toxic myopathy caused by ingestion of ionophores or toxic plants such as *Senna occidentalis*[3]. Based on a strong index of suspicion for ionophore toxicosis, feed samples were submitted for testing, revealing 36 ppm of the ionophore salinomycin.

Several ionophores including monensin and lasalocid are approved for use in growing turkeys in Canada as an aid in the prevention of coccidiosis caused by *Eimeria adenoides*, *E. meleagrimitis* and *E. gallopavonis*. However, salinomycin, although approved for use in chicken broilers, is excluded from this list as it is known to be toxic to turkeys even at very low levels. A caution on the Canadian salinomycin label reads: "Do not allow turkeys, dogs or horses access to this drug. It is known to be toxic to these species. Extra care should be taken to avoid contamination of feeds for these animals[2]". We have no further details as to how and when the salinomycin-contaminated feed was introduced to this specific flock of breeding turkeys, however, in most cases, there is a feed mill or on-farm feed mixing error, or salinomycin-medicated broiler feed is mistakenly fed to the turkeys.

Salinomycin can rapidly cause high mortality in affected flocks. In one recent case report, feed containing salinomycin was given to 13.5 weeks-old turkeys on May 29th. On June 2nd, the error was discovered and the salinomycin-medicated feed was removed but by June 3rd, more than 60% of the total mortality of 34.5% had already occurred[6]. The producer in the current case presented here lost almost all of the turkeys in this breeder flock as a result of ionophore toxicosis. Typical clinical signs include depression, stiffness, weakness, recumbency with extended legs, paralysis and death. The live turkeys in this case were described as panting and panting or dyspnea has been also been previously noted in turkeys with ionophore toxicosis[1]. Microscopic changes are reported in skeletal muscle and in some instances heart. Birds with respiratory signs often have lesions in tracheal muscles[3], and these were noted on histology in this case, although lesions in the myocardium were minimal. Ionophores interfere with ion transfer at the cell membrane, facilitating movement of K+ ions out of myocytes and increasing Ca++ uptake. Toxicity is a result of skeletal muscle damage; type I fibers appear to be selectively affected[3]. Ionophore toxicity is dose dependent, species and age-dependent, and simultaneous use of other drugs may also augment toxicity in some cases[1].

Evaluation of serum CK levels can be helpful in providing rapid confirmation of a skeletal myopathy when dealing with field

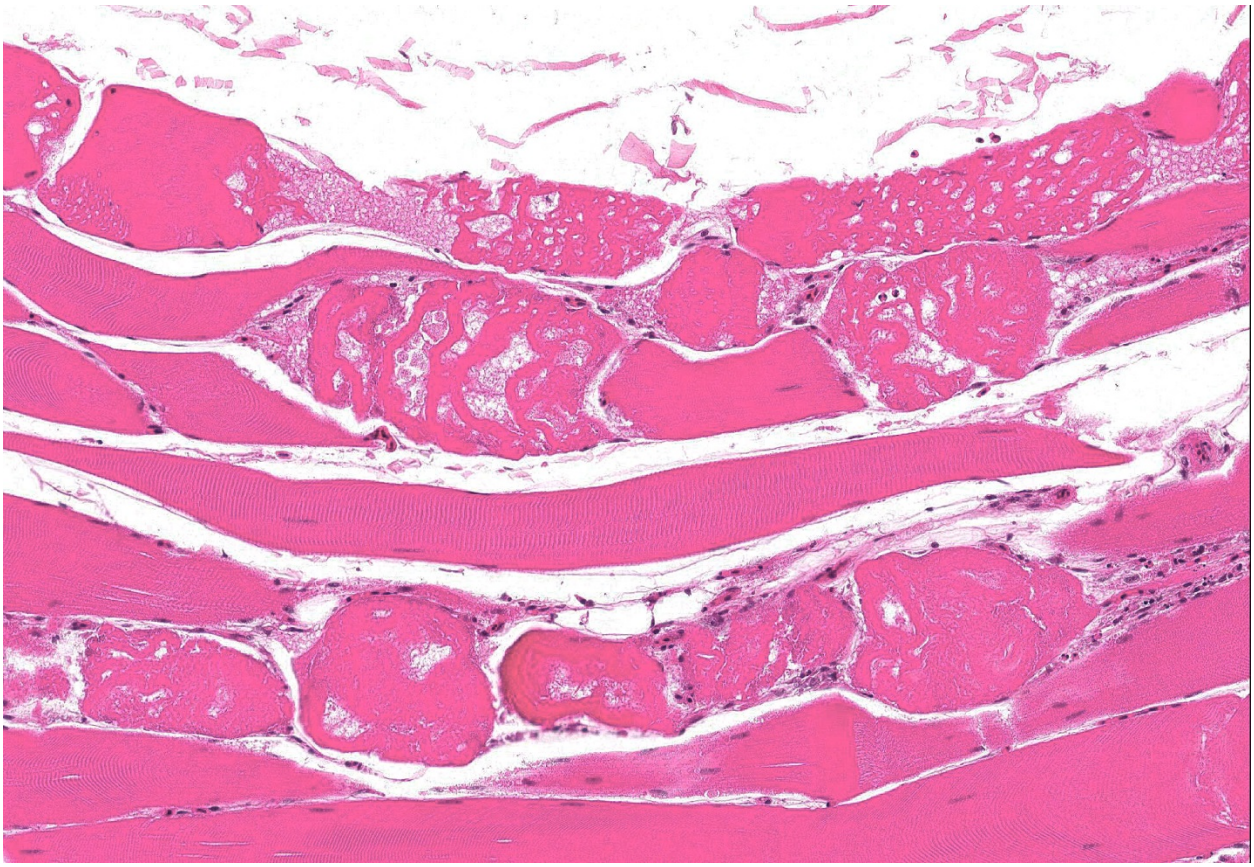

Skeletal muscle, turkey. Throughout the section, randomly scattered groups of myofibers are swollen, vacuolated, and exhibit contraction bands (degeneration and necrosis). (HE, 256X)

cases of recumbency in turkeys, as differential diagnoses include botulism[4].

JPC Diagnosis: Skeletal muscle: Degeneration and necrosis, multifocal, moderate, *Meleagris gallopavo*, avian.

Conference Comment: In domestic animals, toxic myopathies are generally caused by ingestion of ionophores, toxic plants, and plant-origin toxins. As a metabolically active organ system, skeletal muscle is highly susceptible to toxic injury resulting from membrane damage, altered protein synthesis, increased intracellular calcium concentration, or mitochondrial damage. Cases of myotoxicosis have variable clinical signs including: elevated serum concentrations of skeletal muscle cytoplasmic enzymes (CK and AST); severe muscle pain with or without myoglobinuria; or severe muscle weakness, recumbency and myoglobinuria. Animals often die from damage to cardiac muscle from the same toxin.[3]

Ionophores such as monensin, lasalocid, salinomycin, narasin, and maduramicin are compounds that alter membrane permeability to electrolytes by influencing transmembrane transport and function at low concentrations as a coccidiostat in birds and other animals. Monensin is the most common cause of ionophore toxicosis, and is produced by the fermentation of *Streptomyces cinnamonensis*. In addition to its function as a coccidiostat, monensin also promotes growth in ruminants. Toxicity results when animals are fed high concentration rations due to mixing errors,

or when fed to monogastric animals that have a reduced tolerance to the drug; when medications are added to rations (tiamulin, triacetyloleandomycin, or sulfonamides) the toxic effects of ionophores are potentiated. Maduramicin is another ionophore antibiotic and a common coccidiostat in poultry that has demonstrated cardiotoxicity in cattle and sheep. With ionophore toxicity clinical signs can vary; however, with the administration of large single doses, birds may present with lethargy, stiffness, muscular weakness, and recumbency within 24-hours of ingestion. Toxic effects are cumulative with the ingestion of smaller doses, culminating in myocardial lesions and cardiac failure within 2-3 weeks. Myocardial lesions predominate in horses, in contrast to sheep and pigs where skeletal muscle damage with myoglobinuria is more prevalent. . In cattle, both skeletal and cardiac muscles appear equally affected. Microscopically, ionophore toxicity is characterized by multifocal monophasic necrosis of both types 1 and 2 muscle fibers with macrophage infiltration within 48 hours of ingestion; this differs from nutritional myopathies which cause polyphasic necrosis. Ultrastructurally, mitochondria are swollen and degenerate due to disruption of the membrane transport of sodium and potassium, leading to increased intracellular calcium and mitochondrial failure.[3]

Common plants that result in toxic myopathy are: *Cassia occidentalis* or *C. obtusifolia* (senna or coffee senna beans) and *Karwinskia humboldtiana* (coyotillo). Similar to ionophores, ingestion of these plants leads to weakness and eventual recumbency with skeletal muscle pallor, and microscopic multifocal monophasic myonecrosis.[3]

Gossypol is a polyphenolic substance found in cottonseeds (*Gossypium* spp.) that is toxic to most domestic animals (particularly, swine), causing lesions in several organs including the heart, skeletal muscle, liver, and lung. Similar to the aforementioned toxins, death is due to cardiac failure and monophasic myonecrosis; also, there is hepatic centrilobular necrosis and pulmonary edema.[3]

Additionally, the following plants have been known to cause toxic myopathy in select species: *Diaporthe toxica* (lupinosis in sheep), *Cicuta douglasii* (sheep with water hemlock), *Thermopsis montana* (calves with false lupine), *Ageratina* spp. (horses and ruminants with white snake root), *Isocoma pluriflora* (rayless goldenrod), *Acer negundo* (horses ingesting hypoglycin A found in the box elder tree), and selenium toxicosis in pigs, cattle, sheep and other domestic species.[3]

Unless there is known history of ingestion or the presence of the toxin in the intestinal tract, these toxic myopathies are impossible to differentiate.

Contributing Institution:
Animal Health Laboratory
University of Guelph
Guelph, Ontario, Canada
http://ahl.uoguelph.ca

References:

1. Andreasen JR, Schleifer JH. Salinomycin toxicosis in male breeder turkeys. *Avian Dis*.1995; 39 (3):638-642.
2. Bayley A. Bio-Cox 120 G. In: Inglis S, ed. *Compendium of Veterinary Products*. 11th ed. Hensall, ON: North American Compendiums, Ltd; 2009: 288.
3. Cooper BJ, Valentine BA. Muscle and tendon. In: Maxie MG, ed. *Jubb, Kennedy, and Palmer's Pathology of Domestic Animals*. Vol. 1. 6th ed. Philadelphia, PA; Elsevier: 218-220.

4. Fulton RM. Other toxins and poisons. In: Saif YM, ed. *Diseases of Poultry*. 12th ed. Ames, IA: Blackwell Publishing; 2008:1231-1258.
5. Neufeld J. Salinomycin toxicosis of turkeys: serum chemistry as an aid to early diagnosis. *Can Vet J*.1992; 33: 677.
6. Williams S. Muscular system. In: Fletcher OJ, ed. *Avian Histopathology*. 3rd ed. Madison, WA: American Association of Avian Pathologists;2008:80-95.
7. VanAssen EJ: A case of salinomycin intoxication in turkeys. *Can Vet J*. 2006; 47 (3): 256-258.

Trachea, peacock. There is diffuse circumferential loss of mucosal epithelium and expansion of the underlying submucosa by a cellular infiltrate and edema. A fibrinonecrotic membrane covers the denuded mucosa and there is a plug of necrotic exudate in the lumen. (HE, 6X)

CASE IV: T17-14880 (JPC 4101090).

Signalment: Adult, peacock, *Pavo cristatus*, avian.

History: The bird and others in the same flock had respiratory symptoms with rapid breathing and purulent ocular discharge.

Gross Pathology: Pasty to dry exudate was present on the conjunctiva of the eyes. Upon opening the carcass, the bird was found in a fair body condition. The oropharynx was rough and crusty. The crop was empty. Liver, kidney and lungs were congested. There was no other grossly visible lesion.

Laboratory results: Oropharyngeal/tracheal tissues were positive for herpesvirus by PCR. The sequenced amplicon showed identity to Gallid herpesvirus-1.

Microscopic Description: Trachea and larynx: The lesions vary from section to section. In all sections the tracheal mucosa is variably infiltrated with abundant lymphocytes, macrophages, scattered multinucleated syncytial cells and heterophils. The inflammatory cells trans-migrate the epithelium and also extend to the submucosa. Scattered epithelial cells contain eosinophilic intranuclear inclusions. The laryngeal mucosa (sections not included) is ulcerated and large numbers of lymphocytes, macrophages, plasma cells and occasional heterophils infiltrate the submucosa. Large numbers of lymphocytes, plasma cells and scattered heterophils are also observed in the submucosa of palpebral conjunctiva (sections not included). In a focally extensive area, abundant lymphocytes, macrophages and several multinucleated giant (syncytial) cells infiltrate a section of bronchus (sections not included), extend to the adjacent pulmonary parenchyma and variably fill the parabronchus and air capillaries. Scattered epithelial cells contained eosinophilic intranuclear inclusions.

Contributor's Morphologic Diagnosis:

Trachea and larynx: Lymphoplasmacytic and heterophilic to pyogranulomatous tracheitis and laryngitis (laryngotracheitis) with syncytial cells and intranuclear inclusion bodies.

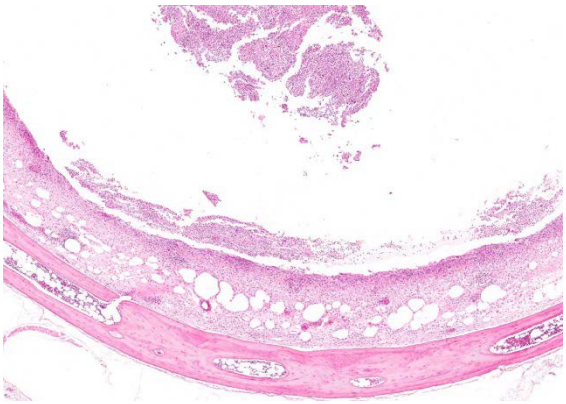

Trachea, peacock. Higher magnification of the trachea. The outer ring of bone may be seen in sections taken close to the larynx. (HE, 62X)

Contributor's Comment: The lesion is consistent with infectious laryngotracheitis due to gallid herpesvirus-1. Infectious laryngotracheitis (ILT) is a highly contagious respiratory disease of poultry reported in most countries around the world and causes significant economic losses in the poultry industry worldwide.[1, 4, 7] ILT virus (ILTV) belongs to alphaherpesviridae and the Gallid herpesvirus-1 species.[7] Different strains of the virus are recognized. In US infectious laryngotracheitis virus (ILTV) strains and field isolates were genotyped by polymerase chain reaction and restriction fragment length polymorphism (PCR-RFLP) into nine different genotypes.[5]

Natural transmission of ILTV is via respiratory and ocular routes. All ages of chickens including pheasants, pheasant-bantam crosses, and peafowl are affected, but chickens older than 3 weeks are most susceptible. The sources of ILTV are clinically affected chickens, latent infected carriers, contaminated dust, litter, beetles, drinking water and fomites.[7] The ILT virus can be spread by the transportation of animals, personnel, and equipment. In one study it was indicated that one of the critical points identified as a potential source of virus transmission was roads that were frequently used by the poultry industry within the outbreak area.[6]

Clinical signs can be severe or mild. Dyspnea and bloody mucus and high morbidity and mortality could be seen in severe forms. In the mild form depression, reduced egg production and weight gain, conjunctivitis, swelling of the infraorbital sinuses (almond shaped eyes), and nasal discharge are observed. The mild form is the most commonly seen type in the US and is called "silent, vaccinal, or almond-shape eye" ILT.[7] Clinical cases with the history of the pump handle type of respiration, conjunctivitis, coughing up of blood and mortality up to 80% is often reported by poultry farmers and veterinarians in India.[2]

Gross lesions are observed in the larynx and trachea. With the severe form, the mucosa of the respiratory tract shows inflammation and necrosis with hemorrhage. A characteristic feature is intranuclear inclusion bodies in epithelial cells. Inclusion bodies are generally present for a few days at the early stage of infection before epithelial cells die. Epithelial cells also form multinucleated cells (syncytia). Laboratory diagnosis (virus isolation and DNA detection) is required to confirm ILT, and rule out other diseases such as infectious bronchitis, Newcastle disease, avian influenza, infectious coryza, and mycoplasmosis that may have similar clinical signs and lesions.

Vaccination is effective to prevent ILTV infection. However, vaccine viruses can create latent infected carrier, which could be a source for spread of virus to non-

vaccinated flocks. Therefore, it is recommended that ILT vaccines be used only in endemic areas. It is important to avoid contact between vaccinated or recovered field virus infected birds with non-vaccinated chickens. It is also critical to remove contaminated fomites for prevention and control of ILTV infection. To control ILTV outbreaks, improved biosecurity and management practice are necessary.[7] Previous studies have demonstrated that the most effective way to prevent or control an ILT outbreak is through enhanced biosecurity, and implementation of an appropriate vaccination program.[6] However, although vaccination may have an important role in controlling ILT in outbreak areas, problems may occur when vaccine is administered incorrectly, vaccination fails to provide immunity to most birds in a flock, and biosecurity measures fail to prevent spread of vaccine virus to unvaccinated flocks.[3]

Recombinant viruses which possess significantly higher virulence and replication capacity were found to emerge as a result of recombination between live vaccine strains

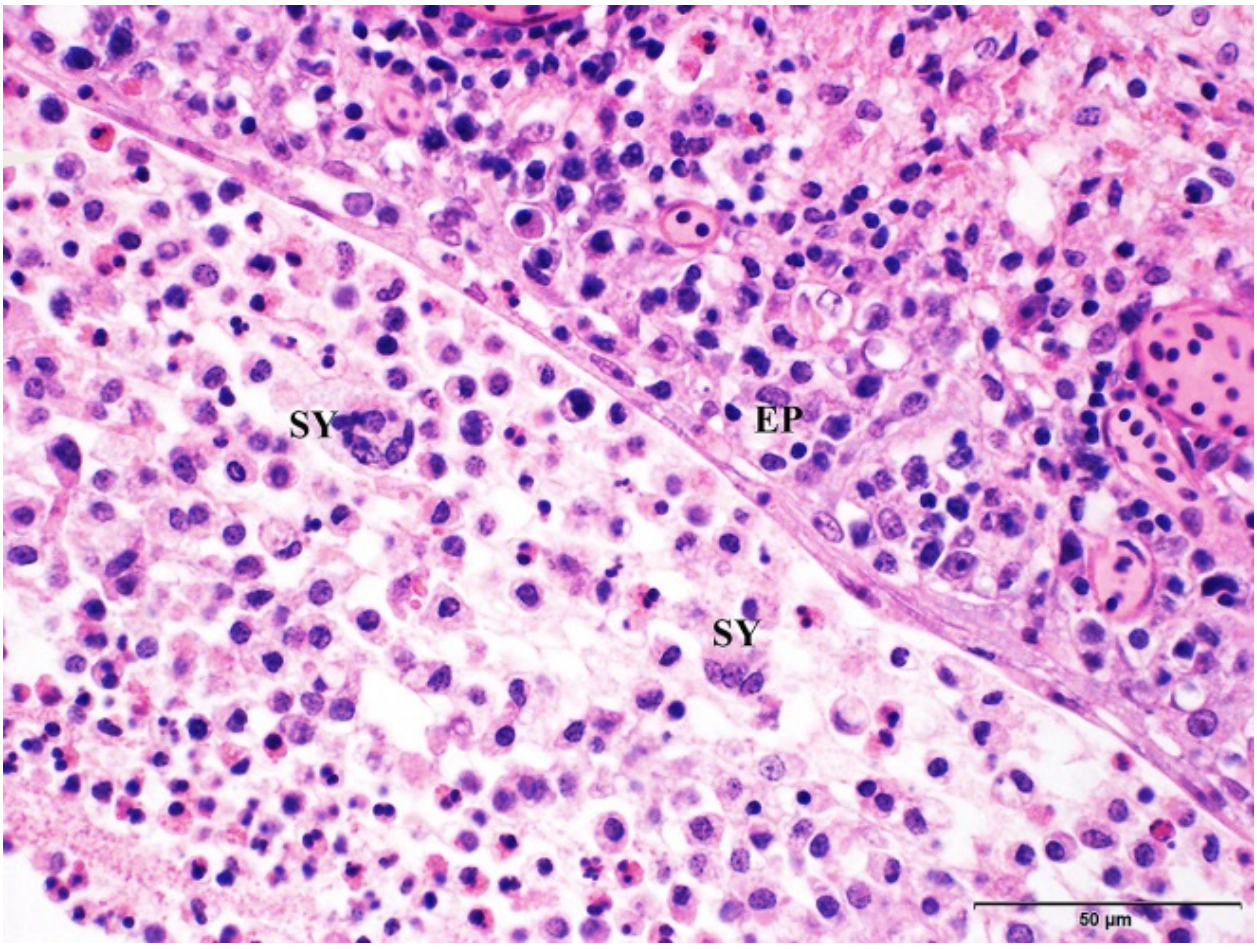

Trachea, peacock. The necrotic membrane is composed of numerous sloughed mucosal epithelium, admixed with heterophils, and polymerized fibrin. The mucosa is covered by attenuated epithelium. The luminal exudate contains occasional syncytial cells (SY). EP= tracheal Epithelium. (HE, 400X) (Photo courtesy of: The University of Georgia College of Veterinary Medicine, Department of Pathology,
Tifton Veterinary Diagnostic & Investigational Laboratory, Tifton, GA 31793, http://www.vet.uga.edu/dlab/tifton/index.php)

(SA2 and A20), and another live vaccine strain (Serva) introduced into Australia in 2007. Interestingly, many of the ILT outbreaks occurred in vaccinated flocks. It is possible that these cases resulted from an inadequate vaccine dose or improper vaccine handling or administration.[1] Replication and spread of vaccine viruses is potentiated by vaccine administration that fails to provide immunity to all the birds in a flock (e.g., via drinking water) and when biosecurity measures fail to prevent spread to unvaccinated flocks.[3]

JPC Diagnosis: Trachea: Tracheitis, necrotizing and lymphohistiocytic, circumferential, severe with multinucleated viral syncytia and intranuclear eosinophilic viral inclusions, *Pavo cristatus*, avian.

Conference Comment: Several gross differentials were discussed in the conference, including: infectious bronchitis, Newcastle disease, avian influenza, infectious coryza, and mycoplasmosis.

Infectious bronchitis (IBV), caused by a coronavirus, occurs naturally in chickens of all ages. IBV has many different serotypes and with the current vaccine there is little cross-protection between serotypes compounding that with a high mutation rate makes this disease difficult to control and diagnose. Gross lesions include upper respiratory tract infections with or without airsacculitis. Some serotypes affect the kidneys (nephrotropic strains) and can result in swollen kidneys (interstitial nephritis histologically) with uric acid crystals in renal tubules and ureters. Microscopically, the tracheitis is characterized by mucosal edema, cilia loss, degeneration and necrosis of mucosal epithelial cells, and inflammation.[6]

Exotic Newcastle disease (ND), caused by avian paramyxovirus-1 (APMV-1), occurs most commonly in chickens and less often in turkeys (although most poultry are susceptible) of all ages. There are three main strains of APMV-1: (1) Lentogenic strains which are mildly pathogenic strains; (2) Mesogenic strains which are moderately pathogenic; and (3) Velogenic strains which are markedly pathogenic strains. Usually, "enzootic" strains of ND are lentogenic or mesogenic and result in mild respiratory infections with occasional nervous signs (abnormal positions of the head and neck, AKA "star gazers", paralysis, prostration). Velogenic strains cause two main pathotypes: (1) Neurotropic velogenic which cause respiratory and nervous signs with high mortality and (2) Viscerotropic velogenic which cause hemorrhagic intestinal lesions with high mortality. With velogenic strains, gross lesions can be diverse and may consist of one or more of the following: diphtheritic laryngotracheitis; conjunctival hemorrhage; air sacculitis; facial edema with hemorrhage of the comb and wattles; hemorrhages on the mucosa of the proventriculus or gizzard, Peyer's patches, cecal tonsils, and large intestine; multifocal splenic necrosis; egg yolk in the abdominal cavity; and deformed eggs.[6]

Avian influenza (AIV) is caused by a type A influenza virus in the Orthomyxoviridae family which has two important surface antigens which help in identification and subtyping of the virus: hemagglutinin (H) which aids in viral attachment and neuraminidase (N) which cleaves sialic acid residues on host cells and mediates virion release. There are many different strains of influenza that are classified into two categories: low pathogenic (LPAI, cause little to no clinical signs) and high pathogenic (HPAI, which cause severe clinical signs and high mortality).

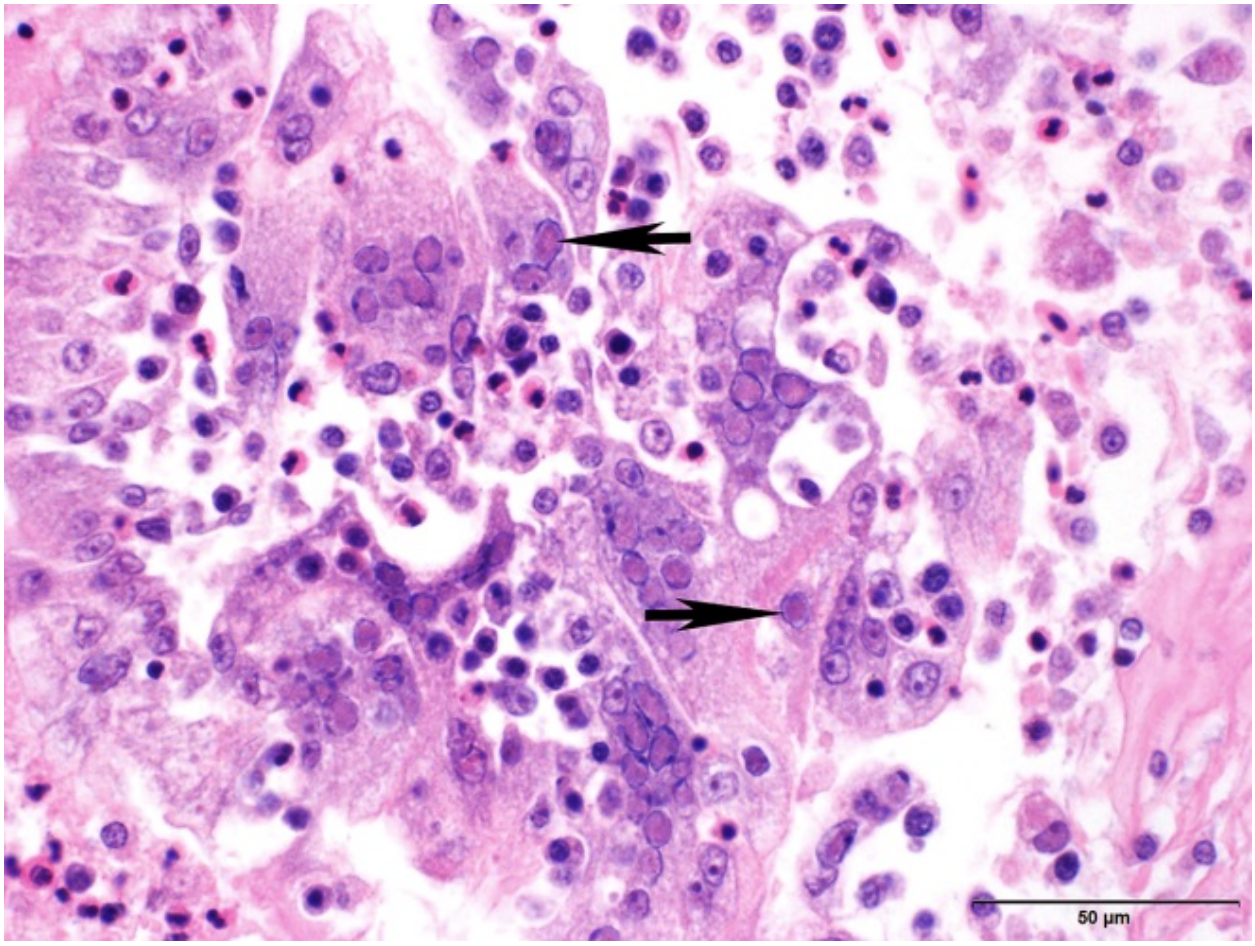

Parabronchus, peacock. The parabronchus contains numerous syncytial cells with multiple nuclei, many of which contain a single prominent eosinophilic herpesviral intranuclear inclusion. (HE, 400X) (Photo courtesy of: The University of Georgia College of Veterinary Medicine, Department of Pathology, Tifton Veterinary Diagnostic & Investigational Laboratory, Tifton, GA 31793,
http://www.vet.uga.edu/dlab/tifton/index.php)

Additionally, HPAI is subcategorized if they are highly pathogenic and "notifiable" strains (HPNAI). Wild reservoirs are waterfowl and shorebirds that are commonly asymptomatic and excrete the virus in their feces for many years. Once introduced into a farm, AIV is transmitted by direct and indirect contact through respiratory secretions and excrement and can be transferred from farm to farm on fomites. Gross lesions associated with LPAI outbreaks include: mild tracheitis, sinusitis, air sacculitis, and conjunctivitis and fibrino-purulent bronchopneumonia can occur with secondary bacterial infections. With HPNAI outbreaks, gross lesions are generally more severe to include: fibrinous exudates on airsacs, in the peritoneum, or pericardial sac; multifocal areas of necrosis externally on the skin, comb, and wattles or internally on the liver, kidney, spleen, or lungs, blotchy, red discoloration of the shanks, hemorrhage and petechiae on mucosal and serosal surfaces of the proventriculus and gizzard. In turkeys, encephalitis and pancreatitis have been reported as well.[6]

Infectious coryza, caused by *Avibacterium paragallinarium*, primarily affects chickens but has been rarely reported in pheasants

and guinea fowl with upper respiratory tract infections often complicated by other agents like *Mycoplasma gallisepticum* which leads to chronic respiratory disease. Transmission of infectious coryza probably occurs through inhalation of infectious droplets or ingestion of infected feed materials. *A. paragallinarium* cannot exist long outside the host and is easily eliminated by disinfectants or environmental extremes. Typical gross lesions are catarrhal inflammation in the sinuses with nasal discharge, conjunctivitis with caseous exudate, edema of the face and wattles, and tracheitis, pneumonia, or air sacculitis in cases complicated by secondary pathogens.[2]

Mycoplasma gallisepticum is the causative agent of chronic respiratory disease in chickens and infectious sinusitis in turkeys. It is initially transmitted transovarially and can then be spread by aerosol transmission to other chicks or through contaminated feed. As with all mycoplasma infections, clinical signs take time to develop and show more profound lesions in broilers 4-8 weeks old. Gross lesions are similar to the other diseases listed above and include: catarrhal inflammation of the sinuses and upper airways, airsacculitis with hyperplastic lymphoid follicles, fibrinous perihepatitis, and adhesive pericarditis.[2]

Due to the similarities in gross and microscopic findings among the diseases discussed above, laboratory diagnosis (virus isolation and DNA detection) is required for definitive diagnosis.

Contributing Institution:

The University of Georgia
College of Veterinary Medicine
Department of Pathology
Tifton Veterinary Diagnostic & Investigational Laboratory
Tifton, GA 31793
http://www.vet.uga.edu/dlab/tifton/index.php

References:

1. Agnew-Crumpton R, Vaz PK, Devlin JM, et al. Spread of the newly emerging infectious laryngotracheitis viruses in Australia. *Infect Genet Evol*. 2016; 43:67-73.
2. Fulton RM. Bacterial diseases. In: Boulianne M, ed. *Avian Disease Manual*. 7th ed. Jacksonville, FL: American Association of Avian Pathologists, Inc.; 2013:103-108.
3. Gowthaman V, Koul M, Kumar S. Avian infectious laryngotracheitis: a neglected poultry health threat in India. *Vaccine*. 2016; 34:4276-4277.
4. Guy JS, Barnes HJ, Morgan LM. Virulence of infectious laryngotracheitis viruses: comparison of modified-live vaccine viruses and North Carolina field isolates. *Avian Dis*. 1990; 34(1):106-113.
5. Lee SW, Hartley CA, Coppo MJ, et al. Growth kinetics and transmission potential of existing and emerging field strains of infectious laryngotracheitis virus. *PLoS One*. 2015; 10: e0120282.
6. Ojkic D, Brash ML, Jackwood MW, Shivaprasad HL. Viral diseases. In: Boulianne M, ed. *Avian Disease Manual*. 7th ed. Jacksonville, FL: American Association of Avian Pathologists, Inc.; 2013:52-53, 62-66.
7. Oldoni I, Rodríguez-Avila A, Riblet SM, et al. Pathogenicity and growth characteristics of selected infectious laryngotracheitis virus strains from the United States. *Avian Pathol*. 2009; 38(1):47-53.
8. Pitesky M, Chin RP, Carnaccini S, et al. Spatial and temporal epidemiology of infectious laryngotracheitis in central California: 2000–2012. *Avian Diseases*. 2014; 58 (4):558-565.

9. Shan-Chia Ou, Giambrone JJ. Infectious laryngotracheitis virus in chickens. *World J Virol*. 2012; 1(5): 142–149.

Self-Assessment - WSC 2017-2018 Conference 6

1. Which of the following does NOT cause lymphoma in chickens?
    a. Reticuloendotheliosis virus
    b. Avian coronavirus
    c. Gallid herpesvirus-2
    d. Avian leukosis virus

2. Which of the following has often been associated with chicken adenovirus infection?
    a. Avian retrovirus
    b. Avian birnavirus
    c. Avian coronavirus
    d. Avian influenzavirus

3. Which of the following is not true about ionophore toxicity?
    a. They facilitate potassium loss and calcium uptake.
    b. Type II myofibers are preferentially affected.
    c. Simultaneous administration of other drugs may increase toxicity
    d. Monogastric animals have reduced tolerance for these drugs

4. Which of the following is not considered a gross differential for infectious laryngotracheitis in poultry*?*
    a. Aspergillosis
    b. Avian influenza
    c. Mycoplasmosis
    d. Infectious bronchitis

5. Which of the following is not true concerning infectious laryngotracheitis in chickens?
    a. The fusion protein in gallid herpesvirus 1 is responsible for syncytia formation.
    b. Reduced egg production may be seen in mild forms.
    c. Intranuclear inclusions may not be visualized in later stages of the disease.
    d. Vaccination may result in a latent carrier state.

Please email your completed assessment to Ms. Jessica Gold at Jessica.d.gold2.ctr@mail.mil for grading. Passing score is 80%.This program (RACE program number) is approved by the AAVSB RACE to offer a total of 0.5 CE Credits, with a maximum of 12.5 CE Credits being available to any individual Veterinary Medical Professionals for the 2017-2018 Wednesday Slide Conference. This RACE approval is for the subject matter categories of: SCIENTIFIC using the delivery method of NON-INTERACTIVE DISTANCE. This approval is valid in jurisdictions which recognize AAVSB RACE; however, participants are responsible for ascertaining each board's CE requirements.
RACE does not "accredit", "endorse" or "certify" any program or person, nor does RACE approval validate the content of the program.

Joint Pathology Center
Veterinary Pathology Services

WEDNESDAY SLIDE CONFERENCE 2017-2018

Conference 7

18 October 2017

CASE I: F1753191 (JPC 4101076).

Signalment: 9-year-old, female intact, Rock Alpine goat, *Capra aegagrus hircus*, caprine.

History: A 9-year-old, female intact Rock Alpine goat presented to Colorado State University Veterinary Teaching Hospital two months prior to necropsy with a three-day history of hyporexia and lethargy which had progressed to lateral recumbency and complete anorexia. The referring veterinarian had previously diagnosed the doe with louse infestation, endoparasites and a heart murmur. Bloodwork by the referring veterinarian revealed a regenerative anemia, stress leukogram and hypoproteinemia characterized by hypoalbuminemia and the goat was treated with ivermectin. Bloodwork at CSU revealed hyperglycemia and elevated creatinine, creatine kinase and aspartate aminotransferase levels. A fecal floatation revealed heavy loads of coccidia, strongyles and *Trichuris* spp**.** During a nine day hospitalization, the doe was treated with intravenous fluids, kaopectate, thiamine, fenbendazole, sulfadimethoxine, oxy-tetracycline and multiple blood transfusions. After significant improvement of her clinical signs and bloodwork, including partial resolution of the dermatitis, the doe was

Haired skin goat. The skin was dry, alopecia, and covered with hyperkeratotic crusts and ulcers. (Photo courtesy of: Colorado State University, Microbiology, Immunology, and Pathology Department, College of Veterinary Medicine and Biomedical Sciences, http://csucvmbs.colostate.edu/academics/mip/Pages/default.aspx)

discharged.

Two months later, the goat presented with a one month history of progressive scaling and ulceration over the withers, dew claws, and coronary bands and acutely progressive lethargy. On physical exam, the doe was febrile, tachypneic and tachycardic. Thoracic radiographs showed a large space-occupying mass which filled the cranial mediastinum and caudally displaced the heart. The doe appeared to be significantly painful, exhibiting shifting leg lameness and refusing to lie down. Humane euthanasia was elected.

Gross Pathology: Presented for postmortem examination was the carcass of a 9-year-old, female intact Alpine goat in good body condition with mild autolysis. Approximately 60% of the skin was markedly dry, thickened and alopecic with exfoliating epithelial crusts which were often tangled within scant remaining hairs. This lesion most severely affected the skin over the epaxials, the ventral abdomen and teats, coronary bands and dew claws. Lesions were multifocally ulcerated with a reddened hemorrhagic underlying dermis. Occupying approximately 40% of the thoracic cavity was a large 12x8x8cm white, multilobular and cystic mass located cranial to the heart within the mediastinal space. An 8 cm in diameter cystic cavity in the mass was filled with translucent yellow fluid. The heart was caudally displaced and the pericardial sac contained approximately 200 mL of serous fluid. Small strands of fibrin were attached to regions of the pleura and pericardial sac which were in contact with the mass. All other organ systems were grossly within normal limits.

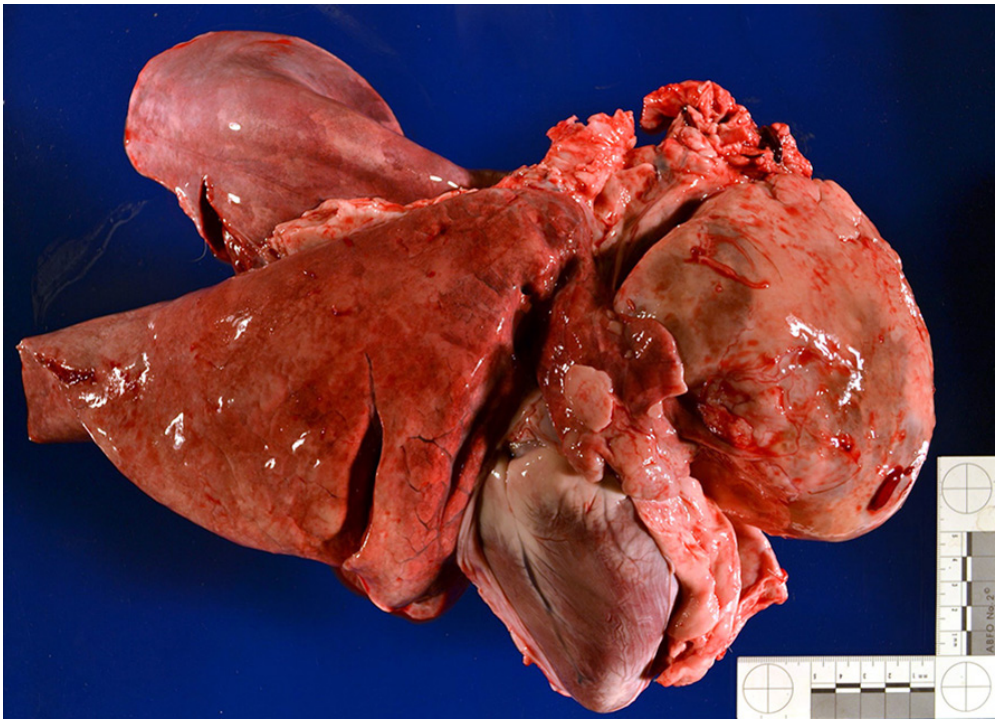

Haired skin goat. An 8cm cystic mass within the cranial mediastinum displaces the heart caudally. (Photo courtesy of: Colorado State University, Microbiology, Immunology, and Pathology Department, College of Veterinary Medicine and Biomedical Sciences, http://csucvmbs.colostate.edu/academics/mip/Pages/default.aspx)

Laboratory results (clinical pathology, microbiology, PCR, ELISA, etc.)**:** Bloodwork was performed at CSU during the doe's second hospitalization.

Initial PCV was 30% with a total protein of 6.5 G/dl. CBC showed neutrophilia (12.2; 2-6 x 10^3/ul) and no ongoing evidence of anemia. Chemistry showed hypoalbuminemia (2.2; 3.3-4.2 g/dL), mild

hyperglobulinemia (5.0; 3.4-4.8 g/dL), hyperglycemia (207; 45-75 mG/dL), hypomagnesemia (1.4; 2.2-2.9 mg/dL), mild hypokalemia (3.67; 3.8-6.3mEQ/L), mild hypochloremia (105.0; 109-117 mEQ/L) and hypoferremia (51; 110-200 uG/dL)

Microscopic Description: Haired skin: The epidermal-dermal junction and perifollicular interstitium are multifocally infiltrated by moderate numbers of lymphocytes. The superficial dermis is expanded by a moderately dense band of lymphocytes with occasional plasma cells, macrophages and neutrophils. Low numbers of mixed inflammatory cells (lymphocytes, plasma cells, neutrophils and macrophages) are present in the dermis. The epidermis is multifocally acanthotic with orthokeratotic and parakeratotic hyperkeratosis. Folli-culosebaceous units are decreased in number (variable in sections). Remaining units are variably atrophied. Individual keratinocytes and basal cells and rare follicular epithelial cells are shrunken with hypereosinophilic cytoplasm and pyknotic or lost nuclei and there is occasional satellitosis. Basal cells are occasionally swollen with abundant vacuolated cytoplasm. There is multifocal ulceration and a thick crust composed of numerous degenerate neutrophils, hair shaft fragments and keratin flakes admixed with abundant eosinophilic debris and occasional serum lakes. Scattered throughout this crust are numerous colonies of 1-3 micron cocci, 2-4 micron long asymmetrically peanut-shaped budding yeasts and rare ruminal contents.

Cranial mediastinal mass: Examined is an encapsulated, highly cellular neoplasm. The neoplasm is composed of loose cords of large polygonal epithelial cells supported by a delicate fibrovascular stroma. Cells have distinct cell borders and abundant eosinophilic cytoplasm. Cell nuclei are

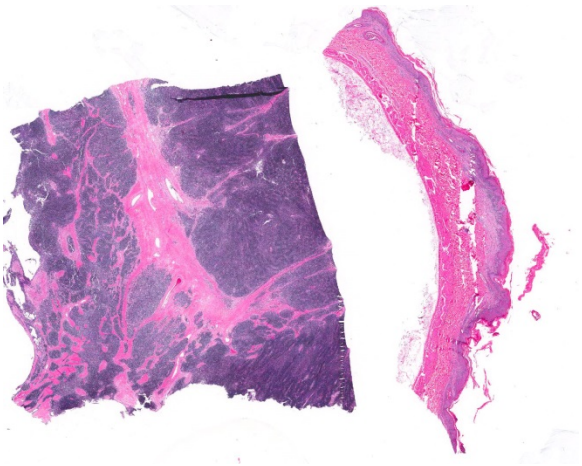

Thymus, skin, goat. A segment of the mediastinal mass and thickened skin are presented for examination. (HE, 5X)

ovoid with finely stippled chromatin and indistinct nucleoli. Anisocytosis and anisokaryosis are marked. Mitoses are rare. The neoplasm is infiltrated and frequently obscured by sheets of numerous small mature lymphocytes.

Immunohistochemistry for cytokeratin, CD3, and CD79a was performed on the cranial mediastinal mass. Neoplastic epithelial cells demonstrated strong, diffuse cytoplasmic immunoreactivity for cytokeratin. Approximately 95% of lympho-cytes infiltrating the mass are CD3 immunoreactive. Rare infiltrating lympho-cytes are immunoreactive for CD79a within the cytoplasm.

In serial sections of skin, a GMS preparation highlighted superficial argyrophilic asymmetric 2-4 micron long, peanut-shaped yeasts and a Gram stain highlighted 1-3umgram positive cocci.

Contributor's Morphologic Diagnoses:

1. Haired skin: Dermatitis and folliculitis, interface, lymphocytic, chronic active, severe with rare keratinocyte, basal cell and follicular

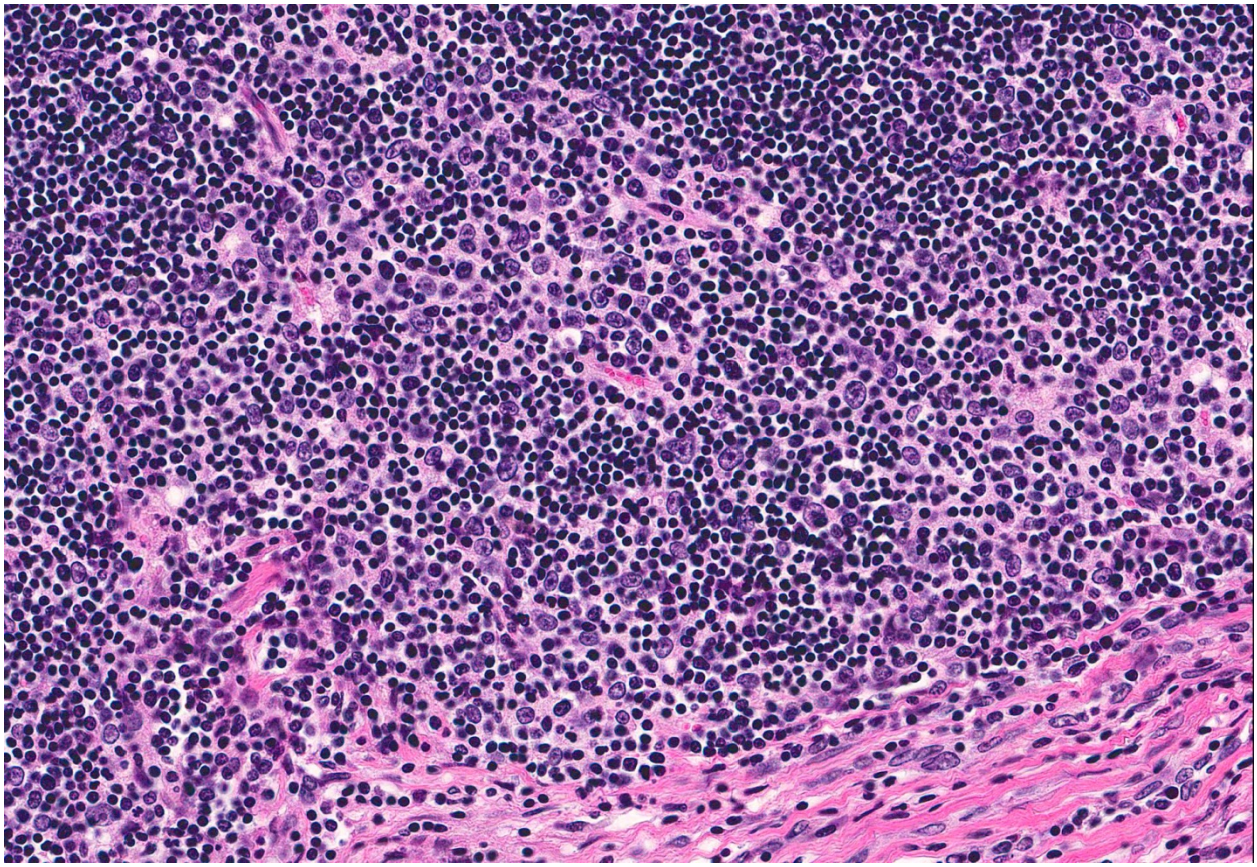

Thymus, goat. Admixed with numerous lymphocytes is a background of neoplastic epithelial cells with large open-faced nuclei and prominent nucleoli. (HE, 400X)

epithelial cell apoptosis and superficial cocci and yeasts.

2. Cranial mediastinal mass: Thymoma, lymphoepithelial (mixed).

Name of Disease: Thymoma-associated exfoliative dermatitis

Contributor's Comment: Thymomas arise from the epithelial components of the thymus. They are classified as epithelial, lymphocytic or lymphoepithelial (mixed), based on the degree of infiltration by non-neoplastic lymphocytes. In one survey of 102 tumors in goats, thymomas represented the third most common tumor.[6] Dairy breeds may be predisposed.[5] These tumors tend to be benign, although there is a report of thymic carcinoma in one goat with metastases to the lung and spleen.[7] Frequently thymomas are an incidental finding in goats with no associated clinical signs; however, reported sequelae include congestive heart failure and megaesophagus.[8,9]

Thymoma-associated exfoliative dermatitis is an established paraneoplastic syndrome of cats.[1, 4, 10, 11] The syndrome has also been reported in rabbits.[3] It has been posited that the mechanism of the dermatologic lesion is rooted in the tumor-supported development of a population of autoreactive T cells which target keratinocytes.[4] The classic feline cutaneous lesion has been previously described as a cell–poor interface dermatitis with telogenization of follicles.[4] However, in a case series of five cats as well as this goat, the lesion is significantly cell-rich,

forming large bands of inflammation at the epidermal-dermal interface.[10] Other paraneoplastic syndromes which have been associated with thymomas include myasthenia gravis, polymyositis and granulocytopenia.[11]

Gross lesions in this case were quite striking. Extensive regions of alopecia, erythema and ulceration with large exfoliative flakes affected the dorsum, ventrum and even the teats and dew claws. Histologically, the lesion is characterized by transepidermal and follicular apoptosis, interface dermatitis and hyperkeratosis. The inflammatory infiltrates are composed of lymphocytes, plasma cells, macrophages and superficially located neutrophils. In some cases, sebaceous glands are lost. The lesion can be quite subtle; however, in this case there are regions which are severely affected. The presence of cocci and yeasts consistent with *Malassezia spp.* varied between sections of the tissue. Secondary infection with bacteria and yeasts can exacerbate the dermatitis and induce pruritus.[2]

Given the prevalence of thymomas in goats and the frequent lack of directly associated clinical signs, this case is of diagnostic interest for dermatologic lesions in goats. As thymoma-associated exfoliative dermatitis can be histologically similar to erythema multiforme and lupus erythematosus, diagnosis is contingent on the clinical diagnosis of a thymoma. Interestingly, post-thymectomy resolution of the dermatologic lesion has been reported in some cases in cats.[1, 2]

JPC Diagnosis: 1. Thymus: Thymoma (lymphocytic type), Rock Alpine goat (*Capra aegagrus hircus)*, caprine.
2. Skin: Dermatitis, lymphocytic, interface, diffuse, mild to moderate with multifocal

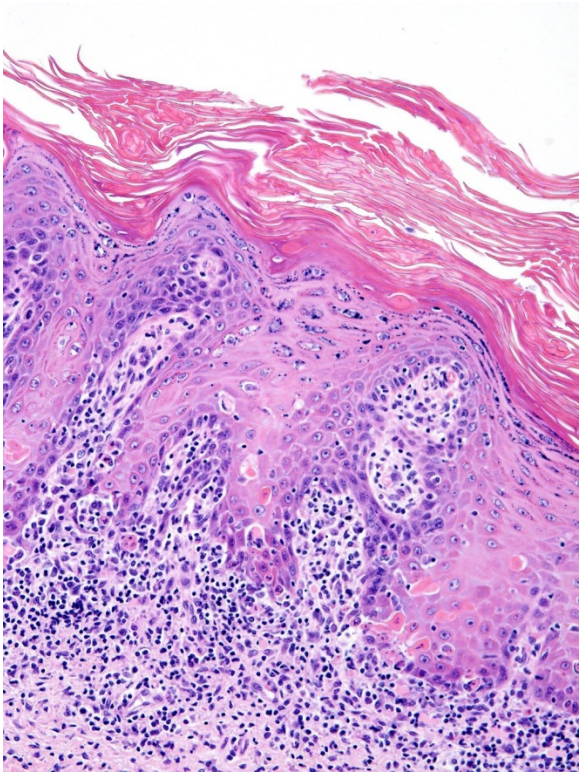

Haired skin, goat. There is a prominent lymphocytic infiltrate in the surperficial dermis. Shrunken, hypeosinophilic keratinocytes (arrows) are present at all levels of the dermis, and there is a thick layer of orthokeratotic hyperplasia overlying the dermis. (HE, 400X)(Photo courtesy of: Colorado State University, Microbiology, Immunology, and Pathology Department, College of Veterinary Medicine and Biomedical Sciences, http://csucvmbs.colostate.edu/academics/mip/Pages/default.aspx)

epithelial hyperplasia, keratinocyte apoptosis, intracorneal pustules, and orthokeratotic and parakeratotic hyperkeratosis.

Conference Comment: Paraneoplastic syndromes are systemic conditions caused most commonly by excessive production of a "normal" hormone by neoplastic cells. The clinical signs they produce are often quite remarkable and are usually the reason the animal is brought to the veterinarian. Clinically, they serve as convenient markers for diagnosticians, and may serve to indicate neoplastic response to treatment. One or more of the following criteria must be met in

order to classify a clinical syndrome as paraneoplastic: (1) when the neoplasm is removed or treated, the concentration of the hormone decreases, (2) after removal of the normal gland producing the hormone, the concentration remains the same or increases, (3) there is a positive arteriovenous concentration of the hormone across the tumor, (4) there is production and secretion of the hormone product *in vitro*. In veterinary literature, the first criterion is most common.

There are several proposed pathogenic mechanisms of paraneoplastic syndromes including: (1) gene de-repression, resulting in the production of active hormones that are usually repressed; (2) ectopic receptor production by a tumor, resulting in displaced hormonal activity (an example is acetylcholine receptors produced by thymomas resulting in anti-acetylcholine receptor antibodies produced by the host immune system, leading to muscle weakness and megaesophagus that characterizes myasthenia gravis); (3) exposure to normally "hidden" substances which the immune system perceives as foreign andmounts a type III hypersensitivity reaction against, with formation of immune complexes. Cachexia is the most common paraneoplastic response and occurs secondary to any neoplastic process because it is caused by rapid tumor growth and utilization of nutrients at the expense of the animal. It is hypothesized to be related the effects of the following pro-inflammatory mediators: tumor necrosis factor (TNF), interleukins 1 and 6 (IL-1 and IL-6) and interferon gamma and alpha (IFNγ and IFNα).[2]

Table 1: Common paraneoplastic syndromes in veterinary species[2, 15]

Paraneoplastic syndrome	**Associated neoplasm**
Endocrine	
Hypercalcemia of malignancy	Lymphoma Apocrine gland carcinoma of the anal sac gland Mammary carcinoma Thymoma
Hypoglycemia	Hepatocellular carcinoma Salivary gland carcinoma Leiomyoma/leiomyosarcoma Plasma cell tumor Lymphoma
Ectopic ACTH	Pulmonary carcinoma
Cutaneous	
Pemphigus	Lymphoma
Alopecia	Pancreatic carcinoma (cat)
Exfoliative dermatitis	Thymoma (cat, rabbit)
Necrolytic migratory erythema	Glucagonoma
Hematologic	
Hypergammaglobulinemia	Multiple myeloma

	Lymphoma
Anemia	Numerous neoplasms
Erythrocytosis	Renal carcinoma
Neurologic	
Myasthenia gravis	Thymoma
Peripheral neuropathy	Insulinoma
Renal	
Glomerulonephritis	Multiple myeloma Polycythemia vera
Gastrointestinal	
Gastroduodenal ulceration	Mast cell tumors Gastrinoma
Miscellaneous	
Hypertrophic osteopathy	Pulmonary carcinoma Other thoracic masses Urinary bladder rhabdomyosarcoma
Cachexia	Numerous neoplasms

Thymomas have been rarely reported in most domestic animal species and present as a lobulated mass in the cranial mediastinum in adult to older animals and commonly replace one lobe with thymic remnant compressed at the periphery. In addition to the classification based on cell type and atypia listed above (epithelial, lymphocytic, or mixed) a more accurate classification has been based on two main benign phenotypes: type A (composed of spindle shaped cells) and type B (composed of epithelioid cells). Type B thymomas are more common in dogs and are further subdivided into three subtypes: (1) type B1 which resembles normal thymus with extensive lymphocyte proliferation (may be mistaken for a lymphoid neoplasm), (2) type B2 with neoplastic epithelial cells that are more plump, with vesiculate nuclei that are more easily discernible on a dense background of lymphocytes, and (3) type B3 which contain large sheets of neoplastic epithelial cells and very few lymphocytes. Type AB thymomas are plausibly a mix of the two with both epithelial neoplastic cells and lymphocytes mixed together. In goats and sheep, type AB are most common and present as striking space occupying masses in older females which are often incidental findings during necropsy.[16] Clinical signs associated with thymomas include respiratory distress and ventral head and neck edema as well as several paraneoplastic conditions often associated with some form of autoimmunity. The most common is myasthenia gravis which results in generalized muscle weakness and megaesophagus (mechanism described above). Secondary neoplasias such as osteosarcoma and mammary tumors, immune-mediated skin diseases, hypercalcemia, and polymyositis have also been reported.[15] Hypercalcemia is due to production of PTHrp which results in increased osteoclastic activity and increased calcium reabsorption in the proximal and distal convoluted tubules of the kidney.[11] In human medicine, the mechanism of

increased autoimmunity has been worked out and is explained in the following sentences. The thymus, under normal conditions, plays a central part in the development of immunity and prevention of autoimmunity. Thymic epithelial cells express MHC I and MHC II antigens that react with circulating T-lymphocytes. Thymomas enhance thymic lymphopoiesis; expression of autoantigens and reduced expression of MHC molecules and autoimmune regulator molecules (AIRE) on neoplastic epithelial cells results in unreliable negative selection and release of autoreactive T lymphocytes.[15]

For the lesions in the skin, conference participants also considered erythema multiforme (EM) which is an autoimmune skin disorder that has been anecdotally reported in the goat. EM has been reported in association with a number of disorders, including: adverse drug reactions, infectious diseases (parvovirus infection in dogs, *Equid herpesvirus*-5, feline herpesviral infections), and in cats, thymoma-associated exfoliative dermatitis has been equated to EM in the literature. Grossly, EM presents as erythematous papules and plaques with a central area of clearing. The classic microscopic presentation is cytotoxic (interface) dermatitis with necrotic keratinocytes scattered throughout all layers of the epidermis and follicular epithelium often surrounded by lymphocytes (satellitosis).[8]

Contributing Institution:
Colorado State University
Microbiology, Immunology, and Pathology Department
College of Veterinary Medicine and Biomedical Sciences
http://csucvmbs.colostate.edu/academics/mip/Pages/default.aspx

References:

1. Cavalcanti J, Moura M, Monteiro F. Thymoma associated with exfoliative dermatitis in a cat. *J Feline Med Surg*. 2014;16(12):1020-1030.
2. Cullen JM, Breen M. An overview of molecular cancer pathogenesis, prognosis, and diagnosis. In: Meuten DJ, ed. *Tumors of Domestic Animals.* 5th ed. Ames, IA: John Wiley & Sons, Inc.; 2017:15-16.
3. Forster-Van Hijfte MA, Curtis CF, White RN. Resolution of exfoliative dermatitis and Malassezia pachydermatis overgrowth in a cat after surgical thymoma resection. *J Small Anim Pract*. 1997;38(10):451-454.
4. Florizoone K. Thymoma-associated exfoliative dermatitis in a rabbit. *Vet Dermatol*. 2005;16(4):281-284.
5. Gross TL. Ihrke PJ. Walder EJ, et al. *Skin Diseases of the Dog and Cat*. 2nd ed. Ames, IA: Blackwell Science Ltd; 2005:68-70, 78-79
6. Hadlow WJ. High prevalence of thymoma in the dairy goat report of seventeen cases. *Vet Pathol*. 1978;15:153-169.
7. Löhr C V. One hundred two tumors in 100 goats. *Vet Pathol*. 2012;50(4):668-675.
8. Mauldin EA, Peters-Kennedy J. Integumentary system. In: Maxie MG, ed. *Jubb, Kennedy, and Palmer's Pathology of Domestic Animals*. Vol. 1. 6th ed. St. Louis, MO: Elsevier; 2016:609-610.
9. Olchowy T, Toal R, Brenneman K, Slauson D, McEntee M. Metastatic thymoma in a goat. *Can Vet J*. 1996;37(3):165-167.
10. Parish SM, Middleton JR, Baldwin TJ. Clinical megaoesophagus in a goat with thymoma. *Vet Rec*. 1996;139:94.
11. Rosol TJ, Meuten DJ. Tumors of the endocrine glands. In: Meuten DJ, ed.

Tumors of Domestic Animals. 5th ed. Ames, IA: John Wiley & Sons, Inc.; 2017:816-821.
12. Rostkowski CM, Stirtzinger T, Baird JD. Congestive heart failure associated with thymoma in two nubian goats. *Can Vet J*. 1985;26:267-269.
13. Rottenberg S, Tscharner C Von, Roosje PJ. Thymoma-associated exfoliative dermatitis in cats. *Vet Pathol*. 2004;41(4):429-433.
14. Singh A, Boston SE, Poma R. Thymoma-associated exfoliative dermatitis with post-thymectomy myasthenia gravis in a cat. *Can Vet J*. 2010;51.
15. Valli VE, Bienzle D, Meuten DJ. In: Meuten DJ, ed. *Tumors of Domestic Animals.* 5th ed. Ames, IA: John Wiley & Sons, Inc.; 2017:305-307.
16. Valli VEO, Kiupel M, Bienzle D, Wood RD. Hematopoietic system. In: Maxie MG, ed. *Jubb, Kennedy, and Palmer's Pathology of Domestic Animals*. Vol. 3. 6th ed. St. Louis, MO: Elsevier; 2016:151-158.

CASE II: 17-14227 (JPC 4102437).

Signalment: 11-year-old female spayed Siberian husky, *Canis familiaris*, canine.

History: Two months prior to surgery, the patient presented to its primary veterinarian for labored breathing after an altercation with another dog. Radiographs at that visit revealed a thoracic mass cranioventral to the heart. The patient was referred to the cardiology service for an echocardiogram which showed mild pericardial effusion and confirmed the presence of an extra-pericardial, thin-walled, fluid-filled structure cranial to the heart with no associated blood flow. A thoracic CT scan found a 5.9 cm x 4.9 cm x 4.2 cm oval, well-defined, thin-walled soft tissue attenuating mass in the cranial mediastinum with a tubular structure that communicated with the pericardial lumen. Cytology of the fluid within the mass revealed malignant cohesive cells suggestive of carcinoma, but mesothelioma could not be ruled out. The patient presented two months later for tachypnea at which visit moderate pericardial fluid with cardiac tamponade as well as mild pleural effusion was found on cardiac ultrasound. Clinical improvement was short lived (< 5 days) after pericardiocentesis. At that time, a subtotal pericardiectomy was elected to remove the cystic mass.

Gross Pathology: Intra-operative findings: The pericardial cystic mass was connected to the pericardium by a 1.5cm orifice at its craniodorsal aspect. On sectioning of the mass, multifocal nodules with an irregular, granular surface extend from the wall of the cystic mass. The affected and adjacent pericardium was mildly thickened.

Laboratory results (clinical pathology, microbiology, PCR, ELISA, etc.)**:** Cytology of fluid from the cystic mass was consistent with carcinoma with evidence of hemorrhage; cytomorphologic features

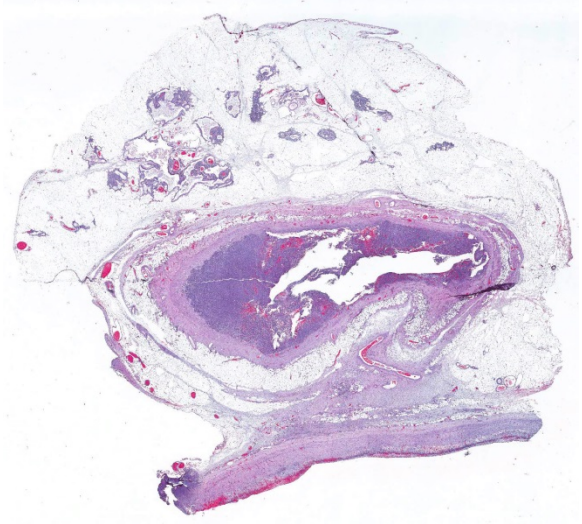

Pericardium, dog. At subgross magnification, there is a densely cellular neoplasm circumferentially lining a sleeve of pericardium. (HE, 5X)

suggest carcinoma (adenocarcinoma) or possible mesothelioma.

Microscopic Description: Pericardial mass: Focally expanding the pericardial adipose tissue is an encapsulated, well-vascularized mass with a large central cavitation. At the periphery, there are multifocal nodules of densely packed sheets of neoplastic polygonal cells with rare papillary formations supported by a small fibrovascular core. Neoplastic cells exhibit marked anisocytosis and anisokaryosis as well as moderate nuclear pleomorphism. Nuclei contain lacy chromatin with distinct, sometimes multiple nucleoli. Cells contain a moderate amount of eosinophilic, variably vacuolated cytoplasm. There are 24 mitotic figures in 10 high power fields with frequent bizarre mitotic figures. Binucleation and karyomegaly are occasionally present. Intra-capsular (not represented on chosen slides) and lymphatic invasion are present. There is multifocal coagulative necrosis and mild hemorrhage. Within the surrounding adipose tissue there are multiple tubular structures lined by simple, ciliated cuboidal epithelium supported by a small amount of fibrous connective tissue which is associated with numerous lymphocytes and plasma cells. The lumens of these tubules contain amorphous, sometimes beaded, eosinophilic material mixed with foamy macrophages and varying number of lymphocytes and plasma cells. The pericardium is markedly expanded by highly cellular collagenous tissue with abundant neovascularization and hemorrhage mixed with mild

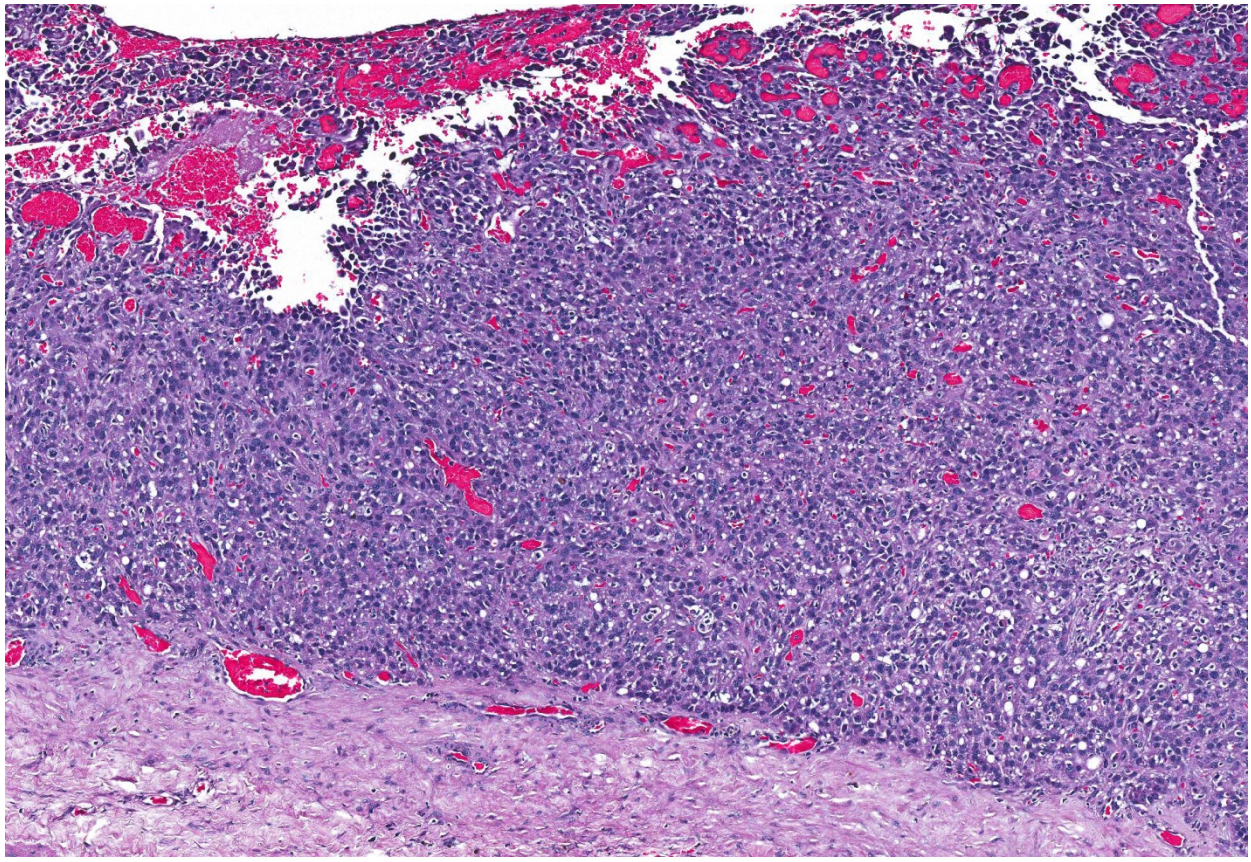

Pericardium, dog. Neoplastic cells arise from the pericardium and are arranged in sheets, forming papillary and micropapillary projections into the lumen. (HE, 112X)

lymphoplasmacytic and histiocytic inflammation. Histiocytes often contain course golden-brown pigment (interpreted as hemosiderin).

By immunohistochemistry, the neoplastic cells of the pericardial mass exhibit weak diffuse cytoplasmic immunoreactivity for cytokeratin (wide spectrum, WSS) in approximately 5% of tumor cells (mostly cells located centrally and those that are dissociated). Over 80% of cells have moderate to intense diffuse cytoplasmic vimentin staining (staining is most intense centrally within the mass).

Contributor's Morphologic Diagnoses:

1. Mesothelioma, solid variant, with capsular and lymphatic invasion
2. Persistent branchial pouch (embryologic remnants)

Contributor's Comment: Mesothelioma is a rare neoplasm in domestic animal species, which typically arise from serosa of the pleura, peritoneum or tunica vaginalis, though pericardial mesotheliomas have been documented with relative frequency in the dog[7-9,11,14]. Based on their immunohistochemical profile, mesotheliomas are believed to arise from proliferating multipotent subserosal progenitor cells which are immunopositive for both vimentin and cytokeratin (AE1/AE3 in this study).[12] Their resting counterparts are immunopositive for vimentin but not cytokeratin. Conversely, terminally-differentiated surface mesothelium is immunopositive for cytokeratin but not vimentin.

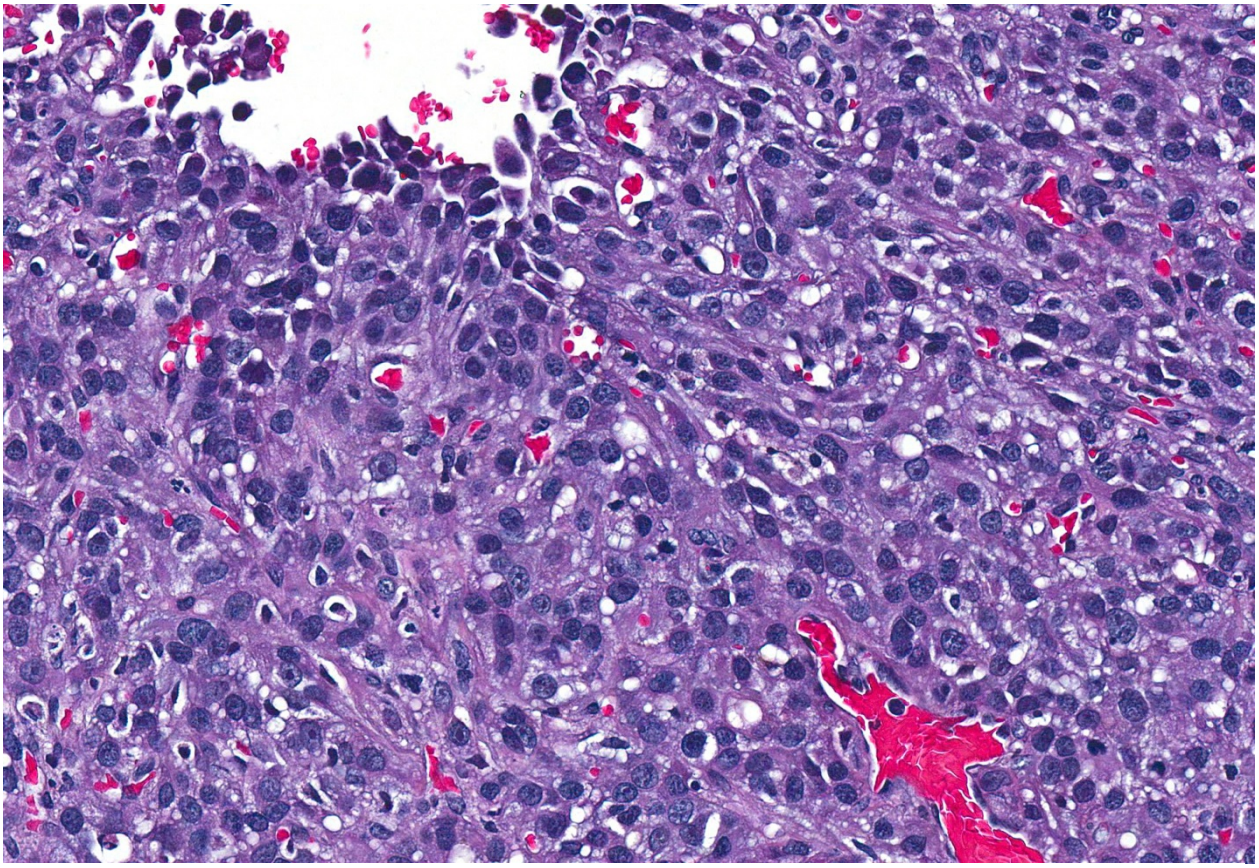

Pericardium dog. Neoplastic cells have indistinct cell borders with moderate amounts of vacuolated eosinophilic cytoplasm. There is moderate anisokaryosis and prominent nucleoli. Lymphocytes are scattered throughout the neoplasm. (HE, 400X)

Several histological subtypes have been categorized: epithelial, spindle and mixed.[11] Further classification of the epithelial subtype has been described by Harbison and Godleski in which there are: 1) papillary form supported by abundant fibrous stroma, 2) less organized papillary form with scant stroma and 3) anaplastic form which makes solid sheets.[10] Based on these findings, we have subclassified this particular neoplasm as a solid or anaplastic variant. To our knowledge, histologic subtype has not been found to be prognostically significant.

In addition to being both cytokeratin- and vimentin-positive, mesothelial cells stain with Alcian blue due to their production of hyaluronic acid, a mucopolysaccarhide.[15] Common ultrastructural features of mesotheliomas include the presence of long microvilli at their surface, desmosomes and tonofilaments.[10]

Biological behavior of pericardial mesotheliomas is similar to mesotheliomas that arise at other sites in that they spread via transplantation, local extension and regional metastasis, with distant metastases occurring rarely.[10] The presence of clusters of atypical mesothelial cells in lymph nodes of patients with pericardial effusion should be interpreted with caution, as embolized mesothelial cells have been found in regional lymph nodes in dogs with non-neoplastic pericardial effusion.[15,19] It is purported that the local inflammation results in widening of intercellular stomata within the mesothelium, through which des-quamated reactive mesothelial cells can enter the subserosal stroma and sub-sequently enter regional lymph nodes by way of subserosal lymphatics.[19]

An underlying cause for the development of mesothelioma in dogs remains to be

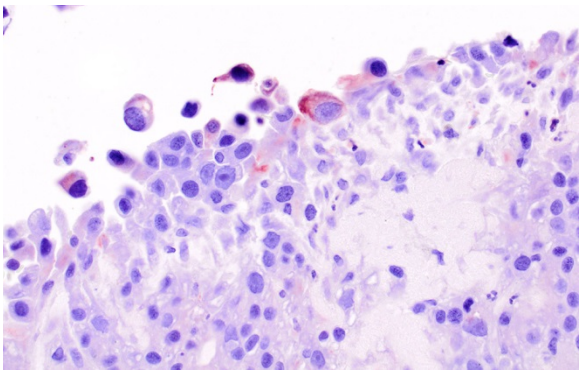

Pericardium, dog. Scattered neoplastic cells exhibit moderate cytoplasmic immunoreactivity for cytokeratin. (anti-AE1/AE3, 400X) (Photo courtesy of: Oregon Veterinary Diagnostic Laboratory, Oregon State University College of Veterinary Medicine, http://vetmed.oregonstate.edu/diagnostic)

elucidated. Spontaneous mesothelioma of the tunica vaginalis has been well-characterized in male Fisher 344/N rats.[4] In humans, inhalation of asbestos and exposure to Simian virus 40 (SV40) have been linked to mesothelioma.[6,10] With regard to pericardial mesothelioma in dogs, asbestos might be a potential contributing factor, particularly for those living in urban settings.[10] A causal relationship between asbestos and mesothelioma has not been established, however, and many cases of canine mesothelioma do not have any known exposure to asbestos. In addition, there is a case series of golden retrievers who developed pericardial mesotheliomas after protracted histories of idiopathic hemorrhagic pericardial effusion, suggestive of a chronic inflammatory pathogenesis.[11]

Based on the unusual clinical description of this lesion, another one interpretation might be malignant transformation of a pericardial cyst. Sisson et al. describes intrapericardial cysts as unilocular or multilocular cysts lined by reactive mesothelium supported by a small amount of fibrous stroma.[17]

Another differential for mediastinal neoplasia is ectopic thyroid carcinoma.

Investigation into intrapericardial neoplasia in dogs found a single case of ectopic thyroid carcinoma as well as a single case of mesothelioma.[8] Development of a papillary carcinoma from ectopic thyroid tissue within a branchial cyst has been documented in humans.[13] Branchial pouches are embryologic structures that develop into various parts of the head and neck, including medullary C-cells of the thyroid gland.[1] Medullary and follicular thyroid carcinomas have been found to be both cytokeratin and vimentin positive using immuno-histochemistry.[4,5,16] Expression of vimentin in carcinomas is believed to facilitate in tumor progression, namely the phenomenon of epithelial-mesenchymal transformation (EMT). Immunohistochemistry for thyroglobulin and calcitonin was not performed on this mass.

JPC Diagnosis: 1. Pericardium: Mesothelioma, Siberian husky (*Canis familiaris)*, canine.
2. Pericardial fat: Branchial cysts, multiple.

Conference Comment: Mesotheliomas have been reported arising from the pleura, pericardium, and peritoneum, as well as the mesothelial lining of the visceral vaginal tunic (an invagination of the peritoneum) of the testis.[2, 14, 19] Of the four locations, mesotheliomas of the peritoneum are most common in domestic animals. Affected animals typically present for peritoneal fluid (ascites), which is characterized cytologically by reactive epithelial-like or mesenchymal-like cells. Cytologic distinction between reactive and neoplastic mesothelial cells is notoriously difficult.

As mentioned by the contributor above there are three recognized histologic subtypes of mesothelioma: epithelioid, spindloid (sarcomatous), and mixed. As with cytology,

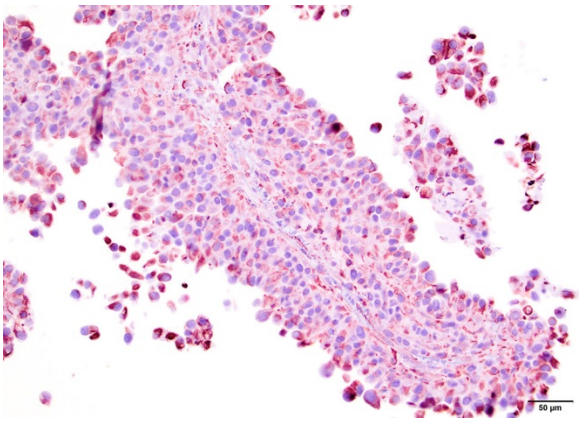

Pericardium, dog. Scattered neoplastic cells exhibit strong cytoplasmic immunoreactivity for vimentin. (anti-vimentin, 400X) (Photo courtesy of: Oregon Veterinary Diagnostic Laboratory, Oregon State University College of Veterinary Medicine, http://vetmed.oregonstate.edu/diagnostic)

histologic differentiation between reactive mesothelium and neoplasia is difficult and is dependent on four factors: (1) invasion of the underlying tissue, (2) the presence of neoplastic mesothelial cells in draining lymph nodes or distant organs, and (3) multiple masses within a body cavity. In addition, mesothelial neoplasia appears much thicker and irregularly arranged, whereas reactive mesothelium generally appears as a single layer of regularly arranged cells. Cellular morphology is generally not helpful because both reactive and neoplastic mesothelial cells can appear either well-differentiated or anaplastic. While many specific immunohistochemical (IHC) stains, including epithelial membrane antigen, desmin, glucose transporter protein-1, p53, and Ki67 have proven diagnostically unreliable, mesothelial cells are somewhat unique in that they exhibit dual expression of vimentin and cytokeratin. Thus the combination of histologic pattern and IHC features are necessary for diagnosis of mesothelioma.[14] Testicular mesotheliomas are quite rare in most domestic species but are described in dogs, bulls, and rats (Fisher 344 strain).[3] Once diagnosed, a presumed

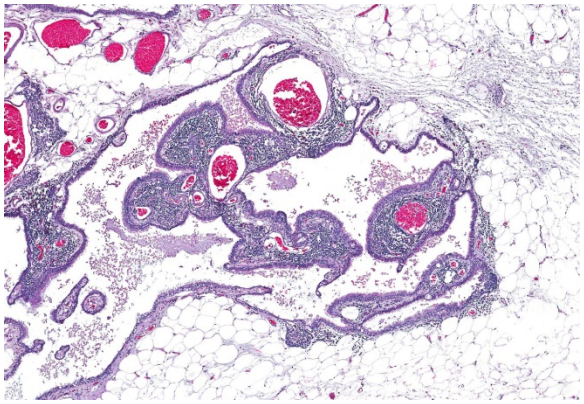

Heart base, dog. The adjacent pericardial fat contains a large multilocular brachial cyst. These cysts are lined by tall columnar ciliated epithelium. (HE, 400X)

primary mesothelioma of the testis must be differentiated from a metastatic mesothelioma that started in one of the other primary locations.[2]

Conference participants discussed the difficult tissue identification in this case, but most noted that the presence of branchial pouch cysts was beneficial. Branchial pouch cysts are congenital and though rare, are usually found in brachycephalic dog breeds. These cysts are often found in the cranial mediastinum (as in this case), close to thymic tissues, and are lined by a single layer of cuboidal epithelial cells.[7]

Contributing Institution:
Oregon Veterinary Diagnostic Laboratory
Oregon State University
College of Veterinary Medicine
http://vetmed.oregonstate.edu/diagnostic

References:

1. Adams A, Mankad K, Offiah C, Childs L. Branchial cleft anomalies: A pictorial review of embryological development and spectrum of imaging findings. *Insights Imaging*. 2016;7:69–76.
2. Agnew DW, MacLachlan NJ. Tumors of the genital systems. In: Meuten DJ, ed. *Tumors of Domestic Animals.* 5th ed. Ames, IA: John Wiley & Sons, Inc.; 2017:713.
3. Barthold SW, Griffey SM, Percy DH. Rat. In: *Pathology of Laboratory Rabbits and Rodents.* 4th ed. Ames, IA: John Wiley & Sons, Inc.; 2016:169.
4. Blackshear PE, Pandiri AR, Ton TT, Clayton NP, Shockley KR, Peddada SD, Gerrish KE, Sills RC, Hoenerhoff MJ. Spontaneous mesotheliomas in F344/N rats are characterized by dysregulation of cellular growth and immune function pathways. *Toxicol Pathol.* 2014;42(5): 863-876.
5. Calangiu MC, Simionescu CE, Stepan AE, Cernea D, Zavoi RE, Margaritescu C. The expression of CK19, vimentin and E-cadherin in differentiated thyroid carcinomas. *Rom J Morphol Embryol*. 2014;55(3): 919-925.
6. Carbone M, Pass HI, Miele L, Bocchetta M. New developments about the association of SV40 with human mesothelioma. *Oncogene*. 2003;22: 5173-5180.
7. Caswell JL, Williams KJ. Respiratory system. In: Maxie MG, ed. *Jubb, Kennedy, and Palmer's Pathology of Domestic Animals.* 6th ed. Vol. 2. St. Louis, MO: Elsevier; 2016:502.
8. Fathi A. The role of immunohistochemical markers in diagnosis and prognosis of medullary thyroid carcinoma. *Egypt J Path*. 2013;33: 13–17.
9. Girard C, He'lie P, Odin M. Intrapericardial neoplasia in dogs. *J Vet Diag Invest*. 1999;11: 73-78.
10. Harbison ML, Godleski JJ. Malignant mesothelioma in urban dogs. *Vet Pathol*. 1983; 20: 531-540.
11. Machida N, Tanaka R, Takemura N, Fujii Y, Ueno A, Mitsumori K. Development of pericardial mesothelioma in golden retrievers with a long-term history of idiopathic

haemorrhagic pericardial effusion. *J Comp Path*. 2004;131: 166-175.
12. McDonough SP, MacLachlan NJ, Tobias AH. Canine pericardial mesotheliomas. *Vet Pathol.* 1992;29: 256-260.
13. Mehmood RK, Basha SI, Ghareeb E. A case of papillary carcinoma arising in ectopic thyroid tissue within a branchial cyst with neck node metastasis. *Ear Nose Throat J.* 2006;85(10): 675-676.
14. Munday JS, Lohr CV, Kiupel M. Tumors of the alimentary tract. In: Meuten DJ, ed. *Tumors of Domestic Animals.* 5th ed. Ames, IA: John Wiley & Sons, Inc.; 2017:592-595.
15. Peters M, Tenhunfeld J, Stephan I, Hewicker-Trautwein M. Embolized mesothelial cells within mediastinal lymph nodes of three dogs with idiopathic haemorrhagic pericardial effusion. *J Comp Path*. 2003;128: 107-112.
16. Pineyro P, Vieson MD, Romas-Vara JA, Moon-Larson M, Saunders G. Histopathological and immunohistochemical findings of primary and mestastatic medullary thyroid carcinoma in a young dog. *J Vet Sci*. 2014;15(3): 449-453.
17. Sisson D, Thomas WP, Reed J, Atkins CE, Gelberg HB. Intrapericardial cysts in the dog. *J Vet Int Med.* 1993; 7(6): 364-369.
18. Stepien RL, Whitley NT, Dubielzig RR. Idiopathic or mesothelioma-related pericardial effusion: clinical findings and survival in 17 dogs studied retrospectively. *J Sm Anim Pract*. 2000;41: 342-347.
19. Wilson DW. Tumors of the respiratory tract. In: Meuten DJ, ed. *Tumors of Domestic Animals.* 5th ed. Ames, IA: John Wiley & Sons, Inc.; 2017:495.

CASE III: S9004764 (JPC 4019378).

Signalment: 7-week-old, male, Holstein calf, *Bos taurus*, bovine.

History: A live, 7-week-old, male calf with history of diarrhea, knuckling of the fetlocks, incoordination and stiffness was submitted for necropsy. Some animals in the group showed dyspnea and coughing. Animals were treated with a broad spectrum antibiotic for 4 days.

Gross Pathology: The calf was in good nutritional condition. The abdomen was moderately distended with gas. Tissues were in good state of postmortem decomposition. The forestomachs and abomasum contained a mixture of ingested feed (grain and green forage). There was about 3 liter of straw-colored fluid with fibrin strands in thoracic and abdominal cavities; thick loosely-adherent sheets of yellow fibrin on serous surfaces; and copious amounts of yellowish fibrinous exudates in multiple joints (polyarthritis). Three other in-contact calves had similar necropsy findings

Laboratory results (clinical pathology, microbiology, PCR, ELISA, etc.)**:**

Brainstem, calf: A section of brainstem with 4th ventricle (at right) is presented for examination. (HE, 5X)

Aerobic culture from liver yielded mixed coliforms
Salmonella culture on the colon and liver was negative
Chlamydia culture on tissue pool was negative (guinea pig inoculation, chicken embryos and cell culture).
Virus isolation on tissue pool (lung, brain, spleen) was negative
Immunofluorescent test for *Chlamydia* on the liver and spleen was negative
Immunofluorescent test for bovine corona virus, IBR, BVD was negative
Immunology for IBR was negative (1:4); and BVD was 1:32.
Heavy metal screen, selenium (liver) and cholinesterase (brain) had normal background levels.

Immunohistochemistry using genus-specific *Chlamydia* antiserum on brain and liver sections from parafinized tissue blocks (archived for 22 years): Positive for *Chlamydia* (new name, C*hlamydophila*) elementary bodies.
Microscopic Description: Brain: Thromboembolic malacia, multifocal, with proliferation of glial cells, vasculitis, perivascular cuffing, axonal degeneration, meningitis; lymphocytic, moderate to severe.

Immunohistochemistry (IHC) staining of the brain is positive for elementary bodies (EB) of *Chlamydophila*; presumptive, *Cp. pecorum*. Photomicrograph of brain IHC is included (see positive staining of elementary

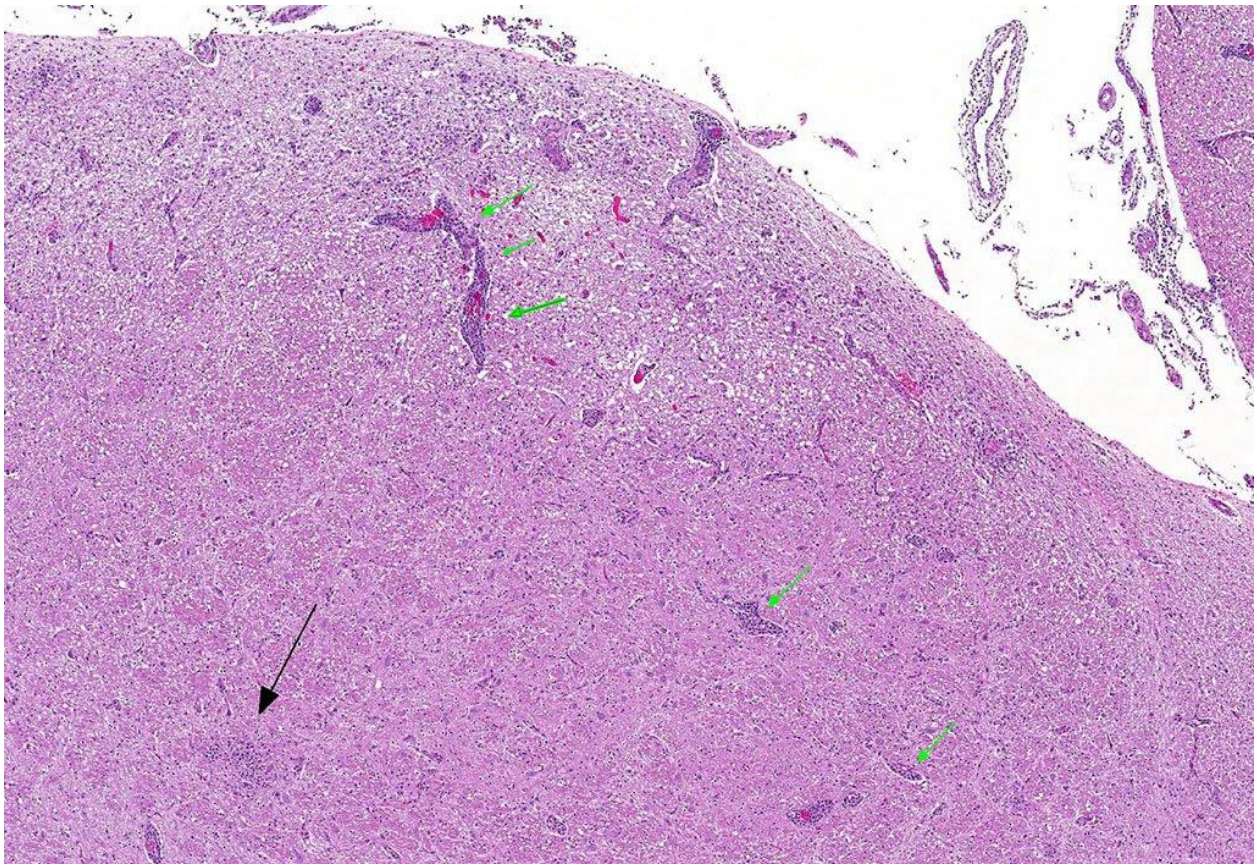

Brainstem, calf: Throughout the section, there is prominent cellular expansion of Virchow-Robin's space (green arrows), and there is pallor of the submeningeal parenchyma. Glial nodules are scattered randomly throughout the section (black arrows) (HE, 40X)

bodies in macrophages and endothelial cells).

Contributor's Morphologic Diagnoses:
Brain: Encephalitis, lymphocytic, multifocal with thromboembolic malacia, vasculitis, perivascular cuffing and meningitis; moderate to severe.

Contributor's Comment: When this case was submitted about 22 years ago, a presumptive diagnosis of sporadic bovine encephalomyelitis was made based on clinicopathological findings. the attempt to isolate chlamydial agent was negative, perhaps because of medication with broad-spectrum antibiotics. Serum sample from another sick calf in the group with similar clinical signs and lesions was positive by complement fixation test for *Chlamydia* antibodies. Recently, because of the availability of IHC, the paraffin block of the brain was retrieved from our repository and tested. We detected positive staining elementary bodies of *Chlamydophila (*new name for *Chlamydia)* using genus-specific *Chlamydia trochomatis* (MONOTOPE™) antiserum.[9] According to the manufacturer, the antiserum has cross reactivity with *C. pneumoniae* and *C. psittaci.*

Intracellular bacteria of the order *Chlamydiales* were first associated with diseases of cattle (*Bos taurus*) when McNutt isolated such organisms from feedlot cattle with sporadic bovine encephalomyelitis.[6] Menges[7] and Wenner[10] in 1953 studied the disease further and proved it was due to an agent belonging to the psittacosis-lymphogranuloma group of viruses. There are currently four families, six genera and 13 species within the order *Chlamydiales* that have valid published names.[4] Two species of the genus *Chlamydophila* cause disease in ruminants: *Cp. abortus* (formerly *Chlamydia psittaci* serotype 1) and *Cp. pecorum*

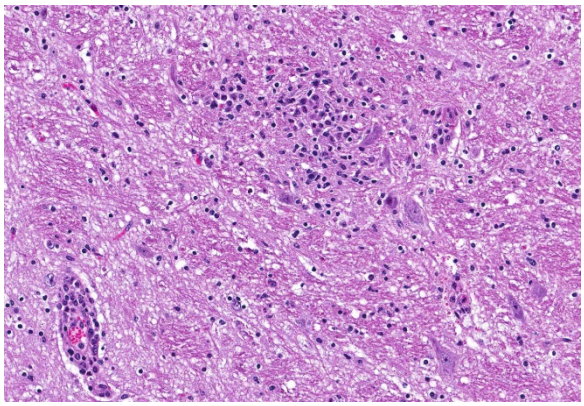

Brainstem, calf: Higher magnification of glial nodule. (HE, 175X).

(formerly *Chlamydia pecorum*).[8] Jee et al reported that the prevalence of *C. pecorum* in calves to be approximately five times as high as that of *C. abortus*, with the highest detection rate being with vaginal swabs, compared to rectal or nasal swabs.[3] The intestinal chlamydial infection may represent the initial event in the pathogenesis of such disease syndrome as polyarthritis, pneumonia, and encephalomyelitis and probably also trans-placental infection and abortion.[2]

Chlamydophila pecorum is a small, obligate intracellular gram-negative bacterium that grows in eukaryotic cells. It has many characteristics of a gram-negative bacterium but it differs in that it lacks peptidoglycan. *C. pecorum* infects certain mammalian hosts like goats, koalas, sheep, swine and cattle. Because *C. pecorum* grows slowly within the natural host, actual disease syndromes are not as evident until later in the infectious process. *C. pecorum* is found mostly in mammals like cattle, sheep, goats, koalas and swine. In koalas, it causes urinary tract disease, infertility, and reproductive diseases. In other mammals, it is associated with abortion, conjunctivitis, encepha-lomyelitis, pneumonia, polyarthritis and enteritis.[5]

JPC Diagnosis: Brainstem and cerebellum (sections varied): Meningoencephalitis, lymphohistiocytic and neutrophilic, multifocal, moderate with necrotizing vasculitis, Holstein (*Bos taurus)*, bovine.

Conference Comment: Sporadic bovine encephalomyelitis (SBE) is caused primarily by *Chlamydophila pecorum* (although *C. psittaci* has also been reported and causes identical disease) which induces severe, diffuse meningoencephalomyelitis in young calves (cattle and buffalo) less than six months old. *C. pecorum* is an obligate intracellular gram-negative bacterium that has a tropism for blood vessels, mesenchymal tissue, and serous membranes which explains its range of clinical syndromes: encephalomyelitis, polyarthritis, metritis, conjunctivitis, and pneumonia. Microscopically, vasculitis and polyserositis are hallmark lesions. Grossly, serofibrinous inflammation of serosal membranes (most commonly the peritoneum) and synovia are characteristic.

Gross lesions in the brain are typically sparse with possible fibrin tags and mild congestion of the meninges, which contrasts the remarkable microscopic findings of diffuse meningoencephalomyelitis, particularly severe around the base of the brain. Meningeal inflammation is composed predominately of histiocytes and plasma cells which expand Virchow-Robbins spaces, resulting in marked perivascular cuffing. Prolonged inflammation results in endothelial damage and encephalitis. Small numbers of chlamydiae can be found as elementary bodies within the cytoplasm of mononuclear cells. .[1]

Microscopic differentials in this case are: *Histophilus somni* (thrombotic meningoencephalitis), *Listeria monocytogenes*, and bovine herpesvirus-5.

Histophilus somni, the only member of the genus *Histophilus* in the family *Pasteurellaceae*, is a facultative anaerobic gram-negative coccobacillus which is normal flora of the male and female genital tracts and nasal cavity. *H. somni* initially begins as a septicemic process which may result in acute death, but if the animal lives, it can spread throughout the body causing widespread petechiation and necrosis. Images and literature often focus on the cerebral lesions because they are the most intense; however, microscopically, the hallmark of this disease is vasculitis with secondary thrombosis. Grossly, there is multifocal hemorrhage and necrosis throughout the brain and spinal cord.The pathogenesis is largely unknown, but there are several known important virulence factors: lipo-oligosaccharide (LOS), immunoglobulin Fc-binding proteins, inhibition of oxygen radicals, and intracellular survival. There are two proposed mechanisms of the vasculitis characteristic of this disease: (1) LOS induces activation of caspase-3 and subsequent apoptosis of endothelial cells and (2) LOS activates host platelets which initiate endothelial cell apoptosis by direct activation of caspase-8 and 9. Apoptosis is further boosted by endothelial cell cytokine production, adhesion molecule expression, and production of reactive oxygen species. Additional lesions include: synovitis with petechiae (atlanto-occipital common), pneumonia (when associated with the bovine respiratory complex), ulcerative laryngitis, , retinal hemorrhages, abscesses in the papillary muscles of the left ventricular free wall of the heart, and, less often, otitis externa/media, mastitis, and abortion.[1]

Listeria monocytogenes is a facultative anaerobic gram-positive bacillus that is

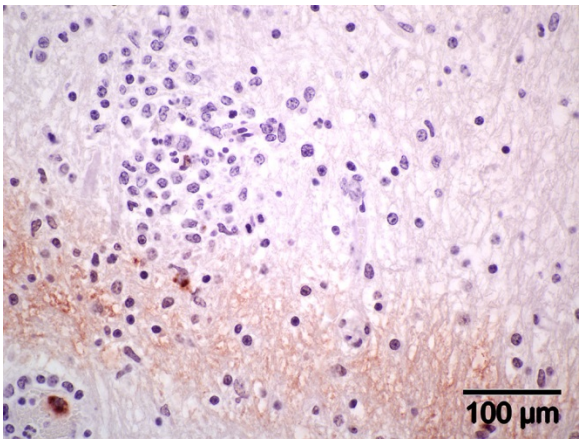

Brainstem, calf: Elementary bodies of chlamydiae are labeled using genus-specific antibodies. (anti-C. trachomatis, 400X)

ubiquitous and able to withstand extreme environmental conditions. *L. monocytogenes* is an intracellular bacteria that lives in macrophages, neutrophils, and epithelial cells, and has several important virulence factors: internalin (allows it to overcome intestinal, placental, and blood-brain barriers by internalizing with E-cadherin) and cholesterol-binding hemolysin (lysing phagosomes). Subsequently, the bacterium replicates in the cytoplasm of the host cell, and uniquely utilizes host cell actin to transfer from one cell to another. There are three distinct syndromes associated with listeriosis: (1) abortion from infection of the pregnant uterus, (2) septicemia and (miliary????) visceral abscesses, and (3) encephalitis. The septicemic form occurs in neonates and aborted fetuses due to multisystemic bacterial colonization. The encephalitic form occurs in the form of outbreaks of adult animals that have eaten partially fermented silage with a pH of 5.5 or above. The bacteriaenter through wounds in the mucosa (from rough feed) and travels via axons to the trigeminal nerve to the brain, with an unusual affinity for the brainstem. Gross lesions are rarely observed; however, microscopically, there are numerous microabscesses composed of viable and degenerate neutrophils, glial nodules, and marked lymphohistiocytic perivascular cuffing.[1]

Finally, bovine herpesvirus-5 (BoHV-5), the causative agent of bovine necrotizing meningoencephalitis, occurs as a sporadic disease in young calves. Bovine herpesvirus-5 is antigenically related to bovine herpesvirus-1 (the causative agent of infectious bovine rhinotracheitis), an alphaherpesvirus; both share a tropism for nervous tissue, are latent in the trigeminal ganglion, and exhibit viral recrudescence. Once the organism is introduced nasally or reactivated, it travels via olfactory nerves to the grey matter of the rostral cerebrum (including the olfactory bulb) where it causes severe necrotizing nonsuppurative meningoencephalitis, with marked gliosis. Gross lesions are rare; however, microscopically there is marked lymphoplasmacytic perivascular cuffs, typically more than 6 cell layers thick. There is neuronal necrosis with occasional intranuclear viral inclusions within neurons and astrocytes.[1]

Contributing Institution:

California Animal Health and Food Safety Laboratory
School of Veterinary Medicine
University of California, Davis
105 W. Central Ave.
San Bernardino, CA 92408
www.cahfs.ucdavis.edu

References:

1. Cantile C, Youssef S. Nervous system. In: Maxie MG, ed. *Jubb, Kennedy, and Palmer's Pathology of Domestic Animals*. Vol. 1. 6th ed. St. Louis, MO: Elsevier; 2016:362-365, 381, 391-392.
2. Doughri AM, Yong S, Storz J. Pathologic changes in intestinal

chlamydial infection of newborn calves. *Am J Vet Res.* 1974; 35(7):939-944.
3. Greub G. (2010). – International Committee on Systematics of Prokaryotes Subcommittee on the Taxonomy of the Chlamydiae: minutes of the inaugural closed meeting, 21 March 2009, Little Rock, Arkansas, United States of America. *Int. J. Syst. Evolut. Microbiol.*, 60, 2691–2693. doi: 10.1099/ijs.0.028225–0.
4. Jee JB, Degraves FJ, Kim TY, and Kaltenboeck B. High prevalence of natural *Chlamydophila* species infection in calves. *J Clin Microbiol*. 2004; 42(12): 5664–5672.
5. Mohamad KY, Rodolakis A. Recent advances in the understanding of *Chlamydophila*
6. *pecorum* infections, sixteen years after it was named as the fourth species of the Chlamydiaceae family. *Vet. Res*. 2010; 41:27.
7. McNutt SH, and Waller EF. Sporadic bovine encephalomyelitis. *Cornell Vet*. 1940; 30**:**437-448.
8. Menges RW, Harshfield GS, Wenner HA. Sporadic bovine encephalomyelitis. Studies on pathogenesis and etiology of the disease. *J Am Vet Med Assoc*. 1953; 122 (913): 294-299.
9. Osman KM, , Ali HA, ElJakee JA, & Galal HM. Infección de cabras y ovejas por *Chlamydophila psittaci* y *Chlamydophila pecorum* en Egipto. *Rev. Sci. Tech. Off. Int. Epiz.*, 2011; 30 (3): 939-948.
10. ViroStat. Immunochemical for Infectious Disease Research. http://www.virostat-inc.com/
11. Wenner HA, Harshfield GG, Chang TW, and Menges RW. Sporadic bovine encephalomyelitis II. Studies on the etiology of the disease. Isolation of nine strains of an infectious agent from naturally infected cattle. *Amer. J. Hyg*. 1953; 57: 15-29.

CASE IV: L17-994 (no label) (JPC 4100736).

Signalment: 4-month-old, female spayed, Domestic shorthair, *Felis catus*, feline.

History: The kitten presented weak and dehydrated with a packed cell volume (PCV) of 12%. Several other kittens had already died over the past 3-4 months.

Gross Pathology: A spayed female Domestic shorthair kitten presented for postmortem examination in fair body condition, weighing 1.55 Kg, with minimal postmortem autolysis. Small amount (1 ml) of blood-tinged, yellow, clear fluid was present within the thoracic cavity and moderate amount (approx. 35 ml) of similar fluid mixed with some strands of fibrin was present within the abdominal cavity. Dark brown fluid was present within the upper and lower respiratory tract (interpreted as terminal aspiration). The lungs were mottled pink and red. Minimal amount of dark brown fluid was also present throughout most of the digestive tract, extending from the oral cavity to the small intestines. The colon was distended with abundant dark red to black, soft feces. The gastrointestinal mucosa was unremarkable. The mesenteric lymph nodes were moderately enlarged. The liver had an accentuated lobular pattern and multiple, up to 3 mm diameter, tan to white, smooth foci that were best apparent on the capsular surface. The omentum, ileum, and colon had multiple, 1-2 mm diameter, white, slightly raised nodules on the serosal surface.

Laboratory results (clinical pathology, microbiology, PCR, ELISA, etc.)**:**

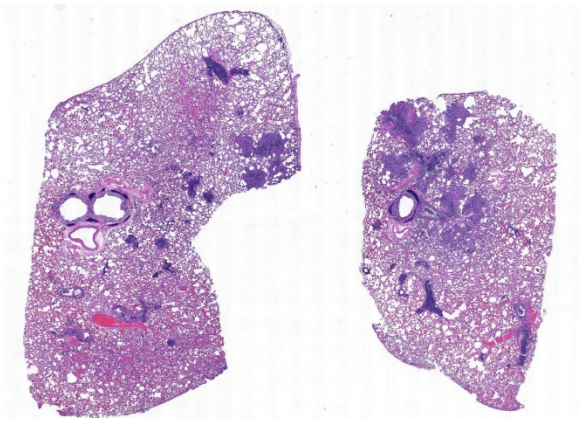

Lung, kitten. Bronchioles multifocally contain a dense cellular infiltrate which extends into surrounding alveolar spaces. (HE, 6X)

Bacterial culture (aerobic): Lung: *Bordetella* sp. (heavy growth)

Special stain (Gram stain): Lung: Moderate numbers of cilia-associated or free gram-negative coccobacilli are within the bronchial and bronchiolar lumen.

Fluorescent antibody test: Lung, liver, intestine, and mesenteric lymph node: Positive for Feline Coronavirus; Intestine, mesenteric lymph node, and spleen: Negative for Feline Parvovirus

Immunohistochemistry for Feline Coronavirus: Lung: Within a focus of peribronchiolar inflammatory cell infiltrate, moderate numbers of macrophages have strong brown (positive) cytoplasmic labeling.

Microscopic Description: Lung: The bronchiolar lumina are filled with abundant viable and degenerate neutrophils inter-spersed with sloughed epithelial cells. Abundant cilia-associated and free gram-negative coccobacilli are present in the inflamed airways. The alveoli surrounding the inflamed bronchioles are frequently distended by abundant fibrin, neutrophils, and macrophages. Pulmonary vessels are diffusely acutely congested. There is also mild to moderate, diffuse alveolar edema.

Colon, mesenteric lymph nodes, liver, and spleen (not submitted): In multifocal areas, the serosal surface of the colon, the mesenteric perinodal adipose tissue, and the capsular surface of the liver and spleen are variably expanded by abundant fibrin mixed with numerous viable and degenerate neutrophils and macrophages. In the most severely affected areas, the fibrinous to pyogranulomatous infiltrate extends into the outer longitudinal layer of the tunica muscularis of the colon, the cortical sinuses of the mesenteric lymph nodes, and the hepatic parenchyma.

Contributor's Morphologic Diagnoses:

1. Lung: Bronchopneumonia, suppurative, acute, with gram-negative cilia-associated and free bacteria.
2. Lung: Pneumonia, fibrino-suppurative and histiocytic, multifocal, with intrahistiocytic feline coronaviral antigen.
3. Intestine, mesenteric lymph node, liver, and spleen (not submitted): Inflammation, fibrinosuppurative to pyogranulomatous.

Contributor's Comment: *Bordetella bronchiseptica* pneumonia is particularly important in kittens <12 weeks of age[1] and in puppies between 7-35 weeks of age[2] due to a greater severity of clinical disease that ensues at this age with a potential of fatal outcome. *B. bronchiseptica* is also important because of its zoonotic potential, particularly for people with immunosuppression.[3] A well-recognized virulence attribute of this pathogen is its adherence to cilia.[4] This

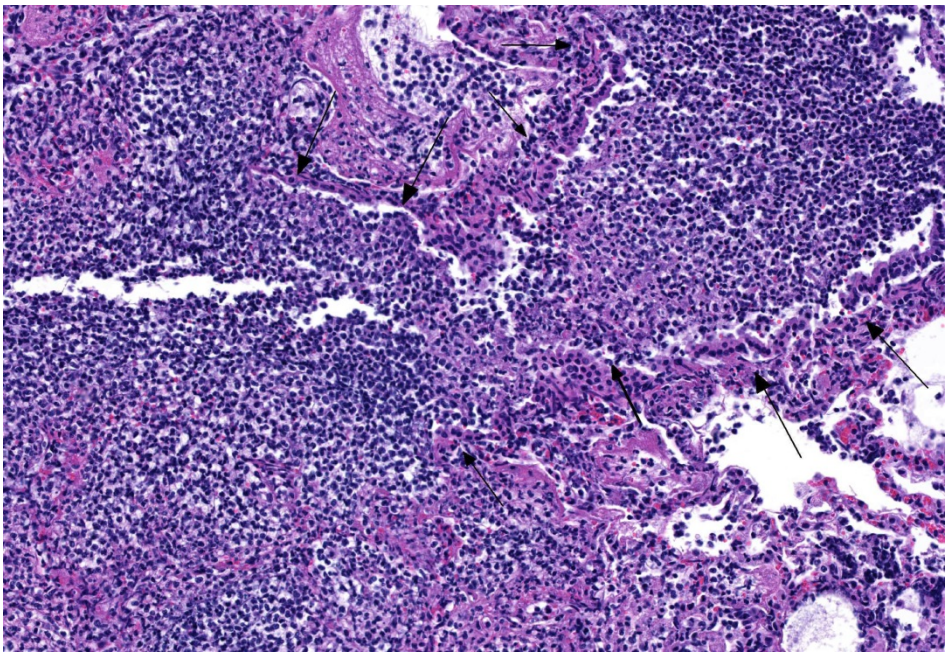

Lung, kitten. The bronchiole (outlined by arrows) is filled with an exudate composed of innumerable degenerate neutrophils admixed with abundant cellular debris. The airway epithelium is multifocally necrotic and lost. (HE, 150X)

adherence is determined by Bvg-regulated expression of filamentous hemagglutinin and pertactin, fimbriae, as well as by adenylate cyclase-hemolysin toxin.[5] The histologic detection of bronchial and bronchiolar cilia-associated bacteria is a significant feature of the diagnosis of *B. bronchiseptica* as a cause of broncho-pneumonia.[6] Along these lines, we detected cilia-associated and free gram-negative bacteria in the lower airways in the histologic lung sections of this kitten. This, combined with the heavy growth of *Bordetella* sp. from the lung, confirms *B. bronchiseptica* as the primary cause of the respiratory disease in this case.

Although the lung lesions in this case were largely attributed to the *Bordetella* sp. bronchopneumonia, the fibrinosuppurative and histiocytic inflammatory alterations in the surrounding alveoli together with the immunohistochemical detection of FCoV antigen in multiple macrophages in one area suggests that there was at least partial contribution of this virus to the respiratory disease of this kitten.

Fibrinosuppurative to pyogranulomatous inflammation associated with feline coronavirus antigen detected by fluorescent antibody testing was also present in several other tissues of this kitten, namely the colon, mesenteric lymph nodes, liver and spleen, consistent with the diagnosis of Feline Infectious Peritonitis (FIP). FIP is a fatal systemic disease of wild and domestic felids caused by feline coronavirus (FCoV), a member of the family Coronaviridae and genus *Coronavirus*, an enveloped, positive-strand RNA virus that spreads via fecal-oral route. Characteristic lesions of FIP include granulomatous phlebitis, fibrinous to granulomatous serositis, and pyogranulomatous inflammation of multiple organs.[7] Cats that present with FIP are usually less than 2 years of age and come from a multi-cat environment.[8] This was true in our case as well, in which the kitten was only 4 months old and came from a multi-cat environment where other kittens had already died. Cats with FIP are lymphopenic,[7] which may have predisposed this kitten to the respiratory bordetellosis. The clinically noted anemia was attributed to gastric bleeding and melena, although gastric erosions and/or ulcers were not apparent on gross and histologic examination.

JPC Diagnosis: Lung: Bronchopneumonia, necrosuppurative, diffuse, marked, with diffuse fibrinous interstitial pneumonia, vascular thrombosis, and numerous cilia-associated bacteria, Domestic shorthair (*Felis catus)*, feline.

Conference Comment: Conference participants agreed with the contributor's presupposition that the majority of the lesions in the lung are caused by *Bordetella bronchiseptica* (which was identified lined up parallel to cilia within large airways using Gram's stain). In the sections distributed to the participants, there are no vascular or other lesions that could be directly atrributable to coronavirus infection, but the participants discussed that immuno-suppression by FIPV predisposed this kitten to developing a respiratory bacterial infection.

Bordetella bronchiseptica is a normal commensal in the upper respiratory tract of most domestic animals but can act as a primary pathogen resulting in tracheo-bronchitis which can progress to pneumonia in more chronic cases. In pigs, it is the primary cause of nonprogressive atrophic rhinitis resulting in mild nasal discharge and sneezing. Certain strains of *B. bronchiseptica* can adhere to nasal cilia and tonsilar epithelium and produce toxins that cause distortion and loss of cilia, submucosal edema, and resorption of the turbinate bone. This process is completely reversible, but predisposes the animal to developing progressive atrophic rhinitis caused by *Pasteurella multocida* type D. This gram negative bacterium produces a cytotoxin, dermonecrotic toxin (encoded on the toxA gene), that results in nonreversible changes to the snout. Similar lesions occur in the epithelium and submucosa with one key difference: this cytotoxin causes proliferation of nearby fibroblasts which

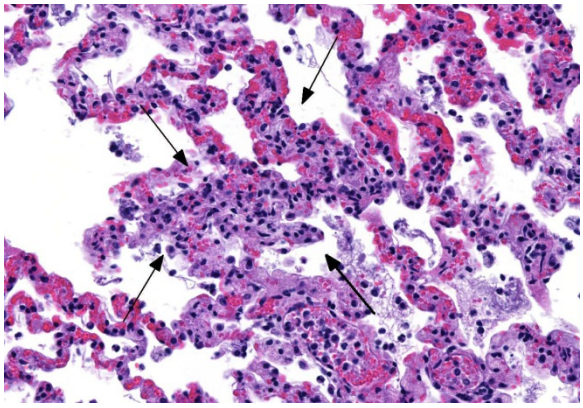

Lung, kitten. Diffusely, alveolar septa are expanded by abundant congestion and fibrin, and there are multifocal areas of septal necrosis (arrows). (HE, 360X)

secrete mediators that induce hyperplasia and increased function of osteoclasts (reabsorbing bone) and decreased function of osteoblasts (reduced formation of bone).[2]

Expression of virulence factors mediated by the Bordetella virulence gene (bvg) operon allows for extensive variability among strains of *B. bronchiseptica*. The bvg operon encodes the following: (1) proteins necessary for attachment to host cells (adhesive proteins filamentous hemagglutinin (FHA), pertactin, fimbriae which aide in adhesion to ciliated cells) and (2) proteins that allow for bacterial survival (iron scavenging, motility mediation, urease and phosphatase activity). However, the most important contributors to the pathogenicity of *B. bronchiseptica* is the secreted adenylate cyclase toxin (hemolysin) which is of the RTX family related to *Mannheimia haemolytica* leukotoxin and *Actinobacillus pleuropneumoniae* Apx toxin. This potent toxin forms pores in target cells, generally leukocytes, to allow transfer of the adenylate cyclase component, resulting in increased cyclic AMP production, which impairs phagocytosis and oxidative burst and leads to cell death forming the characteristic "oat cells" seen microscopically composed of streaming nuclear debris.[2]

Contributing Institution:
Louisiana Animal Disease Diagnostic Laboratory
http://www1.vetmed.lsu.edu/laddl/index.html

References:

1. Anderton TL, Maskell DJ, Preston A. Ciliostasis is a key early event during colonization of canine tracheal tissue by *Bordetella bronchiseptica*. *Microbiology*. 2004; 150: 2843-2855.
2. Caswell JL, Williams KJ. Respiratory system. In: Maxie MG, ed. *Jubb, Kennedy and Palmer's Pathology of Domestic Animals*. Vol. 2. 6th ed. New York, NY: Saunders Elsevier; 2016:533, 578-579, 589.
3. Edwards JA, Groathouse NA, Boitano S. *Bordetella bronchiseptica* adherence to cilia is mediated by multiple adhesin factors and blocked by surfactant protein A. *Infect Immun*. 2005; 73: 3618–3626.
4. Kipar A, Meli ML: Feline infectious peritonitis: still an enigma? *Vet Pathol*. 2014; 51: 505-526.
5. Radhakrishnan A, Drobatz KJ, Culp WT, King LG. Community-acquired infectious pneumonia in puppies: 65 cases (1993–2002). *J Am Vet Med Assoc*. 2007; 230: 1493–1497.
6. Taha-Abdelaziz K, Bassel LL, Harness ML, Clark ME, Register KB, Caswell JL. Cilia-associated bacteria in fatal *Bordetella bronchiseptica* pneumonia of dogs and cats. *J Vet Diagn Invest*. 2016; 4: 369-376
7. Uzal FA, Plattner BL, Hostetter JM. Alimentary system: Feline infectious peritonitis. In: Maxie MG, ed. *Jubb, Kennedy and Palmer's Pathology of Domestic Animals*. Vol. 2. 6th ed. New York, NY: Saunders Elsevier; 2016:253-255.
8. Welsh RD. *Bordetella bronchiseptica* infections in cats. *J Am Anim Hosp Assoc*. 1996; 32: 153–158.
9. Yacoub AT, Katayama M, Tran J, Zadikany R, Kandula M, Greene J. *Bordetella bronchiseptica* in the immunosuppressed population—a case series and review. *Mediterr J Hematol Infect Dis*. 2014; 6:e2014031.

Self-Assessment - WSC 2017-2018 Conference 7

1. Which of the following paraneoplastic syndromes has not been associated with thymoma?
    a. Dysautonomia
    b. Granulocytopenia
    c. Polymyositis
    d. Myasthenia gravis

2. Which of the following stains would not be contributory in the diagnosis of mesothelioma?
    a. Cytokeratin
    b. Vimentin
    c. Synaptophysin
    d. Alcian blue

3. Which of the following cysts is most often found in the cranial mediastinum?
    a. Rathke's pouch
    b. Branchial
    c. Ultimobranchial
    d. Thyroglossal

4. Which of the following is true concerning *Chlamydia pecorum*?
    a. It is a small, obligate intracellular gram-positive bacterium.
    b. It is primarily a parasite of avian species.
    c. Because *C. pecorum* grows slowly within the natural host, actual disease syndromes are not as evident until later in the infectious process.
    d. In koalas, it causes life-threatening encephalitis, which has resulted in massive die-offs.

5. Which of the following histologic findings is not associated with *Bordetella bronchiseptica* infection?
    a. Severe neutrophilic bronchiolitis
    b. Presence of visible bacilli among cilia on airway epithelium
    c. Pyogranulomatous vasculitis
    d. Oat cell formation

Please email your completed assessment to Ms. Jessica Gold at Jessica.d.gold2.ctr@mail.mil for grading. Passing score is 80%.This program (RACE program number) is approved by the AAVSB RACE to offer a total of 0.5 CE Credits, with a maximum of 12.5 CE Credits being available to any individual Veterinary Medical Professionals for the 2017-2018 Wednesday Slide Conference. This RACE approval is for the subject matter categories of: SCIENTIFIC using the delivery method of NON-INTERACTIVE DISTANCE. This approval is valid in jurisdictions which recognize AAVSB RACE; however, participants are responsible for ascertaining each board's CE requirements.
RACE does not "accredit", "endorse" or "certify" any program or person, nor does RACE approval validate the content of the program.

Joint Pathology Center
Veterinary Pathology Services

WEDNESDAY SLIDE CONFERENCE 2017-2018

C o n f e r e n c e 8

25 October 2017

Kurt Williams, DVM, PhD, DACVP
Department of Pathobiology and Diagnostic Investigation
Michigan State University
East Lansing, MI 48824

CASE I: 11111437 (JPC 4019838).

Signalment: 10-year-old, gelding, Thoroughbred, *Equus caballus*, equine.

History: Horse presented to the Veterinary Teaching Hospital with a two month history of anorexia, weight loss and multiple oral ulcers. He was treated by the referring veterinarian with antibiotics, anti-inflammatory drugs and immune stimulants (dosages and types not provided by owner). On ultrasound, multiple pulmonary masses were noted distributed throughout all lung fields. Differential diagnoses included infection vs. neoplasia. Owner opted for euthanasia over further diagnostics and treatment. Patient was euthanized and submitted for necropsy.

Gross Pathology: The lungs are firm throughout, with prominent pleural vessels on the pleura and sub-pleura. Approximately 80% of the lung tissue is tan-to-white and matte; these regions are large and irregular. The remaining 20% of the lung tissue has multifocal, coalescing lesions, ranging from 1-5mm in diameter, also tan-to-white and matte. Yellow-brown purulent material is occasionally present in the bronchi on the left side. Bronchial lymph nodes are diffusely, severely enlarged and on cut surface are homogeneous and tan.

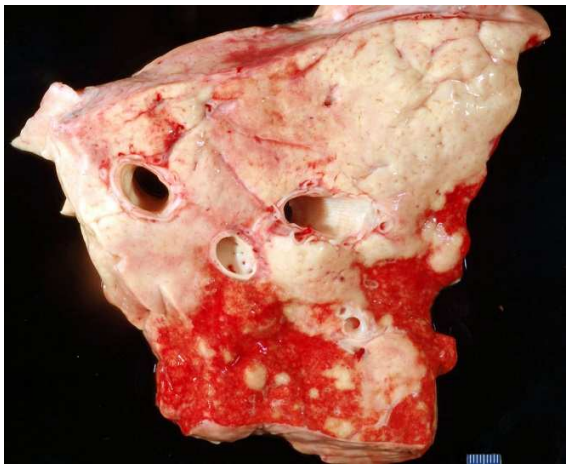

Lung, horse. Approximately 80% of the lung was replaced by white-tan fibrous tissue; the remaining 20% contain numerous fibrotic nodules. (Photo courtesy of: Department of Veterinary Pathobiology, Center for Veterinary Health Sciences, Oklahoma State University, Rm 250 McElroy Hall, Stillwater OK 74078 USA www.cvhs.okstate.edu)

Laboratory results: None performed.

Microscopic Description: Lung: Within severely affected areas of the lung, alveolar septa are widely expanded due to dense mature fibrous connective tissue. There is moderate to marked pneumocyte hyperplasia that partially to completely line alveoli, and most lumens contain foamy macrophages interspersed with cell debris and other inflammatory cells including neutrophils, both viable and degenerate. Bronchiolar epithelium is hyperplastic and lumens contain debris, neutrophils, mucus, and foamy macrophages. Multifocally, within more normal areas, foamy macrophages are present within alveoli and bronchioles. Interalveolar septa are often mildly expanded due to fibrous connective tissue. Hemosiderin-laden macrophages are numerous within alveolar lumens and within septal walls.

The normal architecture of the bronchial lymph node is effaced by thick bands of fibrous connective tissue throughout the node. The cortex and medulla are not distinct, sinusoids are small and cellular, and lymphocytes throughout are mainly small lymphocytes. There is moderate extension of lymphocytes through the capsule.

The spleen (sections not provided) exhibits marked hemosiderosis of the red pulp. In white pulp, the lymphocytes are widely separated. Small lymphocytes predominate and are interspersed with a few large mononuclear cells that contain moderate cytoplasm and large round to oval, dense nuclei. Within some of these cells, there is chromatin margination and equivocal, centrally-located, viral-type inclusion body.

Contributor's Morphologic Diagnosis:
Lung: Multinodular, interstitial pneumonia with marked interstitial fibrosis.

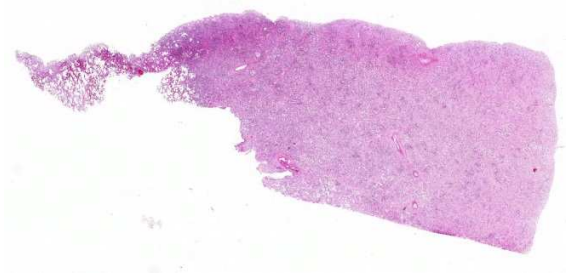

Lung, horse. Approximately 95% of the section is composed of a fibrotic process which effaces normal pulmonary parenchyma. A small area of normal tissue is present at the upper left. (HE, 5X)

Contributor's Comment: The lung lesions are consistent with the equine multinodular pulmonary fibrosis (EMPF) syndrome described by Williams et al. in the United States.[5] The syndrome has also been observed within horses in the UK.[4] This unique disease has been associated with infection by equine herpesvirus-5 (EHV-5).

Clinically, horses with multinodular pulmonary fibrosis syndrome have a mean age of 13-14 years and there is no sex or breed predilection.[5] The patients present with a variable display of tachypnea, tachycardia, respiratory difficulty, cough, and anorexia and weight loss.[5] Clinical pathology often shows a leukocytosis secondary to a mature neutrophilia and elevations of the acute phase inflammatory protein fibrinogen (hyperfibrinogenemia). Lymphopenia, characteristic of acute viral infection, is found in some EMPF horses.[5]

Grossly, there are two morphological forms of the disease.[3] Most common are large, individual to coalescing nodules of fibrosis that typically leave little to no normal lung left. A less common gross presentation are individual, disseminated nodules of fibrosis separated by normal lung tissue; this presentation can be confused with a metastatic, neoplastic process, which was a clinical differential in the current case. The

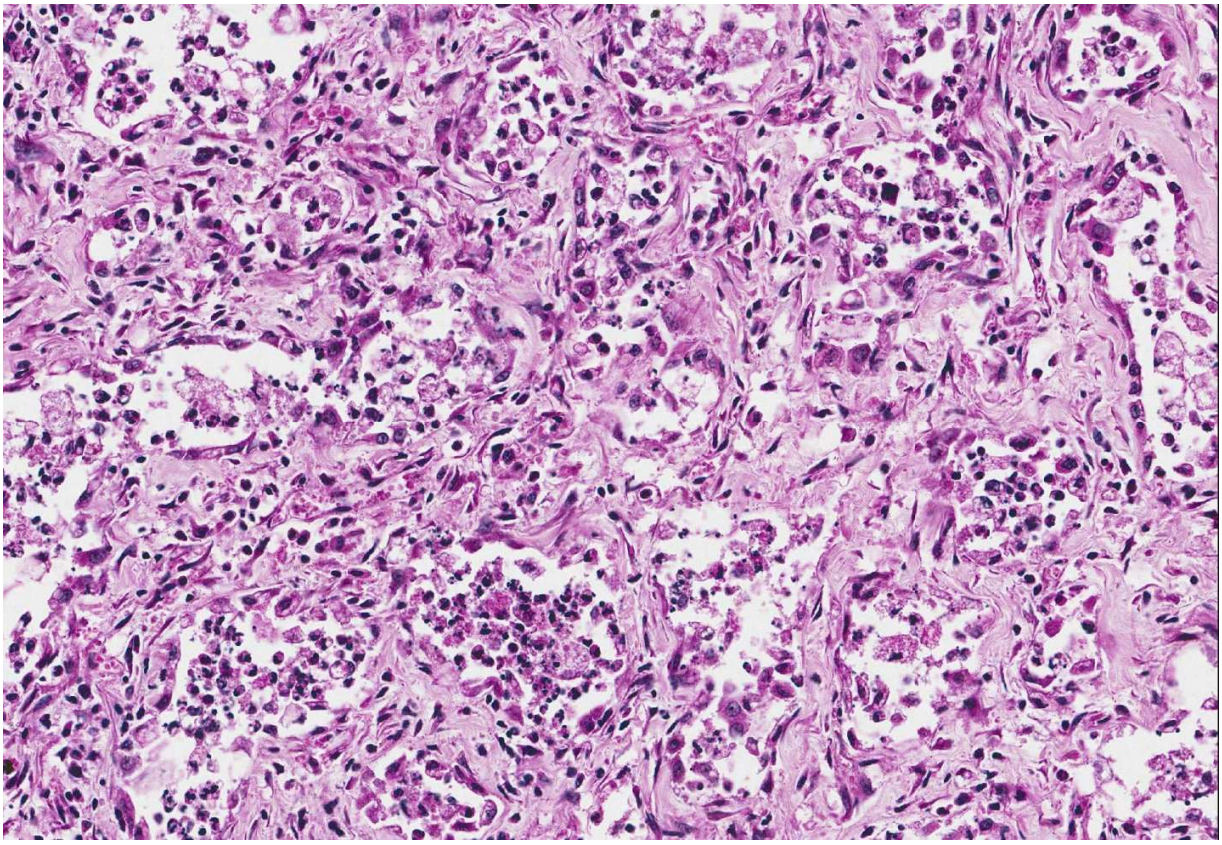

Lung, horse. Alveolar septa are markedly expanded by mature collagen and lined by cuboidal cells which resemble type II pneumocytes. Alveoli are variably filled by moderate numbers of neutrophils and foamy macrophages. (HE, 200X)

current case exhibited more of the "common" gross lesion characterized by near effacement of the lung by coalescing masses of fibrosis.

Histologically, there is marked interstitial fibrosis that can either retain the open alveolar architecture or efface it by less well organized bundles of fibrous connective tissue deposition. Retained airways are often filled with inflammatory cells. Bronchial lymph node lesions recognized by Williams et al.[5] included reactive lymphoid hyperplasia. In the current case, the lymph node was partially effaced by broad sweeping bands of fibrous connective tissue that obscured the corticomedullary junction and otherwise lacked the reactive hyperplasia of the original report.

EMPF has been associated with EHV-5 infection. Intranuclear viral inclusions consistent with herpesvirus are seen primarily within macrophages located in the lesions.[3] In the present case, definitive inclusion bodies were not seen in any organ; however, equivocal inclusion bodies were seen within macrophages of the spleen. The spleen otherwise had no significant microscopic lesions. Although the pathogenesis of EMPF and relationship with EHV-5 has not yet been elucidated, murine models of pulmonary fibrosis may shed some clues. When pulmonary fibrosis is induced in mice infected with MHV68 (gammaherpesvirus) virally infected mice exhibit exacerbation of pulmonary fibrosis over non-infected controls.[6] This observation is accompanied by increased in the production of CCL-2 and CCL-12,

chemokines important for fibroblast recruitment.

JPC Diagnosis: Lung: Fibrosis, interstitial, focally extensive, severe with marked type 2 pneumocyte hyperplasia and rare intra-nuclear intrahistiocytic viral inclusions with marked intra-alveolar inflammation, Thoroughbred (*Equus caballus*), equine.

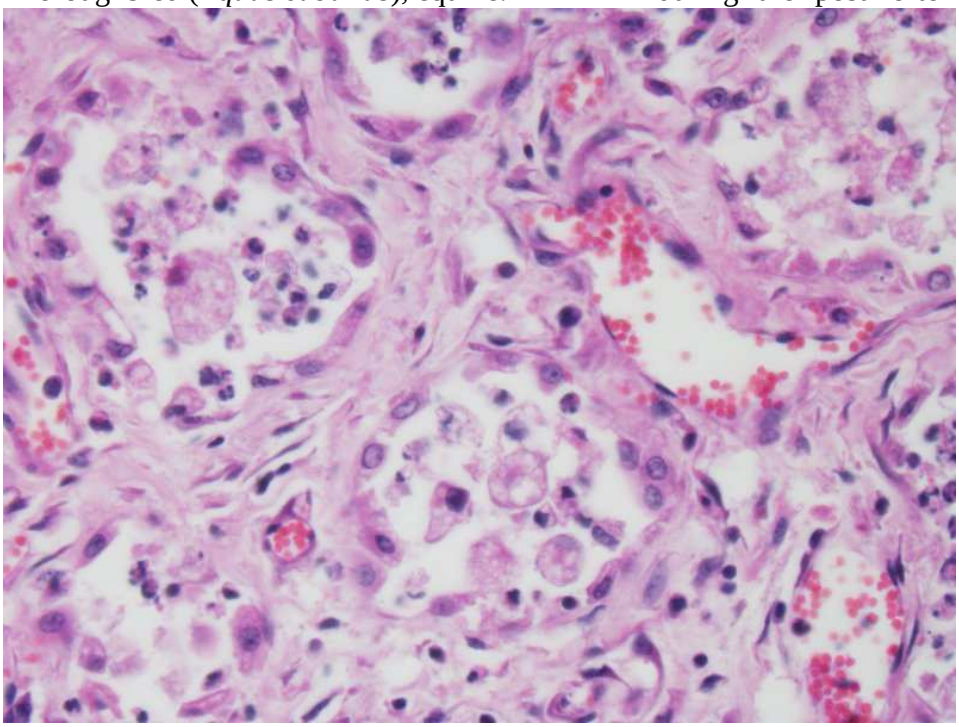

Lung, horse. Rare macrophages contain intranuclear viral inclusions consistent with equine herpesvirus-5. (HE, 400X)

Conference Comment: Conference participants discussed the extensive alveolar remodeling and the possibility that the cuboidal cells lining the airspaces were not type II pneumocytes but another cell type altogether. It was decided that type II pneumocyte hyperplasia was the most accurate option for the morphologic diagnosis because type II pneumocytes are the progenitor cells within the lung parenchyma. These cells repair damaged alveolar epithelium by covering the surface, repopulating the epithelium, secreting new basement membrane, and eventually differentiating into type I pneumocytes.[1]

The conference moderator (who discovered this entity) referred to a study by Marenzoni, et al. that identified *Equine herpesvirus 5* (EHV-5) using bronchoalveolar lavage and biopsy specimens antemortem and then during the postmortem examination were able to use quantitative real-time PCR on several tissues to identify the EHV-5 DNA load in those tissues. They concluded that the viral load was greatest in areas of fibrosis of lung and that higher viral burden resulted in more severe lesions.[2]

In this case, although the contributor only identified inclusions in the spleen (not submitted), the moderator and conference attendees were able to identify several convincing intranuclear viral inclusion bodies within swollen alveolar macrophages.

One remarkable aspect of this disease is the lack of temporal heterogeneity of the lesions. There is no progression in maturity of the lesions and they all appear to have begun at the same time. The conference moderator did not have an explanation for this finding and indicated it is an interesting aspect for future investigation.

Contributing Institution:
Department of Veterinary Pathobiology
Center for Veterinary Health Sciences
Oklahoma State University
Rm 250 McElroy Hall
Stillwater OK 74078 USA
www.cvhs.okstate.edu

References:

1. Caswell JL, Williams KJ. Respiratory system. In: Maxie MG, ed. *Jubb, Kennedy, and Palmer's Pathology of Domestic Animals.* 6th ed. Vol. 2. St. Louis, MO: Elsevier; 2016: 409, 509.
2. Marenzoni ML, Passamonti F, Lepri E, Cercone M, et al. Quantification of Equid herpesvirus 5 DNA in clinical and necropsy specimens collected from a horse with equine multinodular pulmonary fibrosis. *J Vet Diagn Invest*. 2011; 23(4):802-806.
3. McMillan TR, Moore BB, Weinberg JB, Vannella KM, et al. Exacerbation of established pulmonary fibrosis in a murine model by gammaherpesvirus. *Am J Respir Crit Care Med.* 2008; 177:771-780.
4. Soare T, Leeming G, Morgan R, Papoula-Pereira R, et al. Equine multinodular pulmonary fibrosis in horses in the UK. *Vet Rec.* 2011; 169: 313-315.
5. Williams KJ, Maes R, Del Piero F, Lim A, et al. Equine multinodular pulmonary fibrosis: a newly recognized herpesvirus-associated fibrotic lung disease. *Vet Pathol*. 2007; 44: 849-862.
6. Wong DM, Belgrave RL, Williams KJ, Del Piero F, et al. Multinodular pulmonary fibrosis in five horses. *J Vet Med Assoc.* 2008; 232: 898-905.

CASE II: N450-14 (JPC 4101759).

Signalment: 16-year-old, female, spayed, domestic crossbred, *Felis catus*, feline.

History: The cat had polyuria, polydipsia, anorexia, severe dyspnea, lethargy and progressive weight loss. In light of the clinical signs, a diagnosis of uncontrolled diabetes mellitus was suspected. The cat was hospitalized and treated to correct the fluid deficit and the increased electrolyte levels and received intramuscular insulin treatment (0.2 IU/ kg q24h). On the 10th day of hospitalization, after the acute onset of severe dyspnea, the cat died.

Gross Pathology: The lungs were swollen and heavy with a firm elastic consistency and were severely congested and slightly hemorrhagic. At the entrance to the right and left main bronchi there was a large quantity of friable, black material, interspersed with yellow foci that obstructed the bronchial lumen.

Laboratory results: Anaemia (hematocrit 21%, reference range [RR] 24-45%),

Bronchus, cat. The tracheal bifurcation is occluded by a friable aggregate of black and yellow material. (Photo courtesy of: Setor de Patologia Veterinária, Universidade Federal do Rio Grande do Sul, Brazil, http://www.ufrgs.br/patologia/).

leucopenia (4.0 x 10^9 /l; RR 5.0-19.5 109 /l), neutropenia (1.07x109 /l; RR 2.5-12.5 109 /l) and increased fructosamine (533.7 µmol/l; RR 219-247 µmol/l) and glucose (46.0 mmol/l; RR 4.05-7.43 mmol/l) levels were found. Urinalysis showed a moderate level of protein and a high level of glucose, with a specific gravity of 1.018 (RR >1.035). An ultrasound examination revealed a diffuse increase in the size and echogenicity of the liver and pancreas, likely resulting from hepatic lipidosis secondary to diabetes mellitus and pancreatitis. Sections of the lymph nodes and bone marrow underwent immunohistochemical evaluation for detection of feline immunodeficiency virus, feline calicivirus, and feline leukemia virus (FeLV). No viral antigen was observed in these tissues.

Microscopic Description: Lung: The pulmonary parenchyma and bronchial lumen revealed numerous septated, acute-angled or dichotomous branching hyphae (3-4 mm diameter). In addition, biseriate conidial heads with brown phialides and metulae, encompassing the entire surface, as well as smooth-walled, hyaline or darkened conidiophores, were found. The metulae developed in a double series and produced dark brown to black globose to subglobose conidia with rough walls (3-4 mm diameter). Septate hyphae occupied numerous air spaces and infiltrated the alveolar septa. An

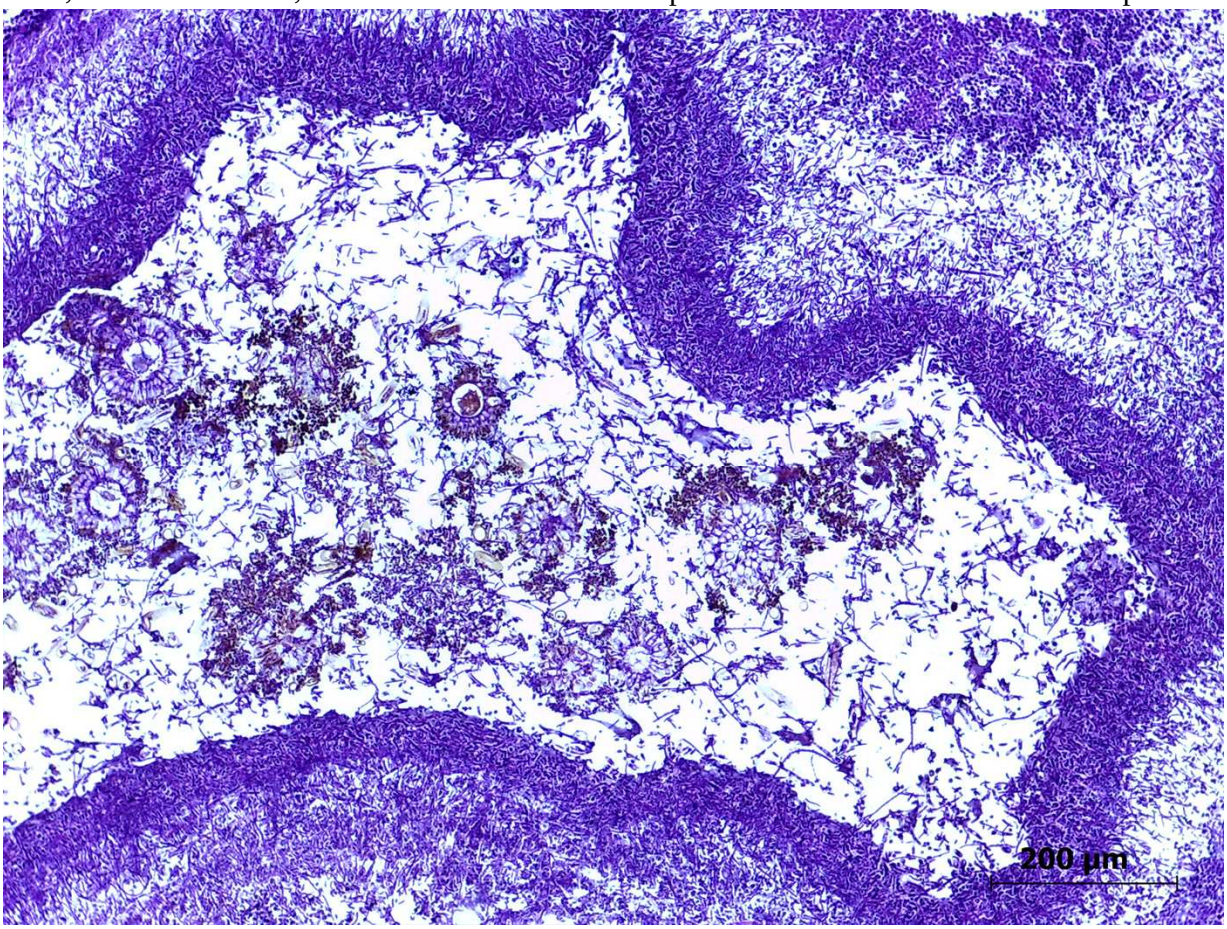

Bronchus, cat. The obstructive material was composed of a thick multilayered mat of fungal hyphae surrounding a moderate number of fruiting bodies (conidia). (Photo courtesy of: Setor de Patologia Veterinária, Universidade Federal do Rio Grande do Sul, Brazil, http://www.ufrgs.br/patologia/). (HE, 100X)

intense infiltrate that consisted predominantly of neutrophils and macrophages with fibrin deposition, associated with necrosis of the bronchial epithelium, and thrombosis was also observed. A methenamine silver stain was performed on the lung sections to highlight the fungi. Sections of the pulmonary parenchyma and bronchi were viewed under polarized light and revealed a high number of birefringent crystals with radiating spokes, consistent with calcium oxalate. No other tissue had evidence of fungal infection.

Contributor's Morphologic Diagnosis: Lung: Bronchopneumonia, pyogranulomatous necrotizing, chronic-active, multifocal and extensive, severe, with intralesional fungi showing conidial heads and dichotomous branching hyphae of *Aspergillus* section *Nigri* and oxalate crystals.

Contributor's Comment: There was a second cat with similar signs which also had diabetes and that had been sent, after its death, to necropsy. Fungal isolation was performed (only in the second case) by seeding samples and arranging tissue fragments in Sabouraud's agar and malt agar. Fungal disease was not suspected in the first cat and unfortunately, no samples were collected for culture. The cultures from the second cat were incubated with chloramphenicol at 37ºC for 7 days for the isolation of *Aspergillus* spp. Identification of the fungal genus and section was performed by observing both the gross and the microscopical aspects of the colonies, which showed a fungus with an aerial black-stained mycelium and colorless reverse, identified as *Aspergillus* section *Nigri*.

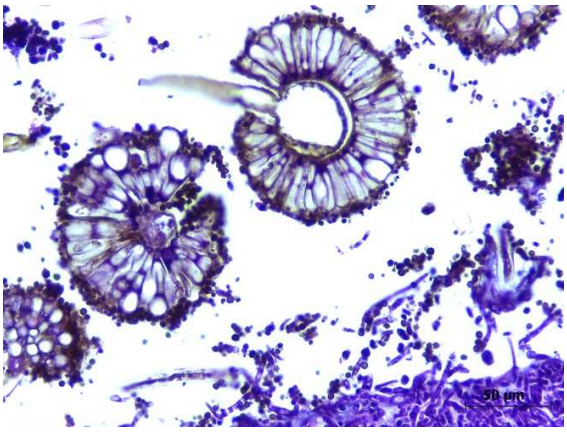

Bronchus, cat. High magnification image of the conidial heads of Aspergillus niger. (Photo courtesy of: Setor de Patologia Veterinária, Universidade Federal do Rio Grande do Sul, Brazil, http://www.ufrgs.br/patologia/). (HE, 400X)

Infections caused by *Aspergillus* spp. result in significant mortality in man and animals. Despite their ubiquitous distribution in indoor and outdoor environments, species in the *Nigri* section are not the most frequent cause of aspergillosis.[8] Compared with species in the *Fumigati* section, species in the *Nigri* section have larger conidia, which allow easy uptake by the host mucociliary system and alveolar macrophages. The conidia of *Aspergillus* spp. develop from mycelia under high oxygen tension or severe infection, and they are not usually observed in histological sections.[1] Fungal pneumonia caused by *A. niger* has been identified in horses by fungal culture,[3] in dogs by molecular analysis[6] and in man by fungal culture;[8] however, there have been no reports of *A. niger*-mediated pneumonia in cats.

A. niger is part of a complex that includes many species, and it is difficult, if not impossible, to distinguish other species phenotypically, except using molecular identification by polymerase chain reaction and sequencing.[10] The finding of calcium oxalate crystals in affected tissue is not recognized commonly in domestic animals, although it has been reported in human cases

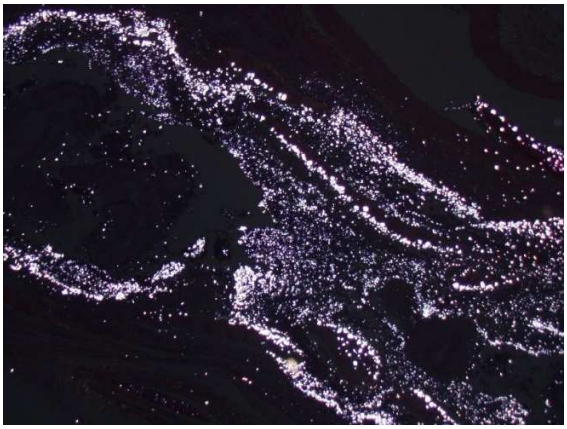

Bronchus, cat. At subgross magnification, there are innumerable birefringent crystals at the periphery of the fungal lesion. (HE, 100X)

and has been considered a classical feature of *A. niger* infection.[7,8] Both calcium oxalate crystals and numerous conidia were observed in the lung tissues of both cats, confirming *A.* section *Nigri* as the etiological agent. Oxalic acid is toxic and can damage tissues and the surrounding blood vessels, which explain the associated inflammatory infiltrate, composed mostly of neutrophils. However, the presence of oxalate crystals is most likely to be compatible with chronic inflammation.

No breed or gender predisposition is apparent for invasive focal or disseminated feline aspergillosis, and cats with sinonasal/sino-orbital aspergillosis can be of any age.[2] Additionally, systemic immuno-compromise due to co-morbidities (e.g. feline parvovirus, FeLV or feline infectious peritonitis virus infection, or prolonged corticosteroid treatment), has been considered supportive evidence of aspergillosis.[2] In this report, diabetes mellitus identified as a risk factor for the development of aspergillosis in cats, may have triggered and/or favoured the development of fungal infection in the lower respiratory tract.[5] Previous reports in man indicate that prolonged diabetes mellitus, prolonged exposure to fungi and old age can predispose patients to mycosis because these patients provide a favourable environment for the growth of *Aspergillus* spp..[11] All of these features are similar to those observed in the present cases.

In man, invasive pulmonary aspergillosis occurs predominantly in immunocompromised hosts; however, the number of cases has increased among immunocompetent patients who have certain pulmonary abnormalities, such as lung neoplasia, as occurred in the first of the present cases. Diabetes mellitus is a metabolic disease that can trigger a series of systemic complications. Furthermore, infections accompanied by high morbidity and mortality are common in diabetic patients. Susceptibility to infection results from immune dysfunction, including reduced cytokine production, immune cell function and migration. Several studies have also indicated an association between secondary toxic metabolites, aspergillosis and immunosuppression of the host.[9] Invasive aspergillosis caused by *A.* section *Nigri* is rare, and the cases described here demonstrate the aggressive nature of species of this section and the potential to cause opportunistic infection in immunocompromised cats. Based on the gross and microscopical findings of fungal hyphae combined with calcium oxalosis and mycological examination, the diagnosis of chronic invasive pulmonary aspergillosis due to *Aspergillus* section *Nigri* was confirmed in two diabetic cats. Not all sections contain conidiophores, however all of them have hypha within bronchial lumina.

JPC Diagnosis: Lung: Bronchitis, pyogranulomatous and necrotizing, severe, with bronchiectasis, numerous fungal hyphae, pigmented conidia, and calcium

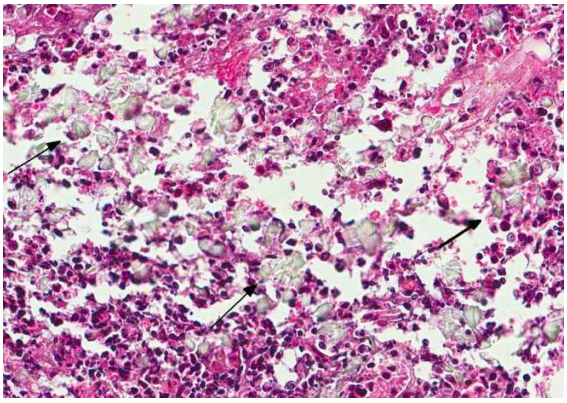

Bronchus, cat. Higher magnification demonstrates numerous fan-shaped oxalate crystals at the periphery of the lesion, enmeshed in fibrin and degenerate neutrophils. (HE, 400X)

oxalate crystals, domestic shorthair, (*Felis catus)*, feline.

Conference Comment: The conference moderator reviewed the typical gross appearance of these lesions and referred to them as "aspergillomas" or "fungal balls".[4] These lesions occur in areas of the respiratory tract with high oxygen tension (often in the nasal cavity, nasopharynx, or large conducting airways where a high oxygen tension allows for mycelial growth and may result in dyspnea and death. In this case, there were contextual clues indicating chronic disease, specifically, loss of cartilaginous basophilia and collapse of the parenchyma at the periphery of the bronchus.

Aspergillus sp. rarely causes lung disease in domestic animals. Of note, *Aspergillus fumigatus* and *A. flavus* can cause chronic destructive bronchitis in German Shepherd dogs. The lesions generated are similar to this case: erosion of the epithelium, neutrophil infiltration, and granulation tissue formation in ulcerated airways. There are mild microscopic differences in the morphology of the fungus (mentioned above by the contributor). This condition is very severe locally, but there have been no reports of progression to invasive systemic aspergillosis in dogs.[4]

Contributing Institution:
Setor de Patologia Veterinária
Universidade Federal do Rio Grande do Sul, Brazil
http://www.ufrgs.br/patologia/

References:

1. Anila KR, Somanathan T, Mathews A, Jayasree K. Fruiting bodies as *Aspergillus*: an unusual finding in histopathology. *Lung India.* 2013; 30: 357-359.
2. Barrs VR, Talbot JJ. Feline aspergillosis. *Vet Clin North Am Small Anim Pract.* 2014; 44: 51-73.
3. Carrasco L, Tarradas MC, Gómez-Villamandos JC, Luque I, Arenas A, Méndez. Equine pulmonary mycosis due to *Aspergillus niger* and *Rhizopus stolonifera. J Comp Pathol*. 1997; 117: 191-199.
4. Caswell JL, Williams KJ. Respiratory system. In: Maxie MG, ed. *Jubb, Kennedy, and Palmer's Pathology of Domestic Animals.* 6th ed. Vol. 2. St. Louis, MO: Elsevier; 2016: 502.
5. Furrow E, Groman RP. Intranasal infusion of clotrimazole for the treatment of nasal aspergillosis in two cats. *J Am Vet Med Assoc.* 2009; 235: 1188-1193.
6. Kim SH, Yong HC, Yoon JH, Yoshioka N, Kano R, Hasegawa A. *Aspergillus niger* pulmonary infection in a dog. *J Vet Med Sci.* 2003; 65: 1139-1140.
7. Procop WG, Johnston WW. Diagnostic value of conidia associated with pulmonary oxalosis: evidence of an *Aspergillus niger* infection. *Diagn Cytopathol.* 1997; 17: 292-294.
8. Person AK, Chudgar SM, Norton BL, Tong BC, Stout JE. *Aspergillus niger*: an

unusual cause of invasive pulmonary aspergillosis. *J Med Microbiol.* 2010; 59: 834-838.
9. Tomee JF, Kauffman HF. Putative virulence factors of *Aspergillus fumigatus*. *Clin Exp Allergy*. 2000; 30: 476-484.
10. Varga J, Frisvad JC, Kocsubé B, Brankovics B, Tóth B, Szigeti G, Samson RA. New and revisited species in *Aspergillus* section *Nigri*. *Stud Mycol*. 2011; 69: 1-17.
11. Wijesuriya TM, Kottahachchi J, Gunasekara TD, Bulugahapitiya U, et al. *Aspergillus* species: an emerging pathogen in onychomycosis among diabetics. *Indian J Endocrinol Metab*. 2015; 19: 811-816.

CASE III: P1270-11 (JPC 4018605).

Signalment: 10-year-old, male, neutered, domestic, *Felis catus*, feline.

History: This cat appeared to be in good health at 1 :00pm; the owner reported he had appeared to sleep more than usual for the last few days. At 1:00am that night, the owner found his cat in severe respiratory distress with sialorrhea. The cat died after an hour with no change in his condition, on its way to the veterinarian.

Gross Pathology: The cat was in good body condition. There were numerous firm whitish nodules, 0.5 to 2 mm in diameter, distributed extensively throughout both lungs, with multifocal atelectasis. A mild amount of mucoid material filled the distal trachea.

Laboratory results: Routine bacteriology on the lungs was not significant (rare contaminants), and negative on liver and kidney.

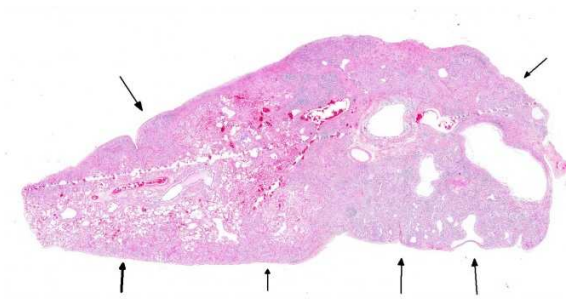

Lung cat. A section of lung with multiple subpleural nodules (arrows) is presented for examination. (HE, 5X)

Microscopic Description: Lung: There is extensive multifocal remodeling of the pulmonary parenchyma, more severe in subpleural areas. The alveolar septa and distal airways are distorted and moderately expanded by dense collagen (fibrosis), smooth muscle bundles and, variably, clusters of mesenchymal cells (fibroblasts/myofibroblasts); they are lined by cuboidal to columnar epithelial cells, and multifocally form larger tubular structures (honeycomb pattern). The alveoli and bronchioles in affected areas are occasionally filled with plump macrophages, and rare to few neutrophils. The epithelium of several, usually larger bronchioles have several goblet cells (mucous metaplasia) and a few foci of squamous metaplasia are visible. There are multifocal moderate lymphoplasmacytic interstitial and subpleural infiltrates. The pleura is multifocally covered by cuboidal to low columnar (hypertrophied) mesothelial cells. There is some variation between the 2 sections/slides submitted. In one of the sections, there is a focal bronchiolo-alveolar proliferation with minimal stroma, suggesting bronchiolo-alveolar adenoma or carcinoma, and focal mucopurulent bronchitis. In the other section, there is multifocal mineralization.

Contributor's Morphologic Diagnosis: Lung: Extensive, multifocal, moderate to marked interstitial pulmonary fibrosis with smooth muscle hyperplasia/metaplasia, epithelial hyperplasia/metaplasia, and fibroblast/myofibroblast foci (probable bronchiolo-alveolar adenoma or carcinoma in one section).

Contributor's Comment: The histological changes in this lung are consistent with feline idiopathic pulmonary fibrosis (FIPF), a previously reported feline interstitial lung disease. Interstitial lung diseases (ILDs) are a heterogeneous group of disorders affecting the pulmonary interstitium, more precisely the alveolar wall, with a variety of etiologies; however, the cause often remains unknown. Most ILDs result from exaggerated inflammatory and reparative responses to an initial insult, which may be infectious, toxic or environmental[2]. Immune-mediated connective tissue disorders result in ILDs in humans and perhaps in dogs; a similar role in feline pulmonary disease has been suggested but has not been proven[2]. In veterinary medicine, lung diseases with a prominent fibrotic component of unknown etiology are often called idiopathic pulmonary fibrosis (IPF). In humans, at least four distinct entities used to be classified as IPF, including usual interstitial pneumonia (UIP)[4]. A consensus statement established by the American Thoracic Society and the European Respiratory Society defined the criteria for the diagnosis of IPF in humans and eliminated all but UIP from the

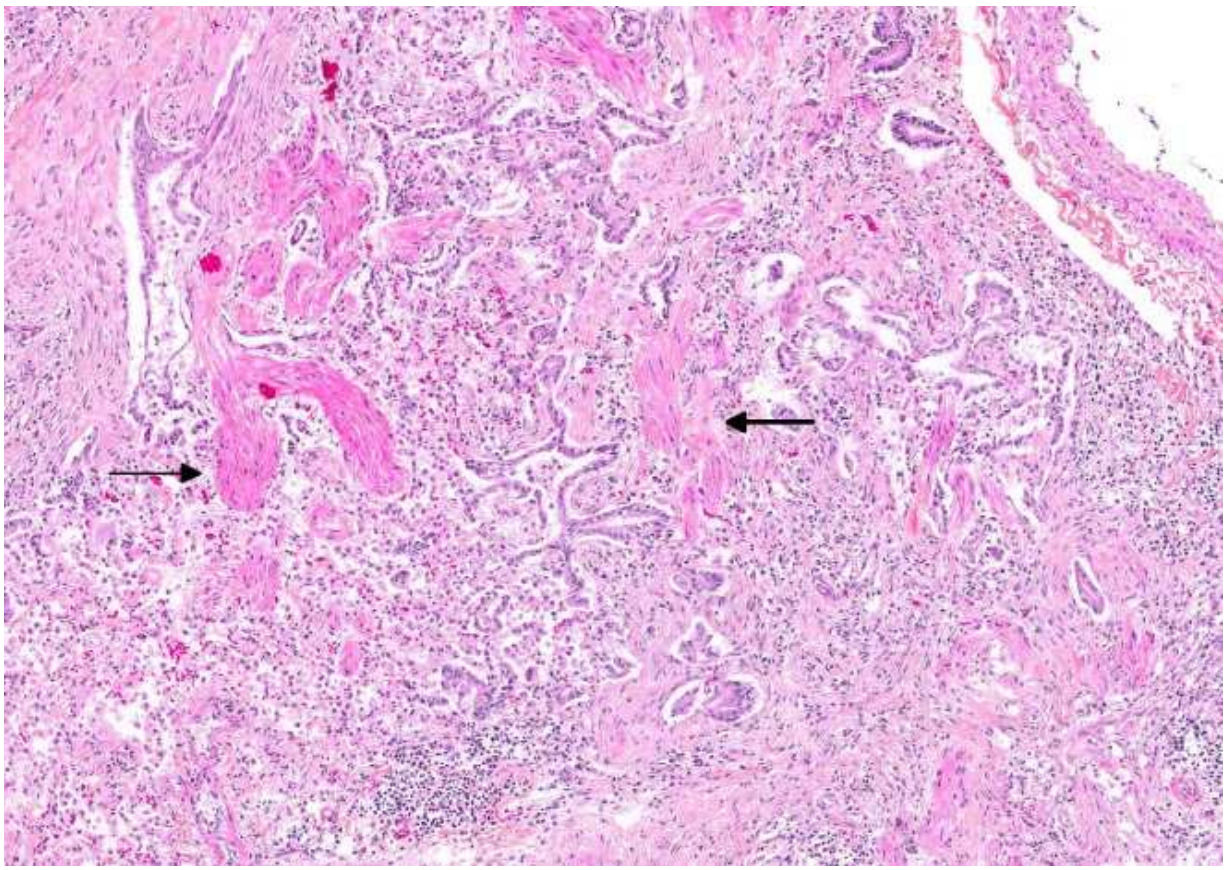

Lung cat. Large areas of fibrosis efface normal pulmonary architecture. Distorted airways and associated smooth muscle (arrows) remain. (HE, 88X)

definition of IPF. The histologic features of UIP lungs are temporal heterogeneity of lung remodeling, with the primary changes being interstitial fibrosis and ongoing fibroblast/myofibroblast proliferation, metaplasia of the alveolar epithelium (honeycomb change with enlarged airspaces lined by prominent variable epithelium), and scant inflammation[4].

Feline idiopathic pulmonary fibrosis (FIPF) is an uncommon chronic interstitial lung disease associated with chronic progressive tachypnea, respiratory distress and cough in middle-aged to older cats[2]. Contrary to other ILDs, IPF is believed to be a fibroproliferative disorder. FIPF type II pneumocyte ultrastructure revealed abnormal dense cytoplasmic lamellar body-like inclusions; this finding is similar to a heritable form of human IPF and is possibly related to a defect in type II pneumocyte biology[4]. FIPF is defined by histopathologic characteristics of usual interstitial pneumonia (UIP). Lesions can be diffuse or patchy. Type II pneumocyte and myofibroblasts are important cellular constituents of feline IPF. Williams reported that myofibroblasts were prominent in foci, beneath honeycombing and hyperplastic epithelium, and in alveolar septa away from the remodeling[4]. An association between pulmonary fibrosis and carcinoma is recognized in humans and animals. Cohn described an IPF-like condition with a coincident pulmonary neoplasia in 6 of 23 cats[2]. These pulmonary neoplasms were generally located in areas of marked fibrosis

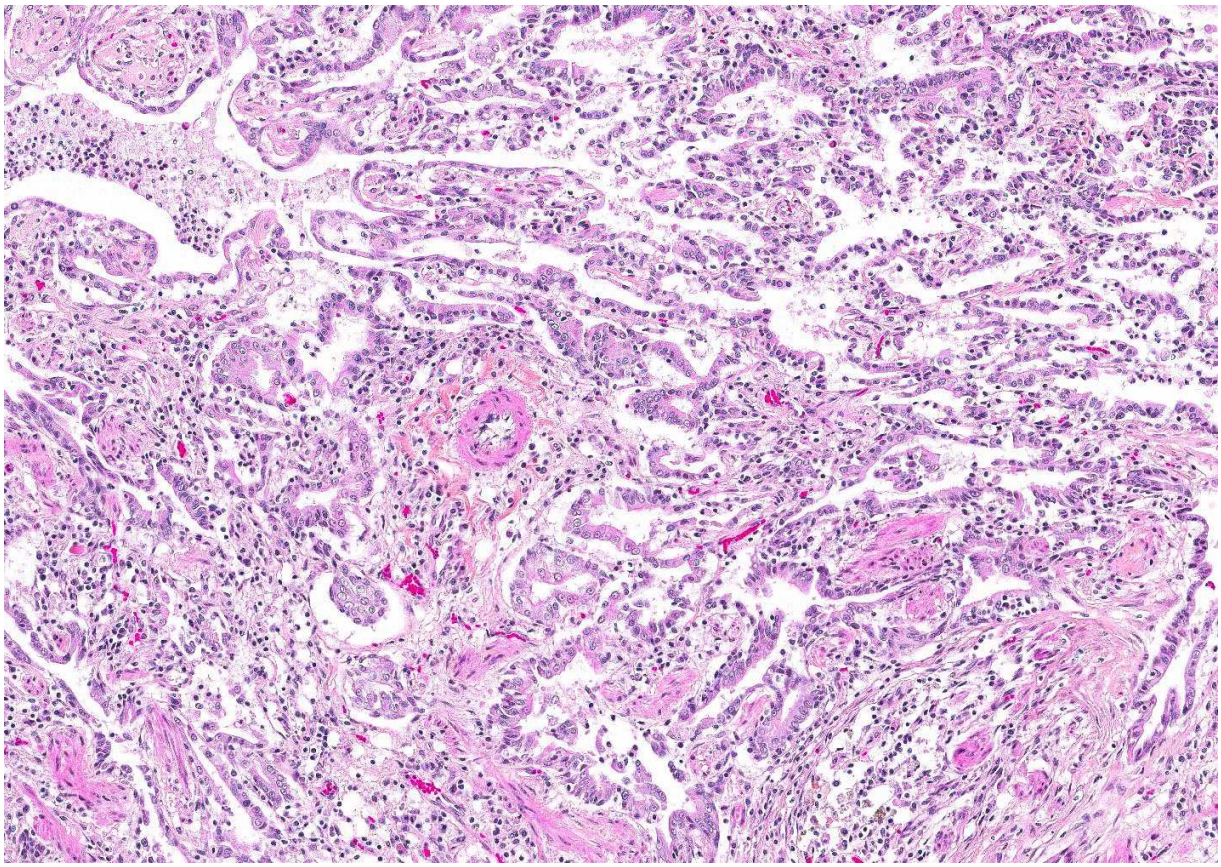

Lung cat. In a focally extensive area of the lung, numerous tortuous airways, lined by hyperplastic epithelium impart a characteristic "honeycomb" appearance to the lung. (HE, 106X)

but the neoplastic foci were limited in extent. Hypotheses to explain coexistence of lung cancer and fibrotic ILD include progression of epithelial hyperplasia to neoplasia, shared etiologic risk factors, and induction of carcinogenesis by diffuse inflammation.

Another idiopathic ILD, diagnosed as the desquamative form of cryptogenic fibrosing alveolitis has been described in a single cat[3]. Idiopathic fibrotic ILD has been described in the dog (West Highland White Terrier). It is characterized by progressive and poorly responsive interstitial fibrosis[1]. However, the condition in dogs is not histologically equivalent to UIP since it lacks alveolar metaplasia, smooth muscle hyperplasia or metaplasia and foci of ongoing fibrosis[2]. Equine multinodular pulmonary fibrosis is another progressive fibrotic lung diseases that has been associated with an EHV-5 virus[1].

JPC Diagnosis: Lung: Fibrosis, interstitial, subpleural, multinodular, severe with marked alveolar loss, bronchiolarization and bronchiolar epithelial metaplasia, and arteriolar and bronchiolar smooth muscle hyperplasia, domestic (*Felis catus)*, feline.

Conference Comment: In contrast with case I (equine multinodular pulmonary fibrosis), this disease entity results in progressive fibrosis with areas of less mature fibrous connective tissue adjacent to mature collagen. The moderator commented that there is very little inflammation in these cases which rules out the possibility of post-inflammatory remodeling. There is also occasional traction bronchiectasis present which is caused by contraction of the fibrous connective tissue pulling apart bronchioles.

There were no pulmonary adenomas or adenocarcinomas in our sections, although it is entirely possible that it was present in the sections viewed by the contributor. Commonly, epithelial hyperplasia associated with this entity is mistaken for a neoplasm; however, IPF can predispose cats to pulmonary adenocarcinoma due to chronic fibrosis and remodeling of the airways.[1]

Contributing Institution:
University of Montreal
College of Veterinary Medicine

References:

1. Caswell JL, Williams KJ. Respiratory system. In : Maxie MG, ed. *Jubb, Kennedy, and Palmer's Pathology of Domestic Animals.* 5th ed. Vol. 2. Philadelphia, PA: Saunders Elsevier; 2007; 496, 523-653.
2. Cohn LA, Norris CR, Hawkins EC, et al. Identification and characterization of an idiopathic pulmonary fibrosis-like condition in cats. *J Vet Intern Med.* 2004;**18:**632–641.
3. Rhind SM, Gunn-Moore DA. Desquamative form of cryptogenic fibrosing alveolitis in a cat. *J Comp Pathol.* 2000;123:226–229.
4. Williams K, Malarkey D, Cohn L, et al. Identification of spontaneous feline idiopathic pulmonary fibrosis morphology and ultrastructural evidence for a type II pneumocyte defect. *Chest*. 2004;125:2278–2288.

CASE IV: H17-0145J (JPC 4100435).

Signalment: Unknown age, female, *Vicugna pacos*, alpaca.

History: A single deceased, female alpaca, which had recently given birth to a

Lung alpaca. The cranioventral regions of the right lung lobes were dark red and firm and oozed dark watery fluid. (Photo courtesy of: Veterinary Pathology Department, School of Veterinary and Life Sciences, Murdoch University, 90 South Street, Murdoch, Western Australia. http://www.murdoch.edu.au/School-of-Veterinary-and-Life-Sciences/)

premature cria, was submitted to the anatomic pathology service. 23 alpacas had died on the property in the previous week. All ages of animals were affected. Death occurred within approximately 48h after the onset of clinical signs, which included ataxia, respiratory distress, dark brown bloody nasal and oral discharge and abortions. Three deceased alpacas were submitted a day earlier to the Department of Agriculture and Food Western Australia. The farmer reported a history of heavy rainfall 7-10 days prior to the animals becoming ill, and that the property had not had animals on it for 5 years before the alpacas were moved on to the property.

The submitted alpaca was previously treated at The Animal Hospital at Murdoch University with intranasal oxygen and intravenous fluids, however, it was found deceased the next morning and submitted to Murdoch University pathology department.

Gross Pathology: On gross necropsy examination the alpaca was in lean body condition (2/5) and had hundreds of approximately 1-3mm diameter dark red foci throughout its oral and conjunctival mucosae, subcutaneous tissues and thoracic pleura.

Diffusely the left lung lobes were mottled dark red to black, firm and oozed a moderate amount of dark red, watery, turbid fluid. Multifocally scattered throughout the left lung lobes there were fewer than ten, multifocal to coalescing, approximately 1-10cm diameter, firm, irregularly shaped nodules, which ranged from pale tan to

black. Approximately 10-20% of the cranioventral region of the right lung lobes was discoloured dark red and firm and oozed a small amount of dark red watery fluid. Approximately 600mL of pale yellow, clear fluid, which contained moderate amounts of pale tan, easily broken down, stringy material was present within the thoracic cavity.

Approximately 500mL of pale yellow, clear fluid, which contained moderate amounts of pale tan, easily broken down, stringy material was present within the abdomen. Approximately 20mL of a similar fluid was present within the pericardial space.

The duodenal mesenteric lymph nodes measured approximately 3cm x 4cm x 5cm to 4cm x 4cm x 7cm respectively with replacement of the normal architecture by moderate amounts of pale tan, thick, turbid fluid and pale tan, firm to crumbly material.

Laboratory results: *Burkholderia pseudomallei* was isolated from aseptically collected samples of both the lung and mesenteric lymph node.

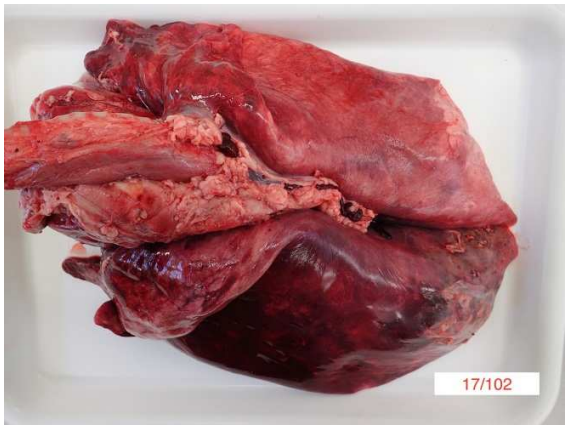

Lung alpaca. Scattered through the left lung lobe are >10 1-10cm tan to black nodules. (Photo courtesy of: Veterinary Pathology Department, School of Veterinary and Life Sciences, Murdoch University, 90 South Street, Murdoch, Western Australia. http://www.murdoch.edu.au/School-of-Veterinary-and-Life-Sciences/)

Microscopic Description: Lung: Multifocally disrupting and infiltrating the pulmonary architecture are variably dense aggregates of large numbers of frequently degenerate neutrophils, low numbers of foamy macrophages and large amounts of pale eosinophilic fibrillar material (fibrin) intermixed with moderate amounts of amorphous eosinophilic and karyorrhectic debris (necrosis). Multifocally present within the cytoplasm of occasional macrophages and occasionally free within the tissue there are low numbers of approximately 2µm in length, 1µm in diameter, gram-negative bacilli. The pulmonary pleura is multifocally expanded and infiltrated by large amounts of pale eosinophilic fibrillar material (fibrin), intermixed with moderate numbers of degenerate neutrophils and fewer lymphocytes and macrophages. Within the remaining pulmonary parenchyma,alveoli contain and are occasionally filled by moderate amounts of a similar inflammatory infiltrate intermixed with moderate numbers of extravasated erythrocytes (haemorrhage)

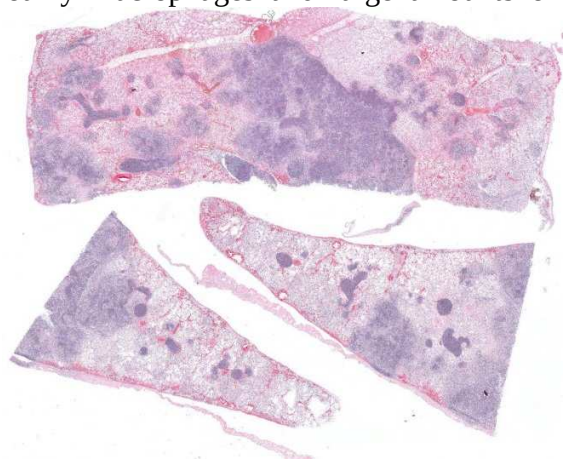

Lung alpaca. Three sections of lung are submitted for examination. (HE, 5X)

and moderate numbers of macrophages, which frequently contain one to two intracytoplasmic erythrocytes.

Contributor's Morphologic Diagnosis: Lung: Severe, acute, multifocal to coalescing, necrosuppurative and fibrinous bronchopneumonia with haemorrhage, fibrinous pleuritis and intra- and extracellular gram-negative bacilli.

Contributor's Comment: This case represents a case of fatal melioidosis, caused by the bacterium *Burkholderia pseudo-mallei*, in an unusual geographic location within Australia. In addition to the alpaca submitted to our diagnostic necropsy service, three additional alpacas from the same property were also involved in the initial outbreak and confirmed to have similar gross and histopathologic changes with a positive culture of *B. pseudomallei*. Furthermore, a single macaw from a neighboring property, which was co-infected with *Chlamydia psittaci*, was also found dead with similar gross necropsy changes and positive *B. pseudomallei* culture.

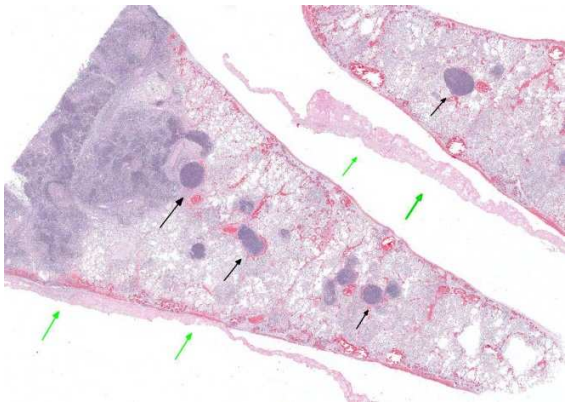

Lung, alpaca. At higher magnification, bronchioles are outlined by a dense cellular exudate (black arrows). Alveoli at left are filled with a similar exudate in a geographic pattern at left. The pelura is covered by a thick mat of fibrin. (HE, 10X)

Differentials for pneumonia reported in alpacas, particularly neonatal alpacas, include bovine respiratory syncytial virus, Parainfluenza type 3 virus, *Pasteurella multocida*, and *Mannheimia haemolytica*. The aforementioned infectious agents have been described in crias to elicit variable gross and histologic pneumonias ranging in severity (mild to severe), distribution (focal to diffuse) and pathologic processes (e.g. necrotizing, fibrinous, suppurative).[14] Additionally bovine diarrhea virus, bovine herpesvirus-1, influenza virus A and *Mycoplasma spp*. have been shown to be associated with lower respiratory diseases in alpacas.[14]

Melioidosis is typically considered endemic to northern Australia and Southeast Asia with endemic and sporadic cases also reported in various countries within South and North America, Africa, the Middle East and Oceania in addition to China, India Puerto Rico, Haiti, Guadeloupe, Haiti and Martinique.[6,15] The location of the outbreak reported in this case is unusual, considering its geographic occurrence within the southwestern wheatbelt region of Western Australia. Further investigation revealed historical evidence of previous outbreaks of melioidosis on the same property. It is thought that the reported heavy rainfall, atypical for the season, immediately prior to this outbreak lead to a re-emergence of the bacterium.

B. pseudomallei is a saprophytic gram-negative motile non-spore forming bacillus which is able to survive in soil and water for many years and in adverse environmental conditions including low pH and high temperatures.[7,10] Infection typically occurs from inhalation of contaminated dust, ingestion of contaminated water or introduction of contaminated soil or water into skin wounds.[10] Horizontal transmission

between infected animals and people has not been reported; however, vertical transmission through the placenta has been reported.[9] Whilst no evidence of zoonotic transmission for *B. pseudomallei* has been demonstrated, indirect transmission from animals and animal products has been argued to pose a possible risk to human health.[8]

Incidence of infections within endemic areas is highest within monsoonal seasons, following high rainfall events. [1,2] The hypothesized cause of this is the contribution of warm, wet conditions to the rapid proliferation of the bacterium within the soil after it has been brought to the surface by a rising water table. [1] Infection has been reported in humans, domestic and non-domestic animal species.[13] Reported cases in domestic species are most prevalent in ruminants and swine, with swine having been reported to be less susceptible to the disease than goats and sheep.[11,13] Additional reports of melioidosis within the literature include horses, cats, dogs, iguanas, rodents, camels, alpacas, horses, deer, tree kangaroos, wallabies, koalas, crocodiles, numerous avian species, captive marine mammals and a number of non-human primates.[12,13,16,17] Clinical disease and necropsy findings in all species are highly variable, depending on the infection entry site, bacterial strain and immune status of the animal.[15] In pigs, melioidosis is frequently asymptomatic with lesions detected upon routine abattoir inspection of carcasses.[11] In other species, pneumonia and chronic, localized infections are most commonly reported, however bacteremia leading to septic shock, neurologic symptoms and mastitis have also been documented.[15,16] Gross and histopathologic changes can range from acute necro-suppurative foci present within multiple organs to chronic, well-formed granulomas.[16] It is important to note that *B. pseudomallei* can be misidentified as a contaminant, as *Pseudomonas spp*. or other non-pathogenic *Burkholderia spp*. by standard identification methods.[9] Furthermore *B. pseudomallei* do not typically colonize the skin and, thus,

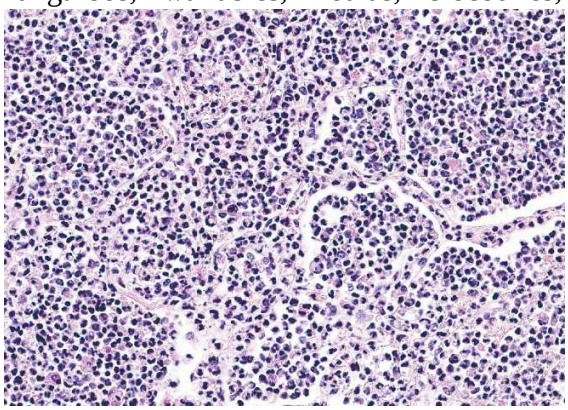

Lung, alpaca. Higher magnification of the affected alveoli, which are filled with an exudate of numerous viable and degenerate neutrophils, fewer macrophages and cellular debris. Alveolar septa are likewise expanded by large numbers of similar cells, edema and fibrin. (HE, 280X)

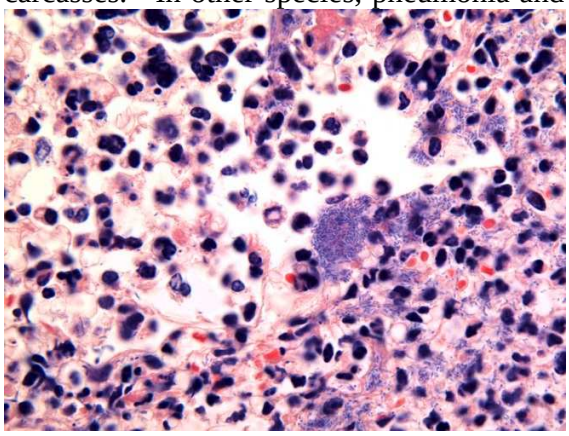

Lung, alpaca. Alveoli contain numerous intra- and extracellular gram-negative bacilli. (Gram, 400X) (Photo courtesy of: Veterinary Pathology Department, School of Veterinary and Life Sciences, Murdoch University, 90 South Street, Murdoch, Western Australia. http://www.murdoch.edu.au/School-of-Veterinary-and-Life-Sciences/)

identification of the organisms should always be considered as a true infection.[9]

Whilst any animal is potentially susceptible to infection, increased risk of infection, particularly fatal infection, with *B. pseudomallei* is found in people with underlying medical conditions including diabetes mellitus, renal dysfunction, immunosuppression, excessive alcohol intake, pulmonary disease, malnutrition and thalassemia.[9,15] Infection in people can undergo a period of latency, which has been reported to last up to 62 years, with reactivation of latent melioidosis to clinical disease which is well documented in patients with immunosuppression.[3,10] An investigation into the immunologic factors inferring susceptibility to *B. pseudomallei* has been performed using BALB/c-C57BL/6 mouse models. Major findings in this study demonstrated *in vivo* depletion of macrophages rendered C57BL/6 mice highly susceptible to intranasal infection with *B. pseudomallei* and that increased bacterial loads and higher mortality rates were observed for TNF-a, TNFR1 and TNFR2 knockout mice.[4]

Given the above information, the number of alpacas affected the severity of disease and the involvement of a potentially immuno-suppressed macaw in the outbreak has raised a question regarding the susceptibility, including the mechanisms of susceptibility, of alpacas to this disease. This would require

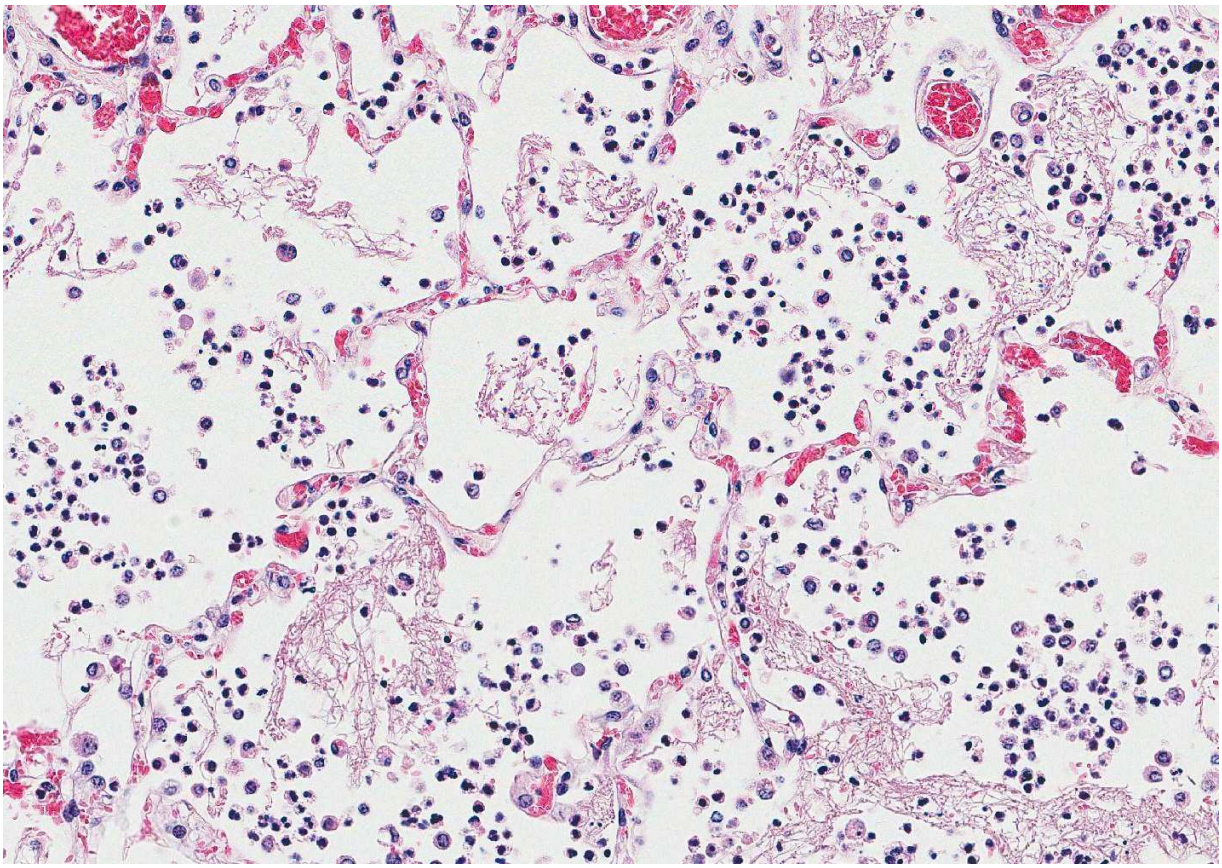

Lung, alpaca. Damage to alveolar septa throughout the lung has resulted in extrusion of edema flue and polyermized fibrin both within the septa and into surrounding alveoli, due to the endotoxin release from damage B. pseudomallei. (HE, 224X)

further investigation and is a topic for potential future research.

JPC Diagnosis: Lung: Bronchopneumonia, necrosuppurative and fibrinous, diffuse, severe, with fibrinous pleuritis, alveolar necrosis, and rare intra-and extracellular bacilli, *Vicugna pacos*, alpaca.

Conference Comment: *Burkholderia pseudomallei* (details described above) result in either acute or chronic disease patterns. In acute disease, which is more common in younger animals, initially the lungs are infected followed by systemic infection. The chronic pattern is more frequent and is characterized by abscesses in multiple organs which are often incidental findings at slaughter. Due to the zoonotic risk, care must be taken at slaughter, as these abscesses are not characteristic and are often mistaken for caseous lymphadenitis (*Corynebacterium pseudotuberculosis*) and glanders (*Burkholderia mallei*). Brain lesions must be differentiated from listeriosis. Besides its endotoxin (typical of a gram-negative bacterium), *B. mallei* has several virulence factors including: malleobactin (an iron-scavenging protein), secreted proteases to degrade tissues, a polysaccharide capsule that protects them from phagocytic killing, and *Burkholderia* lethal factor 1 which inhibits translation and causes death of host cells.

Discussion in this case also covered the two superimposed lesions within the submitted tissue – both a necrotizing broncho-pneumonia as well as a diffuse fibrinous pleuropneumonia, both likely resulting from the presence of *B. pseudomallei*. Protease secretion of the bacterium results in the severe bronchopneumonia; killing of the bacteria results in liberation of endotoxin, diffuse damage to the pulmonary and pleural endothelium, and a fibrinous interstitial pneumonia and pleuritis.

Contributing Institution:
http://www.murdoch.edu.au/School-of-Veterinary-and-Life-Sciences/

References:

1. Baker AL, Ezzahir J, Gardiner C, Shipton W, Warner JM. Environmental attributes influencing the distribution of *Burkholderia pseudomallei* in Northern Australia. *PloS one.* 2015;10(9)**:**e0138953.
2. Baker AL, Warner JM. *Burkholderia pseudomallei* is frequently detected in groundwater that discharges to major watercourses in northern Australia. *Folia microbiologica.* 2016;61(4)**:**301-305.
3. Barnes JL, Ketheesan N. Development of protective immunity in a murine model of melioidosis is influenced by the source of *Burkholderia pseudomallei* antigens. *Immunology and cell biology.* 2007;85(7)**:**551-557.
4. Barnes JL, Williams NL, Ketheesan N. Susceptibility to *Burkholderia pseudomallei* is associated with host immune responses involving tumor necrosis factor receptor-1 (TNFR1) and TNF receptor-2 (TNFR2). *FEMS Immunology & Medical Microbiology.* 2008;52(3)**:**379-388.
5. Caswell JL, Williams KJ. Respiratory system. In : Maxie MG, ed. *Jubb, Kennedy, and Palmer's Pathology of Domestic Animals.* 6th ed. Vol. 2. Philadelphia, PA: Saunders Elsevier; 2016; 563.
6. Elschner MC, Hnizdo J, Stamm I, El-Adawy H, Mertens K, Melzer F. Isolation of the highly pathogenic and zoonotic agent *Burkholderia pseudomallei* from a pet green Iguana in Prague, Czech Republic. *BMC veterinary research.* 2014;10(1)**:**283.

7. Galyov EE, Brett PJ, DeShazer D. Molecular insights into *Burkholderia pseudomallei* and *Burkholderia mallei* pathogenesis. *Annual review of microbiology*. 2010;64**:**495-517.
8. Höger A, Mayo M, Price EP, Theobald V, Harrington G, Machunter B, et al. The melioidosis agent *Burkholderia pseudomallei* and related opportunistic pathogens detected in faecal matter of wildlife and livestock in northern Australia. *Epidemiology and infection.* 2016;144(09)**:**1924-1932.
9. Kelser EA, Melioidosis: A Greater Threat Than Previously Suspected?, *Microbes and Infection* (2016), doi: 10.1016/j.micinf.2016.07.001.
10. Lee S-H, Chong C-E, Lim B-S, Chai S-J, Sam K-K, Mohamed R, et al. *Burkholderia pseudomallei* animal and human isolates from Malaysia exhibit different phenotypic characteristics. *Diagnostic microbiology and infectious disease.* 2007;58(3)**:**263-270.
11. Millan JM, Mayo M, Gal D, Janmaat A, Currie BJ. Clinical variation in melioidosis in pigs with clonal infection following possible environmental contamination from bore water. *The Veterinary Journal.* 2007;174(1)**:**200-202.
12. Parkes HM, Shilton CM, Jerrett IV, Benedict S, Spratt BG, Godoy D, et al. Primary ocular melioidosis due to a single genotype of *Burkholderia pseudomallei* in two cats from Arnhem Land in the Northern Territory of Australia. *Journal of feline medicine and surgery.* 2009;11(10)**:**856-863.
13. Ritter J, Sanchez S, Jones T, Zaki S, Drew C. Neurologic melioidosis in an imported pigtail macaque (*Macaca nemestrina*). *Veterinary Pathology Online.* 2013;50(6)**:**1139-1144.
14. Rosadio R, Cirilo E, Manchego A, Rivera H. Respiratory syncytial and parainfluenza type 3 viruses coexisting with *Pasteurella multocida* and *Mannheimia hemolytica* in acute pneumonias of neonatal alpacas. *Small Ruminant Research.* 2011;97(1)**:**110-116.
15. Sommanustweechai A, Kasantikul T, Somsa W, Wongratanacheewin S, Sermswan RW, Kongmakee P, et al. Environmental management procedures following fatal melioidosis in a captive chimpanzee (*Pan troglodytes*). *Journal of Zoo and Wildlife Medicine.* 2013;44(2)**:**475-479.
16. Tonpitak W, Sornklien C, Chawanit M, Pavasutthipaisit S, Wuthiekanun V, Hantrakun V, et al. Fatal melioidosis in goats in Bangkok, Thailand. *The American journal of tropical medicine and hygiene.* 2014;91(2)**:**287-290.
17. Zehnder AM, Hawkins MG, Koski MA, Lifland B, Byrne BA, Swanson AA, et al. *Burkholderia pseudomallei* isolates in 2 pet iguanas, California, USA. *Emerging infectious diseases.* 2014;20(2)**:**304.

Self-Assessment - WSC 2017-2018 Conference 8

1. Equine multinodular pulmonary fibrosis is associated with which of the following viruses?
    a. Equine papillomavirus-1
    b. Equine herpesvirus-1
    c. Equine herpesvirus-5
    d. Equine rhabdovirus

2. Which other animal species exhibits viral-associated pulmonary fibrosis?
    a. Cattle
    b. Chickens
    c. Guinea pigs
    d. Mice

3. Which of the following has been identified as a predisposing factor for cats with respiratory aspergillosis?
    a. Immunocompromise
    b. Gender
    c. Breed
    d. Age

4. True or false – Feline idiopathic pulmonary fibrosis is characterized by post-inflammatory remodeling.
    a. True
    b. False

5. Which of the following histologic findings is not true about *Burkholderia pseudomallei*?
    a. It is a saprophytic gram-negative bacterium.
    b. Infections increase during wet seasons, especially after high rainfall.
    c. It only can survive for a short time outside a suitable host.
    d. Horizontal transmission between infected animals and people has not been reported.

Please email your completed assessment to Ms. Jessica Gold at Jessica.d.gold2.ctr@mail.mil for grading. Passing score is 80%.This program (RACE program number) is approved by the AAVSB RACE to offer a total of 0.5 CE Credits, with a maximum of 12.5 CE Credits being available to any individual Veterinary Medical Professionals for the 2017-2018 Wednesday Slide Conference. This RACE approval is for the subject matter categories of: SCIENTIFIC using the delivery method of NON-INTERACTIVE DISTANCE. This approval is valid in jurisdictions which recognize AAVSB RACE; however, participants are responsible for ascertaining each board's CE requirements.
RACE does not "accredit", "endorse" or "certify" any program or person, nor does RACE approval validate the content of the program.

Joint Pathology Center
Veterinary Pathology Services

WEDNESDAY SLIDE CONFERENCE 2017-2018

C o n f e r e n c e 9

1 November 2017

Lauren R. Brinster, V.M.D., DACVP
NIH, Bldg. 28A, Rm. 117
9000 Rockville Pike - MSC 5230
Bethesda, MD 20892

CASE I: 17-38-W (JPC 4101294).

Signalment: 26-week-old, male, FVB/N, *Mus musculus*, mouse.

History: This mouse harbored 3 transgenes: Twist1-tetO7-luc, CCSP-rtTA, and tetO-Kras^{G12D}. The mouse had been administered doxycycline in the drinking water since 5 weeks of age to induce transgenes and promote lung tumorigenesis. The doxycycline-treated water was replaced weekly during this time. This mouse was unexpectedly found dead just prior to the intended sacrifice date.

Gross Pathology: The lungs contained numerous white-tan, firm, lung tumors that ranged from pinpoint to 3 x 3mm diameter in all lobes. Additionally, there was a 3 x 4x 0.75cm multilobulated, mass expanding the left abdominal body wall adjacent to the diaphragm (Fig 1). On cut section, the mass was composed of numerous variably sized air and blood-filled cysts. A crackling sound could be elicited upon compression of this body wall mass (subcutaneous crepitation), even post-fixation.

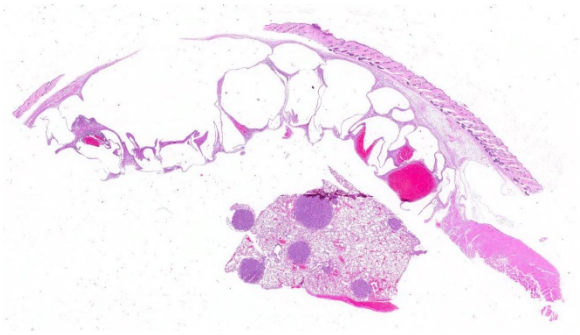

Lung and skin, mouse. The lung contains multiple nodular neoplasms within the parenchyma. The submitted section of haired skin contains numerous clear pseudocytes, some containing hemorrhage. (HE, 6X)

Laboratory results: None performed.

Microscopic Description: Lung: Compressing adjacent pulmonary parenchyma are multifocal, variably-sized, up to 3mm diameter, unencapsulated, well-demarcated, expansile, neoplastic foci composed of one or more layers of cuboidal to columnar epithelial cells arranged in

disorganized glands and packets, supported by a fine fibrovascular stroma. Neoplastic cells have variably-distinct cell borders, scant to moderate amounts of fibrillar eosinophilic to amphophilic cytoplasm, and round to oval nuclei moderately pleomorphic nuclei with finely-stippled chromatin, and 0-4 variably distinct nucleoli. The mitotic rate is less than 1 per 10 HPF. Occasionally, neoplastic cells with prominent nuclear invaginations are present. Within some neoplastic foci, there are areas of necrosis characterized by sloughed and/or pyknotic neoplastic cells, degenerative neutrophils, and cell debris. Necrotic foci are most common in the central portions of larger neoplasms. Smaller neoplastic foci can be seen extending from alveolar or bronchiolar epithelium. Within the adjacent parenchyma, alveoli often contain red blood cells and fibrin. In some sections, there are numerous alveolar macrophages containing red blood cells and/or hemosiderin.

Haired skin, body wall: Diffusely expanding the subcutis and underlying skeletal muscle, are numerous round to irregular cysts (up to 3mm in diameter) filled with clear space (air) and occasionally red blood cells, and/or inflammation and necrosis characterized by neutrophils and macrophages with fibrin and cell debris. Cystic spaces are separated by elongated collagen bundles, pre-existing skeletal muscle bundles, foci of fibroblasts, hemorrhage, and the previously described inflammation and necrosis. The skeletal muscle in this region is multifocally characterized by sarcoplasm that is pale and swollen with internalized nuclei (degeneration), or brightly eosinophilic with loss of cross striations (necrosis).

Contributor's Morphologic Diagnosis:

1. Lung: Adenocarcinoma, multifocal.
2. Haired skin and body wall: Emphysema, subcutaneous and intermuscular, with hemorrhage, and subacute myositis.

Contributor's Comment: Most human lung cancers are adenocarcinomas carrying

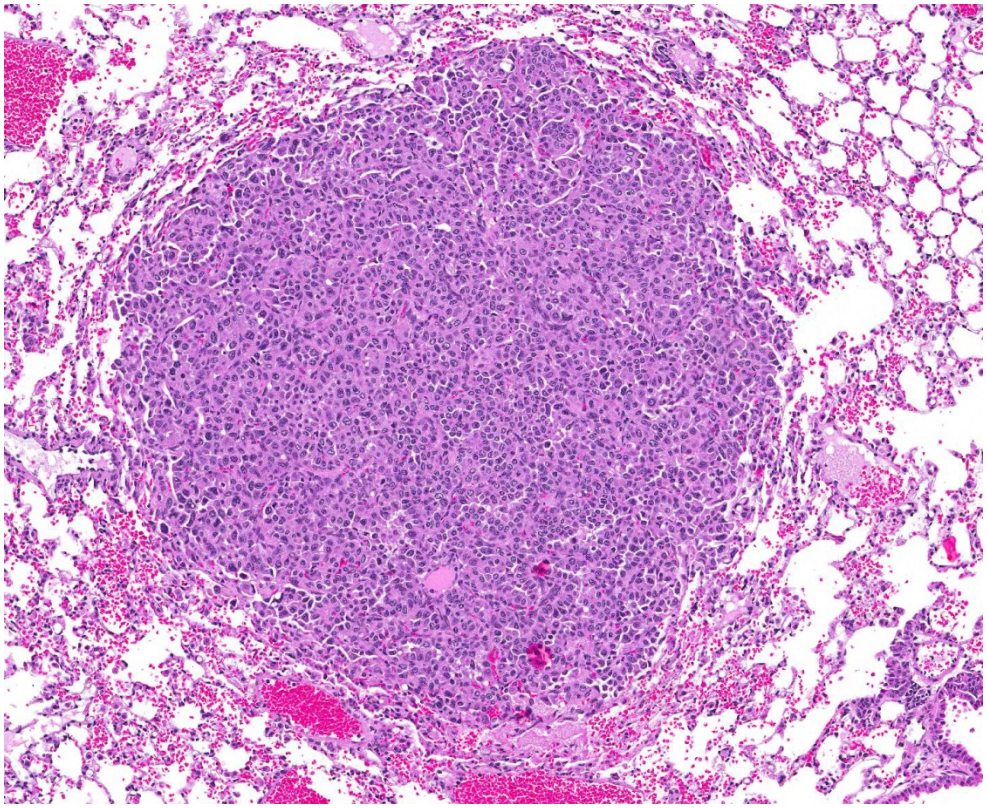

Lung, mouse. Pulmonary neoplasms are less than <3mm in diameter, and are composed of columnar epithelium which line and fill alveolar spaces, often forming papillary projections and rare glands. The neoplasms extend into, but also compress adjacent alveoli, suggesting a slow rate of growth; mitoses are rare. (HE, 112X)

somatic mutations in the genes that encode the EGFR/KRAS/BRAF pathway.[4] Mouse models utilizing the expression of these transgenes are commonly utilized as models for the human disease. Rat Clara cell secretory protein (Ccsp)-rtta activator mice were described in 2000, and provide models in which expression is conditionally controlled in respiratory epithelial cells in the lung, altering lung morphogenesis, differentiation, and proliferation.[10] Additionally, it has been shown that Twist1 plays an important role in both the acceleration and maintenance of $Kras^{G12D}$ - induced autochthonous lung tumorigenesis.[11] As can be expected based on the individual role of each of these transgenes, induction of Twist1-tetO7-luc, CCSP-rtTA, and tetO-$Kras^{G12D}$ in the mouse produces model that may be used to study tumorigenesis in human adenocarcinoma and develop potential treatments.

Subcutaneous edema is often seen in the neck, mediastinum, and retroperitoneal soft tissues secondary to trauma.[7] Additionally, it can be generated by gas forming bacteria secondary to infection or it may arise spontaneously when the pressure gradient between the air-filled alveoli and their surrounding interstitial space is sufficient to cause alveolar rupture.[7]

In this case, the emphysema developed as a bronchocutaneous fistula that presumably occurred after the rupture of one of the many adjacent lung tumors. Bronchocutaneous fistulas can occur in human lung cancer patients. They are a very rare complication, and are the extended version of a bronchopleural fistula, a direct communication between the pleura and bronchial system or the lung parenchyma.[5] Most bronchopleural fistulae are postoperative complications of surgical

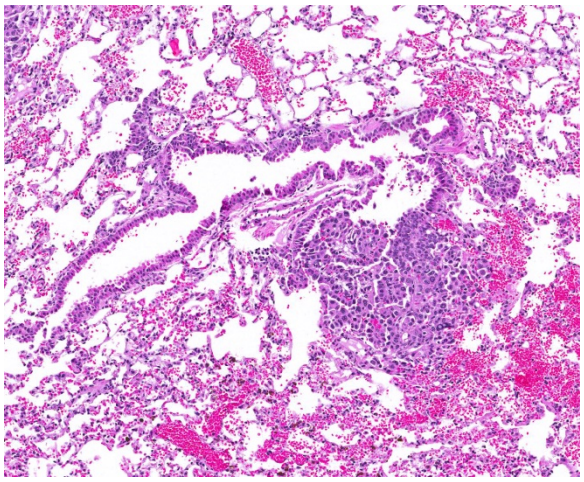

Lung, mouse. Neoplasms occasionally appear to be arising from the airway lining terminal bronchioles. (HE, 136X)

resections of lung, secondary to chemotherapy, radiation treatment, chronic inflammation or infection or a result of internal or external chest trauma.[5,8] Although rare, there are reports of bronchocutaneous fistulas developing in patients that have not received surgical resections, chemotherapy or radiotherapy.[6]

The development of numerous pulmonary adenocarcinomas was expected in the mouse, but the large area of subcutaneous emphysema in the abdominal body wall was not. This has never been described as a potential complication in an inducible lung tumor mouse models. Perhaps, with the continued use of transgenic lung tumor mouse models, rare complications like these may be seen more often by the evaluating comparative pathologists.

JPC Diagnosis: 1. Lung: Pulmonary adenomas, multiple, FVB/N (*Mus musculus)*, mouse.
2. Haired skin and subcutis: Emphysema, diffuse, subacute, severe.

Conference Comment: In mice, primary pulmonary adenomas and adenocarcinomas are the most frequent tumor. In highly susceptible strains, such as A strain mice, tumors can become apparent by 3-4 months old with 100% prevalence by 18-24 months. The high susceptibility of this strain is due to activation of K-ras in the tumors that affect their K-ras allele. In less susceptible strains such as: Outbred Swiss, FVB, BALB/c, 129, and B6:129 hybrids, a predisposition for tumor growth comes from infection with various viral infections (such as Sendai virus) or chemical carcinogens.[1] Primary pulmonary tumors are considered benign until they reach 3mm in diameter, after which they are considered adenocarcinomas or carcinomas. In this case, regardless of the mouse strain, we relied on the INHAND (International Harmonization of Nomenclature and Diagnostic Criteria for Lesions in Rats and Mice) method and determined the size of the tumors to be less than 3mm and, therefore, categorized them as adenomas.[9]

In domestic animal species, primary pulmonary neoplasms are most common in dogs and cats and epithelial tumors are the most common type. Of note, intrapulmonary metastasis is common, and therefore the presence of neoplastic cells within vessels of a pulmonary tumor is not necessarily helpful in distinguishing a primary from a secondary

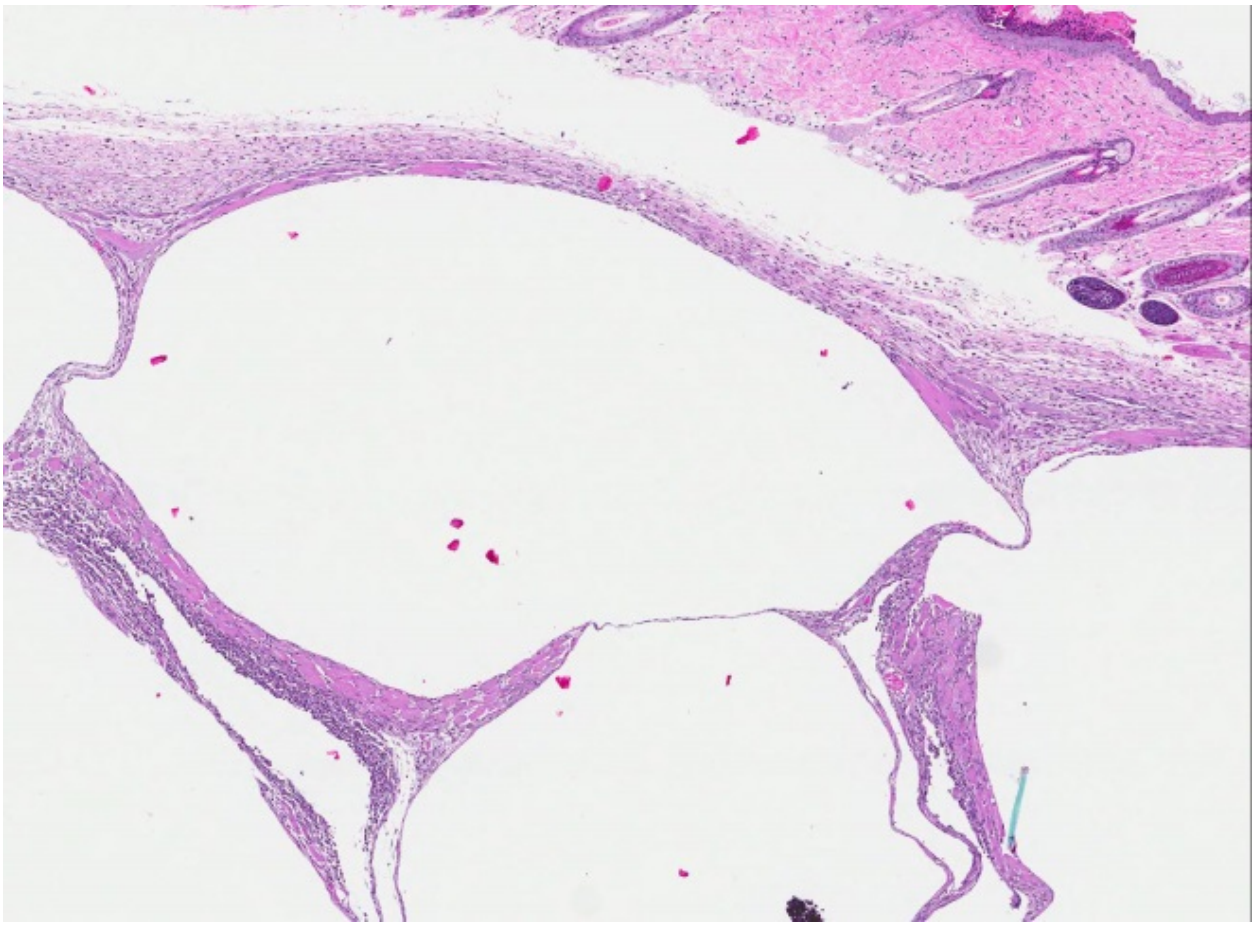

Haired skin, mouse. The dermis is expanded by large clear pseudocysts which separate the deep dermal collagen and skeletal muscle. There is a mild neutrophilic and lymphocytic infiltrate between skeletal muscle bundles reacting to degenerative changes within the muscle. (HE, 58X)

neoplasm. The histologic characteristics that support a primary neoplasm are as follows: Absence of a primary tumor in another organ, presence of single large mass with or without smaller metastases, detection of thyroid transcription factor-1 (TTF-1), mucous production or ciliated cells (both of which are rare in primary tumors).[3] Recently, a study comparing the efficacy of immunohistochemistry of surfactant protein A (SP-A), napsin A, and TTF-1 in diagnosing canine pulmonary carcinomas found that SP-A and napsin A are both useful markers, but that SP-A is the most sensitive and specific and should be paired with napsin-A or TTF-1 to improve detection and differentiation of pulmonary carcinomas from tumors metastatic to the lung.[2] The most frequent lung tumors in dogs are minimally invasive, lepidic predominant, and papillary predominant adenocarcinomas. The grading system in dogs is based on the following criteria: differentiation, degree of nuclear pleomorphism, mitotic rate, nucleolar size, tumor necrosis, fibrosis, and demarcation of the mass. The parameters most predictive of outcome are degree of differentiation, mitotic rate (cutpoints of >1 and >3 per high-power field), necrosis (> 50% of the tumor), and nucleolar size. Staging provides prognostic information, at least in dogs, and is based on number of tumors present (>1=T2), invasion of adjacent tissues (T3), or neoplastic cells present in lymph nodes or other organs (metastasis), both of which indicate a poor prognosis. With pulmonary tumors, invasion refers to neoplastic cells extending into tumor stroma, blood or lymphatic vessels, or pleura, but not extension into adjacent lung tissue. In older cats, pulmonary adenocarcinoma is quite common with a unique pattern of metastasizing to the digits, specifically the dermis on the dorsum of the distal phalanx and beneath the footpad.[3]

Contributing Institution:
Division of Laboratory Animal Resources
University of Pittsburgh
http://www.dlar.pitt.edu/

References:

1. Barthold SW, Griffey SM, Percy DH. *Pathology of Laboratory Rodents and Rabbits.* Ames, IA: John Wiley & Sons, Inc.; 2016:112-113.
2. Beck J, Miller MA, Frank C, DuSold D, et al. Surfactant protein a and napsin a in the immunohistochemical characterization of canine pulmonary carcinomas: comparison with thyroid transcription factor-1. *Veterinary Pathology.* 2017;54(5):767-774.
3. Caswell JL, Williams KJ. Respiratory system. In: Maxie MG, ed. *Jubb, Kennedy, and Palmer's Pathology of Domestic Animals*. Vol. 2. 6th ed. St. Louis, MO: Elsevier; 2016:495-497.
4. Ding L, Getz G, Wheeler DA, Mardis ER, et al. Somatic mutations affect key pathways in lung adenocarcinoma. *Nature.* 2008; 455: 1069–1075.
5. Fraser A, Nolan RL. Malignant bronchosubcutaneous fistula presenting as subcutaneous emphysema. *J Thorac Imag.* 2002; 17: 319–321.
6. Kumar A, Foden AP. Spontaneous subcutaneous emphysema secondary to a malignant bronchocutaneous fistula in a patient who had not received chemotherapy or radiotherapy. *Am J Respir Crit Care Med.* 2012; 185: A4391.
7. Maunder RJ, Pierson DJ, Hudson LD. Subcutaneous and mediastinal emphysema. Pathophysiology, diagnosis, and management. *Arch Intern Med*. 1984; 144(7): 1447-1453.
8. Powner DJ, Bierman MI. Thoracic and extrathoracic bronchial fistulas. *Chest.* 1991; 100: 480–486.

9. Renne R, Brix A, Harkema J, Herbert R, et al. Proliferative and nonproliferative lesions of the rat and mouse respiratory tract. *Toxicologic Pathology*. 2009;37(7 Suppl):5S-73S.
10. Tichelaar JW, Lu W, Whitsett JA. Conditional expression of fibroblast growth factor-7 in the developing and mature lung. *J Biol Chem*. 2000; 275(16): 11858-11864.
11. Tran PT, Shroff EH, Burns TF, Thiyagarajan S, et al. Twist1 suppresses senescence programs and thereby accelerates and maintains mutant Kras-induced lung tumorigenesis. *PLoS Genet*. 2012;8(5):e1002650.doi: 10.1371/journal.pgen.1002650.

CASE II: DX17-0022 (JPC 4101486).

Signalment: Unknown age, female, NSG mouse (NOD.*Cg-Prkdc*^{scid}*Il2rg*^{tm1Wjl}/SzJ), *Mus musculus*, mouse.

History: The mouse was part of a tumor xenograft study and was removed based on predetermined study endpoints for the pathology evaluation.

Gross Pathology: A small-sized, white firm single mass was observed within the wall of the horn of the uterus. No other gross lesions were noted at the time of necropsy.

Laboratory results:
Immunohistochemistry was performed on the mass:

MAC2: Diffuse, membranous to cytoplasmic labeling of >95% of tumor cells
CD68: Diffuse, membranous to cytoplasmic labeling of >95% of tumor cells
Lysozyme: Diffuse, cytoplasmic labeling of >95% of tumor cells
S100: Negative – diffuse, cytoplasmic labeling with blush intensity that is consistent with background; Scattered cells representing neutrophils are positively labeled
Langerin: Negative; Positive control, Haired skin: Scattered immune cells representing dendritic cells in the epidermis have positive cytoplasmic labeling
CD163: Negative; Scattered cells representing tumor infiltrating macrophages are positively labeled
CD45R/B220: Negative

Microscopic Description: An un-encapsulated, nodular mass expands a portion of the endometrium. Neoplastic cells are arranged in tight bundles and streams that are situated within a collagenous stroma. Neoplastic cells are spindle-shaped, have moderate amounts of eosinophilic cytoplasmic and have fusiform, reticulated nuclei with 1-2 prominent nucleoli. There is moderate anisocytosis and anisokaryosis. Mitoses number from 0-1 per 400x/HPF. Low numbers of neutrophils are present throughout the neoplasm. Metastatic lesions are not

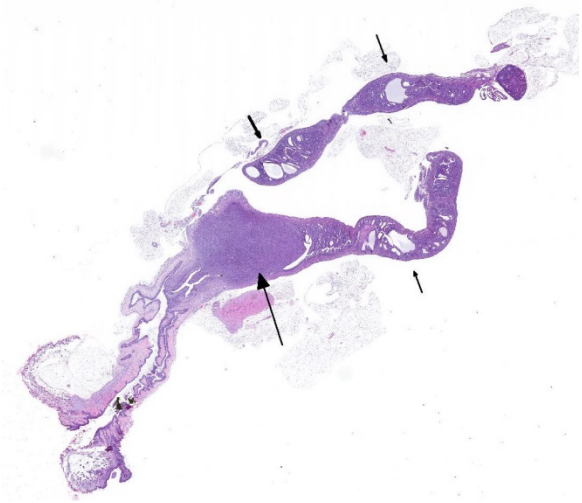

Uterus, mouse. A large mass is present at the juncture of the uterine horns and body (large arrow). The uterine horns contains multiple cysts (cystic hyperplasia) (small arrows). (HE, 6X)

observed.

Contributor's Morphologic Diagnosis: Uterus, endometrium: Histiocytic sarcoma.

Contributor's Comment: Histiocytic sarcomas arising in the uterus of laboratory mice are well-described, vary greatly in morphologic patterning, occur infrequently (~12%) and often involve other organs.[4,6] The putative cells of origin for histiocytic sarcomas for both humans and animals are considered to be CD34+ myeloid dendritic cells that have immunophenotypic characteristics of mature tissue histiocytes and possible shared clonal origins as other leukemias.[3]

In the mouse, several markers may be used to distinguish histiocytic sarcomas from other hematopoietic tumors, especially histiocyte-rich neoplasms. The markers that have shown good reproducibility by immuno-histochemistry (IHC) include: CD163, IBA1, CD68, F4/80, lysozyme and MAC2. The latter five markers are reported to be expressed by histiocytic sarcomas of variable frequency. Histiocytic sarcomas in mice and humans are frequently reported to be negative for the following lineage markers, (where applicable by species): Langerhans cell markers (e.g., Langerin/CD207, CD1A), follicular dendritic cells (CD21/CD35), T-cell related markers (e.g., CD3), common myeloid cell markers (e.g., MPO), melanocytic markers

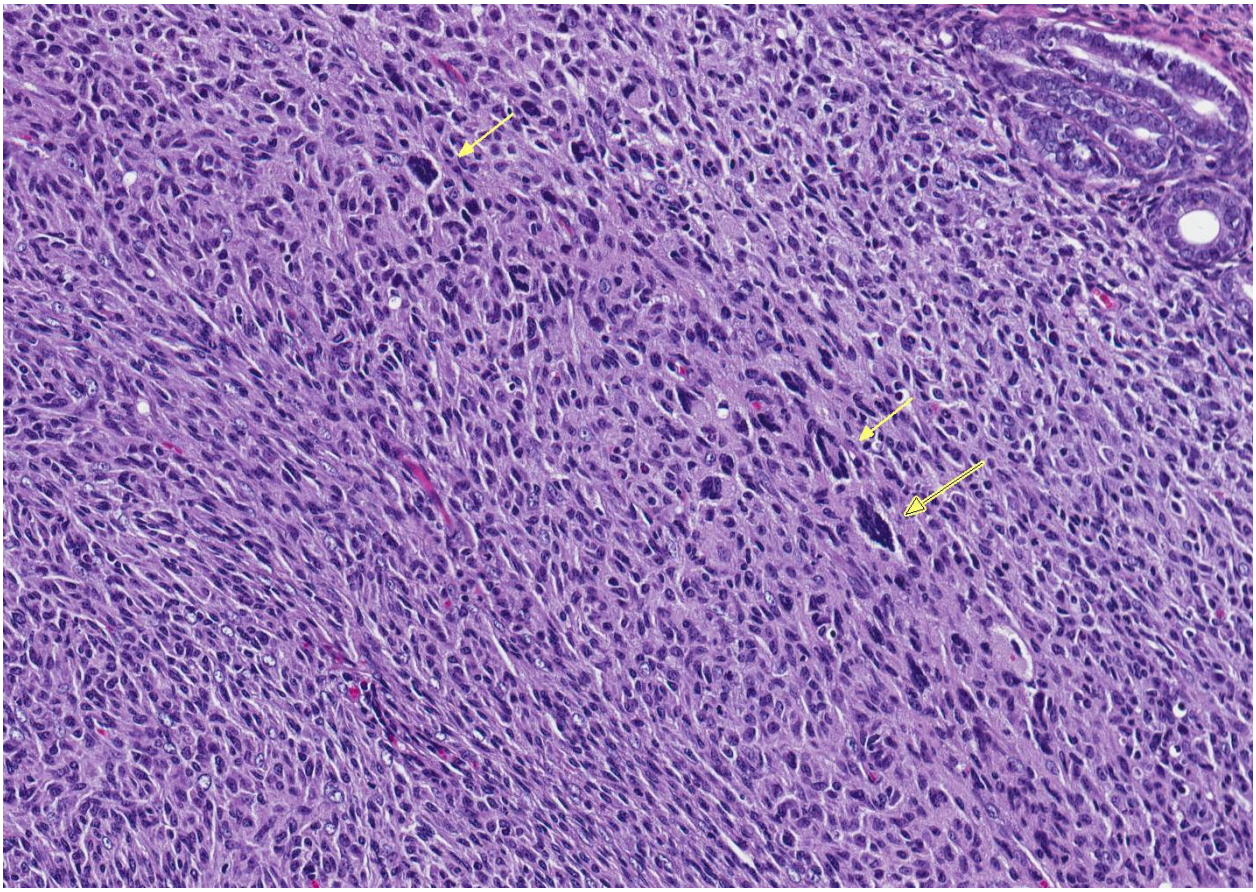

Uterus, mouse. Neoplastic cells are spindled to polygonal, and at one edge, there are low numbers of multionucleated cells, often with nuclei arranged in a ring (yellow arrows) (HE, 200X)

and epithelial cell markers.[7,8,9] The lack of CD163 expression suggests this sarcoma is not derived from tissue macrophages. However, the sarcoma expresses combinations of common histiocyte markers that may include both Langerhans and dendritic cell populations and is most consistent with tumor cells that have originated from a common bone marrow derived histiocytic progenitor.

NSG mice are deficient in mature lymphocytes and NK cells, survive beyond 16 months of age, and are relatively resistant to lymphoma development making this strain useful for long-term engraftment studies using human cells.[11] Because this strain of mouse has been developed relatively recently the incidence of spontaneously arising tumors is only starting to be documented. At least one MAC2 positive histiocytic sarcoma with multi-organ involvement has been reported.[10] Because this strain is used for engraftment studies understanding the incidence of spontaneously arising tumors, especially involving the neoplastic transformation of hematopoietic stem/progenitor cell populations is necessary for determining study related outcomes.

JPC Diagnosis: 1. Uterine body: Histiocytic sarcoma, NSG mouse (NOD.*Cg-Prkdc*^{scid}*Il2rg*^{tm1Wjl}/SzJ) (*Mus musculus)*, mouse.
2. Uterus, endometrium: Hyperplasia, cystic, diffuse, moderate.

Conference Comment: Histiocytic sarcomas (HS) arise from cells of the mononuclear-phagocytic lineage, and therefore, may be arise in any tissue of the body. Gross findings generally include enlargement of the spleen with nodular lesions in any number of additional organs (liver, uterus, vagina, kidney, lung ovaries). Neoplastic cells are large within irregular deeply basophilic nuclei, pale fibrillar cytoplasm, and fairly distinct cell borders. Often giant nuclei and multinucleated cells are present. Cells vary in "roundness" and may appear somewhat elongate, forming interlacing streams and bundles palisading along pre-existing stroma, particularly when located within the uterine wall.[1] These neoplasms are often mistaken for malignant schwannomas. In the liver, HS cells are often seen phagocytizing red blood cells (erythrophagocytosis). When HS are in lymph nodes, they are difficult to differentiate from histiocyte-associated diffuse large B-cell lymphomas and immunohistochemistry is required for definitive diagnosis. There are many markers for cells of dendritic origin (listed above) but CD18 positive membrane staining of suspected cells is diagnostic for HS.[2] Certain strains of mice (B6 and SJL) and rats (SD) are prone to HS.
An interesting associated lesion in mice is hyaline droplets within the cytoplasm of renal tubular epithelial cells which represent lysozyme released from apoptotic neoplastic histiocytes.[5] In hamsters, there has been an association noted between development of hepatic HS and *Helicobacter* spp. related hepatitis.[1]

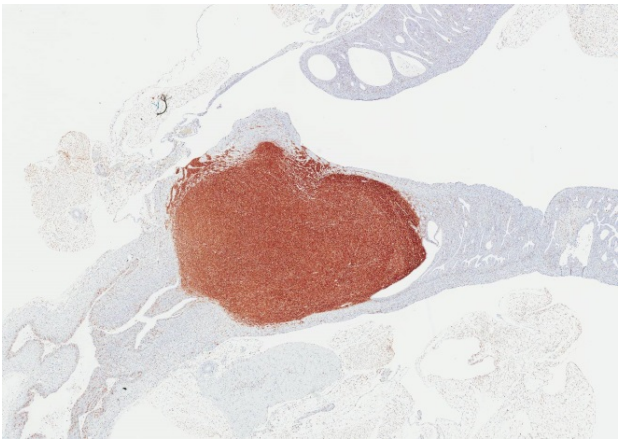

Uterus, mouse. Neoplastic cells are strongly cytoplasmically positive for MAC-2. (anti-MAC-2, 200X)

In dogs, HS are the most commonly occurring joint tumors with many breed predispositions (Bernese Mountain Dogs, Rottweilers, Bullmastiffs, golden Retrievers, Labrador Retreivers, and Flat-Coated Retrievers) as well as environmental factors that predispose such as joint damage from arthritis or ruptured cruciate ligaments. HS in dogs has a different gross appearance and is more lobulated, filling the joint cavity, and infiltrating adjacent soft tissue. Microscopically, cells have a more vacuolated cytoplasm which has led to mistaken identification as liposarcomatous neoplastic cells. Cells have a similar appearance as was previously described for rodents, but joint HS have a more favorable prognosis than those originating in the spleen.[2]

Attendees noted the cystic changes in the endometrium, and while most attendees attributed them to cystic endometrial hyperplasia - the moderator suggested that these may also simply be present as a result of compression from the mass.

The moderator also noted that NSG mice are immune-deficient, and similar to nude mice, are susceptible to hyperkeratotic skin diseases caused by *Corynebacterium*, *Staphylococcus aureus* or *S. xylosus* (ulcerative dermatitis). *C. bovis* grows within keratin due to its lipophilic nature and can persist in the environment within keratin flakes. Microscopically, they have diffuse hyperkeratosis with little dermal inflammation and gram-positive rods can be easily identified among the layers of keratin. *S. aureus* and *S. xylosus* are both commensal bacteria and are common in the environment. In immunosuppressed mice and rats, they can colonize the outer dermis and produce numerous proteins (hemolysins, nucleases, proteases, lipases, hyaluronidase, and collagenase) and exotoxins (exfoliative toxins, leukocidin, superantigens) which damage the skin and produce burn-like features.[1]

Contributing Institution:

St. Jude Children's Research Hospital
Department of Pathology
MS 250, Room 5031
262 Danny Thomas Place
Memphis, TN, 38105-3678
https://www.stjude.org/research/departments-divisions/pathology.html

References:

1. Barthold SW, Griffey SM, Percy DM. *Pathology of Laboratory Rodents and Rabbits.* Ames, IA: John Wiley & Sons, Inc.; 2016:67-70, 103, 110-111, 167-168, 183.
2. Craig LE, Dittmer KE, Thompson KG. Bones and joints. In: Maxie MG, ed. *Jubb, Kennedy, and Palmer's Pathology of Domestic Animals*. Vol. 1. 6th ed. St. Louis, MO: Elsevier; 2016:159-160.
3. Feldman AL, Minniti C, Santi M, Downing JR, Raffeld M, Jaffe ES. Histiocytic sarcoma after acute lymphoblastic leukaemia: a common clonal origin. *The Lancet Oncology*. 2004; 5(4)**:** 248-250.
4. Hao X, Fredrickson TN, Chattopadhyay SK, Han W, Qi CF, Wang Z, et al. The histopathologic and molecular basis for the diagnosis of histiocytic sarcoma and histiocyte–associated lymphoma of mice. *Veterinary Pathology*. 2010; 47(3)**:** 434-445.
5. Hard GC, Snowden RT. Hyaline droplet accumulation in rodent kidney proximal tubules: an association with histiocytic sarcoma. *Toxicologic Pathology*. 1991;19(2):88-97.
6. Lacroix-Triki M, Lacoste-Collin L, Jozan S, Charlet J-P, Caratero C,

Courtade M. Histiocytic sarcoma in C57BL/6J female mice is associated with liver hematopoiesis: review of 41 cases. *Toxicologic Pathology.* 2003; 31(3)**:** 304-309.

7. Pileri SA, Grogan TM, Harris NL, Banks P, Campo E, Chan JKC, et al. Tumours of histiocytes and accessory dendritic cells: an immunohistochemical approach to classification from the International Lymphoma Study Group based on 61 cases. *Histopathology.* 2002; 41(1)**:** 1-29.
8. Rehg JE, Bush D, Ward JM: The utility of immunohistochemistry for the identification of hematopoietic and lymphoid cells in normal tissues and interpretation of proliferative and inflammatory lesions of mice and rats. *Toxicologic Pathology.* 2012; 40(2)**:** 345-374.
9. Rehg JE, Ward JM. Applications of immunohistochemistry-toxicologic pathology of the hematolymphoid system, In: Parker G, ed. *Immunopathology in Toxicology and Drug Development: Volume 1, Immunobiology, Investigative Techniques, and Special Studies.* 1st ed. Cham, Switzerland: Humana Press; 2017: 489-551.
10. Santagostino SF, Arbona RJR, Nashat MA, White JR: Pathology of aging in NOD scid gamma female mice. *Veterinary Pathology.* 2017; 54(5): 855-869.
11. Shultz LD, Lyons BL, Burzenski LM, Gott B et al.: Human lymphoid and myeloid cell development in NOD/LtSz-scid IL2R γ null mice engrafted with mobilized human hemopoietic stem cells. *The Journal of Immunology.* 2005; 174(10)**:** 6477-6489.

CASE III: MS 15-2723 (JPC 4103775).

Signalment: 2-month-old, female, Swiss Webster, *Mus musculus*, mouse.

History: Mouse observed to have severe head tilt to the right and rolling in bedding.

Gross Pathology: A small-sized, white firm single mass was observed within the wall of the horn of the uterus. No other gross lesions were noted at the time of necropsy.

Laboratory results: None submitted.

Microscopic Description: Liver (multiple sections submitted) – Multifocal to coalescing, peri-portal to portal accumulations of one to multiple larvated parasitic eggs (live, dead, fragmented, egg casing only) surrounded by numerous layers of macrophages, and an outer layer of fibrosis with moderate numbers of neutrophils, eosinophils, and occasional plasma cells and lymphocytes are observed. A rare egg is observed attached to the endothelial lining of a portal vein along with an attached granuloma. Numerous black pigment-laden Kupffer cells (hemozoin) and multiple small accumulations of extra-medullary hematopoiesis are observed.

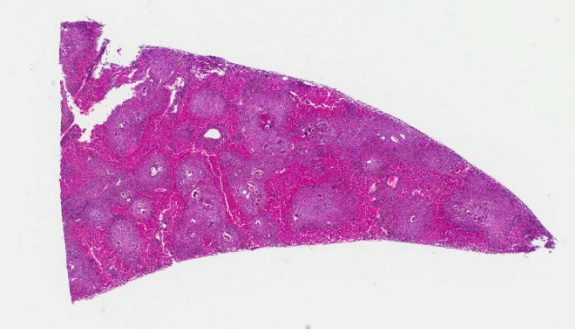

Liver, mouse. At low magnification, approximately 66% of the parenchyma is replaced by discrete, occasionally coalescing granulomas. (HE, 5X)

Contributor's Morphologic Diagnosis: Liver, hepatitis, periportal and portal, granulomatous to pyogranulomatous and eosinophilic, multifocal to coalescing, severe, chronic with multiple parasitic eggs consistent with Schistosomes.

Contributor's Comment:
Schistosomiasis affects more than 230 million people worldwide[2]. *S japonicum* infects a wide range of mammalian host including dogs, pigs and cattle. *S. mansoni* can infect rodents and non-human primates[2]. Schistosomiasis, also known as bilharzia/bilharziasis, is a disease caused by the trematode *Schistosoma*, with *S. mansoni*, *S. japonicum*, and *S. haematobium* being the most prevalent. Schistosomes, usually referred to as blood flukes, are part of the phylum *Platyhelminthes* (flatworms), Class *Trematoda*, and family *Schistosomatidae*. *Schistosoma*, or split body, refers to the appearance of the adult male's lateral edges that fold to form a groove (gynecophoral canal) where the female worm resides. Schistosomes differ from other trematodes in that there are distinct male and female adult worms. *S. haematobium* affects the urogenital tract, while the other two are hepatobiliary and intestinal parasites.[3]

A cercaria is a free-living, actively swimming stage, with a body and a tail. The body contains the acetabulum (ventral sucker); the tail serves to propel, and act as a fulcrum when trying to enter into the skin of a definitive host. Fatty acids (i.e; linoleic acid) and amino acids (i.e; arginine) are chemoattractants to the cercariae.

The cercariae will search for surface skin irregularities associated with hairs, ridges or wrinkles. Once attached to the host, they secrete proteolytic penetrating enzymes by the acetabulum glands; upon entering the skin, the tail detaches and they become known as schistosomules (schistosomulum). At this point, the parasite has changed morphologically and resides in the skin from one to several days before entering the dermal vasculature, after which they begin to feed and mature into the the adult worm stage. Sexes can then be distinguished. Interestingly, the male can develop fully without the female, but the female does not reach sexual maturity in the absence of the male. The female must lie within the male's gynecophoral canal for physical and reproductive development. It is believed the adult worms copulate in the liver before migrating to the mesenteric vein.

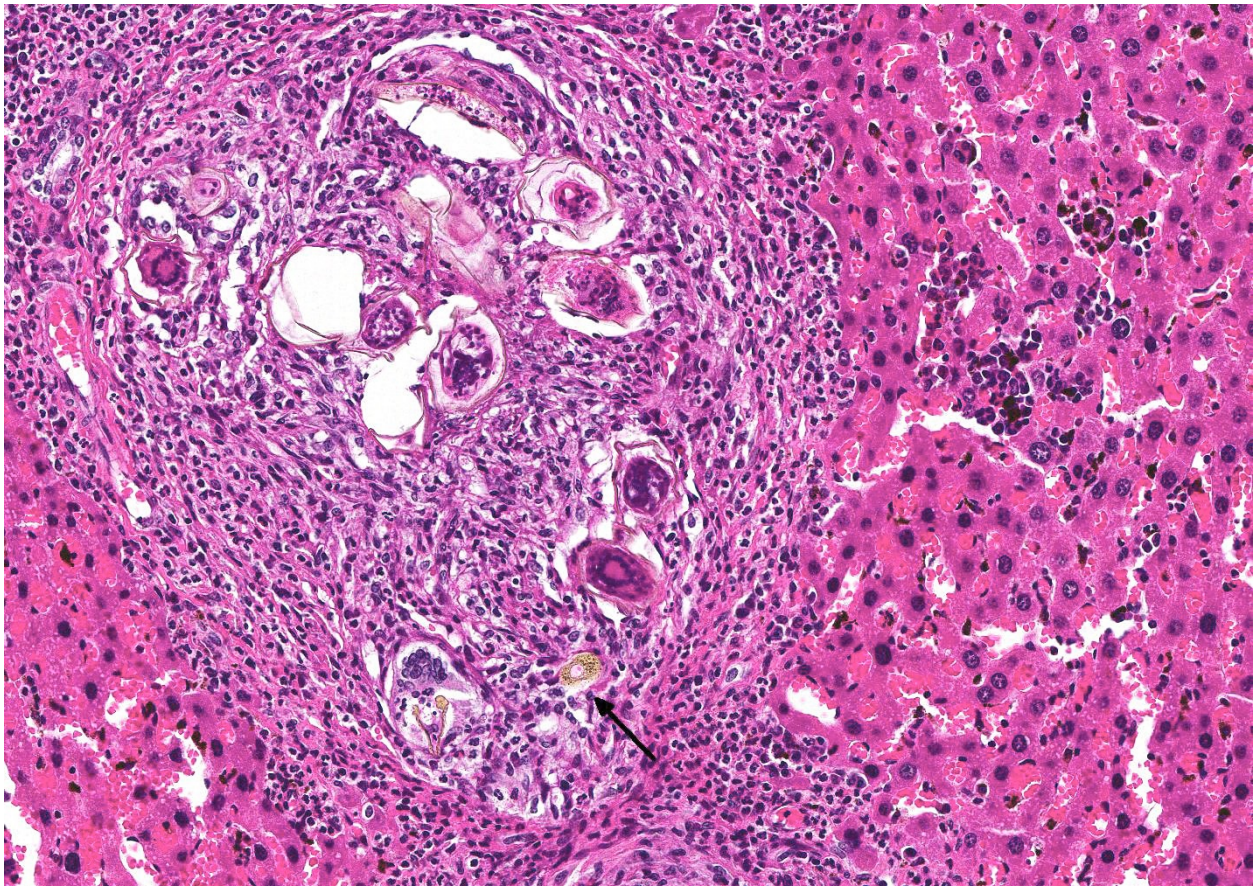

Liver, mouse. Granulomas are centered on numerous schostosome eggs with a refractile brown shell, which contain a multinucleated miracidium. Cross sections of the ends of eggs are brownish yellow (arrow). The surrounding hepatic parenchyma contains numerous hypertrophic Kupffer cells which often contain brownish granular pigment (hemozoin). There is a focus of extramedullary hematopoiesis within the liver parenchyma at right. (HE, 114X)

The male will then anchor the pair to the mesenteric venules by its powerful suckers and muscular body. Females can produce up to 300 embryonated eggs/day, each containing a miracidium. Eggs are released vessel walls, penetrating via egg-released enzymes, and/or by the host' own immune response (granuloma formation), resulting in intestinal tract entry. Many eggs do not enter the vasculature and end up in tissues eliciting an inflammatory response; if they enter the intestine, they are shed in the feces.

In fresh water, the egg shell ruptures, releasing motile, multiciliated miracidia, which have approximately 12 hours to find a snail host. Once inside the snail, they lose their cilia and transform into a primary sporocyst – a sac-like, asexual breeding chamber with numerous secondary sporocysts. . After approximately 2 weeks, the secondary sporocysts escape the primary sporocyst, and migrate to the snail's hepatopancreas and gonads. After another 2 weeks, secondary sporocysts give rise to thousands of cercariae. Once fully developed, the cercariae emerge from the secondary sporocysts, migrate to the anterior of the snail, and are released into the surrounding water to repeat the life cycle. [4].

Schistosomiasis is the condition in which parasitic eggs lodge in the tissues of the definitive host and elicit an chronic inflammatory response. In humans, eggs can

also lodge in the intestinal mucosa and/or submucosa leading to the formation of granulomatous pseudopapillomas or pseudo-polyps which can cause luminal obstruction, ulceration and/or hemorrhage. [2,3,5,7]. Eggs trapped in pre-sinusoidal portal venules secrete soluble egg antigens which are taken up by antigen presenting cells.

Antigen presentation stimulates Th1 cells to secrete IL-2, IFN-gamma and TNF which in turn ilicit a cell mediated response. As the granuloma becomes more organized, Th1 cells are replaced by Th2 cells which produce IL-4, IL-5, IL-10, and IL-13, and the synthesis of IgE, completing granuloma maturation. As the lesions persist, fibroblasts are stimulated by egg products and T-cell cytokines, and produce collagen. Over time, there is downregulation of the Th2 response, resulting in the reduction in the size of newly-formed granulomas. This immunomodulation may be driven by cytokines IL-10 and TGF-beta, induce T-regulatory cells and regulate Th1/Th2 responses. T-regulatory cells and B cells are known sources of IL-10, a key regulator of the egg induced granulofibrotic response.

Marked eosinophilia is a common feature of acute schistosomiasis and may occur before egg deposition. The migration of eosinophils from the circulation to site of infection is primarily induced by CCL11. Under the influence of the Th2 response, the combined effect of IL-5 and GM-CSF contribute to increase in eosinophilia.

Hepatic stellate cells (HSC) are one of the main sources of collagen in the liver and play a crucial role in schistosome-induced fibrogenesis. When activated by IL-13, they differentiate into myofibroblasts, producing collagen. Chemokines associated with HSC recruitment include CXCL1, CCL7, CCL12, and CCL21. Schistosome eggs can inhibit the differentiation of HSC into myo-fibroblasts; *S. mansoni* has the ability to reverse HSC differentiation to their quiescent state[1].

Chronic schistosomiasis leads to extensive periportal fibrosis, a condition known as Symmer's pipestem fibrosis. Portal fibrosis leads to portal hypertension which contributes to splenomegaly, and esophageal and gastric varices[5,7]. Exsanguination by esophageal variceal bleeds is the major cause of death in humans[7].

JPC Diagnosis: Liver: Hepatitis, granulomatous and eosinophilic, random to portal, with numerous schistosome eggs and moderate intrahistiocytic fluke excrement, Swiss Webster (*Mus musculus)*, mouse.

Conference Comment: Schistosomiasis, a fluke infection utilizing snails as intermediate hosts, is prevalent in domestic animals in Asia, Africa, and tropical areas; interestingly this condition does not often cause clinical disease. Generally, damage caused by flukes is due to the orientation of adults and eggs within the vasculature of the liver; lungs, gastrointestinal tract, urinary tract, and nasal cavity. The schistosome's life cycle is similar to other flukes and outlined nicely by the contributor.

Heterobilharzia americana causes clinical disease in dogs, particularly in the southern United States (Louisiana and Texas). The raccoon serves as the definitive host, while dogs and a multitude of other species (bobcat, armadillo, Brazilian tapir, beaver, coyote, mountain lion, mink, nutria, opossum, red wolf, swamp rabbit, and white-tailed deer) serve as accidental hosts. *H. americana* causes hepatic granulomatous lesions which may result in a variety of clinical signs including: mucoid to bloody diarrhea, lethargy, weight loss, vomiting,

anorexia, and ascites. In some cases, dogs experience hypercalcemia due to release of 1,25-dihydroxycholecalciferol from macrophages resulting from the chronic inflammatory process. Microscopically, liver lesions are characterized by multifocal lymphoplasmacytic, eosinophilic to granulomatous inflammation surrounding mineralized eggs that are often arranged in linear arrays. PCR is required to differentiate *H. americana* from other schistosomes by identification of specific subunit ribosomal RNA.[6]

In this case, the species of *Schistosoma* is unknown. Dr. Chris Gardiner, Consultant for Veterinary Parasitology, Joint Pathology Center, reviewed the case and was also unable to specify which type.

There was spirited discussion during the conference about what to call the brown granular pigment within Kupffer cells. It is a fluke byproduct which may represent blood pigment, fluke excrement, or a combination of both.

Contributing Institution:
Veterinary Pathology
Division of Veterinary Resources
Office of Research Services
National Institutes of Health
https://www.ors.od.nih.gov/sr/dvr/drs/Pages/default.aspx

References:

1. Chuah C, Jones MK, Burke ML, McManus DP, Gobert GN. Cellular and chemokine-mediated regulation in schistosome-induced hepatic pathology. *Trends Parasitol*. 2014;30(3):141-150.
2. Colley DG, Bustinduy AL, Secor WE, King CH. Human schistosomiasis. *Lancet.* 2014:383:2253-2264.
3. Elbaz T, Esmat G. Hepatic and intestinal schistosomiasis: review. *J Adv Res*. 2013:4:445-452.
4. Lewis FA, Tucker MS. Schistosomiasis. In: Toledo R, Fried B, eds. *Digenetic Trematodes, Advances in Experimental Medicine and Biology*. New York, NY: Springer Science+Business Media; 2014:47-75.
5. Olveda DU, Olveda RM, McManus DP, Cai P, et al. The chronic enteropathogenic disease schistosomiasis. *Int J Infect Dis.* 2014; 28:193-203.
6. Robinson WF, Robinson NA. Cardiovascular system. In: Maxie MG, ed. *Jubb, Kennedy, and Palmer's Pathology of Domestic Animals*. Vol. 3. 6th ed. St. Louis, MO: Elsevier; 2017: 91-94.
7. Shaker Y, Samy N, Ashour E. Hepatobiliary schistosomiasis. *J Clinic Transl Hepatol.* 2014;2:212-216.

CASE IV: MS17-3649 (JPC 4104252).

Signalment: 3-month-old, male and female, AG129, *Mus musculus*, mouse.

History: Mice received one foot pad injection of Zika virus. Seven to ten days later, the mice were submitted to necropsy due to weight loss or having been found dead. At presentation, live mice were scruffy, some were unstable on their rear legs and others had developed hind limb paralysis. The animals were in thin - lean body condition with variable hydration status.

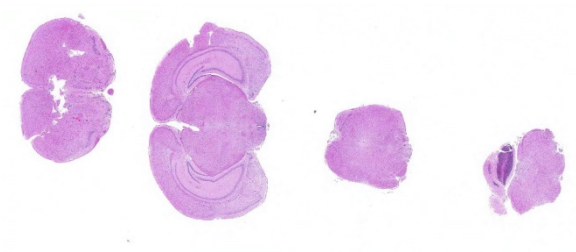

Cerebrum, mouse. 4 sections of brain, from rhinencephalon (left) to cerebellar vermis (right) are presented for examination. (HE, 5X)

Gross Pathology: No gross lesions were present.

Laboratory results: None submitted.

Microscopic Description: Inflammatory changes in the brain were present primarily in the cerebrum and were composed of multifocal, random aggregates of neutrophils, necrotic cells [presumed to be astrocytes] with minimal gliosis. Inflammation varied from minimal - mild and occasionally there were solitary necrotic cells without associated inflammation or interstitial change. Neuronal necrosis varied from none to foci of necrotic neurons. Few vessels had smooth muscle hypertrophy with acute – subacute vasculitis. There was variable ependymal cell necrosis. Similar inflammatory and vascular changes were present in the spinal cord. Some sections of cerebellum had mild granular layer necrosis. Purkinje cells appeared to be spared.

There is variation of the severity of the lesions in some slides.

Acute orchitis with seminiferous tubule cell necrosis was the only other microscopic lesion. [Not submitted]

Transmission Electron Microscopy: In the cytoplasm of cerebral axons and dendrites, there were areas with highly expanded and convoluted endoplasmic reticulum (Image #48). Within the endoplasmic reticulum, there were membrane-bound vesicles with numerous unenveloped, 35- 45 nm, round, dark cored particles. Some virions were heavily clustered while others were widely dispersed within the vesicle. There was adjacent cellular debris with a few degenerated mitochondria. (Image #91) The adjacent tissue was unaffected. (Image #55). Bar = 500 nm.

Contributor's Morphologic Diagnosis: Meningoencephalitis and myelitis, multifocal, minimal to moderate, subacute with neuronal necrosis and vasculitis.

Contributor's Comment: Zika virus is an 11 kb ssRNA Flaviviridae carried by *Aedes* spp. mosquitoes. Other flaviviruses to which it is related are West Nile, Dengue, and yellow fever. Zika virus infection was first described in 1952 where it was isolated from a febrile sentinel rhesus macaque in the Zika forest of Uganda.[3] Since then, the virus has spread to Asia and caused outbreaks in Micronesia in 2007 and French Polynesia in 2013. In 2015, the first case was reported in Brazil.[4,7] Since then, there has been widespread infection, 440,000 – 1.3 million, reported in Central and South America, the

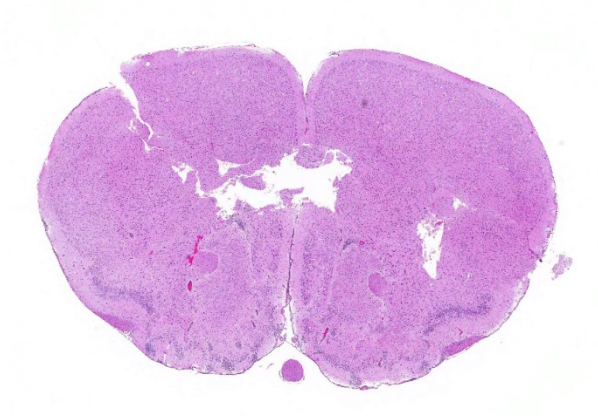

Brain, mouse. The rhinencephalon shows marked hypercellularity within the neuropil, particularly in the ventral regions. (HE, 18X)

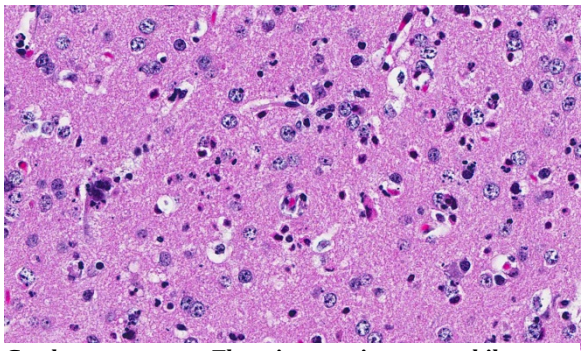

Cerebrum, mouse. There is extensive neutrophil infiltration of the parenchyma throughout the brain, which is most severe in the rhinencephalon. Neutrophils both individually and in small clusters undergo degeneration ad necrosis. (HE, 400X)

Caribbean, and Miami.[2,5,8] The Ministry of Health of Brazil has reported there has been a 20-fold increase in microcephaly.[6]

Infection via Aedes spp. mosquitoes is the most common route of infection. Viral replication occurs within mosquitos which, when taking a blood meal, then infect humans. Nonhuman primates and other mammals may serve as reservoir hosts. Aedes' range is global but most species are concentrated in tropical and subtropical areas. The virus can also be transmitted as a congenital/perinatal or sexual infection. [6,7,8] Transmission via blood transfusion also has been reported.[7]

It is thought that after a mosquito bite, the virus enters through fibroblasts, keratinocytes and immature dendritic cells, migrates to lymph nodes and blood.[8] Once in the cell, the virus induces marked proliferation of the endoplasmic reticulum, rearrangement of the ER membranes, and formation of vesicles, typical of flaviruses. The virus then replicates within the vesicles to form immature virions. The vesicle passes into the Golgi apparatus, becomes glycosylated in and then, being released from it, undergoes final maturation in cytoplasmic vesicles and is released as a mature virion.[7]

Approximately 80% of Zika virus infections are asymptomatic. Infection may be associated with fever, rash, arthralgia, myalgia, headache and conjunctivitis and signs tend to resolve in 2 weeks.[4,6,7] Similar symptoms can also be seen Dengue and Chikungunya virus infection. Individuals may go on to develop meningitis and meningoencephalitis. Additional reported sequelae include hearing loss, hema-tospermia, hypotension and genitourinary symptoms. Infection in Asia and the Americas has been associated with an increase in Guillain-Barré syndrome. Death is not common but has been reported in debilitated/immune-suppressed individuals.[2,8]

Tests to detect Zika can be performed on: CSF, blood, serum, amniotic fluid, fetal and placental tissues, urine, and saliva. During the acute phase of infection, RT-PCR is the best test in which to confirm for Zika virus. However, the period that RNA is present may be as short as 5 days. Serology may also be used but results may be confounded by previous flaviviral infection and time between infection and testing.[8]

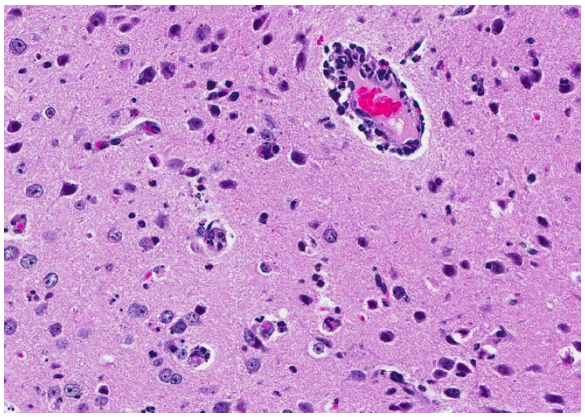

Cerebrum, mouse. In areas of necrosis, vessel walls often contain neutrophils and cell debris (vasculitis). (HE, 400X)

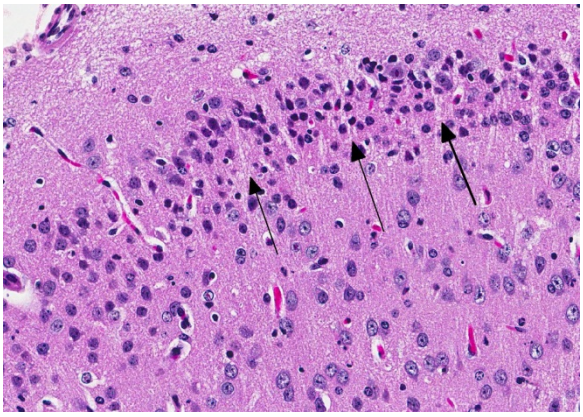

Cerebrum, mouse. There is necrosis of neurons within the cerebrum; in the submeningeal grey matter, it is segmental (arrows). (HE, 400X)

Autopsy findings in a small cohort of ten term neonates included low brain weight, microcephaly with thinning of cerebral cortices with overlapping sutures, pachygyria or agyria and increased ventricle size; thin corpus callosum and optic chiasm; thickening of the leptomeninges; and calcifications between grey and white matter. Other findings included aqueduct stenosis, cerebellar hypoplasia, brainstem abnormalities, and thin, distorted spinal cords. All the neonates had arthrogryposis and some were microphthalmic.[2] Infectious agents that are known to cause similar lesions in infants: intrauterine growth restriction, microcephaly and calcifications, conjunctivitis, hearing loss, rash, hepatosplenomegaly, or thrombocytopenia, are known by the acronym TORCH: Toxoplasmosis, Other (syphilis, varicella-zoster, parvovirus B19, HIV), Rubella, Cytomegalovirus (CMV), and Herpes.

Microscopic lesions appeared to be secondary to abnormal migration and cerebral neuronal/glial loss. Neurons were seen in abnormal locations, as immature cell aggregates around the ventricles, with astrocytosis and calcification. Myelin fibers were decreased or absent. Axonal changes included degeneration, spheroid formation, and loss of orientation. Branching tubes replaced the normal aqueduct. The spinal cord was small due to small cortico-spinal tracts with nerve cell degeneration, loss, gliosis and calcification. Dorsal root ganglia were preserved but ventral ganglia were not. Inflammation was not a prominent feature and when seen, was composed of lymphocytic meningitis, perivascular cuffing and histiocytes and gliosis. Electron microscopy revealed numerous intra-vesicular virions. Muscle atrophy, mild hepatitis and pituitary, retinal and lens mineralization rarely were seen.

Placentas were small for gestational age with inflammation of the villi, fetal membranes and decidua, stromal fibrosis, smooth muscle hyperplasia of villous vessels, chorionic vasculitis, increased vascularity and stromal calcification. In this study, maternal infection in the first or early second trimester led to more severe congenital anomalies.[2]

Until recently, mouse models of Zika have been few. Wild type B6, CD-1, BALB/C mice tend be resistant to Zika infection. However, they can be made to be

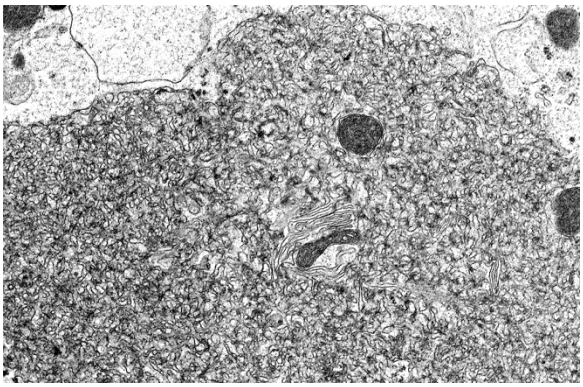

Cerebrum, mouse. In the cytoplasm of cerebral axons and dendrites, there were areas with highly expanded and convoluted endoplasmic reticulum. (Photo courtesy of: Veterinary Pathology, Division of Veterinary Resources, Office of Research Services, National Institutes of Health, https://www.ors.od.nih.gov/sr/dvr/drs/Pages/default.aspx)

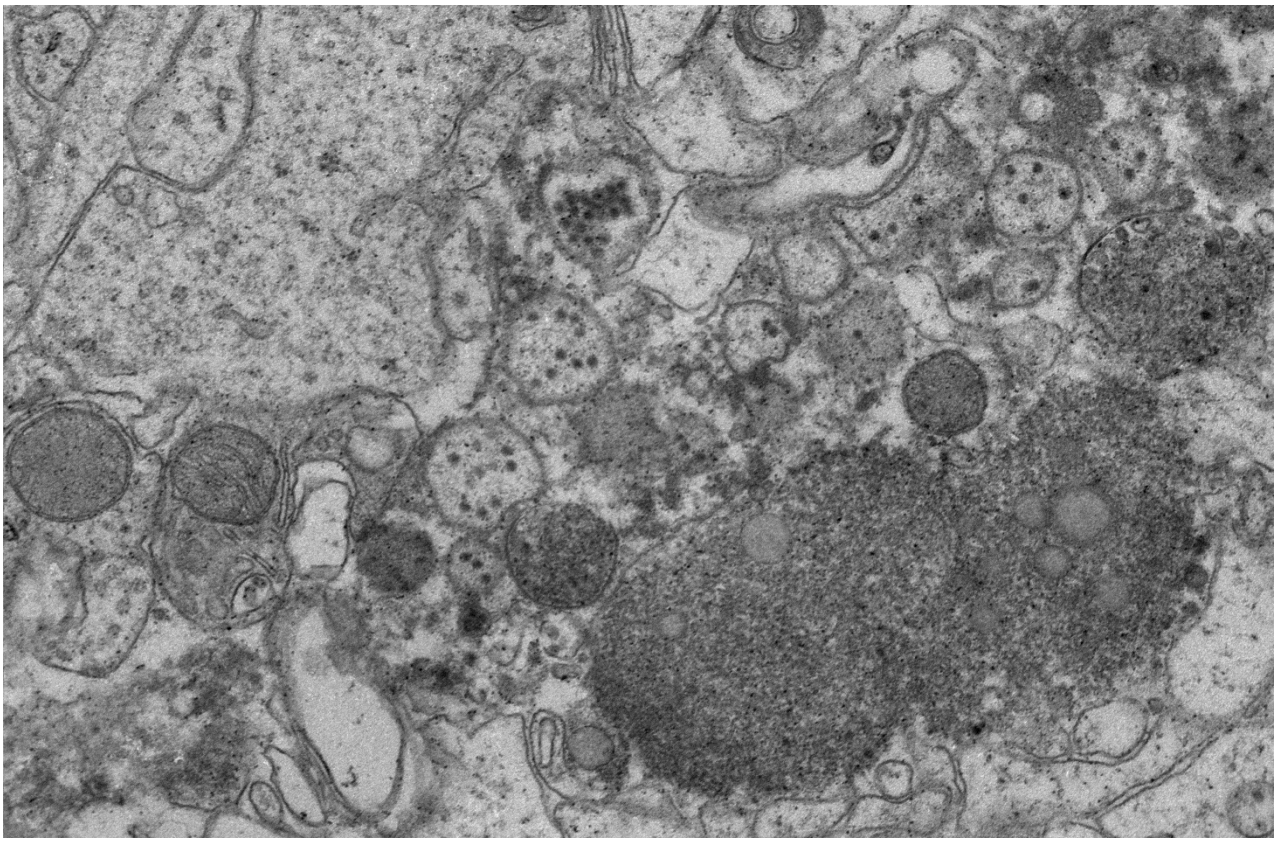

Cerebrum, mouse: Within the endoplasmic reticulum, there were membrane-bound vesicles with numerous non-enveloped, 35- 45 nm, round, dark cored particles. Some virions were heavily clustered while others were widely dispersed within the vesicle. There was adjacent cellular debris with a few degenerated mitochondria. (Photo courtesy of: Veterinary Pathology, Division of Veterinary Resources, Office of Research Services, National Institutes of Health, https://www.ors.od.nih.gov/sr/dvr/drs/Pages/default.aspx)

susceptible by treatment with steroids or mAbs directed against interferon α/β receptors.[5] AG129 mice lack interferon α/β and γ receptors and A129 mice (lacking interferon α/β receptor) are susceptible to Zika infection. As seen in our mice, AG129 mice develop neurologic signs, weight loss and subsequently die but have no gross lesions. Microscopic lesions were limited to the CNS[1]. In some studies, the testis is also affected.[5] The mice have high viral loads are found in brain, spinal cord, spleen and testes and may be studied to determine the pathogenesis of viral dissemination.[5]

JPC Diagnosis: Brain, multiple levels: Meningoencephalitis, necrotizing and neutrophilic, diffuse, moderate with marked neuronal and glial necrosis, AG129 (*Mus musculus*), mouse.

Conference Comment: The conference moderator, who also submitted the case, reviewed the key clinical, gross, and microscopic features of Zika virus (see contributor's comment above). Conference attendees noted necrotic cells randomly arranged throughout the submitted samples (no spinal cord was included) and aggregates of viable and degenerate neutrophils and necrotic cellular debris. Cells are so shrunken it is difficult to determine cell type but most attendees suspect the majority of necrotic cells are

glial cells. The conference moderator showed images from additional tissues including spinal cord and testis. Both of which had a remarkable infiltration of neutrophils and associated necrosis. Within the testis the interstitial space is expanded up to 4 times by neutrophilic inflammation and the spinal cord has degenerative neurons, neuronal necrosis, and spongiosis predominately within the grey matter. There are also numerous astrocytes and neurons that contain eosinophilic intranuclear inclusions, attendees assumed they were viral inclusions. Transmission electron microscopy (TEM) images were provided that clearly identified virions within the cytoplasm but not within the nucleus of affected cells. The pink material seen microscopically cannot be accounted for yet and will most likely be the subject of continued investigation.

Contributing Institution:
Veterinary Pathology
Division of Veterinary Resources
Office of Research Services
National Institutes of Health
https://www.ors.od.nih.gov/sr/dvr/drs/Pages/default.aspx

References:

1. Aliota MT, Caine EA, Walker EC, Larkin KE, Camacho E, Osorio JE. Characterization of lethal Zika virus infection in AG129 mice. *PLoS Negl Trop Dis*. 2016; 10(4):19.
2. Chimelli L, Melo ASO, Avvad-Portari E, Wiley CA, et al. The spectrum of neuropathological changes associated with congenital Zika virus infection. *Acta Neuropathol*. 2017;133(6):983-999.
3. Dick, GW. Zika virus. II. Pathogenicity and physical properties. *Trans R Soc Trop Med Hyg*. 1952;46(5):521-34.
4. Driggers RW, Ho CY, Korhonen EM, Kuivanen S, et al. Zika virus infection with prolonged maternal viremia and fetal brain abnormalities. *N Engl J Med*. 2016;374(22):2142-2151.
5. Morrison, TE, Diamond, MS. Animal models of Zika virus infection, pathogenesis, and immunity. *J Virol*. 2017;91(8):29.
6. Mlakar J, Korva M, Tul N, Popović M, et al. Zika virus associated with microcephaly. *N Engl J Med*. 2016;374(10):951-958.
7. Offerdahl DK, Dorward DW, Hansen BT, Bloom ME. Cytoarchitecture of Zika virus infection in human neuroblastoma and Aedes albopictus cell lines. *Virology*. 2017;501:54-62.
8. Plourde AR, Bloch EM. A literature review of Zika virus. *Emerg Infect Dis*. 2016;22(7):1185-1192.

Self-Assessment - WSC 2017-2018 Conference 9

1. Which of the following inbred strains of mice has an almost 100% incidence of development of pulmonary adenocarcinoma?
    a. A strain
    b. FVB
    c. DBA
    d. C57bl

2. Which of the following Immunohistochemical markers would be expected to be negative in histiocytic sarcomas in mice?
    a. CD163
    b. AE1/AE3
    c. IBA-1
    d. Lysozyme

3. In mice with histiocytic sarcoma, hyaline droplets are most often seen in which tissue?
    a. Ependymal cells
    b. Hepatocytes
    c. Erythrocytes
    d. Renal tubular epithelium

4. The intermediate host for schistosomes is a:
    a. Crayfish
    b. Aquatic mammal
    c. Fish
    d. Snail

5. Which of the following is NOT true about Zika virus ?
    a. About 80% of infections are asymptomatic.
    b. In utero infections may be associated with microcephaly.
    c. In the acute phase of infection, serology is the best diagnostic test.
    d. The testis in an additional target in the mouse.

Please email your completed assessment to Ms. Jessica Gold at Jessica.d.gold2.ctr@mail.mil for grading. Passing score is 80%.This program (RACE program number) is approved by the AAVSB RACE to offer a total of 0.5 CE Credits, with a maximum of 12.5 CE Credits being available to any individual Veterinary Medical Professionals for the 2017-2018 Wednesday Slide Conference. This RACE approval is for the subject matter categories of: SCIENTIFIC using the delivery method of NON-INTERACTIVE DISTANCE. This approval is valid in jurisdictions which recognize AAVSB RACE; however, participants are responsible for ascertaining each board's CE requirements.
RACE does not "accredit", "endorse" or "certify" any program or person, nor does RACE approval validate the content of the program.

Joint Pathology Center
Veterinary Pathology Services

WEDNESDAY SLIDE CONFERENCE 2017-2018

C o n f e r e n c e 10

29 November 2017

CASE I: H12/1754 (JPC 4019375).

Signalment: 3.5-year-old, Aberdeen angus, *Bos primigenius taurus*, bovine.

History: Out of a group of 6 animals, one cow showed chronic, profuse diarrhea and severe, progressive emaciation. The bacteriologic investigation of the feces tested positive for acid-fast rods and negative for Salmonella. Because of the suspicion of paratuberculosis, the cow was
euthanized and submitted for post-mortem investigation.

Presentation, ox. One of a group of 6 cattle displayed effortless and profuse diarrhea with concurrent emaciation. (Photo courtesy of: Institute of Animal Pathology, University of Berne, Länggassstrasse 122, Postfach 8466, CH-3001 Bern, Switzerland , http://www.itpa.vetsuisse.unibe.ch/htm)

Gross Pathology: The animal was moderately emaciated. The muscle masses were reduced, and the ribs were easily palpated. Body fat depots were present. The mucosa of the small intestine, from the duodenum to the ileum was moderate to severe thickened, corrugated, nodular shaped and were light brown. The large intestine content was watery and brown, becoming slightly mucoid in the rectum. No lesions in the colonic mucosa were noted grossly. The mesenteric lymph nodes were moderately enlarged. The rumen pH was 6.5, and the fibers of the content were up to 15 cm long.

Laboratory results:
Blood parameters:

Hematology: (changed parameters)					
Banded Neutrophils	0.54	10^9/l	0	-	0.2
Segmented Neutrophils	6.25	10^9/l	1.0	-	3.5
Lymphocytes	2.05	10^9/l	2.5	-	5.5
Monocytes	0.93	10^9/l	0	-	0.33
Eosinophils	0.00	10^9/l	0.3	-	1.5

Chemistry: (changed parameters)					
Na	116	mmol/l	135	-	165
K	1.50	mmol/l	3.0	-	6.0
Cl	68	mmol/l	90	-	110
Urea	23.99	mmol/l	1.67	-	7.50
Creatinine	183	µmol/l	88	-	133
Bilirubin	23.0	µmol/l	0.85	-	8.6
ASAT (SGOT)	79	IU	117	-	234
GGT	67	IU	10	-	27
GLDH	46	IU	0	-	17

Serology Bovine viral diarrhea (during Swiss eradication program): negative.

Microscopic Description: Small intestine: The intestine is thickened and puts the mucosa in folds. About 90% of the lamina propria and the submucosa are diffusely infiltrated by large numbers of epitheloid macrophages, lymphocytes, plasma cells, eosinophils and fewer neutrophils with numerous multinucleated giant cells of the Langhans and foreign body type. The infiltration distorts and expands the lamina propria of villi. Multifocally, the crypts are moderate to severe extended, lined by an elongated and flattened epithelium. They contain accumulations of cellular debris, mucous and crystalline material (dystrophic calcification) (cryptitis). Crypt epithelium piles up with cells 3-5 deep and with a high nuclear to cytoplasmic ratio (hyperplasia). The lamina propria, the submucosa and the serosa are diffusely widened and pale (edema). The submucosal and serosal lymphatics are diffusely moderately to severely dilated and surrounded by lymphocytes, plasma cells and fewer macrophages. Rarely epitheloid macrophages and multinucleated giant cells plug the lumen of the lymphatics (lymphangitis).

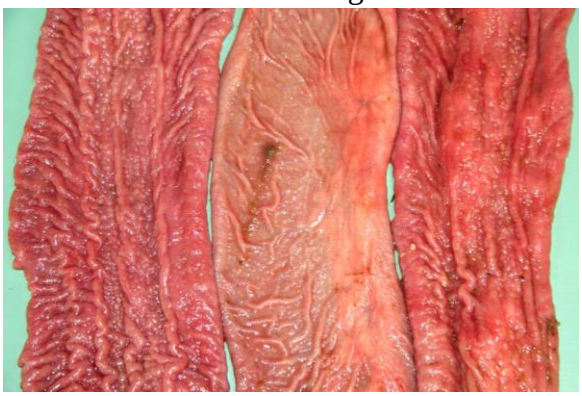

Intestine, ox. The intestinal mucosa is thickened, corrugated, and a segmentally light brown. (Photo courtesy of: Institute of Animal Pathology, University of Berne, Länggassstrasse 122, Postfach 8466, CH-3001 Bern, Switzerland, http://www.itpa.vetsuisse.unibe.ch/htm)

Contributor's Morphologic Diagnosis:
Small intestine: Granulomatous enteritis and lymphangitis with multinucleated giant cells, diffuse, severe, chronic.

Contributor's Comment: Lesions extended from the duodenum to the colon. During necropsy we were impressed about the classic lesion, as it is rarely seen in our necropsy room. The classic histologic picture likewise was a treat. Ziehl-Neelson stained (ZN) many acid-fast rods within the macrophages. The cow had a mild histiocytic lymphadenitis of the mesenteric lymph nodes with ZN-positive rods as well.

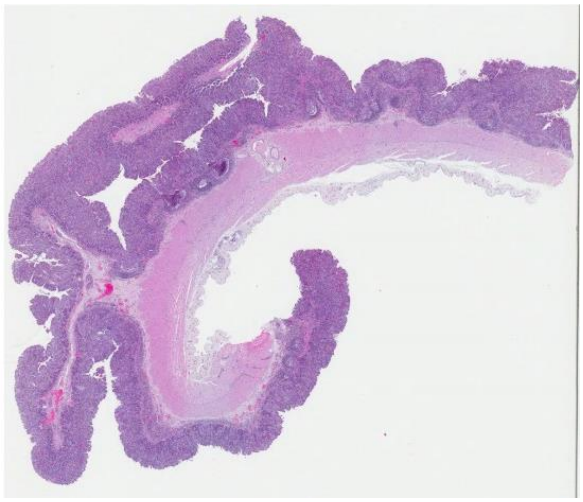

Intestine, ox. A section of thickened, hypercellular intestine is submitted for examination. (HE, 6X)

The diagnosis is paratuberculosis or Johne's disease. Although other infections can be seen on top of mycobacteriosis (e.g. salmonellosis), further bacteriologic investigation was not done.

Johne's disease (JD) or paratuberculosis, caused by *Mycobacterium (M.) avium* subsp. *paratuberculosis (Map)*, causes chronic diarrhea in ruminants. As in our case, typical gross lesions are thickened mucosa, thrown into transverse rugae which will not disappear when the intestinal tract is stretched. Typical microscopic lesions were granulomatous enteritis of the small intestine and lymphadenitis of the draining lymph nodes.

The bacteria are taken up orally by young animals. Susceptibility to infection is greatest in the first 30 days of life. The incubation period of JD is protracted and clinical symptoms are usually detected in cattle 2-5 years-old. Chronic villous involvement leads to malabsorption, protein loss and profuse chronic diarrhea and severe emaciation. The pathogenesis of JD is best understood in cattle. It is assumed to be similar in other ruminants, except that in sheep and goats the enteric gross lesions are often milder. *Map* can be produced in pigs. Spontaneous disease occurs in a number of free-ranging and captive wild ruminants, camelids, rarely in equines and captive primates. Numerous species of wild mammals and several species of wild birds are naturally infected, though not necessarily diseased.[1]

Map has been suspected to play a role in Crohn's disease (CD), a chronic inflammatory bowel disease in humans. Initial suggestion of Map involvement was based on the similarity of the clinical appearance of CD and JD. *Map* has been detected in multiple CD studies, but it is difficult to isolate *Map* from patients with CD. Genetically, over 30 Map genes have been identified in human disease, but no specific association has been shown so far.

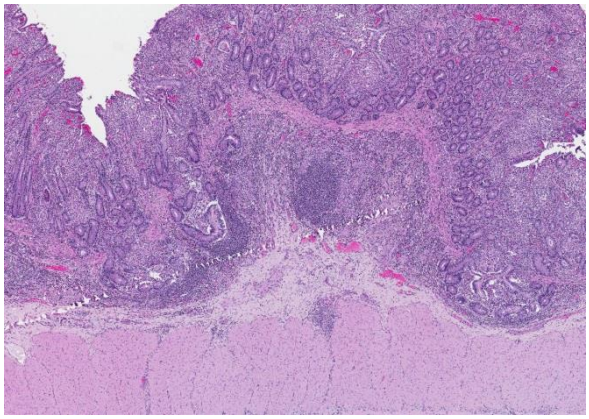

Intestine, ox. There is overall thickening of the intestinal mucosa with loss of villi and crypts, which are replaced by a dense cellular infiltrate. A few remaining hyperplastic crypts extend down into underlying Peyer's patches. (HE 35X)

JD is used as a bovine model of CD. Studies in cattle suggest the early immune response may be similar to the immune response to *M. tuberculosis (Mtb)* during the latent stage of infection. *Map* affords an opportunity to examine the immune response during the early and late stages of infection. These data would also provide insight into how mycobacterial pathogens could contribute to the pathogenesis of CD.[2]

JPC Diagnosis: Small intestine: Enteritis, granulomatous and lymphocytic, diffuse, marked with villar blunting, crypt abscessation and loss, and moderate lymphangitis, Aberdeen angus (*Bos primigenius Taurus)*, bovine.

Conference Comment: Johne's disease in cattle, sheep, and goats is caused by *Mycobacterium avium* ssp. *paratuberculosis* (MAP) and induces granulomatous inflammation of the lepromatous (diffuse) type. The immune response is characterized by a Th2 type of adaptive immune response and appears microscopically as diffuse sheets of macrophages and multinucleated giant cells rather than distinct granulomas as would be expected with a Th1 response.

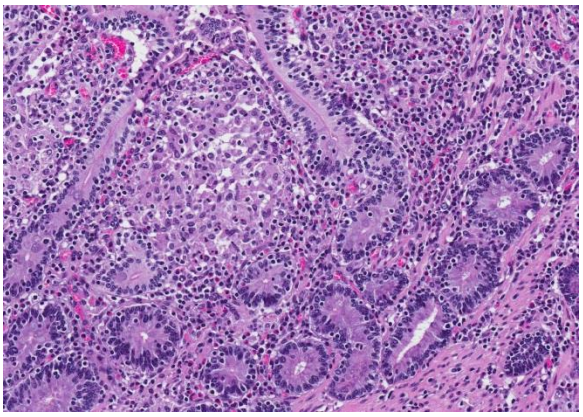

Intestine, ox. The cellular infiltrate extends into the underlying submucosa and tracks vessels. The infiltrate which replaces crypts is composed of numerous polygonal epithelioid macrophage admixed with fewer neutrophils. (HE, 1 56X)

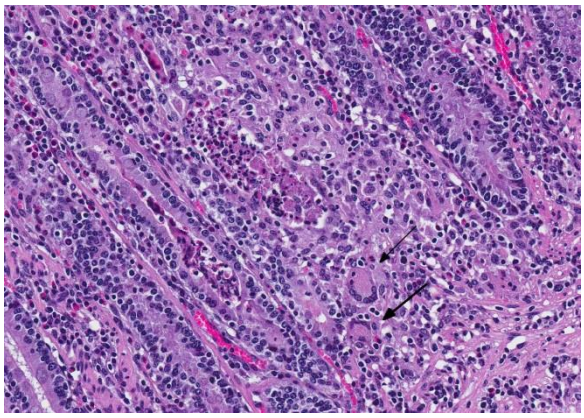

Intestine, ox. Two Langhans-type giant cell macrophages (arrows) are present within the histiocytic infiltrate adjacent to two crypt abscesses. (HE, 228X)

Lesions are most common in the ileum, colon, and mesenteric lymph nodes. Bacteria, which are often numerous, can be identified within macrophages and extracellularly with acid-fast stains. Johne's disease causes injury to cells in three ways: (1) lysis of epithelial cells and extracellular matrix proteins that form cell junctional barriers in the small intestinal mucosa, (2) dysfunction of afferent lymphatic drainage in the small intestinal villi, and (3) lysis of monocyte-macrophage cells and other cells within the lamina propria of infected intestinal villi from chronic inflammatory mediators.[3]

Grossly, affected small intestinal walls are thickened with a cerebriform appearance and mesenteric lymph nodes are enlarged with coalescing areas of yellow-white caseous exudate which occasionally mineralizes. Lymphangitis is common resulting in thickened cords of lymphatic vessels coursing through the mesentery. Additionally, there is marked muscle loss and wasting with intermandibular edema (attributable to hypoproteinemia), fluid accumulation in body cavities, plaques of mineralization and fibrosis within the tunica intima of the thoracic aorta, and diffuse, watery diarrhea. Young animals are most susceptible, and are infected through

ingestion of the bacterium which binds to receptors on the luminal surfaces of M (microfold) cells (which lack a mucous covering). Bacteria are then translocated across the cell into the underlying Peyer's patches and subsequently phagocytosed by tissue macrophages. MAP requires iron for growth and secretes iron-chelating proteins known as exochelins, iron-reductases, and siderophores as virulence factors to acquire iron from ferritin stored in macrophages. Additionally, mycobacterium species can: (1) inhibit acidification of the phagosome, fusion of the phagosome and lysosome, and lysosomal enzyme activities through the production of peroxidases; (2) block injury from reactive oxygen and nitrogen intermediates; and (3) suppress macrophage activation by cytokines (IFN-γ).[3]

There was apathetic debate amongst conference attendees regarding the use of granulomatous versus lymphoplasmacytic versus histiocytic to describe the inflammatory infiltrate in this case, a debate which has been oft-repeated over the years, especially when cases of Johne's disease are

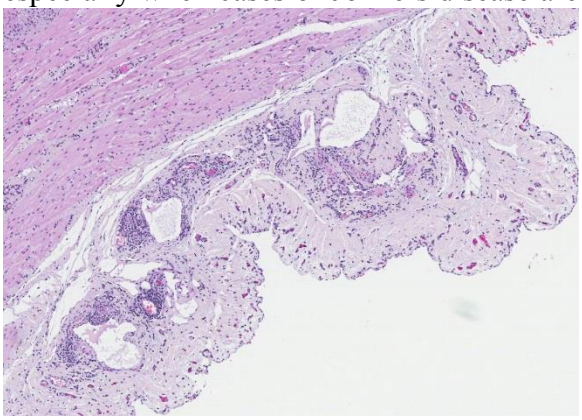

Intestine, ox. Dilated lymphatics within the edematous serosa are surrounded by low to moderate numbers of lymphocytes and fewer histiocytes and plasma cells (lymphangitis). (HE, 80X)

discussed. In this particular case, the presence of multinucleated giant cells and epithelioid macrophages suggest a granulomatous process, their presence

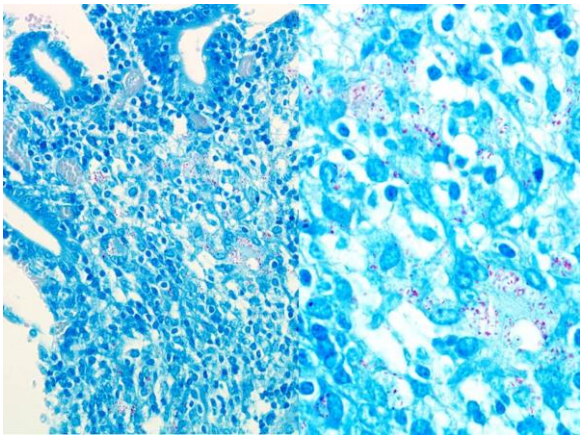

Intestine ox: Mucosal histiocytes contain moderate numbers of acid fast bacilli consistent with M. paratuberculosis. (Ziehl-Nielsen, 400X)

however, was restricted to the submucosa and further out, especially around lymphatics. Lymphocytes, however, predominate in the lesion. Ultimately, the group decided that the presence of numerous epithelioid macrophages in the mucosa as well as the multinucleated macrophages warranted the use of granulomatous in this particular instance.

Contributing Institution:

Institute of Animal Pathology, University of Berne
Länggassstrasse 122, Postfach 8466, CH-3001 Bern, Switzerland
http://www.itpa.vetsuisse.unibe.ch/htm

References:

1. Brown CC, Baker DC, Barker IK. Alimentary system. In Maxie MG, ed. *Jubb, Kennedy, and Palmer's Pathology of Domestic Animals*. 5th ed. Vol. 2. Philadelphia, PA: Elsevier; 2007:222-225.

2. Davis WC, Madsen-Bouterse SA. Crohn's disease and *Mycobacterium avium* subsp. *paratatuberculosis*: The need for a study is long overdue. *Vet. Immunol. Immpathol*. 2012;145:1-6.

3. Zachary JF. Mechanisms of microbial infections. In: Zachary JF, ed.

Pathologic Basis of Veterinary Disease. 6th ed. St. Louis, MO: Elsevier; 2017:162-163.

CASE II: JCP-TAMU-1 2017 (JPC 4102431).

Signalment: 1.5-year-old, Domestic shorthair, *Felis catus*, feline.

History: This 1.5-year-old, castrated-male DSH (*Felis catus*) was taken to the rDVM on a Tuesday for anorexia, vomiting, and not being as "vocal" as normal. He was treated with an anti-emetic (maropitant and cerenia) and sent home. He hid under the bed all day and had a "seizure." The cat returned to the rDVM on Wednesday where he had a seizure and was hypersalivating. The RDVM did a serum chemistry diagnosing renal failure (Creatinine >20mg/dL (0.3-2.1 mg/dL) and BUN>200 mg/dL (<35 mg/dL)). The cat had elevated serum amylase (2263 U/L (300-1100 U/L)). The cat was referred to TAMU emergency receiving. The cat was dehydrated and quiet but otherwise normal physically. The owner was worried that the cat ate some lilies she had received in Monday. Bloodwork showed severe renal failure. A poor prognosis was given and euthanasia was elected late Tuesday night.

Kidney, cat. The kidney was unremarkable. (Photo courtesy of: Texas A&M University, College of Veterinary Medicine and Biomedical Sciences, (Departmental Web site address): http://vetmed.yamu.edu/vtpb)

Gross Pathology: A 4.9 kg (10.8 lb), 1.5-year-old, castrated-male, orange tabby Domestic Shorthair cat in good body condition is autopsied on January 19, 2017.

INTEGUMENTARY/SPECIAL SENSES: A 4 cm circumferential band on the left antebrachium and 2x2 cm on the plantar surface of the left crus are shaved. A moderate amount of brown debris (cerumen) is in both external ear canals.

RESPIRATORY: The lungs are diffusely dark red, glistening, and wet, and on section, ooze abundant, red, foamy fluid into the airways (pulmonary edema). A 1.5x2 cm, pale pink, hyperinflated area is at the margins of the cranial lung lobes (emphysema).

CARDIOVASCULAR (Heart weight: 26 g; Right ventricular wall: 1.5 mm; Left ventricular wall: 4 mm)**, MUSCULOSKELETAL**, **HEMIC & LYMPHATIC** (Spleen weight: 20 g), **ENDOCRINE**, **URINARY** (Right kidney weight: 20 g; Left kidney weight: 20 g), **GENITAL**, **DIGESTIVE**, **LIVER/PANCREAS** (Liver weight: 106 g), **NERVOUS** (Brain weight: 28 g): No significant findings.

Laboratory results:

Blood pressure 120 mmHg (120-180 mmHg)

Severe acidosis pH=7.158 (7.38-7.49))

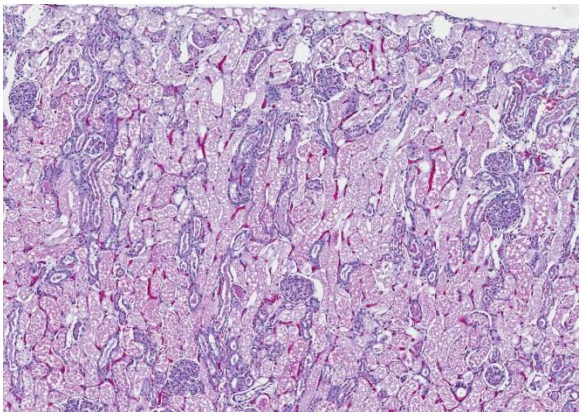

Kidney, cortex. There is extensive necrosis of proximal convoluted tubules and filling of the lumen with light pink proteinaceous and cellular debris. Regenerating tubular epithelium is deeply basophilic. (HE, 50X)

Hypermagnesimic 0.86 mmol/L (0.38-0.52 mmol/L)
Moderate hyperkalemia 5.09 mmol/L (3.91-4.4 mmol/L),
Azotemia = elevated BUN (250 mg/dL (7-32 mg/dL)) and creatinine 12 mg/dL (0.6-1.9 mg/dL))
Hyperosmotic = osmolarity 377.8 mOsm/kg (291-309 mOsm/kg)

Kidney scraping at necropsy: few birefringent (oxalate presumed) crystals (physiologic normal)

Macroscopically the kidneys were unremarkable.

Microscopic Description: Kidney: The section of kidney contains the cortical surface through to the collecting tubules. The proximal tubules are uniformly affected with necrosis and sloughing of tubular cells to fill their lumens. The denuded basement membranes remain intact. Glomeruli are unaffected, and the interstitium is expanded in patches of tubules and around large vessels. Moving toward the cortico-medulary junction, tubules begin to have a granular content, and surviving, attenuated tubular cells surround granular cell debris (granular casts). The regenerating tubular cells often have karyomegaly, and the lining cells progressively become more numerous in tubular profiles. Occasionally, deep blue homogeneous orbs are in cell debris (presumed nucleic acid cohesions). In the medullary tubules and collecting ducts the lining cells are normal and tubules contain occasional granular casts. The medulla has a few foci of nephrocalcinosis. Few, presumed, pre-existing foci of interstitial mononuclear inflammation are noted**.**

Contributor's Morphologic Diagnosis:
Kidney: Severe subacute proximal tubular necrosis/nephrosis, severe subacute proximal tubular injury; granular tubular casts; tubular regeneration.

Contributor's Comment: This is a straight forward case of lily intoxication in a cat. [1-3, 6-7, 9] Early onset of vomition, anorexia, hypersalivation, and apathy with rapid progression and later, seizures is usually reported. Unfortunately, as in this case, if early, immediate, rigorous gastric cleansing and fluid diuresis are not instituted, these cases are fatal. The renal lesion is acute proximal tubular necrosis with rupture and sloughing of lining cells leaving tubules full of indistinct cell debris. Ultrastructurally, the cells are characterized by early (<8 hours post exposure) disruption of apical crista, nuclear pyknosis, megamitochondria and some lipid droplet formation.[8] The lesions are thought to be the result of hypoxia related to mitochondrial intoxication, and the megamitochondria are the product of mitochondrial fusion. The actual toxins are thought to be several steroidal glycoalkaloids, but are undefined.[10] Aqueous extracts of all parts are toxic, and flowers are believed to be more toxic than leaves. Actual experimental cat experiments are limited, but the toxicity curve is steep and different fractions of aqueous extracts, though toxic, are of variable toxicity.

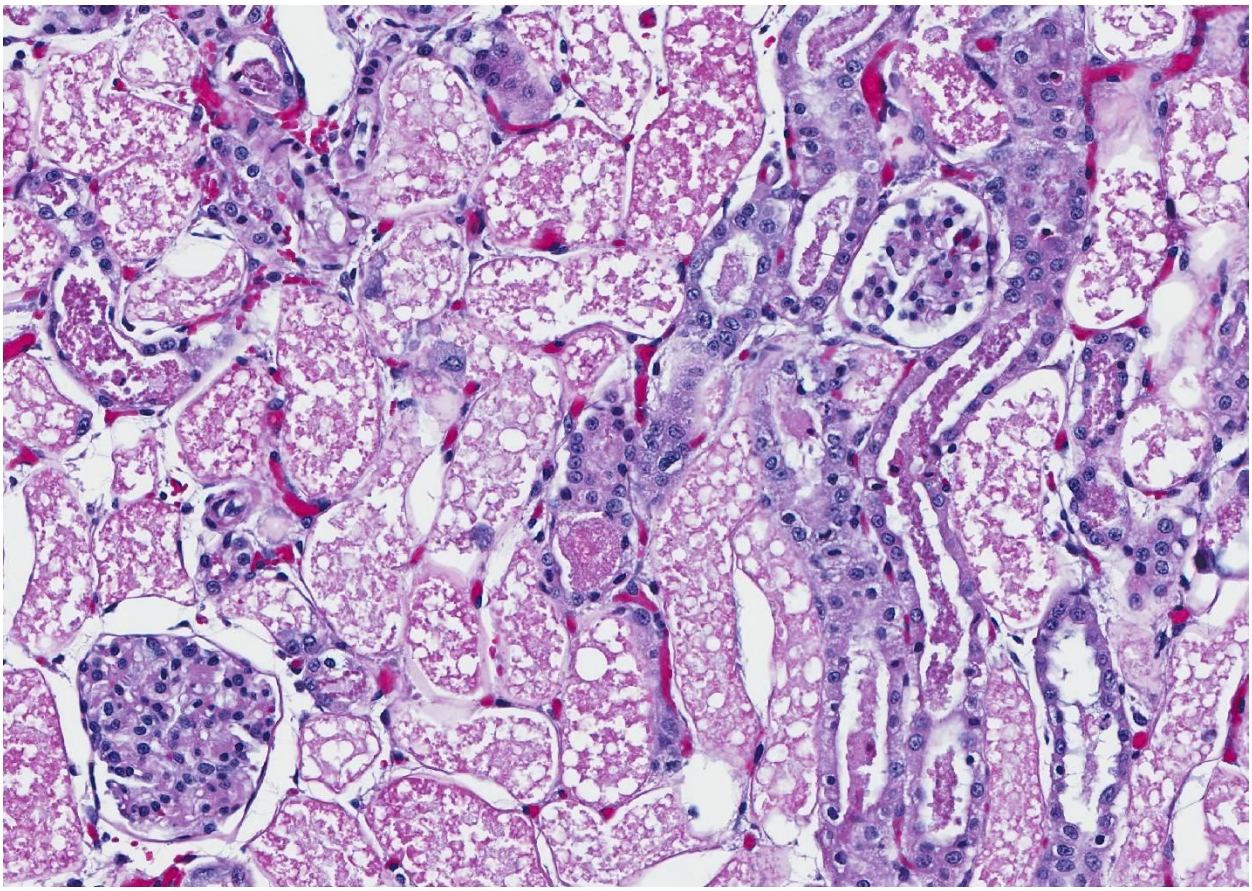

Kidney, cortex. Higher magnification of the diffuse tubular epithelial necrosis. Approximately 15% of the epithelium has begun to regenerate. Glomeruli are within normal limits. (HE, 176X)

Another lesion seen in cats is pancreatic acinar cell degeneration. [3, 8] It is a subtle lesion consisting of numerous, small vacuoles especially prominent in the basophilic cytoplasmic zone of acinar cells which was seen in this cat. Ultra-structurally, these vacuoles presumably represent lipid vacuoles, again, the result of hypoxia. The increase in amylase reported in some cases, including the one presented, is thought to reflect the acinar cell damage.

Seizuring is reported terminally as in this cat. Although thought to be the result of uremia, the cause of seizuring is felt by some to be more complicated and perhaps involves the effect of the toxin because these seizures are triggered by handling.[8]

Exposure to lilies inevitably occurs in households with cats that have lilies of many species (growing or delivered as gifts) because cats will seek them out.[9] A tragic but fascinating condition.

JPC Diagnosis: Kidney, proximal convoluted tubules: Necrosis, diffuse with regeneration and granular cast formation, Domestic shorthair (*Felis catus*), feline.

Conference Comment: Several members of the *Liliaceae* family affect domestic animals, namely, *Lilium* spp. in cats and *Narthecium ossifragum* (bog asphodel) in ruminants. Cats and ruminants are affected by ingestion of leaves or flowers of the plants and present with acute onset polyuria, polydipsia, glucouria, proteinuria,

isosthenuria, and azotemia.[5] The toxic ingredient is unknown, but the acute proximal tubular necrosis that occurs in the kidneys is most likely a result of hypoxia. The most common genera of lily plants, the Easter lily (Lilium longiflorum), affects cats seasonally when plants are brought into their environment; other species: day lily (Hemerocallis spp.), tiger lily (Lilium sp.), Japanese show lily (Lilium hybridum), and rubrum lily (Lilium rubrum) also cause identical renal lesions in cats.[4] Additionally, cats have acute pancreatic necrosis and elevated creatinine kinase. Renal tubular epithelial cells have swollen mitochondria, megamitochondria, and accumulation of lipid droplets ultrastructurally.[5]

The presence of intact basement membranes was demonstrated in the conference with a periodic acid-Schiff with methenamine (PAMS) stain. This stain may be useful in demonstrating tubulorrhexis (induced by ischemia), or its absence (suggestive of acute toxicities). Other differentials for this particular lesion which were briefly discussed included heavy metals, acetaminophen, trimethylprim sulfa, bee or snake venom, various chemotherapeutics, and ethylene glycol. Ethylene glycol could be immediately ruled out in this case because of a lack of intratubular crystal formation.

The blue "orbs" mentioned by the contributor were noticed and admired by conference participants. We agree that they are most likely nucleic acid deposition and are reminiscent of nuclear debris seen in acute tumor lysis syndrome, although their

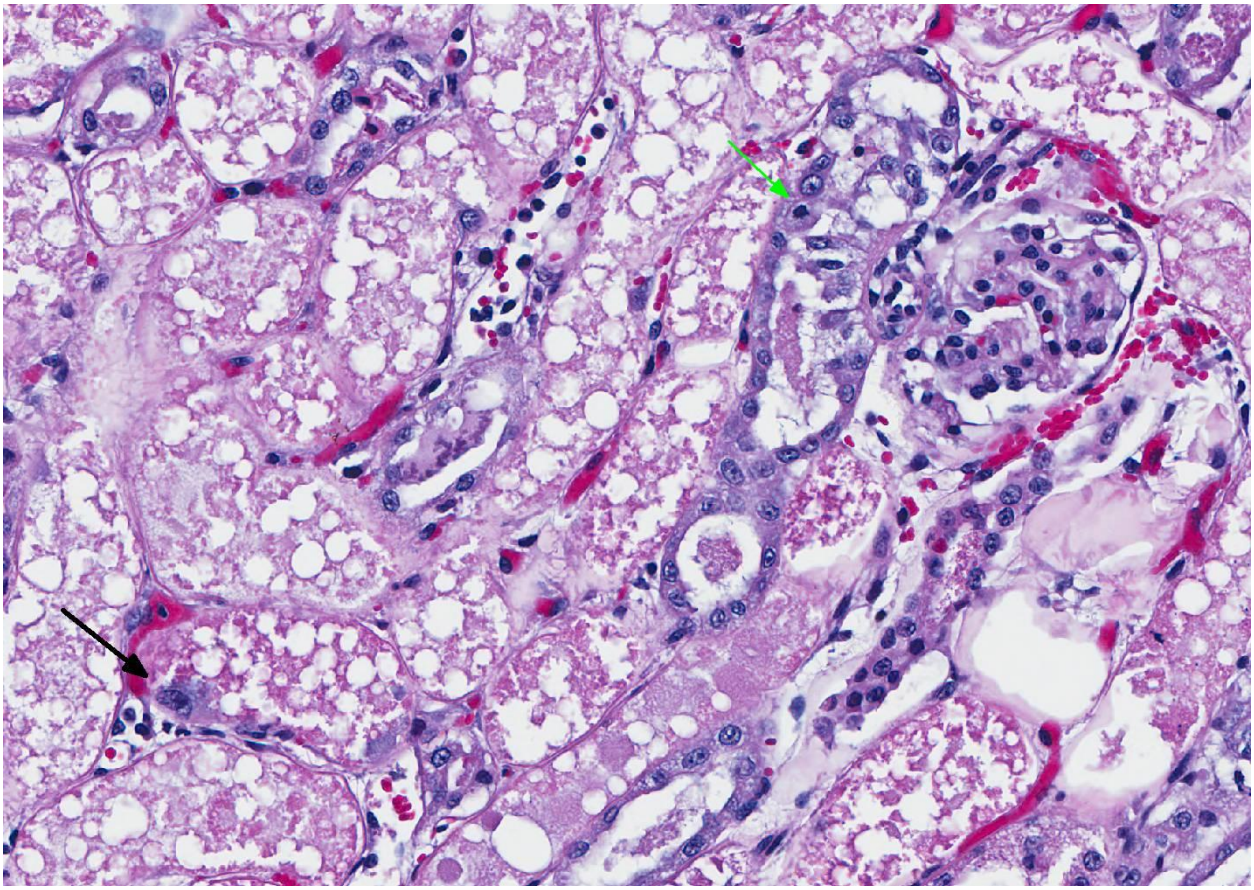

Kidney, cortex. Regenerating epithelium displays mitotic figures (green arrow) and karyomegaly (black arrow). (HE, 202X)

presence in renal tubules is unique.

Contributing Institution:
Texas A&M University
College of Veterinary Medicine and Biomedical Sciences
http://vetmed.tamu.edu/vtpb

References:

1. Bennett AJ, Reineke EL. Outcome following gastrointestinal tract decontamination and intravenous fluid diuresis in cats with known lily ingestion: 25 cases (2001–2010). *J Am Vet Med Assoc.* 2013;242:1110–1116.
2. Berg RIM, Francey T, Segev G. Resolution of acute kidney injury in a cat after lily (*Lilium lancifolium*) intoxication. *J Vet Intern Med*. 2007;21:857–859.
3. Brady MA, Janovitz EB. Nephrotoxicosis in a cat following ingestion of Asiatic hybrid lily (*Lilium* sp.). *J Vet Diagn Invest*. 2000;12:566–568.
4. Breshears MA, Confer AW. The urinary system. In: Zachary JF, ed. *Pathologic Basis of Veterinary Disease.* 6th ed. St. Louis, MO: Elsevier; 2017:681.
5. Cianciolo RE, Mohr FC. Urinary system. In: Maxie MG, ed. *Jubb, Kennedy, and Palmer's Pathology of Domestic Animals.* Vol. 2. 6th ed. St. Louis, MO: Elsevier; 2016:428.
6. Fitzgerald KT. Lily toxicity in the cat. *Topics Comp Anim Med.* 2010;25:213-217.
7. Langston CE. Acute renal failure caused by lily ingestion in six cats. *J Am Vet Med Assoc*. 2002;220:49–52.
8. Rumbeiha WK, Francis JA, Scott D, et al. A comprehensive study of Easter lily poisoning in cats. *J Vet Diagn Invest*. 2004;16:527–541.
9. Slater MR, Gwaltney-Brant S. Exposure circumstances and outcomes of 48 households with 57 cats exposed to toxic lily species. *J Am Anim Hosp Assoc*. 2011;47:386–390.
10. Uhlig S, Hussain F, Wisløff H. Bioassay-guided fractionation of extracts from Easter lily (*Lilium longiflorum*) flowers reveals unprecedented structural variability of steroidal glycoalkaloids. *Toxicon.* 2012;92:42-49.

CASE III: N-103/17 (JPC 4102670).

Signalment: 7-year-old, male, neutered, Doberman pinscher, *Canis familiaris*, canine.

History: This 7-year-old Doberman was presented with recurrent peritoneal and pleural effusions of 3 weeks duration. Echocardiography was performed without heart alterations. Blood biochemical examination revealed increased hepatic enzymes and decreased albumin parameters. A marked lack of coagulation factors was also detected without improvement after plasma transfusions. No more clinical information was supplied.

Gross Pathology: Mucous membranes were icteric and the abdomen was visibly distended. Approximately 9 litres of clear yellowish free fluid in the abdominal cavity were observed, and 3 litres of similar fluid was present in the thoracic cavity. The liver was diffusely yellow to tan, decreased in size and showed multiple multifocal to coalescing micro-nodulations.

Laboratory results:
None provided.

Liver, dog. The liver is small with numerous regenerative nodules. On cut section, the liver is yellow-tan, and nodular regeneration is even more obvious . (Photo courtesy of: Veterinary Pathology Department, Veterinary Faculty, Autonomous University of Barcelona, 08193 Bellaterra, Barcelona, Spain.)

Microscopic Description: Liver: Diffusely affecting all the section there is a severe chronic degenerative process together with multifocal nodules of hepatic regeneration. There is a markedly reduction of the diameter of hepatic lobules because of loss of numerous hepatocytes. Marked portal-to-portal bridging is observed. Which is composed of moderate biliary hyperplasia and mild fibrosis along with severe

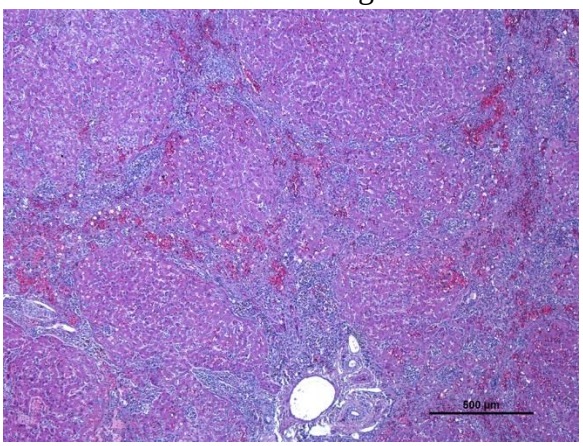

Liver, dog. There is marked periloabular fibrosis and a reduction in the size of the lobules with loss of periportal hepatocytes and edema. (HE, 40X) (Photo courtesy of: Veterinary Pathology Department, Veterinary Faculty, Autonomous University of Barcelona, 08193 Bellaterra, Barcelona, Spain.)

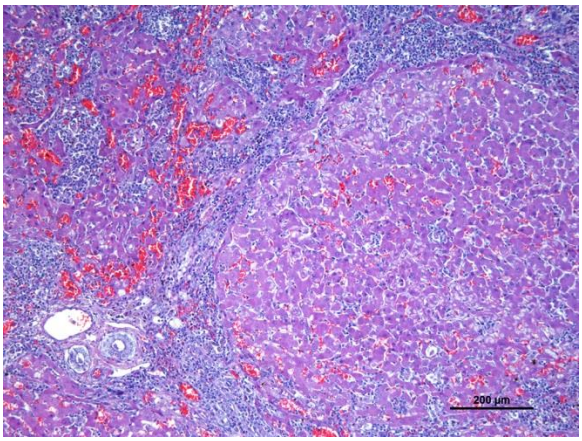

Liver, dog. Higher magnification of a regenerative nodule with periportal fibrosis and inflammation. (HE, 100X) (Photo courtesy of: Veterinary Pathology Department, Veterinary Faculty, Autonomous University of Barcelona, 08193 Bellaterra, Barcelona, Spain.)

inflammatory infiltrate mainly compose of macrophages (most of them arranged in aggregates) and abundant lympho-plasmacytic cells. Numerous biliary ducts contain moderate amount of amorphous yellowish material in the lumen and small bile casts are located in canaliculi (cholestasis). Biliary pigment is also located

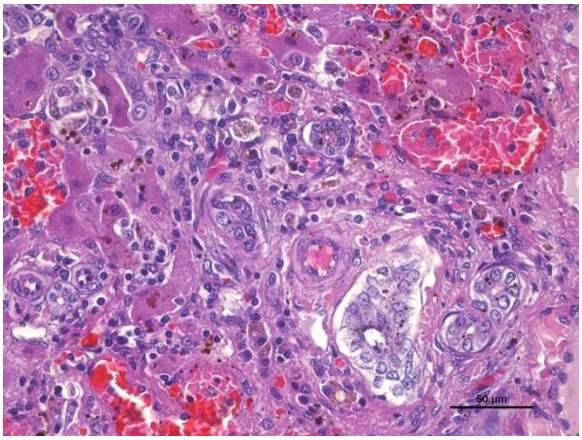

Liver, dog. Portal areas contain numerous biliary profiles as well as individual and aggregates of macrophages with brown intracytoplasmic pigment. Fibrosis surrounds and entraps periportal hepatocytes, with also contain brown granular pigment, and sinusoids are multifocally dilated. (HE, 400X) (Photo courtesy of: Veterinary Pathology Department, Veterinary Faculty, Autonomous University of Barcelona, 08193 Bellaterra, Barcelona, Spain.)

in the cytoplasm of Kupffer cells and hepatocytes. Multifocally sinusoids are distorted, dilated and markedly congested. Numerous hepatocytes appear enlarged with marked eosinophilic nucleolus. Degenerated changes of centrilobular hepatocytes can be seen: intracytoplasmic non-stained, well-defined micro vacuoles (lipid vacuoles) and cytoplasm rarefaction (hydropic degeneration). Also, scattered hepatocytes appear individualised, hypereosinophilic and karyorrhectic (apoptotic hepatocytes). There are multifocal areas of hepatic regeneration consistent of well-delimitated nodules of viable hepatocytes surrounded by fibrous tissue. Cells of the hepatic capsule appear plump and reactive.

SPECIAL STAINS: Rubeanic acid stain was performed and abundant green granular pigment observed in the cytoplasm of numerous hepatocytes in periportal areas.

Contributor's Morphologic Diagnosis:
Liver: Chronic, diffuse, severe hepatocellular degeneration and loss, with intrahepatocellular copper, severe bile stasis, nodular regeneration and moderate lipidosis (end-stage liver (cirrhosis)), Doberman, canine.

Contributor's Comment: The alteration of clinical parameters observed in this case (hypoalbuminemia, hepatic enzymes increased and lack of coagulation factors) was secondary to chronic hepatic failure. Hypoalbuminemia lead to multiple effusions in body cavities and jaundice was secondary to a severe biliary stasis.

In this case, acid rubeanic tissue staining revealed numerous intracytoplasmic green granules in hepatocytes. Therefore, the primary cause of the chronic hepatic failure and the end-stage liver was the chronic copper accumulation and toxicity.

Hepatic injury in copper poisoning of domestic animals frequently is the result of progressive accumulation of copper within

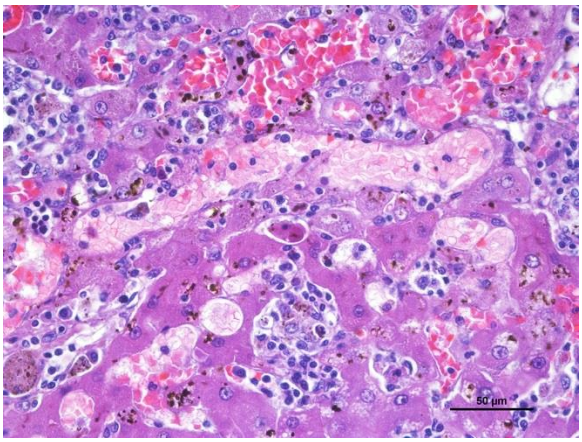

Liver, dog. Occasional hepatocytes (center) are disassociated, hypereosinophilic, and shrunken (apoptosis). (HE, 400X) (Photo courtesy of: Veterinary Pathology Department, Veterinary Faculty, Autonomous University of Barcelona, 08193 Bellaterra, Barcelona, Spain.)

the liver. Hepatic copper toxicosis can result from a primary metabolic defect in hepatic copper metabolism, altered hepatic biliary excretion of copper, or from excess dietary intake of the element.[2]

Hepatic copper accumulation in association with chronic hepatitis has been documented in Doberman, but apart from the recognized genetic mutation in the COMMD1 gene in Bedlington Terriers, leading to a primary copper storage disease with impaired copper excretion, the pathogenesis of the Doberman copper accumulation remains unclear.[2,4]

Copper is an essential trace element of all cells, but even a modest excess of copper can be life-threatening because copper must be properly sequestered to prevent toxicosis. Normally, serum copper is bound to ceruloplasmin and the majority of hepatic copper is bound to metallothionein and stored in lysosomes. Excess copper can lead to the production of reactive oxygen species that initiate destructive lipid peroxidation reactions that affect the mitochondria and other cellular membranes.[1]

In cases of chronic hepatitis caused by copper accumulation, the liver is usually small, often with an accentuated lobular pattern; severely affected livers are characterized by architectural distortion, which ranges from a coarsely nodular texture to an end-stage liver. Chronic hepatitis, depending on the duration of inflammation and injury, is characterized by portal and periportal mononuclear cell inflammation and fibrosis of portal areas that may extend into adjacent periportal areas of the lobule, leading to the prominent lobular pattern. Small aggregates of pigmented macrophages, containing copper and lipofuscin, surrounded by mononuclear inflammatory cells are a reliable feature of copper excess. With progression, hyperplastic nodules and bridging fibrosis develop.[3]

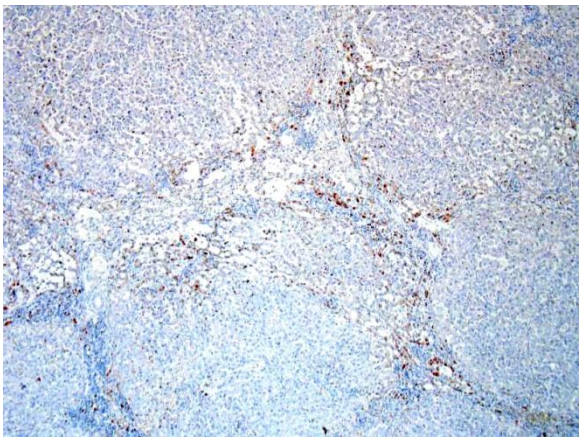

Liver, dog. Low magnification view of copper-laden hepatocytes within hepatic parenchyma separating regenerative nodules. (Rhodanine, 100X)

JPC Diagnosis: Liver: Fibrosis, bridging and portal, diffuse, severe with macronodular hepatocellular regeneration, piecemeal necrosis, cholestasis, siderosis, and sinusoidal capillarization, Doberman pinscher (*Canis familiaris*), canine.

Conference Comment: Doberman Pinchers are one of a number of dog breeds (Bedlington Terrier, West Highland White Terrier, Labrador Retriever, American and English Cocker Spaniel, Skye Terrier, Standard Poodle, Dalmatian, and English Springer Spaniel) that are predisposed to chronic hepatitis. In some of the aforementioned breeds genetic mutations have been identified (Bedlington Terriers with mutations in the COMMD1 gene are described above) but the majority of them are idiopathic. There is an association between excess copper accumulation and chronic liver disease but the exact mechanism has not been worked out yet.[2] Sheep are especially sensitive to excess copper because they don't efficiently regulate copper storage. Although copper is a necessary element for cellular metabolism,

it is far from innocuous, and must be sequestered to prevent toxicosis. In serum, it is bound to ceruloplasmin, and in the liver, it is bound to metallothionein and stored in lysosomes. Even small amounts of unbound, excess copper, results in the production of reactive oxygen species that lead to lipid peroxidation causing mitochondrial and cell membrane damage. Copper toxicosis can occur by the following mechanisms: (1) dietary excess (especially in sheep); (2) inadequate molybdenum in feed which normally antagonizes copper; (3) ingestion of pyrrolizidine alkaloids (*Heliotropium, Crotalaria, Senecio* species) which prevent hepatocyte mitosis which increases copper load on surviving hepatocytes; (4) disorders in copper metabolism (mentioned above).[1]

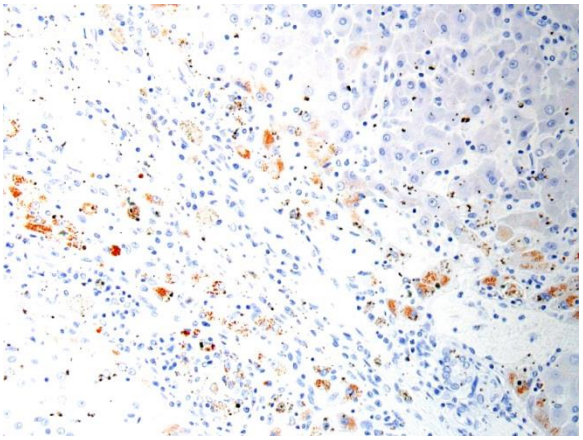

Liver, dog. Higher magnification of copper-laden hepatocytes. (Rhodanine, 200X)

This case engendered spirited discussion concerning the location of the copper and its causality of the chronic changes in this animal. In this individual, the copper is located exclusively in periportal regions, as is seen in many cases of chronic hepatitis. The majority of the parenchyma that is replaced by nodules of regenerating hepatocytes has not accumulated copper; relegating the demonstration of copper to the small amount of "original" liver present in the slide. Whether regenerative nodules do not accumulate copper as a result of an adaptive response or simply as a result of their relatively recent maturation, has not been conclusively determined.[2] However, at this point in lesion development, the attendees believe that it is difficult, if not impossible to determine the link between the copper accumulation in hepatocytes and its causality, if any, to the ongoing cirrhotic process.

Another very interesting change in this liver is the dilation of periportal sinusoids, which resembles "sinusoidal capillarization", a change described in chronic hepatitis in humans.

In the normal animal, liver sinusoidal endothelium varies markedly from capillary endothelium in other organs, as it exhibits fenestration, lacks a basement membrane, and does not express factor VIII-related antigen , platelet endothelial cell adhesion molecules (PECAM-1), CD-34, or E-selectin. In addition, affected sinusoids exhibit decreased compliance with sinusoidal blood flow (likely resulting in the dilation noted in this slide in periportal sinusoids) and possibly contributing to portal hypertension.[4]

Contributing Institution:

Veterinary Pathology Department,
Veterinary Faculty,
Autonomous University of Barcelona,
08193 Bellaterra, Barcelona, Spain.

References:

1. Brown DL, Van Wettere AJ, Cullen JM. Hepatobiliary system and exocrine pancreas. In: Zachary JF, ed. *Pathologic Basis of Veterinary Disease*. 6th ed. St Louis, MO: Elsevier Mosby; 2017: 440.
2. Cullen JM, Stalker MJ. Liver and biliary system. In: Maxie MG, ed. *Jubb, Kennedy and Palmer's Pathology of Domestic Animals*. Vol. 2. 6th ed. St

Louis, MO: Elsevier Mosby; 2016: 302-303, 342.
3. Mandigers PJ, Van den Ingh TS, Spee B, Penning LC, Bode P, Rothuizen J. Chronic hepatitis in doberman pinschers: a review. *Vet Q*. 2004;26(3):98-106.
4. Xu B, Broome U, Uzumel S, Ge, X, Kumaga-Baaesch M, Huttenby K, Christenson B, Ericzon B, Holgersson J, Sumitran-Holgersson S. Capillarization of hepatic sinusoid by liver endothelial cell-reactive autoantibodies in patients with cirrhosis and chronic hepatitis. *Am J Pathol* 2003 163(4) 1275-1289.

CASE IV: 2014 Case 1 (JPC 4050142).

Signalment: Adult, female, breed unspecified, *Bos taurus*, bovine.

History: The bovine was presented for slaughter at a USDA Food Safety Inspection Service (FSIS) inspected slaughter facility and passed antemortem inspection. The carcass was retained for further diagnostic testing after green, caseous-appearing lesions were observed in the liver and portal lymph nodes during postmortem inspection.

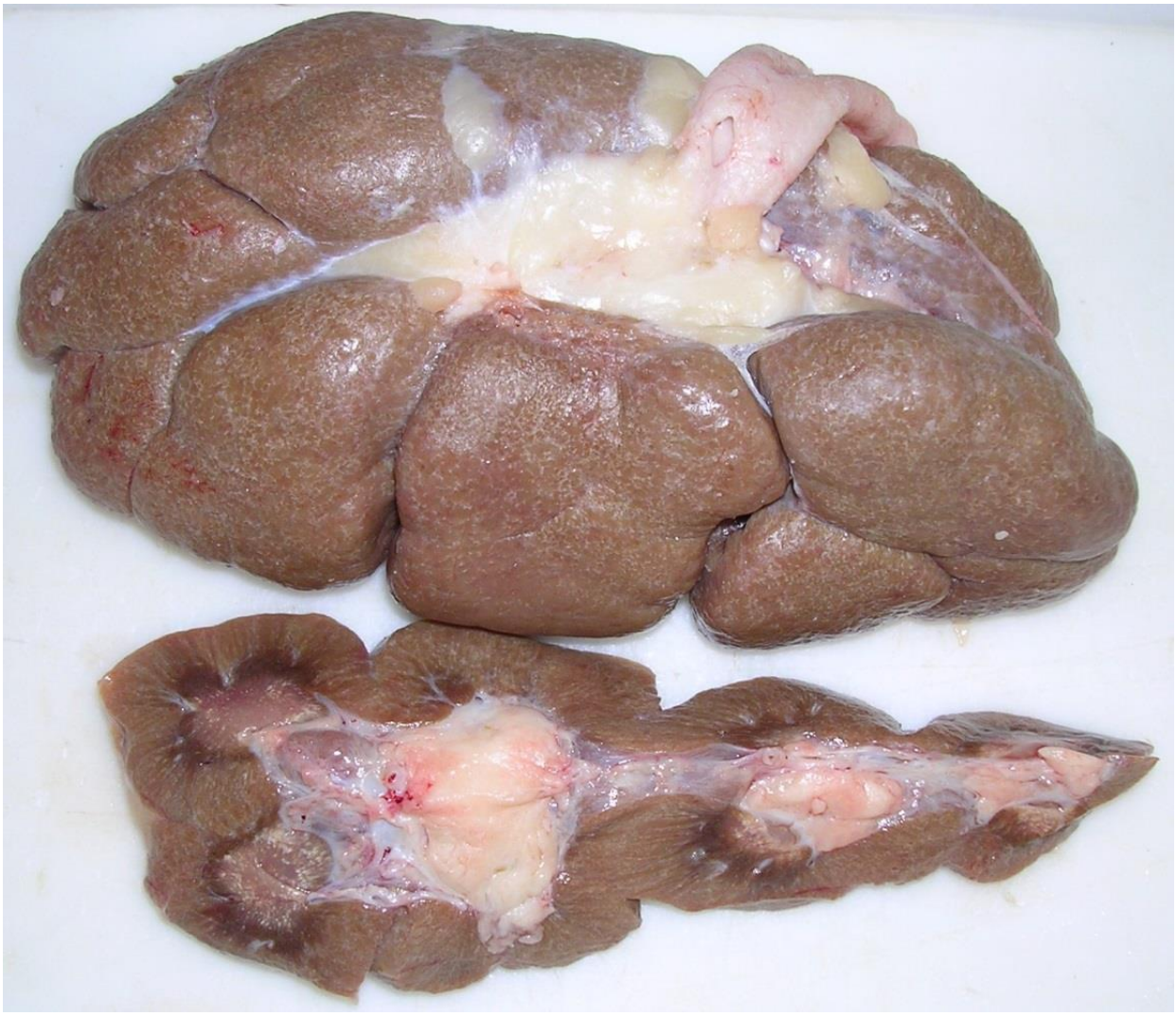

Kidney, ox. Greenish discoloration of the renal cortex of an ox at slaughter. (HE, 5X)

Gross Pathology: Green, caseous-appearing lesions in the liver and portal lymph nodes.

Laboratory results:
None provided.

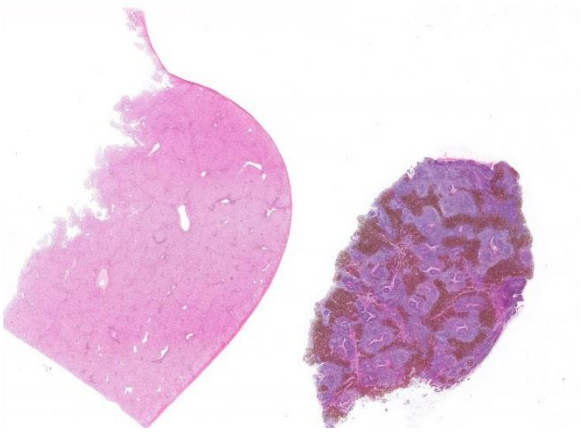

Lymph node and kidney. The medullary sinuses of the lymph node contains abundant brown granular pigment; small aggregates of pigment are present within the renal cortex. (HE, 6X)

Microscopic Description: Liver: Predominantly in portal areas, macrophages contain intracytoplasmic light green to light tan crystalline material which is birefringent when viewed under polarized light. Individual crystals are irregular to rod-shaped and range in size from <1µm to approximately 3µm in length and aggregates can be >100µm in diameter. Small numbers of crystals are found within scattered hepatocytes. Occasionally surrounding the affected cells are clusters of free erythrocytes that obscure the parenchyma. Sinusoids in the adjacent areas are often congested. There is variable subcapsular hemorrhage present.

Lymph node: Cortical and medullary sinuses are expanded by moderate to large numbers of macrophages engorged with intracytoplasmic material identical to that described in the liver.

Contributor's Morphologic Diagnosis:

1. Liver: Accumulation of refractile material consistent with 2,8-dihydroxyadenine, *Bos taurus*, bovine.
2. Lymph node: Cortical and medullary histiocytic accumulation of refractile material consistent with 2,8-dihydroxyadenine.

Contributor's Comment: 2,8-dihydroxyadeninosis or "green liver disease" is a rare condition of bovines that is caused by the tissue deposition of 2,8-dihydroxyadenine (2,8-DHA), an insoluble green crystalline material. Accumulation of 2,8-DHA is most commonly seen in the liver and hepatic lymph nodes, but has also been reported in the kidney, and the renal, mediastinal, intercostal, and gastric lymph nodes.[7] The crystals appears as a light green to light tan mottling on the liver surface and parenchyma. Larger coalescing foci of 2,8-DHA are present in the hepatic lymph nodes. Renal lesions, if present, consist of light green mottling or streaking on the surface and on cut section or as concretions in the renal pelvis. The condition in bovines was initially reported about 20 years ago

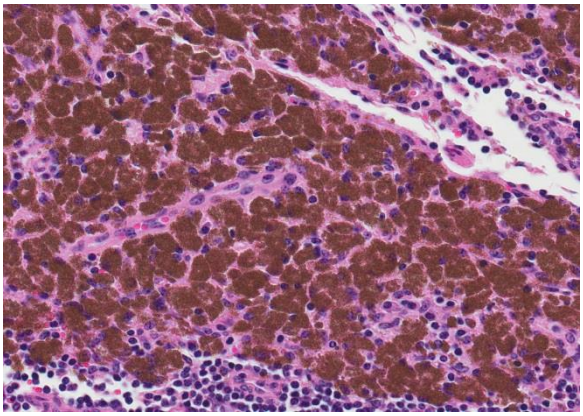

Lymph node, ox. Higher magnification of pigment laden macrophages within the medullary sinuses.

after unusual green lesions were observed during postmortem examination at federally inspected abattoirs. Although the condition is rare, FSIS personnel are trained to recognize it since even rare conditions can be observed during the postmortem exam of the 30 million head of cattle that undergo federal inspection in the US every year.[9]

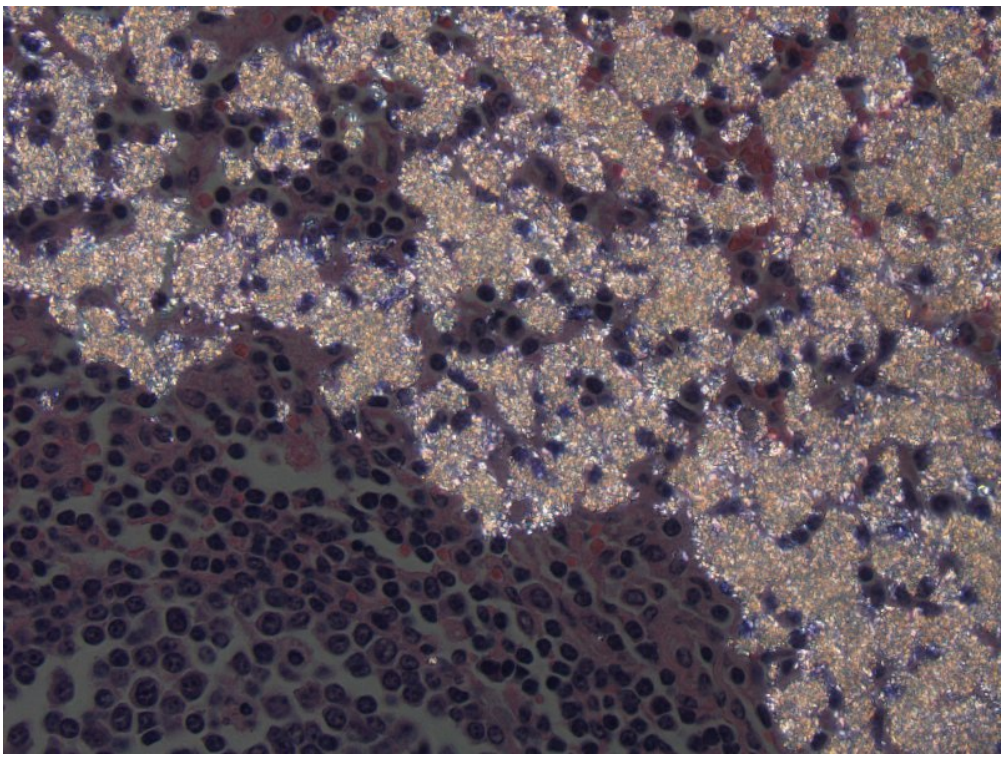

Lymph node, ox. The pigment is strongly birefringent. (HE, 400X)

Bovines with 2,8-dihydroxyadeninosis are thought to have an enzyme deficiency affecting purine catabolism. Normally, adenine is phosphorylated to adenine monophosphate in the first step of adenine catabolism. In the absence of the enzyme adenine phosphoribosyltransferase (APRT), adenine may instead be hydroxylated by the enzyme xanthine oxidase to 2,8-DHA, which precipitates in tissues as an insoluble crystal.[7] The light green to light tan color of the precipitate is retained throughout processing, embedding, and staining.

Deposits of 2,8-DHA in the renal tubules and lower urinary tract have been reported in humans, dogs, and APRT knockout mice. Uroliths and tubular casts can block the urinary tract, and lead to renal failure in these species.[5]

Other causes of grossly green discoloration in bovine tissues include green algal lymphadenitis (chlorellosis),[4] exogenous green pigment in lymph nodes draining tattoo ink from skin,[6] eosinophilic myositis,[10] green liver cell adenomas,[1,3] and bile imbibition. Green discoloration has been noted in injection site lesions in cuts of beef in modified-atmosphere packages.[8]

JPC Diagnosis:

1. Lymph node, medullary sinus: Sinus histiocytosis with intrahistiocytic birefringent pigment, breed unspecified (*Bos Taurus*), bovine.
2. Lymph node: Reactive lymphoid hyperplasia, diffuse, moderate.
3. Liver, portal areas: Histiocytosis, multifocal, mild with abundant intrahistiocytic birefringent pigment.

Conference Comment: An extremely rare condition, 2,8 dihydroxyadenine accumulation in cattle, has only been reported on once in veterinary literature,[7] but results in striking gross and microscopic

lesions that are worth mentioning. Adenine is a purine that is normally found in all tissues of the body (as it serves as one of the bases for the nucleic acids that form DNA and RNA) and is converted to adenylate by an enzyme called adenine phospho-ribosyltransferase. If this enzyme is lacking, adenine is excreted in the urine (resulting in crystalluria) or oxidized by xanthine oxidase to form 2,8-dihydroxyadenine. This substance is not soluble in water and at the body's pH precipitates to form crystals. Grossly, these crystals give tissues a light green hue and are most prominent around the portal triads of the liver and medullary sinuses of lymph nodes. When lymph nodes are incised, the surface of the knife becomes covered in a green, mucoid material. Rarely, there are light-green urinary calculi found within the renal pelvis or anywhere throughout the entirety of the lower urinary tract.[2] In this study[7], the most remarkable microscopic changes were in the portal triads of the liver, which were so enlarged by crystals, macrophages, and multinucleated giant cells that they comprised up to 30 percent of the hepatic mass. Crystal laden macrophages were also present in the medullary sinuses of regional lymph nodes. To date, the pathogenesis of 2,8-dihydroxyadenine accumulation has not been ascertained.

Contributing Institution:
National Centers for Animal Health, Ames, IA
www.ars.usda.gov/main/site_main.htm?modecode=36-25-30-00
www.aphis.usda.gov/nvsl

References:

1. Chu HH, Moon WS. Beta-catenin activated hepatocellular adenoma. *Clin Mol Hepatol*. 2013;19: 185-189.
2. Cianciolo RE, Mohr FC. Urinary system. In: Maxie MG, ed. *Jubb, Kennedy, and Palmer's Pathology of Domestic Animals*. Vol. 2. 6th ed. St. Louis, MO: Elsevier; 2016:429.
3. De Kock G, Fourie P. Green liver cell adenoma in a bovine. Digitized by the University of Pretoria, Library Services.
4. Hafner S, Brown CC, Zhang J. Green algal peritonitis in 2 cows. *Vet Pathol*. 2013;50:256-259.
5. Houston DM, Moore AE, Mendonca SZ, Taylor JA. 2,8-Dihydroxyadenine uroliths in a dog. *J Am Vet Med Assoc*. 2012;241:1348-1352.
6. Ladds PW. *A Colour Atlas of Lymph Node Pathology in Cattle*. Ames, IA: Iowa State University Press; 1986.
7. McCaskey PC, Rigsby WE, Hinton DM, Friedlander L, Hurst VJ. Accumulation of 2,8 dihydroxyadenine in bovine liver, kidneys, and lymph nodes. *Veterinary Pathology Online*. 1991;28:99-109.
8. Roeber DL, Belk KE, Engle TE, Field TG, et al. The effect of vitamin E supplementation on discoloration of injection-site lesions in retail cuts and the greening reaction observed in injection-site lesions in muscles of the chuck. *J Anim Sci*. 2003;81:1885-1894.
9. USDA-NASS: Livestock Slaughter 2012 Summary; 2013.
10. Vangeel L, Houf K, Geldhof P, De Preter K. Different *Sarcocystis* spp. are present in bovine eosinophilic myositis. *Vet Parasitol*. 2013;197:543-548.

Self-Assessment - WSC 2017-2018 Conference 10

1. Which of the statements is not true concerning Johne's disease?
   a. It can be produced in pigs as well as large and small ruminants.
   b. The mucosal inflammation is a response to a Th1 type of adaptive immune response.
   c. Cattle are most sensitive to infection in the first 30 days of life.
   d. M*. avium var paratuberculosis* has been postulated to play a role in human Crohn's disease.

2. True or false: Mycobacterium avium var. paratuberculosis gains entry by translocation across the columnar absorptive mucosal epithelium?
   a. True
   b. False

3. Which of the following is NOT associated with lily toxicity in cats?
   a. Development of megamitochondria
   b. Pancreatic necrosis
   c. Hemolytic anemia
   d. Renal tubular epithelial necrosis

4. Which of the following binds copper in the serum:
   a. COMMD1
   b. Hepcidin
   c. Ceruloplasmin
   d. Metallothonein

5. Which of the following is the purported mechanism of action of 2,8-dihydroxyadeninosis ?
   a. Excess intake of the chemical from contaminated silage.
   b. Kreb's cycle abnormalities in macrophages.
   c. Enzyme abnormalities in purine metabolism.

Excessive breakdown of biliary precursors within hepatocytes.

Please email your completed assessment to Ms. Jessica Gold at Jessica.d.gold2.ctr@mail.mil for grading. Passing score is 80%.This program (RACE program number) is approved by the AAVSB RACE to offer a total of 0.5 CE Credits, with a maximum of 12.5 CE Credits being available to any individual Veterinary Medical Professionals for the 2017-2018 Wednesday Slide Conference. This RACE approval is for the subject matter categories of: SCIENTIFIC using the delivery method of NON-INTERACTIVE DISTANCE. This approval is valid in jurisdictions which recognize AAVSB RACE; however, participants are responsible for ascertaining each board's CE requirements.
RACE does not "accredit", "endorse" or "certify" any program or person, nor does RACE approval validate the content of the program.

Joint Pathology Center
Veterinary Pathology Services

WEDNESDAY SLIDE CONFERENCE 2017-2018

C o n f e r e n c e 11

6 December 2017

CASE I: SQ (JPC 4048071).

Signalment: Adult, female, eastern fox squirrel, *Sciurus niger*, squirrel.

History: This squirrel was found being bitten by a dog. The squirrel died after extrication and the dog's owner presented the squirrel for necropsy due to its unusual external appearance.

Gross Pathology: Distributed throughout the skin, there were numerous (approximately 100), well-demarcated, ovoid to circular, raised nodules ranging from approximately 3 to 35 mm in diameter. The nodules were alopecic, tan to gray, and irregularly smooth surfaced, to variably eroded and ulcerated. On cut section, the nodules consisted of white to tan proliferative soft tissue expanding the dermis. The palpebral fissure of the right eye was narrowed by nodular expansion of the upper eyelid.

The thoracic cavity was filled with blood (hemothorax) and the right thoracic wall had two penetrating, blood-rimmed, tracts (dog bite wounds).

Laboratory results:
PCR using primers targeting the poxviral DNA polymerase and subsequent sequencing had 99% identity with GenBank squirrel fibroma virus isolates.

Microscopic Description: Haired skin: The cutaneous nodular lesions were fairly well-demarcated, broad-based, and raised, consisting of nonencapsulated proliferations of spindloid mesenchymal cells expanding and mildly infiltrating the superficial to deep dermis, with regionally moderate epidermal and follicular epithelial hyperplasia. The epidermis had prominent acanthosis, mild irregular granulosis, and mild laminar orthokeratosis, as well as low numbers of multifocally desquamating devitalized superficial keratinocytes. Some sections had mild multifocal superficial erosion associated with focal parakeratosis and sero-cellular crusting, and other sections (not submitted) had regionally extensive ulceration with dense surface crusting and interspersed coccoid bacteria. Moderate numbers of individualized keratinocytes, mainly in the stratum spinosum, had prominent cytoplasmic swelling and pallor (hydropic change, ballooning degeneration), and some of these keratinocytes also contained single to multiple variably sized,

Haired skin, squirrel. Head and neck (cranioventral view) and perineum (caudoventral view with hind limbs retracted toward bottom of image), Squirrel: Numerous raised, alopecic, and variously eroded to ulcerated, cutaneous nodules are distributed throughout the skin. The right upper eyelid is notably markedly enlarged by one of the nodular expansions. (Photo courtesy of: Michigan State University, Diagnostic Center for Population and Animal Health, www.animalhealth.msu.edu)

eosinophilic, globular cytoplasmic poxviral inclusions (approximately 8 to 20 micrometers in diameter). The proliferative spindloid cells were arranged in dense, interweaving, bundles amidst fine collagenous supporting stroma. These cells had small to moderate quantities of eosinophilic cytoplasm, indistinct cell borders, ovoid nuclei, finely stippled chromatin, and 1 to 2, small, indistinct nucleoli. Low to moderate numbers of the cells contained smaller (approximately 6-12 micrometer diameter), paler eosinophilic, cytoplasmic viral inclusions. Anisocytosis and anisokaryosis were mild to moderate, and mitotic cells were rare. Low to moderate numbers of lymphocytes and plasma cells were mixed with the dermal mesenchymal cell proliferation, especially at the deep margin, where they extended perivascularly into the adjacent dermis and hypodermis. In some regions, the superficial dermis also contained few interspersed neutrophils, free erythrocytes (hemorrhage), and scattered shrunken cells with pyknotic and karyorrhectic nuclei.

Contributor's Morphologic Diagnosis:
Haired skin: Multifocal dermal fibromas, with moderate epidermal hyperplasia, ballooning degeneration, intraepithelial and intramesenchymal cell cytoplasmic poxviral inclusions, and mild lymphoplasmacytic dermatitis.

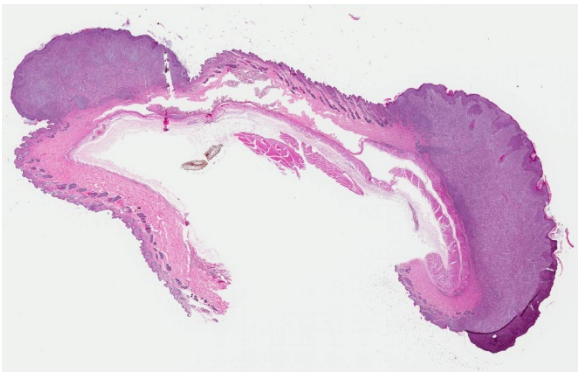

Haired skin, squirrel. There are two dome shaped neoplasms expanding the dermis of the submitted section of haired skin. (HE, 6X)

Contributor's Comment: Squirrel fibromatosis results from infection by squirrel fibroma virus, a poxvirus in the *Leporipoxvirus* genus, closely related to rabbit fibroma virus. The disease has been reported in North American eastern gray, western gray, red, and fox squirrels, and is generally sporadic in occurrence, with rare epizootics.[1] The gross lesions are considerably distinctive, consisting of single to multiple, alopecic, dermal soft tissue nodules that often occur on the face, trunk, limbs, and genital region.[1,9] Involvement of the eyelids has been reported as a common finding[9] (as in Image 1), and nodular lesions in internal organs are less common.[1,7]

Histologically, cutaneous squirrel fibromatosis lesions consist of a combination of typical poxviral epidermal changes and underlying dermal mesenchymal fibroblast-like cell proliferation.[1,9] The epidermal changes are characterized by epithelial hyperplasia, keratinocyte ballooning changes, and eosinophilic intracytoplasmic poxviral inclusions. The proliferative dermal spindle cells have mild cellular pleomorphism and fewer, smaller, intracytoplasmic viral inclusions. Mixed dermal inflammation (consisting of lymphocytes, neutrophils, and macrophages), as well as epidermal erosion, ulceration, and crusting are variable.[1,9] In fewer cases, widespread mesenchymal and epithelial proliferations with intra-cytoplasmic viral inclusions have also been reported to occur at extracutaneous sites, including the lungs, liver, kidney, and lymph nodes.[1,7]

The cutaneous lesions of squirrel fibromatosis are reported to often regress spontaneously, but mortality can occur with debilitation and/or systemic disease. Immunocompetence may play a role in disease susceptibility and the severity of lesions.[1,9] Routes of viral transmission are thought to include biting insects and direct contact, and multifocal lesions may arise from viremia and/or additive cutaneous exposures.[1,9]

Other species-selective poxviral infections of tree squirrels are squirrelpox virus (also previously termed "squirrel parapoxvirus") and the newly described Canadian squirrelpox virus.[1,2,5] In contrast to squirrel fibromatosis, the squirrelpox diseases are characterized by exudative and ulcerative dermatitis lacking nodular dermal mesenchymal proliferations. Furthermore, the squirrelpox diseases have a fatal clinical course (albeit the Canadian disease is limited to a single case report), and the

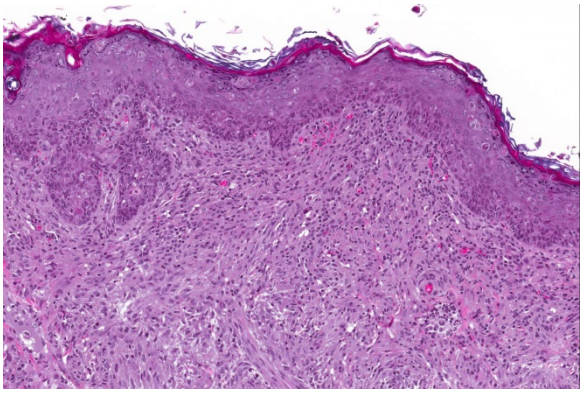

Haired skin, squirrel. The neoplasms are composed of short interlacing streams and bundles of proliferating fibroblasts. (HE, 140X)

causative poxviruses are distinct from the currently named poxviral genera.[1,2,3,5] Although serologic findings support exposure of North American eastern gray squirrels to the squirrelpox virus of the United Kingdom/Ireland, the gray squirrels do not develop clinical disease. Evidence suggests that the virus was introduced to the UK with the eastern gray squirrels and it now threatens the survival of European red squirrels.[4,5]

Table 1. Relevant details of squirrel-selective poxviral infections[1,2,3,5]

Disease Name	**Virus (Viral Genus)**	**Main Host(s) [Geography]**	**Clinical Outcome**	**Gross Lesions**	**Histologic Features**
Squirrel fibromatosis (SQFV)	Squirrel fibroma virus [*Leporipoxvirus*]	Eastern gray squirrels, also western gray, red, and fox squirrels [Eastern North America]	Lesions often regress, occasional mortality	Cutaneous and lesser visceral nodules	Epithelial hyperplasia and mesenchymal (fibroblast) proliferation; ballooning keratinocyte degeneration; ICIB in proliferative epithelial and mesenchymal cells
Squirrelpox (SQPV)	UK squirrelpox virus [*Novel genus within chordopoxvirinae, not yet named*]	European red squirrel (Gray squirrels clinically resistant) [United Kingdom and Ireland]	Fatal	Exudative dermatitis	Epidermal hyperplasia with ulceration, crusting, and necrsuppurative dermatitis; ballooning degeneration and ICIB in keratinocytes
	Canadian squirrelpox virus *[unassigned, most closely related to parapoxviruses]*	North American red squirrel (only 1 case) [Canada, Yukon territory]	Fatal	Exudative dermatitis (more like SQPV than SQFV)	(As above for SQPV) [more like SQPV than SQFV; virus identified only in epithelial cells]

Poxviruses are enveloped DNA viruses that are prominently epitheliotropic and commonly induce epithelial hyperplasia (acanthosis), epithelial cell swelling (ballooning degeneration), and intracytoplasmic inclusion bodies. Grossly, the archetypal cutaneous lesions progress through macule, papule, vesicle, pustule, crust and scar phases.[11] Ultrastructurally, poxviral particules are brick-shaped, enveloped, smooth-surfaced, electron-dense virions (approximately 200-300 nm), with a biconcave (dumb-bell shaped) nucleocapsid core and adjacent lateral bodies.[1] The family *Poxviridae* is classified into two subfamilies: *Entomopoxvirinae*, which infect insects, and *Chordopoxvirinae*, which infect a wide range of vertebrates. Poxviruses that induce cutaneous tumors include squirrel fibroma virus, rabbit fibroma virus, rabbit myxoma virus, yaba monkey tumor virus, lumpy skin disease virus, and sheeppox virus.

Table 2. *Chordopoxvirinae* genera, major viruses, and some notable features[11,JPC archives]

Genus	Major Viruses
Avipoxvirus	Fowlpox virus, Canarypox virus, Pigeonpox virus, Quailpox virus, Turkeypox virus - Characteristic histologic intracytoplasmic inclusion bodies: "Bollinger bodies"
Capripoxvirus	Sheeppox virus, Goatpox virus, Lumpy skin disease virus - All cause systemic disease, mortality/economic loss can be high, especially with sheeppox - "Sheeppox cells" accumulate in lesions: mononuclear cells (macrophages/monocytes, fibroblasts) with vacuolated nuclei/marginated chromatin and ICIB
Cervidpoxvirus	Deerpox virus
Crocodylidpoxvirus	Nile crocodilepox virus
Leporipoxvirus	Rabbit (Shope) fibroma virus, Rabbit myxoma virus, Squirrel fibroma virus - Rabbit (Shope) fibroma virus: causes rabbit fibromatosis (like squirrel fibroma virus) o Atypical dermal mesenchymal proliferation, epidermal hyperplasia, ballooning degeneration, ICIB in epithelium and mesenchymal cells o Benign, self-limiting disease - Rabbit myxoma virus: causes cutaneous myxomatosis ("bighead") o Atypical myxomatous mesenchymal proliferation, epidermal hyperplasia, ballooning degeneration, ICIB in epithelial cells only o Local/benign lesion in American rabbits, but systemic/severe in European rabbits
Molluscipoxvirus	Molluscum contagiosum virus - Infects horses, donkeys, kangaroos, etc.; large ICIB: "molluscum bodies"
Orthopoxvirus	Cowpox virus, Ectromelia (mousepox) virus, Monkeypox virus, Rabbitpox virus, Horsepox virus, Camelpox virus, Vaccinia virus, Variola (smallpox)

	virus - Cowpox virus: teat/udder lesions in cows, but not common; infects others including cats - Monkeypox virus: systemic disease in monkeys and rodents - Ectromelia virus: also causes splenic and hepatic necrosis o A-type inclusions (Marchal bodies): eosinophilic, occur late in disease, common in epidermis (not liver) o B-type inclusions (Guarnieri bodies): basophilic, occur early in disease, present in all infected cells - Rabbitpox: only been reported in laboratory populations - Vaccinia virus: used in vaccines to eradicate smallpox; no disease in domestic animals
Parapoxvirus	Ovine parapoxvirus (contagious ecthyma, contagious pustular dermatitis, Orf, sore mouth), Pseudocowpox virus, Bovine popular stomatitis virus - Ovine parapoxvirus: sheep, goats, cattle, less commonly others; zoonotic o Inclusions only briefly detected in vesicular stage - Pseudocowpox virus: lesions in milking cows, zoonotic to humans: "Milker's nodules" - Bovine popular stomatitis virus: lesions more often mouth/muzzle, transmission to humans looks comparable to "milker's nodules"
Suipoxvirus	Swinepox virus - Host specific, sucking louse (*Haematopinus suis*) contributes to mechanical transmission
Yatapoxvirus	Yaba monkey tumor virus, Tanapox virus - Yabapoxviral dermatitis: benign, dermal tumor, regress; previously termed "histiocytomas"; ICIB in proliferating dermal mesenchymal cells - Tanapox virus: causes "benign epidermal monkey pox"; ICIB in keratinocytes

JPC Diagnosis: Haired skin: Viral fibropapillomas, multiple, eastern fox squirrel (*Sciurus niger)*, squirrel.

Conference Comment: Squirrel fibroma virus belongs to the *Leporipoxvirus* genus of the *Poxviridae* family of viruses and is related to rabbit (shope) fibroma virus and rabbit myxoma virus. The different poxvirus genera are concisely described by the contributor above. Of historical interest, Richard Edwin Shope was an American virologist and physician who identified Shope papillomavirus in 1933 which was the first human virus discovered[6]. This discovery assisted later researchers in linking papillomaviruses to warts and cervical cancer[8]. Among other pathologies, he identified *Influenzavirus* A in pigs (1931) and cultured it from a human in 1933 later identifying it as the virus that circulated in the 1918 pandemic[10]. Interestingly, his son, Robert Shope, was also a virologist that specialized in arthropod-borne viruses[6].

As is always the case when leporipox-driven entities appear in the Wednesday Slide Conference, vigorous debate surrounded the morphologic diagnosis. Emboldened by the recent identification of the neoplastic cells

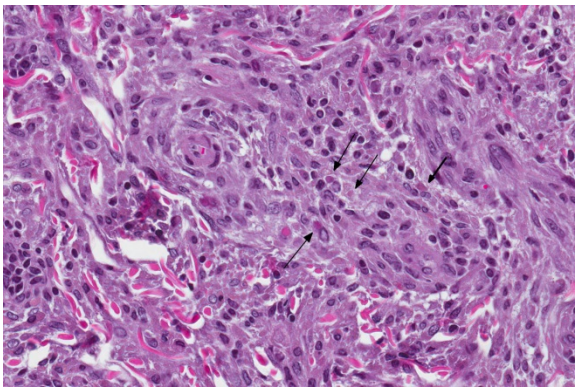

Haired skin, squirrel. Proliferating fibroblasts occasionally contain a single 4-10um intracytoplasmic round viral inclusion. (HE, 400X)

within the dermis as fibroblasts[12], the staff of the Joint Pathology Center threw off the yoke of conservatism exemplified by its longstanding diagnosis of "atypical mesenchymal hyperplasia" and, noting the presence of viral inclusions in both the epidermis and dermis, unanimously endorsed that of "viral fibropapilloma".

Contributing Institution:
Michigan State University
Diagnostic Center for Population and Animal Health
www.animalhealth.msu.edu

References:

1. Bangari DS, Miller MA, Stevenson GW, Thacker HL, Sharma A, and Mittal SK. Cutaneous and systemic poxviral disease in red *(Tamiasciurus hudsonicus)* and gray *(Sciurus carolinensis)* squirrels. Vet Pathol 2009;46:667-672.
2. Himsworth CG, McInnes CJ, Coulter L, Everest DJ, and Hill JE. Characterization of a novel poxvirus in a North American red squirrel (*Tamiasciurus hudsonicus*). J Wildl Dis 2013;49:173-179.
3. Himsworth CG, Musil KM, Bryan L, and Hill JE. Poxviral infection in an American Red Squirrel (*Tamiasciurus hudsonicus*) from northwestern Canada. J Wildl Dis 2009;45:1143-1149.
4. McInnes CJ, Counter L, Dagleish MP, Daene D, Gilray J, Percival A, Willoughby K, Scantlebury M, Marks N, Graham D, Everest DJ, McGoldrick M, Rochford J, McKay F, and Sainsbury AW. The emergence of squirrelpox in Ireland. Anim Conserv 2013;16:51-59.
5. McInnes CJ, Wood AR, Thomas K, Sainsbury AW, Gurnell J, Dein FJ, and Nettleton PF. Genomic characterization of a novel poxvirus contributing to the decline of the red squirrel (*Sciurus vulgaris*) in the UK. J Gen Virol 2006;87:2115-2125.
6. Murphy FA, Calisher CH, Tesh RB, Walker DH. In memoriam: Robert Ellis Shope: 1929–2004. *Emerging Infectious Diseases*. 2004;10(4):762–765.
7. O'Conner DJ, Diters RW, and Nielsen SW. Poxvirus and multiple tumors in an eastern gray squirrel. J Am Vet Med Assoc 1980;177: 792-795.
8. Shope RE, Hurst EW. Infectious papillomatosis of rabbits: with a not on the histopathology. *J. Exp. Med*. 1933;58(5):607–624.
9. Terrell SP, Forrester DJ, Mederer H, and Regan TW. An epizootic of fibromatosis in gray squirrels (*Sciurus carolinensis*) in Florida. J Wildl Dis 2002;38:305-312.
10. Van Epps HL. Influenza: Exposing the true killer. *J Exp Med*. 2006;203(4):803.

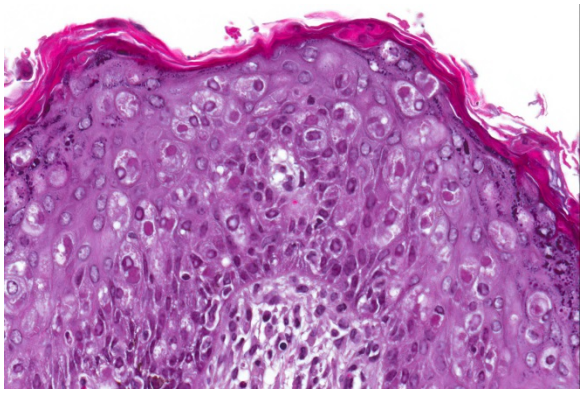

Intestine, ox. The overlying epithelium is hyperplastic, and the cells of the stratum spinosum exhibit ballooning degeneration with one or more 4-10um intracytoplasmic viral inclusions. There is mild orthokeratotic hyperkeratosis. (HE, 1 56X)

11. Zachary JF and McGavin MD. *Pathologic Basis of Veterinary Disease*. 5th ed. St. Louis, MO: Elsevier; 2012: 230-231, 326, 1020-1024.
12. Barthold SW, Griffey SM, Percy DP. *Pathology of Laboratory Rodents and Rabbits, 4th ed.* Oxford, UK: Wiley Blackwell; 2016:263-264.

CASE II: 14/160 (JPC 4048228).

Signalment: Unknown age, adult, female, *Ambystoma mexicanum*, axolotl.

History: The animal was euthanized because of exophthalmia and poor condition due to a mass in the head which extends to the oral cavity.

Gross Pathology: On the head, between the eyes is a firm mass of about 2 x 2 x 1 cm in diameter, which reaches the oral cavity and has a multinodular appearance. The cut surface of the mass is firm, well-delineated and white. The right eye is exophthalmic.

Laboratory results:
None submitted.

Microscopic Description: From the superficial dermis, extending to the cut borders, there is a poorly demarcated, nonencapsulated, infiltratively growing, cell rich neoplastic mass. The cells are polygonal to elongated, arranged in rosettes (Flexner-Wintersteiner-like rosettes), nests and packets and are supported by moderate amount of delicate septa of fibrovascular stroma. The neoplastic cells are 10-15 µm in diameter, have variably less distinct cell borders, moderate amount of eosinophilic, granular cytoplasm and a round to elongated nucleus with finely stippled chromatin and up to 4 nucleoli. The anisocytosis and anisokaryosis are moderate and there are 3-4 mitoses per 400X high power fields. Multifocal in the neoplasia necrosis is present. The surrounding dermis is edematous.

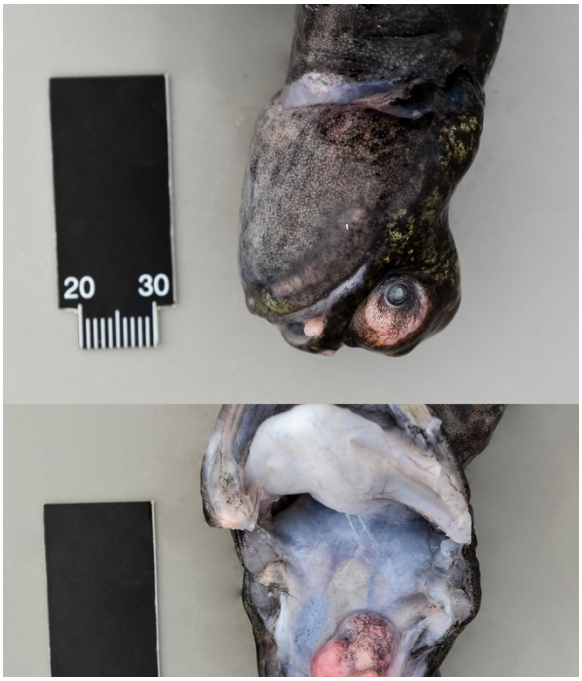

Skin, axolotl. A poorly pigmented neoplasm extends from between the eyes oral cavity. (Photo courtesy of: Vetsuisse Faculty, University of Bern, Institute of Animal Pathology, Laenggassstrasse 122, PF 8466, 3001 Bern Switzerland, http://www.itpa.vetsuisse.unibe.ch/content/index_eng.html)

Contributor's Morphologic Diagnosis:
Head: Neuromastoma (Neuroepithelioma).

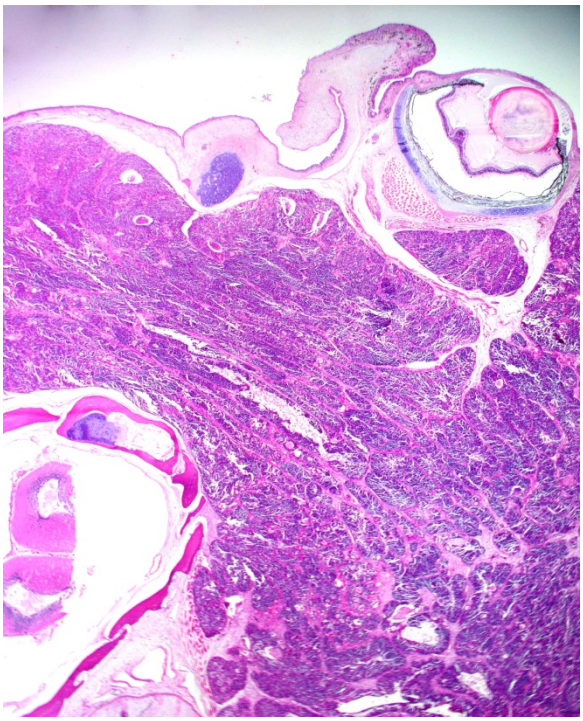

Skin, axolotl. The neoplasm extends beneath the right eye and infiltrates underlying cranium. (Photo courtesy of: Vetsuisse Faculty, University of Bern, Institute of Animal Pathology, Laenggassstrasse 122, PF 8466, 3001 Bern Switzerland, http://www.itpa.vetsuisse.unibe.ch/content/index_eng.html) (HE, 2X)

Contributor's Comment: Neoplastic disorders in amphibians are rare and limited to specific species [orders: Anura (frogs and toads), Urodela (salamander), Gymnophiona (caecilians)].[7] The axolotl belongs to the Urodela and has become popular in cancer research, regenerative biology and immunology.[6] Spontaneous tumors described in axolotl are melanophoroma, epithelioma, neuroepithelioma, lymphangiosarcoma, mast cell tumor, fibropapilloma, sertoli cell tumor and teratoma.[4,6,7]

In our case, the axolotl had a mass on the head between the eyes reaching to the oral cavity. Histologically, the neoplastic cells formed rosettes which lead to the suspicion of a neuroendocrine tumor. In a previous report from an axolotl, a mass with the same distribution and similar histological pattern was described and referred to as a neuromastoma.[4] Neuromastoma (neuroepithelioma) is a neoplasia originating from neuromast cells.[4] These cells are distributed on the head and body and are the end organs of the lateral line system, which is a sensory system in all fishes and permanently aquatic amphibians.[2] On the head of axolotl, tumors like fibropapilloma, mast cell tumor and olfactory neuroblastoma can occur.[4,6,7] These are macroscopical differential diagnoses in our case. Fibropapillomas are common in urodeles[6], but in the histologic examination, fibropapilloma was excluded due to lack of the distinctive histological pattern of proliferative neoplastic fibroblasts. Mast cell tumors are common

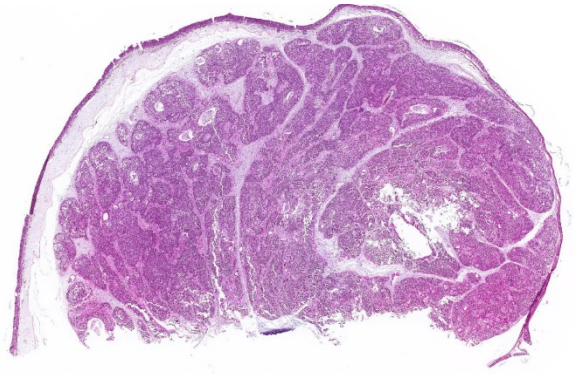

Skin, axolotl. The submitted section of skin shows a multilobular neoplasm within the deep dermis. There are large areas of necrosis and dropout scattered throughout. (HE, 6X)

neoplasias on the head of *A. mexicanum*, often with ulceration of the overlying epidermis.[4] In our histological examination, there was no indication of mast cells in the toluidine blue staining. Olfactory neuroblastoma and neuromastoma may have similar neuroectodermal origin, share similar histological and immunohistochemical features and are not easily distinguished from each other.[4,6] Considering the similar location and histological features of the previous report

of neuromastoma[4], we diagnosed the tumor in our case was diagnosed as a neuro-mastoma.
Only few cases of neuromastoma have been reported and only in Laurenti`s alpine newt and axolotl.[4] It has a prolonged course and the tumor localization impacts the health status of the animal.[7]

Amphibians share the same cell types as other animals, and any cell type can develop neoplastic changes.[7] The knowledge about neoplasia in wild amphibians is incomplete and inconsistent due to insufficient diagnoses and misdiagnoses and difficulty to interpret the neoplasias.[7] The best known amphibian neoplasm is the Lucké renal adenocarcinoma caused by ranid herpesvirus-1 (Lucké`s herpesvirus) and is endemic in the northern leopard frog (*Rana pipiens*) population.[4,7] Interestingly, some anuran species possess anticancer secretory products and cytoprotective capabilities which make them relatively resistant to carcinogens, and the regenerative capacity of urodels is hypothesized to explain the low tumor rate in these amphibians.[7]

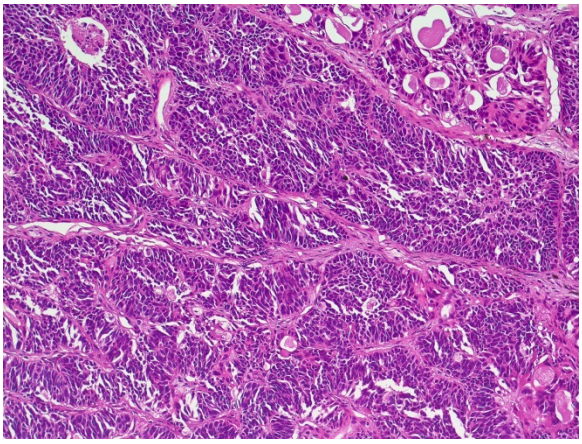

Skin, axolotl. Neoplastic cells are separated into distinct lobules, and are pyramidal, often palisading along the outer edge of each lobule. (HE, 40X) (Photo courtesy of: Vetsuisse Faculty, University of Bern,

Table 1. Spontaneous neoplasias in amphibians: from Stacy et. al 2004

Organ system	Tumor type	Species
Integument and soft tissues	Epidermal papilloma	Urodele species
	Squamous cell carcinoma	Northern leopard frog (*R. pipiens*)
	Dermal gland tumors	Grass frogs (*R. temporaria*) Pond frogs (*R. ridibunda*)
	Melanophoroma	Urodele and anura species
	Fibropapilloma, Fibrosarcoma	Western tiger salamander (*A. mavortium*)
	Neuroepithelial tumors	Axolotl (*A. mexicanum*) Alpine newt (*T. alpestris*)
	Mast cell tumor	Urodele species

Hemolymphatic system	Lymphoma	African clawed frog (*X. laevis*) Axolotl (*A. mexicanum*)
	Granulocytic leukemia	Toads (*Bufo* sp.)
Hepatobiliary system	Hepatocellular adenoma	Barking tree frog (*H. gratiosa*)
Alimentary system	Gastric adenocarcinoma	African clawed frog (*X. laevis*)
	Intestinal adenocarcinoma	Marine toad (*B. marinus*)
Urogenital system	Lucké renal adenocarcinoma	Northern leopard frog (*R. pipiens*)
	Nephroblastoma	Urodele and anura species
	Renal carcinoma	Urodele and anura species
	Sertoli cell tumor	Urodele and anura species
	Cystadenocarcinoma Granulosa cell tumor	Northern leopard frog (*R. pipiens*) Ornate horn frog (*C. ornata*)
	Ovarian teratoma	Northern leopard frog (*R. pipiens*)
Endocrine system	Pancreatic carcinoma	African clawed frog (*X. laevis*) *Rana* species

JPC Diagnosis: Oral mucosa: Neuroepithelioma (neuromastoma), *Ambystoma mexicanum*, axolotl.

Conference Comment: Amystomatidae, or mole salamanders, is a family of North American amphibians that contain approximately 30 species. The axolotl, *Ambystoma mexicanum*, is the most common aquatic species kept in captivity and has been used for many years in biomedical research. Axolotls exhibit a distinguishing feature termed "neoteny" which is the retention of juvenile characteristics. The Anderson's axolotl (*Amystoma andersoni)* are also neotenic and are common zoo residents. The Mexican axolotl is considered endangered due to habitat loss, pollution, and the introduction of fish into their habitats that predate larval axolotls[4].

Neuromastomata, aptly described above, have historically been transplanted successfully, and induced experimentally by numerous carcinogens.[3,4] Sensory cells of the lateral line system are found on the head, body, and tail of larval and adult aquatic amphibians. Specific cells in ampullary organs of the head in *A. mexicanum* contain similar cells that are called electroreceptors. It is not currently possible to distinguish olfactory, neuromastic, or electroreceptor cells from one another and neoplasms are often diagnosed as neuroepitheliomas. The lateral line and pit organs function as mechanoreceptors, while the ampullary organs are electroreceptors. The pit and ampullary organs are located only on head

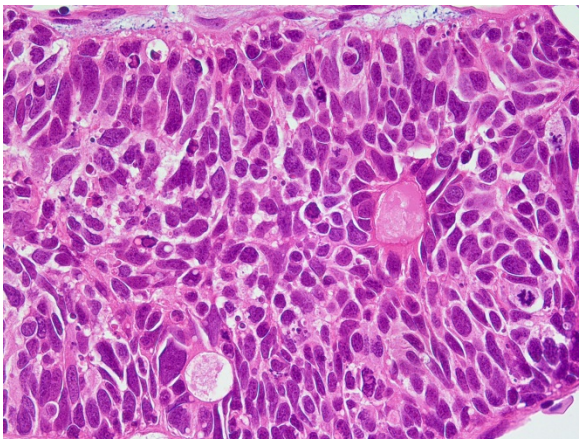

Skin, axolotl. Higher magnification of neoplastic cells. Neoplastic cells occasionally form rosettes around a lumen filled with homogenous to fibrillar proteinaceous material. Neoplastic cells (HE, 40X) (Photo courtesy of: Vetsuisse Faculty, University of Bern, Institute of Animal Pathology, Laenggassstrasse 122, PF 8466, 3001 Bern Switzerland, http://www.itpa.vetsuisse.unibe.ch/content/index_eng.html)

and the lateral line usually extends from head to tail on each side of the body. In the axolotl, specifically, there are three pairs of lateral lines (similar to the northern leopard frog, *Rana pipens*) and only the middle pair extend all the way to the tail.[4] Oral neuroepitheliomas (neuromastomas) were first described in axolotls by Drs. Brunst and Roque in 1967 and there have been few reports since[1].

Contributing Institution:
Vetsuisse Faculty, University of Bern
Institute of Animal Pathology
Laenggassstrasse 122
PF 8466
3001 Bern Switzerland
http://www.itpa.vetsuisse.unibe.ch/content/index_eng.html

References:

1. Brunst VV, Roque AL. Tumors in amphibians histology of a neuroepithelioma in *Siredon mexicanum*. *J Natl Cancer Inst.* 1967;38(2):193-204.
2. Coombs S, Braun CB, Donovan B. The orienting response of Lake Michigan mottled sculpin is mediated by canal neuromasts. *J Exp Biol*. 2001;204:337-348.
3. Darquenne J. Cancerologie experimentale: actions de substances cancerigenes sur le regenerat de la queue de *Triturus alpestris* Laur. Comptes Rendus de l'Academie des Sciences, Paris 273D:1460-1462.
4. Green DE, Harshbarger JC. Spontaneous neoplasia in Amphibia. In: Wright KM, Whitaker BR, eds. *Amphibian Medicine and Captive Husbandry*. Malabar, FL: Krieger Publishing Company; 2001:7, 335-400, 469.
5. Matz G. Tumeurs spontanees et experimentales observes chez *Triturus alpestris* (Laurent) (Salamandridae). Proceedings of 1st International Colloquium on Pathology of Reptiles and Amphibians. 1982:129-133.
6. Shioda C, Uchida K, Nakayama H. Pathological features of olfactory neuroblastoma in an axolotl (*Ambystoma mexicanum*). *J Vet Med Sci.* 2011;73:1109-1111.
7. Stacy BA, Parker JM. Amphibian oncology. *Vet Clin North Am Exot Anim Pract.* 2004;7:673-695.

CASE III: 17-1539 (JPC 4102429).

Signalment: Adult,male, *Stenella coeruleoalba*, dolphin.

History: An adult male dolphin (*Stenella coeruleoalba*) was found dead on the beach with multiple signs of trauma and sent to Oregon State University for necropsy.

Gross Pathology: The animal was in good body condition and had numerous full thickness lacerations throughout the skin.

Spinal cord, dolphin. At subgross magnification, the leptomeninges and inner half of the dura is expanded by a prominent cellular infiltrate. There is a large area of cavitation within the grey matter. Within the vertebral canal, the walls of adjacent arteries are thickened. (HE, 6X)

Adjacent to both testes, there was a 3cm diameter abscess. The animal's rectum contained dozens of well circumscribed, firm parasitic nodules.

Laboratory results:
Brucella ceti was isolated from brain tissue.

Microscopic Description: Spinal cord: All tissues represented by the slide are affected by variable degrees of inflammation, necrosis and degenerative changes. Diffusely, submeningeal spaces are markedly expanded and disrupted by dense infiltrates composed of copious amounts of lymphocytes admixed with fewer macrophages and plasma cells admixed with fibrin. Mononuclear infiltrates extend into the dura and surround nerve roots and blood vessels (perivascular cuffs). In the spinal cord, most blood vessels throughout the white and gray matter are surrounded by inflammatory cells. In many slides, the central region of gray matter is rarefied and, in severe cases, undergoes liquefactive necrosis. The dorsal root ganglion (displayed on some slides) has multifocal areas of satellitosis associated with chromatolysis and neuronophagia. Multifocally, blood vessels within the vascular plexus are completely occluded by subintimal proliferations of spindle cells, hematoidin deposits or fibrinous thrombi. Throughout the section, numerous blood vessels undergo fibrinoid necrosis.

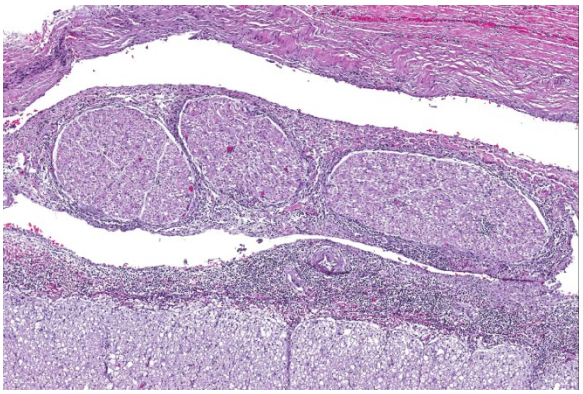

Spinal cord, dolphin. The inflammatory infiltrate expands the leptomeninges as well as surrounds the adjacent spinal nerves. There is some infiltration of the spinal nerves as well. (HE, 74X)

Contributor's Morphologic Diagnosis:
Spinal cord: Severe, diffuse, chronic-active lymphocytic meningomyelitis with poly-radiculoneuritis, pachymeningitis, vasculitis, and myelomalacia.

Contributor's Comment: Brucellosis is a zoonotic and endemic disease that affects a diverse array of land and aquatic mammals in many world regions including the Middle East, Asia, Africa, and North and South America. Domestic and wildlife species can become chronically infected, thus playing an important role disseminating the disease and acting as reservoirs[4,12].

Brucella are nonmotile, un-encapsulated, facultative intracellular, gram-negative coccobacilli. Taxonomically, the *Brucella* genus is divided into ten species according to their host specificity. Four out the ten, *Brucella* abortus, *B. melitensis*, *B. suis*, and *B. canis* are pathogenic to humans[4].

Their lifecycle contains three phases: incubation, acute and chronic infection. The bacterium enters the host via contact with mucosal surfaces and is phagocytized by macrophages and dendritic cells that reach the lymphatic system. Systemic infection follows replication in peripheral and visceral lymph nodes[6]. Once in the host phagocytic cell, the bacterium forms the *Brucella*-containing vacuole (BCV). Derived from the endoplasmic reticulum; the BCV permits the bacteria to evade the immune response, allowing it to survive and replicate with consequent progression to the acute phase where the bacterium infects non-phagocytic cells[13].

Brucella have a tropism for the reticuloendothelial system, bone marrow, reproductive organs, and mammary glands, but the central and peripherial nervous system can also be infected[6]. The pathophysiology behind the initial neurological infection is not completely elucidated. It is known that the inflammation associated with the initial infection is the key contributor to the lesions associated with neurobrucellosis. In the literature, a robust body of evidence shows that, in vivo and in-vitro, *Brucella*'s lipoproteins infect endothelial and glial cells activating the CNS innate immunity leading to secretion of matrix metalloproteases, nitric oxide, cytokines, and upregulation of Toll-like receptors exacerbating and promoting a severe inflammatory response[15].

In marine mammals, *Brucella sp.* infections were initially reported in 1994, and since then, numerous reports associating

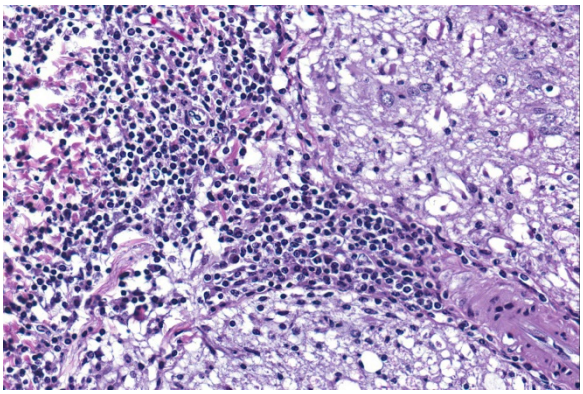

Spinal cord, dolphin. The inflammatory infiltrate, which extends downward along Virchow-Robin's spaces is composed of numerous lymphocytes and fewer histiocytes, neutrophils and plasma cells. (HE, 400X)

cetaceans' neurological lesions with *B. ceti* and *B. pinnipedialis* infection were widely documented[14].

In cetaceans, *Brucella* associated neurological lesions include meningo-encephalitis, meningitis, choroiditis, spinal discospondylitis, altered cerebrospinal fluid and remodeling of the occipital condyles[2,7,8,9,11].

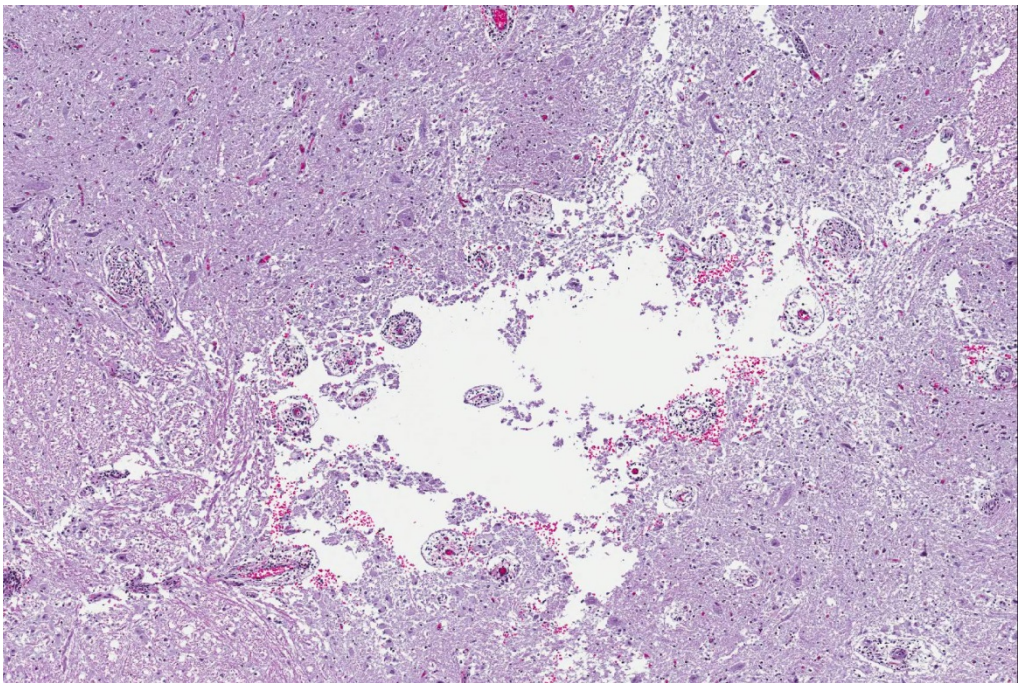

Spinal cord, dolphin. There is a large area of cavitation (malacia) within the central area of the grey matter. (HE, 62X)

The incidence of neurological involvement in cetaceans with brucellosis is not known, we speculate that the large vascular plexus inside the cranial vault with anastomosing arteries and veins along the vertebrae and base of the skull, predispose these animals to develop neurobrucellosis. Worthy of note in this case particularly is the pattern of malacia with minimal inflammation in the gray matter. This lesion is broadly characteristic of vascular compromise and ischemia due to the exquisite sensitivity of the gray matter to hypoxia. The extensive vascular involvement observed in this lesion is highly consistent with the gray matter lesion.

The zoonotic potential of marine mammal *Brucella sp*. is still not clear. There are few reports which describe the isolation of marine mammal *Brucella sp* from humans exposed to the pathogen that further developed granulomatous lesions. However, characterization and comparison of *Brucella* sp. Strains from naturally infected marine mammals and isolates from exposed humans differed[10,16,18]. Therefore, more research is needed to characterize their true zoonotic potential.

Although *Brucella* sp. is now a well-recognized etiological agent for cetacean's nonsuppurative neurological disease, other infectious agents are can also develop similar lesions such as *Herpesviruses*, *Toxoplasma gondii*, West Nile virus, and *Morbillivirus*.

JPC Diagnosis:

1. Spinal cord: Meningomyelitis, lymphohistiocytic, diffuse, severe with focal grey matter necrosis, lymphohistiocytic radiculoneuritis and fibrinoid vasculitis, *Stenella coeruleoalba*, dolphin.

2. Spinal canal: Arteriosclerosis, proliferative, multifocal, moderate to severe.

Conference Comment: A wide range of marine mammals are exposed to or infected with *Brucella* sp. The biovars of *Brucella sp.* that infect marine mammals are genetically distinct from those affecting terrestrial species; however, there have been reported cases of human brucellosis caused by marine mammal serovars[3]. Clinical disease in cetaceans is most common among marine mammals with pinnepeds being the most sensitive. In cetaceans, *Brucella ceti*, is the most common infectious culprit resulting in vertebral osteomyelitis and abortions particularly in bottlenose dolphins[2]. In these cases, atlanto-occipital joints were filled with inspissated, caseous material and there was a chronic, nonsuppurative meningo-encephalitis characterized by patchy congestion of meningeal blood vessels and mononuclear cell cuffing of blood vessels in the brain and meninges. A recent article described *Brucella* spp. Infections in endangered Hector's dolphins that are currently declining in population[1]. A total of 27 dolphins found dead on the New Zealand coastline were evaluation for lesions associated with brucellosis. Of note, *Brucella pinnipedialis* was the most common isolate and resulted in reproductive disease in affected animals which may be a contributing factor to the dwindling numbers in this species.

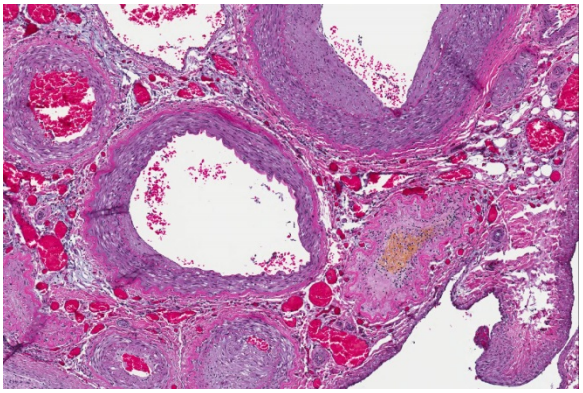

Spinal canal. There are extensive mural changes in arteries in the adjacent spinal canal include subintimal fibrosis (vessels at center and 2'oclock), occlusion and thrombosis with hematoidin deposition (4 o'clock), as well as smooth hyperplasia and recanalization (6 o'clock). (HE, 80X)

Conference participants had an energetic dialogue regarding the association of the grey matter necrosis, inflammatory meningoencephalitis, and the lesions in the adjacent arteries; even a temporal thread does not connect these acute, subacute, and chronic lesions, respectively. Athero-sclerosis has been reported in marine mammals, specifically aged dolphins, and is most likely an incidental finding in this case[17].

Contributing Institution:
Oregon Veterinary Diagnostic Laboratory-College of Veterinary Medicine
Oregon State University, Corvallis, Oregon
http://vetmed.oregonstate.edu/diagnostic

References:

1. Buckle K, Roe WD, Howe L, Michael S, et al. Brucellosis in endangered Hector's dolphins (*Cephalorhynchus hectori). Vet Pathol.* 2017; 54(5):838-845.
2. Dagleish M, et al. Isolation of *Brucella* species from a diseased atlanto-occipital joint of an Atlantic white-sided dolphin *(Lagenorhynchus acutus). Veterinary Record.* 2007;160(25):876-877.
3. Davison NJ, Barnett JEF, Perrett LL, et al. Meningoencephalitis and arthritis association with *Brucella ceti* in a short-beaked common dolphin. *J Wildl Dis.* 2013 49(3): 632-636.
4. de Figueiredo P, et al. Pathogenesis and immunobiology of Brucellosis: review of Brucella–host interactions. *The*

American Journal of Pathology. 2015;185(6):1505-1517.
5. Dold C. Cetacea (whales, dolphins, porpoises). In: Miller RE, Fowler ME, eds. *Fowler's Zoo and Wildlife Medicine*. Vol. 8. St. Louis, MO: Elsevier; 2015:431, 446-447.
6. Franco, M.P., et al. Human brucellosis. *The Lancet infectious diseases*. 2007;7(12):775-786.
7. Godfroid J, et al. From the discovery of the Malta fever's agent to the discovery of a marine mammal reservoir, brucellosis has continuously been a re-emerging zoonosis. *Veterinary Research*. 2005;36(3):313-326.
8. González L, et al. Chronic meningoencephalitis associated with *Brucella* sp. infection in live-stranded striped dolphins *(Stenella coeruleoalba)*. *Journal of Comparative Pathology*. 2002;126(2-3):147-152.
9. Hernández-Mora G, et al. Neurobrucellosis in stranded dolphins, Costa Rica. *Emerging infectious diseases*. 2008;14(9):1430.
10. McDonald W, et al. Characterization of a *Brucella* sp. strain as a marine-mammal type despite isolation from a patient with spinal osteomyelitis in New Zealand. *Journal of Clinical Microbiology*. 2006;44(12):4363-4370.
11. Nymo IH, Tryland M, Godfroid J. A review of *Brucella* infection in marine mammals, with special emphasis on *Brucella pinnipedialis* in the hooded seal *(Cystophora cristata)*. *Veterinary Research*. 2011;42(1):93.
12. Pappas G, et al. The new global map of human brucellosis. *The Lancet infectious diseases*. 2006;6(2):91-99.
13. Pizarro-Cerdá J, et al. Virulent *Brucella abortus* prevents lysosome fusion and is distributed within autophagosome-like compartments. *Infection and immunity*. 1998;66(5):2387-2392.
14. Ross H, et al. *Brucella* species infection in sea-mammals. *Veterinary Record*. 1994;134(14):359-359.
15. Samartino CG, et al., *Brucella abortus* induces the secretion of proinflammatory mediators from glial cells leading to astrocyte apoptosis. *The American Journal of Pathology*. 2010; 76(3):1323-1338.
16. Sohn A, et al. Human Neurobrucellosis with intracerebral granuloma caused by a marine mammal. *J. Vet. Rec*. 2003;13:1342-1353.
17. Sotnikov L. Comparative characteristics of the pathological anatomy of spontaneous atherosclerosis in representative of various classes of animals. *Arkh Patol*. 1967;29(9):61-67.
18. Whatmore AM, et al. Marine mammal *Brucella* genotype associated with zoonotic infection. *Emerging Infectious Diseases*. 2008;14(3):517.

CASE IV: WSC 2017-2018 Rhinoceros (JPC 4101227).

Signalment: 48-year-old female, southern white (*Ceratotherium simum)*, rhinoceros.

History: This 48-year-old, female southern white rhinoceros was housed at a zoologic institution. The animal was humanely euthanized due to quality of life concerns including progressive right forelimb lameness that had become poorly responsive to medical management.

Gross Pathology: At necropsy, both adrenal medullas were markedly enlarged relative to the adrenal cortices (cortex: medulla thickness ratio approximately 1:8). The right adrenal medulla contained a well demarcated, 4cm diameter, slightly firm, round, tan to pink mass that focally compressed the adjacent cortex. Also

Adrenal glands, rhinoceros. Both adrenal medullas are markedly enlarged (cortex:medulla ratio approximately 1:8). There are multiple expansile nodules within both medullas which compress the adjacent medulla and cortex. (Photo courtesy of: Johns Hopkins University School of Medicine, Department of Molecular and Comparative Pathobiology, http://www.hopkinsmedicine.org/mcp/)

present within the right medulla, were two, well demarcated, 1-1.5cm diameter, soft, ovoid masses that were mottled light tan to dark red. Approximately 90% of normal tissue in the left adrenal medulla was replaced by an irregular, multilobulated, approximately 8cm diameter mass that was light tan and soft, with multiple areas that were dark red, shiny, and friable.

Additional gross findings in this animal included severe osteoarthritis affecting all appendicular joints examined, multiple uterine leiomyomas, sclerotic kidneys with numerous cysts, severe dental disease, and a pedunculated mesenteric lipoma.

Laboratory results:
None submitted.

Microscopic Description: The tissue consists of a single section from the right adrenal gland. Within the medulla are two, distinct, neoplastic masses that are well-demarcated, partially encapsulated, and variably compress the adjacent parenchyma. One mass is composed of mature adipocytes and hematopoietic precursor cells arranged in sheets on a scant fibrovascular stroma. All three blood cell lineages (erythroid, myeloid, and lymphoid) are represented. There are also abundant mature red blood cells admixed with small amounts of eosinophilic proteinaceous fluid and scattered, golden to dark brown pigment-laden macrophages. Cellular atypia is minimal and mitotic figures are rare in this mass (<1 per 10 HPF). The second mass is composed of neoplastic cells arranged in nests and packets on a highly-vascularized fibrous stroma. Neoplastic cells frequently palisade around blood vessels (pseudorosette formation). Neoplastic cells are polygonal with distinct cell borders, abundant finely granular, basophilic cytoplasm, and round nuclei with finely stippled chromatin and one distinct nucleolus. There is minimal anisocytosis and anisokaryosis. Mitoses average less than 1 per 10 HPF. Affecting approximately 30% of the mass is an area of central coagulation necrosis and mineralization. Multiple medium-caliber arteries within the medulla contain intraluminal aggregates of neoplastic cells (vascular invasion).

Additional note: The large mass in the left adrenal medulla was histologically identical to the first mass described above, with areas of hematopoietic precursor cells and mature adipose tissue.

Contributor's Morphologic Diagnosis:

1. Adrenal gland, pheochromocytoma, unilateral, with necrosis and vascular invasion
2. Adrenal gland, myelolipoma, multifocal, bilateral
3. Adrenal gland, medullary hyperplasia, diffuse, unilateral, marked (gross diagnosis)

Right adrenal gland, rhinoceros. The right adrenal gland contains one 4cm mass and two smaller 1-1.5cm mass . (Photo courtesy of: Johns Hopkins University School of Medicine, Department of Molecular and Comparative Pathobiology, http://www.hopkinsmedicine.org/mcp/)

Contributor's Comment: This case documents the presence of bilateral adrenal myelolipoma with concurrent unilateral pheochromocytoma and adrenal medullary hyperplasia in a rare species.

Myelolipomas are benign, hormonally inactive, extra-marrow tumors composed of mature adipose tissue and hematopoietic elements. While myelolipomas are not uncommon in humans, they are relatively rare in veterinary species. Reports of myelolipomas in animals are limited to dogs,[20] domestic and non-domestic cats (most notably cheetahs),[2] rodents,[3,18] opossums,[13] and Old and New World monkeys.[9] In animals, they are most commonly reported in the liver, spleen, and adrenal cortex; additional sites include the subcutis (birds),[7] extradural space (dog),[11] and eye (dog).[21]

The etiology of adrenal myelolipomas remains unclear; however there are three proposed mechanisms of development: (1) distant seeding of bone marrow via hematogenous emboli, (2) maturation of embryonic mesenchymal rests, and (3) metaplasia of the adrenal cortex due to chronic hormonal imbalance or adrenocorticotropic hormone (ACTH) secretion.[5] Support for hypothesis #3 comes from controlled experiments in rats, which demonstrated that prolonged administration of testosterone and ACTH induced transformation of the inner zona fasciculata to tissue resembling bone marrow.[19] Additionally, myelolipomas frequently occur in people concurrently suffering from Cushing's disease, hypertension, diabetes and obesity, further suggesting a link with hormonal imbalance or chronic stress.[6] Myelolipomas are rarely reported in conjunction with pheochromocytomas in both people[22] and non-human primates.[10]

Pheochromocytomas are tumors of the chromaffin cells in the adrenal medulla; these are the cells which synthesize and secrete catecholamines (norepinephrine, epinephrine, and dopamine). They are the most common tumor of the adrenal medulla in animals, have been reported in a wide variety of mammals, and are best documented in humans, dogs, bulls, and rats.[15] There is a single previous report of pheochromocytoma a white rhinoceros.[1] While most pheochromocytomas in animals are reportedly non-functional,[14] functional tumors can be associated with hypertension

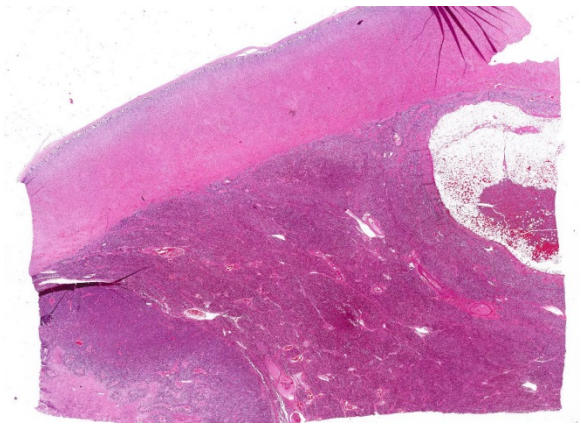

Right adrenal gland, rhinoceros. At low magnification, the submitted section contains two expansile masses (at left and right). (HE, 6X)

and cardiomyopathy due to high circulating levels of catecholamines.[4,24] The previous report of pheochromocytoma in a rhinoceros documented increased serum epinephrine and norepinephrine, as well as histologic changes consistent with systemic hypertension.[1] Hormone levels were not tested in this animal, however medial hypertrophy of arteries and arterioles in multiple organs and a focally extensive area of myocardial fibrosis at the junction of the right and left ventricles, suggest that the pheochromocytoma may have been functional. Histologic grading of pheochromocytomas in humans is based on a scoring system (Pheochromocytoma of the Adrenal gland Scaled Score) in which points are assigned for characteristics including vascular invasion, capsular invasion, local invasion, necrosis, mitoses, and nuclear pleomorphism.[8] While vascular invasion and necrosis were observed in the present case, there was no evidence of local invasion or distant metastases.

Grossly, the right adrenal gland of this rhinoceros had a cortical to medullary thickness ratio of roughly 1:8, suggestive of generalized medullary hyperplasia and / or cortical atrophy. The ratio in the left adrenal gland was similar, but this may have been due to replacement and expansion of normal medullary tissue by the large myelolipoma. While normal ratios for white rhinos are not well established, a previous morphologic study reported that the medulla accounted for only 20% of the mass of the entire adrenal gland.[14] Medullary hyperplasia in veterinary species can be associated with pheochromocytoma and multiple endocrine neoplasia (MEN was not documented in this case).[12]

JPC Diagnosis:

1. Adrenal gland: Pheochromocytoma, Southern white (*Ceratotherium simum)*, rhinoceros.
2. Adrenal gland: Myelolipoma.

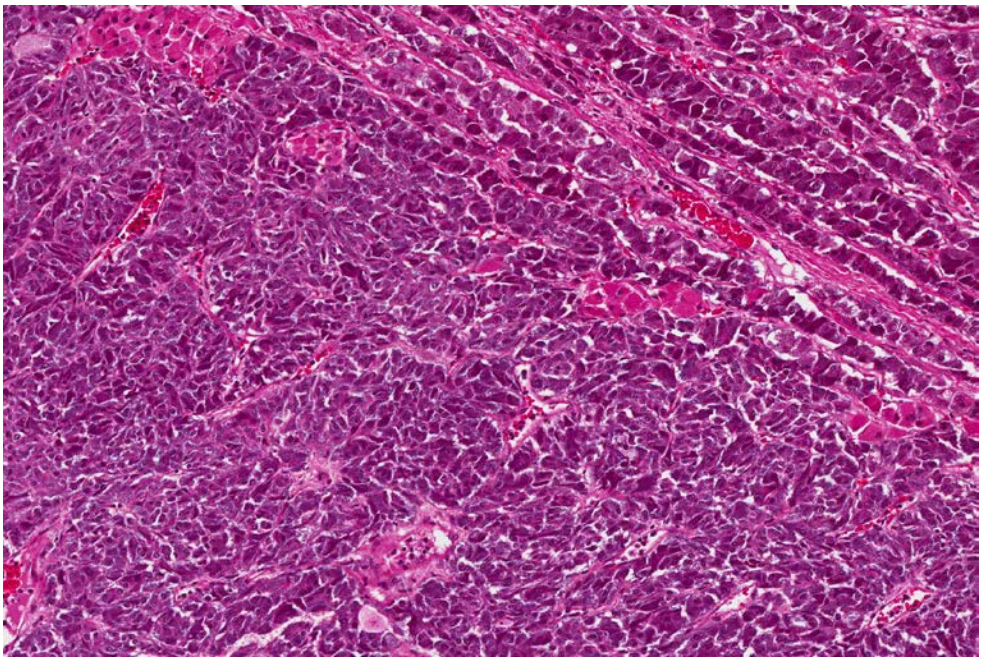

Right adrenal gland, rhinoceros. The nodule at left is composed of large nests of medullary epithelium morphologically similar to that present outside the compression capsule (consistent with a pheochromocytoma). (HE, 176X)

Conference Comment: In prehistoric times, rhinoceroses were the most common large herbivores in North America, and today, they are one of the most primitive of the world's large mammals. There are five species that exist in four genera: in Africa there are white (*Ceratotherium simum)* and black (*Dicero bicornis*) rhinos, in Asia there are Sumatran

(*Dicerorhinus sumatrensis*), Indian (*Rhinoceros unicornis*), and Javan (*Rhinoceros sondaicus*) rhinos. Of the five species, Sumatran are the most primitive and predate the wooly rhino (*Coelodonta antiqitatis*), now extinct, which inhabited northern Europe and Asia during the last Ice Age. In Africa, white rhinos prefer to live on flat terrain which short grasses and black rhinos live in areas with shrubs and young trees, these preferences are associated with their dietary requirements. Regardless, all species of rhino are hindgut fermenters with fast transit times who require regular access to water to cool off, keep their skin free of external parasites, and stay hydrated. Of the five species, white rhinos have the largest world population estimate at 20,143 (2012). The skin of a rhinoceros is extremely thick, with the white rhino's skin reaching a thickness of five centimeters.[11]

In rhinoceroses, neoplasia is fairly uncommon. There have been reported cases of squamous cell carcinoma in white, black, and Indian rhinos as well as cutaneous melanoma in black and Indian rhinos. Rare cases of thyroid carcinoma, hepatocellular carcinoma, and acute lymphoblastic leukemia have been reported in black rhinos.[11]

Myelolipomas are benign tumors that are most often encountered in the adrenal glands of cattle, nonhuman primates, and occasionally other species composed of aggregates of mature adipocytes, reactive fibroblasts, and myeloid and erythroid hematopoietic cells. Occasionally, fibroblasts undergo osseous differentiation and areas of osseous metaplasia occur within the tumor. These tumors are thought to originate from metaplastic transformation of adrenal cortical cells, although their exact origin in currently unknown.[16,23]

Pheochromocytomas are the most common neoplasm arising in the adrenal medulla of domestic animals, but are more frequent in cattle and dogs. Microscopically, they arise from the chromaffin cells of the adrenal medulla, are either unilateral or bilateral, and generally have abundant hemorrhage and necrosis. Macroscopically, the Henle chromaffin reaction can be used to detect the tumor using either potassium dichromate or iodate. When Zenker's solution is applied to a flat surface of freshly cut tumor, there is

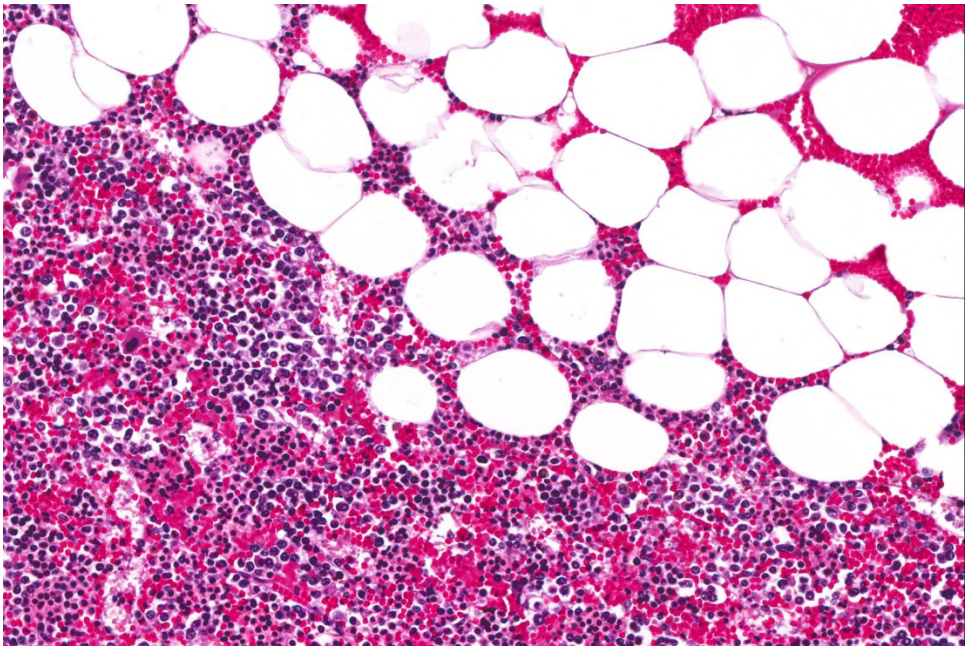

Right adrenal gland, rhinoceros. The nodule at right is composed of adipocytes (right) and trilinear marrow elements (left) . (HE, 264)

oxidation of the catecholamines, and a dark brown pigment that forms within 20 minutes. Ultrastructurally, pheochromocytomas are composed of epinephrine secreting cells, norepinephrine secreting cells, or a combination of the two. The cells that secrete epinephrine have many low electron density granules with a narrow submembranous space. Conversely, the norepinephrine secreting cells have secretory granules with an eccentric electron dense core surrounded by a prominent submembranous space. With chronicity, tumor cells can grow into the caudal vena cava and form a neoplastic thrombus that can occlude drainage from caudal extremities. Metastasis occurs in about 50% of affected dogs to the liver, regional lymph nodes, spleen, and lungs. Since they are of endocrine origin, pheochromocytomas, when functional, can have serious systemic effects related to excessive catecholamine secretion such as: tachycardia, edema, cardiac hypertrophy, arteriolar sclerosis, and medial hyperplasia of arterioles.[16,17]

When discussing the adjacent "normal" adrenal medullary tissue, attendees reached an impasse. Some believed it to be truly hyperplastic, as evidenced by the gross images submitted by the contributor, while others believed that the thinned cortex was due to the mass of two neoplasms expanding the medulla and compressing and stretching the cortex. In short, it was difficult to make a definitive diagnosis of medullary hyperplasia with the single slide available to conference participants; however, if the contributor's other sections of the medulla revealed increased amounts of normal medullary tissue histologically, we support the contributor's gross diagnosis of medullary hyperplasia.

Contributing Institution:

Johns Hopkins University School of Medicine
Department of Molecular and Comparative Pathobiology
http://www.hopkinsmedicine.org/mcp/

References:

1. Bertelsen MF, Steele SL, Grondahl C, Baandrup U. Pheochromocytoma in a white rhinoceros (*Ceratotherium simum*). *J Zoo Wildl Med.* 2011;42(3)**:**521-523.
2. Cardy RH, Bostrom RE. Multiple splenic myelolipomas in a cheetah. *Veterinary Pathology.* 1968;15**:**556-558.
3. Dixon D, Yoshitomi K, Boorman G, Maronpot RR. "Lipomatous" lesions of unknown cellular origin in the liver of B6C3F1 mice. *Veterinary Pathology.* 1994;31**:**173-182.
4. Edmondson EF, Bright JM, Halsey CH, Ehrhart EJ. Pathologic and cardiovascular characterization of pheochromocytoma-associated cardiomyopathy in dogs. *Vet Pathol.* 2015;52(2)**:**338-343.
5. Ishay A, Dharan M, Luboshitzky R. Combined adrenal myelolipoma and medullary hyperplasia. *Horm Res.* 2004;62(1)**:**23-26.
6. Khater N, Khauli R. Myelolipomas and other fatty tumours of the adrenals. *Arab J Urol.* 2011;9(4)**:**259-265.
7. Latimer KS, Rakich PM. Subcutaneous and hepatic myelolipomas in four exotic birds. *Veterinary Pathology.* 1995;32**:**84-87.
8. LDR T. Pheochromocytoma of the adrenal gland scaled score (PASS) to separate benign from malignant neoplasms. *The American Journal of Surgical Pathology.* 2002;26(5)**:**551-566.
9. Lowenstine LJ, McManamon R, Terio KA. Comparative pathology of aging great apes: Bonobos, Chimpanzees,

Gorillas, and Orangutans. *Vet Pathol.* 2016;53(2)**:**250-276.
10. Miller AD, Masek-Hammerman K, Dalecki K, Mansfield KG, Westmoreland SV. Histologic and immunohistochemical characterization of pheochromocytoma in 6 cotton-top tamarins (*Saguinus oedipus*). *Vet Pathol.* 2009;46(6)**:**1221-1229.
11. Miller MA, Buss PE. Rhinoceridae (rhinoceroses). In: Miller RE, Fowler ME, eds. *Fowler's Zoo and Wildlife Medicine*. Vol. 8. St. Louis, MO: Elsevier; 2015:538-539, 544.
12. Miller MA. Endocrine system. In: Zachary JF, ed. *Pathologic Basis of Veterinary Disease*. 6th ed. St. Louis, MO: Elsevier; 2017:709.
13. Newman SJ, Inzana K, Chickering W. Extradural myelolipoma in a dog. *Journal of veterinary diagnostic investigation.* 2000;12**:**71-74.
14. Peng K, Song H, Liu H, Zhang J, Lu Z, Liu Z, et al. Histologic study of the adrenal gland of African White Rhinoceros. *Pakistan Veterinary Journal*. 2011;32(3)**:**394-397.
15. Pope JP, Donnell RL. Spontaneous neoplasms in captive Virginia opossums (*Didelphis virginiana*): a retrospective case series (1989-2014) and review of the literature. *Journal of Veterinary Diagnostic Investigation.* 2017;29(3)**:**1-7.
16. Rosol TJ, Grone A. Endocrine glands. In: Maxie, MG, ed. *Jubb, Kennedy, and Palmer's Pathology of Domestic Animals*. Vol. 3. 6th ed. St. Louis, MO: Elsevier; 2016:343-344, 349-352.
17. Rosol TJ, Meuten DJ. Tumors of the endocrine glands. In: Meuten DJ, ed. *Tumors in Domestic Animals*. Ames, IA: John Wiley and Sons, Inc.; 2017:787-791.
18. Schardein JL, Fitzgerald JE, Kaump DH. Spontaneous tumors in holtzman-source rats of various ages. *Veterinary Pathology.* 1968;5**:**238-252.
19. Selye H, Stone H: Hormonally induced transformation of adrenal into myeloid tissue. *American Journal of Pathology.* 1950;26(2)**:**211-233.
20. Spangler WL, Culbertson MR, Kass PH: Primary mesenchymal (nonangiomatous/nonlymphomatous) neoplasms occurring in the canine spleen: anatomic classification, immunohistochemistry, and mitotic activity correlated with patient survival. *Veterinary Pathology.* 1994;31**:**37-47.
21. Storms G, Janssens G. Intraocular myelolipoma in a dog. *Veterinary Ophthalmology*. 2013;16**:**183-187.
22. Ukimura O, Inui E, Ochiai A, Kojima M, Watanabe H. Combined adrenal myelolipoma and pheochromocytoma. *Journal of Urology*. 1995;154**:**1470.
23. Valli VE, Bienzle D, Meuten DJ. Tumors of the hemolymphatic system. In: Meuten DJ, ed. *Tumors in Domestic Animals*. Ames, IA: John Wiley and Sons, Inc.; 2017:317-318.
24. Zuber SM, Kantorovich V, Pacak K. Hypertension in pheochromocytoma: characteristics and treatment. *Endocrinol Metab Clin North Am.* 2011;40(2)**:**295-311, vii.

Self-Assessment - WSC 2017-2018 Conference 11

1. Which of the statements is not true concerning squirrel fibromatosis?
    a. It is caused by a parapoxvirus
    b. Viral inclusions may be seen in both mesenchymal and epithelial cells.
    c. Nodular lesions may also be seen in internal organs.
    d. It may infect grey, red, and fox squirrels.

2. Which of the following diseases is not caused by a poxvirus?
    a. Myxomatosis
    b. Molluscum contagiosum
    c. Milker's nodules
    d. Carppox

3. In amphibians, neuromast cells are associated with what function?
    a. Cutaneous taste
    b. Lateral line system
    c. Cloacal respiration
    d. Innate immune response

4. Which of the following is NOT associated *Brucella ceti* in cetaceans?
    a. Vertebral osteomyelitis
    b. Neurobrucellosis
    c. Granulomatous hepatitis
    d. Abortion

5. Which of the following neoplasms are USUALLY hormonally active?
    a. Myelolipomas
    b. Pheochromocytomas
    c. Both of the above
    d. Neither of the above

Please email your completed assessment to Ms. Jessica Gold at Jessica.d.gold2.ctr@mail.mil for grading. Passing score is 80%.This program (RACE program number) is approved by the AAVSB RACE to offer a total of 0.5 CE Credits, with a maximum of 12.5 CE Credits being available to any individual Veterinary Medical Professionals for the 2017-2018 Wednesday Slide Conference. This RACE approval is for the subject matter categories of: SCIENTIFIC using the delivery method of NON-INTERACTIVE DISTANCE. This approval is valid in jurisdictions which recognize AAVSB RACE; however, participants are responsible for ascertaining each board's CE requirements.
RACE does not "accredit", "endorse" or "certify" any program or person, nor does RACE approval validate the content of the program.

Joint Pathology Center
Veterinary Pathology Services

WEDNESDAY SLIDE CONFERENCE 2017-2018

C o n f e r e n c e 12

13 December 2017

Mark T. Butt, DVM, DACVP
President, Tox Path Specialists (TPS), LLC
8420 Gas House Pike, Suite G
Frederick, MD 21701

CASE I: 16L-2815 (JPC 4102118).

Signalment: 8 year-old, mare, Irish sport horse, *Equus caballus*, equine.

History: The animal presented with clinical signs consistent with cauda equina syndrome from 29th November 2015. Clinical neurological manifestations were an inability to pass feces and a progressive reduction in tail, anal and vaginal tone. Posteriorly there was a bilateral muscle atrophy of the muscles of the proximal hind limbs and the muscle of the tail head. Unilateral paresis of the right hind limb appeared and developed into a paraparesis. Steroids and non-steroidal anti-inflammatory drugs in combination with neuromodulator treatment were administered.

Gross Pathology: The lumbosacral spinal cord and extradural nerve roots (cauda equina) were markedly enlarged by an abundant grey to whitish irregular material with variable consistency and occasionally a nodular pattern. This material was consistently attached to the epineurium of the sacral nerve roots and was present from the *Conus medulari*, and between the nerve prolongations of the fillum terminale and cauda equina.

Laboratory results:
None provided.

Microscopic Description: Cauda equina: There are multiple cross sections of nerve roots, epidural adipose tissue and connective tissue. The majority of the fibrous tissue corresponds to the epineurium which is markedly expanded by an increased volume of dense irregular connective tissue (severe fibrosis). The fibrotic epineurium is infiltrated by a moderate to severe, multifocal inflammatory infiltrate composed of epithelioid macrophages, often surrounded by large numbers of lymphocytes, fewer plasma cells and occasional Langhans type multinucleated giant cells; there is multifocally mild hemorrhage. The majority of nerve roots are affected by a similar inflammatory process, the severity of these changes ranging from

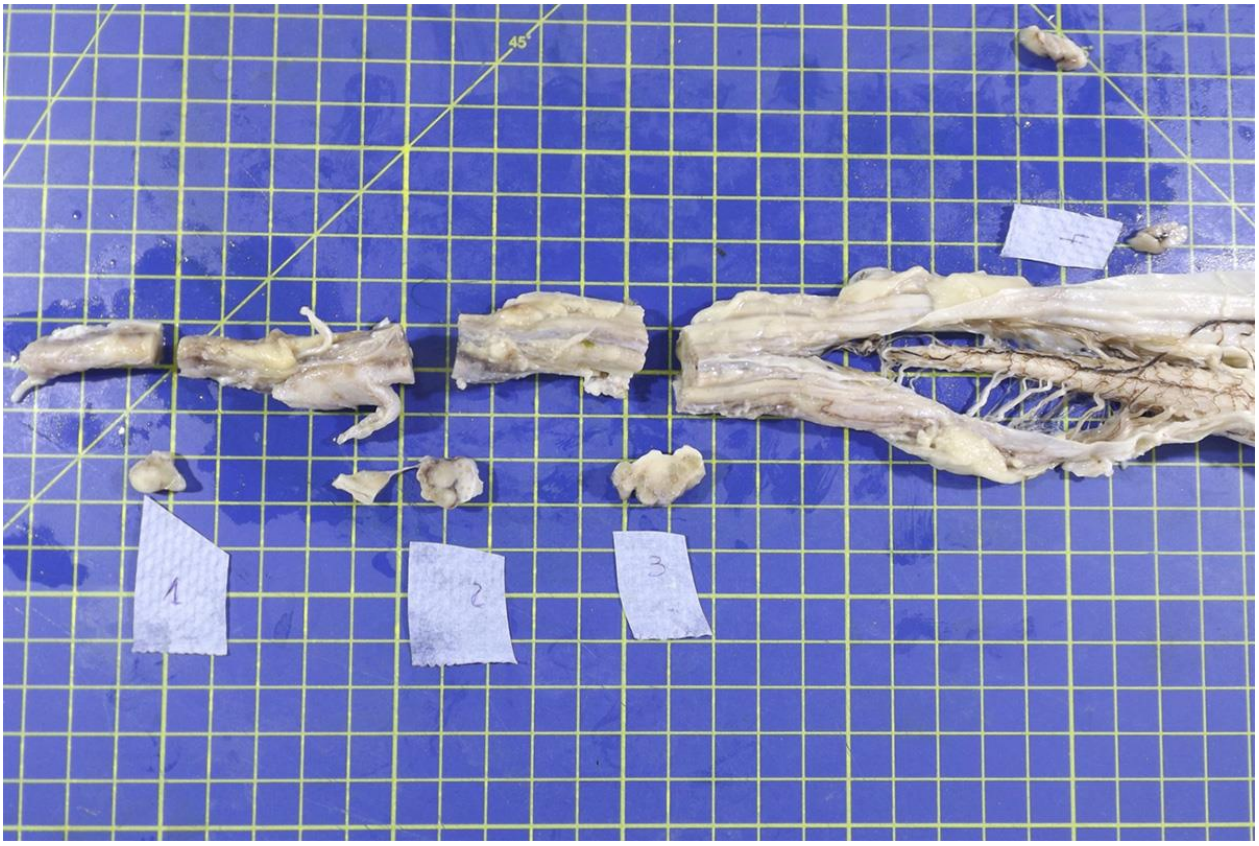

Cauda equina, horse. The lumbosacral spinal cord (right) and spinal roots are expanded and fused by abundant, variably mature fibrous connective tissue. (Photo courtesy of: Department of Veterinary Pathology, Infection and Public Health, Institute of Veterinary Science, University of Liverpool, Leahurst Campus, Chester High Road, Neston, CH64 7TE.

minimal to severe. The most severely affected nerve roots are entirely effaced by multifocal areas of necrosis characterized by large amounts of eosinophilic and basophilic amorphous material (myelin debris) and infiltrated by large numbers of inflammatory cells (macrophages, lymphocytes), and intact axons and myelin sheaths are rarely observed. In those nerves less severely affected, the epineurium and perineurium are markedly enlarged due to high number of infiltrating macrophages and lympho-cytes. There is a reduction of nerve fibers numbers, and nerves variably exhibit swollen axons (spheroid), moderately distended myelin sheets and occasionally phagocytic cells within areas of myelin degradation (digestion chambers). Other peripheral nerves are minimally affected or are unremarkable.

Contributor's Morphologic Diagnosis:
Horse, lumbosacral spinal nerve roots (cauda equina, fillum terminale): Multifocal, severe, chronic, granulomatous poly-radiculoneuritis with multifocal nerve necrosis, Wallerian axonal degeneration and epineurial fibrosis.

Contributor's Comment: Polyneuritis equi (cauda equina neuritis) is an uncommon sporadic disease of the horse of an unknown etiology but is considered likely to be an autoimmune or immune-mediated disorder; it is considered by some authors to be reactive condition from previous inflammatory or infectious episodes[2].

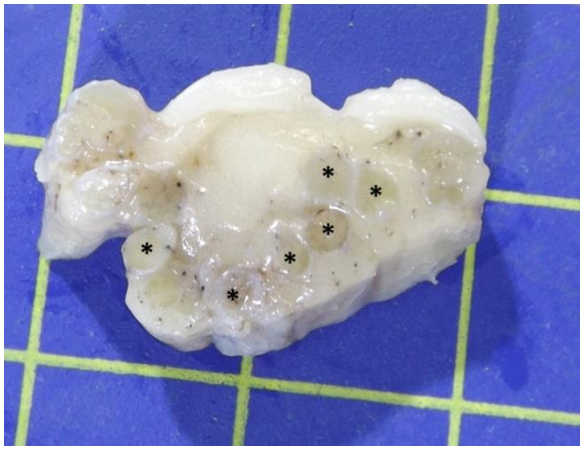

Cauda equina, horse. The entrapped spinal roots (asterisk) are fused within an irregular mass of proliferating fibrous connective tissue. (Photo courtesy of: Department of Veterinary Pathology, Infection and Public Health, Institute of Veterinary Science, University of Liverpool, Leahurst Campus, Chester High Road, Neston, CH64 7TE.)

Clinically, animals exhibit a slowly progressive peripheral neurological disorder, localizing to the sacrococcygeal nerves (cauda equina syndrome) and is most commonly observed in females[9]. Formerly known as cauda equina neuritis in horse, the name of the disease was updated to polyneuritis equi (PNE) based on descriptions in which the involvement of spinal nerves at various levels of the spine and cranial nerves were also reported[11].

Clinical examination allows the neuro-localization of lesions to the level of spinal nerve roots, frequently of the sacral spinal segments[4]. It represents an exclusion diagnosis with and is considered to be of idiopathic origin[1]. A case of verminous migration by *Halicephalobus gingivalis* has been described in association with the typical inflammatory reaction of cauda equina neuritis, however[5]. Equine neurotropic viruses such as equine herpesvirus 1 (EHV1) and West Nile virus have been ruled out as causes in cases reported in recent literature[1]. Some older studies have demonstrated an association between the lesion of PNE and infectious agents such EHV1, equine adenovirus type 1, equine arteritis virus, and *Streptococcus equi* ssp. *equi* with the suggestion that the lesion may have evolved through a bystander mechanism in which the presence of the inflammatory infiltrate damages the nerves, rather than the direct actions of these organisms as causal agents[9]. Additionally, exclusion of traumatic, developmental, neoplastic or toxic diseases should be ruled out before confirming the diagnosis[11].

The typical gross and microscopic lesions that characterize this disease are very much in keeping with the case we present. Typical gross lesions include thickening of the nerve roots of the sacral and coccygeal nerves which may be discolored by acute and / or chronic hemorrhage. Histologically a severe granulomatous neuritis with marked fibrosis and degenerative / necrotizing changes to nerve fibers is described[2].

Cauda equina syndrome also is described in dogs with a higher incidence in large breeds[9]. Nonetheless in this species it is defined as a compression of the spinal cord

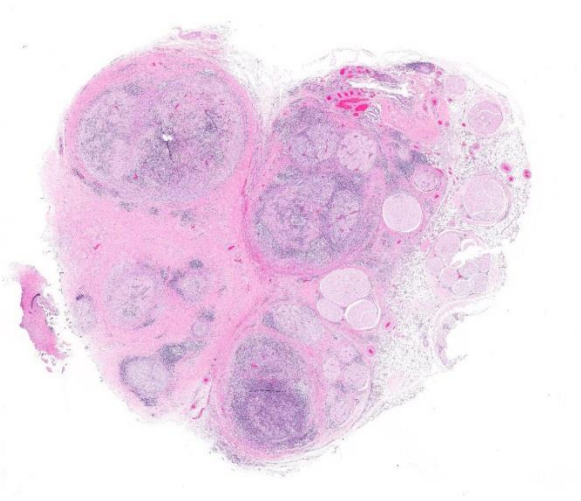

Cauda equina, horse. The epineurium of spinal nerve bundles is markedly expanded and fused with that of other nerve bundles, and the nerves are variably effaced by a cellular infiltrate. (HE, 6X)

due to stenosis of the lumbosacral central canal. Dogs and cats also develop acute polyradiculoneuritis with presumed autoimmune origin and low frequent affectation of the cauda equina[9].

In humans and laboratory animals, Guillain-Barre syndrome (GBS) and allergic neuritis (EAN) constitute infectious autoimmune diseases that have been compared with PNE in horses and acute polyneuritis in dogs. Descriptive studies including the characterization of the histopathological lesions in horses[3,10] are indicative of immune reactions against myelin in PNE. A 2008 study into the composition of the inflammatory infiltrates of PNE[9] demonstrated that both T and B lymphocytes were present within the lesions, along with macrophages. The authors consider the question as to whether there is a T-cell mediated immune response against myelin, or if the B-cells are producing an antibody against the P2 protein of myelin, or there may be a combination of both mechanisms. A 2015 study[3] of equine protozoal myeloencephalitis, caused by *Sarcocytis neurona*, demonstrated that some horses with antibodies against this organism also produce antibodies against myelin protein peptide. This suggests one possible aetiological relationship between an infectious organism and an immune-mediated peripheral neuritis.

JPC Diagnosis: Spinal cord, cauda equina: Polyradiculoneuritis, granulomatous, chronic, diffuse, severe with marked epineurial fibrosis and widespread axonal degeneration, Irish sport horse (*Equus caballus*), equine.

Conference Comment: The cauda equina is composed of roots of the sacral and coccygeal spinal nerves and is present in all mammalian species except for birds, whose

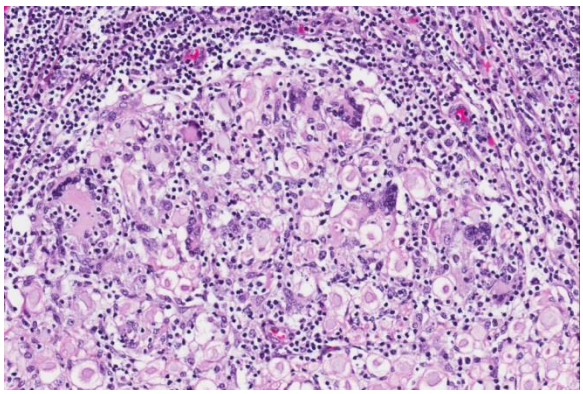

Cauda equina, horse. Cross section of an infiltrated nerve. Numerous lymphocytes and histiocytes infiltrate the nerve root endomysium occasionally replacing axons. Remaining axons sheaths are mildly dilated. There are moderate numbers of foreign body and Langhans type multinucleated macrophages. The encircling epineurium is expanded by numerous lymphocytes, fewer histiocytes and proliferating vessels, fibroblasts and collagen. (HE, 288X)

spinal cord extends throughout the entire spinal canal. These nerves exit the caudal end of the spinal cord and travel through the remainder of the spinal canal longitudinally to reach their intended intervertebral foramina. The cauda equina develops after birth as the vertebral column continues to grow, resulting in cranial displacement of spinal cord segments relative to their corresponding vertebrae (whereas during gestation the spinal cord segments are aligned with their corresponding vertebrae)[7].

First described in 1897 by Dexler as a combination of tail and anal sphincter paralysis due to chronic inflammation and fibrosis of the extradural portions of the nerve roots of the cauda equina, neuritis of the cauda equina has been identified throughout the years in numerous adult horses and ponies of various breeds. Many of the clinical signs (most of which are listed above) including urinary and fecal incontinence, perineal anesthesia, tail paralysis, muscle atrophy and weakness, and hind limb ataxia can be attributed to affected sacrocaudal nerve roots. However, animals often have additional clinical signs

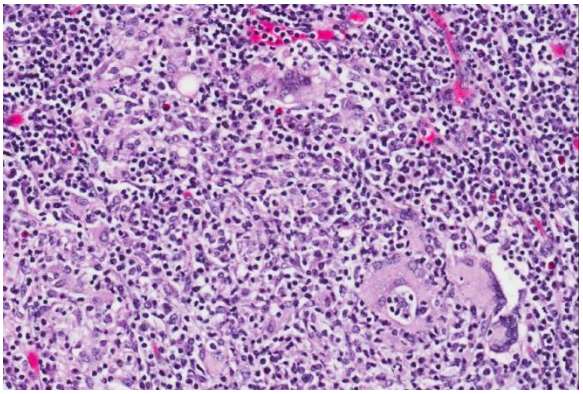

Cauda equina, horse. Higher magnification of the infiltrate within an effaced nerve. No intact axons remain. (HE, 324X)

attributable to cranial nerve roots being affected such as facial paralysis, head tilt, and wasting of the masticatory muscles. The variety of affected nerves led to this syndrome being more aptly named "polyneuritis equi"[8]. In this case, attendees noted the variation of maturity of fibrous connective tissue throughout the lesion - ranging from hypertrophied fibroblasts and loosely packed immature fibrous connective tissue to dense mature collagen, denoting the diseases development over time.

Contributing Institution:

Department of Veterinary Pathology, Infection and Public Health
Institute of Veterinary Science
University of Liverpool
Leahurst Campus
Chester High Road
Neston
CH64 7TE

References:

1. Aleman M, Katzman SA, Vaughan B, Hodges J, et al. Antemortem diagnosis of polyneuritis equi. *J Vet Intern Med.* 2009;23(3):665-8.
2. Cantile C, Youssef S. Nervous system. In: Maxie MG, ed. Jubb, Kennedy, and Palmer's Pathology of Domestic Animals. Vol 1. 6th ed. St. Louis, MO: Elsevier; 2016:374-375.
3. Ellison S, Kennedy T, Schweiss L. Serum antibodies against a reactive site of equine myelin protein 2 linked to polyneuritis equi found in horses diagnosed with EPM. *Intern J Appl Res Vet Med.* 2015;13(3):164-170.
4. Hahn CN. Miscellaneous disorders of the equine nervous system: Horner's syndrome and polyneuritis equi. *Clin Tech Equine Pract.* 2006;5:43–48.
5. Johnson JS, Hibler CP, Tillotson KM, Mason GL. Radiculomeningomyelitis due to *Halicephalobus gingivalis* in a horse. *Vet Pathol.* 2001;38:559-561.
6. Meij BP, Bergknut N. Degenerative lumbosacral stenosis in dogs. *Vet Clin North Am Small Anim Pract.* 2010; 40:983–1009.
7. Stoffel MH, Oevermann A, Vandevelde M. Functional neuroanatomy. In: Bolon B, Butt MT, eds. *Fundamental Neuropathology for Pathologists and Toxicologists: Principles and Techniques.* Hoboken, NJ: John Wiley & Sons, Inc.; 2011:18-19.
8. Summers BA, Cummings JF, de Lahunta A. Diseases of the peripheral nervous system. In: Duncan L, McCandless PJ, eds. *Veterinary Neuropathology.* St. Louis, MO: Mosby; 1995:432-434, 454-455.
9. Vandevelde M, Higgins RJ, Oevermann A. Inflammatory diseases. *Veterinary Neuropathology: Essentials of Theory and Practice.* New York: Willey – Blackwell; 2012.
10. Van Galen G, Cassart D, Sandersen C, Delguste C, et al. The composition of the inflammatory infiltrate in three cases of polyneuritis equi. *Equine vet. J.* 2008;40(2):185-188.
11. Vatistas N, Mayhew IG. Differential diagnosis of polyneuritis equi. *In Practice.* 1995;17:26–29.

CASE II: N2015-0602 (JPC 4084210).

Signalment: 1.8 year-old, male, African pygmy hedgehog, *Atelerix albiventris*, hedgehog.

History: This hedgehog had an approximate 3-month history of progressive depression, weight loss, worsening limb tremors, paresis, and hunched posture. Clinical decline persisted despite supportive care and analgesic therapy (Meloxicam). The animal was euthanized.

Gross Pathology: The hedgehog was in good body and postmortem condition. Mild abrasions were present along the ventral trail. Absent gastric content and mild gall bladder distention suggested recent anorexia. There were no other significant gross findings.

Laboratory results:
None provided.

Microscopic Description: Multiple sections along the brain and spinal cord (cerebrum, thalamus, midbrain, cerebellum, brainstem, and spinal cord) were examined. Submitted slides include cerebrum and brainstem.

Cerebrum, pygmy hedgehog. There is extensive bilateral vacuolation of the white matter of the corona radiata. The very slight tangential section affects the amount of this structure at left. (HE, 6X)

Affecting white matter throughout the examined sections of central nervous system are regions of myelin degeneration. These areas are characterized predominantly by multifocal to clustered, variably sized (approximately 6-60 um-diameter), clear vacuoles (spongiosis), with occasional wispy residual eosinophilic myelin strands and subtle regional pale staining (rarefaction). There are mildly increased interspersed small basophilic glial cells (astrocytosis) with occasional satellitosis, few eosinophilic swollen axons (spheroids), rare vacuolated gitter cells and digestion chambers, and rare eosinophilic reactive astrocytes (gemistocytes). The myelin vacuolation is marked and variably symmetrical within the brainstem, is moderate and more unilaterally predominant within the cerebral cortex corona radiata, and is mild and scattered within the internal capsule, thalamus, midbrain, cerebellar white mater, spinal cord (thoracic, predominantly ventral funiculi), and optic nerve.

Contributor's Morphologic Diagnosis:
Brain and spinal cord, white matter: Myelin degeneration, multifocally extensive, mild (thalamus, optic nerve, spinal cord) to moderate (cerebral cortex, cerebellum) to marked (brainstem), with prominent spongiosis, mild gliosis, and rare axonal degeneration.

Contributor's Comment: This case demonstrates lesions of leukoencephalomyelopathy typical of "Wobbly Hedgehog Syndrome", characterized by demyelinating changes affecting the brain

and spinal cord. This syndrome is a progressive neuropathy of unknown etiology that affects African hedgehogs and is considered to have a familial tendency.

Wobbly Hedgehog Syndrome (WHS) has been recognized since the mid-1990s and is reported to affect approximately 10% of pet African hedgehogs in North America. The predominant clinical signs of WHS are progressive ataxia and paralysis, with onset often under two years of age. Disease progression is variable, but complete paralysis often occurs within 15 months. Other noted clinical abnormalities include tremors, exophthalmos, scoliosis, seizures, muscle atrophy, and self-mutilation.[4] In most cases, the progression of paralysis is ascending to tetraplegia. Weight loss is common and may relate to dysphagia in later stages of disease. Skin abrasions affecting feet and ventral body can relate to loss of motility. As in this case, affected animals are often euthanized due to quality of life concerns.

Histopathology is required for definitive diagnosis of WHS, with characteristic vacuolation of the white matter tracts of the brain (cerebrum, cerebellum, and brainstem) and spinal cord. Lesions are considered to begin with myelin loss, and progress variably to secondary axonal and even neuronal degeneration. In this case, myelin degeneration predominated, with minor axonal degeneration variably evident across sections. Degeneration of lower motor neurons of the ventral horns of the spinal cord, demyelination of ventral spinal rootlets, and neurogenic muscle atrophy are

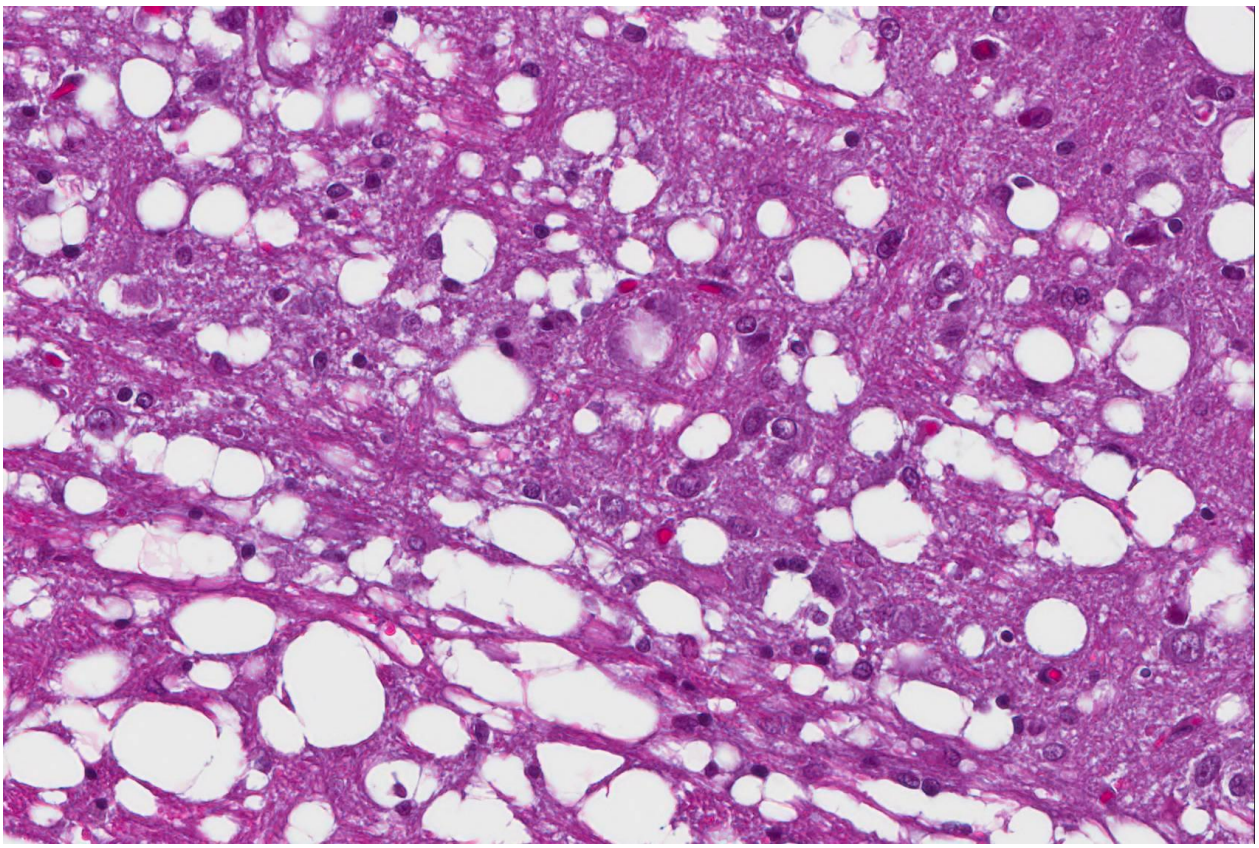

Cerebrum, pygmy hedgehog. Vacuoles are distinct, range up to 40 um in diameter, and often have a single compressed hyperchromatic nucleus at the periphery, suggesting that the vacuoles represent markedly dilated myelin sheaths. (HE, 400X)

also reported.[4] The peripheral nervous system is unaffected. Hepatic lipidosis of varying severity has also been reported in some cases; in the animal of this report hepatocellular lipid vacuolation was mild.

The etiology of WHS is unknown. However, clustered cases and pedigree analysis suggest a hereditary basis. Relatives of this affected hedgehog had also succumbed to neurologic disease with pathologic findings supportive of WHS. Due to familial tendency, breeding hedgehogs with signs of WHS or their close relatives has been discouraged.[4] No treatments (antibiotics, vitamins and supplements, physical therapy regimes, etc.), have been confirmed to alter the course of disease.

Although there are no reports of WHS transmission between unrelated hedgehogs, an infectious cause is not entirely excluded. A similar paralytic and demyelinating syndrome has also been reported in European hedgehogs, but with slightly different histologic and epidemiologic features, for which a viral etiology was suspected.[7] More recently, nonsuppurative encephalitis with vacuolation of the white matter was reported in conjunction with positive detection of pneumonia virus of mice (family paramyxoviridae) in an African hedgehog suspected of WHS, but the relationship between the disease findings and links to causality require further investigation.[6]

Demyelinating conditions of animals and humans may be acquired or inherited/genetic. These diseases result from abnormalities affecting myelin sheaths or myelin forming cells. Axonal or neuronal degeneration is a secondary occurrence. Causes of acquired demyelination include: infectious agents (e.g., canine distemper virus and small ruminant lentiviruses), immune-mediated inflammation (e.g., multiple sclerosis in humans), metabolic derangements (e.g., central pontine myelinosis associated with rapid correction of hyponatremia in various species, and hepatic encephalopathy in various species), and toxic exposures (e.g., hexachlorophene, stypandrol, and others in various species).[2,4-6] In some cases, hypoxia/ischemia and compressive lesions may also predominantly affect oligodendrocytes and myelin sheaths.[5] Hereditary demyelinating conditions include identified genetic defects in humans (e.g., Canavan's disease leukodystrophy due to mutation causing deficiency of aspartoacylase enzyme) and animals (e.g., canine spongiform leukoencephalomyelopathy in Shetland sheepdogs and Australian cattle dogs associated with cytochrome b mitochondrial DNA mutation; and maple syrup urine disease in Hereford, polled Hereford, and polled Shorthorn calves, linked to autosomal recessive mutation causing deficiency in branched-chain alpha-ketoacid decarboxylase complex). Additionally, multiple other presumed heredofamilial conditions causing myelin vacuolation in animals are reported for which specific genetic links are yet to be confirmed (e.g., in horned and polled Hereford calves, Samoyed and Border Terrier puppies, Egyptian Mau and ragdoll cats, and Silver Foxes).[2,4]

Other reported causes of progressive neurologic signs in hedgehogs include brain tumors (e.g., astrocytoma, microglioma, mixed glioma), intervertebral disk disease, and systemic diseases such as hepatic encephalopathy.[1,4,8] None of these conditions was apparent in this case.

JPC Diagnosis: There were two different sections submitted:

1. Brainstem, white matter: Myelin degeneration, bilaterally symmetrical, severe with neuronal degeneration and gliosis, African pygmy hedgehog (*Atelerix albiventris*), hedgehog.
2. Cerebrum, diencephalon, corona radiata: Myelin degeneration, bilaterally symmetrical, moderate.

Conference Comment: Hedgehogs and gymnures belong to the order *Insectivora* and make up the *Erinaceidae* family. There is very little reported infectious diseases in the African (*Atelerix albiventris*) or European (*Erinaceius europaeus*) hedgehog. Of note, enteritis caused by *Salmonella* sp., pneumonia caused by *Corynebacterium* sp., and upper respiratory disease caused by *Pasteurella* sp. and *Bordetella bronchiseptica* are the most frequent offenders. Additionally, insectivores are potential reservoirs for bloodborne pathogens that are transmitted by parasite vectors such as: *Rickettsia* spp., *Borrelia burgdorferi*, *Babesia microti*, and *Anaplasma phagocytophilum*. Fungal diseases reported include: adiaspiromycosis, cryptococcosis, paecilomycosis, histoplasmosis, and dermatophytosis. Viral diseases are extremely rare, but there have been reported cases of infection with herpes simplex virus 1 in African and European hedgehogs.[3]

Neoplasia is the most common of the noninfectious diseases in hedgehogs with malignant mammary adenocarcinoma, lymphoma, and oral squamous cell carcinoma being most frequent. In African hedgehogs specifically males over one-year-old there is a high incidence of cardiomyopathy which is usually diagnosed late in the disease process at which time it is often fatal.[3]

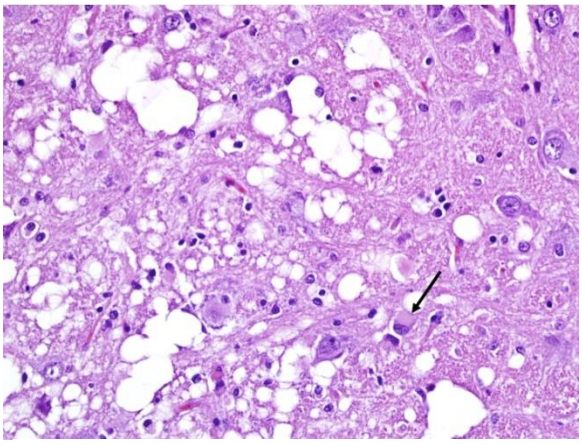

Brainstem, pygmy hedgehog. Within vacuolated areas, there are rare gemistocytes. (Photo courtesy of: Wildlife Conservation Society , www.wcs.org) (HE, 400X)

Clinical neurologic signs in hedgehogs (incoordination, inability to roll into a ball, seizures, paralysis) are often diagnosed (even in clinical settings) as "wobbly hedgehog syndrome" which is a progressive and potentially hereditary disease that results in myelin degeneration in the central nervous system. An important differential diagnosis is intervertebral disk disease which is much less common but has been reported in hedgehogs.[3]

Within examined sections of cerebral cortex, there are multifocal areas within the superficial cortex and pyriform lob which contain numerous bright red, shrunken neurons which were interpreted by the JPC staff and moderator as acutely necrotic; a minimal glial reaction was present. This change is most consistent with ischemic neuronal necrosis; the necrotic neurons do not appear to be associated with areas of white matter degeneration and may represent a second concurrent disease process.

Contributing Institution:
Wildlife Conservation Society
www.wcs.org

References:

1. Benneter SS, Summers BA, Schulz-Schaeffer WJ, et al. Mixed glioma (oligoastrocytoma) in the brain of an African hedgehog (*Atelerix albiventris*). *J Comp Pathol*. 2014;151:420-424.
2. Cantile C, Youssef S. Nervous system. In: Maxie MG, ed. *Jubb, Kennedy, and Palmer's Pathology of Domestic Animals*. Vol. 1. 6th ed. St. Louis, MO: Elsevier; 2016:250-406.
3. D'Agostino J. Insectivores (insectivora, macroscelidea, scandentia). In: Miller RE, Fowler ME, eds. *Fowler's Zoo and Wild Animal Medicine.* Vol. 8. St. Louis, MO: Elsevier; 2015:275-281.
4. Graesser D, Spraker TR, Dressen P, et al. Wobbly hedgehog syndrome in African pygmy hedgehogs (*Atelerix* spp.). *J Exotic Pet Med*. 2006;15(1):59-65.
5. Love S. Demyelinating diseases. *J Clin Pathol*. 2006;59:1151-1159.
6. Madarame H, Ogihara K, Kimura M, et al. Detection of pneumonia virus of mice (PVM) in an African hedgehog (*Atelerix arbiventris*) with suspected wobbly hedgehog syndrome. *Vet Microbiol*. 2014;173:136-140.
7. Palmer AC, Blakemore WF, Franklin RJM, et al. Paralysis in hedgehogs (*Erinaceus europaeus*) associated with demyelination. *Vet Rec.* 1998;143:550-552.
8. Raymond JT, Aguilar R, Dunker F, et al. Intervertebral disc disease in African hedgehogs (*Atelerix albiventris*): four cases. *J Exotic Pet Med*. 2009;18(3):220-223.

CASE III: C973 (JPC 4020995).

Signalment: 9 year-old male neutered greyhound, *Canis familiaris*, canine.

History: The animal presented with a 2-month history of progressive generalized ataxia and hypermetria in all 4 limbs. Multifocal left forebrain, cerebellar and brainstem signs were observed. Magnetic resonance imaging revealed multifocal white and grey matter lesions, notably worse on the left parietal lobe. Cerebrospinal fluid analysis revealed no significant abnormalities. Serology was positive for *Toxoplasma gondii* at 1:200 and *Neospora caninum* at 1:800. Treatment with steroids and clindamycin was initiated; however the dog deteriorated and was subsequently euthanized. Brain tissue was polymerase chain reaction (PCR) positive for *Neospora caninum*.

Gross Pathology: The brain was submitted for post mortem examination. The cerebral hemispheres appeared slightly asymmetrical. Prosection revealed expansion of the left frontal dorsal white matter. In multiple sections, the dorsal and lateral cerebral cortices were focally thinned and discoloured with a tan to brown appearance.

Laboratory results:
Serology was positive for *Toxoplasma gondii* at 1:200 and *Neospora caninum* at 1:800. Treatment with steroids and clindamycin was initiated; however the dog deteriorated and was subsequently euthanized. Brain tissue was polymerase chain reaction (PCR) positive for *Neospora caninum*.

Cerebrum, dog. Serial sections of the fixed cerebrum demonstrate irregularly but markedly thinned and darkened superficial gray matter in the dorsal and lateral cortex. (Photo courtesy of: The Royal Veterinary College, Hatfield, England)

Microscopic Description: Multiple brain sections revealed a widespread, bilateral necrotizing inflammatory lesion affecting mainly the dorsal and dorsolateral cerebral cortices, characterised by multifocal extensive cerebrocortical necrosis. The necrotic grey matter was replaced by fibrillary gliosis or cavitated and contained many gitter cells, with some slides exhibiting more destructive lesions than others. Multifocal moderate to marked lymphocytic and lesser plasmacytic aggregates were seen within the lepto-meninges and the necrotic cortices, forming variably sized perivascular cuffs. Multiple reactive (proliferating) vessels were observed. The corona radiata in areas appeared degenerate or necrotic with many areas of myelin vacuolation.

Found within and adjacent to the areas of cerebrocortical necrosis and more widely in the brain were abundant round to oval protozoal cysts measuring up to 90 um in diameter with a 2-4 um thick eosinophilic cyst wall enclosing numerous 2-3 um basophilic bradyzoites.

<u>Additional sections</u>

Minimal to milder inflammation and gliosis was observed surrounding the lateral, third and fourth ventricles and deeper tissue and within the mesencephalon. Severe bilateral degeneration characterised by myelin vacuolation, few intramyelinic macro-phages, and gliosis was noted in the crus cerebri and pyramids. A small area of the cerebellar vermis exhibited vacuolation and some disruption of the cortex with mild loss of Purkinje neurons.

Immunohistochemistry: cysts within sections of the cerebrum were positive in stains for *N. caninum*.

Contributor's Morphologic Diagnosis:
Brain, cerebral cortex: Meningoencephalitis, necrotizing, chronic-active, multifocally extensive, severe, with protozoal cysts.

Contributor's Comment: *Neospora caninum* is a cyst-forming coccidian parasite in the phylum Apicomplexa, family Sarcocystiidae and like other coccidians, is an obligate intracellular parasite[12,13].

Cerebrum, dog. The superficial grey matter is thin and demonstrates segmental pallor (arrows). 3-3.

Molecular analysis shows that *N. caninum* is closely related to *Toxoplasma gondii*[12]. Both coccidian parasites have proliferative (tachyzoite) and tissue cyst (bradyzoite) phases with tachyzoites proliferating by endodyogeny. Some differences in morphology and life cycle exist; *N. caninum* has a thicker cyst wall and does not develop within a host cell parasitophorous vacuole as does *Toxoplasma gondii*. Differentiation by light microscopy alone is unreliable. Electron microscopy, immunohisto-chemistry and molecular techniques are required for definitive diagnosis[15]. Co-infection with *T. gondii* can theoretically occur and it should be considered as a differential diagnosis[8].

Naturally occurring neosporosis has been reported in a variety of animals including dogs, cats, cattle, sheep, goats, deer, water buffalo, antelope, a rhinoceros and horses (*Neospora hughesi*). In general, neosporosis is primarily a disease of cattle and dogs where the parasite causes abortion and CNS/PNS/muscle disease respectively[5,6,7,15]. The domestic dog is the definitive host for the parasite; however, experimental studies have shown that the Australian dingo and the coyote are also definitive hosts[8,15]. The mechanism of natural infection in dogs is incompletely understood, however ingestion of neural and muscle tissue containing cysts is considered the most likely source of infection[8]. In cattle, *N. caninum* is very efficiently transmitted transplacentally (vertically) but consumption of bovine foetal membranes can also act as a source of infection in dogs[7]. Transplacental transmission in the terminal stages of gestation and post-natal transmission via milk occurs in dogs. Infected dogs produce environmentally resistant oocysts which play an important role in the epidemiology of neosporosis[14]. To date, viable fecal oocysts have been demonstrated only in naturally infected dogs and the gray wolf[8]. The ingestion of sporulated *N.caninum* oocysts from the environment is the natural method of infection in juvenile and adult cattle which are the main intermediate hosts[14].

The *Neospora* lifecycle involves three infectious stages: (1) Oocysts produced in the feces of dogs following ingestion of bradyzoites; (2) The tachyzoite, a rapid multiplying stage which initiates lesion development by multiplying in and rupturing cells; (3) with onset of host immune defense, tachyzoites differentiate into bradyzoites to form tissue cysts mainly in the central nervous system (CNS) and muscle of dogs and in the intermediate host[2].

N. caninum tachyzoites can invade a variety of cell types in many organs including those of the monocyte-macrophage system. The most likely method of spread to the CNS occurs through infected leukocytes crossing the blood-brain barrier. Findings typical of pathogens with endothelial tropism such as vascular swelling and injury, tissue ischemia

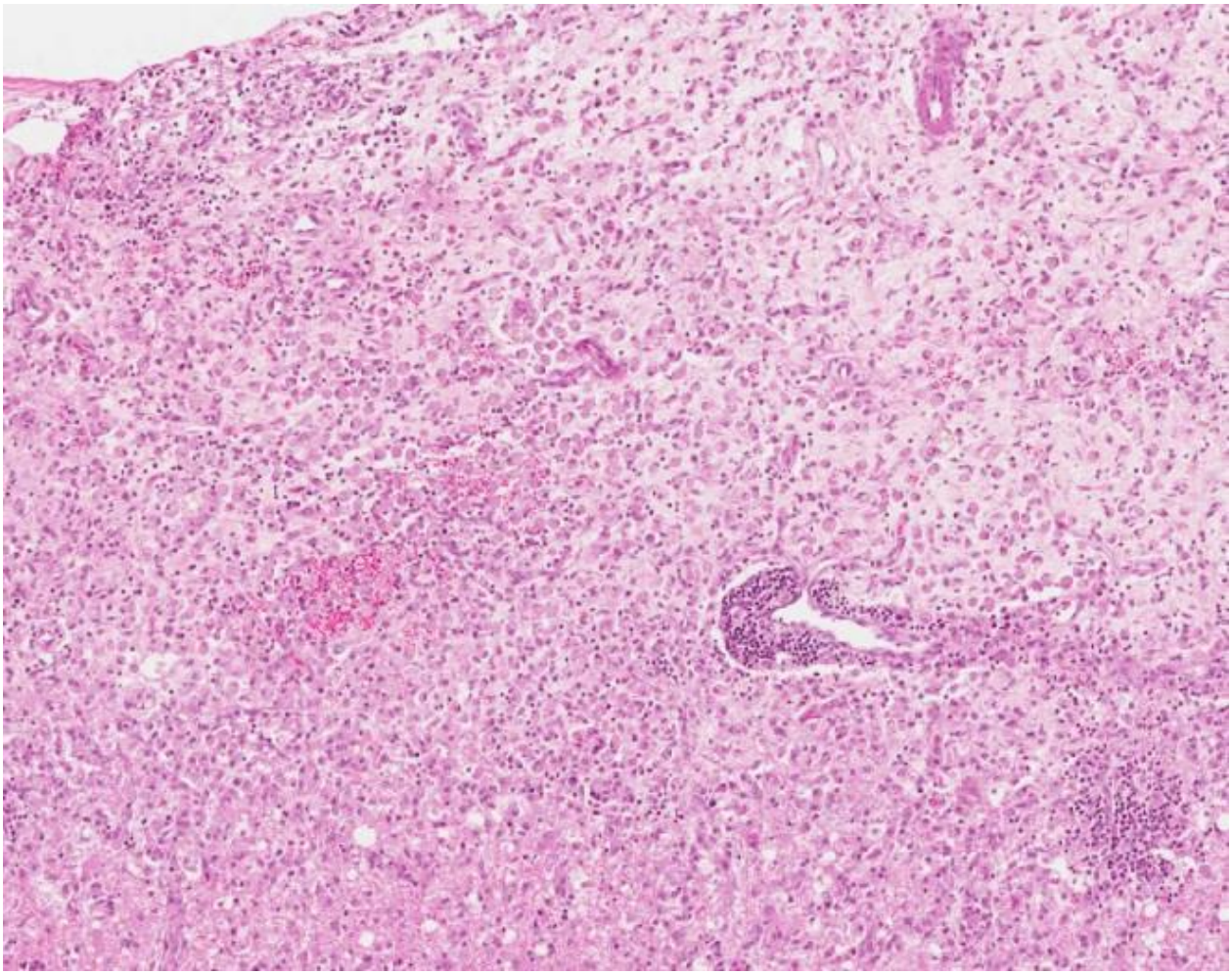

Cerebrum, dog. The superficial gray matter is markedly hypercellular, with infiltration of numerous Gitter cells, multifocal hemorrhage, and numerous lymphocytes and plasma cells within Virchow-Robins space. (HE, 69X)

and multifocal infarction are often observed in CNS lesions caused by *N. caninum*[14,15].

Clinical disease can affect dogs of all ages, however the most severe cases of *N. caninum* typically occur in congenitally infected puppies over 3 weeks of age[8], involve several animals in a litter and present as a progressive ascending neuromuscular paralysis caused by encephalomyelitis, polymyositis and especially polyradiculitis[1]. Neurological signs are dependent on the site that is parasitized and may include such features as; rigidity following muscle denervation and contracture leading to rigid hyperextension of the pelvic limbs, cervical weakness, and dysphagia[1,5]. Pelvic limb contracture is one of the most consistently reported signs in pups[8]. Widespread involvement of the CNS and other organs occurs in adult dogs with signs of disseminated disease including pneumonia, polymyositis, myocarditis, dermatitis, and hepatitis[1,5,15].

Gross CNS lesions can be present throughout the white and/or gray matter with the periventricular white matter being affected in some cases. Peracute lesions

consist of foci of hemorrhage and necrosis adjacent to blood vessels. Chronic lesions have a granular yellow-brown to grey appearance. Early microscopic lesions include tachyzoite infection of and proliferation within endothelial cells, leading to ischemia and necrosis of surrounding neuropil[15]. Later lesions are characterized by nonsuppurative encephalomyelitis and the presence of tachyzoites and tissue cysts in neurons and neuropil with the amount of necrosis, gliosis, neovascularization and white matter injury dependent on the duration of the lesion[1]. More chronic lesions contain prominent lymphocytic and histiocytic perivascular and leptomeningeal aggregates. Over time, due to host immune defense mechanisms tachyzoites change to bradyzoites that replicate more slowly and form tissue cysts[15].

Diagnosis of neosporosis involves histological detection of lesions, immuno-histochemistry illustrating tachyzoite and bradyzoite phases, PCR detection of parasite DNA and serology[8].

Treatment with corticosteroids is con-traindicated in cases of neosporosis[11] as immunosuppressed dogs may shed more oocysts than immunocompetent dogs[7]. In this greyhound, the numerous cysts within the CNS were presumably a consequence of corticosteroid treatment. In studies, dogs that had been given corticosteroids shed more than 100,000 oocysts after being fed with infected murine brains. Various pathological manifestations of neosporosis have been reported in dogs on immuno-suppressive therapy, including cerebellar inflammation and atrophy (which can occur in the absence of steroid treatment), the presence of tachyzoites in cerebrospinal fluid and protozoal hepatitis[9,10,11]. Treatment with currently available drugs including clindamycin is considered only partially effective. None of the currently available drugs are considered capable of killing tissue cysts[8].

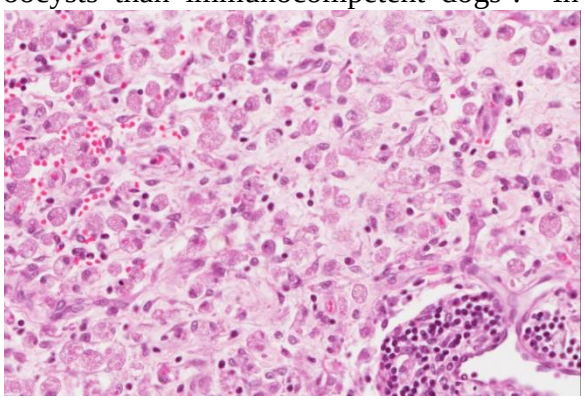

Cerebrum, dog. Higher magnification of the gray matter, showing the large number of Gitter cells within an edematous neuropil with numerous proliferating capillaries lined by hypertrophic endothelium. (HE, 69X)

The predominant cerebrocortical distribution is an unusual neuroanatomic pattern for this infection. We believe that the white matter degeneration within the crus cerebri is secondary following the cerebral cortical necrosis while focal Purkinje cell loss in the midvermis is probably due to brain herniation. While the neocortical inflammation and necrosis in this case is due in large part to the parasites, prolonged seizures may also have contributed to this pattern of necrosis.

JPC Diagnosis: Cerebrum: Meningo-encephalitis, necrotizing, segmental, severe with numerous intracellular and extracellular apicomplexan cysts, Greyhound (*Canis familiaris*), canine.

Conference Comment: The protozoal organisms in the phylum Apicomplexa that result in encephalomyelitis are *Toxoplasma*, *Hammonidia*, *Sarcocystis*, and *Neospora*. Of the four, *Neospora* is the most recent addition. First identified in 1988 by Drs. Dubey, Carpenter, and Speer[4,6] canine

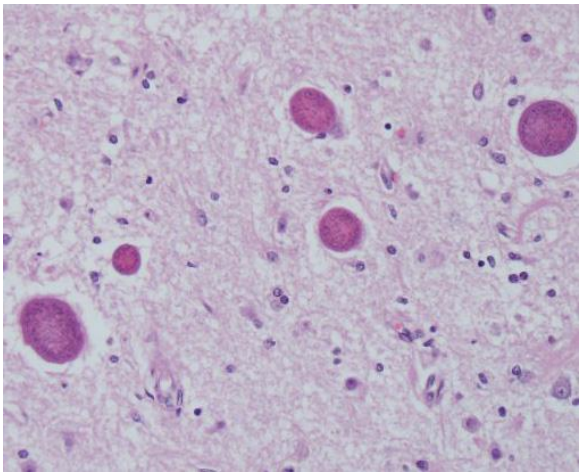

Cerebrum, dog. There are numerous apicomplexan cysts scattered throughout the gray and white matter consistent with Neosporum caninum. (HE, 400X)

protozoan encephalomyelitis was originally thought to be caused by *Toxoplasma.*

Toxoplasma gondii which is still an important differential diagnosis (as mentioned above) uses domestic cats and other Felidae as its definitive host, whereas all other warm-blooded animals can act as intermediate host. Interestingly, cats can also act as intermediate hosts where the parasite continues in an extraintestinal cycle. Infection can occur in one of three ways: (1) ingestion of meat containing tissue cysts, (2) ingestion of food contaminated with cat feces which contain sporulated oocysts, and (3) infection in utero. Transplacental infection is most common in sheep, among domestic animals, where infection begins as a primary placentitis affecting predominately the cotyledons with progressive seeding of the organism to the fetus. Late abortions are common with tissue cysts present in the fetal brain and myocardium. Areas of mineralization may accompany cysts in the brain most likely due to hypoxia from placental insufficiency during pregnancy. Following ingestion of oocysts or tissue cysts by intermediate hosts, the organism forms tissue cysts within the CNS, skeletal and heart muscles most commonly. These cysts may survive for the life of the host and can either: (1) become latent and cause no clinical signs or (2) result in acute, necrotizing disseminated infections affecting CNS, lung, myocardium, liver, pancreas, skeletal muscle, and lymph nodes. The organ affected depends mostly on the host. For instance, in cats severe interstitial pneumonia is common, and in adult dogs, concurrent polymyositis and encephalomyelitis is the most common scenario. In puppies and young dogs, however, polyradiculoneuritis is the most common pattern. In the case of latent infections, tissue cysts may show up as incidental findings on necropsy or, if the animal is immune suppressed, may convert to an active infection. There is an association in dogs with *Morbillivirus* infection and toxoplasmosis, presumably because of the immunosuppressive action of the virus.[13]

Neospora caninum was identified by Dubey and his colleagues in a retrospective study of 23 cases of canine "toxoplasmosis" in which this new organism was distinguishable from *Toxoplasma* only by electron microscopy and immunohistochemistry[4,6]. Ultrastructurally, *Neospora* tachyzoites lack

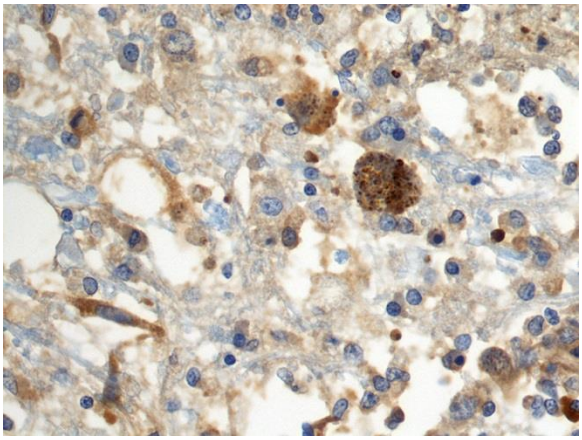

Cerebrum, dog. Cysts are immunopositive for N. caninum . (anti-N. caninum, 400X)Photo courtesy of: The Royal Veterinary College, Hatfield, England) (HE, 400X)

micropores, but have numerous micronemes and more rhoptries than *Toxoplasma gondii*. Additionally, *Toxoplasma* replicates exclusively in parasitophorous vacuoles, whereas, *Neospora* can use a parasitophorous vacuole or replicate free within the cell cytoplasm[3].

Contributing Institution:
The Royal Veterinary College
Hatfield, England

References:

1. Brown CC, Baker DC, Barker IK. Alimentary system. In: Maxie MG, ed. *Jubb, Kennedy, and Palmer's Pathology of Domestic Animals.* 5th ed. Vol. 2. St. Louis, MO: Elsevier; 2007:272.
2. Buxton D, McAllister MM, Dubey JP. The comparative pathogenesis of neosporosis. *Trends in Parasitology*. 2002;18:546-552.
3. Cheville NF. Pathogenic protozoa. In: *Ultrastructural Pathology The Comparative Cellular Basis of Disease.* 2nd ed. Ames, IA: John Wiley & Sons; 2009:555.
4. Dubey JP. A review of *Neospora caninum* and *Neospora*-like infections in animals. *J Protozool Res.* 1992;2:40-52.
5. Dubey JP. Review of *Neospora caninum* and neosporosis in animals. *Korean J Parasitol*. 2003;41:1-16.
6. Dubey JP, Carpenter JL, Speer CA, et al. Newly recognized fatal protozoan disease of dogs. *J Am Vet Med Assoc.* 1988;192:1269-1285.
7. Dubey JP, Schares G, Ortega-Mora LM. Epidemiology and control of neosporosis and *Neospora caninum. Clin. Microbiol*. 2007;20:323-367.
8. Dubey JP, Schares G. Neosporosis in animals--the last 5 years. *Vet Parasitol.* 2011;180:90-108.
9. Fry DR, McSporran KD, Harvey C. Protozoal hepatitis associated with immunosuppressive therapy in a dog. *J Vet Intern Med.* 2009;23**:**366-368.
10. Galgut BI, Janardhan KS, Grondin TM, Harkin KR, Wight-Carter MT. Detection of *Neospora caninum* tachyzoites in cerebrospinal fluid of a dog following prednisone and cyclosporine therapy. *Vet Clin Pathol.* 2010;39:386-390.
11. Garosi L, Dawson A, Couturier J, Matiasek L, et al. Necrotizing cerebellitis and cerebellar atrophy caused by *Neospora caninum* infection: magnetic resonance imaging and clinicopathologic findings in seven dogs. *J Vet Intern Med.* 2010;24:571-578.
12. Howe DK, Sibley LD. Comparison of the major antigens of *Neospora caninum* and *Toxoplasma gondii*. *International Journal for Parasitology*. 1999;29:1489-1496.
13. Summers BA, Cummings JF, de Lahunta A. Inflammatory diseases of the central nervous system. In: Duncan L, McCandless PJ, eds. *Veterinary Neuropathology*. St. Louis, MO: Mosby; 1995:162-169.
14. Taylor MA, Coop RL, Wall RL. Parasites of cattle. In: Taylor MA, ed. *Veterinary Parasitology*. 3rd ed. West Sussex, UK: Wiley-Blackwell; 2007:121.
15. Zachary JF. Nervous system. In: McGavin MD, Zachary JF, eds. *Pathologic Basis of Veterinary Diseases.* 5th ed. St. Louis, MO: Elsevier; 2007:809.

CASE IV: O291/16 (JPC 4101762).

Signalment: 8 month-old, female, intact, Pug, *Canis familiaris*, canine.

History: The dog had two generalized seizures within a week. On clinical

Cerebrum, dog. There is segmental primarily perivascular hypercellularity of the deep superficial cortex (arrows) at the junction of gray and white matter. (HE, 6X).

examination, the dog presented with abnormal posture and right-sided circling. The dog also had generalized muscle twitching, most notably in the face. Menace response was absent. The dog was subsequently admitted to the animal hospital for intensive care treatment with phenobarbital, glucocorticosteroids and clindamycin, after which it became semi-comatose. As symptoms did not subside, the dog was humanely euthanized.

Gross Pathology: The dog was brought directly to necropsy. No gross findings were evident.

Laboratory results:
Hematology, biochemistry, electrolytes and C-reactive protein (CRP) were within normal reference ranges. Toxoplasma serology was negative.

Microscopic Description: Brain, parietal cortex: In the grey-white matter interface, with predominance in the cortical grey matter and sparing of deep cortical white matter, there are multifocal to diffuse inflammatory lesions, distributed within the neuropil and centered around perivascular spaces (perivascular cuffs). The neuronal parenchyma exhibits moderate to severe vacuolation (rarefaction) with scattered glial cells and vessels outlined by hypertrophic endothelium. Perivascular inflammatory infiltrates are composed primarily of lymphocytes, plasma cells, macrophages and occasional binucleated cells. These cells can also be seen in the leptomeninges and around meningeal vessels.

Multifocally, phagocytic cells engulfing neuronal debris (neuronophagia) are evident (not in all slides), as well as neurons exhibiting pyknotic nuclei, with shrunken cellular outline and hypereosinophilic cytoplasm (neuronal necrosis). Glial nodules and diffuse gliosis can be seen throughout the aforementioned areas, as well as neuronal loss and satellitosis. Clefting of perivascular spaces from surrounding parenchyma is also observed (perivascular edema).

Contributor's Morphologic Diagnosis:
Brain: Polioencephalitis and meningitis, non-purulent and necrotizing, multifocal to coalescing, severe.

Name the Condition: Necrotizing meningoencephalitis

Contributor's Comment: Necrotizing meningoencephalitis (NME), formerly known as "pug dog encephalitis", is an idiopathic disorder primarily affecting small breed dogs such as Pugs, and less commonly Pekingese,[3] Chihuahua,[8] Maltese,[3] Shih Tzu and other small breed species[4]. Dogs present

with neurological signs at ages ranging between 6 months to 7 years, with a mean age of onset at 29 months.[18] Affected Pug dogs often present at a median age of 18 months, and the disease is most often seen in young females.[9] Occasional reports of NME in large breed dogs exist, but is a rare occurrence.[5] Affected dogs usually present with sudden onset of prosencephalic clinical signs including seizures and depression, often with fatal outcome.[18]

A commonly discussed differential diagnosis of NME is granulomatous meningoencephalomyelitis (GME). GME also affects small breed dogs, such as terriers and toy breeds, but may occur in larger breeds as well, with an age range of 6 months to 12 years.[3]

The anatomical distribution of lesions in NME and GME varies. NME usually affects the cortical grey matter, with relative sparing of deeper periventricular tissues. The lesions are often confluent over large areas, and may be evident grossly (but not always). Multifocal swelling and yellow foci of malacia can be observed bilaterally, but asymmetrically, in the cerebral hemispheres. GME usually produces milder gross changes, but granulomatous foci are occasionally seen.[17] Another variant of idiopathic necrotizing meningoencephalitis is necrotizing leukoencephalitis (NLE). NLE is a condition primarily affecting Yorkshire terriers, Boston terriers and Chihuahuas.[3] As for NLE, malacic foci are observed but, in contrast to NME, are centered in the white matter of the cerebral hemispheres.

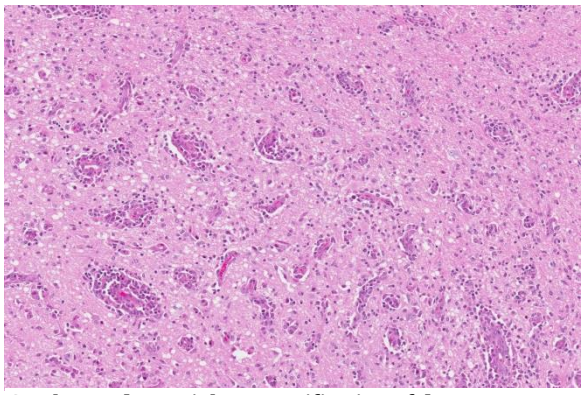

Cerebrum, dog. Higher magnification of deep gray matter with cuffing of small vessels by 2-4 layers of histiocytes, lymphocytes, and fewer neutrophils. Inflammatory cells migrate in low numbers into the adjacent vacuolated neuropil. (HE, 144X).

Histologically, NME primarily affects the cortical grey matter. Areas of rarefaction, vacuolation and neuronal necrosis are significant features of the disease, accompanied by non-purulent inflammatory infiltrates of lymphocytes, plasma cells and macrophages, arranged diffusely and as perivascular cuffs.[3] In contrast, histologic changes in GME are multifocal and patchy, with lesions centered in the basal parts of the brain, particularly the white matter of the brain stem and spinal cord.[18] GME often produces a more cellular infiltrate consisting of numerous macrophages and giant cells, with or without mitotic activity.[3] These infiltrates may be arranged in a granulomatous fashion with formation of epithelioid cells.[17] However, large malacic foci are rarely seen in GME, and for this reason, GME may be hard to distinguish from brain malignant histiocytosis.[3]

Histopathological evaluation is required to distinguish between all subsets of idiopathic meningoencephalitis.[18]

A definitive etiology has not been identified for either NME or GME. For NME and GME, immune-mediated reactions against brain tissue have been suggested, including anti-astrocyte antibodies in NME and GME,[10] and anti-GFAP antibodies specifically in NME patients.[11] GFAP has been found to be one of the more commonly targeted auto-antigens in Pug dogs.[16] According to immunohistochemical studies, a predominance of CD3- positive T-cells has been detected in GME.[12] CD163-positive

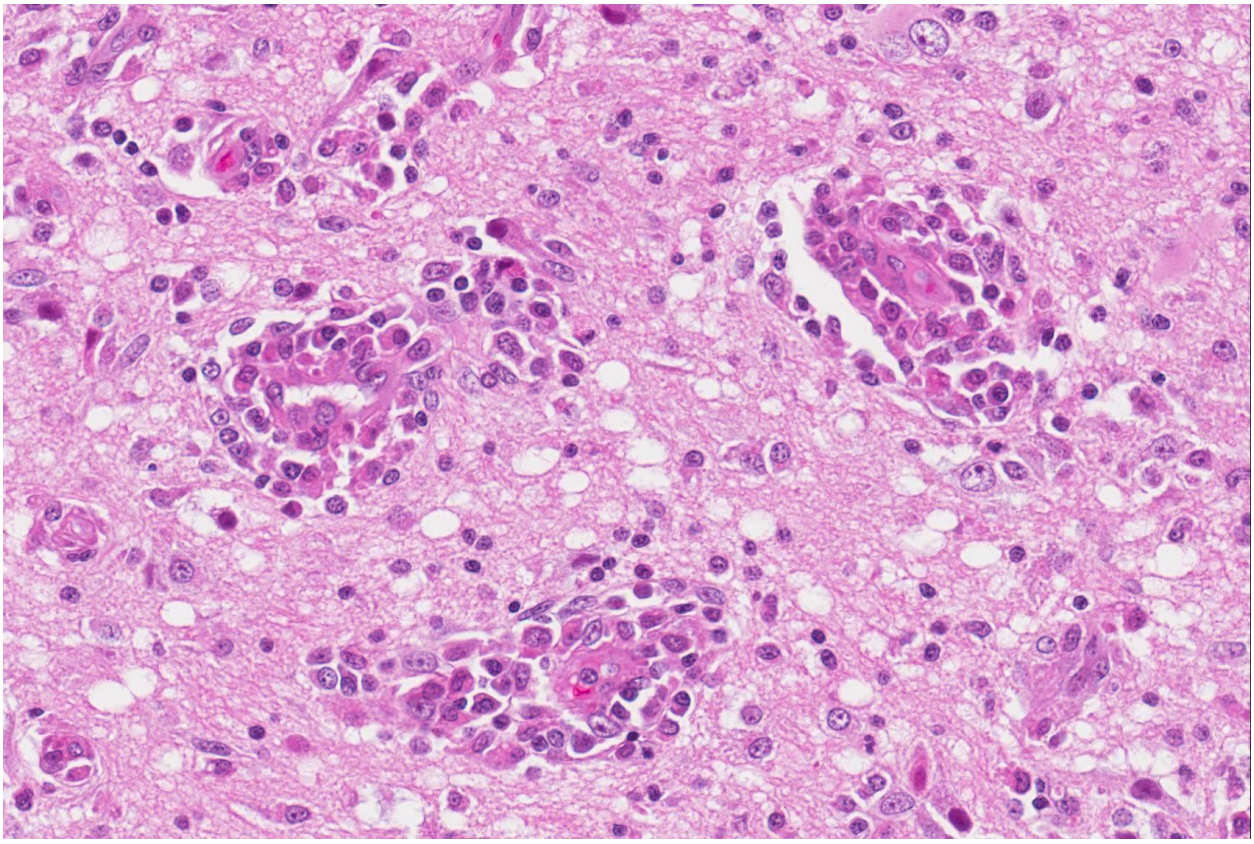

Cerebrum, dog. Still higher magnification of deep gray matter. Inflammatory cells around vessels are of normal morphology. There is vacuolation of the intervening neuropil, likely the result of edema and a mild gliosis with occasional hypertrophic astrocytes (arrow) (HE, 400X).

cells (macrophages) can be detected in both NME and GME,[12] but lysozyme immuno-reactive cells are more abundant in NME than GME.[17] However, the distribution of the macrophage cell population varies from diffuse in NME to granulomatous and perivascular in GME.[12] On protein level, a marked increase of IFN-γ and IL-17 has been observed in NME and GME, respectively.[13]

The inheritance pattern of NME has been investigated. Two loci have been identified in NME-affected dogs, one of these being associated with dog leukocyte antigen class II.[2, 7] Common genetic backgrounds have been proposed in dogs with NME regardless of breed. However, the implication of these traits may differ between dog breeds.[15] In Pug dogs specifically, a strong familial inheritance pattern has been demonstrated.[6]

Infectious etiologies for these encephalitides have also been discussed. According to one study, *Mycoplasma canis* has been identified in some cases of NME and GME (4/25 and 1/25 respectively).[1] However, the role of *Mycoplasma* in the pathogenesis of these diseases remains uncertain. Regarding viral causes, alpha-herpesviruses are proposed as possible agents.[3] However, no association between NME and viral pathogens such as herpes-, adeno- or parvoviruses has been found in many studies, including one pertaining to approximately 5000 studied individuals.[1,6,14]

JPC Diagnosis: Cerebrum: Meningo-encephalitis, lymphohistiocytic, multifocal

to coalescing, moderate with edema, neuronal loss, and astrocyte hypertrophy, Pug (*Canis familiaris*), canine.

Conference Comment: Necrotizing meningoencephalitis (NME, fully described above) results in malacia of the cerebral cortex and mononuclear cell infiltration in the meninges and perivascular spaces that is bilateral but asymmetrical and mostly affecting the gray matter. The main differential, granulomatous meningoencephalitis (GME), is characterized by histiocytic inflammation predominately within the cerebral white matter that can form granulomas with chronicity.[3]

Both NME and GME have currently unidentified causes and are active areas of research. Many recent works are detailed above, and a recent study in pug dogs reviewed individuals that had undergone extrahepatic portosystemic shunt attenuation surgery to identify if there were increased postoperative neurologic complications, including NME. Only four dogs were necropsied, none of which had evidence of NME.[20]

In this case, attendees were not certain that this represented a case of NME as no definitive areas of necrosis were present in the submitted slide. Given the lack of demonstrable parenchymal necrosis and the extent of concurrent white matter lesions, conference participants discussed the possibility that this may actually case represent a case of GME. Another topic of discussion not mentioned by the contributor is the presence of numerous clustered hypertrophic astrocytes clustered which demonstrated large vesicular nuclei and abundant pink cytoplasm. Participants discussed whether the term "Alzheimer type 2 astrocytes" was appropriate in this case, a term has been traditionally reserved for reactive astrocytes in hepatic encephalopathies which are induced by accumulation of ammonia and other endogenous toxins, or cases involving cerebral amyloid.[3] Preferring to be conservative in such matters which are known to enflame true neuropathologists, the "hypertrophic astrocytes" was settled upon in this case.

Contributing Institution:
Swedish University of Agricultural Sciences
Department of Biomedical Sciences and Veterinary Public Health, Section of Pathology
BOX 7028
SE 750 07, Uppsala, Sweden
https://www.slu.se/en/departments/biomedical-sciences-veterinary-public-health/

References:

1. Barber RM, Porter BF, Li Q, et al. Broadly reactive polymerase chain reaction for pathogen detection in canine granulomatous meningoencephalomyelitis and necrotizing meningoencephalitis. *J Vet Intern Med.* 2012;26(4):962-968.
2. Barber RM, Schatzberg SJ, Corneveaux JJ, et al. Identification of risk loci for necrotizing meningoencephalitis in Pug dogs. *J Hered*. 2011;102, Suppl 1:S40-46.
3. Cantile C, Youssef S. Nervous system. In: Maxie MG, ed. *Jubb, Kennedy, and Palmer's Pathology of Domestic Animals*. Vol. 1. 6th ed. Philadelphia, PA:Saunders Elsevier; 2016:262, 344, 392-394.
4. Cooper JJ, Schatzberg SJ, Vernau KM, et al. Necrotizing meningoencephalitis in atypical dog breeds: a case series and literature review. *J Vet Intern Med.* 2014;28(1):198-203.
5. Estey CM, Scott SJ, Cerda-Gonzalez S. Necrotizing meningoencephalitis in a

large mixed-breed dog. *J Am Vet Med Assoc.* 2014;245(11):1274-1278.
6. Greer KA, Schatzberg SJ, Porter BF, et al. Heritability and transmission analysis of necrotizing meningoencephalitis in the Pug. *Res Vet Sci.* 2009;86(3):438-442.
7. Greer KA, Wong AK, Liu H, et al. Necrotizing meningoencephalitis of Pug dogs associates with dog leukocyte antigen class II and resembles acute variant forms of multiple sclerosis. *Tissue Antigens.* 2010;76(2):110-118.
8. Higgins RJ, Dickinson PJ, Kube SA, et al. Necrotizing meningoencephalitis in five Chihuahua dogs. *Vet Pathol.* 2008;45(3):336-346.
9. Levine JM, Fosgate GT, Porter B, et al. Epidemiology of necrotizing meningoencephalitis in Pug dogs. *J Vet Intern Med.* 2008;22(4):961-968.
10. Matsuki N, Fujiwara K, Tamahara S, et al. Prevalence of autoantibody in cerebrospinal fluids from dogs with various CNS diseases. *J Vet Med Sci*. 2004;66(3):295-297.
11. Matsuki N, Takahashi M, Yaegashi M, et al. Serial examinations of anti-GFAP autoantibodies in cerebrospinal fluids in canine necrotizing meningoencephalitis. *J Vet Med Sci.* 2009;71(1):99-100.
12. Park ES, Uchida K, Nakayama H, . Comprehensive immunohistochemical studies on canine necrotizing meningoencephalitis (NME), necrotizing leukoencephalitis (NLE), and granulomatous meningoencephalomyelitis (GME). *Vet Pathol.* 2012;49(4):682-692.
13. Park ES, Uchida K, Nakayama H, .Th1-, Th2-, and Th17-related cytokine and chemokine receptor mRNA and protein expression in the brain tissues, T cells, and macrophages of dogs with necrotizing and granulomatous meningoencephalitis. *Vet Pathol.* 2013;50(6):1127-1134.
14. Schatzberg SJ, Haley NJ, Barr SC, et al. Polymerase chain reaction screening for DNA viruses in paraffin-embedded brains from dogs with necrotizing meningoencephalitis, necrotizing leukoencephalitis, and granulomatous meningoencephalitis. *J Vet Intern Med.* 2005;19(4):553-559.
15. Schrauwen I, Barber RM, Schatzberg SJ, et al. Identification of novel genetic risk loci in Maltese dogs with necrotizing meningoencephalitis and evidence of a shared genetic risk across toy dog breeds. *PLoS One.* 2014;9(11):e112755.
16. Shibuya M, Matsuki N, Fujiwara K, et al. Autoantibodies against glial fibrillary acidic protein (GFAP) in cerebrospinal fluids from Pug dogs with necrotizing meningoencephalitis. *J Vet Med Sci.* 2007;69(3):241-245.
17. Suzuki M, Uchida K, Morozumi M, et al. A comparative pathological study on canine necrotizing meningoencephalitis and granulomatous meningoencephalomyelitis. *J Vet Med Sci*. 2003;65(11):1233-1239.
18. Talarico LR, Schatzberg SJ. Idiopathic granulomatous and necrotizing inflammatory disorders of the canine central nervous system: a review and future perspectives. *J Small Anim Pract.* 2010;51(3):138-49.
19. Uchida K, Park E, Tsuboi M, Chambers JK, Nakayama H. Pathological and immunological features of canine necrotizing meningoencephalitis and granulomatous meningoencephalitis. *Vet J.* 2016;213:72-77.
20. Wallace ML, MacPhail CM, Monnet E. Incidence of postoperative neurologic complications in pugs following portosystemic shunt attenuation surgery. *J Am Anim Hosp Assoc.* 2017 Nov

13:Epub ahead of print. doi: 10.5326/JAAHA-MS-6534.

Self-Assessment - WSC 2017-2018 Conference 12

1. True or false? Horses affected with cauda equine syndrome often have cranial nerve deficits.
    a. True
    b. False

2. Which of the following is NOT true about "Wobbly Hedgehog Syndrome"?
    a. It affects approximately 10% of pet African hedgehogs in North America.
    b. The primary lesion is vacuolation of the white matter tracts of the spinal cord.
    c. It is considered an infectious disease with a long latency period similar to prion diseases.
    d. The peripheral nervous system is unaffected.

3. Which of the following statements is true concerning neosporosis?
    a. Cats are the definitive host.
    b. *N. caninum* has a thicker cyst wall and does not develop within a host cell parasitophorous vacuole as does *Toxoplasma gondii*.
    c. Unlike Toxoplasma gondii, it is not transmitted across the placenta.
    d. Treatment with corticosteroids decreases shedding of oocysts and may be used to decrease outbreaks.

4. Neospora was first identified by Dr. JP Dubey in which of these species?
    a. Dogs
    b. Cats
    c. Horses
    d. Cattle

5. Which of the following breeds have not been identified at risk for necrotizing meningoencephalitis (NME)?
    a. Pugs
    b. French bulldogs
    c. Pekingese
    d. Maltese

Please email your completed assessment to Ms. Jessica Gold at Jessica.d.gold2.ctr@mail.mil for grading. Passing score is 80%.This program (RACE program number) is approved by the AAVSB RACE to offer a total of 0.5 CE Credits, with a maximum of 12.5 CE Credits being available to any individual Veterinary Medical Professionals for the 2017-2018 Wednesday Slide Conference. This RACE approval is for the subject matter categories of: SCIENTIFIC using the delivery method of NON-INTERACTIVE DISTANCE. This approval is valid in jurisdictions which recognize AAVSB RACE; however, participants are responsible for ascertaining each board's CE requirements.
RACE does not "accredit", "endorse" or "certify" any program or person, nor does RACE approval validate the content of the program.

Joint Pathology Center
Veterinary Pathology Services

WEDNESDAY SLIDE CONFERENCE 2017-2018

C o n f e r e n c e 13

3 January 2017

Kim Newkirk, DVM, PhD, DACVP
Associate Professor, Anatomic Pathology
Biomedical and Diagnostic Sciences
College of Veterinary Medicine
University of Tennessee
2407 River Dr., Rm A205
Knoxville, TN 37996

CASE I: 14/327 (JPC 4050462).

Signalment: 12 year-old, male, Cairn terrier, *Canis familiaris*, canine.

History: The dog was examined at the veterinary school at Norwegian University of Life Sciences due to eye problems and was diagnosed clinically with ocular melanosis/melanocytic glaucoma bilaterally but more extensive in the right eye. Eye examination revealed right side buphthalmos +2, right side moderately mydriatic irresponsive pupil, left side iatrogenic miosis, IOP 37/23, diffuse endothelial edema; right side +2-3 and left side +1-2, vitreous prolapse right side and posterior lens luxation, and dorsally ectatic and black pigmented sclera was noted. Black pigmentation also involved conjunctiva. Attempts at controlling the intraocular pressure in the right eye was not successful, and the right eye was enucleated. The owners were informed that lesions also in the left eye most likely would progress.

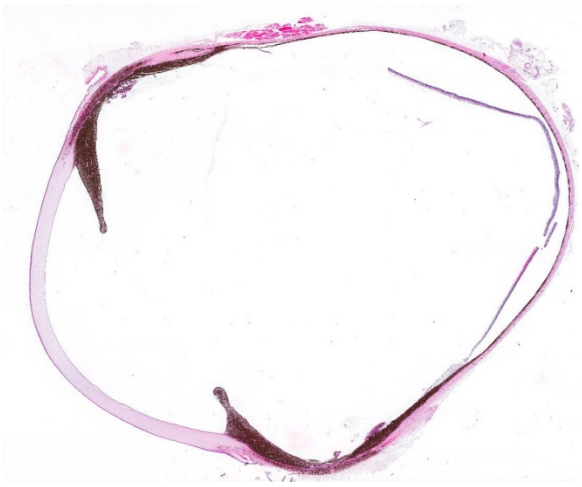

Eye, dog. A cross section of the globe demonstrates thickening of the iris with pigment laden cells that expand the adjacent uvea and infiltrate the sclera. (HE, 5X)

Gross Pathology: An enucleated right eye was received for histopathologic evaluation. The globe measured 2.5 cm in diameter. In

the medial canthus of the eyelids, there was a 3mm exophytic tumor with a black surface. The third eyelid was diffusely black without discernible thickening of the tissue. In the globe there were four slightly bulging areas in the anterior portion of the sclera, each 3-4 mm in diameter, with black discoloration of the surface of the sclera, and trans-scleral black discoloration on the cut surface. Anterior vitreous prolapse was not obvious after sectioning of the eye and the lens was detached (thus not included in the sections). A few small opaque areas were detected in the periphery of the lens.

Laboratory results:
None provided.

Microscopic Description: In the iris, ciliary body and filtration angle there was a diffuse infiltration of large round plump pigmented cells. Close to the filtration angle, the cells also focally infiltrated the cornea, between Descemet's membrane and corneal stroma. At the anterior portion of the sclera, at the level of iris and ciliary body, there was transscleral infiltration of pigmented cells with separation and loss of scleral connective tissue. Pigmented cells also extended into episclera in some areas. The pigmented cells had abundant cytoplasm with numerous dark brown granules that was bleached by potassium permanganate and a central or peripheral round vesicular nucleus with a small nucleolus. The mitotic index was <1 per 10 HPFs, and minimal anisocytosis and anisokaryosis. The retina was detached (artifact). There was degeneration and loss of neurons in the ganglion layer, moderate thinning of the inner granular layer and mild multifocal fusion of inner and outer nuclear layer in the retina. In the anterior and posterior chambers a pale blue material (vitreous) with some free pigmented cells.
In the lens (not submitted) there was multifocal degeneration of stroma on the anterior side and swollen lens fibers (Morgagnian globules) and large eosinophilic swollen cells (bladder cells).
On the rim of the eyelid from medial canthus there was a focal hyperplasia of sebaceous glands with lobules of well differentiated glandular tissue surrounding a centrally located duct (not submitted). In the surrounding dermis in this area and diffusely in the medial conjunctiva, including the third eyelid, there was multifocal to confluent infiltration of pigmented cells as described above.

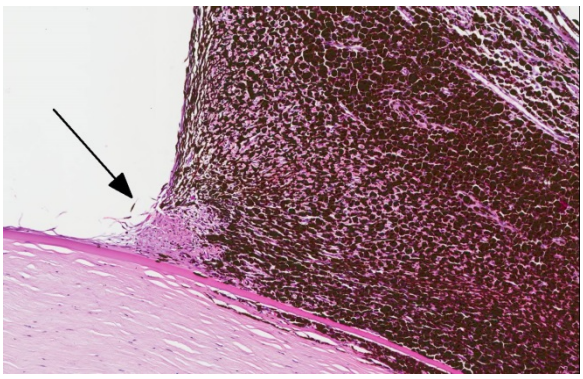

Eye, dog. The iris root is markedly thickened pigment-laden macrophages. The drainage angle (arrow) is closed by few spindle and pigment-laden cells admixed win a collagenous matrix. (HE, 144X)

The globe was re-embedded in a standard size tissue block, and this caused an artificial dorsoventral flattening of the globe.

Contributor's Morphologic Diagnosis:
Eye: Ocular melanosis with secondary glaucoma.

Contributor's Comment: The lesions in this specimen are consistent with the condition called ocular melanosis of Cairn terriers. In a study describing the clinical presentation of 114 Cairn terriers diagnosed with ocular melanosis, the earliest lesions was dark-colored thickening of the iris root followed by scleral/episcleral pigment

plaques, release of pigment into the aqueous and deposition in the drainage apparatus, especially ventrally.[3] In advanced cases, secondary glaucoma develops, and 3 of the 114 dogs developed uveal melanocytic neoplasms.[3]
Ocular melanosis is characterized by diffuse infiltration of plump pigment-laden cells mainly in anterior segments of the eye including the iris, ciliary body, sclera/episclera overlying the filtration angle and the peripheral deep layers of the cornea, but posterior segments may also be involved.[4]

An important differential diagnosis is uveal or limbal melanocytoma in the dog, as the pigmented cells infiltrating ocular tissue in ocular melanosis are histologically similar to such tumor cells. However the growth pattern is reported to be different; in ocular melanosis the pigmented cells infiltrate diffusely in the tissues, as opposed to uveal or limbal melanocytomas in which the tumor cells are expected to result in an expanding mass.[4]

The origins of the pigment-laden cells have been controversial, and the main cell population has been described to be dominated by either melanophages or melanocytes. Van de Sandt et al[6] described the ultrastructural morphology of most of the cells to be consistent with melanophages and some cells appearing to be melanocytes. In this paper, the specific origin of ocular tissue chosen for electron microscopy study was not indicated. In another study[4] where iridal and ciliary body tissue was ultra-structurally investigated, the main cell population was described as melanocytes containing melanosomes in stage III or IV of development, but some cells that probably represented melanophages were also observed. Both Van de Sandt et al[6] and Petersen-Jones et al[4] reported the cells to be negative for the common melanocyte marker Melan A. However, Petersen-Jones et al[4] described most but not all cells to be immunohistochemically positive for HMB45, an antibody that recognizes gp100, which is a melanosome organelle specific marker localized in stage II and III melanosomes. Some cells were also positive for MITF, a melanocytic nuclear transcription factor. Most eyes contained some pigmented cells positive for CD18 suggestion they were macrophages that had engulfed pigment, but in 1 globe which was markedly inflamed, out of 8 globes investigated immunohistochemically, there were abundant CD18 positive pigmented cells.[4]

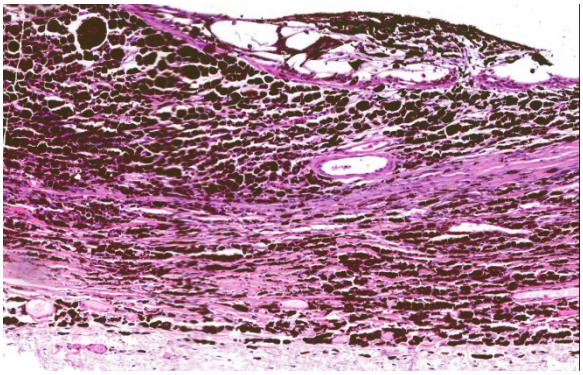

Eye, dog. The choroid at left, sclera (bottom), and peripheral retina (upper right) are all infiltrated and expanded by pigment-laden macrophages. (HE, 120X)

The cause of the disease is unknown. The disease is reported to be inherited with a possible autosomal dominant mode of inheritance.[3] In one study examining 11 potential candidate genes, none of the selected candidate genes were likely to be the gene locus for ocular melanosis in Cairn terriers.[7]

JPC Diagnosis: Globe, anterior uvea, choroid, and sclera: Melanosis with anterior synechae formation and drainage angle occlusion with mild to moderate diffuse retinal atrophy, Cairn terrier, canine.

Conference Comment: Ocular melanosis, also known as pigmentary glaucoma, most commonly occurs in the Cairn terrier breed and results in excessive pigmentation of the uvea which disrupts the contour of the uvea particularly prominent at the iris base, anterior ciliary body and limbal sclera. The pigmented cells have been identified through electron microscopy and immuno-histochemistry to be melanocytes or melanophages (described in more detail above). The thickened limbal scleral and episclera can give the impression of neoplasia; however, melanocytoma (the most likely differential) can be distinguished from melanosis by the presence a regional mass that compresses adjacent tissues. In contrast, melanosis is more diffuse and often bilateral in the Cairn terrier. Ocular melanosis has also been identified in other breeds such as the Boxer and Labrador Retriever, and in these breeds is clinically and morphologically similar, varying only in the distribution. In other breeds, melanosis is usually unilateral and composed pre-dominately of melanophages based on limited electron microscopic studies.[2]

The eyelid and brow may also be involved, in which the condition is known as oculodermal melanocytosis, which correlates with a high risk for melanoma in Caucasian patients.[2] In dogs, there have been occasional reports of melanocytoma or malignant uveal melanoma occurring in eyes simultaneously affected with melanosis. A recent article[1] reports a Golden Retriever with diffuse ocular melanosis and extension into the bulbar conjunctiva and orbital space forming a pigmented, necrotic mass diagnosed as a limbal melanocytoma. Remarkably, there was also a pigmented mass in the third eyelid of the opposite eye that was also diagnosed as a melanocytoma.

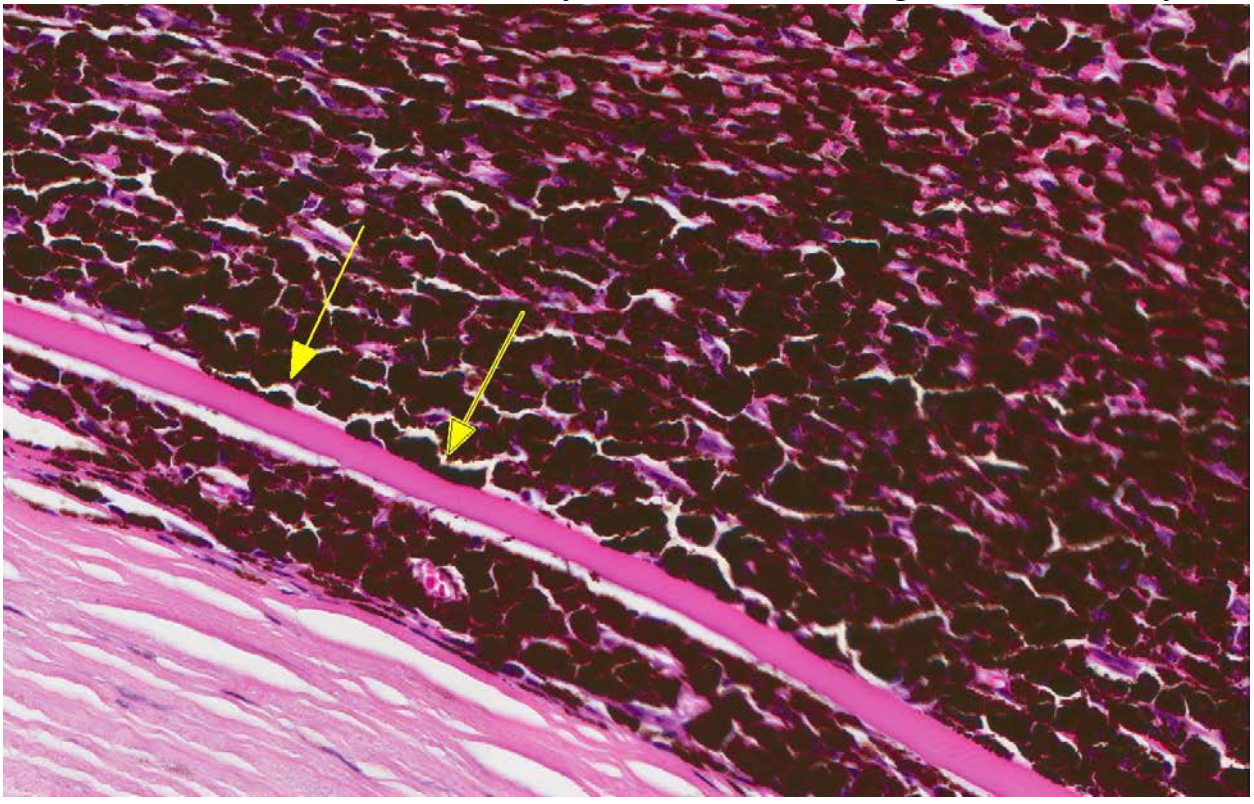

Eye, iris and peripheral cornea. Large pigment-laden macrophages efface iridal architecture and infiltrate the cornea underneath Descemet's membrane (yellow arrows). (HE, 400X)

Cases such as this give weight to the belief of some pathologists that ocular melanosis is merely diffuse melanocytoma.[2]

Ocular melanosis results in a slowly progressive chronic glaucoma associated with compression of and accumulation of pigmented cells within the filtration angle and scleral venous plexus. Free melanin granules are often present and are phagocytized by local macrophages and trabecular endothelial cells within outflow tracts. Secondary glaucoma of this nature is not responsive to medical or surgical treatment because melanophages and melanocytes continue to proliferate and eventually abrogate the treatment by obstructing whatever therapeutic intervention was initiated.[5] In humans, ocular melanosis occurs rarely and results in unilateral heterochromia of the iris and a darkened choroid.

Canine glaucomas are classified based on the following criteria: possible cause (primary, secondary, or congenital), gonioscopic appearance of the filtration angle, and duration or stage of disease. Primary glaucomas are characterized by intra-ocular pressure (IOP) increases without any concurrent disease; these are often hereditary in certain breeds (reported in over 45 breeds, of which the most notable are Beagle, Basset Hound, Welsh springer spaniel and Great Dane) and can occur bilaterally. Primary glaucomas often occur due to pectinate ligament dysplasia or consolidation of ligaments into sheets (mesodermal dysgenesis) or abnormal metabolism of the trabecular cells of the outflow system or pupillary blockage. Secondary glaucomas result from increased IOP associated with concurrent ocular disease, such as uveitis, lens luxations, intumescent cataracts, phacolytic or clastic uveitis, hyphema, intraocular neoplasia or melanosis, which obstruct aqueous outflow pathways. Several breeds are predisposed to lens luxation, most commonly Fox Terrier, Sealyham Terrier, Border Collie, Tibetan Terrier, Cairn Terrier, Welsh Corgi, and Jack Russell Terrier. In Jack Russell Terriers, Miniature Bulldogs, and Lancashire Heelers, a mutation of the ADAMTS17 gene has been associated with lens luxation. Finally, in congenital glaucoma increased IOP is caused by multiple anterior segment anomalies resulting in decreased aqueous humor outflow and develops soon after birth. Congenital glaucoma is exceedingly rare in dogs, whereas, primary (breed-related) and secondary glaucomas are most common.[5]

Conference participants described peripheral anterior synechiae (Descemet's membrane extends into the ciliary body), ectropion uveae due to a thin pre-iridal fibrovascular membrane, and evidence of secondary glaucoma (thin sclera and retina). The moderator discussed a proposed grading scheme that has not been published yet for ocular melanosis: increased melanin-containing cells (grade I), increased melanin-containing cells and distortion (grade II), and melanin-containing cells increased and invading sclera (grade III).

Contributing Institution:
www.nmbu.no

References:

1. Dees DD, Maclaren NE, Teixeira L, Dubielzig RR. An unusual case of ocular melanosis and limbal melanocytoma with benign intraorbital extension in a dog. *Vet Ophthalmol*. 2013;16(suppl 1):117-122.
2. Dubielzig RR, Ketring KL, McLellan GJ, Albert DM. The uvea. In: *Veterinary Ocular Pathology a Comparative*

Review. New York, NY: Saunders Elsevier; 2010:280-282.
3. Petersen-Jones SM, Forcier J, Mentzer AL. Ocular melanosis in the Cairn terrier: clinical description and investigation of mode in inheritance. *Vet Ophthalmol*. 2007;10(suppl.1):63-69.
4. Petersen-Jones SM, Mentzer AL, Dubielzig RR, Render JA, Steficek BA, Kiupel M. Ocular melanosis in the Carin terrier: histopathological description of the condition, and immunohistochemical and ultrastructural characterization of the characteristic pigment-laden cells. *Vet Ophthalmol*. 2008;11(4):260-268.
5. Plummer CE, Regnier A, Gelatt KN. The canine glaucomas. In: Gelatt KN, Gilger BC, Kern TJ, eds. *Veterinary Ophthalmology*. 5th ed. Vol. 2. Ames, IA: John Wiley & Sons, Inc.; 2013: 1053-1054, 1075-1077, 1100-1101.
6. van de Sandt RR, Boevé MH, Stades FC, Kik MJ. Abnormal ocular pigment deposition and glaucoma in the dog. *Vet Ophthalmol*. 2003;6(4):273-278.
7. Winkler PA, Bartoe JT, Quinones CR, Venta PJ, Petersen-Jones SM. Exclusion of eleven candidate genes for ocular melanosis in Cairn terriers. *J Negat Results Biomed*. 2013;12(6).

CASE II: K13-8163-B (JPC 4070254).

Signalment: 8 year-old castrated male Saint Bernard, *Canis familiaris*, canine.

History: Firm, non-pruritic, non-seasonal, longer than a year infiltrative disease within the eye; discrete symmetrical, 1-5 cm (an enucleated globe was received for histopathologic evaluation).

Gross Pathology: None.

Laboratory results:

Globe, dog. At subgross magnification, there is a large, pigmented, densely cellular neoplasm arising from the ciliary body, effacing the anterior and posterior changes and displacing the lens backward. There is extensive hemorrhage the anterior and posterior chambers as well as within the optic nerve at left. (HE, 6X)

None provided.

Microscopic Description: The slide contains a partial cross section of a canine globe. The globe has an unencapsulated mass arising from the ciliary body within the anterior uveal tract between the iris and lens. The mass is composed of tightly packed sheets and cords of polygonal cells and supported by a very fine vascular stroma. Neoplastic cells have indistinct cell borders, moderate to abundant eosinophilic cytoplasm and oval nuclei with finely stippled chromatin. Pseudorosettes and occasional large bone formation are present. There is moderate anisokaryosis and anisocytosis. Mitotic figures are 7 in 5 HPF. There are variably-sized cavitated spaces containing blood or eosinophilic material and melanophages throughout the mass. The mass is not invading the sclera but is filling the iridocorneal angle and displacing the lens posteriorly. There is abundant hemorrhage filling the posterior and anterior chamber occasional associated to hematin-laden macrophages and fibrosis. The retina exhibits atrophy of the nerve fiber and ganglion cell layers. The lens has few eosinophilic spherical globules (Morgagnian globules) and bladder cells within

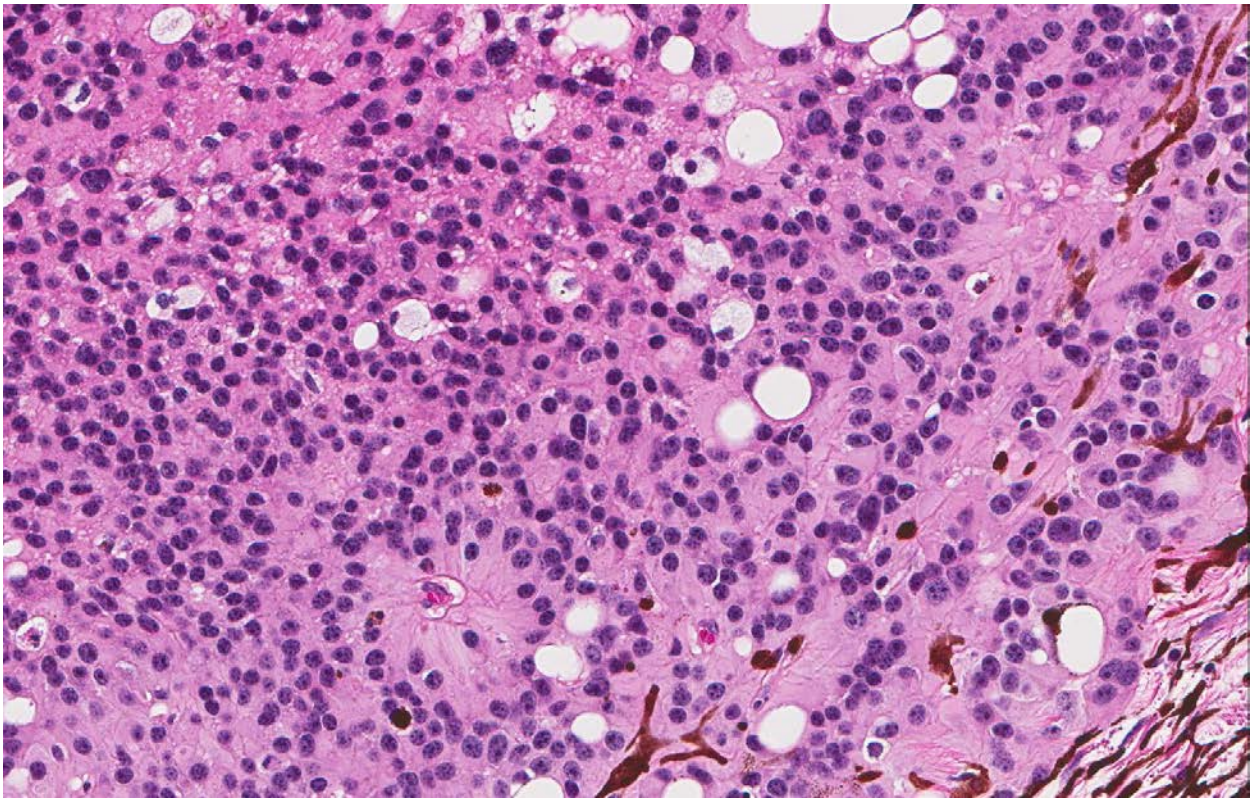

Globe, dog. Neoplastic cells are polygonal with distinct cell borders and abundant eosinophilic granular to vacuolated cytoplasm. Nuclei are variably sized with finely clumped chromatin and 1-2 basophilic nuclei. There are large areas of hemorrhage and necrosis throughout the mass.

subcortical areas. The special stain PAS reveals a complex network of delicate PAS positive basement membranes surrounding groups of neoplastic cells.

Contributor's Morphologic Diagnoses:

1. Eye: Pigmented iridociliary adenoma.
2. Eye: Secondary glaucoma and retinal atrophy with cataractous change.

Contributor's Comment: Histopathological features are most consistent with a benign iridociliary adenoma in this case. The tumor is considered benign because is not invading the sclera or choroid, and lacks cellular pleomorphism. Iridociliary adenomas and adenocarcinomas arise from the pigmented or non-pigmented epithelium of the ciliary body and iris, which are of neuroectoderm origin.[2,7] They are the second most common primary intraocular tumor of dogs, occasionally seen in cats and infrequently seen in other species.[2,5] In general, morphologic patterns for iridociliary epithelial tumors include papillary, solid, palisading ribbons or ribbon-cord, tubular, cystic and anaplastic. The most common secondary abnormality detected with these tumors is glaucoma.[5] However; other complications include uveitis, cataract, loss of vision and, less frequently, retinal detachment, lens luxation and corneal decompensation.[1] Although, iridociliary adenocarcinomas are extremely rare and usually do not metastasize, metastasis is a late stage phenomenon and unlikely in the absent of extensive scleral invasion.[8] Iridociliary epithelial tumors, benign and malignant, can be diagnosed based on histopathological features; however,

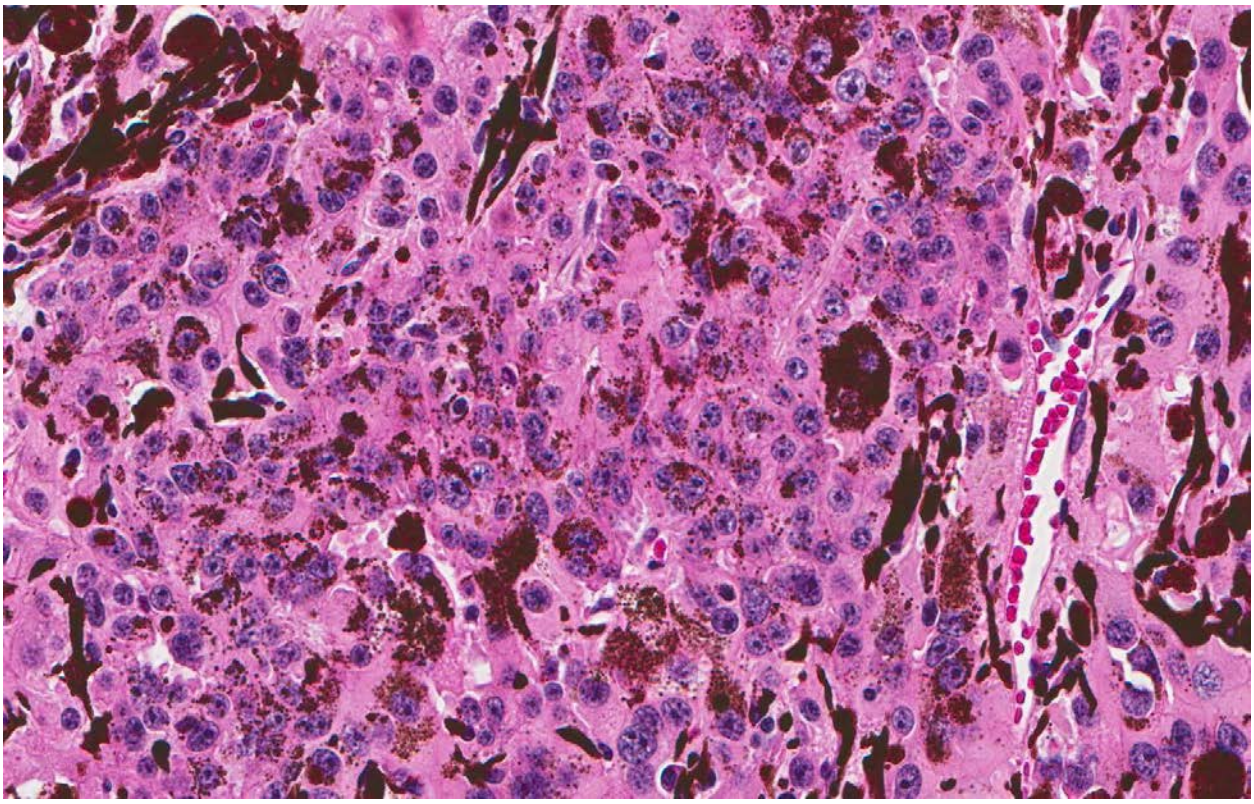

Globe, dog. In an extensive area of the mass, neoplastic cells also contain dark brown globular intracytoplasmic pigment.

adenomas were indistinguishable from adenocarcinomas by biopsy in one study.[1] Additionally, these tumors almost always retain abundant basement membrane production that can be accentuated with PAS staining.[3] An unique characteristic is the positive staining for vimentin and negative for cytokeratin in adenomas.[6] The cells also stain for S-100 and neuron-specific enolase.[6] On the other hand, the malignant version is vimentin and cytokeratin AE1/AE3 positive.[8]

JPC Diagnosis:

1. Globe: Pigmented iridociliary adenoma with drainage angle occlusion, hyphema and subretinal hemorrhage, and retinal detachment and atrophy, Saint Bernard, canine.
2. Retina, vessels: Ferrugination, multifocal, severe.

Conference Comment: Iridociliary epithelial tumors are of neuroectodermal origin and arise from the epithelial cells of either the iris or ciliary body. Primary iridociliary epithelial tumors generally exhibit one of the following criteria: noninvasive growth of epithelial cells that extends into the aqueous adjacent to the iris or ciliary body, pigmented epithelial cells, or thick basement membrane structures on the cell surface.

The incidence of benign (adenoma) and malignant (adenocarcinoma) iridociliary epithelial tumors are about equal; however, ocular melanomas are about twice as common as iridociliary tumors and are the most frequent primary intraocular tumor in the dog. Adenomas are easier to distinguish from melanomas because they are often limited to the ciliary body, whereas, adenocarcinomas, like melanomas, are characterized by a more invasive growth

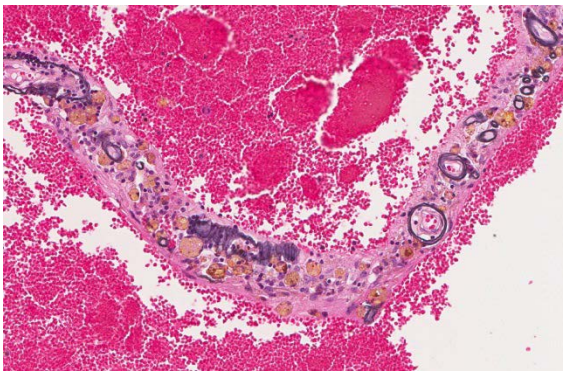

Globe, dog. The detached retina is floating in the markedly hemorrhagic vitreous. The markedly atrophic retina has lost nuclei within all layers. Vessel walls are mineralized, and the retina contains hemosiderin-laden macrophages.

pattern, may extend through the iris base or pupil and are potentially metastatic. The typical microscopic growth patterns of iridociliary adenoma and adenocarcinoma are described by the contributor above. The key microscopic difference between the two depends on extension into the sclera and the presence of anaplasia. If present, these features support a diagnosis of iridociliary adenocarcinoma.

Interestingly, these tumors often appear non-pigmented grossly, regardless of the extent of microscopic pigmentation. In addition to the immunohistochemical characteristics noted above, Alcian blue can often be used to identify hyaluronic acid secretions, which are commonly associated with cells of iridociliary epithelial origin.[4] Historically, tumors of the ciliary body have been induced in laboratory beagles via intravenous injection of ^{226}Ra and ^{228}Ra. These tumors were not identified as of neural crest origin, ruling out melanoma, and were assumed to represent unique radium-induced neoplasms arising from the pigmented epithelium of the ciliary body.[4]

The conference moderator also discussed the significance of the location of new vessels within the corneal stroma. Vascularization of the deep corneal stroma (as seen in this case) tends to be associated with intraocular disease, while more external vessel formation is typically due to corneal trauma. Additionally, a prominent cyclitic membrane was noted by conference participants, arising from the ciliary body and extending to the posterior aspect of the lens. Finally, conference participants discussed the extensive hemorrhage within the posterior segment of the eye. Although the reason for this is unclear, some

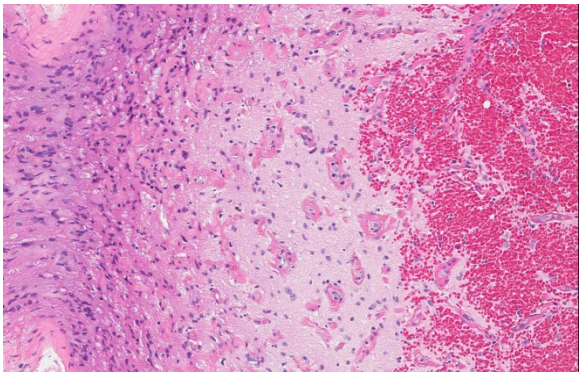

Globe, dog. There is marked hemorrhage in the optic nerve (right), and edema centrally which separates degenerating nerve fibers. (HE, 256X)

participants postulated that the patient was hypertensive, while others suggested the possibility of trauma to a non-sighted eye. Of note, within the retinal remnant vessel walls often appear deeply basophilic and are highlighted with Prussian-blue stain, which suggests accumulation of iron-containing material, a process known as "ferrugination". This could be associated with the chronic hemorrhage noted above.

Contributing Institution:
State of Tennessee
Department of Agriculture
Consumer and Industry Services
Kord Animal Health Diagnostic Laboratory
http://www.tn.gov/agriculture

References:

1. Beckwith-Cohen B, Bentley E, Dubielzig RR. Outcome of iridociliary epithelial tumour biopsies in dogs: a retrospective study. *Vet Record.* 2015;176(6):147. doi:10.1136/vr.102638
2. Dubielzig RR. Tumors of the eye. In: Meuten DJ, ed. *Tumors in Domestic Animals*. Ames, IA: Iowa State Press; 2002:749-750.
3. Dubielzig RR, Steinberg H, Gavin H, Deehr A. J, Fisher B. Iridociliary epithelial tumors in 100 dogs and 17 cats: a morphological study. *Vet. Ophthal*. 1998;1:223-231.
4. Hendrix D. Diseases and surgery of the canine anterior uvea. In: Gelatt KN, Gilger BC, Kern TJ, eds. *Veterinary Ophthalmology*. 5th ed. Vol. 2. Ames, IA: John Wiley & Sons, Inc.; 2013:1181-1182.
5. Njaa B, Wilcock B. The ear and eye. In: Zachary JF, McGavin MD, eds. *Pathologic Basis of Veterinary Disease*. 5th ed. St. Louis, MO: Elsevier Saunders; 2012:1229-1230.
6. Wilcock B. Eye and ear In: Maxie MG, ed. *Jubb, Kennedy, and Palmer's Pathology of Domestic Animals*. Vol 1. 5th ed. Philadelphia, PA: Saunders; 2007:542.
7. Wilcock B, Dubielzig RR, Render JA. *Histological Classification of Ocular and Otic Tumors of Domestic Animals*. Second series. Vol IX. Washington, D.C.: Armed Forces Institute of Pathology/ American Registry of Pathology; 2002:25.
8. Zarfoss MK. and Dubielzig RR. Metastatic iridociliary adenocarcinoma in a Labrador retriever. *Vet Path.* 2007;44:672-676.

CASE III: 719/16 (JPC 4095576).

Signalment: Adult, female, *Cavia porcellus*, guinea pig.

History: The animal stems from a large colony kept in a zoo and was euthanized due to an overall poor body condition. At necropsy the ocular lesion was an incidental finding.

Gross Pathology: On external examination the left eye presented with an irregularly shaped, well-demarcated whitish-grey mass at the limbal region of the iris, which encircled the pupil entirely. On cut section there was a marked thickening of the ciliary body with a bone-like structure and projections extending into the anterior chamber. Otherwise the eye was unremarkable.

Laboratory results:
None provided.

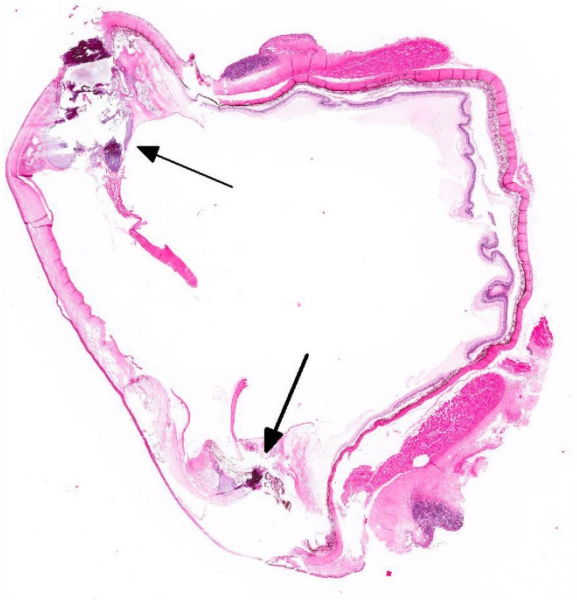

Globe, guinea pig. The globe is artifactually flattened in the anterior-posterior plane. The ciliary body contains well-formed spicules of bone. (HE, 6X)

Microscopic Description: Eye: Expanding and replacing the stroma of the ciliary body and the iris is a proliferation of regularly formed lamellar bone containing multiple central cavities filled by hematopoietically active bone marrow. The bone is partially surrounded by a fine fibrous layer. Multifocally in the subepithelial connective tissue of the bulbar conjunctiva there are nodular infiltrates composed of large numbers of lymphocytes and few plasma cells.

Contributor's Morphologic Diagnoses:

1. Eye: Heterotopic bone formation of the ciliary body.
2. Eye: Lymphoplasmacytic conjunctivitis, multifocal, chronic, mild.

Contributor's Comment: Heterotopic bone formation, also known as osseous choristoma, is a sporadic, usually incidental finding in the eye of guinea pigs.[5,10] Heterotopic bone formation of the ciliary body can be found in young as well as aged guinea pigs of both sexes and it might occur uni- or bilaterally.[10,12] In general, affected animals don't show any clinical symptoms, however, development of secondary open-angle glaucoma by blockage of the iridocorneal filtration angle has been reported with chronic exposure keratitis being the most notable associated sequelae.[10] Other authors on the contrary found no elevation of the intraocular pressure inside eyes displaying heterotopic bone formation of varying degrees compared to unaffected eyes.[8,12]

The etiology of this condition has not been fully determined yet. Bone in the eye can

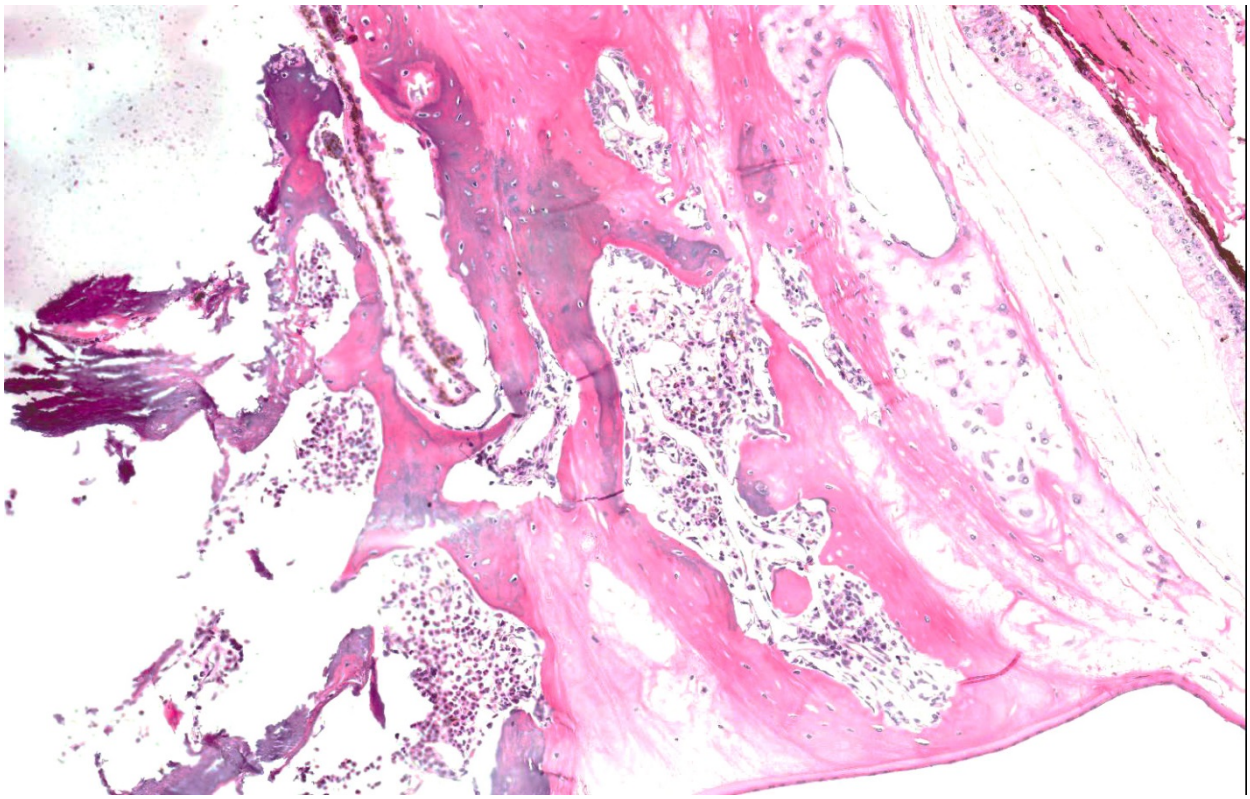

Globe, guinea pig. The spicules of bone within the ciliary body are mineralized (at left) and at right contain marrow elements. (HE, 84X)

arise within metaplastic or neoplastic processes particularly in phthisic eyes.[5] In most affected guinea pigs, however, no previous ocular trauma or disease has been reported.[5,10,12] Due to their slow-growing nature and well-differentiated appearance, they originally have been classified as choristoma, which is defined as histologically normal tissue arising in ectopic positions and considered a benign congenital neoplasm, therefore resulting of an incorrect embryogenesis.[7]

It has also been noted that the role of the ciliary epithelium in transporting and concentrating plasma ascorbic acid into the aqueous humor might be a pivotal factor for development since ascorbic acid positively influences trabecular bone formation by modifying the expression of several bone matrix genes in osteoblasts.[1,13] Osseous metaplasia and mineralization are common findings in other organs of guinea pigs, especially the lungs.[8]

Similar ocular lesions have also been described in other species including dogs and also humans.[6] In humans the location differs in that mainly choroidal structures are affected.[5,11]

JPC Diagnosis: Eye, anterior uvea: Osseous choristoma (heterotropic bone) with fibrovascular membrane formation, drainage angle occlusion, iris bombe, and diffuse mild retinal atrophy, *Cavia porcellus*, guinea pig.

Conference Comment: There have been several reports within the past 30 years detailing individual cases of osseous choristoma in guinea pigs with little additional information about this benign lesion which is considered an embryologic remnant that is left behind and grows as the animal ages.[2, 3, 4, 5, 6, 10, 12]

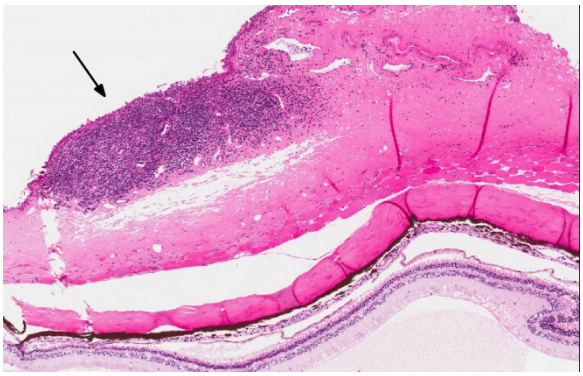

Conjunctiva, guinea pig. There are numerous lymphocytes and fewer plasma cells within the conjunctiva. HE, 84X)

Bone is a normal feature of the eyes, particularly the sclera of birds and some reptiles, but not of the eye of mammals. Osseous metaplasia may result from trauma. Additionally, bone may develop as ossification within a pre-existing choroidal hemangioma.[5] These causes can be ruled out by an otherwise normal ocular anatomy and no evidence of pre-existing vascular lesions or ocular trauma.

Osseous choristomas within the ciliary body appear microscopically as replacement and elevation of ciliary body tissue with mature bony spicules surrounded by a thin fibrous envelope. Frequently, the bone will contain vascular spaces and hematopoietically active bone marrow.[5]

Guinea pigs are particularly susceptible to ectopic mineralization, possibly related to the high calcium content of commercial guinea pig diets and alfalfa. In addition to heterotopic bone formation within the ciliary body of the eye, guinea pigs may develop ectopic ossification within the lungs and urolithiasis from high calcium within urine. Like rabbits, guinea pigs' main mode of calcium homeostasis is renal excretion, thus, chronic renal disease predisposes animals to ectopic mineralization.[9] Ectopic

mineralization is different that an osseous choristoma, which is mature bone in an abnormal location.

In addition to the findings listed above by the contributor, conference attendees identified peripheral anterior synechiae, posterior synechiae, thinning of the sclera, and multifocal atrophy of the ganglion cell layer. Microscopic evidence for glaucoma was considered, and there was spirited discussion related to the cause, whether it was due to the pre-iridial fibrovascular membrane or compression of the trabecular meshwork by the osseous choristoma. Additional discussion centered on the presence of numerous lymphocytes within the conjunctiva and as to whether they represented true conjunctivitis or mucosal-associated lymphoid tissues which is commonly found at this site in older rodents.

Contributing Institution:
Institute of Veterinary Pathology
Faculty of Veterinary Medicine
LMU Munich
Veterinaerstr. 13
80539 Muenchen
http://www.patho.vetmed.uni-muenchen.de/index.html

References:

9. Aghajanian P, Hall S, Wongworawat MD, Mohan S. The roles and mechanisms of actions of vitamin C in bone: new developments. *J Bone Miner Res*. 2015;30:1945-1955.
10. Brooks DE, McCracken MD, Collins BR. Heterotopic bone formation in the ciliary body of an aged guinea pig. *Lab Anim Sci*. 1990;40(1):88-90.
11. Cullen CL, Grahn BH, Wolfer J. Diagnostic ophthalmology. Right superficial corneal ulcer with secondary anterior uveitis and osseous choristoma in a guinea pig. *Can Vet J*. 2000;41(6):502-503.
12. Donnelly TM, Brown C, Donnelly TM. Heterotopic bone in the eyes of a guinea pig: osseous choristoma of the ciliary body. *Lab Anim (NY)*. 2002;31(7):23-25.
13. Griffith JW, Sassani JW, Bowman TA, Lang CM. Osseous choristoma of the ciliary body in guinea pigs. *Vet Pathol*. 1988;25(1):100-102.
14. Lynch GL, Scagliotti RH. Osseous metaplasia in the eye of a dog. *Vet Pathol*. 2007;44(2):222-224.
15. Meuten DJ, ed. *Tumors in Domestic Animals*. 4th ed. 2002:28.
16. Percy DH, Barthold SW. *Pathology of Laboratory Rodents and Rabbits*. 3rd ed. Ames, IA: Blackwell Publishing; 2007:219.
17. Percy DH, Barthold SW. *Pathology of Laboratory Rodents and Rabbits*. 4th ed. Ames, IA: Blackwell Publishing; 2016: 216.
18. Schaffer EH, Pfleghaar S. Secondary open angle glaucoma from osseous choristoma of the ciliary body in guinea pigs. *Tierarztl Prax*. 1995;23:410–414.
19. Shields JA, Shields CL. *Intraocular Tumors: An Atlas and Textbook*. 2nd ed. Philadelphia, PA: Lippincott Williams & Wilkins;2008:264.
20. Williams DL, Sullivan A. Ocular disease in the guinea pig (*Cavia porcellus*): A survey of 1000 animals. *Vet Ophthalmol*. 2010;13Suppl:54–62.
21. Williams DL. The guinea pig eye. In: Williams DL, ed. *Ophthalmology of Exotic Pets*. 1st ed. Oxford, UK: Wiley-Blackwell; 2012: 67-69.

CASE IV: NE 17-399 (JPC 4101750).

Signalment: 8.5 year-old, female, African black-footed (jackass) penguin (*Spheniscus demersus)*.

History: This penguin was presented for acute inability to walk 2 days after laying an egg. Radiographs showed a large shelled egg in the coelom and diffuse osteopenia compared to an age-matched, control penguin. She was treated with calcium, butorphanol, meloxicam, enrofloxacin, and subcutaneous fluids, but died several hours later.

Gross Pathology: The body was in good nutritional condition (body condition score 3/5). The ribs were irregular, soft and serpentine, and cut easily with a scalpel blade. Both the left and right parathyroid glands were enlarged; the left measured 9x4x1.5mm and the right measured 10x4x1.5mm. There was an 89.7g egg in the oviduct near the cloaca. The eggshell was pale blue-green and hard. There was a complete fracture of the spine at the synsacral-thoracic junction with associated hemorrhage.

Laboratory results:
None provided.

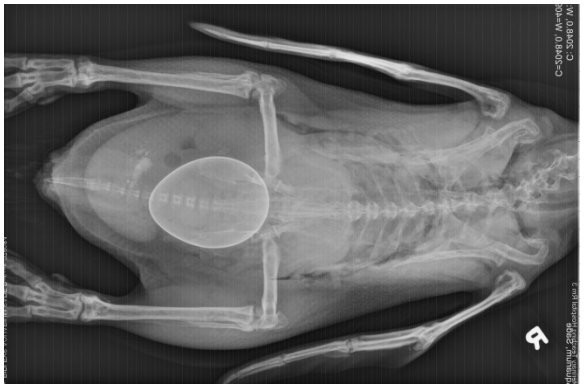

Whole body radiograph, penguin. The cadaver displays diffuse osteopenia as well as a well formed shelled egg within the uterus. (HE, 6X). (Photo courtesy of: University of Tennessee College of Veterinary Medicine, Department of Biomedical and Diagnostic Sciences, 2407 River Drive, Room A205, Knoxville, TN 37996, https://vetmed.tennessee.edu/departments/Pages/biomedical_diagnostic_sciences.aspx)

Microscopic Description: The hematopoietic and adipose tissue of the marrow of the scleral ossicles is variably replaced by fibroblasts and osteoclasts. The numerous osteoclasts and their Howship's lacunae are forming a scalloped endosteal margin and thin cortex.

Contributor's Morphologic Diagnoses:
Scleral ossicles: Marked osteolysis with fibroplasia (fibrous osteodystrophy).

Ribs, penguin. The ribs are irregular, twisted, and cut easily with a scalpel. (Photo courtesy of: University of Tennessee College of Veterinary Medicine, Department of Biomedical and Diagnostic Sciences, 2407 River Drive, Room A205, Knoxville, TN 37996 https://vetmed.tennessee.edu/departments/Pages/biomedical_diagnostic_sciences.aspx

Contributor's Comment: This was a case of nutritional secondary hyperparathyroidism with widespread fibrous osteodystrophy and vertebral fracture. The lesions in the scleral ossicles were also present in the femur, ribs, and vertebrae (all other bones examined).

This penguin was part of an indoor colony at an aquarium. The diet consisted of capelin and a daily avian multivitamin. At one time this bird was supplemented with calcium carbonate during times of egg production, but due to her habit of only laying a single egg per season, the supplementation was discontinued. It is common for penguins to lay two eggs per clutch. After the death of

this bird, serum from other birds in the collection was tested for calcium and vitamin D3 levels; both were low and the birds are now supplemented.

Nutritional hyperparathyroidism and fibrous osteodystrophy has been reported in juvenile penguins.[1] It also occurs in laying hens, where the physiology of parathyroid hormone (PTH) is like that in mammals. PTH responds to hypocalcemia by stimulating osteoclasts (directly and indirectly via osteoblasts) to remove bone.[3] The response is especially rapid in birds, where in response to PTH, osteoclasts increase their cell spread area by 40% within 2-4 minutes.[3] Osteoclasts also increase their ruffled border and acid production in response to PTH.[3]

JPC Diagnosis: Eye, scleral ossicles: Osteolysis, diffuse, severe with fibroplasia (fibrous osteodystrophy), African black-footed (jackass) penguin (*Spheniscus demersus).*

Conference Comment: Fibrous osteodystrophy is a metabolic bone disease characterized by bone resorption with proliferation of adjacent fibrous tissue and poorly mineralized immature bone. This condition is due to chronically elevated plasma parathyroid hormone (PTH) or hyperparathyroidism and occurs in horses, pigs, dogs, cats, ferrets, goats, reptiles, and non-human primates (sheep and goats are relatively unaffected). PTH can be elevated due to any one of the following: functional parathyroid gland adenoma (primary hyperparathyroidism), hypercalcemia of malignancy (production of parathyroid hormone-related peptide (PTHrP)), reduced renal clearance of phosphate and thus low calcium due to their inverse relationship (renal secondary hyperparathyroidism), dietary deficiency of calcium, excess of phosphorus, or in association with vitamin D deficiency (nutritional secondary hyperparathyroidism).[2]

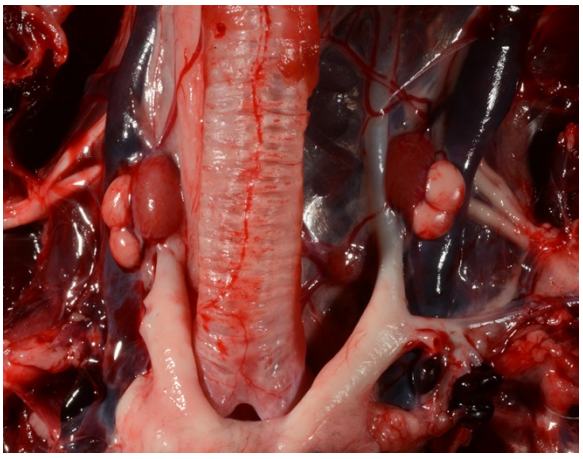

Parathyroid glands, penguin. Bilaterally, the parathyroid glands are markedly enlarged. (Photo courtesy of: University of Tennessee College of Veterinary Medicine, Department of Biomedical and Diagnostic Sciences, 2407 River Drive, Room A205, Knoxville 37996 https://vetmed.tennessee.edu/departments/Pages/biomedical_diagnostic_sciences.aspx)

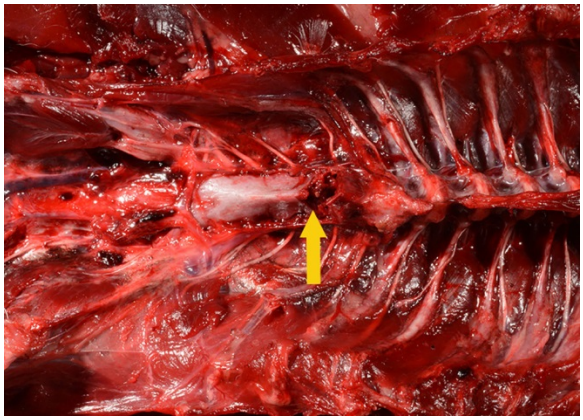

Vertebral column, penguin. There was a complete fracture of the spine at the synsacral-thoracic junction (yellow arrow) with associated hemorrhage. (Photo courtesy of: University of Tennessee College of Veterinary Medicine, Department of Biomedical and Diagnostic Sciences, 2407 River Drive, Room A205, Knoxville, TN 37996, https://vetmed.tennessee.edu/departments/Pages/biomedical_diagnostic_sciences.aspx)

Primary hyperparathyroidism is characterized by autonomous secretion of PTH resulting in persistent hypercalcemia and hypophosphatemia (due to increased

urinary secretion of phosphate). This clinical pathology finding distinguishes primary from secondary hyperparathyroidism. In all cases of secondary hyperparathyroidism, plasma total calcium concentrations are normal or slightly decreased. Animals with primary hyperparathyroidism often suffer from polyuria and polydipsia, generalized muscle weakness, and widespread mineralization of soft tissues including nephrocalcinosis, which may result in the death of the animal even before skeletal changes are evident. Hereditary and familial primary hyperparathyroidism has been reported in German shepherd puppies and Keeshond dogs, respectively. Hypercalcemia of malignancy due to elevated PTHrP is most common in lymphoma and apocrine gland adeno-carcinoma of the anal sac.[2]

Renal secondary hyperparathyroidism develops when impaired glomerular filtration leads to decreased excretion of phosphate. Hyperphosphatemia and is more common in dogs and cats. Subsequently, hypocalcemia develops (due to complexing of calcium with phosphate) which stimulates the release of PTH. Additionally, the hypocalcemia is exacerbated by released of FGF23 from osteocytes (triggered by hyperphosphatemia) with increases renal excretion of phosphate and suppresses 1α-hydroxylase which leads to decreased production and breakdown of $1,25(OH)_2D_3$. Adult dogs with renal failure are most commonly affected with renal secondary hyperparathyroidism, but, as mentioned above, skeletal lesions are usually not as clinically important as the manifestations of uremia.[2]

Finally, nutritional secondary hyper-parathyroidism is most commonly caused by diets with low calcium and a high concentration of phosphorus. In most

Globe, penguin. The scleral ossicles (arrows) are prominent; one scleral ossicle (two arrows) is thickened and hypercellular. (HE 5X)

species, this affects primarily young, rapidly growing animals except in horses that are extremely sensitive to the effects of high phosphorus. In horses, nutritional secondary hyperparathyroidism, colloquially known as "bran disease" usually occurs after several months of a maintenance diet high in grain or tropical grasses high in oxalate, such as: *Setaria sphacelata*, *Cenchrus ciliaris* (buffel grass), *Brachiaria mutica* (para grass), *Digitaria decumbens* (pangola grass), *Pennisetum clandestinum* (kikuyu grass), and *Panicum* spp. These are dangerous because oxalate binds calcium and makes it unavailable for absorption. The characteristic gross finding in horses is "big head" or bilateral enlargement of the maxilla and mandible.[2] In captive birds with fibrous osteodystrophy, nutritional imbalances in calcium, phosphorus, and vitamin D are often compounded by inadequate amounts of unfiltered sunlight, which provides ultraviolet light required for birds to make vitamin D. The lighting conditions of the penguin in this case are unknown.

Contributing Institution:

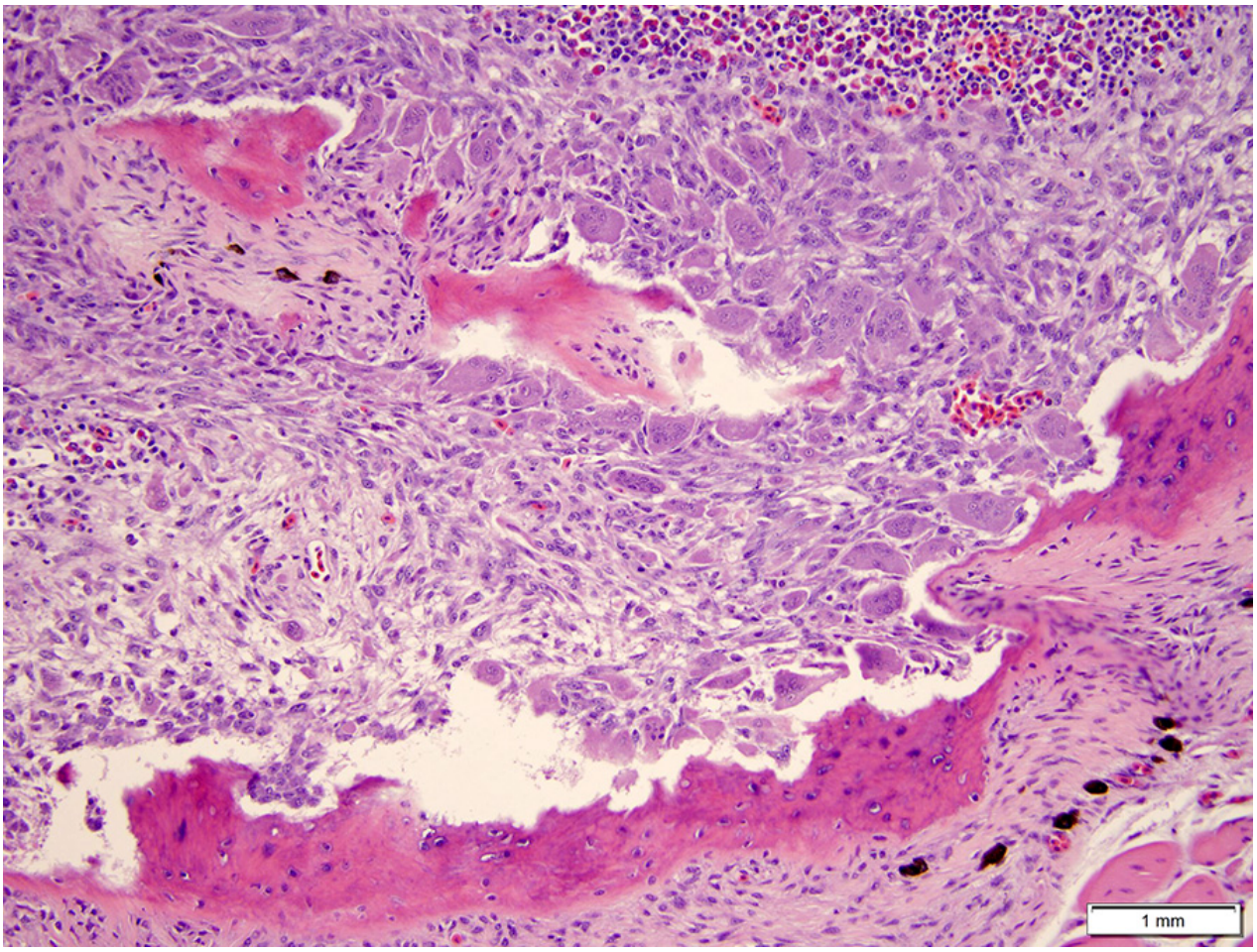

Scleral ossicle, penguin. (100X) The lamellar and trabecular bone of the scleral ossicle is markedly decreased and has a scalloped edge. The cellular contents of the marrow spaced is replaced by a combination of osteoclasts (often in Howship's lacunae on the remaining bone) as well as plump fibroblasts. A small amount of marrow is present at upper right. (Photo courtesy of: University of Tennessee College of Veterinary Medicine, Department of Biomedical and Diagnostic Sciences, 2407 River Drive, Room A205, Knoxville, TN 37996, https://vetmed.tennessee.edu/departments/Pages/biomedical_diagnostic_sciences.aspx)

University of Tennessee College of Veterinary Medicine
Department of Biomedical and Diagnostic Sciences
2407 River Drive, Room A205
Knoxville, TN 37996
https://vetmed.tennessee.edu/departments/Pages/biomedical_diagnostic_sciences.aspx

References:

22. Adkesson MJ, Langan JN. Metabolic bone disease in juvenile Humboldt penguins (*Spheniscus humboldti*): investigation of ionized calcium, parathyroid hormone, and vitamin D3 as diagnostic parameters. *J Zoo Wildl Med.* 2007;38:85-92.
23. Craig LE, Dittmer KE, Thompson KG. Bones and joints. In: Maxie, MG ed. *Jubb, Kennedy, and Palmer's Pathology of Domestic Animals.* 6th ed. Vol. 1. St. Louis, MO: Elsevier; 2016:74-80.
24. Dacke CG. The parathyroids, calcitonin, and vitamin D. In: Whittow CG, ed. *Sturkie's Avian Physiology.* 5th ed. San Diego Academic Press; 2000;473-477.

Self-Assessment - WSC 2017-2018 Conference 13

1. Which of the following is the major factor in differentiating ocular melanosis from uveal melanocytoma?
    a. Amount of pigment
    b. Pattern of growth
    c. Immunohistochemical findings
    d. Portions of the eye affected

2. Which of the following is NOT characteristic of primary iridociliary epithelial tumors?
    a. Noninvasive growth of epithelial cells that extends into the aqueous adjacent to the iris or ciliary body
    b. Thick basement membrane structures on the cell surface.
    c. Numerous cytoplasmic invaginations into the nucleus
    d. Pigmented epithelial cells

3. Which of the following statements is true concerning the formation of heterotopic bone in the eyes of guinea pigs?
    a. It is the result of chronic renal disease.
    b. It may be seen in young as well as old animals.
    c. Most cases are associated with blindness.
    d. They usually follow some form of ocular trauma.

4. True or false. Fibrous osteodystrophy is the result of a chronic decrease in parathyroid hormone?
    a. True
    b. False

5. Nutritional secondary hyperparathyroidism is most commonly the result of which of the following diets?
    a. Low calcium, low phosphorus
    b. High calcium, low phosphorus
    c. Low calcium, high phosphorus
    d. High calcium, high phosphorus

Please email your completed assessment to Ms. Jessica Gold at Jessica.d.gold2.ctr@mail.mil for grading. Passing score is 80%.This program (RACE program number) is approved by the AAVSB RACE to offer a total of 0.5 CE Credits, with a maximum of 12.5 CE Credits being available to any individual Veterinary Medical Professionals for the 2017-2018 Wednesday Slide Conference. This RACE approval is for the subject matter categories of: SCIENTIFIC using the delivery method of NON-INTERACTIVE DISTANCE. This approval is valid in jurisdictions which recognize AAVSB RACE; however, participants are responsible for ascertaining each board's CE requirements.
RACE does not "accredit", "endorse" or "certify" any program or person, nor does RACE approval validate the content of the program.

Joint Pathology Center
Veterinary Pathology Services

WEDNESDAY SLIDE CONFERENCE 2017-2018

Conference 14

10 January 2017

CASE I: BB364/11 (JPC 4019414).

Signalment: 9-year-old, female, spayed, Collie cross, *Canis familiaris*, canine.

History: This dog was referred to the Royal (Dick) School of Veterinary Studies, University of Edinburgh, with a two-month history of persistent watery diarrhea, weight loss and vomiting. The dog had been imported from Italy under the UK's Pet Passport Scheme in 2001. On initial presentation, the dog was bright and alert but thin. The only other physical abnormality was palpable thickening of a loop of bowel in the cranial abdomen. On routine hematology there was lymphopenia and a single biochemical abnormality of a moderately increased ALT (310 IU/l, ref 21–102 IU/L). Abdominal ultrasound confirmed thickening of the jejunal wall. Exploratory celiotomy confirmed marked thickening of one third of the jejunum but found no evidence of obstruction. Biopsies were taken on two separate occasions. The first set consisted of small, full-thickness biopsies from which the initial diagnosis was made; the second set consisted of three portions originating from an 80cm resected segment of thickened jejunum. The dog recovered well and has remained asymptomatic.

Intestine, dog. In the affected segment, the mucosa is circumferentially thickened by firm, pale yellow tissue thickening the intestinal wall up to 3.5cm. (Photo courtesy of: Veterinary Pathology Unit, Division of Veterinary Clinical Sciences, Roslin Institute and Royal (Dick) School of Veterinary Studies, The University of Edinburgh, Easter Bush Veterinary Centre, Roslin, Midlothian, EH25 9RG, UK http://www.ed.ac.uk/schools-departments/vet/services/pathology)

Gross Pathology: Gross lesions were most appreciable in the portions of resected jejunum taken at the second surgery. In the most severely affected segment, the wall was thickened up to 3.5cm. On transverse

section, this thickening was circumferential and consisted of firm, pale yellow tissue.

Laboratory results:
Immunohistochemistry with antibody against NSE confirmed the abnormal presence of neural elements in the small intestinal lamina propria, most notably clusters of neuronal cell bodies but also streaming bundles of axons.

Microscopic Description: Small intestine (jejunum): Numerous well differentiated neuronal cell bodies are scattered throughout the intercryptal lamina propria. The cell bodies are polygonal with faintly visible cell borders, a moderate amount of cytoplasm, large, oval, eccentrically located, hypo-chromatic, vesiculated to open-faced nuclei and clearly visible nucleoli. There are numerous short streams and nodular aggregates of elongated cells with abundant eosinophilic, fibrillar to foamy cytoplasm, compatible with bundles of axons or Schwann cells. They form nests within the subcryptal area but extend as streams into the mid lamina propria. The myenteric and submucosal plexuses are increased in number and size. There is moderate goblet cell hyperplasia and the lumen contains abundant fibrillar, eosinophilic, mucinous material (mucus). In some sections, rare dilated crypts contain small amounts of necrotic cell debris.

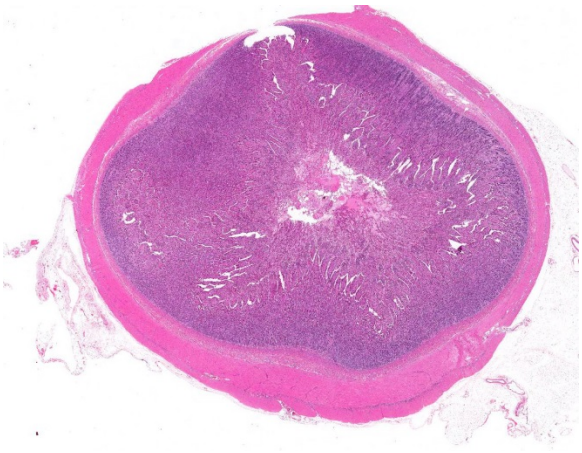

Intestine, dog. Subgross of the affected segment. (HE, 5X)

Note: Sections from the most severely thickened portion were a little different (not included here). In addition to the above lesions, there was marked superimposed mucosal hyperplasia, characterized by an increased number of well differentiated but elongated or branching crypts, often lined by numerous goblet cells. Some crypts were distended by necrotic cell debris and/or mucus. Crypt rupture had led to release of lakes of mucus and necrotic cell debris into the lamina propria. There was also marked villous blunting and fusion, with ulceration.

Contributor's Morphologic Diagnosis:
Jejunum: Intestinal ganglioneuromatosis

Contributor's Comment: Intestinal ganglioneuromatosis (GN) is a rare condition in which there is hyperplasia of all components of the intestinal ganglia. It has some similarities with ganglioneuroma, which is also the result of neuronal and axonal proliferation but is considered neoplastic.[7] However, in contrast to ganglioneuroma, which tends to be well defined and mass-like, GN is poorly demarcated and more diffuse.[5] In humans, diffuse GN presents in one of two forms, transmural or mucosal. Transmural lesions also have a more guarded prognosis due to their link with multiple endocrine neoplasia (MEN) IIb and neurofibromatosis 1 (NF1).[5,19] GN usually arises in the colon or rectum in humans, though one report described lesions extending from lips to rectum.[3,19] Reported clinical signs have included vomiting, weight loss, diarrhea or constipation, hematochezia, melena and abdominal pain.[1,4] Similar clinical presentations have been described in veterinary patients.[7,8]

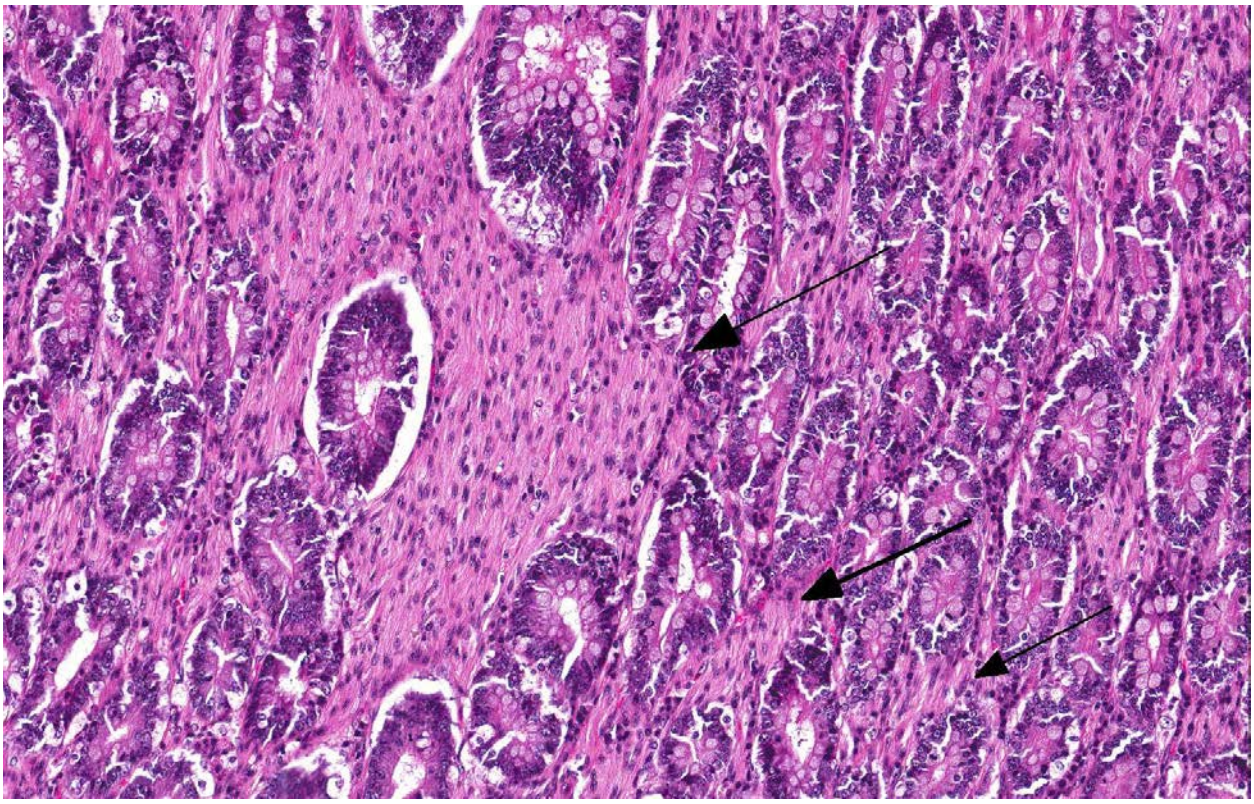

Intestine, dog. Intestinal crypts are separated and occasionally replaced by nerve bundles (arrows) with accompanying Schwann cells. (HE, 200X)

The few previous reports of canine GN have been in juveniles and have typically only involved the colon.[2,7] Small intestinal GN is very rare in the dog, with only one report in the literature.[8] In general, alimentary GN in the dog tends to mirror the transmural form in humans, involving the submucosa and intestinal wall, with relative sparing of the mucosa. Our case was a little different in that the lesion arose in a mature dog with no prior history of gastrointestinal disease; it predominantly affected the mucosal lamina propria of the small intestine; and it was successfully treated. In all prior cases it has been speculated that the lesions are probably congenital, based upon the age of the patient and the slowly progressive nature of the disease.[2]

As mentioned above, MEN IIb, which is the result of a point mutation in the RET proto-oncogene, accounts for the majority of intestinal GN cases in humans. However, the exact pathogenesis of GN is still unclear. Proposed theories include overexpression of neural growth factor leading to proliferation of one nerve fiber type; hyperplasia of multiple nerve fibers, rather than "clonal expansion" of a single subtype; decreased expression of the tumor suppressor gene, PTEN; and increased expression of glial cell line-derived neurotrophic factor (GDNF) and a related neurotrophic factor, neurturin.[6,9,12,16] In humans, clinical signs attributable to GN develop within the first weeks of life and are followed by skeletal abnormalities, thickened lips, mucosal neuromas, and a Marfanoid habitus. Multiple endocrine neoplasms occur in later life, including medullary thyroid carcinoma and pheochromocytoma.[10] There were no clinical signs to suggest multiple endocrine neoplasia in this case and the adrenal glands were ultrasonographically normal. The

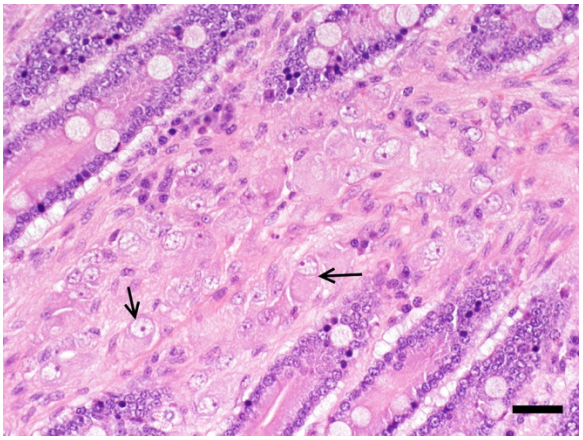

Intestine, dog. Well-differentiated neurons are scattered through the neuronal tissue within the lamina propria (arrows). (HE, 400X) (Photo courtesy of: Veterinary Pathology Unit, Division of Veterinary Clinical Sciences, Roslin Institute and Royal (Dick) School of Veterinary Studies, The University of Edinburgh, Easter Bush Veterinary Centre, Roslin, Midlothian, EH25 9RG, UK http://www.ed.ac.uk/schools-departments/vet/services/pathology)

etiology of diarrhea associated with neural tumors is still unclear. Increased levels of vasoactive intestinal polypeptide (VIP) have been identified in some cases of human GN, resulting in the clinical syndrome of watery diarrhea, hypokalemia and achlorhydria.[11] Alternative mechanisms for the diarrhea include altered intestinal motility, hypersecretion and malabsorption.

JPC Diagnosis: Jejunum: Ganglio-neuromatosis.

Conference Comment: Intestinal ganglio-neuromas arise in peripheral ganglia and are composed of well-differentiated neurons and nerve processes, Schwann cells, and enteric glial cells. Exceedingly rare in domestic animals, intestinal ganglioneuromatosis (GN) is characterized as regional or segmental proliferation of ganglio-neuromatous tissue and has only been reported in dogs, a Boer goat[18], a piglet[17], and a horse[15]. Immuno-histochemical stains aid in the identification of the individual cell types, with neurons positive for neuron specific enolase (NSE) and S-100 and Schwann and enteric glial cells positive for S-100 and glial fibrillary acidic protein (GFAP).[15] These benign proliferative lesions occur predominately in the ileum or colon with few reports of small intestinal infiltration[13] and can usually be associated microscopically with the myenteric plexus from which they either extend through the outer portion of the tunica muscularis to the serosal surface[15] or through the inner portion of the tunica muscularis, submucosa, and muscularis mucosa, and into the lamina propria[13] where it can result in chronic-intestinal pseudoobstruction (CIPO) due to polypoid to segmental expansion of the lamina propria.[14] The pathogenesis of GN is currently unknown; however, researchers have identified deletion of PTEN in the enteric nervous system (ENS) of affected mice which corresponds to abnormally low PTEN expression in humans with enteric GN causing CIPO. PTEN is a phosphatase that controls cell growth, proliferation, and death. In these mice, the clinical changes of CIPO were reversed by administration of a

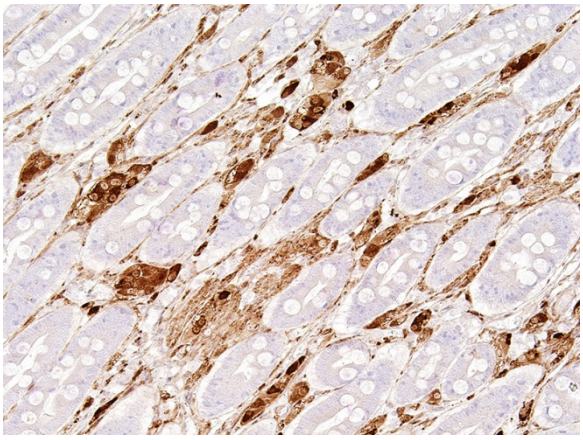

Intestine, dog. Neurons stain immunopositively for neuron-specific enolase. (Photo courtesy of: Veterinary Pathology Unit, Division of Veterinary Clinical Sciences, Roslin Institute and Royal (Dick) School of Veterinary Studies, The University of Edinburgh, Easter Bush Veterinary Centre, Roslin, Midlothian, EH25 9RG, UK http://www.ed.ac.uk/schools-departments/vet/services/pathology)

pharmacological inhibitor of the PI3K/PTEN-AKT-S6K signaling pathway, indicating a potential therapeutic target for ganglioneuromatous forms of CIPO.[14] Additionally, current literature reveals that segmental GN can be removed surgically resulting in resolution of clinical signs and a successful outcome.[13]

Contributing Institution:

Veterinary Pathology Unit
Division of Veterinary Clinical Sciences
Roslin Institute and Royal (Dick) School of Veterinary Studies
The University of Edinburgh
Easter Bush Veterinary Centre
Roslin
Midlothian
EH25 9RG
UK
http://www.ed.ac.uk/schools-departments/vet/services/pathology

References:

1. Atluri DK, Ganesan S, Ferguson RD. Education and imaging. Gastrointestinal: intestinal ganglioneuromatosis. *J Gastroenterol Hepatol.* 2008;23:160.
2. Bemelmans I, Kury S, Albaric O, et al. Colorectal hamartomatous polyposis and ganglioneuromatosis in a dog. *Vet Pathol.* 2011;48:1012-1015.
3. Carney JA, Go VL, Sizemore GW, Hayles AB. Alimentary-tract ganglioneuromatosis — a major component of the syndrome of multiple endocrine neoplasia, type 2b. *N Engl J Med.* 1976;295:1287-1291.
4. Cohen MS, Phay JE, Albinson C, et al. Gastrointestinal manifestations of multiple endocrine neoplasia type 2. *Ann Surg.* 2002;235:648-654.
5. D'Amore ESG, Manivel JC, Pettinato G, Niehans GA, Snover DC: Intestinal ganglioneuromatosis: mucosal and transmural types. A clinicopathologic and immunohistochemical study of six cases. *Hum Pathol.* 1991;22:276–286.
6. DeSchryver-Kecskemeti K, Clouse RE, Goldstein MN, et al. Intestinal ganglioneuromatosis. A manifestation of overproduction of nerve growth factor. *N Engl J Med.* 1983;308:635-639.
7. Fairley RA, McEntee MF. Colorectal ganglioneuromatosis in a young female dog (Lhasa Apso). *Vet Pathol.* 1990;27:206-207.
8. Hazell KLA, Reeves MP, Swift IM. Small intestinal ganglioneuromatosis in a dog. *Aust Vet J*. 2011;89:15-18.
9. Lee NC, Norton JA. Multiple endocrine neoplasia type 2b: Genetic basis and clinical expression. *Surg Oncol.* 2000;9:111–118.
10. Moline J, Eng C. Multiple endocrine neoplasia type 2: an overview. *Genet Med.* 2011;13:755-764.
11. Moon SB, Park KW, Jung SE, et al. Vasoactive intestinal polypeptide-producing ganglioneuromatosis involving the entire colon and rectum. *J Pediatr Surg.* 2009;44:e19-21.
12. O'Donnell AM, Puri P. A role for PTEN in paediatric intestinal dysmotility disorders. *Pediatr Surg Int.* 2011;27:491-493.
13. Paris JK, McCandlish IA, Schwartz T, Simpson JW, Smith SH. Small intestinal ganglioneuromatosis in a dog. *J Comp Pathol.* 2013;148(4):323-328.
14. Piug I, Champeval D, De Santa Barbara P, Jaubert F, Lyonnet S, Larue L. Deletion of Pten in the mouse enteric nervous system induces gangloneuromatosis and mimics intestinal pseudoobstruction. *J Clin Invest.* 2009;119(12):3586-3596.
15. Porter BF, Storts RW, Payne HR, Edwards JF. Colonic ganglioneuromatosis in a horse. *Vet Pathol.* 2007;44(2):207-210.

16. Qiao S, Iwashita T, Ichihara M, et al. Increased expression of glial cell line-derived neurotrophic factor and neurturin in a case of colon adenocarcinoma associated with diffuse ganglioneuromatosis. *Clin Neuropathol.* 2009;28:105-112.
17. Quiroga MA, Lozada MO, Madariaga G, Cappucio JA, et al. Ileal ganglioneuromatosis in a piglet: histopathological and immunohistochemical studies. *J Comp Pathol.* 2014;151(4):380-383.
18. Sheley MF, Higgins RJ, Mete A. Transmural ileal ganglioneuromatosis in a young Boer goat (*Capra hircus). J Comp Pathol.* 2014;151(2-3):190-194.
19. Thway K, Fisher C. Diffuse ganglioneuromatosis in small intestine associated with neurofibromatosis type 1. *Ann Diag Pathol.* 2009;13:50–54.

CASE II: 2 (salmon colored slide) (JPC 4101493).

Signalment: 6-year-old, female, Epagneul Breton (French Brittany), *Canis familiaris*, canine.

History: The dog was found dead at home 23 days after parturition. The owner reported that delivery was normal and the dog gave birth to three puppies.

Gross Pathology: At the necropsy, the dog was emaciated and moderate hemorrhagic enteritis and diffuse pulmonary edema were observed. The endometrium was hemorrhagic and thickened by the presence of brown ellipsoidal enlargements (previous placental attachment) distributed in the left and right uterine horns. The uterine lumen contained small amounts of serosanguinous fluid. The cause of death was attributed to development of acute pneumonia.

Laboratory results:
None provided.

Microscopic Description: Uterus, placental sites: The uterine mucosa is expanded by irregular, multilobulated, eosinophilic projections that compress the adjacent endometrium.
The mass is composed by large amount of fibrillary pale eosinophilic dense material (collagen), finely beaded meshwork of fibrillary, pale eosinophilic material (fibrin), moderate amount of extravasated erythrocytes (hemorrhage), and necrotic and karyorrhectic debris accumulating prevalently in the proximal 1/3rd the projections. Between the deepest portion of the eosinophilc matrix and the glandular zone, there are variable numbers of polygonal multinucleated giant cells with an epithelioid appearance characterized by abundant eosinophilic cytoplasm, often vacuolated (decidual cells/syncytial trophoblast). These cells were often oriented

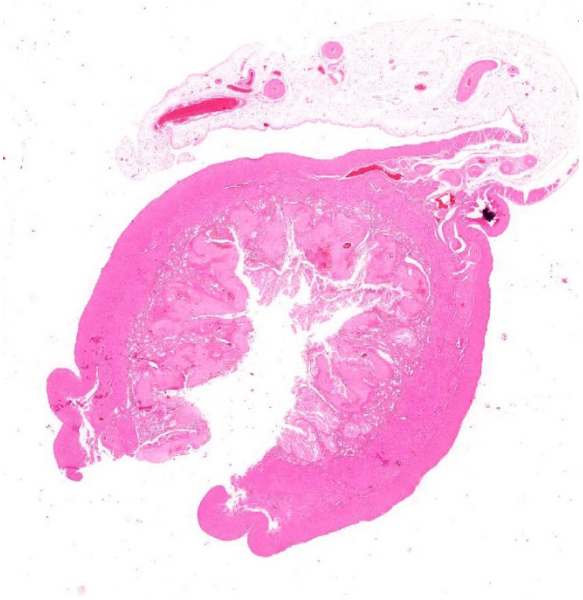

Uterus, dog. A cross section of uterine horn with a markedly thickened endometrium is presented for examination. (HE, 4X)

around vascular structures that were characterized by hyaline walls (vascular degeneration). The glandular zone is characterized by reduced number of endometrial glands, that are multifocally variably dilated and filled with moderate amount of eosinophilic fluid and necrotic and karyorrhectic debris. Within the endometrial mucosa, lamina propria is fibrotic and moderate numbers of mature lymphocytes, plasma cells, and lesser numbers of hemosiderin laden macrophages were also present (mild chronic endometritis). Multifocally, the superficial mucosa lining is sloughed, but when present is organized in papillary projections lined by swollen columnar epithelial cells with abundant, clear, foamy vacuolated cytoplasm and apically located vesicular nuclei (progestational epithelium).

Additional findings (not in the slides): numerous follicles and large corpora lutea were present both ovaries.

Contributor's Morphologic Diagnosis:
Uterus, placental site: Coagulative necrosis, subacute, locally extensive, moderate, with retention of trophoblasts/decidual cells, hemorrhages and mild chronic lympho-plasmacytic endometritis (involution of placental sites).

Contributor's Comment: In dogs, normal involution of the genital tract, after whelping is a slower process compared to other species. More rapid initial involution occurs during the first 4-6 week post-partum. During this period odorless green or dark brown vaginal discharge called "lochia" can be observed (as it was for this dog).

Histologically, placental site involution

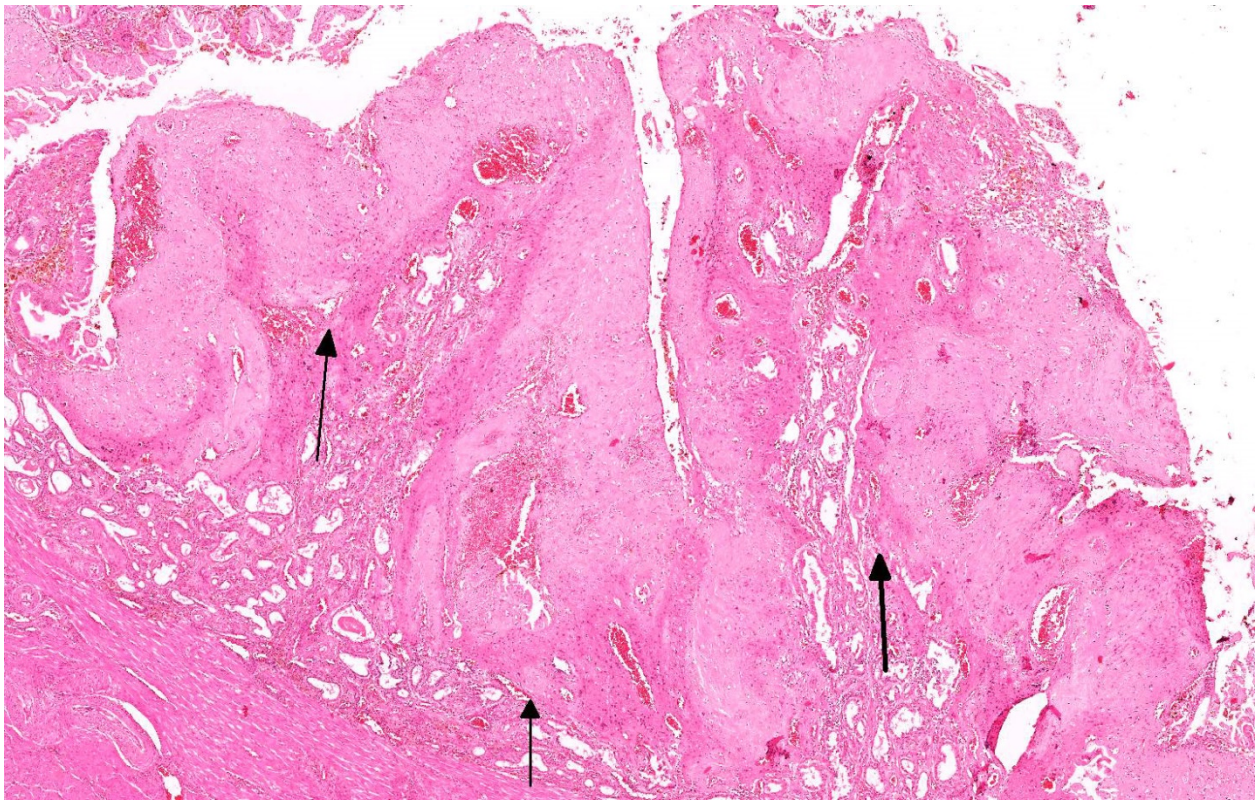

Uterus, dog. Approximately half of the endometrium is replaced by large, coalescing plaques of collagen, remnant trophoblasts, and cellular debris. (HE, 30X)

starts with massive epithelial sloughing into the uterine lumen. Sloughing is at the level of attachment to the endometrial lamina propria that is also expanded by the presence of inflammatory cells (lymphocytes, plasma cells and macrophages).[2] Trophoblasts, on the surface of the uterine mucosa and scattered throughout the lamina propria, are numerous, often necrotic and degenerated, and according to Orfanou et al.,[7] can be observed even at 84 days post-partum. The area of detachment is soon regenerated and covered by a single layer of columnar epithelial cells. During involution, the majority of the uterine glands return to normal size and shape. By the commencement of the eighth week almost all of the collagen masses have sloughed into the lumen. This process continues until the end of the twelfth week and finally, the uterus can be classified as anestrus from the thirteenth week postpartum.[2,7]

Subinvolution of placental sites (SIPS) is a disorder of young, primiparous bitches that causes a sanguineous vulvar discharge any time after the fourth week postpartum. In bitches with SIPS, there is a failure or delay in normal uterine involution or a delay of fetal trophoblasts to regress physiologically.[1,8]

Usually, young bitches are affected, even if the exact etiology of the condition is unknown but factors thought to play a role include failure of thrombus formation and occlusion of endometrial blood vessels due the continuous invasion of trophoblast-like cells into the endometrium and myometrium and the decreased influence of decidual cells on them.[1] SIPS has also been reported in women, and although placentation is hemochorial in humans (versus endotheliochorial in dogs), the pathogenesis of SIPS seems similar. In humans, it has been suggested that important factors in the pathogenesis of SIPS include poor interaction between extravillous cytotrophoblasts and maternal decidual tissue, the absence of immunoglobulins and complement proteins in subinvoluted vessels, and persistent expression of the anti-apoptosis protein Bcl-2, which prevents apoptosis and thereby promotes maintenance of utero-placental vessels.[3,12]

A consistent histological feature is retention and invasion of trophoblast like cells into the underlying stroma and even into the myometrium,[1] together with the presence of abundant collagen mass, largely necrotic and hemorrhagic, that can extended down to involve the whole mucosa or even part of the myometrium. Moreover, the retained trophoblastic cells do not regress or degenerate, but continue to invade the deep glandular layer or even the myometrium, preventing normal thrombus formation in endometrial blood vessels[6] and can be the reason for the prolonged duration of vulvar discharge observed clinically.

The timing of persistence of trophoblast-like cells in physiological involution and subinvolution of placental sites is debated. According to Al-Bassam and co-workers[1] these cells would be present during the first 2 weeks postpartum but in the case of SIPS they persist for a longer period of time. A recent study however, shows that these cells persist on the surface of the uterine epithelium, the placental tissues, as well as in smears of vulvar discharge during the whole period of involution even up to 84 days postpartum in normal involution of the uterus in the bitch.[7]

Clinically, a chronic post-parturient serous or sanguineous discharge (4 to 16 weeks after parturition or even until the beginning of the next estrous) without any systemic illness is the most common presentation.[6]

Affected animals can become anemic, and the uterus is prone to ascending infections.

Spontaneous regression of normal placental sites usually occurs in bitches in good health without significant anemia.[9] However, dogs should be closely monitored weekly or biweekly with clinical, hematologic and ultrasonographic examinations because of the risk of uterine perforation and peritonitis, albeit rare.[6]

In cases of severe bleeding, blood transfusions and ovariohysterectomy should be immediately considered. Usually the affected bitches are not predisposed to recurrence of the disorder as this is a condition that only affects primiparous bitches.[11]

JPC Diagnosis: Uterus, placental site: Normal placental site involution, Epagneul Breton (French Brittany), canine.

Conference Comment: This case accentuates the importance of a good clinical history. Subinvolution of placental sites (SIPS) looks histologically identical to normal involution.

SIPS occurs in young, primiparous bitches and is characterized clinically by prolonged blood-tinged vaginal discharge due to failure of trophoblasts to regress postpartum resulting in delayed re-epithelialization of the endometrium. Sources vary as to duration postpartum that normal uterine bleeding ceases, some say past 7-10 days[10] and others 1-6 weeks[5], and placental sites should be involuted by the 12th week. Nevertheless, the clinical and microscopic manifestations are diagnostic for this syndrome which currently has an unknown cause.[5] Grossly, the uterine horns (cornua) contain segmental, ellipsoidal, irregular, grey to brown thickenings in areas where the placenta previously attached. The adjacent endometrium is normal grossly and microscopically. Microscopically, these thickenings are composed of a combination of amorphous eosinophilic matrix, fibrin, degenerating placental tissue, and regenerating endometrium.[5] Trophoblasts are more numerous than in normal involuting placental sites and are often aggregated at the base of the fibrous masses and extend into the myometrium even penetrating the serosa and allowing leakage of uterine contents into the peritoneum. The overlying surface epithelium often has a heavily vacuolated cytoplasm indicating the influence of progesterone. Corpora lutea are consistently present in the ovary but progesterone levels are low.[10] Sequella to SIPS are ascending infections, open pyometras, and endometritis. Additionally, in dogs with pre-existing bleeding disorders, like von Willebrand's disease, rapid exsanguination is a gruesome reality.[5]

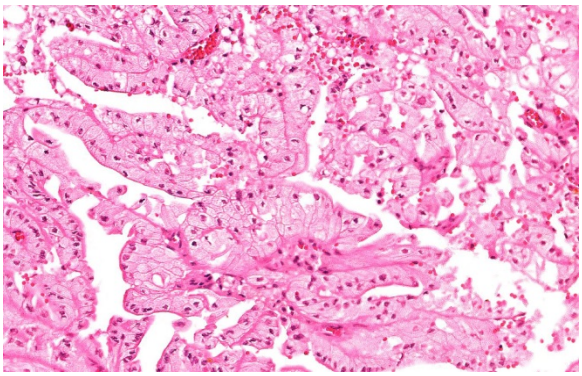

Uterus, dog. Remaining glands are often lined by hypertrophic epithelium with abundant vacuolated cytoplasm (progestational influence). (HE, 226X)

The composition of the large pink masses largely replacing endometrial tissue within the involuting uterus was a subject of spirited discussion, with some favoring a necrotic coagulum and others favoring a collagenous plaque. In truth, the correct answer is a combination of both. During involution, at approximately 2-3 weeks large

plaques of collagen are formed in the involuting endometrium; these plaques are generally sloughed around 8 weeks.[1] this is consistent with the clinical history in this case of a uterus at 23 days post-partum.

Hamsters and other rodents (see below) have a labryrinthine hemochorial placenta in which the trophoblast cells are in direct contact with the maternal vasculature. Therefore, they routinely have giant trophoblastic cells in the myometrial arteries (they have tropism for arterial blood) and rarely in the pulmonary arteries during gestation and up to 3 weeks postpartum.[4]

Table 1: Placental types by species[4,5,10]

Species	**Distribution of contact**	**Classification by maternal cell layers**	**Maternal-fetal interdigitation**
Mare, Sow	Diffuse	Epitheliochorial	Villi (horse: "cups", pig: folded villi)
Ruminant	Cotyledonary	(Syn)epitheliochorial (combination)	Villi
Bitch, Queen	Zonary	Endotheliochorial	Labyrinth
Rhesus macaque	Double discoid	Hemochorial	Villi
Ape, human	Discoid	Hemochorial	Villi
Rabbits, rodents	Discoid	Hemochorial	Labyrinth

Contributing Institution:
DIMEVET –Anatomical Pathology Section
Faculty of Veterinary Medicine of Milan, Italy
http://www.dimevet.unimi.it/ecm/home

References:

1. Al-Bassam MA, Thomson RG and O'Donnell L. Involution abnormalities in the postpartum uterus of the bitch. *Veterinary Pathology*. 1981;18:208–216.
2. Al-Bassam MA, Thomson RG and O'Donnell L. Normal postpartum involution of the uterus in the dog. *Canadian Journal of Comparative Medicine*. 1981;45:217–232.
3. Andrew A, Bulmer JN, Morrison L, Wells M, Buckley CH. Subinvolution of the uteroplacental arteries: an immunohistochemical study. *Int J Gynecol Pathol*. 1993;12:28–33.
4. Barthold SW, Griffey SM, Percy DH. Hamster. In: *Pathology of Laboratory Rodents and Rabbits*. 4th ed. Ames, IA: Wiley Blackwell; 2016:174.
5. Foster RA. Female reproductive system and mammae. In: Zachary JF, ed. *Pathologic Basis of Veterinary Disease*. 6th ed. St. Louis, MO: Elsevier; 2016:1189.
6. Johnston SD, Kustritz MVR and Olson PNS. Subinvolution of placental sites. In: Johnston SD, Kustritz MVR, Olson PNS, eds. *Canine and Feline Theriogenology*. 1st ed. Philadelphia, PA: Saunders; 1991:139–141.
7. Orfanou DC, Ververidis HN, Pourlis A, Fragkou IA, Kokoli AN, Boscos CM, Taitzoglou IA, Tzora A, Nerou CM, Athanasiou L, Fthenakis GC. Post-partum involution of the canine uterus – gross anatomical and histological features. *Reproduction in Domestic Animals*. 2009;44 (Suppl 2):152–155.
8. Reberg SR, Peter AT, Blevins W. Subinvolution of placental sites in dogs.

Compendium on Continuing Education for the Practicing Veterinarian. 1992;14:789–796.
9. Schall WD, Duncan JR, Finco OR, Knecht CD. Spontaneous recovery after subinvolution of placental sites in a bitch. *Journal of the American Veterinary Medical Association.* 1971;159:1780–1782.
10. Schlafer DH, Foster RA. Female genital system. In: Maxie MG, ed. *Jubb, Kennedy, and Palmer's Pathology of Domestic Animals.* Vol. 3. 6th ed. St. Louis, MO: Elsevier; 2016:441.
11. Sontas HB, Stelletta C, Milani C, Mollo A, Romagnoli S. Full recovery of subinvolution of placental sites in an American Staffordshire terrier bitch. *J Small Anim Pract.* 2011;52:42-45.
12. Weydert JA, Benda JA. Subinvolution of the placental site as an anatomic cause of postpartum uterine bleeding: a review. *Arch Pathol Lab Med.* 2006;130:1538–1542.

CASE III: N-1238 (JPC 4102671).

Signalment: 3-month-old, female and male, Boer, *Capra hircus*, caprine.

History: Progressive flaccid paralysis was observed in the hind limbs of 30 out of 40 Boer goat kids over a period of seven days. Age of onset of clinical signs ranged from five to twelve weeks of age; there was no neonatal ataxia. On examination, the kids were affected to varying degrees of severity from hind limb weakness through to an inability to stand. Four kids were found in sternal recumbency. All had normal mentation with intact reflexes and motor function. The mildly affected kids were still suckling. Six animals were euthanized. The herd had no mineral supplementation.

The farm also kept a flock of 120 mixed breed sheep; these had no mineral supplementation and showed no signs of ataxia.

Gross Pathology: Four goat kids were submitted for post-mortem examination (two males [goats A and B] and two females [goats C and D]). They were in relatively good body condition. The lungs were mildly and multifocally mottled red and there was a moderate amount of froth in the trachea (pulmonary congestion and edema). There was a moderate amount of vegetative material within the rumen and well-formed feces in the rectum. Brain and spinal cord were grossly unremarkable.

Laboratory results:

Liver mineral analysis in the four goat kids:

[Reference ranges used from ovine liver (µmol/kg DM) assuming DM 280g/kg:
Mn 130 – 286 µmol/kg DM; Fe 1919 – 19186 µmol/kg DM; Cu 1405 - 5619 µmol/kg DM; Zinc 1639 - 4096 µmol/kg DM; Se 11.3 - 67.8 µmol/kg DM; Molybdenum 11 - 45 µmol/kg DM; Cd 1 – 44 µmol/kg DM; Pb 1- 14 µmol/kg DM; Co 2 -5 µmol/kg DM]

	Mn µmol/kg DM	Fe µmol/kg DM	Cu µmol/kg DM	Zn µmol/kg DM	Se µmol/kg DM	Mo µmol/kg DM	Cd µmol/kg DM	Pb µmol/kg DM	Co µmol/kg DM
Goat A	177	32182	57 **L***	3872	3.6 **L**	33.7	0.1 **L**	6.7	3.9
	166	31061	53 **L**	3734	3.2 **L**	33.6	0.1 **L**	6.7	6.6 **H***
Goat B	227	18608	57 **L**	2658	4.4 **L**	22.7	0.1 **L**	1.3	2.7
	238	19274	69 **L**	2785	5.0 **L**	23.6	0.1 **L**	1.2	2.9
Goat C	124 **L**	19243	43 **L**	2073	4.3 **L**	26.5	0.1 **L**	2.4	3.5
	140	23758	125 **L**	2377	4.3 **L**	31.5	0.1 **L**	3.1	5.0
Goat D	159	22351	31 **L**	3276	3.9 **L**	26.7	0.1 **L**	2.3	1.4 **L**
	189	29184	28 **L**	4045	3.7 **L**	33.8	0.1 **L**	3.3	1.5 **L**

*L: Low; H: High.

Microscopic Description: The severity of the lesions varies slightly depending on the slide. The cervical spinal cord has bilateral, symmetrical and severe degenerative lesion that affects both grey and white matter. Within the ventral funiculi (mainly the ventromedial tracts) and, less severely, the lateral funiculi, myelin sheaths are markedly distended and often contain axonal fragments and/or few macrophages within its lumen (digestion chambers, Wallerian degeneration). Rare spheroids are also observed. Moderate numbers of neurons located within both the ventral horns and the intermediate area, are swollen and rounded and show loss of Nissl granules which are only remaining at the periphery, with its nucleus displaced towards the periphery (central chromatolysis). Some neurons show karyorrhexis, karyolysis and hypereosinophilia (necrosis). Few small haemorrhages are seen within the grey matter. No inflammatory reaction is observed.

Spinal cord, goat A section of spinal cord is presented for examination. There is bilateral spongiosis of the dorsal aspects of the ventral funiculi. (HE, 6X)

Similar lesions were observed in sections from cervical, thoracic and lumbar spinal cord from all the goat kids as well as within the brainstem from 2 of them (A and D).

Contributor's Morphologic Diagnosis: Spinal cord (cervical): Severe, multifocal Wallerian degeneration with moderate, multifocal neuronal chromatolysis.

Contributor's Comment: A diagnosis of enzootic ataxia was made based on the histological findings and low liver copper levels, and was supported by the signalment and clinical presentation. Caprine arthritis and encephalitis virus (CAEV) was initially considered as a differential diagnosis, but the lack of inflammatory reaction within the nervous tissue suggested that it was not involved in the development of these lesions. The pulmonary edema observed in all four goats was most likely secondary to the euthanasia.

Enzootic ataxia, also known as delayed swayback, is a copper deficiency myelopathy[1]. Swayback is a congenital form of the disease that affects neonates; this was not observed in this case. Ataxic kids are normal at birth, but develop clinical signs between one week and six months of age.[2,4] There are differences in the metabolism of copper in sheep and goat, and between breeds within species.[6] The delayed form of swayback is frequently seen in goats, while the congenital form is rare in this species.[1,3] The Angora and Boer breeds of goats have been suggested as being particularly susceptible to low copper levels.[1,4,5]

The disease is thought to be caused by a deficiency in the intake of copper by the dam during pregnancy.[1] Most commonly this is a primary deficiency due to inadequate intake from the diet, but a secondary form can occur where dietary molybdenum, zinc and cadmium impair the absorption of copper.[1,6] The exact diet of the does during pregnancy in this case is unknown, but reportedly no mineral supplementation was provided. In this case, all four kids had liver molybdenum and zinc levels within the normal ranges while cadmium levels were low. In addition to the copper deficiency, all goats showed low levels of selenium and cadmium.

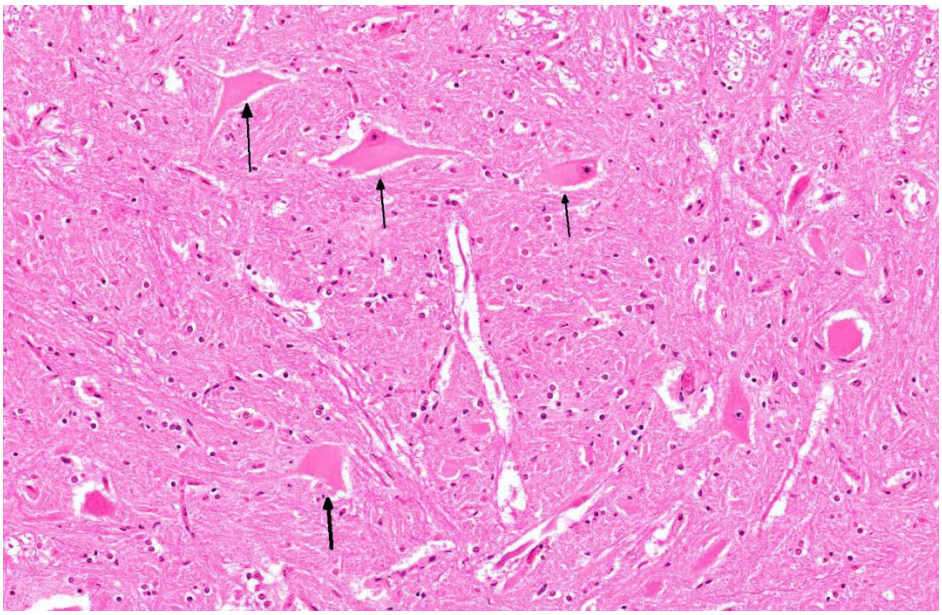

Spinal cord, goat. Neurons (arrows) within the ventral horns are often swollen with dissolution of Nissl substance (central chromatolysis). (HE, 136X)

The exact pathogenesis of enzootic ataxia remains unclear, mainly due to the unknown mechanism of action of copper in the developing nervous system.[3,6] Albeit, copper is required for the activity of several enzymes that are essential for neural

function, including cytochrome oxidase and superoxide dismutase, amongst others. The effects of copper deficiency on the central nervous system occur in utero and during early neonatal life.[2,3,6] Copper deficiency leads to suppression of mitochondrial respiration and reduced phospholipid synthesis. This energy failure is likely to play a role in the axonal and neuronal degeneration that is observed histologically.[3] The generation of reactive oxygen species (ROS) have also been implicated in these changes. . Despite the aforementioned changes, the animal's ability to metabolize copper is not impaired; therefore, tissue concentrations in affected animals may return to normal after dietary correction.[3]

Gross lesions associated with enzootic ataxia in kids are few and not consistent,[3,6] correlating with the lack of relevant gross findings in this case. Microscopic lesions affect the grey and white matter of both the spinal cord and brainstem. In the spinal cord, the dorsolateral aspect of lateral funiculus and the ventromedial tracts of the ventral funiculi are most commonly affected, as evident in this case. . Goat kids show a particularly high incidence of cerebellar degeneration compared to lambs[3], which was however not observed in the here presented case.

JPC Diagnosis: Spinal cord, white matter, ventral and lateral funiculi: Neuroaxonal degeneration, bilaterally symmetrical, multifocal, moderate, with ventral horn neuronal chromatolysis.

Conference Comment: Copper is an essential element for many cellular functions: antioxidant activity (superoxide dismutase), mitochondrial respiration (cytochrome oxidase), catecholamine synthesis (dopamine β-hydroxylase), melanin synthesis (tyrosinase), and iron hemostasis (ceruloplasmin). Copper deficiency causes disease in lambs, goat kids, and piglets and manifests as either absolute primary due to dietary deficiency, or conditioned secondary (most common) due to reduced intestinal absorption, reduced tissue availability, or enhanced secretion. There are several minerals that act as antagonists to copper including: molybdenum, sulfate, iron, and zinc. Ruminants are specifically affected by molybdenum and sulfate which limit copper absorption by forming complexes with copper in the rumen called thiomolybdates. Iron mechanism of antagonism is unknown.[3,6,8]

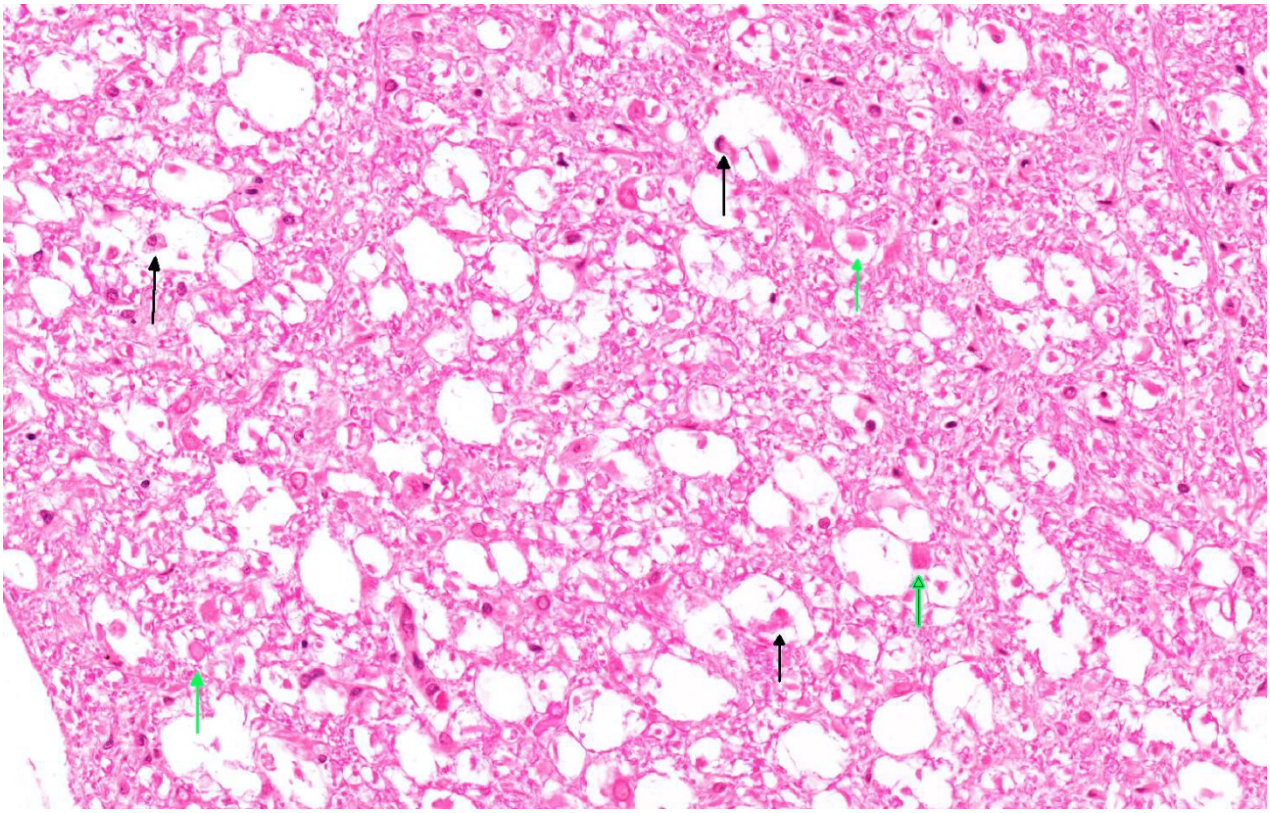

Spinal cord, goat. Within the ventral funiculi, myelin sheaths are markedly dilated and contain swollen axons (green arrows), and gitter cells (black arrows). (HE, 136X)

Clinically, there are two forms of copper deficiency in lambs and goat kids: swayback which is congenital and mainly affects lambs and enzootic ataxia which has a delayed onset and affects lambs between 1 week and several months of age. Affected animals develop progressive neurologic signs such as swaying, falling, spastic paralysis or ascending hindlimb paralysis[7], ataxia, blindness, or deafness. Grossly, only lambs with congenital swayback have lesions that are apparent in the cerebral white matter, evident as bilaterally symmetrical cavitation within the occipital pole or entire corpus medullare. Lambs with delayed enzootic ataxia may develop lesions at any part of the neuraxis in the gray or white matter, but those lesions have not been clearly defined. In both forms, the microscopic changes in the spinal cord are the most characteristic and consist with Wallerian degeneration in the dorsolateral and ventromedial tracts throughout the spinal cord, a pattern suggestive of a distal axonopathy. Additionally, there are degenerative neuronal changes within the red, lateral vestibular, medullary reticular, and dorsal spinocerebellar nuclei in Clarke's column, and in the spinal motor neurons of the intumescences.[3,6,8]

The pathogenesis for these syndromes is not fully understood, but most likely represents the culmination of numerous factors to include energy failure from altered function of mitochondrial cytochrome oxidase and subsequent neuronal degeneration and/or inadequate function of copper-zinc superoxide dismutase leading to oxidative damage.[3,6,8]

In piglets, many of the white matter changes associated with copper deficiency are similar to kids and lambs; however, there are additional neuronal changes. They also can develop skeletal and elastin abnormalities leading to fractures and arterial rupture.[3,6,8] In addition to the neurological manifestations of copper deficiency, sheep also develop "steely wool" (wiry, poor hair coat), hypopigmentation of black wool, and osteoporosis. Poor hair coat and achromotrichia are particularly prominent in cattle which may develop pale colored hair around their eyes, called "spectacles".

Contributing Institution:
School of Veterinary Medicine & Science
University of Nottingham, UK
https://www.nottingham.ac.uk/vet/servicesfortheveterinaryprofession/pathology.aspx

References:

1. Allen AL, Goupil BA, Valentine BA. A retrospective study of spinal cord lesions in goats submitted to 3 veterinary diagnostic laboratories. *Can Vet J*. 2012;53:639–642.
2. Banton MI, Lozano-Alarcon F, Nicholson SS, et al. Enzootic ataxia in Louisiana goat kids. *J Vet Diagn Invest.* 1990;2:70–73.
3. Cantile C, Youssef S. Nervous system. In: Maxie MG, ed. *Jubb, Kennedy and Palmer's Pathology of Domestic Animals*. 6th ed. Vol. 1. St. Louis, MO:Elsevier Ltd; 2016:328–329.
4. Harwood D. Diseases of dairy goats. *In Pract*. 2004;26:248–259.
5. McKay M, Bone P, Kendall N. Establishing the plasma copper reference range in Boer goats. *Vet Rec*. 2010;167:499.
6. Miller AD, Zachary JF. Copper deficiency. In: Zachary JF, ed. *Pathologic Basis of Veterinary Disease*. 6th ed. St. Louis, MO:Elsevier Ltd; 2017:887–888.
7. No authors listed. Delayed swayback diagnosed in lambs with hindlimb paresis. *Vet Rec.* 2015;176(5):118-121.
8. Summers BA, Cummings JF, de Lahunta A. Degenerative diseases of the central nervous system. In: Duncan L, McCandless PJ, eds. *Veterinary Neuropathology.* St. Louis, MO: Mosby; 1995:273-277.

CASE IV: 2 (white colored slide) (JPC 4065579).

Signalment: 1.5-year-old, female, *Cavia porcellus*, guinea pig.

History: The animal was a pet that developed severe abdominal enlargement. At surgery one of the ovaries was massively enlarged (approximately 6X4 cm).

Gross Pathology: None provided.

Laboratory results: None provided.

Microscopic Description: Almost 100% of the ovary (part of the tumor submitted) is replaced by an irregularly round, unencapsulated, poorly demarcated, densely cellular, pleomorphic, expansile neoplasm that extends to the cut borders of the sample provided. (The lesion was delimited by the ovarian capsule).

Neoplasm is composed of variably arranged cells with a derivation from both mature and embryonal elements of all three primordial germ cell layers, embedded in a variable amount of fibrovascular stroma.

Approximately 60% of the neoplasm consists of neuroectodermal neoplastic cells that multifocally palisade around either central areas composed of brightly

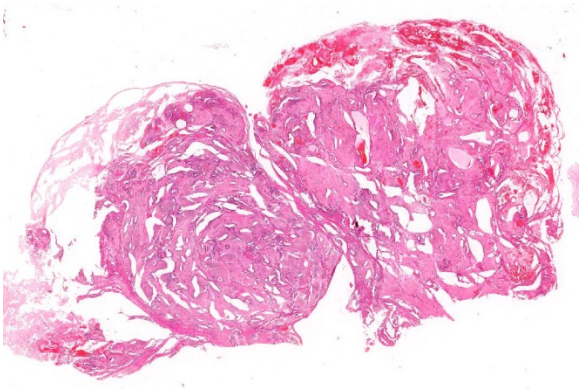

Ovary, guinea pig. The ovary is replaced by an expansile, multilobular, cystic neoplasm. (HE, 4X)

eosinophilic, homogeneous protein-rich material (neuroepithelial rosettes mimicking ventricular spaces and ependyma) surrounded by sheets of glial cells (mimicking glial production zone) or around blood vessels (pseudo-rosettes). Neoplastic cells are oval to cylindrical, 15-20 micron in diameter, have indistinct borders, high N/C ratio and central or palisading hyperchromatic oval nuclei with indistinct nucleoli. There are scattered larger (30-40 micron in diameter), polygonal to stellate cells with abundant, pale basophilic, granular cytoplasm and a central round nucleus with single prominent nucleolus (well differentiated neurons) embedded in an abundant, pale eosinophilic, vaguely fibrillar to vacuolated background substance (neuropil).
Ectoderm is represented by few tubules and cystic spaces lined by single or multiple layers of cuboidal to columnar, 20-24 micron in diameter, epithelial cells with distinct cell borders, polarized nuclei and evident apical capitation of the cytoplasm (consistent with apocrine gland origin).

Mesodermal elements include bundles of fusiform cells 30-35 micron in length with indistinct cell borders, abundant pale eosinophilic cytoplasm and central, cigar shaped nuclei (well differentiated smooth muscle tissue), multiple focal islands of oval to stellate cells loosely embedded in abundant pale basophilic, myxoid matrix (consistent with myxoid to embryonal cartilage- not included in all sections) and rare, small multifocal areas of mineralized lamellar bone with intralacunar round to oval osteocytes (not included in all sections).

Endoderm comprises multiple, variably sized, cystic spaced, up to 0,5 mm in diameter, filled with variable amounts of amphophilic, fibrillar to granular material (mucus), lined by pseudostratified epithelium composed of columnar to bottle-shaped cells, with basal to centrally located nucleus and apical ciliated border (consisting of respiratory epithelium) or few acini and tubules of epithelial polygonal cells with pale eosinophilic cytoplasm expanded by secretory pale vacuoles and flattened basal nuclei (consisting with salivary or goblet cells).

Cellular atypia such as anisocytosis anisokaryosis are mild in all cell populations; occasional multinucleated, undifferentiated neoplastic elements are seen; mitoses are fewer than 1 per 10 HPF.

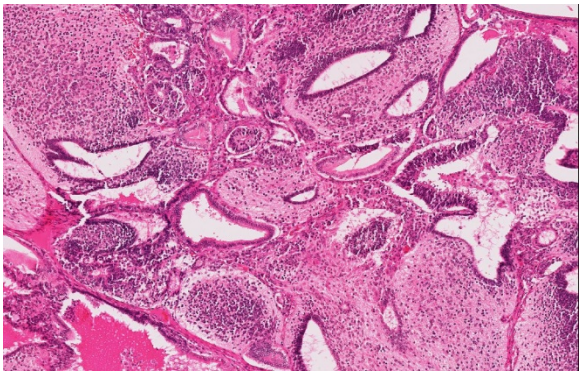

Ovary, guinea pig. At higher magnification, the mass is largely composed of neural tissue with condensation of primitive neuroepithelium forming ependymal-like rosettes. (HE, 80X)

Almost 25% of the mass is composed of elevated numbers of extravasated erythrocytes (hemorrhages) admixed with a meshwork of fibrillar lightly eosinophilic extracellular material (fibrin) and foci of pale eosinophilic, granular to amorphous extracellular material mixed to karyorrhectic cell debris (liquefactive necrosis).

Contributor's Morphologic Diagnosis: Ovary, ovarian teratoma, guinea pig (*Cavia porcellus*)

Contributor's Comment: Teratomas are complex neoplasms composed of tissues representative of at least two, (sometimes all three) primordial germinal layers that are the ectoderm (nervous tissue skin including adnexa), mesoderm (connective tissue, muscle, bone, cartilage, and urogenital and cardiovascular system), and endoderm (gastrointestinal and respiratory epithelium, including their glandular structures).[9] Teratomas are tumors considered to emerge from proliferation of totipotent stem cells occurring physiologically in gonads and that sometimes may reside in abnormal location due to anomalous migration or lack of regression of midline embryonic rest. Such cells have the capacity to differentiate into any of the cells types of the adult body.[6] Teratomas usually occur in the gonads[9,16] and more frequently in the ovary where they may cause spherical to ovoid severe enlargement with a gross aspect of solid and cystic areas on cut surface[9] but reports about extragonadal teratomas, involving cutaneous structures, the alimentary tract, the kidneys, and retroperitoneal and retrobulbar spaces, as well as other systems, also exist.

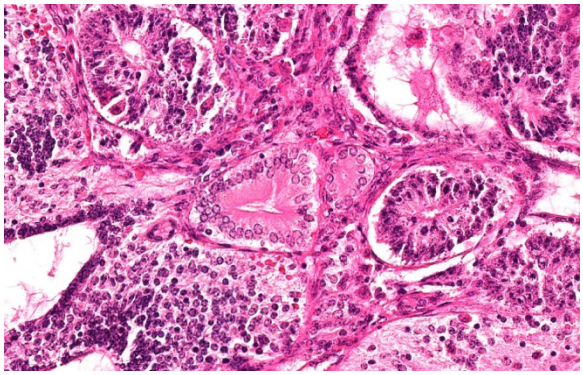

Ovary, guinea pig. Scattered among the ependymal rosettes are nests of ciliated columnar epithelium resembling respiratory epithelium. (HE, 324X)

Teratomas are considered uncommon in domestic animals[9,16] and have been reported in humans, nonhuman primates, dog, cat, horse (base of the ear), sheep, ox, rabbit, swine, laboratory rodents, ferret (adrenal gland), poultry, a blue heron, frogs, hares, squirrel, a spot-necked otter, a woodchuck, turtles, porpoise, hedgehog, red-eared slider and a giraffe.[4,10,11,12,15,17,20] In guinea pigs, primary tumors of the reproductive tract represent approximately 25% of spontaneous tumors.[13] Among these, teratoma is the most frequent.[19,21] Differential diagnosis in guinea pigs include cystic rete ovarii seen commonly in older sows.[13] Teratomas in mice have been rarely reported in B6C3F1, LT/Sv, CD1, C3H strains, with the exception of inbred strain 129 mice. Indeed, approximately 1/3 of 129 teratoma substrain male mice develop spontaneous testicular teratomas.[14] An ovarian teratoma with associated trisomy of chromosome 16 has been reported in a baboon.[10]

Classification of a teratoma as benign or malignant is based largely on the relative amount of primitive, undifferentiated cell content and type of tissues within the tumor: when all the components are well differentiated they are classified as benign (mature) teratomas; on the contrary, if undifferentiated cells/tissue are predominant, and immature neuro-ectodermal elements are over-represented, the tumor is termed teratocarcinoma and is considered malignant.[6] In general, the

presence of undifferentiated cells aggravates the prognosis, and teratomas with incompletely differentiated tissues should be considered potentially malignant.[7,16] However, in the present case, despite the major composition by variably differentiated neuro-ectodermal tissue and the complete substitution of the ovarian parenchyma, a final diagnosis of teratoma and not of teratocarcinoma was made, due to the presence of several well differentiated and recognizable cell lines and absence of neoplastic emboli or distant metastasis. In animals most ovarian and prepuberal testicular teratomas are considered benign, whereas most post pubertal testicular tumors in men are malignant, suggesting a differential origin from benign and malignant cells respectively.[8] The difference may reside in the human tolerance for parthenogenetic development of immature somatic ovarian cells into three germ layers while suppressing neoplastic cells, in contrast to the human male that differentiates malignant immature somatic cells less efficiently in the embryo.[18] The k-FGF gene, a member of the family of fibroblast growth factor genes, is considered as a marker for murine malignant, testicular, teratoma.[5]

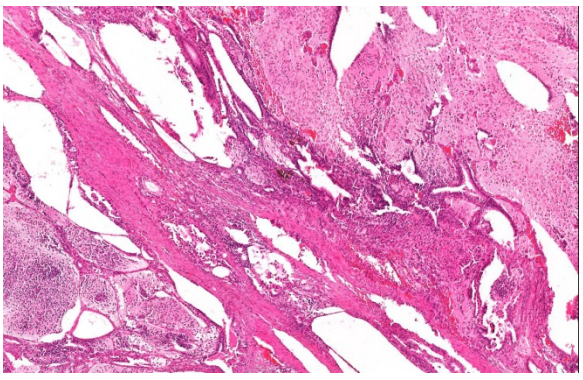

Ovary, guinea pig: Dense bands of smooth muscles course through the neoplasm. (HE, 288X)

JPC Diagnosis: Ovary: Teratoma, *Cavia porcellus*, guinea pig.

Conference Comment: As an excellent review of teratomas is provided by the contributor, our conference comment will focus on ovarian tumors in general.

Ovarian tumors are classified based on embryologic origin: (1) epithelial (surface epithelium of modified mesoderm, rete ovarii, or subsurface epithelial structures (SES, in bitches); (2) germ cells; (3) ovarian stroma (sex cord stromal or gonadostromal). More specifically, sex cord stromal elements are the theca and granulosa cells and their luteinized derivatives which are essential to the formation of primary follicles.[1] A review of ovarian follicle progression is prudent at this juncture. Primordial follicles (the most immature) are plentiful in the adult ovary located deep to the tunica albuginea and composed of a central oocyte surrounded by a layer of simple squamous follicle cells. Hormonal stimulation induces maturation to a primary follicle composed of the central oocyte which is developing, surrounded by a layer of cuboidal cells which proliferate to form a multilaminar (late primary) follicle. An antrum progressively forms as the follicle cells conjoin and leave an open fluid filled space as the zona pellucida forms around the outside of the follicle. The

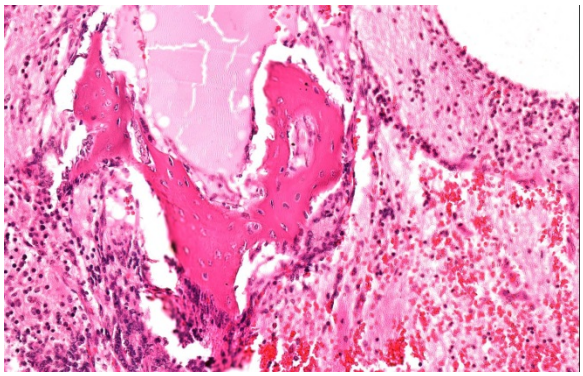

Ovary, guinea pig. Spicules of well-differentiated bone are scattered throughout the neoplasm. (HE, 196X).

follicle is termed “secondary” once the antrum has widened into a C-shape. At this point, the follicle cells are called membrana granulosa and a layer of stromal cells form around the outer zona pellucida called the theca folliculi. The theca folliculi has two layers: the interna (a more cellular, inner vascular layer) and the externa (an outer layer of connective tissue). Finally, continued stimulation and growth leads to Graafian (tertiary) follicle formation in which the oocyte is surrounded by several layers of membrana granulosa cells auspiciously termed the cumulus oophorus. Following ovulation, granulosa and theca interna cells multiply, hypertrophy, and differentiate into granulosa and theca lutein cells which form the corpus luteum and produce progesterone. Assuming there is no pregnancy, the corpus luteum regresses during the end of diestrus to form a corpus albicans followed by atresia and resorption of the remaining structure.[2]

Ovarian epithelial tumors are most common in the bitch, arising from the SES, and tend to form cystic nodules that elevate the surface of the ovary. Metastasis of carcinomas occurs via implantation with ascites. Sex cord stromal tumors, on the other hand, are more common in the mare, cow, and queen and are named according to the originating cell type of the ovarian endocrine scheme (granulosa cell tumor, granulosa-theca cell tumor, thecoma, luteoma, Sertoli cell tumor of the ovary or lipid cell tumor). These tumors, being endocrine in origin, frequently produce hormones such as progesterone, estrogen, or inhibin resulting in systemic effects like anestrus, persistent estrus (nymphomania), masculinization, and blood dyscrasias. Granulosa cell tumors are the most common sex cord stromal tumor and are composed of aggregates of granulosa cells with the vague appearance of follicle formation surrounded and separated by a supporting stroma of spindle cells. Some tumors (more frequent in horses) contain Cal-Exner bodies, homogenous eosinophilic deposits within the center of the follicular structures, which are a useful microscopic feature. In dogs, granulosa cell tumors may appear to be composed of Sertoli cells. For that reason, this type is called Sertoli cell tumor of the ovary. Finally, germ cell tumors of the ovary can be broken down into two main categories: dysgerminoma or teratoma. Dysgerminomas are extremely rare in domestic animals and are composed of broad sheets of large cells with prominent nuclei and scant cytoplasm. Grossly, they are large, grey to white, and firm. Teratomas (described in detail above) are, by definition, composed of two or more germinal layers.[1] The germ cell layers are ectoderm, mesoderm, and endoderm and form the components listed below.

Table 1: Germ cell layer derivatives[3]

Ectoderm	Mesoderm	Endoderm
Epidermis of skin and its derivatives (sweat glands, hair follicles)	Notochord	Epithelial lining of digestive tract
Epithelial lining of mouth and anus	Skeletal system	Epithelial lining of respiratory system
Cornea and lens of eye	Muscular system	Lining of urethra, urinary bladder, and reproductive system
Nervous system	Muscular layer of stomach and intestine	Liver
Sensory receptors in epidermis	Excretory system	Pancreas
Adrenal medulla	Circulatory and lymphatic systems	Thymus
Tooth enamel	Reproductive system (except germ cells)	Thyroid and parathyroid glands
Epithelium of pineal and pituitary glands	Dermis of skin	
	Adrenal cortex	

Conference attendees discussed the potential locations for this tumor because there was no apparent normal tissue present. One participant pointed out that even within completely effaced ovaries, there is at usually SES and surface epithelium remaining. It is unclear whether SES are present in guinea pig ovaries since available resources only confirmed their presence in canine ovaries.[2,13] However, in some sections there were remnants of surface epithelium suggesting the submitted slide was truly ovarian in nature.

Contributing Institution:
DIVET-University of Milano
Via Celoria 10
20133 Milano Italy
http://eng.divet.unimi.it/ecm/home

References:

1. Agnew DW, MacLachlan NJ. Tumors of the genital systems. In: Meuten DJ, ed. *Tumors in Domestic Animals.* 5th ed. Ames, IA: John Wiley & Sons, Inc.; 2017:690-698.
2. Bacha WJ, Bacha LM. Female reproductive system. In: *Color Atlas of Veterinary Histology.* 2nd ed. Ames, IA: Blackwell; 2006:221-223.
3. Banks WJ. Epithelia. In: Reinhardt RW, Steube M, eds. *Applied Veterinary Histology.* 3rd ed. St. Louis, MO: Mosby; 1993:48.
4. Barlow AM, Couper D. Cutaneous teratoma in a wild roe deer. *Vet Rec.* 2006;159:211-212.
5. De Anta JM, Monzó M, Peris B, Ruano. k-FGF protooncogene expression is associated with murine testicular teratogenesis but is not involved during mouse testicular development. *Histol Histopathol*. 1997;12:33-41.

6. Ellenson LH, Pirog EC. The female genital tract. In: Robbins and Cotran, eds. *Pathologic Basis of Disease*. 8th ed., Philadelphia, PA: Saunders Elsevier; 2010:1047-1048.
7. Klein MK. Tumors of the female reproductive system. Germ cell tumors. In: *Withrow SJ, Vail DM, Withrow & MacEwen's Small Animal Clinical Oncology*. 4th ed. St. Louis, MO: Saunders Elsevier; 2007: 610-611.
8. Lakhoo K. Neonatal teratomas. *Early Hum Develop*. 2010; 86:643-647.
9. MacLachlan NJ, Kennedy PC. Tumors of the genital systems. In: Meuten DJ, ed. *Tumors in Domestic Animals*. 3rd ed. Ames, IA: Iowa State Press; 2002:554-555, 565-567.
10. Moore CM, McKeand J, Witte SM, e al. Teratoma with trisomy 16 in a baboon (*Papio hamadryas*). *Am J Primatol*. 1998; 46:323-32.
11. Murai A, Yanai T, Kato M, et al. Teratoma of the umbilical cord in a giraffe (*Giraffa camelopardalis reticulata*). *Vet Pathol*. 2007; 44:204-6.
12. Newman SJ, Brown CJ, Patnaik AK. Malignant ovarian teratoma in a red-eared slider (*Trachemys scripta elegans*). *J Vet Diagn Invest*. 2003; 15:77-81.
13. Percy DH, Barthold SW. Guinea Pig. In: Percy DH, Barthold SW, eds. *Pathology of Laboratory Rodents and Rabbits*. 3rd ed. Oxford, UK: Blackwell Publishing; 2007:248-249.
14. Percy DH, Barthold SW. Mouse In: Percy DH, Barthold SW, eds. *Pathology of Laboratory Rodents and Rabbits*. 3rd ed. Oxford, UK: Blackwell Publishing; 2007:121.
15. Schelling SH, Morton D. An extragonadal teratoma in a female cynomolgus monkey (*Macaca fascicularis*). *J Med Primatol*. 2015;44:113-5.
16. Schlafer DH, Miller RB. Female genital system. In: Maxie MG, ed. *Jubb, Kennedy, and Palmer's Pathology of Domestic Animals*. 5th ed., Vol 3, Philadelphia, PA: Saunders Elsevier; 2007:450, 453-454.
17. Shelling SH. Retrobulbar teratoma in a great blue heron. *J Vet Diagn Invest*. 1994; 6:514-516.
18. Ulbright TM. Germ cell tumors of the gonads: a selective review emphasizing problems in differential diagnosis, newly appreciated, and controversial issues. *Modern Path*. 2005;18:S61-79.
19. Vink HH. Ovarian teratomas in guinea-pigs: a report of ten cases. *J Pathol*. 1970;102:180-182.
20. Williams BH, Yantis LD, Craig SL et al. Adrenal teratoma in four domestic ferrets (*Mustela putorio furo*). *Vet.Path*. 2001, 38:328-331.
21. Willis RA. Ovarian teratomas in guinea-pigs. *J Pathol Bacteriol*. 1962; 84:237-239.

Self-Assessment - WSC 2017-2018 Conference 14

1. Which of the following is a feature that distinguishes ganglioneuromatosis from ganglioneuroma?
    a. Ganglioneuromas are well-defined and mass-like.
    b. Ganglioneuromatosis lacks the presence of all components of the intestinal ganglia.
    c. Ganglioneuromatosis tends to be transmural in the dog.
    d. Ganglioneuromatosis is considered an intestinal malignancy.

2. How many weeks does it take for the normal placenta to involute?
    a. 6
    b. 12
    c. 18
    d. 24

3. Enzootic ataxia is caused by the deficiency of what trace mineral?
    a. Magnesium
    b. Cobalt
    c. Cadmium
    d. Copper

4. Which of the following does not inhibit the absorption of copper?
    a. Molybdenum
    b. Calcium
    c. Zinc
    d. Cadmium

5. Which of the following tissues is NOT of ectodermal origin?
    a. Adrenal medulla
    b. Tooth enamel
    c. Pancreas
    d. Nervous tissue

Please email your completed assessment to Ms. Jessica Gold at Jessica.d.gold2.ctr@mail.mil for grading. Passing score is 80%.This program (RACE program number) is approved by the AAVSB RACE to offer a total of 0.5 CE Credits, with a maximum of 12.5 CE Credits being available to any individual Veterinary Medical Professionals for the 2017-2018 Wednesday Slide Conference. This RACE approval is for the subject matter categories of: SCIENTIFIC using the delivery method of NON-INTERACTIVE DISTANCE. This approval is valid in jurisdictions which recognize AAVSB RACE; however, participants are responsible for ascertaining each board's CE requirements.
RACE does not "accredit", "endorse" or "certify" any program or person, nor does RACE approval validate the content of the program.

Joint Pathology Center
Veterinary Pathology Services

WEDNESDAY SLIDE CONFERENCE 2017-2018

Conference 15

17 January 2018

CASE I: S16-1796 (JPC 4101316).

Signalment: 21-week-old, male, Eagle owl, *Bubo bubo*, avian.

History: The animal's general condition was reduced (sunken eyes, bristling of the feathers, anorexia) and got constantly worse over 3 days. The animal died subsequently despite treatment with glucose and activated charcoal. The animal originated from a falconry, was kept in an aviary with the possibility of free flight and was mostly fed on chicken and pigeons.

Gross Pathology: The animal was in moderate body condition. The liver had a light brown to beige color. On the surface, randomly distributed on all lobes, small (<1 mm in diameter), sharply demarcated, whitish-yellowish foci were found. On the mucosa of the small intestine, randomly distributed, round, 2 mm in diameter, well demarcated, whitish-yellowish foci were detected. The spleen was considerably swollen and showed a dark red to light violet color. Round, whitish-yellowish foci were also detected on the surface of the spleen.

Laboratory results:
Bacteriological examination of liver (culture): Negative.

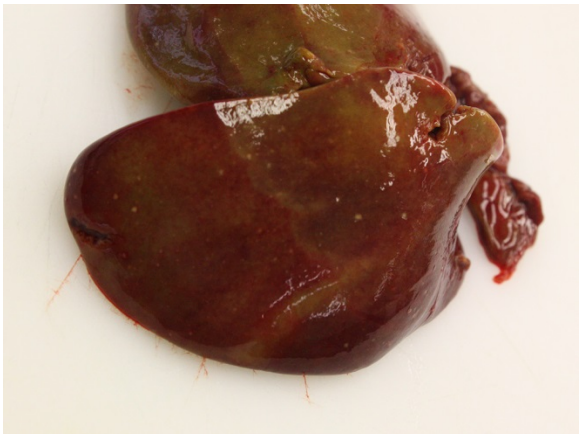

Liver, owl. There are multiple well-demarcated areas of necrosis scattered through the liver parenchyma. (Photo courtesy of: Institute of Veterinary Pathology Vetsuisse-Faculty (University of Zurich), Winterthurerstrasse 268, CH-8057 Zurich, Fax number +41 44 635 89 34, www.vetpathology.uzh.ch)

Parasitological examination of feces: Negative.

Microscopic Description: Liver: Approximately 70% of the liver had multifocal to coalescing randomly distributed foci of coagulative necrosis, characterized by hypereosinophilic hepatocytes with karyopyknosis and karyorrhexis. The inflammatory response surrounding foci of necrosis was minimal and consisted of a few macrophages. Intra-nuclear eosinophilic inclusion bodies and

chromatin margination occurred in hepatocytes bordering the necrotic areas.

Contributor's Morphologic Diagnosis:
Liver: Hepatitis, multifocal, acute, necrotizing, severe with intranuclear eosinophilic inclusion bodies within hepatocytes.

Contributor's Etiologic Diagnosis:
Columbid herpesvirus 1

Contributor's Comment: Gross and histologic lesions in this owl were highly suspicious of an infection with herpesvirus and this was confirmed by the detection of the characteristic intranuclear inclusion bodies in hepatocytes bordering the necrotic foci. In addition to necrotizing hepatitis, necrotizing splenitis and necrotizing enteritis was seen in this animal. The owl has been kept in an aviary and fed on chicken and pigeons, the latter being the most likely source of infection; pigeons are often subclinically infected with columbid Herpesvirus 1 that can cause disease in owls.[8]

In 1932 in North America herpesvirus was first reported in owls and subsequently in prairie falcons (*Falco mexicanus*), American kestrels (*Falco sparverius*) and the peregrine falcon (*Falco peregrinus*).[8] Originally herpesvirus isolates from falcons and owls have been considered as distinct viruses, namely falconid herpesvirus 1 (FHV-1) and strigid herpesvirus 1 (StHV-1). However, serologic studies showed cross-reactivity among FHV-1, StHV-1 and columbid herpesvirus-1 (CoHV-1) as well as that CoHV-1 and FHV-1 are indistinguishable and finally PCR studies confirmed that inclusion body hepatitis in falcons and owls is caused by columbid herpesvirus-1.[3]

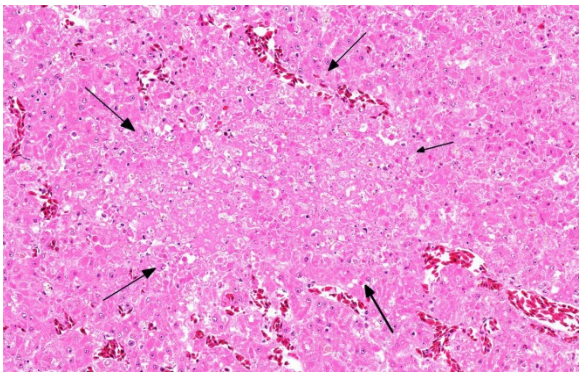

Liver, owl. Areas of largely coagulative necrosis are scattered throughout the section (delimited by arrows). The lack of inflammatory cells suggests an acute lesion. (HE, 168X)

In owls, falcons, and eagles, the disease is known as hepatosplenitis. The disease usually has an acute to subacute course. Clinical signs are nonspecific, including weakness, anorexia and depression.[7] Characteristic gross lesions in falcons are small white hepatic and splenic foci representing necrosis and similar foci in the bone marrow of falcons.[3] Histologically, areas of coagulative necrosis are detectable in the spleen, liver and bone marrow, usually with only little associated inflammation.[3] Intranuclear eosinophilic inclusion bodies within hepatocytes or macrophages bordering the necrotic areas can frequently be detected.[3] Lesions caused by CoHV-1 are not restricted to the liver and spleen; often the small intestine and the kidney are also involved.[6] The progression of the disease is associated with rapid virus multiplication and organ dysfunction. Most reported cases of disease in falcons and owls involve prior documented or possible ingestion of pigeons or by direct contact with the infected bird.[4,8]

In pigeons, Hhrpesvirus-induced disease was first described in Rock Pigeons (*Columbia livia*) and was called "inclusion body disease" or "inclusion body hepatitis".[3] Herpesvirus is prevalent in the pigeon population and has little to no effect on the

health of this species. Pigeons, especially those kept in captivity, are common subclinical carriers of the virus. However, disease occurs in squabs aged ten to sixteen weeks. Clinical signs such as depression, anorexia, conjunctivitis, oral and pharyngeal ulceration, dyspnea, and diarrhea with a duration of a few hours to as long as one week are reported, but not always present. Histological lesions include hepatic and splenic necrosis as reported in owls and falcons. In addition upper respiratory tract inflammation with ulceration and upper gastrointestinal tract inflammation with ulceration is described. Epithelial and parenchymal cells bordering the necrotic areas contain eosinophilic intranuclear inclusions.[3,4]

The disease is transmitted to squads by chronically infected male and female breeding pigeons when feeding regurgitated crop milk during the first weeks of life of the squabs.[5] Contact during courtship, preening and mutual feeding of adult pairs during mating does not result in virus transmission. Ingested virus replicates in the oropharynx region, followed by short-term viremia and virus multiplication in all internal organs. Squabs show severe epithelial lesions in the pharynx, esophagus and crop. Infection by pigeon herpesvirus only rarely results in clinically overt forms of disease in adults and adult pigeons usually do not present any clinical signs except depression, anorexia or conjunctivitis.[5] Exact data on the prevalence of herpesvirus disease in pigeons is not available. Numerous reports provide evidence for the presence of the pigeon herpesvirus in all European countries and many pigeon lofts. Pigeon herpesvirus has

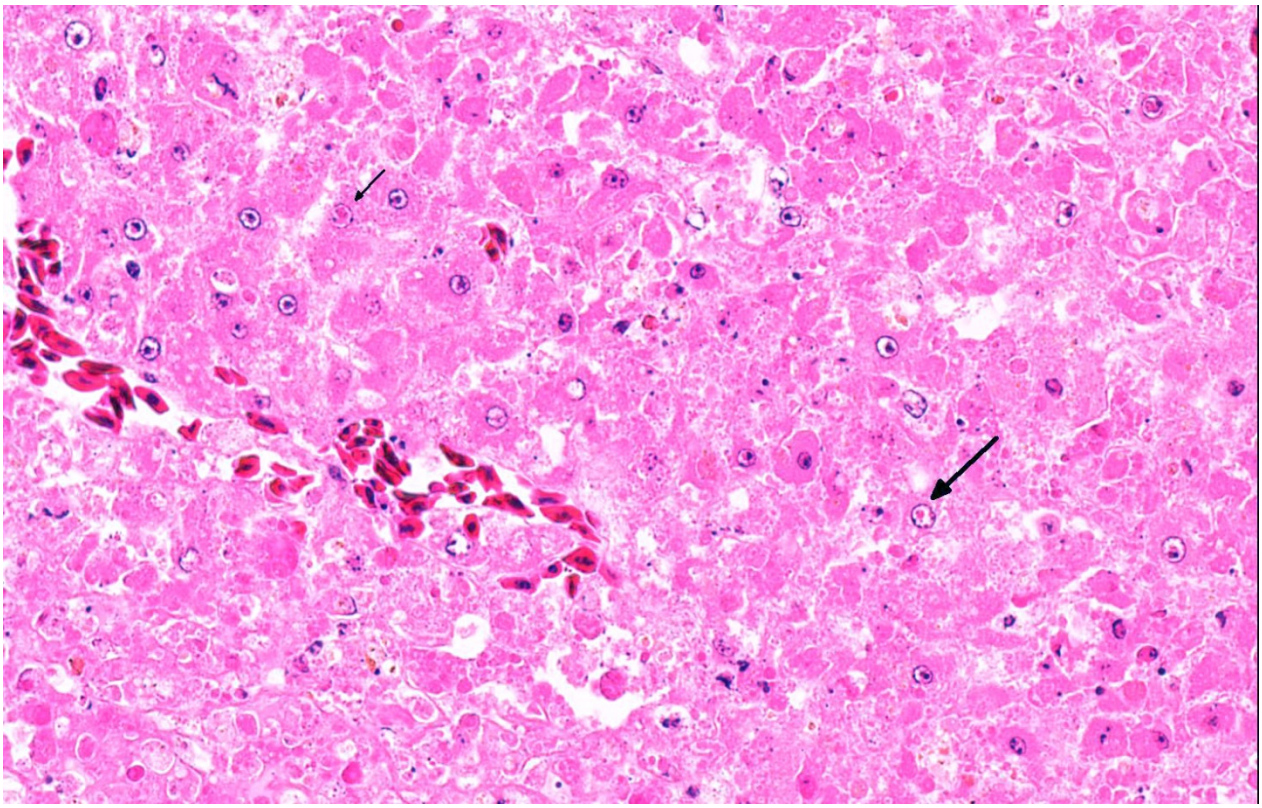

Liver, owl. At the edge of the areas of necrosis, degenerating hepatocytes often contain a single eosinophilic intranuclear inclusions. (HE, 400X)

been detected in all breeds of domestic pigeons (*Columba livia f. domestica*), feral pigeons, and other members of the family Columbidae.[5]

JPC Diagnosis: Liver: Hepatitis, necrotizing, random, multifocal to coalescing, moderate with intranuclear eosinophilic viral inclusion bodies, Eagle owl (*Bubo bubo)*, avian.

Conference Comment: Hepatosplenitis caused by herpesvirus in owls (OHV) and falcons (FHV) are genetically similar and are both pathogenic for owls, ring-necked doves (*Streptopelia* sp.) and kestrels (Eurasian and American).[2] In a comprehensive review of OHV, Drs. Burtscher and Sibalin reviewed the wide spectrum of hosts affected and identified the tawny owl and barn owl as being resistant.[1] Herpesviral disease in birds of prey is often Peracute, resulting in rapid fatalities. However, subclinical cases do occur and are characterized by lethargy, anorexia, diarrhea, and a progressive leukopenia. Gross lesions include hepatomegaly and splenomegaly with pharyngeal and intestinal lesions in owls. Microscopically, there is hepatic necrosis with prominent intranuclear inclusion bodies most prominent at the edge of the necrotic tissue.[2]

The virus is often spread through infected pigeons,as in this case, and is a risk to both captive and free-living birds of prey around the world. Diagnosis is usually based on gross lesions and identification of the characteristic eosinophilic intranuclear inclusion bodies microscopically which are pathognomonic for this disease.[9] There is no successful treatment for viral hepatitis and most often infected birds are culled to prevent spread of the disease. In comparison to psittacine herpesviruses, falcon and owl herpesviruses are more resistant to chemical disinfectants.[2]

The main differential for liver and intestinal lesions in raptors with prominent intranuclear inclusion bodies would be adenovirus. However, most of these animals are subclinically infected and diagnosis is often made at necropsy.[2]

Conference participants noted that there was some slide variation with mixed colonies of bacteria in areas of necrosis on some slides (presumed postmortem overgrowth) and intranuclear inclusion bodies in bile duct epithelial cells.

Contributing Institution:
Institute of Veterinary Pathology
Vetsuisse-Faculty (University of Zurich)
Winterthurerstrasse 268, CH-8057 Zurich
Fax number +41 44 635 89 34
www.vetpathology.uzh.ch

References:

1. Burtscher H, Sibalin M. Herpesvirus stringis: host spectrum and distribution in infected owls. *J Wildl Dis.* 1975;11(2):164-169.
2. Cooper JE. Infectious diseases, excluding macroparasites. In: *Birds of Prey Health & Disease.* 3rd ed. Oxford, UK: Blackwell Science Ltd.; 2002:101-102.
3. Gailbreath K, Oaks L. Herpesviral inclusion body disease in owls and falcons is caused by the pigeon herpesvirus (Columbid herpesvirus-1). *J Wildlife Dis.* 2008;44:427-433.
4. Kaleta E, Docherty D. Avian herpesviruses. In: Thomas N, Hunter D, eds. *Infectious Disease of Wild Birds*. Ames, IA: Blackwell Publishing; 2007:63-86.

5. Kaleta EF. Herpesviruses of birds- a review. *Avian Pathology*. 1990;19(2):193-211.
6. Mozos E, Hervas J, Moyano T, Diaz J, Gomez-Villamandos JC. Inclusion body disease in a peregrine falcon (*Falco peregrinus*): histological and ultrastructural study. *Avian Pathology*. 1994;23(1):175-181.
7. Pinkerton M, Wellehan J, Johnson A, Childress A, Fitzgerard S, Kinsel M. Columbid herpesvirus-1 in two Cooper's hawks (*Accipiter cooperii*) with fatal inclusion body disease. *J Wildl Dis*. 2008; 44:622-628.
8. Rose N, Warren Al, Whiteside D, Bidulka J, Robinson JH, Illanes O, Brookfield C. Columbid herpesvirus-1 mortality in great horned owls (*Bubo virginianus*) from Calgary, Alberta. *Can Cet J*. 2012;53:265-268.
9. Scott DE. Infectious diseases. In: Raptor Medicine, Surgery, and Rehabilitation. 2nd ed. Oxfordshire, UK: CABI; 2017:117-118.

CASE II: E 6940/16 (JPC 4100856).

Signalment: 4-week-old, female, Chilean flamingo, *Phoenicopterus chilensis*, avian.

History: A 4-week-old, female flamingo from the zoo showed a multinodular, ulcerated, wart-like proliferation of approximately 5 x 4 x 3 cm extension in the skin at the right tibiotarsal joint. The proliferated tissue was surgically resected, fixed in 10% neutral buffered formalin and submitted for histological examination.

Gross Pathology: The submitted tissue was partially ulcerated and had a tan color. On cut surface it appeared multilobulated.

Laboratory results:

Formalin-fixed paraffin-embedded tissue (FFPE) was used for molecular sequencing of the gene encoding the 4b-protein. Phylogenetic analysis revealed a sequence homology of 99.9% with the ATCC strain of canarypox (genus: avipoxvirus).

Microscopic Description: Glaborous skin: The epidermis of the featherless skin is irregularly proliferated and severely thickened with increased layers of spinosum cells (acanthosis). There are multifocal superficial or complete losses of the epidermis associated with extravascular erythrocytes and few heterophilic granulocytes. Underneath the stratum corneum there are multifocal accumulations of partly degenerated heterophilic granulocytes, erythrocytes, proteinaceous fluid and bacteria. Particularly, cells of the spinosum layer display severe diffuse hypertrophy with intracellular edema (hydropic degeneration). Eosinophilic inclusion bodies up to 15 µm in diameter are present in the cytoplasm (Bollinger's inclusion bodies). Within the dermis, there is a diffuse mild to moderate infiltration of heterophilic granulocytes and few macrophages. Furthermore, numerous blood vessels are markedly extended and filled with red blood cells. Multifocally there are moderate accumulations of extravascular erythrocytes (hemorrhages) and eosinophilic, fibrillary material (fibrin).

Contributor's Morphologic Diagnosis:
Skin: Dermatitis, erosive and ulcerative, heterophilic, acute, diffuse, severe with epidermal hyperplasia, pustules, hydropic degeneration of keratinocytes and cytoplasmic, eosinophilic inclusion bodies (Bollinger's inclusion bodies) consistent with poxvirus infection.

Contributor's Comment: The morphological findings are consistent with a

Glabrous skin, flamingo. There is a 5 x 4 x 3 cm multinodular, ulcerated, wart-like cutaneous mass at the right tibiotarsal joint. (Photo courtesy of: Department of Pathology, University of Veterinary Medicine Hannover, Buenteweg 17, D-30559 Hannover, Germany, http://www.tiho-hannover.de/kliniken-institute/institute/institut-fuer-pathologie)

poxvirus infection that was confirmed by transmission electron microscopy. Molecular analysis revealed a canarypox strain of the genus avipoxvirus (APV). The histologic key lesions include epidermal hyperplasia and hydropic degeneration of keratinocytes with large, cytoplasmic, eosinophilic inclusion bodies (Bollinger's inclusion bodies). Using the pop-off technique,[11] transmission electron microscopy (TEM) revealed biconcave brick-shaped virions measuring 250 x 320 nm. Virus particles exhibited, depending of the sectioning plane, a biconcave core, two lateral bodies and an envelope consistent with avipox virions.[15]

Macroscopically, an exophytic ulcerated multinodular proliferation was present on the featherless skin at the tibiotarsal joint. This wart-like lesion represents the proliferative or cutaneous form of an APV infection ("dry pox").[8] It is characterized by nodular proliferations on featherless skin such as legs, feet, eyelids and base of the beak. Scars may be visible after recovery and healing. Another manifestation of APV infections is termed diphtheritic/diphtheroid or "wet" form that is characterized by proliferative and fibrino-necrotic lesions of the mucous membranes, predominantly of the tongue, pharynx and larynx.[4,8,20] Birds may also show both forms. The mortality rate of the diphtheritic form is reported to be higher compared to the cutaneous form. However, secondary bacterial infections may significantly increase the mortality rate in the cutaneous form.[20] Rarely, a septicemic form develops that is characterized by acute onset of ruffled plumage, somnolence, cyanosis and anorexia. This form may cause mortality rates of up to 99% and is seen

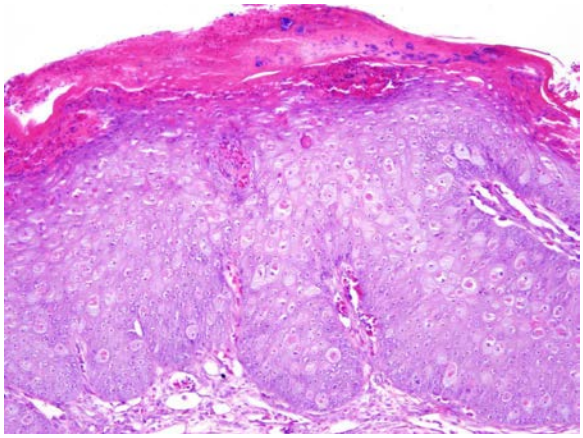

Glabrous skin, flamingo. . There is irregular, frond-like proliferation of the featherless skin with a markedly thickened stratum spinosum . Numerous keratinocytes contain large round intracytoplasmic viral inclusions. (Photo courtesy of: Department of Pathology, University of Veterinary Medicine Hannover, Buenteweg 17, D-30559 Hannover, Germany, http://www.tiho-hannover.de/kliniken-institute/institute/institut-fuer-pathologie)

predominantly in canaries and canary-finch crosses.[8]

Avian poxviruses belong to the genus *Avipoxvirus* which is a member of the subfamily *Chordopoxvirinae* with the family of *Poxviridae*. Avian poxviruses are large, brick-shaped, enveloped viruses with a double-stranded DNA. In infected cells, they replicate in the cytoplasm.[10,19] Transmission occurs through latently infected birds and biting arthropods. In addition, direct transmission of the virus may be facilitated by small traumatic injuries caused by territorial behavior. Furthermore, virus may be transmitted through aerosols via mucous membranes of the eyes or the upper respiratory and digestive tracts.[4,8,10,12] Mosquitos may retain infectious virus in the salivary glands for 2 to 8 weeks.[8] Dry scabs can harbor the virus for many months.[15]

Birds of all ages are susceptible, however, mostly young individuals are affected. The incubation period varies from 7 to 14 days.[14] The virus is usually named by the species in which it was originally isolated. Most investigations about mortality and morbidity of APV infections are based on single APV isolates, which make it difficult to find general information on pathogenicity of particular APV isolates in different species. For example, canaries are highly susceptible to canary poxviruses but they are resistant to pigeon pox, turkey pox and fowl pox.[19] Nevertheless, APV can also cross species barriers and may infect taxonomically different species.[10] Avian poxvirus has a worldwide distribution and infection is described in over 232 avian species in 23 orders.[2] Disease can arise in domestic, pet and wild birds of many different species.[19]

Avipoxvirus infections have been described in various flamingo species in different countries of the world.[10,13,16,20] American flamingos (*Phoeniconais ruber*) were infected in the USA and Portugal,[10,13] Lesser flamingos (*Phoenicopterus minor*) in South Africa,[16] and Greater flamingos (*Phoenicopterus roseus*) in Japan.[16] In the presented case, a Chilean flamingo (*Phoenicopterus chilensis*) was affected. In all published cases, infection occurred in young individuals up to 4.5 months of age. They all suffered from the cutaneous form of avian poxvirus infection.[8,11,16,20] In Portugal, Japan and the USA, single animals were affected,[4,10,13] whereas in South Africa 30% of the fledgling flamingos displayed the cutaneous form.[20]

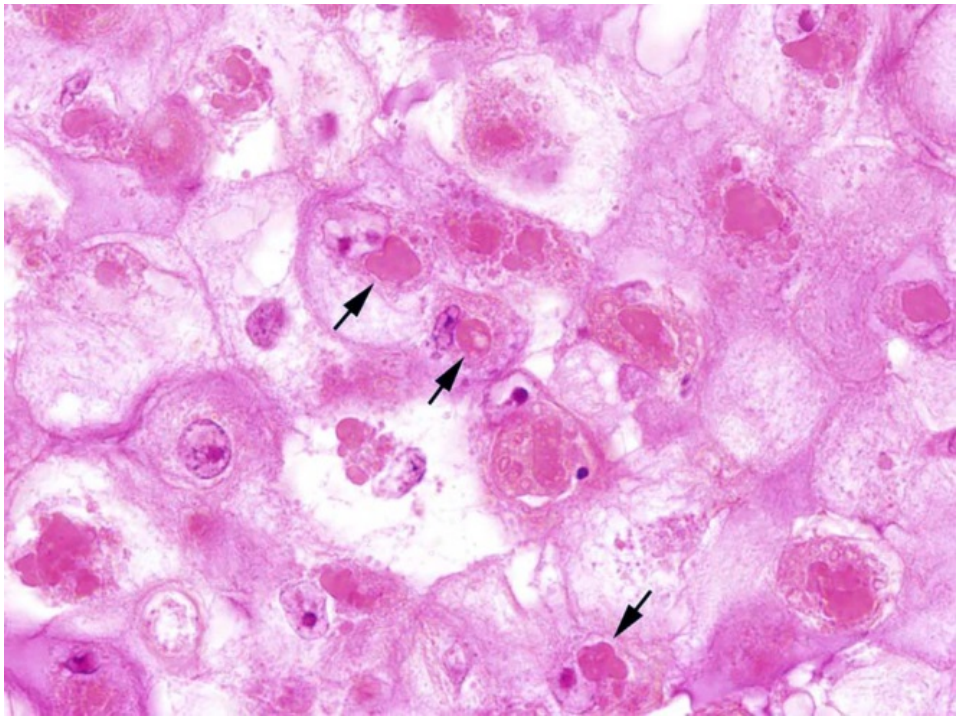

Glabrous skin, flamingo. Keratinocytes of the stratum spinosum are swollen as a result of intracytoplasmic edema (ballooning degeneration) and often contain one or more irregularly round intracytoplasmic viral inclusions (Bollinger bodies) (arrows). (Photo courtesy of: Department of Pathology, University of Veterinary Medicine Hannover, Buenteweg 17, D-30559 Hannover, Germany, http://www.tiho-hannover.de/kliniken-institute/institute/institut-fuer-pathologie) (HE, 400X)

Identification and differentiation of various Avipoxvirus species is mainly based on sequencing of the 4b core polypeptide. This gene is composed of 1971 nucleotides and encodes a protein that has a molecular weight of 75.2 kDa.[1,18] For the isolation of Avipoxvirus, the chorioallantoic membrane (CAM) of specific-pathogen-free (SPF) chicken embryos is inoculated. Within this culture system the virus forms type A cytoplasmic inclusions.[2,10,13]

As morphological differential diagnoses neoplastic proliferations, granulomatous inflammation as well as exuberant granulation tissue have to be considered.

JPC Diagnosis: Skin: Dermatitis, necrotizing and proliferative, focally extensive, severe, with ballooning degeneration, and intracytoplasmic eosinophilic viral inclusion bodies (Bollinger bodies), Chilean flamingo (*Phoenicopterus chilensis)*, avian.

Conference Comment: The term fowlpox was initially used to describe poxvirus infections of all birds, but as the number of species affected grew, it became used specifically for the disease in chickens.[3] Avianpox is an old disease that was previously thought to be related to human small pox and chicken pox. While this disease does not affect the human population, it does affect numerous avian species that we know of (chickens, turkeys, pigeons, canaries, psittacines, and wild birds) but perhaps all bird species are susceptible.[17]

The first USDA license issued for a poultry product was for the fowlpox vaccine in 1918.[5] To this day, the pox vaccine is the primary method of disease control and prevention with initial vaccination of birds at 4 weeks of age or at any age if necessary. The fowl pox vaccine is currently being used as a vector for recombinant vaccines due to its efficacy and prevalence.[17] The characteristic inclusion bodies of poxviruses (described above) represent the site of DNA synthesis and packing of the infectious virus particles. Avianpox viruses contain

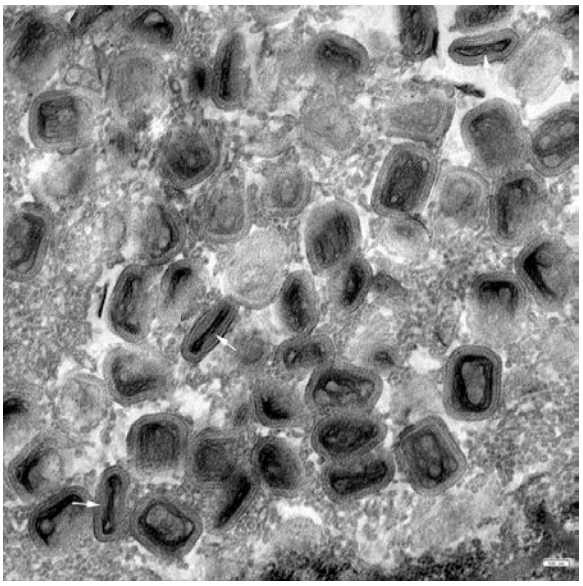

Glabrous skin, flamingo. Ultrastructurally, infective keratinocytes contain numerous biconcave brick-shaped virions measuring 250 x 320 nm. (Photo courtesy of: Department of Pathology, University of Veterinary Medicine Hannover, Buenteweg 17, D-30559 Hannover, Germany, http://www.tiho-hannover.de/kliniken-institute/institute/institut-fuer-pathologie)

numerous genes for DNA replication, repair, and processing, as well as a specific enzyme (CPD photolyase) that repairs UV-induced DNA damage using visible light as a source of energy. This may help explain the virus' environmental durability. Poxviruses encode proteins that affect host cells such as vaccinia virus growth factor (VGF) which stimulates proliferation of keratinocytes using epidermal growth factor receptors (EGFRs). Still other proteins inhibit complement mediated cell lysis and the host inflammatory response. All of these factors function to not only provide the virus a safe environment to replicate in, but also provide fertile soil for secondary bacterial infections.[3]

Gross differentials for cutaneous (dry) pox include mite infections and bacterial pododermatitis. *Cnemidokoptes mutans* ("scaley leg mite") lives primarily in unfeathered skin and causes thick, hyperkeratotic shanks with white, scaly crusts, and *Cnemidokoptes gallinae* ("depluming mites") lives in basal feather shafts and causes breakage or complete loss of feathers and intense irritation.[6] Finally, bacterial pododermatitis ("bumblefoot") most commonly caused by *Staphylococcus aureus* results in purulent abscesses on the plantar surface of the foot due to penetrating wounds.[7]

Conference participants noted variable serocellular crust formation in some sections with prominent colonies of superficial bacteria admixed with hemorrhage.

Table 1: Select genera of the family Poxviridae.[9,12]

Genus	**Virus/Disease**	**Major Hosts**
Orthopoxvirus	Vaccinia virus Buffalopox/Rabbitpox virus*	Numerous: cattle, buffalo, swine, rabbits
	Cowpox*	Rodents (reservoir), cattle, cats, elephants, rhinos
	Camelpox	Camels
	Ectromelia (Mousepox)	Mice, voles
	Monkeypox*	NHPs, squirrels, anteaters
Capripoxvirus	Goatpox	Goats, sheep

	Sheeppox	Sheep, goats
	Lumpy skin disease virus	Cattle, cape buffalo
Suispoxvirus	Swinepox virus	Swine (vector= *Hematopinus suis*)
Leporipoxvirus	Myxoma virus	Rabbits (*Oryctolagus* & *Sylvilagus* spp.)
	Rabbit fibroma virus, Hare fibroma virus	Rabbits
	Squirrel fibroma virus	Grey and red squirrels
Avipoxvirus	Fowlpox, canarypox, quailpox, etc	Chickens, turkeys, peacocks, etc.
Parapoxvirus	Caprine parapoxvirus (Orf; contagious ecthyma)*	Sheep, goats
	Bovine parapox (bovine papular stomatitis virus)*	Cattle
	Pseudocowpox*	Cattle
	Sealpox*	Seals
	Parapoxvirus of red deer	Red deer
Molluscipoxvirus	Molluscum contagiosum virus*	NHPs, birds, dogs, kangaroos, equids
Yatapoxvirus	Yabapox virus & tanapoxvirus*	NHPs
Unclassified	Squirrel poxvirus, fish (carp edema), horsepox	

*zoonotic

Contributing Institution:
http://www.tiho-hannover.de/kliniken-institute/institute/institut-fuer-pathologie

References:

1. Binns MM, Boursnell ME, Tomley FM, Campbell J. Analysis of the fowlpoxvirus gene encoding the 4b core polypeptide and demonstration that it possesses efficient promoter sequences. *Virology*. 1989; 170:288–291.
2. Bolte AL, Meurer J, Kaleta EF. Avian host spectrum of avipoxviruses. *Avian Pathol*. 1999; 28:415–432.
3. Boulianne M. Viral diseases. In: *Avian Disease Manual*. 7th ed. Jacksonville, FL: American Association of Avian Pathologists, Inc.; 2013: 46-49.
4. El-Abasy MA, El-Khyate FF, Adayel SA, Hefny HY, El-Gohary AEA. Ostrich pox virus infection in farms at some Northern Egyptian governorates. *Alexandria J Vet Sci*. 2016; 49:80–89.
5. Espeseth DA, Lasher H. Early history of regulatory requirements for poultry biologics in the United States. *Avian Dis.* 2010;54(4):1136-1143.
6. Fitz-Coy SH. Parasitic diseases. In: *Avian Disease Manual*. 7th ed.

Jacksonville, FL: American Association of Avian Pathologists, Inc.; 2013: 154-155.
7. Fulton RM. Bacterial diseases. In: *Avian Disease Manual*. 7th ed. Jacksonville, FL: American Association of Avian Pathologists, Inc.; 2013: 134-135.
8. Gerlach H. Viruses. In: Ritchie BW, Harrison GJ, Harrison LR, eds. *Avian Medicine: Principles and Application*. Lake Worth, FL: Wingers Publishing; 1994:862–948.
9. Hargis AM, Myers S. The integument. In: Zachary JF, ed. *Pathologic Basis of Veterinary Disease.* 6th ed. St. Louis, MO: Elsevier; 2017:1039-1040.
10. Henriques AM, Fevereiro M. Avian poxvirus infection in a flamingo of the Lisbon Zoo. *J Zoo Wildl Med*. 2016;47:161–174.
11. Lehmbecker A, Rittinghausen S, Rohn K, Baumgärtner W, Schaudien D. Nanoparticles and pop-off technique for electron microscopy a known technique for a new purpose. *Toxicol Pathol*. 2014;42:1041–1046.
12. Mauldin EA, Peters-Kennedy J. Integumentary system. In: Maxie, MG, ed. *Jubb, Kennedy, and Palmer's Pathology of Domestic Animals.* Vol. 1. 6th ed. St. Louis, MO: Elsevier; 2016:616-625.
13. Mondal SP, Lucio-Martínez B, Buckles EL. Molecular characterization of a poxvirus isolated from an American Flamingo (*Phoeniconais ruber rubber*). *Avian Dis*. 2008;52:520–525.
14. Pledger A. Avian pox virus infection in a mourning dove. *Can Vet J*. 2005;46:1143–1145.
15. Ritchie BW. *Avian Viruses: Function and Control*. Lake Worth, FL: Winger's Publ.; 1995:285–311.
16. Terasaki T, Kaneko M, Mase M. Avian poxvirus infection in flamingos (*Phoenicopterus roseus*) in a zoo in Japan. *Avian Dis*. 2010;54:955–957.
17. Tripathy DN, Reed WM. In: Swayne DE, ed. *Diseases of Poultry*. 13th ed. Ames, IA: Wiley-Blackwell; 2013: 333-349.
18. Weli SC, Traavik T, Tryland M, Coucheron DH, Nilssen O. Analysis and comparison of the 4b core protein gene of avipoxviruses from wild birds: evidence for interspecies spatial phylogenetic variation. *Arch Virol*. 2004;149:2035–2046.
19. Weli SC, Tryland M. Avipoxviruses: infection biology and their use as vaccine vectors. *Virol J*. 2011;8:49.
20. Zimmermann D, Anderson MD, Lane E, van Wilpe E, Carulei O, et al. Avian poxvirus epizootic in a breeding population of Lesser Flamingos (*Phoenicopterus minor*) at Kamfers Dam, Kimberley, South Africa. *J Wildl Dis*. 2011;47:989–993.

CASE III: LJ84 (JPC 4101222).

Signalment: 1-year-old, male, Indian rhesus macaque, *Macaca mulatta*, primate.

History: Received bivalent pneumococcal/salmonella vaccination a year prior and 100 TCID50 of SIVmac251 intravenously five months prior to submission. Initially presented with soft stool and distended abdomen 2 weeks prior to being discovered recumbent with nystagmus and head tilt.

Abdomen, rhesus macaque The pancreas is hemorrhagic and diminished in size. (Photo courtesy of: Tulane National Primate Research Center, www2.tulane.edu/tnprc/)

Gross Pathology: The abdomen contains 20-30 ml of blood-tinged fluid. The pancreas is enlarged (5.5 x 8 x 3 cm) and hemorrhagic (Fig 1). There is edema of the capsule of the left kidney and the serosa of the duodenum. Formed feces noted in the colon.

Laboratory results:

	RBC	Hgb	Hct	WBC
PMN	Eo	Bas	Mon	Lym
Plt	Retic			
- 5 months	5.18	12.1	39.1	8.55
41.6	1.6	0.2	7.1	49.5
404K	0			
Presented	3.77	8.0	26.2	29.4
90.0	0	0	6.0	4.0
138K	10.3			

Blood chemistry is unremarkable.

Microscopic Description: Pancreas: The capsule of the pancreas is edematous and diffusely hemorrhagic and infiltrated with numerous neutrophils and small numbers of eosinophils and macrophages. Fibrin tags containing neutrophils are attached to the peritoneal surface. Large zones of the acinar pancreas are necrotic with multifocal hemorrhage and infiltration of variable numbers of neutrophils and small numbers of macrophages. Some blood vessels contain fibrin thrombi; vascular walls contain segmental foci of degeneration with PMN infiltration or complete necrosis. Surviving epithelial cells are swollen and many contain slightly enlarged nuclei with marginated chromatin and glassy basophilic intranuclear inclusions. IFA staining with anti-adenoviral monoclonal antibody confirms the presence of adenovirus in epithelial cell nuclei and cytoplasm. Stroma is edematous.

Contributor's Morphologic Diagnosis:
Pancreas: Pancreatitis, acute hemorrhagic, necrotizing, Adenovirus with fibrinous peritonitis and necrotizing vasculitis.

Contributor's Comment: Acute pancreatitis in humans is most often (80%) associated with biliary tract disease and alcoholism.[5] Clinical signs include epigastric abdominal pain (80-95%), nausea and vomiting (40-80%), and abdominal distension (21-46%) with some displaying fever, jaundice, ascites, and pleural

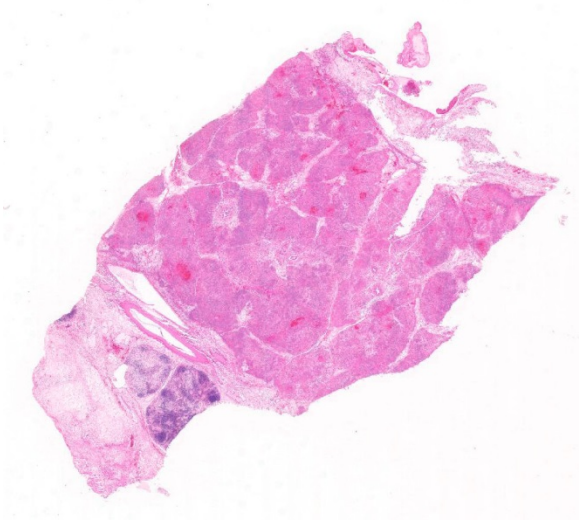

Pancreas, rhesus macaque. A section of pancreas, and adjacent mesentery and lymph node is presented. The pancreas, while maintaining its overall lobular architecture, lacks the characteristic basophilia of a healthy pancreas. (HE, 5X)

effusion.[2] In most instances, gallstones and/or inflammation reduces outflow of digestive proenzymes, allows back-diffusion of these secretions across the pancreatic ducts, and activation of the proenzymes.[5] High ethanol concentrations can induce spasm or edema of the sphincter of Oddi, as well as induce production of secretin from the small intestine triggering more pancreatic secretions.[7] Protease inhibitors like alpha-1-antitrypsin, alpha-2-macroglobulin, c-1-esterase inhibitor, and pancreatic secretory trypsin inhibitor in body fluids and tissues protect against activation of nascent proenzymes stored and transported in membrane bound granules. However, protection is incomplete since, in the presence of calcium, trypsin bound to inhibitor still has some tryptic activity that activates other proenzymes.[7] Damage to acinar cell membranes, ducts and blood vessels rapidly compounds the injury adding hemorrhage and anoxia.

Other causes of acute pancreatitis include drugs, hyperlipidemia, hypercalcemia, viral infections (mumps, coxsackievirus, hepatitis B, CMV, varicella, herpes simplex, adenovirus, HIV), bacterial and fungal infections (Mycoplasma, Legionella, Leptospira, Salmonella, Aspergillus, Toxoplasma, Cryptosporidium), vascular diseases, pregnancy and ascariasis.[6] Drugs like the thiazide diuretics induce hypercalcemia; estrogens and HIV protease inhibitors induce hypertriglyceridemia with production of toxic free fatty acids, vascular damage and thrombosis.[6] Blood and bone marrow transplantation have been linked to acute pancreatitis by a variety of mechanisms including drug toxicity, graft-versus-host-disease, and adenoviral infection.[3]

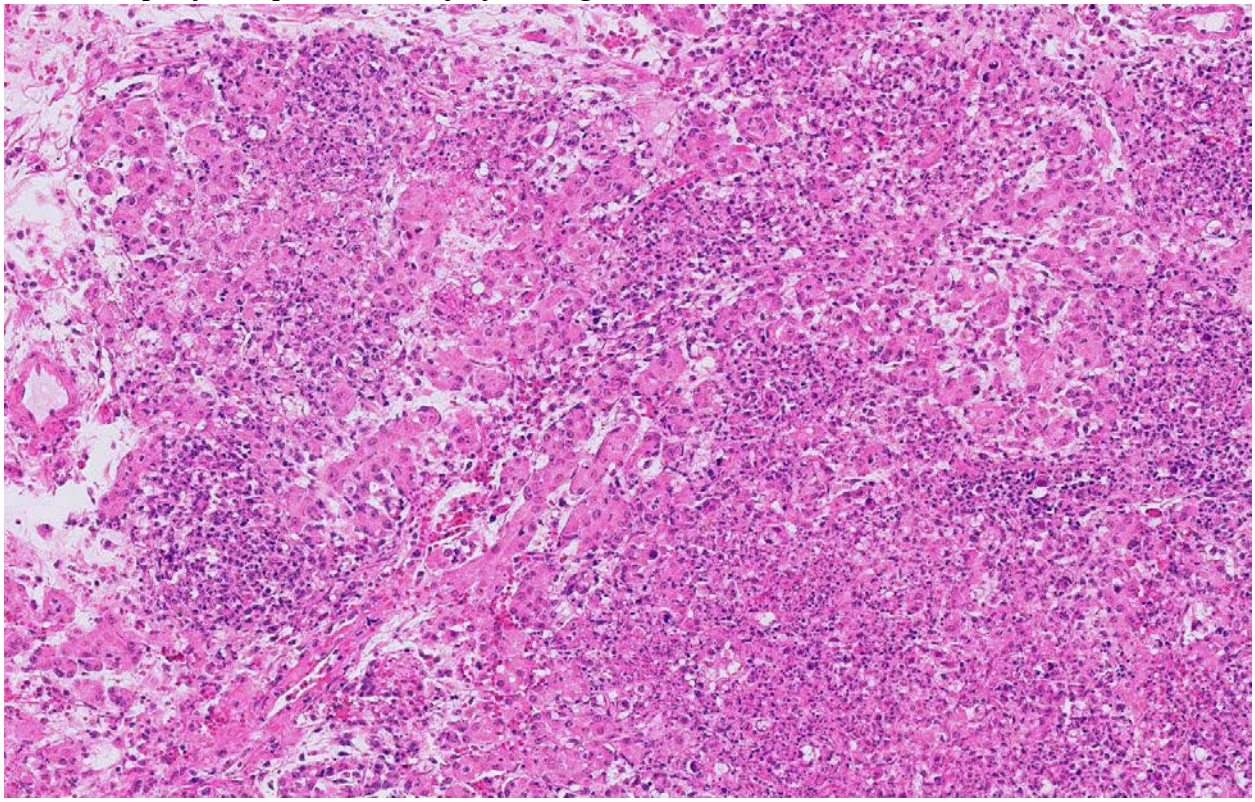

Pancreas, rhesus macaque. There is extensive lytic necrosis of the acinar pancreas with loss of architecture and infiltration of numerous viable and degenerate neutrophils, admixed with abundant cellular debris (HE, 260X)

More specific to simian research, pancreatitis is rarely reported but half the cases are associated with adenovirus.[4] We have found most adenoviral infections to be associated with SIV infection (91%) with 45% of these presenting with acute pancreatitis (unpublished). Adenoviral replication with movement of virus to the cytoplasm accounts for the extensive liver necrosis observed in chick embryos[1] and

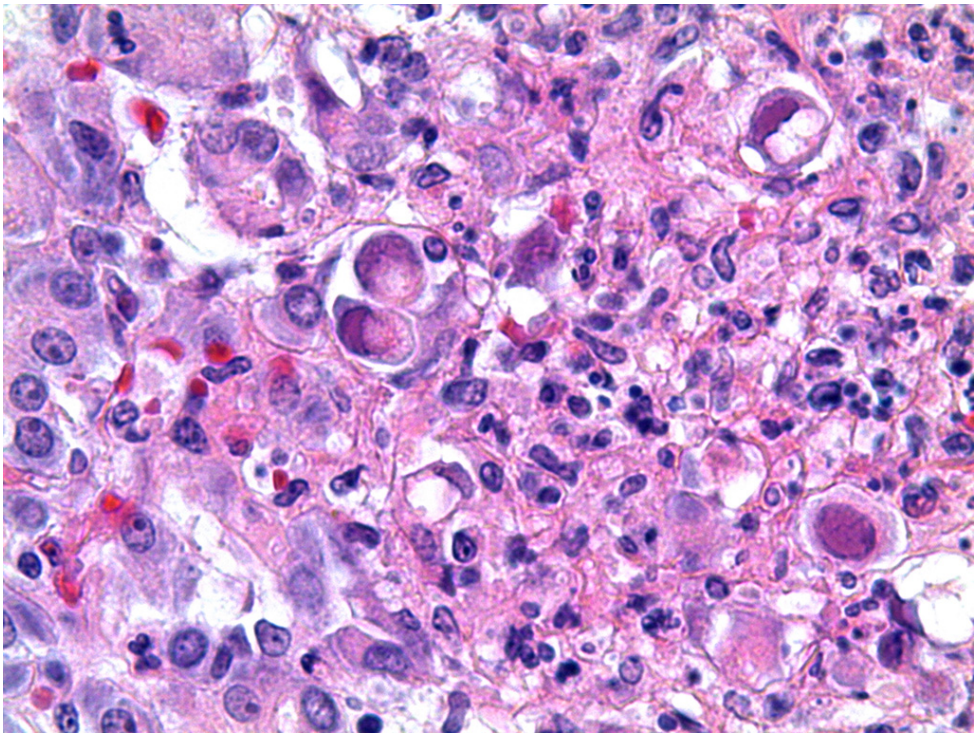

Pancreas, rhesus macaque. Degenerating acinar cells are karyomegalic with single large glassy basophilic intranuclear adenoviral inclusion. (HE, 400X)

given the large amounts of virus detected by IFA in the submitted case, in is not hard to speculate that cell lysis could easily overwhelm the protective inhibitors in tissue fluids.

Recent work with an acute pancreatitis mouse model induced by starvation has shown a critical role for small GTPase Rab7 in intracellular vesicle transport of lysosomes involved in autophagy and endocytosis.[8] Pancreas-specific-Rab7-deficient mice exhibited enhanced disease due to blockade of endosome maturation suggesting that Rab7 may be a therapeutic target.

JPC Diagnosis: Pancreas: Pancreatitis, necrotizing, diffuse, severe with mild necrotizing steatitis and ductal and acinar intranuclear basophilic viral inclusion bodies, Indian rhesus macaque (*Macaca mulatta)*, primate.

Conference Comment: Within the family Adenoviridae, of which there are numerous ubiquitous viruses that affect a wide number of species, the genus *Mastadenovirus* contains the human and nonhuman primate isolates. The name "adenovirus" is derived from adenoid, meaning the lymphoid tissue of the nasopharynx, because the first isolates were obtained from those locations in military recruits suffering from upper respiratory tract infections. There are over 50 serotypes of adenovirus that has been isolated from nonhuman primate species (macaques, African green monkeys, baboons, chimpanzees, gorillas, orangutans, squirrel monkeys, owl monkeys, and cotton-topped tamarins), and they tend to cause respiratory or enteric disease in immune suppressed animals. In fact, adenoviruses have been isolated from healthy animals,

suggesting that persistent infections are common.[9]

When on immunosuppressive drugs or infected concomitantly with immunosuppressive viruses (SIV and betaviruses) respiratory tract infections with adenovirus results in necrosis of epithelial cells of the trachea, bronchi, bronchioles, and alveoli. The gastrointestinal tract is the second most common organ system infected, characterized microscopically by mucosal erosion or ulceration with necrotic enterocytes containing prominent adenoviral inclusions. There have been numerous reports of adenoviral-induced pancreatitis which seem to occur most frequently in young macaques, as in this case, that have been severely immunocompromised by SRV-1, SRV-2, and SIV.[4] Even less common are necrotizing lesions of the liver, kidney, and urinary bladder which microscopically appear as necrotizing hepatitis, tubulointerstitial nephritis, and hemorrhagic cystitis with the aforementioned intranuclear inclusions. Although these inclusions are prominent in infected animals, they may resemble CMV and SV40 which also produce basophilic intranuclear inclusions, albeit resulting in significant nucleomegaly and cytomegaly.[9]

Conference participants commented on additional changes within these tissues. Within the remaining areas of intact pancreas (which were rare), there was evidence of acinar atrophy with cell shrinkage, loss of zymogen granules, and an overall increase in the acinar luminal size. , Vasculitis and thrombosis was identified in and away from areas of necrosis. In areas of necrosis, it was easier to attribute vascular necrosis to the ongoing devastation in the surrounding tissues. In areas away from the necrosis, participants searched for adenoviral inclusions within endothelium,

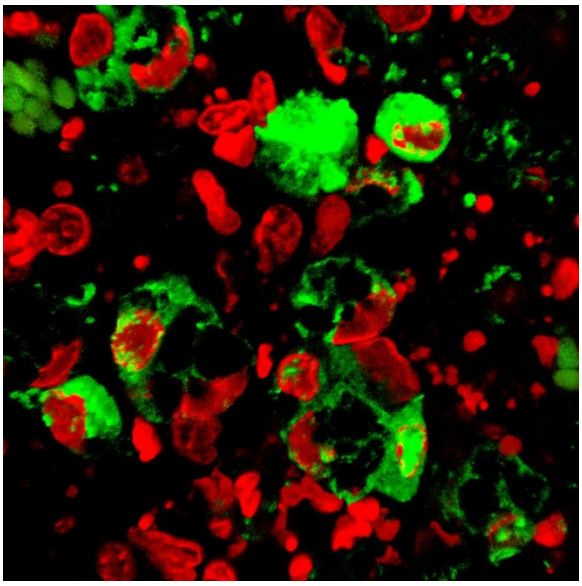

Pancreas, rhesus macaque, IFA. Adenovirus (green) demonstrated in nuclei and cytoplasm of many epithelial cells. Stains: anti-adenovirus IgG2, Chemicon cat#MAB8052, secondary goat-anti-mouse IgG1 with Alexa 488 Life Technologies cat# A21121, Topro3 counter stain (red) Thermo Fisher.

but none were identified. Finally, participants identified changes within the adjacent pancreatic lymph node which included edema and increased numbers of neutrophils within cortical and medullary sinuses, but rather than suggest a separate necrotizing process in the lymph node, participants decided that the lymph node was simply draining the adjacent area of inflammation.

Contributing Institution:
Tulane National Primate Research Center
www.tulane.edu/tnprc/

References:

1. Alemnesh W, Hair-Bejo M, Aini I, Omar AR. Pathogenicity of fowl adenovirus in specific pathogen free chicken embryos. *J Comp Path*. 2012;146:223-229.
2. Bai HX, Lowe ME, Husian SZ. What have we learned about acute pancreatitis

in children? *J Pediatr Gastroenterol Nutr*. 2011;52(3):2262-270.
3. Bateman CM, Kesson SM, Shaw PJ. Pancreatitis and adenoviral infection in children after blood and marrow transplantation. *Bone Marrow Transplantation*. 2006;38:807-811.
4. Chandler FW, McClure HM. Adenoviral pancreatitis in rhesus monkeys: current knowledge. *Vet Pathol*. 1982;Suppl 7:171-180.
5. Cotran RS, Kumar V, Collins T. *Robbins and Cotran Pathologic Basis of Disease*. 6th ed. Philadelphia, PA: Elsevier; 1999:904-907.
6. Hung WY, Lanfranco OA. Contemporary review of drug-induced pancreatitis: A different perspective. *World J Gastointestinal Pathophys*. 2014;5(4):405-415.
7. Rubin E, Farber JL. *Pathology*. Philadelphia, PA: Lippincott Williams & Williams; 1988:812-816.
8. Takahashi K Mashima H, Miura K, Maeda D, Goto A, Goto T, Sun-Wada G, Wada Y, Ohnishi H. Disruption of small GTPase Raby exacerbates the severity of acute pancreatitis in experimental mouse models. *Science Reports*. 2017;7(2817):1-16.
9. Wachtman L, Mansfield K. Viral diseases of nonhuman primates. In: Abee CR, Mansfield K, Tardif S, Morris T, eds. *Nonhuman Primates in Biomedical Research: Diseases*. Vol. 2. Waltham, MA: Academic Press; 2012:27-30.

CASE IV: 401343 (JPC 4103279).

Signalment: 4-year-old, female, Scottish blackface sheep, *Ovis aries*, ovine.

History: The animal was referred for ill thrift and respiratory distress.

Presentation, sheep. Tipping the JRSV-infected sheep with placement of head downwards ("wheelbarrow test") releases large amounts of clear, white fluid from the respiratory tract. (Photo courtesy of: Division of Pathology, Public Health and Disease Investigation , Veterinary Diagnostic Services, School of Veterinary Medicine, College of Medical, Veterinary and Life Sciences, University of Glasgow (Garscube Campus), 464 Bearsden Road, Glasgow G61 1QH, Scotland, http://www.gla.ac.uk/schools/vet/)

Gross Pathology: This animal is in poor body condition (BCS: 1.5/5). Small amounts of white froth are noted at the nares and within the lumen of the trachea. In a multifocal to coalescing distribution and affecting predominantly the right middle and caudal pulmonary lobes, the pulmonary parenchyma is effaced by multiple, reasonably well-demarcated, pale pink to grey, firm masses. On cut surface, small amounts of clear fluid run from the surface of the masses, which have a grey, granular appearance.

Laboratory results: None provided.

Microscopic Description: Lung: Affecting approximately 50% of the pulmonary parenchyma are multiple, well-demarcated, yet infiltrative, moderately to highly cellular, multifocal to coalescing neoplastic masses composed of epithelial cells arranged in a predominantly lepidic, rarely acinar or even papillary pattern, which are supported by small amounts of poorly to moderately cellular collagenous stroma. Lining the alveoli is an, in most cases, single layer of cuboidal to columnar neoplastic cells with distinct cell borders, moderate to large amounts of eosinophilic, often also vacuolated cytoplasm, a round to oval basal nucleus with ropey, clumped and vesiculated chromatin and a small, basophilic nucleolus. There is minimal to mild anisocytosis and anisokaryosis, and four mitotic figures are present in 10 HPF, some of which are bizarre. Multifocally present within the lumina of the neoplastic-lined alveolar spaces or acini are small to moderate amounts of pale eosinophilic material and small numbers of neutrophils, macrophages, occasional small to moderately sized accumulations of extravasated erythrocytes (hemorrhage) and sloughed epithelial cells. The supporting stroma multifocally exhibits mildly dispersed collagenous fibers (edema), small numbers of extravasated red blood cells (hemorrhage) and in a multifocal to coalescing distribution contains small to moderate numbers of lymphocytes, plasma cells and smaller numbers of neutrophils. The alveolar spaces in the periphery of the neoplastic nodules also contain moderate numbers of alveolar macrophages, smaller numbers of neutrophils, occasional lymphocytes and multifocally, moderate to large numbers of extravasated erythrocytes. Multifocally, surrounding the bronchioles are small to moderate numbers of lymphocytes and plasma cells in a multifocal to coalescing distribution.

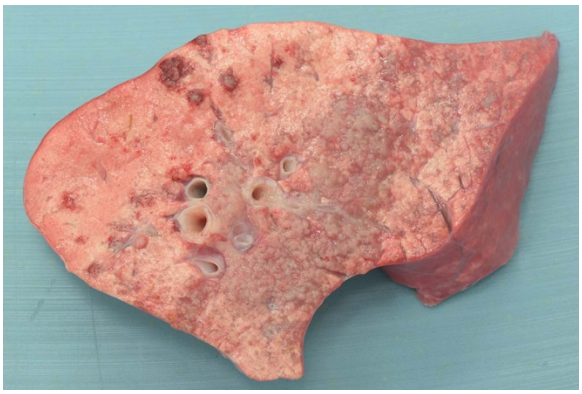

Lung sheep. The cut section of the affected lung in this animal exhibits multifocal to coalescing, small, grey, granular masses. (Photo courtesy of: Division of Pathology, Public Health and Disease Investigation, Veterinary Diagnostic Services, School of Veterinary Medicine, College of Medical, Veterinary and Life Sciences, University of Glasgow (Garscube Campus), 464 Bearsden Road, Glasgow G61 1QH, Scotland, http://www.gla.ac.uk/schools/vet/)

Contributor's Morphologic Diagnosis: Lung: Pulmonary adenocarcinoma, multifocal to coalescing.

Contributor's Comment: Ovine pulmonary adenocarcinoma (OPA; also known as Jaagsiekte or ovine pulmonary adenomatosis) is an infectious and contagious neoplastic disease caused by a beta retrovirus, Jaagsiekte sheep retrovirus (JSRV), an enveloped RNA virus that primarily targets sheep but also, rarely goats. This disease is present worldwide, and is particularly common in South America, South Africa and Scotland with certain breeds of sheep exhibiting a predisposition. It is absent in Australia and New Zealand and has been eradicated in Iceland.[5,9]

Affected animals typically present with progressive dyspnea, tachypnea, nasal discharge, coughing and weight loss.[5] A characteristic feature of this disease is the production of excessive amounts of frothy to milky fluid (surfactant proteins) from the nostrils especially when the head is lowered (wheelbarrow test), although it has been

reported the amounts of fluid produced can be variable between individuals.[7]

Multifocal or locally extensive neoplasms are found in the pulmonary parenchyma with metastases to the regional lymph nodes occurring in approximately 0.3-25% of cases. More distant metastases are rare but when present, they can spread to different organs with in order of frequency: liver, kidneys, skeletal muscle, digestive tract, spleen, skin and adrenal glands.[11]

JRSV induces oncogenic transformation of type II pneumocytes, Clara cells and progenitor cells of the pulmonary airway epithelia[8,9], however the exact pathogenic mechanisms of viral neoplastic transformation are poorly understood. It has been reported that attachment of the virus to the host cell is mediated through the binding of the SU subunit of the viral Env protein (envelope protein) to a specific cell surface receptor, Hyal2 on the host cell[9,12], which in turn mediates the entry of the virus into the cell via endocytosis.[3] As with all RNA viruses, reverse transcription, where the single-stranded RNA genome is converted into a double-stranded, DNA genome, then takes place within the cytoplasm, which is essential for integration of the virus into the host genome.[9] The Env protein has been shown to be able to induce similar tumors in immunodeficient mice and has also been shown to induce oncogenesis in rat fibroblasts, however as stated previously, the mechanisms are not clearly known.[12]

Spread of JRSV between sheep occurs through respiratory secretions from affected sheep. Additionally, lambs can be infected through their dams from the ingestion of infected colostrum.[4]

Two forms of OPA have been described, the classical and the atypical form. In the

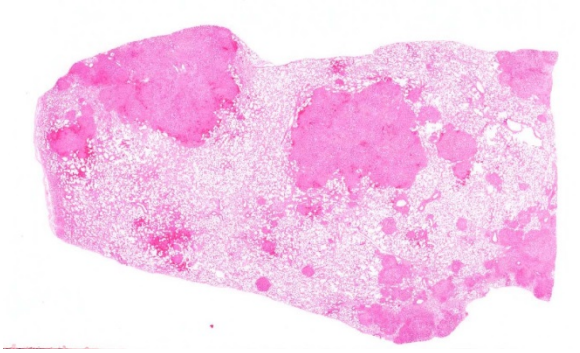

Lung, sheep. The submitted section of lung contains numerous well-demarcated neoplastic nodules ranging up to 5mm in diameter. (HE, 5X)

classical form, sheep present with the clinical signs as described above and typically contain multifocal to coalescing neoplastic lesions in the cranioventral pulmonary lung lobes. Grossly, the lungs are heavy, wet and fail to collapse. On cut surface, the tumors often have a grey, granular appearance and large amounts of fluid run from the surface. In contrast, the atypical form often follows a subclinical course and grossly, neoplasms are seen in the diaphragmatic lung lobes. Tumors in the atypical form are dry, white and have a multifocal distribution.[9,11]

Microscopically, the histopathological features of both the classic and the atypical form are similar with several patterns including the lepidic pattern where the alveoli are lined by either cuboidal or columnar neoplastic cells. Other patterns include the papillary and acinar patterns.[5,9] The atypical form differs from the classical one by having more well-demarcated neoplastic lesions which are associated with larger numbers of mononuclear cells, in particular CD4 and CD8 T-cell subsets, as well as increased amounts of fibrous tissue. It has been suggested that infiltration of mononuclear cells into the tumors of atypical cases may be due to an immunological response to tumorigenesis, whereas in the classical form, there is suppression of such infiltration.[2,13]

Neoplastic processes can be complicated by the presence of concurrent infections including Maedi-Visna, a viral infection caused by a non-oncogenic retrovirus and resulting in interstitial pneumonia with the formation of prominent lymphoid nodules as well as interstitial fibrosis and hypertrophy of smooth muscle. In addition, bacterial infections are prevalent in a large number of sheep affected by OPA, such as those caused by *Mycoplasma* spp, and may contribute to death of the animal.[6,9]

Although rare, non-viral pulmonary carcinomas are difficult to distinguish from ovine pulmonary adenocarcinoma based on the gross and histological lesions alone and immunohistochemistry is required to detect the JSRV envelope glycoprotein for definitive confirmation.[5]

Clinically, a further viral-induced epithelial tumor, however present in the nasal cavity, can produce similar clinical signs of increased fluid production from the nostrils. The enzootic nasal tumor is also caused by a retrovirus, the enzootic nasal tumor virus type 1 (ENTV-1) in sheep and the enzootic nasal tumor virus type 2 (ENTV-2) in goats, which infects the secretory epithelial cells of the nasal glands and here leads to the formation of nasal epithelial masses with abundant secretion of mucus.[9,14]

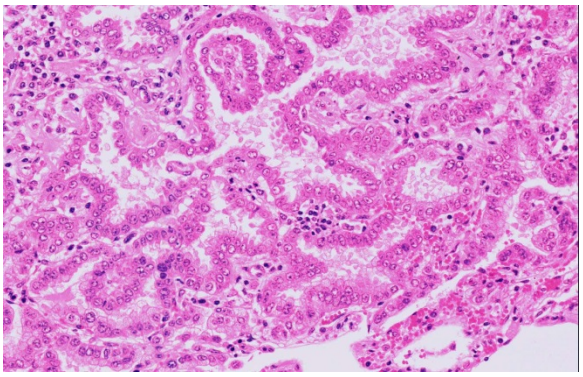

Lung, sheep. Neoplastic columnar epithelium is arranged in a lepidic pattern along alveolar septa and occasionally form papillary projections into alveolar lumina. There is infiltration of low to moderate numbers of lymphocytes, macrophages, and few few neutrophils within the edematous stroma. (HE, 256X)

JPC Diagnosis: Lung: Pulmonary adenocarcinoma, Scottish blackface sheep (*Ovis aries)*, ovine.

Conference Comment: Jaagsiekte sheep retrovirus (JSRV) belongs to the family *Retrovirdae*, subfamily *Orthoretrovirinae*, and genus *Betaretrovirus.* JSRV (as described above) is the causative agent of contagious lung tumors in sheep called ovine pulmonary adenocarcinoma. The term "jaagsiekte" is taken from the Afrikaans words for "chase" (jag) and "sickness" (siekte) describing the common clinical scenario of sheep that exhibit respiratory distress from being chased. The infectious "exogenous" form of JRSV has an endogenous counterpart (enJRSVs) which is present in the genome of healthy sheep and goats.[15] Sheep have approximately 27 copies of enJRSVs that are able to block the JSRV replication cycle and have an essential role in fetal development and formation of the placenta.[1]

JRSV is transmitted via respiratory droplets and infect respiratory epithelial cells (type II pneumocytes or Clubb cells) as well as lymphocytes and myeloid cells, but replicates most in alveolar type II pneumocytes and Club cells.[10] This virus has the typical "gag", "pol", and "env" genome arrangement bordered on each end by a long terminal repeat (LTR). The "gag" portion encodes the internal structural matrix, capsid, and nucleocapsid proteins. "Pol" encodes the RT and integrase enzymes. Most importantly, "env" encodes surface and transmembrane envelope glycoproteins which aid in viral cellular

entry and directly stimulate neoplastic transformation of type II pneumocytes and/or Club cells.[9]

An interesting feature of JRSV infection is lack of host immune response. There are two possible explanations for this phenomenon. (1) The sheep may be immunologically tolerant to JRSV due to the already present enJRSV that would be expressed in the fetal thymus during T-cell development. Thus, any anti-JRSV reactive T-cells would be removed via self-tolerance mechanisms. (2) Another possibility is that tumor cells downregulate their expression of MHC-I. This hypothesis is supported by research that has identified an absence of virus-specific cytotoxic T-cells.[9]

Contributing Institution:

Division of Pathology, Public Health and Disease Investigation
Veterinary Diagnostic Services
School of Veterinary Medicine
College of Medical, Veterinary and Life Sciences
University of Glasgow (Garscube Campus)
464 Bearsden Road
Glasgow G61 1QH, Scotland
http://www.gla.ac.uk/schools/vet/

References:

1. Arnaud F, Varela M, Spencer TE, Palmarini M. Coevolution of endogenous betaretroviruses of sheep and their host. *Cell. Mol. Life Sci*. 2008;65(21):3422–3432.
2. Azizi S, Tajbakhsh E, Fathi F. Ovine pulmonary adenocarcinoma in slaughtered sheep: A pathological and polymerase chain reaction study. *J S Afr Vet Assoc*. 2014;85:932.
3. Bertrand P, Cote M, Zheng Y-M, et al. Jaagsiekte sheep retrovirus utilizes a pH-dependent endocytosis pathway for entry. *J Virol*. 2008;82:2555-2559.
4. Borobia M, De las Heras M, Ramos JJ, et al. Jaagsiekte sheep retrovirus can reach Peyer's patches and mesenteric lymph nodes of lambs nursed by infected mothers. *Vet Pathol*. 2016;53:1172-1179.
5. Caswell JL, Williams KJ. Respiratory system. In: Maxie MG, ed. *Jubb, Kennedy and Palmer's Pathology of Domestic Animals*. 6th ed. Vol. 2: St. Louis, MO: Elsevier Ltd; 2016:560-562.
6. Cousens C, Gibson L, Finlayson J, et al. Prevalence of ovine pulmonary adenocarcinoma (Jaagsiekte) in a UK slaughterhouse. *Vet Rec*. 2015;176:413.
7. Cousens C, Thonur L, Imlach S, et al. Jaagsiekte sheep retrovirus is present at high concentration in lung fluid produced by ovine pulmonary adenocarcinoma-affected sheep and can survive for several weeks at ambient temperature. *Res Vet Sci*. 2009;87:154-156.
8. De las Heras M, de Martino A, Borobia M, et al. Solitary tumours associated with Jaagsiekte retrovirus in sheep are heterogenous and contain cells expressing markers identifying progenitor cells in lung repair. *J Comp Pathol*. 2014;150:138-147.
9. Griffiths DJ, Martineau HM, Cousens C. Pathology and pathogenesis of ovine pulmonary adenocarcinoma. *J Comp Pathol*. 2010;142:260-283.
10. Lopez A, Martinson SA. The respiratory system. In: McGavin MD, Zachary JF, eds. *Pathologic Basis of Veterinary Disease*. 6th ed. St. Louis, MO: Elsevier;2016:553-554.
11. Minguijon E, Gonzalez L, De las Heras M, et al. Pathological and aetiological studies in sheep exhibiting extrathoracic metastases of ovine pulmonary adenocarcinoma (Jaagsiekte). *J Comp Pathol*. 2013;148:139-147.

12. Rai SK, Duh FM, Vigdorovich V, et al. Candidate tumor suppressor HYAL2 is a glycosylphosphatidylinositol (GPI)-anchored cell-surface receptor for Jaagsiekte sheep retrovirus, the envelope protein of which mediates oncogenic transformation. *Proc Natl Acad Sci USA*. 2001;98:4443-4448.
13. Summers C, Benito A, Ortin A, et al. The distribution of immune cells in the lungs of classical and atypical ovine pulmonary adenocarcinoma. *Vet Immunol Immunopathol.* 2012;146:1-7.
14. Walsh SR, Linnerth-Petrik NM, Yu DL, et al. Experimental transmission of enzootic nasal adenocarcinoma in sheep. *Vet Res.* 2013;44:66.
15. York DF, Querat G. A history of ovine pulmonary adenocarcinoma (jaagsiekte) and experiments leading to the deduction of the JSRV nucleotide sequence. *Curr. Top. Microbiol. Immunol*. 2003;275:1–23.

Self-Assessment - WSC 2017-2018 Conference 15

1. What is the most likely foodborne source for herpesviral infection in owls?
    a. Chickens
    b. Mice
    c. Sparrows
    d. Pigeons

2. A septicemic form of avian poxviral infection which has up to 99% mortality is seen in what species of birds?
    a. Ducks and geese
    b. Canaries and finches
    c. Chickens
    d. Emus

3. Which of the following viruses has not been associated with adenoviral-induced pancreatitis?
    a. Simian immunodeficiency virus
    b. Simian retrovirus-1
    c. Simian retrovirus-2
    d. Simian lymphocryptovirus

4. Which of the following cell types best support replication of JRSV in the lung?
    a. Type I pneumoncytes
    b. Airway epithelium
    c. Respiratory gland epithelium
    d. Type II pneumocytes

5. Which of the following is not characteristic of the atypical form of JRSV?
    a. There is minimal fluid formation
    b. Type I pneumocytes are infected and become neoplastic
    c. The atypical form follows a subclinical course.
    d. Neoplasms are seen in diaphragmatic lobes

Please email your completed assessment to Ms. Jessica Gold at Jessica.d.gold2.ctr@mail.mil for grading. Passing score is 80%.This program (RACE program number) is approved by the AAVSB RACE to offer a total of 0.5 CE Credits, with a maximum of 12.5 CE Credits being available to any individual Veterinary Medical Professionals for the 2017-2018 Wednesday Slide Conference. This RACE approval is for the subject matter categories of: SCIENTIFIC using the delivery method of NON-INTERACTIVE DISTANCE. This approval is valid in jurisdictions which recognize AAVSB RACE; however, participants are responsible for ascertaining each board's CE requirements.
RACE does not "accredit", "endorse" or "certify" any program or person, nor does RACE approval validate the content of the program.

Joint Pathology Center
Veterinary Pathology Services

WEDNESDAY SLIDE CONFERENCE 2017-2018

Conference 16

24 January 2018

CASE I: F16-0079.3 (JPC 4101317).

Signalment: 5-year-old, male, Green tree python, *Morelia viridis*, reptile.

History: The animal showed acute respiratory distress and discharge of mucus from the oral and nasal cavity. Two days after the onset of symptoms the animal was found dead.

Gross Pathology: A marked thickening of the lung parenchyma and a severe accumulation of clear mucus in the upper and distal airways (larynx, trachea, lung, air sacs) were noted at gross examination. The animal was in moderate body condition and the carcass was slightly dehydrated. All other internal organs showed no macroscopic changes.

Laboratory results: The presence of nidoviral RNA (Morelia viridis Nidovirus, "MVNV") was confirmed through RT-PCR of the affected lung tissue and intracellular nidoviral protein was detected via immunohistochemistry in respiratory and faveolar epithelial cells of the lungs. Infected epithelial cells were also found in the trachea and the nasal cavity. A markedly increased proliferative activity was noted in all epithelial cell layers of the diseased lung via a PCNA marker. Additionally, the immunohistochemical examination for the detection of active-caspase 3 revealed an increased number of apoptotic epithelial cells in the lung of the infected animals.

Microscopic Description: The two histologic hallmarks are the epithelial thickening in the entire lung and excess mucus in the lumen of lungs and airway. The multilayered respiratory epithelium covering the smooth muscle at the luminal end of the trabeculae displays increased cellularity with an increase in cell layers and irregular cell arrangement (hyperplasia). In the faveolar space, the epithelium is characterized by patchy to diffuse proliferations of cuboidal to columnar cells carrying short microvilli (type II pneumocytes) and rare flat cells with short

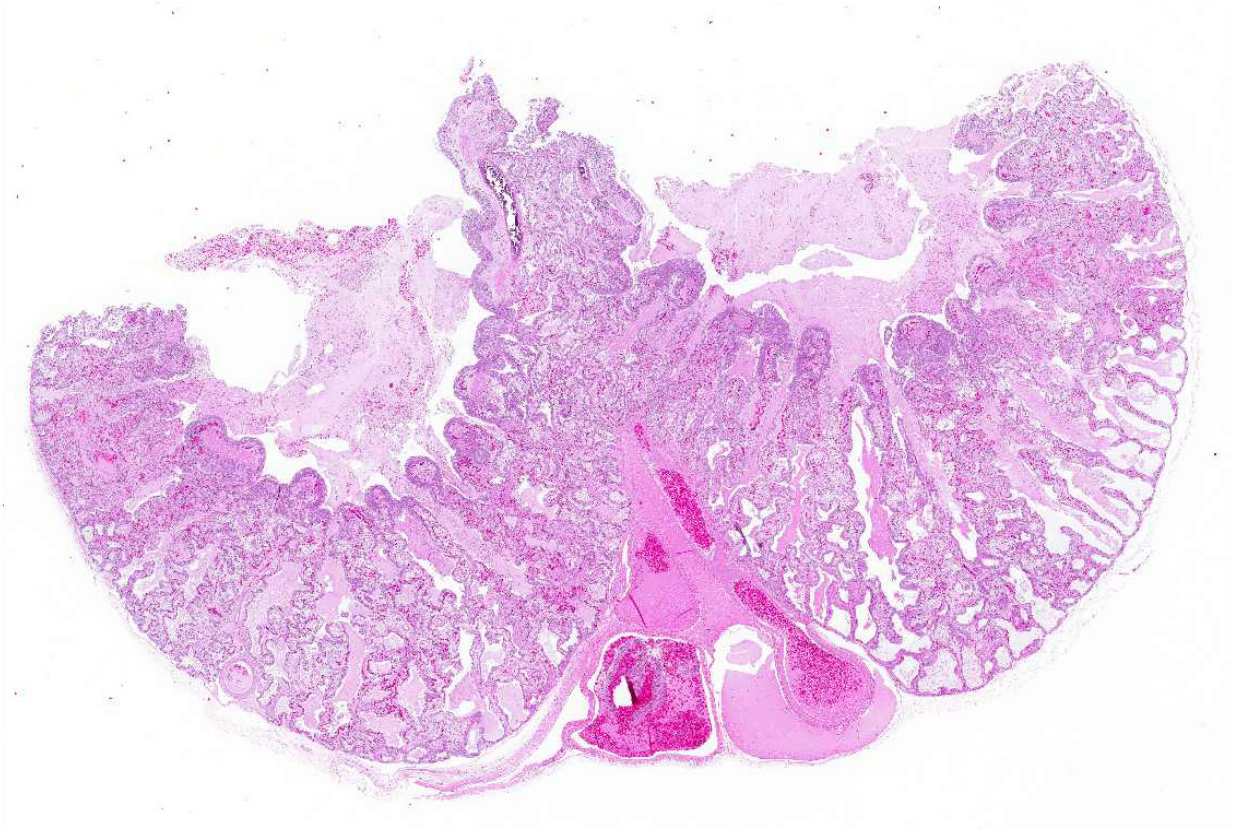

Lung, green tree python. Subgross image of the lung demonstrates marked edema within the airway and faveolae. Faveolar septa are markedly expanded and the respiratory epithelium is markedly hyperplastic. (HE, 400X).

cytoplasmic projections covering the capillaries (type I pneumocytes). The inflammatory component is represented by moderate, multifocal to diffuse interstitial infiltration of lymphocytes, plasma cells and heterophilic granulocytes. Multifocal heterophilic granulocytes and lymphocytes also infiltrate the respiratory epithelium. The lymphoid aggregates (equivalent to the mammalian bronchiolar-associated tissue) are activated. Abundant homogenous eosinophilic fluid (mucus) is filling the faveolar space, admixed with numerous heterophilic granulocytes, erythrocytes and cell debris.

Contributor's Morphologic Diagnosis:
Lung: Proliferative pneumonia, severe, diffuse with type II pneumocyte hyperplasia and mucus accumulation in the faveolar space.

Contributor's Comment: The *Morelia viridis* nidovirus belongs to the subfamily of the Torovirinae (Family Coronaviridae), which have so far mainly been associated with enteric diseases (humans, horses, cattle, swine).[4,11,13,16] However, recent studies on toroviruses have shown that they can be both entero- and pneumotropic.[14] In the last two years snake nidoviruses have been identified as the causative agent of a severe respiratory disease in ball pythons, green tree pythons[3] and Indian pythons.[2,8,9,12] Nidoviruses were also identified in the lungs of cattle and wild shingleback lizards with pneumonia, though their direct association with disease has so far not been examined.[9,14]

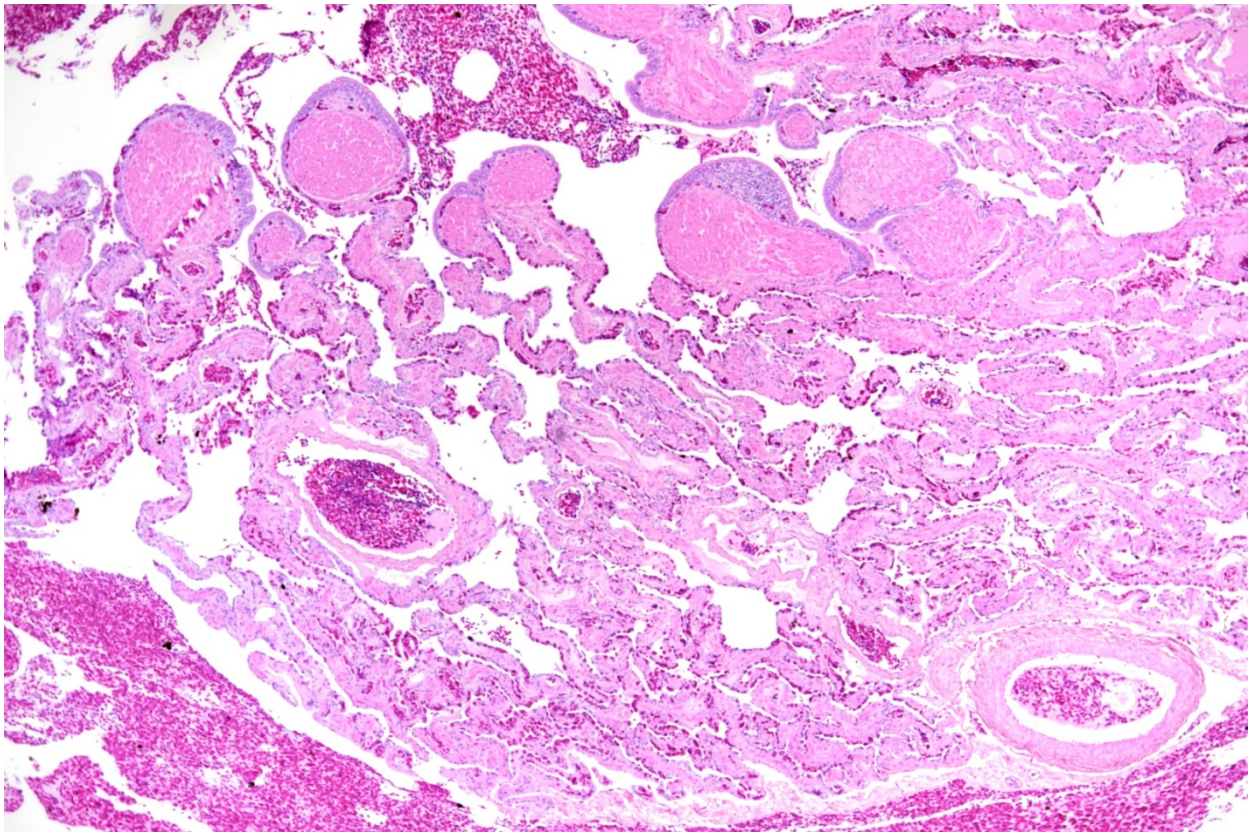

Lung, green tree python. Histological appearance of a healthy snake lung (HE, 400X). (Photo courtesy of: Institute of Veterinary Pathology Vetsuisse-Faculty (University of Zurich), Winterthurerstrasse 268, CH-8057 Zurich, Fax number +41 44 635 89 34, www.vetpathology.uzh.ch)

In the python lung, nidovirus infection is associated with a distinct proliferative activity and a degree of apoptotic cell death of both type I and type II pneumocytes, leading to an increased epithelial turnover and hyperplasia.[3]

In the faveolar space of the healthy snake lung, thin cytoplasmic extensions of the type I pneumocytes cover the capillary walls, forming the gas-blood barrier.[10] This case nicely demonstrates a marked replacement of type I pneumocytes by type II pneumocytes in the faveolar space, known as an unspecific regenerative response of snakes to infectious agents, similar to response to lung injury in mammals.[5] In the healthy reptilian lung, lamellated bodies containing surfactant can be demonstrated through electron microscopy in type II pneumocytes. Following the nidoviral infection, "transformed" type II pneumocytes containing intracytoplasmic serous/mucous granules are noted ultrastructurally in the faveolar space.[3] This epithelial cell type has been previously described in various reptile species and is likely to explain the pathognomonic excess in mucus production in nidoviral pneumonia[7,10] and indicate an decrease in surfactant production.[3] In the present case viral protein could be detected in the epithelium of the entire respiratory tract (nasal cavity, larynx, trachea, lung and air sacs) and indicates a respiratory transmission (droplet) as the most likely infection route. Nidoviruses cause sudden outbreaks with high mortality in breeding collections, symptoms prior to deceasing/death are rare.

JPC Diagnosis: Lung: Pneumonia, bronchointerstitial, necrotizing, diffuse, mild with marked respiratory and type II pneumocyte hyperplasia and faveolar edema, Green tree python (*Morelia viridis*), reptile.

Conference Comment: Nidoviruses are a diverse group, affecting humans and a growing population of veterinary species including: snakes, wild shingleback lizards, cattle, and nematodes. Nidoviruses that affect animal species are from the *Coronaviridae* family and *Torovirinae* subfamily. Specifically, the *Torovirus* genus affects mammals and the little known *Bafinivirus* genus affects ray-finned fish. There have been disagreements regarding the classification of reptile nidoviruses which have not been formally classified to date.[1] Regardless of the phylogenetic differences, toroviruses all share similar tissue tropism for the gastrointestinal and respiratory tracts.

Snake-associated nidoviruses were first identified in ball pythons (*Python regius*) and Indian rock pythons (*P. molurus*) in 2014[2,12,15] and green tree pythons (*Morelia M. viridis*) in 2017.[3] Gross findings in these snakes include: stomatitis, sinusitis, pharyngitis, tracheitis, esophagitis, and proliferative pneumonia with abundant mucus secretion.

More and more over the past several years, nidovirus infection has been associated with fatal respiratory disease in several species of python, but Koch's postulates had not

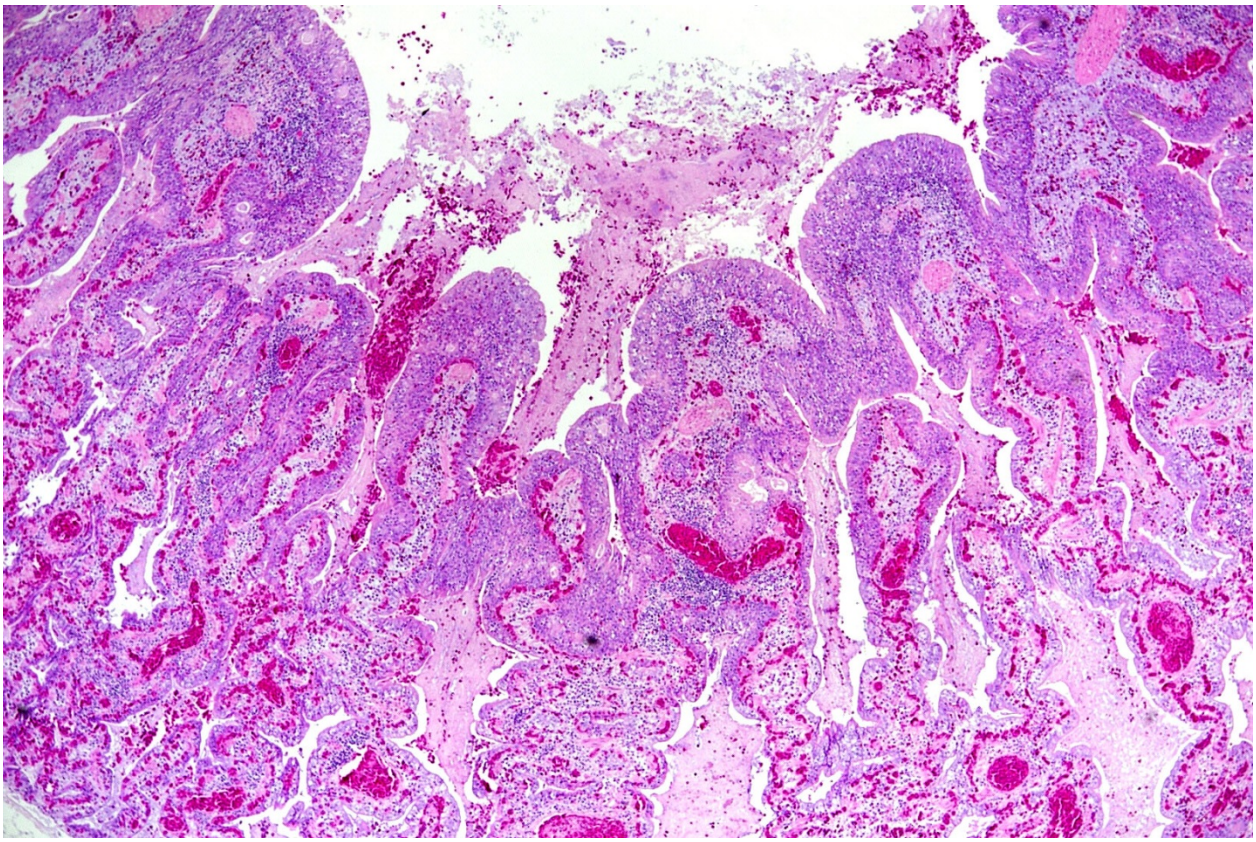

Lung, green tree python. Marked thickening of the entire epithelium (hyperplasia) with a moderate mixed-cellular interstitial inflammation and accumulation of mucus, cell debris and heterophils in the lung lumen (HE, 400X) (Photo courtesy of: Institute of Veterinary Pathology Vetsuisse-Faculty (University of Zurich), Winterthurerstrasse 268, CH-8057 Zurich, Fax number +41 44 635 89 34, www.vetpathology.uzh.ch)

definitively proven that it was the cause. In a recent study,[6] it was demonstrated through experimental infection of three ball pythons (*Python regius*) that nidovirus infection results in mucinous chronic inflammation and proliferative interstitial pneumonia. Possible transmission routes were suggested by identifying infectious virus in oral secretions and fecal material. Additionally, it was suggested that choanal and oral swabs were the best sample locations for antemortem diagnosis.

Conference participants thought there was enough necrosis within the submitted sections to include it as a modifier in the morphologic diagnosis. Morphologically, the participants suggested that the material present within the faveolar spaces suggested proteinaceous edema fluid rather than mucus. The location descriptor of bronchopneumonia as used in the JPC morphologic is based on the presence of hyperplastic and inflammatory changes in the respiratory epithelium at the tips of the faveolar septa as well as the type II pneumoncyte hyperplasia deep in the faveolae.

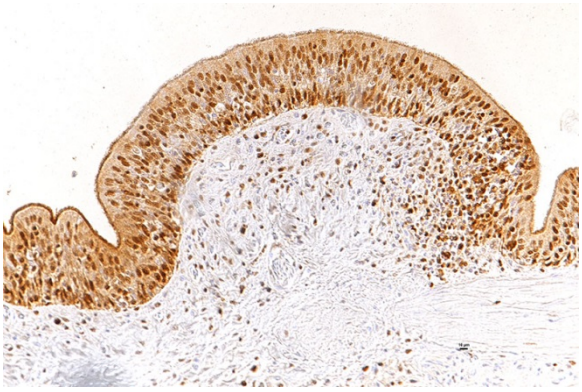

Lung, green tree python. Evidence of proliferative activity in all epithelial cell layers of the multilayered respiratory epithelium (PCNA, 200X). (Photo courtesy of: Institute of Veterinary Pathology Vetsuisse-Faculty (University of Zurich), Winterthurerstrasse 268, CH-8057 Zurich, Fax number +41 44 635 89 34, www.vetpathology.uzh.ch)

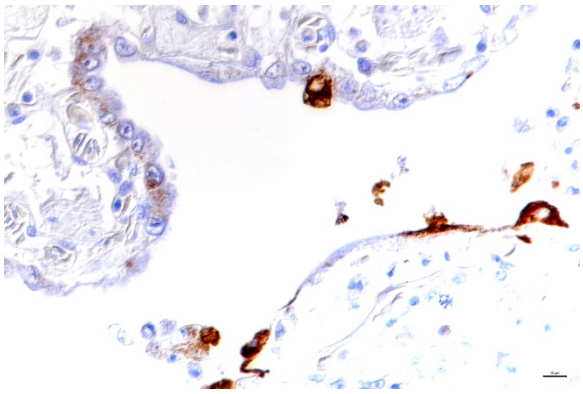

Lung, green tree python. Multifocal infected type I and type II pneumocytes (Immunohistochemistry for nidoviral-antigen, 400X). (Photo courtesy of: Institute of Veterinary Pathology Vetsuisse-Faculty (University of Zurich), Winterthurerstrasse 268, CH-8057 Zurich, Fax number +41 44 635 89 34, www.vetpathology.uzh.ch)

Contributing Institution:

Institute if Veterinary Pathology
Vetsuisse-Faculty (University of Zurich)
Winterthurerstrasse 268, CH-8057 Zurich
Fax number +41 44 635 89 34
www.vetpathology.uzh.ch

References:

1. Adams MJ, Lefkowitz EJ, King AMQ, et al. Changes to taxonomy and the international code of virus classification and nomenclature ratified by the international committee on taxonomy of viruses. *Arch. Virol.* 2017;162:2505-2538.
2. Bodewes R, Lempp C, Schurch AC, et al. Novel divergent nidovirus in a python with pneumonia. *The Journal of General Virology*. 2014;95(Pt 11):2480-2485.
3. Dervas E, Hepojoki J, Laimbacher A, Romero-Palomo F, Jelinek C, Keller S, Smura T, Hepojoki S, Kipar A, Hetzel U. Nidovirus-associated proliferative pneumonia in the green tree python (*Morelia viridis*). (under review in *Journal of Virology*, 2017).
4. Draker R, Roper RL, Petric M, Tellier R. The complete sequence of the bovine

torovirus genome. *Virus Research*. 2006;115(1):56-68.
5. Fehrenbach H, Kasper M, Tschernig T, et al. Keratinocyte growth factor-induced hyperplasia of rat alveolar type II cells in vivo is resolved by differentiation into type I cells and by apoptosis. *The European Respiratory Journal*. 1999;14(3):534-544.
6. Hoon-Hanks LJ, Layton ML, Ossiboff RJ, et al. Respiratory disease in ball pythons (*Python regius*) experimentally infected with ball python nidovirus. *Virology*. 2018 [Epub ahead of print]. doi: 10.1016/j.virol.2017.12.008.
7. Jacobson ER, Adams HP, Geisbert TW, Tucker SJ, Hall BJ, Homer BL. Pulmonary lesions in experimental ophidian paramyxovirus pneumonia of Aruba Island rattlesnakes, *Crotalus unicolor*. *Veterinary Pathology*. 1997;34(5):450-459.
8. Marschang RE, Kolesnik E. Nachweis von nidoviren bei lebenden pythons und boas. *Tierarztliche Praxis. Ausgabe K, Kleintiere/Heimtiere*. 2017;45(1):22-26.
9. O'Dea MA, Jackson B, Jackson C, Xavier P, Warren K. Discovery and partial genomic characterisation of a novel nidovirus associated with respiratory disease in wild shingleback lizards (*Tiliqua rugosa*). *PloS one*. 2016;11(11):e0165209.
10. Pastor García LM, Murcia Ud, Publicaciones Sd. *Histology, ultrastructure and immuno-histochemistry of the respiratory organs in non-mammalian vertebrates*. [Murcia]: Secretariado de Publicaciones de la Univesidad de Murcia [etc.]; 1995.
11. Steele AD, Bos P, Alexander JJ. Clinical features of acute infantile gastroenteritis associated with human rotavirus subgroups I and II. *Journal of Clinical Microbiology*. 1988;26(12):2647-2649.
12. Stenglein MD, Jacobson ER, Wozniak EJ, et al. Ball python nidovirus: A candidate etiologic agent for severe respiratory disease in *Python regius*. *mBio*. 2014;5(5):e01484-14.
13. Sun H, Lan D, Lu L, Chen M, Wang C, Hua X. Molecular characterization and phylogenetic analysis of the genome of porcine torovirus. *Archives of Virology*. 2014;159(4):773-778. http://dx.doi.org/10.1007/s00705-013-1861-x.
14. Tokarz R, Sameroff S, Hesse RA, et al. Discovery of a novel nidovirus in cattle with respiratory disease. *The Journal of General Virology*. 2015;96(8):2188-2193.
15. Uccellini L, Ossiboff RJ, Matos REC de, et al. Identification of a novel nidovirus in an outbreak of fatal respiratory disease in ball pythons (*Python regius*). *Virology Journal*. 2014;11:144.
16. Weiss M, Steck F, Horzinek MC. Purification and partial characterization of a new enveloped RNA virus (Berne virus). *Journal of General Virology*. 1983;64(9):1849-1858.

CASE II: 1704 0830 (JPC 4101141).

Signalment: 1-year-old, female, Suri alpaca, *Vicugna pacos*, alpaca.

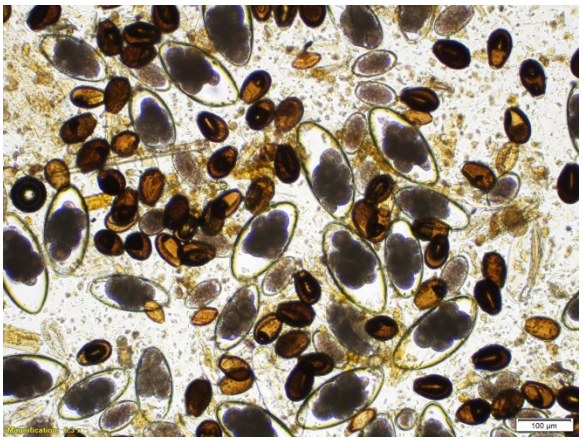

Fecal flotation, alpaca. Higher magnification of an Eimeria macusaniensis oocyst. The oocyst is pyriform shaped with a distinct brown-colored wall and has a micropyle and micropylar cap. (Scale=20µm) (Photo courtesy of: Dr. Y. Nagamori. Oklahoma Animal Disease Diagnostic Laboratory)

History: The alpaca was recently found depressed with decreased appetite. She had free access to a small Bermuda grass pasture but no known exposure to any toxic plants. She had no history of any medical treatment. Upon presentation, she was weak, dyspneic, recumbent and unable to stand. Physical examination showed dilated pupils with absence of pupillary light reflexes. Euthanasia followed by necropsy examination was elected by the owner with the aim of identifying any potential herd health problems.

Gross Pathology: The wall of the ileum was mildly and subjectively thickened, but the mucosa was grossly unremarkable. In multiple segments of the spiral colon, the mucosa was uniformly reddened and mildly thickened with multifocal dark red, ulcerative foci overlain by a moderate amount of fibrin. The liver was diffusely pale with an accentuated lobular pattern and greasy texture on cut surfaces (hepatic lipidosis) with multiple petechial and occasional ecchymotic hemorrhages scattered throughout the hepatic parenchyma. In the heart, multifocal petechial hemorrhages were present in the endocardium and myocardium of the left ventricle.

Laboratory results: An iStat Chem 8 biochemical analysis performed upon presentation revealed mild acidemia (AnGap 36 mEq/L; reference interval: 14-21 mEq/L), mild hypoglycemia (89 mg/dL; reference interval: 102-149 mg/dL) and azotemia (creatinine of 6.3 mg/dL; reference interval: 1-2.4 mg/dL).

Fecal flotation revealed numerous *Eimeria macusaniensis* oocysts, *Nematodirus* sp. eggs, and moderate numbers of Trichostrongyle-type of eggs, *Capillaria* sp. eggs and *Trichuris* sp. eggs. *Eimeria macusaniensis* oocysts were also observed in the direct fecal smears.

Aerobic bacterial culture recovered very large numbers of *Escherichia coli* and the anaerobic culture recovered very large numbers of *Clostridium perfringens* from the ulcerated spiral colon. The bacterial culture for *Salmonella* spp. was negative.

Microscopic Description: Small intestine: The lamina propria is moderately expanded by inflammatory infiltrates, predominantly lymphocytes, plasma cells and eosinophils, as well as large numbers of intra-epithelial, intracytoplasmic protozoan schizonts,

Fecal flotation, alpaca. Numerous parasitic eggs of different types are observed, including Eimeria macusaniensis oocysts. (Scale=100µm) (Photo courtesy of: Dr. Y. Nagamori. Oklahoma Animal Disease Diagnostic Laboratory)

gamonts, and oocysts. Most of these protozoa are located in the deep mucosa. The protozoa are present in the cytoplasm of cryptal epithelial cells, compressing the nuclei of the host cells. Schizonts are 70-100 µm in diameter, round to elliptical, and are surrounded by a large, clear parasitophorous vacuole. Within schizonts, numerous small, basophilic merozoites and occasional blastophores are discernible. The microgamonts are 120-200 µm in diameter and contain multiple highly condensed nuclei arranged in irregular bands, anastomosing trabeculae or circular patterns with prominent blastophores formation. Fully-developed microgamonts contain numerous linear or needle-shaped microgametes. In comparison, the macrogamonts are relatively small (50-90 µm in diameter) and are surrounded by a prominent parasitophorous vacuole. The developing macrogametes exhibit multiple, large, variably-sized, characteristic wall-forming bodies at the periphery of the cytoplasm. A few non-sporulated oocysts, approximately 80 x 55 µm, are seen in the epithelial cells or free in the intestinal lumen. The oocysts are pyriform with thick (8-10 µm) walls and have a visible micropyle and micropylar cap. The mucosa associated lymphoid tissues (Peyer's patches) are prominent and hypercellular.
Spiral colon: Multiple mucosal erosions are accompanied by acute necrosis of surface epithelial cells characterized by shrunken, pyknotic nuclei and hypereosinophilic cytoplasm. The erosive foci are overlain by karyorrhectic cellular debris intermingled with degenerate neutrophils, fibrin, mucus, erythrocytes and bacterial colonies. There are mildly increased numbers of lymphocytes, plasma cells and eosinophils present in the lamina propria of the affected segments.

Contributor's Morphologic Diagnosis:

Ileum: Moderate, subacute, diffuse lymphocytic and eosinophilic ileitis with numerous intralesional protozoan schizonts, gamonts and oocysts (morphologically consistent with *Eimeria macusaniensis*).

Ileum, colon: There are no obvious abnormalities on subgross examination. (HE, 4X)

Spiral colon: Moderate, acute, multifocal erosive colitis, with intralesional bacterial colonies.

Contributor's Comment: This is a presumed case of acute sepsis secondary to erosive colitis with coexistence of intestinal *Eimeria macusaniensis*. *E. macusaniensis* has been recognized as a significant intestinal pathogen in alpacas and llamas.[1,2,4,5,6] Along with the other 5 species of *Eimeria* known to infect camelids (*E. lamae*, *E. alpacae*, *E. punoensis*, *E. peruviana*, and *E. ivitaensis*), coccidiosis in alpacas was generally considered subclinical and only occasionally caused disease in young animals.[5] However, recent reports suggest *E. macusaniensis* infection in both adults and juveniles can cause varying degrees of clinical disease and death, either by sole infection, co-infection with other *Eimeria* spp., or complicated by secondary bacterial infections.2-4 It appears *E. macusaniensis* infected animals may be predisposed to other diseases.[1] A relationship between enterotoxemia caused by *Clostridium perfringens* and *E. macusaniensis* infection in alpacas has been

proposed and described.[4,6] In the present case, the erosive colitis, potentially caused by *C. perfringens* overgrowth, may have been predisposed by the heavy burden of *E. macusaniensis*.

Although the small intestine was grossly unremarkable except for subjective, mild thickening of mucosa of the ileum, large numbers of asexual and sexual stages of *E. macusaniensis* were revealed histologically. *E. macusaniensis* is recognized by the distinct, relatively large oocysts with average sizes of 75.5 µm by 54.9 µm during endogenous stages in tissue sections[7] and 106.6 µm by 80.5 µm in the feces.6 The oocysts are pyriform shape, with brown, 9-10 µm thick walls, a micropyle and a micropylar cap.[7,8] Other endogenous stages of *E. macusaniensis* (schizont, macrogamont and microgamont) are reported to be relatively indistinguishable from other *Eimeria* spp. in camelids.[5,7]

Antemortem diagnosis of *E. macusaniensis* can be challenging due to several factors, including nonspecific clinical signs, relatively long pre-patent period (≧30 days), and variable numbers of oocysts shed in the feces of affected animals. In addition, the oocysts of *E. macusaniensis* have a relatively high specific gravity, which makes it possible for them to be missed by routine fecal flotation methods and requires specific techniques (e.g. saturated sugar solution or flotation solutions with higher specific gravity) to achieve a better detection rate.[2,4] Therefore, the prevalence of *E. macusaniensis* may sometimes be underestimated.

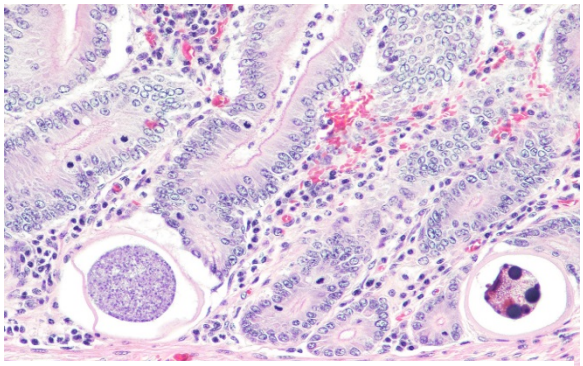

Ileum, alpaca. Schizont (left) containing numerous merozoites is surrounded by a prominent parasitophorous vacuole. The developing macrogamont (right) shows multiple distinct wall-forming bodies at the periphery of cytoplasm. (HE, 200X) (Photo courtesy of: Oklahoma State University, Department of Veterinary Pathobiology, College of Veterinary Medicine, 250 McElroy Hall, Stillwater, OK 74078, https://cvhs.okstate.edu/Veterinary_Pathobiology)

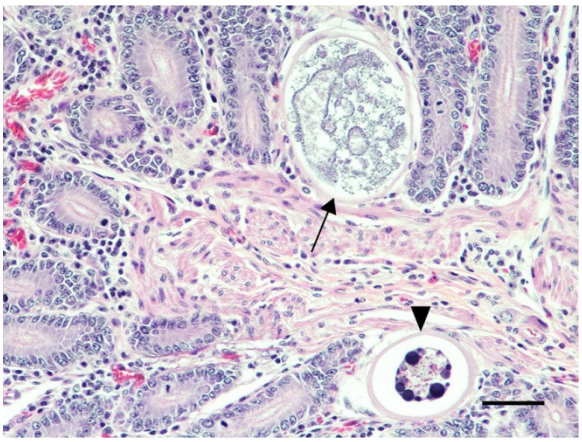

Ileum, alpaca. The developing microgamont (arrow) contains multiple irregularly arranged, highly condensed nuclei with blastophore formation. Note the macrogamont (arrowhead) is relatively small and encompassed by a prominent parasitophorous vacuole. (HE, 200X) (Photo courtesy of: Oklahoma State University, Department of Veterinary Pathobiology, College of Veterinary Medicine250 McElroy Hall, Stillwater, OK 74078, https://cvhs.okstate.edu/Veterinary_Pathobiology)

In a report of 34 alpacas and 15 llamas,[2] the most commonly reported clinical signs of animals infected by *E. macusaniensis* include lethargy, anorexia and weakness with few cases presented with diarrhea and colic. It is also important to note that there is no significant age or sex predisposition, although juveniles and females at breeding ages comprise a considerable subset among the infected population, which is hypothesized to be associated with the depressed immune status of the animals.[2]

JPC Diagnosis:

1. Ileum: Intraepithelial apicomplexan schizonts, gamonts, and oocysts with minimal lymphocytic inflammation, Suri alpaca (*Vicugna pacos*), alpaca.
2. Spiral colon: No abnormal findings.

Conference Comment: There are innumerable species of the genus *Eimeria* which demonstrats a direct coccidian life cycle characterized by both sexual and asexual reproduction. The Eimerian life history is prototypical and may be used as a basis for understanding the life cycle of all other coccidians. Rare exceptions include coccidians that utilize blood-feeding arthropods as hosts (*Hepatozoon* or *Schllackia*) where the oocysts develop in the arthropod and the mammalian host is infected by ingesting the infected arthropod.[1]

The life cycle begins when an infective sporulated oocyst is ingested by an appropriate host. There the sporozoites emerge, and schizogony, or asexual replication, begins. Free sporozoites enter cells of the lamina propria or enterocytes within the duodenum, form round trophozoites, and divide to become first-generation schizonts (same as meronts). It is worth noting that all intracellular forms of *Eimeria* (trophozoite, schizont, etc.) are all located within a parasitophorous vacuole which is best seen on electron microscopy. The first-generation schizont subsequently forms first-generation merozoites that burst out of the infected cell and infect adjacent cells to become second-generation schizonts. Schizogony continues in a cyclical fashion for two to three generations and then final merozoites (telomerozoites) infect a final naïve host cell and develop into either a female macrogamont or male microgamont. At this point sexual replication, or gametogony, can occur. When gamonts mature, they are called gametes. The female macrogamete is unicellular and fills the entire parasitized cell, whereas the male microgamont undergoes multiple divisions and eventually contains biflagellated microgaametes which exit the microgametocyte to fertilize the macrogamete and form zygotes. Oocysts develop which are leased by rupture of the host cell and passed out with the feces to undergo sporulation, be ingested, and start its life cycle all over again.[1]

Generally, *Eimeria* sp. can be identified based on host specificity and oocyst form (see chart below), and identified postmortem using direct smears of intestinal contents or H&E stained histologic sections. Wright's or Giemsa stain can be useful in identifying sporozoites. Simply identifying coccidian oocysts in animal feces is not enough to implicate disease since healthy animals may have large numbers. The history and clinical signs must fit with a diagnosis of coccidiosis: bloody diarrhea, weight loss, and ill thrift.[1,9]

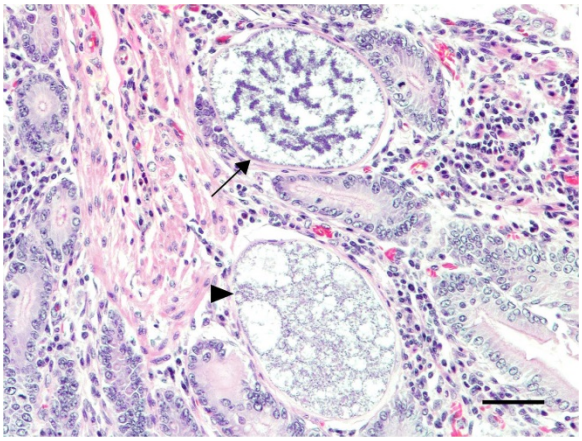

Ileum, alpaca. The developing microgamont (arrow) exhibits irregular bands and anastomosing trabeculae. A fully-grown microgamont (arrowhead) contains numerous microgametes. (HE, 200X) (Photo courtesy of: Oklahoma State University, Department of Veterinary Medicine250 McElroy Hall, Stillwater, OK 74078, https://cvhs.okstate.edu/Veterinary_Pathobiology)

Of interest, recent paleoparasitological investigation into the pre-incan to pre-hispanic contact period in northern Chile identified *Eimeria macusaniensis* as well as three other parasite eggs (*Enterobius vermicularis, Trichostrongylus* sp.*,* and *Trichuris* sp.*)* within human coproliths (fossilized feces).[3] The presence of *E. macusaniensis* in human fecal matter is related to the use of llamas as food, transportation, and sacrificial offerings, and underscores the importance of llamas and alpacas to societal evolution.

Table 1: *Eimeria* sp. by host and organs affected[9]

Animal	**Coccidia**	**Organ affected/Clinical signs**
Birds		
Chickens	*E. acervulina*	Duodenum/enteritis
	E. necatrix/maxima	Jejunum/enteritis
	E. brunette	Ileum/enteritis
	E. tenella	Ceca/typhylitis
Turkey	*E. meleagridis*	Cecum
	E. adenoeides	Cecum, ileum
	E. meleagrimitis	Upper intestine
	E. gallopavonis	Ileum, large intestine
Geese & ducks	*E. truncata*	Kidney/anorexia, depression
	E. anseris/nocens	Intestine
Sandhill/whooping cranes	*E. reichenowi*	Disseminated
	E. psittaculae	Intestine
Parrots		
Cattle	*E. bovis/zuernii*	Cecum and colon/diarrhea
	E. alabamensis	Small intestine
Sheep	*E. ahsata/christenseni*	SI
	E. brakuensis	SI
	E. crandallis	SI
	E. ovinoidalis	Cecum, colon
Goats	*E. christenseni*	SI
	E. arloingi	SI
	E. hirici	SI
	E. ninakohlyak-imovea	LI
Equine	*E. leukarti*	SI
	Klossiella equi	
Swine	*E. debliecki*	SI (in 1-3 week old piglets)
Canine	*I. canis*	Ileum, colon occasionally
Feline	*I. felis*	SI, colon occasionally

Mice	*Klossiella muris* *E. falciformis* *E. vermiformis* *E. papillata* *E. ferrisi*	kidney Colon Intestine Intestine Intestine
Rabbit	*E. stiedae* *E. intestinalis* *E. flavescens*	Bile ducts Ileum & cecum Ileum & cecum
Ferret	*E. furonis*	SI

The sections made available to participants did not contain eosinophils in the small intestine, or bacterial colonies and ulceration within the large intestine. Attendees vigorously debated the severity of the parasitism, inflammation, and crypt hyperplasia within the small intestine and concluded that it would not be severe enough to induce ulcer formation and secondary bacterial infections further down the alimentary tract. Therefore, an additional pathogen is suspected.

Contributing Institution:

Oklahoma State University
Department of Veterinary Pathobiology
College of Veterinary Medicine
250 McElroy Hall
Stillwater, OK 74078
https://cvhs.okstate.edu/Veterinary_Pathobiology

References:

1. Bowman DD. *Georgis' Parasitology for Veterinarians*. 10th ed. St. Louis, MO: Elsevier; 2014: 98-103.
2. Cebra CK, Valentine BA, Schlipf JW, Bildfell RJ, McKenzie E, Waitt LH, et al. *Eimeria macusaniensis* infection in 15 llamas and 34 alpacas. *J Am Vet Med Assoc.* 2007;230(1):94-100.
3. De Souza MV, Da Silva LGR, Silva-Pinto V, et al. New paleoparasitological investigations form the pre-inca to hispanic contact period in northern Chile. *Acta Trop.* 2018;178:290-296.
4. Johnson AL, Stewart JE, Perkins GA. Diagnosis and treatment of *Eimeria macusaniensis* in an adult alpaca with signs of colic. *Vet J*. 2009;179(3):465-467.
5. Palacios CA, Perales RA, Chavera AE, Lopez MT, Braga WU, Moro M. *Eimeria macusaniensis* and *Eimeria ivitaensis* co-infection in fatal cases of diarrhoea in young alpacas (*Lama pacos*) in Peru. *Vet Rec.* 2006;158(10):344-345.
6. Rosadio R, Londone P, Perez D, Castillo H, Veliz A, Llanco L, et al. *Eimeria macusaniensis* associated lesions in neonate alpacas dying from enterotoxemia. *Vet Parasitol.* 2010;168(1-2):116-120.
7. Schrey CF, Abbott TA, Stewart VA, Marquardt WC. Coccidia of the llama, *Lama glama*, in Colorado and Wyoming. *Vet Parasitol.* 1991;40(1-2):21-28.
8. Taylor MA, Coop RL, Wall RL. *Veterinary Protozoology Veterinary Parasitology*. 4th ed. Hoboken, NJ: John Wiley & Sons, Inc.; 2015:129-138.
9. Uzal FA, Plattner BL, Hostetter JM. Alimentary system. In: Maxie MG, ed. *Jubb, Kennedy, and Palmer's Pathology of Domestic Animals.* Vol. 2. 6th ed. St. Louis, MO: Elsevier; 2017:227-235.

CASE III: H15-0067L (JPC 4067142).

Signalment: Unknown age, male, Bilby, *Macrotis lagotis*, marsupial.

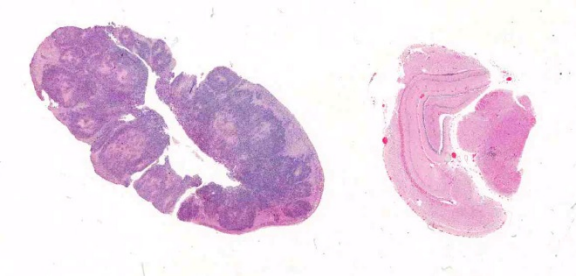

Adrenal gland left (right); cross section through diencephalon (right), bilby: The normal architecture of the adrenal gland is effaced by a densely cellular inflammatory infiltrate as well as multiple foci of inflammation in the cerebrum and thalamus. (HE 5X)

History: A captive young adult male bilby (*Macrotis lagotis*) was euthanized at a wildlife park following the onset of severe lethargy and was subsequently presented to the anatomic pathology service at Murdoch University Veterinary Hospital for necropsy examination. Approximately two months prior, the bilby was captured for an annual health check. He was healthy and weighed 2098 grams. On that day he was transferred to a neighboring enclosure which contained 10 other bilbies, including one young male and nine adult and sub-adult females. Approximately seven weeks later, the bilby became lethargic and was recaptured. He weighed 1630 grams. He was isolated and euthanized three days later following no improvement. A zoo keeper was bitten during capture.

Gross Pathology: On gross examination, the bilby was emaciated with a focal circular, ulcerated skin lesion on the dorsal tail base. Dozens of variably sized, poorly demarcated, red to tan nodules were present throughout the lungs and kidneys. The adrenal glands were markedly enlarged, pale tan and soft with loss of corticomedullary distinction.

Laboratory results: Samples of aseptically collected lung and spleen were stored at 4^0C prior to submission for fungal culture. Tissue cultures isolated *Sporothrix schenckii* demonstrating thermal dimorphism. At 26^0C the isolates were expanding, crumbly and grey in color and at 36^0C an atypical yeast-like organism was identified. Microscopically, organisms were characterized by clavate conidia arranged predominantly terminally on erect conidophores attached by fine denticles. Dematiaceous sessile conidia were also observed. Subsequent sequencing of the internal transcribed spacer (ITS) regions confirmed the isolate as *Sporothrix schenckii sensu lato*.

Microscopic Description: Adrenal glands: Diffusely effacing the normal medullary architecture and extensively infiltrating and effacing over 90% of the cortex, are large numbers of degenerate neutrophils and epithelioid macrophages admixed with moderate numbers of multinucleate giant cells, and large amounts of eosinophilic and karyorrhectic debris (necrosis). Admixed are frequent pleomorphic 2-15 μm diameter yeast. These organisms are predominately intracellular within the cytoplasm of macrophages and multinucleate giant cells,

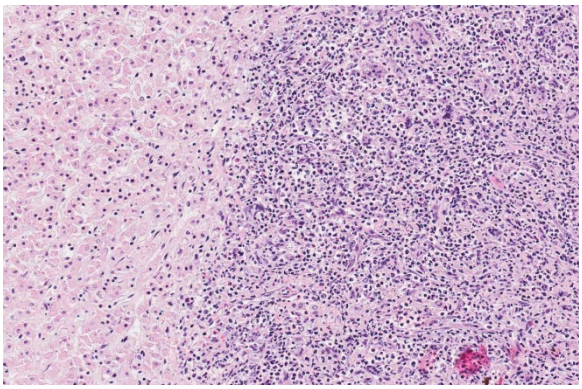

Adrenal cortex, bilby. The adrenal cortex (left) is replaced by a dense pyogranulomatous infiltrate composed of numerous macrophages, viable and degenerate neutrophils, and scattered multinucleated giant cell macrophages (HE, 80X)

but are also present in fewer numbers extracellularly within areas of necrosis. Yeasts are round, oval or elongate (cigar-shaped) and larger yeast (10-15 μm diameter) are round to oval with rare narrow-based budding. Yeasts are sometimes surrounded by a clear thin halo and/or a slightly refractile clear cell wall, and stain intensely positive with periodic acid-Schiff (PAS). The smaller forms (2-9 μm diameter) are elongate, cigar-shaped to oval and stain intensely positive with PAS and are also Gram positive.

Brain: In multiple regions of brain, including the cerebrum, hippocampus and midbrain, the neuropil and leptomeninges are disrupted by multifocal to coalescing, randomly distributed foci of pyogranulomatous inflammation as previously described. Low numbers of the previously described fungal yeast are present scattered throughout the inflammatory foci. Mildly increased numbers of glial cells are present immediately surrounding these inflammatory foci.

Similar inflammatory foci are also present within the kidneys, lungs, testes, lymph nodes, heart, liver, spleen, salivary glands and tail wound.

Contributor's Morphologic Diagnosis:

Adrenal glands: Severe, regionally extensive, subacute, pyogranulomatous and necrotizing adrenalitis with numerous intrahistiocytic and extracellular fungal yeast.

Brain: Moderate, multifocal to coalescing, random, subacute, pyogranulomatous meningoencephalitis with occasional intrahistiocytic and extracellular fungal yeast and mild gliosis.

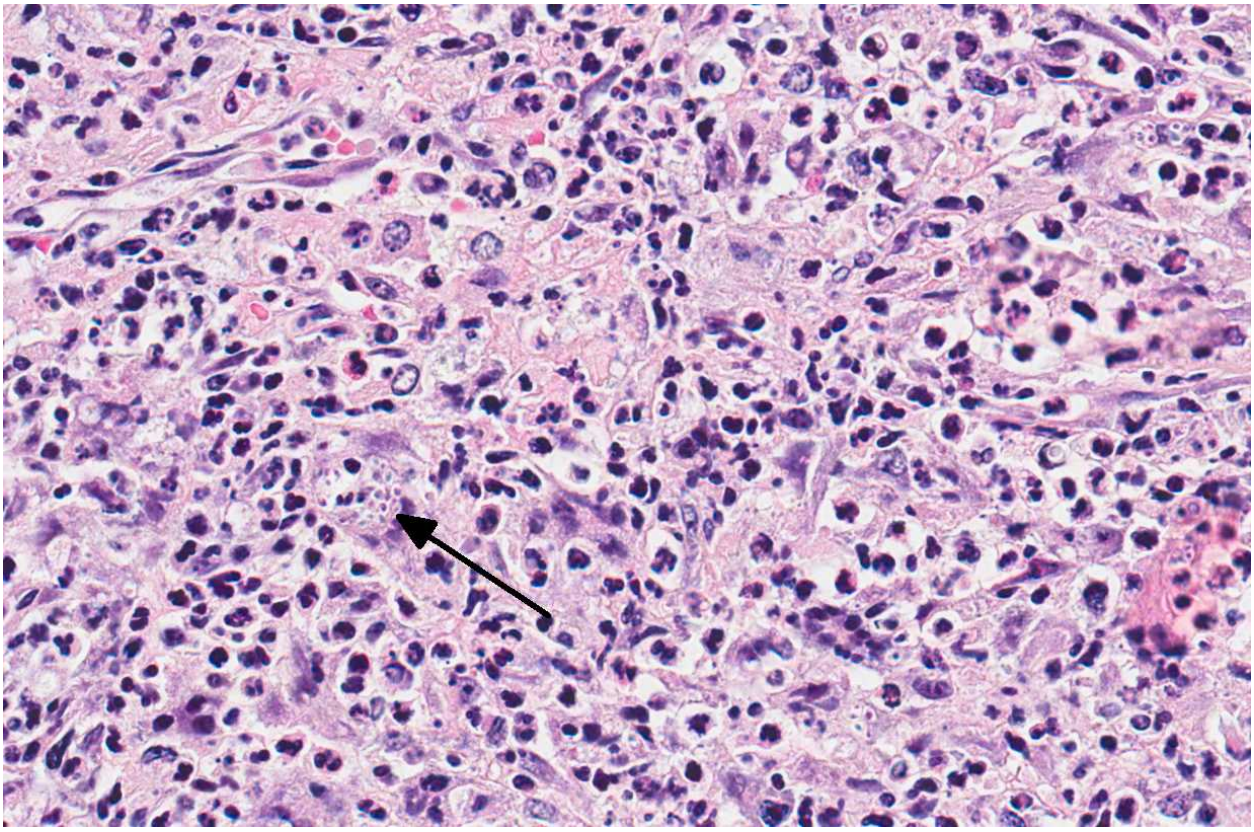

Adrenal cortex, bilby. Macrophages and multinuclearted giant cell macrophages cotnin one or more intracytoplasmic 3-5um, round to ellipsoid yeasts. (HE, 400X)

Contributor's Comment: The histological and fungal culture findings are consistent with disseminated sporotrichosis, an uncommon fungal disease of humans and animals which, outside of Brazil, is usually caused by the fungus *Sporothrix schenkii*. Gene sequencing of isolates from Brazil have shown the most common species as *S. brasiliensis*, with *S. globosa, S. albicans*, *S. luriei* and *S. Mexicana* also isolated.[1,5] *Sporothrix* spp. are thermally dimorphic, cosmopolitan fungi found in soil, hay and decaying plant matter.

Based on the size and pleomorphic nature of the yeast, *Sporothrix schenckii* was strongly suspected following initial microscopic evaluation; however, other yeast that can appear morphologically similar include *Cryptococcus* spp. and *Blastomyces dermatitidis* (see table below for summary of common fungal yeast pathogens).

Given the presence of the organism within the chronic skin wound on the tail base, the most likely route of infection in this case was considered to be either wound inoculation or direct inoculation from a penetrating wound, with subsequent dissemination via hematogenous or lymphatic spread to numerous internal organs.

Diencephalon, bilby. There are two foci of inflammation in the diencephalon – one in the internal capsule and one in the thalamus (arrows). (HE, 10X)

Although multiple cases of fungal disease have been described in a variety of native Australian marsupials and monotremes, to our knowledge this is the first reported case of sporotrichosis in a native Australian marsupial. *Trichophyton* spp. and *Microsporum* spp. have been described as the cause of dermatophytosis in both native Australian macropods and koalas. *Mucor amphibiorum* causes significant morbidity and mortality in the platypus, with severe ulcerative dermatitis, occasional spread to underlying muscle and dissemination to other organs. *Candida* spp. have been reported to cause gastrointestinal infections in macropods and koalas and *Cryptococcus gatii* and *C. neoformans var grubii* have been associated with cryptococcal meningitis, pulmonary and disseminated cryptococcosis in a number of macropod species, koalas and a single dusky antechinus (*Antechinus swainsonii*).

In the veterinary literature, sporotrichosis has been reported in a variety of animals. Cats are the most commonly affected domestic species; however, cases in dogs, horses, cattle, pigs, fish, rodents and armadillos have also been reported.[6,12] In cats, sporotrichosis typically presents as ulcerated, nodular cutaneous lesions, most commonly on the head and ears. Respiratory mucosal involvement is common; ascending lymphangitis and dissemination are reported less frequently.[8,13] Disseminated disease is rare in all species, with human cases occurring most often in immuno-compromised patients. In cats, however, it usually occurs in the absence of immunosuppression.[8,11,13] Feline sporotrichosis is an important source of zoonotic sporotrichosis in humans, with cases in Brazil associated with bites and scratches from infected domestic cats (Felis catus). *S. schenkii* has been isolated from the

nail beds of healthy cats.[4] Human infections resulting from bites or scratches from rodents, armadillos, and a single opossum have also been reported.[3,12] In this case, zoonotic infection did not occur following the bilby bite.

Table 1. Summary of common fungal yeast pathogens.[10]

Features	Sporothrix spp	Cryptococcus neoformans	Blastomyces dermatidis	Coccidioides immitis	Histoplasma capsulatum	Histoplasma farciminosum
Histopathology						
Tissue morphology Budding	Pleomorphic cigar shaped yeast cells Narrow base	Oval yeast cells with prominent thick capsule Narrow base	Thick walled yeast cells Broad base & unipolar	Spherules containing endospores	Oval yeast cells within macrophages Narrow base	Oval yeast cells within macrophages Narrow base
Size (diameter)	3-6 µm	4-8 µm	8-10 µm	Spherules 10-80 µm, endospores 2-5 µm	2-5 µm	2-5 µm
Staining	PAS, silver stains, small forms: Gram positive	PAS, silver stains, capsule: mucicarmine	PAS, silver stains	PAS, silver stains	PAS, silver stains	PAS, silver stains
Epidemiology & clinical disease						
Disease Species most affected Environmental habitat Geographical distribution Site of lesions Route of infection	Sporotrichosis Horses, cats, dogs & humans Decaying vegetation, soil, moss Worldwide, mainly tropical and subtropical Lymphocutaneous, occasional dissemination Traumatic implantation	Cryptococcosis Cats horses and humans Soil enriched with bird faeces & Australian red gum trees Worldwide Nasal cavity, lungs, brain, eye, skin Inhalation	Blastomycosis Dogs and humans Acidic soil rich in organic matter North America, India and the Middle east Lungs with metastasis to skin and other tissues Usually inhalation	Coccidiomycosis Dogs, horses and humans Arid or semi-arid soil in low-lying areas Southwestern USA, Central and South America Lungs with metastasis to bones Usually inhalation	Histoplasmosis Dogs, cats and humans Soil enriched with bird and bat faeces Endemic to Mississippi and Ohio river valleys with sporadic cases in other countries Lungs with occasional dissemination Inhalation	Epizootic lymphangitis Equidae Soil Africa, the Middle East and Asia Skin, lymphatic vessels and nodes Traumatic implantation
Mycological characteristics						
Fungal culture	Dimorphic 25ºC mould colonies white to black/brown, wrinkled and leathery; conidia pear shaped arranges in rosettes on conidiophores 35-37ºC yeast colonies cream to tan	37ºC mucoid colonies with capsules, urease activity; brown colonies on birdseed agar	Dimorphic 25-35ºC mould colonies white and cottony producing pear shaped conidia borne on conidiophores or hyphae 37ºC yeast colonies cream to tan, wrinkled and waxy	25-30ºC mould colonies shiny moist and grey to white and cottony; septate hyphae with barrel shaped arthrospores separated by empty cells	Dimorphic 25-30ºC white to buff colonies with cottony aerial hyphae; septate hyphae bear small conidia and sunflower-like macroconidia 37ºC yeast colonies cream to tan, round and mucoid	Dimorphic similar to H. capsulatum

JPC Diagnosis:

1. Adrenal gland: Adrenalitis, pyogranulomatous, multifocal to coalescing, severe with numerous intracellular and extracellular yeasts, Bilby (*Macrotis lagotis*), marsupial.
2. Brain, diencephalon: Encephalitis, pyogranulomatous, multifocal, moderate with rare intracellular yeasts.

Conference Comment: Sporotrichosis is a subacute to chronic disease of animals and humans caused by fungi of the *Sporothrix* spp. of which *Sporothrix schenckii* is the most common. *S. schenckii* is a dimorphic fungus, meaning it is in its mycelial form at room temperature and when at 37 ^{0}C (body temperature) it develops into the yeast form. Microscopically, the yeast form is oval to cigar-shaped with a thin refractile cell wall, 2-6 um in diameter by 2-10 um in length, exhibit narrow based budding, and may intracellular (within multinucleated giant cells or macrophages) or extracellular. Like many other types of fungi, *Sporothrix* elicits a diffuse or nodular pyogranulomatous response. When cutaneous, the epidermis is often hyperplastic or ulcerated and often accompanied by fibrosis. In some cases, yeasts are surrounded by Splendore-Hoeppli material or asteroid bodies, but this is not pathognomonic for sporotrichosis and can be seen when there is antigen-antibody complex formation surrounding other organisms or foreign objects.[2,9]

Sporotrichosis has been reported in cats, dogs, horses, mules, donkeys, cattle, goats, swine, camels, and humans. As discussed in this case, sporotrichosis carries a risk of zoonotic transmission, and the most common route is from cats to humans.[2] Disease is more common in cats, horses, and dogs living in temperate and tropical zones; particularly in intact male outdoor cats and hunting dogs. Infection is acquired via puncture wounds,

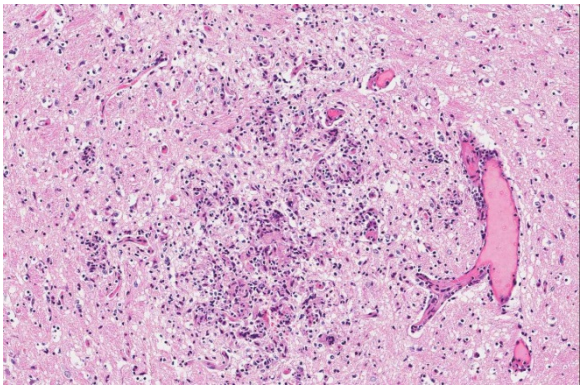

Diencephalon, bilby. Within the thalamus, there is a focus of pyogranulomatous inflammation with marked perivascular inflammation and edema. (HE, 200X)

and pulmonary infection occurs rarely via inhalation of spores. Sporothrix spores are quite hardy and can survive for months or years in soil, vegetation, and wood. The human form of disease is termed “rose handler’s disease” which illustrates that point.[2] Clinically, there are three forms of sporotrichosis: (1) Primary cutaneous form; (2) Cutaneous-lymphatic form; and (3) Extracutaneous or disseminated form.[9]

The primary cutaneous form is most likely a result of strong host immunity and results from puncture wounds with the organism confined to the point of entry. This form tends to be chronic and clinically appears as multiple scattered raised, alopecic, ulcerated or crusted nodules along the head or distal extremities. Infected cats can spread the organism around their own epidermis through autoinoculation by grooming.[9]

The cutaneous-lymphatic form is the most common form in horses and humans and involves the skin and subcutis with spread through associated lymphatics. Affected lymphatic vessels become thickened and rope-like, regional lymph nodes are enlarged, and often nodules break open resulting in oozing sores. In this form, lesions are often along the proximal forelimbs, chest, and thighs.[9]

Finally, the extracutaneous or disseminated form occurs most frequently in cats and may involve a single extracutaneous tissue or multiple organs. This form develops often as a sequela to cutaneous-lymphatic infection or following inhalation of spores. In affected cats, no immunosuppressive factors have been identified and it is unclear what causes *Sporothrix* to disseminate. Clinically, affected cats are febrile, depressed, and anorexic.[9]

Microscopically, the cigar-shaped yeast is characteristic, and can be readily identified using standard fungal stains (GMS or PAS) or Gram stain (gram-positive),[2] but there are times when the cigar-shaped form is not present. In those cases, common differentials would include *Cyptococcus neoformans* or *Histoplasma capsulatum*. However, *Cryptococcus neoformans* can be much larger (up to 20um) with a very thick 2um capsule that stains with mucicarmine, and *Histoplasma capsulatum* is always intracellular.[9]

Contributing Institution:
http://www.murdoch.edu.au/Services/Veterinary-Hospital/About-us/Services/Pathology-and-Clinical-Pathology/

References:

1. Alves SH, Boettcher CS, de Oliviera DC, et al. *Sporothrix schenckii* associated with armadillo hunting in Southern Brazil: epidemiological and antifungal susceptibility profiles. *Revista da Sociedade Brasileira de Medicina Tropical*. 2010;43:523-525.
2. Chandler FW, Kaplan W, Ajello L. Sporotrichosis. In: *Color Atlas and Text of the Histopathology of Mycotic Diseases.* Chicago, IL: Year Book Medical Publishers, Inc.; 1980: 112-115.
3. da Rosa ACM, Scroferneker ML, Vettorato R, et al. Epidemiology of sporotrichosis: a study of 304 cases in Brazil. *Journal of the Americal Academy of Dermatology*. 2005;52:451-459.
4. de Souza L, Nascente P, Nobre M, et al. Isolation of *Sporothrix schenkii* from the nails of healthy cats. *Brazilian Journal of Mycology*. 2006;37:372-374.
5. Gremiao IDF, Menezes RC, Schubach TMP, et al. Feline sporotrichosis: epidemiological and clinical aspects. *Medical Mycology*. 2015;53:15-21.
6. Ladds P. *Pathology of Australian Native Wildlife*. Collingwood, AUS: CSIRO Publishing. 2009:155-167.
7. Lopez-Romero E, Reyes-Montes M, Perez-Torres A, et al. *Sporothrix schenckii* complex and sporotrichosis, an emerging health problem. *Future Microbiology*. 2011;6:85-102.
8. Mata-Essayag S, Delgado A, Colella MT, et al. Epidemiology of sporotrichosis in Venezuela. *International Journal of Dermatology*. 2013;52:974-980.
9. Mauldin EA, Peters-Kennedy J. Integumentary system. In: Maxie MG, ed. *Jubb, Kennedy, and Palmer's Pathology of Domestic Animals*. Vol 1. 6th ed. St. Louis, MO: Elsevier; 2016: 655-657.
10. Quinn P, Markey B, Carter M, et al. *Veterinary Microbiology and Microbial Disease*. Oxford, UK: Blackwell Publishing. 2010:235-245.
11. Schubach A, de Lima Barros MB and Wanke B. Epidemic sporotrichosis. *Current Opinion in Infectious Diseases*. 2008;21:129-133.
12. Teixeira MM, de Almeida LGP, Kubitschek-Barreira P, et al. Comparative genomics of the major fungal agents of human and animal

sporotrichosis: *Sporothrix schenckii* and *Sporothrix brasiliensis*. *BMC Genomics*. 2014;15:943-964.
13. Wenker CJ, Kaufman L, Bacciarini LN, et al. Sporotrichosis in a nine-banded armadillo (*Dasypus novemcinctus*). *Journal of Zoo and Wildlife Medicine*. 1998;29:474-478.

CASE IV: WSC 2017-2018 Case I (JPC 4100648).

Signalment: Adult, male, African green monkey, *Chlorocebus sabaeus*, primate.

History: This monkey was in a study to determine the efficacy of a therapeutic drug for treating pneumonic plague. All of the monkeys in this study were exposed to a lethal dose of aerosolized *Yersinia pestis*. Once an individual animal began displaying clinical signs, twice daily treatments were initiated with either a placebo (control group) or the therapeutic drug (experimental group). This monkey was in the experimental group and it developed clinical signs necessitating euthanasia on Day 15 after bacterial challenge. Note: All of the control animals died on Day 4 or Day 5.

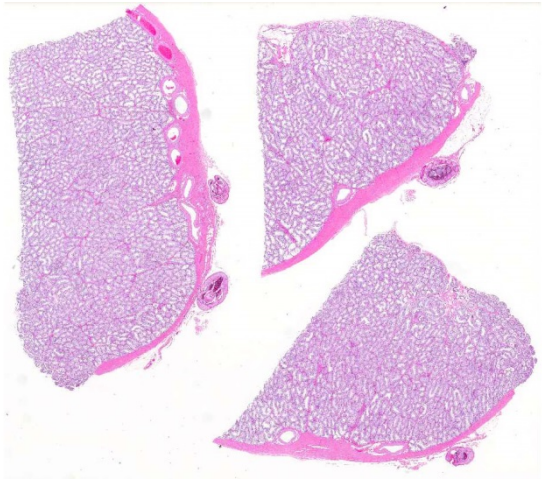

Testis, African Green monkey. Within the fused vaginal tunics, there are multiple cross sections of larval acanthocephalan parasites. (HE, 5X)

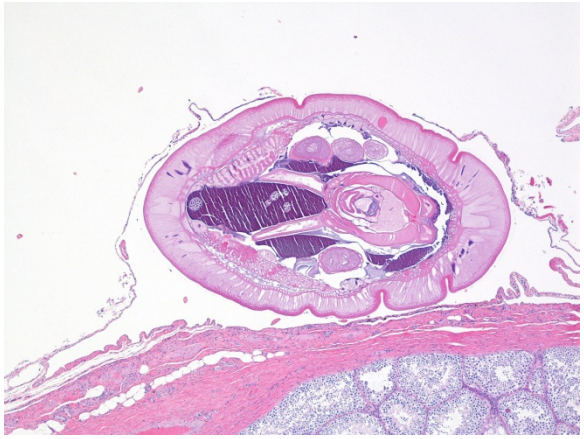

Testis, African Green monkey. Section of testis with an approximately 2 mm diameter metazoan parasite encysted in the tunica vaginalis. (HE, 40X) (Photo courtesy of: US Army Medical Research Institute of Infectious Diseases, Pathology Division, Fort D Detrick, MD http://www.usamriid.army.mil/)

This monkey was part of a research project conducted under an Institutional Animal Care and Use Committee (IACUC) approved protocol in compliance with the Animal Welfare Act, PHS Policy, and other federal statutes and regulations relating to animals and experiments involving animals. The facility where this research was conducted is accredited by the Association for Assessment and Accreditation of Laboratory Animal Care, International and adheres to principles stated in the 8th edition of the Guide for the Care and Use of Laboratory Animals, National Research Council, 2011.

Gross Pathology: There were multiple fibrous adhesions between the left testis and the inner lining of the scrotum. In the areas of adhesion, numerous oval white nodules, measuring 1-2 X 2-3 mm, were located in the connective tissues over the tunica albuginea of this testis and within the surrounding scrotum. There were several fibrous adhesions between the right middle lung lobe

and the mediastinum and between the right inferior lung lobe and the thoracic wall. An approximately 1 cm diameter firm nodule was palpated within the middle of the right inferior lung lobe.

Laboratory results: None provided.

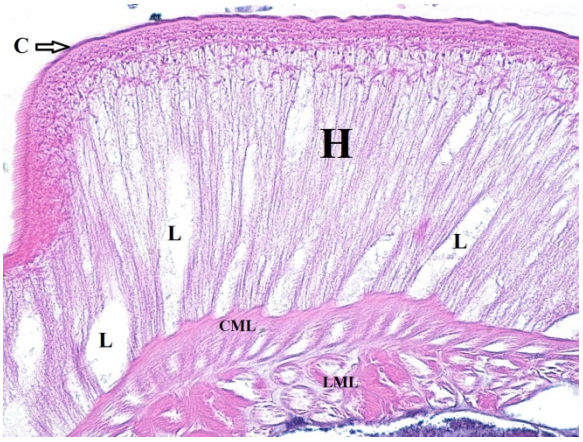

Testis, African Green monkey. High magnification of the wall of the parasite showing it has an outer cuticle (C), a thick hypodermis (H) containing lacunae (L), a circular muscle layer (CML), and a longitudinal muscle layer (LML). (HE, 400X) (Photo courtesy of: US Army Medical Research Institute of Infectious Diseases, Pathology Division, Fort Detrick, MD http://www.usamriid.army.mil/)

Microscopic Description: Testis (3 sections): Adjacent to the tunica albuginea, within the tunica vaginalis, there are four sections of a metazoan parasite measuring 1.5–2.5 mm in greatest diameter. The parasites have a cuticle, a wide hypodermis (100-200 µm thick) containing multiple lacunae, and two layers of muscle (circular and longitudinal) that border a pseudocoelom. In one section of the parasite, there is a retracted proboscis with spines. In other sections, the pseudocoelom contains oval muscular structures, measuring <100 X <200 µm, which have peripheral muscles and a central canal; these are consistent with lemnisci. Neither a digestive tract nor mature eggs are evident. Multifocally, the tunica vaginalis is fused with the tunica albuginea which results in the parasites being encysted. In other tissue sections (not present on the scanned slide), the parasites reside in pseudocysts present in the left epididymis and the wall of the scrotum.

Contributor's Morphologic Diagnosis: Testis/tunica vaginalis; multiple encysted larval acanthocephalan parasites

Contributor's Comment: The anatomic features of the parasites in this monkey that are characteristic of the phylum Acanthocephala include: (1) a cuticle; (2) a thick hypodermis; (3) a pseudocoelom; (4) the lack of a digestive tract; (5) a proboscis with spines; and (6) the presence of lemnisci (pleural of lemniscus).[4,5] No other types of parasites have lemnisci.[5]

As adults, Acanthocephelans are parasites of the intestinal tract of vertebrate hosts and different species have been reported in all classes of vertebrates (i.e. fish, amphibians, reptiles, birds, and mammals).[4] The adult worm everts it spiny proboscis and this is used for attachment to the host's intestinal wall. This proboscis is responsible for the common names for Acanthocephalans:

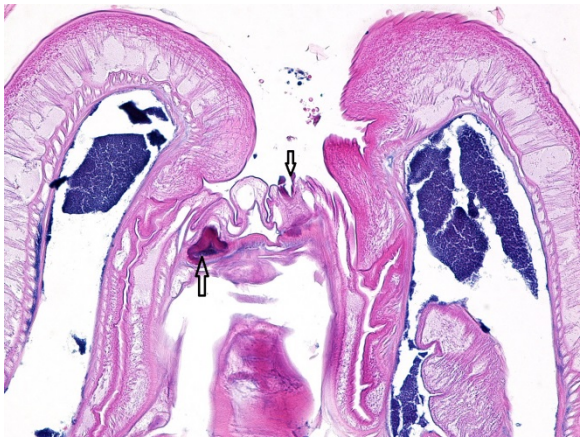

Testis, African Green monkey. Section of the parasite with a retracted proboscis that has spines (arrows). (HE, 200X)(Photo courtesy of: US Army Medical Research Institute of Infectious Diseases, Pathology Division, Fort Detrick, MD http://www.usamriid.army.mil/)

"thorny-headed" or "spiny-headed" worms.[4,5] Lacking a digestive tract, the worms absorb nutrients through their body wall and the channels (lacunae) in the hypodermis probably aid in transporting absorbed nutrients.[4]

Adult female worms produce eggs, each containing a larva called an acanthor,[2,4] which are passed in the feces of the host. The larvated eggs are ingested by an invertebrate intermediate host (usually an arthropod) in which the parasites develop and encyst at a stage called a cystacanth.[2,4] Usually, the life cycle is completed when the definitive host ingests the infected intermediate host and the cystacanths are then released and develop into adults in the intestines of the definitive host.

However, cystacanths can occasionally use vertebrates as paratenic hosts.[2,4,5] This occurs when a cystacanth-infected intermediate host is ingested by a vertebrate that is not a final host species; the cystacanths then encyst in the tissues of the paratenic host without any further maturation. The parasites in this monkey are consistent with cystacanths and the monkey is a paratenic host. A full necropsy was performed on this monkey and

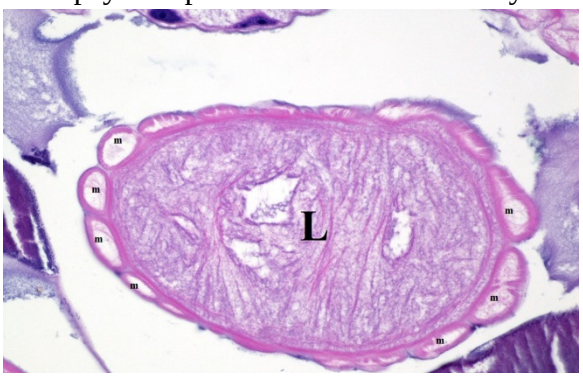

Testis, African Green monkey. High magnification of the parasite showing a lemniscus (L) within the pseudocoelom. Around its periphery are compressor muscles (m). (HE, 400X) (Photo courtesy of: US Army Medical Research Institute of Infectious Diseases Pathology Division, Fort Detrick, MD http://www.usamriid.army.mil/)

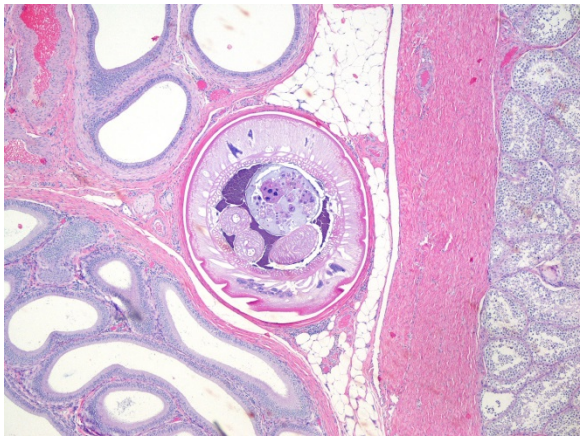

Testis, African Green monkey. Section of testis and epididymis (from a different histology slide). The parasite is contained within a pseudocyst within the epididymis. (HE, 40X) (HE, (Photo courtesy of: US Army Medical Research Institute of Infectious Diseases, Pathology Division, Fort Detrick, MD http://www.usamriid.army.mil/)

the only locations that these parasites were found were in the connective tissues around the left testis and epididymis. These parasites were deemed to be incidental findings of no clinical significance. The lung lesions noted grossly in this animal were areas of subacute to chronic inflammation attributable to the experimental bacterial challenge.

This African green monkey originated from a semi-feral colony on the island of St. Kitts in the Caribbean. The monkeys on St. Kitts are believed to have descended from escaped or intentionally-released "pets" on slave-trading ships in the 1600's.[1] They became established on the island (as well as the Caribbean islands of Nevis, Anguilla, Saint Maarten, and Barbados) and their population increased to a level so that their crop-raiding tendencies caused them to be described as a "pest species" on St. Kitts as early as 1700,[1] where they are still considered to be an invasive pest.

The species of Acanthocephala in this monkey was not determined. However, the

monkey most likely had plenty of opportunities to be exposed to potential intermediate hosts on St. Kitts before it was brought to the United States. Adult acanthocephalans in the genus *Prosthenorchis* have been reported in a variety of New World primates (NWPs) and cystacanths of these parasites have also been found encysted in the peritoneal membranes of NWPs.[2,6] However, it is unlikely that the parasites in the monkey of this report are a species of *Prosthenorchis* because NWPs do not occur on St. Kitts. It is interesting to note that feral pigs are present on St. Kitts; this suggests the possibility that the parasites in this monkey might be cystacanths of the "thorny-headed worm" of pigs: *Macracanthorhynchus hirudinaceus*.

Note: Opinions, interpretations, conclusions, and recommendations are those of the author and are not necessarily endorsed by the U.S. Army.

JPC Diagnosis: Testis, tunica vaginalis: Multiple encysted acanthocephalans, African green monkey (*Chlorocebus sabaeus*), primate.

Conference Comment: Acanthocephalans were first described by Italian author Francesco Redi in 1684. The name "Acanthocephala" (which is derived from the Greek *akanthos*, thorn and *kephale*, head) was coined by scientist Joseph Koelreuter in 1771 but not formalized until 1809. Acanthocephalans are simple parasites that lack many internal organs for increased efficiency. For instance, they lack a mouth or gastrointestinal tract, and the adult stages of the parasite live in the intestines of their host where they uptake nutrients that have been digested by the host. Thorny-headed worms have marked variation in size from species to species depending on the host and can reach up to 65 centimeters in length

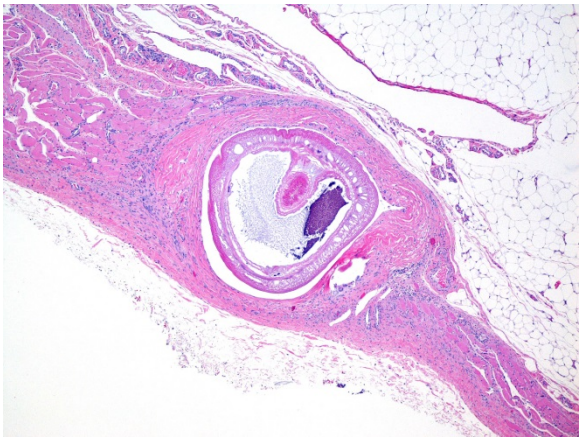

Testis, African Green monkey. Section of scrotum (from a different histology slide). The parasite is contained within a pseudocyst and there is disruption, mild mononuclear inflammation, and fibrosis of the tunica dartos (40X)(Photo courtesy of: US Army Medical Research Institute of Infectious Diseases, Pathology Division, Fort Detrick, MD http://www.usamriid.army.mil/)

(*Gigantorhynchus gigas*). In addition to their physical size, there is variation in the size of many of their adult cells. Polyploidy is common with some species having up to 343n. Finally, some species of thorny-headed worms have an interesting life cycle and have been referred to by some as "body snatchers". Generally, Acanthocephalans begin their life cycles within invertebrates, such as earthworms or crustaceans that live near water systems. When these invertebrates are infected, the thorny-headed worms cause the invertebrates to go towards the light (*i.e.* surface of the water or soil), where they will inevitably be eaten by a definitive host and allow for continuation of the life cycle.[3]

Contributing Institution:
US Army Medical Research Institute of Infectious Diseases
Pathology Division
Fort Detrick, MD
http://www.usamriid.army.mil/

References:

1. Anonymous. The History of the St. Kitts Vervet Monkey. www.stkittsheritage.com/wp-content/uploads/2013/12/Vervet-Monkey-article.pdf.
2. Bowman DW. Helminths. In: Bowman DW, ed. *Georgis' Parasitology for Veterinarians*. 10th ed. St. Louis, MO: Elsevier Saunders; 2014; 227-229.
3. Crompton D, Thomasson W, Nickol BB. *Biology of the Acanthocephala*. Cambridge, UK: Cambridge University Press; 1985:27.
4. Eberhard ML. Histopathologic diagnosis. In: Bowman DW, ed. *Georgis' Parasitology for Veterinarians*. 10th ed. St. Louis, MO: Elsevier Saunders; 2014; 430.
5. Gardiner CH, Poynton SL. *An Atlas of Metazoan Parasites in Animal Tissues*. Washington, DC; Armed Forces Institute of Pathology; 1999.
6. Strait K, Else JG, Eberhard ML. Parasitic diseases of nonhuman primates. In: Abee CR, Mansfield K, Tardif SD, Morris T, eds. *Nonhuman Primates in Biomedical Research: Diseases*. Vol. 2. 2nd ed. Boston, MA: Academic Press; 2012; 258-260.

Self-Assessment - WSC 2017-2018 Conference 16

1. Nidoviruses are members of which virus family?
    a. Picornaviridae
    b. Togaviridae
    c. Coronaviridae
    d. Circoviridae

2. The effects of *Eimeria macusaniensis* in camelids may be worsened with which of the following conditions?
    a. Bovine pestivirus
    b. Clostridium perfringens
    c. Clostridium septicum
    d. Mycobacterium paratuberculosis

3. Which of the following forms of sporotrichosis is most often seen in horses?
    a. Ocular
    b. Primary cutaneous
    c. Cutaneous-lymphatic
    d. Disseminated

4. Which of the following yeasts is significantly larger than the others in tissue section?
    a. Sporothrix sp.
    b. Cryptococcus neoformans
    c. Histoplasma capsulatum
    d. Coccidioides immitis

5. Which of the following is not seen in acanthocephalans?
    a. A reproductive tract
    b. A hypodermis
    c. A digestive tract
    d. A cuticle

Please email your completed assessment to Ms. Jessica Gold at Jessica.d.gold2.ctr@mail.mil for grading. Passing score is 80%.This program (RACE program number) is approved by the AAVSB RACE to offer a total of 0.5 CE Credits, with a maximum of 12.5 CE Credits being available to any individual Veterinary Medical Professionals for the 2017-2018 Wednesday Slide Conference. This RACE approval is for the subject matter categories of: SCIENTIFIC using the delivery method of NON-INTERACTIVE DISTANCE. This approval is valid in jurisdictions which recognize AAVSB RACE; however, participants are responsible for ascertaining each board's CE requirements.
RACE does not "accredit", "endorse" or "certify" any program or person, nor does RACE approval validate the content of the program.

Joint Pathology Center
Veterinary Pathology Services

WEDNESDAY SLIDE CONFERENCE 2017-2018

C o n f e r e n c e 17

31 January 2018

CASE I: 186 (JPC 4079216).

Signalment: Adult, freshwater crocodile, *Crocodylus johnsoni*, reptile.

History: Found dead. No preceding clinical signs.

Gross Pathology: None

EM Image Description:
The image shows multiple intact nucleated red blood cells and centrally a cell with a parasitopherous vacuole containing numerous spores. The higher magnification image of a single spore shows it to have a thick, multilayered wall composed of an electron-dense outer layer (exospore) an electron-lucent inner layer (endospore) and a plasma membrane enclosing the cytoplasm. At the posterior end of the cytoplasm there is a distinct nucleus to the center, a poorly defined posterior vacuole and multiple coils of the polar filament to the periphery. At the anterior end there is an anchoring disc underlying which are the membranes of the polaroplast. The anchoring disc is connected to the polar filament.

Contributor's Morphologic Diagnosis: Intrahepatic microsporidiosis

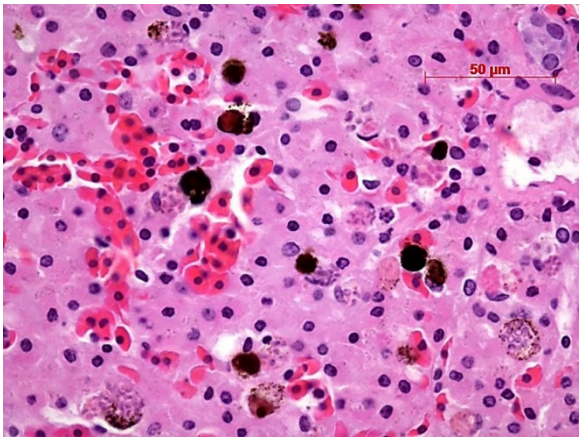

Liver, freshwater crocodile. Almost all Kupffer cells contained numerous (often up to 20) phagocytosed, slightly refractile, oval to round organisms approximately 2-3 um in diameter (Photo courtesy of: Gribbles Pathology, 1868 Dandenong Rd, Clayton, Victoria 3168, Australia) (HE, 400X).

Molecular diagnostics:
Sequencing of product amplified by Universal Microsporidian primers produced a 96% match across 276 base pairs to *Encephalitozoon hellem* (Animal Health Laboratories, Department of Agriculture and Food, Western Australia).

Contributor's Comment: The ultrastructural features of this organism are consistent with mature spores of *Microsporidia* spp.. The extrusion apparatus, composed of the coiled polar filaments and

anchoring disc, are characteristic of this organism.[11] The number and arrangement of the coils of the polar filament vary among genera and species.[4] The polar filament is discharged through the anterior end of the spore, penetrating a new host cell and inoculating the infective sporoplasm. The spore has a thick wall with three distinct layers including a proteinaceous exospore, a chitinous endospore and a plasma membrane making it resistant in the environment. Initial histology on the liver of this crocodile showed almost all Kupffer cells contained numerous (often up to 20) phagocytosed, slightly refractile, oval to round organisms approximately 2-3 um in diameter. In addition, similar organisms were present within macrophages in the mesentery associated with moderate chronic inflammation and occasional organisms were present within splenic macrophages (identified by special stains). The organisms were positive for PAS, ZN and GMS stains.

Microsporidia are unicellular and spore forming obligate parasites which cannot grow & divide outside the host cell. They belong to the phylum Microsporia which has over 150 genera. These organisms were originally classified as fungi, reclassified as protozoa and then again as fungi. Microsporidia have chitin and trehalose which are fungal components, heat shock proteins similar to those of fungi and fungal α- and β-tubulins.[11] All stages of the life-cycle occur within the parasitophorous vacuole. The most common microsporidia are: *Enterocytozoon bieneusi*, *Encephalitozoon hellem*, *Encephalitozoon intestinalis* (previously *Septata intestinalis*), and *Encephalitozoon cuniculi*.

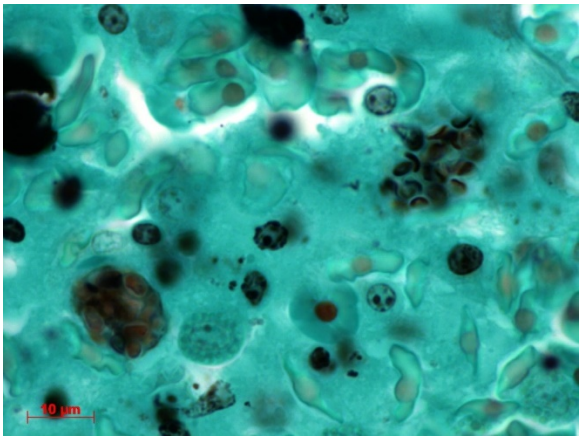

Liver, freshwater crocodile. Phagocytosed organisms within Kupffer cells (Photo courtesy of: Gribbles Pathology, 1868 Dandenong Rd, Clayton, Victoria 3168, Australia) (GMS, 1000X).

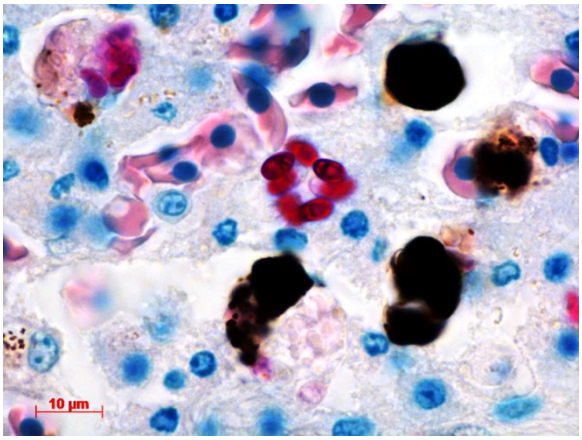

Liver, freshwater crocodile. Phagocytosed organisms within Kupffer cells (Photo courtesy of: Gribbles Pathology, 1868 Dandenong Rd, Clayton, Victoria 3168, Australia) (ZN, 1000X).

As common pathogens of arthropods and fish, Microsporidia are responsible for economic losses in the fish farming and bee-keeping industries.[11] *Encephalitozoon cuniculi* is the most commonly encountered microsporidial infection in veterinary practice. This infection was problematic for research rabbit colonies until screening for infection was introduced; however, it remains a common cause of fatal encephalitis in pet rabbits. *E. cuniculi* has also been described in farm-raised foxes and domestic dogs as well as spontaneous infection in numerous other domestic and wild species.[11]

Microsporidial infections have been described in numerous species of reptiles,[10]

most commonly bearded dragons which typically develop multisystemic granulomatous disease.[9] Infection in crocodiles has not previously been described.[10] Disseminated *E. hellem* infection has been described in a captive Egyptian fruit bat with the primary lesion being active cholangiohepatitis and acute renal tubular nephrosis associated with organisms.[3] Microsporidial infection has been described in psitticine birds with histological changes ranging from hepatic necrosis in budgerigars associated with organisms[1] to unilateral keraoconjunctivitis in a cockatoo.[8]
Multiple microsporidia have been identified as causative agents of disease in immunocompromised humans however *Enterocytozoon bieneusi* is the most commonly diagnosed.[11]

JPC Diagnosis: Granular leukocyte: Multiple Microsporidian spores, intracytoplasmic, freshwater crocodile (*Crocodylus johnsoni*), reptile.

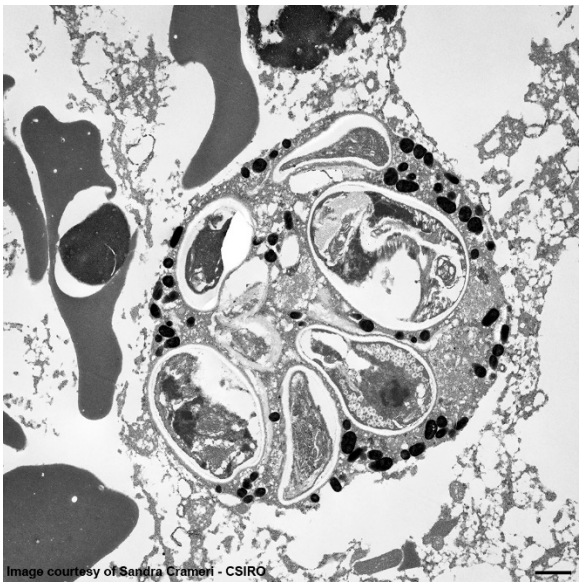

Liver, freshwater crocodile. A granulated leukocyte (presumably a Kupffer cell) contains numerous microsporidian spores within its cytoplasm. (Photo courtesy of: Gribbles Pathology, 1868 Dandenong Rd, Clayton, Victoria 3168, Australia)

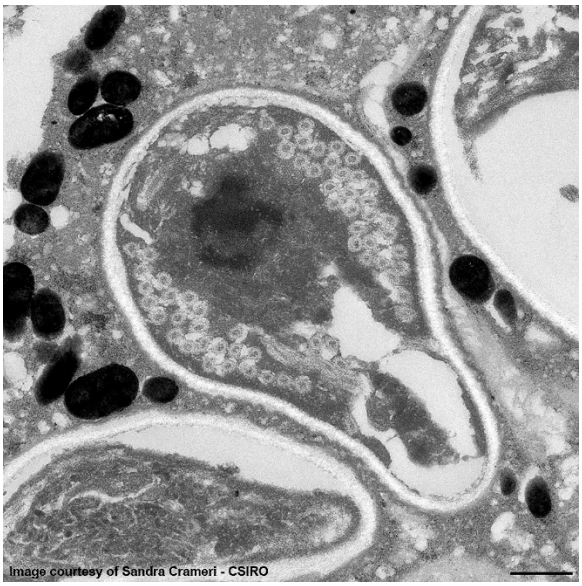

Liver, freshwater crocodile. Higher magnification of a spore. The spore has a trilaminar wall composed of an outer exospore and inner endospore delimited by a plasma membrane. There are numerous coils of the polar filament at the periphery of the spore and a dissolute nucleus centrally. The anterior end of the spore contains a poorly defined anchoring disk, and a posterior vacuole at the other end. (Photo courtesy of: Gribbles Pathology, 1868 Dandenong Rd, Clayton, Victoria 3168, Australia)

Conference Comment: There are over 100 genera and 1000 species within the phylum Microsporidia which affect many invertebrates and all vertebrates, particularly if they are immunosuppressed.[5] Microsporidians only reproduce asexually and are obligate intracellular eukaryotic organisms most closely related to fungi genomically. Infection follows injection of the sporoplasm into the host cell, where there is a proliferative merogenic phase, and eventually forming a sporont with a complex internal structure that lives within a parasitophorous vacuole. Spores are acid fast (carbol fuchsin), gram positive, luna positive, and contain a PAS positive polar granule.[2]

In reptiles, in addition to *Encephalitozoon* sp., *Pleistophora* sp. have been identified in lizards and snakes. In these populations of reptiles, organisms are identified

intracytoplasmically within renal tubules, hepatocytes, alveolar epithelial cells, gastric mucosal epithelial cells, enterocytes, capillary endothelial cells, macrophages, and ventricular ependymal cells in the brain.[5]

Drs. LaDouceur and Murphy have recently identified microsporidian in peppermint shrimp (*Lysmata* spp.) which resulted in grossly swollen, opaque, pale tan nodules within skeletal musculature containing numerous microscopic microsporidian spores with minimal tissue inflammation.[6]

In fish, two common microsporidial infections are *Loma salmonae* and *Pseudoloma neurophilia* which cause pathologic changes in the gills and central nervous system, respectively. *L. salmonae* predominately affects salmonids and *P. neurophilia* commonly affects Zebrafish and neon tetra. In fact, *P. neurophilia* is the most common pathogen in zebrafish research facilities and results in emaciation and spinal curvature of affected animals giving credence to the common name "skinny disease". Microscopically and often macroscopically, aggregates of microsporidia can be seen, and are termed "xenomas"; these cysts can be seen grossly on the gills of salmonids infected with *L. salmonae* and in the CNS of zebrafish infected with *P. neurophilia.*[7]

A common differential for *Encephalitozoon* spp., especially in mammals, is *Toxoplasma gondii* or *Neospora caninum.* Key differences are listed in the chart below.[2]

***Toxoplasma* spp.**	***Encephalitozoon* spp.**
Small cysts (60 µm)	Pseudocysts are large (up to 120 µm)
Spores not acid fast	Spores are acid fast (Carbol fuchsin)
Gram negative	Gram positive
Giemsa: cytoplasm is granulated	Giemsa: cytoplasm is light blue
Stains well with H&E	Stains poorly with H&E
Larger organism (2-6 µm)	Smaller organism (1.5 x 2.5 µm)
Tend to invoke necrosis	Necrosis not a common finding
Luna stain negative	Luna stain positive

Contributing Institution:
Gribbles Pathology
1868 Dandenong Rd
Clayton, Victoria 3168
Australia

References:

1. Black SS, Steinohrt LA, Bertucci DC, Rogers LB, Didier ES. *Encephalitozoon hellem* in budgerigars (*Melopsittacus undulatus*).*Vet Pathol*. 1997;34(3):189-198.
2. Cantile C, Youssef S. Nervous system. In: Maxie, MG, ed. *Jubb, Kennedy, and Palmer's Pathology of Domestic Animals.* Vol. 1. 6th ed. St. Louis, MO: Elsevier; 2016:385-386.
3. Childs-Sanford SE, Garner MM, Raymond JT, Didier ES, Kollias GV. Disseminated microsporidiosis due to *Encephalitozoon hellem* in an Egyptian fruit bat (*Rousettus aegyptiacus*). *J Comp Pathol*. 2006;134(4):370-373.
4. Franzen C, Müller A. Molecular techniques for detection, species

differentiation, and phylogenetic analysis of Microsporidia. *Clin. Microbiol. Rev*. 1999;12:243-285.
5. Jacobson ER. Parasites and parasitic diseases of reptiles. In: Jacobson ER, ed. *Infectious Diseases and Pathology of Reptiles*. Boca Raton, FL: CRC Press; 2007:580-581.
6. LaDouceur EEB, Murphy BG. Microsporidiosis in peppermint shrimp (Decapoda: Hippolytidae: *Lysmata* spp.). *J Zoo Wildl Med*. 2017;48(4):1223-1229.
7. Noga EJ. *Fish Disease Diagnosis and Treatment*. 2nd ed. Ames, IA: Wiley-Blackwell; 2010:247-253.
8. Phalen DN, Logan KS, Snowden KF. *Encephalitozoon hellem* infection as the cause of a unilateral chronic keratoconjunctivitis in an umbrella cockatoo (*Cacatua alba*). *Vet Ophthalmol*. 2006;9(1):59-63.
9. Richter B, Csokai J, Graner I, Eisenberg T, Pantchev N, Eskens HU, Nedorost N. Encephalitozoonosis in two inland bearded dragons (*Pogona vitticeps*). *J Comp Pathol*. 2013;148(2-3):278-282.
10. Scheelings TF, Slocombe RF, Crameri S, Hair S. *Encephalitozoon hellem* infection in a captive juvenile freshwater crocodile (*Crocodylus johnstoni*). *J Comp Pathol*. 2015;153(4):352-356.
11. Wasson K, Peper RL. Mammalian Microsporidiosis. *Vet Pathol*. 2000;37:113-128.

CASE II: 12-294 (JPC 4021148).

Signalment: Stillborn, male, Welsh-cross pony, *Equus caballus*, equine.

History: Animal presented for necropsy following stillbirth.

Gross Pathology: This male Welsh-cross pony fetus presented for necropsy to the Frederick Diagnostic Laboratory. The periocular and oral mucous membranes tissues were yellow and there was meconium pasted on the hair and skin (fetal distress). The subcutaneous tissues were discolored yellow (icterus) and there was marked subcutaneous edema in the intermandibular space (bottlejaw), at the thoracic inlet, and in the inguinal/femoral region. Additionally approximately 1L of clear yellow fluid was noted in the peritoneal cavity. The liver was markedly enlarged, rubbery pink/purple with rounded lobe margins. The kidneys were bilaterally brown and the adrenal glands both had multifocal acute cortical hemorrhages. The epicardium contained few, small (2-5mm) scattered hemorrhages in the left and right ventricular free walls and there was multifocal to coalescing, bright red subendocardial hemorrhages in both right and left ventricles extending into the myocardium.

Subcutaneous tissues, neck, equine fetus. The affected foal exhibited icterus and marked edema of the cervical tissues. (Photo courtesy of: Maryland Veterinary Diagnostic Laboratory, Frederick, MD.)

Laboratory Results (clinical pathology, microbiology, PCR, ELISA, etc.):

1. Equine Herpes Virus FAT Lung POSITIVE; Liver POSITIVE
2. Equine Viral Arteritis FAT Lung NEGATIVE

Thorax, equine fetus. There is extensive effusion within the pleural cavity, and the liver is markedly enlarged, brownish, and rubbery in texture. (Photo courtesy of: Maryland Veterinary Diagnostic Laboratory, Frederick, MD.)

Microscopic Description:

Adrenal gland: Primarily within the superficial cortex, there are multifocal to coalescing areas of necrosis and hemorrhage. Subcapsularly, there are numerous multinucleated synctial cells that are occasionally necrotic. Multifocally within cortical and synctial cells, there are 5-10 um eosinophilic intranuclear viral inclusion bodies that frequently peripheralize the chromatin. Multifocally occluding the sinusoids of both the cortex and the medulla, there are rare fibrin thrombi. The adjacent ganglion is essentially normal.

Contributor's Morphologic Diagnosis:

Adrenal gland: Cortical necrosis, multifocal with moderate cortical hemorrhage, subcapsular syncitiae, rare medullary sinusoidal thrombosis and eosinophilic, intranuclear viral inclusions

Contributor's Comment: Equine herpesvirus type 1 (EHV-1) typically results in a multisystemic vasculitis which is almost invariably fatal in equine fetuses and neonates. The virus can be subdivided into two subtypes both of which cause neonatal disease and respiratory disease, however, the most common subtype isolated in aborted foals is subtype 1 and this type is also felt to be the only subtype which will result in the neurologic form of the disease. Abortion frequently occurs in animals that have been exposed to the disease at an earlier point, potentially as a mild respiratory form of the disease. The virus is transmitted to the foal via leukocytes within the bloodstream and subsequently to the placenta. Fetal death typically occurs at the point of a sudden abortion without the mare showing premonitory signs.[9]

Aborted fetuses have diagnostic pathological lesions which were observed in this case. Affected animals often have significant subcutaneous and fascial edema as well as both thoracic and abdominal effusions. Additionally, icterus is a common finding. Histopathological findings characteristically are multiorgan hemorrhagic necrosis with acidophilic intranuclear inclusions within many tissues, but specifically within the bronchiolar and alveolar epithelium.[2,3,9]

This case of adrenal necrosis and hemorrhage in association with systemic EHV-1 and peri-

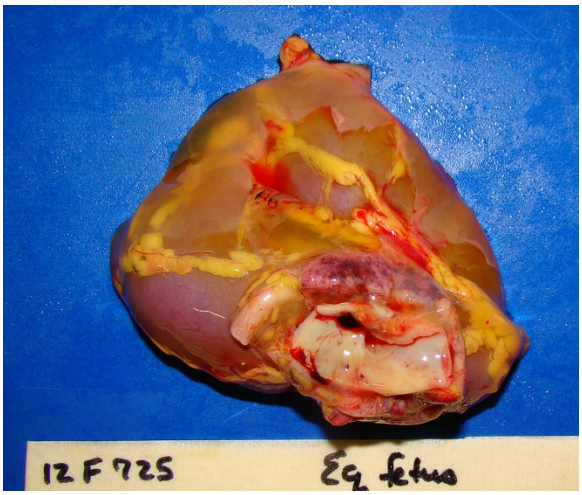

Adrenal gland, equine fetus. There are acute cortical hemorrhages on the adrenal gland.

partum stress is also interesting in its microscopic presentation which is similar to that seen in cases of endotoxic shock in humans and certain domestic species.[4] These instances are variably described in the literature as the Waterhouse-Fredrickson (Friderichsen) syndrome specific to the adrenal gland or in more general terms as the Shwartzman reaction in which endotoxic shock during late gestation results in multiorgan thrombosis and hemorrhage. The former syndrome has been reported as associated with endotoxin induced adrenocortical necrosis and hemorrhage which then causes adrenal insufficiency.[6] While the latter is used as a model for endotoxin induced disseminated intra-vascular coagulation (DIC).[8]

The Shwartzman phenomenon was described in the 1940s and1950s in humans relating to multi-organ infarction secondary to septic shock and endotoxin. Studies examining acute and severe hemorrhagic necrosis of the adrenal in rabbits used intravenous injection of endotoxin following pretreatment with adrenocorticotropic hormone (ACTH).[5] The resultant pathological changes occurred primarily in the zona fasciculata of the adrenal cortex and mimicked the Shwartzman reaction. Studies of localized Shwartzman reaction has been shown to be

Adrenal gland, equine fetus. There are multifocal to coalescing areas of necrosis and hemorrhage replacing about 33% of the cortex. (HE, 5X)

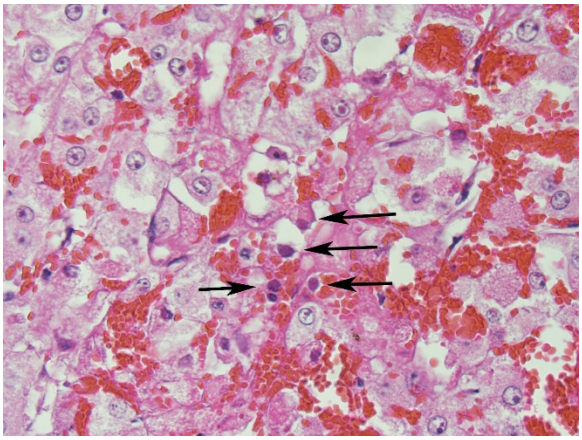

Adrenal gland, cortex, equine fetus. Within the areas of necrosis, the nuclei of degenerating adrenocortical cells contain glassy eosinophilic viral inclusions which fill the nucleus and peripheralize the chromatin. (HE, 400X)

due to massive releases of TNF-α by IFN-γ-activated macrophages, and results in microthrombi throughout the vasculature. While this particular case of abortion is theorized to be due to the effects of EHV-1 and not one of endotoxin related septic shock, the fetal stress associated with systemic equine herpesvirus infection likely resulted in a significant ACTH and substantial cortisol release with subsequent adrenal insufficiency. This priming by ACTH may have created a histopathological picture similar to that seen with the Shwartzman reaction in humans and the Waterhouse-Fredrickson syndrome described in septic calves and in baboons.[1,4] Interestingly, there is a report of fatal cytomegalovirus associated adrenal insufficiency in an immunocompromised human receiving steroid therapy in which histopathological examination of the adrenal glands noted a necrotizing adrenalitis with adrenocortical hemorrhage and intranuclear viral inclusions consistent with cytomegalovirus.[10]

This case and its associated photographs were generously contributed by Dr. Virginia Pierce, Director of the Frederick Diagnostic Laboratory.

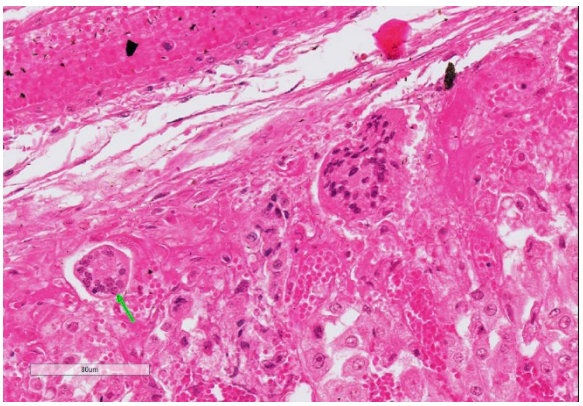

Adrenal gland, cortex, equine fetus. Primarily within the zone glomerulosa, there are numerous large viral syncytia; the nuclei of which contain viral inclusions as well. (HE, 400X)

JPC Diagnosis: Adrenal gland, cortex: Adrenalitis, necrohemorrhagic, multifocal to coalescing, moderate with intranuclear viral inclusions, viral syncytia, and capsular, cortical, and medullary thrombi, multifocal, moderate, Welsh-cross pony (*Equus caballus*), equine.

Conference Comment: Viral infections have been postulated to result in disseminated intravascular coagulation (DIC) by three mechanisms: viral or antiplatelet antibody-mediated platelet aggregation; directly by causing endothelial damage (the most likely mechanism in this case); or immune complex formation inducing activation of Hageman factor (factor XII). Hageman factor, the initiator of the intrinsic coagulation cascade, simultaneously converts plasminogen to plasmin which cleaves fibrinogen and fibrin to yield fibrin/fibrinogen degradation products (FDPs). These FDPs inhibit thrombin activity, fibrin polymerization, and platelet aggregation. Under normal circumstances, these two processes (coagulation and fibrinolysis) exist in equilibrium to limit thrombosis. Clinical manifestations of DIC include: generalized Schwartzman-like reaction (GSR); hemorrhagic adrenal necrosis (Waterhouse-Friderichsen syndrome); microangiopathic hemolytic anemia (MHA); acrocyanosis and gangrene; or hemolytic-uremic syndrome (HUS).[7]

The generalized Schwartzman-like reaction is characterized by bilateral hemorrhagic renal cortical necrosis which can cause oliguric renal failure especially in septicemic postpartum cows. Likewise, Waterhouse-Friderichsen syndrome, causes hemorrhagic adrenal necrosis in septicemic calves. MHA is a result of intravascular fragmentation of erythrocytes also commonly seen in septicemic calves which frequently also exhibit acrocyanosis and gangrene of the distal extremities. Finally, HUS occurs when disseminated coagulation is combined with acute renal failure. This syndrome is well documented in humans, and has also been documented in Greyhound dogs with a condition colorfully named “Alabama rot” in which there is idiopathic cutaneous and renal glomerular vasculopathy.[7]

Microscopically, animals in DIC have microthrombi in numerous organs, but are most easily detected in cerebral capillaries, renal glomeruli, adrenals, lungs, and myocardium. Generally, microthrombi are classified as hyaline thrombi (composed of fibrin), granular thrombi (composed of platelets), or hyaline globules/”shock bodies” (composed of FDPs). In cases with suspected DIC a prompt postmortem examination is imperative as fibrinolysis continues after death and most microthrombi will be lysed within 3 hours. Special stains for micro-thrombi include: Martius-scarlet-blue which stains fibrin red, or phosphotungstic acid hematoxylin (PTAH) which stains fibrin purple. Unfortunately, these stains only identify polymerized fibrin, however, fibrin strands can be identified in small vessels on

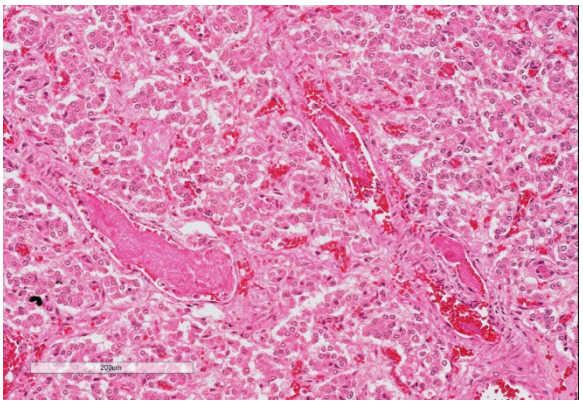

Adrenal gland, medulla. Within the medulla, and to a lesser extend within the cortex and capsule, small vessels are occluded by fibrin thrombin. (HE, 400X)

H&E that often contain entrapped fragmented red blood cells, termed schistocytes, which serves as an indirect indicator of DIC.[7]

Conference attendees enthusiastically discussed the contributor's suggestion that the necrosis and hemorrhage in the adrenal was a result of the Schwartzman reaction or Waterhouse-Friderichsen syndrome. However, as endotheliotropism and vascular thrombosis is well-documented in equine herpesvirus-1 infections, were unable to ascribe the lesions in the adrenal to other concurrent conditions in the absence of a more extensive clinical history or sections of other target tissues for these alternate possibilities.

Contributing Institution:
Armed Forces Radiobiology Research Institute (AFRRI)
Uniformed Services University of the Health Sciences (USUHS)
www.afrri.usuhs.mil

References:

1. Cary M, Kosanke S, White G. Spontaneous Waterhouse-Friderichsen syndrome in a gang-housed baboon. *J Med Primatol*. 2001;30:185-187.
2. Del Piero F, Wilkins PA, Timoney PJ, Kadushin J,Vogelbacker H, Lee JW, Berkowitz SJ, La Perle KMD. Fatal nonneurological EHV-1 infection in a yearling filly. *Vet Pathol*. 2000;37:672–676.
3. Hamir AN, Vaala W, Heyer G, Moser G. Disseminated equine herpesvirus-1 infection in a two-year-old filly. J Vet Diagn Invest. 1994;6:493-496
4. Hoffmann R. Adrenal lesions in calves dying from endotoxin shock, with special reference to the Waterhouse-Friderichsen syndrome. *J Comp Path*. 1977;87:231-239.
5. Levin J, Cluff LE. Endotoxemia and adrenal hemorrhage: a mechanism for the Waterhouse-Friderichsen syndrome. *J Exp Med*. 1965;121:247–260.
6. Maitra A. The endocrine system. In: Kumar V, Abbas A, Fausto N and Aster JC eds. *Robbins and Cotran: Pathological Basis of Disease.* 8th ed. Philadelphia, PA: Elsevier Saunders. 2010:1155.
7. Robinson WF, Robinson NA. Cardiovascular system. In: Maxie, MG, ed. *Jubb, Kennedy, and Palmer's Pathology of Domestic Animals.* 6th ed. Vol. 3. Philadelphia, PA: Elsevier; 2016:64-66.
8. Rosenberg HF. The Shwartzman reaction repealed. *J Leuk Biol*. 2007;81:623-624.
9. Schlafer DH, Miller RB. Female genital system. In: Maxie MG, ed. *Jubb, Kennedy and Palmer's Pathology of Domestic Animals*. 5th ed. Vol 3. Philadelphia, PA: Elsevier Saunders; 2007:532-534.
10. Uno K, Konishi M, Yoshimoto E, Kasahara K, Mori K, Maeda K, Ishida E, Konishi N, Murakawa K, Mikasa K. Fatal cytomegalovirus-associated adrenal insufficiency in an AIDS patient receiving corticosteroid therapy. *Intern Med*. 2007;46:617-620.

CASE III: S-13-1538 (JPC 4085535).

Signalment: 2-year-old, female, Aberdeen Angus, *Bos taurus*, bovine.

History: Seventy, 1.5- to 2-year-old Aberdeen Angus, Hereford and mixed breed steers and heifers were grazing a mixed pasture composed of *Festuca arundinacea*, *Lotus corniculatus*, and *Trifolium repens* and supplemented with *Trifolium pretense* haylage. The herd was managed in a rotational grazing system, and paddocks were sprayed with a commercial liquid formula for bloat prevention. The animals had access to an old abandoned building lodging waste material, including an unlabeled bucket containing an unidentified gray-white powder. Over a period of 21 days, 14 animals (20%) became sick, 10 (14%) died, and 4 recovered. Affected animals had diarrhea, melena, mild ataxia, and/or difficulty standing. The clinical course in fatal cases was 12-18 hrs.

Omasum, ox: There is extensive hemorrhage of the omasum with focal areas of ulceration (arrows0 and mucosal sloughing. (Photo courtexy of: Plataforma de Investigación en Salud Animal, Instituto Nacional de Investigación Agropecuaria (INIA), Uruguay, , www.inia.uy)

Gross Pathology: Three cattle were autopsied. The main gross findings included severe diffuse congestion and hemorrhage of the mucosa of the abomasum, omasum and rumen, with multifocal extensive mucosal/epithelial sloughing, erosions and ulcers in the forestomachs. The submucosa of the abomasum and forestomachs was moderately expanded by red-tinged gelatinous material (edema and hemorrhage). In one of the animals there was diffuse bilateral pallor of the cortical renal parenchyma.

Laboratory Results (clinical pathology, microbiology, PCR, ELISA, etc.):

The arsenic concentration (DM) in the liver of three animals were 20, 31 and 24 ppm, and lead concentrations were 8.3, 25 and 9.4 ppm, respectively. Mercury was no detected in any case.

Microscopic Description:

Examined is a section of the *vela abomasica* (omaso-abomasal ostium).

Omasum: Frequently, the mucosa is ulcerated with abundant necrotic cells, debris, fibrin, edema, hemorrhage, plant material and mixed bacterial colonies. Multifocally in more preserved areas, where the aforementioned changes are more superficial and do not reach the mucosal basement membrane, the basal layer of the epithelium is detached, and the basal cells are swollen and have a clear eosinophilic vacuolated cytoplasm, or exhibit individual cells necrosis. Multifocally, there are large intraepithelial spaces filled with abundant neutrophils, edema and fibrin (pustules). The submucosa underlying the ulcerated areas is multifocally expanded by edema and fibrin, extravasated erythrocytes, and viable and

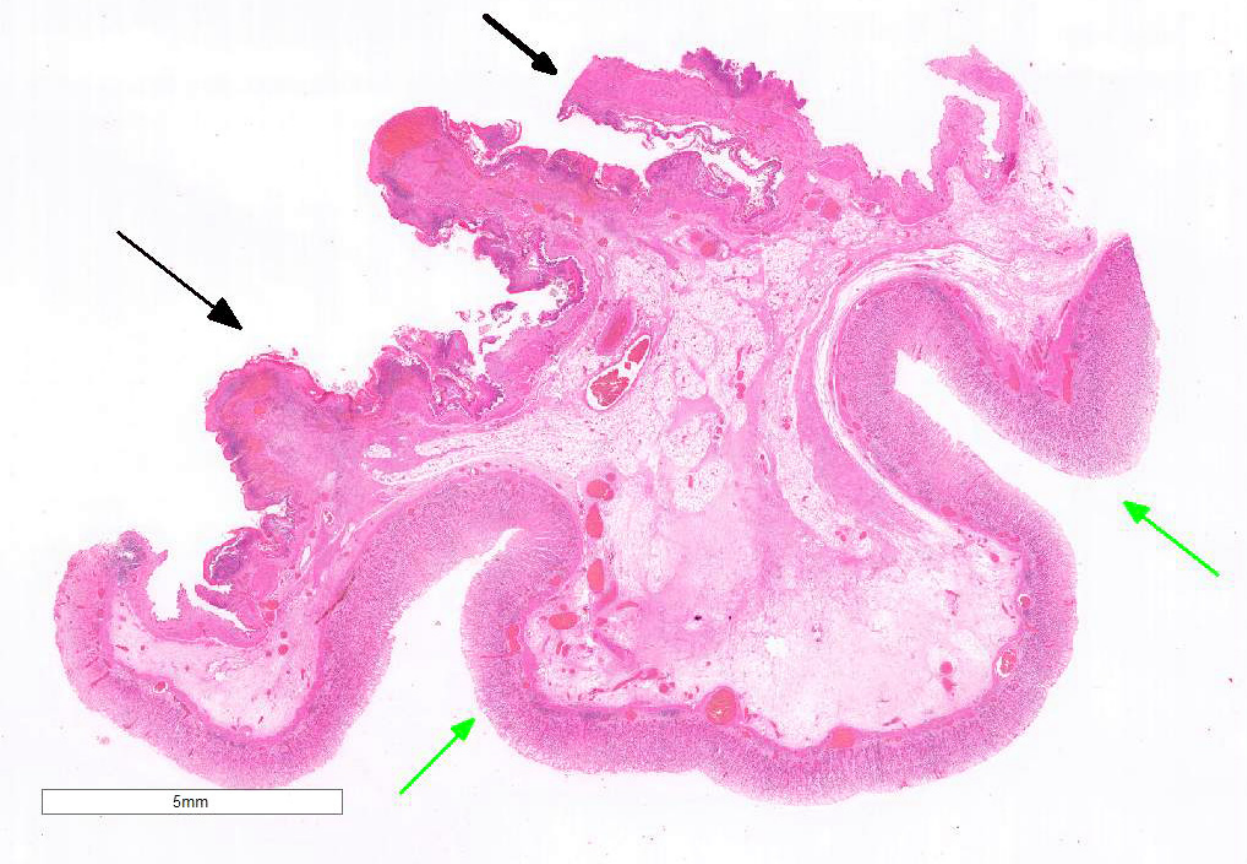

Forestomachs, ox. A single section taken at the omaso-abomasal ostium is submitted. There is necrosis and hemorrhage with mucosal sloughing of the omasum (black arrows) but minimal change in the mildly autolytic abomasum (green arrows). (HE, 5X)

degenerate neutrophils. The submucosal blood vessels are either congested and lined by hypertrophic endothelial cells, or occluded by fibrin thrombi and lined by endothelial necrotic cells. The tunica muscularis and adventitia are variably expanded by abundant edema and moderate numbers of viable and degenerate neutrophils. Lymphatic vessels are multifocally ectatic.

Abomasum: Diffusely, mucosal and submucosal vessels are congested and there is multifocal extravasation of erythrocytes. Edema and few infiltrating eosinophils, neutrophils and lymphocytes are observed in the lamina propria. Some scattered parietal and chief cells exhibit degeneration or necrosis. Occasionally, glands in the deeper aspect of the mucosa are mildly ectatic, lined by attenuated epithelium and filled with small amounts of sloughed necrotic epithelial cells. The submucosa is diffusely expanded by edema and neutrophils. Note: in most sections there is variable autolysis in the mucosa of the abomasum.

Contributor's Morphologic Diagnosis:

1. Omasum: omasitis, necrohemorrhagic, suppurative, ulcerative, diffuse, severe, acute.
2. Abomasum: abomasitis, necrohemorrhagic, diffuse, severe, acute.

Contributor's Comment: The disease was diagnosed as arsenic poisoning. The results indicated arsenic intoxication and lead

exposure. A sample of the powder found in the buckets in the abandoned building present in the paddock was submitted to a laboratory for determination of its chemical composition, and proved to be lead arsenate, an inorganic insecticide that used to be extensively used in agriculture.[5] Retrospectively, it was found out that the farm where this outbreak occurred used to be an orange orchard a few decades ago. The current property owner had purchased the farm in recent years, and was unaware of the presence of this insecticide in this building. In several occasions the farmer had seen cattle entering the abandoned building where the insecticide had been inadvertently stored.

Arsenic is a ubiquitous toxic element that is concentrated in the environment as a result of industrial activities. Before the 1960s, arsenic was used extensively in pesticides, herbicides, fungicides, paint, and leather and wood preservatives.[2,4] Arsenic has 3 oxidative stages, and intoxication is associated with either the trivalent (arsenite) or pentavalent (arsenate) forms. The pentavalent form is reduced to the trivalent form in the rumen. In cattle, the lethal dose 50% after ingestion is 1-25 mg/kg for trivalent arsenic, and 30-100 mg/kg for the pentavalent form.[2]

Although acute arsenic poisoning is uncommon nowadays, it should be considered in some particular epidemiological conditions that allow animals to access areas where the elements persist.[2,6] Arsenic poisoning is due to sulfhydryl group binding, and inhibition of cellular metabolic activity.[3] Arsenic is also a low-grade corrosive and irritant. Signs and

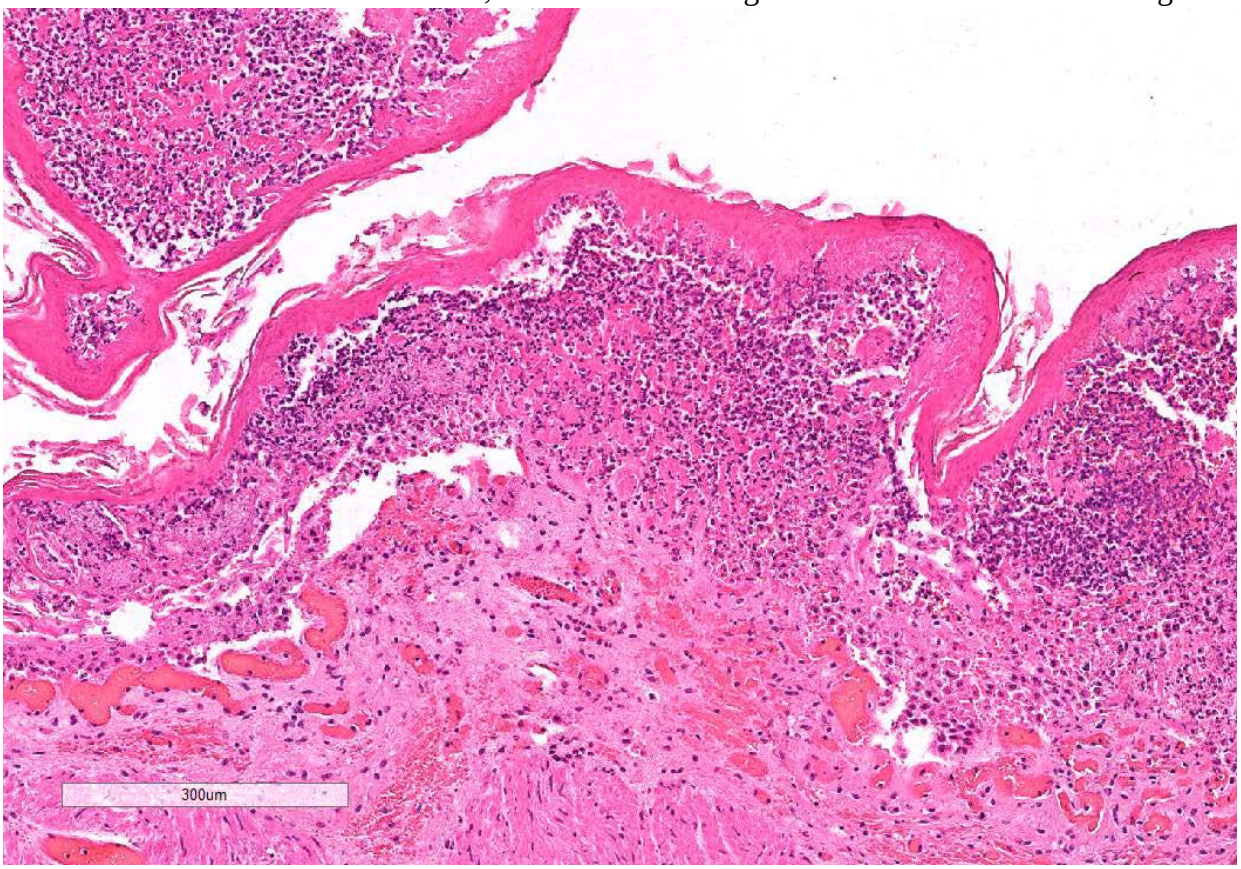

Omasum, ox. ***The necrotic mucosa is lifted off the underlying lamina propria by an infiltrated of large numbers of degenerate neutrophils admixed with hemorrhage, fibrin edema, and abundant cellular debris. (HE, 81X)***

lesions of acute arsenic poisoning in domestic animals are referable to the gastrointestinal tract (congestion, edema, hemorrhage, necrosis), liver (hepatocellular necrosis), and kidney (tubular necrosis). Skin and nervous lesions and signs occur in subacute to chronic poisoning, and include edema and petechiation of the brain (mediated by vascular injury), and dermatitis.[2-6] In addition to the alimentary tract lesions presented in this conference, the microscopic examination of the kidneys in two of the examined cattle revealed diffuse nephrosis, which was supportive of systemic arsenic poisoning.

The main differential diagnosis for necrohemorrhagic and ulcerative lesions of the forestomachs in cattle in Uruguay is *Baccharis coridifolia* poisoning, which causes necrohemorrhagic lesions in the digestive tract; however no toxic plants were found in the pasture.[1] Other differential diagnoses include viral agents such as bovine viral diarrhea virus (BVDV, mucosal disease), bovine herpesvirus-1 (BHV-1), malignant catarrhal fever (MCF) virus, and bluetongue disease virus. BVDV and BHV-1 infection were ruled out by immuno-histochemistry in the omasum in this case.

JPC Diagnosis: Omasum: Omasitis, necrotizing, diffuse, severe with marked submucosal edema, Aberdeen Angus (*Bos taurus*), bovine.

Conference Comment: Arsenic poisoning may occur orally or percutaneously, with the percutaneous route having a lower toxic dose which is potentiated by high body temperature. Common sources of arsenic for animals include insecticides and herbicides, more specifically sodium arsenite, lead arsenate (the agent in this case), and arsenic pentoxide. The most susceptible organs are the brain, lungs, liver, kidney, and alimentary mucosa due to their high metabolic requirements. In general, the pattern of lesions corresponds to the route of intoxication except in pigs where the signs are only referable to the nervous system.[3]

There are two types of arsenicals, inorganic and organic, which each have trivalent and pentavalent forms. Of the two, inorganic arsenite (As^{3+}) is the most toxic, followed by inorganic arsenate (As^{5+}), trivalent organics, and pentavalent organics. In general, inorganics and trivalent organics affect the alimentary tract and vasculature, and pentavalent organics lead to neurologic signs. The main mechanism of action of arsenic is combination with an inactivation of sulfhydryl groups which results in systemically decreased metabolic activity. The clinical signs for inorganic arsenite (As^{3+}), inorganic arsenate (As^{5+}), and trivalent organics are similar. In the peracute form, very large amounts can result in sudden death within 24 hours with no gross lesions. In the acute form, less poison is ingested and there are several days after ingestion and before onset of clinical signs which include: vomiting, colic, weakness, staggering, ataxia, recumbency, watery diarrhea, rumen and gastrointestinal atony, shock, collapse, and eventually death. Microscopically, the lesions associated with acute toxicity can be attributed to vascular injury with marked gastric and intestinal mucosal and submucosal congestion, edema, hemorrhage, and ulceration. Liver and kidney are affected too with multifocal hepatic and renal proximal tubular necrosis. The subacute and chronic forms have the same distribution as the acute form with more severe clinical signs (fatigue, intense thirst, brick-red mucus membranes, and swollen joints) and, microscopically, glomerular changes which include capillary dilation which results in ischemia, proteinuria, and tubular necrosis eventually culminating in tubular fibrosis. In

pigs specifically, organoarsenical phenylarsonic acid derivatives (arsanilic acid or 3-nitro-4-hydroxyphenylarsonic acid) are frequently used as feed additives to encourage growth and control of intestinal disease (ie. Swine dysentery). Toxic doses of either results in a spectrum of lesions from white matter edema in the central nervous system to Wallerian degeneration of the peripheral nerves.[3]

The differentials discussed above by the contributor can be ruled out based on the location of gross lesions and microscopic appearance. For instance, malignant catarrhal fever (bovine gammaherpesvirus) generally has ocular and oral lesions, and microscopically there will be perivascular lymphoproliferative lesions of predominately CD8+ T-cells. Bovine herpesvirus-1, or bovine rhinotracheitis, would have lesions in the mouth, pharynx, and trachea with eosinophilic intranuclear inclusion bodies microscopically. Finally, the mucosal disease form of bovine pestivirus and bluetongue (orbivirus) generally produce oral and nasal mucosal ulceration also.[3]

Conference attendees carefully considered the contributor's morphologic diagnosis of necrohemorrhagic abomasitis; however the absence of hemorrhage or inflammatory infiltrates (other than aggregates of lymphocytes and plasma cells in the deep mucosa) or underlying vascular changes led to a unanimous consensus that the abomasal mucosal changes were the result of autolysis.

Contributing Institution:
Plataforma de Investigación en Salud Animal
Instituto Nacional de Investigación Agropecuaria (INIA), Uruguay
www.inia.uy

References:

1. Barros CSL. Livestock poisoning by *Bacharis coridifoia*. In: Garland T, Barr AC (ed).*Toxic Plants and other Natural Toxicants*. New York, NY: CAB International; 1998:569-572.
2. Bertin FR, Baseler LJ, Wilson CR, Kritchevsky JE, Tylor SD. Arsenic toxicosis in cattle: meta-analysis of 156 cases. *J Vet Intern Med*. 2013; 27: 977–981.
3. Cantile C, Youssef S. Nervous system. In: Maxie, MG, ed. *Jubb, Kennedy and Palmer's Pathology of Domestic Animals*. Vol. 1. 6th ed. Philadelphia, PA: Elsevier; 2015:327-328.
4. Neiger R, Nelson N, Miskimins D, Caster J, Caster L. Bovine arsenic toxicosis. *J Vet Diagn Invest*. 2004;16:436–438.
5. Peryea FJ. Historical use of lead arsenate insecticides, resulting soil contamination and implications for soil remediation. *Proceedings of the 16th World Congress of Soil Science, Montpellier, France*. 1998. Available at: soils.tfrec.wsu.edu/leadhistory.
6. Selby LA, Case AA, Osweiler GD, Hayes HM Jr. Epidemiology and toxicology of arsenic poisoning in domestic animals. *Environ Health Perspect*. 1977; 19:183–189.

CASE IV: 2017 B (JPC 4101690).

Signalment: 3-year-8-month-old, female, Holstein, *Bos taurus*, bovine.

History: An idiopathic disease occurred in 4 of 80 dairy cows during the month of April. The affected cows showed anorexia, and dystaxia and/or astasia. Three of the affected cows were slaughtered; a fourth was submitted for necropsy. Clinically, this cow had sudden astasia 5 days before necropsy,

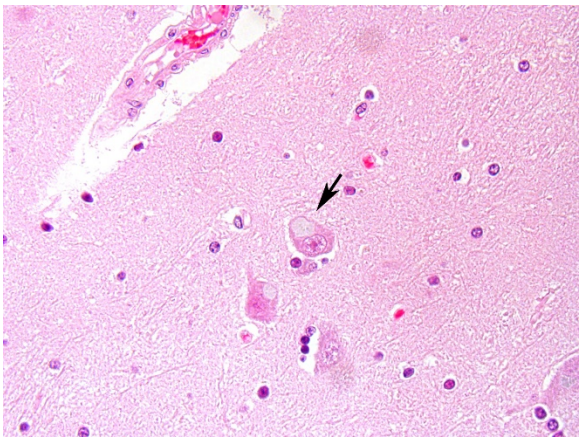

Pons, ox. Within numerous neurons, especially within perikarya, there are single discrete irregularly round amphophilic inclusions. (HE, 5X)

and became hyposensitive. The cow stretched its forelimbs frequently and often had spasms in the left hindlimb.

Gross Pathology: Mild congestion was observed in the brain. Muscles in the left hindlimb, in which spasms had been observed, were dark-red.

Laboratory Results (clinical pathology, microbiology, PCR, ELISA, etc.): None provided.

Microscopic Description: After hematoxylin and eosin (HE) staining, numerous basophilic inclusion bodies approximately 15 µm in diameter were observed in the perikarya and neuropil. The inclusion bodies in the perikarya were round to cauliflower-shaped, and some had dense cores. Bodies in the neuropil were round and occasionally concentric, and stained homogenously. They were positive on PAS stain and resistant to diastase and β-amylase digestion, but partly sensitive to α-amylase digestion. Further, these bodies stained red with Best's carmine, brown with iodine, clear blue with Alcian blue pH2.5 and blue with colloidal iron. The bodies were mostly negative on Nissl stain, but the cores of some bodies were positive.

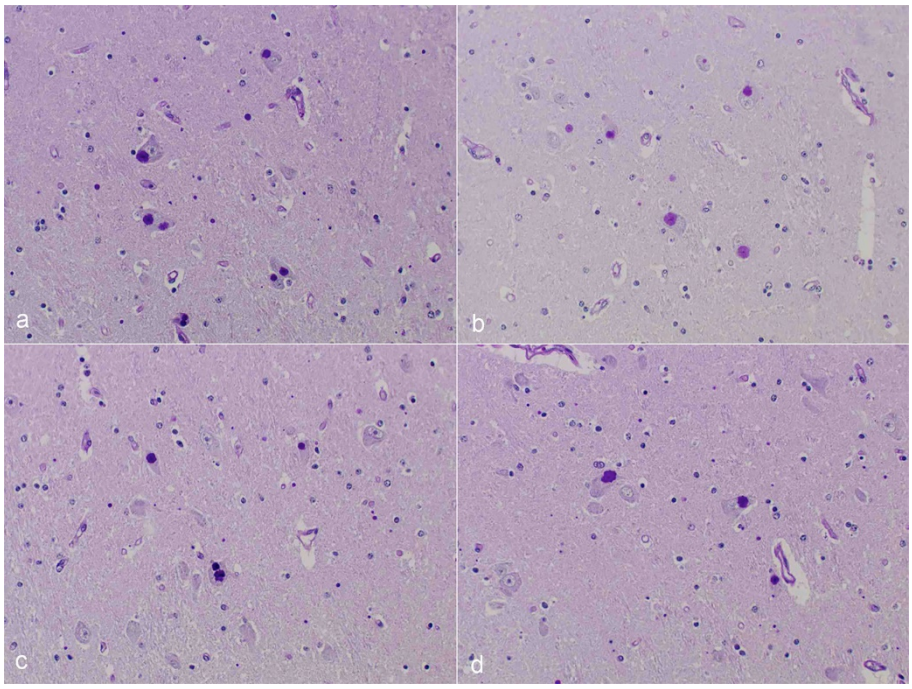

Pons, ox. Neuronal inclusions are positive on PAS (upper left) mildly resistant to alpha-amylase digestion (upper right) and resistant to and resistant to diastase and beta- amylase. (Photo courtesy of: National Institute of Animal Health, National Agriculture and Food Research Organization (NARO), 3-1-5Kannondai, Tsukuba, Ibaraki 3050856, Japan, (WSC ID95), http://www.naro.affrc.go.jp/english/niah/index.html)

The inclusion bodies in perikarya were numerous in the diencephalons, especially in the dorsal region of the thalamus. In neuropil, the bodies were observed throughout the central nervous system (CNS), but few were observed in the cerebellum or spinal cords. Such lesions were seen only in the CNS.

Immunohistochemical examination was performed using anti-ubiquitin polyclonal antibodies and anti-GFAP antibodies. The inclusion

bodies were slightly reactive with anti-ubiquitin antibodies. In sections with anti-GFAP antibodies, the inclusion bodies were not surrounded by GFAP-positive cells, indicating they rarely occur in astrocytes.

On transmission electron microscopy, the inclusion bodies in the neuronal perikarya and neuropils consisted of filamentous components. The width of the filaments was approximately 10nm. The inclusion bodies were not surrounded by membranes. Occasionally, filamentous components aggregated in the center and radially distributed to the periphery. The inclusion bodies in the neuropils were not surrounded by the myelin sheath.

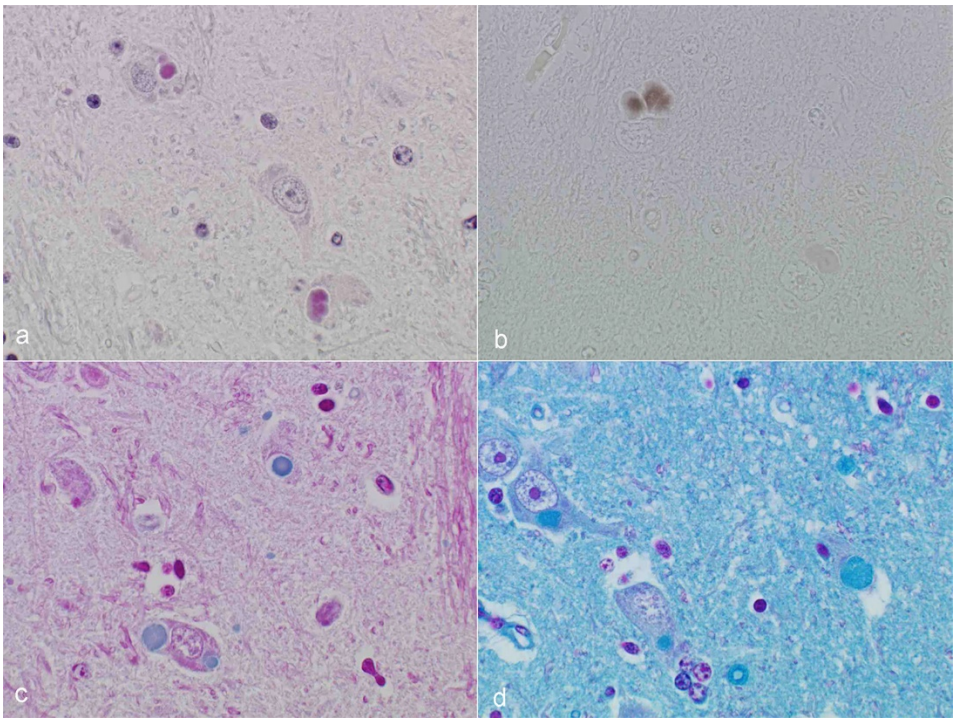

Pons, ox. Neuronal inclusions stain red with Best's carmine (upper left) brown with iodine (upper right), clear blue with Alcian blue 2.5 (lower left) and blue with colloidal iron (lower right). (Photo courtesy of: National Institute of Animal Health, National Agriculture and Food Research Organization (NARO), 3-1-5Kannondai, Tsukuba, Ibaraki 3050856, Japan, (WSC ID95), http://www.naro.affrc.go.jp/english/niah/index.html))

Contributor's Morphologic Diagnosis:

Diencephalon: Lafora-like bodies (polyglucosan bodies), intra-perikarya and intra-dendrites, numerous, Holstein, bovine

Contributor's Comment: Several types of the inclusion bodies of the CNS have been recognized in humans and animals. The polyglucosan body is a one of these inclusions. In this case, the inclusion bodies seen in the CNS were considered to be polyglucosan bodies based on morphological and histochemical features. Polyglucosan bodies are classified into Lafora bodies and corpora amylacea based on their location in the tissue.[6] Lafora bodies are localized in the perikarya and process of nerve cells; corpora amylacea are localized to within axons and /or astrocytes. In the present case, the inclusion bodies were primarily observed in perikarya, which identified them as Lafora bodies.

Lafora disease is a progressive myoclonic epilepsy in humans associated with an autosomal recessive hereditary defect.[2,6] Histopathologically, the bodies were, amorphous to cauliflower-like, and some had core, slightly basophilic, cytoplasmic inclusion bodies, which are identified as Lafora bodies if seen in the CNS, heart, and liver. In animals, Lafora bodies in the CNS have been reported in dogs,[8] cat,[3] and cattle.[5,9] Although hereditary

spread has been reported in canines, the etiology of Lafora disease in cattle is obscure.

In addition, polyglucosan bodies in the CNS associated with aging have been reported in several animals.[4,10] However, the present case was considered to be too young to have such age-related lesions. Although the genetic background and the association with age cannot be proven, the similarity of this case to human Lafora disease was considered interesting.

JPC Diagnosis: Pons, perikarya: Polyglucosan (Lafora) bodies, numerous, Holstein (*Bos taurus*), bovine.

Conference Comment: In humans, non-viral inclusion bodies have been further classified as Hirano, Pick, Lewy, Lafora, and Bunina bodies based on ultrastructural differences. Hirano-like bodies are more elongated microscopically and ultrastructurally are composed of beaded filaments. Bunina bodies are much smaller (2-5 µm) and are often arranged in clusters or chains. Bodies resembling Hirano and Bunina have been identified in horses and dogs, and although their pathogenic potential has not been investigated, there are a not uncommon feature of equine motor neuron disease. Finally, Lafora bodies are the most commonly identified non-viral inclusion in domestic animals and appear to be age related. They are located within neuronal parikarya, neuropil, and axons and are typically an incidental finding. These basophilic to amphophilic inclusions are strongly PAS-positive and metachromatic. Ultrastructurally, they are a mixture of branching filaments, non-membrane bound electron-dense bodies, and glycogen. Lafora bodies are generated due to abnormalities of carbohydrate metabolism which lead to the

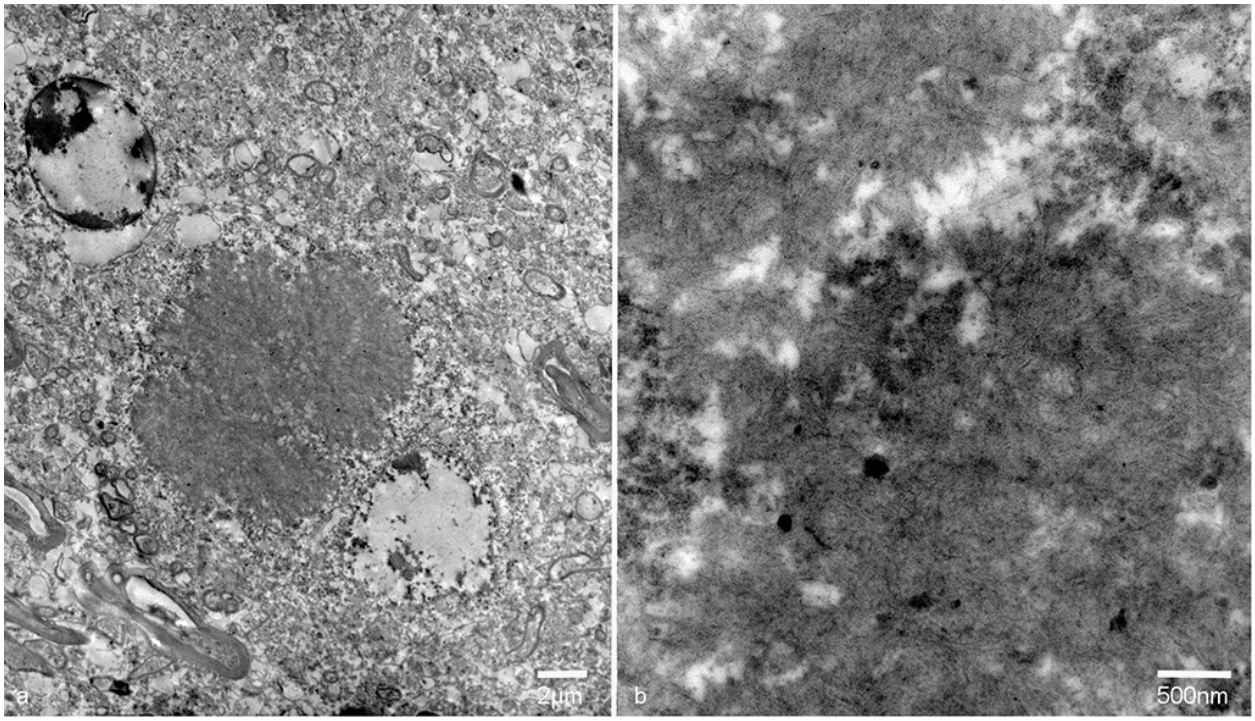

Pons, ox. Neuronal inclusions consist of mats of 10nm filaments located adjacent to the nucleus. (Photo courtesy of: National Institute of Animal Health, National Agriculture and Food Research Organization (NARO), 3-1-5Kannondai, Tsukuba, Ibaraki Ibaraki 3050856, Japan, (WSC ID95), http://www.naro.affrc.go.jp/english/niah/index.html).

production of glucose polymers termed polyglucosans. When present in large numbers, they may be due to Lafora disease, which is analogous to the autosomal recessive form of human Lafora disease and has been reported in Basset Hounds, Poodles, Beagle dogs, and Miniature Wire-haired Dachshunds. In the Dachshund, it has the highest incidence and is a triplet repeat disorder (the first discovered in domestic animals).[1] In a 2014 study, 50% of the study's cohort carried at least one copy of the EPM2B mutation, which is one of the gene mutations in the human form of Lafora disease.[7] In Lafora disease, the polyglucosan bodies are most numerous in Purkinje cells, and neurons of the caudate, thalamic, and periventricular nuclei. Clinically, these animals exhibit progressive myoclonus.[1]

Contributing Institution:

National Institute of Animal Health,
National Agriculture and Food Research Organization (NARO)
3-1-5Kannondai, Tsukuba, Ibaraki 3050856, Japan
http://www.naro.affrc.go.jp/english/niah/index.html

References:

1. Cantile C, Youssef S. Nervous system. In: Maxie, MG, ed. *Jubb, Kennedy and Palmer's Pathology of Domestic Animals*. Vol. 1. 6th ed. Philadelphia, PA: Elsevier; 2015:255, 292.
2. Cavanagh JB. Corpora-amylacea and the family of polyglucosan disease. *Brain Res Rev*. 1999;29:265-295.
3. Hall DG, Steffens WL, Lassiter L. Lafora bodies associated with neurologic signs in a cat. *Vet Pathol*. 1998;35:218-220.
4. Kamiya S, Suzuki Y. Polyglucosan bodies in the brain of cat. *J Comp Path*. 1989;101:263-267.
5. Kreeger JM, Frappier DC, Kendall JD. Systemic glycoproteinosis resembling Lafora's disease in a cow. *Cornell Vet*. 1991;81:215-221.
6. Minassian BA. Lafora's disease: towards a clinical, pathologic, and molecular synthesis. *Pediatr Neurol*. 2001;25:21-29.
7. Sainsbury R. DNA screening for Lafora's disease in miniature wire-haired dachshunds. *Vet Rec*. 2014; 175(22):568.
8. Schoeman T, Williams J, Wilpe EV. Polyglucosan storage disease in a dog resembling Lafora's disease. *J Vet Intern Med*. 2002;16:201-207.
9. Simmons MM. Lafora disease in the cow. *J Comp Path*. 1994;110:389-401.
10. Yanai T, Masegi T, Iwanaka M, et al. Polyglucosan bodies in the brain of a cow. *Acta Neuropathol*. 1994;88:75-77.

Self-Assessment - WSC 2017-2018 Conference 17

1. Microscpoiridia are derivative forms of what family?
    a. Fungi
    b. Bacteria
    c. Viruses
    d. Protozoa

2. Which of the following is NOT a common gross finding in equine fetuses aborted due to EHV-1 ?
    a. Subcutaneous and fascial edema
    b. Icterus
    c. Thoracic and abdominal effusion
    d. Fibrinous polyarthritis

3. Which of the following is NOT a clinical manifestation of DIC?
    a. Waterhous-Friedrichsen syndrome
    b. Hemolytic-uremic syndrome
    c. Generalized Schwartzman-like reaction
    d. Caval syndrome

4. Which of the following is integral to the pathogenesis of arsenic toxicity?
    a. Inhibition of the Embden-Meyerhof pathway
    b. Binding to sulfhydryl groups
    c. Inhibition of lysyl hydroxylase
    d. Formation of pyrrol esters

5. Which of the following is not a form of neuronal inclusion?
    a. Polyglucosan body
    b. Councilman body
    c. Lafora body
    d. Corpora amylacea

Please email your completed assessment to Ms. Jessica Gold at Jessica.d.gold2.ctr@mail.mil for grading. Passing score is 80%.This program (RACE program number) is approved by the AAVSB RACE to offer a total of 0.5 CE Credits, with a maximum of 12.5 CE Credits being available to any individual Veterinary Medical Professionals for the 2017-2018 Wednesday Slide Conference. This RACE approval is for the subject matter categories of: SCIENTIFIC using the delivery method of NON-INTERACTIVE DISTANCE. This approval is valid in jurisdictions which recognize AAVSB RACE; however, participants are responsible for ascertaining each board's CE requirements.
RACE does not "accredit", "endorse" or "certify" any program or person, nor does RACE approval validate the content of the program.

Joint Pathology Center
Veterinary Pathology Services

WEDNESDAY SLIDE CONFERENCE 2017-2018

C o n f e r e n c e 18

7 February 2018

Elizabeth A. Mauldin, DVM, Dipl. ACVP & ACVD
Professor of Dermatopathology
Academic Head of PennVet Laboratory of Pathology and Toxicology
Ryan Veterinary Hospital, Rm 4035
3900 Delancey St, Philadelphia, PA 19104

CASE I: 1704415 (JPC 4101081).

Signalment: 21-year-old, female, American Quarter Horse (*Equus caballus*), equine.

History: The mare had a well-circumscribed hairless mass in the right nuchal region. The mass was reported to be pruritic and was excised surgically and submitted whole for histopathologic evaluation.

Gross Pathology: The submitted formalin-fixed sample consisted of haired skin with an approximately 14 mm diameter, slightly firm, tan, raised and hairless mass that markedly expanded the superficial dermis and elevated the epidermis.

Laboratory Results (clinical pathology, microbiology, PCR, ELISA, etc.):
None provided.

Microscopic Description:
The superficial dermis is focally expanded by an unencapsulated, multilobulated and densely cellular neoplasm that replaces adnexal units and elevates the epidermis. The neoplastic cells have variable arrangements,

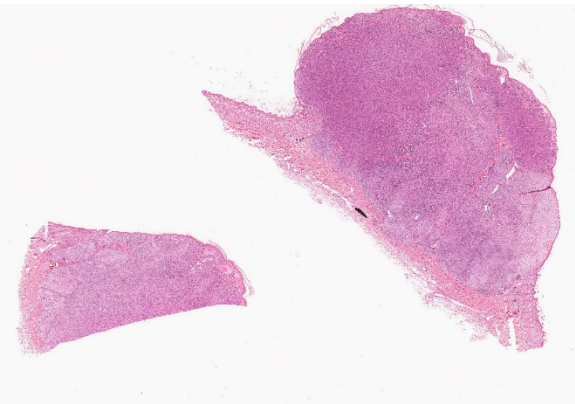

Haired skin, horse. Glomus tumor, horse, haired skin. A multilobulated, highly cellular neoplasm expands the dermis and elevates the epidermis. (HE, 7X) (Photo courtesy of: University of Pennsylvania, School of Veterinary Medicine, Department of Pathobiology http://www.vet.upenn.edu/research/academic-departments/)

ranging from dense sheets and nests to trabeculae or thin ribbons separated by a delicate fibrovascular stroma. Multifocally throughout the neoplasm, cells closely abut or palisade along vascular channels and impinge on the lumina without disrupting the endothelium. The cells are cuboidal to polygonal with variably distinct cell borders,

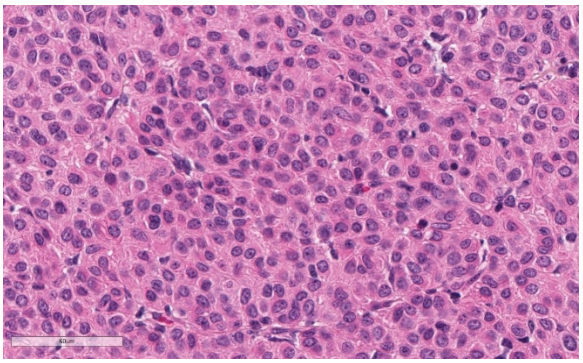

Haired skin, horse. Typical rounded glomus cells with pale eosinophilic cytoplasm and a round nucleus with finely stippled chromatin and one inconspicuous nucleolus. (HE, 400X) (Photo courtesy of: University of Pennsylvania, School of Veterinary Medicine, Department of Pathobiology http://www.vet.upenn.edu/research/academic-departments/)

a moderate amount of pale eosinophilic cytoplasm, and a round to ovoid or irregular nucleus with finely stippled chromatin and a small inconspicuous nucleolus. Occasionally, the cells have abundant hypereosinophilic cytoplasm that peripheralizes the nucleus (epithelioid-type cells). Anisocytosis and anisokaryosis are mild to moderate and mitotic figures are infrequent, with an average of 0 to 1 per single high power field (12 per 50 consecutive 40X high power fields). Binucleation and individual cell necrosis are occasionally observed. Low numbers of lymphocytes and plasma cells multifocally infiltrate the intervening stroma. The overlying epithelium is mildly hyperplastic with orthokeratotic hyperkeratosis and is focally ulcerated.

A periodic acid-Schiff (PAS) stain highlights a thin PAS-positive basement membrane surrounding individual or small nests of cells.

Immunohistochemistry:
The neoplastic cells exhibit diffuse and strong positive cytoplasmic immuno-reactivity for alpha-smooth muscle actin (α -SMA), vimentin, and desmin, and are negative for pancytokeratin (AE1/AE3) and CAM 5.2.

Contributor's Morphologic Diagnosis:
Horse, cutaneous mass: glomus tumor

Contributor's Comment: Glomus tumors (GT) are rare, typically benign neoplasms that are thought to arise from the modified perivascular smooth muscle cells of the glomus body, a structure that plays a role in body temperature regulation by allowing arterio-venous shunting of blood and is most commonly found in the subungual regions, subcutis of the extremities, or other specific locations such as the precoccygeal region.[5,9]

Glomus tumors in humans are usually solitary tumors that appear as small circumscribed nodules in the deep dermis or subcutis of the upper and lower extremities, with the subungual region of the finger being the most common location. Many other, less common locations have been described, such as the gastrointestinal tract, penis, urinary bladder, lungs etc.[5]

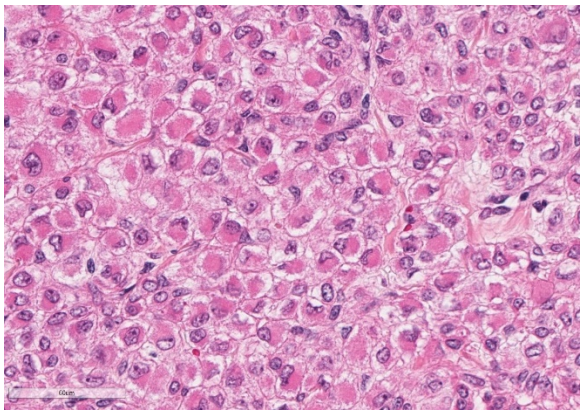

Haired skin, horse. Epithelioid-type glomus cells with abundant eosinophilic cytoplasm and a peripheral nucleus. Binucleation is occasionally noted. (HE, 400X) (Photo courtesy of: University of Pennsylvania, School of Veterinary Medicine, Department of Pathobiology http://www.vet.upenn.edu/research/academic-departments/)

The clinical diagnosis in humans is based on the typical red-blue appearance, combined with a history of paroxysmal pain from cold exposure and light touch, regardless of the size of the tumor.[4,5] Depending on their histologic appearance, GT are classified as classic (or sporadic/solid), glomangiomas, glomangiomyomas, glomangiomatosis and symplastic GT, which have a higher grade of nuclear atypia.[4] The classic GT are by far the most common type and account for approximately 75% of tumors.[5] Although predominantly benign, a small subset of tumors displays clinical or histological features of malignancy.[3] Folpe et al., in 2001, proposed the following classification system for this subset of tumors. Malignant GT, or glomangiosarcoma, are tumors larger than 2 cm in diameter and located deep in the subcutis and underlying tissues, or that have atypical mitotic figures, or a moderate to high nuclear grade and ≥ 5 mitotic figures/50 consecutive 40x high power fields. Symplastic GT have a high nuclear grade in the absence of other malignancy features. Tumors that lack the criteria for malignant GT or symplastic GT, but exhibit one of the following characteristics, high mitotic activity and superficial location, or large size, or deep location only, are classified as GT of uncertain malignant potential. Finally, glomangiomatosis are tumors resembling diffuse angiomatosis with increased numbers of glomus cells. Only malignant GT were associated with metastasis, which included the brain, bone, lung, liver, small intestine, mediastinal lymph nodes, and bowel mesentery.[3]

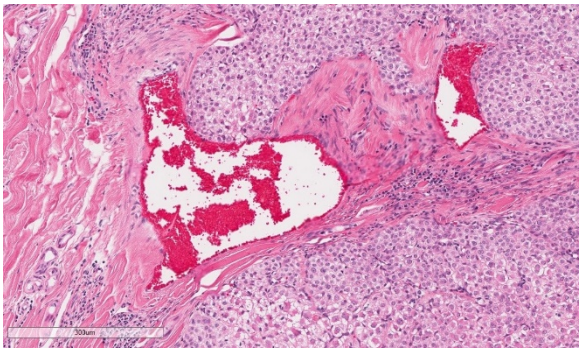

Haired skin, horse. Neoplastic cells multifocally impinge on vascular lumina beneath an intact endothelial lining (HE, 100X) (Photo courtesy of: University of Pennsylvania, School of Veterinary Medicine, Department of Pathobiology, http://www.vet.upenn.edu/research/academic-departments/)

Histologically, classic glomus tumors are well-defined, multilobulated, often partially encapsulated neoplasms composed of nests of small rounded cells often closely associated to capillaries and supported by a hyalinized or myxoid stroma. Cells have eosinophilic cytoplasm and a round, centrally located nucleus.[4] A more oncocytic or epithelioid appearance of cells is occasionally reported.[4] Cellular and nuclear pleomorphism and mitoses are not prominent features.[4] Immunohistochemical staining is consistently positive for α-smooth muscle actin and vimentin.[8]

Similarly to humans, glomus tumors in domestic animals are rare and typically benign, and have been described in non-human primates, cats, dogs, cows, and horses.[7,10,11] In horses, these tumors have been reported to occur in the subcutis of the head and neck and in the foot.[1,2] A single case of glomus tumor with neuroendocrine differentiation was reported in the maxilla of a 13-year-old Icelandic crossbred mare.[10] Most cases reported in horses displayed features of malignancy, either by local invasion, or by cytological criteria, according to the human classification of malignant glomus tumors.[1-3,10] However, no metastasis to the local lymph nodes or distant sites were reported.

In the case presented herein, the preliminary diagnosis of a trichoblastoma was ruled out based on negative immunoreactivity for

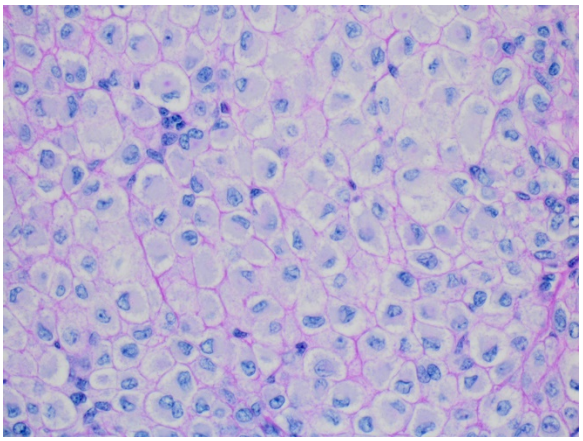

Haired skin, horse. A thin basement membrane surrounds individual or small groups of neoplastic cells. (PAS, 400X) (Photo courtesy of: University of Pennsylvania, School of Veterinary Medicine, Department of Pathobiology, http://www.vet.upenn.edu/research/academic-departments/)

pancytokeratin (AE1/AE3) and CAM 5.2, while the positive immunoreactivity for alpha-smooth muscle actin (α-SMA), vimentin, and desmin instead supported a diagnosis of glomus tumor. Given the mitotic activity and nuclear pleomorphism, the tumor in this horse would be classified as a malignant glomus tumor (glomangiosarcoma) based on the human classification criteria. The malignant behavior of glomus tumors reported in horses was typically associated with increased cellular pleomorphism and the difficulty to achieve a complete surgical excision.[1,2,10] In the present case, the small circumscribed nature of the neoplasm and complete surgical excision suggest a favorable prognosis.

JPC Diagnosis: Haired skin: Glomus tumor, American Quarter Horse (*Equus caballus*), equine.

Conference Comment: Glomus tumors arise (not surprisingly) from glomus cells which are specialized modified smooth muscle cells controlled by the sympathetic nervous system. They are typically associated with arteriovenous shunts or anastomoses that act to regulate flow within the shunt vessels and influence temperature regulation. In humans, these are frequently found in extremities.[6] In animals, glomus tumors are most frequently reported in dogs where they also tend to occur along extremities. Additionally, there have been isolated reports in cats, horses, non-human primates, and several cows.[2,7,9,11] In horses, there appears to be a predisposition for the head or neck (as seen in this case); however, examination of additional cases is necessary to determine whether there is indeed a true site predilection.[2] A recent case described in a Holstein-Friesian cow identified a large primary glomus tumor within the liver.[7]

Microscopically, glomus tumors are well-demarcated, dermal or subcutaneous masses with a fibrous capsule that often contains subcapsular vessels and nerve fibers. In domestic animals and humans, most are considered round cell type, or glomus tumor proper, in which round cells are densely packed with centrally located, prominent nuclei and moderate amounts of pale eosinophilic cytoplasm. Rarer are the spindle cell type in which cells are more elongated with oval nuclei. In both types, mitotic figures and multinucleated cells are few, and each cell or groups of cells is surrounded by a PAS-positive basement membrane. Ultrastructurally, the basement membrane can be seen as well as actin-like filaments, cytoplasmic dense bodies, pinocytotic vesicles, and glycogen granules.[6]

Differentials for the round cell type of glomus tumor include: Merkel cell tumors, plasma cell tumors, nonepitheliotropic lymphomas, histiocytomas, mast cell tumors, and transmissible venereal tumors (TVTs). In general, all of the above differentials lack the association with peripherally located blood vessels and nerve fibers that are prominent in

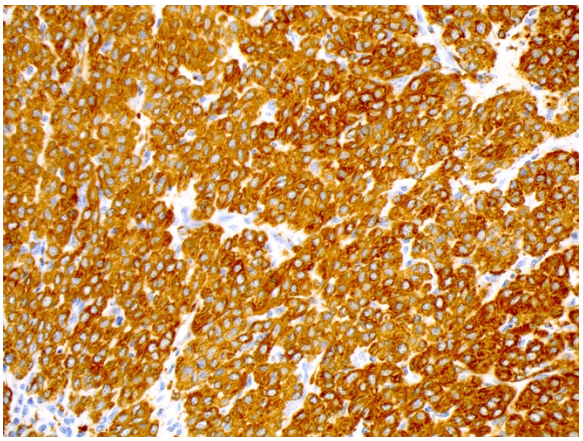

Haired skin, horse. Neoplastic cells exhibit strong positive cytoplasmic immunoreactivity to α-SMA. (IHC for α-SMA, DAB chromogen, 200X) (Photo courtesy of: University of Pennsylvania, School of Veterinary Medicine, Department of Pathobiology, http://www.vet.upenn.edu/research/academic-departments/)

glomus tumors. Additionally, Merkel and plasma cell tumors have prominent "packeting" of cells which are separated by a fine stroma and not surrounded by basement membrane. The location of the nuclei can separate glomus tumors from plasma cell tumors and histiocytomas. Also, histiocytomas have a characteristic "top heavy" appearance and often have intraepidermal neoplastic cells. Mast cells can be clearly identified using toluidine blue or Giemsa stains to highlight metachromatic cytoplasmic granules. Finally, lymphomas and TVTs are most difficult to distinguish based on H&E cytologic characteristics alone. Due to its smooth muscle origin, glomus cell tumors retain positivity for vimentin, α-smooth-muscle actin, and pan-muscle-specific actin which will be negative in lymphomas and TVTs.[6]

Contributing Institution:
University of Pennsylvania
School of Veterinary Medicine
Department of Pathobiology
http://www.vet.upenn.edu/research/academic-departments/

References:

1. Brounts SH, Adams SB, Vemireddi V, Holland CH. A malignant glomus tumour in the foot of a horse. *Equine Vet Educ*. 2008;20:24-27.
2. Burns RE, Pesavento PA, McElliott VR, Ortega J, Affolter VK. Glomus tumours in the skin and subcutis of three horses. *Vet Dermatol*. 2011;22:225–231.
3. Folpe AL, Fanburg-Smith JC, Miettinen M, Weiss SW. Atypical and malignant glomus tumors: analysis of 52 cases, with a proposal for the reclassification of glomus tumors. *Am J Surg Pathol*. 2001;25:1-12.
4. Folpe AL, Brems H, Legius E. Glomus tumours. In: Fletcher CDM, Bridge JA, Hogendoorn PCW, Mertens F. *World Health Organization Classification of Tumours: WHO Classification of Tumours of Soft Tissue and Bone*, 4th ed., Lyon, France: International Agency for Research on Cancer; 2013:116-117.
5. Goldblum JR, Folpe AL, Weiss SW. Perivascular Tumors In: *Enziger and Weiss's Soft Tissue Tumors*, 6th ed., Philadelphia, PA: Saunders Elsevier; 2014:749-765.
6. Gross TL, Ihrke PJ, Walder EJ, Affolter VK. Perivascular tumors. In: *Skin Diseases of the Dog and Cat Clinical and Histopathological Diagnosis.* 2nd ed. Ames, IA: Blackwell Science Ltd.; 2005:759-762.
7. Horiuchi N, Komagata M, Shitamura K et al. Glomus tumor of the liver in a cow. *J Vet Med Sci*. 2015;77:729–732.
8. Mravic M, LaChaud G, Nguyen A, Scott MA, Dry SM, James AW. Clinical and histopathological diagnosis of glomus tumor: an institutional experience of 138 cases. *Int J Surg Pathol*. 2015;23:181–188.
9. Park CH, Kozima D, Tsuzuki N, Ishi Y, Oyamada T. Malignant glomus tumour in

a German shepherd dog. *Vet Dermatol*. 2009;20:127-130.
10. Peters M, Grafen J, Kuhnen C, Wohlsein P. Malignant glomus tumour (glomangiosarcoma) with additional neuroendocrine differentiation in a horse. *J Comp Pathol*. 2016;154:309-313.
11. Roperto S, Borzacchiello G, Brun R et al. Multiple glomus tumors of the urinary bladder in a cow associated with bovine papillomavirus type 2 (bpv-2) infection. *Vet Pathol*. 2008;45:39–42.

CASE II: NP-20/17 (JPC 4102669).

Signalment: 3-day-old male piglet (*Sus scrofa domesticus*), porcine.

History: This was one of two piglets that came from a farm of 1100 sows and 3000 suckling piglets. 24-48 hours post-birth the piglets showed diffuse inflammation and cyanosis of the head, lethargy and they died 12 to 24 hours after the first clinical signs appeared. The clinical signs affected one or few of the piglets from a same litter and all the affected animals died. The problem occurred in litters of both gilts and sows. Teeth shaving or trimming of piglets is not a general procedure in this farm.

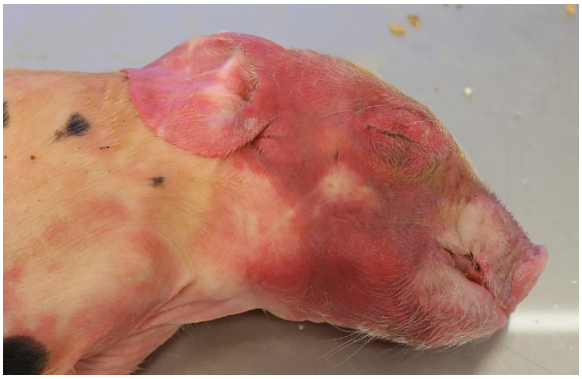

Face and neck, skin, piglet. There is diffuse erythema and swelling of the skin and the subcutaneous tissue of the face, the head and the cranial portion of the neck. (Photo courtesy of: Veterinary Pathology Department, Veterinary Faculty, Autonomous University of Barcelona, 08193 Bellaterra, Barcelona, Spain.)

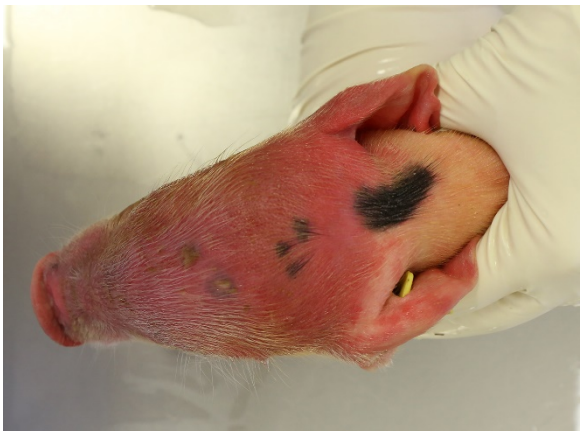

Subcutaneous tissue of the face and submandibular lymph node. The subcutaneous tissue and the hypodermis, and regional lymph nodes are markedly edematous. (Photo courtesy of: Veterinary Pathology Department, Veterinary Faculty, Autonomous University of Barcelona, 08193 Bellaterra, Barcelona, Spain.)

Gross Pathology: Both piglets submitted for necropsy presented an intense and diffuse swelling of the skin and the subcutaneous tissue of the face, the head and the cranial portion of the neck. The skin also had a diffuse reddish coloration. In the frontal aspect of the face, in the cutaneous surface there were two small irregular epithelial erosions covered with crusts. After removing the skin of the head and neck there was moderate amount of clear, fluid to gelatinous material in the subcutaneous tissue and the hypodermis, interpreted as edema. The regional lymph nodes (submandibular and retropharyngeal lymph nodes) appeared diffusely edematous and reddened. In both animals teeth were intact. In the rest of the body there were not significant alterations. The stomach was filled with clotted milk.

Laboratory Results (clinical pathology, microbiology, PCR, ELISA, etc.):

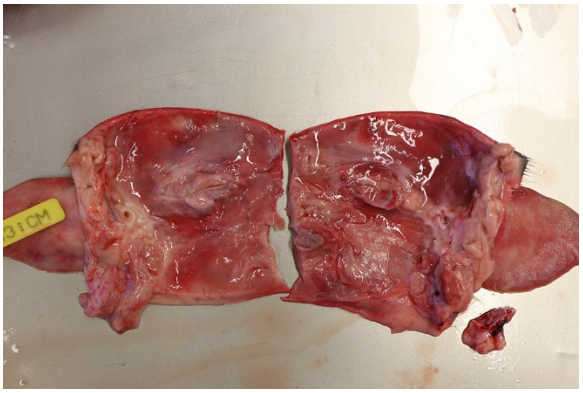

Face and neck, skin, piglet. In the surface frontal part of the face there are two small irregular epithelial erosions covered with crusts. (Photo courtesy of: Veterinary Pathology Department, Veterinary Faculty, Autonomous University of Barcelona, 08193 Bellaterra, Barcelona, Spain.)

Microbiology: *Pasteurella multocida* was isolated on bacterial culture of the skin and subcutaneous tissue, liver and spleen of both animals.

Tissue gram stain: Abundant numbers of coccobacillary gram-negative bacteria in the deeper dermis and subcutaneous tissue. There were also large quantities of gram positive bacterial cocci on the epidermal surface.

Microscopic Description:
Multifocally, the skin shows areas of loss of continuity of the epidermis (ulcers) and substitution by moderate amounts of necrotic debris, degenerated neutrophils, extravasated erythrocytes and occasional aggregates of cocci (serocellular crust). The dermis is entirely expanded by abundant interstitial edema and hemorrhage, together with large amount of inflammatory infiltrate composed mainly by neutrophils and in lesser extend macrophages and lymphocytes that reach the subcutaneous muscle and adipose tissue. In these localizations, there are abundant coccobacilli distributed diffusely and forming small clusters. Additionally the deep dermis there are multifocal areas of necrosis composed by eosinophilic amorphous material with cellular debris and abundant bacterial colonies. The blood vessels are markedly congested and contain abundant bacterial emboli in their lumen.

Contributor's Morphologic Diagnosis:

1. Haired skin: Dermatitis, cellulitis and panniculitis, necrotizing and suppurative, diffuse, acute, severe with gram-negative bacteria consistent with *Pasteurella multocida*.
2. Haired skin: Dermatitis, ulcerative and suppurative, multifocal, acute, severe with gram-positive bacteria.

Contributor's Comment: This case is consistent with a condition known as facial necrosis (facial pyemia),[2,8] a common condition in suckling pigs less than one week of age characterized by bilateral necrotic ulcers that are often covered by hard brown crusts and that extent from the side of the face to the lower jaw area, especially on the lips and cheeks.

The condition is the result of infection of wounds inflicted by piglets on each other with their sharp teeth while suckling from the sow. Lacerations to the sides of the face become infected with organisms such as *F. necrophorum*, *Streptococcus* spp., and *B. suis*, among others.[2,5]

Facial skin, piglet. The dermis and subcutis is markedly thickened by edema and hemorrhage, and vessels are surrounded by a cellular infiltrate. (HE, 6X)

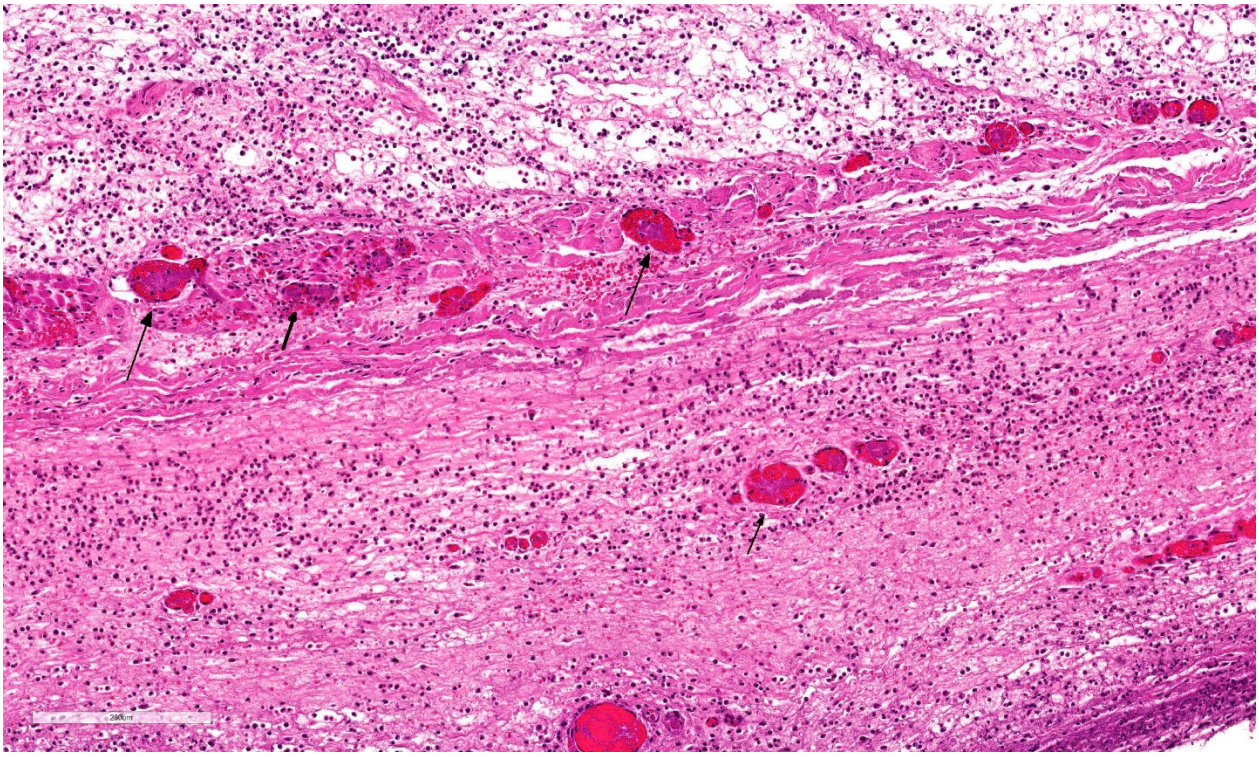

Facial skin, piglet. The deep dermis, panniculus carnosus, and subcutis are markedly expanded by edema, fibrin, and innumerous viable and degenerate neutrophils. Blood vessels contain large colonies of bacilli (arrows). (HE, 155X).

In this case, none of the above bacteria was cultured but *Pasterella multocida* was isolated in pure culture. This case represents an especially severe form of the disease, complicated by cellulitis and panniculitis. This may be associated with the effects of *Pasteurella multocida* dermonecrotic toxin.[12]

Facial necrosis is commonly seen in large litters and especially in the disadvantaged weaker piglets and when milk letdown is slow such as when sows suffer from mastitis, metritis, agalactia syndrome (MMA syndrome). In these cases there is an increase in competitition between piglets and lacerations and bites do occur.

Since 2013, there is a European legislation that regulates the shaving or trimming of teeth in suckling piglets. The aim of the regulation is to avoid teeth shaving as a general procedure, but it can be still considered in specific or individual litters when a facial necrosis situation suddenly occurs.

Facial necrosis occurs during the first few days of life and any number of piglets in a litter can be affected. Initially, lesions can be seen as striated lacerations caused by bites from other piglets. The lesions become infected, resulting in shallow ulcerations covered with hard browns crusts and can predispose to outbreaks of exudative epidermitis.

In this case there was a septicemic pasteurellosis since *Pasteurella multocida* was isolated from skin, liver and spleen. Septicemic pasteurellosis has a sudden onset with mortality ranging from 5% to 40%. Clinical signs include high fever, dyspnea, prostration, edema of the throat and lower

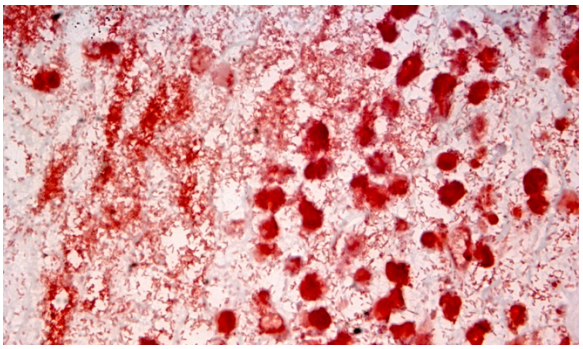

Facial skin, piglet. There are innumerable gram-negative bacilli within the tissue, admixed with degenerate neutrophils. (Photo courtesy of: Veterinary Pathology Department, Veterinary Faculty, Autonomous University of Barcelona, 08193 Bellaterra, Barcelona, Spain.) (Gram stain, 400X)

jaw and purplish discoloration of the abdomen, suggesting endotoxic shock.[5,10,12]

JPC Diagnosis: Haired skin and subcutis: Dermatitis and cellulitis, necrosuppurative, diffuse, severe with vasculitis, thrombosis, and numerous intravascular and extracellular bacilli, piglet (*Sus scrofa domesticus*), porcine.

Conference Comment: *Pasteurella multocida*, a gram-negative nonmotile cocco-bacillus, was first identified in 1878 as the causative agent of fowl cholera. It was isolated by Louis Pasteur in 1880, in whose honor it is named.[9] Strains of *P. multocida* are currently divided into five serogroups (A, B, D, E, F) based on capsular composition and somatic serovar.[6] *P. multocida* is a ubiquitous pathogen and is often part of the normal respiratory flora in mammals, but can cause a wide range of diseases such as: fowl cholera in poultry, atrophic rhinitis in pigs[12], pneumonia in various species, and bovine hemorrhagic septicemia in cattle and buffalo.[7] In humans, it is a common cause of zoonotic infections following animal bites or scratches.

As a gram-negative bacterium, *P. multocida* expresses the variable carbohydrate surface molecule, lipopolysaccharide (LPS) and a polysaccharide capsule which has been shown to aide in resistance to phagocytosis by host immune cells (serotypes A and B) as well as complement-mediated lysis (serotype A).[1,4] Strains that cause atrophic rhinitis (serotype D) also produce *P. multocida* toxin (PMT) which is a dermonecrotic toxin encoded on bacteriophages that initially stimulates osteoblasts. Then, as toxin levels increase, PMT blocks the function of osteoblasts and increases the activity of osteoclasts, leading to osteolysis of nasal turbinates.[12]

In a laboratory setting, *P. multocida* will grow at 37 °C on blood, chocolate, or high-strength agars, but will not grow on MacConkey agar. Bacterial growth is accompanied by a “mousy” odor due to metabolic products produced by the bacterium. Environmental endurance can be strengthened by adding salt.[3]

Contributing Institution:
Veterinary Pathology Department
Veterinary Faculty
Autonomous University of Barcelona
08193 Bellaterra, Barcelona, Spain

References:

1. Boyce JD, Adler B. The capsule is a virulence determinant in the pathogenesis of *Pasteurella multocida* M1404 (B:2). *Infect Immun.* 2000;68(6):3463-3468.
2. Cameron R. Integumentary system: Skin, hoof and claw. In: Zimmerman JJ, Karriker LA, Ramirez A, Schwartz KJ, Stevenson GW, eds. *Diseases of Swine*. 10th ed. Ames, IA: John Wiley & Sons, Inc. 2012:257.
3. Casolari C, Fabio U. Isolation of *Pasteurella multocida* from human clinical specimens: first report in Italy.

European Journal of Epidemiology. 1988;4(3):389-390.
4. Chung JY, Wilkie I, Boyce JD, Townsend KM, Frost AJ, Ghoddusi M, Adler B. Role of capsule in the pathogenesis of fowl cholera caused by *Pasteurella multocida* serogroup A. *Infect Immun*. 2001;69(4):2487-2492.
5. Hargis AM, Myers S. The integument. In: Zachary JF. *Pathologic Basis of Veterinary Disease*. 6th ed. St Louis, MO: Elsevier Mosby; 2017:1129.
6. Kuhnert P, Christensen H. *Pasteurellaceae: Biology, Genomics and Molecular Aspects.* Bern, Switzerland: Caister Academic Press; 2008:34-39.
7. Lopez A, Martinson SA. Respiratory system, mediastinum, and pleurae. In: Zachary JF. *Pathologic Basis of Veterinary Disease*. 6th ed. St Louis, MO: Elsevier Mosby; 2017:528, 530, 542, 550.
8. Nimmo-Wilkie J. Skin. In: Sims LD, Glastonbury JRW. *Pathology of the Pig-A Diagnostic Guide*. 1st ed. Barton, A.C.T.: Pig Research and Development Corporation, Victoria, Australia. 1996:351.
9. Pasteur L. The attenuation of the causal agent of fowl cholera. *Immunology*. 1880:126-131.
10. Register KB, Brockmeier SL, de Jong MF, Pijoan C. Pasteurellosis. In: Zimmerman JJ, Karriker LA, Ramirez A, Schwartz KJ, Stevenson GW, eds. *Diseases of Swine*. 10th ed. Ames, IA: John Wiley & Sons, Inc. 2012:803.
11. Ujvári B, Szeredi L, Pertl L, Tóth G, Erdélyi K, Jánosi S, Molnár T, Magyar T. First detection of *Pasteurella multocida* type b:2 in Hungary associated with systemic pasteurellosis in backyard pig. *Acta Veterinaria Hungarica*. 2015;63:141–156.
12. Zachary J F. Mechanisms of microbial infection. In: Zachary JF. *Pathologic Basis of Veterinary Disease*. 6th ed. St Louis, MO: Elsevier Mosby; 2017:173-174.

CASE III: V165/17 (JPC 4102987).

Signalment: 1.5-year-old, male, castrated, domestic shorthair (*Felis catus*), feline.

History: Plaques, erosions and erythema have been present bilaterally for one year on the concave pinna around the entrance to the ear canal. There has been no response to various treatments.

Gross Pathology: The inner aspect of the pinna is thickened by plaques covered by thick dark brown-black exudate which occludes the entrance to the ear canal.

Laboratory Results (clinical pathology, microbiology, PCR, ELISA, etc.):
None provided.

Microscopic Description:
The skin is covered by a thick crust composed of keratin and proteinaceous debris, large collections of lytic granulocytes (neutrophils and eosinophils), RBC and scattered bacterial colonies. There is severe diffuse hyperplasia of the epidermis and outer root sheath with widespread spongiosis. Dead keratinocytes with shrunken, angular, hypereosinophilic cytoplasm and pyknotic nuclei are present predominantly in the hyperplastic outer root sheath. They occur either as individual cells or form small groups and are often found in the upper layers of the epidermis or outer root sheath. There is prominent luminal folliculitis characterized by pronounced infundibular dilation, parakeratotic hyperkeratosis and formation of coalescing eosinophilic and neutrophilic pustules. The debris in the follicular lumen is continuous with the superficial crust. Keratinocytes with pale cytoplasm form an irregular layer below

Pinna and vertical ear canal, cat: Plaques of a thick dark exudate largely occlude the vertical ear canal and spread outward over the inner surface of the pinna. (Photo courtesy of: Department of Veterinary Resources, Weizmann Institute of Science, Rehovot 76100, Israel, http://www.weizmann.ac.il/vet/)

the disturbed stratum corneum of the most severely dilated hair follicle in this sample. A low number of eosinophils and probable lymphocytes migrate through the hyperplastic epidermis and outer root sheath. In the superficial and perifollicular dermis there is moderate to severe multifocal to coalescing infiltration of eosinophils, mast cells, neutrophils, a few lymphocytes, plasma cells and occasional macrophages with intracytoplasmic light brown granular pigment consistent with secretory material.

Contributor's Morphologic Diagnosis:
Severe eosinophilic and mastocytic proliferative, hyperkeratotic and necrotizing dermatitis and folliculitis

Contributor's Comment: This rare and distinctive skin disease of cats was first reported as "Proliferative necrotizing otitis of kittens" in the 2nd edition of Gross et. al..[1] It was initially reported to affect cats <1 year-old, but a later publication describes cases also in adult cats.[1,2]

Clinically, the disease presents as bilateral, sharply demarcated, thick brown crusts usually on the inner surface of the proximal pinna and around the entrance to the ear canal.[1,2,3] In some cases the vertical ear canal is involved.[2,3] The proliferative tissue is friable leading to erosion, ulceration and in some case occlusion of the ear canal.[1,2] The condition may regress spontaneously (by 1 to 2 years-old)[1] or persist for a long time (e.g. 4.5 years)[2]. In the initial report, cats were described as indifferent to the lesions or demonstrated evidence of only mild pruritus when ulceration is present.[1] More significant pruritus was noted in the cats of the 2nd report which had concurrent otitis due to bacterial or yeast infection.[2]

Gross et al. classify this condition as a necrotizing disease of the epidermis.

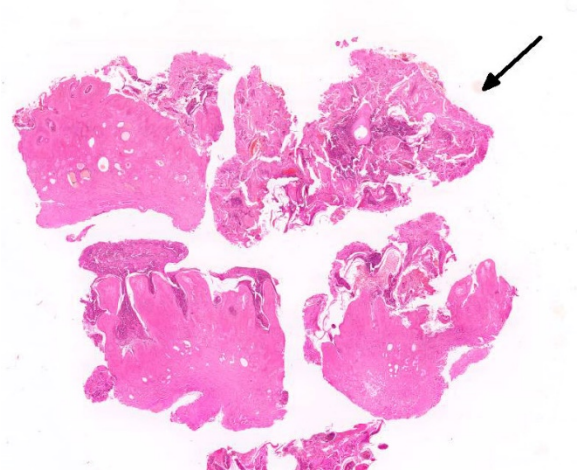

Vertical ear canal, cat. Multiple biopsies of ear pinna and overlying crust (black arrow) are submitted for examination. (HE, 7X)

Vertical ear canal, cat. There is diffuse marked epithelial hyperplasia. The epidermis is covered by a thick serocellular crust which extends down into follicles (green arrows). (HE, 28X)

Diseases in this group are characterized by death of keratinocytes either by necrosis or apoptosis. Since, the morphologic features of dead keratinocytes do not allow distinction between the two processes, the convention is that apoptosis is considered to be the underlying mechanism when death affects individual keratinocytes (e.g. erythema multiforme) and necrosis when death affects many confluent cells (e.g. toxic epidermal necrolysis). To complicate matters, dyskeratotic cells are also indistinguishable from dead keratinocytes.[1] According to Mauldin et al. dead keratinocytes are limited to the outer root sheath and are not present in the interfollicular epidermis. The embedding of our samples is unfortunately oblique, but to the degree that we were able to pursue this point we tend to agree with Mauldin et. al. possibly with rare minor exceptions.

The cause of this condition is unknown. The possibility of viral infection was investigated by PCR and IHC but to date no evidence of viral involvement has been found.[1,2] The two main references for this condition describe keratinocytes with abundant pale eosinophilic cytoplasm[1,2], a finding which is present to a limited degree in the submitted sample (around the most dilated hair follicle). However, we did not identify enlarged nuclei with marginated chromatin without inclusion bodies.[2]

Individual keratinocyte death, presumably by apoptosis, suggests an immunologic basis[1], and this is supported by the good response to treatment with Tacrolimus® (FK -506), an inhibitor of T-cell-mediated cytokines.[2,5] Immunohistochemical analysis done on one case showed a close association between CD3+T cells and caspase-3-stained keratinocytes, which suggests that

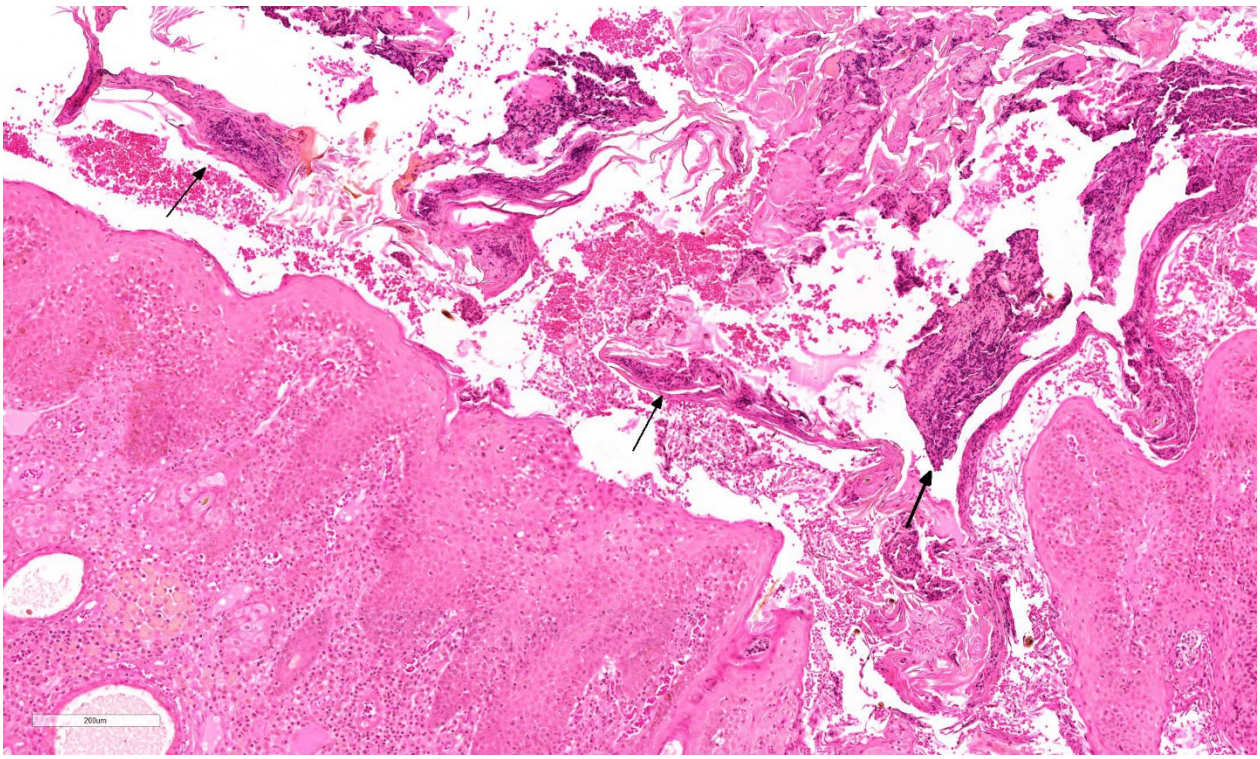

Vertical ear canal, cat. The serocellular crust contains numerous pustules (black arrows). The underlying epithelium is markedly hyperplastic and there is a profound neutrophilic infiltrate of the superficial dermis. (HE, 111X)

keratinocyte apoptosis is induced by epidermal infiltrating T cells, but the reason this occurs is unknown.[5]

JPC Diagnosis: Haired skin (external ear canal): Otitis externa, proliferative and hyperkeratotic with luminal folliculitis and keratinocyte apoptosis, domestic shorthair (*Felis catus*), feline.

Conference Comment: Proliferative and necrotizing otitis of kittens is a rare disorder that was first described in a 2007 academic journal by the moderator, Dr. Elizabeth Mauldin[2], which characteristically presents as well-demarcated, erythematous plaques with adherent keratinaceous debris on the inner aspect of the pinna extending into the pre-auricular regions of the face. Although the gross appearance is unique and largely diagnostic, lesions can be easily confirmed via biopsy. Microscopically, the lesions are characterized by a markedly hyperplastic epidermis with brightly eosinophilic, shrunken keratinocytes (apoptotic or dyskeratotic) scattered subjacent to areas of prominent parakeratotic hyperkeratosis that contains layers of viable and degenerate neutrophils. Adjacent hair follicles may also be involved and are often plugged with keratinaceous debris and inflammatory cells.[1,4]

Histologically, this lesion is similar to hyperkeratotic erythema multiforme (EM), with several distinct differences: (1) affected keratinocytes are not routinely surrounded by lymphocytes (ie. satellitosis) and are only present in areas with prominent hyperkeratosis (suggesting that they may be dyskeratotic rather than apoptotic); and (2) there is minimal to mild epithelial hyperplasia and neutrophilic crusting, as

evident with proliferative and necrotizing otitis. .[1,4]

Contributing Institution:
Department of Veterinary Resources,
Weizmann Institute of Science
Rehovot 76100, Israel
http://www.weizmann.ac.il/vet/

References:

1. Gross TL et al. *Skin Diseases of the Dog and Cat*. 2nd ed. Oxford, UK: Blackwell Science; 2005:75, 79-80.
2. Mauldin EA et al. Proliferative and necrotizing otitis externa in four cats. *Vet Dermatol*. 2007;18:370-377.
3. Momota Y et al. Proliferative and necrotizing otitis externa in a kitten: successful treatment with intralesional and topical corticosteroid therapy. *J Vet Med Sci*. 2017;78(12):1883–1885.
4. Stevens BJ, Linder KE. Pathology in practice. Proliferative and necrotizing otitis externa. *J Am Vet Med Assoc*. 2012;241(5):567-569.
5. Vidémont E, Pin D. Proliferative and necrotising otitis in a kitten: first demonstration of T-cell-mediated apoptosis. *J Small Anim Pract*. 2010;51:599-603.

CASE IV: S 504/16 (JPC 4102124).

Signalment: 6-year-old, female, Warmblood (*Equus ferus caballus*), equine.

History: Severe, subcutaneous edema affected all four limbs, the ventral abdomen, and the head. Multifocal petechial and ecchymotic hemorrhages were visible on all mucous membranes including the mouth and the vagina. The rectal temperature was 39.7°C (reference interval 37,0 – 38,0°C) and white blood cell count was elevated (15.7 x 109/l, reference value 5 – 10 x 109/l). The horse was treated with antibiotics, flunixin (nonsteroidal anti-inflammatory drug) and high dosages of dexamethasone. The horse rapidly deteriorated and was humanely euthanized upon the owner's request.

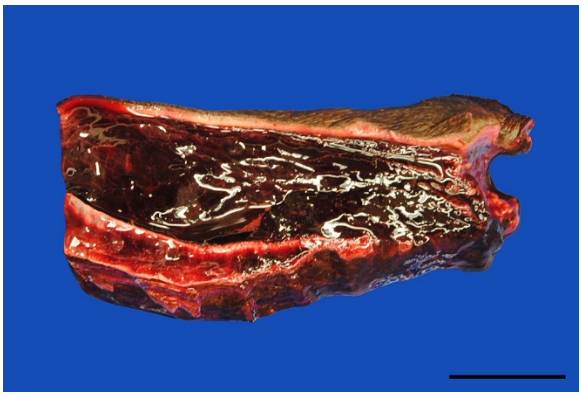

Haired skin and subcutis, horse. The subcutis is markedly expanded by edema and hemorrhage. (Photo courtesy of: Department of Veterinary Pathology, Freie Universitaet Berlin, http://www.vetmed.fu-berlin.de/en/einrichtungen/institute/we12/index.html)

Gross Pathology: In addition to the mucous membranes, petechial to ecchymotic hemorrhages were striking in the parietal and visceral pleura, the lung, myo- and pericardium as well as the mediastinum. Small proportions of pus drained from the cut surface of the right retropharyngeal lymph node. The subcutis of the ventral body parts including the legs, ventral abdomen and scrotum was severely thickened up to 5 cm by edema.

Laboratory Results (clinical pathology, microbiology, PCR, ELISA, etc.):
Streptococcus equi ssp. equi was isolated from the right retropharyngeal lymph node.

Microscopic Description:
Skin: The subcutis is severely thickened by a mainly homogenous and partially fibrillary pale eosinophilic material, clear space (edema) and extravascular erythrocytes (acute hemorrhages). Surrounding blood vessels, high numbers of leukocytes are present, predominantly degenerate

neutrophils and fewer numbers of macrophages. Almost all blood vessels are multifocally disrupted and expanded by moderate deposition of a loosely arranged eosinophilic homogenous to fibrillar material (fibrin) admixed with few degenerate neutrophils and cellular and karyorrhectic debris (fibrinoid necrosis). The endothelial lining is partially lost or endothelium cell nuclei are prominent and oval in shape (endothelial activation). The fibrinoid necrosis of the blood vessels and the perivascular infiltration expand into the surrounding dermis. The epidermis is normal.

Contributor's Morphologic Diagnosis:
Skin, subcutis: Vasculitis, severe, acute, diffuse, leukocytoclastic with severe edema, multifocal hemorrhage and dermal necrosis.

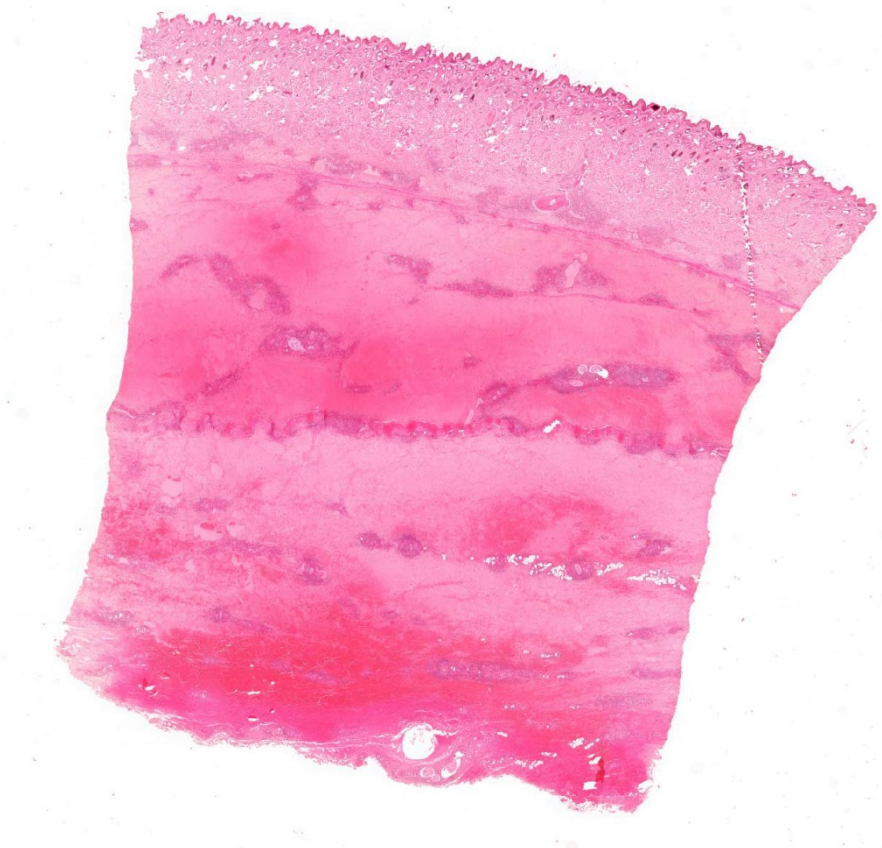

Haired skin and subcutis, horse. Subgross examination reveals the extent of the hemorrhage and edema of the subcutis. There is a markedly cellular infiltrate surrounding all vessels. (HE, 5X)

Contributor's Comment: The syndrome purpura hemorrhagica, formerly known as *morbus maculosus equorum*, is consistent with a generalized leukocytoclastic vasculitis almost always including the skin.[14] It is clinically characterized by subcutaneous edema of ventral body parts and petechial or ecchymotic hemorrhages in the visible mucous membranes, i.e mouth and vagina. Underlying hemorrhagic diathesis is caused by endothelial and / or vascular damage in context of a generalized vasculitis. The latter is considered to result from a type III hypersensitivity with deposition of antigen-antibody immune-complexes in blood vessel walls. Activation of complement components and a subsequent recruitment and activation of leukocytes is responsible for the damage of the blood vessels. Considering the pathogenesis, the syndrome is not primarily caused by a specific infectious agent and hence not transmissible. However, in most cases, a previous infection provokes the hypersensitivity reaction. Most commonly, as in the current case, a preceding infection with *Streptococcus equi* spp. *equi* (Strangles) can be referred as the initiating cause of purpura hemorrhagica. It has been detected in approximately 5.4 to 6.5% of the infected horses, typically 2 to 4 weeks post infection.[4,14] Although the pathogenesis of *Streptococcus equi* spp.

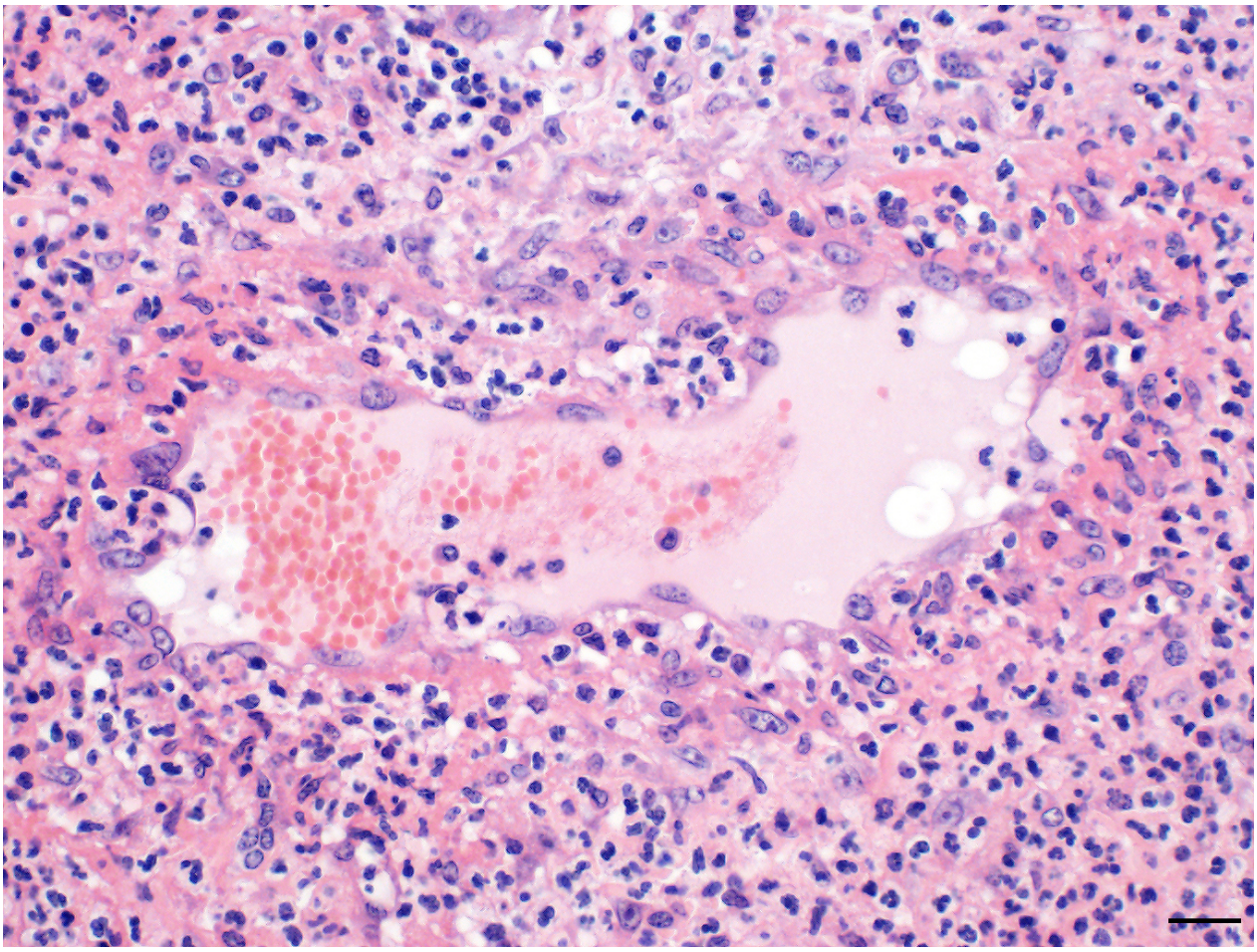

Haired skin and subcutis, horse. Vessel walls are expanded by numerous neutrophils, cellular debris, and fibrin (vasculitis) and numerous viable neutrophils have migrated into the surrounding tissue. (HE, 400X) (Photo courtesy of: Department of Veterinary Pathology, Freie Universitaet Berlin, http://www.vetmed.fu-berlin.de/en/einrichtungen/institute/we12/index.html)

equi associated purpura hemorrhagica is not fully understood, high serum concentrations of IgA antibodies and low serum concentrations of IgG antibodies seem to favor the development of immune complexes on the basis of the M-like protein of *Streptococcus equi* (SeM).[14] Vaccination with SeM may trigger purpura hemorrhagica.[6] Furthermore, additional infectious agents are discussed as possible cause of this syndrome including viruses (equine influenza virus, equine herpes viruses, equine arteritis virus) and bacteria (*Corynebacterium pseudo-tuberculosis*, *Streptococcus equi* spp. *zooepidemicus*, *Rhodococcus equi*).[2,11,16]

Purpura hemorrhagica, i.e, a leukocytoclastic vasculitis, may be diagnosed antemortem by full-thickness punch skin biopsies.[11,16] However, biopsies should be taken prior to treatment with corticosteroids as these may tremendously reduce the severity of the vasculitis and even suppress any histological evidence whatsoever.[11]

The prognosis of purpura hemorrhagica is difficult to predict, however may be favorable with an immediate and aggressive therapy including immunosuppression with corticosteroids.[6] Complications like laryngeal edema (dyspnea), dermal necrosis,

thrombophlebitis, glomerulonephritis, and infarctions of skeletal musculature, lung, skin and the intestinal tract as well as colic due to severe edema, gastric rupture, intestinal intussusception, torsion and prolapse recti, may occur.[5,8,9,13,14]

JPC Diagnosis: Haired skin and dermis: Vasculitis, necrotizing, diffuse, severe with marked hemorrhage, edema, and moderate neutrophilic dermatitis and cellulitis, Warmblood (*Equus ferus caballus*), equine.

Conference Comment: Purpura hemorrhagica (from the Latin meaning "purple") is a type of immune-mediated vasculitis characterized grossly as red or purple areas of hemorrhage of the skin and mucus membranes with subsequent edema. Microscopically, affected vessels are surrounded by neutrophils that cause destruction of vascular walls (leuko-cytoclastic vasculitis), perivascular edema, hemorrhage, and fibrin. Commonly associated with previous infection with *Streptococcus equi* (usually involving the respiratory tract with abscessation), *Corynebacteirum pseudotuberculosis*, or vaccination with *S. equi* M protein (SeM); purpura hemorrhagica is classified as a type III hypersensitivity reaction and is caused by immune complexes (antigen and immuno-globulins) that deposit on the walls of small blood vessels (resulting in vasculitis) or renal glomerular capillaries and vessels (resulting in glomerulonephritis).[6,7,12]

Clinically, edema is well-demarcated and most often noticed in the distal limbs, followed by the ventrum and head with fever, tachycardia, tachypnea, anorexia, and depression. Clinical signs vary based on the organ system involved and can include all of the following: colic, lameness, neurologic signs, renal dysfunction, small intestinal intussusceptions, and muscular infarcts. Clinical pathology abnormalities include: leukopenia or leukocytosis, anemia, thrombocytopenia, hypergamma-globulinemia, increased acute phase proteins, and increased muscle enzyme activities. Diagnosis is based on a combination of history, clinical signs, antibody titers (very high Se-M specific titers), and skin biopsies (to confirm leukocytoclastic vasculitis). Treatment is based on supportive care, immune suppression, and removal of the underlying cause.[6,12]

Differentials for purpura hemorrhagica include endotheliotropic viruses such as: equine viral arteritis, African horse sickness (*Orbivirus*), Hendra virus, or equine herpesvirus-1. Equine viral arteritis virus, an *Arterivirus*, is transmitted in contaminated body fluids via venereal or respiratory routes. The virus targets mononuclear and endothelial cells; clinical signs are usually associated with vasculitis. Clinical signs include: fever, leukopenia, depression, periorbital and supraorbital edema, conjunctivitis, lacrimation, petechiae, respiratory signs, colic or diarrhea, and abortion.[6] African horse sickness (AHS) is a foreign animal disease (never currently been reported in the United States) that results in edema, predominately of the nuchal ligament and supraorbital fossa, pulmonary edema, and myocardial failure. Equine *Orbivirus* is transmitted by *Culicoides imicola* and is endotheliotropic (related to the causative agent of bluetongue). In Africa, all equids are susceptible, with horses being the most susceptible, followed by mules, donkeys, and zebras. Hendra virus causes fatal pneumonia, encephalitis, and rarely subcutaneous edema in horses and humans (zoonotic).[3] Finally, equine herpesvirus-1, though most often associated with the central nervous system, is also an endotheliotropic virus and with chronicity rarely causes petechial

hemorrhage and edema in cutaneous and subcutaneous tissues.[1]

Contributing Institution:
Department of Veterinary Pathology
Freie Universitaet Berlin
http://www.vetmed.fu-berlin.de/en/einrichtungen/institute/we12/index.html

References:

1. Aleman M, Nout-Lomas YS, Reed SM. Disorders of the neurologic system. In: Reed SM, Bayly WM, Sellon DC, eds. *Equine Internal Medicine.* 4th ed. St. Louis, MO: Elsevier; 2018:645-652.
2. Aleman M, Spier SJ, Wilson WD, Doherr M. *Corynebacterium pseudotuberculosis* infection in horses: 538 cases (1982-1993). *JAVMA*. 1996;209:804-809.
3. Davis E. Disorders of the respiratory system. In: Reed SM, Bayly WM, Sellon DC, eds. *Equine Internal Medicine.* 4th ed. St. Louis, MO: Elsevier; 2018:345-346.
4. Duffee LR, Stefanovski D, Boston RC, Boyle AG. Predictor variables for and complications associated with *Streptococcus equi* subsp *equi* infection in horses. *JAVMA*. 2015;247:1161-1168.
5. Dujardin C. Multiple small-intestine intussusceptions: a complication of purpura haemorrhagica in a horse. *Tijdschrift voor diergeneeskunde.* 2011;136:422-426.
6. Dunkel B. Disorders of the hematopoietic system. In: Reed SM, Bayly WM, Sellon DC, eds. *Equine Internal Medicine.* 4th ed. St. Louis, MO: Elsevier; 2018:1011,1012.
7. Hargis AM, Myers S. The integument. In: Zachary JF. *Pathologic Basis of Veterinary Disease*. 6th ed. St Louis, MO: Elsevier Mosby; 2017:1120-1121.
8. Jaeschke G, Wintzer H. Ein Beitrag zum Krankheitsbild des Morbus maculosus equorum. *Tieraerztliche Praxis*. 1988:385-394.
9. Kaese HJ, Valberg SJ, Hayden DW, Wilson JH, Charlton P, Ames TR, Al-Ghamdi GM. Infarctive purpura hemorrhagica in five horses. *JAVMA*. 2005;226:1893-1898.
10. Mealey RH, Long MT. Mechanisms of disease and immunity. In: Reed SM, Bayly WM, Sellon DC, eds. *Equine Internal Medicine*. 4th ed. St. Louis, MO: Elsevier; 2018:46.
11. Pusterla N, Watson JL, Affolter VK, Magdesian K, Wilson W, Carlson G. Purpura haemorrhagica in 53 horses. *The Veterinary Record.* 2003;153:118-121.
12. Rashmir-Raven AM. Disorders of the skin. In: Reed SM, Bayly WM, Sellon DC, eds. *Equine Internal Medicine.* 4th ed. St. Louis, MO: Elsevier; 2018:1196.
13. Roberts M, Kelly W. Renal dysfunction in a case of purpura haemorrhagica in a horse. *The Veterinary Record.* 1982;110:144-146.
14. Sweeney C, Whitlock R, Meirs D, Whitehead S, Barningham S. Complications associated with *Streptococcus equi* infection on a horse farm. *JAVMA*. 1987;191:1446-1448.
15. Sweeney CR, Timoney JF, Newton JR, Hines MT. *Streptococcus equi* infections in horses: guidelines for treatment, control, and prevention of strangles. *Journal of Veterinary Internal Medicine*. 2005;19:123-134.
16. Wiedner EB, Couëtil LL, Levy M, Sojka JE. Purpura hemorrhagica. *Comp Clin Educ Practicing Vet – Equine Ed.* 2006;1(2):82-93.

Self-Assessment - WSC 2017-2018 Conference 18

1. Glomus tumors are positive for which of the following immunohistochemical markers?
    a. Cytokeratin
    b. Smooth muscle actin
    c. CAM 5.2
    d. Synaptophysin

2. The causative agent in facial pyemia in pigs is?
    a. F. necrophorum
    b. Pasteurella multocida
    c. Streptococcus suis
    d. Brucella suis

3. Which of the following is true concerning proliferative and necrotizing otitis externa of kittens?
    a. CD3-positive lymphocytes surround apoptotic keratinocytes.
    b. There is minimal hyperplasia of the affected epithelium.
    c. The syndrome affects surface epithelium, but not hair follicles.
    d. This lesion may affected cats over 1 year of age.

4. Which of the following is often a trigger for purpura hemorrhagica?
    a. Streptococcus equi v. equi
    b. Brucella abortus
    c. Staphylococcus aureus
    d. Equine herpesvirus-1

5. Purpura hemorrhagica is classified as which type of hypersensitivity?
    a. Type I
    b. Type II
    c. Type III
    d. Type IV

Please email your completed assessment to Ms. Jessica Gold at Jessica.d.gold2.ctr@mail.mil for grading. Passing score is 80%.This program (RACE program number) is approved by the AAVSB RACE to offer a total of 0.5 CE Credits, with a maximum of 12.5 CE Credits being available to any individual Veterinary Medical Professionals for the 2017-2018 Wednesday Slide Conference. This RACE approval is for the subject matter categories of: SCIENTIFIC using the delivery method of NON-INTERACTIVE DISTANCE. This approval is valid in jurisdictions which recognize AAVSB RACE; however, participants are responsible for ascertaining each board's CE requirements.
RACE does not "accredit", "endorse" or "certify" any program or person, nor does RACE approval validate the content of the program.

Joint Pathology Center
Veterinary Pathology Services

WEDNESDAY SLIDE CONFERENCE 2017-2018

C o n f e r e n c e 19

4 April 2018

Donald Meuten, DVM, PhD, DACVP (Anatomic and Clinical Pathology)

CASE I: P46/14 (JPC 4048933).

Signalment: 8-year-old, female, spayed, Bernese Mountain Dog (*Canis lupus familiaris*), canine.

History: 8-year old spayed Bernese mountain dog with hypercalcemia and elevated levels of parathyroid hormone. An enlarged parathyroid gland (9x13mm) and a slightly enlarged thyroid gland were found on the right side with ultrasound. The left parathyroid and thyroid gland were considered to be within normal variation. The right parathyroid and thyroid were removed with surgery.

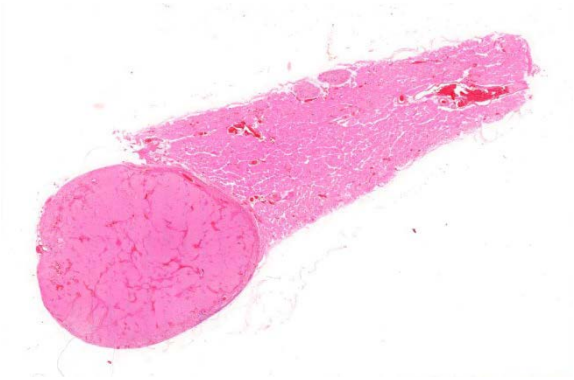

Thyroid gland, dog. At one edge of the section, expanding the parathyroid gland, there is a 1.1cm round expansile neoplasm. (HE, 4X)

Gross Pathology: The parathyroid gland was markedly enlarged, had a hard texture and was firmly attached to the thyroid gland.

Laboratory Results (clinical pathology, microbiology, PCR, ELISA, etc.): see below

Before surgery

// RHA

Analys:	Värde	Enhet	Referensvärde	Sign
Utlåtande				
S-Fosfat	0,7	mmol/L	0,8 1,9	KLAB
S-Kalcium	3,2	mmol/L	2,3 2,8	KLAB
S-Kreatinin	121	umol/L	46 115	KLAB

// RHA

Analys:	Värde	Enhet	Referensvärde	Sign
Utlåtande				
S-Glukos		mmol/L		

// RHA

Bilddiagnostik

Buk ,

U-pH	8		6 7	KLAB
U-Densitet, profil	1,012	kg/l		KLAB
U-protein profil	0			KLAB
U-hemoglobin	0		0	KLAB
U-glukos	0		0	KLAB
U-aceton	0		0	KLAB
U-Leukocyter	0	/synfält	0 3	KLAB
U-Erytrocyter	0	/synfält	0 3	KLAB
U-Cylindrar	0	/synfält	0 2	KLAB
U-Kristaller	0	/synfält		KLAB
U-Epitel	0	/synfält		KLAB

// RHA

Lab

Analys:	Värde	Enhet	Referensvärde	Sign
Utlåtande				
Provtagningsavgift blod	-			
ABL90 joniserat Ca	-			
iCa2+	1,56		1,29 1,46	iåm

// IÅM

Lab

Analys:	Värde	Enhet	Referensvärde	Sign
Utlåtande				
C-reaktivt protein CRP (hund)	<5		< 5	KLAB
S-Albumin	31	g/L	27 37	KLAB
S-Protein	66	g/L	56 75	KLAB
S-Kalcium	3,1	mmol/L	2,3 2,8	KLAB
S-Fosfat	0,8	mmol/L	0,8 1,9	KLAB

// EJI

Analys:	Värde	Enhet	Referensvärde	Sign

ENDOCRINOLOGY

Parathyroid Hormone * 144 pg/ml 20-65
Canine reference range = 20 - 65 pg/mL

PTH related protein (PTHrP) * 1.2 pmol/l <0.5
Ref. Range Note: >1.0 suggestive of malignancy

EDTA plasma sample received at Lab frozen 28th January

Authorised By : Ms Helen Evans BSc (Hons)
Laboratory Manager

Incomplete Tests : None
Test Codes : PTHR

AFTER SURGURY

Analys:	Värde	Enhet	Referensvärde	Sign
Utlåtande				
S-Kalcium	2,6	mmol/L	2,3 2,8	KLAB
S-Kreatinin	115	umol/L	46 115	KLAB
S-Urea	4,3	mmol/L	2,5 8,8	KLAB
S-Fosfat	1,1	mmol/L	0,8 1,9	KLAB

// EJI

Analys:	Värde	Enhet	Referensvärde	Sign
Utlåtande				
Provtagningsavgift blod				
ABL90 blodgaser/syrabas				
pH	7,468		7,33 7,46	ebo
kl.13.30				
HCO3-	23,0		22,2 - 27,2	ebo
pCO2	30,0		31,8 54	ebo
pO2	42,1		26,4 66,8	ebo
sO2	85,2		50 97,9	ebo
Htk	57,9		40,7 67,1	ebo
Hb	189		133 219	ebo
Na+	147		146 152	ebo
K+	4,4		3,6 4,8	ebo
Cl-	115		112 118	ebo
Ca2+	1,28		1,29 1,46	ebo

Glu	4,8		3,8 5,8	ebo
Lakt	1,2		0,8 2,2	ebo
BE	-2,0		-2,5 4,9	ebo
Aniongap	10,7		3,8 11	ebo

// EJI

Analys:	Värde	Enhet	Referensvärde	Sign
Utlåtande				
S-Kalcium	2,7	mmol/L		SE
S-Kreatinin	122	umol/L		SE

Analys:	Värde	Enhet	Referensvärde	Sign
Utlåtande				
Provtagningsavgift blod				
Tyreoidea pkt hd f-T4, TT4, TS				
Fritt T4 i paket	9,3	pmol/L		KA
Totalt T4 i paket	24	nmol/L		KA
TSH i paket	36	mU/L		KA

// LLE

Analys:	Värde	Enhet	Referensvärde	Sign
Utlåtande				
Provtagningsavgift blod	*			KLD
ABL90 joniserat Ca	*			KLD
iCa2+	1,37		1,29 1,46	KLD

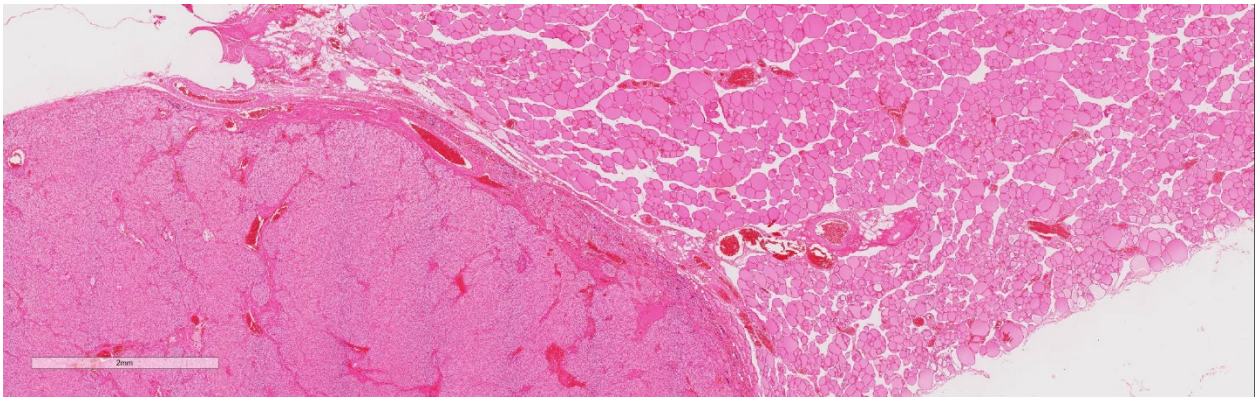

Thyroid gland, dog. The border of neoplasm forms compresses the adjacent follicles and the advancing front forms a compression capsule from pre-existent stroma. (HE, 9X)

Microscopic Description: Adjacent to the thyroid gland is a large, well circumscribed, encapsulated expansive nodular neoplasia. The neoplasm mildly compresses the adjacent thyroid and focally neoplastic cells infiltrate the surrounding fibrous capsule. The neoplasm shows sheets of densely packed round cells (principally "chief" cells) and a moderate stroma consisting of thin fibrovascular tissue. Multifocally in the neoplasm are thicker bands of fibrovascular tissue and adjacent to these the neoplastic cells are arranged in a slight trabecular pattern with cords of cells palisading around thin fibrovascular septa. Scattered within the fibrous tissue are mononucleated cells with intracytoplasmic golden brown clumped pigment. The neoplastic cells reveal a mild pleomorphism with mild anisokaryosis and mild anisocytosis. The cells have a round nucleus, scant often vacuolated cytoplasm and indistinct cell borders. Mitotic index is low (5 mitoses/HPA) with presence of few atypical mitoses. Multifocally in the periphery of the neoplasm are groups of cells with hyperchromatic nuclei and no discernable cytoplasm believed to represent remnants of active dark principal cells. Additional parathyroid tissues are present in the periphery of the thyroid gland.

Contributor's Morphologic Diagnosis: Parathyroid gland, parathyroid carcinoma

Contributor's Comment: Parathyroid carcinomas are uncommon in domestic animals but have been observed in dogs and occasionally in cats, the etiology remains unknown. Among dogs, the tumor occurs most commonly in older animals.[1,7] The tumor arises from parenchymal chief cells resulting in unregulated secretion of parathyroid hormone that cause hyper-calcemia. The main differential diagnoses are the more common parathyroid adenoma and parathyroid hyperplasia. Anaplastic thyroid neoplasia and more rarely metastases of renal cell carcinoma should also be excluded.[1,4,5,8]

Clinical symptoms are due to hypercalcemia and include weakness, lethargy, polyuria, polydipsia and gastrointestinal disorders.[2,7,9] The most common symptom in dogs with parathyroid carcinoma appear to be weakness while in primary hyper-parathyroidism due to hyperplasia or adenoma polyuria and polydipsia seems to be more prone.[7] However it is difficult to distinguish between benign and malignant etiology since the clinical symptoms are similar. Most deaths related to parathyroid carcinoma are caused by hypercalcemia.[4]

Parathyroid carcinoma is not only a clinically challenging diagnosis but is also a difficult histopathological diagnosis since an overlap exists between pathologic features of parathyroid adenomas and carcinomas. Grossly, parathyroid carcinomas are larger than adenomas; the tumor is characteristically hard and greyish in appearance and is seemingly lacking surrounding fatty tissue more characteristic of adenoma. Histologically, parathyroid carcinoma commonly invades its surrounding capsule and adjacent structures. In carcinomas, there are usually greater degrees of cellular pleomorphism than in adenomas with more frequent mitotic figures and atypical mitoses. Since mitotic figures will sometimes be encountered in parathyroid adenomas, their presence alone is not be pathognomonic of carcinoma. Moreover, in carcinomas the chief cells form a trabecular pattern with thick fibrous bands and microscopic evidence of capsular and vascular invasion.[1,2,4,5,8] Carcinomas may metastasize to regional lymph node and lung but metastases are uncommon and usually occur late in the course of the disease.[2]

Surgery remains the primary management in treatment of parathyroid carcinoma. Neoplastic parathyroid tissue, both benign and malignant, is known to easily reimplant, to establish a new blood supply and marginal surgical excision is adequate for treatment.[2,4] Long term prognosis in dogs after surgery is often good.[7]

JPC Diagnosis: Parathyroid gland: Parathyroid adenoma, Bernese mountain dog (*Canis lupus familiaris*), canine.

Conference Comment: Both parathyroid adenomas and carcinomas can secrete parathyroid hormone (PTH) resulting in primary hyperparathyroidism. PTH functions to regulate ionized calcium in the blood in the following ways: (1) promoting excretion of phosphorus and retention of calcium in the renal distal convoluted tubules, (2) activation of osteocytic and osteoclastic bone resorption, and (3) retention of calcium in the intestines. Bony lesions are often most prominent in the bones of the maxilla and mandible of horses resulting in a condition known as “bran disease” or fibrous osteodystrophy where there is concurrent osteolysis and replacement with fibrous connective tissue. However, bone lesions are often more pronounced in secondary hyperparathyroidism, due to renal failure or nutritional imbalance.[6]

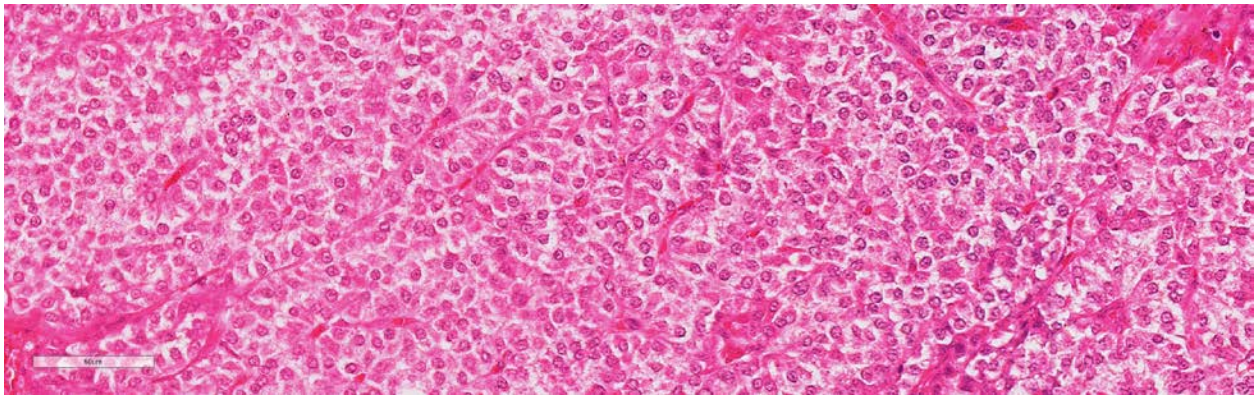

Thyroid gland. A monomorphic population of neoplastic cells is arranged in nests and packets with indistinct cell borders and a moderate amount of finely granular eosinophilic cytoplasm. Mitotic figures are rare. (HE, 335X)

Parathyroid gland adenomas are much more common than carcinomas in domestic animals. Certain breeds have familial tendencies, like Keeshond dogs, who are approximately fifty times more likely to develop parathyroid adenomas than other dog breeds due to an autosomal dominant trait. Microscopically, adenomas are composed of chief cells that are subdivided into smaller groups by a fine fibrovascular stroma. Chief cells can take one of two morphologies: (1) small amounts of lightly eosinophilic cytoplasm, or (2) large amounts of vacuolated, clear cytoplasm ("water clear cells"). The amount of cytoplasm (i.e. the morphology) is suggestive of the level of PTH secretion. More cytoplasm suggests more PTH synthesis and secretion.[6]

Chief cell hyperplasia can cause elevated PTH, but these lesions are often multifocal[6] and not one large compressive mass as this case.

As mentioned by the contributor above, parathyroid carcinomas are often larger than adenomas and characterized by invasion into the capsule, adjacent thyroid gland or other tissues, and veins or lymphatics. Microscopically, chief cells are often more irregularly arranged, pleomorphic, and have higher mitotic rates. In cats, chief cell carcinomas are often multinodular with numerous cysts lined by attenuated chief cells.[6]

Attendees discussed whether this lesion is a neoplasm or parathyroid hyperplasia. Based on the number of mitotic figures and size, it is more consistent with a neoplasm. Additionally, the neoplasm, though quite large and compressive, does not appear to be invasive. Therefore, we respectfully disagree with the contributor and prefer the diagnosis of adenoma rather than a carcinoma, although this generated much discussion. There was normal parathyroid gland that was compressed against the capsule adjacent to the neoplasm which some attendees thought might have been neoplastic invasion, but the general consensus was that it was normal parathyroid gland based on a slight difference in cellular organization and a thin septum between it and the neoplasm. Participants found it curious that the interior parathyroid gland is not atrophied, which would be expected with a PTH-producing adenoma and makes the laboratory findings perplexing (elevated pre-operative PTH with resolution of calcium and phosphorus levels after surgery).

In the normal parathyroid gland, attendees described aggregates of basophilic nuclei with cells that appeared to be fused. Some thought them to be lymphocytes, but the moderator properly identified those cells as normal cells which appear fused due to fixation artifact. The moderator explained that those cells had initially been identified as syncytial cells due to the fused plasma membranes identified ultrastructurally.[3] However, a few years later it was discovered that there are several parathyroid cell variants that occur secondary to immersion fixation.[10]

Finally, the moderator commented about clinical implications of measuring peptide hormones such as measuring PTH and calcium in surgery after the parathyroid tumor is removed but before the surgery is complete. These peptide hormones can change within minutes and return to normal. If this doesn't happen, the surgeon can check the contralateral gland for more tumors.

Contributing Institution:
Department of Biomedical Sciences and Veterinary Public Health, Section of Pathology, SLU (Swedish University of Agricultural Sciences)

http://www.slu.se/en/departments/biomedical-sciences-veterinary-public-health/

References:

1. Capen CC. Endocrine glands. In: Maxie MG, ed. *Jubb, Kennedy and Palmer´s Pathology of Domestic Animals*. Vol. 3. 5th ed. St. Louis, MO: Saunders Elsevier; 2007:368.
2. Marocci C, Cetania F, et al. Review: Parathyroid carcinoma. *Journal of Bone and Mineral Research*. 2008; 23(12):1869-1879.
3. Meuten DJ, Capen CC, Thompson KG, Segre GV. Syncytial cells in canine parathyroid glands. *Vet Pathol*. 1984; 21(5):463-468.
4. Randall P, Owen, et al. Parathyroid carcinoma: a review. *Head & Neck*. 2011; 33:429-436.
5. Rodrigueze C, Nadér S, Hans C, Badoual C. Parathyroid carcinoma: a difficult histological diagnosis. *European Annals of Otorhinolaryngology, Head and Neck Diseases*. 2012; 129: 157-159.
6. Rosol TJ, Meuten DJ. Tumors of the endocrine glands. In: Meuten DJ, ed. *Tumors in Domestic Animals*. 5th ed. Ames, IA: John Wiley & Sons, Inc.; 2017:809-815.
7. Sawyer ES, Nortrup NC, et al. Outcome of 19 dogs with parathyroid carcinoma after surgical excision. *Veterinary and Comparative Oncology*. 2011; 10(1): 57-64.
8. Thomson L. Malignant neoplasms of the parathyroid gland. In: *Head and Neck Pathology: Foundations in Diagnostic Pathology*. 2nd ed. Philadelphia, PA: Elsevier; 2012. 653-668.
9. Van Vonderen IK, Kooistra HS, et al. Parathyroid hormone immuno-histochemistry in dogs with primary and secondary hyper-parathyroidism: the question of adenoma and primary hyperplasia. *J. Comp. Path*. 2003; 129: 61-69.
10. Wild P, Kelliner SJ, Schraner EM. Parathyroid cell variants may be provoked during immersion fixation. *Histochemistry*. 1987; 87(3):263-271.

CASE II: 3855-16 (JPC 4101305).

Signalment: 13-year-old female spayed Australian shepherd (*Canis familiaris*), canine.

History: This dog had a soft tissue mass on the dorsal left chest wall. The mass was deep and attached to chest wall muscles and invaded into adjacent fat. The surgeon dissected around mass and removed muscle where it was attached.**Gross Pathology:** Mass measured 5 x 4 x 3 cm

Laboratory Results (clinical pathology, microbiology, PCR, ELISA, etc.): None provided.

Microscopic Description:

A 5 x 4 x 3 cm subcutaneous mass from behind the left shoulder blade is examined in four sections representing a cross section and lateral margins. The specimen has two distinct masses with a line of demarcation at their collision point. The peripheral mass is densely cellular, poorly circumscribed, and unencapsulated and is infiltrating into the adjacent subcutaneous adipose tissue. The mass consists of spindle-shaped cells arranged in bundles, streams, storiform patterns and whorls accompanied by collagen; the collagenous stroma varies from delicate to thick bands, in different regions of the tumor. The neoplastic cells are medium-sized with indistinct cellular margins and small amounts of fibrillar eosinophilic cytoplasm which blends with the stroma. The nuclei are medium-sized and oval with stippled chromatin and 1-5 nucleoli. Eleven mitotic figures are seen in ten high powered fields including a few atypical mitotic

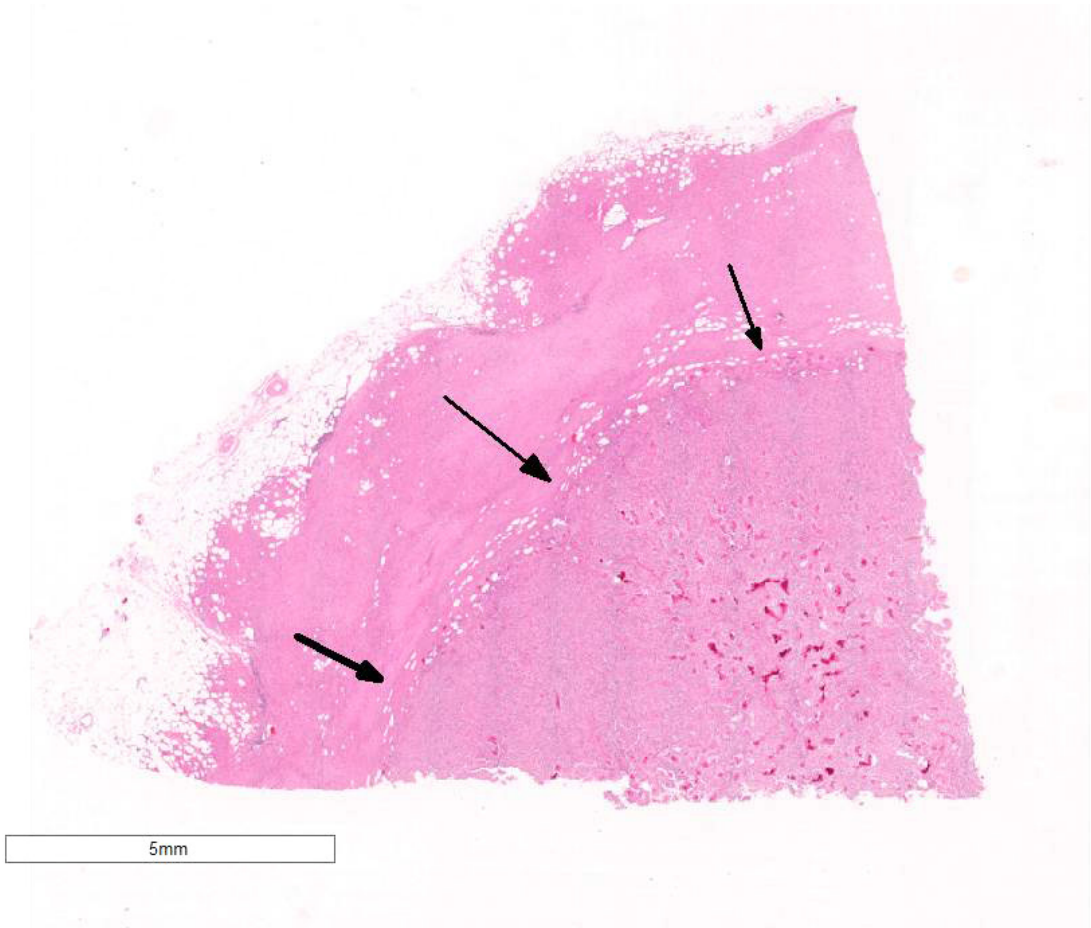

Soft tissue, chest wall: A single mass composed of two independent neoplasms is separated by a distinct border (arrows). (He, 5X)

figures. The central mass is densely cellular, circumscribed, unencapsulated, and slightly compresses the surrounding malignant peripheral nerve sheath tumor. The mass consists of plump spindle-shaped cells arranged in short streams and sheets accompanied by osteoid matrix. The neoplastic cells are medium to large with distinct cellular margins and moderate to large amounts of finely granular to fibrillar eosinophilic cytoplasm. The nuclei are large and oval with vesicular chromatin and 1-5 nucleoli. Thirty-two mitotic figures are seen in ten high powered fields, including a few atypical mitotic figures. The mass has moderate anisocytosis and anisokaryosis with rounded multinucleated giant cells occasionally scattered throughout it. The mass touches the deep and lateral margins.

Contributor's Morphologic Diagnosis:
Malignant peripheral nerve sheath tumor and osteosarcoma – collision tumor

Contributor's Comment: This neoplastic mass has a very unique histological appearance where the outer part has differentiated into a malignant peripheral nerve sheath tumor and the inner part has differentiated into an osteosarcoma. As there is a distinct junction between the two masses, this neoplasm was classified as a collision tumor.

Collision tumors are the result of two tumors in the same anatomic site which abut one

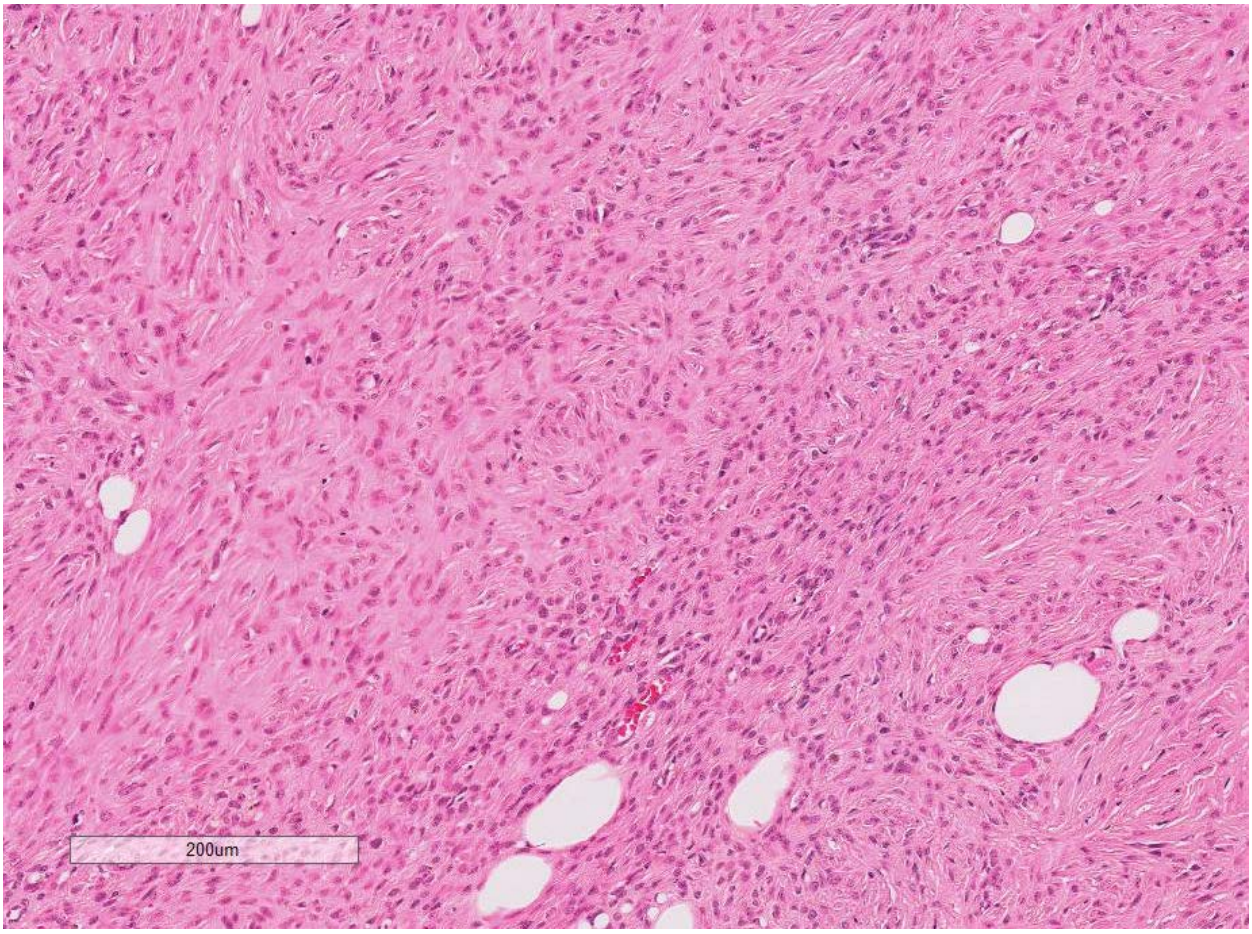

Soft tissue, chest wall: The first tumor (at upper left of the ubgross section,) is composed of moderate numbers of spindled cells forming tight bundles (storiform pattern). (HE, 120X.)

another but have a distinct demarcation between the two. Collision tumors are rare in domestic animals. Compared to collision tumors, biphasic or mixed tumors exist in which there are two intermixing phenotypically distinct populations of neoplastic cells. Reports of collision tumors involving melanomas are common.[3,6,8] Additionally, mixed Sertoli-seminoma tumors in the testes of dogs comprised nearly seven percent of all tumors in one study.[7] These collision and mixed tumors present a diagnostic dilemma as to how they arise, particularly if the tissue of origin is embryologically different.

It is uncertain if this case represents a mass with growth of each neoplasm de novo, resulting in a collision of the two tumors or if there was metaplasia leading to development of a second tumor with characteristics of malignancy. Peripheral nerve sheath tumors are a heterogeneous group of tumors and their classification is confusing.[5] As the various classifications imply, there may be mesenchymal origin of these tumors that may undergo metaplasia. An example of cartilaginous differentiation exists.[5] It is feasible osseous metaplasia may, too, occur and develop into what appears to be a collision tumor.

JPC Diagnosis: 1. Fibrovascular tissue: Sarcoma (favor peripheral nerve sheath tumor), Australian shepherd (*Canis familiaris*), canine.
2. Fibrovascular tissue: Osteosarcoma.

Conference Comment: There have been several collision tumors reported in the veterinary literature within the last five years, including: malignant trichoblastoma/melanoma in a rabbit,[2] oral squamous cell carcinoma/malignant melanoma in a dog,[8] uterine adenocarcinoma/leiomyosarcoma in a goat,[1] perianal gland carcinoma/hemangiosarcoma in a dog,[9] and fibrosarcoma/mast cell tumor in a dog.[9] In most cases of collision tumors, the authors postulate that one tumor is primary and a second separate tumor occurs due to chronic inflammation, repetitive mitotic stimulation, and eventual neoplastic transformation of various local cell types. This differentiates collision tumors from mixed tumors, which are single tumors that include a mixture of different neoplastic cell types.

Collision tumors are also recognized in humans where much research is being done regarding their genetic profiles. For instance, it has been shown that intracranial collision tumors are composed of two distinct components. In the case of a combined meningioma and oligodendroglioma, there is deletion of chromosome 22q and 19q in both tumors initiating neoplastic transformation of both cell types.[4]

Attendees discussed the use of cytology with ALP staining for rapid diagnosis of

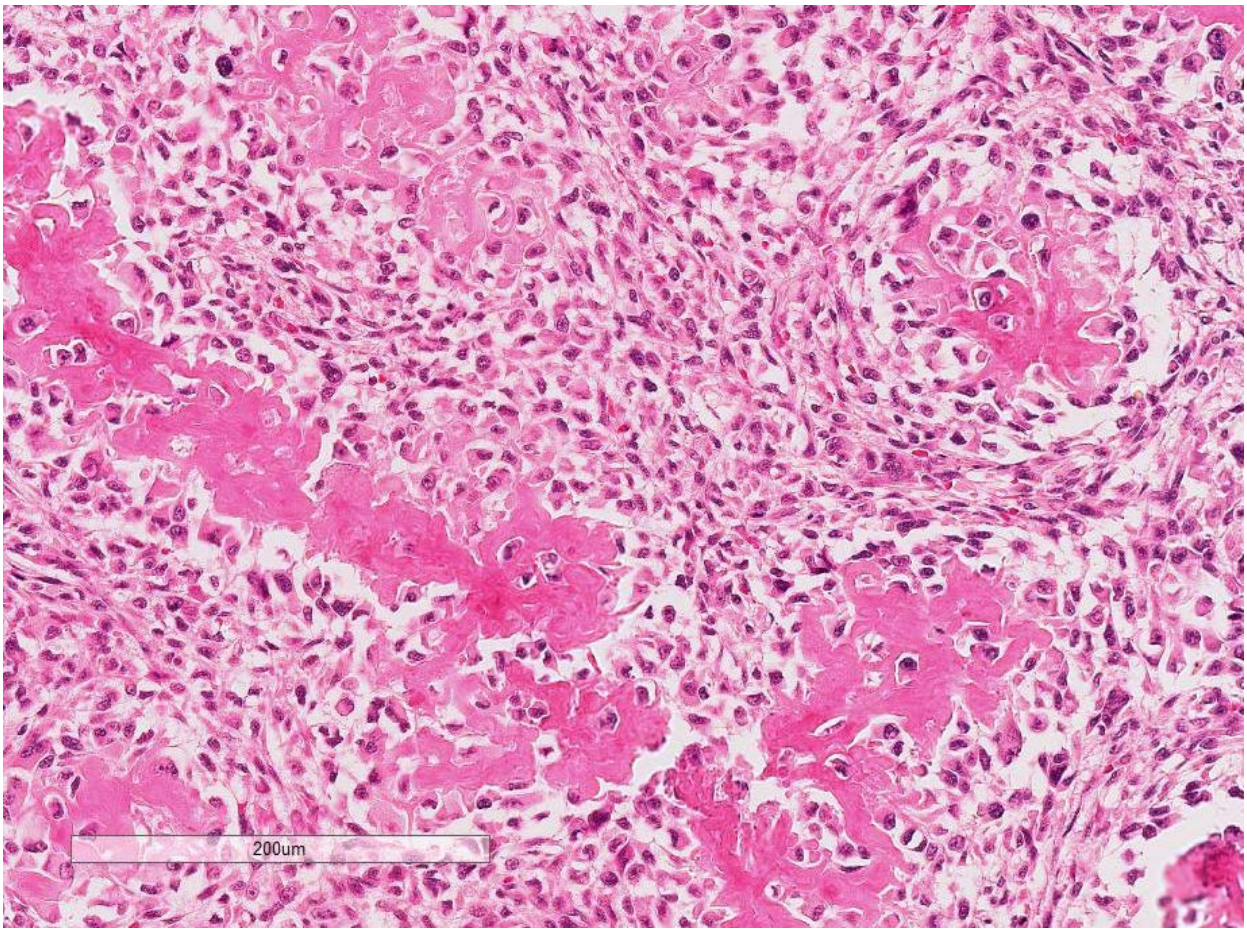

Soft tissue, chest wall. The second tumor (lower right of the Subgross image) is composed of plump active osteoblasts creating large amounts of osteoid. (HE, 155X)

osteosarcoma during surgery, remarking that sometimes biopsies can resemble reactive bone, especially if the sample is obtained from the periphery of the neoplasm. Additionally, participants discussed the special stains utilized in this case, including S-100, which exhibited strong, intra-cytoplasmic immunoreactivity for the spindle cell population of the sarcoma.

Contributing Institution:
Veterinary Diagnostic Center
School of Veterinary Medicine and Biomedical Sciences
University of Nebraska-Lincoln
http://vbms.unl.edu/nvdls

References:

1. Dockweiler JC, Cossic B, McDonough ST, Fubini SL, et al. Tumor collision of uterine adenocarcinomoa and leio-myosarcoma in a goat. *J Vet Diagn Invest.* 2017; 29(5):696-699.
2. Golbar HM, Izawa T, Kuwamura M, Fujita D, et al. A collision tumor consisting of malignant trichoblastoma and melanosarcoma in a rabbit. *J Comp Path.* 2014; 151(1): 63-66.
3. Jakab C, Balka G. First report of malignant collision skin tumor with malignant melanoma and anaplastic sarcoma components in a dog. *Acta Vet Hung*. 2012; 60:245-255.
4. Kearney H, Cryan JB, Looby S, Brett FM, et al. The DNA copy number landscape of a collision tumor. *Clin Neuropathol.* 2018;37(2):68-73.
5. Koestner A, Higgins RJ. Tumors of the nervous system. In: Meuten DJ, ed. *Tumors in Domestic Animals*. 4th ed. Ames, IA: Iowa State Press; 2002:697–738.
6. Muscatello LV, Avallone G, Benazzi C, Sarli G, Porcellato I, Brachelente C, Brunetti B. Oral squamomelanocytic tumor in a dog: a unique biphasic cancer. *J Comp Path*. 2016; 154:211-214.
7. Patnaik AK, Mostofi FK. A clinicopathologic, histologic, and immunohistochemical study of mixed germ cell-stromal tumors of the testis in 1 dogs. *Vet Path*. 1993; 30:287-295.
8. Rodríguez F, Castro P, Ramírez GA. Collision Tumor of squamous cell carcinoma and malignant melanoma in the oral cavity of a dog. *J Comp Path.* 2016; 154:314-318.
9. Scott JE, Liptak JM, Powers BE. Malignant collision tumors in two dogs. *J Am Vet Med Assoc.* 2017; 251(8):941-945.

CASE III: W1161-16 (JPC 4102120).

Signalment: 15-year-old, male, neutered, Saluki (*Canis familiaris*), canine.

History: The dog had been previously diagnosed with hyperadrenocorticism based on low-dose dexamethasone suppression test, and treatment with trilostane was initiated. The dog was transported a long distance by plane and subsequently became in appetent. The animal was found collapsed in a kennel and taken to the University of Melbourne

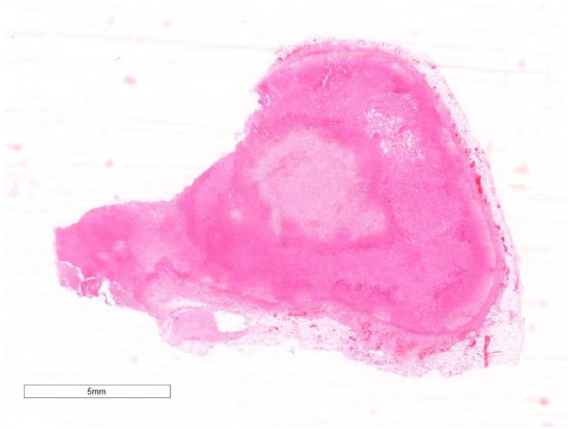

Adrenal gland, dog: The entire adrenal cortex and large areas of the medulla are effaced by necrosis and hemorrhage. Israel, http://www.weizmann.ac.il/vet/)

veterinary referral service. At admission, the animal was recumbent and obtunded, with normal cranial nerve assessment. The dog was markedly tachycardic (180bpm) with a grade 1/6 left sided systolic heart murmur; an ECG revealed intermittent supraventricular tachycardia and occasional 2nd degree heart block. Body temperature was 39.8 ºC. Biochemistry, hematology and urinalysis results are presented below. The owner elected for the dog's euthanasia following consultation.

Gross Pathology: The liver was enlarged with rounded lobe margins and mottled red-brown coloration. The parenchyma was faintly nodular in structure and very friable. Within both adrenals there were multiple poorly-defined, variably sized, tan to beige colored soft tissue nodules, and multifocally within the adrenal parenchyma there were regions of dark red to black discoloration. The renal surface was irregularly indented, and underlying the indented areas there were wedge-shaped foci of parenchymal pallor extending through the cortex into the medulla.

Laboratory Results (clinical pathology, microbiology, PCR, ELISA, etc.): see below

Haematology	**Value**	**Canine Ref Values**
PCV %	**66**	37-55
RBC ($x10^{12}$/L)	**10.13**	5.65-8.87
Hb g/dL	**24.9**	8-12
MCV (fL)	64.9	61.6-73.5
MCH (pg)	23.2	21.2-25.9
MCHC (g/dL)	35.9	32.0-37.9
Neut ($x10^9$/L)	8.53	2.95-11.64
Lymph ($x10^9$/L)	1.29	1.05-5.10
Mono ($x10^9$/L)	0.42	0.16-1.12
Eosino ($x10^9$/L)	0.6	0.06-1.23
Baso ($x10^9$/L)	0.01	0.0-0.1
Platelet (K/µL)	325	148-484
PT	16	14-19
aPTT	88	75-105

Biochemistry		
Urea (mmol/L)	**26.9**	2.5-9.6
Crea (µmol/L)	**460**	44-159
Phos (mmol/L)	**2.85**	0.81-2.2
TP (g/L)	61	52-82
Albumin (g/L)	29	22-39
Globulin (g/L)	32	25-45
ALT (U/L)	**239**	10-125
ALKP (U/L)	88	23-212
GGT (U/L)	0	0-11
T Bil (µmol/L)	6	0-15
Chol (mmol/L)	5.48	2.84-8.26
Amylase (U/L)	1485	500-1500

Lipase (U/L)	422	200-1800
Glu (mmol/L)	4.6	3.3-6.1
Lactate (mmol/L)	1.3	<2.0
K^+ (mmol/L)	**5.9**	3.6 – 5.8
Na^+ (mmol/L)	**140**	145 – 158
Ca^{2+} (mmol/L)	2.42	1.98-3.00
Cl^- (mmol/L)	115	105 – 122

Blood gases		
FiO2 %	.21	
A or V	V	V
pH	7.314	7.405
pCO2 mmHg	25.2	36.6
pO2 mmHg	34.5	52
HCO3 mEq/L	12.4	22
Anion Gap mmol/L	17.7	<24

Urinalysis: USG 1.018, pH 6, trace protein. Rare casts and no bacteria noted on urine sediment exam.
LDDST: Cortisol 228 nmol/L at 0h (28-150 nmol/L), 128 nmol/L at 4h (<30 nmol/L), and 220 nmol/L at 8h (<30 nmol/L). (References in parenthesis)

Microscopic Description: Diffusely throughout the adrenal cortex there is loss of cellular detail, eosinophilic parenchymal homogeneity, and effacement of normal tissue architecture (necrosis). Multifocally

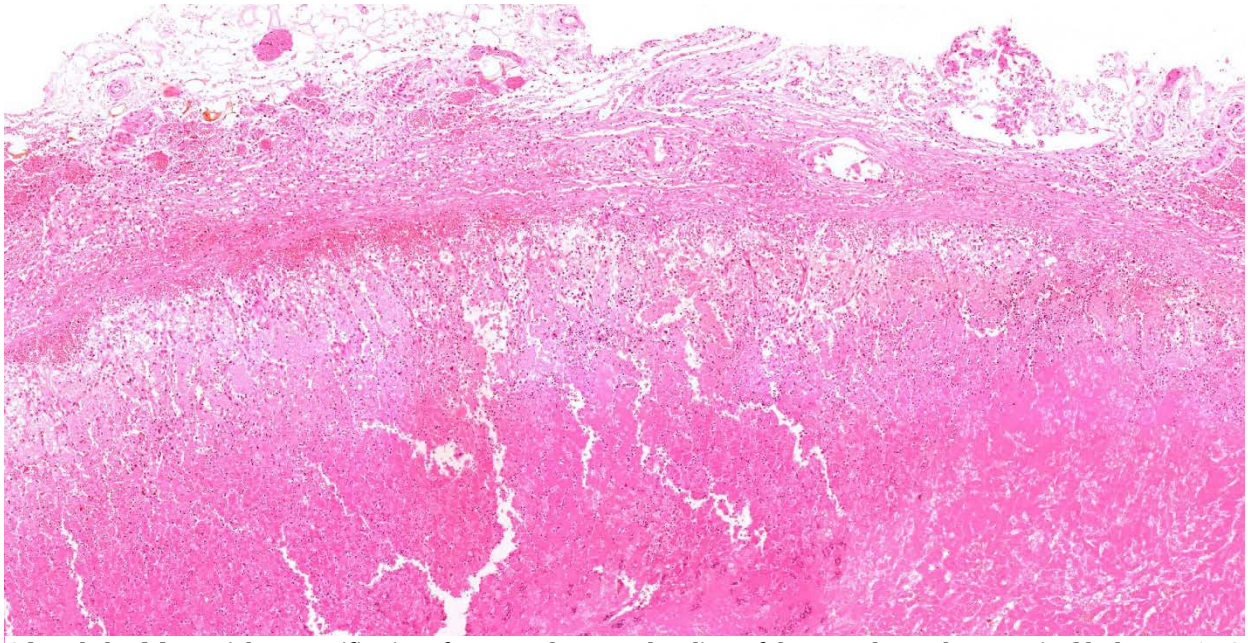

Adrenal gland dog. Higher magnification of cortex. The stromal outlines of the zona glomerulosa remain (black arrows). A line of hemorrhage, delineates them from the overlying edematous and hemorrhagic capsule, and the zona fasciculata and glomerulosa at bottom, are diffusely necrotic and largely effaced by hemorrhage. (HE, 69X)

within the affected areas there are deposits of lacy basophilic material (chromatin strands) and cellular debris which sometimes displays fine acicular clefting (cholesterol deposits), and there are also large regions that are suffused by extravasated erythrocytes (hemorrhage). Cortical cells in residual viable areas are poorly cohesive and are often swollen with cytoplasmic clearing (ballooning degeneration). There is relative sparing of the adrenal medullary structure, but the vasculature is moderately engorged and chromaffin cells display cytoplasmic eosinophilia (not present in all sections).

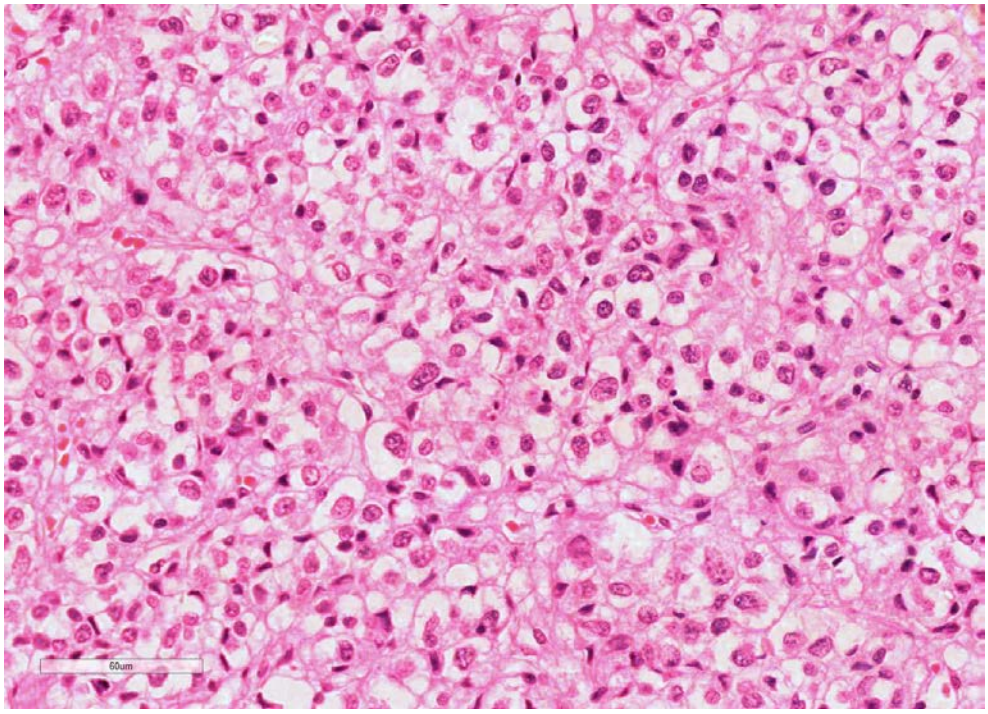

Adrenal gland dog. The majority of the adrenal medulla remains viable. (HE, 373X)

Surrounding the areas of necrosis, there is a marked infiltrate of neutrophils (predominantly degenerate) and macrophages, which extends beyond the capsule, and there is also a poorly organized population of fibroblasts within early granulation tissue. The connective tissue surrounding the adrenal is expanded and rarefied (edematous) with engorged vessels, multifocal hemorrhage and deposits of lacy eosinophilic material (fibrin).

Contributor's Morphologic Diagnosis:
Adrenal: Adrenocortical necrosis, severe, bilaterally diffuse, subacute

Contributor's Comment: Adrenal necrosis is infrequently identified in domestic species, with foci of necrosis identified in 1.8% of cats (n=159) and 3.0% of dogs (n=101) in a recent survey.[5] The necrosis in this case was attributed to an idiosyncratic response to trilostane therapy, resulting in secondary adrenocortical insufficiency and Addisonian crisis. Trilostane is commonly used for medical treatment of canine hyperadrenocorticism, and has superseded op'DDD as the drug of choice for control of this condition. It is a steroid analogue that reversibly inhibits adrenal steroidogenesis through blockade of 3β-hydroxysteroid dehydrogenase, thereby preventing the conversion of 3β-hydroxysteroids (pregenolone, 17-hydroxypregnenolone, and dehydroepiandrosterone) to 3-ketosteroids (progesterone, 17-hydroxyprogesterone, and androstenedione).[10] Administration inhibits both mineralocorticoid and glucocorticoid synthesis, and sex hormone synthesis may also be impaired, although typically to a lesser degree. The metabolism of trilostane

has not been examined in detail in dogs, but in rats the drug is partially converted to ketotrilostane by the liver before being excreted fecally, while urinary excretion predominates in monkeys.[9]

There are multiple published reports of adrenal necrosis in dogs associated with trilostane administration.[2,11,12] Reutsch *et. al.* identified adrenal necrosis in five of seven dogs treated with trilostane for hyper-adrenocorticism.[12] This side-effect is not readily explained by the known effects of trilostane within the adrenal gland, and it has been proposed that the adrenal necrosis observed during trilostane therapy may reflect excessive secretion of adreno-corticotropic hormone (ACTH), rather than direct effects of the drug or its metabolites. This hypothesis is supported by trials demonstrating the development of adreno-cortical hemorrhage and vacuolization in rats treated with ACTH, whereas treatment with trilostane alone produced no histological lesions.[1] Moreover, adrenal hemorrhage has been observed clinically in humans receiving exogenous ACTH therapy.[7] The exact role of trilostane in the pathogenesis of adreno-cortical degeneration remains uncertain; however, it is possible that trilostane may promote hypersecretion of ACTH, or alternatively sensitizes adrenocortical cells to the toxic effects of ACTH. In the present case, we speculate that the stress of the flight prior to presentation may have precipitated excessive ACTH secretion and development of subsequent adrenal necrosis.

There are a large range of other chemicals capable of causing adrenal toxicity, as indicated in the table 1. The adrenal cortex is relatively susceptible to toxic effects due to its well-developed and highly permeable blood supply, its robust lipid metabolic pathways with strong uptake of lipophilic substances, and its abundance of cytochrome P450 enzymes for bio-transformation. Toxins may be selective in the region of the adrenal affected, even within the different cortical zones, and thus identifying the affected regions may aid in determining the causative agent. Compounds such as aniline and sulfated muco-polysaccharides pre-dominantly target the zona glomerulosa, whereas the effects of toxins such carbon tetrachloride, acrylonitrile, clotrimazole and op'-DDD are largely confined to the zonas fasciculata and reticularis.[13] Toxicity affecting the adrenal medulla is relatively uncommon but has been reported with compounds such as reserpine, thiouracil and xylitol; cellular proliferative changes appear to be the most common manifestation of medullary toxicity.[13]

Non-toxic causes of adrenal degeneration may also occur. Hemorrhage and necrosis predominantly affecting the adrenal cortex has been observed in association with septic infections in humans, in particular those caused by *Neisseria meningitidis*, *Staphylococcus aureus* and streptococci. The pathogenesis of this condition - known as Waterhouse-Friederichsen Syndrome – is poorly understood, but it has been proposed that adrenaline release may induce both platelet aggregation and marked adrenal vasoconstriction, predisposing to venous thrombosis and infarction within the gland, particularly in association with concurrent disseminated intravascular coagulation.[9] Similar changes may be observed in septicemic horses[5] and calves[15], as well as in young lambs dying from exposure. Although possibly not completely analogous, adrenocortical hemorrhage may also be present in horses that die of during marked exertion. Adrenal hemorrhage has been induced experimentally in rabbits through intravascular endotoxin administration[8], but it is interesting to note that adrenocortical hemorrhage does not develop in

hypophysectomized animals treated with endotoxin, suggesting that the pathogenesis of Waterhouse-Friederichsen syndrome requires pituitary signaling. Thus, aberrant ACTH secretion may be a common factor in the pathogenesis of both trilostane toxicity and septic adrenal hemorrhage.

Table 1. Adrenal toxins (from Colby[4])

Acrylonitrile	Dilantin	Polyglutamic acids
ACTH	Dimethylbenzanthracenes	Ponceau SX
Aflatoxin	Estrogens	Pyrazole
Aminoglutethimide	Ethanol	Spironolactone
Aniline	Etomidate	Sulfated mucopolysaccharides
Bromocripitine	Fluphenazine	Suramin
Carbon tetrachloride	Hexadimethrine bromide	Tamoxifen
Chenodeoxycholic acid	Iprindole	Tetrachlorvinphos
Chloroform	Ketoconazole	Testosterone
Chlorphentermine	Mefloquine	Thioacetamide
Clotrimazole	Methanol	Thioguanine
Cyproterone	Nitrogen oxides	Toxaphene
Cysteamine hydrochloride	Parathion	Triparanol
op'-DDD	PBBs, PCBs	Urethane
Danazol	Polyanthosulfonate+ aminocaprionic acid	Zimelidine

JPC Diagnosis: Adrenal gland: Necrosis, cortical and medullary, diffuse, severe with hemorrhage, Saluki (*Canis familiaris*), canine.

Conference Comment: The word “adrenal” comes from the Latin for near (*ad-*) and kidney (*renes*) thus named for its relative location to the kidneys. An Italian anatomist, Bartolomeo Eustachi, is the individual credited with their discovery in 1563. However, his works were not received publicly until years later because they were secluded in the papal library. Eustachius (as he was known) along with Vesalius are considered the fathers of human anatomy. Due to religious restrictions on anatomists through the Renaissance, his anatomy book became a bestseller more than a century after his death.[3] His works are broken down into 17 “plates” in which he describes and illustrations the kidneys, ear, heart (including the vena azygous and vena cava, both named by him), thoracic and abdominal viscera, brain, spinal cord, and detailed descriptions of peripheral nerves.[14] In order to more clearly see the intimate structure and detail of these organs, Eustacius created magnifying glasses (early microscopes) and used different fluids to break down tissues. As you may expect, he also had extended knowledge of the inner ear, naming the Eustacian tube and diagraming the malleus, stapdius, and cochlea.[16]

The conference moderator discussed the submitted laboratory work, initially keying in on the azotemia (in which creatinine and urea are markedly increased), the elevated PCV (dehydration), and the urine specific gravity indicating dilute urine (1.018) with casts. Due to those findings, he favored renal rather than pre-renal azotemia. Conversely, he also

pointed out that there was no stress leukogram, which is abnormal for a sick dog and favors Addison's disease. After discussion with the contributor and reviewing the gross description of the kidney, the moderator concluded that this patient must have had concurrent renal disease which is what caused the clinical pathological findings. Additionally, he favors infarction of the gland rather than the toxic effects of trilostane administration. Conference attendees noted that trilostane is contraindicated in renal failure even though it is metabolized by the liver and excreted fecally.

Contributing Institution:

Veterinary Anatomic Pathology
Faculty of Veterinary and Agricultural Sciences
The University of Melbourne
Victoria, Australia

References:

1. Burkhardt WA, Guscetti F, Boretti FS, Ivos Todesco A, Aldajarov N, Lutz TA, et al. Adrenocorticotropic hormone, but not trilostane, causes severe adrenal hemorrhage, vacuolization, and apoptosis in rats. *Domest Anim Endocrinol*. 2011; 40(3): 155-164.
2. Chapman PS, Kelly DF, Archer J, Brockman DJ, Neiger R. Adrenal necrosis in a dog receiving trilostane for the treatment of hyperadrenocorticism. *J Small Anim Pract.* 2004; 45(6): 307-310.
3. Choulant L. *History and Bibliography of Anatomic Illustration.* Translated and annotated by Mortimer Frank. New York, NY: Hafner; 1962:200-204.
4. Colby HD. Adrenal-gland toxicity - chemically-induced dysfunction. *Journal of the American College of Toxicology*. 1988; 7(1): 45-69.
5. Hart KA, Barton MH. Adrenocortical insufficiency in horses and foals. *Vet Clin North Am Equine Pract*. 2011; 27(1): 19-34.
6. Herbach N, Wiele K, Konietschke U, Hernmanns W. Pathologic alterations of canine and feline adrenal glands. *Open Journal of Pathology*. 2016; 6: 140-153.
7. Kornbluth AA, Salomon P, Sachar DB, Subramani K, Kramer A, Gray CE, et al. ACTH-induced adrenal hemorrhage: a complication of therapy masquerading as an acute abdomen. *J Clin Gastroenterol*. 1990; 12(4): 371-377.
8. Levin J, Cluff LE. Endotoxemia and adrenal hemorrhage. A mechanism for the Waterhouse-Friderichsen syndrome. *J Exp Med*. 1965; 121: 247-260.
9. Piccioli A, Chini G, Mannelli M, Serio M. Bilateral massive adrenal hemorrhage due to sepsis: report of two cases. *J Endocrinol Invest.* 1994; 17(10): 821-824.
10. Ramsey IK. Trilostane in dogs. *Vet Clin North Am Small Anim Pract.* 2010; 40(2): 269-283.
11. Ramsey IK, Richardson J, Lenard Z, Tebb AJ, Irwin PJ. Persistent isolated hypocortisolism following brief treatment with trilostane. *Aust Vet J*. 2008; 86(12): 491-495.
12. Reusch CE, Sieber-Ruckstuhl N, Wenger M, Lutz H, Perren A, Pospischil A. Histological evaluation of the adrenal glands of seven dogs with hyperadrenocorticism treated with trilostane. *Vet Rec*. 2007; 160(7): 219-224.
13. Ribelin WE. The effects of drugs and chemicals upon the structure of the adrenal gland. *Fundam Appl Toxicol.* 1984; 4(1): 105-119.
14. Roberts KB. Eustachius and his anatomical plates. *Newsletter of the Canadian Society for the History of Medicine*. 1979; Apr: 9-13.
15. Rosol TJ, Grone A. Endocrine glands. In: Maxie G, ed. *Jubb, Kennedy & Palmer's*

Pathology of Domestic Animals. Vol. 3. 6th ed. St. Louis, MO: Elsevier Health Sciences; 2015: 269-357.
16. Schmidt JE. *Medical Discoveries: Who and When*. Thomas Publishing; 1959: 9-10.

CASE IV: 4079-14 (JPC 4048433).

Signalment: Neonatal, male and female, Dorper (*Ovis aires*), ovine.

History: Of 36 pregnant ewes, 14 have lambed in the last week. The lambs (2) with goiters died within 10 minutes of birth. The normal lamb also died after birth. Examination of the ewe reveals a possible small thyroid swelling. All lambs were frozen before submission.

Gross Pathology: Examined at necropsy are two term affected lambs and an unaffected lamb. The lambs had been frozen and thawed prior to examination. The affected lambs externally have a large subcutaneous bulge in their anterior neck behind the larynx. The affected lambs are a female of body weight 2.2 kg and crown-rump length 31.1 cm and a male weighing 2.7 kg and having a crown rump length of 35.3 cm. The female affected lamb has a brachygnathic mandible. The unaffected lamb is a female of body weight 2.15kg and crown-rump length of 33.5 cm.

The unaffected lamb has a well-developed thick hair coat all over its body. The female affected lamb has no hair on the anterior aspects of the lower extremities, ventral abdomen or trunk. The only relatively normal hair is present on the neck, although there is also some hair on the posterior aspects of the legs below the elbow and stifle. The male affected lamb has similar alopecia on the anterior aspects of the front and rear legs, ventral body, and particularly scrotum, and a sparse, poorly developed hair coat on the trunk, especially on the posterior trunk. Hair on the head and neck is more normal.

The female affected lamb has enlarged thyroids that are 7 cm long X 2.5 cm in greatest diameter and weigh 26.6 grams. The male's thyroids are 7 cm long X 3 cm in greatest diameter and weigh 2.15 grams. The enlarged thyroids are dark red in color and fleshy in texture. The left thyroid of the female contained a simple well defined cyst of 0.8 cm diameter located in the middle of the gland. The thyroids of the unaffected lamb are 2 X 0.7 cm and weigh 0.6 grams.

No visceral abnormalities are noted, including in the adrenals or pituitary. The eyes and brain are proportionally of normal size. The white matter of the spinal cord is a similar intensity of white between the affected and unaffected lambs.

Laboratory Results (clinical pathology, microbiology, PCR, ELISA, etc.): None provided.

Microscopic Description:

Thyroid gland: The thyroid follicles in both affected lambs are enlarged, sometimes spanning several 4X fields. The colloid has

Thyroid gland, lamb. Two lambs (unaffected at top) are presented for examination. The affected lamb at bottom is alopecic over the anterior aspects of the lower extremities, ventral abdomen and trunk (Photo courtesy of: Veterinary Medical Diagnostic Lab, University of Missouri, www.VMDL.missouri.edu)

decreased eosinophilia and increased granularity. The follicular cells are frequently detached, although they remain at the periphery of follicles (freezing artifact). Interstitial cells are difficult to appreciate. The thyroid from the unaffected lamb has isomorphic follicles containing moderately eosinophilic colloid and a layer of cuboidal cells lining each. There is mild to moderate sloughing of colloidal epithelium (freezing artifact).

Skin: Affected lambs have reduced numbers of hairs protruding from the follicles. In some affected sections the epidermis is thinner and the hairs are farther apart, with mild myxedema of the deep dermis. In some sections there is basophilic ground substance consistent with myxedema in the upper dermis as well.

Contributor's Morphologic Diagnosis:
Colloid goiter
Epidermal atrophy with alopecia
Contributor's Comment: This case demonstrates congenital goiter and the alopecic skin disease that often is present.

Goiter or thyroid hyperplasia can result from multiple mechanisms: iodine deficiency, ingestion of goitrogenic compounds that interfere with thyroxine production, excess iodide and genetic mechanisms that interfere with biosynthesis of thyroid hormones.[2] All of these etiologies result in activation of the hypothalamus as a result of low T3 and T4, with the result of increasing TSH. Common goitrogenic plants include thiouracil, sulfonamide and plants of the Brassica group. Offspring of deficient dams develop severe bilateral thyroid enlargement as in this case, with hyperplasia and hypertrophy of thyroid follicular cells and enlargement of interstitial blood vessels. Increased iodide blocks release of T3 and T4, resulting in enhanced TSH secretion.[2]

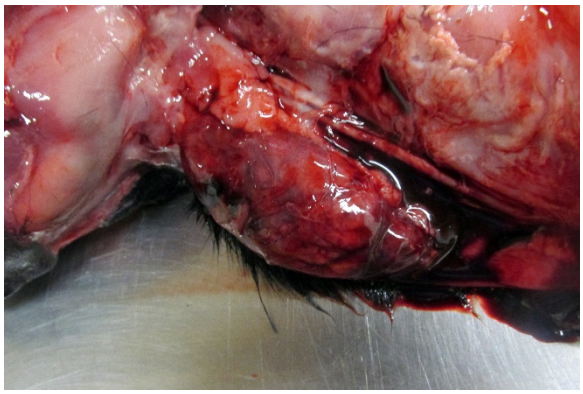

Thyroid gland, lamb. Thyroids in the affected glands are dark red, fleshy, and measure 7cm in length. (Photo courtesy of: Veterinary Medical Diagnostic Lab, University of Missouri, www.VMDL.missouri.edu)

Hypothyroidism in animals, including sheep, and people can result in abortions, stillbirths and congenital abnormalities.[2]

In hyperplastic goiter, follicles vary in size; colloid is hypereosinophilic and may be vacuolated. Follicles are lined by one or more layers of epithelium, with small basal nuclei. Finger-like projections of cytoplasm may protrude into the follicle lumens. In these lambs, the colloid was pale and several large cysts were present. Following correction of the problem, the gland may become pale, as reduced TSH reduce endocytic resorption of colloid and condition is called colloid goiter.[4]

Thyroxine or T4 is the major product of the thyroid gland but is not active as an effective transcription factor. T4 must be deiodinated to T3 before it can bind to the nuclear receptor and the reaction regulated the bioavailability. Sulfation may also play a role in fetal thryoxine metabolism, as the addition of sulfate accelerates deiodination to inactive metabolites. Sulfation is upregulated during gestation in sheep during the last trimester and may regulate the supply of fetal T3 and facilitate maternal-fetal exchange. Iodine is concentrated by the placenta during fetal life.[7] Glucuronidation of thyroxine occurs in

liver and precedes biliary-fecal excretion. Stimulation of glucuronidation by various drugs can produce goiter in rats, but not humans.[7]

Congenital dyshormonogenetic goiter is inherited as an autosomal recessive trait in Corriedale, Dorset Horn, Merino and Romney sheep,[3,5] Afrikaner cattle, and dwarf Saanen goats. Dorset horn sheep form part of the Dorper lineage. Inheritance is believed to be autosomal recessive in sheep. The most obvious changes in these sheep, besides thyroid enlargement, were abnormalities of the skin. Affected fetuses have abnormal hair coat, myxedema of the subcutis, weakness, and most die after birth. Thyroid follicles are described as collapsed due to lack of colloid,[2] because there is increased endocytic activity and diminished ability to synthesize thyroglobulin. Iodine uptake is increased but blood T3 and T4 are low. The antibody used to stain for thyroglobulin was not optimized for sheep, but there was at least some staining of affected lambs' thyroids. Unfortunately freezing and thawing of the tissue caused considerable artifact, which may have interfered with staining.

Under long term TSH stimulation, albumin and other proteins are iodinated by the thyroid. Iodine supplements restore normal thyroid hormone levels in affected sheep, even though thyroglobulin is absent. However, affected offspring die shortly after birth. Thyroglobulin RNA transcripts are incorrectly processed and no full-length protein results, yet the product is immuno-reactive with anti-thyroglobulin polyclonal antibodies[3] and IHC may not be a definitive differentiating test.

Few studies have been done on the histogenesis of fetal skin lesions during maternal hypothyroidism. Primary changes in rat skin include a significant decrease in epidermal thickness and reduction of hair follicle numbers.[1] In addition, there is increased laminin deposition in the dermis and particularly the basement membrane.[1] Laminin is important in connecting the dermis and epidermis. Hypothyroid rat pups developed increased laminin by 10 days of age. Number of hair follicles decreased and myxedema is present as in the skin of these lambs. Laminin is important to hair follicle development; T3 increases hair follicle survival in vivo considerably.

JPC Diagnosis: 1. Thyroid gland, follicular epithelium: Hyperplasia, diffuse, severe, Dorper (*Ovis aires*), ovine.
2. Haired skin, superficial dermis: Myxedema, diffuse, moderate.

Conference Comment: Synthesis of thyroid hormone is unique among the other endocrine organs because hormone assembly occurs extracellularly within the lumen of the thyroid follicle. Iodide ions (I^-) are collected from plasma by follicular cells, transported to the follicular lumen, and oxidized to iodine (I_2). Thyroglobulin, a high-molecular-weight glycoprotein, is synthesized by follicular cells and contains tyrosine, which is an essential component of thyroid hormones and

Thyroid gland, lamb. The affected lamb has a subcutaneous bulge in the ventral neck. . (Photo courtesy of: Veterinary Medical Diagnostic Lab, University of Missouri, www.VMDL.missouri.edu)

aids in their assembly as follows: Iodine binds tyrosyl residues in thyroglobulin to form monoiodotyrosin (MIT) followed by diiodotyrosine (DIT) which are coupled together to form T4 and T3 which is secreted by the thyroid gland in response to the hypothalamic-pituitary-thyroid axis (HPTA). The hypothalamus initiates the process by secreting thyrotropin-releasing hormone (TRH) which acts on the pituitary which releases thyroid stimulating hormone (TSH). TSH stimulates secretion of T3 and T4 from thyroid follicles. T3 and T4 act as a negative feedback mechanism to inhibit TSH release from the pituitary and induce somatostatin release from the hypothalamus which also inhibits TSH release from the pituitary. Additionally, T4 is converted to T3 within the pituitary gland and hypothalamus.[6]

Non-neoplastic and noninflammatory hyperplasia of the thyroid gland is termed "goiter" and is due to several pathogenic mechanisms: iodine deficiency or excess, goitrogenic compounds that interfere with thyroid hormone synthesis, and genetic enzyme defects in thyroid hormone synthesis. It is interesting that both deficiency of and excess iodine result in goiter. This is because iodine is required for synthesis of thyroid hormones, but, conversely, excess iodine interferes with fusion of colloid droplets and lysosomal bodies, blocking the release of thyroid hormones.[6] The rest of these pathogenic mechanisms are described in detail by the contributor.

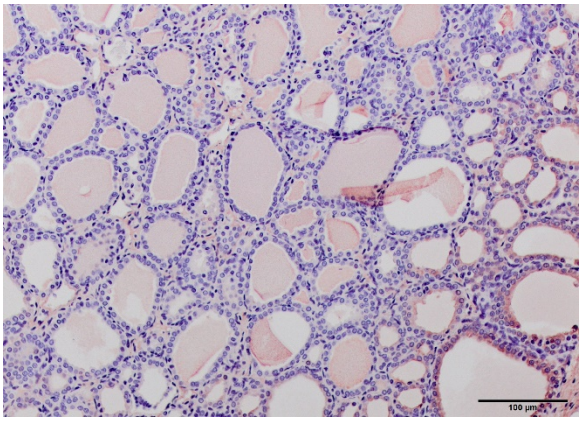

Thyroid gland, lamb. Follicles are larger than in the unaffected lamb, isomorphic and colloid-filled, but (Photo courtesy of: Veterinary Medical Diagnostic Lab, University of Missouri, www.VMDL.missouri.edu)

Newborns with goiter have unique gross characteristics such as: myxedema, alopecia, swollen tongue and laryngeal edema. The latter often contribute to death in newborns with goiter due to asphyxia and suffocation. The effect on the dam is often minimal except for prolonged gestation, dystocia, and retained placenta on occasion.[6]

True diffuse goiter must be distinguished from nodular hyperplasia, which is a fairly common finding in older horses, cats and dogs, appearing grossly as variably sized white nodules. In most animals, these nodules are not hormonally active, except in cats where they are typically functional.[6]

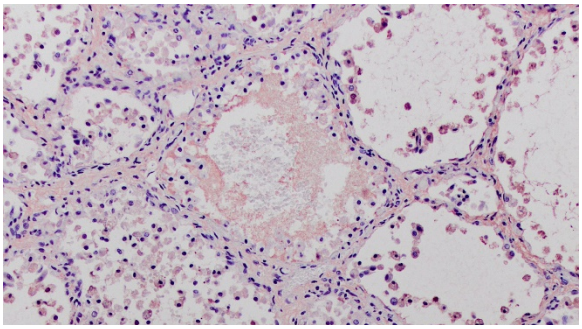

Thyroid gland, lamb. Previous freezing has resulted in detachment of colloid epithelium and colloid granularity in some areas of the slide. (Photo courtesy of: Veterinary Medical Diagnostic Lab, University of Missouri, www.VMDL.missouri.edu)

The diffuse myxedema within the superficial dermis is prominent in the submitted sections of skin from the affected animal. Evaluation of hair follicles in the absence of age-matched control or the unaffected lamb proved more problematic for attendees. While there are some focal areas in which hair follicles appear decreased in number,

follicles do not show obvious signs of hypoplasia.

Contributing Institution:
Veterinary Medical Diagnostic Lab
University of Missouri
www.VMDL.missouri.edu

References:

1. Amerion M, Tahajjodi S, Hushmand Z, et al. The effect of maternal thyroid disorders (hypothyroidism and hyper-thyroidism) during pregnancy and lactation on skin development in Wister rat newborns. *Iranian J Basic Med Sci*. 2012;16:665-674.
2. Capen CC. Endocrine Glands. In: Maxie MG, ed. *Jubb, Kennedy, and Palmer's Pathology of Domestic Animals*. Vol. 3. 5th ed. St. Louis, MO: Elsevier-Saunders; 2007:389-393.
3. Falconer IR, Roitt IM, Seamark RF, et al. Studies on congenitally goitrous sheep. *Biochem J*. 1970;117:417-424.
4. Hetzel BS, Mano MT. A review of experimental studies on iodine deficiency during fetal development. *J Nutrition*. 1988;119:145-151.
5. Jones BR, Greenway RM; Jolly RD, et al. A defect in thyroglobulin synthesis in an inherited ovine goiter: possible neonatal respiratory dist4ress syndrome. *NZ Vet J*. 1986;34:145-148.
6. Rosol TJ, Grone A. Endocrine glands. In: Maxie MG, ed. *Jubb, Kennedy, and Palmer's Pathology of Domestic Animals.* Vol. 3. 6th ed. St. Louis, MO: Elsevier; 2016:310-326.
7. WuS-y, Green WL, Huang W-s, et al. Alternate pathways of thyroid hormone metabolism. *Thyroid*. 2006;15:943-958.

Self-Assessment - WSC 2017-2018 Conference 19

1. Which of the following is true concerning parathyroid adenomas in the dog?
    a. The most common symptom in dogs with parathyroid carcinoma is polyuria.
    b. Parathyroid carcinomas release high levels of calcitonin resulting in hyperparathyroidism.
    c. Like thyroid follicular tumors, parathyroid carcinomas are more common than adenomas in the dog
    d. Most deaths related to parathyroid carcinomas are caused by hypercalcemia.

2. True or false. Collision tumors and mixed tumors are the same thing.
    a. True
    b. False

3. Which of the following compounds does NOT target the adrenal cortex in the dog?
    a. Carbon tetrachloride
    b. Xylitol
    c. op'- DDD
    d. Clotrimazole

4. Which of the following often accompanies congenital goiter in newborn lambs?
    a. Chronic hepatic congestion
    b. Alopecia
    c. Coloboma
    d. Intestinal atresia

5. Which of the following is true?
    a. T4 may be converted within the pituitary gland to T3.
    b. Thyrotropin-releasing hormone stimulates T3 and T4 from thyroid follicles.
    c. T3 must be deiodinated to T4 before it can bind to nuclear receptors.
    d. Hypothyroid rat skin has decreased amounts of dermal laminin.

Please email your completed assessment to Ms. Jessica Gold at Jessica.d.gold2.ctr@mail.mil for grading. Passing score is 80%.This program (RACE program number) is approved by the AAVSB RACE to offer a total of 0.5 CE Credits, with a maximum of 12.5 CE Credits being available to any individual Veterinary Medical Professionals for the 2017-2018 Wednesday Slide Conference. This RACE approval is for the subject matter categories of: SCIENTIFIC using the delivery method of NON-INTERACTIVE DISTANCE. This approval is valid in jurisdictions which recognize AAVSB RACE; however, participants are responsible for ascertaining each board's CE requirements.
RACE does not "accredit", "endorse" or "certify" any program or person, nor does RACE approval validate the content of the program.

Joint Pathology Center
Veterinary Pathology Services

WEDNESDAY SLIDE CONFERENCE 2017-2018

C o n f e r e n c e 20

6 April 2018

John M. Cullen, VMD, PhD, DACVP, FIATP
Alumni Distinguished Professor of Pathology
North Carolina College of Veterinary Medicine
1060 William Moore Drive
Raleigh, NC 27607

CASE I: T16-13553 (JPC 4084197).

Signalment: 10-year-old, female, spayed, American bulldog (*Canis familiaris*), canine.

History: Acute (sudden death). No additional history was available. A formalin-fixed tissue described as from a gallbladder mass was received.

Gross Pathology: Abdominal (gallbladder mass) was observed on gross examination.
Laboratory Results (clinical pathology, microbiology, PCR, ELISA, etc.): None provided.
Microscopic Description:
A formalin-fixed tissue from a gallbladder mass was received. A non-demarcated, non-capsulated neoplasm effaced the architecture of the gall bladder. The neoplasm is composed of closely packed sheets and nests of round cells supported on fine to ample fibrovascular stroma The neoplastic cells had indistinct cell borders and moderate, occasionally vacuolated, finely granular, eosinophilic cytoplasm. The nuclei were round, variably sized and had stippled

Gallbladder, dog. A large multilobular neoplasm has effaced the wall of the gallbladder (HE, 4X)

nuclear chromatin. Occasional nuclei were hyperchromatic. Nucleoli were small to indistinct. Mitotic cells were very rare (<1 per 10x HPF). Anisocytosis and anisokaryosis were mild to moderate. Multifocally, aggregates of lymphocytes were observed in some sections. Dark staining cytoplasmic granules were demonstrated by special stains (Churukian-Schenk) for argyrophilic granules.

Contributor's Morphologic Diagnosis: Neoplasm, neuroendocrine tumor (carcinoid), gallbladder

Contributor's Comment: Carcinoid tumors are uncommon neoplasms in humans and animals. The tumors arise from dispersed cells of the neuroendocrine system in the gastrointestinal tract, biliary system, pancreas and lungs. In dogs, hepatic, gastrointestinal and pulmonary carcinoids have been reported. Carcinoid tumors are reported in both sexes, several different breeds, and over an age range of 9-13 years. Extrahepatic biliary (gallbladder) carcinoid tumors are rare tumors in humans and very rare in dogs.[3,5,6,8] Carcinoid tumors in humans are potentially malignant and are usually slow growing tumors with a 5-year survival rate of 94% if localized, 64% if regional metastasis is present and 18% if distant metastasis has occurred during diagnosis.[7] Metastasis of carcinoids is also common in domestic animals and demonstrating the malignancy of the tumor. The tumor metastasizes in a similar manner to adenocarcinomas, through lymphatics and hematogenous routes. In dogs, small intestinal carcinoids frequently spread to the lung and pleura, liver, regional lymph nodes and pancreas.[3]

Since reports on canine primary gallbladder carcinoid are very rare, adequate information is unavailable to determine malignancies of

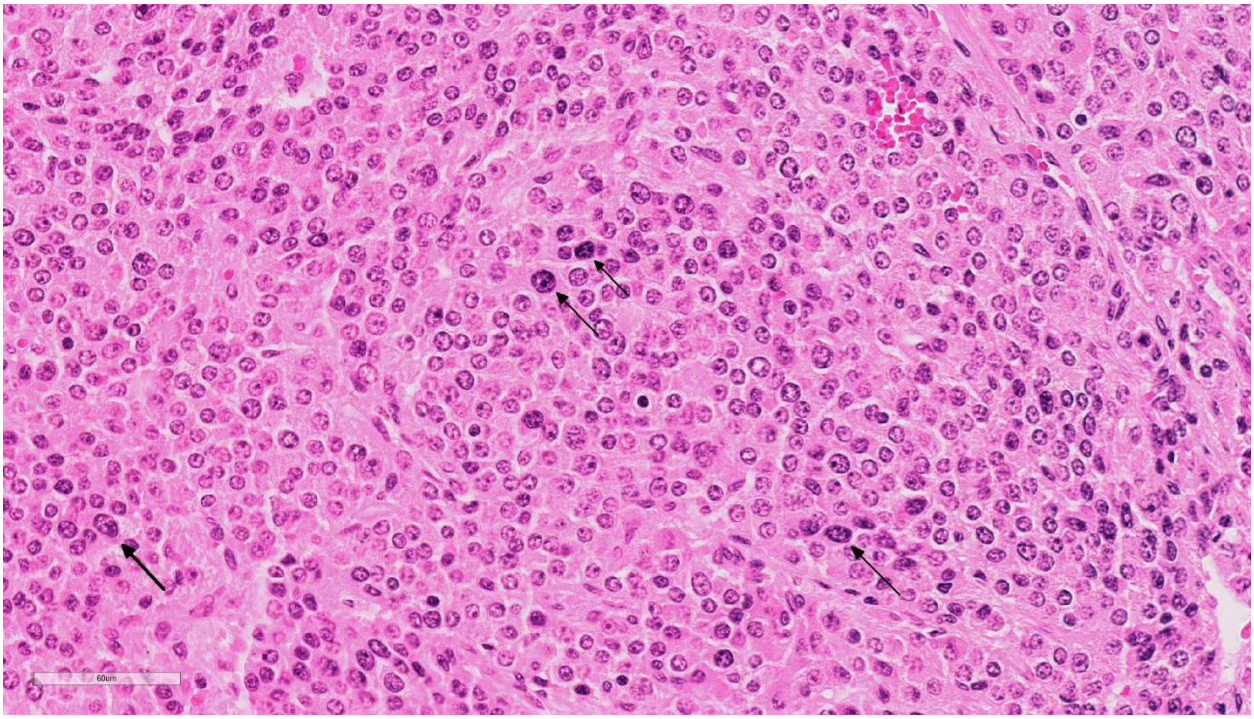

Gallbladder, dog. Neoplastic cells are polygonal and arranged in nests and packets. Karyomegalic cells are scattered throughout the section. Mitoses are rare. (HE, 400X)

primary gallbladder carcinoids in dogs. However, in one report, the presence of neoplastic cells within vessels of the gallbladder was suggested to indicate the potential of canine gallbladder carcinoid for metastatic dissemination.[8] Carcinoid tumors release various secretory products that often govern a clinical syndrome. For example, vasoactive amines released from the tumors may result in diarrhea, skin flushing, or cyanosis, hypertension, bronchoconstriction, pulmonary valvular stenosis, and right heart failure. Typical carcinoid syndrome as reported in humans has not been reported in domestic animals.[3]

Carcinoid tumors are commonly misdiagnosed especially if the tumor occurred in uncommon sites. Definitive diagnosis of carcinoid tumors requires immunohistochemistry, or special stains for argyrophilic granules or electron microscopy.[8] Immunohistochemistry against chromogranin A, synaptophysin and neuron specific enolase are often applied. The cytoplasmic granules stain positive with argyrophilic stains such as Churukian-Schenk and Grimelius stains. Therefore, special stains, such as Churukian-Schenk and Grimelius stains, which are readily available, are relatively inexpensive and should be applied in suspected cases of a carcinoid tumor.

JPC Diagnosis: Gallbladder: Carcinoid, American bulldog (*Canis familiaris*), canine.

Conference Comment: Carcinoids arise from neuroendocrine cells within mucosa of various organs, but most often the stomach and intestine. In animals, those neuroendocrine cells either secrete low-molecular-weight polypeptide hormones like secretin, somatostatin, and cholecystokinin or are part of a larger amine precursor uptake decarboxylation (APUD) group which produces serotonin among other compounds. Although carcinoids are rare in animals, the most commonly reported locations in dogs are the duodenum, colon, and rectum. They are even more scarcely reported in other organs such as the lungs (more common in humans), liver, and gallbladder as in the present case.[2,11] As noted above by the contributor, there have been three recent reports of gallbladder carcinoids, all in dogs.[5,8] Historically, they have also been reported in the gallbladder of cats and cattle.

Within the liver, carcinoids arise from the neuroendocrine cell population associated with biliary epithelium and hepatic parenchyma; therefore tumors may form within the liver, extrahepatic bile ducts, or gallbladder.[2] Clinically, carcinoids most frequently cause secondary bowel obstruction and anemia from ulceration with subsequent hemorrhage. They can also be easily mistaken for polyps, especially when located at the anorectal junction. Diarrhea may be another associated finding, as a result of release of functional polypeptide hormones.[11]

Grossly, carcinoids are lobulated, firm, dark red to tan, and rarely larger than a few centimeters in diameter. They arise deep within the mucosa, commensurate with the location of neuroendocrine cells, causing submucosal nodules with ulceration and erosion of the overlying mucosa and often infiltrating transmurally into the mesentery.[11] In the liver, there is frequent intrahepatic spread with metastasis to local lymph nodes, peritoneum, and lung.[2]

Microscopically, carcinoids are composed of round to oval polygonal cells with abundant amounts of finely granular eosinophilic to finely vacuolated cytoplasm with round vesiculate nuclei and prominent nucleoli. In typical neuroendocrine fashion, the cells are

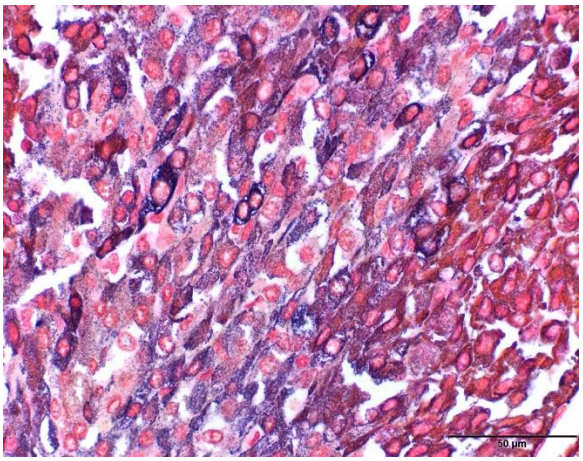

Gallbladder, dog. Neoplastic cells contain numerous dark argyrophilic granules (Churukian-Schenk, 400X) (Photo courtesy of: The University of Georgia, College of Veterinary Medicine, Department of Pathology, Tifton Veterinary Diagnostic and Investigational Laboratory, Tifton, GA 31793, USA http://www.vet.uga.edu/dlab/tifton/index.php)

arranged in nests, and packets expanding the mucosa, submucosa, and muscularis; packets are surrounded by a fine fibrovascular stroma. Additional findings include: amyloid in between cells and adjacent to stromal blood vessels and megalocytes or multi-nucleated neoplastic cells. A potential histologic differential diagnosis is intestinal mast cell tumor, owing to the presence of numerous granules.

Ultrastructurally, carcinoid cells have numerous dense, round to oval, variably sized, membrane-bound intracytoplasmic secretory granules with abundant rough endoplasmic reticulum (RER) and a plasma membrane with interdigitating processes.[11] Mast cell tumors have less dense granules that can vary from homogenous to scroll-like admixed with large clear vacuoles (degranulation) and less RER.

The diagnosis of carcinoids is based on the following: neuroendocrine microscopic pattern, cytoplasmic granules which are argentaffinic (reduce silver solution to metallic silver after formalin fixation) and argyrophilic (reduce silver solution to metallic silver after being exposed to a pre-reduction step)[10] granularity, immuno-histochemical identification of secretory products, and unique ultrastructural appearance. Histochemical and immuno-histochemical (IHC) reactivity can vary, especially if there is significant autolysis prior to fixation (common in the gastro-intestinal tract). However, in decent quality specimens, carcinoid cells are positive for neuron-specific enolase (NSE) and chromogranin as well as immunopositive for peptides being produced (e.g. serotonin). Those peptides may also be identified in circulation further supporting an endocrine diagnosis. Carcinoid cells are negative for periodic acid-Schiff and the granules do not exhibit metachromasia with Giemsa stains, further differentiating carcinoid from intestinal mast cell tumor.[11]

In humans, several paraneoplastic syndromes have been identified, such as: cutaneous flushing, diarrhea, bronchospasm, and systemic fibrosis. Fibrosis is concerning as it can lead to dysfunction of the pulmonary and tricuspid valves followed by regurgitation and right heart failure. This syndrome, termed “carcinoid syndrome”, is most common in patients that develop carcinoids in their respiratory tract. The right side of the heart is affected because monoamine oxidases in the lungs fail to inactivate vasoactive substances, and these vasoactive substances lead to the aforementioned cutaneous flushing and bronchospasm which are key clinical indicators.[9] The mechanism of fibrosis in humans is unclear but is postulated to result from interactions between tumor cells and fibroblasts or hormones and peptides secreted by the carcinoid.[4]

Conference participants discussed the differences between benign and malignant carcinoids, which, according to the

moderator, are much more common in the liver (in his experience). In this case, with a history of a single mass and no evidence of vascular invasion in the submitted sections, this carcinoid is likely benign. Additionally, attendees reviewed the origin of carcinoid tumors and the moderator cited an article[1] which stated that proliferating cholangiocytes may take on a neuroendocrine phenotype, as well as initiate vessel proliferation, which may facilitate metastasis.[1] Shunt dogs, for example, tend to have proliferation of cholangiocytes and arterioles at the same time.

Contributing Institution:
The University of Georgia
College of Veterinary Medicine
Department of Pathology
Tifton Veterinary Diagnostic and Investigational Laboratory
Tifton, GA 31793, USA
http://www.vet.uga.edu/dlab/tifton/index.php

References:

1. Alvaro D, Mancino MG, Glaser S, Gaudio E, et al. Proliferating cholangiocytes: a neuroendocrine compartment in the diseased liver. *Gastroenterology*. 2007; 132(1):415-431.
2. Cullen JM, Stalker MJ. Liver and biliary system. In: Maxie MG, ed. *Jubb, Kennedy, and Palmer's Pathology of Domestic Animals*. Vol. 2. 6th ed. St. Louis, MO: Elsevier; 2016:349.
3. Head KW, Else RW, Dubielzig RR. Tumors of the alimentary tract. In: Meuten DJ, ed. *Tumors in Domestic Animals*. 4th ed. Ames, IA: Iowa State Press; 2002: 468-470.
4. Laskaratos FM, Rombouts K, Caplin M, Toumpanakis C, Thirlwell C, Mandair D. Neuroendocrine tumors and fibrosis: An unsolved mystery?. *Cancer*. 2017; 123(24):4770-4790.
5. Lippo NJ, Williams JE, Brawer RS, Sobel KE. Acute hemobilia and hemocholecyst in 2 dogs with gallbladder carcinoid. *J Vet Intern Med*. 2008; 22 (5):1249-52.
6. Mezi S, Petrozza V, Schillaci O, et al. Neuroendocrine tumors of the gallbladder: a case report and review of the literature. *J Med Case Reports*. 2011; 5:334
7. Modlin IM, Sandor A. An analysis of 8305 cases of carcinoid tumors. *Cancer*. 1997; 79:813-829.
8. Morrell CN, Volk MV, Mankowski JL. A carcinoid tumor in the gallbladder of a dog. *Vet Pathol*. 2002; 39 (6):756-8.
9. Shinn BJ, Tafe LJ, Vanichakarn P. A case of carcinoid syndrome due to malignant metastatic carcinoid tumor with carcinoid heart disease involving four cardiac valves. *Am J Case Rep*. 2018; 19:284-288.
10. The internet pathology laboratory for medical education. Hosted by The University of Utah Eccles Health Science Library. https://library.med.utah.edu/WebPath/HISTHTML/STAINS/STAINS.html . Published 1994. Updated 2018. Accessed March 29, 2018.
11. Uzal FA, Plattner BL, Hostetter JM. Alimentary system. In: Maxie MG, ed. *Jubb, Kennedy, and Palmer's Pathology of Domestic Animals*. Vol. 2. 6th ed. St. Louis, MO: Elsevier; 2016:105-106.

CASE II: 20327-15 A or C (JPC 4099033).

Signalment: 2-year-old male neutered Cocker spaniel (*Canis familiaris*), canine.

History: In the 6-months prior to death, the dog had periodic bouts of inappetence, dark stools, and jaundice. The submitting veterinarian performed a necropsy and

Liver, dog: A rectangular section of liver is presented for examination. There is a vague nodularity even at low magnification. (HE, 5X)

submitted formalin-fixed liver to ALPC for examination.

Gross Pathology: Liver: Small and firm with numerous 1-2 mm, nodules throughout the surface.

Laboratory Results (clinical pathology, microbiology, PCR, ELISA, etc.):
ALT 168 (12-118 U/L)
ALP 172 (5-131 U/L)
Total Bilirubin 2.4 (0.1-0.3 mg/dL)
Albumin 1.6 (2.7-4.4 g/dL)
BUN 4 (6-31 mg/dL)
Urine bilirubin 3+
Bile acids pre-meal: 18.8 (<10.0 umol/L)
Bile aids post-meal: 21.8 (<20.0 umol/L)
Leptospirosis titers: Negative
Copper: 1460.0 ppm (dry weight)
Measurement was performed on formalin-fixed tissue.
COPPER DIAGNOSTIC LEVEL: Canine: Liver (DW) – normal 120-400 ppm; deficient < 80 ppm; toxic > 1,500 ppm.
**Several profiles were run throughout the 6-month duration of the illness. The most significant of these results are listed above.

Microscopic Description:
Liver: Diffusely, the normal hepatic architecture is replaced by numerous regenerative nodules that are up to 3.5 mm in diameter. Regenerative nodules are separated and surrounded by bridging tracts of fibrous connective tissue. Fibrous tracts contain a moderate proliferation of bile ducts and/or oval cells that are frequently mixed with individual or small clusters of hepatocytes. Small numbers of lymphocytes and plasma cells, few macrophages, and rare neutrophils are also multifocally scattered throughout fibrous tracts. Diffusely, there is marked loss of portal triads with few recognizable portal triads remaining within fibrous tracts. Bile canaliculi throughout the regenerative nodules are frequently expanded with bile. Multifocally, hepatocytes and Kupffer cells within nodules and fibrous tracts contain small to moderate amounts of yellow-gold to gold-brown pigment. Small to moderate numbers of hepatocytes within regenerative nodules and fibrous tracts exhibit macrovesicular vacuolation, characterized by single or small numbers of discrete, clear, intracytoplasmic vacuoles. Occasionally, portal veins and lymphatics are markedly dilated, and occasionally, sinusoids exhibit mild congestion.

HALLS BILE: Bile canaliculi, hepatocytes, and Kupffer cells within regenerative nodules and to a lesser extent fibrous tracts are often distended with bile pigment.

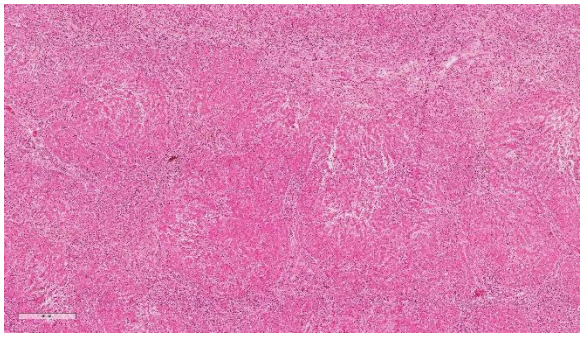

Liver, dog: At higher magnification, the parenchyma contains numerous regenerative nodules bounded by fibrous connective tissue. (HE, 70X)

RHODANINE: Frequently, hepatocytes and Kupffer cells within regenerative nodules and fibrous tracts contain small to moderate amounts of copper.

MASSON'S TRICHROME: Diffusely, delicate strands of collagen separate and surround individualized hepatocytes and hepatocyte clusters within fibrous tracts.
PRUSSIAN BLUE: Small numbers of Kupffer cells scattered throughout regenerative nodules and the fibrous tracts contain small to moderate amounts of iron pigment.

GOMORI'S RETICULIN: Diffusely, the normal lobular architecture is lost within both the regenerative nodules and the fibrous tracts. Reticulin fibers within the fibrous tracts are more numerous than the reticulin fibers within regenerative nodules and are also haphazardly arranged. Reticulin fibers within the fibrous tracts often separate and surround collagen bundles and dissect between or completely surround individual and small groups of hepatocytes and/or inflammatory cells.

Contributor's Morphologic Diagnosis:
Liver: Multifocal, widespread lobular dissecting hepatitis with marked fibrosis; mild, mixed inflammation; diffuse micronodular regeneration; moderate cholestasis; and occasional lymphatic ectasia

Contributor's Comment: The arrangement of the reticulin fibers within fibrous tracts indicates lobular dissection of the parenchyma. The lobular dissection and the proliferation of bile ducts within fibrous tracts is compatible with a diagnosis of lobular dissecting hepatitis, a form of cirrhosis most often seen in young adult dogs.[2,3,5,6] This form of chronic hepatitis has recently been reported in the American Cocker Spaniel.[3] Cocker Spaniels are at

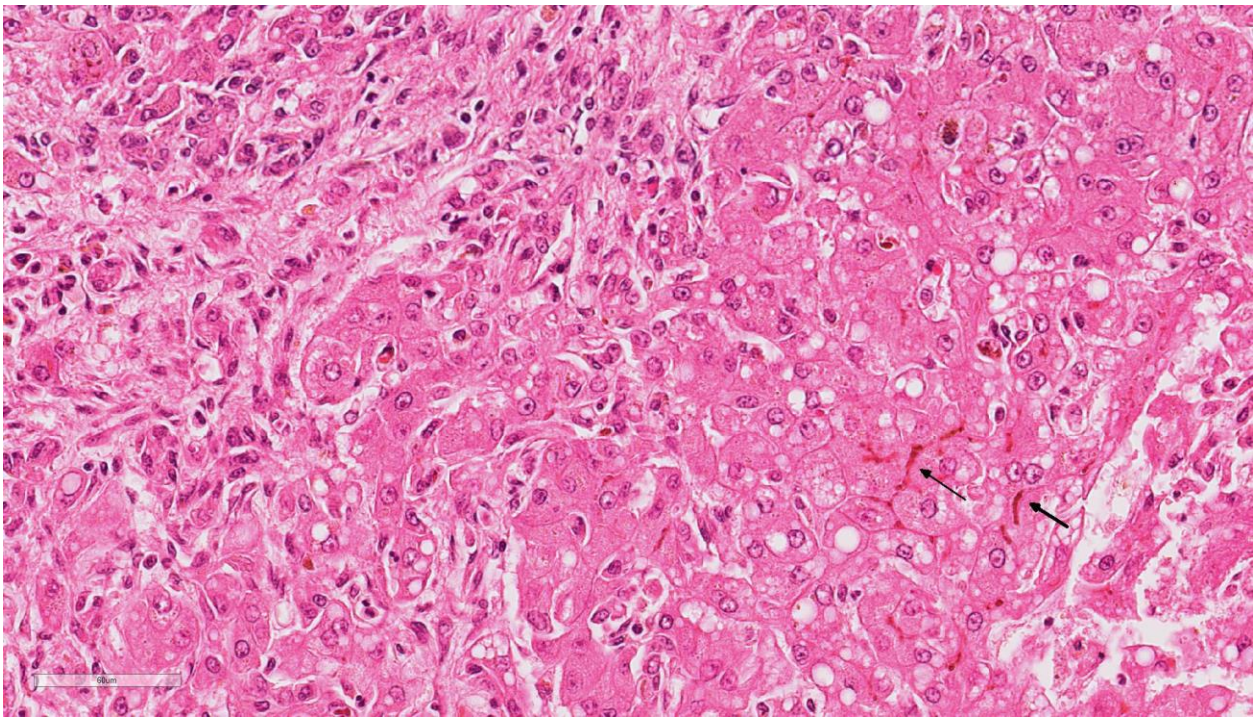

Liver, dog: High magnification demonstrates the extensive portal fibrosis and minimal inflammation at upper left, and adjacent dissection of small groups of hepatocytes. Small groups of dissected hepatocytes are often bordered directly by fibroblasts. There is cholestasis at the edge of the regenerative nodule (arrows). (HE, 400X)

increased risk for early onset chronic hepatitis that quickly becomes cirrhotic. Males are preferentially affected, and most of these dogs are diagnosed as young adults.[6] Disease is typically advanced at presentation, and most of these dogs lack signs of liver disease prior to the development of portal hypertension and ascites, the most common presenting sign.[3,6] Since disease is typically advanced at presentation, most dogs die within a few months of diagnosis.[6] In addition to cirrhosis, the condition is characterized by marked bile duct proliferation, a mild necroinflammatory response, and inconsistent copper retention.[2,3,5,6] Hepatic copper retention may occur as a primary injury or secondary to cholestasis. Since copper retention is inconsistent in this condition, most cases are attributed to cholestasis (which was prominent in this case).[2,6] The cause of chronic hepatitis in the Cocker Spaniel remains unknown. Because of the breed association, a genetic component has been postulated, and an α1-antitrypsin deficiency has been suggested, but remains unproven.[2,3,6]

JPC Diagnosis: Liver: Bridging fibrosis, diffuse, severe with marked micronodular hepatocellular regeneration, biliary hyperplasia, cholestasis, and diffuse hepatocellular lipidosis, Cocker spaniel (*Canis familiaris*), canine.

Conference Comment: Chronic hepatitis has frequently been reported in English and American Cocker Spaniels and English Springer Spaniels. Recently, American Cocker Spaniels have been reported to have lobular dissecting hepatitis, a distinct pattern of chronic hepatitis which has been most frequently identified in young dogs with ascites and acquired portosystemic shunts resulting from portal hypertension. Grossly, these two conditions have distinct differences. Chronic hepatitis and cirrhosis appears grossly as small, firm livers with multiple regenerative nodules, whereas, in lobular dissecting hepatitis, the liver is also small and pale with fewer hyperplastic nodules.[1]

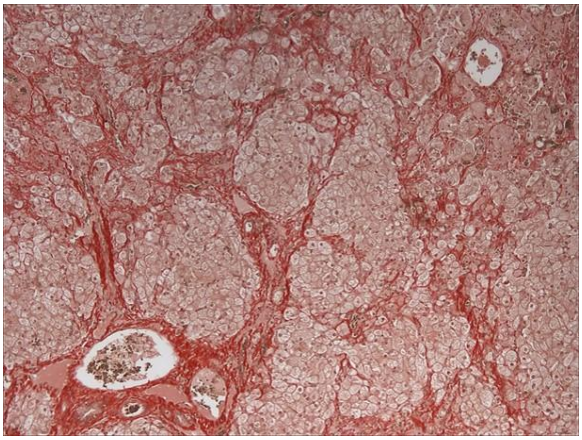

Liver, dog: A reticulin stain at low magnification demonstrates thick bands of reticulin fibers often following portal areas which divides the parenchyma into regenerative nodules. (Reticulin, 40X)

Microscopically, there is also variation in pattern between these two conditions. Chronic hepatitis is characterized by moderate to severe portal hepatitis with inflammatory infiltrates (lymphocytes, plasma cells and fewer neutrophils) and variable degrees of portal and bridging fibrosis. Lobular dissecting hepatitis, on the other hand, is characterized by dissection of hepatic parenchyma by reticulin and fine collagen fibers, subdividing individualized and small groups of hepatocytes. Fibroblasts, suspected of hepatic stellate origin, are prominent along sinusoids. Regenerative nodules may also be present, but not as consistently as with chronic hepatitis. In contrast with chronic hepatitis, portal inflammation and periportal fibrosis is not a prominent feature in lobular dissecting hepatitis.[1]

As mentioned by the contributor above, α1-antitrypsin deficiency has been suggested to

play a role in English Cocker Spaniels. α1-antitrypsin, a plasma glycoprotein, is a member of the serine proteinase inhibitor superfamily, and an inhibitor of neutrophil elastase. In humans, α1-antitrypsin deficiency leads to misfolded forms of α1-antitrypsin which accumulate in the rough endoplasmic reticulum of hepatocytes and form PAS-positive globules. The damage of hepatocytes resulting from accumulation of this protein has been associated with neonatal hepatitis, juvenile cirrhosis, and adult hepatocellular carcinoma in humans.[1]

A recent study of this condition identified the spindle cells producing reticulin and collagen fibers as myofibroblasts, as a result of their immunopositivity for anti-α-smooth muscle actin and anti-vimentin antibodies. Additionally, the reticular fibers produced by these cells were strongly positive for anti-collagen type III and type IV antibodies with positivity to anti-fibronectin and anti-laminin antibodies continuously along the basement membrane of the sinusoids of remaining hepatic cords and in between hepatocytes.

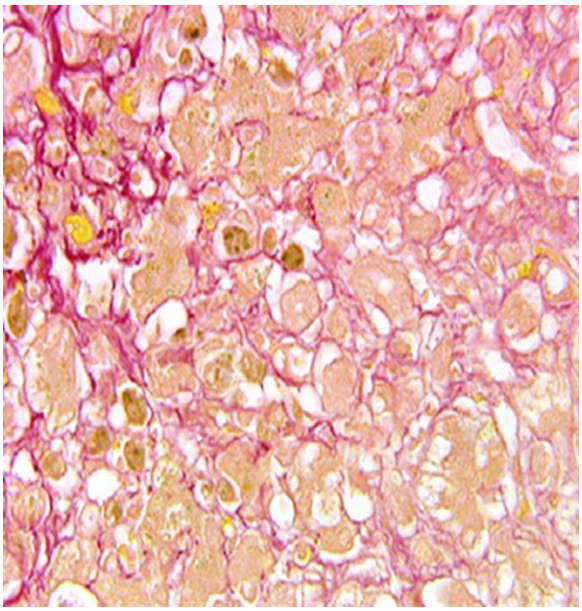

Liver, dog: A reticulin stain at high magnification demonstrates fibers often following surrounding individualized hepatocytes. (Reticulin, 400X)

This study also suggests that expression of fibronectin and laminin occurs before the deposition of reticulin between hepatocytes indicating an active extracellular matrix which contributes to the architectural damage.[4]

During the conference, the moderator reviewed patterns of cholestasis, observing that extrahepatic obstruction leads to circumferential fibrosis around bile ducts and biliary hyperplasia. The cholestasis in this case is likely due to fibrosis (intrahepatic obstruction) within the liver.

Conference attendees reviewed a case report[3] about American cocker spaniels with lobular dissecting hepatitis and noted that those dogs frequently have ascites that does not affect them as rapidly as other dogs with chronic hepatitis. Additionally, this report subdivides lobular dissecting hepatitis. According to this particular classification, the moderator believes that this particular casecase would fall in the subcategory of bridging fibrosis or micronodular cirrhosis. One unusual finding was the moderate amount of copper present in this case, whereas the dogs in the case study did not have any copper accumulation.

Contributing Institution:
http://www.aad.arkansas.gov/veterinary-diagnostic-lab

References:

1. Cullen JM, Stalker MJ. Liver and biliary system. In: Maxie MG, ed. *Jubb, Kennedy, and Palmer's Pathology of Domestic Animals.* Vol 2. 6th ed. St. Louis, MO: Elsevier; 2016:302-305.
2. Kahn CM, Line S, et al. *The Merck Veterinary Manual*. 10th ed. Whitehouse Station, NJ: Merck & Co., Inc.; 2010:423-428.
3. Kanemoto H, Sakai M, Sakamoto Y, Spee B, Van den Ingh TSGAM,

Schotanus BA, Ohno K, Rothuizen J. American cocker spaniel chronic hepatitis in Japan. *J Vet Intern Med*. 2013;27:1041-1048.
4. Mizooku H, Kagawa Y, Matsuda K, Okamoto M, Taniyama H. Histological and immunohistochemical evaluations of lobular dissecting hepatitis in American cocker spaniel dogs. *J Vet Med Sci.* 2013; 75(5):597-603.
5. Van den Ingh TSGAM, Van Winkle TJ, Cullen JM, et al. Morphological classification of parenchymal disorders of the canine and feline liver. In: Rodenhuis J, ed. *WSAVA Standards for Clinical and Histological Diagnosis of Canine and Feline Liver Diseases*. St. Louis, MO: Elsevier Saunders; 2006:94-98.
6. Willard MD. Inflammatory canine hepatic disease. In: Ettinger SJ, Feldman EC, eds. *Textbook of Veterinary Internal Medicine*. 7th ed. St. Louis, MO: Elsevier Saunders; 2010:1637-1642.

CASE III: 10621-16 (JPC 4101304).

Signalment: 15-year-old male neutered Domestic shorthair (*Felis catus*), feline.

History: Necropsy organ samples were submitted to the Diagnostic Laboratory from a euthanized cat with a history of emaciation, jaundice, and difficulty breathing.

Gross Pathology: None provided.
Laboratory Results (clinical pathology, microbiology, PCR, ELISA, etc.): None provided.
Microscopic Description:
In the lung, many of the alveoli are filled with solid sheets of small cells containing scant amounts of cytoplasm with round to oval nuclei. In some areas, there is marked anisokaryosis. Approximately six mitotic

Liver, cat: At low magnification, portal tracts are accentuated by a cellular infiltrate. (HE, 9X)

figures can be seen in ten high powered fields. Along with these neoplastic cells, there are numerous and scattered aggregates of lymphocytes and plasma cells. Numerous airways are partially filled with plugs of desquamated cells mixed with mucus and inflammatory cells. Marked alveolar emphysema is also observed in these sections.

In the liver, periportal areas are markedly expanded due to the presence of large numbers of a mixed population of leukocytes. Limiting plates of lobules are disrupted by this inflammatory infiltrate. Lymphocytes and plasma cells extend into adjacent sinusoids from the periportal areas. Additionally, there is disseminated cholangiolar hyperplasia. Surrounding numerous cholangioles, there is a marked scirrhous response. Some of the larger cholangioles are markedly undulating due to the hyperplastic change and contain a few neutrophils and desquamated epithelial cells in their lumens. A few small aggregates of macrophages containing small cytoplasmic lipid vacuoles are present near the areas of portal inflammation.

In the pancreas, multiple foci of nodular hyperplasia can be seen. These nodules are separated from normal pancreatic parenchyma by slender fibrous septae. Modest disorganization of exocrine pancreas

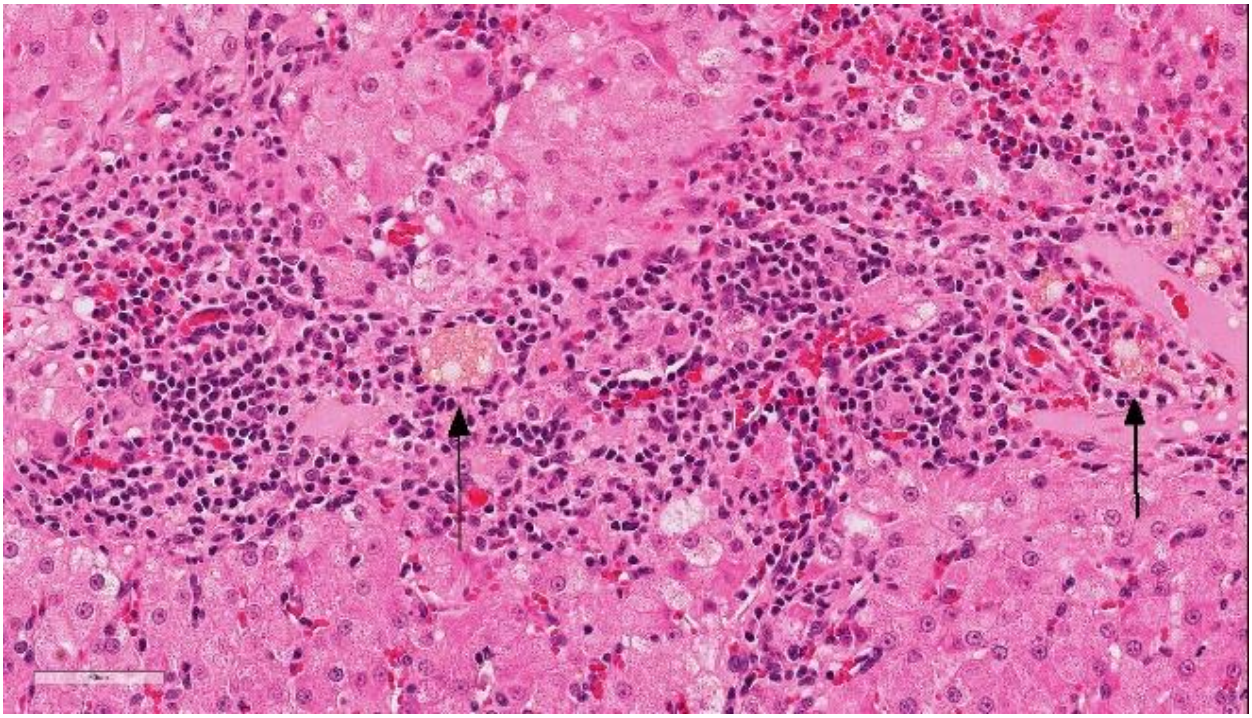

Liver, cat: Affected portal tracts display ductopenia as well as the formation of lipogranulomas. (HE, 315X)

is observed in these hyperplastic areas. There is moderate duct epithelial hyperplasia with small cystic formation in a major pancreatic duct. Occasional small lymphoplasmacytic aggregates can be seen in the interstitium of the pancreas and are sometimes associated with pancreatic islets.

Contributor's Morphologic Diagnosis:

1. Anaplastic small cell carcinoma – lung
2. Severe, chronic, lymphoplasmacytic, cholangitis
3. Marked multifocal nodular hyperplasia – pancreas
4. Mild multifocal lymphoplasmacytic pancreatitis

Contributor's Comment: While cholangitis is a relatively common set of liver diseases in cats[4,5] the overall prevalence is not well established as definitive diagnosis requires a biopsy and many cases are clinically unapparent during the early stages. In our case, the liver disease was identified coincidentally at necropsy as the cat was euthanized due to its lung cancer. This is a common finding as cholangitis does not typically result in mortality, but rather animals succumb to a concurrent disease process.[2]

Lymphocytic cholangitis in cats is a slowly progressive inflammatory lesion primarily of older animals that does not have a sex predisposition.[9] There have been a number of different pseudonyms used to describe the condition, although there is a proposal to standardize the classification scheme by the World Small Animal Veterinary Association (WSAVA) Liver Standardization group. Using their classification, the types of cholangitis can be subdivided into the following four groups: neutrophilic cholangitis, lymphocytic cholangitis, destructive cholangitis, and chronic cholangitis associated with liver fluke infestation.[8]

The most common type of cholangitis in cats is neutrophilic or suppurative cholangitis and the pathogenesis is through ascending bacterial biliary infections from the gastrointestinal tract.[5,8] These cases have portal neutrophilic infiltrates being the primary component during the acute infections and mixed infiltrates including lymphoplasmacytic infiltrates during the chronic stages. Secondary changes include biliary fibrosis and biliary hyperplasia, as well as a low risk of hepatic abscesses.[8]

Lymphocytic cholangitis is the second most common type of cholangitis, [8] although other studies have ranked it more prevalent than the neutrophilic variant.[4] An etiology has not been established for this condition, although it has been associated with inflammatory bowel disease and pancreatitis, suggesting that it may have an immune-mediated component. Clinically ,lymphocytic cholangitis tends to be slowly progressive without overt clinical signs during the initial development. Liver enzymes, although they may be elevated, are not directly correlated to the degree of inflammation.[2] Lesion severity is not uniform across all liver lobes. [2] Some cases can also histologically mimic hepatic lymphoma[8,9] although there are notable key differences which delineate these entities. These differences include bile duct targeting, ductopenia, peribiliary fibrosis, portal B-cell aggregates, and portal lipogranulomas, which are features that are associated with inflammatory rather than neoplastic infiltrates.[9]

Destructive cholangitis is typically reported in dogs rather than cats and is associated with drug reactions, biliary toxins, and some viral infections. Unlike neutrophils and lymphocytic cholangitis, this variant can cause severe cholestasis up to the point of bile obstruction.

Liver fluke infestation can cause chronic cholangitis is cats. These cases tend to have dilated bile ducts with fibrosis and papillary hyperplasia and pleocellular inflammation and can predispose to the eventual development of biliary carcinomas.[8]

JPC Diagnosis: 1. Liver: Cholangitis, lymphocytic, chronic, diffuse, severe, Domestic shorthair (*Felis catus*), feline.
2. Liver, bile duct: Cholangitis, neutrophilic, proliferative, focally extensive.

Conference Comment: Feline cholangitis is relatively common and presents in three different varieties: neutrophilic, lymphocytic, and chronic (due to liver flukes). A fourth variety, destructive cholangitis, is most common in dogs and briefly discussed by the contributor above. Microscopically, aside from the inflammatory cell population, they all have similar effects on the hepatic parenchyma: inflammatory infiltrates within portal regions and subsequent periportal to bridging fibrosis and bile duct or oval cell proliferation.

Clinically, these three have distinct presentations. Neutrophilic cholangitis is caused by bacterial cholecystitis, pancreatitis, and inflammatory bowel disease. These cats typically present with an acute history of lethargy, inappetence, pyrexia, and jaundice. Liver fluke infestations in cats is variable depending on the animal's environment, but they infrequently cause clinical disease and are usually incidental findings at necropsy.[1] The literature frequently associates chronic fluke infections with pancreatitis, however, a recent study conducted on cats on St. Kitts debunked that theory. They found that cats infected with *Platynosomum* sp. Rarely induces pancreatic damage in cats, and that any chronic pancreatitis present was subtle

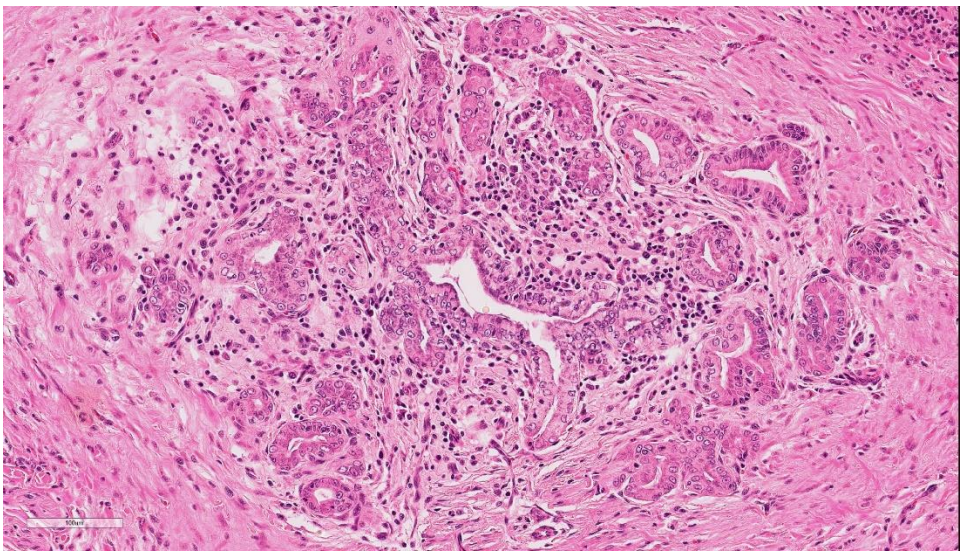

Liver, cat. The section contains a central focus of proliferating bile ducts with irregular cuboidal to columnar biliary epithelium, mild lymphocytic inflammation, and marked circumferential fibrosis. (HE, 215X)

and most likely not related to the pathogenesis of platynosomosis.[6]

Lymphocytic cholangitis in cats is a relatively new condition characterized by lymphocytic infiltrates within portal regions and a biliary response with hyperplasia and duct destruction. The pathogenesis is unclear, but an immune-mediated disease has been proposed. One study identified T-cells as the predominant cell type with fewer B-cells admixed (at times forming secondary follicles). This study did not recognize eubacteria (using FISH) which rules out chronic bacterial cholangitis as the cause. Additionally, in cats, where T-cell hepatic lymphoma is common, this study found five microscopic features that distinguish lymphocytic cholangitis from lymphoma: (1) bile duct targeting, (2) peribiliary fibrosis, (3) portal B-cell aggregates, and (4) portal lipogranulomas.[9] Additional diagnostics include T-cell receptor (TCR) clonality assays.[3] However, this test may not be as reliable as previously supposed, Warren et al.[9] found unanticipated results in which a portion of cases with lymphocytic cholangitis were clonal to oligoclonal as were their lymphoma cases. However, most (83%) lymphocytic cholangitis cases were polyclonal as expected.

Recent studies have sought to distinguish lymphocytic from neutrophilic cholangitis in cats with the least invasive modality. Unfortunately, ultrasonographic findings are identical for both conditions: diffuse liver and gallbladder hyperechogenicity and enlarged pancreas.[7]

During the conference, the moderator identified circumferential fibrosis around bile ducts which are disproportionately small and lined by irregular biliary epithelium. In addition, some sections (not all) contained a single aggregate of irregularly shaped bile ducts with degenerating epithelial cells and neutrophils (resulting in the second conference morphologic diagnosis above). As one of the potential causes of lymphocytic cholangitis is chronic neutrophilic cholangitis, the moderator speculated that this focus of atypical neutrophilic cholangitis might have been contributory to the overall condition. He further articulated that this focus does not appear neoplastic, and although there is a scirrhous response, the cells have normal organization and damaged biliary epithelium frequently produces that type of tissue response. Regarding the possibility of fluke infection in this case, the moderator stated that fluke lesions are large, often macroscopic, and result in marked

ductal fibrosis. Finally, he noted that it is important to rule out chronic neutrophilic cholangitis, a condition treatable with antibiotics, by culturing bile solids in these cases.

Contributing Institution:
Veterinary Diagnostic Center
School of Veterinary Medicine and Biomedical Sciences
University of Nebraska-Lincoln
http://vbms.unl.edu/nvdls

References:

1. Boland L, Beatty J. Feline cholangitis. *Vet Clin North Am Small Anim Pract.* 2017;47(3):703-724.
2. Callahan JE, Haddad JL, Brown DC, Morgan MJ, et al. Feline cholangitis: a necropsy study of 44 cats (1986-2008). *J Feline Med Surg*. 2011; 13:570-576.
3. Cullen JM, Stalker MJ. Liver and biliary system. In: Maxie MG, ed. *Jubb, Kennedy, and Palmer's Pathology of Domestic Animals.* Vol. 2. 6th ed. St. Louis, MO: Elsevier; 2016:308.
4. Gagne JM, Weiss DJ, Armstrong PJ. Histopathologic evaluation of feline inflammatory liver disease. *Vet Pathol.* 1996; 33:521-526.
5. Hirose N, Uchida K, Kanemoto H, Ohno K, Chambers JK, Nakayama H. A retrospective histopathological survey on canine and feline liver diseases at the University of Tokyo between 2006 and 2012. *J. Vet. Med. Sci*. 2014; 76(7):1015-1020.
6. Koster LS, Shell L, Ketzis J, Rajeev S, Illanes O. Diagnosis of pancreatic disease in feline platynosomosis. *J Feline Med Surg.* 2017;19(12):1192-1198.
7. Marolf AJ, Leach L, Gibbons DS, Bachand A, Twedt D. Ultrasonographic findings of feline cholangitis. *J Am Anim Hosp Assoc.* 2012; 48(1):36-42.
8. M van den Ingh TSGA, Cullen JM, Twedt DC, Van Winkle T, Desmet JV, Rothuizen J. Morphological classification of biliary disorders of canine and feline liver. In: Rothuizen J, Bunch SE, Charles JA, et al. eds. *WSAVA Standards for Clinical and Histological Diagnosis of Canine and Feline Liver Diseases*. Edinburgh, UK: Saunders Elsevier; 2006:61-76.
9. Warren A, Center S, McDonough S, Chiotti R, et al. Histopathologic features, immunophenotyping, clonality, and eubacterial fluorescence in situ hybridization in cats with lymphocytic cholangitis/cholangiohepatitis. *Vet Pathol.* 2011; 48(3):627-641.

CASE IV: 2012911922 (JPC 4032913).

Signalment: 11-year-old, female, spayed, Chihuahua (*Canis familiaris*), canine.

History: The dog was presented with a chief complaint of abdominal bloating. By abdominal ultrasonography, a large hepatic mass and hypoechoic lesion filling the peritoneal cavity were detected.

Gross Pathology: From surgical finding, the cystic mass originated from the hepatic left lateral lobe and filled the entire peritoneal cavity. The mass was the size of larger than 10 cm in diameters and was very soft and semitransparent milky to yellowish white mixed with blood. When made a cut in, a lot of mucus leaked, and the mass lost shape. The cut surface showed extensive myxomatous area. The site of liver attachment of the mass was harder and whiter than other area.
Laboratory Results (clinical pathology, microbiology, PCR, ELISA, etc.): None provided.
Microscopic Description:

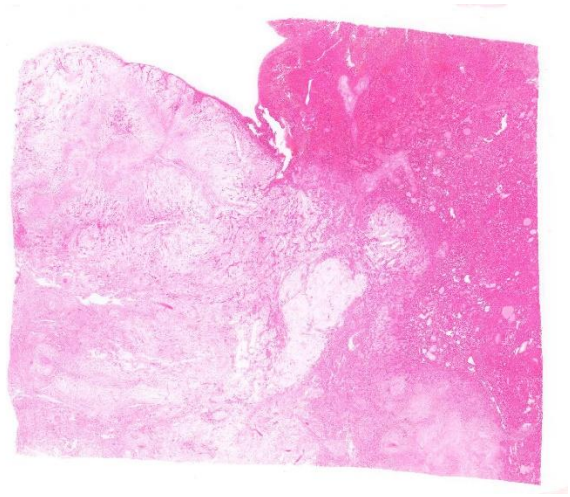

Liver, dog. Approximately 66% of the section of liver is effaced by a poorly cellular, markedly infiltrative neoplasm. (HE, 6X)

Spindle-shaped tumor cells chiefly proliferated in sheet or bundle with collagen fibers and mucinous matrix. Round or pleomorphic tumor cells also mingled with spindle-shaped tumor cells. The spindle-shaped tumor cells and collagen fiber were arranged in a concentric pattern in the perivascular areas. The tumor cells had round or oval nuclei of varying size with one or a few small to large distinct nucleoli. The cytoplasm of majority spindle shaped tumor cells was poor-marginated scant to abundant eosinophilic cytoplasm. Some pleomorphic to round tumor cells had several small or large vacuoles or a single giant vacuole like signet-ring-cell. Signet-ring shaped cells had usually thin cytoplasm compressed by a large vacuole and peripherally located nuclei. A few multinucleated tumor cells and large round cells were also observed. Mitotic figures were often seen. Hepatic cords and bile ducts were often remained between tumor cells within the mass, and the bile ducts were showed mild to moderate reactive hyperplasia. Mild hemorrhage and inflammatory cell infiltration were also seen. In the peripheral area of mass, thin spindle-shaped tumor cells proliferated with amounts of collagen fibers and invaded between hepatic cords.

On a Masson's trichrome stain, spindle-shaped tumor cells and collagen fibers were stained weak blue in contrast with dark blue at the edges of hepatic cords. However, vacuolated round tumor cells were unstained.

Immunohistochemically, spindle-shaped and vacuolated round tumor cells were strongly to moderately positive for vimentin. The spindle-shaped tumor cells were variably positive for alpha-smooth muscle actin. But all tumor cells were negative for desmin. Tumor cells of both types were intracellular strongly positive for laminin. The extracellular matrix was often weakly positive for vimentin, alpha-smooth muscle actin and laminin.

Contributor's Morphologic Diagnosis:
Liver: Ito cell tumor, malignant

Contributor's Comment: Mesenchymal tumors in liver are rare in human and animals. Hemangiosarcoma and leiomyosarcoma appear more commonly in animals.[7,12]

The normal liver tissue consists of four types of sinusoidal lining cells; endothelial, Kupffer, pit and hepatic stellate (Ito) cells.

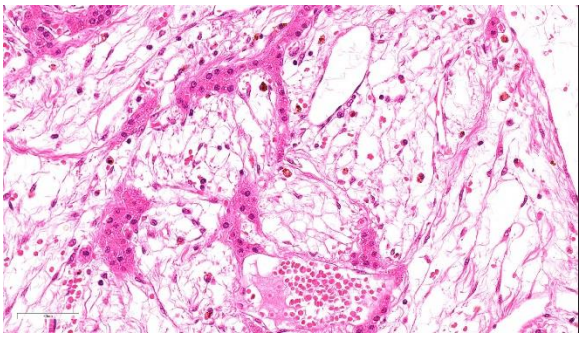

Liver, dog. The neoplasm is composed of widely-spaced spindle cells producing abundant mucinous ground substance. Neoplastic cells separated markedly atrophic cords of hepatocytes. (HE, 155X)

Stellate (Ito) cell also called perisinusoidal cell, vitamin A-storing cells, fat-storing cells, lipocytes, and interstitial cells. It is difficult to distinguish between each cell types by the routine light microscopy, so immuno-histochemical stains and ultrastructural analysis are helpful.

Stellate (Ito) cells contain lipid droplets in cytoplasm, store vitamin A in lipid droplets, and play a role in the storage and regulation of vitamin A.[8] These cells have also another major role to produce extracellular matrix proteins.[11] During the proliferating process, stellate (Ito) cells lost fat droplets and vitamin A with myofibroblast-like appearance, and produce great amounts of extracellular matrix.[8,11] In immunohistochemical stains, stellate (Ito) cells without fat droplets and vitamin A are positive for desmin and actin/alpha-smooth muscle actin. It supports to identify proliferating stellate (Ito) cells as cells have myofibroblastic function.[4,8,11]

Present tumor was consisted of two principal histological types of tumor cells: spindle-shaped and vacuolated round. Those tumor cells proliferate within remaining hepatic cords and bile ducts and invaded hepatic parenchyma, producing collagen fibers. It seemed that this tumor arose from the hepatic sinusoid.

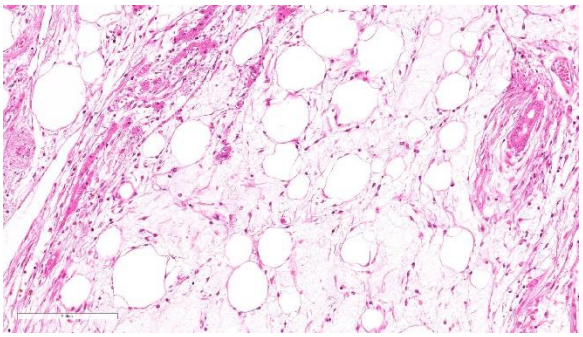

Liver, dog. Multifocally within the neoplasm, neoplastic cells are expanded by a large clear vacuole, resembling adipocytes. (HE, 350X)

Similar proliferative lesions have been reported rarely in animals[1,4,10,14,15] and humans.[13] These reports concluded or suggested stellate (Ito) cell origin from not only morphohistochemical features but also immunohistochemical and ultrastructural features.[1,4,10,15] Tumor cells in previous reports were immunoreactive for vimentin, desmin, α-smooth muscle actin, laminin,

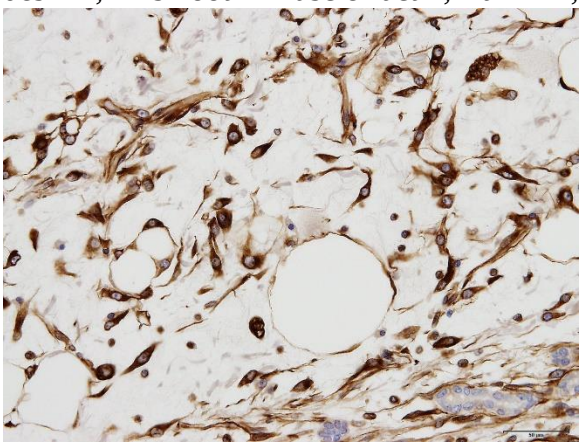

Liver, dog. Neoplastic cells exhibit strong cytoplasmic immunoreactivity for vimentin. Hepatocytes are negative. (anti-vimentin, 400X)

tenascin, and alpha B-crystallin. Tumor cells of present tumor show immunoreaction similar to previous reports with the exception desmin, suggesting that the present tumor originated from stellate (Ito) cells. Those previous reports suspected hepatic stellate (Ito) cell tumor was benign.[1,4,10,15] However, our present tumor had cellular atypia and many mitotic figures suggesting a malignant tumor.

Tumors suspected hepatic stellate (Ito) cell origin were diagnosed by use of various diagnostic term[1,4,10,13,15] because stellate cell had a lot of synonym. We diagnosed present tumor as malignant Ito cell tumor by references from the discussion of Stroebel P et al.[15]

Myxoid liposarcoma should be considered in the differential diagnosis.[17] Some tumor cells

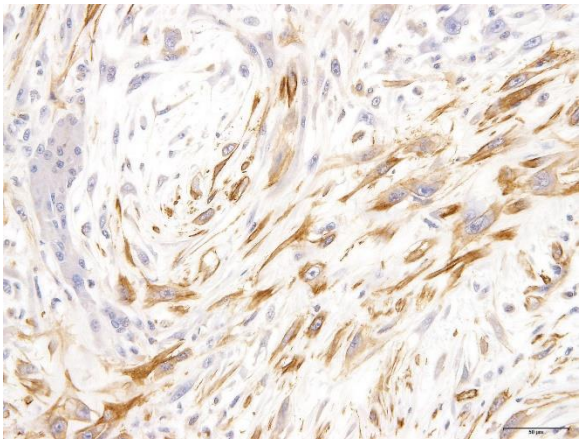

Liver, dog. Neoplastic cells exhibit moderately strong cytoplasmic immunoreactivity for smooth muscle actin. Unfortunately, the same stain run at the JPC was negative. (anti-smooth muscle actin, 350X)

of present case had small to large fat vacuoles in their cytoplasm. These tumor cells were suspended individually in a myxoid matrix similar to that seen in myxoid liposarcoma. However, the immunohistochemical profile including smooth muscle actin and laminin was different from our present case. Especially, laminin is a major compound of the hepatic extracellar matrix. In the repair processes of focal hepatic injury, laminin positive interstitial matrix are increased with Ito cells proliferation after infiltration of various inflammation cells.[12] Intra- and extra- cellular laminin expression were seen in the previous Ito cell origin tumors.[10,16] In addition, hepatic cords often remained in the tumor tissues. It seems that the tumor arise between hepatic cords and proliferated with separation of them. The histomorphologic and immunohistochemical characteristics supported that present tumor originated from Ito cells.

JPC Diagnosis: Liver: Sarcoma, poorly differentiated, with myxoid differentiation, Chihuahua (*Canis familiaris*), canine.

Conference Comment: Hepatic stellate (Ito) cells are remarkably diverse mesenchymal cells found between hepatocytes in the space of Disse and serve primarily as storage cells for lipid and vitamin A in large round vacuoles. The functionality of stellate cells does not end there, they also play a role in the following arenas: hepatic fibrosis, cytokine release, blood flow, and antigen presentation.[5]

When the liver is damaged, stellate cells become activated and take on a myofibroblastic phenotype, evidenced by the presence of immunohistochemically measurable α-smooth muscle actin, with concomitant loss of lipid vacuoles. In addition to the production of collagen and other extracellular matrix components (proteoglycans, fibronectin, and hyaluronin) activated stellate cells also release cytokines which are proinflammatory, profibrogenic, and promitotic.[5]

Stellate cells can affect sinusoidal blood flow by producing matrix and narrowing sinoisoidal lumina and by constriction of myofibroblastic stellate cells around endothelial cells. This act of constriction is induced by increased production of endothelin-1 by sinusoidal endothelial cells, which, in health, is balanced by vasodilation stimulated by nitric oxide also released by sinusoidal endothelial cells.[5]

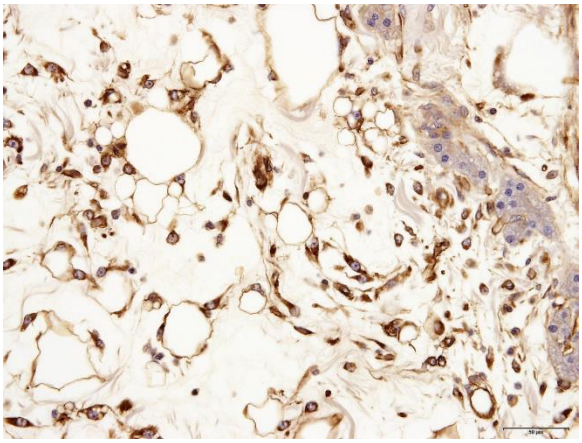

Liver, dog. Neoplastic cells exhibit strong cytoplasmic immunoreactivity for laminin. (anti-laminin, 400X)

Finally, stellate cells act as antigen-presenting cells in the liver much the same as Kupffer cells. In this realm, they mostly function to present lipid antigens to CD1-restricted T lymphocytes (like natural killer T-cells), but also present antigenic peptides to CD4+ and CD8+ T-cells with priming of CD8+ T-cells.[18]

Stellate (Ito) cell tumors are more common in mice than other domestic animals but are still rare.[3] Gross lesions are described as moderately firm, pale white nodules found within the liver parenchyma. Microscopically the nodules are composed of nodular aggregates of round to spindle cells that have dark oval nuclei and variably sized clear cytoplasmic vacuoles on a myxomatous matrix. These vacuoles are positive for oil red O and Sudan black staining, identifying them as lipid. Tumor cells are positive for vimentin, actin, desmin, and proliferating cell nuclear antigen. Additionally, the extra-cellular matrix stains positive for laminin and tenascin.[16] A key differential in rodents is Ito cell hyperplasia which is described associated with *Helicobacter* sp. infection and numerous other circumstances. The main difference is with hyperplasia there is usually concurrent Kupffer cell hyperplasia as well.[3]

The conference participants as well as the moderate (an internationally renowned hepatic specialist) had difficulty precisely diagnosing the neoplasm as well as identifying it as of Ito cell origin. The moderator first cited the gross findings which state that mucus leaked out of the mass when it was incised; in his experience, stellate cell tumors rarely have that much myxomatous material present. To further underscore the difficulty in attributing the origin to that of Ito cells, the moderator cited several articles. The first one discussed morphologic characterization of myofibroblastic cells in the liver – the portal myofibroblasts and stellate cells.[9] They found that desmin was

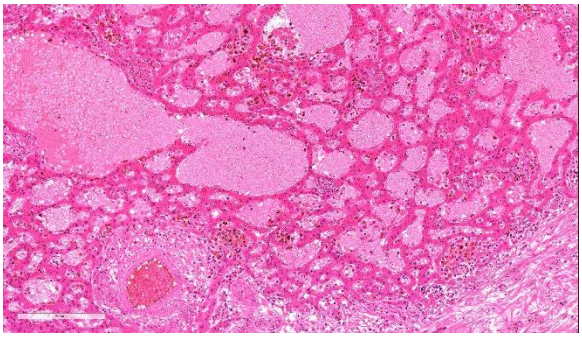

Liver, dog. There is marked sinusoidal dilation for at the periphery of the neoplasm as a result of markedly aberrant vascular flow and massive chronic congestion. (HE, 107X)

unreliable in differentiating between the two, but that stellate cells were generally negative for vimentin. This fact is in stark contrast with the present case, in which the neoplastic cells are vimentin-positive. Further, the moderator elaborated on the presence of abundant mucin grossly which he stated may be more representative of a hemangio-pericytoma, which like many types of mesenchymal neoplasma may demostrate a myxoid variant that is desmin negative (similar to this case).[2] Finally, mesenchymal hamartomas may have a similar appearance to this neoplasm with a loose stroma surrounding ducts. Mesenchymal hama-rtomas are developmental anomalies in the biliary system of horses and have also been reported in humans. Considering all facts, the moderator would prefer sarcoma (myxoid variant) rather than being specific about cell type.

In an effort to be as specific as possible, a battery of histochemical and immuno-histochemical stains were run including: Alcian blue, S-100, GFAP, smooth muscle actin, and desmin. The myxomatous matrix within the neoplasm is Alcian blue-positive but all other stains are negative. including smooth muscle actin, but which was positive for the contributor. In our stain, there is good internal control with strong intracytoplasmic

immunoreactivity of the smooth muscle cells in vessels and myoepithelial stellate cells within portal regions, but the neoplastic cells are diffusely negative. Furthermore, we consulted M.D. gastrointestinal pathology subspecialists who admittedly had not seen an Ito cell tumor and could find no report of such a neoplasm in the human literature. In their experience, this is consistent with a myxoid fibrosarcoma, but had poorly differentiated liposarcoma as a differential due to the presence of fat.

Contributing Institution:

Department of Pathology
Faculty of Pharmaceutical Sciences
Setsunan University
45-1 Nagaotohge-cho
Hirakata, Osaka 573-0101, Japan
http://www.setsunan.ac.jp/~p-byori/

References:

10. Adkison DL, Sundberg JP. "Lipomatous" hamartomas and choristomas in inbred laboratory mice. *Vet Pathol*. 1991;28: 305-312.
11. Avallone G, Helmbold P, Caniatti M, Stefanello D, Nayak RC, Roccabianca P. The spectrum of canine cutaneous perivascular wall tumors: morphologic, phenotypic, and clinical characterization. *Vet Pathol.* 2007;44(5):607-620.
12. Barthold SW, Griffey SM, Percy DH. Mouse. In: *Pathology of Laboratory Rodents and Rabbits.* 4th ed. Ames, IA: John Wiley & Sons, Inc.; 2016:101,114.
13. Carpino G, Morini S, Ginanni Corradini S, et al. Alpha-SMA expression in hepatic stellate cells and quantitative analysis of hepatic fibrosis in cirrhosis and in recurrent chronic hepatitis after liver transplantation. *Dig Liver Dis*. 2005;37: 349-356.
14. Cullen JM, Stalker MJ. Liver and biliary system. In: Maxie MG, ed. *Jubb, Kennedy, and Palmer's Pathology of Domestic Animals.* Vol. 2. 6th ed. St. Louis, MO: Elsevier; 2016:288-289.
15. Dixon D, Yoshitomi K, Boorman GA, et al. "Lipomatous" lesions of unknown cellular origin in the liver of B6C3F1 mice. *Vet Pathol*. 1994;31: 173-182.
16. Head K CJ, Dubielzig R, Else R, et al. *Histological Classification of Tumors of the American System of Domestic Animals*. 2nd ed. Vol. X. Washington, DC: Armed Forces Institute of Pathology in cooperation with the American Registry of Pathology and the Worldwide Reference on Comparative Oncology; 2003:119-133.
17. Higashi N, Sato M, Kojima N, et al. Vitamin A storage in hepatic stellate cells in the regenerating rat liver: with special reference to zonal heterogeneity. *Anat Rec A Discov Mol Cell Evol Biol*. 2005;286: 899-907.
18. Ijzer J, Roskams T, Molenbeek RF, Ultee T, et al. Morphological characterization of portal myofibroblasts and hepatic stellate cells in the normal dog liver. *Comparative Hepatology*. 2006; 5:7-15.
19. Mohr U. International classification of rodent tumors the mouse. Hannover: *WHO International Agency for Research on Cancer;* 2001: 76-77.
20. Nelson V, Fernandes NF, Woolf GM, et al. Primary liposarcoma of the liver: a case report and review of literature. *Arch Pathol Lab Med*. 2001; 125: 410-412.
21. Ogawa K, Suzuki J, Mukai H, et al. Sequential changes of extracellular matrix and proliferation of Ito cells with enhanced expression of desmin and actin in focal hepatic injury. *Am J Pathol*. 1986;125: 611-619.
22. Patnaik AK, Hurvitz AI, Lieberman PH. Canine hepatic neoplasms: a clinicopathologic study. *Vet Pathol*. 1980; 17: 553-564.
23. Shintaku M, Watanabe K. Mesenchymal hamartoma of the liver: a proliferative

lesion of possible hepatic stellate cell (Ito cell) origin. *Pathol Res Pract*. 2010; 206: 532-536.
24. Stroebel P, Mayer F, Zerban H, et al. Spongiotic pericytoma: a benign neoplasm deriving from the perisinusoidal (Ito) cells in rat liver. *Am J Pathol*. 1995;146: 903-913.
25. Tillmann T, Kamino K, Dasenbrock C, et al. Ito cell tumor: immunohistochemical investigations of a rare lesion in the liver of mice. *Toxicol Pathol*. 1999; 27: 364-369.
26. Weiss SW GJ. *Soft Tissue Tumors*. 5th ed. St. Louis, MO: Mosby; 2008: 477-516.
27. Winau F, Hegasy G, Weiskirchen R, Weber S, et al. Ito cells are liver-resident antigen-presenting cells for activating T cell responses. *Immunity*. 2007;26(1):9-10.

Self-Assessment - WSC 2017-2018 Conference 20

1. Which of the following is not useful in the diagnosis of carcinoid tumors?
    a. Positive staining for chromogranin A
    b. Positive staining with argentaffinic stains
    c. Positive staining for argyrophilic stains
    d. Metachromasia with Giemsa staining

2. Which of the following is defining characteristic of lobular dissecting hepatitis in the dog?
    a. Formation of regenerative nodules
    b. Presence of reticulin fibers around individual and small groups of hepatocytes
    c. α1-antitrypsin deficiency
    d. Cholestasis due to extrahepatic obstruction

3. Which of the following is usually the result of bacterial infection?
    a. Neutrophilic cholangitis
    b. Destructive cholangitis
    c. Chronic cholangitis
    d. Lymphocytic cholangitis

4. Which of the following is NOT associated with lymphocytic cholangitis?
    a. Portal T-cell aggregates
    b. Bile duct targeting
    c. Portal lipogranulomas
    d. Peribiliary fibrosis

5. Which of the following is not a documented function of Ito cells?
    a. Vitamin A storage
    b. Detoxification of xenobiotics
    c. Production of extracellular matrix proteins
    d. Myofibroblastic functions

Please email your completed assessment to Ms. Jessica Gold at Jessica.d.gold2.ctr@mail.mil for grading. Passing score is 80%.This program (RACE program number) is approved by the AAVSB RACE to offer a total of 0.5 CE Credits, with a maximum of 12.5 CE Credits being available to any individual Veterinary Medical Professionals for the 2017-2018 Wednesday Slide Conference. This RACE approval is for the subject matter categories of: SCIENTIFIC using the delivery method of NON-INTERACTIVE DISTANCE. This approval is valid in jurisdictions which recognize AAVSB RACE; however, participants are responsible for ascertaining each board's CE requirements.
RACE does not "accredit", "endorse" or "certify" any program or person, nor does RACE approval validate the content of the program.

Joint Pathology Center
Veterinary Pathology Services

WEDNESDAY SLIDE CONFERENCE 2017-2018

Conference 21

11 April 2018

Timothy K Cooper DVM, PhD, DACVP
Research Pathologist Charles River Laboratories
National Institute of Allergy and Infectious Diseases (NIAID) Integrated Research Facility
Division of Clinical Research
8200 Research Plaza - Fort Detrick
Frederick, MD 21702

CASE I: Case 1 G9312 (JPC 4085100).

Signalment: 6-year-old, male, mouse lemur (*Microcebus murinus*), non-human primate.

History: Within a captive, indoor housed colony of grey mouse lemurs (*Microcebus murinus*), a male intact, six-years-old animal presented with acute onset of clinical symptoms including hematuria, decreased general condition, weight loss, and inappetence. General examination revealed a poor body condition and blood-smeared coat in the genital region. Injuries were not detected. Therefore, an acute hemorrhagic cystitis was suspected. Therapy consisted of parenteral application of enrofloxacin, meloxicam, fluid therapy, as well as vitamins and supplementary food as supportive care. Two days after initial presentation, the lemur was found dead.

Gross Pathology: At necropsy, hemorrhages were found within different organs. Hemorrhages were most prominent within lung parenchyma and urinary bladder and less severe within renal pelvis and the subcutis. Furthermore, there was splenomegaly.

Thoracic viscera, mouse lemur. Sections of heart and lung are submitted for examination. At low magnification, thick cuffs of a cellular exudate surround pulmonary arteries. (HE, 4X)

Laboratory Results (clinical pathology, microbiology, PCR, ELISA, etc.):

Bacteriology: culture: negative

Virology: PCR for agents inducing respiratory disease (Influenza, Paramyxovirus, Human Metapneumovirus, Respiratory syncytial virus, Adenovirus): negative

Special stains used for histology: Ziehl-Neelsen stain for acid fast bacteria: negative; PAS reaction: negative; silver impregnation: negative

Microscopic Description:
The main histologic finding within the lung parenchyma was a severe granulomatous inflammation of small- and medium-sized arteries. The intima of affected vessels showed mild fibrinoid necrosis and proliferation. The tunica media and adventitia were heavily infiltrated with a mixed cellular infiltrate. Giant cells of foreign body and Langhans' type represent the dominant cell type. Eosinophilic cells were also present in high numbers. The lesions were accompanied by alveolar hemorrhage and histiocytosis. Comparable vascular alterations of milder degree were found within the kidneys. In the kidneys, giant cells were missing. Furthermore a mild lymphocytic interstitial myocarditis was found. Reactive extramedullary hematopoiesis was prominent within the spleen and with lesser extent within the liver.

Contributor's Morphologic Diagnosis:
Lung: vasculitis, chronic, granulomatous and eosinophilic, multifocal, severe, with prominent giant cell formation, alveolar histiocytosis and alveolar hemorrhage, idiopathic, non-human primate.

Contributor's Comment: A unique case of an idiopathic granulomatous generalized vasculitis in a mouse lemur is described. The cause of disease remains unclear. The most

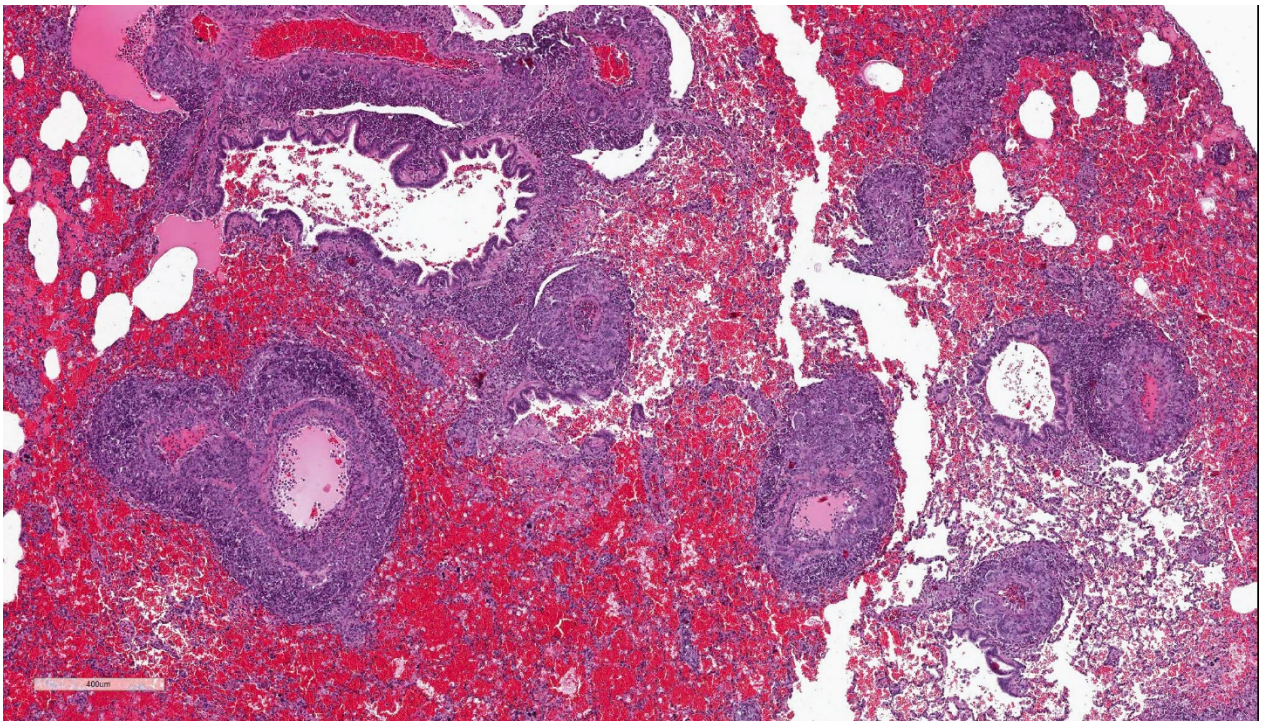

Lung, mouse lemur. A dense cellular infiltrate expands the adventitia of medium-sized arterioles. There is also expansion of bronchiolar-associated lymphoid tissue. Surrounding alveoli are filled with acute hemorrhage. (HE, 45X)

important infectious agents inducing granulomatous inflammation such as tuberculosis, leprosy, aspergillosis and leishmaniasis were ruled out histologically by special stains. No hints were found for a foreign body reaction or foreign body disease by histologic investigation. A drug induced vasculitis could be excluded because the animal did not receive drugs like propylthiouracil, methimazole, sulfasalazine, D-penicillamine, or minocycline capable to induce microscopic polyangitis. Therefore, an autoimmune or allergic disorder was suspected.

Several forms of idiopathic disseminated giant cell arteritis are recognized in humans and should be discussed as differential diagnosis for this case (Table 1). They mainly differ in their distribution, and a rough classification can be done according to the type of vessels involved. On this basis, arteritis temporalis (classic giant cell arteritis Horton) and Takayasu arteritis could be excluded in the present case because they mainly affect the aorta and other large-sized vessels. With the same argumentation polyarteritis nodosa (PAN), an idiopathic multisystemic necrotizing vasculitis, could be excluded too, because it mainly affects medium-sized vessels and rarely lung vasculature. The disease is well recognized in humans, and a PAN-like syndrome has been observed in a number of other species. In non-human primates, the disease is only described in cynomolgus monkeys (*Macaca fascicularis*).[1,6] The two case reports describe a necrotizing arteritis affecting vessels in the kidney, small intestine, colon, heart, spleen, mesentery, urinary bladder, and pancreas. The pulmonary vasculature was not involved. The lesions were segmental in distribution

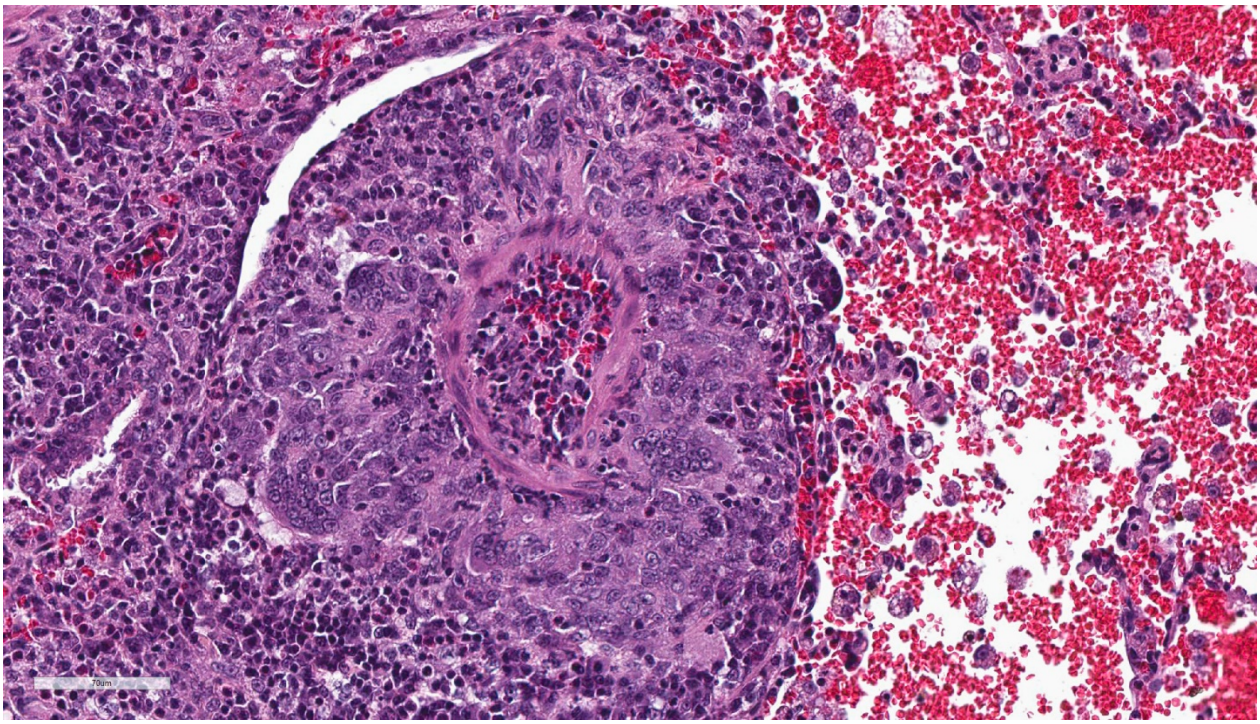

Lung, mouse lemur. At higher magnification, the adventitia of affected arteries is expanded and effaced by large numbers of epithelioid macrophages and fewer multinucleated giant cell macrophages, neutrophils, and eosinophils. Adjacent alveolar septa are hyperpcellular with increased numbers of activated intravascular macrophages and neutrophils. Hemorrhage is present within alveoli. (HE, 45X)

and of varying severity and stage of development. A transmural mixed inflammatory cell infiltrate was present, often accompanied by fibrinoid necrosis of the tunica media.[6] Main differences to the present case exist in the lack of giant cells and the amount of fibrinoid necrosis. For the given reasons, PAN was excluded as a diagnosis in the present case.

The eosinophilic nature of the lesions are indicative for another form of idiopathic vasculitis called eosinophilic granulomatosis with polyangitis or Churg-Strauss vasculitis. This is an autoimmune condition associated with asthma.[3] The clinical history of the diseased animal gives no evidence for a preexisting asthmatic syndrome. The inflammatory character of Churg-Strauss vasculitis is predominantly eosinophilic, whereas giant cells are more prominent in the present case. For these reasons, Churg-Strauss vasculitis was also excluded as a diagnosis in the present case.

The described lesion shows more similarities with the entity granulomatosis with polyangitis (GPA), previously known as Wegener granulomatosis. The disease is an idiopathic vasculitis of medium and small arteries of the respiratory tract with coexisting glomerulonephritis. As in the presented case, hematuria is a frequent finding. The main histologic criteria are presence of giant cells and fibrinoid necrosis of the vessel wall. GPA is generally characterized by anti-neutrophil cytoplasmic antibodies (ANCA).[8]

Nevertheless, the most probable diagnosis in this case is disseminated visceral giant cell arteritis, a giant cell arteritis of extracranial arteries and arterioles. Histologic similarities are the presence of giant cells, a mixed inflammatory infiltrate with eosinophils and less extend of fibrinoid necrosis of the vessel wall.[5]

The pathogenesis of all vasculitides discussed above is poorly understood and most likely involves immunopathogenic mechanisms. Most speculation centers on immune complex deposition, with subsequent activation of the complement cascade, neutrophil and monocyte chemotaxis, and the release of lysosomal enzymes, oxygen-free radicals, and proinflammatory mediators. Anti-neutrophil cytoplasmic antibodies (ANCA) have been identified in patients suffering from some forms of vasculitis. The identification of ANCA antibodies may help to discriminate among the different forms. In the present case, there was no possibility for further investigations. Therefore, the final diagnosis and pathogenesis remains speculative.

Table 1: Disseminated visceral giant cell arteritis, differential diagnoses.[5]

Pathologic entity	**Principle affected vessel**	**Giant cells**	**Fibrinoid necrosis**	**Eosinophilic infiltrates**	**ANCA**
Arteritis temporalis (Classic giant cell arteritis Horton)	cranial arteries occasionally large systemic arteries	+	±	±	
Takayasu arteritis	aorta and aortic arch branches	±	-	-	
Polyarteritis nodosa	medium sized and small arteries	±	+++	+++	negative

Eosinophilic granulomatosis with polyangitis (Churg-Strauss vasculitis)	extracranial small arteries and veins, perivascular tissue	+	+++	+++	positive
Granulomatosis with polyangiitis (Wegener granulomatosis)	small vessel of upper respiratory tract, lung, kidney	+++	+++	+++	positive c-ANCA
Disseminated visceral giant cell arteritis	extracranial small arteries and arterioles	+++	±	-	negative

Legend: -: absent; ±: occasionally present; +: usually present; +++: always present; (adapted from Lie, 1977)

JPC Diagnosis:

1. Lung, small and medium caliber pulmonary arteries: Arteritis, granulomatous, segmental, severe with diffuse, severe alveolar hemorrhage and edema, mouse lemur (*Microcebus murinus*), non-human primate.
2. Heart, aorta and coronary artery: Arteritis and periarteritis, granulomatous, segmental, moderate with multifocal aortic valvular endocarditis.
3. Heart: Myocardial degeneration and necrosis, multifocal, mild.

Conference Comment: In humans, there are two common vasculitides of medium to large vessels that can cause both peripheral and coronary artery disease: Takayasu's arteritis and giant-cell arteritis. Giant-cell arteritis typically affects older females (greater than 50 years old) and has two variants: cranial giant-cell arteritis and large-vessel giant-cell arteritis. Clinical signs for cranial giant-cell arteritis include headaches, scalp pain, jaw claudication, and loss of vision. Patients with large-vessel giant-cell arteritis generally suffer from aortic dissection or aneurysm, claudication of the limbs, myocardial ischemia, and acute aortic insufficiency.[4]

Ultrasound can raise suspicion of giant-cell arteritis by identifying the "halo sign" which represents diffuse edema of the vessel wall with adjacent normal vascular wall (known as "skip lesions"). Diagnosis is by temporal-artery biopsy, but this method can result in false-negatives for two reasons: (1) sampling of the "skip lesion" region or (2) the temporal artery is not involved. The latter is fairly common in large-vessel giant-cell arteritis, in which 40% of patients do not have temporal artery involvement.[4]

The most commonly recommended treatment for giant-cell arteritis in humans is glucocorticoids with many patients requiring long-term treatment to prevent worsening of the arteritis and eventually occlusion of large vessels.[4] New research has shown the efficacy of tocilizumab (an interleukin-6 receptor alpha inhibitor) in combination with glucocorticoids in sustaining disease remission in patients and avoiding the side effects of long-term glucocorticoid use.

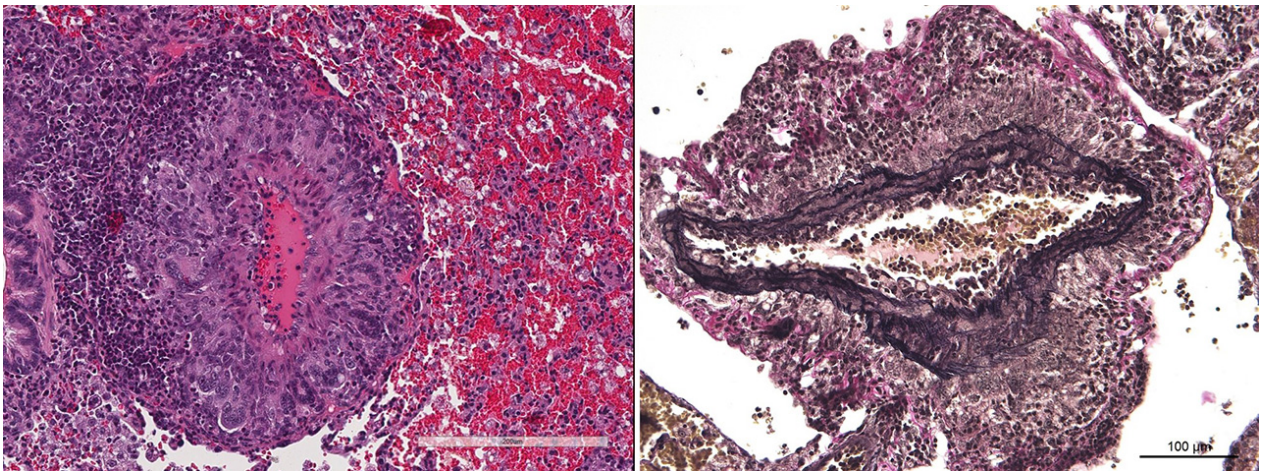

Lung, mouse lemur. Affected artery on left, with demonstration of the elastin network of the unaffected tunica intima and media on the right. The cellular infiltrate is present within the adventitia, indicating a periarteritis rather than a true arteritis. (HE and Movat pentachrome , 200X)

Elevated serum levels of interleukin-6 result in increased concentration of C-reactive protein and other acute phase proteins which correlate with disease severity. Tocilizumab, an interleukin-6 receptor alpha inhibitor, allows for reduced concentrations of glucocorticoids and decreased levels of acute phase proteins.[7]

There is significant variability between the submitted unstained slides and the digital slide provided to conference recipients. The moderator thought the only vessels affected were small and medium-sized pulmonary arteries because on the digital slide, the aorta and coronary arteries were not involved, but they were inflamed in our stained slide. Conference participants noted the recent article written about this case, which states that the aorta was unremarkable.[2] The moderator theorized that the article was written based on initial cuts from the block, and emphasized the segmental and stochastic nature of many vasculitides.

Two special stains were run, Verhoff van Giesson and Masson's trichrome. In the elastin stain, the tunica media of the medium pulmonary arteries generally has intact elastic lamina with smooth muscle cells in between. In the Masson's trichrome, surprisingly no fibrosis is identified within the tunica intima or media of affected arteries. In many arteries the lesions are more of a periarteritis because the tunica intima and media are largely spared. A discussion of the abundant acute hemorrhage in the alveoli included possible pulmonary hypertension leading to rupture of small alveolar capillaries. This condition is characterized by small arteries that exhibit medial hyperplasia and fibrosis, as well as pathognomonic plexiform lesions, and right ventricular hypertrophy, none of which were identifiable in this case.

In humans, the current vasculitis nosology (the Chapel Hill consensus) was revised in 2012[4] and is subdivided by: vessel type, characteristics of the infiltrate, and if the individual has ANCA antigen (anti-neutrophil cytoplasmic antibodies). The moderator believes the closest classification for the entity presented here is Wegener granulomatosis and Churg-Strauss vasculitis (see chart above), but that trying to pigeon hole this into a human classification may not

be useful. Certain features vary slide to slide, and the amount of fibrinoid vasculitis is a minor component in the slides examined.

Contributing Institution:
German Primate Center
Kellnerweg 4, 37077
Göttingen, Germany
www.dpz.eu

References:

1. Albassam MA, Lillie LE, Smith GS. Asymptomatic polyarteriitis in a cynomolgus monkey. *Lab Anim Sci* 1993;43**:** 628–629.
2. Cichon N, Lampe K, Bremmer F, Becker T, Matz-Rensing K. Unique case of granulomatous arteritis in a grey mouse lemur (*Microcebus murinus*) – first case description. *Primate Biology*. 2017; 4:71-75.
3. Cottin V, Cordier J-F. Churg-Strauss syndrome. *Allergy* 1999;4:535-551.
4. Kelly NP, Gerhard-Herman M, Desai AS, Miller AL, Loscalzo J. An unusual cause of leg pain. *New England Journal of Medicine*. 2017; 377(23): 2267-2272.
5. Lie J T. Disseminated visceral giant cell arteriitis. Histopathologic description and differentiation from other granulomatous vasculitides. *Am J Clin Pathol* 1978;69: 299-305.
6. Porter BF, Frost P, Hubbard GB. Polyarteriitis nodosa in a cynomolgus macaque (*Macaca fascicularis*). *Vet Pathol* 2003;40:570-503.
7. Stone JH, Tuckwell K, Dimonaco S, Klearman M, et al. Trial of Tocilizumab in giant-cell arteritis. *New England Journal of Medicine*. 2017; 377(15): 1493-1494.
8. Wojciechowska J, Krajewski W, Krajewski P, Kręcicki T. Granulomatosis with polyangiitis in otolaryngologist practice: A review of current knowledge. *Clinical and Experimental Otorhinolaryngology* 2016; 9: 8-13.

CASE II: F1755364 (JPC 4101079).

Signalment: 18-year-old, male, castrated, domestic shorthair (*Felis catus*), feline.

History: An 18-year old male castrated domestic short-haired cat presented acutely non-responsive to the emergency veterinarian. The cat had an approximately 1 year history of intermittent neurologic signs including ataxia, right-sided head tilt, paresis and paralysis, as well as progressive weight loss. Previous diagnoses included chronic kidney disease and systemic hypertension (180-220mmHg systolic). Fundic evaluation at a prior examination revealed microhemorrhages and partial retinal detachment. The cat was euthanized due to poor prognosis.

Gross Pathology: Extending from the left mid-thalamus caudally through the brainstem to the level of the obex is a poorly demarcated 4 x 1.5 x 1.0 cm region of hemorrhage with softening of the neural parenchyma (malacia) (Figure 1). Hemorrhage extends along the leptomeninges of the cerebellum, caudal cortex, and ventral brainstem. The ventral cervical and lumbar spinal cord has multifocal linear dark red foci on midline, centered on the ventral spinal artery.

Bilaterally, the kidneys are small (half normal size), pale, and firm, with diffusely pitted capsular surface that correlates with linear white streaks of fibrosis radiating from the medulla to the cortical surface.

Laboratory Results (clinical pathology, microbiology, PCR, ELISA, etc.):

Clinical Pathology: BUN 54 mG/dL (normal 18-35 mG/dL); Creatinine 3.6

Cerebellum and brainstem, cat: There is a large focus of acute hemorrhage and malacia within the brainstem extending from the thalamus to the obex. (HE, 5X) (Photo courtesy of: Colorado State University, , http://csu-cvmbs.colostate.edu/academics/mip/Pages/default.aspx)

mG/dL (normal 0.8-2.4 mG/dL); urine specific gravity: 1.015.

Microscopic Description:

Cerebellum/brainstem: Multifocal meningeal and parenchymal arteries and arterioles are segmentally to diffusely thickened by bright eosinophilic amorphous, hyalinized, and occasionally granular material admixed with rare mural karyorrhectic debris (hyaline degeneration to fibrinoid necrosis). Endothelial cells are often plump with large nuclei and open chromatin (reactive) or vacuolated (degeneration). Multifocal vessels within the ventral leptomeninges and central brainstem are disrupted and replaced by severe regionally extensive hemorrhage partially organized by fibrin strands. Hemorrhage focally effaces approximately 40% of the brainstem cross-sectional area and tracks along the leptomeninges. Neuropil abutting the regions of hemorrhage is moderately vacuolated with edema and infiltrated by minimally increased numbers of glial cells. Multifocal neurons contain finely granular golden brown cytoplasmic lipofuscin pigment. There is rare mild meningeal and choroidal mineralization.

Spinal cord (not shown): Elsewhere along the spinal cord there were several similar sites of hemorrhage, each associated with similar vascular changes as those previously described. Some of these sites were more subacute to chronic with deposits of hematoidin and a more developed parenchymal reaction.

Kidney (not shown): The capsule is bossellated with multifocal depressions that correspond to radiating regions of marked interstitial fibrosis which dissect, separate,

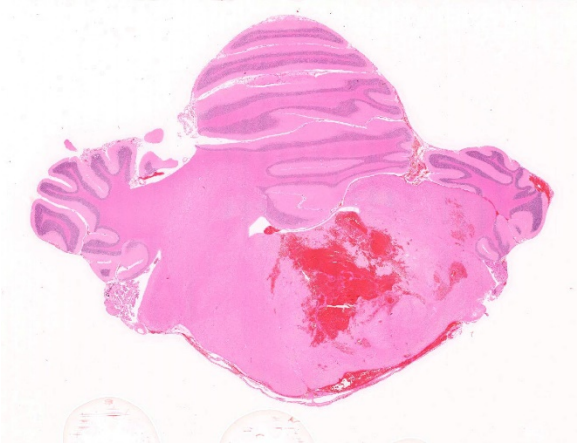

Cerebellum and brainstem, cat. Multiple areas of hemorrhage are present within the brainstem, and the adjacent meninges and 4th ventricle. (HE, 7X)

and replace approximately 40% of cortical tubules and glomeruli. Concentric perivascular, periglomerular, and peritubular fibrosis is frequent. High numbers of lymphocytes and plasma cells infiltrate the fibrous connective tissue. Glomeruli are often shrunken and sclerotic and Bowman's capsules are moderately to markedly thickened and occasionally lined by plump reactive parietal cells. Tubules have moderately to severely thickened basement membranes and exhibit one or more of the following changes: tubular ectasia lined by attenuated epithelium, swollen vacuolated epithelium (degeneration), plump slightly basophilic epithelial lining (regeneration), or rare individual necrotic epithelial cells with shrunken cell borders, hypereosinophilic cytoplasm, and pyknotic nuclei. Tubules often contain proteinaceous fluid, occasional mineral or rare refractile crystals.

Contributor's Morphologic Diagnosis:
Brainstem, cerebellum and spinal cord, arterioles: Severe chronic hyaline degeneration and fibrinoid necrosis with acute severe perivascular hemorrhage and necrosis (malacia).

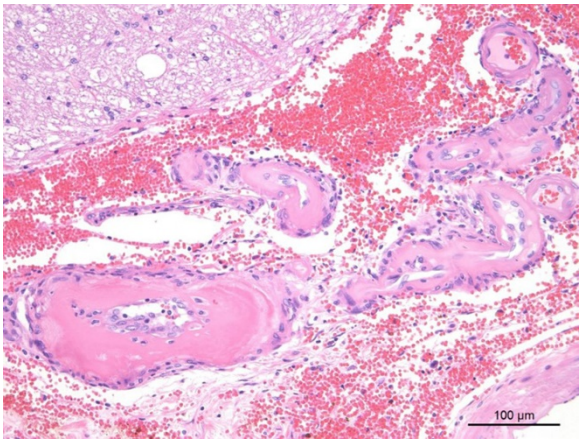

Brainstem, cat: High magnification image of the arterioles at the base of the brainstem. The arteriolar walls are diffusely replaced with collagen, which appears hyaline on HE. (HE, 400X)

Kidney (not shown): Severe chronic tubulointerstitial nephritis with marked interstitial fibrosis, glomerulosclerosis, and tubular proteinosis.

Contributor's Comment: Hyaline degeneration of arteries is a non-specific pathologic change that refers to loss of normal cellular structure and deposition of amorphous material of the intima and media of a muscular artery or arteriole. The hyalinized appearance is a result of deposition of plasma protein, amyloid deposits, and/or necrosis of vascular smooth muscle.[5] Hyaline degeneration can be

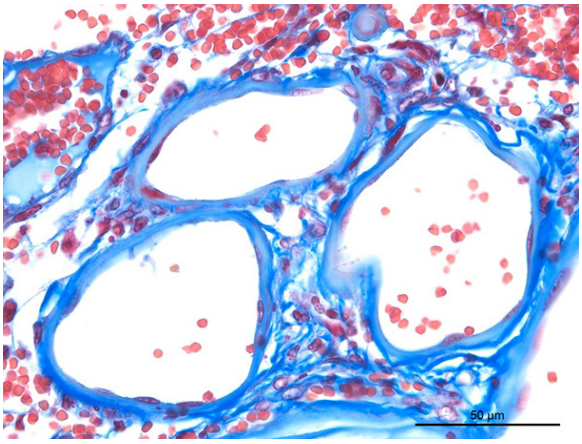

Brainstem, cat: A Masson's trichrome demonstrates the wall of affected arterioles are replaced by collagen, rather than protein. The arteriolar walls are diffusely replaced with collagen, which appears hyaline on HE. (HE, 400X)

associated with hypertension, uremia, diabetes mellitus, aging, hepatosis dietetica, organomercurial poisoning, mulberry heart disease, and cerebrospinal angiopathy/edema disease (among others).[4,5]

In this case, vascular changes are secondary to persistent hypertension (hypertensive vasculopathy) and chronic kidney disease. Other conditions that may result in secondary hypertension include: hyperthyroidism, diabetes mellitus, hyperaldosteronism, pheochromocytoma, chronic anemia (cats),

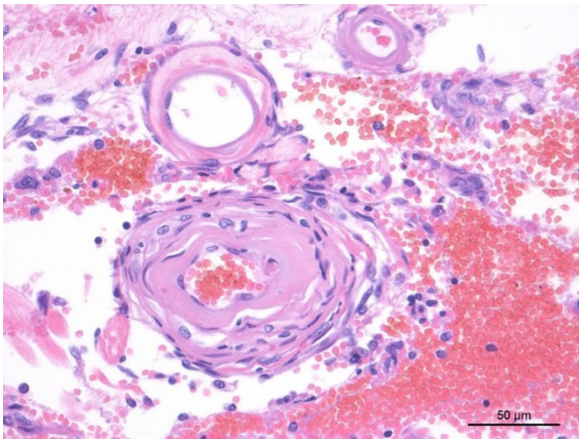

Brainstem, cat: In addition to collagen replacement of the arteriolar smooth muscles, there is whorling of fibroblasts with interspersed mature collagen around small arterioles. (HE, 400X)

hypothyroidism (dogs), erythropoietin therapy, and acute and chronic laminitis (cattle, horses).[5] Hypertension can also be essential (primary). Essential hypertension is characterized by an increase in total peripheral vascular resistance due to a primary decrease in lumen diameter and increase in media thickness.

Renal disease is a common cause of hypertension in dogs and cats and contributed to the systemic hypertension identified in this case. Renal disease can be both a cause and effect of hypertension, complicating the pathogenesis in individual cases. Chronic renal disease results in impaired sodium and water excretion and thus increased blood volume. Furthermore, a hypertension-induced decrease in renal perfusion activates the renin-angiotensin-aldosterone system, which also results in increased blood pressure. Impaired renal perfusion and progressive vascular injury further exacerbates chronic kidney disease.

A common clinical presentation of animals with hypertensive vasculopathy is acute blindness secondary to retinal arterial degeneration with associated retinal vascular tortuosity, intraocular hemorrhage, and retinal detachment (hypertensive retinopathy).[3] In cats and people a similar manifestation involving arteries of the central nervous system (hypertensive encephalopathy) has also been rarely described.[1] Under normal conditions the vascular tone of cerebral arteries and arterioles are tightly regulated to maintain constant and appropriate perfusion of the brain. When systemic blood pressure reaches the upper limit of the capacity of cerebral autoregulation, the cerebral arterioles segmentally constrict and dilate. The appropriate autoregulatory response is maintained in constricted regions. In dilated regions, however, vascular overdistension disrupts endothelial tight junctions, allows leakage of plasma proteins into the extracellular space (vasogenic edema), activates endothelial cells into increase expression of adhesion molecules (ICAM-1, PCAM-1) and cytokines (IL-1, IL-6, IL-8, TNF-α), induces neutrophil and monocyte adhesion and migration, and over time results in repetitive injury to the endothelium and vascular wall with subsequent vascular degeneration, necrosis and hemorrhage.[1,7] This case exhibits an end-stage response to chronic vascular damage as a result of persistent systemic hypertension. The intermittent nature of neurologic signs is consistent with repetitive small hemorrhages within the central nervous system and subsequent resolution. In fact, several other sites of more chronic hemorrhage were identified histologically in this cat's spinal cord. These had deposition of hematoidin and a more developed tissue reaction. A final massive hemorrhage within the brainstem ultimately yielded the patient non-responsive.

JPC Diagnosis: Brainstem, arteries: Hyaline vascular necrosis, multifocal, moderate with perivascular fibrosis, multifocal, severe, acute parenchymal and meningeal

hemorrhage, domestic shorthair (*Felis catus*), feline.

Conference Comment: There are three key terms regarding arterial degeneration to bear in mind: arteriosclerosis, atherosclerosis, and arteriolosclerosis.[2]

Arteriosclerosis (from the Greek, *arterio-* for artery and *-sclerosis* for hardening) is a chronic change consisting of: lumen narrowing, hardening, and loss of elasticity. Arteriosclerosis most commonly occurs in the abdominal aorta and points of arterial branching in older horses, ruminants, and carnivores secondary to a proliferative and degenerative change rather than inflammatory. A key feature is the lack of lipid deposition, which is a feature of atherosclerosis. The pathogenesis of plaque formation has not been fully explained but there are two main theories: (1) platelet microthrombi form in areas of turbulence or endothelial damage leading to release of platelet-derived growth factor (PDGF) and transforming growth factor-β, the former resulting in migration and proliferation of smooth muscle cells; and (2) the damage to the endothelium results in the endothelial cells themselves producing mitogens like PDGF. In reality, the pathogenesis is most likely a combination of the two. Microscopically, those mitogens cause migration of smooth muscle cells (or myointimal cells) from the media to the intima which act similarly to fibroblasts surrounding arteries by producing the matrix that forms the plaque composed of: collagen, elastic tissue, and proteoglycans.[6]

Atherosclerosis, which is characterized by the formation of an atheroma, a focal, raised, intimal fibrofatty plaque composed of cholesterol esters, is most common in humans and is only applicable to domestic animals in relation to animal models of

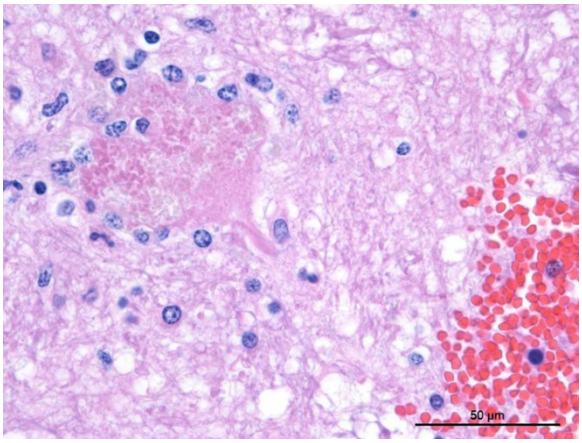

Brainstem, cat: Adjacent to an area of hemorrhage, a swollen, degenerating neuron is surrounded by astrocyte nuclei. (HE, 400X)

human disease. Some animals are susceptible to the formation of atheromas (rabbits, chickens, and pigs) and are thus, good animal models for research purposes. Dogs, cats, cattle, goats, and rats, on the other hand, are atheroresistant (with few exceptions, see below). In general, pigs and non-human primates are the most widely used large-animal models and variations of genetically modified mice are becoming available as well. Clinically, atherosclerosis in humans often results in myocardial infarction, stroke, and peripheral vascular resistance. More common in domestic animals are fatty streaks, another type of intimal lesion, which are often found in the aorta and larger arteries of ruminants and swine. These appear grossly as soft, smooth, flat lesions of varying sizes that are stained bright orange with Sudan IV. There is no known correlation of fatty streaks with the formation of atherosclerotic plaques. The cause of atherosclerosis is multifactorial and explained by the "response to injury" hypothesis which states that endothelial injury or dysfunction can result from hyperlipidemia (mainly cholesterol from low-density lipoprotein and very-low-density lipoprotein). The following steps (platelet adhesion and smooth muscle migration and proliferation) are the same as for

arteriosclerosis. As mentioned above, the key microscopic feature differentiating the two is the presence of lipid, which can be extracellular or intracellular (within activated macrophages or smooth muscle cells) called "foam cells". In fatty streaks, lipid in activated macrophages is most prevalent and in atherosclerosis, lipid in smooth muscle cells predominates. In pigs, atheromas most frequently form in the aorta and extramural coronary arteries, cerebral and iliac arteries. The main predisposing factor is a diet containing excess cholesterol and the plaques, unlike humans, rarely lead to fully occlusive thrombus formation. Dogs, although generally atheroresistant, can develop atherosclerosis secondary to hypercholesterolemia from hypothyroidism or diabetes mellitus. Additionally, Miniature Schnauzers have a genetic predisposition towards idiopathic hyperlipoproteinemia which often results in atherosclerosis. Microscopically, in dogs the lipid accumulates in the tunica media, whereas, in humans, it is present in the intima. As an aside, historically the term "xanthomatosis" has been used to describe this condition in animals. Current literature dictates that xanthomas are accumulation soft lipid-laden foam cells in the subcutaneous and cutaneous tissues only, and is a well-known condition in cats deficient in lipoprotein lipase.[6]

Finally, arteriolosclerosis describes a variable group of lesions in arterioles which may be predominantly hyaline or hyperplastic, both of which are initiated by endothelial damage. Hyalinosis or hypertrophic hyalinization is characterized by brightly eosinophilic, amorphous material which expands vessel walls, and results from leakage of plasma proteins. In domestic animals, hyalinosis is most frequently seen in older dogs, and pigs within splenic arterioles. Additionally, in dogs, hyaline deposition may affect the intramural coronary arteries, meningeal arteries, and cerebral arteries. In the heart, it can result in multifocal intramural myocardial infarction (MIMI) which leads to congestive heart failure when paired with valvular endocardiosis (commonly found in older dogs). In pigs, pathologic changes associated with hyaline arteriolar deposits occurs with organomercurial poisoning (meninges), edema disease (gastric and colonic submucosa and cerebellar folia), and hepatosis dietetica and mulberry heart disease (heart). Hyperplastic arteriolosclerosis, is characterized by intimal changes (smooth muscle proliferation and concentric fibrosis, AKA "onion skinning") with fibrinoid necrosis of the tunica media.[6]

In humans, the most common cause of arteriolosclerosis is systemic hypertension which can occur via primary or secondary means. In domestic animals, the most common cause of systemic hypertension is primary renal disease which is associated with primary or secondary hypertension. Primary systemic hypertension leads to decreased renal perfusion, subsequent activation of the renin-angiotensin-aldosterone system, and additional hypertension. Conversely, chronic renal disease can result in secondary hypertension by poor excretion of sodium and water and increased blood volume. One important and dangerous feature of hypertension is that it is self-perpetuating and can result in the death of the animal. The causes of hypertension and main clinical signs are described above by the contributor.[6]

In this case, side-by-side viewing of the affected arterioles on HE and with a Masson's trichrome deomonstrated the marked fibrosis of the vessel wall, which appeared as simple hyaline change on HE. The Masson's trichrome identified abundant collagen (type I or III) that has effaced the

tunica intima and media, smooth muscle cells. Additionally the Masson's trichome helped to demonstrate the perivascular whorling of fibrocytes around the adventitia of smaller arterioles, in an attempt to stabilize them against the systemic hypertension.

Contributing Institution:
Colorado State University
http://csu-cvmbs.colostate.edu/academics/mip/Pages/default.aspx

References:

9. Brown CA, Munday JS, Mathur S, Brown SA: Hypertensive Encephalopathy in Cats with Reduced Renal Function. *Vet Pathol.* 2005;42(5):642-649.
10. Fishbein MC, Fishbein GA. Arteriosclerosis: facts and fancy. *Cardiovasc Pathol.* 2015;24(6):335-342.
11. Maggio F, DeFrancesco TC, Atkins CE, Pizzirani S, Gilfer BC, Davidson MG: Ocular lesions associated with systemic hypertension in cats: 69 cases (1985-1998). *JAVMA*. 2000;217(5):695-702
12. Maxie MG, Youssef S: Nervous system. In: Maxie MG, ed. *Jubb, Kennedy, and Palmer's Pathology of Domestic Animals*. 5th ed., vol. 1. Elsevier Science Direct E-Books. 2007: 335–343.
13. Maxie MG, Robinson WF: Cardiovascular system. In: Maxie MG, ed. *Jubb, Kennedy, and Palmer's Pathology of Domestic Animals*. 5th ed., vol 3. Elsevier Science Direct E-Books. 2007: 56-93
14. Robinson WF, Robinson NA. Cardiovascular system. In: Maxie MG, ed. *Jubb, Kennedy, and Palmer's Pathology of Domestic Animals*. 6th ed. Vol. 3. St. Louis, MO: Elsevier; 2016:56-60.
15. Suzuki K, Masawa M, Takatama M. The pathogenesis of cerebrovascular lesions in hypertensive rats. *Med Electron Microsc*. 2001; 34(4):230-9.

CASE III: G071 (JPC 4100982).

Signalment: 4-week-old, female, outbred Hartley guinea pig (*Cavia porcellus*), guinea pig.

History: Experimentally infected with Ebola virus (guinea pig adapted Mayinga isolate) by intraperitoneal route 8 days prior to necropsy.

Gross Pathology: The animal was mildly dehydrated. The liver was pale and friable. Lungs were mottled and multifocally hemorrhagic. The gastrointestinal tract was filled with digested blood.

Laboratory Results (clinical pathology, microbiology, PCR, ELISA, etc.): None provided.

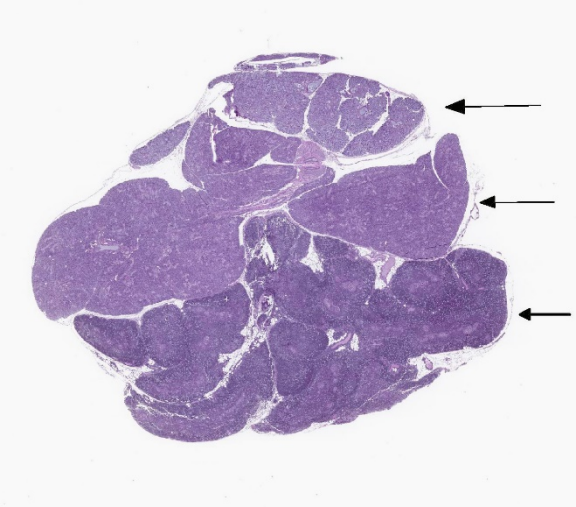

Salivary gland and thymus: *In the guinea pig, the cervical location of the thymus puts it in apposition with salivary glands (Sublingual salivary gland (top arrow), parotid salivary gland (middle arrow), thymus (bottom arrow). (HE, 6X)*

Microscopic Description: Slide contains sections of thymus and sublingual and parotid salivary glands. In the thymus, there is moderate diffuse lymphocytolysis with tingible body macrophages containing apoptotic cellular debris in the cortex and medulla, with blurring of the distinction between the two. Low numbers of macrophages with abundant vacuolated cytoplasm and small to large eosinophilic intracytoplasmic inclusion bodies are present in the medulla and occasionally cortex. Within the center of the Hassall's corpuscles, there is pyknotic nuclear dust admixed with viable and degenerate heterophils and cornified epithelial cells, with scattered rare coarse mineralized concretions (normal feature of this species).

Within the both salivary glands there are low numbers of individual necrotic ductal cells. There are scattered individual and small clusters of apoptotic and necrotic acinar cells with rare ICIB. There are low numbers of vacuolated and inclusion bearing macrophages and fibroblasts in the interacinar and periductal interstitium. Within several small and medium ducts in the parotid gland, there are karyomegalic ductal epithelial cells containing very large eosinophilic to amphophilic (owl's eye) intranuclear inclusions with a clear halo and peripheral margination of the chromatin (Cowdry type A). In both salivary glands there are several medium ducts that are mildly dilated and filled with wispy (sublingual) to homogenous (parotid) pale basophilic acellular material (inspissated saliva).

Contributor's Morphologic Diagnosis:

1. Thymus, lymphocytolysis, diffuse, moderate, with intrahistiocytic intracytoplasmic inclusion bodies
2. Salivary glands, parotid and sublingual, sialoadenitis, necrotizing and histiocytic, multifocal, acute, mild with intracytoplasmic inclusion bodies
3. Salivary gland, parotid, ductal epithelial cell karyomegaly, multifocal, mild with intranuclear inclusion bodies

Contributor's Comment: Ebola virus, a filovirus, is an important high consequence pathogen causing significant human disease outbreaks, most recently in West Africa from 2014 to 2016, and again in 2017. Guinea pigs remain an important model for infectious disease research, and have a number of unique anatomical features. The guinea pig thymus is located in the cervical region, and the pustule like appearance of the Hassall's corpuscles is normal for this species.[1] Lesions in the thymus are consistent with experimental manipulations.[4,5] Macrophages are a main target cell type of Ebola virus infection, with frequent (and often severe)

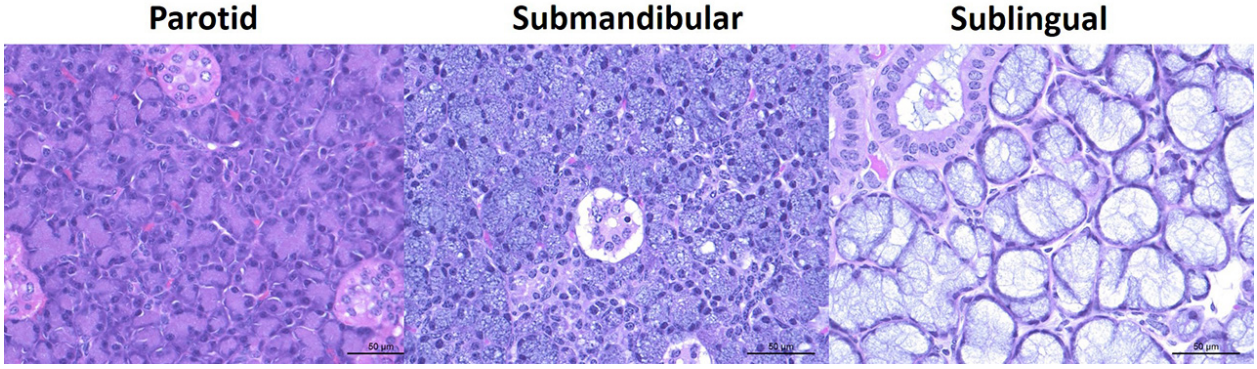

Salivary glands, guinea pig. Histologic differences in the salivary glands of the guinea pig. (HE, 315X)

bystander necrosis of lymphocytes. Ebola does not infect lymphocytes.[9,10] Lympho-cytolysis of the thymic cortex can be seen in a number of infectious disease processes, as well as corticosteroid administration or stress.

Lesions in the salivary glands represent two distinct processes, and are a mixture of experimental manipulation and adventitious spontaneous (background) infection. There is apoptosis and necrosis of ductal and acinar epithelial cells, with viral cytoplasmic inclusions present in acinar epithelial cells as well as interstitial fibroblasts and macro-phages. These lesions are consistent with experimental Ebola virus infection, and saliva may transmit the virus during acute infections. Saliva is also one of several fluids that may remain positive for the Ebola genome in convalescent human disease survivors, although virus generally cannot be isolated from the saliva.[2] Human disease transmission via semen from recovered individuals has been documented.[3]

Intranuclear inclusions in the parotid ductal epithelium are consistent with *caviid betaherpesvirus-2* (guinea pig cytomegalovirus).[1] In other species (rat, mouse), polyomavirus would be a differential etiology; guinea pigs have no described polyomavirus. *Caviid betaherpesvirus-2* is not excluded by the supplier of these animals, and CMV is typically an incidental finding in this species. Systemic disease can occur in pregnant or weaned pigs. There were no CMV type inclusions in any other organ sampled in this guinea pig, nor in any of the other pigs in this study.

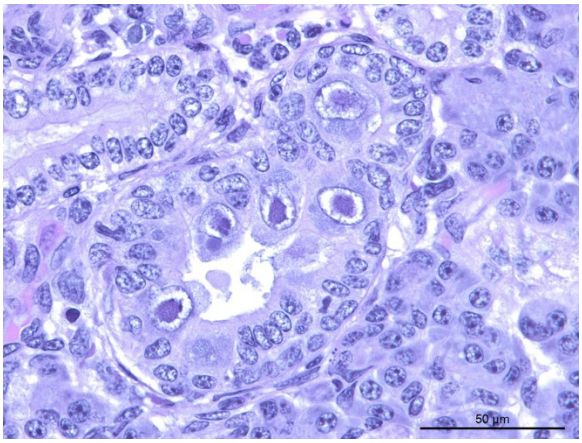

Salivary gland, guinea pig. Ductal epithelial nuclei are swollen by a large viral inclusion consistent with cytomegalovirus. (HE, 400X)

JPC Diagnosis:

1. Thymus, lymphocytes: Apoptosis, diffuse, moderate, with numerous tingible body macrophages, outbred Hartley guinea pig (*Cavia porcellus*), guinea pig.
2. Thymus & salivary gland, macrophages: Intracytoplasmic viral inclusions, occasional.
3. Salivary gland, glandular epithelium: Necrosis, multifocal, minimal to mild.
4. Salivary gland, ductal epithelium: Rare, intranuclear, karyomegalic viral inclusions.

Conference Comment: The family *Filoviridae* (negative-sense RNA viruses) has three genera: *Marburgvirus* (Marburg and Ravn viruses), *Ebolavirus* (Sudan virus, Ebola virus, Reston virus, Bundibugyo virus, and Tai Forest virus), and *Cuevavirus* (Lloviu virus). Filoviruses enter cells via macropinocytosis with subsequent binding to Niemann-Pick C1 (NPC1) receptor protein (a

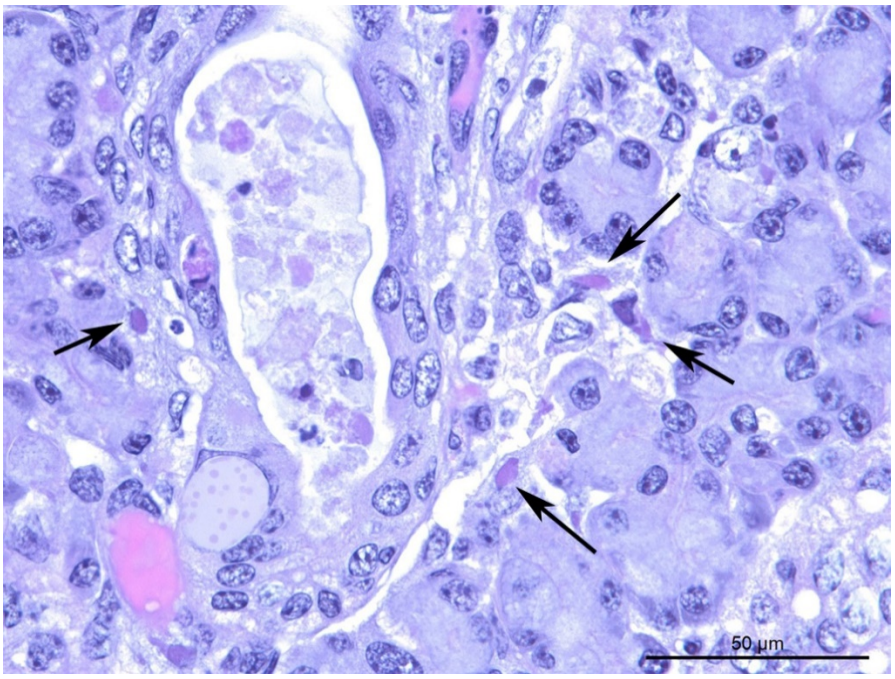

Salivary gland, guinea pig. Fibroblasts and macrophages within the salivary gland contain irregular eosinophilic viral inclusions consistent with filoviral inclusions (arrows). The duct contains necrotic cellular debris, likely from glandular necrosis

host cholesterol transport protein). Other cellular attachment molecules include: C-type lectins, phosphatidylserine, actin filaments, and cellular microtubules. Virus replication takes place in the cytoplasm and form prominent intracytoplasmic inclusion bodies. Viral maturation occurs via budding of preassembled nucleocapsids from the plasma membrane. As RNA viruses, Filoviruses mutate rapidly within infected individuals or reservoirs (different species of fruit bats).[7] The mutation rate has been calculated to be similar to seasonal influenza at 2.0 x 10^{-3} substitutions per site per year.[6]

Non-human primates (NHPs) are highly susceptible to filovirus infections with outbreaks reported in wild gorillas (*Gorilla gorilla*) and chimpanzees (genus *Pan*). The incubation period is about 3-6 days, followed by onset of clinical disease characterized by petechiae, ecchymoses, hemorrhagic pharyngitis, hematemesis, melena, and prostration. The pathogenesis of filovirus infections is similar in NHPs and humans but the clinical course of disease in NHPs is shorter and almost always ends in death. Mice and guinea pigs are not susceptible to field strains of Marburg virus or Ebola virus but rodent-adapted strains have been developed for vaccine and therapeutics testing.[8]

In experimentally infected NHPs, filoviruses replicate in macrophages, dendritic cells, and endothelium resulting in dissemination throughout the body and necrosis of various organs which is most flagrant in the liver. Infected monocytes, macrophages, and dendritic cells also release inflammatory mediators like tumor necrosis factor and interleukin-8, as well as, nitric oxide which effect vascular permeability and coagulation, and tissue factor from infected macrophages and monocytes. Additionally, loss of functional hepatocytes yields reduced synthesis of clotting factors and further aggravation of dysfunctional hemostasis dramatically ending with disseminated intravascular coagulation.[8]

Conference participants failed to recognize the eosinophilic intracytoplasmic viral inclusion bodies in macrophages and fibroblasts within the salivary gland. According to the moderator (who is also the contributor of this case), viral inclusions were seen in the glandular epithelial cells as well with immunohistochemistry; the saliva is also a way that this virus may be spread. ,potentially contributing to virus spread via

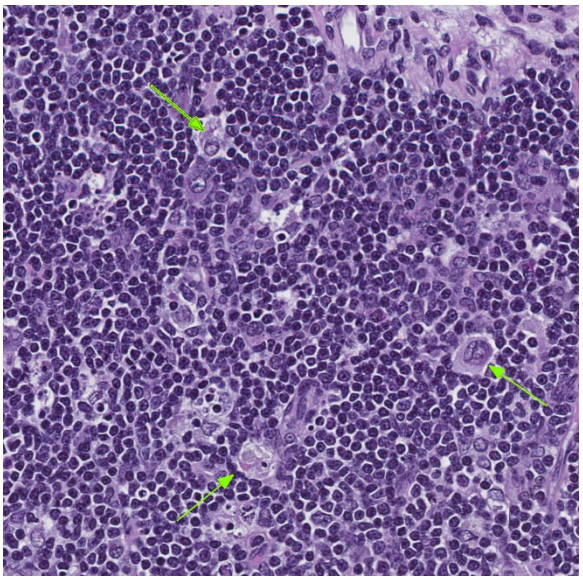

Thymus. Tingible body macrophages contain irregular cytoplasmic viral inclusions consistent with filoviral inclusion (arrows). There is an increased number of tingible body macrophages as a result of increased lymphocyte turnover. (HE, 400X)

saliva. Ebolavirus results in lymphocytolysis in the thymic cortex indirectly as "bystander necrosis". The main microscopic differential for this lesion is stress-induced lymphocytolysis.

Contributing Institution:
Pathology Department
NIH/NIAID
Integrated Research Facility
https://www.niaid.nih.gov/about/integrated-research-facility

References:

1. Barthold, S.W., S.M. Griffey, and D.H. Percy, *Guinea Pig*, in *Pathology of Laboratory Rodents and Rabbits*, S.W. Barthold, S.M. Griffey, and D.H. Percy, Editors. 2016, Wiley Blackwell: Ames, IA. p. 213-252.
2. Brainard, J., et al., *Presence and Persistence of Ebola or Marburg Virus in Patients and Survivors: A Rapid Systematic Review*. PLoS Negl Trop Dis, 2016. 10(2): p. e0004475.
3. Christie, A., et al., *Possible sexual transmission of Ebola virus - Liberia, 2015*. MMWR Morb Mortal Wkly Rep, 2015. 64(17): p. 479-81.
4. Connolly, B.M., et al., *Pathogenesis of experimental Ebola virus infection in guinea pigs*. J Infect Dis, 1999. 179 Suppl 1: p. S203-17.
5. Cross, R.W., et al., *Modeling the Disease Course of Zaire ebolavirus Infection in the Outbred Guinea Pig*. J Infect Dis, 2015. 212 Suppl 2: p. S305-15.
6. Jenkins GM, Rambaut A, Pybus OG, Holmes EC. Rates of molecular evolution in RNA viruses: A quantitative phylogenetic analysis. *Journal of Molecular Evolution*. 2002; 54(2): 156-165.
7. Klapper, CE. The development of the pharynx of the guinea pig with special emphasis on the morphogenesis of the thymus. *Am J Anat*. 1946;78:139-180.
8. MacLachlan NJ, Dubovi EJ. Filoviridae. In: *Fenner's Veterinary Virology*. 5th ed. San Diego, CA: Elsevier; 2017:373-380.
9. Prescott, J.B., et al., *Immunobiology of Ebola and Lassa virus infections*. Nat Rev Immunol, 2017. 17(3): p. 195-207.
10. Younan P, Iampietro M, Bukreyev A. Disabling of lymphocyte immune response by Ebola virus. *PLoS Pathog*. 2018;14(4):e1006932.

CASE IV: 16N-3473 (JPC 4101312).

Signalment: 6-month-old, female, Quarter horse (*Equus caballus*), equine.

History: This filly came from a farm at which two other horses reportedly had neurologic disease over the past five years. The patient was grade 4/5 ataxic. Cervical radiographs were unremarkable. She was down in the trailer and was unable to stand without assistance upon arrival to the

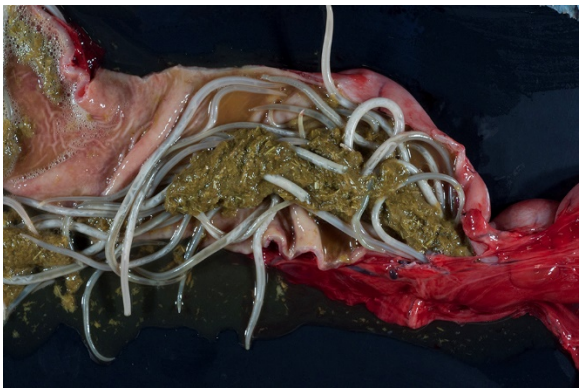

Small intestine, horse. Numerous adult ascarids (Parascaris equorum) were present within the small intestine of this individual. (Photo courtesy of: UC Davis School of Veterinary Medicine, http://www.vetmed.ucdavis.edu/index.cfm)

clinic. Neuroaxonal dystrophy was suspected. The animal was eventually euthanized due to the poor prognosis. Deworming and vaccination history were unknown.

Gross Pathology: Four 0.4- to 0.5-cm in diameter ulcers were present on squamous epithelium of the cardia. Hundreds of large robust nematodes consistent with *Parascaris equorum* filled the duodenum and jejunum. Approximately fifty slender elongate, white nematodes consistent with strongyle larvae were present in the large intestine, most notably in the right dorsal colon. The abdominal aorta at the level of the root of the cranial mesenteric artery was segmentally thickened. Other lesions were insignificant and/or were not relevant to the presenting complaints or the slide shown here.

Laboratory Results (clinical pathology, microbiology, PCR, ELISA, etc.): None provided.

Microscopic Description:
Aorta: The artery is asymmetrically thickened, and the intima is expanded and partially effaced by multifocal to coalescing necrosis, inflammation and multiple cross-sections of nematodes. The nematodes are covered by a superficial layer of fibrin with abundant erythrocytes neutrophils and small amounts of cellular debris. Endothelial cells are commonly plump and crowded along the affected surface. Endothelium is often absent in regions lined by the thrombus with adjacent nematodes. The nematodes are approximately 400 um in diameter with a smooth, glassy eosinophilic, 8.0-um-thick cuticle, platymyarian muscle, a pseudo-coelom, and a large central intestine lined by a few multinucleated cells with a bright-eosinophilic brush border. The reproductive tracts are not visible or are underdeveloped (consistent with larval forms). The adjacent internal elastic lamina appears disrupted and the nearby tunica media and adventitia are multifocally vacuolated and distorted with moderate to abundant numbers of infiltrating lymphocytes, plasma cells and neutrophils. This region also contains multifocal small areas of necrotic cellular debris and some scattered erythrocytes. Similar, small aggregates leucocytes are scattered throughout the adjoining adipose tissue. The adventitia of the smaller nearby arteries are occasionally cuffed by small numbers of lymphocytes and plasma cells.

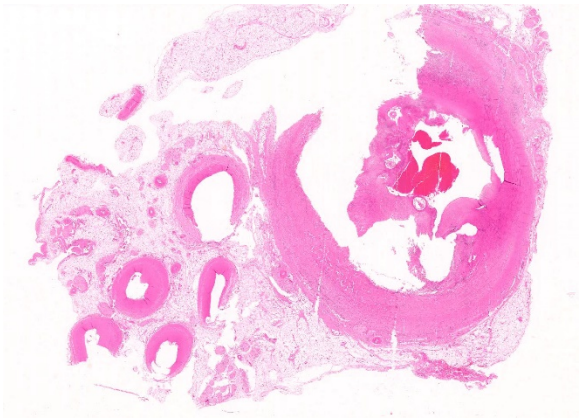

Muscular artery, horse. A cross-section of the cranial mesenteric artery contains a large fibrin thrombus and cross sections of larval nematodes in the lumen. (HE, 5X)

Contributor's Morphologic Diagnosis:
Aorta (at the junction of root of cranial mesenteric artery): Severe, multifocal to coalescing, neutrophilic, lymphoplasmacytic, endarteritis with luminal thrombosis and larval nematodes (presumed *Strongylus vulgaris* larvae)

Contributor's Comment: The lesions in the abdominal aorta at the junction with the cranial mesenteric artery described above are secondary to *Strongylus vulgaris* larvae invasion. Of the nematodes that affect horses, the small strongyle group, or cyathostomins, are found most commonly. However, *S. vulgaris* is the most important strongyle species affecting horses, as it causes the most damage to the host. *S. vulgaris* develops uniquely as it's the only strongylid that completes a stage of larval maturation in the arterial system of the horse. L3 larvae are ingested from contaminated fields and penetrate through the mucosa to the submucosa in the ventral colon or cecum. The larvae mature and molt to the L4 stage which invade the submucosal arterioles. L4 larvae migrate in or along the intima to the cranial mesenteric artery where they mature for the next 3 to 4 months until molting into the L5 stage. L4 larvae are unable to penetrate the internal elastic lamina and therefore cannot invade the media of vessels. Blood flow to the intestinal subserosal arteries transports the L5 larvae back to the subserosa of the cecum and colon where they are encapsulated forming nodules. When nodules rupture, adult worms return to the gut lumen where they become sexually mature in another 6 to 8 weeks.[6]

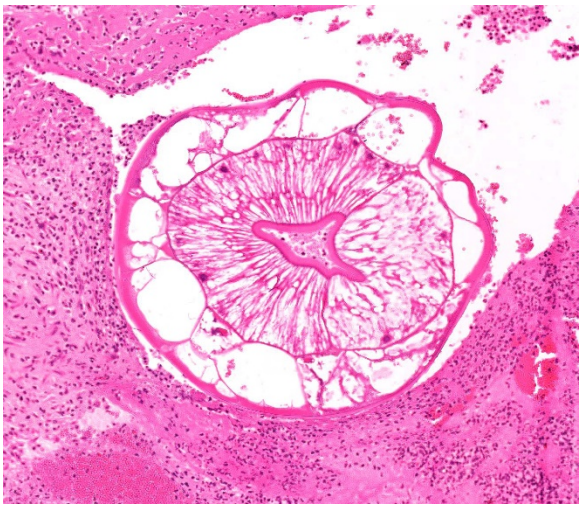

Muscular artery, horse. A cross section of a larval nematode (consistent with Strongylus vulgaris) is embedded in a fibrinocellular thrombus. The nematode has a thick cuticle, a pseudocoelom, platymyarian-coelomyarian musculature, and a large intestine with multinucleate columnar epithelial cells. (HE, 175X)

The cranial mesenteric artery and a communicating branch, the ileo-cecocolic artery, are the vessels most commonly affected by *S. vulgaris* migration. Lesions associated with *S. vulgaris* migration have also been identified in the aorta, the celiac artery and its branches, the renal arteries, and the spermatic vessels. Lesions range from common but incidental tortuous intimal tracks to uncommon occlusive thrombosis resulting in non-strangulating intestinal infarction leading to severe colic signs. Other possible outcomes of larval migration include thickening of mesenteric vessels leading to increased pressure on the abdominal autonomic plexi, which interferes with intestinal innervation. Toxins produced from degenerating larvae can also lead to signs of colic. Aberrant migration of *S. vulgaris* larvae can cause CNS signs, hind limb lameness, or even renal infarction.[6]

Characteristic histologic findings of *S. vulgaris*-induced endarteritis are present in the current case and include proliferation of the intima, adventitia and endothelium; associated fibrin deposition; regions of hemorrhage and necrosis within the vessel wall, and chronic ongoing inflammation of the intima associated with the nematodes. This case also exhibits area of internal elastic lamina disruption with subsequent thickening

of the media and associated inflammation. The nematode larval characteristics include a thick cuticle, platymyarian musculature, a pseudocoelom, prominent lateral cords, and an intestinal tract lined by only a few multinucleated cells with a prominent, bright-eosinophilic brush border.[4]

Broad-spectrum anthelmintics, primarily the macrocyclic lactones, have been used to control the effects of *S. vulgaris* on for approximately the last 50 years.[7] Nematode control has followed interval treatment regimens involving the frequent administration of anthelmintic products based on established times for the re-appearance of strongyle eggs in feces after treatment. This interval-based treatment has been successful in significantly reducing the prevalence of strongyle infections and the incidence of large strongyle-associated disease.[5] Anthelmintic drug resistance, however, has been an unfortunate side-effect of this type of therapy, and there are now several reports of resistance in stronglyes after ivermectin or moxidectin administration in numerous countries.[1,5,6,7]

Due to recent regulatory changes in Denmark, anthelmintics can only be acquired with a veterinarian prescription, and only after parasitological diagnosis.[4] Veterinarians in Denmark now have a more active role in regulating responsible anthelmintic drug use to reduce drug resistance. Regular interval-based treatment without attaining fecal egg counts is still commonly practiced in most countries, many of which are reporting anthelmintic drug resistance. Recently, there has been increased support for implementation of similar regulations in some of these countries.[6]

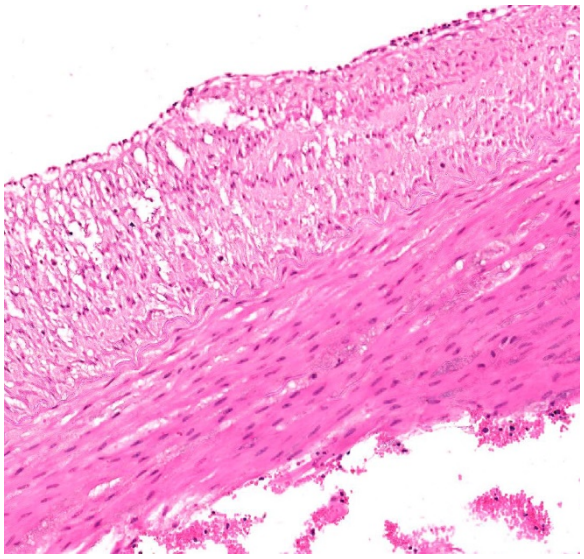

Muscular artery, horse. The tunica intima is thickened to 250um by fibrous connective tissue. (HE, 200X)

The presenting clinical signs in this horse were suggestive of neuroaxonal dystrophy (NAD), and lesions in the medulla oblongata and thoracolumbar regions found on postmortem histologic examination were consistent with NAD. Inflammation of the intestinal lamina propria as well as lymphadenopathy were secondary to infestation with *Parascaris equorum*, *S. vulgaris*, and small *Strongyles* in the small and large intestine.

JPC Diagnosis: Muscular artery: Arteritis, proliferative and necrotizing, transmural, chronic, severe with mural thrombosis and numerous larval strongyles, Quarter horse (*Equis caballus*), equine.

Conference Comment: Verminous arteritis is most often caused by larvae of the *Strongylus* and *Ascaris* genera.[6]

Table 1: Causes of verminous arteritis[3,6]

Nematode	Location	Species affected
Angiostrongylus vasorum	Pulmonary arteries	Dogs
Spirocerca lupi	Thoracic aorta; esophagus	Dogs
Dirofilaria immitis	Pulmonary arteries; right heart	Dogs
Strongylus vulgaris	Cranial mesenteric and ileo-cecocolic arteries	Horses
Oncocerca armillata	Aorta	Cattle, water buffaloes, goats, camels
Elaeophora poeli	Aorta	Cattle and related species
Elaeophora schneideri	Common carotid arteries	Mule deer, black-tailed deer
Elaeophora bohmi	Arteries and veins of the metacarpus, metatarsus, more distal extremities	Austrian horses
Crassicauda magna	Mesenteric and gastroepiploic arteries; thoracic and abdominal aorta	Cuvier's beaked whales (*Ziphius cavirostris*)[3]

Equine strongylosis is caused by members of the family *Strongylidae* which are common nematode parasites of the cecum and colon and often present in mixed infections. There are two subfamilies: *Strongylinae* (large strongyles – genera *Strongylus, Triodontophorus, Oesophagodontus,* and *Craterostomum*) and *Cyathostominae* (small strongyles). The large strongyles are plug feeders or blood suckers, of which *Strongylus* sp. undergoes extensive migration with wide-reaching effects. The small strongyles feed on intestinal contents and are mostly non-pathogenic in adults.[9]

Of the large strongyles, *Strongylus vulgaris* is the most significant. Larval forms cause endoarteritis in mesenteric vessels leading to arterial infarction of the large bowel and colic. Adult forms cause anemia and ill-thrift. The terms "endoarteritis" and "endarteritis" are often used interchangeably, however, endarteritis implies that end arteries are primarily affected.[6] Verminous endoarteritis is succinctly summarized by the contributor above. The other large strongyles, *S. edentatus and S. equinus,* rarely cause lesions. However, subserosal hemorrhagic plaques, termed hemomelasma ilei, are often attributed to trauma by migrating *S. edentatus* larvae but could be caused by any migrating strongyle.[9]

The cyathostomins, or small strongyles, are non-pathogenic as adults, but as larvae cause a clinical syndrome called larval cyathostominosis. This syndrome is caused by simultaneous emergence of larva from the deep mucosa or submucosa of the cecum and large colon. Emergence corresponds to the climate favorability for the parasites; hypobiosis or developmental inhibition occurs during cold or very hot months. It is only in late winter, spring, and early summer that encysted larvae emerge collectively to continue their development in the intestinal lumen.[9]

Conference participants viewed a Masson's trichrome and the remarkable amount of fibrosis and granulation tissue that effaces the muscular artery, as well as the intimal hyperplasia seen in the section. According to the moderator, the reviewed specimen is likely the cranial mesenteric artery because it is a muscular artery. The aorta, on the other

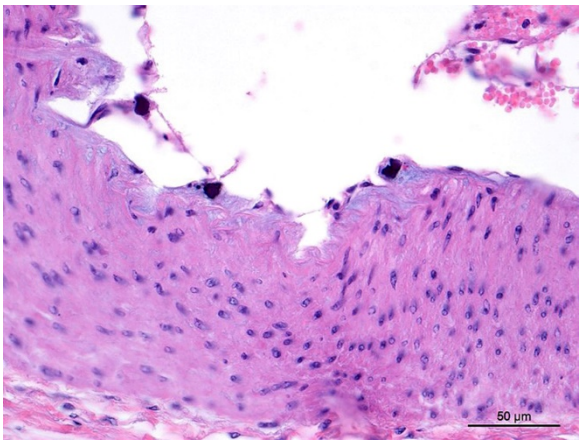

Muscular artery, horse. Asteroid bodies are common mineralized concretions in the intima of intestinal arteries of horses. (HE, 400X)

hand, is an elastic artery. Paucity of medial elastic lamina was demonstrated in this specimen using a Movat's pentachrome stain which highlights elastin. Additionally, the presence of intimal bodies along the endothelium was noted, a common finding in large arteries of horses.[2]

Contributing Institution:
UC Davis School of Veterinary Medicine
http://www.vetmed.ucdavis.edu/index.cfm

References:

1. Canever RJ, et al. Lack of Cyathostomin sp. reduction after anthelmintic treatment in horses in Brazil. *Veterinary Parasitology*. 2013; 194: 35-39.
2. de Oliveira AC, Rosenbruch M, Schulz LC. Intimal asteroid bodies in horses: light and electron microscopic observations. *Vet Pathol*. 1985;22(3):226-31.
3. Diaz-Delgado J, Fernandez A, Xuriach A, Sierra E, et al. Verminous arteritis due to *Crassicauda* sp. in Cuvier's beaked whales (*Ziphius cavirostris*). *Vet Pathol*. 2016;53(6):1233-1240.
4. Gardiner CH, Poynton SL. Strongyles. In: *An Atlas of Metazoan Parasites in Animal Tissues*. Washington, DC; Armed Forces Institute of Pathology. 2006: 22-24.
5. Matthews JB. Anthelmintic resistance in equine nematodes. *International Journal for Parasitology: Drugs and Drug Resistance*. 2014; 4: 310-315.
6. Robinson WF, Robinson NA. Cardiovascular system. In: Maxie MG, ed. *Jubb, Kennedy, and Palmer's Pathology of Domestic Animals*. Vol 3. 6th ed. St. Louis, MO: Elsevier; 2016:85-87.
7. Sallé G and Cabaret J. A survey on parasite management by equine veterinarians highlights the need for a regulation change. *Veterinary Record Open*. 2015: e000104.
8. Scott I., Bishop RM, and Pomroy WE. Anthelmintic resistance in equine helminth parasites–a growing issue for horse owners and veterinarians in New Zealand? *New Zealand Veterinary Journal*. 2015; 63: 188-198.
9. Uzal FA, Plattner BL, Hostetter JM. Alimentary system. In: Maxie MG, ed. *Jubb, Kennedy, and Palmer's Pathology of Domestic Animals*. Vol 3. 6th ed. St. Louis, MO: Elsevier; 2016:216-217.

Self-Assessment - WSC 2017-2018 Conference 21

1. Which of the following is NOT characterized by the presence of fibrinoid necrosis?
    a. Polyarteritis nodosa
    b. Arteritis temporalis
    c. Wegener granulomatosis
    d. Takayasu arteritis

2. Which of the following is defining characteristic of lobular dissecting hepatitis in the dog?
    a. Formation of regenerative nodules
    b. Presence of reticulin fibers around individual and small groups of hepatocytes
    c. α1-antitrypsin deficiency
    d. Cholestasis due to extrahepatic obstruction

3. Which of the following is usually the result of bacterial infection?
    a. Neutrophilic cholangitis
    b. Destructive cholangitis
    c. Chronic cholangitis
    d. Lymphocytic cholangitis

4. Which of the following is NOT a site of replication of filoviruses?
    a. Dendritic cells
    b. Endothelium
    c. Macrophages
    d. Lymphocytes

5. True or false. Large strongyle adults suck blood from the host.
    a. True
    b. False

Please email your completed assessment to Ms. Jessica Gold at Jessica.d.gold2.ctr@mail.mil for grading. Passing score is 80%.This program (RACE program number) is approved by the AAVSB RACE to offer a total of 0.5 CE Credits, with a maximum of 12.5 CE Credits being available to any individual Veterinary Medical Professionals for the 2017-2018 Wednesday Slide Conference. This RACE approval is for the subject matter categories of: SCIENTIFIC using the delivery method of NON-INTERACTIVE DISTANCE. This approval is valid in jurisdictions which recognize AAVSB RACE; however, participants are responsible for ascertaining each board's CE requirements.
RACE does not "accredit", "endorse" or "certify" any program or person, nor does RACE approval validate the content of the program.

Joint Pathology Center
Veterinary Pathology Services

WEDNESDAY SLIDE CONFERENCE 2017-2018

C o n f e r e n c e 22

18 April 2018

Amy Durham MS, VMD, DACVP
Associate Professor, Department of Pathobiology
University of Pennsylvania, School of Veterinary Medicine
MJR-VHUP, Room 4041
3900 Delancey Street,
Philadelphia, PA 19104

CASE I: 15L-2067C (JPC 4066542).

Signalment: 3-year-old, male, Warmblood (*Equus caballus*), equine.

History: Acute signs of colic, poor general condition

Gross Pathology: Diffuse thickening and white discoloration of the caudal 2/3 of the small intestine, evident from the serosal surface.

Laboratory Results (clinical pathology, microbiology, PCR, ELISA, etc.):

- CD3: Diffusely well-differentiated small lymphocytes show moderate to strong immunopositivity for CD3. Large blastic cells show diffuse moderate membranous positive signal for CD3. CD3 positive cells represent >95% of the lymphoid cells recognized.
- CD79a: Scattered very rare small well-differentiated lymphocytes are positive for CD79a antibody. Large blastic cells are negative. CD79a positive cells represent <5% of the lymphoid cells recognized.
- CD20: Large blastic cells are diffusely negative for CD20 antibody. CD20 positive cells represent <5% of the lymphoid cells recognized.

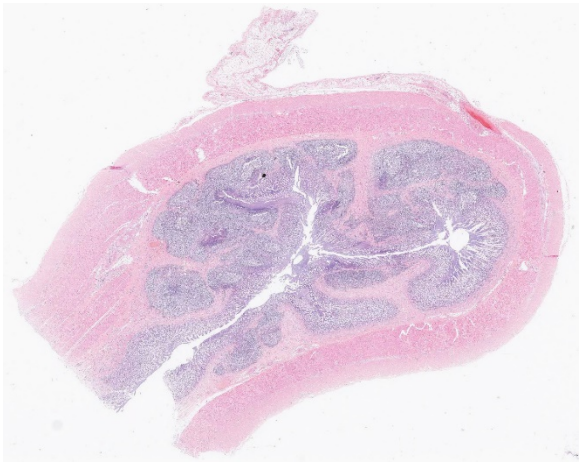

Ileum, horse. A neoplastic infiltrate extends from the Peyer's patches into the surrounding mucosa and submucosa. (HE, 4X)

- Synaptophysin: An intense strong cytoplasmic positive stain is detected in the scattered remaining neurons of the Auerbach's and Meissner's plexuses

Microscopic Description:
Ileum – The intestinal epithelium is diffusely effaced by amorphous eosinophilc material and nuclear debris (post mortem autolysis – artifact). Multifocally, some crypts are expanded by eosinophilic and basophilic amorphous material (cellular and nuclear debris/crypt abscesses) with occasional areas characterized by granular basophilic material (mineralization – dystrophic). The autonomic ganglia of the submucosa (Meissner's) and tunica muscularis (Auerbach's) exhibited a marked reduction in numbers of neuronal bodies which occasionally appear hyper-eosinophilic with rounded cell margins and peripheralized hyperchromatic nuclei (chromatolysis). Within the plexuses an increased number of satellite cells is also recognized. Expanding from the submucosal gut associated lymphoid tissue (GALT), and diffusely infiltrating and effacing the mucosa, submucosa and occasionally reaching the superficial tunica muscularis of the ileum there is a densely cellular, poorly demarcated, unencapsulated and infiltrative proliferation of round cells arranged in sheets within a fine fibrous stroma. Cells are 20-25 μm in diameter, round with distinct cell borders. They exhibit scant to moderate lightly basophilic cytoplasm and central round nuclei with finely stippled to vesicular chromatin and one to three nucleoli. The follicular structure of GALT is diffusely effaced or lost. Mitotic index is 1-4 mitosis per high power field and occasional bizarre mitoses are recognized. Large numbers of small well-differentiated lymphocytes are infiltrating in between the atypical blastic cells. Large numbers of atypical lymphoid cells are found infiltrating lymphatic vessels and/or veins of the lamina propria,

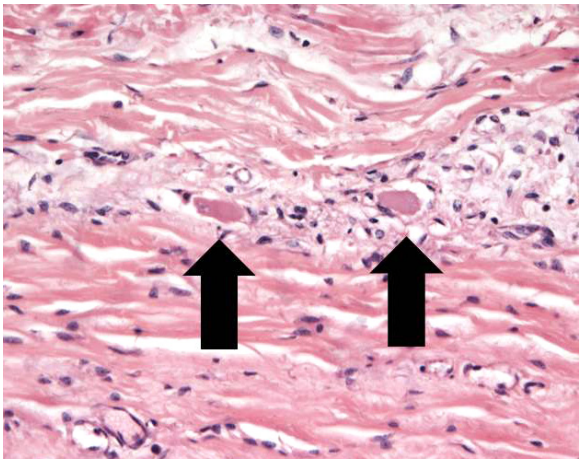

Ileum, horse. There is a significant reduction of numbers of neurons within the Auerbach's and myenteric plexi. Remaining neurons exhibit chromatolysis. (HE, 400X) (Photo courtesy of: of Liverpool, Leahurst Campus, Chester High Road, Neston, Wirral, UK, CH64 7TE.)

submucosa, muscularis and serosa. Scattered basophilic, star-shaped bodies (mineralization – asteroid bodies) are recognized within the intima of medium sized to large submucosal arteries (incidental finding).

Contributor's Morphologic Diagnosis:
Ileum, diffuse sub-acute severe Meissner's and Auerbach's plexuses chromatolysis and neuron loss.
Ileum, atypical lymphoproliferative disorder consistent with intestinal lymphoma.
Name of the condition: Equine dysautonomia
Name of the disease: Equine grass sickness

Contributor's Comment: In the present case, the submucosal (Meissner's) and myenteric (Auerbach's) plexuses showed severe neuronal chromatolysis (de-generation) consistent with equine grass sickness (equine dysautonomia). Immuno-histochemical staining with an anti-synaptophysin antibody revealed a marked reduction in numbers of neurons within the neuronal ganglia of the Meissner's and Auerbach's plexuses and a highly increased

immune-signal within the soma of remnant neurons indicative of neuronal degeneration.[3,20]

Equine grass sickness is a polyneuronopathy of the central and peripheral nervous system that only affects grazing horses, ponies and donkeys. It is a seasonal disease with peak of incidence between April-July in the northern hemisphere. This pathological condition was first described in Scotland in 1909, since then equine grass sickness has been described in numerous Northern European countries, Cyprus, Falkland Islands and Australia.[17] Although the etiology is still unknown, toxins produced by *Clostridium* spp. are suspected to play a role in the disease as low serum antibody levels for this bacterium were found to be a risk factor.[10] The most common gross pathological manifestations are fluid distention of the proximal gastrointestinal tract (stomach and small intestine) and large intestine impaction with dry and corrugated digesta often coated by copious mucus.[1] Histologically the main findings consist in neuronal chromatolysis of the peripheral nervous system and central nervous system, with changes particularly severe in the peripheral autonomic ganglia and enteric neurons. Whilst less significant, different studies also have identified involvement of the central nervous system including degeneration of cranial nerves (III, V, VI, VIII, XII), dorsal motor nucleus of the X, accessory cuneate nucleus, red nucleus and reticular formation.[17] The histological appearance of the chromatolytic neurons consists in swelling of cell body (soma), loss and/or peripheralization of Nissl substance, central eosinophilic spheroid bodies, foamy cytoplasm and peripheral margination and flattening of the nucleus.[9] The best gastrointestinal location to identify these changes is the ileum (submucosal and myenteric plexuses), especially in acute cases.[13] Nonetheless, chromatolysis has been also reported in stomach, duodenum, jejunum, caecum, large colon, small colon and rectum,[17] and the duodenum has been identified as the best location to identify degenerated neurons in chronic cases.[13] Neuronal lesions have been documented in the following ganglia of the autonomic system: ciliary ganglion, cranial cervical ganglion, caudal mesenteric ganglion, stellate ganglion, thoracic and abdominal sympathetic trunk, celiaco-mesenteric, caudal mesenteric ganglion and parasympathetic terminal cardiac ganglion.[17] Additionally, loss of interstitial cells of Cajal have also been reported in cases of acute grass sickness, suggesting the loss of these pacemarkers may also contribute to development of the dysmotility.[6] The only way to diagnose equine grass sickness ante mortem is by mean of an ileal biopsy which allows the identification of neuronal loss and / or neuronal chromatolysis with 100% sensitivity and specificity.[12] Anti-synaptophysin immunostaining has been proposed as a good diagnostic tool to identify degenerating neurons which show an increase of synaptophysin signal within the cytoplasm.[3,20]

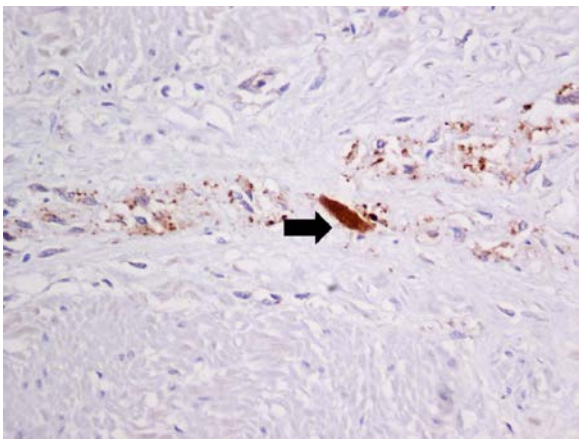

Ileum, horse. Enhanced synaptophysin immunopositivity is consistent with neuronal degeneration. (HE, 400X) (Photo courtesy of: University of Liverpool, Leahurst Campus, Chester High Road, Neston, Wirral, UK, CH64 7TE.)

Associated with the typical features of equine dysautonomia, an atypical proliferation of the lymphoid tissue arising from the GALT was also recognized in this case, that can explain the grossly observed focally extensive thickening and white discoloration of the intestine, which is not a usual feature of equine grass sickness per se. In our opinion there are several features that support the diagnosis of a lymphoma against a lymphoid hyperplasia: grossly the intestinal wall was diffusely severely thickened and white in color. Histologically the blastic lymphoid cells exhibited features of atypia (large cellular size, with vesicular to finely stippled chromatin, occasional nuclear membrane indentations and scattered bizarre mitotic figures) and the infiltrative behavior (invasion of the lamina propria and vessels) with loss of follicular structure of numerous GALT areas. On the basis of the morphological appearance provided by the H&E the tumor was provisionally classified as a T-cell rich B-cell lymphoma.

Immunohistochemichal results however identified a constant CD3 positivity in both small and blastic lymphoid cells, with lack of positivity for B markers (CD79a / CD20). CD3 positive cells were also detected within vessels. On this basis a T cell lympho-proliferative disorder consistent with a T cell lymphoma was the final diagnosis in this case. Unfortunately no other organ was available for examination to further investigate the possible leukemic phase of the neoplasm as suggested by the vascular invasion, in distant organs. A clonality test was not available to test the clonality of the proliferation.

Alimentary lymphoma is a commonly reported tumor of the gastrointestinal system in horse.[1] The mean age of presentation of

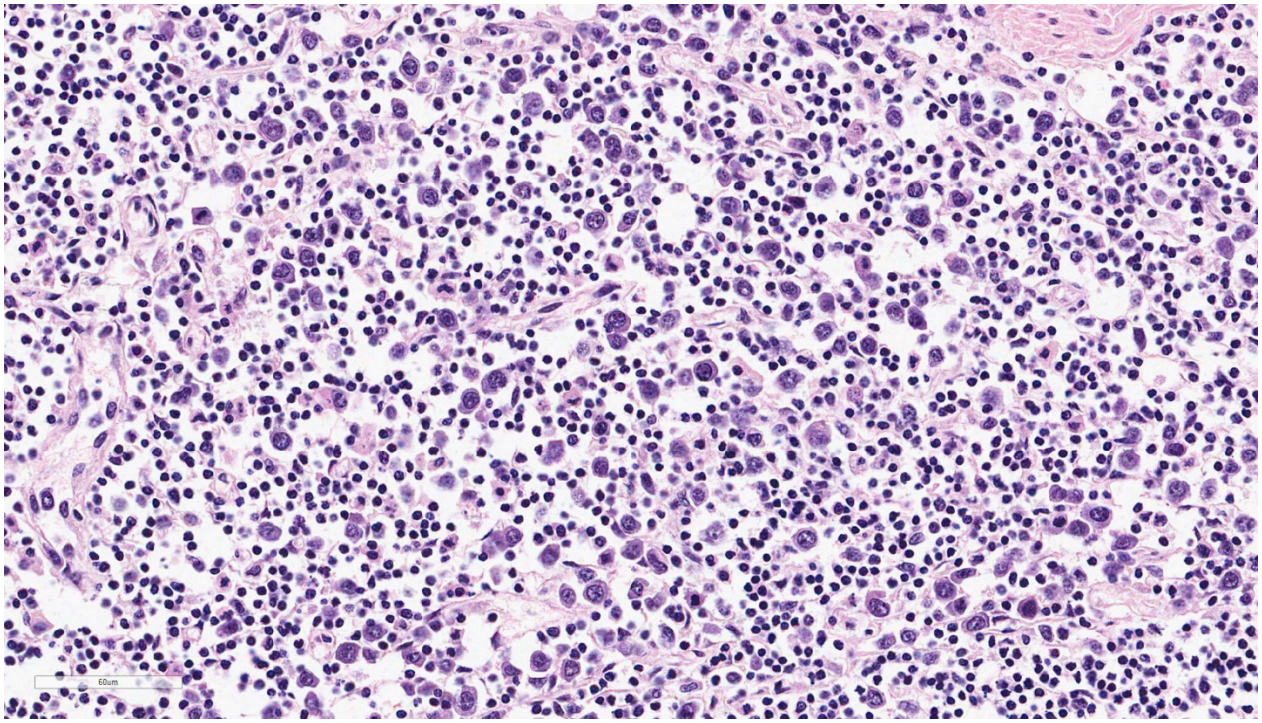

Ileum, horse. The presence of small numbers of large lymphocytes in a sea of smaller mature T-cells is consistent with T-cell rich B-cell lymphoma. (HE, 400X)

intestinal lymphoma is 16 years. This information, gained from a recent publication[19], differs from older papers of equine lymphoma in which the mean age was 7.5-10 years.[5,14,15] This difference may suggest alimentary lymphoma is more represented in older animals compared to other lymphomas or perhaps life expectancy of horses has increased during recent years.[19] The major clinical signs are weight loss, ventral edema and ascites probably due malabsorption and protein loss, lethargy, occasionally diarrhea, pyrexia, and abdominal pain with sings of colic.[1,5] In one study lymphoma was found as the most common diagnosis in a group of horses showing frequent recurrent episodes of colic with high mortality, lymphoma was the fourth most common etiology in horses showing chronic colic signs.[4,8] The most affected anatomical region is the small intestine closely followed by the large intestine, although segmental distribution is also described usually associated with younger animals.[19] The gross appearance of this tumor consists of diffuse thickening of the intestinal wall, enlargement of the regional lymph nodes and sometimes nodular bulges in the serosal surface.[1,5,18] Histologically it is commonly characterized by diffuse infiltration of the mucosa and submucosa and sometimes the tunica muscularis.[1] The cytological features of the tumor may vary depending on phenotype of the primary neoplastic lymphocytes.[7,11]

Alimentary lymphoma has been traditionally correlated with B-cell neoplastic proliferation since it is thought to arise from GALT, therefore large centroblastic cells are the predominant cell population.[1,18] Other subtypes of lymphoma have been later documented such as epitheliotrophic T-cell lymphoma[16] and T-cell rich B-cell lymphoma (TCRBCL), been this latter the most common lymphoma subtype according to a recent publication.[2] Histologically TCRBCL is composed of two cell populations, the

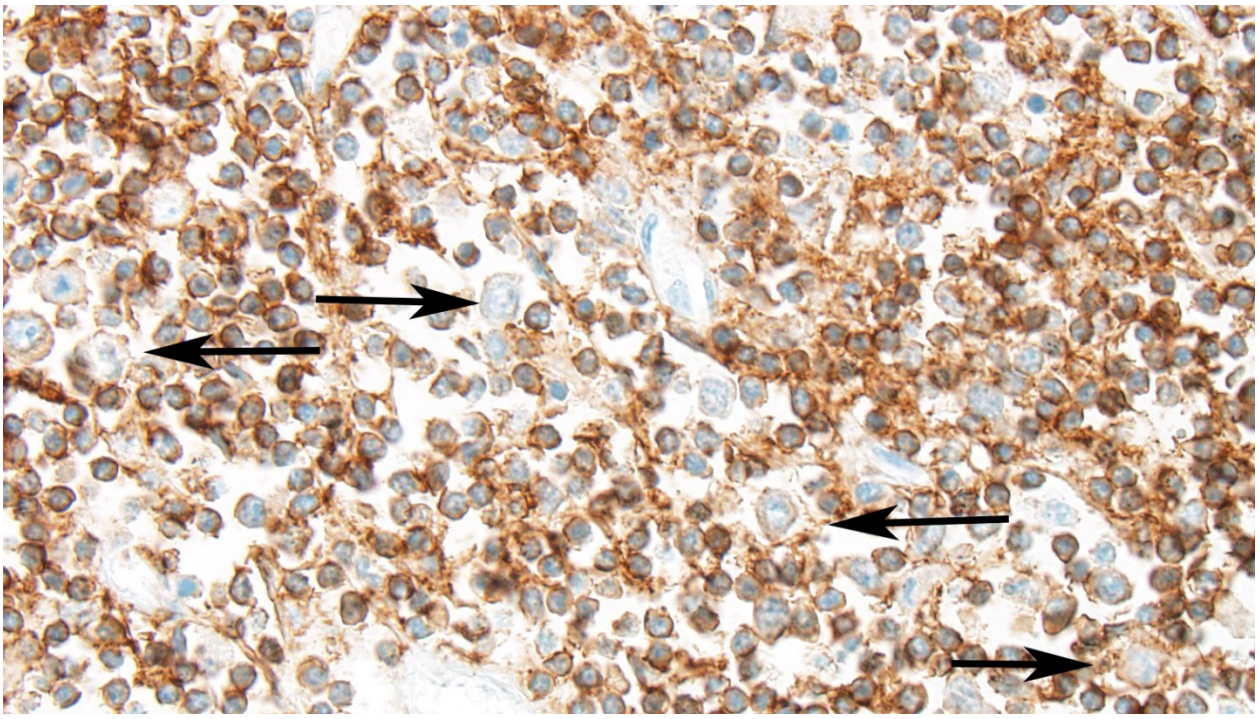

Ileum, horse. T-cells are strongly positive for CD3; larger B-cells are not. (HE, 400X)

predominant one is characterized by well-differentiated small T-lymphocytes, inter-mingled within these T-cells there are large neoplastic cells ~2-3 times the size of the aforementioned cells which are derived from B-lymphocytes.[2,7] Most of T-cell lymphomas are characterized by small to medium T-lymphocyte cell population infiltrating lamina propria and mucosa occasionally showing epitheliotropsim.[16] In all lymphomas there is a marked shortening and fusion of the villi.

JPC Diagnosis: 1. Small intestine (ileum per contributor): Lymphoma (consistent with TCRBCL), Warm blood (*Equus caballus*), equine.
2. Small intestine (ileum per contributor), neurons: Neuronal degeneration and loss, multifocal, moderate.

Conference Comment: Gastrointestinal lymphomas are discussed by the contributor and were reviewed by conference attendees including: enteropathy-associated T-cell lymphomas, type I and II (EATL), diffuse large B cell lymphomas, and large granular lymphocyte (LGL) lymphoma. EATL is most common in the jejunum of dogs and cats. EATL type I is composed of intermediate to large T-cells, whereas EATL type II is composed of small T-cells (often with histologic overlap with inflammatory bowel disease early in disease process).LGL lymphoma is composed of large cells with brightly eosinophilic granules that contain granzymes. The granules are much easier to see cytologically, so an impression smear done by the surgeon prior to formalin fixation is often high yield.
In this case, there are large cells (that are often mitotic) admixed with a reactive population of small lymphocytes. In the horse, this mixed cell population is most consistent with T cell rich large B cell lymphoma (TCRBCL), which is the most common subtype of lymphoma in this species. For this reason, we re-ran special stains to take a second look at the two cell populations. CD3, a marker for T-cells, was positive (with strong intracytoplasmic immunoreactivity) for the majority of the cells, particularly the cells that expand the lamina propria; CD20 and Pax-5, markers for B-cells were positive (with strong intracytoplasmic immunoreactivity) for the smaller population of large neoplastic cells admixed among the T-cell aggregates or forming germinal centers (presumed to be residual GALT) or was non-contributory, respectively. It is ideal to use more than one B-cell marker in suspected lymphoma cases. CD79a was not run in this case as it has not been proven effective in the horse. Two other B-cell markers (CD20 and Pax-5) This immunohistochemical pattern is compatible of TCRBCL. PARR was discussed as an option for diagnosis, but the paucity of neoplastic cells and the abundance of small reactive T cells may confound this test.

Contributing Institution:
University of Liverpool,
Leahurst Campus,
Chester High Road,
Neston, Wirral, UK, CH64 7TE

References:

1. Brown CC, Barker IK. Alimentary system. In: Maxie MG, ed. *Jubb, Kennedy, and Palmer's Pathology of Domestic Animals*, 5th ed.Vol 2. Philadelphia, PA:Elsevier Saunders;2007:1-296.
2. Durham AC, Pillitteri CA, San Myint M, et al. Two hundred three cases of equine lymphoma classified according to the World Health Organization (WHO) classification criteria. *Vet Pathol*. 2013;50:86-93.
3. Hilbe M, Guscetti F, Wunderlin S, et al. Synaptophysin: an immunohistochemical

marker for animal dysautonomias. *J Comp Pathol*. 2005;132:223-227.
4. Hillyer MH, Mair TS. Recurrent colic in the mature horse: a retrospective review of 58 cases. *Equine Vet J*. 1997;29:421-424.
5. Hillyer TSMaMH. Clinical features of lymphosarcoma in the horse: 77 cases. *Equine vet Educ*. 1991;4:108-113.
6. Hudson N, Mayhew I, Pearson G. A reduction in interstitial cells of Cajal in horses with equine dysautonomia (grass sickness). *Auton Neurosci.* 2001;92:37-44.
7. Kelley LC, Mahaffey EA. Equine malignant lymphomas: morphologic and immunohistochemical classification. *Vet Pathol.* 1998;35:241-252.
8. Mair TS, Hillyer MH. Chronic colic in the mature horse: a retrospective review of 106 cases. *Equine Vet J*. 1997;29:415-420.
9. Vandevelde RJH, Oevermann A. *Veterinary Neuropathology: Essentials of Theory and Practice*. New York, NY:Wiley-Blackwell; 2012:15-16.
10. McCarthy HE, French NP, Edwards GB, et al. Equine grass sickness is associated with low antibody levels to *Clostridium botulinum*: a matched case-control study. *Equine Vet J*. 2004;36:123-129.
11. Meyer J, Delay J, Bienzle D. Clinical, laboratory, and histopathologic features of equine lymphoma. *Vet Pathol*. 2006;43:914-924.
12. Milne EM, Pirie RS, McGorum BC, et al. Evaluation of formalin-fixed ileum as the optimum method to diagnose equine dysautonomia (grass sickness) in simulated intestinal biopsies. *J Vet Diagn Invest.* 2010;22:248-252.
13. Murray A, Pearson GT, Cottrell DF. Light microscopy of the enteric nervous system of horses with or without equine dysautonomia (grass sickness): its correlation with the motor effects of physostigmine. *Vet Res Commun.* 1997;21:507-520.
14. Neufeld JL. Lymphosarcoma in the horse: a review. *Can Vet J*. 1973;14:129-135.
15. Neufeld JL. Lymphosarcoma in a mare and review of cases at the Ontario Veterinary College. *Can Vet J*. 1973;14:149-153.
16. Pinkerton ME, Bailey KL, Thomas KK, et al. Primary epitheliotropic intestinal T-cell lymphoma in a horse. *J Vet Diagn Invest*. 2002;14:150-152.
17. Pirie RS, Jago RC, Hudson NP: Equine grass sickness. *Equine Vet J*. 2014;46:545-553.
18. Platt H: Alimentary lymphomas in the horse. *J Comp Pathol.* 1987;97:1-10.
19. Taylor SD, Pusterla N, Vaughan B, et al. Intestinal neoplasia in horses. *J Vet Intern Med*. 2006;20:1429-1436.
20. Waggett BE, McGorum BC, Shaw DJ, et al. Evaluation of synaptophysin as an immunohistochemical marker for equine grass sickness. *J Comp Pathol.* 2010;142:284-290.

CASE II: P636-14 (JPC 4066540).

Signalment: 8-week-old, intact, female, Braque francais (French pointer) (*Canis familiaris*), canine.

History: This puppy was presented to a veterinary clinic for a sudden onset of drooling (sialorrhea), vomiting, tremors and seizures. Due to the severity and rapid evolution of the clinical signs, the owner

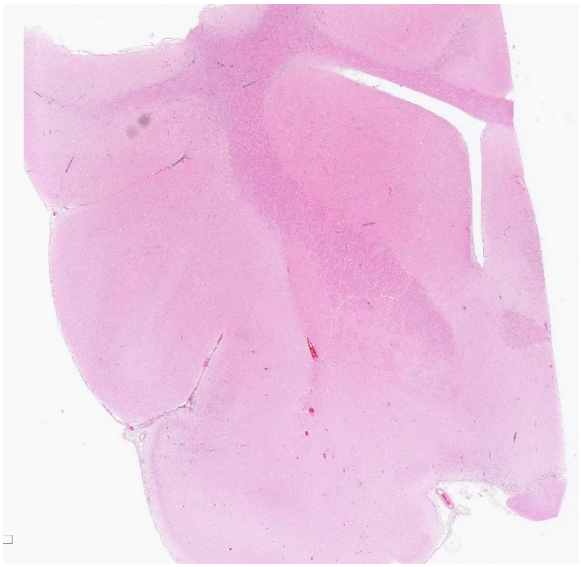

Cerebrum, puppy: A section of cranial diencephalon was submitted for examination. (HE, 4X)

elected for euthanasia without any further investigation. The dog was submitted to our diagnostic laboratory and a complete necropsy was performed.

Gross Pathology: The dog was in good body condition and there were no remarkable findings on gross examination.

Laboratory Results (clinical pathology, microbiology, PCR, ELISA, etc.): The dog's brain tested negative for rabies (immuno-peroxidase) and herpesvirus (PCR → panherpesvirus/DNA polymerase on FFPE tissue).

Microscopic Description: Similar lesions were observed throughout the brain and the cranial portion of the cervical spinal cord, with relatively minor variations in intensity. The submitted sections are from the cerebrum. Multifocally in the neuro-parenchyma and, to a lesser degree, the leptomeninges (subarachnoid space), there is a population of relatively monomorphic lymphoid cells that have a mainly perivascular and, in the neuroparenchyma, vascular distribution (Fig.1). In the neuroparenchyma, these cells are located in the Virchow-Robin spaces (up to 8 cells thick) and/or the vascular walls in both white and grey matter; in the latter case, there is sometimes associated edema, fibrin and/or erythrocytes (Figs 1 and 2). Multifocally, especially around affected blood vessels, the neuropil has an increased cellularity due to the presence of apparently similar lymphoid cells and possibly glial cells (some of which are reactive) (Fig.1). The lymphoid cells are small (nuclei ≤ 1.5 RBC), and are characterized by scant eosinophilic cytoplasm, a round to oval nucleus with finely stippled chromatin. There are several to numerous cells, interpreted as lymphoid cells, that are karyorrhectic or sometimes pyknotic (apoptosis). Anisocytosis and anisokaryosis are minimal, and no mitoses were detected. Immunohistochemistry (IHC) for CD3 and CD79a was performed on sections of the brain. The overwhelming majority (> 99%) of lymphoid cells, including in the hypercellular neuropil, were strongly positive for CD3 (Figs.3 and 4), with very rare cells (< 1%) positive for CD79a. There were no significant changes in other organs examined, including the eyes.

Contributor's Morphologic Diagnosis:
Primary CNS T-cell lymphoma (PCNSL)

Contributor's Comment: Although a diagnosis of viral mononuclear/lymphocytic meningoencephalomyelitis was initially considered and investigated (CDV and herpesvirus), primary CNS T-cell lymphoma was the final diagnosis based on the morphologically monomorphic nature of the lymphocytic infiltrate (including the absence of plasma cells) that was confirmed to be almost purely of T cell nature, and its angiocentric nature; although not assessed by IHC, macrophages did not seem to be present, at least in significant numbers, and glial nodules were not observed. Assessment of T-cell clonality by either T-cell antigen receptor gene rearrangement analysis (PCR)

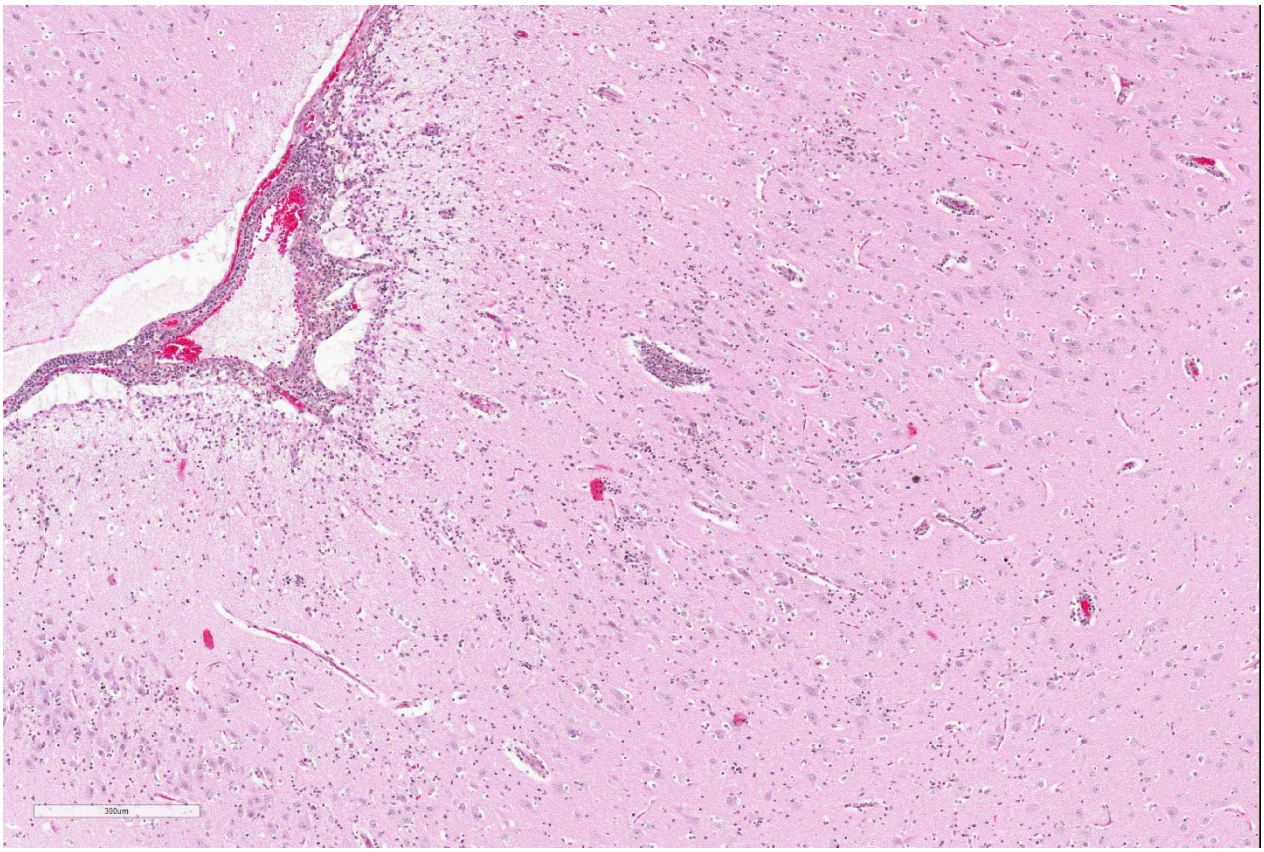

Cerebrum, puppy: Multifocally, the meninges (upper left) as well as Virchow-Robins spaces are expanded by numerous lymphocytes. Lymphocytes also infiltrate the gray matter as well. (HE, 100X)

or X-chromosome inactivation pattern (XCIP) analysis was not performed. Demonstration of clonality would have further supported our diagnosis, although it is not totally confirmative; the XCIP technique has more limitations, especially with regards to gender (females) and hematopoietic neoplasms.[9]

Primary CNS lymphomas (PCNSL) are uncommon to rare neoplasms defined as non-Hodgkin lymphomas that are confined, at least initially, to the CNS and/or the eye.[1,3,12,13] In the CNS, they can involve the neuroparenchyma and/or the meninges. Primary ocular lymphomas included in the PCNSLs in humans are vitreoretinal lymphomas (PVRL); 65-90% of patients with PVRLs develop lymphoma in the CNS.[2] In contrast to PCNSLs, secondary CNS lymphomas represent a metastatic process from a lymphoma outside the CNS, and are more common.[1,3,4,13] In humans and cats, 5% of patients with systemic lymphomas have CNS involvement, predominantly in the leptomeninges.[8,13] PCNSLs are neoplasms mainly seen in humans, dogs and, to a lesser degree cats, but they have also been described in ruminants, a dolphin and a harbor seal;[1,3-5,7,8,12,13] there is a probable case reported in a horse.[11] In humans and dogs, the reported incidence is about 3% of intracranial neoplasms; in humans they account for 1-2% of all non-Hodgkin lymphomas. In cats, most PCNSLs involve the spinal cord.[4] In animals, the majority of PCNSLs are of T-cell lineage, in contrast with humans in which 80-95% are large B-cell lymphomas which differ from their systemic counterparts with regards to behavior and treatment.[1,3,7,12] The etiology is

unknown in both animals and humans, except in cats in which FeLV is often involved and in immunocompromised humans in which the Epstein-Barr virus (EBV) plays a major role (EBV has not been associated with PCNSL in immunocompetent human patients).[1,12] Most PCNSL cases have gross lesions and the diagnosis of lymphoma is straightforward on microscopic examination, but in a few reported cases in cats and dogs,[4,5,7,8] there were no conspicuous masses and histopathology could not readily differentiate between lymphoma and mononuclear/ lymphocytic inflammation. In human PCNSLs, neoplastic lymphocytes in the neuroparenchyma characteristically invade walls of small blood vessels, accumulate in perivascular spaces and spread into the neuropil.[1,3]

In the present case, the age of the animal, absence of gross lesions and, histologically, absence of "masses" of lymphoid cells, atypia and mitosis initially led to a diagnosis of mononuclear (non-suppurative) meningo-encephalomyelitis of probable viral origin. Other infectious diseases (e.g. neosporosis), granulomatous meningoencephalitis (GME) and necrotizing meningoencephalitis (NME) were included in the initial differential diagnosis, but the histopathologic findings were not consistent with these conditions. Based on aforementioned findings (homogenous infiltrate, angiocentrism and

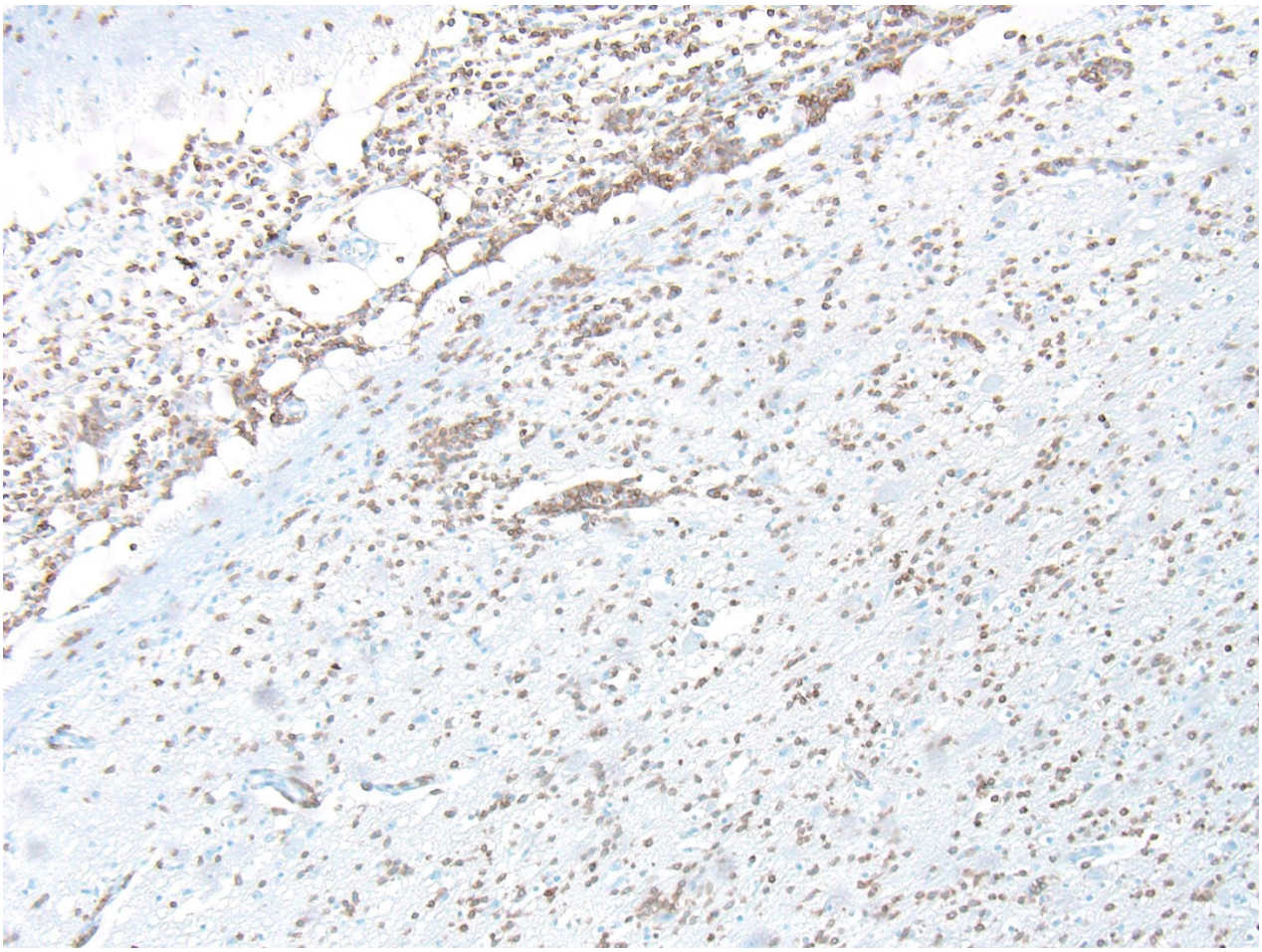

Cerebrum, puppy: The majority of the infiltrating lymphocytes stain strongly positive for CD-3. (anti-CD3, 100X)

IHC), some published veterinary cases and a consultation with a veterinary neuropathologist, we finally concluded to a PCNSL. An equine case with similarities to our case was termed "lymphoproliferative disease with features of lymphoma in the CNS".[11] In human pathology, small-cell lymphomas have been distinguished from mononuclear encephalitides by two morphologic criteria: 1) encephalitis generally has a more polymorphous infiltrate with at least some plasma cells, and 2) vascular invasion by lymphocytes, characteristic in lymphomas, is not a feature of encephalitis.[3] The age of the animal is also not typical of canine lymphomas which are mostly seen in middle-aged dogs, even though they have been seen in puppies as young as 4 months. In the bovine species, lymphomas have been reported in aborted fetuses and neonatal calves.[6]

JPC Diagnosis: Cerebrum: Meningoencephalitis, lymphocytic, multifocal to coalescing, moderate, Braque francais (French pointer) (*Canis familiaris*), canine.

Conference Comment: As described by the contributor above, primary central nervous system (CNS) lymphoma is rare in humans and animals. In humans the majority are large B-cell variants, whereas, in animals most of the reported cases have been T-cell variants. Microscopically, the diagnosis of lymphoma

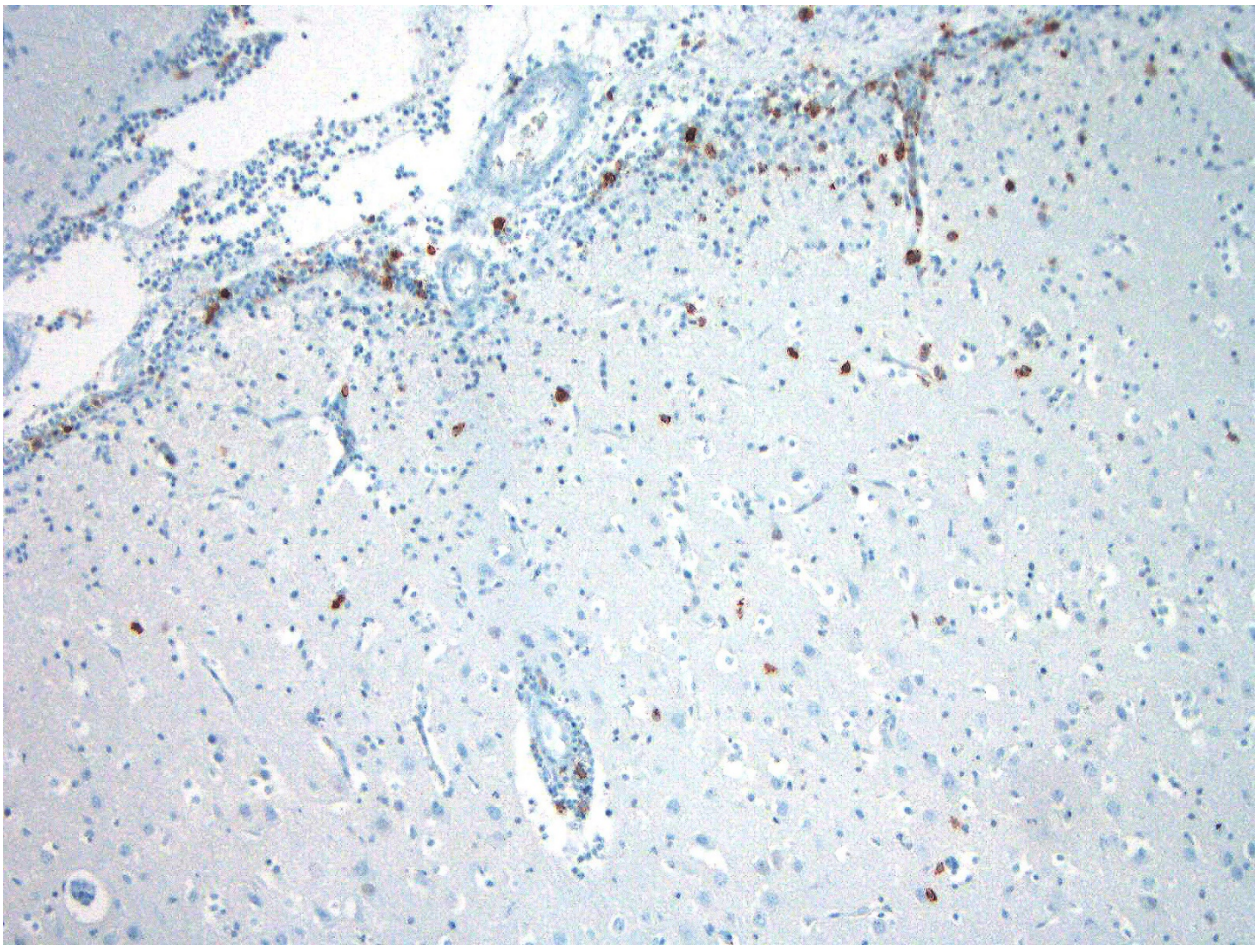

Cerebrum, puppy: CD20-positive B cells are present within the infiltrate around vessels as well as in the parenchyma. (anti-CD20), 100X

is challenging because the perivascular and periventricular distribution of neoplastic cells may be confused with an inflammatory response (e.g. viral encephalitis). However, inflammatory responses often have several other cell types depending on chronicity, exhibiting neutrophilic infiltrates initially, followed by plasma cells, lymphocytes, and potentially histiocytes as the infection progresses. In humans, an atypical variant of CNS lymphoma has been described termed "lymphomatosis cerebri" which is characterized by diffuse infiltration of deep cerebral white matter by individualized lymphoma cells with no mass formation. Another differential which has been reported in humans and domestic animals is lymphomatoid granulomatosis, a rare primary pulmonary lymphoproliferative disease which has had CNS involvement described in late stages. This is characterized microscopically by angiocentric and angiodestructive atypical lymphoid cells with rare binucleate and multinucleate cells.[10]

The conference attendees discussed the alternative diagnoses, given the clinical presentation (young puppy). Conference attendees reviewed common viral encephalitides (distemper, alphaviruses, West Nile virus, rabies, canine herpesvirus-1) with their microscopic characteristics. It was noted that immunohistochemistry for B cells or tests for T-cell clonality were not performed as part of the workup. Several immunohistochemical stains were run by the JPC in this case to further classify the cell type in these specimens. While the majority of cells exhibited strong cytoplasmic positivity for T-cells, a number of lymphocytes both in perivascular and parenchymal locations stained positively for CD20, a B-lymphocyte marker. PARR testing was discussed as an important next step to determine if this represents a clonal expansion of T cells. Based on the morphologic appearance of the lesion, the relatively frequency of both subclinical viral infections in puppies versus the frequency of primary T-cell lymphomas (the age of this puppy notwithstanding), the presence of B-cells within the lesion, and the absence of evidence of clonality, the moderator and attendees favored a diagnosis of inflammatory disease in this case rather than T-cell lymphoma.

Contributing Institution:
Faculty of veterinary medicine,
Université de Montréal,
St-Hyacinthe, Quebec, Canada
http://www.medvet.umontreal.ca

References:

1. Arbelo M, Espinosa de los Monteros A, Herraez P, et al. Primary central nervous system T-cell lymphoma in a common dolphin (Delphinus delphis). *J Comp Path*. 2014; **150**:336-340.
2. Chan CC, Rubenstein JL, Coupland SE, et al. Primary vitreoretinal lymphoma: a report from an International Primary Central Nervous System Lymphoma Collaborative Group symposium. *Oncologist*. 2011;16:1589-99
3. Ellison D, Love S, Chimelli L, et al. Primary CNS lymphomas. In: *Neuropathology: a reference text of CNS pathology*. Second edition. Mosby, Philadelphia, PA, 2004: 689-694.
4. Fondevila D, Vilafranca M, Pumarola M. Primary central nervous system T-cell lymphoma in a cat. *Vet Pathol*. 1998;**35**:550-3.
5. Guil-Luna S, Carrasco L, Gómez-Laguna J, et al. Primary central nervous system T-cell lymphoma mimicking meningoencephalomyelitis in a cat. *Can Vet J*. 2013;**54**:602-5.
6. Jacobs RM, Messick JB, Valli VE. Tumors of the hemolymphatic system. In:

Tumors in domestic animals. Fourth Edition. Iowa State Press, Ames, IA, 2002:119-198.
7. Kim NH, Ciesielski T, Kim JH, et al. Primary central nervous system B-cell lymphoma in a young dog. *Can Vet J*. 2012; **53**:559-564.
8. Long SN, Johnston PE, Anderson TJ. Primary T-cell lymphoma of the central nervous system in a dog. *J Am Vet Med Assoc*. 2001;**218**:719-22.
9. Mochizuki H, Goto-Koshino Y, Takahashi M, Fujino Y, Ohno K, Tsujimoto H. Demonstration of the cell clonality in canine hematopoietic tumors by X-chromosome inactivation pattern analysis. *Vet Pathol*. 2015 Jan;**52**(1):61-9
10. Morita T, Kondo H, Okamoto M, Park CH, Sawashima Y, Shimada A. Periventricular spread of primary central nervous system T-cell lymphoma in a cat. *J Comp Pathol.* 2009;140(1):54-58.
11. Morrison LR, Freel K, Henderson I, et al. Lymphoproliferative disease with features of lymphoma in the central nervous system of a horse. *J Comp Pathol*. 2008;**139**:256-61.
12. Nigo M, Richardson S, Azizi E, et al. Ventriculitis Caused by Primary T-Cell CNS Lymphoma in an Immunocompetent Patient. J Clin Oncol. 2014 Nov 17 (Epub ahead of print).
13. Vandevelde M, Higgins RJ, Oevermann A. Neoplasia. In: *Veterinary Neuropathology: essentials of theory and practice*. First edition. Ames, Iowa: Wiley-Blackwell, 2012: 129-156.

CASE III: 15-23253 (JPC 4066861).

Signalment: 7-year-old, spayed, female, Bullmastiff (*Canis familiaris*), canine.

History: A 7 year old spayed female Mastiff was referred to the Cornell University Hospital for Animals Emergency Service for evaluation of hemoabdomen and a two day history of weakness, lethargy, and in appetence. On presentation, the patient was febrile with tachycardia and tachypnea. Abdominal ultrasound and abdominocentesis confirmed a hemorrhagic effusion. Platelet numbers were moderately decreased, and coagulation parameters were within normal limits. The patient also had a one month history of an ulcerated mass on the right

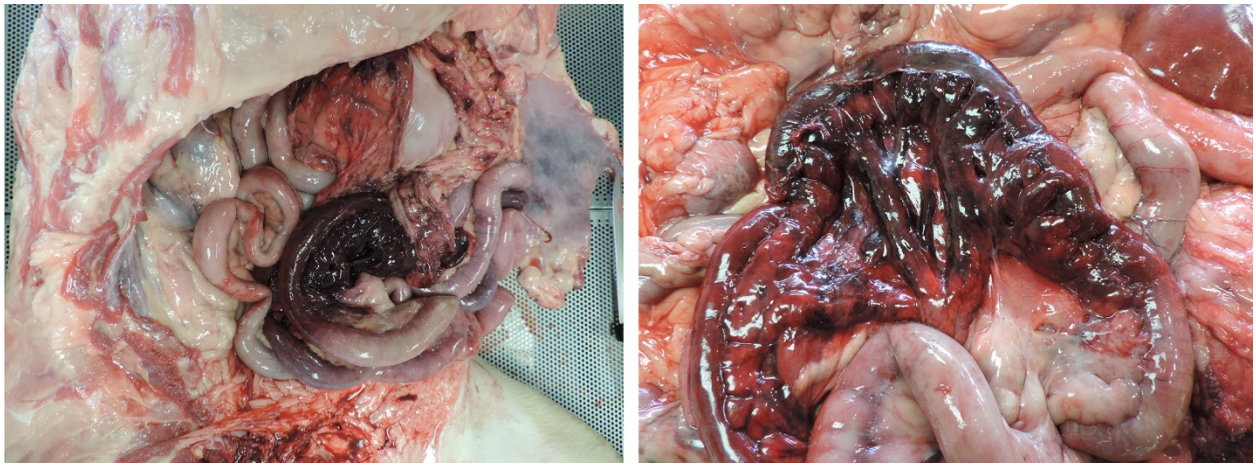

Intestine, dog: ***There is extensive infarction and hemorrhage of the small intestine (Photo courtesy of: Department of Anatomic Pathology, Cornell University College of Veterinary Medicine http://www.vet.cornell.edu/biosci/pathology/)***

lateral thigh that had been unresponsive to treatment with antimicrobials.

While hospitalized the patient developed neurologic signs, including a vestibular episode with nystagmus and ataxia, circling, head-pressing, and knuckling. Her neurologic signs progressed to tetraplegia, and she became obtunded. The patient's condition further declined, and she died in the hospital.

Gross Pathology: Gross examination confirmed hemoabdomen and focal cutaneous ulceration at the lateral right thigh. Examination further revealed multiple sites of acute infarction and hemorrhage in the meninges and cerebrum, small intestine, lung, and a mesenteric lymph node. More chronic sites of infarction were found in the kidney and myocardium.

Laboratory Results (clinical pathology, microbiology, PCR, ELISA, etc.): None provided.

Microscopic Description:

The submitted slide includes a section of liver. Distending portal and central veins and expanding sinusoids are sheets and clusters of intravascular neoplastic cells. Neoplastic cells are round with a high nuclear to cytoplasmic ratio. Nuclei are up to twice the diameter of a neutrophil and have distinct cell margins, scant amphophilic to pale basophilic cytoplasm, and an often eccentric, round or indented nucleus with coarsely clumped chromatin and 1-3 magenta nucleoli. There is marked anisocytosis and anisokaryosis and up to 4 mitotic figures per high magnification (400x) field. There are scattered apoptotic neoplastic cells. Sinusoids also contain increased numbers of circulating neutrophils and lymphocytes. Hepatic cords are thin with mildly dilated sinusoidal spaces (atrophy). Portal and central vein lymphatics are occasionally dilated.

Cerebrum, dog: There is multifocal to coalescing hemorrhage within the cerebral meninges. (Photo courtesy of: Department of Anatomic Pathology, Cornell University College of Veterinary Medicine, http://www.vet.cornell.edu/biosci/pathology/)

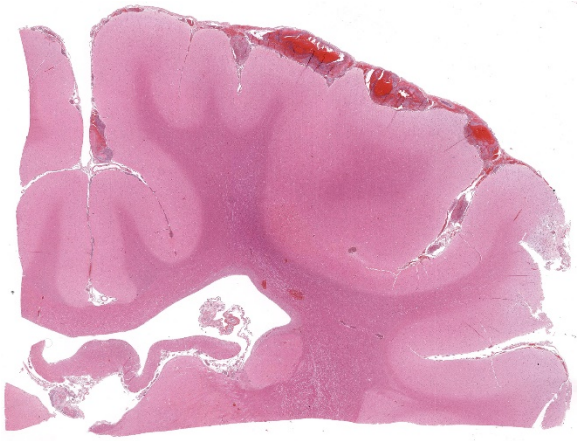

Cerebrum, dog: At subgross magnification, there is focally extensive meningeal hemorrhage as well as multiple hemorrhages in the periventricular white matter. (HE, 6X) (Photo courtesy of: Department of Anatomic Pathology, Cornell University College of Veterinary Medicine http://www.vet.cornell.edu/biosci/pathology/)

Immunohistochemistry revealed positive reactivity for CD3, consistent with a T cell origin. Similar intravascular neoplastic populations were observed in the lung, heart, kidney, jejunal mesentery, pancreas, mesenteric lymph node, skin, and brain, often associated with thrombosis and infarction.

Contributor's Morphologic Diagnosis:
Liver: Intravascular lymphoma, large T cell

Contributor's Comment: Intravascular lymphoma (IVL) is a rare large-cell lymphoma, defined by its confinement within blood vessel lumina in the absence of leukemia or a primary extravascular mass. Typical clinical and pathologic features are related to vascular occlusion, injury, and fibrin thrombosis, often with central nervous system signs. In a review of 17 cases of IVL in dogs, predominant clinical signs included spinal cord ataxia, seizures, vestibular disease, lethargy, diarrhea, and fever.[4] Skin involvement was apparent in one of the cases.[4] IVL accounted for the spectrum of clinical findings in this dog, including the neurologic signs (due to cerebral thrombosis and infarction), hemoabdomen (small intestinal infarction), and ulcerative dermatitis. No extravascular lymphomatous masses were found at necropsy, and ante-mortem blood work was not consistent with leukemia.

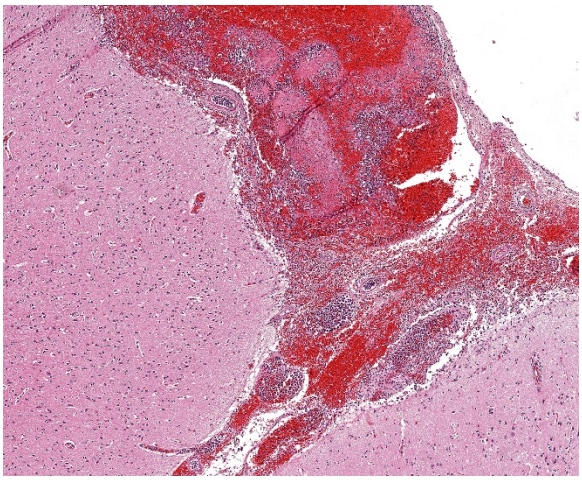

Cerebrum, dog: Within the meninges, there is extensive hemorrhage, vessels are dilated and by cellular fibrinocellular thrombi. (HE, 40X) (Photo courtesy of: Department of Anatomic Pathology, Cornell University College of Veterinary Medicine, http://www.vet.cornell.edu/biosci/pathology/)

Intravascular lymphoma was first described in the dog as angioendotheliomatosis, under the assumption that the neoplastic cells were derived from the endothelium, but subsequent immunohistochemical data determined the lymphocyte-derivation.[4,6,7] Refinement of understanding of intravascular lymphoma in dogs was supported by work on immunohistochemical and ultrastructural data on similar human neoplasms.[6] While the

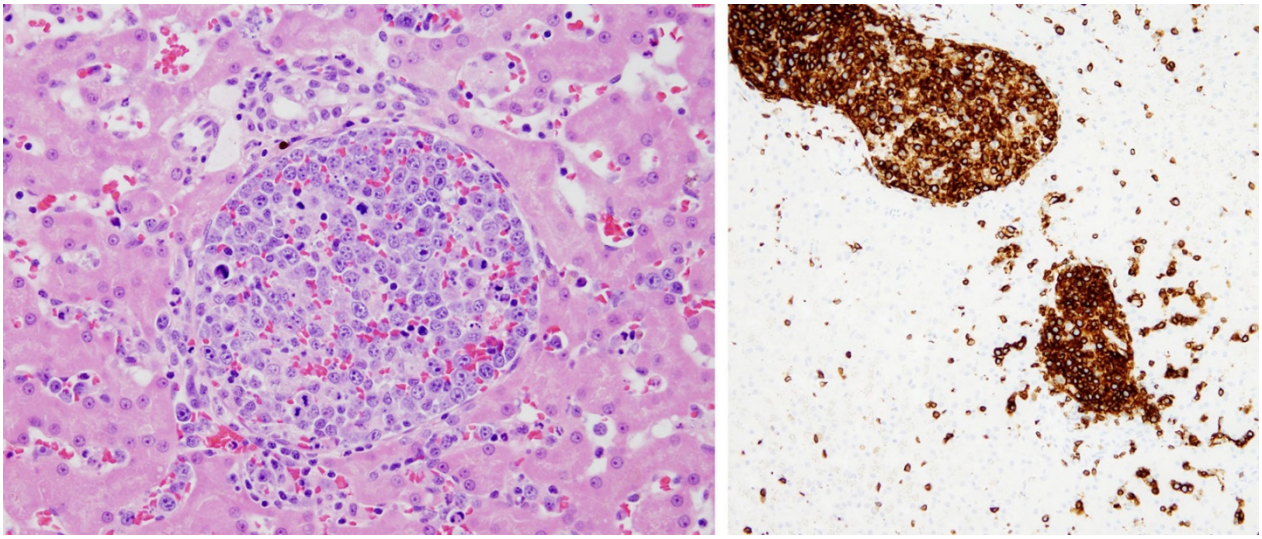

Liver, dog: Portal veins are expanded by accumulations of numerous neoplastic lymphocytes, which stain strongly positive for CD-3, indicated T-cell origin. (Left: HE, 400X, right: anti-CD-3, 400X) (Photo courtesy of: Department of Anatomic Pathology, Cornell University College of Veterinary Medicine, http://www.vet.cornell.edu/biosci/pathology/)

majority of human cases are derived from B cells, most reported intravascular lymphomas in dogs are derived from T cells or non-B, non-T lymphocytes.[2,4,8] Human and canine cases show a similar predilection for nervous system involvement, but cutaneous presentation appears to be more common in humans.[4]

Neoplastic lymphocytes are generally most abundant in capillaries and small to medium veins, but also appear in smaller numbers within arteries.[4] The mechanism for the selective intravascular growth of IVL is unknown, but defective cell-to-cell adhesion between the neoplastic lymphocytes and endothelial cells has been proposed.[1,5]

JPC Diagnosis: Liver, veins, arteries, and sinusoids: Intravascular lymphoma, multifocal, Bull mastiff (*Canis familiaris*), canine.

Conference Comment: Angiotropic intravascular lymphoma, previously also referred to as malignant angioendotheliomatosis, is a rare tumor in humans and dogs, and has been reported a cat. Microscopically, it is characterized by a proliferation of neoplastic lymphocytes within the lumen and wall of blood vessels with no primary extravascular mass. In most human cases, these cells have been identified as B-cells, but in canine and feline cases, the majority are of T-cell origin.[3,4] Clinically, most of these cases present with neurologic signs and microscopically neoplastic cells are seen occluding cerebral arteries and veins. The vessels of the lungs are also commonly affected. In the affected cat,[3] there was severe involvement of the kidneys and cerebrum with absence of neoplastic cells in other visceral organs. Diagnosis usually follows the onset of neurologic signs and is typically postmortem. There are no neoplastic cells identified in routine blood samples. In humans, even with chemotherapy, prognosis is poor. There is no treatment data in domestic animals.[3]

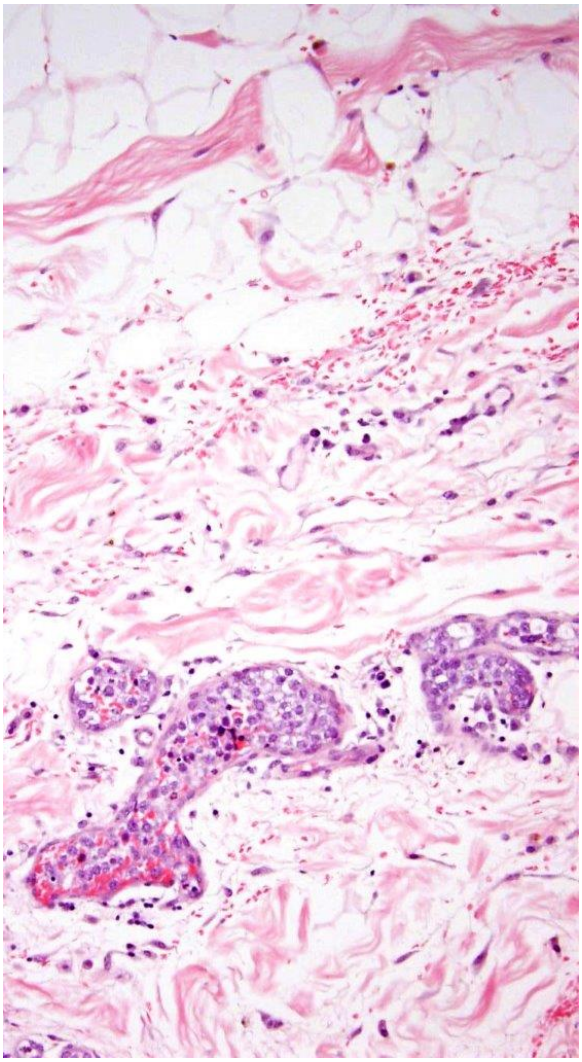

Skin, dog: Vessels in the skin are also occluded by numerous T-cells. (HE, 200X) (Photo courtesy of: Department of Anatomic Pathology, Cornell University College of Veterinary Medicine, http://www.vet.cornell.edu/biosci/pathology/)

The moderator shared a case that she had also of a female Bullmastiff that had intravascular lymphoma who presented with neurologic signs, acute renal failure, antibiotic-resistant urinary tract infection, and autoimmune hemolytic anemia. She then graciously reviewed images of the case and features of the entity.

Contributing Institution:
Anatomic Pathology
Cornell University College of Veterinary Medicine
http://www.vet.cornell.edu/biosci/pathology/

References:

1. Jalkanen S, Aho R, Kallajoki M et al. Lymphocyte homing receptors and adhesion molecules in intravascular malignant lymphomatosis. *Int J Cancer.* 1989;**44**:777–782.
2. Lane LV, Allison RW, Rizzi TR et al. Canine intravascular lymphoma with overt leukemia. *Vet Clin Pathol.* 2012;**41**:84–91.
3. LaPointe JM, Higgins RJ, Kortz GD, Bailey CS, Moore PF. Intravascular malignant T-cell lymphoma (malignant angioendotheliomatosis) in a cat. *Vet Pathol*. 1997;34(3):247-250.
4. McDonough SP, Van Winkle TJ, Valentine BA, et al. Clinciopathological and immunophenotypical features of canine intravascular lymphoma (malignant angioendotheliomatosis). *J Comp Path.* 2002;**126**:277–288.
5. Ponzoni M, Arrigoni G, Gould VE et al. Lack of CD 29 (β1 integrin) and CD 54 (ICAM-1) adhesion molecules in intravascular lymphomatosis. *Hum Pathol*.2000;**31**:200–226.
6. Sheibani K, Battifora H, Winberg CD et al. Further evidence that "malignant angioendotheliomatosis" is an angiotropic large-cell lymphoma. *N Engl J Med*. 1986;314:943–948.
7. Summers BA, deLahunta A. Cerebral angioendotheliomatosis in a dog. *Acta Neuropathologica.* 1985;**68**:10–14.
8. Zuckerman D, Seliem R, Hochberg E. Intravascular lymphoma: the oncologist's "great imitator". *The Oncologist.* 2006;**11**:496–502.

CASE IV: #1 (JPC 4101495).

Signalment: 12-year-old, neutered male, European domestic shorthair (*Felis catus*), feline.

History: Mass developing rapidly in the right mid-thigh. Previous history of multiple antibiotic and vaccine injection on the site were reported by the referring veterinarian.

Gross Pathology: Subcutaneous soft mass of large diameter, white tan, blending in the muscle

Laboratory Results (clinical pathology, microbiology, PCR, ELISA, etc.): CBC, Serum biochemistry, urine analysis unremarkable. Clinical staging negative for internal disease.

Microscopic Description:
Haired skin (not always present): The deep dermis, the panniculus and the skeletal muscles are characterized by a variably cellular neoplastic infiltration associated with areas of necrosis. The tumor is not encapsulated, infiltrative, and extending to the borders of the biopsy.

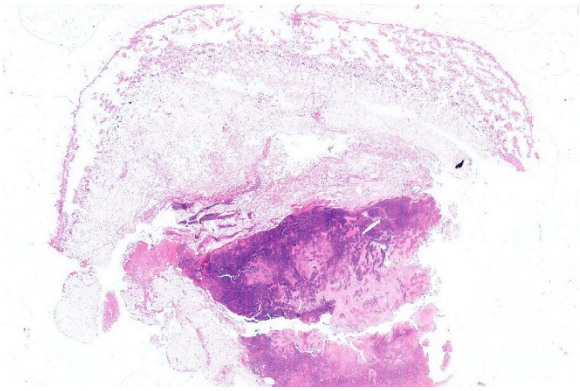

Hared skin and subcutis, cat: The subcutis and underlying skeletal muscle contains a nodular and half-necrotic round cell neoplasm. (HE, 4X)

The neoplasm is composed by round neoplastic organized in variably dense sheets or that tightly encircle and invade blood vessels walls (angiocentric and angioinvasive pattern) in association with locally extensive to coalescing areas of necrosis.

Neoplastic cells range from 20 to 35 microns in diameter, are round, with variably distinct cell borders, high N/C ratio, complete rim of variably eosinophilic homogeneous cyto-plasm. Nuclei are round, oval indented, paracentral, 15-30 micron in diameter, with finely granular chromatin and 1 to 4 round, prominent, basophilic nucleoli. Anisocytosis and anisokaryosis are severe. Mitoses are common and range from 2-6 per HPF and are often atypical. Tingible body macrophages range from 1 to 4 per HPF.

Contributor's Morphologic Diagnosis:
Angiocentric angiodestructive large cell subcutaneous lymphoma (injection site type) with necrosis

Contributor's Comment: Lymphomas represent more than 50% of all tumors in cats, with a prevalence of approximately 1.6% of the general feline population and 4.7% of hospitalized sick cats.[11,23] Primary cutaneous lymphomas account for 0.2 to 3%[21] of all feline lymphomas. Cutaneous, non-epitheliotropic lymphomas seem more frequent in cats[10] than dogs and include indolent T cell lymphoma, also referred to as cutaneous lymphocytosis,[6,7] diffuse T cell lymphoma, T cell rich large B cell lymphoma, and lymphoplasmacytic lymphoma.

In this case, microscopic features parallel descriptions and history of injection site lymphoma in cats.[15,17] Primary cutaneous lymphomas developing following injection have been reported in cats.[15,17] These lymphomas exhibit several peculiarities, including clinical presentation as a solitary dermal to subcutaneous nodule, development at confirmed previous injection sites (lateral thorax, interscapular region, thighs), microscopical presence of necrosis leading to central cavitation, peripheral inflammation, angiocentric, angioinvasive and angiodestructive growth patterns,[15,17] and presence of peripheral inflammation characterized by perivascular nodular lymphoid cell aggregates.[17] An additional unusual feature of feline injection site primary cutaneous lymphomas as a group is the prevalence of large B cell lymphomas with centroblastic, immunoblastic and anaplastic morphology[17] that are considered rare to exceptional tumors in cats.[7,10,21,23]

Primary cutaneous diffuse large B cell lymphomas (DLBCL) in man manifest as a solitary nodule or as multiple tumors restricted to one anatomic area (regional disease) and have a relatively poor prognosis compared with other primary cutaneous lymphomas, with a 5-year survival rate of 20-55%.[19] The most common morphological variants of human DLBCL are centroblastic, immunoblastic and anaplastic.[19] All these features are shared by a large prevalence of feline injection site skin lymphomas.[17]

The microscopic angiocentric, angioinvasive and angiodestructive pattern described for cutaneous feline injection site lymphomas resembles descriptions of human angiocentric lymphomas (ALs).[18] In man, primary cutaneous ALs represent a localized disease with propensity to relapse developing primarily in male patients.[18] Distinctively, human ALs are also characterized by extensive tissue necrosis and/or severe inflammation that often obscures the tissue and the neoplastic process itself.[16]

Pathogenesis of feline cutaneous injection lymphomas may also resemble pathogenesis of human lymphomas emerging in the

context of chronic inflammation with transformation of lymphoid cells.[4,5,8,9] Chronic inflammation has long been linked to emergence of a wide range of human malignancies and is now generally accepted as a risk factor for development of a variety of cancers including hematopoietic malignancies such as cutaneous T and B cell lymphomas in man.[5,8,9] In cats, the development of sarcomas at injections sites (e.g. rabies vaccine, long acting antibiotics or steroids) or at sites of implanted foreign material (non-absorbable suture material, microchip implants, retained surgical sponges or trauma) have been well documented and their pathogenesis has been attributed to the chronic inflammation elicited.[12] Progression of chronic inflammation to feline cutaneous lymphoma has also been hypothesized.[17] Previously, cutaneous lymphomas have been reported to arise in areas of feline injection site sarcomas following chemotherapy or radiation therapy of the primary tumor, and lymphomagenesis in these cases was hypothesized to derive from the mutagenic action of chemotherapy or radiation treatment.[14]

Many primary human cutaneous lymphomas including ALs and DLBCL have been consistently associated with inflammation and EBV infection.[2,5] DLBCL associated with chronic inflammation (DLBCL-ACI) is a B cell lymphoma included in the WHO classification as a specific entity[2] This tumor develops in the context of long standing inflammation associated most frequently with EBV infection.[2,4] Most cases of DLBLC-ACI have been described in patients with pyothorax resulting from artificial pneumothorax prescribed for pleural tuberculosis.[2] DLBLC-ACI is also angiocentric and, similarly to feline injection site lymphoma, is more frequent in middle aged to old male patients and develops after a long latency period of over 10 years from terminally differentiated B cells.[2] In these instances, inflammation has been implicated in the reactivation and proliferation of EBV transformed B cells and seems to be the most accredited pathogenesis for DLBCL-ACI.[2] Chronic inflammation enables virally transformed B cells to escape from host immune surveillance trough production of IL-10 and providing autocrine and paracrine cell growth stimuli via IL-6 production. Noteworthy, also for other DLBCL occurring in settings of long standing inflammation such as osteomyelitis, metallic implants, and chronic skin ulceration, EBV positivity of neoplastic cells has been demonstrated. All the above observations parallel the finding of inflammation and concurrent FeLV positivity documented in several cases of CFIL.[17] While Feline injection site sarcoma seems not related with a specific viral etiology[10,12] the role of FeLV in lymphoma development has been well established.[11,13] Overall, approximately 70 percent of cats with lymphoma have FeLV antigenemia. Rate of FeLV serological positivity has been correlated with the anatomical form of lymphoma with percentages of positive cats maximal for mediastinal lymphoma (90%) and multicentric lymphoma (80%) and decreasing to less than 10% for cutaneous lymphoma.[11,13]

In feline injection site lymphomas, expression of FeLV p27 capsidic and gp70 envelope proteins has been detected in neoplastic cells.[13] Expression of p27 indicates that viral infection has occurred but does not confirm viral assembly (nonproductive infection) thus, p27 detection

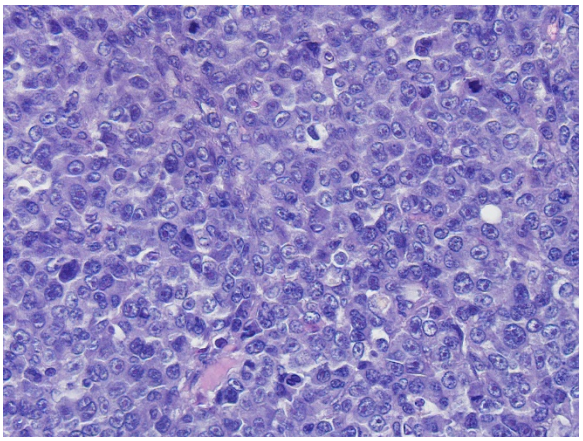

Hared skin and subcutis, cat: High magnification of neoplastic cells reveals a diffuse infiltrate numerous large neoplastic lymphocytes with a high mitotic rate. Unfortunately, unstained slides were not available for immunophenotyping, and immunophenotyping results were not included by the contributor. (HE, 4X)

does not imply that FeLV infection is in progress. Gp70 expression denotes viral particle assembly confirming viral integration, viral replication and productive infection.[20] In FeLV latent infection, cats are seronegative but FeLV provirus has been demonstrated in peripheral blood and bone marrow cells by PCR. Thus, old seronegative cats may still bear the virus in their genome, but the virus may be inserted and not transcribed until reactivation and/or neoplastic transformation of infected cells occurs. Like what is described for DLBCL-ACI in man, chronic inflammation elicited by the injection may have contributed to FeLV reactivation and transcription with neoplastic transformation of lymphoid cells. The most likely hypothesis linking persistent antigenic stimulation with chronic inflammation and lymphoma development derives from the nature of the lymphoid proliferation. During chronic antigenic stimulation, lymphoid cell proliferation and gene rearrangements of TCR and BCR increase with increasing production of normal cells or cells with genetic mutations or translocations.

JPC Diagnosis: Haired skin (not present on all sections) and subcutis: Lymphoma with angioinvasion, angiodestruction, and coagulative necrosis, European domestic shorthair (*Felis catus*), feline.

Conference Comment: Throughout the 20th century, lymphomas in domestic animals were classified based on the non-Hodgkin lymphoma classification system in humans. The Rappaport classification, designed in 1966, was one of the earliest systems used in veterinary medicine, especially the dog. This system was based solely on morphologic characteristics (which fallaciously classified many large cell lymphomas as histiocytic). It wasn't until the advancement of immunohistochemical practices that classification systems were again updated. The Lukes-Collins (North America) and Kiel (Europe) classification systems were published based on immunologic more than morphologic concepts, but often yielded different diagnoses. To unify lymphoma classification, in 1982, the National Cancer Institute initiated a broad study oriented on clinical outcome rather than morphologic features and published the Working Formulation. This classification system was even more unreliable because survival times were based on human clinical trials. Finally, an updated Kiel classification was produced which until recently was the most useful prognostic tool for canine malignant lymphomas.[22]

The current system used is based on the WHO classification system for hema-topoietic neoplasms which has been applied to lymphomas in multiple veterinary species. These classification schemes characterized each type of lymphoma as a specific disease entity. The WHO classification for lymphoma diagnosis in domestic animals entails grouping subtypes based on pattern (diffuse or nodular), cell size, grade,

postulated normal cell counterpart, and defining histopathologic features.[1,22] Cell size is determined based on the size of a red blood cell (RBC) with large lymphocytes being greater than twice the size of an RBC, intermediate lymphocytes being 1.5 times the size of an RBC, and small lymphocytes being 1 to 1.25 times the size of an RBC. Grade is determined by the mitotic count per 400x field with indolent being 0-1/HPF, low grade being 2-5/HPF, medium 6-10/HPF, and high greater than 10 mitotic figures per 400x HPF. Cell size can be difficult to appreciate, secondarily, chromatin pattern can be used to distinguish between different forms of lymphoma. For example, small cell lymphomas have very dense chromatin and intermediate in a few subtypes have prominent nucleoli (Burkitt-like subtype) whereas others have hazy chromatin with indistinct nucleoli (lymphoblastic lymphomas). Immunohistochemically, there are several available B-cell markers (e.g CD20, CD79a or b, Pax5), and it is optimal to use more than one in order to capture the distinct maturation phases of B-cells. CD3 is an excellent pan-T-cell marker. It is important to note that PARR is a genotyping test for clonality, and must always be run in concurrence with immunophenotyping protocols (e.g. IHC, ICC, flow cytometry).

The moderator briefly discussed cancer arising in an inflammatory background. Inflammation is causally related to cancer via: genotoxicity, aberrant tissue repair, proliferative responses, invasion, and metastasis. For example, STAT3 and NF-kB pathways are involved in diffuse large B-cell lymphoma oncogenesis. Additionally, tumor cells secrete soluble growth factors, and render inflammatory cells suppressive against host immune responses. Finally, some microbial organisms are causative agents of cancer inducing inflammation, and commensal microbiota, if altered, can predispose to neoplastic transformation.[3]

Unfortunately, the unstained slides submitted contained a different tissue than what was submitted on H&E with the tumor. We were therefore unable to fully subtype the lymphoma in this case.

Contributing Institution:
DIMEVET, Faculty of Veterinary Medicine of Milan, Italy
http://www.dimevet.unimi.it/ecm/home

References:

1. Boes KM, Durham AC. Bone Marrow, blood cells, and the lymphoid/lymphatic system. In: Zachary JF, ed. *Pathological Basis of Veterinary Disease.* 6th ed. Philadelphia, PA: Mosby Elsevier Inc.; 2017:724-803.
2. Chan JKC, Aozasa K, Gaulard P. DLBCL associated with chronic inflammation. In: Swerdlow SH, Campo E, Harris NL, et al, eds. *WHO Classification of Tumors of Haematopoietic and Lymphoid Tissues*. Lyon, France: IARC Press; 2008: 245-246.
3. Elinav E, Nowarski R, Thaiss CA, Hu B, Jin C, Flavell RA. Inflammation-induced cancer: crosstalk between tumours, immune cells, and microorganisms. *Nat Rev Cancer*. 2013;13(11):759-771.
4. Engels EA. Infectious agents as causes of non-Hodgkin lymphoma. *Cancer Epidemiol Biomarkers Prev*. 2007 Mar;16(3):401-404.
5. Ferreri AJM, Ernberg I, Copie-Bergman C. Infectious agents and lymphoma development: molecular and clinical aspects. *J Internal Med*. 2009;265(4)**:** 421-438.
6. Gilbert S, Affolter VK, Gross TL, Moore PF, Ihrke PJ. Clinical, morphological and immunohistochemical characterization of

cutaneous lymphocytosis in 23 cats. *Vet Dermatol.* 2004;15(1): 3-12.
7. Gilbert S, Affolter VK, Schmidt P, et al. Clonality studies of feline cutaneous lymphocytosis. *Vet Dermatol.* 2004*;* 15 (Suppl 1): 24.
8. Grivennikov SI, Greten FR, Karin M. Immunity, inflammation, and cancer. *Cell. 2010;*140(6)**:** 883-899.
9. Grivennikov SI, Karin M. Inflammation and oncogenesis: a vicious connection. *Curr Opin Genet Dev.* 2010; 20(1):65-71.
10. Gross TL, Ihrke PJ, Walder EJ, Affolter VK. Lymphocytic tumors. In: *Skin Diseases of the Dog and Cat: Clinical and Histopathologic Diagnosis*. 2nd ed. Oxford, UK: Blackwell Science Ltd.; 2005:866-893.
11. Jacobs RM, Messick JB, Valli VE. Tumors of the hemolymphatic system. In: *Lymphoid tumors*. 4th ed. Ames, IA, USA: Iowa State Press; 2002:119-198.
12. Kidney BA. Role of inflammation/wound healing in feline oncogenensis: a commentary. *J Feline Med Surg*. 2008;10(2): 107-108.
13. Louwerens M, London CA, Pedersen NC, Lyons LA: Feline lymphoma in the post-feline leukemia virus era. *J Vet Intern Med.* 2005;**19:** 329-335.
14. Madewell BR, Gieger TL, Pesavento PA, Kent MS. Vaccine site-associated sarcoma and malignant lymphoma in cats: a report of six cases (1997-2002). *J Am Anim Hosp Assoc*. 2004;40(1): 47-50.
15. Meichner K, von Bomhard W. Patient characteristics, histopathological findings and outcome in 97 cats with extranodal subcutaneous lymphoma (2007-2011). *Vet Comp Oncol*. 14 (S1), 8–20.
16. Metgud RS, Doshi JJ, Gaurkhede S, Dongre R, Karle R: Extranodal NK/T-cell lymphoma, nasal type (angiocentric T-cell lymphoma): A review about the terminology. *J Oral Maxillofac Pathol.* 2011;15**:** 96-100.
17. Roccabianca P, Avallone G, Rodriguez A, Crippa L, Lepri E, Giudice C, Caniatti M, Moore PF, Affolter VK. Cutaneous lymphoma at injection site: pathological, immunophenotypical, and molecular characterization in 17 cats. *Vet Pathol.* 2016;53(4):823-832.
18. Savage KJ, Harris NL, Vose JM, Ullrich F, Jaffe ES, Connors JM, Rimsza L, Pileri SA, Chhanabhai M, Gascoyne RD, Armitage JO, Weisenburger DD. International peripheral T-cell lymphoma project. ALK- anaplastic large-cell lymphoma is clinically and immunophenotypically different from both ALK+ ALCL and peripheral T-cell lymphoma, not otherwise specified: report from the International Peripheral T-Cell Lymphoma Project. *Blood.* 2008;111: 5496-5504.
19. Stein H, Warnke R, Chan W, Jaffe E, Chan J, Gatter K, Campo E. Diffuse large B-cell lymphoma, not otherwise specified. In: Swerdlow SH, Campo E, Harris NL, et al, eds. *WHO Classification of Tumors of Haematopoietic and Lymphoid Tissues*. Lyon, France: IARC Press; 2008: 233-237.
20. Suntz M, Failing K, Hecht W, Schwartz D, Reinacher M. High prevalence of non-productive FeLV infection in necropsied cats and significant association with pathological findings. *Vet Immunol Immunopathol*. 2010;136(1-2): 71-80.
21. Valli VE, Jacobs RM, Norris A, et al. The histologic classification of 602 cases of feline lymphoproliferative disease using the National Cancer Institute working formulation. *J Vet Diagn Invest.* 2000;12(4): 295-306.
22. Valli VEO, Kiupel M, Bienzle D, Wood DR. Hematopoietic System. In: Maxie MG, ed. *Jubb, Kennedy and Palmer's Pathology of Domestic Animals*. Vol 3.

6th ed. Philadelphia, PA: Elsevier Saunders; 2016:103-267.
23. Valli V. *Veterinary Comparative Hematopathology*. Ames, IA: Blackwell publishing; 2007.

Self-Assessment - WSC 2017-2018 Conference 22

1. Which of the following is the best location for identifying changes associated with grass sickness in horses?
    a. Duodenum
    b. Jejunum
    c. Ileum
    d. Cecum

2. Which of the following is the most common subtype of lymphoma in the horse?
    a. Diffuse B cell lymphoma
    b. T-cell rich B-cell lymphoma
    c. LGL lymphoma
    d. T-zone lymphoma

3. Which of the following is true concerning primary central nervous system lymphoma?
    a. Most of the reported cases in animals are of T-cell origin.
    b. In humans, they are classified as Hodgkin-type lymphomas.
    c. Secondary CNS lymphomas are more common.
    d. Human primary central nervous system lymphomas are rarely angiocentric.

4. Primary intravascular lymphomas in animals are generally of what celltype?
    a. T-cell
    b. B-cell
    c. NK cell
    d. Non-T, non-B cell

5. Which of the following has NOT been associated with the development of sarcomas in cats?
    a. Implantation of microchips
    b. Injection of long-acting steroids
    c. Trauma
    d. Dental procedures

Please email your completed assessment to Ms. Jessica Gold at Jessica.d.gold2.ctr@mail.mil for grading. Passing score is 80%.This program (RACE program number) is approved by the AAVSB RACE to offer a total of 0.5 CE Credits, with a maximum of 12.5 CE Credits being available to any individual Veterinary Medical Professionals for the 2017-2018 Wednesday Slide Conference. This RACE approval is for the subject matter categories of: SCIENTIFIC using the delivery method of NON-INTERACTIVE DISTANCE. This approval is valid in jurisdictions which recognize AAVSB RACE; however, participants are responsible for ascertaining each board's CE requirements.
RACE does not "accredit", "endorse" or "certify" any program or person, nor does RACE approval validate the content of the program.

Joint Pathology Center
Veterinary Pathology Services

WEDNESDAY SLIDE CONFERENCE 2017-2018

C o n f e r e n c e 23

25 April 2018

Julie Engiles VMD, DACVP
Associate Professor of Pathology
Department of Pathobiology- New Bolton Center Murphy Laboratory
382 West Street Road
Kennett Square, PA 19348

CASE I: 164361-16 (JPC 4100935).

Signalment: 3-year-old, male, castrated, Doberman pinscher (*Canis familiaris*), canine.

History: The patient presented to Cornell University Hospital for Animals (CUHA) Emergency Service for respiratory distress. Nine months prior, he had been evaluated for bilateral swollen carpi and radiographs revealed an aggressive bone lesion; the carpi became progressively worse leading to forelimb lameness, coughing, sneezing and epistaxis. The patient was administered diphenhydramine, 1.25 mg/kg (0.56 mg/lb), PO, q 12 h, as needed and amoxicillin, 25 mg/kg (11.36 mg/lb), PO, q 12 h, for 30 days. Cytological examination of a needle aspirate from an enlarged popliteal lymph node revealed histiocytic inflammation. The patient was administered prednisone, 0.5 mg/kg (0.22 mg/lb), PO, q 12 h for 7 days, then 0.5 mg/kg (0.22 mg/lb), PO, q 24 h for 14 days and doxycycline, 5 mg/kg (0.22 mg/lb), PO, q 12 h for 30 days. Because the carpal swelling continued to increase, the dose of prednisone was increased to 1 mg/kg (0.45 mg/lb), PO, q 12 h, at which point the respiratory signs worsened. Bronchoscopy showed inflamed, hemorrhagic bronchi, and radiographs showed progressive bilateral periosteal reaction and lytic lesions of the right and left distal radius and ulna, and a severe generalized miliary nodular lung pattern.

Radius, dog. The distal radius was expanded up to 5cm with loss of cortical bone.(HE, 4X) (Photo courtesy of: Cornell University School of Veterinary Medicine, Department of Biosciences, 240 Farrier Road, Ithaca, NY 14853, http://www.vet.cornell.edu/biosci/pathology/)

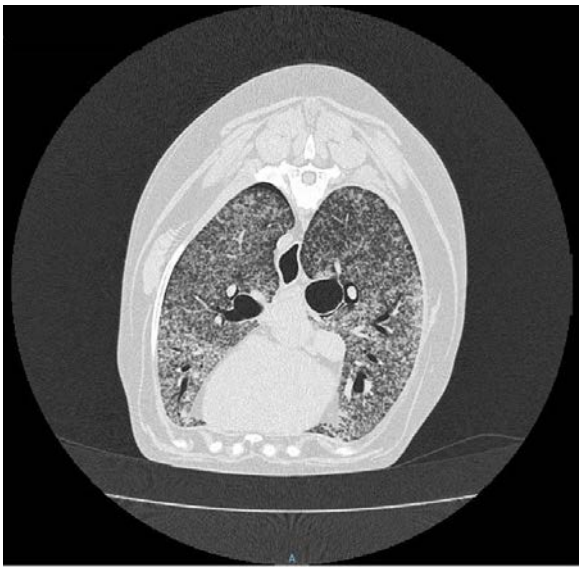

Computed tomography, lungs, dog. A CT scan of the lungs demonstrates a generalized bilateral military nodular pattern. (Photo courtesy of: Cornell University School of Veterinary Medicine, Department of Biosciences, 240 Farrier Road, Ithaca, NY 14853, http://www.vet.cornell.edu/biosci/pathology/)

Gross Pathology: Prior to post-mortem examination, educational computed tomography (CT) scans were recorded of the head, neck and thorax and confirmed the bilateral, generalized miliary nodular pattern within the lungs. The CTs also revealed periosteal new bone formation on the calvaria.

At necropsy, the dog was in good body condition (4 out of 9, Purina scale) with mild postmortem autolysis. Bilaterally, the carpal joints were severely enlarged, with the left being worse than the right. Both carpal joints were hard with focal, soft, depressed areas. On the medial aspect of the right carpus, there was a 0.6 cm diameter full-thickness defect containing 0.1 mL of creamy, soft material (draining tract). Bilaterally, the skeletal musculature of the brachium, predominantly the triceps brachii, was less prominent (atrophy). The left popliteal lymph node was firm.

The lungs were diffusely mottled dark red and light pink, failed to collapse and mildly firm (interstitial pneumonia). Diffusely throughout the lungs were dozens of miliary, white-tan foci that extended into the parenchyma. The trachea contained approximately 2 mL of frothy, red fluid. On cut section, the large airways oozed a small amount of cloudy red to gray mucoid material (exudate).

Bilaterally, the distal one-third of the radius and ulna were expanded approximately 7 cm in diameter on the left and 5 cm in diameter on the right. On cut section, the right and left carpal joints exuded approximately 1 mL of viscous, brown, cloudy fluid (suppurative synovitis and periarthritis). The periarticular fascia on the medial aspect of the right and left carpi had cystic spaces filled with similar brown, cloudy fluid. On sagittal section, the periosteum of the distal one-third of the radius, ulna and carpal bones was gradually expanded towards the carpal joint up to 1.7

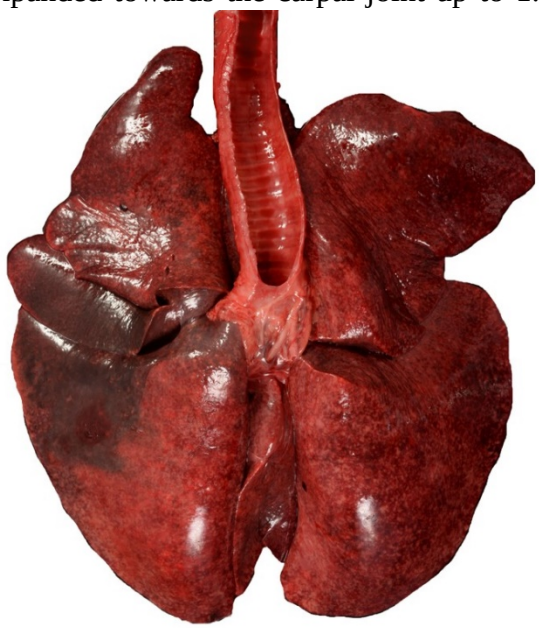

Lung, dog. The lungs were mottled, failed to collapse and contain numerous granulomas throughout the parenchyma. (Photo courtesy of: Cornell University School of Veterinary Medicine, Department of Biosciences, 240 Farrier Road, Ithaca, NY 14853, http://www.vet.cornell.edu/biosci/pathology/)

cm thick. The outer cortical surface was rough and uneven.

Laboratory Results (clinical pathology, microbiology, PCR, ELISA, etc.):
Blastomyces dermatitidis was partially cultured from lung tissue (culture was not finalized due to human health risks). *Blastomyces dermatitidis* infection was confirmed by PCR of the lung tissue.

Microscopic Description:
The cortical bone is expanded by numerous cavities filled with numerous macrophages together with fewer multinucleated giant cells, and rare lymphocytes (osteomyelitis). The inflammatory infiltrate varies, with multiple clusters of neutrophils and degenerated neutrophils in random areas. In multiple areas, the inflammatory cells are centered upon variable size islands of an intensely eosinophilic to magenta, acellular material, with indistinct margins (bone necrosis). The cortical bone is covered by an expanded layer of woven bone that is incompletely mineralized (periosteal reaction) and contains numerous osteocytes. The immature woven bone is lined by a single layer of plump osteoblasts (reactive). Frequently, the edges of the woven bone are scalloped, irregular with adjacent osteoclasts (Howship's lacunae). Randomly scattered in the inflammatory infiltrate are numerous intrahistiocytic and extracellular, 8-20 µm in diameter, round yeast-like organisms with a 2-3 µm thick, clear to lightly basophilic, refractile capsule. The yeast-like organisms frequently exhibit broad-based budding consistent with *Blastomyces spp*. The inflammatory infiltrate extends to the bone marrow spaces and dissects through the periosteal reaction and adjacent skeletal muscles (myositis).

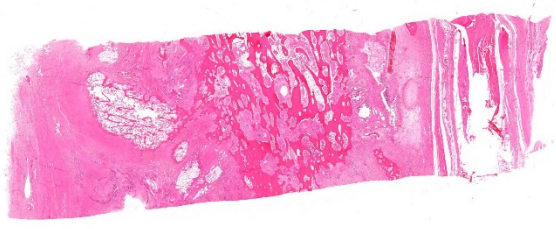

Radius, dog. There is diffuse loss of cortical bone with marked proliferation of anastomosing trabeculae of woven bone and extensive inflammation that extends into the surrounding soft tissue. (HE, 6X)

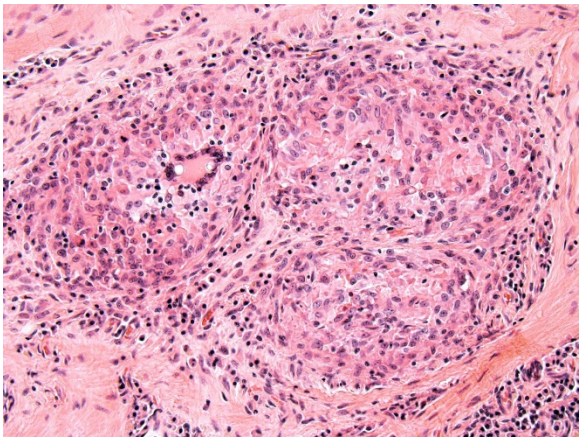

Radius, dog. Numerous poorly formed granulomas populate the bone and adjacent soft tissue. Rare multinucleated giant cell macrophages contain yeasts (arrows). (HE, 200X)

Contributor's Morphologic Diagnosis:
Pyogranulomatous osteomyelitis and myositis, with bone necrosis, woven bone deposition and yeasts consistent with *Blastomyces spp*.

Contributor's Comment: This is a classic case of disseminated blastomycosis caused by infection with *Blastomyces dermatitidis* with severe lung and skeletal involvement. Additionally, histopathology examination of the heart revealed severe, multifocal, chronic degeneration and necrosis of cardiomyocytes with dystrophic mineralization, suggestive of hypoxia attributable to the severe pneumonia. Histopathology examination of decalcified sections of distal radius/ulna and calvaria revealed a severe, chronic osteomyelitis with large numbers of yeast organisms, consistent

with disseminated blastomycosis. Histochemical staining of lung sections using periodic acid-Schiff and Grocott-Gomori's methenamine silver further highlighted the yeast organisms.

Although the classic presentation for fungal pneumonia on radiographs is a generalized, random, miliary nodular pattern, blasto-mycosis can have various presentations ranging from multiple pulmonary nodules, patchy or lobar lung consolidation (alveolar pattern), to a solitary pulmonary mass.[3] Histopathology ruled out other potential causes of pulmonary nodules, such as neoplasia and infection with other mycoses including *Coccidioides immitis*, *Cryptococcus neoformans*, and *Histoplasma capsulatum*.

Blastomycosis is one of the most common systemic mycotic infection of dogs that live in endemic areas including the Ohio and Missouri river valleys, the southern Great Lakes, and southern mid-Atlantic states.[4] In the state of New York, the incidence of blastomycosis in dogs has increased over the past 20 years and is endemic in the Adirondacks where this dog lived.[5] Blastomycosis occurs in dogs and humans and is rare in other animals. Young, male, intact dogs living in endemic areas are at an increased risk of becoming infected.[5] Sporting dogs such as Labrador and Golden retrievers and Doberman Pinschers are more frequently affected.[6,7]

Blastomyces dermatitidis is a saprophytic fungus found in moist acidic or sandy soil, with high organic content.[6] It is a thermally dimorphic fungus, that forms septated mycelia in the environment, but becomes yeast in infected tissues. In its mycelial form, it produces conidia (spores) that are inhaled by the host and then phagocytized by alveolar macrophages.[7] In the presence of higher body temperature, spores become yeast with thick double-contoured outer walls and characteristic broad-based budding.[6,7] The yeast causes local suppurative to pyogranulomatous inflammatory response, which may be self-limiting.[8] However, phagocytized yeasts can be transported into the pulmonary interstitium where they can disseminate hematogenously or through the lymphatic system to other organs.[8] Inoculation directly through a skin wound is also possible, but rare.[8] By contrast with other mycotic diseases such as *Coccidioides immitis* and *Aspergillus sp.* where infectious spores can be easily aerosolized from infected tissues and transmit the disease, the yeasts of *B. dermatitidis* are not infective, and thus, do not require special biosafety precautions during necropsy.

Clinical signs with blastomycosis depend on the organ system most severely affected; however, respiratory signs is the most common clinical presentation.[7,8] In dogs, *B. dermatitidis* often disseminates to the lungs, lymph nodes, skin, eyes, bones, reproductive system, and nervous system.[8] Lameness caused by osteomyelitis or paronychia is reported in 25% of dogs with blastomycosis, and fungal osteomyelitis in 10-15% of cases.

Itraconazole is the treatment of choice at a dosage of 5 mg/kg (2.27 mg/lb) every 24 hours for 60 days. Treatment should be continued for 30-60 days after resolution of clinical signs. Clinical signs often become more severe in the early phase of treatment, as the yeast organisms die off and elicit severe inflammation.[8] Prognosis for blastomycosis is good if severe pulmonary or CNS involvement is not present. Relapse is possible in dogs with initially severe clinical disease or in dogs treated for an insufficient length of time. Prolonged administration of prednisone might have contributed to the severe disseminated disease seen in this case.

JPC Diagnosis: Bone: Osteomyelitis, pyogranulomatous, diffuse, severe with marked cortical and trabecular osteolysis and numerous yeasts, Doberman pinscher (*Canis familiaris*), canine.

Conference Comment: Generally, bacterial osteomyelitis is more common than fungal, but there are three dimorphic fungi that can affect bone: (1) *Blastomyces dermatitidis*, (2) *Coccidioides immitis*, and (3) *Cryptococcus neoformans*. These three are dimorphic fungi, meaning they are in the filamentous form in the environment and yeast form in tissues. *Blastomyces dermatitidis* is fully described by the contributor above.[1,2]

Coccidioides immitis, an endosporulator, is a common inhabitant of the desert climates in the southwestern United States, areas of Mexico, Central, and South America and is transmitted primarily by inhalation of arthroconidia (spores). Once at body temperature, the spores transition into spherules (yeast form) which can migrate along the pleura creating damage by inducing production of arginase I and coccidioidal urease by host tissues. Infection can be subclinical and manifestation in bone often takes years to develop, generally long after respiratory lesions have healed. Dissemination to bone is most common in dogs with the distal diaphysis of long bones affected by isolated nodules. Spherules have an outer wall glycoprotein which acts to modulate host immune responses by compromising cell-mediated immunity and preventing phagocytosis. Grossly, coccidiomycosis forms firm, fibrous nodules often with caseating centers which microscopically are composed of granulomatous to pyogranulomatous inflammation surrounded by a thick fibrous connective tissue capsule. The fungus is often present at various stages of maturation, from the immature spherule (10-20um in diameter)

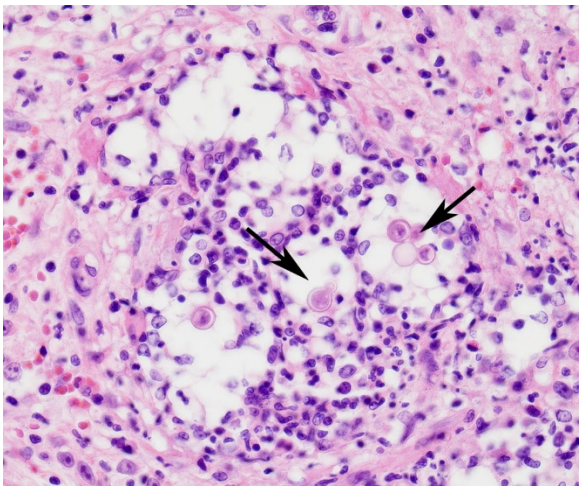

Radius, dog. Areas of pyogranulomatous inflammation within the bone also contain numerous 8-14um yeasts with a 2um hyaline wall and narrow based budding. (arrows). (HE, 400X) (Photo courtesy of: Cornell University School of Veterinary Medicine, Department of Biosciences, 240 Farrier Road, Ithaca, NY 14853, http://www.vet.cornell.edu/biosci/pathology/)

to the mature spherule (up to 200um in diameter) which typically has a double contoured wall and contains numerous endospores (2-5um in diameter). Other organisms that reproduce by endosporulation include: *Rhinosporidium seeberi*, *Prototheca* sp., *Chlorella* sp., and *Batrachochytrium dendrobatidis*.[1,2]

Cryptococcus neoformans is a common inhabitant of pigeon feces and soil which typically affects immunocompetent cats and dogs (cats more so) with transmission via inhalation and primary lesions in the lungs and nasal cavity. In cats, osteolytic lesions occur in the bones of the maxilla with soft tissue swellings over the bridge of the nose. Grossly, lesions appear gelatinous or cyst-like. Microscopically, there are numerous yeast which exhibit narrow based budding, with thick heteropolysaccharide capsules which form a clear halo and characteristic "soap bubble" appearance. Their mucopolysaccharide capsules stain positive with Mayer's mucicarmine and Alcian blue. Inflammation is scarce in these lesions due to

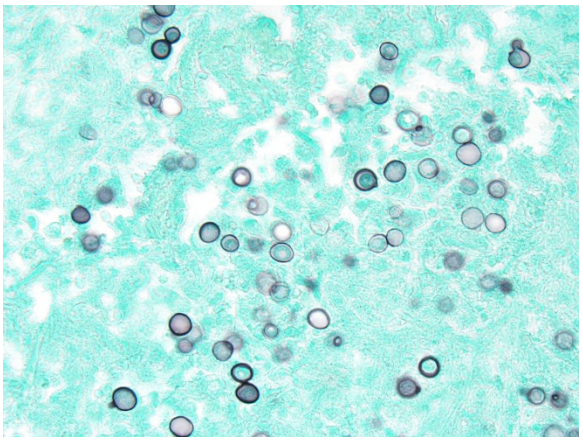

Radius, dog. A silver stain easily discloses large numbers of budding yeasts within the section. (Gomori methenamine silver, 400X)

the action of multiple virulence factors. The polysaccharide (glucuronoxylomannin) capsule prevents phagocytosis as well as inhibiting migration and recruitment of inflammatory cells. Additionally, an enzyme called laccase is produced which forms a melanin-like pigment that acts as an antioxidant. Two other enzymes, serine protease and urease aid in tissue invasion and promote sequestration in microcapillaries, respectively.[1,2]

During the conference, the moderator pointed out the marked loss of cortical bone which had been remodeled by osteoclasts, resulting in a trabecular appearance. Osteoclasts are of monocyte-macrophage lineage and many granulomatous reactions affecting bone result in marked bone loss and remodeling through osteoclastic activation.

Radiographically, osteosarcoma and granulomatous inflammation may appear very similar. A key difference identified by the moderator is that infectious organisms usually cross the joint with abrupt transition from lesion to normal bone, whereas most neoplastic processes generally do not cross joints and have a longer zone of transition from lesion to normal. Additionally, clinically neoplasia is generally one large mass, whereas, with infectious organisms several joints may be infected. Radiographic interpretation and clinical history is essential for accurate histologic diagnosis.

Contributing Institution:
http://vet.cornell.edu/biosci/pathology/

References:

1. Caswell JL, Williams KJ. The respiratory system. In: Maxie MG, ed. *Jubb, Kennedy, and Palmer's Pathology of Domestic Animals*, Vol 2, 6th ed. St. Louis, MO: Elsevier; 2016:582-584.
2. Craig LE, Dittmer KE, Thompson KG. Bones and joints. In: Maxie MG, ed. *Jubb, Kennedy, and Palmer's Pathology of Domestic Animals*, Vol 2, 6th ed. St. Louis, MO: Elsevier; 2016:103-104.
3. Crews JL, Feeney DA, Jessen CR, et al. Radiographic findings in dogs with pulmonary blastomycosis: 125 cases (1989–2006). *J Am Vet Med Assoc*. 2008; 232(2):215-221.
4. Bromel C, Sykes JE. Epidemiology, diagnosis, and treatment of Blastomycosis in dogs and cats. *Clin Tech Small Anim Pract*. 2005; 20(4):233-239.
5. Cote E, Barr SC, Allen C, et al. Blastomycosis in six dogs in New York State. *J Am Vet Med Assoc*. 1997; 210(4):502-504.
6. Woods KS., Barry M, Richardson D. Carpal intra-articular blastomycosis in a Labrador retriever. *Can Vet J*. 2013; 54:167–170.
7. Taboada J, Grooters AM. Systemic Mycoses. In: Ettinger SJ, Feldman EC, eds. *Textbook of Veterinary Internal Medicine*. 6th ed. St. Louis, MO: Saunders Elsevier; 2005:671-690.
8. Legendre AM. Blastomycosis. In: Green CE, ed. *Infectious Diseases of the Dog*

and Cat. 3rd ed. St Louis, MO: Elsevier Inc.; 2006:569-576.

CASE II: UFMG 247/12 (JPC 4018791).

Signalment: 9-month-old, male, mixed breed (*Felis catus*), feline.

History: Initially this cat had a history of lameness of the right hind limb. The owner reported that the lameness started after a surgical procedure (orchiectomy) five months ago. Some days later, the cat returned to the same clinic where the orchiectomy had been performed. The right hid limb of this animal was subjected to radiography (craniocaudal and mediocaudal), and periosteal thickening of the metaphysis of the tibia was observed. Prednisone and enrofloxacin were prescribed, but improvement was not observed. After 50 days, two draining fistulae were observed on the medial tibia and topic rifamycin was prescribed. Fifteen days later, more draining fistulae were detected, and treatment with prednisone and enrofloxacin was reinitiated. Due to poor response to therapy and progressive weight loss, the cat was submitted to the veterinary hospital at the Universidade Federal de Minas Gerais (UFMG). On the clinical examination, the cat had temperature of 39ºC, regular body condition and the right tibia was diffusely thickned. Radiography was performed, and blood was collected for hemogram and biochemical analysis. Radiography revealed marked changes in the metaphysis and diaphysis of the right tibia. Changes were characterized by extensive loss of cortical bone and replacement by irregular and disorganized bone. There was no cortex-medullar definition and irregular radiodensity (osteoproliferation) was observed within marrow bone. In addition, marked periosteal reaction and thickening of the soft tissues lateral to the tibia were observed (Figure 1). Considering the presence of deep dermatitis, myositis, and involvement of the marrow bone (probably osteomyelitis), another therapy was attempted. A treatment with cefazolin, meloxicam, cefovecin sodium, tramadol, and fluid therapy was prescribed. After four days, a new blood test was performed, exudate was collected for bacteriological examination, and a surgical curettage was performed. The cat responded poorly to treatment, and a new blood test did not indicate any recovery. Due

Tibia, cat. A prominent proliferative and lytic lesion extends along the length of the tibia with loss of cortical outline, as well as cortical and medullary differentiation. (Photo courtesy of Universidade Federal de Minas Gerais, Escola de Veterinária, Departamento de Clínica e Cirurgia Veterinárias, Av. Antônio Carlos, 6627; 31270-901. Belo Horizonte, MG, Brazil – www.vet.ufmg.br)

to unfavorable prognosis, amputation of the referred right hid limb was performed. One week after amputation, the clinical condition improved notably and no sign of disease was detected again.

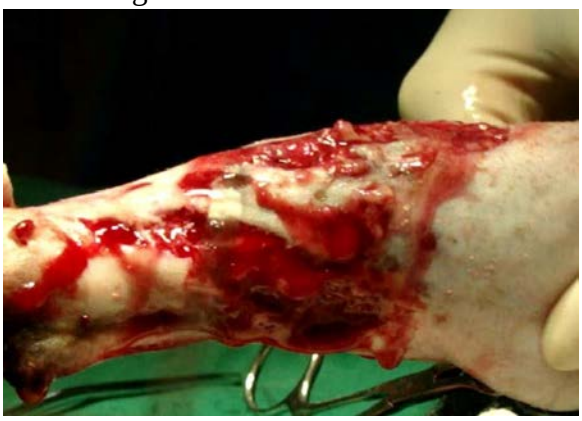

Tibia, cat. The skin along right tibia is multifocally to ulcerated and a red exudate is observed in the underlying subcutis and underlying muscle. (Photo courtesy of Universidade Federal de Minas Gerais, Escola de Veterinária, Departamento de Clínica e Cirurgia Veterinárias, Av. Antônio Carlos, 6627; 31270-901. Belo Horizonte, MG, Brazil – www.vet.ufmg.br)

Gross Pathology: Grossly, the skin along right tibia was intensely and multifocally to coalescing ulcerated. A reddish-yellow viscous exudate was observed in the subcutis and muscles (Figure 2). The right tibia was enlarged with moderate new bone formation along the metaphysis and diaphysis. Longitudinal and transverse sections showed loss of the medullary cavity and replacement with white and firm woven bone with scattered yellowish-white and granular material. There was no evidence of differentiation between medullary cavity and cortical bone.

Laboratory Results (clinical pathology, microbiology, PCR, ELISA, etc.):

Clinical pathology:

- CBC two weeks prior amputation: 4,6 Hgb, 17,0 Hct, 4,0 RBC, 86/34.744 Seg, 08/ 3232 Lym, 03/1212 Mno.
- CBC one day prior amputation: 6,7 Hgb, 24,0 Hct, 6,0 RBC, 90/28.630 Seg, 07/ 1.449 Lym, 01/207 Mno.
- No changes were detected in the biochemical profile.

Microbiology: *Pseudomonas aeruginosa* was isolated from draining purulent exudate.

Microscopic Description: Histologically, the skin was extensively ulcerated and replaced by many neutrophils and cellular debris. In the subjacent dermis, there was multifocal mature granulation tissue and numerous neutrophils and macrophages. Deep in the dermis, multifocal variably-sized areas with colonies of bacteria surrounding by neutrophils, macrophages and giant multinucleated cells are found and irregular format with basophilic centers and eosinophilic filamentous radiating aggregates in the periphery (Splendore-Hoeppli phenomenon). Adjacent to the pyogranulomatous reaction, connective fibrous tissue and neovascularization were observed. The reaction invaded the hypodermis and muscular fascia. Where the infection reaches the muscles, marked necrosis and loss of muscular fibers could be seen. The periosteum of the tibia was thickened due to marked fibrous tissue

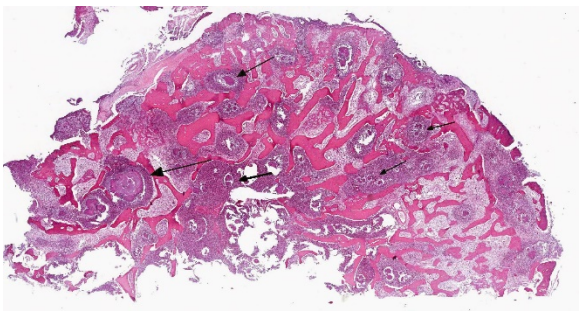

Tibia, cat: A cross section of the tibia is present with areas of trabecular lysis, formation of anastomosing woven bone, and an almost total loss of lamellar cortical bone. An inflammatory infiltrated is present between trabeculae and is centered on variably-sized bacterial colonies (arrows). (HE, 144X)

proliferation and inflammation. The compact bone of cortical was multifocally replaced by an inflammatory reaction and trabecular bone. The Harvey's canals were expanded and there was bone necrosis (loss of osteocytes) and reabsorption. The marrow bone was replaced by multiple Splendore-Hoppli reactions surrounding by neutrophils and giant cells (several containing 20 to 60 nuclei). Many foamy macrophages were infiltrating interconnected trabecular bone containing few osteoblast cells and no mineralized osteoid layer. Multifocal areas with new endosteal bone forming a network were found among remnants trabeculae. Thromboses were observed in the periosteal layer in some slides. Popliteal lymph node presented marked cortical lymphoid hyperplasia. Within lymphatic sinuses, numerous macrophages and giant cells with foamy cytoplasm were observed. Selected tissues from tibia, lymph node and adjacent muscles were subjected at Good Pasture, Giemsa, periodic acid – Schiff (PAS), Ziehl Neelsen and Grocott's methenamine silver (GMS) special stains. Good Pasture stained Gram-positive bacteria within colonies in the marrow bone, periosteum, muscles, fascia, skin and lymph node. A Goodpasture gram stain revealed many coccobacteria grouped in the central area or associated to the filamentous radially arranged material. In the periphery of reaction, cocci grouped in pairs or single chains could be seen. No organisms were identified in identical tissue sections stained by all others special stains aforementioned.

Contributor's Morphologic Diagnosis:

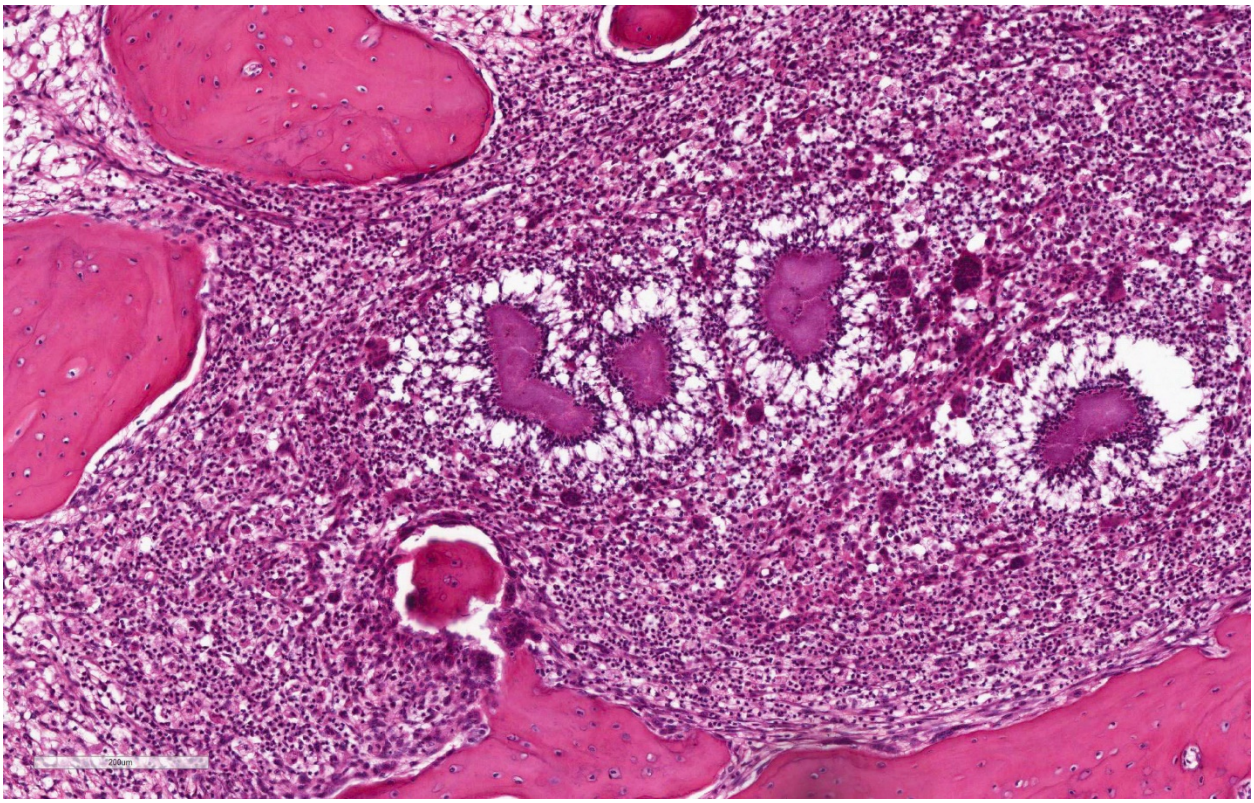

Tibia, cat: Bacterial colonies are surrounded by a layer of neutrophis, and the intertrabecular spaces are filled with numerous neutrophils, epithelioid macrophages, lymphocytes and few plasma cells. Osteoclasts are present within the exudate at a distance from trabeculae, which have numerous reversal lines. (HE, 144X)

1. Bone (tibia): Marked diffuse pyogranulomatous periostitis, osteomyelitis, and marrow osteoproliferation associated with numerous granule formation (Splendore-Hoeppli phenomenon), and multifocal cortical loss, reabsorption, fibroplasia and new endosteal bone formation.
2. Skin and muscles (not included): Marked multifocal to coalescing pyogranulomatous and necrotic dermatitis and myositis associated with numerous granule formation (Splendore-Hoeppli phenomenon)

Contributor's Comment: Bacterial pseudomycetoma (botryomycosis) is a pyogranulomatous skin disease characterized by an unusual, presumed immunologic, reaction to nonfilamentous bacteria[4]. Some specific bacteria elicit Splendore-Hoeppli reaction (an antigen-antibody complex), which are characterized by the presence of radiating, club-shaped eosinophilic material around infectious and non-infectious agents[6]. Grossly, purulent material discharged from fistulae frequently contains white to yellow sand-like granules[3]. The antigen-antibody complex, morphologically unique reaction, was first described in sporotrichosis by Splendore and is schistosomiasis by Hoeppli[6]. Splendore-Hoeppli reaction can be caused by filamentous bacteria including *Actinomyces* spp. and *Nocardia* spp.[4]. Also, nonfilamentous bacteria including *Pseudomonas*, *Proteus*, *Eschericiha coli*[6], *Staphylococcus* and *Streptococcus*[4] are described and should be considered in the differential diagnosis. Gram's stain for bacteria can be used for differential diagnosis among Gram-positive (*Actinomyces, Nocardia, Staphylococcus, Streptococcus)* and Gram-negative (*Pseudomonas, Proteus* and *Eschericiha coli)* organisms[6]. Also, *Nocardia* spp. can be identified by Ziehl Neelsen[5], PAS and GMS stains.[3]
In cats, infectious with *Actinomyces viscosus*[8] and *Nocardia* spp.[5] were reported. However, report of nonfilamentous bacteria causing pyogranulomatous infection in the skin, muscles and bone in cats was not found.

The bacteria isolate in this case (*Pseudomonas aeruginosa*) could not be identified on special stains. Myriads of slightly elongate Gram–positive bacteria arranged in pairs or single chains were suggested of *Streptococcus* spp. infection. However, *Staphylococcus* spp. cannot be excluded. Gram-negative bacilli suggested of *Pseudomonas* spp. were not detected in all tissues evaluated.

Clinically, fungal organisms including *Microsporum canis* causing dermatophytic pseudomycetoma should be considered for differential diagnosis in cats. In fungal infection, the histopathology is very useful for differential diagnosis. Fungal hyphae are visible within granulomatous inflammation in tissue stained by hematoxilin and eosin and are strongly positive using PAS and GMS special stains.[4]

Skin and subcutaneous infections probably to develop as a result of wound contamination or trauma such as bites, lacerations, or puncture wounds with foreign bodies. Thus, infections localized in the skin and subcutis may extend deep to involve bone and muscle.[3] Bacterial infectious of bones usually originates in vascular areas of periosteum (determining periostitis) or medullary cavity (determining osteomyelitis). During bacteremia or septicemia, bacteria can become localized in many organs. In bones, there is a strong predilection for sites of active endochondral ossification within the metaphyses and epiphyses of long bones and vertebral bodies. The medullary sinusoidal

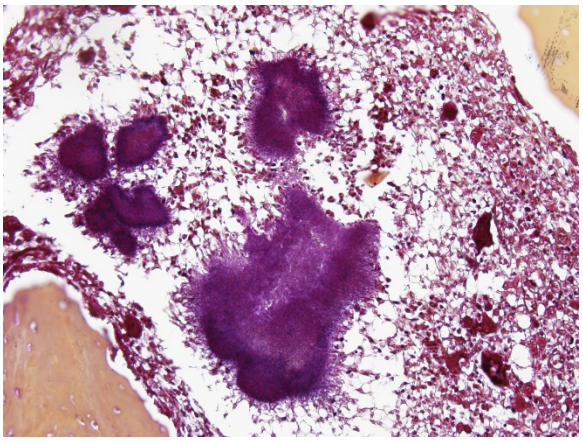

Tibia, cat: Filamentous bacilli are gram-positive. (Brown-Hopps, 400X)

capillaries are fenestrated, permitting ready escape of bacteria into the bone marrow. Thus, a combination of physeal, meta-physeal, or epiphyseal injury and concurrent bacteremia may be involved in the pathogenesis of hematogenous osteo-myelitis.[10] Probably, extension of infection to periosteum and marrow bone from adjacent tissue (skin and muscles) occurred in this animal. Indeed, evidence of other foci of infection was not detected in this cat.

Conversely, bacteria can be localized in the bone marrow and the infection can disseminate to adjacent tissues. Clinical manifestations of osteomyelitis may not develop until several months later when the bone lesion becomes extensive enough to cause pain, disfigurement of the bone, or perhaps result in pathological fracture.[10]

The recognition of reactive conditions associated with Splendore-Hoeppli reactions and differentiation among different agents (bacteria or fungi) are important to therapeutic measures. Also, aseptic collection of exudate and confidence culture following antibiogram is important to obtain success in the treatment.

JPC Diagnosis: Bone: Osteomyelitis, pyogranulomatous, chronic-active with diffuse, severe osteolysis and multifocal woven bone production with numerous colonies of filamentous bacilli, mixed breed (*Felis catus*), feline.

Conference Comment: Osteomyelitis, or inflammation of the medullary cavity and adjacent bone, is most commonly caused by bacteria (rather than fungi). Bacteria can spread to bone by three routes: (1) hematogenously, (2) local extension, or (3) implantation.[1]

Hematogenous spread is most common in young horses and ruminants with omphalophlebitis, however, these animals usually succumb to septicemia before boney lesions become evident. Bacteria seem to prefer areas of active endochondral ossification within metaphyses and epiphyses of long bones and vertebral bodies for two reasons, (1) capillaries there are fenestrated and allow bacteria to enter the bone marrow and (2) they make sharp turns within the growth plate allowing for accumulation of bacteria. Local extension is most common in older animals with severe periodontal disease and secondary bacterial spread into the maxilla and mandible, and implantation of bacteria usually results from adulteration of surgical fracture repair, bite wounds or gunshot injury, or open fractures.[1]

Certain bacteria are partial to bone, like *Staphylococcus aureus*, which invades osteoblasts, protecting it from host immune defense.[1] *Pasteurella multocida* wreaks havoc by retarding the growth and differentiation of osteoblasts and activating osteoblasts to resorption.[2] Moreover, at sites of infection, host defense mechanisms can be counter-productive, for example, cytokine production (IL-1, IL-6, TNF-α) by inflammatory cells induces osteoblasts to

activate osteoclasts to resorb bone.[1] A summary of the numerous manifestations of bacterial osteomyelitis is below for your viewing pleasure.

Table 1: Common manifestations of bacterial osteomyelitis[1]

Location	**Species affected**	**Predisposing factor**	**Route of dissemination**	**Common isolates**
Vertebral body	Horses, livestock	Inadequate passive immunity	Hematogenous (through umbilicus)	*Trueperella pyogenes* (common) Foals: *Escherichia coli, Salmonella enterica* serovar Typhimurium, staphylococci, streptococci, *Rhodococcus equi* Calves: *Fusobacterium necrophorum* Sheep: *Mannheimia haemolytica, F. necrophorum*, staphylococci Pigs: *Erysipelothrix rhusiopathiae*, staphylococci, streptococci
	Piglets, lambs	Inadequate passive immunity	Hematogenous (tail biting or docking)	
Mandible	Cattle "lumpy jaw"	Penetrating injury to oral mucosa	Implantation	*Actinomyces bovis* or *Trueperella pyogenes*
	Numerous	Periodontitis	Local extension	*Fusobacterium necrophorum*, other oral commensals
Numerous locations	Small animals	Open fractures, bite wounds, gunshot injury	Implantation	*Staphylococcus pseudointermedius*, streptococci
Nasal cavity	Pigs	Bacterial toxins	Local extension	*Pasteurella multocida* and *Bordetella bronchiseptica*

Pseudomonas aeruginosa, isolated from the purulent exudate in this case, is traditionally thought of as the causative agent of numerous dermatologic disorders, such as post-grooming furunculosis and otitis externa.[9] However, as a potent gram-negative bacterium, it can cause a myriad of clinical

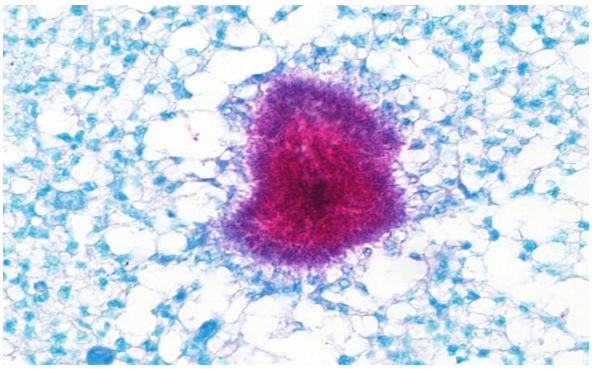

Tibia, cat: Filamentous bacilli are strongly acid-fast (Fite-Furaco, 400X)

syndromes (endometritis (mares), mastitis (cattle), pneumonia (foals and mink), enteritis (primates), and abortion and abnormal fetal development (cattle and horses)) and, in these cases, is often part of a consortium of fellow gram-negative and gram-positive bacteria.[7]

Ruleouts discussed in this case included: *Nocardia* sp. and *Actinomyces* sp. The moderator and conference attendees noted that they didn't appreciate Splendore-Hoeppli material (radiating eosinophilic club-shaped antigen-antibody protein) surrounding bacterial colonies. Gram and acid-fast stains were run to further classify the bacteria which in the submitted unstained sections appear to be gram-positive and acid-fast. In the moderator's and attendee;s cumulative experience, these organisms are most indicative of *Nocardia* sp, which we favor as the causative agent in this case.

Actinomyces sp. and *Nocardia* sp., often lumped together in textbooks, come in cutaneous, subcutaneous, and visceral forms. They generally manifest as nodular ulcerated lesions on the extremities which may arise from underlying bone and are often secondary to wound contamination. Grossly, yellow to green sulfur granules are present corresponding with microscopic aggregates of bacteria with small amounts of adherent neutrophils awash in a sea of suppurative or pyogranulomatous inflammation. Attendees agreed that the aggregates of fulamentous bacilli in these sections are strongly reminiscent of sulfur granules.

Contributing Institution:

Universidade Federal de Minas Gerais
Escola de Veterinária
Departamento de Clínica e Cirurgia Veterinárias
Av. Antônio Carlos, 6627; 31270-901.
Belo Horizonte, MG, Brazil
www.vet.ufmg.br

References:

1. Craig LE, Dittmer KE, Thompson KG. Bones and joints. In: Maxie MG, ed. *Jubb, Kennedy, and Palmer's Pathology of Domestic Animals,* Vol 2, 6th ed. St. Louis, MO: Elsevier; 2016:98-103.
2. Gwaltney SM, Galvin RJ, Register KB, Rimler RB, Ackermann MR. Effects of *Pasteurella multocida* toxin on porcine bone marrow cell differentiation into osteoclasts and osteoblasts. *Vet Pathol.* 1997; 34(5):421-430.
3. Ginn PE, Mansell JEKL, Rakich PM. Skin and appendages. In**:** Jubb, Kennedy & Palmer's Pathology of Domestic Animals, ed. Maxie MG, 5th ed., pp. 553-781, Saunders Elsevier, Toronto, Canada, 2007.
4. Gross TL, Ihrke PJ, Walder EJ, Affolter VK. Skin diseases of the dog and cat: clinical and histopathological diagnosis, second ed., p. 01 – 932, Blackwell Science, Oxford, United Kingdom, 2005.
5. Harada H, Endo Y, Sekiguchi M, Setoguchi A, Momoi Y. Cutaneous nocardiosis in a cat. J Vet Med Sci, **71**:785-787, 2009.
6. Hussein MR. Mucocutaneous Splendore-Hoeppli phenomenon. J Cutan Pathol, **35**: 979-988, 2008.

7. Kahn CM. *The Merck Veterinary Manual.* 9th ed. Whitehouse Station, NJ: Merck & Co., Inc.; 2005:422, 1132, 1544, 1550, 1753.
8. Murakami S, Yamanishi MW, Azuma R. Lymph node abscess due to *Actinomyces viscosus* in a cat. J Vet Med Sci **59**:1079-1080, 1997.
9. Tham HL, Jacob ME, Bizikova P. Molecular confirmation of shampoo as the putative source of *Pseudomonas aeruginosa*-induced postgrooming furunculosis in a dog. *Vet Dermatol.* 2016; 27(4):320-380.
10. Thompson K: Bones and joints. In: Jubb, Kennedy, and *Palmer's Pathology of Domestic Animals*, ed. Maxie MG, 5th ed., pp. 02-184, Saunders Elsevier, Toronto, Canada, 2007.

CASE III: 16-41394 (JPC 4100931).

Signalment: 14-week-old, male, intact, mixed breed (*Canis familiaris*), canine.

History: This animal had an approximately 4-week-long history of intermittent difficulty or inability to walk and/or stand, and vocalization due to pain upon light palpation. Clinical examination revealed positive deep pain on all four limbs and radiographs were unremarkable. Due to the poor quality of life, the animal was humanely euthanized.

Gross Pathology: The animal was in poor nutritional condition, and the costochondral joints from the seventh to thirteenth ribs were moderately enlarged and prominent. Upon longitudinal sectioning of long bones (femur, radius and ulna, tibia and fibula), no evident abnormalities were observed.

Laboratory Results (clinical pathology, microbiology, PCR, ELISA, etc.): None provided.

Microscopic Description:

Long bone (tibia): Diffusely, the metaphysis is severely affected by inflammation accompanied by degeneration and necrosis. The primary spongiosa (ossification zone) is diffusely distorted and infiltrated by a thick band of numerous viable and degenerate neutrophils and fewer macrophages, among abundant pyknotic and karyorrhectic cellular debris and eosinophilic, loose, fibrillar material (fibrin). Inflammatory cells frequently replace the primary spongiosa and expand intertrabecular spaces, separating fragmented remnants of thinned and tortuous trabeculae, composed of amphophilic to hyperbasophilic, finely stippled to amorphous material (mineralized cartilage

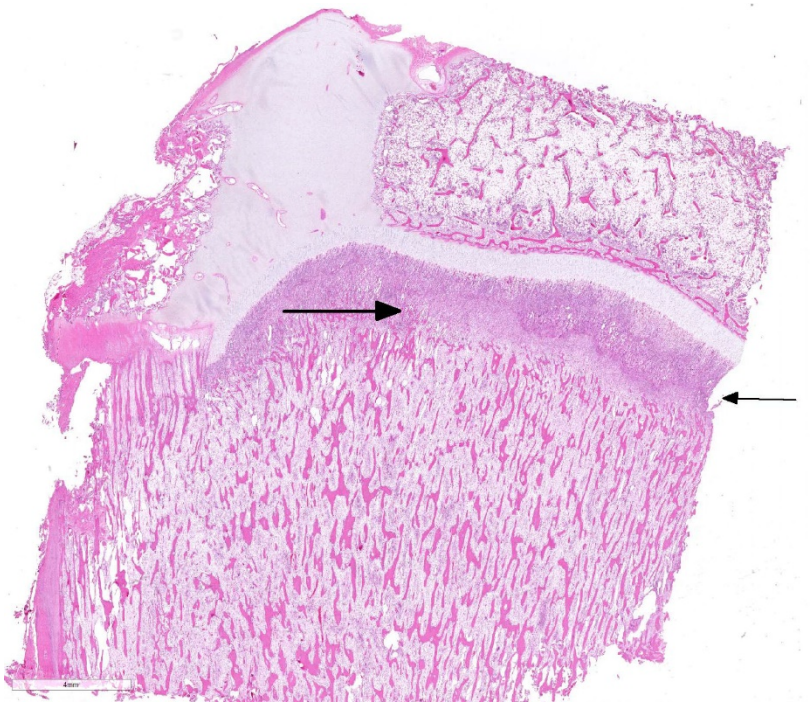

Long bone with growth plate, puppy: Epiphyseal primary spongiosa is basophilic as a result of a cellular infiltrate, and there is an irregular linear area of necrosis at the metaphyseal aspect (arrows). (HE, 6X)

spicules). There is marked paucity to absence of osteoblasts lining the fragmented and sparse trabeculae. There are frequent

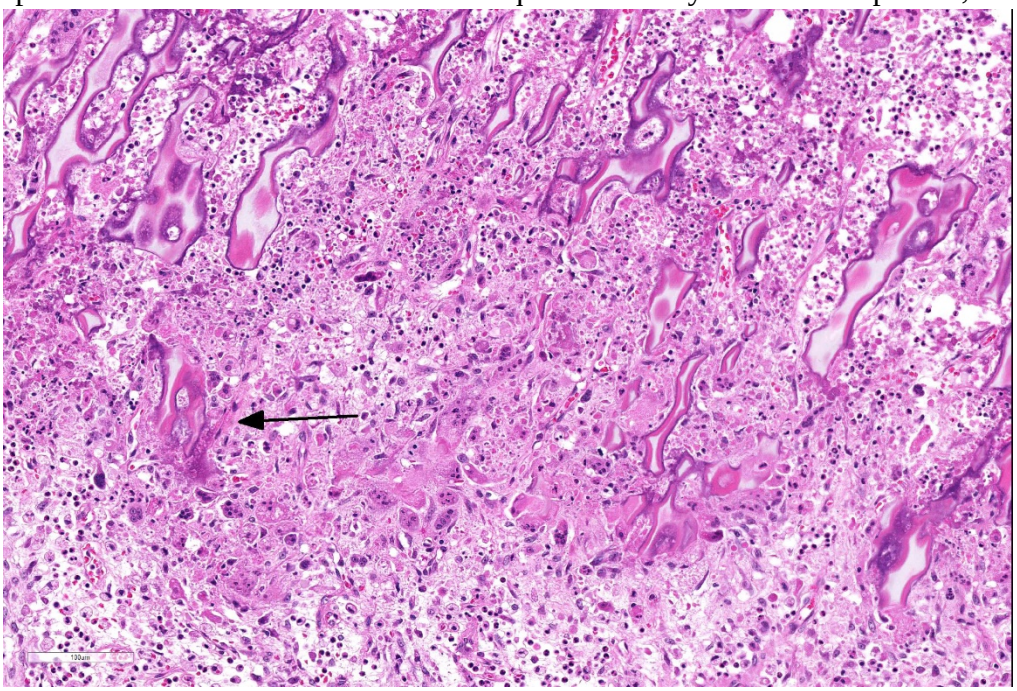

Long bone with growth plate, puppy: Necrotic regions contain fractured trabeculae of the primary spongiosa (arrow) which are minimally lined by osteoid. There is abundant fibrin, edema, infiltrating neutrophils and cellular debris often replacing primary spongiosa and osteoclasts are free within the remaining space. (arrows). (HE, 150X)

osteoclasts scattered among the inflammatory infiltrate, abutting scalloped metaphyseal spicules. The inflammatory cells loosely extend into the underlying secondary spongiosa and, in a lesser extent, into the proximal and mid-diaphyseal medullary cavity. Frequent small caliber and thin walled blood vessels within the medullary cavity present hyaline profile due to bright eosinophilic, fibrillar material concentrically replacing the vascular wall (vascular fibrinoid necrosis).

Contributor's Morphologic Diagnosis:
Metaphysis (tibia): Diffuse, severe, subacute, necrosuppurative osteomyelitis (metaphyseal osteopathy).

Contributor's Comment: Considering the signalment, clinical history and similar histopathology affecting the costochondral joints, femur and tibia in a bilateral and symmetrical pattern, a diagnosis of metaphyseal osteopathy was concluded in this case.

Metaphyseal osteopathy, also known as hypertrophic osteodystrophy (HOD), is a developmental bone disease involving necrosis and suppurative inflammation affecting the metaphyseal region of long bones of rapidly growing young dogs.[1,2] The disease has been reported in over 40 breeds, including mixed breed dogs. However, breed predisposition is commonly reported in Great Danes, Boxers, German Shepherds, Irish Setters, and Weimaraners.[1,4] The latter is reported as the only breed where entire litters and closely related animals have been affected by the disease, strongly supporting a heritable component.[4]

The etiopathogenesis of metaphyseal osteopathy is not fully understood, and proposed mechanisms involving nutritional, infectious or vaccine-related reactions lack supporting scientific evidence.[1] A recent study demonstrated overall overexpression of pro-inflammatory cytokines regulating innate immunity, such as Il-1b, IL-18, GM-CSF, CXCL10, TNF and IL-10, in affected dogs of two different breeds (Irish Setter and

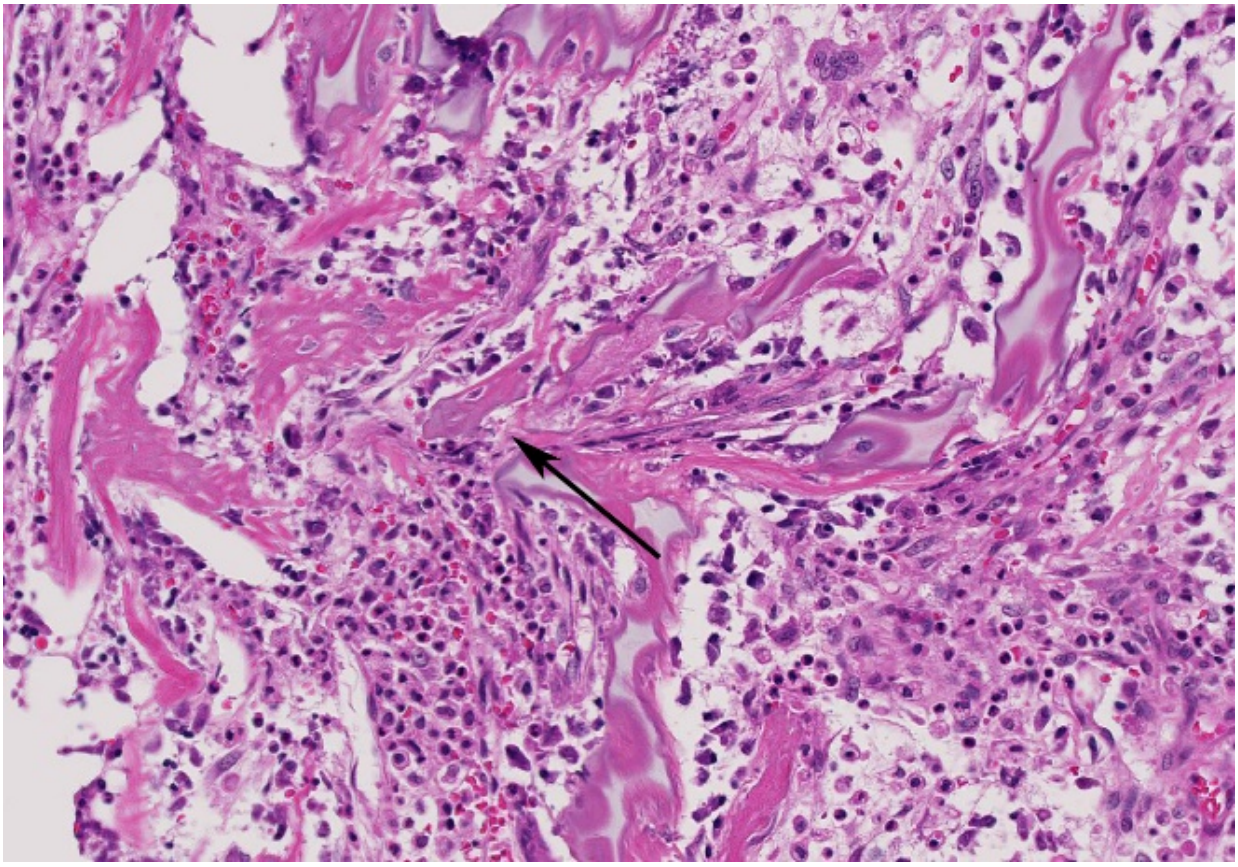

Long bone with growth plate, puppy: Horizontally-oriented trabeculae of primary spongiosa (arrow) are excellent evidence of microfracture. In this field, neutrophils are numerous and there is abundant polymerized fibrin. (HE, 200X)

Weimaraner) supporting the hypothesis of an autoinflammatory disease.[3]

The condition can range from self-limiting with management with corticosteroid therapy to multisystemic involvement, potentially reaching overall debilitation and eventual death or euthanasia[2], as ultimately happened in this case.

JPC Diagnosis: Long bone, metaphysis: Osteomyelitis, metaphyseal, necrotizing and neutrophilic, multifocal, moderate to severe with osteolysis and microfractures of the primary spongiosa, mixed breed (*Canis familiaris*), canine.

Conference Comment: Metaphyseal osteopathy is a condition with an unknown etiology that affects young, growing, large breed dogs (breed predispositions listed above) with relapsing lameness, joint swelling, and pain of the distal radius and ulna most commonly. Radiographically, these areas correspond to the metaphysis parallel to the physis and have alternating linear, parallel radiodense and radiolucent zones. Grossly, lesions are bilaterally symmetrical and characterized by a pale band in the primary spongiosa adjacent to the physis that can develop into small fractures within the boney spicules of the spongiosa. With chronicity, the periosteum thicken to support the dysfunctional ossification within the spongiosa and appears as bulbous dilations. The microscopic appearance is diagnostic for this condition with persistence of the mineralized cartilage lattice of the primary spongiosa, marked neutrophilic inflammation surrounding trabeculae,

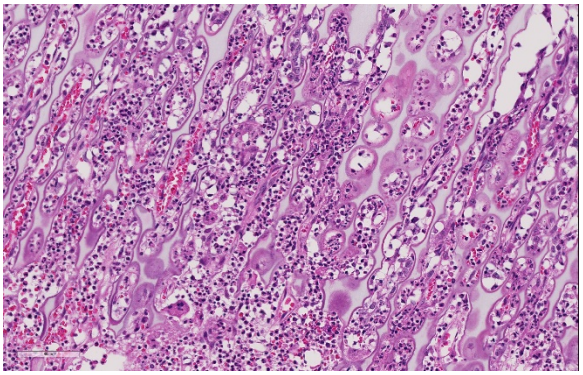

Long bone with growth plate, puppy: Proximal to the area of necrosis, spaces between cartilage columns contain large numbers of neutrophils. In this field, neutrophils are numerous and there is abundant polymerized fibrin. (HE, 275X)

necrosis and loss of osteoblasts, and sometimes increased osteoclasts. Secondarily, as noted grossly, trabeculae frequently fracture and the periosteal bone is markedly thickened. The suppurative inflammation frequently extends into the marrow cavity of the metaphysis resulting in necrosis of marrow contents and fibrin thrombi.[1]

The main differentials for metaphyseal osteopathy include: bacterial osteomyelitis/septic metaphysitis/polyarthritis, hypovitaminosis C, and panosteitis.

All bacterial causes would have a different radiographic appearance and colonies of bacteria microscopically. Hypovitaminosis C, or scurvy, also exhibits decreased osteoid deposition on the cartilaginous trabeculae ("scorbutic lattice") of the primary spongiosa but lacks inflammation and necrosis. Ascorbic acid (vitamin C) is required for hydroxylation of proline and lysine during fibrillary collagen cross-linking. Cartilage that is not properly cross-linked is inherently weak leading to decreased osteoid, increased fragility of blood vessels (hemorrhages), and microfractures in bone.[1]

Finally, panosteitis does not occur within the metaphysis and often appears as cotton-like densities within the medullary space of long bones radiographically. Clinically, panosteitis affects similar ages and breeds as metaphyseal osteopathy, but manifests as "shifting leg lameness" which often resolves on its own as the animal grows. The radiodensities seen radiographically correspond to increasing amounts of fibrovascular tissue with are soon replaced by woven bone within the medullary cavity. There are several subsequent episodes of bone resorption and formation leading to characteristic resting and reversal lines microscopically. Additionally, there is rarely any inflammation present, despite the name "panosteitis".[1]

Contributing Institution:
University of Illinois at Urbana-Champaign
Veterinary Diagnostic Laboratory
http://vetmed.illinois.edu/vet-resources/veterinary-diagnostic-laboratory/

References:

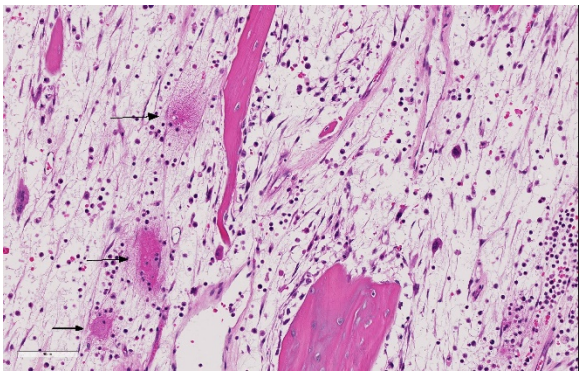

Long bone with growth plate, puppy: Throughout the epiphysis and metaphysis, small vessels exhibit fibrinoid necrosis. (HE, 275X)

1. Craig LE, Dittmer KE, Thompson, KG. Bones and joints. In: Zachary JF, McGavin MD, eds. *Pathologic Basis of Veterinary Disease*. 6th ed. St. Louis, MO: Elsevier Mosby; 2016:83-84, 105-108.
2. Greenwell CM, Brain PH, Dunn AL. Metaphyseal osteopathy in three Australian Kelpie siblings. *Aust Vet J*. 2014; 92(4):115-118.
3. Safra N, Hitchens PL, Maverakis E, et al. Serum levels of innate immunity cytokines are elevated in dogs with metaphyseal osteopathy (hypertrophic osteodytrophy) during active disease and remission. *Vet Immunol Immunopathol*. 2016; 179:32-35.
4. Safra N, Johnson EG, Lit L, et al. Clinical manifestations, response to treatment, and clinical outcome for Weimaraners with hypertrophic osteodystrophy: 53 cases (2009–2011). *J Am Vet Med Assoc*. 2013; 242(9):1260-1266.

CASE IV: 109234-16 (JPC 4100936).

Signalment: 15-week-old female intact Boston terrier (*Canis familiaris*), canine.

History: A 15-week-old intact female Boston Terrier was presented to the Neurology Service of the Cornell University Hospital for Animals with a 7-week history of hyporexia, dysphagia, difficulty ambulating, failure to gain weight, and lethargy. The physical examination revealed dull mentation, poor body condition, non-ambulatory tetraparesis, severe joint laxity, and bilateral corneal opacities. MRI and CT imaging showed evidence of skull malformation, hydrocephalus, cerebral atrophy, severe vertebral and intervertebral disc malformations, and epiphyseal dysplasia. Cytology of the blood, cerebrospinal fluid, and joint fluid revealed cytoplasmic vacuolation and metachromatic cytoplasmic granules in neutrophils, lymphocytes, and macrophages. Based on these findings a presumptive diagnosis of mucopolysaccharidosis (MPS) was made and the owner elected euthanasia due to the poor prognosis.

Vertebrae, puppy: The vertebral bodies are shortened, the intervertebral disc is widened and rounded, and the disc material is loose. (Photo courtesy of: Cornell University School of Veterinary Medicine, Department of Biosciences, 240 Farrier Road, Ithaca, NY 14853, http://www.vet.cornell.edu/biosci/pathology/)

Gross Pathology: Within both corneas were 0.4 cm in diameter, irregularly shaped areas of white-blue opacity. The left and right 10th, 11th, and 12th ribs were widened, flattened, and bulging laterally and ventrally. All four limbs had severe laxity of all of their joints and the left forelimb was externally rotated at the carpus. On the ventral midline at the level of the umbilicus was a small, 0.6 cm in diameter, focal, round, soft, reducible, protrusion (umbilical hernia).

Bilaterally, the proximal epiphyseal plates of the femur and humerus and distal epiphyseal plate of the radius and ulna were displaced and irregular (epiphyseal dysplasia). All vertebral bodies were shortened with thinning of the cortex and an approximate 1:1 ratio of the vertebra to intervertebral disc length. The intervertebral discs were rounded, widened, and hollow at the center and contained clear, loose, gelatinous material (dysplastic nucleus pulposus). The rostral mandible at the level of the symphysis was widened and thickened up to 3.0 x 3.0 x 1.0 cm. The xiphoid process extended 3.0 cm caudal to the last sternebra. On the dorsal

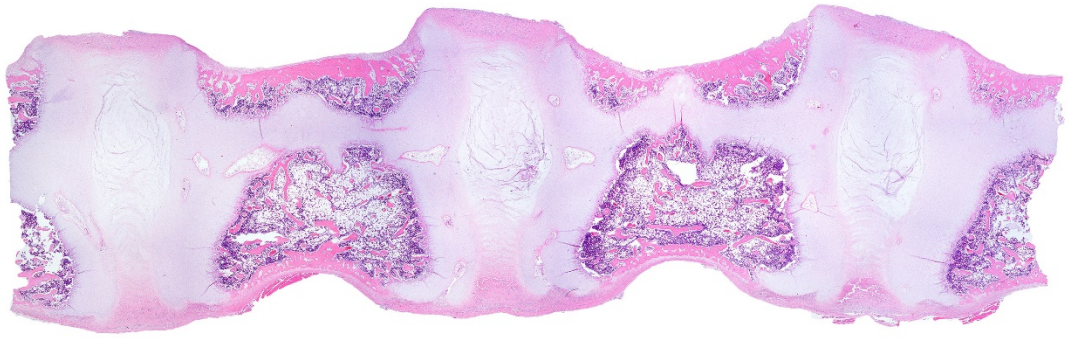

Vertebrae, puppy: Low magnification image of the vertebral bodies demonstrating the bridging trabecular of cartilage between the epiphyses. (HE, 6X) (Photo courtesy of: Cornell University School of Veterinary Medicine, Department of Biosciences, 240 Farrier Road, Ithaca, NY 14853, http://www.vet.cornell.edu/biosci/pathology/)

surface of both carpi and arising between the carpal bones were five (right) and four (left) raised, up to 0.9 x 0.5 x 0.3 cm, well-demarcated, tan to pink, soft, fluctuant, cystic structures continuous with the joint capsules. These cystic structures contained <0.5 mL of slightly opaque, red-tinged fluid. The joints of all four limbs contained mildly increased amounts of cloudy, red-tinged fluid and the joint capsules had increased elasticity.

The heart weighed 26.0 g. The leaflet of the tricuspid valve along the interventricular septum was glistening, smooth, and focally thickened up to 1.0 x 0.6 x 0.2 cm. The mitral valve had seven similar, nodular thickenings up to 0.3 x 0.1 x 0.1 cm.

The meninges were diffusely opaque and moderately thickened. Sectioning of the brain revealed a mild dilation of the lateral ventricles (hydrocephalus).

Laboratory Results (clinical pathology, microbiology, PCR, ELISA, etc.):

Berry urine MPS spot test: Positive

Microscopic Description:

Diffusely, the epiphyseal cartilage is severely thickened with an irregular contour and lacking secondary centers of ossification. Multifocally within, and occasionally crossing the epiphyseal cartilage, are broad tracts that lack cartilage with small blood vessels surrounded by abundant large polygonal cells with foamy cytoplasm and eccentric nuclei (transphyseal vessels). Consistently bridging the medullary space between epiphyseal cartilage are broad columns of cartilage with occasional extensions into the medullary space ventrally and dorsally. Chondrocytes are mildly enlarged, rounded, and have finely vacuolated cytoplasm and are occasionally binucleated. At the chondro-osseous junction is a narrow proliferative and hypertrophic zone with mineralized cartilage and a paucity of osteoclasts. Trabecular bone is sparse and discontinuous with retained cartilage cores. The nucleus pulposus is composed of abundant wispy to frothy basophilic matrix, small numbers of scattered 2 to 4 µm in diameter round, eosinophilic globules, and moderate numbers of large polygonal cells with vacuolated cytoplasm and eccentric nuclei (variable severity between sections). Expanding the collagen fiber matrix of the ventral and dorsal longitudinal ligaments are large numbers of individual and clustered large polygonal cells with foamy cytoplasm and eccentric nuclei.

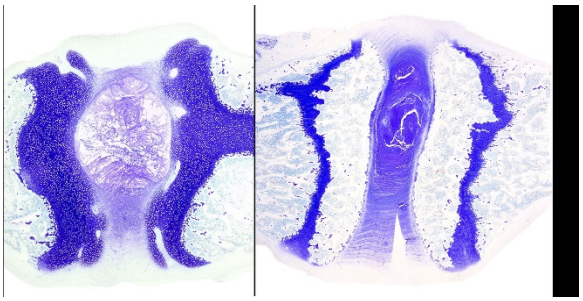

Vertebrae puppy: The toluidine blue stain reveals the cartilage that otherwise stains very pale and highlights the lack of a site of secondary ossification in the epiphysis, the rounding of the epiphysis, the abnormal contents of the nucleus pulposus, and the bridging trabeculae of cartilage in the vertebral metaphysis. (Toluidine blue, 2X) (Photo courtesy of: Cornell University School of Veterinary Medicine, Department of Biosciences, 240 Farrier Road, Ithaca, NY 14853, http://www.vet.cornell.edu/biosci/pathology/)

Contributor's Morphologic Diagnosis:
Lumbar vertebrae:

1. Chondrodysplasia
2. Epiphyseal dysplasia with loss of secondary site of ossification
3. Intervertebral disc dysplasia
4. Osteopenia

Contributor's Comment: The combined clinicopathologic, gross, and histologic findings of this puppy were strongly suggestive of mucopolysaccharidosis (MPS) with features that overlap with other reported cases of MPS in dogs. To confirm the diagnosis, urine was submitted to PennGenn Laboratories at the University of Pennsylvania for a urinary Berry MPS spot test[3]. In addition, a severe deficiency of β-glucuorindase was detected in the serum (personal communication, Dr. Urs Giger). These results were consistent with a Type VII MPS, also known as Sly syndrome in humans. Unfortunately, insufficient samples were available to determine the underlying genetic mutation in this case.

Mucopolysaccharidoses are a group of related lysosomal storage diseases that are the result of genetic deficiencies of key enzymes involved in the normal degradation of mucopolysaccharides. Muco-polysaccharides are glycosaminoglycans; long-chain carbohydrates attached to protein cores that are commonly found in the ground substance of connective tissues throughout the body. Examples of glycosaminoglycans include dermatan sulfate, heparin sulfate, keratin sulfate, and chondroitin sulfate. MPS disorders are broken down into types designated by the underlying enzyme deficiency. For example, Type I MPS is the result of a deficiency in the α-L-iduronidase enzyme and results in the accumulation of dermatan sulfate and heparin sulfate within lysosomes and in the urine. Thus far, only MPS types I, II, IIIA, IIIB, IIIC, IIID, VI, and VII have been identified in domestic animals.

Lysosomes are small organelles within the cytoplasm that are responsible for the breakdown of endogenous and exogenous materials, including byproducts of normal cellular processes[9]. When deficiencies of specific lysosomal acid hydrolases or components of enzyme trafficking occur, substrates are not properly catabolized and

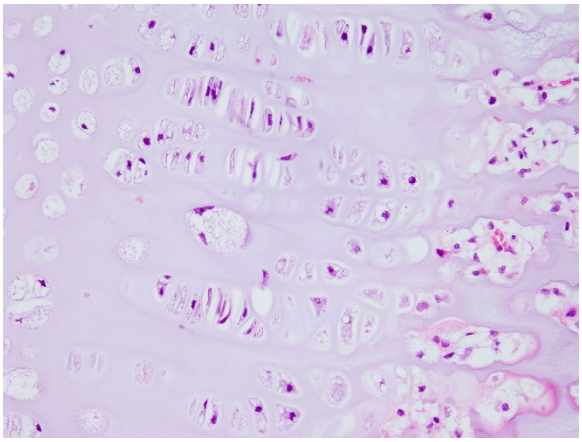

Vertebrae, puppy: Swelling, rounding, and vacuolation of chondrocytes in the growth plate cartilage with vacuolated cells the medullary space between spicules of primary spongiosa. (HE, 400X) (Photo courtesy of: Cornell University School of Veterinary Medicine, Department of Biosciences, 240 Farrier Road, Ithaca, NY 14853, http://www.vet.cornell.edu/biosci/pathology/)

can accumulate within the lysosomes. This accumulation of the substrate is characteristic of lysosomal storage diseases, a heterogeneous group of disorders with a common feature of accumulating metabolites. The buildup of this material can cause lysosomes to become large and hinder normal cellular processes and may even lead to cell death. Errors in lysosomal processing can also result in the accumulation of autophagic substrate during normal cell turnover which can cause altered cellular metabolism and result in apoptosis. Long-lived postmitotic cells, fixed and mobile macrophages, and the cells most active in metabolizing these substrates are most susceptible to storage disease.

The lesions associated with MPS are related to the distribution and functions of the glycosaminoglycans affected by the enzyme deficiency. The key gross findings of this case that are consistent with MPS include skeletal deformities with shortened vertebral bodies, incomplete ossification of the vertebral end plates with subsequent widening of the intervertebral disc spaces, deformed epiphyses of the appendicular skeleton, facial dysmorphism, nodular thickening of the atrioventricular valves, meningeal thickening and opacity, and bilateral corneal opacities. The secondary ossification center of the distal epiphysis of the tibia, for example, is expected to be developed by 10-30 days of age but was completely lacking in this dog[5]. In addition to the vacuolation of chondrocytes, macrophages, and other stromal cells in the vertebral column, vacuolation in the Purkinje cells of the cerebellum, the stromal cells and macrophages of the aorta and trachea, proximal convoluted tubular epithelial cells, and synovium of appendicular joints were also seen in this case. The vacuolation of the epithelial cells of the kidneys is thought to reflect elevated levels of circulating glycosaminoglycans in the blood that are excreted through the glomerulus and reabsorbed in the renal tubular epithelium[11]. Surprisingly, vacuolation of Kupffer cells and hepatocytes

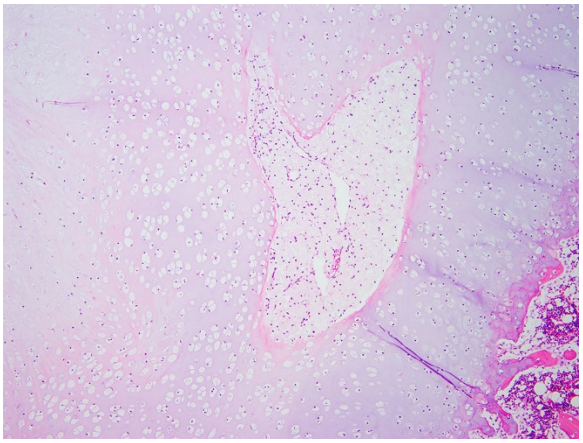

Vertebrae, puppy: A transphyseal vessel is highlighted by expansion of the perivascular space by vacuolated cells. (HE, 400X) (Photo courtesy of: Cornell University School of Veterinary Medicine, Department of Biosciences, 240 Farrier Road, Ithaca, NY 14853, http://www.vet.cornell.edu/biosci/pathology/)

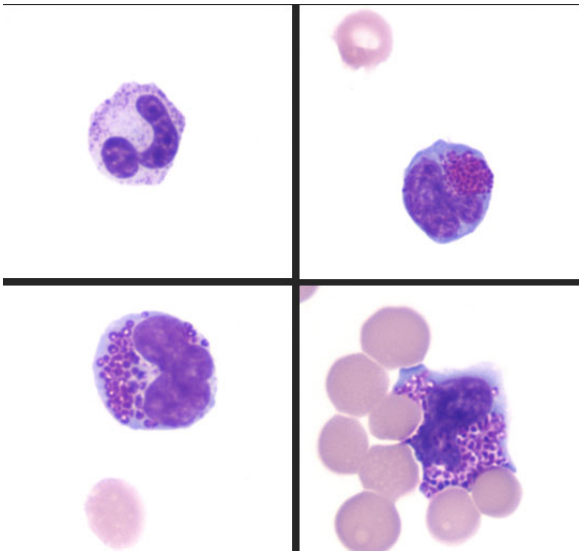

CSF neutrophil/lymphocytes: Large numbers of metachromatic granules in the cytoplasm of a neutrophil and lymphocytes (Alder-Reilly bodies). (Wright-Giemsa, 1000X) (Photo courtesy of: Cornell University School of Veterinary Medicine, Department of Biosciences, 240 Farrier Road, Ithaca, NY 14853, http://www.vet.cornell.edu/biosci/pathology/)

was not a feature in this case despite being reported in another case of type VII MPS[6].

One of the early clues of MPS in this case was the presence of metachromatic intracytoplasmic granules (Alder-Reilly bodies) in neutrophils, lymphocytes, and macrophages in peripheral blood, joint fluid, and cerebrospinal fluid. This is a common finding in cases of MPS and is best observed with Leishman or Wright-Giemsa stains as Diff-Quick-stained smears do not reveal inclusions as readily in some reports[8].

Histochemical staining of the vacuoles was variable with Alcian blue and periodic acid-Schiff; however, it is suspected that the inclusion material can be lost during processing. In this case, the only cells highlighted with Alcian blue stain were within the wall of the aorta. Some reports have suggested that better success is obtained by using these stains on frozen tissues[12]. Electron microscopy could reveal dilated lysosomes that appear empty (electron-lucent), electron dense, or contain lamellar swirls (zebra bodies). Electron microscopy was not performed in this case.

JPC Diagnosis: Vertebral column: Chondrodysplasia, diffuse, severe with epiphyseal dysplasia, loss of secondary ossification sites, intervertebral disc dysplasia, and chondrocytic, fibroblastic and histiocytic vacuolation, Boston terrier (*Canis familiaris*), canine.

Conference Comment: Mucopolysaccharidosis is aptly described by the contributor above.

Table 1: Selected mucopolysaccharidoses in domestic animals [5,11,13,14]

Disease	Storage product(s)	Deficient enzyme(s)	Species	Breed(s)
MPS type I "Hurler's disease"	Different glycosaminoglycans (dermatan sulfate, heparan sulfate, keratin sulfate, chondroitin sulfate)	α-L-iduronidase	Dog, cat	Plott hound Domestic shorthair
MPS type II "Hunter syndrome"		Iduronate-2-sulfatase	Dog	Labrador retriever (1)
MPS type III A, B, D "Sanfilippo syndrome"		Heparan sulfate sulfamidase (SGSH; MPS type IIIA), a-N-acetylglucosaminidase (NAGLU; MPS type IIIB), and N-acetylglucosamine-6-sulfatase (GNS; MPS type IIID)	Dog, cattle, goat	IIIA – Dachshund, New Zealand Huntaway dogs IIIB – Schipperke dogs, cattle, emus IIID – goats
MPS type VI "Maroteaux-Lamy disease"		ARSB (arylsulfatase B)	Dog, cat	Miniature Pinscher, Miniature Schnauzer, Toy Poodle, Welsh Corgi, Chesapeake

				Bay Retriever, Great Dane Domestic shorthair, Siamese
MPS type VII "Sly disease"		B-glucuronidase	Dog, cat	German Shepherd Dog Domestic shorthair

During the conference the moderator noted that the cartilage cores are not running parallel to the axis of the bone but perpendicular, indicating infractions or microfractures in the bone. In general, the bone is weakly mineralized with few primary trabeculae being formed and a disorganized zone of hypertrophy, indicative of a developmental lesion.

Contributing Institution:
Cornell University
240 Farrier Road
Ithaca, NY 14853
http://www.vet.cornell.edu/biosci/pathology/

References:

1. Abreu SJ, Hayden P, Berthold IM, Shapiro S, Decker D, Haskins M. Growth plate pathology in feline mucopolysaccharidosis VI. *Calcified Tissue International Calcif Tissue Int.* 1995; 57(3):185-190.
2. Berry HK. Screening for muco-polysaccharide disorders with the Berry spot test. *Clinical Biochemistry*. 1987; 20:365-371.
3. Burbidge HM, Thompson KC, Hodge H. Post Natal development of canine caudal cervical vertebrae. *Research in Veterinary Science.* 1995; 59(1):35-40.
4. Canine and Feline Epiphyseal Plate Closure and Appearance of Ossification Centers. http://cal.vet.upenn.edu/projects/saortho/appendix_c/appc.htm
5. Cantile C, Youssef S. Nervous system. In: Maxie MG, ed. *Jubb, Kennedy, and Palmer's Pathology of Domestic Animals.* Vol. 1. 6th ed. St. Louis, MO: Elsevier; 2016:289-290.
6. Dombrowski DC, Silverstein K, Carmichael P, Wang P, O'Malley TM, Haskins ME, Giger U. Muco-polysaccharidosis type VII in a German shepherd dog. *Journal of the American Veterinary Medical Association.* 2004; 224(4):553-57.
7. Gitzelmann R, Bosshard NU, Superti-Furga A, Spycher MA, et al. Feline mucopolysaccharidosis VII due to β-glucuronidase deficiency. *Veterinary Pathology*. 1994; 31:435-443.
8. Jolly RD, Hopwood JJ, Marshall NR, Jenkins KS, Thompson DJ, Dittmer KE, Thompson JC, Fedele AO, Raj K, Giger U. Mucopolysaccharidosis type VI in a miniature poodle-type dog caused by a deletion in the arylsulphatase B gene. *New Zealand Veterinary Journal*. 2012; 60(3):183-188.
9. Kumar V, Abbas AK, Aster JC. *Pathologic Basis of Disease*. Philadelphia, PA: Elsevier-Saunders, 2015.
10. Mehta AB, Beck M, Sunder-Plassmann G. *Fabry Disease: Perspectives from 5 Years of FOS*. Ch. 6, Table 1.
11. Palmieri C, Giger U, Wang P, Pizarro M, Shivaprasad HL. Pathological and biochemical studies of mucopolysaccharidosis Type IIIB

(Sanfilippo syndrome type B) in juvenile emus (*Dromaius novaehollandiae*). *Veterinary Pathology*. 2014; 52(1):160-169.

12. Shull RM, Helman, RG, Spellacy E, Constantopoulos G, et al. Morphologic and Biochemical Studies of Canine Mucopolysaccharidosis I. *American Journal of Veterinary Pathology.* 1984; 114(3):487-495.
13. Wang P, Margolis C, Lin G, Buza EL, et al. Mucopolysaccharidosis type VI in a Great Dane caused by a nonsense mutation in the ARSB gene. *Vet Pathol.* 2018; 55(2):286-293.
14. Wilkerson MJ, Lewis DC, Marks SL, Prieur DJ. Clinical and morphologic features of mucopolysaccharidosis type II in a dog: naturally occurring model of Hunter syndrome. *Vet Pathol.* 1998; 35(3):230-233.
15. Yogalingam G, Pollard T, Gliddon B, Jolly RD, Hopwood. Identification of a mutation causing mucopolysaccharidosis type IIIA in a New Zealand huntaway dogs. *Genomics.* 2002; 79(2):150-153.

Self-Assessment - WSC 2017-2018 Conference 23

1. Which of the following dimorphic fungi undergoes endosporulation?
    a. Histoplasma capsulatum
    b. Blastomyces dermatitidis
    c. Coccidioides immitis
    d. Cryptococcus neoformans

2. Which of the following is not considered a common route of spread of bacteria in osteomyelitis?
    a. Hematogenously
    b. Lymphatic spread
    c. Local extension
    d. Implantation

3. Which of the following is the cause of metaphyseal osteopathy in the dog?
    a. Post viral infection
    b. Immune-mediated
    c. Bacterial infection
    d. Currently unknown

4. Which of the following is NOT seen histologically in metaphyseal osteopathy?
    a. Marked neutrophilic inflammation surrounding trabeculae
    b. Retained cartilaginous cores within the metaphysis
    c. Persistence of the mineralized cartilage lattice of the primary spongiosa
    d. Necrosis and loss of osteoblasts

5. True or false. Large strongyle adults suck blood from the host.
    a. True
    b. False

Please email your completed assessment to Ms. Jessica Gold at Jessica.d.gold2.ctr@mail.mil for grading. Passing score is 80%.This program (RACE program number) is approved by the AAVSB RACE to offer a total of 0.5 CE Credits, with a maximum of 12.5 CE Credits being available to any individual Veterinary Medical Professionals for the 2017-2018 Wednesday Slide Conference. This RACE approval is for the subject matter categories of: SCIENTIFIC using the delivery method of NON-INTERACTIVE DISTANCE. This approval is valid in jurisdictions which recognize AAVSB RACE; however, participants are responsible for ascertaining each board's CE requirements.
RACE does not "accredit", "endorse" or "certify" any program or person, nor does RACE approval validate the content of the program.

Joint Pathology Center
Veterinary Pathology Services

WEDNESDAY SLIDE CONFERENCE 2017-2018

C o n f e r e n c e 24

2 May 2018

Jeffrey C. Wolf, DVM, DACVP
Chief Scientific Officer
Manager of Virginia Pathology Experimental Pathology Laboratories, Inc.
45600 Terminal Drive
Sterling, VA 20166

CASE I: AP17-0483 (JPC 4101485).

Signalment: 1-year-old, female, Zebrafish (*Danio rerio*), pisces.

History: A subset of TP53 mutant zebrafish from the colony were found with significantly distended coelomic cavities, which necessitated their removals from the study.

Gross Pathology: The coelomic cavities of the affected fish were grossly distended and, upon opening, contained variably sized, firm, tan masses that compressed and effaced organs and infiltrated the body wall.

Laboratory Results (clinical pathology, microbiology, PCR, ELISA, etc.): None provided.

Microscopic Description:

The coelomic cavity is expanded by a large, unencapsulated neoplasm that is arranged in variably sized and tightly arranged bundles with regions of indistinct nuclear palisading and situated within an eosinophilic, collagenous matrix. Neoplastic cells have poorly defined cellular borders, are spindle-shaped and have moderate amounts of cytoplasm. Nuclei are oval to fusiform in shape and have either reticulated or hyperchromatic patterning with 1 to 2 nucleoli that are variable in prominence based on the orientation of the tumor cells. There is marked anisocytosis and anisokaryosis with atypical giant cells

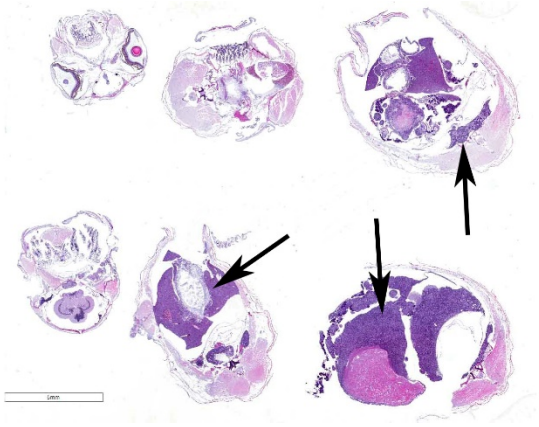

Transverse sections, zebrafish. Several cross-sections of the fish are submitted for examination. 3 0f 6 s4ections contain a large infiltrative partially necrotic (lower left) neoplasm which partially fills the coelomic cavity. (HE, 5X)

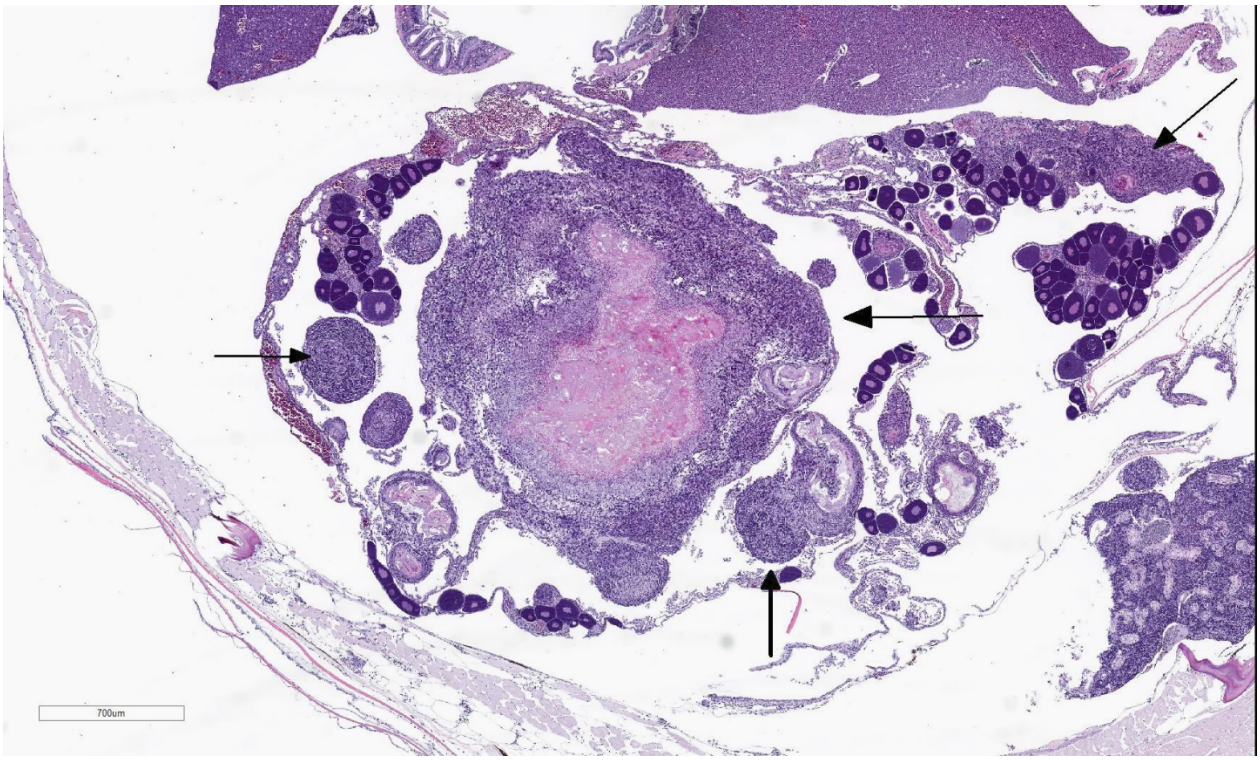

Coelomic cavity, zebrafish. Higher magnification of the neoplasm (arrows) present within the coelomic cavity. Tumor nodules often have large central pink areas of necrosis, and the tumor infiltrates the ovary and separates follicles. (HE, 30X)

scattered throughout the tumor. Mitoses range from 0-4 per 400x/hpf. There are varying combinations and concentrations of small lymphocytes, heterophils and histiocytes that are distributed throughout the neoplasm as well as randomly scattered foci of necrosis that often coalesce together. There are also rare, small sized granulomas that are centered on clear spaces as well as entrapped remnants of ovarian tissues in different states of degeneration. Neoplastic cells contact and extend into portions of the body wall. Metastasis is not observed.

Contributor's Morphologic Diagnosis:
Coelomic cavity: Malignant peripheral nerve sheath tumor, Zebrafish

Contributor's Comment: The tumors that were observed in the *Tp53*-mutant zebrafish are classified as malignant peripheral nerve sheath tumors (MPNSTs) based on cellular pleomorphism, invasiveness, the presence of necrosis, and, most importantly, the clinical course of the disease that was documented for this colony. In humans and animals peripheral nerve sheath tumors (PNSTs) may arise throughout the body and are largely defined by their morphologic patterning and include neurofibromas, schwannomas and perineurinomas. Further subdivision into benign versus malignant tumors is currently based on the degree of cellular differentiation, mitotic count, presence of necrosis and clinical staging. Schwann cells are the putative cells of origin for most PNSTs. Benign PNSTs most consistently express S100, which is frequently used to distinguish them from other neuroepithelial and mesenchymal neoplasms with similar morphologies.[3,5,9] PNSTs are not currently documented in zebrafish outside of experimental manipulations affecting *Tp53* status or ribosomal protein genes, although

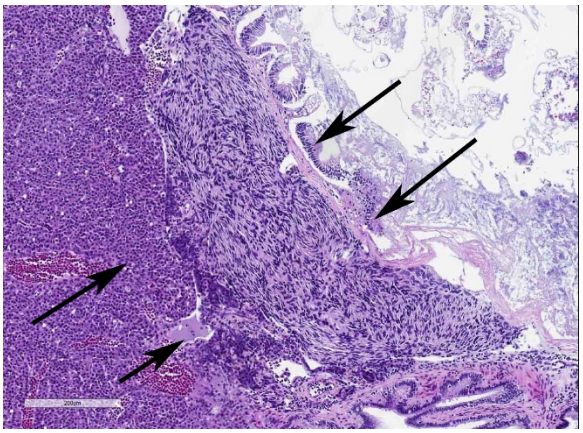

Coelomic cavity, zebrafish. The tumor infiltrates between the liver and intestine. (HE, 40X)

viral infection resulting in neurofibromatosis has been described in damselfish.[1,7,10] One study has confirmed that sarcomas arising in laboratory zebrafish, which had mutations of both T*p53* and B*rca2*, are derived from Schwann cell populations as assessed by the positive labeling of the tumor cells with anti-CD57 and anti-S100 antibodies.[13]

The zebrafish has been an important animal model for studying human MPNSTs, especially in the context of hereditary cancer syndromes, because *t* mutated zebrafish MPNSTs often have comparable genetic alterations as human tumors.[12,14] Since many of the functions of P53 are conserved the spectrum of tumors that may arise from perturbations to P53-mediated cellular processes frequently result in lymphomas, leukemias, sarcomas and carcinomas in both humans and animals. However, there are often species specific differences in the frequencies of certain tumors, such as the predisposition for zebrafish to form malignant rather than benign PNSTs.[6,8,12] These differences suggest that a combination of time and environmental dependent factors are important for the types of P53 dependent tumors that develop and their biological behaviors.[2] While these differences in biology between humans and animal species exist, these dissimilarities are being used to further understand the essential genetic and environmental events that are important for the biology of PNSTs.

JPC Diagnosis: 1. Omentum, ovary, pancreas: Malignant peripheral nerve sheath tumor, Zebrafish (*Danio rerio*), pisces.
2. Kidney, ovaries, omentum: Granulomas, multiple.

Conference Comment: In humans, malignant peripheral nerve sheath tumors (MPNSTs) are rare but devastating tumors, asthey are aggressive and have high rates of relapse following chemotherapy. In approximately half of cases, MPNSTs occur in association with neurofibromatosis type I which results from loss of function mutations to the tumor suppressor neurofibromin. Neurofibromatosis type I, an autosomal dominant condition, is the most common human syndrome which predisposes to cancer. Clinical signs include: cutaneous hyperpigmentation (known as “café-au-lait spots”) and multiple cutaneous neurofibromas which can transform into MPNSTs.

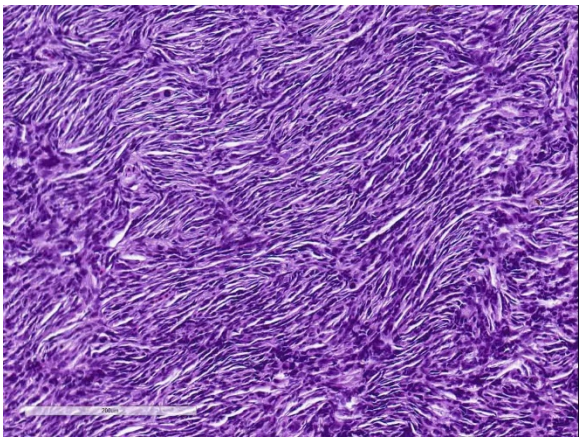

Coelomic cavity, zebrafish. Neoplastic spindle cells are arranged in short streams and bundles. Nuclei are ellipsoid to spindled with moderate anisocytosis and anisokaryosis. (HE, 200X)

In addition to NF-1, TP53 mutations have also been associated with development of MPNSTs – this is where zebrafish are particularly useful.[4] Historically, human cancer studies utilized rodent models. However, disadvantages such as increased time for tumor development and cost encouraged identification of a new model. Zebrafish are more economic and undergo neoplastic transformation and growth quicker. Most importantly, many aspects of carcinogenesis in humans are similarly expressed in zebrafish.

Several methods are used to generate effective models for research including: chemical carcinogenesis, forward or reverse genetics screens, transgenic models, and xenotransplantation in embryos.[11] Currently, zebrafish are used as models for the following types of cancer:

Table 1: Zebrafish models of cancer[11]

Tissue of origin	**Cancer model**
Cutaneous neoplasia	Benign nevus; melanoma; papilloma; epidermal tumors
Muscular, adipocytic, and vascular neoplasia	Embryonal rhabdomyosarcoma; rhabdomyosarcoma; liposarcoma; hemangiosarcoma
Intestinal, pancreatic, and hepatic neoplasia	Intestinal adenoma; malignant intestinal tumors; pancreatic acinar cell adenoma; pancreatic carcinoma; hepatoma; hepatocellular carcinoma
Hematopoietic, lymphoid, and small round blue cell neoplasia	T-cell leukemia; T-cell or B-cell acute lymphocytic leukemia; T-cell lymphoblastic lymphoma; acute myeloid leukemia; myeloproliferative neoplasm; small round blue cell tumors
Neural and neuroendocrine neoplasia	MPNST; neuroblastoma; neuroepithelioma; pituitary corticotroph adenoma; pancreatic neuroendocrine carcinoma

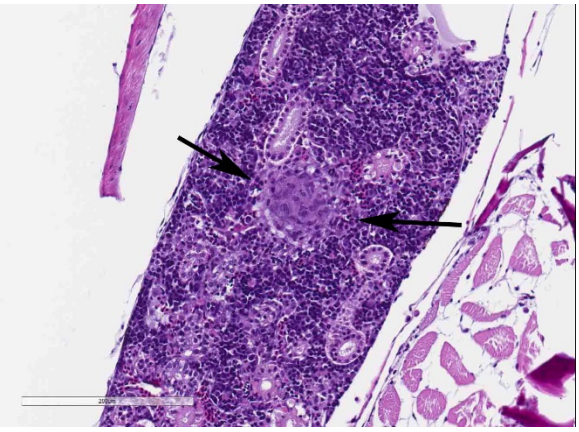

Head kidney: Small granulomas are present within several organs including the kidney, ovary, and omentum. (arrows). (HE, 40X)

Peripheral nerve sheath tumors can be further differentiated as benign and malignant Schwannoma, neurofibroma, or neuro-fibrosarcoma. In most cases, the Schwann cell likely the progenitor cell. A common rule out in fish is chromatophoroma (pigment cell tumors). The bi-color damselfish was once thought to be a naturally-occurring model of neurofibromas before it was discovered they were virally induced.[10]

During the conference, the moderator pointed out that there is increased hematopoietic tissue and vacuolated tubular epithelial cells

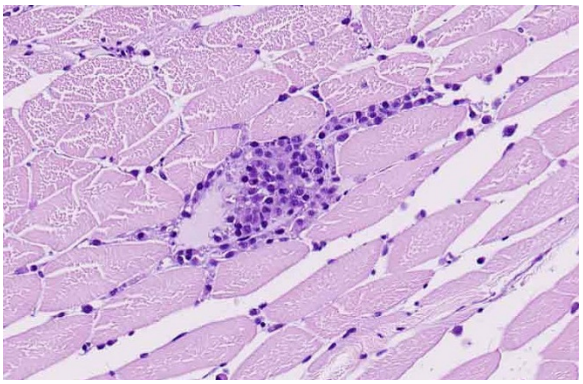

Abdominal wall, zebrafish. Rare muscle fibers are necrotic with infiltration of numerous macrophages. (HE, 100X)

within the anterior kidney, multiple granulomas, and histiocytes focally within skeletal muscle. Conference participants discussed what constitutes a "malignant" PNST and concluded that invasiveness is a key indicator but that spread to other organs via blood or lymphatics is not required.

Contributing Institution:

St Jude Children's Research Hospital
Department of Pathology
MS 250, Room 5031
262 Danny Thomas Place
Memphis, TN, 38105-3678
https://www.stjude.org/research/departments-divisions/pathology.html

References:

1 Amsterdam A, Sadler KC, Lai K, Farrington S, Bronson RT, Lees JA, et al.: Many Ribosomal Protein Genes Are Cancer Genes in Zebrafish. *PLOS Biology* 2004:2(5)**:**e139.

2 Berghmans S, Murphey RD, Wienholds E, Neuberg D, Kutok JL, Fletcher CDM, et al.: tp53 mutant zebrafish develop malignant peripheral nerve sheath tumors. *Proceedings of the National Academy of Sciences of the United States of America* 2005:102(2)**:**407-412.

3 Cantile C, Youssef S: Chapter 4 - Nervous System IN: Maxie, M. Grant *Jubb, Kennedy & Palmer's Pathology of Domestic Animals: Volume 1 (Sixth Edition)*: W.B. Saunders; 2016: 250-406.

4 Farid M, Demicco EG, Garcia R, Ahn L, et al. Malignant peripheral nerve sheath tumors. *The Oncologist.* 2014; 19(2):193-201.

5 Louis DN, Ohgaki, H., Wiestler, O.D., Cavenee, W.K.: WHO Classification of Tumours of the Central Nervous System, Fourth Edition. *IARC WHO Classification of Tumours, No 1* 2007.

6 Lozano G: Mouse Models of p53 Functions. *Cold Spring Harbor Perspectives in Biology* 2010:2(4)**:**a001115.

7 MacInnes AW, Amsterdam A, Whittaker CA, Hopkins N, Lees JA: Loss of p53 synthesis in zebrafish tumors with ribosomal protein gene mutations. *Proceedings of the National Academy of Sciences* 2008:105(30)**:**10408-10413.

8 Olivier M, Hollstein M, Hainaut P: TP53 Mutations in Human Cancers: Origins, Consequences, and Clinical Use. *Cold Spring Harbor Perspectives in Biology* 2010:2(1)**:**a001008.

9 Rodriguez FJ, Folpe AL, Giannini C, Perry A: Pathology of Peripheral Nerve Sheath Tumors: Diagnostic Overview and Update on Selected Diagnostic Problems. *Acta neuropathologica* 2012:123(3)**:**295-319.

10 Schmale MC, Gibbs PDL, Campbell CE: A virus-like agent associated with neurofibromatosis in damselfish. *Diseases of Aquatic Organisms* 2002:49(2)**:**107-115.

11 Shive HR. Zebrafish models for human cancer. *Vet Pathol.* 2013; 50(3):468-482.

12 Storer NY, Zon LI: Zebrafish Models of p53 Functions. *Cold Spring Harbor Perspectives in Biology* 2010:2(8).

13 White LA, Sexton JM, Shive HR: Histologic and Immunohistochemical Analyses of Soft Tissue Sarcomas From

brca2-Mutant/tp53-Mutant Zebrafish Are Consistent With Neural Crest (Schwann Cell) Origin. *Veterinary Pathology* 2017:54(2)**:**320-327.

14 Zhang G, Hoersch S, Amsterdam A, Whittaker CA, Lees JA, Hopkins N: Highly aneuploid zebrafish malignant peripheral nerve sheath tumors have genetic alterations similar to human cancers. *Proceedings of the National Academy of Sciences* 2010:107(39)**:**16940-16945.

CASE II: IP17-300 (JPC 4101145).

Signalment: Juvenile, undetermined sex, Nile tilapia (*Oreochromis niloticus*), pisces.

History: In a group of 50,000 fish, after 21 days of culture, with an approximate weight between 0.8 and 1 gram, a considerable amount of mortality was reported. Some of these fish had difficulty swimming and were found on the pond's surface. There were whitish spots distributed throughout the body. At least 300 fish were found dead on the surface and countless more were found on the pond's bottom. Wet mounts of gills and skin (including fins), were performed to calculate the mean intensity for mono-geneans, trichodinids and *Ichthyo-phthirius multifiliis*; the values obtained were 5, 15 and 47 parasites per infected fish respectively. The prevalence for these same parasites was 46%, 53.3% and 100% respectively.

Gross Pathology: Multifocal to coalescing raised pinpoint 2mm white spots covered most of the skin, gills and oral cavity; in some fish these pinpoint lesions affected the cornea as well.

Laboratory Results (clinical pathology, microbiology, PCR, ELISA, etc.): Wet mounts of gill clippings obtained at necropsy demonstrated large numbers of round, 50-300 µm diameter theronts and trophonts consistent with *Ichthyophthirius multifiliis.*

Presentation, tilapia. Numerous white spots are scattered across the scales, eyes, and fins of affected fish. (Departamento de Patología (Pathology Department). Facultad de Medicina Veterinaria y Zootecnia, Universidad Nacional Autónoma de México. Mexico City, Mexico.
Web site: ***http://fmvz.unam.mx/fmvz/departamentos/patologia/acerca.html)***

Microscopic Description:

Gills: Multifocally, there is moderate hyperplasia of the gill epithelium with blunting and fusion of secondary lamellae and numerous irregularly round, single-cell, up to 200 um diameter, intraepithelial protozoal cysts with a 1-2 um thick hyaline wall, abundant, finely granular to vacuolated basophilic cytoplasm containing numerous host erythrocytes, and a 30 x100 um, crescent-shaped, deeply basophilic macronucleus (trophont). Goblet cell hyperplasia was also observed. Variable amounts of mucus and necrotic debris admixed with filamentous bacteria was present in some sections. Attached to the lamella or freely between them, numerous saucer shaped, hemispheric, dumbbell shaped, or sac like or flattened cylindrical protozoa, consistent with trichonids, were also observed.

Skin and oral cavity: Multifocally, there are nodular foci within the epidermis that are composed of hyperplastic epithelium that

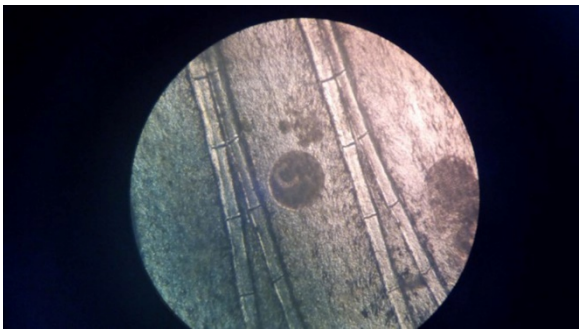

Gill filaments, tilapia. A wet mount of the gill clippings contains a 50-300um theront with a prominent horseshoe nucleus characteristic of Ichthyophthiris multifiliis. (Departamento de Patología (Pathology Department). Facultad de Medicina Veterinaria y Zootecnia, Universidad Nacional Autónoma de México. Mexico City, Mexico. Web site: http://fmvz.unam.mx/fmvz/departamentos/patologia/acerca.html)

piles up to 6 to 9 cell layers. Hyperplastic epithelium often surrounds previously described intraepithelial protozoa.

Contributor's Morphologic Diagnosis:
Gill: Epithelial hyperplasia, nodular, moderate, diffuse, with numerous protozoa (trophonts and theronts) consistent with *Ichthyophthirius multifiliis* and trichodinids.

Skin and oral cavity: Epithelial hyperplasia, nodular, multifocal, moderate with protozoa (trophonts and theronts) consistent with *Ichthyophthirius multifiliis.*

Contributor's Comment: Histologic findings were similar in all fish examined. In addition to proliferative branchitis and dermatitis, affected fish exhibited a similar lesion in the oral cavity associated with organisms identical to those observed in the gills. *Ichthyophthirius multifiliis* is a ciliated protozoan parasite that infects the skin and gills of freshwater fish and causes "Ich" or white spot disease. The life cycle begins with a small migratory and infective stage known as theront attaching to the epidermis and gills, where it feeds and continue its development to a trophont, which elicits a reactive response (epidermal hyperplasia). At this stage, trophonts increase dramatically in size due to enlargement of their macro-nucleus, production of food vacuoles and liposomes, and formation of new mucocysts. The trophont breaks through the epithelium, drops off the host, and forms a capsule (tomont) that adheres to the bottom of the tank. Tomonts undergo binary fission within the cyst to produce tomites which break through the cyst and eventually become infective motile theronts. *Ichthyophthirius multifilis* are 75 μm to 1 mm in diameter and uniformly ciliated with a crescent-shaped nucleus. *I. multifiliis* causes localized lymphocytic infiltration, focal necrosis, and varying degrees of epithelial proliferation in the skin and gills. In severe cases, sloughing of the epidermis has been observed.[1,2,3,10] In experimentally infected channel catfish (*Ictalurus punctatus*), infection of the peritoneal cavity has been reported; three possible enterance routes were speculated: penetration through esophageal wall, penetration of the pneumatic duct (a structure connecting the esophagus and swim bladder), or retrograde migration from the anus.[5] In saltwater fish *Cryptocaryon irritans* has the same life cycle as *I. multifilis*, where it is referred as "marine ich" and produces similar lesions.

Conversely, trichodinas/trichodinids are mobile peritrich ciliates that attach temporarily to the substrate while feeding and have been found in both freshwater and marine fish. They are found in the skin and gills. Although they are typically considered commensal organisms, they may become numerous in stressed or debilitated fish. Depending on the orientation of the parasites in tissue sections, they may appear as saucer shaped, hemispheric, dumbbell shaped, and sac like or flattened cylindrical organisms. Heavy infection with this parasite, has been

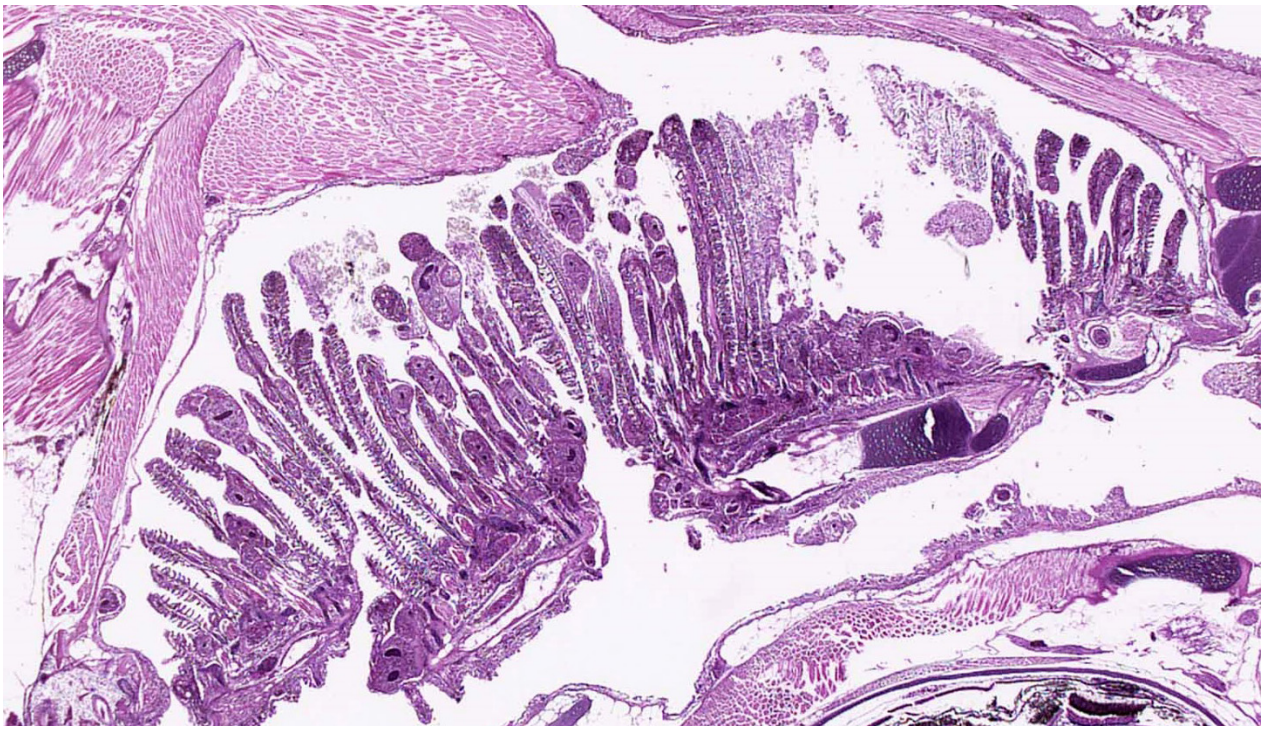

Gill, filaments: Gills are diffusely thickened and variably hypercellular. Many filaments are expanded by the presence of large trophonts with a horseshoe-shaped macronucleus (arrows). (HE, 40X)

associated with excessive secretion of mucous, and can result in hypertrophy and hyperplasia of gill epithelium with subsequent fusion of secondary gill lamellae.[1,2]

In addition to *I. multifilis* and trichodinids, several other potential etiologic agents were observed microscopically that could have contributed to some extent to the lesions in gills, skin and oral cavity. Depending on the slide, there were also few monongeneans, filamentous bacteria and epitheliocystis. In this group of fish, *I. multifilis* is believed to be the primary pathogen when one takes into account the previously stated prevalence and mean intensity.

Fish parasites are an integral part of water ecosystems and they are common in wild and cultured populations of fish. It is well known that fish live in balance with parasites, however, this balance can be broken by stressors such as sudden changes in water quality (i.e. temperature, oxygen, etc) and poor husbandry (i.e. high stocking densities, excessive handling, etc.). Therefore, diseases caused by parasites are much more frequently manifested in cultured fish, which suffer from numerous stress factors that influence their ability to effectively protect themselves against parasitic infections. Infections caused by protozoan and metazoan parasites occur very frequently in cultured fish and can cause significant economic losses to fish farms due to mortality, but parasites may also exert considerable impact on growth and behavior of fish, on their resistance to other stress factors, susceptibility to predation, etc. Many of these parasites can cause severe injury to different organs and tissues and they can provide portals of entry for bacteria in fish, generating co-infections.[4,7,9]

JPC Diagnosis: 1. Gills, pharynx, skin: Epithelial hyperplasia, blunting and fusion of

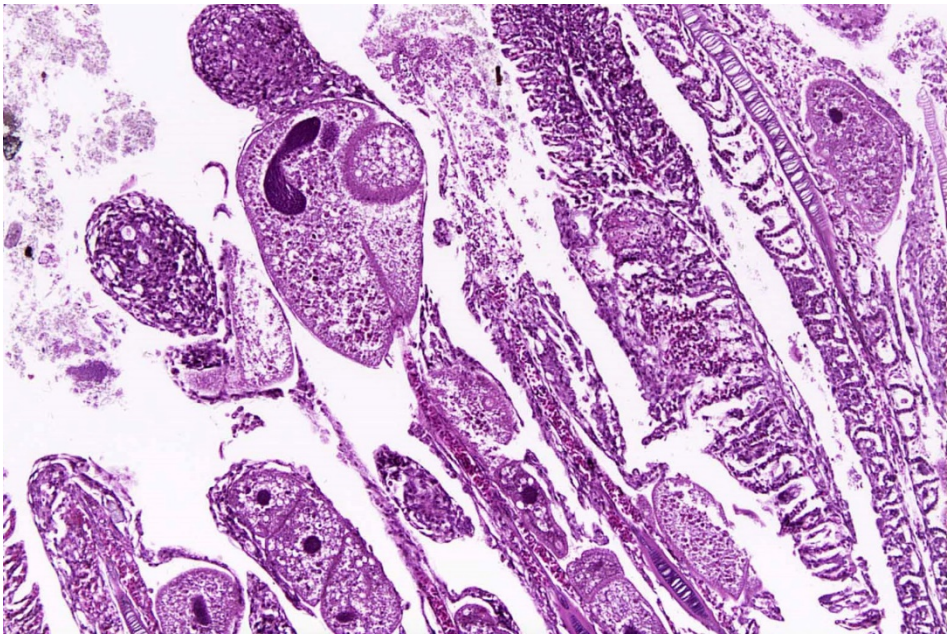

Gill, filaments: Gills are diffusely thickened and variably hypercellular. Many filaments are expanded by the presence of large trophonts with a horseshoe-shaped macronucleus (arrows). (HE, 40X)

secondary lamellae and numerous embedded protozoal ciliates (theronts) consistent with *Ichthyophthirius multifiliis* and free trichodinids, Nile tilapia (*Oreochromis niloticus*), pisces.
2. Gills: Epitheliocystis, rare.
3. Gills: Filamentous bacilli, multifocal.
4. Gills: Monogenean, single.

Conference Comment: The gills of teleosts are the most vulnerable structures they possess; their external location ensures close association with the external environment and any contaminates or parasites that inhabit it. External protozoan and monogenean trematode parasites have a particular affinity for the gills because they have a rich blood supply and thus provide a nutrient-rich environment. Additionally, the gills are often the route of entry for various bacterial and viral agents (lymphocystis or *Herpesvirus salmonis* for example) which spread from the branchial vessels hematogenously and systemically either via leukocyte trafficking or cell-free dissemination. The gills are composed of two main parts: the primary lamellae (which extend out from the branchial arch) and the secondary lamellae (which protrude as smaller projections out from the primary lamellae). Within the primary lamellae are: epithelium, endothelium, pillar cells and supporting stroma (made up of fibrous and cartilaginous connective tissues). Admixed are specialized cells such as: mucous cells, salt cells, eosinophilic granule cells and fixed macrophages. When injured, the inflammatory response is limited, and the earliest microscopic lesions are swelling and degeneration of the lamellar

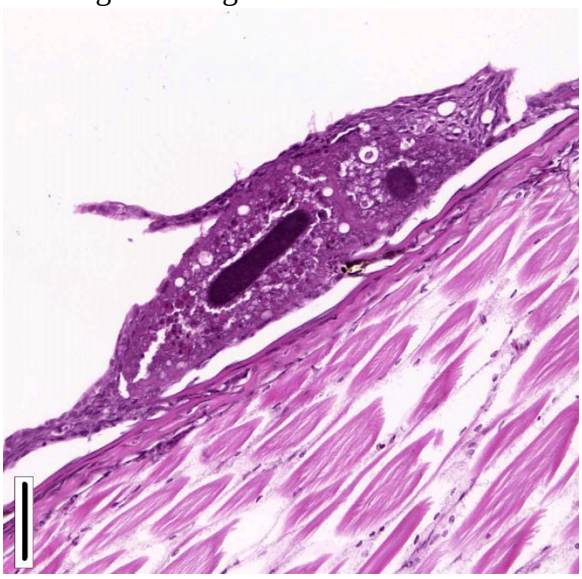

Skin, tilapia: Non -encysted theronts (invasive form) are present on the skin, as well as on the mucosa of the oral and branchial cavity. (HE, 400X)

epithelial cells, or edema of the subepithelial connective tissue. In general, lamellar edema and epithelial necrosis are the result of acute exposure to direct acting toxins or chemical pollutants such as heavy metals, red tides, phytoplankton or jellyfish and ultimately lead to hemorrhage. On the other hand, lamellar hyperplasia often results from chronic exposure to lower levels of a toxicant and can assume several morphologic forms: clubbing of secondary lamellae, mucous cell hyperplasia or metaplasia, and ultimately lamellar fusion. With good water quality and a modicum of time, most gill lesions heal.[6,8]

Table 1: Gross and microscopic differentials for *Ichthyophthirius multifilis*[6,8]

Protozoan		
Cryptocaryon irritans (marine ich)	Saltwater fish	Penetrates the epithelium; saltwater equivalent of *Ichthyophthirius multifilis*
Trichodina spp.	Marine or freshwater fish	Grossly similar to *Ichthyophthirius multifilis*; identified on wet mount as disk shaped organism scooting on the surface of tissues
Chilodonella spp.		Same life cycle and gross pathology as *Ichthyophthirius multifilis*; more severe tissue damage
Amyloodinium sp. (marine velvet disease)	Warm water marine fish (elasmobranches (sharks, rays) and teleost (ray fin fish)	Dinoflagellate; affects gills, skin, and eyes; larger than *Ichthyophthirius multifilis*
Piscinoodinium spp. (freshwater velvet disease, rust disease)	Freshwater fish	Freshwater analogue of Amyloodiniosis
Ichthyobodo spp. (*Ischthyobodo necator* complex)	Immunosuppressed and young fish; freshwater primarily	Smallest ectoparasite of fish (size of red blood cell); epithelial hyperplasia with increased mucus production (makes fish bluer and extra slimey)
Fungal/algae		
Saprolegniales sp. (water mold)	Freshwater (especially estuarine tropical fish)	Cottony, proliferative growth on skin or gills
Bacterial		
Epitheliocystis sp.	Freshwater and marine fish	Intracellular, Gram-negative; causes epithelial and dermal cell enlargement
Viral		

Lymphocystis (pscine iridovirus)		Hypertrophied fibroblasts with basophilic intracytoplasmic inclusion bodies

Icthyophthirius multifilis (also known as "ich" or white spot disease) is the largest protozoan parasite in fish; trophozoites can reach 100 µm in diameter and have a prominent oval or horseshoe-shaped nucleus. Ich is common in aquarium and hatchery-reared freshwater fish and can result in respiratory impairment in severely infected fish. Microscopically, the trophozoites are found in the skin or gill lamellae surrounded by epithelial hyperplasia. *I. multifilis* has a direct life cycle in which encysted trophozoites (trophonts) leave the fish and settle at the bottom of the tank where, in their tomont form, they divide into numerous motile tomites (theronts). It is the motile theront form that infects the skin of the fish. Their total life cycle only takes 4 days but can be quicker in warmer water temperatures.

Trichodina spp. is a saucer-shaped, 50 µm in diameter, peritrichal ciliated protozoan with a macro- and a micronucleus. Microscopically, it appears as a characteristic ring of interlocking denticles. Low numbers are not typically associated with disease and are frequently environmental contaminates. However, in increased numbers, with concurrent disease, or in an immunosuppressed host, they can cause increased skin and gill mucus and respiratory distress. *Trichodina* spp. have a simple life cycle and reproduce by binary fission.[6,8]

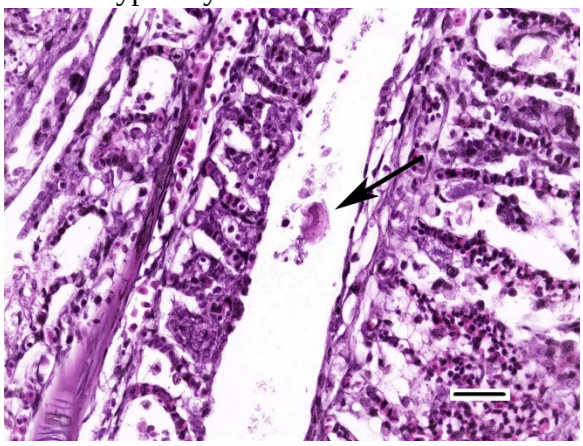

Gills, tilapia: Occasionally trichodinid ciliates are present between hyperplastic gill filaments. (HE, 400X)

Contributing Institution:

Departamento de Patología (Pathology Department)
Facultad de Medicina Veterinaria y Zootecnia
Universidad Nacional Autónoma de México
Mexico city, Mexico
http://fmvz.unam.mx/fmvz/departamentos/patologia/acerca.html

References:

1. Bruno DW, Nowak B, Elliot DG. Guide to the identification of fish protozoan and metazoan parasites in stained tissue sections. *Dis. Aqua. Org*. 2006; 70:1-36.
2. Dar SA, Kaur H, Chishti MZ, Ahmad F, Tak IR, Dar GH**.** First record of protozoan parasites in cyprinid fish, *Schizothorax niger Heckel*, 1838 from Dal Lake in Kashmir Himalayas with study on their pathogenesis. *Microb Pathogenesis*. 2016; 93:100-104.
3. Gardiner CH, Fayer R, Dubey JP. *An Atlas of Protozoan Parasites in Animal Tissues*. 2nd ed. Washington DC: Armed Force Institute of Pathology, American Registry of Pathology, 1998: 16-17.
4. Kotob MH, Menanteau-Ledouble S, Kumar G, Abdelzaher M, El-Matbouli M. The impact of co-infections on fish: a review. *Vet Res*. 2016; 47(98):1-12.
5. Maki JL, Brown CC, Dickerson HW. Occurrence of *Ichthyophthirius multifiliis*

within the peritoneal cavities of infected channel catfish *Ictalurus punctatu. Dis Aquat Org*. 2001; 44:41–45.
6. Noga EJ. *Fish Disease Diagnosis and Treatment*. 2nd Ames, IA: Wiley-Blackwell; 2010:129-148.
7. Pantoja MFW, Neves RL, Dias RDM, Marinho GBR, Montagner D, Tavares-Dias M. Protozoan and metazoan parasites of Nile tilapia *Oreochromis niloticus* cultured in Brazil. *Rev. MVZ Córdoba*. 2012; 17(1):2812-2819.
8. Roberts RJ. *Fish Pathology*. 4 ed. West Sussex, UK: Wiley-Blackwell; 2012: 76-85, 159, 309.
9. Scholz T. Parasites in cultured and feral fish. *Vet Parasitol*. 1999; 84:317-335.
10. Wei JZ, Li H, Yu H. Ichthyophthiriasis: emphases on the epizootiology. *Lett Appl Microbiol*. 2013; 57:91—101.

CASE III: 68197 (JPC 4084211).

Signalment: Nine-month-old, male, Meller's chameleon (*Trioceros melleri*), reptile.

History: A cohort of five Meller's chameleons (two male, three female) were group-housed in an outdoor zoological exhibit for approximately five months during the summer. One month prior to presentation, they were moved to an indoor enclosure for the winter. Routine complete blood cell count and serum chemistry panels performed two months prior to presentation were unremarkable.

Liver, chameleon. There is a diffuse loss of normal hepatic architecture and focal areas of pallor. (HE, 6X)

All five animals died within a span of one month. The first mortality occurred without premonitory signs. One week later, three other individuals in the group presented with acute onset dehydration, lethargy and anorexia. Despite supportive care and environmental changes, these three individuals became moribund and were euthanized ten days after presentation. Two days later, the final group member exhibited intermittent mouth gaping, decreased appetite, and a cutaneous vesicle near the tail base. Blood work performed at that time showed hyperglycemia, hyperphosphatemia, and a leukocytosis with reactive heterophils and monocytes. Despite gavage feedings and treatment with famcylcovir, ceftazadime, subcutaneous fluids, and meloxicam the animal developed serous oculonasal discharge and multifocal oral and dermal petechiae, and was found dead 10 days after onset of clinical signs.

Gross Pathology: All animals presented in thin body condition. The first four animals did not have any other significant gross findings, while the fifth animal exhibited mild transudative coelomic effusion and petechial hemorrhages affecting the tongue and kidneys.

Laboratory Results (clinical pathology, microbiology, PCR, ELISA, etc.): Fixed liver tissue from the first chameleon and a pooled sample of fresh frozen liver from the following three chameleons were sent to the San Diego Zoo Institute for Conservation Research for Ranavirus qPCR testing. All samples were positive for Ranavirus. PCR

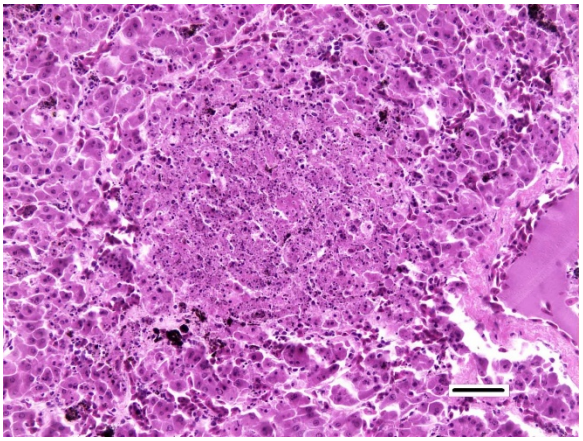

Liver, chameleon. There is diffuse loss of normal plate architecture. Foci of necrosis (center) lytic necrosis contain abundant cellular debris as well as melanin pigment liberated from necrotic melanomacrophages. (HE, 200X)

and sequencing of the neurofilament-like and major capsid protein genes further identified the virus as a member of the Frog Virus 3 (FV3) group.

Microscopic Description:
Liver: Randomly distributed throughout the hepatic parenchyma are numerous, variably-sized areas of necrosis characterized by disruption of chordal architecture and replacement by eosinophilic and karyorrhectic debris admixed with fibrin, mild hemorrhage, and dark brown to black granular material (presumptive melano-macrophage granules). Adjacent hepatocytes are often shrunken and hypereosinophilic with pyknotic to faded nuclei. Throughout the section, hepatocytes and biliary epithelial cells frequently contain one to multiple, variably-sized, basophilic intracytoplasmic viral inclusion bodies. Biliary epithelial cells are also multifocally necrotic, and the periductular connective tissue is often mildly expanded by clear space (edema). Rarely, and with some section variation, the walls of small blood vessels are segmentally disrupted by necrotic cellular debris and brightly eosinophilic fibrillar material (fibrinoid necrosis). Aggregates of small (1-2μm) intravascular rod-shaped bacteria are also present in some sections.

Contributor's Morphologic Diagnosis:
Liver, necrosis, multifocal to coalescing, acute, moderate, with intracytoplasmic viral inclusion bodies and intravascular bacteria

Contributor's Comment: Death in these chameleons is attributed to systemic ranaviral infection. Ranaviruses are increasingly recognized pathogens of fish and amphibians, which have contributed to infection, disease, and die-offs worldwide.[3] As such, ranaviral infection in amphibians is reportable to the World Organization for Animal Health.[12] In reptiles, ranavirus infections are well documented in turtles and tortoises, with sporadic reports in snakes and lizard species.[13] While other iridoviruses have been previously isolated from chameleons[7], to the author's knowledge this is the first documented case of ranavirus-related disease in chameleons. To date, ranavirus infection of mammals and birds has not been reported.

The Ranavirus genus belongs to the family Iridoviridae, which are large viruses (120-300 nm) with double stranded DNA and an icosahedral capsid containing a lipid component.[9] There are six species within the Ranavirus genus, the most well-characterized being Frog Virus 3 (FV3).[5]

In chelonians, ranavirus infection has been associated with sudden death, cervical / palpebral edema, and necroulcerative stomatitis / esophagitis. Histologic lesions generally include fibrinoid vasculitis, hepatic and splenic necrosis, enteritis, and pneumonia.[2,6,9] Reports in snakes are rare; one report in a group of green pythons described nasal mucosal ulceration, hepatic necrosis, and necrotizing pharyngitis.[4] Ranavirus has been detected in a total of 8

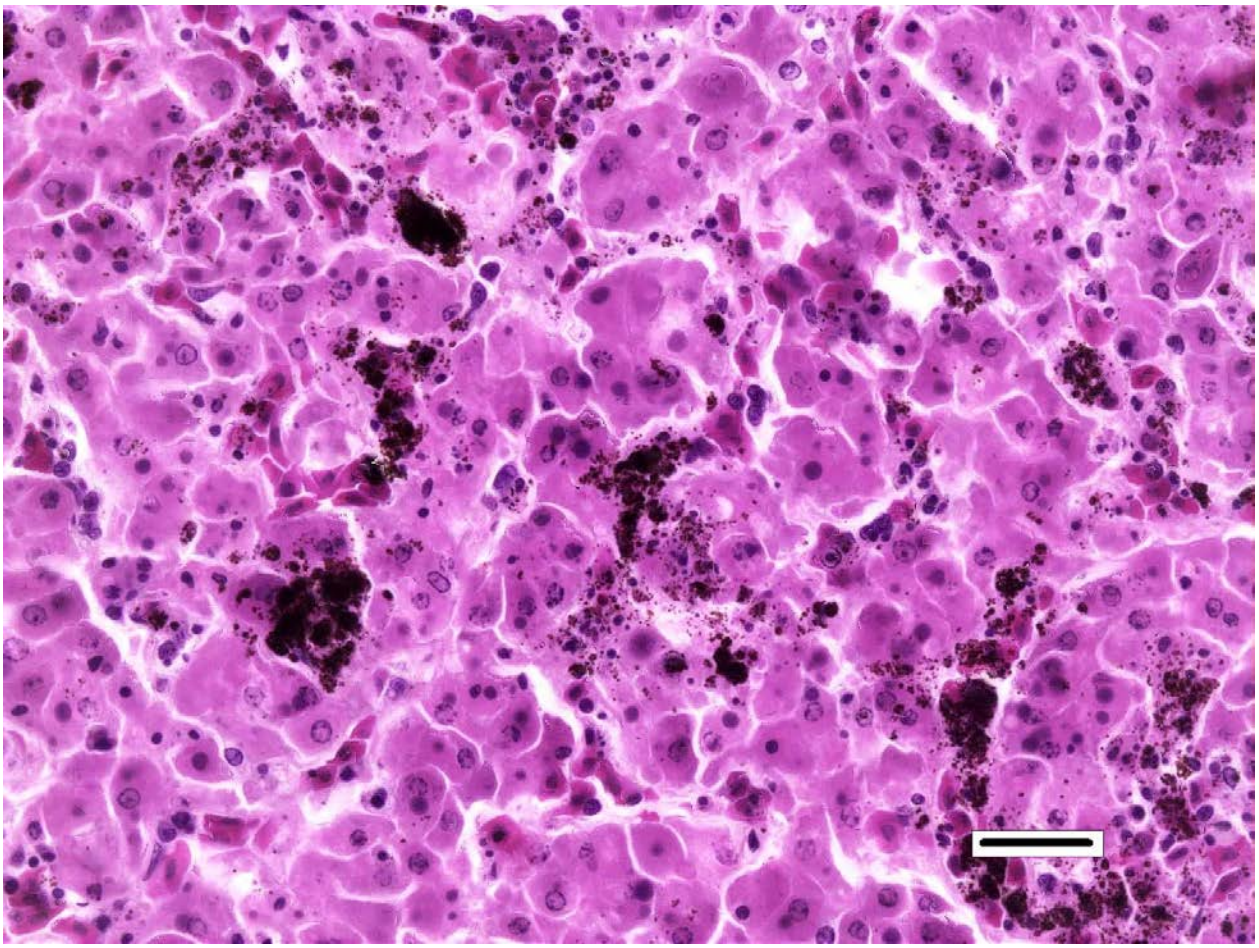

Liver, chameleon. In less affected areas, hepatocytes demonstrate degenerative and necrotic changes. Hepatocytes often contain one of more 2-4um round intracytoplasmic viral inclusions (arrows). (HE, 400X)

lizard species, with signs ranging from no overt disease to granulomatous dermatitis, necroulcerative glossitis, and hepatic necrosis.[1,10,13] A recent report on ranaviral disease in lizards indicates that ranaviral infection may be an important differential diagnosis for skin lesions in lizards.[13] In all hosts, subtle lesions of ranaviral infection may be obscured by secondary bacterial or fungal infection, especially when cytoplasmic inclusions are rare or inapprarent.[11]

The chameleons in this report presented predominately with non-specific clinical signs or sudden death. One animal presented with petechial hemorrhage and multifocal papular epidermitis progressing to vesicle formation and ulceration. The most significant microscopic findings in these cases were multifocal necrosis, most notably affecting the spleen, liver, kidney, adrenal tissues, and nasal cavity. Moderate to abundant numbers of basophilic intracytoplasmic intrahepatocytic and intrahistiocytic viral inclusions were present in the liver and nasal cavity, respectively. While stomatitis was not appreciated in this cohort, all animals exhibited varying degrees of necrotizing rhinitis with secondary bacterial and, in one animal, fungal infection. Occasional intravascular bacterial colonies were also observed in the liver of the

submitted chameleon, suggestive of intercurrent bacteremia/septicemia.

Antemortem diagnostic tests for ranavirus include identification of basophilic intracytoplasmic inclusions in leukocytes, PCR of blood or oral / cloacal swabs, or ELISA of plasma. Postmortem diagnostic tests include necropsy and histologic identification of basophilic intracytoplasmic inclusions, virus isolation, PCR of affected tissues, and electron microscopy. Immuno-histochemistry has been demonstrated in research settings, but is not available commercially[10]. Molecular testing for ranavirus is becoming more readily available, however many tests rely on reactivity with the highly conserved major capsid protein (MCP), which identifies the Ranavirus genus, but is not reliable for speciation. For these chameleons, quantitative polymerase chain reaction (qPCR) targeting the ranavirus MCP gene was followed by sequencing of the MCP and neurofilament-like genes, which further identified the virus as a member of the Frog Virus 3 (FV3) group.

In summary, ranavirus is an emerging disease of fish, amphibians, and reptiles that exhibits high morbidity and mortality. It is becoming increasingly recognized as a pathogen of lizards and thus, should be considered a differential in lizards that present with sudden death, rhinitis, skin lesions, and splenic / hepatic necrosis.

JPC Diagnosis: Liver: Hepatitis, necrotizing, diffuse, severe with numerous intracytoplasmic viral inclusions, Meller's chameleon (*Trioceros melleri*), reptile.

Conference Comment: The family *Iridoviridae* contain viruses which affect a very broad host range (arthropods, fish, amphibians, and reptiles) and produce numerous disorders to include systemic necrosis (genera *Ranavirus* and *Megalocyticirus*), and non-neoplastic skin lesions (genera *Lymphocystivirus*). On electron microscopy, iridoviruses form paracrystalline arrays within the cytoplasm which can be seen microscopically as prominent basophilic intracytoplasmic viral inclusions. Iridovirus virions are structurally similar to those of *Asfarviridae* (the causative agent of

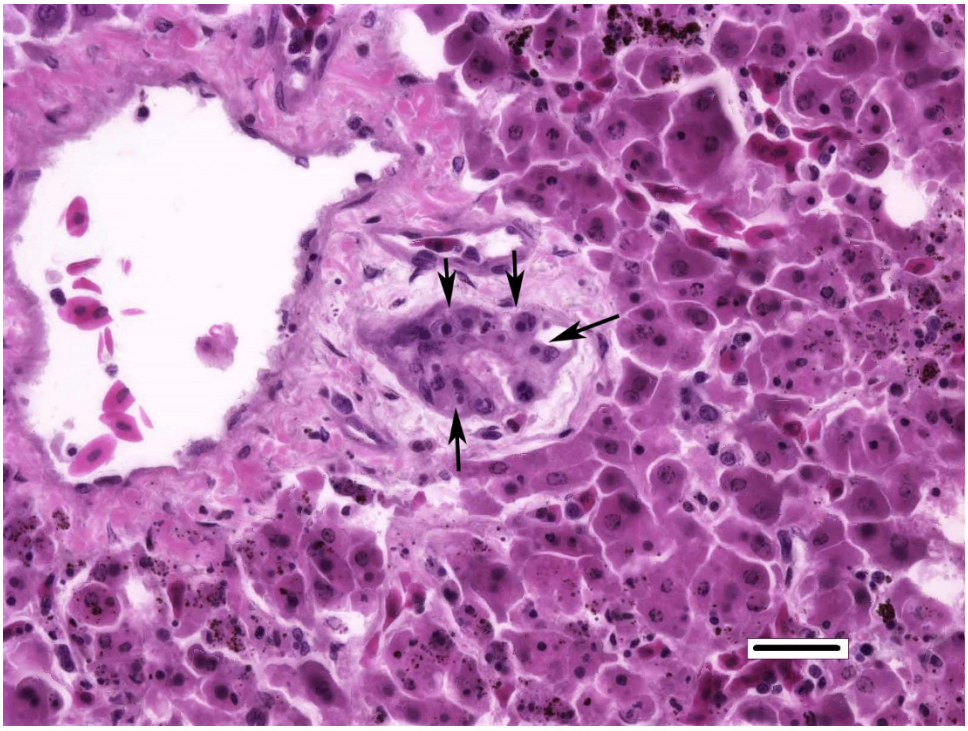

Liver, chameleon. Intracytoplasmic viral inclusions are also present within biliary epithelium as well. (HE, 400X)

African swine fever) and functionally, as there is a limited amount of initial replication which occurs in the nucleus, followed by more extensive replication in the cytoplasm later in the disease.[8]

There are two known strains of ranaviruses in amphibians, ranavirus type I (Frog virus-3) and ranavirus type III (tadpole edema virus).[14]

Frog virus-3 (FV-3, the etiologic agent in this case), the first ranavirus identified, was originally isolated from leopard frogs infected with ranid herpesvirus-1 (Lucke's renal adenocarcinoma). Despite the initial presumption of ranaviruses being a "benign" infectious agent, it became evident that their pathogenicity could cause a wide spectrum of diseases, ranging from cutaneous hemorrhage and necrosis to diffuse necrosis of numerous visceral organs; the aforementioned etiological agent is responsible for mass die-offs in North American frogs. Tadpoles are the most susceptible, but most wild amphibian populations are at risk of widespread epizootics. Affected tadpoles present initially with gross lesions resembling redleg, a common presentation of Gram-negative septicemia.

With ranavirus infections, the most severe lesions are in the kidneys, characterized by glomerular endothelial necrosis and hemorrhage with multifocal tubular necrosis, mild hemoglobin nephrosis, and free melanosomes within glomeruli. Additionally, there are extensive areas of hemorrhage and necrosis in the stomach and periportal to lobar necrosis in the liver. Basophilic intracytoplasmic inclusion bodies are present within glandular epithelial cells in the stomach and hepatocytes.[14]

Tadpole edema virus (TEV), an acute fatal infection of wild tadpoles of bullfrogs (*Rana catesbeiana*), bufonids (*Bufo americanus, Bufo woodhousei fowleri*), and pelobatids (*Scaphiopus intermontana*) has similar gross and microscopic findings to FV-3. [14]

Table 1: Viruses in the family *Iridoviridae*[8]

Genus	**Virus**
Iridovirus	Invertebrate iridescent virus-6, 1, 2, 9, 16, 21, 22, 23, 24, 29, 30, 31
Chloriridovirus	Invertebrate iridescent virus-3
Ranavirus	Frog virus-3 (tadpole edema virus, tiger frog virus) Ambystoma tigrinum virus (regina ranavirus) Bohle iridovirus Epizootic hematopoietic necrosis virus European catfish virus (European sheatfish virus) Santee-Cooper ranavirus (largemouth bass virus, doctor fish virus, guppy virus-6) Singapore grouper iridovirus, Grouper iridovirus
Megalocytivirus	Infectious spleen and kidney necrosis virus
Lymphocystivirus	Lymphocystis disease virus-1
Unclassified	White sturgeon iridovirus; Erythrocytic necrosis virus

Conference participants debated at length regarding the presence of bacteria in vessels and sinusoids and concluded that, although ranavirus commonly occurs in conjunction with other agents, the bacteria was most likely not part of the pathogenesis and excluded it from the morphologic diagnosis.

Contributing Institution:

Johns Hopkins School of Medicine
Department of Molecular and Comparative Pathobiology
733 N. Broadway, Suite 811
Baltimore, MD 21205
http://www.hopkinsmedicine.org/mcp/

References:

1 de Matos AP, Caeiro MF, Papp T, Matos BA, Correia AC, Marschang RE. New viruses from Lacerta monticola (Serra da Estrela, Portugal): further evidence for a new group of nucleo-cytoplasmic large deoxyriboviruses. *Microsc Microanal.* 2011;17(1)**:**101-108.

2 DeVoe R. GK, Elmore S, Rotstein D, Lewbart G, Guy J. Ranavirus-associated morbidity and mortality in a group of captive Eastern box turtles (*Terrapene carolina carolina). J Zoo Wildl Med.* 2004;35(4)**:**534-543.

3 Gray MJ, Chinchar VG. Introduction: history and future of Ranaviruses. In: Gray J, Chinchar, G., ed. *Ranaviruses, Lethal Pathogens of Ectothermic Vertebrates*. 1st Ed.: Springer International Publishing; 2015: 1-7.

4 Hyatt AD, Williamson M, Coupar B, et al. First identification of a Ranavirus from green pythons (*Chondropython viridis*). *Journal of Wildlife Diseases.* 2002;38(2)**:**239-252.

5 Jancovich JK, Steckler NK, Waltzek TB. Ranavirus taxonomy and phylogeny. In: Gray J, Chinchar, G., ed. *Ranaviruses, Lethal Pathogens of Ectothermic Vertebrates*. 1st Ed.: Springer International Publishing; 2015: 59-70.

6 Johnson AJ, Pessier AP, Wellehan JF, Childress A, Norton TM, Stedman NL, et al. Ranavirus infection of free-ranging and captive box turtles and tortoises in the United States. *J Wildl Dis.* 2008;44(4)**:**851-863.

7 Just F, Ahne W, Blahak S. Occurrence of an invertebrate iridescent-like virus (*Iridoviridae)* in reptiles. *J Vet Med B.* 2001;48**:**685-694.

8 MacLachlan NJ, Dubovi EJ. *Fenner's Veterinary Virology*. 5th ed. San Diego, CA: Elsevier; 2017:182-188.

9 Marschang RE. Viruses infecting reptiles. *Viruses.* 2011;3(11)**:**2087-2126.

10 Marschang RE, Braun S, Becher P. Isolations of a Ranavirus from a gecko (*Uroplatus fimbriatus). Journal of Zoo and Wildlife Medicine.* 2005;45(2)**:**295-300.

11 Miller DL, Pessier AP, Hick P, Whittington RJ. Comparative pathology of Ranaviruses and diagnostic techniques. In: Gray J, Chinchar, G., ed. *Ranaviruses, Lethal Pathogens of Ectothermic Vertebrates*: Springer International Publishing; 2015: 171-208.

12 Schloegel LM, Daszak P, Cunningham AA, Speare R, Hill B. Two amphibian diseases, chytridiomycosis and ranaviral disease, are now globally notifiable to the World Organization for Animal Health (OIE): an assessment. *Diseases of Aquatic Organisms.* 2010;92(3)**:**101-108.

13 Stohr AC, Blahak S, Heckers KO, Wiechert J, Behncke H, Mathes K, et al. Ranavirus infections associated with skin lesions in lizards. *Vet Res.* 2013;44**:**84.

14 Wright KM, Whitaker BR. *Amphibian Medicine and Captive Husbandry.* Malabar, FL: Krieger Publishing Company; 2001:418-420.

CASE IV: N17-104-1 (JPC 4101578).

Signalment: 22-year-old, female, intact, red-eared slider (*Trachemys scripta elegans*), reptile.

History: This turtle presented for persistent abnormal egg laying behavior, and had been treated for dystocia with 8 retained eggs several months prior at the referring veterinarian. No remaining eggs were observed on radiographs at presentation, and bloodwork revealed elevated liver enzymes (AST), azotemia, hyperkalemia, and hypoproteinemia. Coeloscopic ovario-hysterectomy was performed and revealed multiple enlarged ovarian follicles with numerous adhesions to the body wall and numerous yolk droplets on serosal surfaces. Due to the inability to completely surgically resect all ovarian tissue and poor prognosis for recurrent coelomitis, euthanasia was elected.

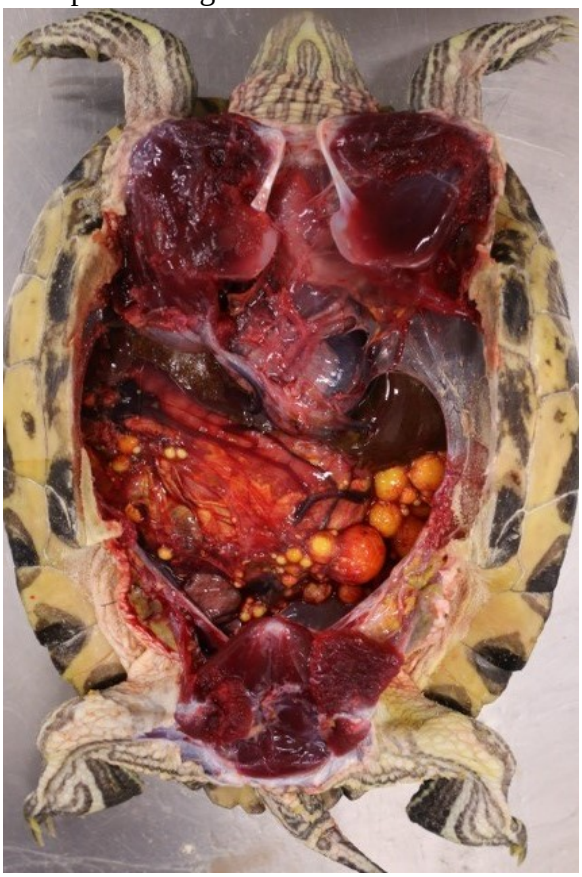

Presentation, turtle: A large reddish-tan mass is present within and expanding ovarian follicles. (Photo courtesy of: Cummings School of Veterinary Medicine at Tufts University, http://vet.tufts.edu/foster-hospital-small-animals/departments-and-services/pathology-service/)

Gross Pathology: Within the caudal coelom, there is a mixture of healthy mature and immature follicles, bilaterally, with an 11 x 6 cm, yellow to tan, soft, friable, fatty, ovoid mass associated with the right-sided ovarian tissue and 2-3 mature follicles embedded within the capsule. On the surface of the opposing coelomic wall are patchy, thin, yellow, fibrinous adhesions. On cut section, the center of the mass is markedly friable and greasy, and homogenously pale tan. Sections of the mass did not float when placed into formalin.

Laboratory Results (clinical pathology, microbiology, PCR, ELISA, etc.): Cytologic impressions of the mass revealed small clusters of markedly pleomorphic, large, round to polygonal cells arranged singly or in loose aggregates on a moderately proteinacous background with scattered red blood cells. Cells range from 20 to 50 um in diameter, with distinct cell borders and contain moderate, pale basophilic, occasionally vacuolated cytoplasm. Nuclei are large and round to oval with reticular chromatin and contain multiple prominent nucleoli. Binucleation and multinucleation is frequent. Anisocytosis and anisokaryosis are marked, and mitotic activity is moderate.

Microscopic Description:

Ovary: Displacing previtellogenic and vitellogenic ovarian follicles, is an un-encapsulated, poorly demarcated, expansile neoplasm composed of sheets of round to polygonal cells, occasionally forming indistinct lobules, separated by very thin collagenous stroma. Neoplastic cells have distinct cell borders and moderate amounts of homogenous, pale eosinophilic cytoplasm.

Ovary, turtle: A tan mass (at left) incorporates numerous follicles. (HE, 6X) (Photo courtesy of: Cummings School of Veterinary Medicine at Tufts University, http://vet.tufts.edu/foster-hospital-small-animals/departments-and-services/pathology-service/)

Nuclei are round to oval, centrally located with vesiculate chromatin pattern and contain 1 to 3, prominent nucleoli. Anisocytosis and anisokaryosis are moderate. There are 19 mitotic figures in 10 hpf. There is frequent multifocal individual cell necrosis and low numbers of scattered lymphocytes.

Contributor's Morphologic Diagnosis:
Ovary, dysgerminoma

Contributor's Comment: Dysgerminomas are germ cell tumors that arise from undifferentiated, pluripotent germ cells in the ovary.[6,12,14,15] Other germ cell tumors, such as teratoma and embryonal carcinoma, are distinguished by somatic differentiation and maturation of neoplastic cells towards an embryonic tissue type(s). In chelonians, germ cell tumors are extremely rare.[3,5,6,9,12] Dysgerminomas have been reported in 2 red-eared sliders and a snapping turtle. Teratomas were reported in a red-eared slider and a snapping turtle. In other veterinary species, dysgerminomas are similarly rare, and have been reported in dogs, cats, horses, maned wolves, Eastern rosella, and mountain chicken frogs.[2,10,15] Maned wolves in captivity have been reported to have an increased prevalence of ovarian tumors, with suspected hereditary predisposition for dysgerminomas.[10] In humans, dysgerminomas can occasionally be hormonally functional and human chorionic

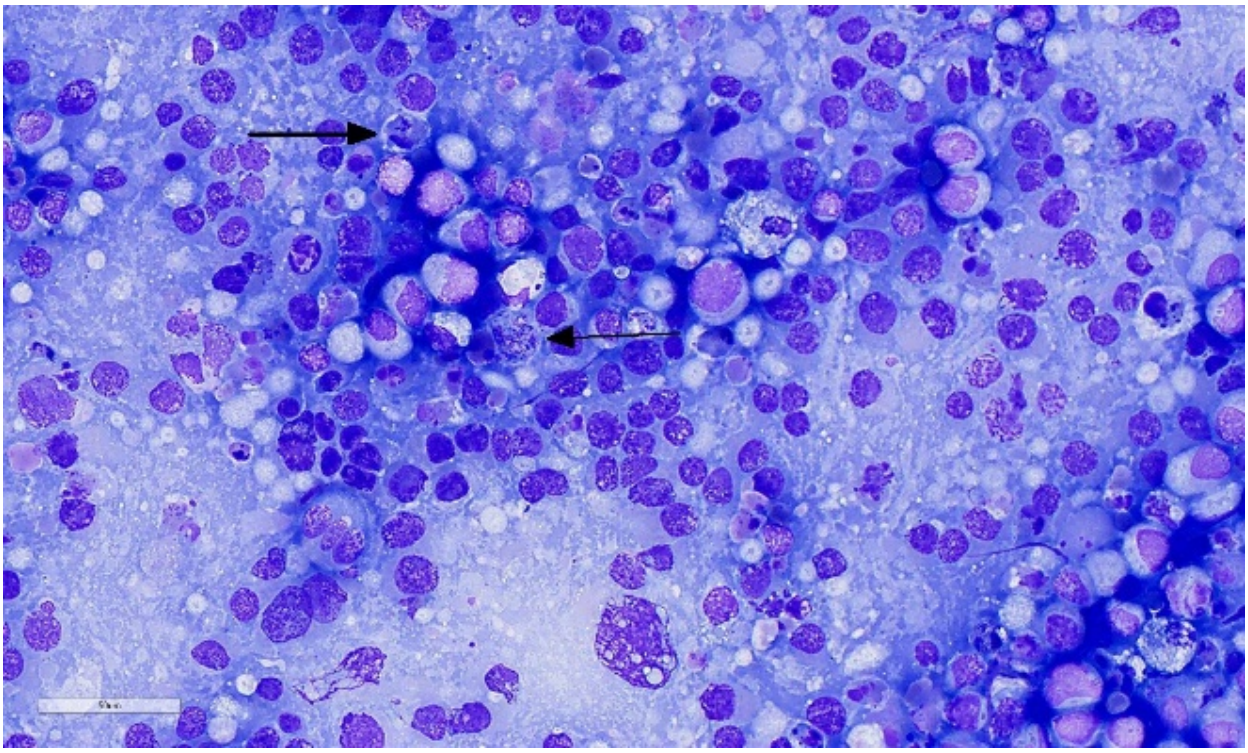

Ovary, turtle: An impression of the mass contain numerous pleomorphic and occasional multinucleated cells with numerous mitotic figures (arrows) on a blue proteinaceous background. (Wrights, 400X)

gonadotropin, produced by syncytio-trophoblastic giant cells, can contribute to aberrant follicular maturation and ovulation and pregnancy-like signs.[11,15] Similar hormonal influence by the tumor contributing to the clinical signs of chronic egg laying behavior in this turtle is speculative. Although dysgerminomas are considered malignant, metastasis is rarely observed.

Clinical signs across all species is largely non-specific, and related to the effects of a space-occupying mass within the abdomen. Turtles have shown signs of anorexia, lethargy, carapace dysecdysis, or inability to swim normally, and, in this case, abnormal egg laying behavior.[3,5,9] Grossly, in chelonians, dysgerminomas appear as unilateral, intracoelomic, white to yellow, friable, fat-like masses, ranging from 4 to 11 cm, and are associated with ovarian tissue. Microscopic examination reveals sheets of round to polygonal cells with large, round to oval vesicular nuclei with prominent nucleoli, and moderate pale eosinophilic cytoplasm. Mitoses are frequent. Scattered lymphocytes and multifocal regions of ischemic necrosis are occasionally noted.

Immunohistochemistry for germ cell tumors have not been established in chelonians, and was not performed in this case. Currently, a diagnosis of dysgerminoma in people is reliant on positive immunoreactivity with placental alkaline phosphatase (PLAP) and vimentin.[8,11] Recent development of germ cell-selective immunohistochemical markers, OCT3/4 and SALL4, are now also recommended for diagnosis. OCT3/4 is a nuclear transcription factor that plays a role in maintaining pluripotency in primordial germ and stem cells. SALL4 is a nuclear factor with which OCT3/4 interacts, and is involved in totipotency. Both OCT3/4 and SALL4 are strongly expressed in dysgerminomas, but, since they are both

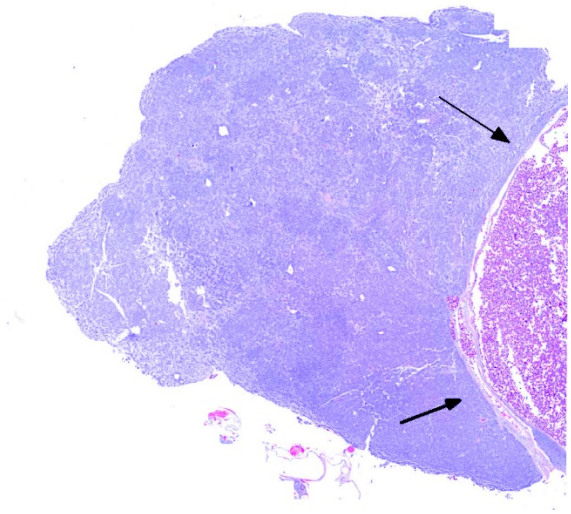

Ovary, turtle. A densely cellular neoplasm opposes a vitellogenic follicle (arrows). (HE, 6X)

markers of pluripotency, they are also expressed in embryonal carcinomas and less differentiated teratomas. CD117 (c-kit) is a proto-oncogene expressed in dysgerminomas, and not in other germ cell tumors. However, only 30% of dysgerminomas demonstrate immuno-reactivity. Dysgerminomas are immuno-negative for α-fetoprotein, inhibin-α, and S-100.

Immunohistochemical markers for dysgerminomas in veterinary literature are variable across species and, in some cases, show similarities to the immunophenotype observed in people.[2,4,15] OCT4 was expressed in dysgerminomas in mountain chicken frogs, but the tumors were immunonegative for vimentin, PLAP, and calretin.[2] In the dog, dysgerminomas do not express c-kit, but are immunopositive for SALL4 with variable expression of PLAP and vimentin. Immunohistochemistry with α-fetoprotein, inhibin-α, and S-100 are negative in dogs.[4]

Based on the gross and microscopic appearance in this case, diagnosis of dysgerminoma is strongly supported. Dysgerminomas should be considered as a differential diagnosis in turtles with a coelomic mass and antemortem identification with cytology may be helpful. As more cases are identified, immunophenotyping for germ cell tumors in turtles can be further elucidated. This is the first report of a red-eared slider with a dysgerminoma showing clinical signs of chronic reproductive behavior, suggesting the possibility of hormonal production by this tumor in this species.

JPC Diagnosis: 1. Ovary: Dysgerminoma, red-eared slider (*Trachemys scripta elegans*), reptile.
2. Cytologic impression: Round cell proliferation with intracytoplasmic, eosinophilic granules and foamy macrophages.

Conference Comment: Two types of germ cell tumors have been reported in female domestic animals: dysgerminomas and teratomas. Germ cells arise in the yolk sac, migrating to the gonadal ridge during differentiation, and associate with sex cords before formation of primary follicles.[1]

Dysgerminoma, a rare ovarian tumor, is most common in the bitch and queen, but have also

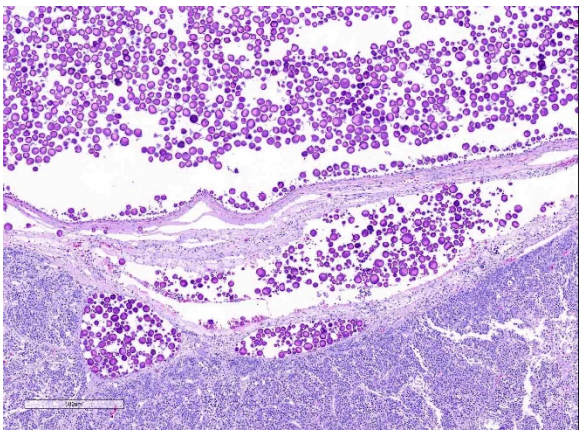

Ovary, turtle. Higher magnification of the mass demonstrates a nesting pattern that is unusual for a dysgerminoma. A mature vitellogenic follicle is at top. (HE, 40X)

been identified in the cow, mare, sow, and maned wolves. Dysgerminomas in fish may contain testicular elements. They correspond to seminomas in the testicle and occasionally are hormonally active, resulting in clinical signs of hyperestrogenism. Grossly, dysgerminomas are large, firm, white or gray homogenous tumors that elevate the ovarian capsule and can contain areas of hemorrhage, necrosis or cystic cavitations.

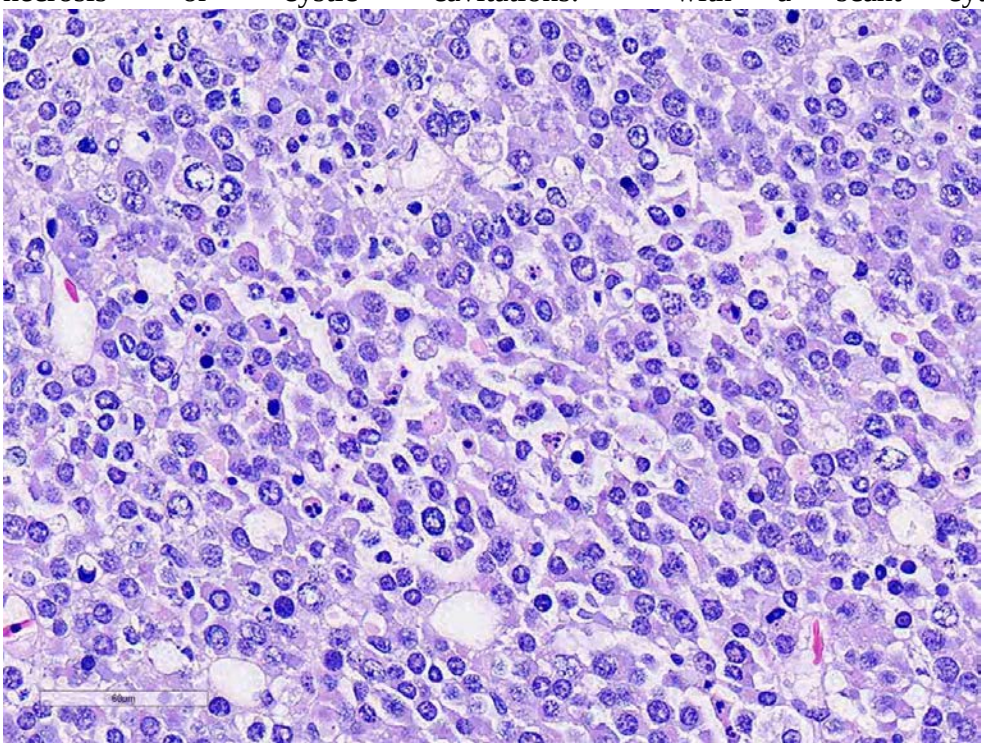

Ovary, turtle. Sheets of round cells with marked anisokaryosis and numerous red cytoplasmic granules composed the mass. There is a high mitotic rate as well as abundant cellular apoptosis. (HE, 200X)

Microscopically, they are densely cellular and composed of primitive germ cells arranged in sheets, cords, and nests separated by a thin connective tissue septa. Neoplastic cells have large vesicular nuclei with prominent nucleoli and scant eosinophilic cytoplasm giving them a blastic appearance. Multinucleated cells and bizarre mitotic figures are common as is metastasis to regional lymph nodes or explantation to adjacent tissues.

Teratomas are less common and are composed of at least two of the germinal layers (endoderm, mesoderm, or ectoderm).

A recent article[7] (discussed during the conference) identified a presumptive ovarian dysgerminoma in an orange-spot freshwater stingray which was composed of sheets of round cells arranged in solid and cystic areas with a scant cytoplasm, moderate anisokaryosis, multiple nucleoli and frequent mitotic figures. Additionally, the moderator shared an interesting case in a medaka in which there was spermatogenic progression within the dysgerminoma. Differentials discussed by conference participants included lymphoma, histiocytic tumor, and sex cord stromal tumor.

Contributing Institution:

Cummings School of Veterinary Medicine at Tufts University
http://vet.tufts.edu/foster-hospital-small-animals/departments-and-services/pathology-service/

References:

1. Agnew DW, MacLachlan NJ. Tumors of the genital systems. In: Meuten DJ, ed. *Tumors in Domestic Animals.* 5th ed. Ames, IA: John Wiley & Sons, Inc.; 2017:690-698.

2. Fitzgerald SD, Duncan AE, Tabaka C, Garner MM, Dieter A, Kiupel M. Ovarian dysgerminomas in two mountain chicken frogs (*Leptodactylus fallax*). *J Zoo Wildlife Med.* 2007; 38(1): 150-153.
3. Frye FL, Eichelberger SA, Harshbarger JC, Cuzzocrea AD. Dysgerminomas in two red-eared slider turtles (*Trachemys scripta elegans*) from the same household. *J Zoo Anim Med*. 1988; 19(3): 149-151.
4. Hara S, Morita R, Shiraki A, et al. Expression of protein gene product 9.5 and Sal-like protein 4 in canine seminomas. *J Comp Path.* 2014; 151: 10-18.
5. Hidalgo-Vila J, Martinez-Silvestre A, Diaz-Paniagua C. Benign ovarian teratoma in a red-eared slider turtle (*Trachemys scripta elegans*). *Vet Rec*. 2006; 159: 122-123.
6. Innis CJ, Boyer TH. Chelonian reproductive disorders. *Vet Clin Exot Anim*. 2002; 5: 555-578.
7. Jafarey YS, Berlinski RA, Hanley CS, Garner MM, Kiupel M. Presumptive dysgerminoma in an orange-spot freshwater stingray (*Potamotrygon motoro). Journal of Zoo and Wildlife Medicine*. 2015; 46(2):382-385.
8. Kaspar HG, Crum CP. The utility of immunohistochemistry in the differential diagnosis of gynecologic disorders. *Arch Pathol Lab Med*. 2015; 139: 41-54.
9. Machotka SV, Wisser J, Ippen R, Nawab E. Report of dysgerminoma in the ovaries of a snapping turtle (Chelydra serpentina) with discussion of ovarian neoplasms reported in reptilians and women. *In Vivo*, 1992 Jul-Aug; 6(4): 349-54.
10. Munson L, Montali RJ. High prevalence of ovarian tumors in maned wolves (*Chrysocyon brachyurus*) at the National Zoological Park. *J Zoo Wildlife Med.* 1991; 22(1): 125-129.
11. Nogales FF, Dulcey I, Preda O. Germ cell tumors of the ovary. *Arch Pathol Lab Med*. 2014; 138: 351-362.
12. Perry SM, Mitchell MA. Reproductive medicine in freshwater turtles and land tortoises. *Vet Clin Exot Anim*. 2017; 20: 371-389.
13. Sever M, Jones TD, Roth LM, Karim FWA, et al. Expression of CD117 (c-kit) receptor in dysgerminoma of the ovary: diagnostic and therapeutic implications. *Mod Path*. 2005; 18: 1411-1416.
14. Solano-Gallego L. Reproductive system. In: Raskin RE, Meyer DJ. *Canine and Feline Cytology: A Color Atlas and Interpretation Guide*. 2nd ed. St. Louis, MO: Elsevier Saunders; 2010: 282-286.
15. Strunk A, Imai DM, Osofsky A, Tell LA. Dysgerminoma in an Eastern Rosella (*Platycercus eximius eximius*). *Avian Diseases*. 2011; 55: 133-138.

Self-Assessment - WSC 2017-2018 Conference 24

1. Which of the following stains has been used to distinguish benign peripheral nerve sheath tumors from other tumors with a similar morphology?
    a. NSE
    b. S-100
    c. GFAP
    d. NFP

2. Which of the following forms of Ichthyphthirius multifiliis invades the skin ?
    a. Tomont
    b. Tomite
    c. Theront
    d. Therite

3. Which of the following appears as haystacks of filaments in the gill of fish?
    a. Flexibacter columnare
    b. Epitheliocystis
    c. Trichodina sp.
    d. Monogenean flukes

4. Which of the following are not affected by ranavirus infection?
    a. Birds
    b. Lizards
    c. Fish
    d. turtles

5. Which of the following proto-oncogenes has been expressed in dysgerminomas but not in other germ cell tumors?
    a. c-myc
    b. c-kit
    c. fas
    d. c-ras

Please email your completed assessment to Ms. Jessica Gold at Jessica.d.gold2.ctr@mail.mil for grading. Passing score is 80%.This program (RACE program number) is approved by the AAVSB RACE to offer a total of 0.5 CE Credits, with a maximum of 12.5 CE Credits being available to any individual Veterinary Medical Professionals for the 2017-2018 Wednesday Slide Conference. This RACE approval is for the subject matter categories of: SCIENTIFIC using the delivery method of NON-INTERACTIVE DISTANCE. This approval is valid in jurisdictions which recognize AAVSB RACE; however, participants are responsible for ascertaining each board's CE requirements.
RACE does not "accredit", "endorse" or "certify" any program or person, nor does RACE approval validate the content of the program.

Joint Pathology Center
Veterinary Pathology Services

WEDNESDAY SLIDE CONFERENCE 2017-2018

Conference 25

9 May 2018

CASE I: 17B-0101 (JPC 4102436).

Signalment: 9-year-old, neutered male, mixed breed (*Canis familiaris*), canine.

History: The dog had an approximately 3 week history of hematuria which improved but did not resolve with antibiotics. Abdominal ultrasound and CT scan revealed a mass lesion involving the left kidney. Cytologic evaluation of the mass lesion revealed spindle cells of uncertain origin (reactive vs. neoplastic). The left adrenal gland was not visualized via imaging or during surgery. Surgical findings reported white streaking along the mesentery suggestive of lymphatic invasion.

Gross Pathology: Received is a 20 x 11 x 10 cm multilobulated mass lesion with multi-focally adhered omentum. The kidney itself is not apparent until sectioning. On cut section, the mass lesion is soft, multilobular, red and tan with a thin rim of remnant kidney representing approximately 10% of the submitted tissue. The adrenal gland is not apparent.

Laboratory results: None provided.

Microscopic Description: Left kidney: Where anatomic borders are apparent, the leading edge of the mass lesion is necrotic and thus, poorly demarcated. Regions of the border are composed of fibrous connective tissue which could either represent tumor capsule or could represent reactive fibrosis of the kidney.

Presentation, dog. Abdominal computed tomography image of mass in region of left kidney. (Photo courtesy of: University of Wisconsin Madison, School of Veterinary Medicine, Pathobiological Sciences, 2015 Linden Dr., Madison, WI 53706)

The mass lesion is composed of multiple lobules of spindle cells usually arranged in streams, but occasionally forming tubules, acini, and rosettes all of which have similar cellular morphology. The fibrovascular stroma is fine. Neoplastic cells have indistinct cell borders, moderate amounts of eosinophilic cytoplasm, and round to oval nuclei with coarsely stippled chromatin. Mitotic figures average 8 in 10 high powered fields examined. Anisocytosis and aniso-karyosis are moderate. Multifocally there is abundant tumor necrosis, variably coagulative and lytic, with multifocal hemorrhage. The tumor is separated from the surgical margin by a single layer of spindle cells. There is no evidence of vascular invasion. The adrenal gland is not histologically apparent.

Contributor's Morphologic Diagnosis: Left kidney: Nephroblastoma

Contributor's Comment: Nephroblastoma is the most common primary renal tumor of swine, chickens and fish, the fifth most common primary renal tumor in dogs, and the fourth most common primary renal tumor in cats.[7] A tumor with similar morphology also occurs in the thoracolumbar spinal column of young dogs.[7]

Kidney, dog. Left kidney with adhered omentum. (Photo courtesy of: University of Wisconsin Madison, School of Veterinary Medicine, Pathobiological Sciences, 2015 Linden Dr., Madison, WI 53706)

The age distribution in veterinary species follows that in people where it is an embryonal, childhood tumor. In this case and other reported cases in dogs, the tumor is discovered in adulthood but is suspected to either be present from a young age or to arise from remnant nephrogenic rests later in life.[2,7]

Despite Dr. Meuten's commentary that "searching sufficient sections will eventually identify a few [glomeruloid structures] that are worthy of the diagnosis or a photograph," numerous DVM and MD pathologists at our institution were unable to do so. Because this tumor did not have classic features of primitive glomeruli, the slides were reviewed with local collaborating MD pathologists with expertise in embryonic renal tumors. Positive immunohistochemical staining for Wilms' tumor 1 (WT1) confirmed the diagnosis of nephroblastoma and ruled out their differential diagnosis of synovial cell sarcoma which, in humans, can be a primary mesenchymal renal tumor diagnosed via

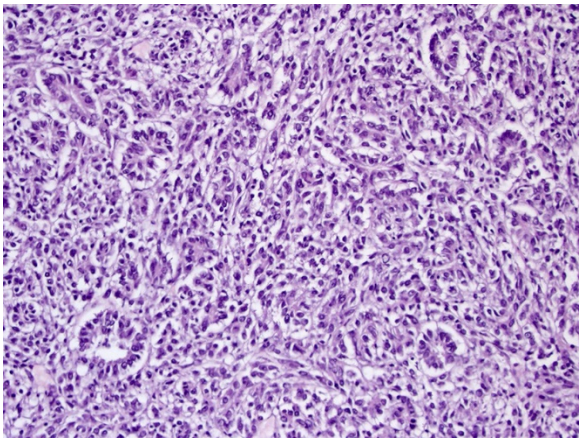

Kidney, dog. The neoplasm is primarily composed of spindled cells, throughout which primitive tubules are scattered. (HE, 400X)

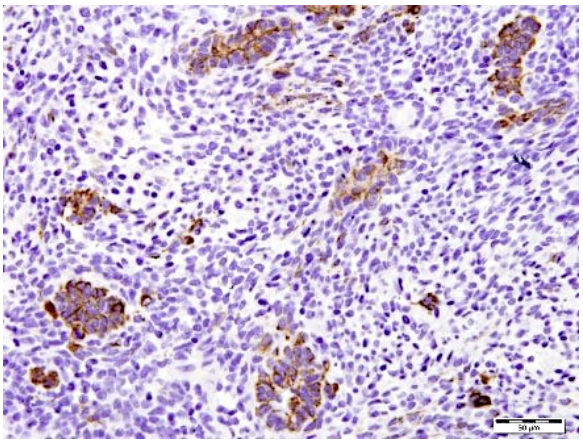

Kidney, dog. Tubular structures show cytoplasmic immunoreactivity for cytokeratin. (anti-cytokeratin, 400X) (Photo courtesy of: University of Wisconsin Madison, School of Veterinary Medicine, Pathobiological Sciences, 2015 Linden Dr., Madison, WI 53706

morphology together with specific chromosomal translocations.[7]

Metastatic risk is considered high in dogs[4,7], but primary source data for this assertion is difficult to confirm, and sample sizes are usually small in published studies. In a 2006 retrospective paper[1] detailing clinical outcome of dogs with primary renal neoplasia, only 5 of 82 dogs had the diagnosis of nephroblastoma. Of those, one reported metastatic disease at the time of diagnosis and three of four from which follow-up was available had metastatic disease at the time of death. The spindle cell variant is also reported to be of higher metastatic potential[4] also without a reference to primary source data. The tumor in the submitted case progressed quickly both locally and distantly in spleen and abdominal lymph nodes within 6 weeks of resection. The blastemal predominant morphology of this tumor has been reported in at least two other single case reports in dogs[9,10], the former representing a benign variant.

Cianciolo and Mohr report tumors with more differentiated tubular and glomerular structures have a better prognosis than those with anaplasia and sarcomatous features[2] although the primary source for this statement is unclear. Diagnosis in this case was challenging in that the characteristic feature of glomeruloid structures were not apparent.

JPC Diagnosis: Kidney: Nephroblastoma, mixed breed (*Canis familiaris*), canine.

Conference Comment: Nephroblastomas are a generally disorganized mixture of three components: epithelial, mesenchymal, and blastemal which arise from the metanephrogenic renal blastema. In different tumors and even different areas within the same tumor one or more of those components can predominate. In humans, the causative factor is mutation of the tumor suppressor gene Wilm's tumor-1 (WT-1) which is located on chromosome 11p13. A genetic cause in animals has not yet been identified. Grossly, nephroblastomas are most often unilateral and isolated to one pole of the kidney, encapsulated, multilobulated, white to tan, and firm with spongy/cystic areas and foci of necrosis and hemorrhage. Microscopically, the epithelial component often forms abortive tubules or primitive glomeruli within tubules surrounded by the mesenchymal components which is

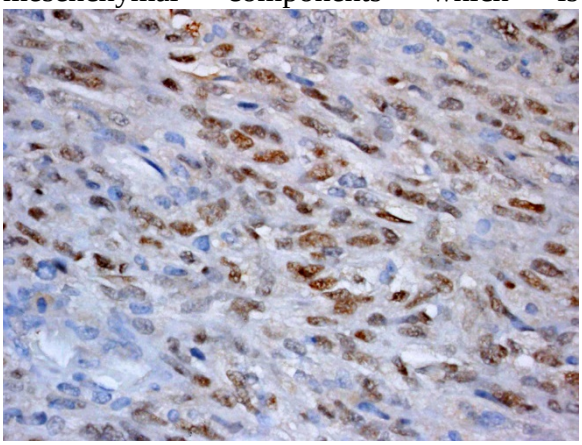

Kidney, dog. Spindle cells are diffusely and strongly positive for WT-1. (anti-WT1, 400X)

organized in long interlacing streams and can differentiate into muscle, fibrous, adipose, cartilage or bone tissues. The blastemal component is often found in clumps between the epithelial and mesenchymal components and are small cells with high nuclear to cytoplasmic ratios and round, hyper-chromatic nuclei.[2,7]

As mentioned above, it has been described that tumors with mesenchymal differentiation often exhibit frequent metastasis.[4] There has been recent publication of a blastemal-predominant canine renal nephroblastoma that had gingival metastasis which suggests that all types of nephroblastomas have metastatic potential. In dogs, a common presentation occurs not in the kidney, but in the thoracolumbar spinal cord, arising from remnants of metapnephric rests located between the dura mater and spinal cord. This condition is most commonly observed in young German Shepherd Dogs and is also called ectopic nephroblastoma. Additionally, there have been rare reports of multifocal spinal cord involvement which may represent metastasis or multifocal generation of the tumor.[3,11] Traditional renal nephroblastomas have been identified in all species but occur with greatest frequency in chickens and pigs.[2] Where in chickens, they are often associated with avian leukosis virus.[8] In fish (Japanese eel and Rainbow trout) and rats (Sprague-Dawley subline) nephroblastomas are induced via carcinogens.[5,6]

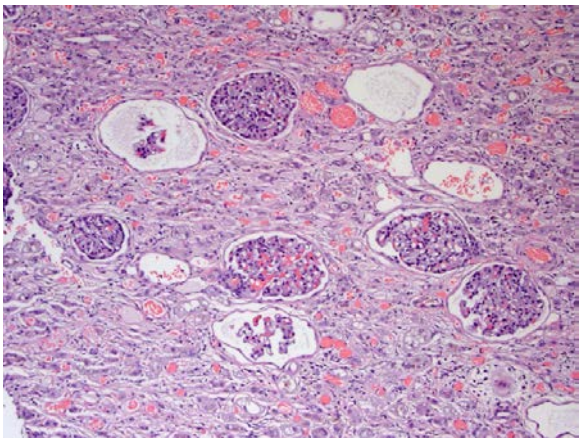

The adjacent neoplasm exhibits marked tubular atrophy, interstitial expansion by mature collagen, and cystic changes to glomeruli. (HE, 200X)

Contributing Institution:
University of Wisconsin Madison
School of Veterinary Medicine
Pathobiological Sciences

References:

1. Bryan JN, Henry CJ, Turnquist SE, Tyler JW, et al. Primary renal neoplasia of dogs. *JVIM*. 2006; 20(5):1155–1160.
2. Cianciolo R, Mohr C. Urinary system. In: Maxie MG, ed. *Jubb, Kennedy & Palmer's Pathology of Domestic Animals*. Vol 2. 6th ed. St. Louis, MO: Elsevier; 2016:376-464.
3. Henker LC, Bianchi RM, Vargas TP, DeOliveira EG, et al. Multifocal spinal cord nephroblastoma in a dog. *J Comp Pathol*. 2018;158:12-16.
4. Ladanyi M. Fusions of the SYT and SSX genes in synovial sarcoma. *Oncogene*. 2001; 20(40):5755-5762.
5. Lombardini ED, Hard GC, Harshbarger JC. Neoplasms of the Urinary Tract in Fish. *Vet Pathol*. 2014;51:1000-1012.
6. Mesfin GM. Intralobar nephroblastematosis: precursor lesions of nephroblastoma in the Sprague-Dawley rat. *Vet Pathol*. 1999;36:379-90.
7. Meuten D, Meuten T. Tumors of the urinary system. In: Meuten DJ, ed. *Tumors in Domestic Animals*. 5th ed. Ames, IA: John Wiley & Sons; 2017:632-688.
8. Nair V, Fadly AM. Neoplastic diseases: Leukosis/sarcoma group. In: Swayne DE, ed. *Diseases of Poultry*. 13th ed. Ames, IA: Wiley-Blackwell Publishing; 2013:578-582.

9. Simpson RM, Gliatto M, Casey HW, Henk WG. The histologic, ultrastructural, and immunohistochemical features of a blastema-predominant canine nephroblastoma. *Vet Pathol*. 1992; 29(3):250-253.
10. Soldati S, Radaelli E, Mazzuti A, Scanziani E. Congenital mesoblastic nephroma in a young basset hound dog. *J Small Anim Pract*. 2012; 53:709–713.
11. Terrell SP, Platt SR, Chrisman CL, et al. Possible intraspinal metastasis of a canine spinal cord nephroblastoma. *Vet Pathol*. 2000;37:94-97.

CASE II: 16A351 (JPC 4101577).

Signalment: Full-term stillborn male rhesus macaque (*Macaca mulatta*), non-human primate.

History: A 4-year-old primiparous, outdoor-housed female rhesus macaque from a large breeding colony presented acutely for clinical signs of dystocia. Ultrasonography revealed an absent fetal heartbeat consistent with *in utero* fetal demise. A caesarean section was subsequently performed; the dam recovered uneventfully. A full-term stillborn male rhesus macaque was submitted for necropsy along with the bidiscoid placenta.

Gross Pathology: Grossly, the crown of the head of the fetus was deformed and exhibited abundant subcutaneous edema and hemorrhage. The face demonstrated moderate edema and congestion. The lungs were diffusely deep red and atelectatic, with scattered 1- 2mm white foci. Gross examination of the primary and secondary placental discs revealed few opaque tan-white foci on the fetal surface with slight thickening of the fetal membranes. Multifocally, there were marginal regions of pallor and infarction on both placental discs.

Presentation, abortus, rhesus macaque. The crown of the head of the fetus was deformed and there is abudant subcutaneous edema and hemorrhage. (Photo courtesy of: Oregon National Primate Research Center, Oregon Health and Science University, Division of Comparative Medicine, Pathology Services Unit, 505 NW 185th Avenue, Beaverton, OR, 97006)

Laboratory results: 4+ beta-hemolytic *Streptococcus* sp. was isolated from the placenta and stomach, with 2+ beta-hemolytic *Streptococcus* sp. cultured from the pleura

Microscopic Description: Two sections of placenta (primary disc) with attached fetal membranes are examined.

Diffusely expanding and infiltrating the subchorionic trophoblast layer is a nearly continuous, thick band of karyorrhectic neutrophils admixed with eosinophilic cellular debris, and few clusters of homogenous eosinophilic material (fibrin). Trophoblasts are vacuolated and necrotic. The chorionic plate is expanded by edema and contains fewer numbers of neutrophils which are often perivascular. The amniotic epithelium is sloughed and replaced by necrotic cellular debris interspersed with wispy strands of eosinophilic material. High numbers of cocci are found at the interface of the amnion and chorion, extending into the subjacent chorionic plate. Chorionic (fetal) blood vessels are infiltrated by karyorrhectic neutrophils and vessel walls are smudgy and

Placenta, rhesus macaque. The primary and secondary placental discs demonstrate few gray-white foci on the fetal surface with mild thickening of the fetal membranes. (Photo courtesy of: Oregon National Primate Research Center, Oregon Health and Science University, Division of Comparative Medicine, Pathology Services Unit, 505 NW 185th Avenue, Beaverton, OR, 97006)

hypereosinophilic (fibrinoid necrosis). Few large- and medium-size vessels contain luminal fibrin thrombi. The fetal membranes are diffusely necrotic and multifocally expanded by high numbers of karyorrhectic neutrophils and eosinophilic cellular debris. The maternal basal plate and decidua contain lower numbers of degenerate neutrophils which occasionally surround maternal blood vessels. Numerous fibrin coagula are also present within the basal plate. There is moderate, multifocally extensive extravasation of red blood cells (acute hemorrhage) along the maternal decidua on both tissue sections.

Contributor's Morphologic Diagnosis: Placenta, fetal membranes: Chorioamnionitis, neutrophilic, necrotizing, acute, diffuse, severe, with subchorionic microabscesses, chorionic necrotizing vasculitis, amniotic epithelial necrosis, mild neutrophilic deciduitis, decidual vasculitis, and gram-positive cocci, rhesus macaque *(Macaca mulatta)*, nonhuman primate.

Other morphologic diagnoses:

- Umbilical cord: Funisitis, neutrophilic, necrotizing, marked, multifocal with segmental necrotizing umbilical arteritis.
- Lung: Bronchopneumonia, pyogranulomatous, subacute, moderate, diffuse with peribronchial hemorrhage, high numbers of intralesional cocci, intra-alveolar squamous cells, mucin, and amorphous debris.

Contributor's Comment: This is a case of acute streptococcal chorioamnionitis with fetal demise. Microbial culture of the placenta yielded 4+ beta-hemolytic *Streptococcus* sp. Gram staining of placenta sections confirmed numerous gram-positive cocci within the fetal membranes. The umbilical cord and umbilical vessels also contained neutrophilic infiltrates and exhibited necrotic changes to umbilical vessel walls. The character and distribution of inflammation within the fetal membranes in this case, is consistent with acute chorioamnionitis (ACA) due to ascending

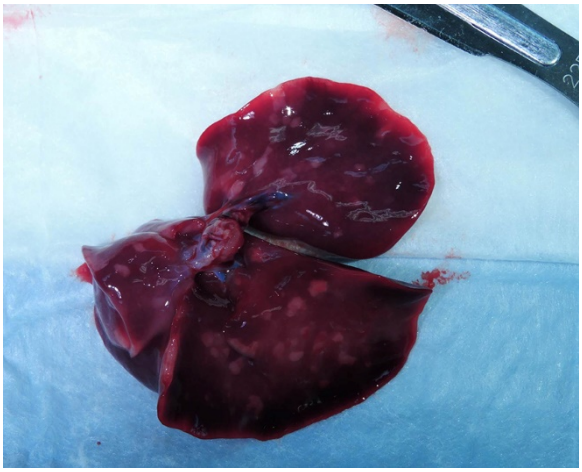

Lungs, rhesus macaque abortus: Numerous 2mm white foci are scattered throughout all lung lobes. (Photo courtesy of: Oregon National Primate Research Center, Oregon Health and Science University, Division of Comparative Medicine, Pathology Services Unit, 505 NW 185th Avenue, Beaverton, OR, 97006)

bacterial infection from the dam's lower genital tract.

In humans and non-human primates, ACA consists of a fetal and maternal acute inflammatory response characterized by diffuse neutrophilic infiltration variably involving the fetal membranes, placenta, and umbilical cord. The initial inflammatory response is maternal, with neutrophils exiting the placental intervillous space and decidual vessels with infiltration of the chorionic plate, later migrating through the fetal membranes and eventually into the amniotic fluid.[1,2] As the maternal inflammatory response progresses, neutrophils become karyorrhectic and apoptotic. In contrast, the fetal inflammatory response varies depending on the gestational age, but may be manifested as chorionic vasculitis, umbilical arteritis and phlebitis, and funisitis as neutrophils transmigrate across the umbilical vessels.

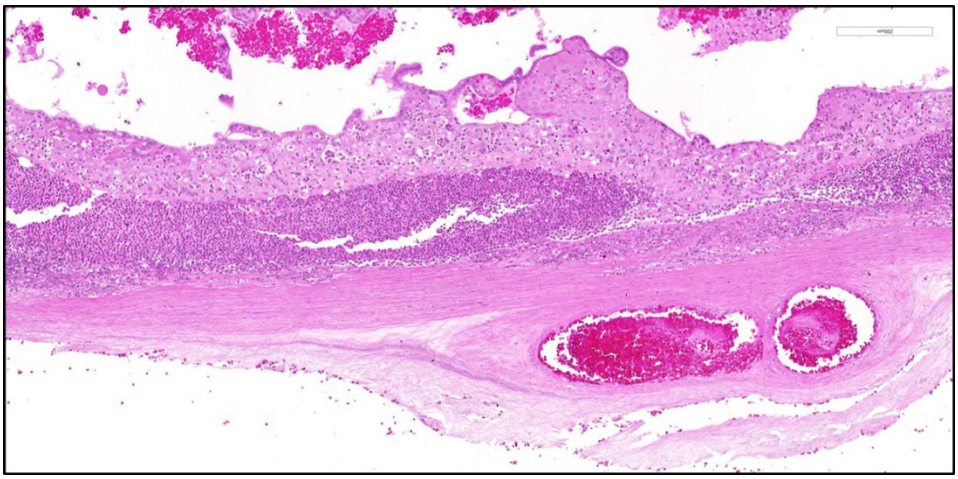

Placenta, rhesus: There is a thick band of degenerate neutrophils and cellular debris lines the deep aspect of the chorioamnionic plate. (HE, 40X)

Most acute chorioamnionitis cases in humans and non-human primates are considered to have an infectious etiology. Ascending microbial invasion from the lower genital tract is the most common route of intrauterine and subsequent intra-amniotic infection.[1,5] Following infection of the amniotic cavity, the fetus may aspirate infected amniotic fluid leading to fetal pneumonia, sepsis, and death in-utero. Infectious pathogens within amniotic fluid may also be swallowed into the gastrointestinal tract or may gain access through the middle ear and tympanic membrane. Commonly isolated microorganisms in human placentas with a histologic diagnosis of ACA include vaginal commensals such as streptococci, staphylococci, *Ureaplasma* sp., and *Mycoplasma hominis*, as well enteric bacteria and anaerobes including *Bacteroides* sp., *E.coli*, and *Fusobacterium* sp..[1,5,7] In addition to commensal organisms from the lower reproductive tract, *Listeria monocytogenes*, a sporadic cause of abortion and stillbirth in captive macaques, may also produce a neutrophilic and necrotizing placentitis characterized by intervillositis and villitis. *L. monocytogenes* undergoes hematogenous spread, gaining access to the placenta through the maternal circulation and intervillous space and eventually invading the villi and fetal circulation.

Acute chorioamnionitis also commonly and indirectly contributes to fetal morbidity and mortality by precipitating preterm labor and birth. Phospholipase production by invading bacteria and neutrophils stimulates the synthesis of prostaglandins, which induce uterine contractions and cervical dilation.[6,7] Increased matrix metalloproteinases (MMP) may contribute to degradation of the

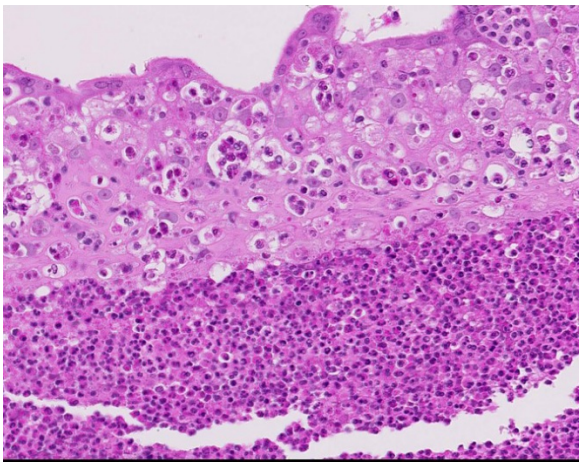

Placenta, rhesus: Trophoblasts superficial to the band of neutrophils are degenerate and/or necrotic; many trophoblasts appear to have phagocytosed degenerate neutrophils. (HE, 320X)

extracellular matrix of the fetal membranes, potentially resulting in premature membrane rupture. Up to one-third of preterm deliveries in women are attributed to ACA.[7]

More frequently, acute chorioamnionitis remains subclinical in the mother with occasional clinical manifestations including pyrexia, leukocytosis, purulent amniotic fluid or vaginal discharge, and uterine tenderness. Maternal sepsis is infrequent and the primary clinical impacts of ACA are the adverse effects on the fetus.[5]

Histologic changes in the present case mirror many of the classic features of ACA found in human placentas. The degree of neutrophil karyorrhexis and amniotic epithelial necrosis coupled with necrotizing funisitis on sections of umbilicus (not included) are indicative of later-stage and more severe infection.[1] Beta-hemolytic *Streptococcus* sp. was isolated from the stomach and pleura of this full-term stillborn rhesus macaque, consistent with ingestion and aspiration of contaminated amniotic fluid. Gram staining of lung sections confirmed high numbers of gram-positive cocci within the alveoli and small airways. Microscopic evaluation of fetal lung tissue showed a pyogranulomatous bronchopneumonia with increased numbers of squamous cells, mucin, and debris. Acute aspiration of meconium was also considered as an etiology for the bronchopneumonia, however, meconium pigment was not appreciated microscopically on lung sections.

Infections due to beta-hemolytic *Streptococcus* sp. in nonhuman primates, including the present case, are considered largely opportunistic and depend on host factors such as age, pregnancy and immune system status, as well as environment and social stress.[3] The most pathogenic streptococcal groups in macaques are beta-hemolytic groups A and B as well as alpha-hemolytic *Streptococcus pneumoniae*, which lacks the Lancefield antigen and serogroup designation. In addition to reproductive loss, streptococcal infections in macaques have also been reported to cause suppurative pneumonia, rhinitis, conjunctivitis, meningoencephalitis, polyarthritis, sepsis, and polyserositis.

JPC Diagnosis: Placental disc and chorioamnionic membrane: Chorio-amnionitis and deciduitis, neutrophilic and

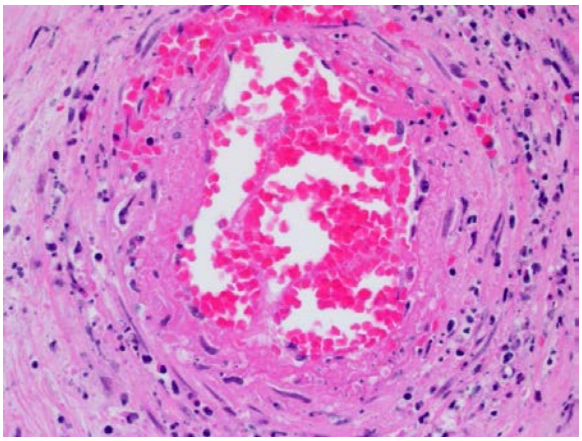

Placenta, rhesus: Chorionic vessels include arterioles, are necrotic, with abundant extruded protein hemorrhage, and cellular debris within their walls. (HE, 320X)

necrotizing, subacute, diffuse, severe, with necrotizing vasculitis, loss of amniotic epithelium and numerous cocci.

Conference Comment: The contributor has done an outstanding job in describing this case.

Streptococci are gram-positive, catalase-negative bacteria which are arranged in pairs or chains and exhibit varying degrees of hemolysis on blood agar which has been used to group the different species. α-Hemolytic streptococci produce a green zone around the colonies from hydrogen peroxide oxidation of hemoglobin to methemoglobin but do not lyse erythrocytes. β-Hemolytic streptococci tend to be the most pathogenic types and cause acute lysis of red blood cells with hemolytic zones around colonies on blood agar. Finally, γ-streptococci are non-hemolytic and non-pathogenic. Another method to divide the over 98 recognized species of *Streptococcus* is using a precipitin test based on extractable carbohydrate antigens called Lancefield groups which are designated A through V (excluding I and J). These groups are further subdivided based on protein antigens, M, R, and T. This is of some importance clinically, as antibodies to Lancefield groups are not protective but antibodies to M, R, or T are protective. M protein, in particular, is an important virulence determinant because it allows the bacterium to evade phagocytosis. For example, the SeM protein of *Streptococcus equi* ssp. *equi* prevents phagocytosis by binding host immunoglobulin and coating the bacterium, masking sites for complement activation and collectin/ficolin binding. Another protein, the FbsA protein is a fibrinogen-binding protein which aids in virulence of *Streptococcus agalactiae*. Other streptococci have analogous proteins, like the FOG protein in group G *Streptococcus dysgalactiae* ssp. *equisimilis*, and the Szp protein of *S. equi* ssp. *zooepidemicus*. Most species of virulent streptococci have a capsule which is either composed of hyaluronic acid (groups A and C) or polysaccharide (groups B, E, and G). The gram-positive cell wall of streptococci contain lipoteichoic acids and peptidoglycan which interact with host macrophages and

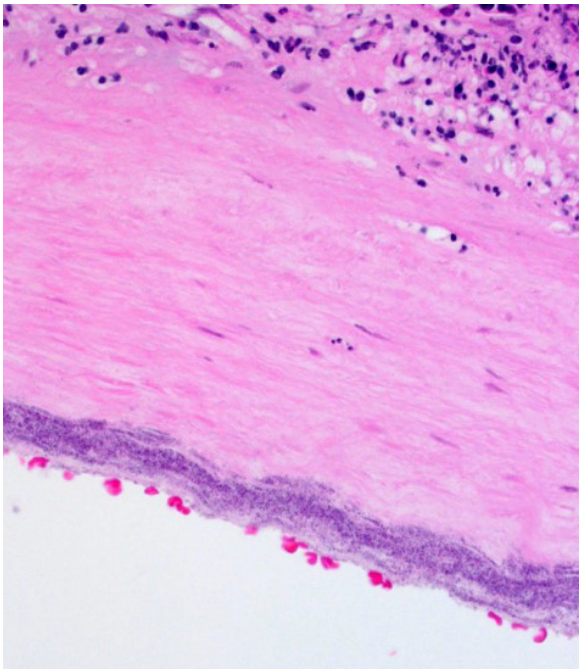

Placenta, rhesus macaque: A band of streptococci lines the deep chorionic plate superficial to the chorioamnionic membrane. (HE, 400X)

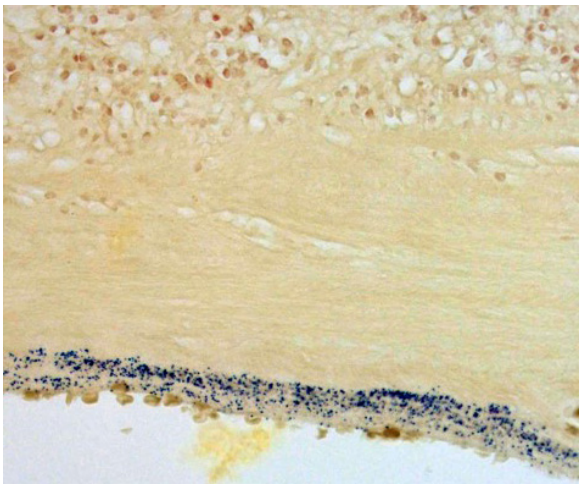

Placenta, rhesus macaque: Gram stain of streptococci in the deep chorionic plate. (Brown-Hopps, 400X)

induce release of proinflammatory cytokines.[9]

Particularly virulent streptococcal species possess pyrogenic toxin superantigens. Superantigens simultaneously bind with major histocompatibility complex class II molecules and T cell receptor molecules on the V-β region resulting in massive activation of antigen-presenting cells and T-cells which proceed to produce overwhelming amounts of cytokines. This so-called "cytokine storm" has detrimental systemic effects and often results in the death of the animal.[9]

Contributing Institution:
Oregon Health & Science University
Oregon National Primate Research Center
Division of Comparative Medicine
Pathology Services Unit
505 NW 185th Avenue Beaverton, OR 97006
www.ohsu.edu/xd/research/centers-institutes/onprc

References:

1. Benirschke K, Burton GJ, Baergen RN. Infectious diseases of the placenta. In: *Pathology of the Human Placenta.* 6th ed. New York, NY: Springer; 2012:557- 581.
2. Chong JK, Roberto R, Chaemsaithong P, et al. Acute chorioamnionitis: definition, pathologic features, and clinical significance. *Am J Obstet Gynecol.* 2015; 213(4 Suppl):529-552.
3. Cline JM, Brignolo L, Ford EW. Urogenital System. In: Abee CR, Mansfield K, Tardif S, Morris T. eds. *Nonhuman Primates in Biomedical Research: Diseases.* 2nd ed. Vol 2. Waltham, MA: Elsevier; 2012:524-527.
4. Egal AS, Ardeshir A, Mariano FV, et al. Contribution of endemic listeriosis to spontaneous abortion and stillbirth in a large outdoor-housed colony of rhesus macaques *(Macaca mulatta). J Am Assoc Lab Animal Sci.* 2015; 54(4):399-404.
5. Gersell DJ, Kraus FT. Diseases of the placenta. In: Kurman RJ, Ellanson LH, Ronnett BM, eds. *Blausteins's Pathology of the Female Genital Tract.* 6th ed. New York, NY: Springer; 2011:1036-1041.
6. Gravett MG, Witkin SS, Novy MJ. A non-human primate model for chorioamnionitis and preterm labor. *Semin Reprod Endocrinol.* 1994; 12(14):246-262.
7. Novy MJ, Duffy L, Axthelm MK et al. *Ureaplasma parvum* or *Mycoplasma hominis* as sole pathogens cause chorioamnionitis, preterm delivery, and fetal pneumonia in rhesus macaques. *Reprod Sci*. 2009;16(1):56-70.
8. Saji F, Samejima Y, Kamiura S, et al. Cytokine production in chorioamnionitis. *J Reprod lmmunol*. 2000; 47(2):185-196.
9. Steward GC. Streptococcus and Enterococcus. In: McVey DS, Kennedy M, Chengappa MM, eds. *Veterinary Microbiology.* 3rd ed. Ames, IA: John Wiley & Sons, Inc.; 2013:194-199.

CASE III: CASE 2 51304 (JPC 4068392).

Signalment: 3-week-old, female, Jersey (*Bos taurus*), bovine.

History: The calf had a reported history of a rotavirus scour and was treated with antibiotics and supportive therapy that consisted of tube-feeding milk by the owner.

Gross Pathology: The calf is in poor body condition and in a fresh state of preservation. The abomasum contains multiple 1-2mm brown/red foci on the mucosal surface and the luminal contents are green-yellow and watery. Several discrete red foci (10-15cm diameter) with fibrin tags are visible on the serosal surface of the rumen. These lesions are transmural and correspond with friable, brown and tan plaques surrounded by a

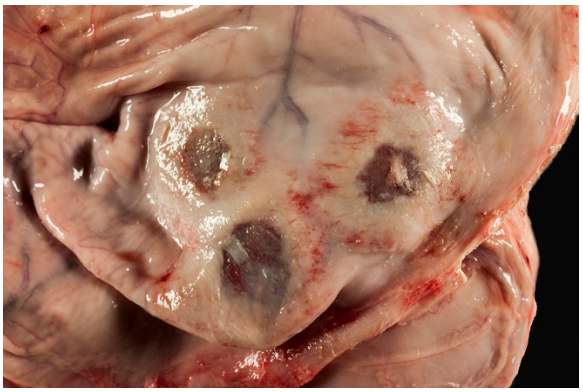

Rumen, calf. Several discrete red foci (10-15cm diameter) with fibrin tags are visible on the serosal surface of the rumen (Photo courtesy of: Massey University, Institute of Veterinary, Animal and Biomedical Sciences, Private Bag 11 222, Palmerston North 4442, New Zealand, http://ivabs.massey.ac.nz http://vet-school.massey.ac.nz)

hyperemic border on the mucosal surface. Approximately 70% of the intervening ruminal mucosa is grey and mildly thickened. The rumen is filled with milky fluid and clots and has a pH of 5. Multiple serosal segments of the small and large intestine are reddened.

Laboratory results: None provided.

Microscopic Description: Rumen: focally and transmurally, the rumen wall is markedly expanded by edema, fibrin and eosinophilic karyorrhectic debris intermixed with numerous inflammatory cells that consist predominantly of intact and degenerate neutrophils, macrophages and smaller numbers of lymphocytes and plasma cells. Multifocally and affecting the serosa and submucosa adjacent the necrotic lesion, there are large numbers of mesenchymal cells admixed with thin strands of collagen. Multiple submucosal blood vessels contain fibrin thrombi and are hyalinized and disrupted by moderate numbers of neutrophils and fungal hyphae that are 5-20um wide, pauci-septate, have thin, non-parallel walls, exhibit irregular, non-dichotomous or right-angled branching and occasionally contain focal bulbous dilatations. Moderate numbers of fungal hyphae are present within the mucosa, submucosa and extending to the serosa. Multifocally, there is mild to moderate hyperkeratosis, erosion and ulceration of the squamous epithelium and there are numerous intraepithelial aggregates of neutrophils (microabscesses). Multifocally between keratin lamellae there are small numbers of basophilic, 2-4um diameter, round to oval and occasionally pseudoseptate fungal organisms. Multifocally there are large numbers of purple bacterial colonies within the superficial mucosa.

Contributor's Morphologic Diagnosis:
Rumen: severe, chronic, focally extensive, necrotizing rumenitis with vasculitis and thrombosis and intralesional fungal hyphae morphologically consistent with zygomycetes. Moderate, chronic, locally extensive ruminal hyperkeratosis with intralesional fungal organisms morphologically consistent with *Candida*.
(Mycotic rumenitis)

Contributor's Comment: Opportunistic fungal organisms such as the zygomycetes of the genera *Mucor*, *Absidia* and *Rhizopus*,

Rumen, calf. Mucosal view of the transmural lesions in the ruminal wall. (Photo courtesy of: Massey University, Institute of Veterinary, Animal and Biomedical Sciences, Private Bag 11 222, Palmerston North 4442, New Zealand, http://ivabs.massey.ac.nz http://vet-school.massey.ac.nz)

Aspergillus, and occasionally *Candida* can cause mycotic rumenitis in calves. The two fungi involved in this case, the zygomycetes and *Candida* require predisposing circumstances such as stress, sepsis, long-term administration of antibiotics or ruminal acidosis to cause disease.[2,9] The zygomycetes are saprophytic and ubiquitous organisms found in the environment, and are common gastrointestinal inhabitants of animals. They are angioinvasive and gain access to the vascular system through injury to mucosal barriers. The yeast *Candida*, in which *C. albicans* is most often implicated in animal disease, is a common inhabitant of the gastrointestinal tract, genital mucosa and upper respiratory tract of mammals. *Candida* exists as a yeast form but can undergo a phenotypic switch to the invasive, filamentous form when there are perturbations to the mucosa or physiological state of an animal.[11] Neither organism should cause disease in an immunocompetent animal.

The incidence of mycotic infections in the forestomach of calves diagnosed at necropsy is relatively low. The incidence rate of alimentary mycosis in calves less than 6-months-old presented to necropsy over a 10-year period is 3%.[4] The most common organisms isolated are the zygomycetes, followed closely by *Aspergillus*. Co-infection, where both organisms are identified, is also reported.[4,8] Isolation of *Candida* is uncommon; however, it is reported to occur in co-infections in adjacent, non-inflamed regions of the mucosa.[8] The most common risk factor for mycotic infection of the forestomachs in these calves is diarrhea that is treated with antibiotics.

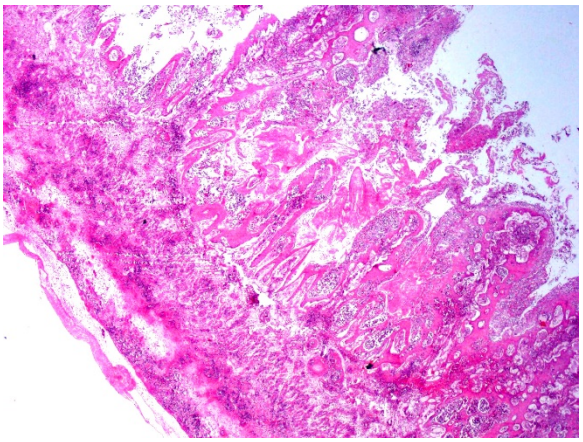

Rumen, calf. There is diffuse transmural necrosis of the ruminal wall with sloughing of the mucosa, extensive infiltration of neutrophils, and widespread necrotizing vasculitis. (HE, 40X)

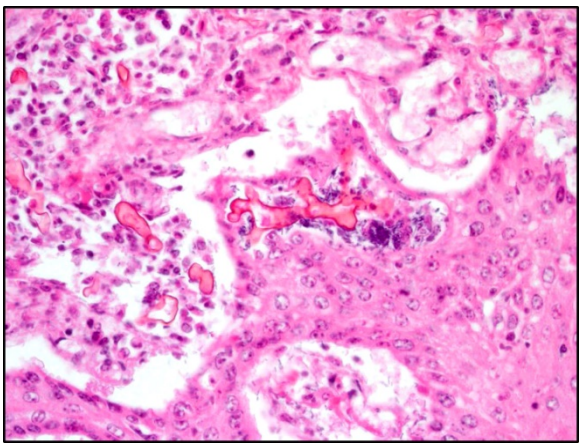

Rumen, calf. Numerous 8-15 um fungal hyphae with non-parallel wall and non-dichotomous branching are present throughout the necrotic mucosa as well as within the walls of vessels. (HE, 400X)

The pH of the ruminal fluid in this calf was 5, which is below normal physiological levels in a milk-fed calf (6.4-7.0).[5] Ruminal acidosis in pre-ruminant calves is primarily caused by esophageal groove dysfunction that results in the spillage and subsequent stagnation and putrefaction of milk in the rumen and reticulum.[6] Risk factors associated with esophageal groove dysfunction include the feeding of milk from a pail or tube, and neonatal diarrhea.[5] Ruminal acidosis causes mild mucosal inflammation, and coupled with the other precipitating factors in this case, such as the antibiotic use and stress, precipitated a high-

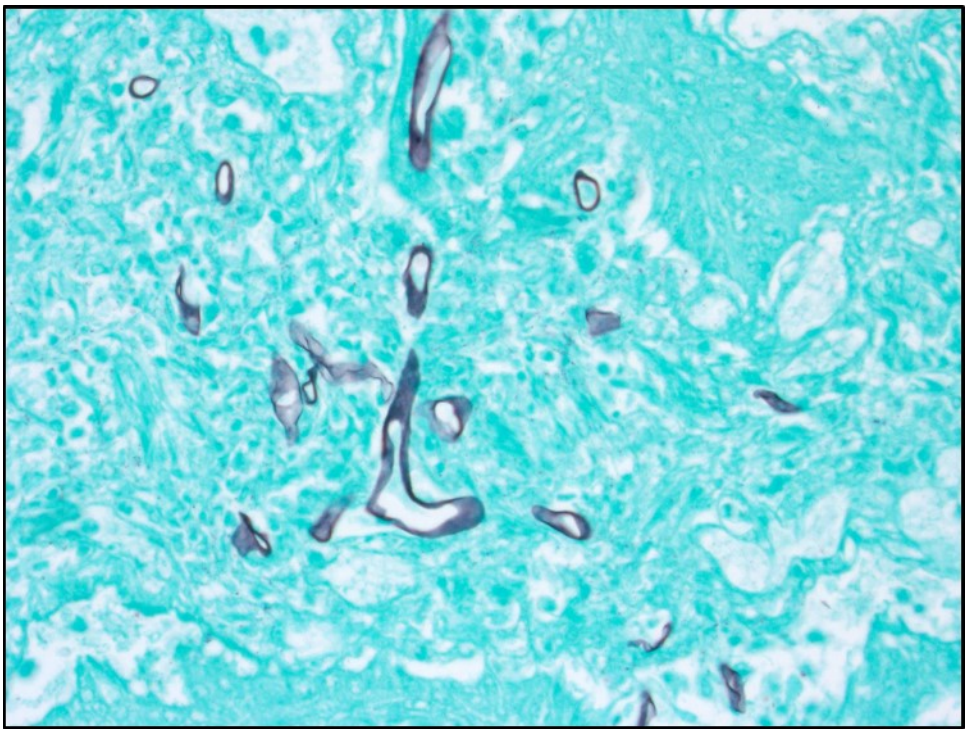

Rumen, calf. A silver stain of the fungal hyphae present in the section. (Gomori methenamine silver, 400X)

risk environment for opportunistic fungal infection.

JPC Diagnosis: Rumen: Rumenitis, necrotizing, focally extensive, severe with necrotizing vasculitis, widespread vascular thrombosis, and numerous fungal hyphae.

Conference Comment: Distinguishing the ruminant forestomachs histologically can be daunting, particularly with advanced disease. Here are a few key features that may simplify the process.

The rumen contains small tongue-shaped papillae which become more substantial as the animal is weaned and begins eating more roughage. The mucosal epithelium has three functions: protection, metabolism, and absorption and is keratinized to protect against rough, fibrous ingesta. Within the deeper strata, short chain volatile fatty acids are metabolized (butyric, acetic, and proprionic acids). Microscopically, what sets the rumen apart is the shape of the papillae and the lack of lamina muscularis extension into the papillae.[1]

Next, the reticulum is composed of long, thin primary lamellae with knob-like projections extending off termed secondary lamellae and permanent interconnecting folds (reticular crests) giving the gross appearance of a honeycomb. The reticulum is also lined by keratinized stratified squamous epithelium and the key microscopic feature are small slits of lamina muscularis within the tips of the primary lamellae.[1]

Finally, the omasum has even more folded lamellae which extend like pages of a book grossly and are lined by keratinized stratified squamous epithelium, all be it not as keratinized as the ruminal papillae. In the omasum, form follows function, and there is a much thicker lamina muscularis beneath the lamina propria that extends into the entire length of the lamellae providing the ability to squeeze ingesta into the abomasum.[1]

Both *Candida* spp. and zygomycetes are normal flora in the ruminant gastrointestinal tract.

Zygomycosis comprises numerous etiologic agents which can manifest clinically as

cutaneous, subcutaneous, systemic (pulmonary or gastrointestinal), or rhinocerebral infections. The microscopic hallmark of all zygomycetes is the invasive mycelial form in tissues which is infrequently septate and exhibits non-dichotomous branching with non-parallel walls and rare bulbous dilatations. The hyphae are often surrounded by eosinophilic granular material (Splendore-Hoeppli phenomenon) and angioinvasion is common particularly with Mucorales. The main microscopic differential for zygomycosis is pythiosis and must be distinguished using immunohisto-chemistry, culture, or PCR. In addition to mycotic rumenitis, zygomycetes are a common cause of abortion in ruminants and a differential for granulomatous lymphadenitis.[3,7,11]

In contrast with zygomycosis, *Candida* spp. are less invasive and often associated with prolonged antibiotic use, immuno-suppression, concurrent disease, or stress. Anorexia in chronically ill animals results in increased keratin along the surface of mucus membranes which may provide a fertile environment for *Candida* to hang on and grow. An important determinant of virulence amongst *Candida* spp. is the presence of adhesins which aide in binding to host tissues. Specifically, yeast bind mannose receptors and hyphae bind complement receptor 3 (CR3) and the Fc-gamma receptor. Adherence and resistance to antifungal drugs is facilitated by biofilm formation. Additionally, *Candida* species produce enzymes to degrade proteins in the extracellular matrix which aides in dissemination (aspartyl proteinases), resist oxidative killing by phagocytes (catalase), and block neutrophil degranulation (adenosine). Microscopically, Candida spp. Are seen in three, often comingling, forms: pseudohyphae, hyphae, and yeast. The pseudohyphal form is composed of chains of

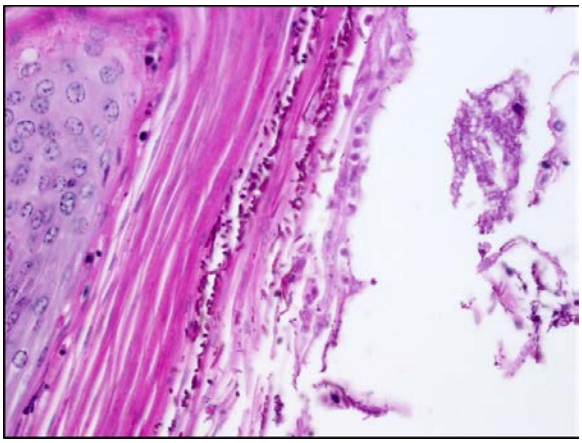

Rumen, calf: Numerous ovoid yeasts are present within the keratin layers of the mucosa. Keratin is commonly seen on the rumenal papillae of nursing calves. (Periodic acid-Schiff, 400X)

blastoconidia and distinguished from the hyphal form by narrowed points of attachment of adjacent yeast. The yeast form can often be seen reproducing by narrow-based budding.[3,10,11]

Conference attendees viewed PAS, GMS, and PTAH immunohistochemical stains to identify organisms and fibrin thrombi present in the section. Polymerized fibrin was identified first at the periphery of affected vessels, plugging endothelial holes, and eventually filling the lumen. While the pathogenicity of the fungal hypehae, present transmurally and often within the walls of necrotic vessels were in doubt, the damage resulting from presumptive yeast forms of *Candida* present largely in the hyperkeratotic layer and mucosa was a source of spirited discussion.

In addition, the possibility of this calf as a “ruminal drinker” (a calf with abnormal closure of the rumenoreticular groove during nursing, which directs milk directly into the stomach) was discussed, the history of tube-feeding was also cited as a possibility for the introduction of milk into the developing rumen, where it might be used as a culture

medium for a range of commensal bacterial and fungal agent.

Contributing Institution:
http://ivabs.massey.ac.nz
http://vet-school.massey.ac.nz

References:

1 Bacha WJ, Bacha LM. *Color Atlas of Veterinary Histology*. 3rd ed. Ames, IA: Wiley-Blackwell; 2012:155-157.
2 Brown CC, Baker DC, Barker IK. Alimentary system. In: Maxie MG, ed. *Jubb, Kennedy, and Palmer's Pathology of Domestic Animals*. 5th ed. London, UK: Saunders; 2007:1-296.
3 Chandler FW, Kaplan W, Ajello L. *Color Atlas and Text of the Histopathology of Mycotic Diseases*. Chicago, IL: Year Book Medical Publishers, Inc.; 1980:42-45, 122-126.
4 Chihaya Y, Furusawa Y, Okada H, Matsukawa K, Matsui Y. Pathological studies on systemic mycoses in calves. *Journal of Veterinary Medical Science*. 1991; 53(6):1051-1058.
5 Dirksen G, Dirr L. Oesophageal groove dysfunction as a complication of neonatal diarrhea in the calf. *Bovine Practitioner*. 1989; 17(4):353-358.
6 Gentile A. Ruminal acidosis in milk-fed calves. *Large Animal Veterinary Rounds*. 2004:4(9).
7 Ginn PE, Mansell JEKL, Rakich PM. Integumentary system. ln: Maxie MG, ed. *Jubb, Kennedy, and Palmer's Pathology of Domestic Animals*. Vol 1. 6th ed. Philadelphia, PA: Elsevier Saunders. 2016:659-660.
8 Neitzke JP, Schiefer B. Incidence of mycotic gastritis in calves up to 30 days of age. *Canadian Veterinary Journal-Revue Veterinaire Canadienne*. 1974; 15(5):139-143.
9 Quinn PJ, Markey BK. Mycology. In: *Concise Review of Veterinary Microbiology*. 1st ed. London, UK: Wiley-Blackwell; 2003:70-87.
10 Uzal FA, Plattner BL, Hostetter JM. Alimentary system. In: Maxie MG, ed. *Jubb, Kennedy and Palmer's Pathology of Domestic Animals*. Vol 2. 6th ed. Philadelphia, PA: Elsevier; 2016:202.
11 Zachary JF. Mechanisms of microbial infection. In: Zachary JF, McGavin MD, eds. *Pathologic Basis of Veterinary Disease*. 5th ed. St. Louis, MO: Elsevier; 2011:147-241.

CASE IV: Case 2 (JPC 4101147).

Signalment: 3.5-month-old, female, CyBB knockout (*Mus musculus*), mouse.

History: The animal had been used as a breeder and was found dead. Dystocia was the top differential diagnosis.

Gross Pathology: There is a mass replacing the caudal right lung lobe that contains inspissated white-tan material (abscess), with few scattered tan pinpoint-1mm foci throughout all lobes. There is bloody discharge from the vulva. The uterus is gravid with 2-3 pups in each horn. The spleen is enlarged 5- fold.

Laboratory results: Bacterial culture yielded positive growth for *Klebsiella pneumoniae ssp pneumonia* from heart blood, as well as swabs from the lung abscess.

Microscopic Description: Lung: There is marked expansion and replacement of architecture by a central region of lytic cell debris, as well as lytic and degenerate neutrophils surrounded by an outer layer of collagen and fibroblasts (abscess). Within some sections, where inflammation is less extensive, there are alveoli lined by cuboidal

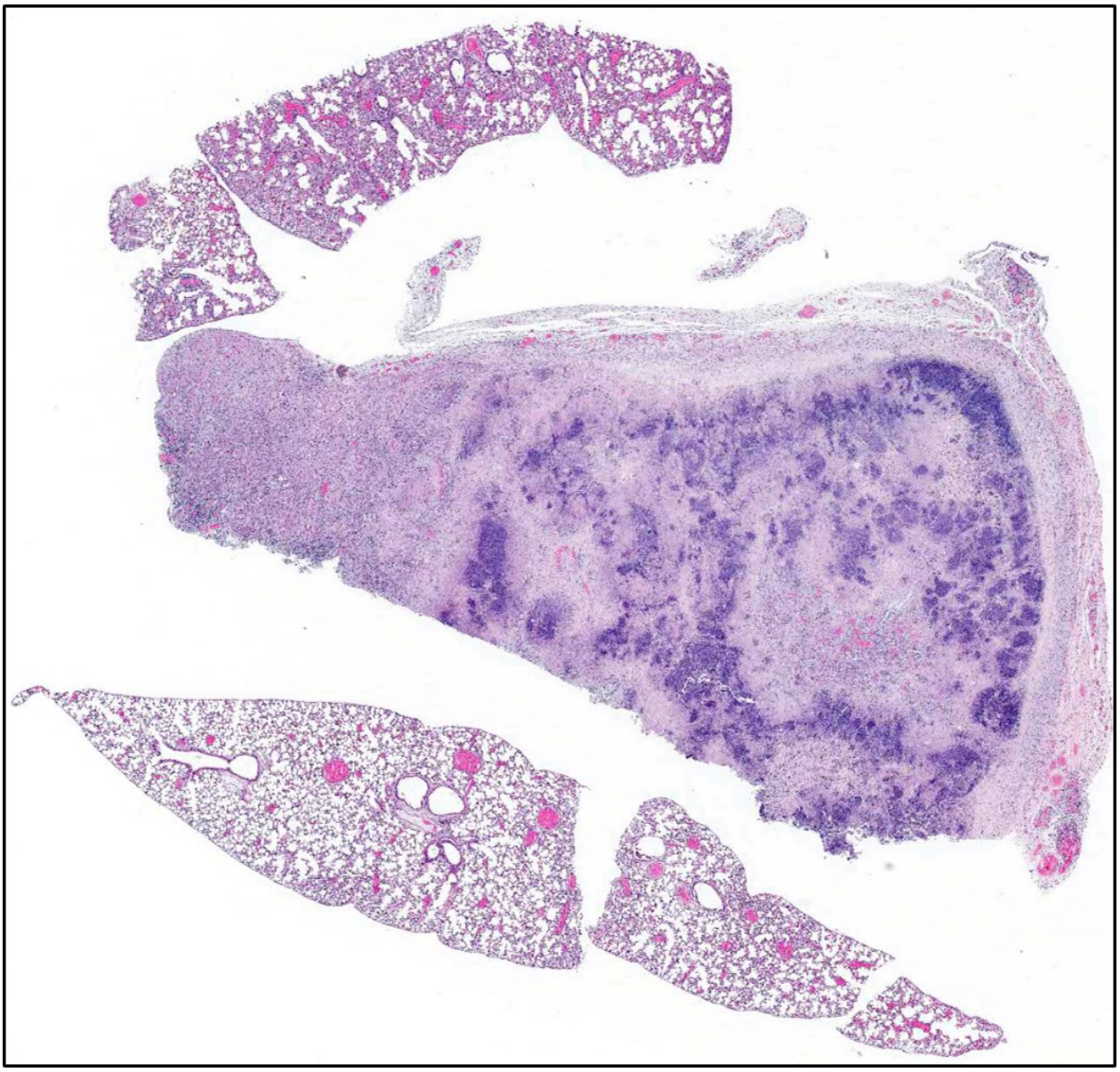

Lung, mouse: Five section of lung are submitted. One section contains a large, subpleural area of necrosis with a prominent basophilic infiltrate of degenerate neutrophils and cellular debris. (HE, 6X)

epithelium (type 2 pneumocyte hyperplasia), and are filled with degenerate neutrophils, epithelioid macrophages and multinucleated giant cells with variably-sized eosinophilic rhomboid crystals. There is compression of adjacent relatively normal parenchyma, where alveoli are filled with similar inflammatory cells containing crystals, which are also present in large numbers in peripheral alveolar spaces in non-abscessed lung sections. Similar crystals are also present free within the lumens of airways. The associated pleura is expanded by immature fibrous connective tissue, macrophages, lymphocytes and plasma cells, and congested small blood vessels.

Contributor's Morphologic Diagnosis:
Lung: Multifocal to coalescing suppurative pneumonia with abscesses; Multifocal to

coalescing granulomatous pneumonia with intracytoplasmic eosinophilic crystals (acidophil macrophage pneumonia)

Contributor's Comment: The submitted slide illustrates two relatively classic lesions seen in mice: bacterial pneumonia with abscessation and acidophil macrophage pneumonia. *Klebsiella pneumoniae* is an enteric commensal bacterium and is considered an opportunistic pathogen. It has been associated with suppurative lesions of the female reproductive tract in aged B6C3F mice, as well as perianal dermatitis, preputial abscesses, otitis and bacteremic disease (leading to pneumonia and abscesses in other organs) in mice of all ages and strains.[1]

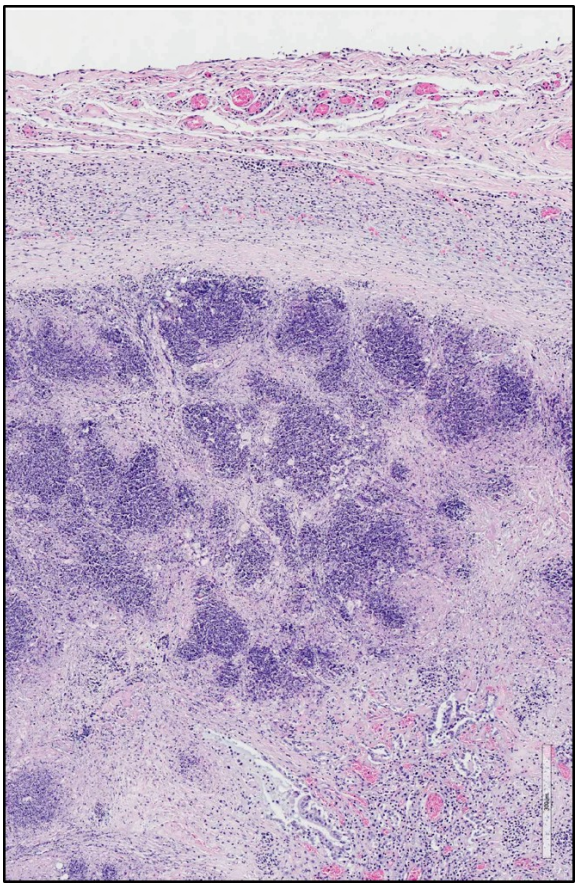

Lung, mouse: Higher magnification of the areas of necrosis, which are partially encapsulated by a fibrous capsule. (HE 88X)

Although not shown, this animal also had necrosuppurative metritis and similar inflammation affecting numerous organs, indicating bacteremia.

Acidophil macrophage pneumonia (AMP), also known as eosinophilic crystalline pneumonia, typically occurs in older animals with B6, 129 and Swiss mice being more susceptible.[1] These crystals have been shown to be composed of iron, α-1 antitrypsin, immunoglobulin and granulocytic breakdown products, as well as Ym1 chitinase.[1,5] AMP is typically an incidental finding, but can cause mortality in severe cases.[1,3]

Both bacterial pneumonia and acidophil macrophage pneumonia, along with splenomegaly, are documented to occur in the present genetically engineered mouse (homozygous null CyBB, or cytochrome b-245, beta polypeptide).[2] This transgenic mouse is used to model chronic granulomatous disease in humans and is considered to be highly susceptible to bacterial infections.[2,4] These mice are also highly susceptible to fungal infections; however, none were observed on H&E stained slides.

JPC Diagnosis: 1. Lung: Pneumonia, necrosuppurative, multifocal to coalescing, severe.
2. Lung, Pneumonia, granulomatous, diffuse, moderate, with numerous intra-histiocytic intracytoplasmic, eosinophilic crystals.

Conference Comment: *Klebsiella* spp. are common commensal bacteria of the gastrointestinal tract of mice in the family Enterobacteriae. These bacteria, although usually quiescent, have the ability to become opportunistic pathogens. In mice (particularly immunodeficient mice), several

disease processes have been linked to *Klebisella* spp. including: suppurative endometritis, perianal dermatitis, preputial abscesses, otitis, tooth infections, urogenital infections, pneumonia, and bacteremic disease (cervical lymphadenopathy, hepatic and renal abscesses, empyema, myocarditis, and thrombosis). Lesions are not characteristic and diagnosis is dependent upon virus isolation with either *Klebsiella pneumoniae* or *K. oxytoca* being the most common isolates.[1]

Acidophilic macrophage pneumonia (AMP) is characterized by accumulation of eosinophilic crystals within macrophages and free within alveolar spaces and is often an incidental finding in certain strains of mice (listed by the contributor above). In severely affected mice, the lungs are grossly red to tan and do no collapse. Ultrastructurally, the crystals are needle-shaped or rhomboidal which a clear lattice structure which repeats every 3-5 nm and are quite complex, composed of Ym1 and Ym2 chitinase, containing iron, alpha-1 antitrypsin, immunoglobulin, and breakdown products of granulocytes. This ultrastructural appearance is similar to Charcot-Leyden crystals associated with eosinophil-rich diseases in humans and non-human primates. Older mice frequently have a small number of alveolar macrophages containing crystals which become pathologic when a disease process impairs clearance of alveolar exudate and the crystal-laden macrophages accumulate and fill vital air spaces leading to dyspnea. Other locations in predisposed mice also contain Ym1 and Ym2 chitinase including: epithelium of the olfactory, nasal respiratory, middle ear, trachea, lung, stomach, gall bladder, bile duct, and pancreatic duct.[1]

Conference participants were hesitant to describe this lesion as an abscess because it is lacking a definitive capsule and there is normal tissue in between areas of lytic necrosis, preferring this to represent multifocal to coalescing areas of lytic necrosis.

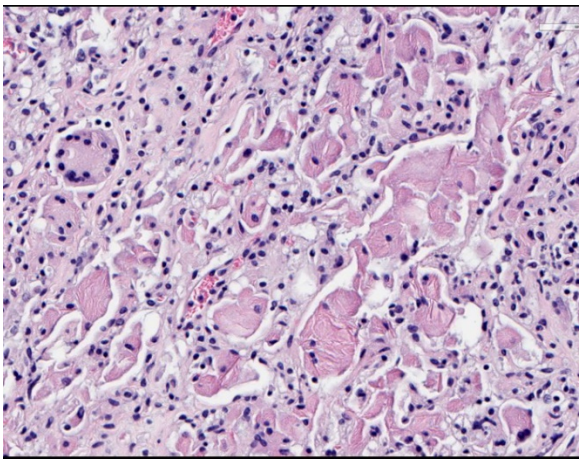

Lung, mouse: Adjacent alveoli (as well as those in other submitted sections), contain numerous epithelioid macrophages and Langhans' type multinucleated macrophages contain numerous acicular eosinophilic crystals. (HE 400X)

Contributing Institution:
http://www.yerkes.emory.edu/research/divisions/pathology/index.html

References:

1. Barthold SW, Griffey SM, Percy DH. *Pathology of Laboratory Rodents and Rabbits*. 4th ed. Ames, IA: Blackwell Publishing Professional; 2007:62, 94-95.
2. Bingel SA. Pathology of a mouse model of x-linked chronic granulomatous disease. *Contemp Top Lab Anim Sci*. 2002; 41(5):33-38.
3. Hoenerhoff MJ, Starost MF, Ward JM. Eosinophilic crystalline pneumonia as a major cause of death in 129S4/SvJae mice. *Vet Pathol*. 2006; 43(5):682-688.
4. Pollock JD, Williams DA, Gifford MA, Li LL, Du X, Fisherman J, Orkin SH, Doerschuk CM, Dinauer MC. Mouse model of X-linked chronic granulomatous disease,

an inherited defect in phagocyte superoxide production. *Nat Genet*. 1995; 9(2):202-209.

5. Ward JM, Yoon M, Anver MR, Haines DC, Kudo G, Gonzalez FJ, Kimura S. Hyalinosis and Ym1/Ym2 gene expression in the stomach and respiratory tract of 129S4/SvJae and wild-type and CYP1A2-null B6, 129 mice. *Am J Pathol*. 2001; 158(1):323-332.

Self-Assessment - WSC 2017-2018 Conference 25

1. In which of the following locations may ectopic nephroblastomas be found in the dog?
    a. Spinal cord
    b. Adrenal gland
    c. Pituitary gland
    d. Prostate

2. Which of the follow is not considered a commensal bacilli from the lower genital tract in primates?
    a. *Streptococcus* sp.
    b. *Ureaplasm*a sp.
    c. Mycoplasma hominis
    d. Listeria monocytogenes

3. Which of the following contain adhesins, which allow binding to host tissues?
    a. *Candida* sp.
    b. Zygomyces sp.
    c. Aspergillus sp.
    d. *Pythium insidiosum*

4. Which of the following is true concerning primary central nervous system lymphoma?
    a. Most of the reported cases in animals are of T-cell origin.
    b. In humans, they are classified as Hodgkin-type lymphomas.
    c. Secondary CNS lymphomas are more common.
    d. Human primary central nervous system lymphomas are rarely angiocentric.

5. Which of the following has NOT been associated with the development of sarcomas in cats?
    a. Implantation of microchips
    b. Injection of long-acting steroids
    c. Trauma
    d. Dental procedures

Please email your completed assessment to Ms. Jessica Gold at Jessica.d.gold2.ctr@mail.mil for grading. Passing score is 80%.This program (RACE program number) is approved by the AAVSB RACE to offer a total of 0.5 CE Credits, with a maximum of 12.5 CE Credits being available to any individual Veterinary Medical Professionals for the 2017-2018 Wednesday Slide Conference. This RACE approval is for the subject matter categories of: SCIENTIFIC using the delivery method of NON-INTERACTIVE DISTANCE. This approval is valid in jurisdictions which recognize AAVSB RACE; however, participants are responsible for ascertaining each board's CE requirements.
RACE does not "accredit", "endorse" or "certify" any program or person, nor does RACE approval validate the content of the program.